Technische Universität München

Lehrstuhl für Anorganische Chemie mit Schwerpunkt Neue Materialien

Investigations on the Reactivity of Nine-Atomic Group 14 Element *Zintl* Anions in Solution

Felix Sebastian Geitner

Vollständiger Abdruck der von der Fakultät für Chemie der Technischen Universität München zur Erlangung des akademischen Grades eines

Doktors der Naturwissenschaften (Dr. rer. nat.)

genehmigten Dissertation.

Vorsitzender:	Prof. Dr. Lukas Hintermann
Prüfer der Dissertation:	1. Prof. Dr. Thomas F. Fässler
	2. Prof. Dr. Shigeyoshi Inoue
	3. Prof. Dr. Eric Rivard (schriftliche Beurteilung) apl. Prof. Dr. Wolfgang Eisenreich (mündliche Prüfung)

Die Dissertation wurde am 25.09.2018 bei der Technischen Universität München eingereicht und durch die Fakultät der Chemie am 08.11.2018 angenommen.

.

für meine Familie & Vesta

„Die Neugier steht immer an erster Stelle eines Problems, das gelöst werden will.“

Galileo Galilei (1564-1642)

Acknowledgements

Mein besonderer Dank geht an meinen Doktorvater

Prof. Dr. Thomas F. Fässler:

Vielen Dank für die Aufnahme in die Arbeitsgruppe, das interessante Forschungsthema, die unentwegte Unterstützung, als auch die konstruktive Zusammenarbeit in angenehmer Arbeitsatmosphäre.

Darüber hinaus wäre diese Arbeit nicht ohne die Unterstützung und Zusammenarbeit mit vielen Kollegen möglich gewesen, welchen ich im Folgenden dafür danken möchte. Mein Dank gilt:

Manuela Donaubauer für die unentwegte und verlässliche Hilfe bei allen organisatorischen Angelegenheiten.

meinem Masteranden **Christoph Wallach**, als auch meinen Forschungspraktikanten **David Mayer**, **Fabian Linsenmann**, **Christoph Wallach**, **Dominik Staude** und **Sebastian Pios** für die engagierte und motivierte Mitarbeit bei meinen Forschungsprojekten.

meinen Laborkollegen **Kerstin Mayer**, **Christina Fischer** und **Christoph Wallach**, als auch meinen Bürokollegen **Maria Müller**, **Christoph Wallach** und **Thomas Wylezich** für die stets angenehme Arbeitsatmosphäre.

Dr. Wilhelm Klein für die geduldige Unterstützung bei der Lösung kristallographischer Probleme.

Dr. Alexander Pöthig, Kerstin Mayer und **Thomas Henneberger** für hilfreiche Diskussionen.

allen Mitgliedern der **Arbeitsgruppen Fässler** und **Nilges** für die angenehme Atmosphäre in der Universität als auch bei Skiausflügen und Wandertouren.

Dr. Richard Weidner, **Dr. Thomas Renner**, **Dr. Jan Tillmann**, **Dr. Elke Fritz-Langhals** von der **WACKER Chemie AG**, als auch allen Mitgliedern des **WACKER Instituts für Silicium Chemie** für den spannenden Austausch verschiedenster Aspekte der Silicium Chemie und die angenehme und produktive Atmosphäre bei den regelmäßigen Treffen.

Prof. T. Don Tilley für die Aufnahme an seinen Lehrstuhl und die Ermöglichung meines Forschungsaufenthaltes an der University of California, Berkeley, als auch allen Mitgliedern seiner Gruppe für die freundliche Aufnahme und hilfsbereite Unterstützung.

Lorenz Schiegerl, **Kerstin Mayer** und **Christina Fischer** für die Unterstützung bei ESI-MS Messungen.

Ulrike Ammari für die Durchführung der Elementaranalysen.

Maria Müller für die Durchführung der EDX Messungen.

Maria Weindl für die Durchführung der VT-NMR Messungen.

Jasmin Dums für die Durchführung der theoretischen Berechnungen.

Dr. Annette Schier für das Korrekturlesen der Manuskripte.

allen Mitarbeitern der **Technischen Universität München**, die zum Gelingen dieser Arbeit beigetragen haben.

Weiterhin möchte ich mich bei all meinen **Aalener** und **Münchner Freunden** für die Aktivitäten Abseits der Promotion bedanken. Ohne euch wäre diese Zeit nicht annähernd so schön gewesen.

Mein besonderer Dank gilt meinen **Eltern Elisabeth** und **Richard**, als auch meinem **Bruder Moritz** für die kontinuierliche und vorbehaltlose Unterstützung während meines Studiums als auch dieser Promotion.

Zum Abschluss gebührt mein allergrößter Dank der wichtigsten Person in meinem Leben: meiner **Freundin Vesta**. Ich danke dir von tiefstem Herzen für die wunderbaren letzten vier Jahre, deine tägliche Unterstützung und den ständigen Rückhalt während meiner Promotion. Ich freue mich auf unsere gemeinsame Zukunft!

List of Abbreviations

[18]crown-6	1,4,7,10,13,16-hexaoxacyclooctadecane
[2.2.2]-cryptand	4,7,13,16,21,24-hexaoxa-1,10-diazabicyclo[8.8.8]hexacosane
Å	Angstrom
A	alkali metal
adamantyl	tricyclo[3.3.1.1]decyl
BTS	copper oxide catalyst for gas regeneration
Bz	benzoyl
cod	cyclooctadiene
coe	cyclooctene
Cp	cyclopentadienyl
Cp*	1,2,3,4,5-pentamethylcyclopentadienyl
Cy	cyclohexyl
δ	chemical shift
d	day
Dipp	2,6-di-*iso*-propylphenyl
dmf	*N*,*N*-dimethylformamide
dppe	1,2-bis(diphenylphosphino)ethane
E	main-group element
EDX	energy dispersive X-ray spectroscopy
en	ethylenediamine
EPR	electron paramagnetic resonance
equiv.	equivalent(s)
ESI-MS	electrospray ionization mass spectrometry
Et	ethyl
eV	electron volt
g	gram(s)
h	hour(s)
^{i}Bu	*iso*-butyl
^{i}Pr	*iso*-propyl
INEPT	insensitive nuclei enhanced by polarisation transfer
IR	infrared spectroscopy
K	Kelvin
m	*meta*
M	transition metal
Me	methyl
MeCN	acetonitrile

Mes	mesityl
mg	milligram(s)
MHz	megahertz
min	minute(s)
mL	millilitre
m/z	mass-to-charge ratio
^{n}Bu	*n*-butyl
NHC	*N*-heterocyclic carbene
NHC^{Dipp}	1,3-di(2,6-di-*iso*-propylphenyl)imidazolylidene
NHC^{iPr}	1,3-di(*iso*-propyl)imidazolylidene
NHC^{Mes}	1,3-di(mesityl)imidazolylidene
NMR	nuclear magnetic resonance spectroscopy
o	*ortho*
p	*para*
PCM	polarizable continuum model
Ph	phenyl
PXRD	powder X-ray diffraction
ppm	parts per million
R	substituent / ligand
r. t.	room temperature
SC-XRD	single crystal X-ray diffraction
^{t}Bu	*tert*-butyl
thf	tetrahydrofuran
TMS	trimethylsilyl
tol	toluene
UV/VIS	ultraviolet-visible spectroscopy

Abstract

The technological progress and the power revolution from fossil fuels to renewable energies are driven by the continuous exploration of novel materials with superior properties. In this context nanoparticles and nanostructured materials of the Group 14 element semiconductors silicon and germanium play a key role. Binary intermetallic compounds of the compositions A_4E_9 (*A*: alkali metal; *E:* Ge-Pb) and $A_{12}E_{17}$ (*A*: alkali metal; *E:* Si-Sn) contain well-defined, nine-atomic Group 14 element *Zintl* clusters, which represent interesting building blocks for the fabrication of such materials. Therefore, within this work the reactivity of soluble $[E_9]^{4-}$ (*E*: Si, Ge, Sn) clusters and silylated $[Ge_9]$ cages towards transition metal complexes and main-group element compounds was investigated. These studies aim for novel methods for the stabilization, functionalization and linkage of the nine-atomic cages in order to make these species available for future applications.

In examinations on the reactivity of $A_{12}Si_{17}$ (*A*: alkali metal) towards a series of coinage metal NHC (*N*-heterocyclic carbene) complexes in NH_3(l) as solvent, the novel complex of a silicide cluster anion **$[NHC^{Dipp}Cu(\eta^4\text{-}Si_9)]^{3-}$** was obtained. The anion is stable at low temperature and can be transferred to pyridine or acetonitrile solutions. However, at room temperature cleavage of the Cu-NHC bond is observed. Analogous reactions of K_4Sn_9 with the coinage metal NHC complexes $NHC^{Dipp}MCl$ (*M*: Cu, Ag, Au) yielded a series of $[M\text{-NHC}]^+$ coordinated $[Sn_9]^{4-}$ clusters **$[NHC^{Dipp}M(\eta^4\text{-}Sn_9)]^{3-}$ (*M*: Cu, Ag, Au)**. Whereas these anions are stable at low temperature for *M* = Cu and Au, for **$[NHC^{Dipp}Ag(\eta^4\text{-}Sn_9)]^{3-}$** cleavage of the Ag-NHC bond under formation of the large intermetalloid aggregate **$[(\eta^4\text{-}Sn_9)Ag(\eta^1\text{-}Sn_9)]^{7-}$** occurs.

Neutral coinage metal NHC decorated $[Ge_9]$ cluster compounds were obtained by conversion of various silylated $[Ge_9]$ clusters with $NHC^{Dipp}MCl$ (*M*: Cu, Ag, Au). Investigations carried out with tris-silylated $[Ge_9]$ clusters bearing silyl groups with varying steric impact yielded **$[NHC^{Dipp}M(\eta^3\text{-}Ge_9\{Si(TMS)_3\}_3)]$ (*M*: Cu, Ag, Au)** and **$[NHC^{Dipp}Cu(\eta^3\text{-}Ge_9\{SiR_3\}_3)]$ (*R*: ^{i}Pr, ^{i}Bu)**. By contrast, analogous reactions with the bis-silylated cluster $[Ge_9\{Si(TMS)_3\}_2]^{2-}$ led to the dinuclear coinage metal compounds **$[(NHC^{Dipp}M)_2(\eta^3,\eta^3\text{-}Ge_9\{Si(TMS)_3\}_2)]$ (*M*: Cu, Ag, Au)**, in which the coinage metal cations are bridged by the $[Ge_9]$ moiety.

Moreover, reactions of $[Ge_9\{Si(TMS)_3\}_n]^{(4-n)-}$ (*n*: 2, 3) with the early transition metal complex $[Cp_2TiCl]_2$ yielded the neutral compound **$[Cp_2Ti(MeCN)(\eta^1\text{-}Ge_9\{Si(TMS)_3\}_3)]$** and the $[Cp_2Ti]^+$ bridged dimeric tri-anion **$[Cp_2Ti(\eta^1\text{-}Ge_9\{Si(TMS)_3\}_2)_2]^{3-}$**. In both species the $[Ge_9]$ clusters approach Ti(III) with single Ge vertex atoms under formation of donor-acceptor interactions.

Further examinations on the reactivity of [Ge_9] clusters towards **Group 13 element** compounds [BrBN(Mes)-CH_2-CH_2-N(Mes)], [BrBN(Dipp)-CH=CH-N(Dipp)], Mes_2BBr and [$^tBu_2AlBr]_2$ yielded a series of mixed-substituted anionic species **[Ge_9{Si(TMS)$_3$}$_2$*ER*$_2$]$^-$** (*E*: B, Al; *R*: substituent).

The functionalization of [Ge_9] clusters with phosphanyl groups was achieved by reactions of chlorophosphines with silylated [Ge_9] clusters, yielding neutral **[Ge_9{Si(TMS)$_3$}$_3$P*RR^I*]** (*R*, *R^I*: small alkyl or alkenyl) or anionic **[Ge_9{Si(TMS)$_3$}$_2$P*RR^I*]$^-$** (*R*, *R^I*: medium or large alkyl, alkenyl, aryl, aminoalkyl) mixed-functionalized [Ge_9] cluster species. The principle of phosphine-functionalization of [Ge_9] was validated by the formation of a series of zwitterions **[(Ge_9{Si(TMS)$_3$}$_2$)*R*$_2$P]CuNHC^{Dipp}** (*R*: medium-sized substituent) comprising P-Cu interactions. However, the isolation of **[NHC^{Dipp}Cu(η^3-Ge_9{Si(TMS)$_3$}$_2$P*R*$_2$)]** (*R*: large substituent) with Ge-Cu interactions revealed that the steric impact of the attached phosphanyl groups is decisive for the reactivity of the mixed-functionalized [Ge_9] cluster anions. Moreover, the formation of the dimeric species **[{Si(TMS)$_3$}$_2$$Ge_9${(^{t}Bu)$_2$PCu}$_2$$Ge_9${Si(TMS)$_3$}$_2$]** proved that the attached phosphanyl groups can also participate in the linkage of [Ge_9] clusters.

Multiple phosphine-functionalized [Ge_9] clusters **[Ge_9{P(N^{i}Pr$_2$)$_2$}$_3$]$^-$** and **[Ge_9{P(N^{i}Pr$_2$)^{t}Bu}$_3$]$^-$** were obtained by heterogenous reactions of K_4Ge_9 with the respective chlorophosphines in MeCN. The anions readily react with NHC^{Dipp}CuCl under formation of the neutral compounds **[NHC^{Dipp}Cu(η^3-Ge_9{P(N^{i}Pr$_2$)$_2$}$_3$)]** or **[NHC^{Dipp}Cu(η^3-Ge_9{P(N^{i}Pr$_2$)^{t}Bu}$_3$)]**. Investigations on the reactivity of **[Ge_9{P(N^{i}Pr$_2$)^{t}Bu}$_3$]$^-$** towards *M*(CO)$_5$(thf) (*M*: Cr, Mo, W) indicated the formation of multiple [*M*(CO)$_5$] fragment coordinated [Ge_9] clusters. Moreover, the formation of the fivefold coordinated [Ge_9] cluster **[(NHC^{Dipp}Cu)$_2$(η^3,η^3-Ge_9{P(N^{i}Pr$_2$)$_2$}$_2$Cr(CO)$_5$)]** in reactions of **[NHC^{Dipp}Cu(η^3-Ge_9{P(N^{i}Pr$_2$)$_2$}$_3$)]** with Cr(CO)$_5$(thf) revealed that the multiple phosphine-functionalized [Ge_9] clusters can also undergo ligand exchange reactions at the [Ge_9] core.

Zusammenfassung

Der technologische Fortschritt und die Energiewende von fossilen Brennstoffen hin zu erneuerbaren Energien werden durch die stetige Entwicklung neuer Materialien mit verbesserten Eigenschaften vorangetrieben. In diesem Zusammenhang spielen Nanopartikel und nanostrukturierte Materialien der Gruppe-14-Element-Halbleiter Silicium und Germanium eine wichtige Rolle. Binäre intermetallische Verbindungen mit der Zusammensetzung A_4E_9 (*A*: Alkalimetall; *E:* Ge-Pb) und $A_{12}E_{17}$ (*A*: Alkalimetall; *E:* Si-Sn) enthalten wohldefinierte, neunatomige Gruppe-14-Element-Cluster, welche interessante Bausteine für den Aufbau solcher Materialien darstellen. Im Rahmen dieser Arbeit wurden Untersuchungen zur Reaktivität von löslichen $[E_9]^{4-}$ (*E*: Si, Ge, Sn) Clustern und silylierten $[Ge_9]$ Clustern gegenüber Übergangsmetallkomplexen und Hauptgruppenelementverbindungen durchgeführt. Dies dient dem Zweck neue Methoden für die Stabilisierung, Funktionalisierung und Verknüpfung der neunatomigen Käfige zu finden und diese für zukünftige Anwendungen verfügbar zu machen.

Bei Untersuchungen zur Reaktivität von $A_{12}Si_{17}$ (*A*: Alkalimetall) gegenüber einer Reihe von Münzmetall-NHC (*N*-heterocyclisches Carben) Komplexen in NH_3(l) als Lösungsmittel wurde der neue Komplex eines Silicid Clusteranions **$[NHC^{Dipp}Cu(\eta^4\text{-}Si_9)]^{3-}$** erhalten. Das Anion ist bei niedriger Temperatur stabil und kann in andere Lösungsmittel wie Pyridin oder Acetonitril überführt werden. Allerdings findet bei Raumtemperatur eine Spaltung der Cu-NHC Bindung statt. Analoge Studien zu Reaktionen zwischen K_4Sn_9 und den Münzmetall-NHC Komplexen $NHC^{Dipp}MCl$ (*M*: Cu, Ag, Au) resultierten in der Bildung einer Reihe von $[M\text{-NHC}]^+$ koordinierten $[Sn_9]^{4-}$ Clustern **$[NHC^{Dipp}M(\eta^4\text{-}Sn_9)]^{3-}$ (*M*: Cu, Ag, Au)**. Während diese Anionen für *M* = Cu und Au bei geringer Temperatur stabil sind, findet im Falle von **$[NHC^{Dipp}Ag(\eta^4\text{-}Sn_9)]^{3-}$** eine Spaltung der Ag-NHC Bindung unter Bildung des großen intermetalloiden Aggregats **$[(\eta^4\text{-}Sn_9)Ag(\eta^1\text{-}Sn_9)]^{7-}$** statt.

Weiterhin wurden neutrale Münzmetall-NHC komplexierte $[Ge_9]$ Cluster durch Umsetzung verschiedener silylierter $[Ge_9]$ Cluster mit $NHC^{Dipp}MCl$ (*M*: Cu, Ag, Au) erhalten. Untersuchungen mit dreifach silylierten $[Ge_9]$ Clustern mit Silylgruppen unterschiedlichem sterischen Anspruchs resultierten in der Bildung von **$[NHC^{Dipp}M(\eta^3\text{-}Ge_9\{Si(TMS)_3\}_3)]$ (*M*: Cu, Ag, Au)** und **$[NHC^{Dipp}Cu(\eta^3\text{-}Ge_9\{SiR_3\}_3)]$ (*R*: ^{i}Pr, ^{t}Bu)**. Im Gegensatz dazu führten Reaktionen mit dem bis-silylierten Cluster $[Ge_9\{Si(TMS)_3\}_2]^{2-}$ zur Bildung von $[Ge_9]$ Cluster verbrückten zweikernigen Münzmetallkomplexen **$[(NHC^{Dipp}M)_2(\eta^3,\eta^3\text{-}Ge_9\{Si(TMS)_3\}_2)]$ (*M*: Cu, Ag, Au)**.

Reaktionen von $[Ge_9\{Si(TMS)_3\}_n]^{(4-n)-}$ (*n*: 2, 3) mit dem frühen Übergangsmetallkomplex $[Cp_2TiCl]_2$ resultierten in der neutralen Verbindung **$[Cp_2Ti(MeCN)(\eta^1\text{-}Ge_9\{Si(TMS)_3\}_3)]$** und der $[Cp_2Ti]^+$ verbrückten dimeren Spezies **$[Cp_2Ti(\eta^1\text{-}Ge_9\{Si(TMS)_3\}_2)_2]^{3-}$**. In beiden Komplexen treten Donor-Akzeptor Wechselwirkungen zwischen einzelnen Ge Clusteratomen und Ti(III) auf.

Untersuchungen zur Reaktivität von [Ge_9] Clustern gegenüber Verbindungen der **13. Hauptgruppe** [BrBN(Mes)-CH_2-CH_2-N(Mes)], [BrBN(Dipp)-CH=CH-N(Dipp)], Mes_2BBr und [$^tBu_2AlBr]_2$ resultierten in der Bildung einer Reihe von anionischen gemischt-substituierten Spezies **[Ge_9{$Si(TMS)_3$}$_2$*ER_2*]$^-$** (*E*: B, Al; *R*: Substituent).

Die Funktionalisierung von [Ge_9] Clustern mittels Phosphanyl Gruppen wurde durch Reaktionen der entsprechenden Chlorphosphane mit silylierten [Ge_9] Clustern erreicht, wobei neutrale **[Ge_9{$Si(TMS)_3$}$_3$P*RR^I*]** (*R*, *R^I*: kleine Alkyl oder Alkenyl Reste) oder anionische **[Ge_9{$Si(TMS)_3$}$_2$P*RR^I*]$^-$** (*R*, *R^I*: mittelgroße und große Alkyl, Alkenyl, Aryl, Aminoalkyl Reste) gemischt-funktionalisierte [Ge_9] Cluster Spezies erhalten wurden. Das Prinzip der Phosphan-Funktionalisierung von [Ge_9] wurde durch die Bildung einer Reihe von zwitterionischen Verbindungen **[(Ge_9{$Si(TMS)_3$}$_2$)*R_2*P]CuNHC^{Dipp}** (*R*: mittelgroße Substituenten) mit P-Cu Interaktionen bestätigt. Die Isolierung von **[NHC^{Dipp}Cu(η^3-Ge_9{$Si(TMS)_3$}$_2$P*R_2*)]** (*R*: große Substituenten) mit Ge-Cu statt P-Cu Wechselwirkungen zeigt, dass der sterische Anspruch der eingeführten Phosphanyl Gruppen entscheidenden Einfluss auf die Reaktivität der funktionalisierten Cluster Anionen hat. Weiterhin konnte durch die Synthese der dimeren Verbindung **[{$Si(TMS)_3$}$_2$$Ge_9${($^tBu)_2$PCu}$_2$$Ge_9${$Si(TMS)_3$}$_2$]** nachgewiesen werden, dass die angebrachten Phosphanyl Gruppen auch zur Verknüpfung von [Ge_9] Clustern genutzt werden können.

Die mehrfach Phosphan-funktionalisierten [Ge_9] Cluster **[Ge_9{$P(N^iPr_2)_2$}$_3$]$^-$** und **[Ge_9{$P(N^iPr_2)^tBu$}$_3$]$^-$** wurden durch heterogene Reaktionen von K_4Ge_9 mit den entsprechenden Chlorphosphanen in Acetonitril erhalten. Die Anionen reagieren mit NHC^{Dipp}CuCl unter Bildung der Verbindungen **[NHC^{Dipp}Cu(η^3-Ge_9{$P(N^iPr_2)_2$}$_3$)]** oder **[NHC^{Dipp}Cu(η^3-Ge_9{$P(N^iPr_2)^tBu$}$_3$)]**. Untersuchungen zur Reaktivität von **[Ge_9{$P(N^iPr_2)^tBu$}$_3$]$^-$** gegenüber *M*$(CO)_5$(thf) (*M*: Cr, Mo, W) deuten auf die Bildung von mehrfach [*M*$(CO)_5$] Fragment koordinierten Addukten der Cluster hin. Weiterhin führten Reaktionen von **[NHC^{Dipp}Cu(η^3-Ge_9{$P(N^iPr_2)_2$}$_3$)]** mit $Cr(CO)_5$(thf) zur Bildung von **[(NHC^{Dipp}Cu)$_2$(η^3,η^3-Ge_9{$P(N^iPr_2)_2$}$_2$$Cr(CO)_5$)]**. Die Isolierung dieser fünffach substituierten Verbindung zeigt, dass die mehrfach Phosphan-funktionalisierten [Ge_9] Cluster auch Ligandenaustausch Reaktionen am [Ge_9] Clusterkern eingehen können.

Table of Contents

Note

This dissertation is written as a publication-based thesis. All articles published in peer-reviewed journals are included in this dissertation. The respective bibliographic data is compiled in chapter 5. Regarding unpublished work, corresponding manuscripts for publication were prepared and are also included in chapter 5. All peer-reviewed publications and their bibliographic data are listed in chapter 6. The relevance of this work for science, a review on relevant literature, as well as the scope and outline of the thesis are presented as introductory part in chapter 1. Details on the synthesis and characterization of materials as well as computational methods are presented in chapter 2. The results and discussion in chapter 3 are presented as summaries of the embedded publications and manuscripts. An overall summary and conclusion is given in chapter 4.

1 Introduction

1.1 Relevance of the Group 14 Elements Si, Ge and Sn in Material Science

The Group 14 elements silicon and germanium are both intrinsic semiconductors and reveal indirect band gaps of 1.12 eV (Si) or 0.67 eV (Ge), respectively.[1] Additionally, both can be n- and p-doped with a range of elements.[2-5] Silicon and germanium can be used as semiconducting materials in transistors or integrated circuits,[6-7] and they are also interesting materials with respect to other application fields such as photovoltaics,[8-9] optoelectronics[10-12] or anode materials in lithium ion batteries, [13-14] which have recently attracted much attention in connection with the energy revolution (replacement of fossil fuels by renewable energies). Since silicon is an abundant (29 % by weight of the Earth's crust)[15] and inexpensive element it has widely replaced its rarer and more expensive congener germanium as a semiconducting material in most electronic devices we are using in our daily lives.[7] However, germanium also reveals superior properties compared to silicon such as an increased electron- and hole mobility, an increased Li-ion diffusivity and tuneable optoelectronic properties, which makes germanium-based materials still especially interesting with respect to lithium ion batteries and optoelectronics.[11, 16-17] Another interesting feature of germanium is its capability to form solid solutions $Ge_{1-x}E_x$ (*E*: Si, Sn) with silicon or tin, which allows for a fine-tuning of the material's properties in dependence of the composition.[18-20] Tin, as the heaviest Group 14 congener dealt with within this work, is mainly applied as component in alloys, which it readily forms with a series of other metals (e. g. bronzes with copper).[21] The alloy Nb_3Sn reveals superconductive properties and finds application in superconductive magnets, and thin layers of tin oxide or tin sulfide can be used as electronically conducting films in optoelectronic devices.[21-24]

Rapid technological progress and the energy revolution from fossil fuels to renewable energies demand the continuous exploration of novel materials with superior properties. In this context, the synthesis of nanoparticles or the fabrication of nanostructured materials with unique morphologies is a promising approach. Regarding the Group 14 element semiconductors silicon and germanium, the application of Group 14 element clusters as tailor-made building blocks for such materials might play a key role in the future. In general, there are different approaches towards Group 14 element clusters in solution, comprising the bottom-up synthesis of clusters from small precursor molecules and the extraction of preformed deltahedral *Zintl* clusters from solid state *Zintl* phases.[25-27] This thesis addresses the extraction of deltahedral $[E_9]^{4-}$ (*E*: Si, Ge, Sn) *Zintl* clusters from solid state *Zintl* phases and the investigation of their reactivity in solution with respect to the stabilization and functionalization of these clusters, as well as their linkage to larger aggregates.

1.2 Different Approaches towards Group 14 Element Clusters in Solution

Bottom-up Approaches

For the bottom-up synthesis of silicon clusters, the reductive coupling of halogenated silanes by complete dehalogenation or the application of nucleophilic Si_2 precursors have been established as methods of choice.[28-33] Initially, these routes evolved due to the rareness of stable low-valent silicon halide precursors, which are available in broader range in the meantime.[34-38] By contrast, for the formation of cage compounds of germanium and tin, the reduction of $R_{4-n}EX_n$ (*E*: tetrel element, *R*: organyl; *X*: halide) under cleavage of *RX,* the reduction of low-valent molecules $E^{II}X_2$ (*E*: tetrel element, *X*: halide) or the disproportionation of metastable Ge(I) or Sn(I) halides *via* co-condensation are the most frequently used approaches.[25, 27] The cage compounds obtained from the described bottom-up syntheses either reveal exclusively ligand bound cage vertices,[39-44] or they contain also ligand-free cluster atoms [Scheme 1.1 (Si),[29-31, 45, 46] Scheme 1.2 (Ge, Sn)].[47-52] In the latter case the number of cage atom to cage atom bonds is higher than the number of cage atom to ligand bonds. With respect to further functionalization of the clusters, or the formation of larger networks or aggregates by connection of several clusters to each other, clusters comprising ligand-free vertex atoms are especially interesting. Regarding silicon cages, the term siliconoid clusters was introduced for unsaturated silicon clusters comprising at least one ligand-free cluster atom with a hemispheroidal coordination sphere.[26, 31, 46] A selection of siliconoid clusters is presented in Scheme 1.1.

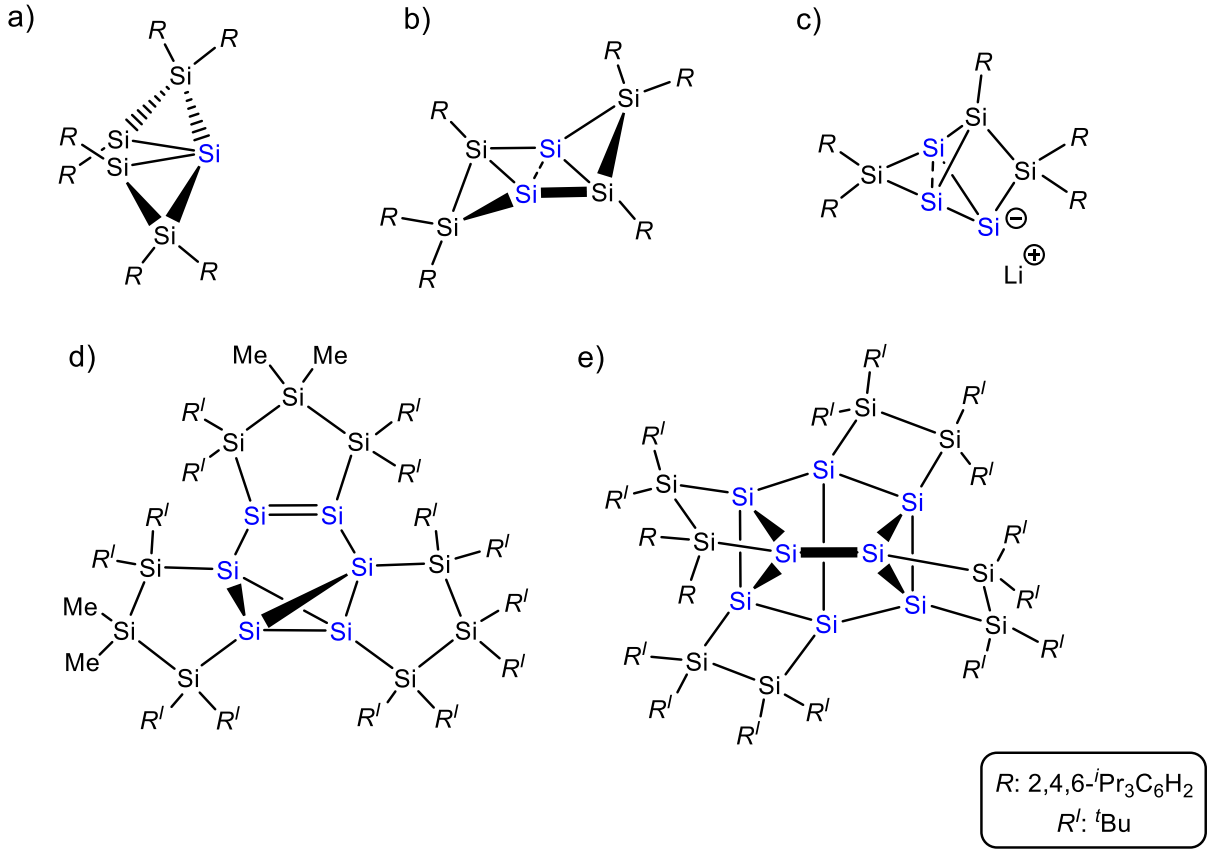

Scheme 1.1: Structures of a selection of siliconoid clusters. Ligand-free silicon atoms are presented in blue colour. a) Si_5 cluster comprising one naked Si atom, which was the first stable isolated siliconoid.[31] b) Tricyclic isomer of hexasilabenzene comprising two ligand free silicon vertices.[45] c) First anionic siliconoid representing the missing link between anionic silicide clusters and siliconoids.[46] d) Cyclopentasilane-fused hexasilabenzvalene comprising six Si atoms, which are exclusively bound to other Si vertices.[29] e) Cyclotetrasilane-fused persilacuneane with eight Si vertices exclusively connected to other Si atoms.[30]

In case of the heavier homologues Ge and Sn, clusters comprising naked uncoordinated vertex atoms are referred to as metalloid clusters, which emphasizes their intermediacy between soluble molecules and solid state bulk structures. The oxidation state of the metal vertices in metalloids is close to zero as in the elemental metals.[53-55] A selection of metalloid Ge or Sn clusters with at least one uncoordinated cluster vertex atom is presented in Scheme 1.2.

The formation of various siliconoid and metalloid cages with different cage sizes and varying structural motifs reveals the huge potential of these bottom-up approaches. However, the synthetic procedures oftentimes suffer from low yield and sometimes several reaction steps are required to obtain the desired cluster species.[25, 26, 29, 30] Moreover, for certain techniques such as co-condensation, special equipment is needed, which prohibits an easy up-scaling of the reactions.[52, 56] Thus, mostly only small amounts of the cage molecules can be isolated by this method.

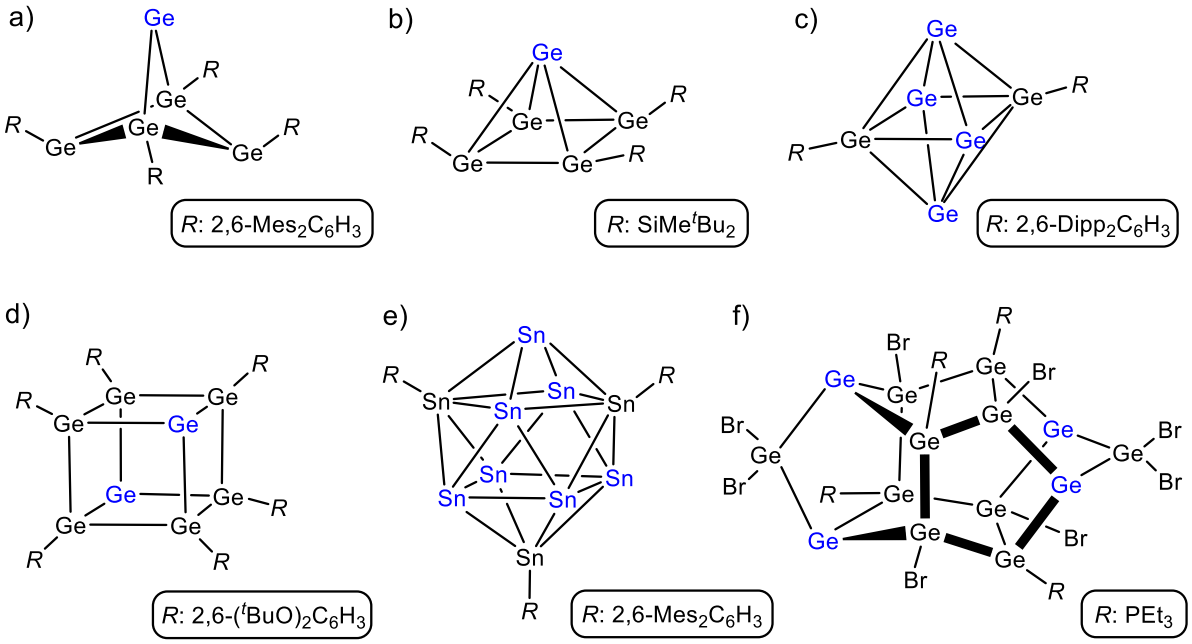

Scheme 1.2: Selection of metalloid Ge and Sn cages comprising uncoordinated cluster vertex atoms (blue) obtained *via* bottom-up synthesis from small precursor molecules. a) $[Ge_5\{2,6\text{-}Mes_2C_6H_3\}_4]$,[47] b) $[Ge_5\{SiMe^tBu_2\}_4]$,[48] c) $[Ge_6\{2,6\text{-}Dipp_2C_6H_3\}_2]$,[49] d) $[Ge_8\{2,6\text{-}(^tBuO)_2C_6H_3\}_6]$,[50] e) $[Sn_{10}\{2,6\text{-}Mes_2C_6H_3\}_2]^+$,[51] f) $[Ge_{14}Br_8(PEt_3)_4]$.[52]

Extraction of Discrete Deltahedral Group 14 *Zintl* Clusters from Solid State *Zintl* Phases

As already stated in the previous section, solid state *Zintl* phases of Group 14 elements represent interesting precursors for discrete deltahedral Group 14 element *Zintl* clusters in solution. In general, *Zintl* phases can be described as salt-like intermetallic compounds in which the valence electrons of the more electropositive component are transferred to the more electronegative element, which results in polyatomic anion substructures. The structure of the formed polyanions can be often derived from the *Zintl-Klemm-Busmann* concept (8-*N* rule).[57-59] *Zintl* phases of the compositions A_4E_9 (*A*: Na-Cs, *E*: Ge,[12, 60-62] Sn,[60, 63] Pb[64-67]) and $A_{12}E_{17}$ (*A*: Na-Cs, *E*: Si,[65, 68] Ge,[60, 65] Sn[65]) are accessible *via* solid state syntheses from the elements, yielding the neat solids in macroscopic yield.[12, 60-68] The A_4E_9 phases which exist for the tetrel elements Ge-Pb, exclusively contain nine-atomic polyanionic $[E_9]^{4-}$ clusters and reveal a decent solubility in highly polar solvents such as ethylenediamine, dmf or NH_3(l). By contrast, the $A_{12}E_{17}$ (*E*: Si-Sn) phases (in case of silicon the only source for $[Si_9]$ clusters, since no phase of the composition A_4Si_9 is known to date) do also contain $[E_4]^{4-}$ tetrahedrons besides the $[E_9]^{4-}$ clusters in a $[E_9]^{4-}$ / $[E_4]^{4-}$ ratio of 1:2 (Figure 1.1). Due to the increased charge per atom ratio in the $[E_4]^{4-}$ tetrahedrons, the $A_{12}E_{17}$ phases reveal a decreased solubility compared to the A_4E_9 phases. The formation of the clusters contained in these *Zintl* phases can only partially be explained with the *Zintl*-Klemm-Busmann concept but follows the *Wade-Mingos* rules (see chapter 1.3.1).

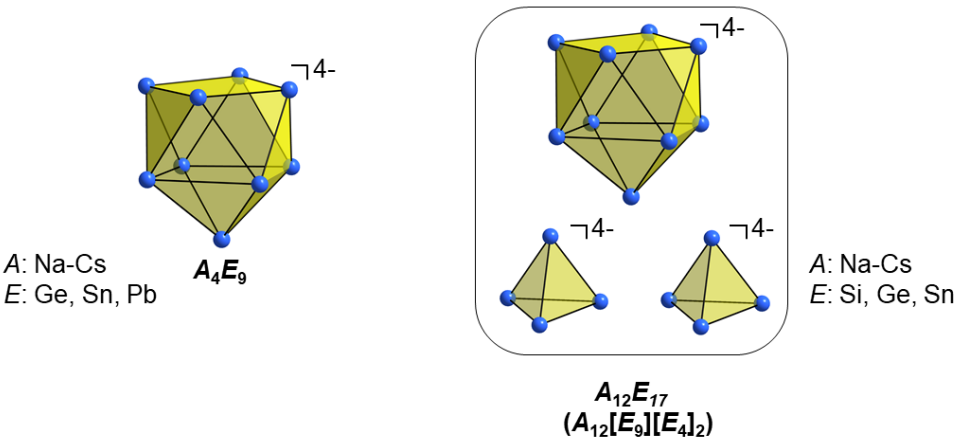

Figure 1.1: *Zintl* clusters contained in *Zintl* phases of the compositions A_4E_9 (*A*: Na-Cs, *E*: Ge-Pb) and $A_{12}E_{17}$ (*A*: Na-Cs, *E*: Si-Sn).

Upon dissolution of *Zintl* phases of the compositions A_4E_9 and $A_{12}E_{17}$, a charge separation occurs, resulting in the presence of discrete anionic *Zintl* clusters in solution, which comprise exclusively uncoordinated tetrel element vertex atoms.[69-72] However, the fourfold negative charge of the polyanions, resulting in low solubility and a highly reductive nature of the clusters, is a major drawback for the application of solid state *Zintl* phases as precursors for well-defined Group 14 element clusters in solution.

Relation between Siliconoids, Metalloids (Ge, Sn) and *Zintl* Clusters of Group 14 Elements

Despite the different synthetic approaches there are recognizable relations between siliconoid or metalloid (Ge, Sn) cages and deltahedral Group 14 element *Zintl* clusters. This is, for example, manifested by the recent synthesis of the first anionic siliconoid cluster, closing the gap between siliconoids and negatively charged silicide *Zintl* clusters (Scheme 1.1),[46] and a computational study which predicted further potential siliconoids by bridging of $[Si_9]$ clusters with sp^3-Si linkers.[73] Moreover, the close relation between metalloid Group 14 element clusters and negatively charged *Zintl* clusters is expressed by the tris-silylated $[Ge_9]$ cluster $[Ge_9\{Si(TMS)_3\}_3]^-$, which can be obtained by co-condensation techniques starting from metastable Ge(I) halogenides and $Li\{Si(TMS)_3\}$ or by the so-called "*Zintl* route" using K_4Ge_9 and $(TMS)_3SiCl$ as starting materials.[56, 74]

1.3 Deltahedral Group 14 Element *Zintl* Clusters and their Reactivity in Solution

This thesis addresses investigations of the reactivity of deltahedral nine-atomic Group 14 element *Zintl* clusters in solution, aiming for novel methods for the stabilization, functionalization and linkage of [E_9] (*E*: Si, Ge, Sn) clusters. Therefore, within this chapter the general properties of nine-atomic deltahedral Group 14 element *Zintl* clusters are discussed in terms of structural and electronic aspects, as well as their dissolution and redox behavior. Moreover, the established reactivity of $[E_9]^{4-}$ (*E*: Si-Pb) clusters towards different reaction partners (transition metal complexes, heavier main-group element compounds or organic reagents) is reviewed.

1.3.1 General Properties of Deltahedral Nine-Atomic Group 14 Element *Zintl* Clusters

Structural and Electronic Aspects

The bonding in nine-atomic *Zintl* anions $[E_9]^{4-}$ (*E*: Si-Pb) cannot be explained by 2-centre-2-electron bonds since the number of bonds every vertex atom of the cluster forms to further tetrel element vertices of the cage is higher than the number of available valence electrons. Therefore, the clusters can be defined as delocalized electron-deficient systems comprising multi-centre-2-electron interactions between the cluster's vertices. In combination with their negative charge, implicating an electron-rich molecule, this results in ambivalent properties of the clusters which can react as nucleophiles or electrophiles, depending on the reaction conditions or the reaction partners. The bonding situation in these Group 14 element *Zintl* clusters can be described by the *Wade-Mingos* rules for cage-like boranes, assuming that every tetrel element contributes two electrons to the cluster framework bonding and every vertex atom comprises an electron lone-pair, which formally substitutes the radial B-H bond occurring in the boranes.[75-78] Accordingly, a $[E_9]^{4-}$ cluster with 22 electrons ($9 \cdot 2e^- + 4e^-$) contributing to the cluster skeleton is expected to form a *nido*-type cluster ($2n + 4$ electrons; *n*: number of cluster vertices) with C_{4v} symmetry, which can be described as capped square antiprism. By contrast, in case of an oxidized $[E_9]^{2-}$ cluster only 20 electrons ($9 \cdot 2e^- + 2e^-$) are involved in the cluster framework, which should result in a D_{3h} symmetric *closo*-type cluster ($2n + 2$ electrons; *n*: number of cluster vertices) with the shape of a tricapped trigonal prism according to the *Wade-Mingos* rules (Figure 1.2). The different symmetries of the [E_9] cages can easily be interconverted into each other (low energy barrier),[79] and a change of the electron count of the clusters e.g. through oxidation of $[E_9]^{4-}$ only results in a slight

transformation of the cluster symmetry, which makes the $[E_9]^{n-}$ (n: 2, 3 ,4) cluster species electronically flexible systems.[27, 80] This property results in an agile redox behavior in solution.

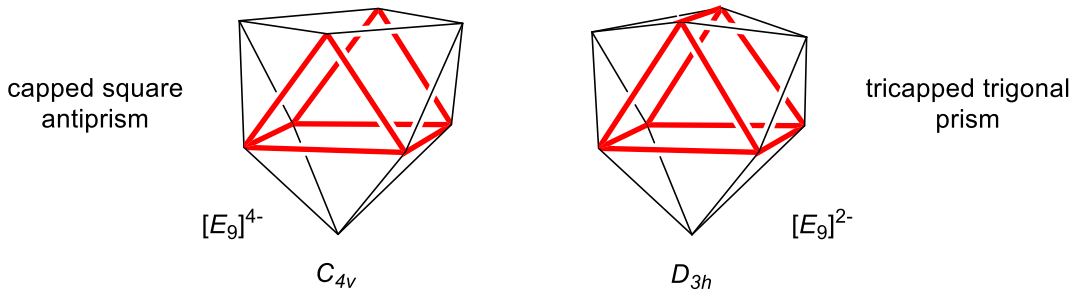

Figure 1.2: Resonance structures of $[E_9]^{n-}$ (n: 2, 3, 4) clusters. Left: Capped square antiprism with C_{4v} symmetry as expected for *nido*-type cluster $[E_9]^{4-}$. Right: Tricapped trigonal prism with D_{3h} symmetry as predicted for *closo*-type cage $[E_9]^{2-}$.

Dissolution and Redox Behaviour

Dissolution of *Zintl* phases and subsequent crystallization of bare *Zintl* clusters from solution was first achieved for K_4Ge_9 and K_4Sn_9 from ethylenediamine.[81, 82] Shortly after, it was found by Corbett that the addition of the sequestering agent [2.2.2]-cryptand enhances both, the solubility of the phases, as well as the crystallization of the obtained materials.[83] This can be explained by the fact that the sequestered cations have a nearly similar size as the cluster anions, which allows for a better packing in the crystal structure. Later on, 18[crown]-6 was introduced as further potential sequestering agent by Fässler.[84] In the meantime, a broad range of different tetrel cluster anions was crystallized from solution (ethylenediamine, NH_3(l) or pyridine). Besides the $[E_9]^{4-}$ (E: Si,[85-87] Ge,[88-91] Sn,[81-83, 92-95] Pb[96-98]) clusters, also other cluster species such as paramagnetic $[E_9]^{3-}$ (E: Si,[99] Ge,[100-104] Sn,[105-108] Pb[98, 100, 106]) cages and diamagnetic $[E_9]^{2-}$ clusters (E: Si,[109] Ge[110, 111]) or clusters of different size $[E_5]^{2-}$ (E: Si,[86, 99] Ge,[112, 113] Sn,[114, 115] Pb[92, 114]) were isolated, which indicated that the $[E_9]^{4-}$ clusters can be easily oxidized in solution. The exact mechanism for the formation of $[E_5]^{2-}$ clusters from $[E_9]^{4-}$ is not completely clear to date. Regarding the nine-atomic cages it was postulated that $[E_9]^{n-}$ (n: 2-4) clusters coexist in solution in equilibria with solvated electrons and that the amount and type of added sequestering agent affects which species crystallize from solution.[80, 116] Another result of the redox activity of the $[E_9]^{4-}$ clusters in solution is the coupling of the nine-atomic cages (Figure 1.3). The simplest coupling product is the dimeric species $[Ge_9\text{-}Ge_9]^{6-}$ (Figure 1.3 a), consisting of two $[Ge_9]^{3-}$ units which are connected by a single exo bond.[72, 88, 104, 117, 118] Similar interactions occur in extended one-dimensional polymer chains consisting of $[Ge_9]^{2-}$ units, which are interconnected by single exo bonds (Figure 1.3 b).[119, 120] By contrast, in the oligomeric species $[Ge_9{=}Ge_9{=}Ge_9]^{6-}$ [121-123] (Figure 1.3 c) and $[Ge_9{=}Ge_9{=}Ge_9{=}Ge_9]^{8-}$ [124, 125] (Figure 1.3 d) delocalized bonding occurs between the single cages, which results in elongated distances between the clusters. Regarding the formation of

$[Ge_9=Ge_9=Ge_9]^{6-}$, a recent UV/VIS study showed the aggregation of the $[Ge_9]^{2-}$ clusters to the trimeric species in dependency of the concentration.[123]

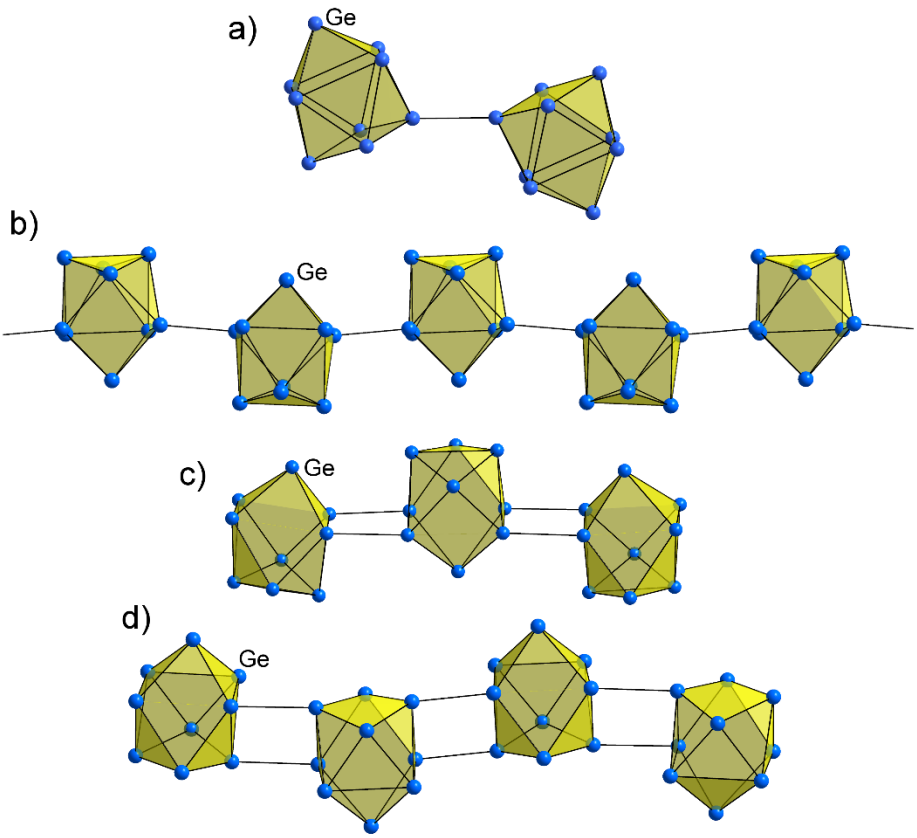

Figure 1.3: Dimeric, oligomeric and polymeric species formed upon oxidative coupling of $[Ge_9]$ clusters. a) $[Ge_9\text{-}Ge_9]^{6-}$,[72, 88, 104, 117, 118] b) $^1_\infty\{[Ge_9]^{2-}\}$,[119, 120] c) $[Ge_9=Ge_9=Ge_9]^{6-}$,[121, 122] d) $[Ge_9=Ge_9=Ge_9=Ge_9]^{8-}$.[124, 125]

1.3.2 Reactivity of Group 14 Element *Zintl* Clusters in Solution

In the previous sections the relevance of tetrel elements in material science has been pointed out (chapter 1.1), and *Zintl* phases have been introduced as valuable sources for discrete, tailor-made tetrel element clusters in solution (chapter 1.2). Moreover, the general structural and electronic properties, as well as the dissolution and the redox behaviour of the deltahedral nine-atomic Group 14 element *Zintl* clusters have been discussed (chapter 1.3.1). These general properties influence the reactivity of the Group 14 element *Zintl* clusters towards other reaction partners. In this chapter the variable reactivity of these clusters towards different reaction partners will be reviewed. Since the evaluation of novel stabilization and functionalization methods for nine-atomic Group 14 element *Zintl* clusters, as well as their connection to larger aggregates are the major aspects of this work, this chapter generally focusses on the reactivity of nine-atomic $[E_9]^{4-}$ (*E*: Si-Sn) clusters. However, in case of the silicide cluster chemistry four-atomic clusters $[Si_4]^{4-}$ are also considered, since phases of the composition $A_{12}Si_{17}$ (*A*: alkali metal), containing both cluster types, are the only source for preformed $[Si_9]^{4-}$ clusters to date. Therefore, the reactivity of the silicide clusters (chapter 1.3.2.1) is discussed separately from the reactivity of the nine-atomic clusters of its heavier congeners (Ge-Pb; chapter 1.3.2.2), which can all be extracted from A_4E_9 phases and reveal comparable reactivity. In chapter 1.3.2.2 the review of the reactivity of the heavier Group 14 element congeners is structured according to the different reaction partners (transition metal complexes, heavier main-group element compounds and organic reagents). Moreover, the prosperous subsequent chemistry of silylated $[Ge_9]$ clusters (introduction in chapter 1.3.2.2), which have recently attracted much attention due to their increased solubility and stability, is reviewed in chapter 1.3.2.3. In this context the formation of completely neutral stabilized or functionalized clusters is of special interest.

1.3.2.1 Reactivity of Silicide *Zintl* Clusters in Solution

Zintl phases of the composition $A_{12}Si_{17}$ (*A*: alkali metal) are the only available precursors known for obtaining $[Si_9]^{4-}$ clusters in solution.[65, 68] Due to the presence of $[Si_4]^{4-}$ clusters besides the nine-atomic silicide cages, these phases reveal a decreased solubility and an increased reductive nature, which limited the silicide cluster chemistry to NH_3(l), from which mainly silicide cluster solvates were crystallized.[85-87, 99, 126] Whereas reactions of silicide clusters with main-group element compounds or organics have not been successful to date, there are three examples in which the introduction of organometallic fragments at silicide clusters was achieved (Figure 1.3). The functionalized silicide anion $[PhZn(\eta^4\text{-}Si_9)]^{3-}$ was obtained by

treatment of $K_{12}Si_{17}$ with [2.2.2]-cryptand in NH_3(l) and subsequent reaction with $ZnPh_2$ in pyridine.[127] In this species the $[ZnPh]^+$ fragment coordinates to the open *pseudo* square plane of the $[Si_9]$ cluster in a η^4-coordination mode (Figure 1.4 a). The reaction of $K_6Rb_6Si_{17}$ with $Ni(CO)_2(PPh_3)_2$ in NH_3(l) led to the formation of the $Ni(CO)_2$ bridged silicon cluster dimer $[Ni(CO)_2(\mu\text{-}Si_9)_2]^{8-}$ with or without addition of [2.2.2]-cryptand as a sequestering agent.[128, 129] In this species the interactions between $Ni(CO)_2$ and the $[Si_9]$ cages occur *via* single Si vertices of the clusters, which reveals that $[Si_9]$ cages can interact with different transition metal fragments in various coordination modes (Figure 1.4 b). The reaction of $K_6Rb_6Si_{17}$ with mesitylcopper in the presence of [18]crown-6 in NH_3(l) resulted in the formation of the first transition metal complex of a silicide tetrahedron $[(MesCu)_2(\eta^3,\eta^3\text{-}Si_4)]^{4-}$, in which the MesCu fragments are attached at the $[Si_4]$ cluster with η^3-coordination to two triangular faces of the tetrahedral cage (Figure 1.4 c).[130] The isolation of $[(MesCu)_2(\eta^3,\eta^3\text{-}Si_4)]^{4-}$ indicated that $[Si_4]^{4-}$ clusters can also be dissolved in NH_3(l), which was later proven by the isolation of further crystals containing bare silicide tetrahedrons,[87, 131] and the monitoring of a ^{29}Si NMR signal assigned to $[Si_4]^{4-}$ in NH_3(l).[132] In recent NMR studies the detection of the elusive $[Si_9]$ clusters was also achieved. The clusters were detected as the protonated species $[Si_9H]^{3-}$ in NH_3(l) solution,[133] or as the di-protonated species $[Si_9H_2]^{2-}$ in pyridine.[134] These investigations implicate a stepwise protonation of the $[Si_9]^{4-}$ clusters, which activates the clusters, enhances their solubility and allows for a targeted separation of the $[Si_4]$ cages. Therefore, this exploration might play a key role in the expansion of $[Si_9]$ cluster chemistry in the future. In the case of $[Si_9H]^{3-}$ the crystallographic characterization revealed the addition of the proton to a Si vertex atom within the open square plane of the $[Si_9]$ cluster.[126, 133] Examinations on the reactivity of silicide clusters towards coinage metal NHC complexes $NHC^{Dipp}MCl$ (*M*: Cu, Ag, Au) resulted in the isolation of the novel complex of a silicide anion $[NHC^{Dipp}Cu(\eta^4\text{-}Si_9)]^{3-}$ (presented in chapter 3.1.2.1 or in the respective publication chapter 5.1).[135]

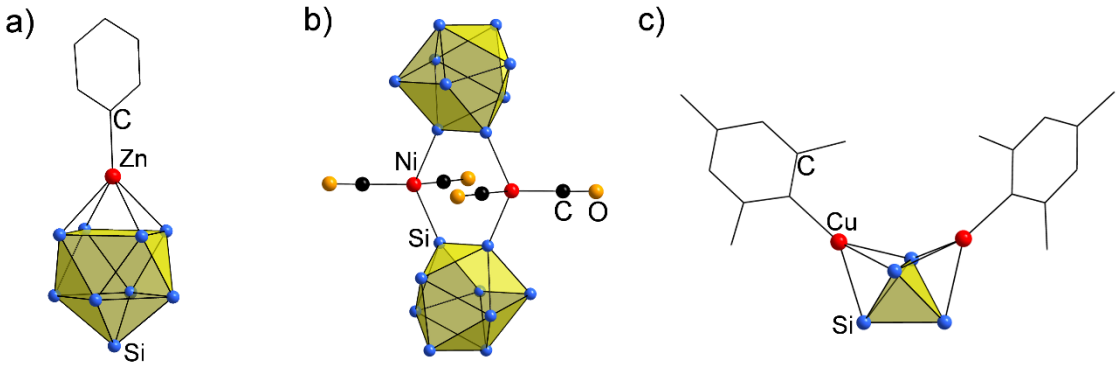

Figure 1.4: All organometallic fragment coordinated silicide clusters reported prior to this thesis. a) $[PhZn(\eta^4\text{-}Si_9)]^{3-}$,[127] b) $[Ni(CO)_2(\mu\text{-}Si_9)_2]^{8-}$, [128, 129] c) $[(MesCu)_2(\eta^3,\eta^3\text{-}Si_4)]^{4-}$.[130] Colour code: Si (blue), transition metals (red), C (black), O (orange).

1.3.2.2 Reactivity of Nine-Atomic *Zintl* Clusters of the Heavier Group 14 Homologues (Ge-Pb) in Solution

Reactivity towards Transition Metal Complexes

The first successful attachment of an organometallic fragment at a $[E_9]^{4-}$ (*E*: Ge-Pb) cluster was achieved by reaction of K_4Sn_9 with $Cr(CO)_3Mes^H$ (Mes^H: mesitylene) in ethylenediamine, yielding $[(CO)_3Cr(\eta^4\text{-}Sn_9)]^{4-}$, in which the $[Sn_9]^{4-}$ cage is approached by the Lewis acidic Cr^0 fragment *via* its *pseudo* square open plane (Figure 1.5 a).[136] Subsequent studies on the reactivity of complexes of late, electron-rich transition metals towards $[E_9]^{4-}$ (*E*: Ge, Sn, Pb) clusters confirmed the preference of this bonding mode by the isolation of $[(CO)_3M(\eta^4\text{-}E_9)]^{4-}$ (*M*: Cr, Mo, W; *E*: Sn, Pb),[136-139] $[(cod)Ir(\eta^4\text{-}E_9)]^{3-}$ (*E*: Sn,[140, 141] Pb[141]), $[R_3PCu(\eta^4\text{-}Ge_9)]^{3-}$ (*R*: ^{i}Pr, Cy),[142] $[PhZn(\eta^4\text{-}E_9)]^{3-}$ (*E*: Ge-Pb)[127] and $[PhCd(\eta^4\text{-}E_9)]^{3-}$ (*E*: Sn, Pb).[143] The formation of these species can either be described by a ligand exchange reaction in the case of the replacement of neutral ligands at the transition metal through the *Zintl* cluster (e.g. CO) or as salt metathesis reactions if the negatively charged ligands (e.g. Cl^-, Ph^-) are substituted by the *Zintl* cluster. Upon coordination to transition metals with its open square plane, a $[E_9]^{4-}$ cluster acts as a six-electron donor, and therefore all of the above listed compounds can be described as 18-valence shell electron complexes.[27, 142] Further interesting representatives revealing similar interactions between a transition metal and $[E_9]^{4-}$ (*E*: Ge, Pb) are $[Ge_9Zn\text{-}ZnGe_9]^{6-}$ (Figure 1.5 b) and $[Pb_9Cd\text{-}CdPb_9]^{6-}$ comprising a Zn-Zn bond or a Cd-Cd bond, respectively.[144, 145] However, $[E_9]^{4-}$ clusters can also interact with transition metal fragments *via* single tetrel vertex atoms with the formation of an *exo* bond to the transition metal. In this case the $[E_9]^{4-}$ cages can be regarded as two-electron donors. This coordination mode has been observed in transition metal compounds of the clusters with varying coordination modes between the clusters and the transition metal, e.g. in the Cu^+ bridged dimeric germanide $[(\eta^4\text{-}Ge_9)Cu(\eta^1\text{-}Ge_9)]^{7-}$ (Figure 1.5 c), [142] in the trimeric species $[(\eta^4\text{-}Ge_9)Zn\text{-}(\eta^1,\eta^1\text{-}Ge_9)\text{-}Zn(\eta^4\text{-}Ge_9)]^{8-}$ or in the polymeric chain $^1_\infty\{Zn[(\eta^4\text{:}\eta^1\text{-}Ge_9)]\}^{2-}$.[144] Moreover, single bond interactions were observed between $[Sn_9]^{4-}$ and an electron-poor $[Cp_2Ti(NH_3)]^+$ fragment in $[Cp_2Ti(NH_3)(\eta^1\text{-}Sn_9)]^{3-}$ (Figure 1.5 d),[146] which was obtained from reaction mixtures of $[Cp_2TiCl]_2$ and K_4Sn_9 in NH_3(l). The isolation of this anion is especially interesting since it indicates that $[Sn_9]^{4-}$ clusters can be stable in solution in the presence of electron-poor transition metals in high oxidation state at low temperature.[146] Further species comprising single bond interactions between $[Ge_9]$ and the transition metal fragments were found in $[Ge_9\{M(CO)_5\}_3]^{4-}$ (*M*: Cr, Mo, W), in which three $M(CO)_5$ moieties are coordinated to single Ge atoms of the cluster core (Figure 1.5 e). The isolation of these species reveals that it is possible to decorate bare $[Ge_9]^{4-}$ clusters with several transition metal fragments.[147]

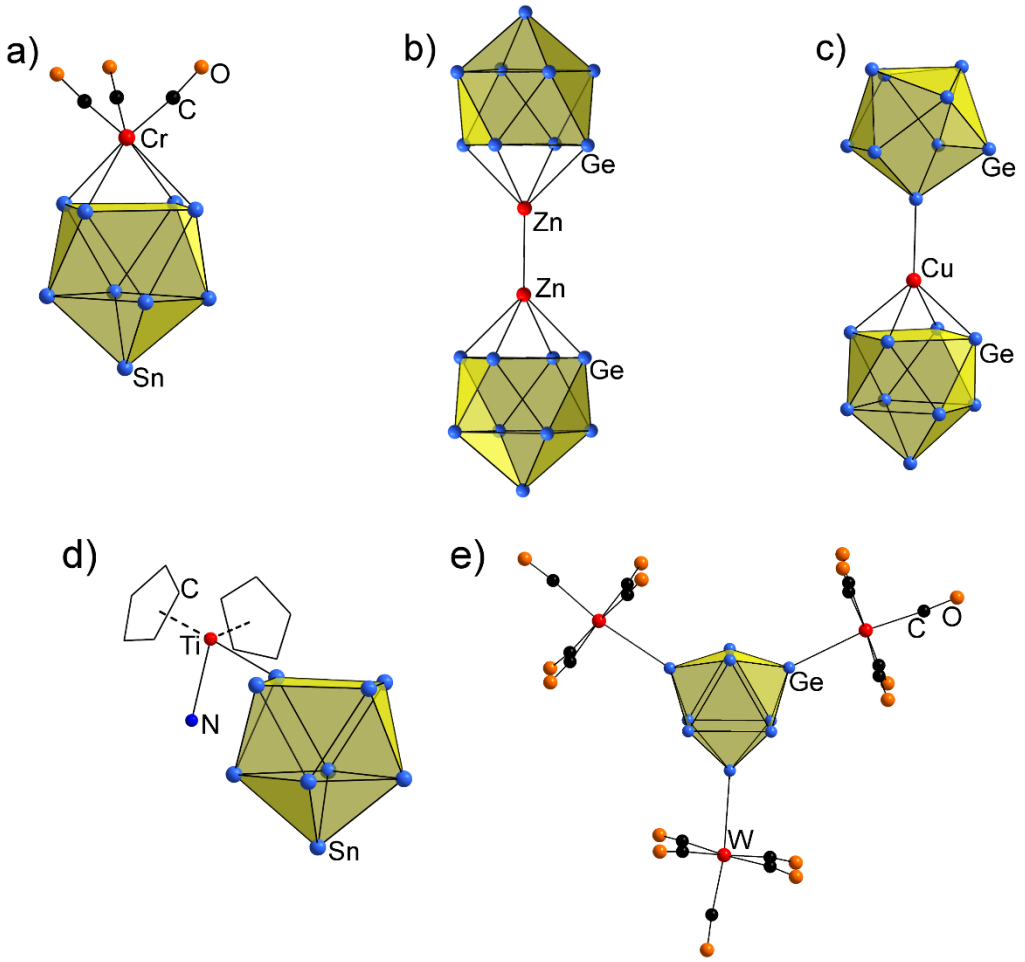

Figure 1.5: Selection of cluster anions obtained from reactions of *Zintl* clusters with transition metal complexes revealing different interactions between the $[E_9]^{4-}$ clusters and the transition metals. a) $[(CO)_3Cr(\eta^4\text{-}Sn_9)]^{4-}$,[139] b) $[Ge_9Zn\text{-}ZnGe_9]^{6-}$,[144] c) $[(\eta^4\text{-}Ge_9)Cu(\eta^1\text{-}Ge_9)]^{7-}$,[142] d) $[Cp_2Ti(NH_3)(\eta^1\text{-}Sn_9)]^{3-}$,[146] e) $[Ge_9\{W(CO)_5\}_3]^{4-}$.[147] Colour code: Ge and Sn (bright blue), transition metals (red), C (black), O (orange), N (dark blue).

Besides the attachment of transition metal fragments to $[E_9]$ (*E*: Ge-Pb) clusters, transition metals or transition metal cations can also migrate into the core of $[E_9]$ (*E*: Ge, Sn, Pb) cages under formation of so-called endohedral clusters. Examples for such species are $[Cu@E_9]^{3-}$ (*E*: Sn, Pb; Figure 1.6 a),[95, 148] or the filled paramagnetic $[Ge_9]^{3-}$ cluster $[Ni@Ge_9]^{3-}$.[149] All of these anions have in common that the incorporated transition metal reveals d^{10}-configuration and does not contribute electrons to the cluster framework. In analogy to their empty congeners, the endohedral clusters can also interact with further transition metal fragments resulting, for example, in $[Ph_3PNi(Ni@Ge_9)]^{2-}$ [150] or $[(CO)Ni(Ni@Ge_9)]^{2-}$.[151] Recently, the extraction of $[Co@Sn_9]^{4-}$ from an intermetallic precursor phase of the composition "$K_5Co_3Sn_9$" and subsequent reaction with a series of transition metal complexes yielded further representatives for such species $[(L)M(Co@Sn_9)]^{3-}$ [(*L*)*M*: (CO)Ni, (C_2H_4)Ni, (Ph_3P)Pt, (Ph)Au].[152] Moreover, a number of endohedral cluster compounds with increased cluster size is known. These species result from the oxidative fragmentation of the $[E_9]^{4-}$ clusters and allow

for the incorporation of either larger transition metals (atomic or ionic radius) or more than one transition metal atom. In the case of ten-atomic clusters different cage shapes were observed. Whereas the $[Pb_{10}]^{2-}$ cluster in $[Ni@Pb_{10}]^{2-}$ can be described as a deltahedral *closo*-type cluster (Figure 1.6 b),[153, 154] the tetrel cages in $[Co@Ge_{10}]^{3-}$ [155] (Figure 1.6 c) and $[Fe@E_{10}]^{3-}$ (*E*: Ge,[156] Sn[157]) reveal a non-deltahedral pentagonal prismatic shape. Ten-atomic deltahedral clusters are also stable without incorporated metal as shown by the isolation of $[Ge_{10}]^{2-}$ and $[Pb_{10}]^{2-}$.[158, 159] In contrast, larger cages were exclusively found with incorporated transition metals stabilizing the cluster skeleton; examples for such species are $[M@Pb_{12}]^{3-}$ (*M*: Mn,[160] Ni,[153] Pd,[153] Pt[153, 161]; Figure 1.6 d), $[Ru@Ge_{12}]^{3-}$ [162] and $[Ir@Sn_{12}]^{3-}$.[140] The latter so-called stannasphere is obtained upon heating a solution of $[(cod)Ir(\eta^4\text{-}Sn_9)]^{3-}$ in ethylenediamine. Further large aggregates were found in $[Ni_2@Sn_{17}]^{4-}$,[163] which can be described as the coupling product of two $[Ni@Sn_9]^{2-}$ units, sharing one Sn cage atom, and $[Pt_2@Sn_{17}]^{4-}$ consisting of a closed polyhedron of 17 tin atoms with an incorporated Pt dumbbell.[164] In the even larger aggregates $[Pd_2@E_{18}]^{4-}$ (*E*: Ge,[165] Sn[166]; Figure 1.6 e) two Pd atoms are incorporated in cocoon-shaped deltahedral clusters, and even three Ni atoms are involved in $[Ni_3@Ge_{18}]^{4-}$.[149]

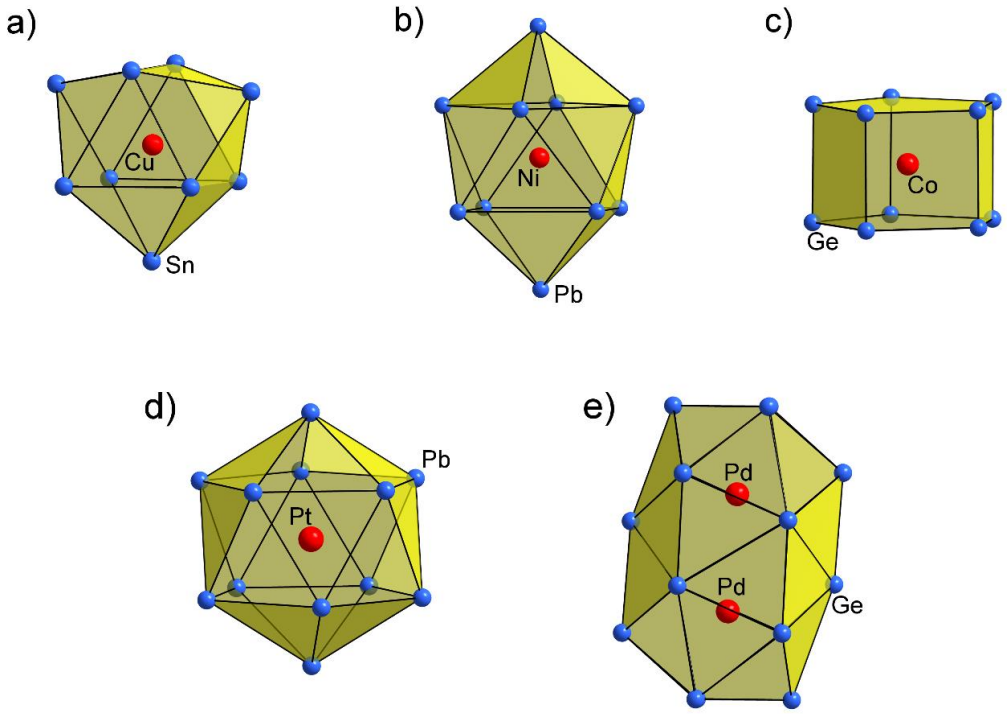

Figure 1.6: Selection of endohedral cluster anions with different cluster sizes and shapes resulting from reactions of $[E_9]^{4-}$ (*E*: Ge-Pb) clusters with transition metal complexes: a) $[Cu@Sn_9]^{3-}$,[148] b) $[Ni@Pb_{10}]^{2-}$,[154] c) $[Co@Ge_{10}]^{3-}$,[155] d) $[Pt@Pb_{12}]^{3-}$,[161] e) $[Pd_2@Ge_{18}]^{4-}$.[165] Colour code: Ge-Pb (blue), transition metals (red).

Oxidation processes can also result in other large intermetalloid species such as $[Au_3Ge_{45}]^{4-}$ (Figure 1.7 a),[167] resulting from the oxidation of $[Au_3Ge_{18}]^{5-}$, which was initially obtained by reaction of K_4Ge_9 with Ph_3PAuCl in ethylenediamine.[168] In the latter, two $[Ge_9]$ cages are bridged by an Au_3 triangle. Moreover, the formation of $[E_9]^{3-}$ (*E*: Ge, Sn) dimers $[Ge_9\text{-}Ge_9]^{6-}$ [169] (Figure 1.7 b) and $[Ag(Sn_9\text{-}Sn_9)]^{5-}$ (Figure 1.7 c),[170] comprising *E*-*E* connections, was observed upon partial oxidation of $[E_9]^{4-}$ (*E*: Ge, Sn) clusters in reactions with Cu^+ or Ag^+ complexes.

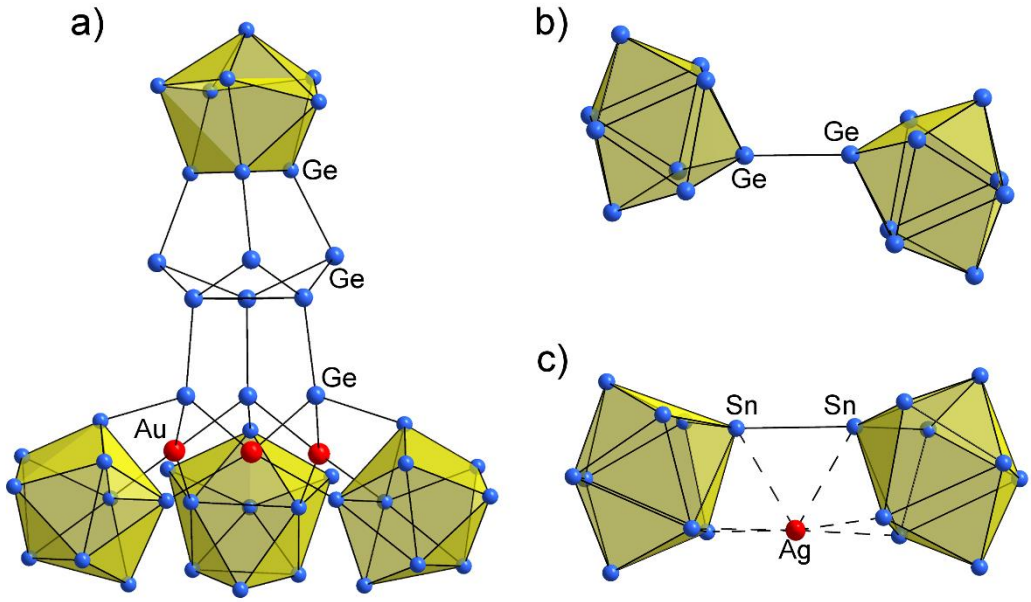

Figure 1.7: Selection of cluster anions resulting from oxidation of the $[E_9]^{4-}$ cages in reactions with transition metal complexes. a) $[Au_3Ge_{45}]^{4-}$,[167] b) $[Ge_9\text{-}Ge_9]^{6-}$,[169] c) $[Ag(Sn_9\text{-}Sn_9)]^{5-}$.[170] Colour code: Ge and Sn (blue), transition metals (red).

Examinations on the reactivity of coinage metal NHC complexes $NHC^{Dipp}MCl$ (*M*: Cu, Ag, Au) towards $[Sn_9]^{4-}$ clusters, resulting in the isolation of $[NHC^{Dipp}M(\eta^4\text{-}Sn_9)]^{3-}$ (*M*: Cu, Ag, Au) and the large intermetalloid $[(\eta^4\text{-}Sn_9)Ag(\eta^1\text{-}Sn_9)]^{7-}$ are discussed in chapter 3.1.2.1 and in the respective publication (chapter 5.2).[171]

Reactivity towards Heavier Main-Group Element Compounds

The introduction of heavier main-group element ligands to $[E_9]^{4-}$ (*E*: Ge, Sn) cages was first achieved by reaction of K_4Ge_9 with $BiPh_3$ in ethylenediamine, yielding the doubly $[Ph_2Bi]$-substituted $[Ge_9]$ cluster $[Ph_2Bi\text{-}Ge_9\text{-}BiPh_2]^{2-}$ (Figure 1.8 a).[172] Subsequently, further similar compounds $[Ph_2Sb\text{-}Ge_9\text{-}SbPh_2]^{2-}$,[172] $[Ph\text{-}Ge\text{-}SbPh_2]^{2-}$,[173] $[Ph_2Sb\text{-}Ge_9\text{-}Ge_9\text{-}SbPh_2]^{4-}$,[173] $[Ge_9\text{-}SnR_3]^{3-}$,[174] $[R_3E\text{-}Ge_9\text{-}ER_3]^{n-}$ (*E*: In, Ge, Sn; *R*: alkyl, Ph; *n*: 2, 4)[174, 175] or $[Ph_3Sn\text{-}Ge_9\text{-}Ge_9\text{-}SnPh_3]^{4-}$ [174] were obtained by reactions of K_4Ge_9 with ER_4, R_3ECl, ER_3^- (*E*: Ge, Sn) or ER_3 (*E*: In, Sb), and reactions of K_4Sn_9 with Cy_3SnCl led to the formation of $[Sn_9\text{-}SnCy_3]^{3-}$.[176] In the case of Sb-, Bi-, Ge- and Sn-based ligands, a nucleophilic interaction

of the main-group element fragments with the $[Ge_9]^{n-}$ (*n*: 2, 3, 4) clusters was established (in accordance with the electron-deficient nature of the clusters; see chapter 1.3.1), whereas an acid-base interaction was proposed in the case of In-based substituents (according to negative charge and nucleophilic character of the clusters; chapter 1.3.1).[172, 173, 175] In the above listed compounds, interactions between $[E_9]^{4-}$ (*E*: Ge, Sn) and the main-group element ligands mainly occur *via* single *exo* bonds between one tetrel vertex of the cluster and the main-group element. Exclusively in $[Ge_9\text{-}SnR_3]^{3-}$ (*R*: Me, Ph) and $[Sn_9\text{-}SnCy_3]^{3-}$, interactions of the attached stannyl ligand with more than one tetrel vertex of the cluster were observed, resulting in multi-centre-2-electron bonds. Moreover, main-group metal bridged $[Ge_9]^{4-}$ dimers $[(\eta^4\text{-}Ge_9)Sn(\eta^3\text{-}Ge_9)]^{4-}$ (Figure 1.8 b),[177] $[(\eta^3\text{-}Ge_9)In(\eta^3\text{-}Ge_9)]^{5-}$ and $[PhIn(Ge_9\text{-}Ge_9)]^{4-}$ (Figure 1.8 c),[175] the latter comprising a Ge-Ge bond, were isolated from ethylenediamine solutions. In these species the clusters interact with the main-group elements *via* triangular or *pseudo* square faces in either a η^3- or η^4-coordination mode. The first threefold substituted $[Ge_9]^{4-}$ cluster $[Ge_9\{Si(TMS)_3\}_3]^-$ was originally obtained by co-condensation reactions using Ge(I)-halides and Li{Si(TMS)$_3$} as starting materials (bottom-up approach; see chapter 1.2).[56]

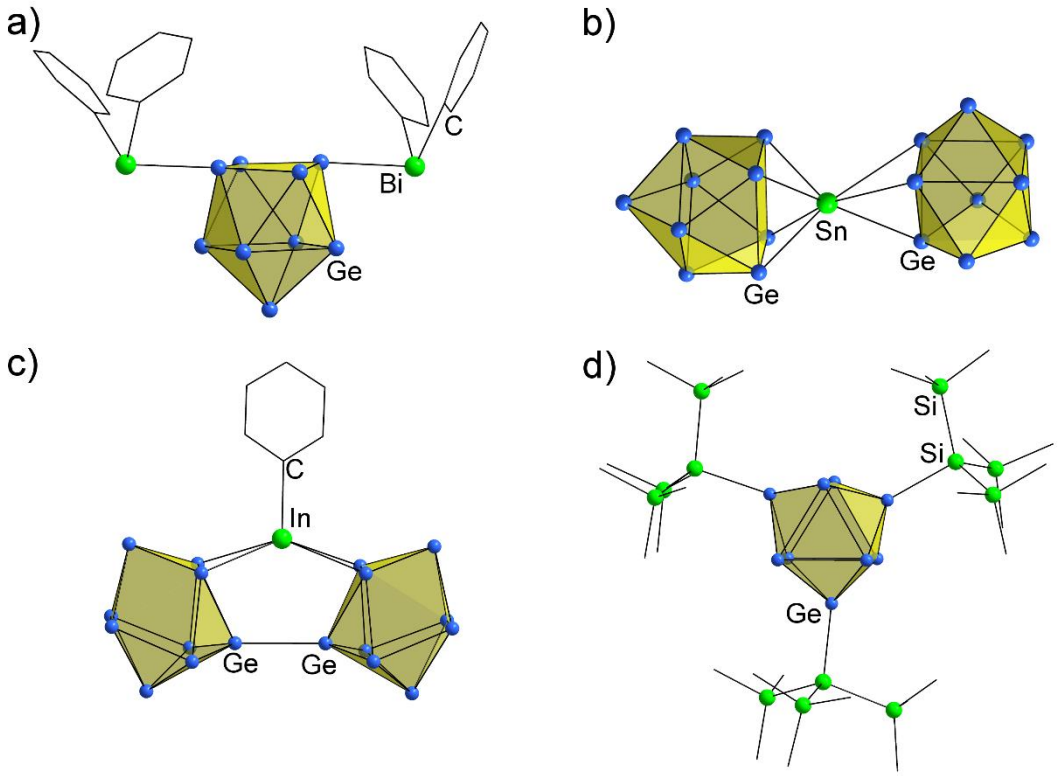

Figure 1.8: Selection of cluster anions resulting from reactions of $[Ge_9]$ clusters with heavier main-group element compounds revealing different interactions between $[Ge_9]^{4-}$ clusters and the main-group element ligands. a) $[Ph_2Bi\text{-}Ge_9\text{-}BiPh_2]^{2-}$,[172] b) $[(\eta^4\text{-}Ge_9)Sn(\eta^3\text{-}Ge_9)]^{4-}$,[177] c) $[PhIn(Ge_9\text{-}Ge_9)]^{4-}$,[175] d) $[Ge_9\{Si(TMS)_3\}_3]^-$.[74] Colour code: Ge (blue), heavier main-group element ligands (green), C (black).

Subsequently, a method to access this species in reasonable yield was found in the heterogenous reaction of K_4Ge_9 with acetonitrile solutions of $(TMS)_3SiCl$.[74] $[Ge_9\{Si(TMS)_3\}_3]^-$, in which the silyl groups are attached to three Ge atoms of the cluster core *via* single *exo* bonds (Figure 1.8 d), is soluble in standard solvents (e. g. MeCN, thf) and reveals increased stability in comparison to bare $[Ge_9]^{4-}$ clusters. However, at the same time it comprises ligand free Ge atoms, which can be approached by potential reaction partners. In follow-up studies $[Ge_9]^{4-}$ clusters were substituted with a broad range of silane ligands of different steric demand, yielding $[Ge_9R_3]^-$ (*R*: $SiEt_3$,[178] $Si(^iPr)_3$,[178] $Si(^iBu)_3$,[178] $SiPh_3$,[179] $Si(TMS)_2(SiPh_3)$,[180] $Si(TMS)_2(Si^iPr_3)$,[181] SiH^tBu_2[181]; Scheme 1.3). Moreover, a method to isolate macroscopic amounts of the bis-silylated $[Ge_9]$ cluster species $[Ge_9\{Si(TMS)_3\}_2]^{2-}$ was reported,[182] and the threefold stannylation of $[Ge_9]$ obtaining $[Ge_9\{SnR_3\}_3]^-$ (*R*: ^{i}Pr, Cy) was achieved.[183, 184] The attachment of the main-group substituents at the $[Ge_9]$ clusters also occurs *via* single *exo* bonds in these species. Due to the prosperous subsequent chemistry of the silylated $[Ge_9]$ clusters, their reactivity towards transition metal complexes, heavier main-group element compounds and organic reagents will be discussed in detail in chapter 1.3.2.3.

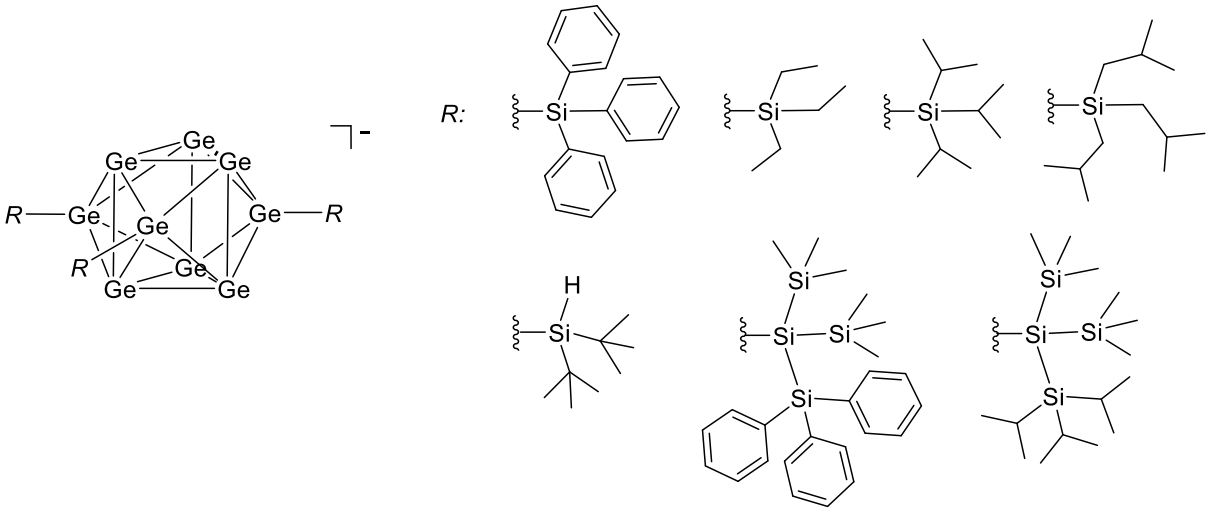

Scheme 1.3: Overview on reported tris-silylated $[Ge_9]$ clusters bearing silane ligands with different steric demand.[178-181]

Investigations on novel Group 14 element cluster functionalization methods, resulting in the synthesis of threefold phosphine-functionalized $[Ge_9]$ cages are presented in chapter 3.2.3.2 or in the respective publication (chapter 5.11).[185]

Reactivity towards Organic Reagents

The most prominent reaction of $[E_9]^{4-}$ (*E*: Ge, Sn) clusters with organics is probably the vinylation reaction with bis(trimethylsilyl)acetylene, yielding the vinylated $[E_9]$ clusters $[E_9\{CH=CH_2\}]^{3-}$ (*E*: Ge,[186-187] Sn[188]), $[Ge_9\{CH=CH_2\}_2]^{2-}$ [186, 187, 189] (Figure 1.9 a) or $[CH_2=CH\text{-}Ge_9\text{-}Ge_9\text{-}CH=CH_2]^{4-}$.[190] Reactions of $[Ge_9]^{4-}$ with further acetylene derivatives resulted in similar structures with variously substituted vinyl ligands attached to $[Ge_9]$,[186, 191, 192] and alkyl rest were introduced at $[Ge_9]^{4-}$ and $[Sn_9]^{4-}$ clusters, yielding $[R\text{-}Ge_9\text{-}Ge_9\text{-}R]^{6-}$ (*R*: ^{t}Bu, ^{i}Bu, ^{n}Bu) [193], $[Sn_9\text{-}^t Bu]^{3-}$ [188] or $[Sn_9\text{-}^i Pr]^{3-}$.[176] Furthermore, $[Ge_9\text{-}Mes]^{3-}$ was obtained upon reaction of K_4Ge_9 with mesitylsilver in ethylenediamine.[187] In all of these anionic species the organic substituents are attached to the $[E_9]$ (*E*: Ge, Sn) cages *via* single *exo* bonds and except $[Ge_9\{CH=CH_2\}_2]^{2-}$, all of the above listed species were only accessible in low yield. Recently, methods for the linkage of two $[Ge_9]^{4-}$ clusters with conjugated organic building blocks were found, which resulted in the isolation of $[R\text{-}Ge_9\text{-}CH=CH\text{-}CH=CH\text{-}Ge_9\text{-}R]^{4-}$ (*R*: $CH=CH_2$,[194] $C(CH_3)=CH\text{-}CH=N(CH_2)_2NH_2$[195]) and $[Ge_9\text{-}CH=CH\text{-}CH=CH\text{-}Ge_9]^{6-}$ (Figure 1.9 b).[196] These novel species are especially interesting with regard to the extension of the conjugated electron system of $[Ge_9]^{4-}$ clusters.

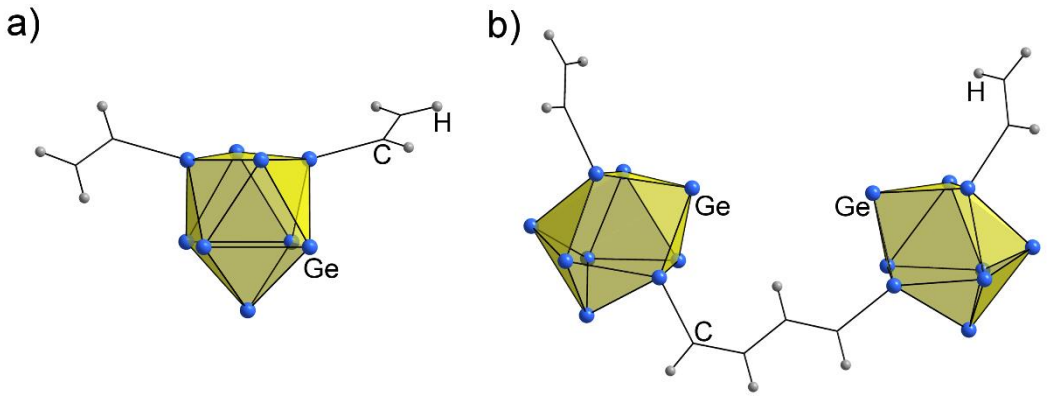

Figure 1.9: Selection of organo-functionalized $[Ge_9]$ clusters resulting from reactions of $[Ge_9]^{4-}$ with organic reagents. a) $[Ge_9\{CH=CH_2\}_2]^{2-}$,[186] b) $[R\text{-}Ge_9\text{-}CH=CH\text{-}CH=CH\text{-}Ge_9\text{-}R]^{4-}$ (*R*: $CH=CH_2$).[194] Colour code: Ge (blue), C (black), H (grey).

1.3.2.3 Reactivity of Silylated [Ge_9] *Zintl* Clusters in Solution

Variously silylated [Ge_9] clusters can be synthesized in reasonable yield by the heterogenous reaction of K_4Ge_9 with the respective chloro trialkylsilanes in acetonitrile (chapter 1.3.2.2).[74, 182] Due to their decreased negative charge, the silylated [Ge_9] clusters are soluble in standard solvents (e. g. MeCN or thf) and reveal a decreased reductive nature. However, these cluster species still contain reactive sites (ligand free Ge vertices), which resulted in a prosperous subsequent chemistry. In the following, the reactivity of silylated [Ge_9] clusters towards transition metal complexes, heavier main-group element compounds and organic reagents is reviewed.

Reactivity towards Transition Metal Complexes

Reactions of $[Ge_9\{Si(TMS)_3\}_3]^-$ with transition metal halides or transition metal complexes bearing labile ligands resulted in a series of transition metal bridged [Ge_9] dimers $[M(\eta^3\text{-}Ge_9\{Si(TMS)_3\}_3)_2]^{n-}$ (*M*: Mn,[197] Cu-Au,[198, 199] Zn-Hg,[200] Pd;[201] *n* = 0-2; Figure 1.10 a). The tricapped trigonal prismatic [Ge_9] cages (the silyl groups are attached at the capping Ge atoms; Scheme 1.3) interact with the transition metals through one of their triangular bases in a η^3-coordination mode. Similar investigations carried out with Cu^+-phosphine complexes or $ZnCp^*_2$ resulted in the neutral compounds $[^iPr_3PCu(\eta^3\text{-}Ge_9\{Si(TMS)_3\}_3)]$,[179] $[Cu(\eta^3\text{-}Ge_9\{Si(TMS)_3\}_3)_2\text{-}Cu\text{-}PPh_3]$ [201] or $[Cp^*Zn(\eta^3\text{-}Ge_9\{Si(TMS)_3\}_3)]$ (Figure 1.10 b),[179] in which at least one of its original ligands remains bound to the transition metal. Reactions of $[Ge_9\{Si(TMS)_3\}_3]^-$ with $Cr(CO)_5(coe)$ (coe: cyclooctene) yielded $[(CO)_5Cr(\eta^1\text{-}Ge_9\{Si(TMS)_3\}_3)]^-$, in which Cr^0 interacts with a single vertex atom of the [Ge_9] cage (Figure 1.10 c).[202] By contrast, reactions of $[Ge_9\{Si(TMS)_3\}_3]^-$ with the more reactive Group 6 element compounds $M(CO)_3(MeCN)_3$ (*M*: Cr, Mo, W) led to $[(CO)_3M(\eta^5\text{-}Ge_9\{Si(TMS)_3\}_3)]^-$ (*M*: Cr, Mo, W), in which the transition metal atom *M* is incorporated in the cluster skeleton and interacts with five Ge atoms (Figure 1.10 d).[202, 203] Further studies on the reactivity of $[Ge_9\{Si(TMS)_3\}_3]^-$ towards a series of M^{2+} cations (*M*: Fe, Co, Ni) resulted in redox reactions, in which the transition metals were reduced by the [Ge_9] clusters. In case of iron and cobalt, no interactions between the reduced metal fragments and intact [Ge_9] clusters occurred, however, in reactions with Fe^{2+} the large metalloid cluster $[Ge_{18}\{Si(TMS)_3\}_6]$ was isolated as oxidation product of $[Ge_9\{Si(TMS)_3\}_3]^-$ (Figure 1.10 e).[204] By contrast, in reactions with Ni^{2+}, the resulting dppe [1,2-bis(diphenylphosphino)ethane] stabilized Ni^+ fragments can coordinate to the triangular bases of the [Ge_9] core, which resulted in mixtures of neutral $[(dppe)Ni(\eta^3\text{-}Ge_9\{Si(TMS)_3\}_3)]$ and the cationic complex $[\{(dppe)Ni\}_2(\eta^3,\eta^3\text{-}Ge_9\{Si(TMS)_3\}_3)]^+$.[197] Moreover, the reactivity of tris-silylated [Ge_9] clusters bearing smaller silane ligands $[Ge_9\{SiR_3\}_3]^-$ (*R*: ^{i}Bu, Ph) towards coinage metal complexes was investigated, which resulted in the formation of the dimeric Au^+

bridged species $[Au(\eta^3\text{-}Ge_9\{Si(^iBu)_3\}_3)_2]^-$ (in analogy to respective reactions with $[Ge_9\{Si(TMS)_3\}_3]^-$) or the twofold $[^iPr_3PCu]^+$ bridged dimer $\{(^iPr_3PCu)_4[Ge_9\{SiPh_3\}_2]_2\}$.[178, 179] The formation of the latter is induced by the cleavage of one of the labile $[SiPh_3]^+$ groups per $[Ge_9]$ cluster. The bridging Cu^+ moieties interact with a triangular face (η^3-coordination mode) of one $[Ge_9]$ cluster and a single Ge vertex atom of the other $[Ge_9]$ core (η^1-coordination mode; Figure 1.10 f). In further studies, reactions of $[Ge_9\{Si(^iPr)_3\}_3]^-$ with $Pd(PPh_3)_4$ yielded the Pd_3 bridged dimeric species $[Ge_{18}Pd_3\{Si(^iPr)_3\}_6]^{2-}$.[184]

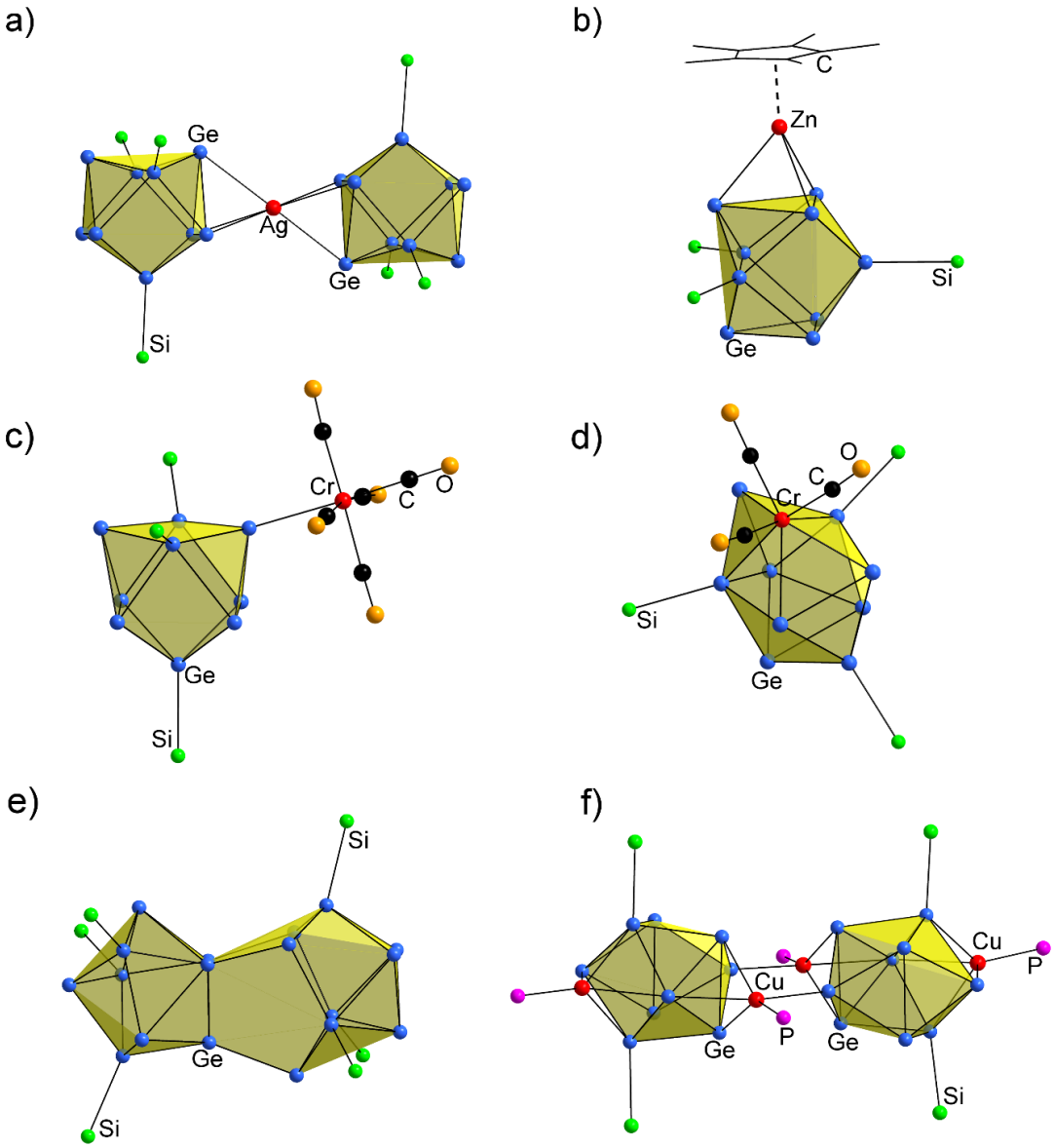

Figure 1.10: Selection of products obtained in reactions of tris-silylated $[Ge_9]$ clusters with transition metal complexes. a) $[Ag(\eta^3\text{-}Ge_9\{Si(TMS)_3\}_3)_2]^-$,[199] b) $[Cp^*Zn(\eta^3\text{-}Ge_9\{Si(TMS)_3\}_3)]$,[179] c) $[(CO)_5Cr(\eta^1\text{-}Ge_9\{Si(TMS)_3\}_3)]^-$, d) $[(CO)_3Cr(\eta^5\text{-}Ge_9\{Si(TMS)_3\}_3)]^-$,[202] e) $[Ge_{18}\{Si(TMS)_3\}_6]$,[204] f) $\{(^iPr_3PCu)_4[Ge_9\{SiPh_3\}_2]_2\}$.[179] For clarity, in a–d the TMS groups of the silyl substituents are omitted and in e) the Ph groups of the silyl substituents as well as the ^{i}Pr groups of the phosphine moieties are omitted. Colour code: Ge (blue), Si (green), transition metals (red), C (black), O (orange), P (purple).

Investigations on the reactivity of coinage metal NHC complexes $NHC^{Dipp}MCl$ (*M*: Cu, Ag, Au) and the Ti(III) complex $[Cp_2TiCl]_2$ towards silylated $[Ge_9]$ clusters, resulting in $[NHC^{Dipp}M(\eta^3\text{-}Ge_9\{Si(TMS)_3\}_3)]$ (*M*: Cu, Ag, Au),[205] $[NHC^{Dipp}Cu(\eta^3\text{-}Ge_9\{SiR_3\}_3)]$ (*R*: ^{i}Pr, ^{i}Bu),[178, 206] $[(NHC^{Dipp}M)_2(\eta^3,\eta^3\text{-}Ge_9\{Si(TMS)_3\}_2)]$ (*M*: Cu, Ag, Au),[206] or $[Cp_2Ti(MeCN)(\eta^1\text{-}Ge_9\{Si(TMS)_3\}_3)]$ and $K_3[Cp_2Ti(\eta^1\text{-}Ge_9\{Si(TMS)_3\}_2)_2]$ are discussed in chapter 3.1.2.2 and chapter 3.1.3 or in the respective publications (chapters 5.3, 5.4, 5.5) and the manuscript for publication (chapter 5.6).

Reactivity towards Heavier Main-Group Element Compounds

Even though threefold silylation of $[Ge_9]$ clusters can be achieved in a single reaction step, the introduction of a fourth silyl group, which would result in a neutral $[Ge_9]$ cluster compound, has not been reported to date. By contrast, reactions of $[Ge_9\{Si(TMS)_3\}_3]^-$ with R_3SnCl (*R*: Me, Ph, ^{n}Bu) readily yield neutral compounds $[Ge_9\{Si(TMS)_3\}_3SnR_3]$ (*R*: Me, Ph, ^{n}Bu; Figure 1.11 a).[207, 208] The $[Ge_9]$ core interacts with the $[SnR_3]^+$ fragments with two or three Ge atoms in one of its triangular faces. Therefore, the Ge-Sn interactions can be described as 2-electron-multi-centre bonds (similar to the observations made for bare $[E_9]^{4-}$ (*E*: Ge, Sn) clusters bearing stannyl substituents; chapter 1.3.2.2). Moreover, reactions of $[Ge_9\{Si(TMS)_3\}_3]^-$ with TlCp led to the formation of the neutral compound $[TlGe_9\{Si(TMS)_3\}_3]$, in which the thallium cation can be regarded as additional cluster vertex (Figure 1.11 b). In the solid state the Tl^+ cation caps a square plane of the $[Ge_9]$ cluster, whereas in solution at least partial dissociation occurs depending on the polarity of the solvent.[208]

Subsequent reactions of the bis-silylated cluster $[Ge_9\{Si(TMS)_3\}_2]^{2-}$ with different chlorosilanes allowed for the synthesis of the mixed-substituted species $[Ge_9\{Si(TMS)_3\}_2\{Si(TMS)_2(SiPh_3)\}]^-$,[182] the introduction of silyl substituents bearing a functional alkenyl moiety $[Ge_9\{Si(TMS)_3\}_2R]^-$ (*R*: $SiPh_2(CH{=}CH_2)$, $SiPh_2\{(CH_2)_3CH{=}CH_2\}$; Figure 1.11 c),[209] and the bridging of two $[Ge_9]$ clusters *via* a silyl group linker $[\{Si(TMS)_3\}_2Ge_9\text{-}SiMe_2\text{-}(C_6H_4)\text{-}SiMe_2\text{-}Ge_9\{Si(TMS)_3\}_2]^{2-}$ (Figure 1.11 d).[210]

Investigations on the attachment of further main-group element substituents at silylated $[Ge_9]$ clusters, yielding $[Ge_9\{Si(TMS)_3\}_2ER_2]^-$ (*E*: B or Al; *R*: substituents) or $[Ge_9\{Si(TMS)_3\}_3PRR^I]$ (*R, R^I*: alkyl or alkenyl groups)[211] and $[Ge_9\{Si(TMS)_3\}_2PRR^I]^-$ (*R*, *R^I*: alkyl, alkenyl, aryl or aminoalkyl substituents)[211, 212] are discussed in chapters 3.2.2 and 3.2.3.1 or in the respective publications (chapters 5.8 and 5.9) and the manuscripts for publication (chapters 5.7 and 5.10).

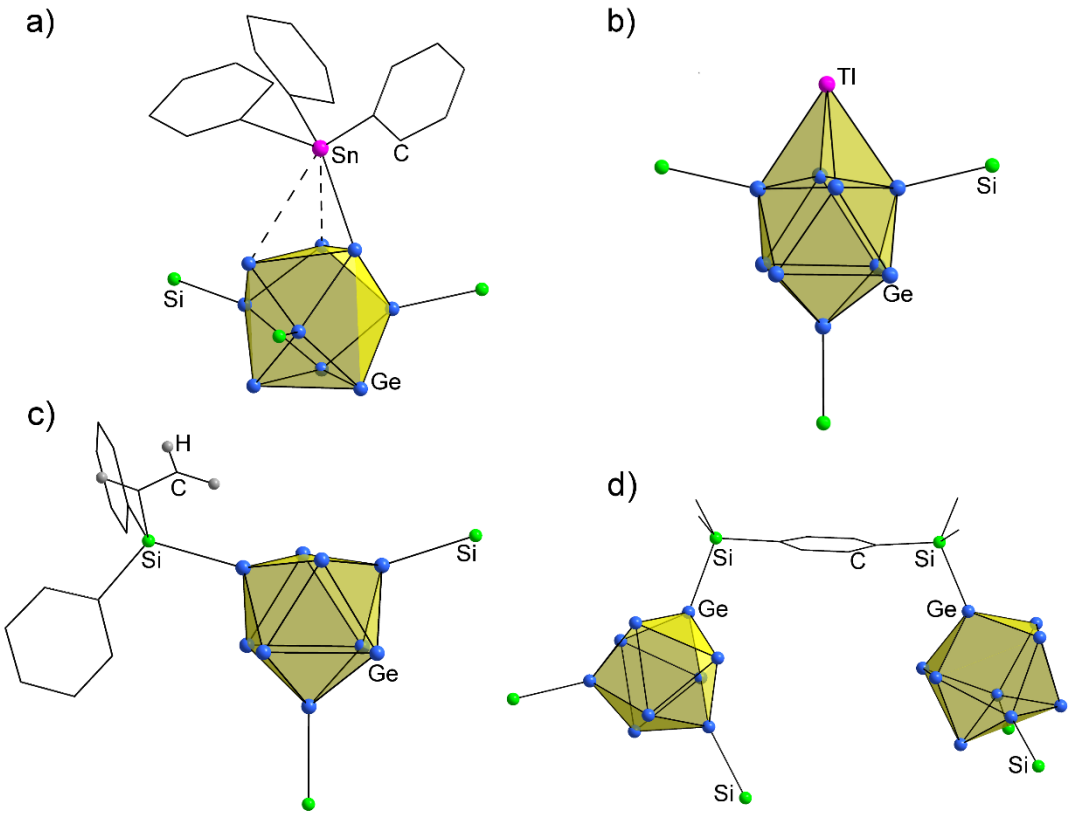

Figure 1.11: Selection of products obtained in reactions of $[Ge_9\{Si(TMS)_3\}_3]^-$ and $[Ge_9\{Si(TMS)_3\}_2]^{2-}$ with heavier main-group element compounds. a) $[Ge_9\{Si(TMS)_3\}_3SnPh_3]$,[207] b) $[TlGe_9\{Si(TMS)_3\}_3]$, [208] c) $[Ge_9\{Si(TMS)_3\}_2SiPh_2(CH{=}CH_2)]^-$,[209] d) $[\{Si(TMS)_3\}_2Ge_9\text{-}SiMe_2\text{-}(C_6H_4)\text{-}SiMe_2\text{-}Ge_9\{Si(TMS)_3\}_2]^{2-}$.[210] For clarity, the TMS groups of the hypersilyl substituents are omitted in a–d. Colour code: Ge (blue), Si (green), other heavier main-group elements (purple), C (black), H (grey).

Reactivity towards Organic Reagents

Reactions of $[Ge_9\{Si(TMS)_3\}_3]^-$ with ethylbromide resulted in the formation of the neutral $[Ge_9]$ cluster compound $[Ge_9\{Si(TMS)_3\}_3Et]$.[208] In contrast to the interactions observed between stannyl ligands and $[Ge_9\{Si(TMS)_3\}_3]^-$ (see: reactions with heavier main-group element compounds), the ethyl group is connected to the $[Ge_9]$ core *via* one Ge vertex in a trigonal base of the $[Ge_9]$ cluster and the Ge-C bond points radially away from the cluster core, manifesting its nature as a 2-centre-2-electron bond. Subsequent reaction of $[Ge_9\{Si(TMS)_3\}_3Et]$ with $Pd(PPh_3)_4$ led to the incorporation of a Pd-PPh_3 moiety into the cluster skeleton, yielding $[\{Si(TMS)_3\}_3EtGe_9Pd(PPh_3)]$ (Figure 1.12 a).[213] In further studies alkenyl groups comprising reactive terminal double bonds were introduced to $[Ge_9\{Si(TMS)_3\}_3]^-$ by reactions with the respective alkenyl halides, yielding the neutral complexes $[Ge_9\{Si(TMS)_3\}_3R]$ (*R*: $CH{=}CH_2$, $(CH_2)_3CH{=}CH_2$; Figure 1.12 b).[214] Moreover, reactions of $[Ge_9\{Si(TMS)_3\}_3]^-$ with various acylchlorides led to the formation of neutral compounds $[Ge_9\{Si(TMS)_3\}_3C(O)R]$ (*R*: Me, ^{i}Pr, ^{t}Bu, Ph, Bz), and for $[Ge_9\{Si(TMS)_3\}_3C(O)^tBu]$ (Figure 1.12 c) a subsequent decarbonylation reaction yielding $[Ge_9\{Si(TMS)_3\}_3{}^tBu]$ was observed.[215]

Reactions of the bis-silylated [Ge_9] cluster $[Ge_9\{Si(TMS)_3\}_2]^{2-}$ with ethylbromide resulted in $[Ge_9\{Si(TMS)_3\}_2Et]^-$, which loses one of its silyl groups during the crystallization process obtaining the mono-silylated species $[Ge_9\{Si(TMS)_3\}Et]^{2-}$.[216]

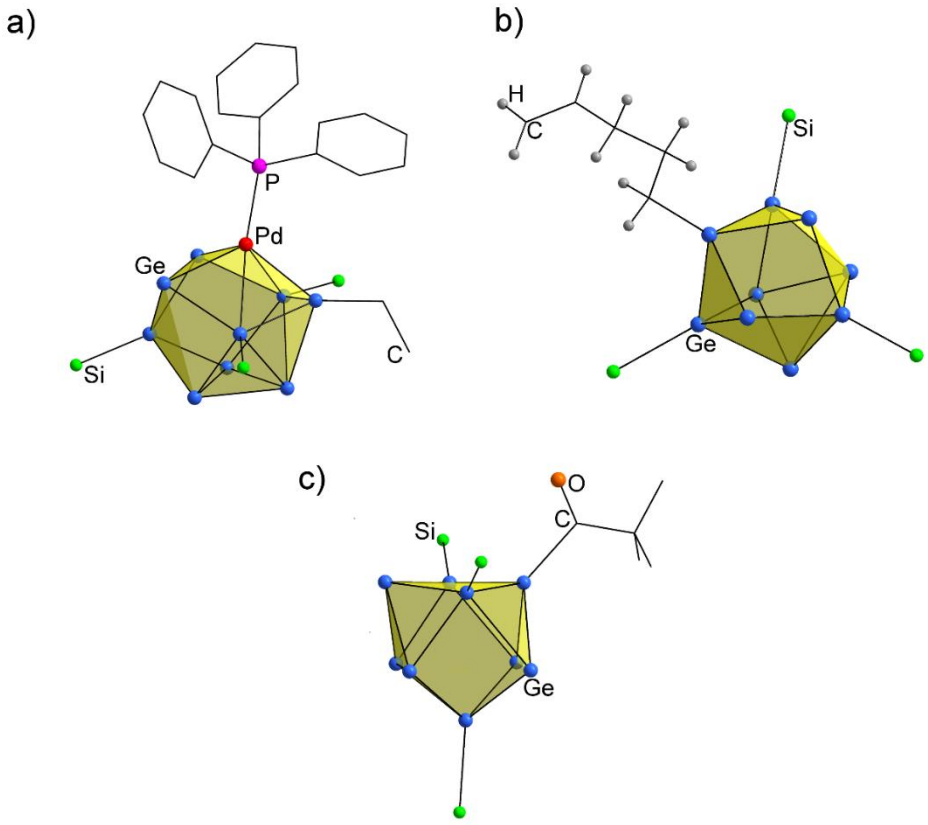

Figure 1.12: Selection of compounds obtained from reactions of $[Ge_9\{Si(TMS)_3\}_3]^-$ with organic reagents (and subsequent reaction with a transition metal complex). a) $[\{Si(TMS)_3\}_3EtGe_9Pd(PPh_3)]$,[213] b) $[Ge_9\{Si(TMS)_3\}_3\{(CH_2)_3CH{=}CH_2\}]$,[214] c) $[Ge_9\{Si(TMS)_3\}_3C(O)^tBu]$.[215] For clarity, in a–c TMS groups of the silyl substituents are omitted. Colour code: Ge (blue), Si (green), C (black), H (grey), O (orange), P (purple), Pd (red).

1.4 Motivation

Silicon- and germanium-based materials are of interest for a broad range of applications comprising electronics,[6, 7] solar cells,[8, 9] optoelectronics[10-12] or anode materials for Li ion batteries,[13, 14] and the application of Group 14 element semiconductors is continuously growing. In this context, nanoparticles or nanostructured materials, providing unique novel morphologies, are particularly interesting with respect to the tunability of the materials' properties, which makes Group 14 element clusters valuable synthons for the future fabrication of such materials.[217-220] *Zintl* phases of the compositions A_4E_9 (*A*: alkali metal, *E*: Ge-Pb) and $A_{12}E_{17}$ (*A*: alkali metal, *E*: Si-Sn) contain well-defined, nine-atomic $[E_9]^{4-}$ clusters and can be synthesized in macroscopic yield *via* solid state reactions.[12, 61-68] Therefore, these binary intermetallic phases represent potential precursors for the solution-based fabrication of nanostructured, semiconducting materials. However, the high negative charge of the contained *Zintl* clusters results in poor solubility and a remarkably reductive nature, which is a drawback in this context. This is especially true for the silicide cluster chemistry, in which $A_{12}Si_{17}$ (*A*: alkali metal) phases are the only available precursors for $[Si_9]^{4-}$ clusters in solution.[27, 80] In order to make $[E_9]^{4-}$ (*E*: Si, Ge, Sn) clusters available for subsequent applications, suitable methods to overcome these solubility and reactivity problems are needed.

Therefore, this thesis addresses investigations on the reactivity of bare $[E_9]^{4-}$ (*E*: Si, Ge, Sn) cages and silylated $[Ge_9]$ clusters towards transition metal complexes and main-group element compounds, aiming for novel methods for their stabilization, functionalization and linkage.

1.5 Outline and Scope

In **chapter 3.1** the stabilization and linkage of bare $[E_9]^{4-}$ (*E*: Si, Sn) cages and various silylated [Ge_9] clusters with transition metal moieties is discussed. **Chapter 3.1.2** deals with the reactivity of nine-atomic Group 14 element *Zintl* clusters towards coinage metal NHC complexes NHC-*M*-Cl (*M*: Cu, Ag, Au). Reactions of bare $[E_9]^{4-}$ (*E*: Si, Sn) cages with the coinage metal NHC complexes at low temperature in NH_3(l) are summarized in **chapter 3.1.2.1**. These investigations resulted in the synthesis of the silicide cluster anion $[NHC^{Dipp}Cu(\eta^4\text{-}Si_9)]^{3-}$. The effect of the $[NHC^{Dipp}Cu]^+$ coordination is discussed in terms of solubility and stability of the novel species. Moreover, the synthesis of a series of $[NHC^{Dipp}M]^+$ (*M*: Cu, Ag, Au) coordinated $[Sn_9]^{4-}$ clusters $[NHC^{Dipp}M(\eta^4\text{-}Sn_9)]^{3-}$ (*M*: Cu, Ag, Au) is described, and the formation of the large intermetalloid $[(\eta^4\text{-}Sn_9)Ag(\eta^1\text{-}Sn_9)]^{7-}$ is discussed with respect to the step-by-step formation of such species in solution. In **chapter 3.1.2.2** investigations on the reactivity of variously silylated [Ge_9] clusters towards $NHC^{Dipp}M$Cl (*M*: Cu, Ag, Au) are presented, which led to the isolation of a series of neutral coinage metal NHC coordinated [Ge_9] clusters $[NHC^{Dipp}Cu(\eta^3\text{-}Ge_9\{Si(TMS)_3\}_3)]$ (*M*: Cu, Ag, Au), $[NHC^{Dipp}Cu(\eta^3\text{-}Ge_9\{SiR_3\}_3)]$ (*R*: ^{i}Pr, ^{i}Bu) and $[(NHC^{Dipp}Cu)_2(\eta^3,\eta^3\text{-}Ge_9\{Si(TMS)_3\}_2)]$ (*M*: Cu, Ag, Au).

By contrast, **chapter 3.1.3** focusses on the reactivity of silylated [Ge_9] clusters towards the early transition metal complex $[Cp_2TiCl]_2$. The syntheses of the neutral compound $[Cp_2Ti(MeCN)(\eta^1\text{-}Ge_9\{Si(TMS)_3\}_3)]$ and the $[Cp_2Ti]^+$ bridged dimeric species $K_3[Cp_2Ti(\eta^1\text{-}Ge_9\{Si(TMS)_3\}_2)_2]$ by reaction of $[Ge_9\{Si(TMS)_3\}_n]^{(4-n)-}$ (*n*: 2, 3) with $[Cp_2TiCl]_2$ are described and the Ge-Ti bonding situation is discussed.

Chapter 3.2 deals with the stabilization and functionalization of [Ge_9] *Zintl* clusters with main-group element moieties. Investigations on the reactivity of silylated $[Ge_9\{Si(TMS)_3\}_n]^{(4-n)-}$ (*n*: 2, 3) cages and bare $[Ge_9]^{4-}$ clusters towards several Group 13 element compounds R_2E-Br (*E*: B, Al; *R*: substituent) are summarized in **chapter 3.2.2**. These studies resulted in the isolation of mixed-substituted clusters $[Ge_9\{Si(TMS)_3\}_2ER_2]^-$ (*E*: B, Al; *R*: substituent), which were characterized by means of NMR spectroscopy and ESI-MS. In **chapter 3.2.3** the phosphine-functionalization of [Ge_9] clusters is presented. **Chapter 3.2.3.1** deals with the synthesis of mixed-functionalized neutral clusters $[Ge_9\{Si(TMS)_3\}_3PRR^I]$ (*R, R^I*: small alkyl, alkenyl) or anionic species $[Ge_9\{Si(TMS)_3\}_2PRR^I]^-$ (*R*, *R^I*: medium or large alkyl, alkenyl, aryl, aminoalkyl). Moreover, the reactivity of the mixed-functionalized [Ge_9] clusters towards NHC^{Dipp}CuCl is discussed with respect to the validation of this [Ge_9] cluster functionalization method. Finally, **chapter 3.2.3.2** focusses on the synthesis of multiple phosphine-functionalized [Ge_9] clusters $[Ge_9\{PRR^I\}_3]^-$ (*R*: N^{i}Pr$_2$; *R^I*: N^{i}Pr$_2$ or ^{t}Bu) and their behaviour in reactions with NHC^{Dipp}CuCl or $M(CO)_5$(thf) (*M*: Cr, Mo, W). The outline and scope of this thesis are illustrated in Scheme 1.4.

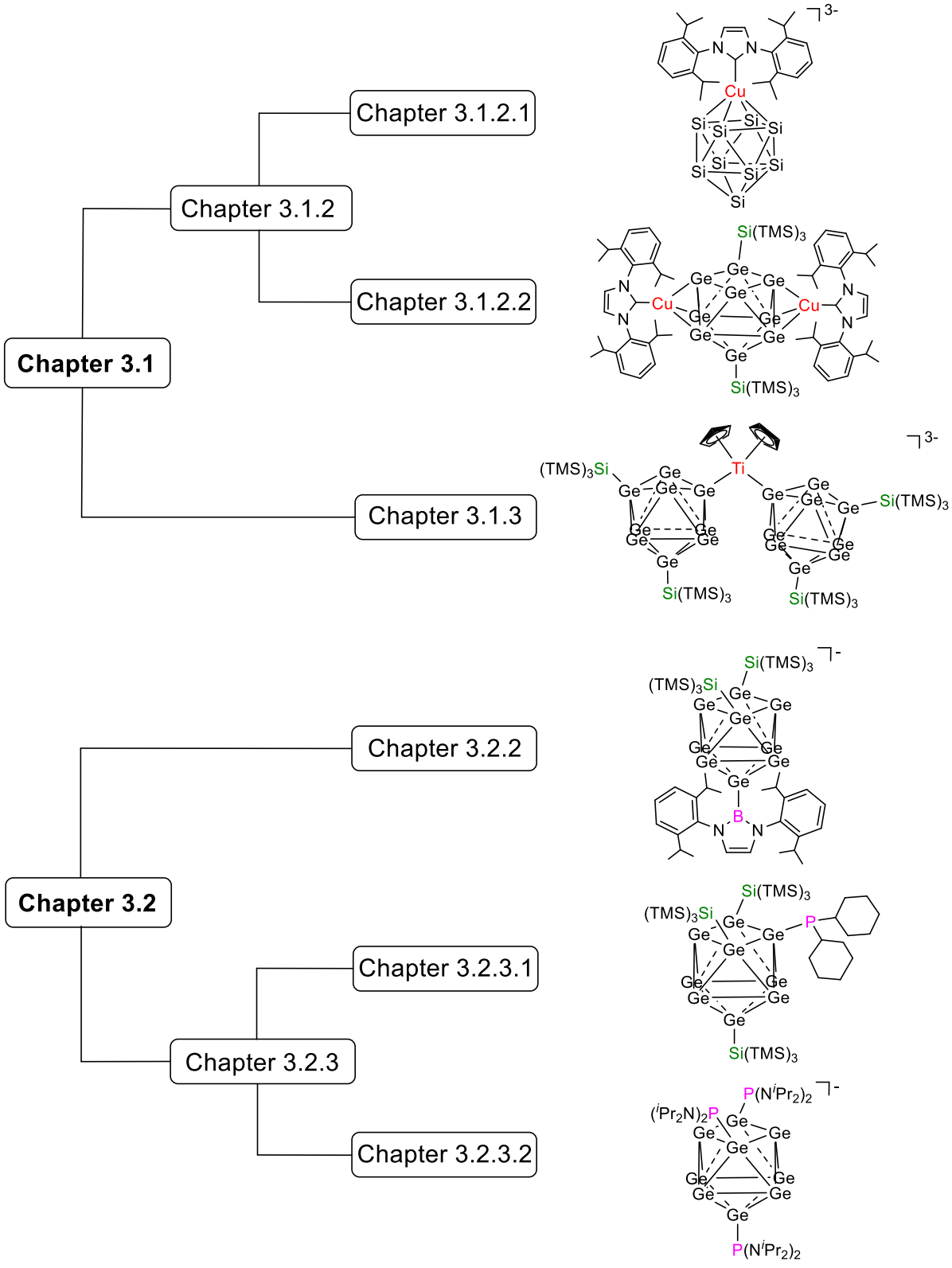

Scheme 1.4: Flowchart illustrating outline and scope of this thesis.

1.6 Literature

[1] C. Papadopoulos, *Solid State Electronic Devices*, Springer, New York, U.S.A, **2014**.
[2] D. M. Chapin, C. Fuller, G. Pearson, *J. Appl. Phys.* **1954**, *25*, 676.
[3] S. Botti, J. A. Flores-Livas, M. Amsler, S. Goedecker, M. A. L. Marques, *Phys. Rev. B* **2012**, *86*, 121204.
[4] A. B. Fowler, W. E. Howard, G. E. Brock, *Phys. Rev.* **1962**, *128*, 1664.
[5] N. Fukata, K. Sato, M. Mitome, Y. Bando, T. Sekiguchi, M. Kirkham, J. I. Hong, Z. L. Wang, R. L. Snyder, *ACS Nano* **2010**, *4*, 3807.
[6] R. Brandes, D. Conrads, E. Döring, P. Döring, H. Gierens, R. Henke, A. Kemnitz, W. Plaßmann, H. Steffen, *Vieweg Handbuch Elektrotechnik*, Springer, **2013**.
[7] C. Claeys, E. Simoen, *Germanium-Based Technologies: From Materials to Devices*, Elsevier Science, Amsterdam, **2011**.
[8] E. C. Cho, S. Park, X. Hao, D. Song, G. Conibeer, S. C. Park, M. A. Green, *Nanotechnology* **2008**, *19*, 245201.
[9] M. G. Kanatzidis, *Adv. Mater.* **2007**, *19*, 1165.
[10] R. A. Bley, S. M. Kauzlarich, *J. Am. Chem. Soc.* **1996**, *118*, 12461.
[11] A. Stein, *Nature* **2006**, *441*, 1055.
[12] A. M. Guloy, R. Ramlau, Z. Tang, W. Schnelle, M. Baitinger, Y. Grin, *Nature* **2006**, *443*, 320.
[13] M. Ashuri, Q. He, L. L. Shaw, *Nanoscale* **2016**, *8*, 74.
[14] J. Liang, X. Li, Z. Hou, T. Zhang, Y. Zhu, X. Yan, Y. Qian, *Chem. Mater.* **2015**, *27*, 4156.
[15] K. H. Wedepohl, *Geochim. Cosmochim Acta* **1995**, *59*, 1217.
[16] R. Pillarisetty, *Nature* **2011**, *479*, 324.
[17] J. Graetz, C. C. Ahn, R. Yazami, B. Fultz, *J. Electrochem. Soc.* **2004**, *151*, A698.
[18] E. Kasper, A. Schuh, G. Bauer, B. Holländer, H. Kibbel, *J. Cryst. Growth* **1995**, *157*, 68.
[19] E. Kasper, *J. Cryst. Growth* **1995**, *150*, 921.
[20] E. Kasper, M. Kittler, M. Oehme, T. Arguirov, *Photon. Res.* **2013**, *1*, 69.
[21] A. F. Holleman, E. Wiberg, N. Wiberg, *Lehrbuch der Anorganischen Chemie*, Walter de Gruyter, **2007**.
[22] J. D. Verhoeven, D. K. Finnemore, E. D. Gibson, J. E. Ostenson, L. F. Goodrich, *Appl. Phys. Lett.* **1978**, *33*, 101.
[23] S.-S. Lin, Y.-S. Tsai, K.-R. Bai, *Appl. Surf. Sci.* **2016**, *380*, 203.
[24] J. Vidal, S. Lany, M. d´Avezac, A. Zunger, A. Zakutayev, J. Francis, J. Tate, *Appl. Phys. Lett.* **2012**, *100*, 032104.
[25] A. Schnepf, *New J. Chem.* **2010**, *34*, 2079.
[26] Y. Heider, D. Scheschkewitz, *Dalton Trans.* **2018**, *47*, 7104.
[27] S. Scharfe, F. Kraus, S. Stegmaier, A. Schier, T. F. Fässler, *Angew. Chem. Int. Ed.* **2011**, *50*, 3630.
[28] D. Nied, R. Köppe, W. Klopper, H. Schnöckel, F. Breher, *J. Am. Chem. Soc.* **2010**, *132*, 10264.
[29] A. Tsurusaki, C. Iizuka, K. Otsuka, S. Kyushin, *J. Am. Chem. Soc.* **2013**, *135*, 16340.
[30] I. Shintaro, O. Kyohei, T. Yuki, K. Soichiro, *Angew. Chem. Int. Ed.* **2013**, *52*, 2507.
[31] D. Scheschkewitz, *Angew. Chem. Int. Ed.* **2005**, *44*, 2954.
[32] D. Scheschkewitz, *Chem. Lett.* **2011**, *40*, 2.

[33] T. Iwamoto, M. Kobayashi, K. Uchiyama, S. Sasaki, S. Nagendran, H. Isobe, M. Kira, *J. Am. Chem. Soc.* **2009**, *131*, 3156.
[34] C.-W. So, H. W. Roesky, J. Magull, R. B. Oswald, *Angew. Chem. Int. Ed.* **2006**, *45*, 3948.
[35] R. S. Ghadwal, H. W. Roesky, S. Merkel, J. Henn, D. Stalke, *Angew. Chem. Int. Ed.* **2009**, *48*, 5683.
[36] Y. Wang, Y. Xie, P. Wei, R. B. King, H. F. Schaefer, P. von R. Schleyer, G. H. Robinson, *Science* **2008**, *321*, 1069.
[37] A. C. Filippou, O. Chernov, B. Blom, K. W. Stumpf, G. Schnakenburg, *Chem. Eur. J.* **2010**, *16*, 2866.
[38] J. Teichmann, M. Wagner, *Chem. Commun.* **2018**, *54*, 1397.
[39] N. Wiberg, C. M. M. Finger, K. Polborn, *Angew. Chem. Int. Ed. Engl.* **1993**, *32*, 1054.
[40] N. Wiberg, *Coord. Chem. Rev.* **1997**, *163*, 217.
[41] H. Matsumoto, K. Higuchi, S. Kyushin, M. Goto, *Angew. Chem. Int. Ed. Engl.* **1992**, *31*, 1354.
[42] A. Sekiguchi, T. Yatabe, C. Kabuto, H. Sakurai, *J. Am. Chem. Soc.* **1993**, *115*, 5853.
[43] P. Kircher, G. Huttner, K. Heinze, G. Renner, *Angew. Chem. Int. Ed.* **1998**, *37*, 1664.
[44] G. Renner, P. Kircher, G. Huttner, P. Rutsch, K. Heinze, *Eur. J. Inorg. Chem.* **2001**, 973.
[45] K. Abersfelder, A. J. P. White, H. S. Rzepa, D. Scheschkewitz, *Science* **2010**, *327*, 564.
[46] P. Willmes, K. Leszczyńska, Y. Heider, K. Abersfelder, M. Zimmer, V. Huch, D. Scheschkewitz, *Angew. Chem. Int. Ed.* **2016**, *55*, 2907.
[47] A. F. Richards, M. Brynda, M. M. Olmstead, P. P. Power, *Organometallics* **2004**, *23*, 2841.
[48] V. Y. Lee, Y. Ito, O. A. Gapurenko, A. Sekiguchi, V. I. Minkin, R. M. Minyaev, H. Gornitzka, *Angew. Chem. Int. Ed.* **2015**, *54*, 5654.
[49] A. F. Richards, H. Hope, P. P. Power, *Angew. Chem. Int. Ed.* **2003**, *42*, 4071.
[50] A. Schnepf, C. Drost, *Dalton Trans.* **2005**, 3277.
[51] A. F. Richards, B. E. Eichler, M. Brynda, M. M. Olmstead, P. P. Power, *Angew. Chem. Int. Ed.* **2005**, *44*, 2546.
[52] T. Kunz, C. Schrenk, A. Schnepf, *Angew. Chem. Int. Ed.* **2018**, *57*, 4088.
[53] A. Schnepf, G. Stösser, H. Schnöckel, *J. Am. Chem. Soc.* **2000**, *122*, 9178.
[54] A. Schnepf, H. Schnöckel, *Angew. Chem. Int. Ed.* **2002**, *41*, 3532.
[55] H. Schnöckel, *Dalton Trans.* **2005**, 3131.
[56] A. Schnepf, *Angew. Chem. Int. Ed.* **2003**, *42*, 2624.
[57] E. Zintl, *Angewandte Chem.* **1939**, *52*, 1.
[58] W. Klemm, *Proc. Chem. Soc.* **1958**, 329.
[59] E. Busmann, *Z. Anorg. Allg. Chem.* **1961**, *313*, 90.
[60] H. G. Von Schnering, M. Baitinger, U. Bolle, W. Carrillo-Cabrera, J. Curda, Y. Grin, F. Heinemann, J. Llanos, K. Peters, A. Schmeding, M. Somer, *Z. Anorg. Allg. Chem.* **1997**, *623*, 1037.
[61] V. Quéneau, S. C. Sevov, *Angew. Chem. Int. Ed.* **1997**, *36*, 1754.
[62] S. Ponou, T. F. Fässler, *Z. Anorg. Allg. Chem.* **2007**, *633*, 393.
[63] C. Hoch, M. Wendorff, C. Röhr, *Acta Cryst. Sect. C* **2002**, *58*, i45.
[64] V. Quéneau, S. C. Sevov, *Inorg. Chem.* **1998**, *37*, 1358.
[65] C. Hoch, M. Wendorff, C. Röhr, *J. Alloys. Compd.* **2003**, *361*, 206.
[66] E. Todorov, S. C. Sevov, *Inorg. Chem.* **1998**, *37*, 3889.
[67] S. Bobev, S. C. Sevov, *Polyhedron* **2002**, *21*, 641.
[68] V. Quéneau, E. Todorov, S. C. Sevov, *J. Am. Chem. Soc.***1998**, *120*, 3263.

[69] A. Harder, E. Zintl, *Z. Phys. Chem. A* **1931**, *154*, 47.
[70] D. Kummer, L. Diehl, *Angew. Chem. Int. Ed. Engl.* **1970**, *9*, 895.
[71] F. H. Smyth, *J. Am. Chem. Soc.* **1917**, *39*, 1299.
[72] A. Nienhaus, R. Hauptmann, T. F. Fässler, *Angew. Chem. Int. Ed.* **2002**, *41*, 3213.
[73] L.-A. Jantke, T. F. Fässler, *Inorganics* **2018**, *6*, 31.
[74] F. Li, S. C. Sevov, *Inorg. Chem.* **2012**, *51*, 2706.
[75] K. Wade, *Chem. Commun.* **1971**, 792.
[76] K. Wade, *Adv. Inorg. Chem. Radiochem.* **1976**, *18*, 1.
[77] D. M. P. Mingos, *Acc. Chem. Res.* **1984**, *17*, 311.
[78] D. M. P. Mingos, R. L. Johnston, *Struct. Bond.* **1987**, *68*, 29.
[79] J. Rosdahl, T. F. Fässler, L. Kloo, *Eur. J. Inorg. Chem.* **2005**, 2888.
[80] S. C. Sevov, J. M. Goicoechea, *Organometallics* **2006**, *25*, 5678.
[81] L. Diehl, K. Khodadadeh, D. Kummer, J. Strähle, *Z. Naturforsch. B* **1976**, *31*, 522.
[82] L. Diehl, K. Khodadadeh, D. Kummer, J. Strähle, *Chem. Ber.* **1976**, *109*, 3404.
[83] J. D. Corbett, P. A. Edwards, *J. Am. Chem. Soc.* **1977**, *99*, 3313.
[84] T. F. Fässler, R. Hoffmann, *Angew. Chem. Int. Ed.* **1999**, *38*, 543.
[85] S. Joseph, C. Suchentrunk, F. Kraus, N. Korber, *Eur. J. Inorg. Chem.* **2009**, 4641.
[86] S. Joseph, C. Suchentrunk, N. Korber, *Z. Naturforsch. B.* **2010**, *65*, 1059.
[87] C. B. Benda, T. Henneberger, W. Klein, T. F. Fässler, *Z. Anorg. Allg. Chem.* **2017**, *643*, 146.
[88] C. Suchentrunk, J. Daniels, M. Somer, W. Carrillo-Cabrera, N. Korber, *Z. Naturforsch. B.* **2005**, *60*, 277.
[89] C. Downie, J.-G. Mao, A. M. Guloy, *Inorg. Chem.* **2001**, *40*, 4721.
[90] W. Carrillo-Cabrera, U. Aydemir, M. Somer, A. Kircali, T. F. Fässler, S. D. Hoffmann, *Z. Anorg. Allg. Chem.* **2007**, *633*, 1575.
[91] M. Somer, W. Carrillo-Cabrera, E.-M. Peters, K. Peters, H. G. von Schnering, *Z. Anorg. Allg. Chem.* **1998**, *624*, 1915.
[92] J. D. Corbett, P. A. Edwards, *J. Chem. Soc.*, *Chem. Commun.* **1975**, 984.
[93] R. Hauptmann, R. Hoffmann, T. F. Fässler, *Z. Anorg. Allg. Chem.* **2001**, *627*, 2220.
[94] R. Hauptmann, T. F. Fässler, *Z. Anorg. Allg. Chem.* **2002**, *628*, 1500.
[95] C. B. Benda, M. Waibel, T. Köchner, T. F. Fässler, *Chem. Eur. J.* **2014**, *20*, 16738.
[96] L. Yong, S. D. Hoffmann, T. F. Fässler, *Inorg. Chim. Acta* **2006**, *359*, 4774.
[97] T. F. Fässler, R. Hoffmann, *J. Chem. Soc.*, *Dalton Trans.* **1999**, 3339.
[98] J. Campbell, D. A. Dixon, H. P. A. Mercier, G. J. Schrobilgen, *Inorg. Chem.* **1995**, *34*, 5798.
[99] J. M. Goicoechea, S. C. Sevov, *J. Am. Chem. Soc.* **2004**, *126*, 6860.
[100] T. F. Fässler, M. Hunziker, *Inorg. Chem.* **1994**, *33*, 5380.
[101] T. F. Fässler, U. Schütz, *Inorg. Chem.* **1999**, *38*, 1866.
[102] V. Angilella, C. Belin, *Faraday Trans.* **1991**, *87*, 203.
[103] C. Suchentrunk, N. Korber, *Inorg. Chim. Acta* **2006**, *359*, 267.
[104] R. Hauptmann, T. F. Fässler, *Z. Kristallogr. NCS* **2003**, *218*, 461.
[105] S. C. Critchlow, J. D. Corbett, *J. Am. Chem. Soc.* **1983**, *105*, 5715.
[106] T. F. Fässler, M. Hunziker, *Z. Anorg. Allg. Chem.* **1996**, *622*, 837.
[107] T. F. Fässler, R. Hoffmann, *Z. Kristallogr. NCS* **2000**, *215*, 139.
[108] L. Yong, S. D. Hoffmann, T. F. Fässler, *Z. Kristallogr. NCS* **2005**, *49*, 220.
[109] J. M. Goicoechea, S. C. Sevov, *Inorg. Chem.* **2005**, *44*, 2654.
[110] C. H. E. Belin, J. D. Corbett, A. Cisar, *J. Am. Chem. Soc.* **1977**, *99*, 7163.
[111] J. Aakerstedt, S. Ponou, L. Kloo, S. Lidin, *Eur. J. Inorg. Chem.* **2011**, 3999.
[112] J. Campbell, G. J. Schrobilgen, *Inorg. Chem.* **1997**, *36*, 4078.

[113] C. Suchentrunk, N. Korber, *New. J. Chem.* **2006**, *30*, 1737.
[114] P. A. Edwards, J. D. Corbett, *Inorg. Chem.* **1977**, *16*, 903.
[115] M. Somer, W. Carrillo-Cabrera, E.-M. Peters, K. Peters, M. Kaupp, H. G. von Schnering, *Z. Anorg. Allg. Chem.* **1999**, *625*, 37.
[116] A. Ugrinov. S. C. Sevov, *Chem. Eur. J.* **2004**, *10*, 3727.
[117] L. Xu, S. C. Sevov, *J. Am. Chem. Soc.* **1999**, *121*, 9245.
[118] R. Hauptmann, T. F. Fässler, *Z. Anorg. Allg. Chem.* **2003**, *629*, 2266.
[119] D. Craig, T. Zhongjia, A. M. Guloy, *Angew. Chem. Int. Ed.* **2000**, *39*, 337.
[120] C. Downie, J.-G. Mao, H. Parmar, A. M. Guloy, *Inorg. Chem.* **2004**, *43*, 1992.
[121] A. Ugrinov, S. C. Sevov, *J. Am. Chem. Soc.* **2002**, *124*, 10990.
[122] L. Yong, S. D. Hoffmann, T. F. Fässler, *Z. Anorg. Allg. Chem.* **2005**, *631*, 1149.
[123] T. F. Fässler, S. Frischhut, J. Machado de Carvalho, A. Karttunen, *Z. Anorg. Allg. Chem.* **2018**, *644*, 1337.
[124] A. Ugrinov, S. C. Sevov, *Inorg. Chem.* **2003**, *42*, 5789.
[125] L. Yong, S. D. Hoffmann, T. F. Fässler, *Z. Anorg. Allg. Chem.* **2004**, *630*, 1977.
[126] T. Henneberger, T. F. Fässler, W. Klein, *Z. Anorg. Allg. Chem.* **2018**, *644*, 1018.
[127] J. M. Goicoechea, S. C. Sevov, *Organometallics* **2006**, *25*, 4530.
[128] S. Joseph, M. Hamberger, F. Mutzbauer, O. Härtl, M. Meier, N. Korber, *Angew. Chem. Int. Ed.* **2009**, *48*, 8770.
[129] S. Gärtner, M. Hamberger, N. Korber, *Crystals* **2015**, *5*, 275.
[130] M. Waibel, F. Kraus, S. Scharfe, B. Wahl, T. F. Fässler, *Angew. Chem. Int. Ed.* **2010**, *49*, 6611.
[131] C. Lorenz, S. Gärtner, N. Korber, *Z. Anorg. Allg. Chem.* **2017**, *643*, 141.
[132] M. Neumeier, F. Fendt, S. Gärtner, C. Koch, T. Gärtner, N. Korber, R. M. Gschwind, *Angew. Chem. Int. Ed.* **2013**, *52*, 4483.
[133] C. Lorenz, F. Hastreiter, J. Hioe, L. Nanjundappa, S. Gärtner, N. Korber, R. M. Gschwind, *Angew. Chem. Int. Ed.* **2018**, *57*, 12956.
[134] L. J. Schiegerl, A. J. Karttunen, J. Tillmann, S. Geier, G. Raudaschl-Sieber, M. Waibel, T. F. Fässler, *Angew. Chem. Int. Ed.* **2018**, *57*, 12950.
[135] F. S. Geitner, T. F. Fässler, *Chem. Commun.* **2017**, *53*, 12974.
[136] B. W. Eichhorn, R. C. Haushalter, W. T. Pennington, *J. Am. Chem. Soc.* **1988**, *110*, 8704.
[137] B. W. Eichhorn, R. C. Haushalter, *Chem. Commun.* **1990**, 937.
[138] J. Campbell, H. P. A. Mercier, H. Franke, D. P. Santry, D. A. Dixon, G. J. Schrobilgen, *Inorg. Chem.* **2002**, *41*, 86.
[139] B. Kesanli, J. Fettinger, B. Eichhorn, *Chem. Eur. J.* **2001**, *7*, 5277.
[140] J.-Q. Wang, S. Stegmaier, B. Wahl, T. F. Fässler, *Chem. Eur. J.* **2010**, *16*, 1793.
[141] D. O. Downing, P. Zavalij, B. W. Eichhorn, *Eur. J. Inorg. Chem.* **2010**, 890.
[142] S. Scharfe, T. F. Fässler, *Eur. J. Inorg. Chem.* **2010**, 1207.
[143] B. Zhou, M. S. Denning, T. A. D. Chapman, J. M. Goicoechea, *Inorg. Chem.* **2009**, *48*, 2899.
[144] K. Mayer, L.-A. Jantke, S. Schulz, T. F. Fässler, *Angew. Chem. Int. Ed.* **2017**, *56*, 2350.
[145] B. Zhou, M. S. Denning, T. A. D. Chapman, J. E. McGrady, J. M. Goicoechea, *Chem. Commun.* **2009**, 7221.
[146] C. B. Benda, M. Waibel, T. F. Fässler, *Angew. Chem. Int. Ed.* **2015**, *54*, 522.
[147] L. Wang, Y. Wang, Z. Li, H. Ruan, L. Xu, *Dalton Trans.* **2017**, *46*, 6839.
[148] S. Scharfe, T. F. Fässler, S. Stegmaier, S. D. Hoffmann, K. Ruhland, *Chem. Eur. J.* **2008**, *14*, 4479.
[149] J. M. Goicoechea, S. C. Sevov, *Angew. Chem. Int. Ed.* **2005**, *44*, 4026.

[150] D. R. Gardner, J. Fettinger, B. W. Eichhorn, *Angew. Chem. Int. Ed. Engl.* **1996**, *35*, 2852.
[151] J. M. Goicoechea, S. C. Sevov, *J. Am. Chem. Soc.* **2006**, *128*, 4155.
[152] C. Liu, L.-J. Li, X. Jin, J. E. McGrady, Z.-M. Sun, *Inorg. Chem.* **2018**, *57*, 3025.
[153] E. N. Esenturk, J. Fettinger, B. Eichhorn, *J. Am. Chem. Soc.* **2006**, *128*, 9178.
[154] E. N. Esenturk, J. Fettinger, B. Eichhorn, *Chem. Commun.* **2005**, 247.
[155] J. Q. Wang, S. Stegmaier, T. F. Fässler, *Angew. Chem. Int. Ed.* **2009**, *48*, 1998.
[156] B. Zhou, M. S. Denning, D. L. Kays, J. M. Goicoechea, *J. Am. Chem. Soc.* **2009**, *131*, 2802.
[157] T. Kramer, J. C. A. Duckworth, M. D. Ingram, B. Zhou, J. E. McGrady, J. M. Goicoechea, *Dalton Trans.* **2013**, *42*, 12120.
[158] M. M. Bentlohner, C. Fischer, T. F. Fässler, *Chem. Commun.* **2016**, *52*, 9841.
[159] A. Spiekermann, S. D. Hoffmann, T. F. Fässler, *Angew. Chem. Int. Ed.* **2006**, *45*, 3459.
[160] B. Zhou, T. Krämer, A. L. Thompson, J. E. McGrady, J. M. Goicoechea, *Inorg. Chem.* **2011**, *50*, 8028.
[161] E. N. Esenturk, J. Fettinger, Y.-F. Lam, B. Eichhorn, *Angew. Chem. Int. Ed.* **2004**, *43*, 2132.
[162] G. Espinoza-Quintero, J. C. A. Duckworth, W. K. Myers, J. E. McGrady, J. M. Goicoechea, *J. Am. Chem. Soc.* **2014**, *136*, 1210.
[163] E. N. Esenturk, J. C. Fettinger, B. W. Eichhorn, *J. Am. Chem. Soc.* **2006**, *128*, 12.
[164] B. Kesanli, J. E. Halsig, P. Zavalij, J. C. Fettinger, Y.-F. Lam, B. W. Eichhorn, *J. Am. Chem. Soc.* **2007**, *129*, 4567.
[165] J. M. Goicoechea, S. C. Sevov, *J. Am. Chem. Soc.* **2005**, *127*, 7676.
[166] F. S. Kocak, P. Zavalij, Y.-F. Lam, B. W. Eichhorn, *Inorg. Chem.* **2008**, *47*, 3515.
[167] A. Spiekermann, S. D. Hoffmann, T. F. Fässler, I. Krossing, U. Preiss, *Angew. Chem. Int. Ed.* **2007**, *46*, 5310.
[168] A. Spiekermann, S. D. Hoffmann, F. Kraus, T. F. Fässler, *Angew. Chem. Int. Ed.* **2007**, *46*, 1638.
[169] S. Scharfe, T. F. Fässler, *Z. Anorg. Allg. Chem.* **2011**, *637*, 901.
[170] J.-Q. Wang, B. Wahl, T. F. Fässler, *Angew. Chem. Int. Ed.* **2010**, *49*, 6592.
[171] F. S. Geitner, W. Klein, T. F. Fässler, *Dalton Trans.* **2017**, *46*, 5796.
[172] A. Ugrinov, S. C. Sevov, *J. Am. Chem. Soc.* **2002**, *124*, 2442.
[173] A. Ugrinov, S. C. Sevov, *J. Am. Chem. Soc.* **2003**, *125*, 14059.
[174] A. Ugrinov, S. C. Sevov, *Chem. Eur. J.* **2004**, *10*, 3727.
[175] D. F. Hansen, B. Zhou, J. M. Goicoechea, *J. Organomet. Chem.* **2012**, *721–722*, 53.
[176] F. S. Kocak, P. Y. Zavalij, Y.-F. Lam, B. W. Eichhorn, *Chem. Commun.* **2009**, 4197.
[177] M. M. Bentlohner, L.-A. Jantke, T. Henneberger, C. Fischer, K. Mayer, W. Klein, T. F. Fässler, *Chem. Eur. J.* **2016**, *22*, 13946.
[178] L. J. Schiegerl, F. S. Geitner, C. Fischer, W. Klein, T. F. Fässler, *Z. Anorg. Allg. Chem.* **2016**, *642*, 1419.
[179] K. Mayer, L. J. Schiegerl, T. F. Fässler, *Chem. Eur. J.* **2016**, *22*, 18794.
[180] O. Kysliak, C. Schrenk, A. Schnepf, *Inorg. Chem.* **2015**, *54*, 7083.
[181] O. Kysliak, T. Kunz, A. Schnepf, *Eur. J. Inorg. Chem.* **2017**, 805.
[182] O. Kysliak, A. Schnepf, *Dalton Trans.* **2016**, *45*, 2404.
[183] L. G. Perla, S. C. Sevov, *J. Am. Chem. Soc.* **2016**, *138*, 9795.
[184] L. G. Perla, A. Muñoz-Castro, S. C. Sevov, *J. Am. Chem. Soc.* **2017**, *139*, 15176.
[185] F. S. Geitner, W. Klein, T. F. Fässler, *Angew. Chem. Int. Ed.* **2018**, *57*, 14509.
[186] M. W. Hull, S. C. Sevov, *J. Am. Chem. Soc.* **2009**, *131*, 9026.
[187] C. B. Benda, J.-Q. Wang, B. Wahl, T. F. Fässler, *Eur. J. Inorg. Chem.* **2011**, 4262.

[188] D. J. Chapman, S. C. Sevov, *Inorg. Chem.* **2008**, *47*, 6009.
[189] M. W. Hull, S. C. Sevov, *Inorg. Chem.* **2007**, *46*, 10953.
[190] C. B. Benda, H. He, W. Klein, M. Somer, T. F. Fässler, *Z. Anorg. Allg. Chem.* **2015**, *641*, 1080.
[191] M. W. Hull, S. C. Sevov, *J. Organomet. Chem.* **2012**, *721–722*, 85.
[192] M. W. Hull, S. C. Sevov, *Chem. Commun.* **2012**, *48*, 7720.
[193] M. W. Hull, A. Ugrinov, I. Petrov, S. C. Sevov, *Inorg. Chem.* **2007**, *46*, 2704.
[194] S. Frischhut, M. M. Bentlohner, W. Klein, T. F. Fässler, *Inorg. Chem.* **2017**, *56*, 10691.
[195] M. M. Bentlohner, W. Klein, Z. H. Fard, L.-A. Jantke, T. F. Fässler, *Angew. Chem. Int. Ed.* **2015**, *54*, 3748.
[196] M. M. Bentlohner, S. Frischhut, T. F. Fässler, *Chem. Eur. J.* **2017**, *23*, 17089.
[197] O. Kysliak, C. Schrenk, A. Schnepf, *Chem. Eur. J.* **2016**, *22*, 18787.
[198] C. Schenk, A. Schnepf, *Angew. Chem. Int. Ed.* **2007**, *46*, 5314.
[199] C. Schenk, F. Henke, G. Santiso-Quinones, I. Krossing, A. Schnepf, *Dalton Trans.* **2008**, 4436.
[200] F. Henke, C. Schenk, A. Schnepf, *Dalton Trans.* **2009**, 9141.
[201] F. Li, S. C. Sevov, *Inorg. Chem.* **2015**, *54*, 8121.
[202] C. Schenk, A. Schnepf, *Chem. Commun.* **2009**, 3208.
[203] F. Henke, C. Schenk, A. Schnepf, *Dalton Trans.* **2011**, *40*, 6704.
[204] O. Kysliak, C. Schrenk, A. Schnepf, *Angew. Chem. Int. Ed.* **2016**, *55*, 3216.
[205] F. S. Geitner, T. F. Fässler, *Eur. J. Inorg. Chem.* **2016**, 2688.
[206] F. S. Geitner, M. A. Giebel, A. Pöthig, T. F. Fässler, *Molecules* **2017**, *22*, 1204.
[207] F. Li, A. Muñoz-Castro, S. C. Sevov, *Angew. Chem. Int. Ed.* **2012**, *51*, 8581.
[208] F. Li, S. C. Sevov, *J. Am. Chem. Soc.* **2014**, *136*, 12056.
[209] K. Mayer, L. J. Schiegerl, T. Kratky, S. Günther, T. F. Fässler, *Chem. Commun.* **2017**, *53*, 11798.
[210] O. Kysliak, C. Schrenk, A. Schnepf, *Inorg. Chem.* **2017**, *56*, 9693.
[211] F. S. Geitner, J. V. Dums, T. F. Fässler, *J. Am. Chem. Soc.* **2017**, *139*, 11933.
[212] F. S. Geitner, C. Wallach, T. F. Fässler, *Chem. Eur. J.* **2018**, *24*, 4103.
[213] F. Li, A. Muñoz-Castro, S. C. Sevov, *Angew. Chem. Int. Ed.* **2016**, *55*, 8630.
[214] S. Frischhut, T. F. Fässler, *Dalton Trans.* **2018**, 47, 3223.
[215] S. Frischhut, W. Klein, M. Drees, T. F. Fässler, *Chem. Eur. J.* **2018**, *24*, 9009.
[216] S. Frischhut, T. F. Fässler, *C. R. Chim.* **2018**, *21*, 932.
[217] L. T. Canham, *Appl. Phys. Lett.* **1990**, *57*, 1046.
[218] L. Venema, *Nature* **2011**, *479*, 309.
[219] B. K. Teo, X. H. Sun, *Chem. Rev.* **2007**, *107*, 1454.
[220] W. Lu, C. M. Lieber, *Nat. Mater.* **2007**, *6*, 841.

2 Experimental Section

2.1 Experimental Procedures

2.1.1 Materials and Equipment

If not stated otherwise, all reactions were carried out in an oxygen and moisture free argon Ar4.8 atmosphere (Westfalen Gas; purity: 99.998 %) using a Schlenk line equipped with a rotary vane vacuum pump (*Vacuubrand* RZ 5; average vacuum $4 \cdot 10^{-2}$ mbar) and a quicksilver pressure control valve or in a glovebox (*MBraun*, average oxygen value < 0.1 ppm; average H_2O value < 0.1 ppm). The Ar4.8 gas was purified by passing a BTS catalyst, silica gel with indicator ("orange gel"), and phosphorous pentoxide with H_2O indicator before usage. All glassware was stored in a drying oven (*Binder*; ED115) at 120 °C. Reactions were carried out in Schlenk tubes or Schlenk flasks equipped with a glass valve and a glass stopper using either silicon-based grease (*Dow Corning*) or teflon paste (*Roth AG*) as lubricants. Before usage, reactions vessels were additionally heated to 650 °C using a heat gun (*Steinel*) in dynamic vacuum and subsequently purged with argon gas (Schlenk line, procedure was repeated three times). Glassware was cleaned in an isopropanol/KOH bath after usage. Plastic syringes and metal cannulas were purged with argon gas three times before usage. Further equipment (NMR- and EPR-tubes, agate mortars, teflon tubing, Whatman filters, teflon syringe filters, *Pasteur* pipettes and stirring bars) were stored in a drying oven for at least 2 h before usage.

2.1.2 Filtrations

Filtrations under exclusion of air and moisture were carried out at the Schlenk line using Whatman filters (*Whatman*, GD 1 UM) attached to teflon tubings with teflon tape (*VWR*) or in the glovebox using either Whatman filter (*Whatman*, GD 1 UM) packed Pasteur pipettes or teflon syringe filters (VWR; diameter 2.5 cm, pore size 0.2 µm).

2.1.3 Reactants and Solvents

Commercially available chemicals were used as received unless otherwise stated. The solvents acetonitrile, diethylether, tetrahydrofuran, toluene, pentane and hexane were obtained from a solvent purification system (*MB-SPS*; *MBraun*) and were subsequently stored over molecular sieves (3 Å) prior to usage. Liquid ammonia was dried over sodium at -78 °C prior to usage (chapter 2.1.5) and ethanol was dried with sodium/diethylphtalate. Table 2.1 summarizes all commercially available reactants and solvents used within this work and provides information about physical state, purity, supplier/producer and storage of the respective chemicals.

Table 2.1: List of commercially available chemicals used within this work.

Substance	Physical state	Purity [%]	Supplier/ Producer	Storage
acetic acid	liquid	97	*Merck*	bench
acetonitrile	liquid	-	*VWR*	SPS
acetonitrile-d_3	liquid	99.8	*Deutero*	glovebox
acetone	liquid	99	*Alfa Aesar*	bench
aluminium tribromide	solid	98	*Merck*	glovebox
ammonia	gas	99.999	*Westfalen*	gas cylinder
antimony trichloride	solid	99	*Alfa Aesar*	glovebox
argon	gas	99.998	*Westfalen*	gas cylinder
benzene-d_6	liquid	99.0	*Deutero*	glovebox
bis-1-adamantylchlorophosphine	solid	97	*Sigma Aldrich*	glovebox
bis-diisopropylaminochlorophosphine	solid	97	*Acros Organ.*	glovebox
bis(*o*-tolyl)chlorophosphine	solid	98	*Alfa Aesar*	glovebox
boron tribromide (1.0 M in hexane)	liquid	-	*Sigma Aldrich*	fridge (6 °C)
5-bromo-1-pentene	liquid	95	*Sigma Aldrich*	fridge (6 °C)
chloroform-d_1	liquid	99.8	*Deutero*	glovebox
chlorotri(*iso*-butyl)silane	liquid	99	*Sigma Aldrich*	glovebox
chlorotri(*iso*-propyl)silane	liquid	97	*Sigma Aldrich*	glovebox
chlorotrimethylsilane	liquid	99	*Sigma Aldrich*	glovebox
chlorotris(trimethylsilyl)silane	solid	95	*TCI*	glovebox
copper(I) chloride	solid	97	*Alfa Aesar*	glovebox
copper(I) bromide	solid	97	*Alfa Aesar*	bench
[2.2.2]-cryptand	solid	99	*Merck*	glovebox
diethylether	liquid	-	*Brenntag*	SPS
dicyclohexylchlorophosphine	liquid	97	*Sigma Aldrich*	glovebox
2,6-diisopropylaniline	liquid	92	*Merck*	Bench
di-*iso*-propylchlorophosphine	liquid	96	*Sigma Aldrich*	glovebox
dimesitylchlorophosphine	solid	95	*Sigma Aldrich*	glovebox
di-*tert*-butylchlorophosphine	liquid	96	*Sigma Aldrich*	glovebox
ethylacetate	liquid	99.9	*VWR*	bench
germanium	solid	99.999	*Evochem*	glovebox
glyoxal (40 % in water)	liquid	-	*Merck*	bench
hexane	liquid	-	*Brenntag*	SPS
hydrogen-tetrachloroaurate(III) trihydrate	solid	99	*Alfa Aesar*	glass ampoule

Substance	Physical State	Purity [%]	Supplier/ Producer	Storage
iodine	solid	99.8	*VWR*	glovebox
iso-propyldichlorophosphine	liquid	96	*Sigma Aldrich*	glovebox
iso-propylmagnesium bromide (2.0 M in thf)	liquid	-	*Acros Organ.*	fridge (6 °C)
lithium	solid	97	*Rockwood Lithium*	glovebox
lithium diisopropylamide (LDA; 2.0 M in thf, *n*-heptane, ethylbenzene)	liquid	-	*Acros Organ.*	fridge (6 °C)
magnesium cuttings	solid	99.9	*ChemPur*	bench
menthol	solid	99	*Sigma Aldrich*	bench
methanol	liquid	99.5	*VWR*	bench
n-butyllithium (1.6 M in hexane)	liquid	-	*Acros Organ.*	fridge (6 °C)
paraformaldehyde	liquid	95	*Merck*	bench
pentane	liquid	-	*Brenntag*	SPS
1,10-phenanthroline	solid	99	*Sigma Alrich*	bench
phosphorus trichloride	liquid	99	*Merck*	glovebox
potassium	solid	98	*ChemPur*	glovebox
silver(I)oxide	solid	99	*Merck*	bench
sodium	solid	99	*ChemPur*	glovebox
sodium *tert*-butoxide	solid	98	*Sigma Aldrich*	bench
tert-butyldichlorophosphine	liquid	98	*Alfa Aesar*	glovebox
tert-butyl lithium (1.9 M in pentane)	liquid	-	*Acros Organ.*	fridge (6 °C)
tert-butylmagnesium bromide (1.0 M in Me-thf)	liquid	-	*Alfa Aesar*	fridge (6 °C)
tetrahydrofuran	liquid	-	*Kraft*	SPS
tetrahydrofuran-d_8	liquid	99.5	*Deutero*	glovebox
tetrahydrothiophene	liquid	99	*Merck*	bench
toluene	liquid	-	*Brenntag*	SPS
triethylamine hydrochloride	solid	99	*Sigma Aldrich*	glovebox
2,4,6-trimethylaniline	liquid	98	*Alfa Aesar*	bench
2,4,6-trimethylphenylbromide	liquid	99	*Alfa Aesar*	bench

2.1.4 Solid State Reactions

K_4E_9 (*E*: Ge, Sn)

In a typical reaction, potassium (1.052 g, 26.9 mmol) and germanium (3.999 g, 55.1 mmol) or tin (6.54 g, 55.1 mmol) were weighted in (glovebox, argon atmosphere) into a stainless-steel cylinder (length: 7 cm, diameter: 1.5 cm), which was placed in a stainless-steel autoclave (length: 9 cm, diameter: 2.5 cm) and the autoclave was closed with a stainless-steel screw cap (Figure 2.1).[1, 2] The sealed autoclave was placed in a corundum tube (length: 60 cm, diameter: 4 cm) under argon atmosphere, which had been evacuated on a Schlenk line for 30 min prior to usage. The corundum tube with the contained steel autoclave was closed with a lubricated glass cap equipped with a rubber balloon for pressure balance and was vertically placed in a tube furnace (*HTM Reetz GmbH*) equipped with a temperature controller (*Eurotherm Deutschland GmbH*). The furnace was heated to the target temperature of 650 °C (*E*: Ge) or 550 °C (*E*: Sn) with a rate of 2 K/min and kept at this temperature for 2 d before it was slowly cooled to room temperature with a rate of 1 K/min. Subsequently, the steel autoclave was removed from the corundum tube and rapidly brought into the glovebox. The product *Zintl* phases were removed from the autoclaves and finely grounded using an agate pestle and mortar. The obtained grey/blue solids were examined for phase-purity by powder XRD in wax sealed glass capillaries prior to usage.

$A_{12}Si_{17}$ or $A_6A^I_6Si_{17}$ (*A*, *A*^{I}: K, Rb)

The syntheses of $A_{12}Si_{17}$ or $A_6A^I_6Si_{17}$ (*A*, *A*^{I}: K, Rb) were conducted in tantalum ampoules (Figure 2.1), which were fabricated by cutting tantalum tubes (*Changsha South Tantalum Niobium Co., LTD.*, diameter 10 mm, wall strength: 0.5 mm) in small cylinders (height approx. 3.5 cm). The cylinders were closed at one end with a tantalum cap and were sealed by arc melting in an arc furnace (MAM 1 *Edmund Bühler*). The ampoules were cleaned by sonication in acetic acid, water and acetone before they were dried in a drying cabinet at 120 °C and stored in the glovebox prior to usage. For the synthesis of the silicide *Zintl* phases, stoichometric amounts of the elements were weighted in into the tantalum ampoules (glovebox, argon atmosphere; Table 2.2), which were afterwards closed with a tantalum cap at their open end and sealed by arc melting.[3] Subsequently, the ampoules were placed in a quartz tube (length: 80 cm, diameter: 4 cm; three ampoules per quartz tube), which was closed with a lubricated glass cap, evacuated, and vertically placed in a tube furnaces (*HTM Reetz GmbH*) equipped with a temperature controller (*Eurotherm Deutschland GmbH*). The furnace was heated to the target temperature of 800 °C at a rate of 2 K/min and was kept at this temperature for 15 h, before it was cooled to room temperature at a rate of 0.5 K/min. The ampoules were removed from the quartz tube and rapidly brought into the glovebox. The

product *Zintl* phases were brought out of the ampoules and finely grounded using an agate pestle and mortar. Subsequently, the obtained grey/blue solids were examined for phase purity by powder XRD in wax sealed glass capillaries prior to usage.

Table 2.2: Typical syntheses of silicide phases $A_{12}Si_{17}$ or $A_6A'_6Si_{17}$ (*A*: K, Rb).

	K	Rb	Si
$K_{12}Si_{17}$	469.0 mg / 12 mmol	-	477.0 mg / 17 mmol
$K_6Rb_6Si_{17}$	191.5 mg / 4.9 mmol	419.0 mg / 4.9 mmol	389.3 mg / 13.9 mmol
$Rb_{12}Si_{17}$	-	836.6 mg / 9.8 mmol	389.3 mg / 13.9 mmol

Figure 2.1: Stainless-steel autoclave and tantalum ampoule as reaction compartments for solid state reactions.

2.1.5 Working with Liquid Ammonia

Ammonia condenses as colourless liquid below -33 °C and can be used as solvent for reactions at low temperature.[4] For working with liquid ammonia, a Schlenk line consisting exclusively of glass components was used (Figure 2.2). Due to the moisture sensitivity of the *Zintl* phases used within this work, it was necessary to remove water traces from ammonia prior to usage. Therefore, ammonia (WESTFALEN Gas; 99.999 %) was condensed from a gas cylinder into an isopropanol/dry ice cooled solvent trap containing elemental sodium and stored there for at least 1 h. The formation of a blue solution (solvated electrons) in the solvent trap indicated that NH_3(l) was dry. For subsequent reactions Schlenk tubes including the reactants were attached at the respective adapters of the Schlenk line and NH_3(l) was condensed into the cooled reaction vessels (-78 °C; isopropanol/dry ice) in static vacuum. Subsequently, the Schlenk tubes were removed from the Schlenk line and were stored in a freezer (*Thermo Fisher Scientific*) at -70 °C.

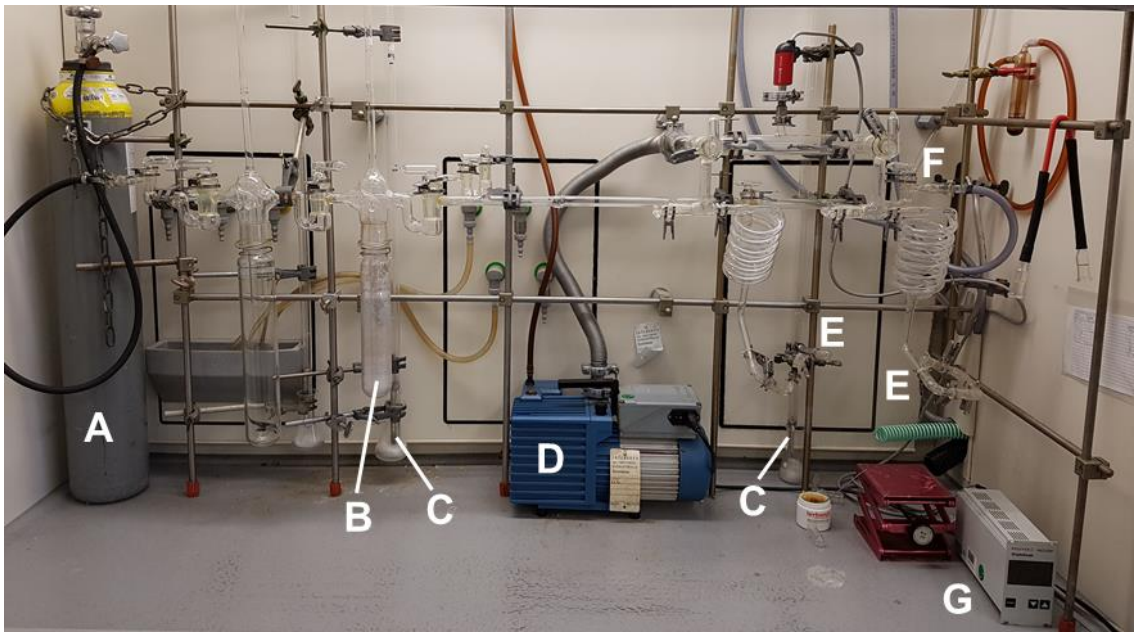

Figure 2.2: Setup used for working with liquid ammonia. (A) gas cylinder containing NH_3(g), (B) solvent trap containing elemental sodium, (C) mercury overpressure valves, (D) vacuum pump, (E) adapters for Schlenk flasks, (F) argon supply, (G) pressure gauge.

2.2 Characterization Methods

2.2.1 Nuclear Magnetic Resonance Spectroscopy (NMR)

NMR spectra were acquired on a *Bruker* Avance Ultrashield 400 MHz spectrometer equipped with an auto sampler. Chemical shifts are reported in parts per million relative to $SiMe_4$ (tetramethylsilane) with the solvent peaks serving as internal reference.[5] Air and moisture sensitive samples were prepared in the glovebox under argon atmosphere and measurements were performed in air-tight J-Young NMR tubes (*Deutero*). Variable temperature NMR experiments (VT-NMR) were carried out by Maria Weindl using a Bruker DRX 400 MHz spectrometer. Abbreviations for signal multiplicities are: s (singlet), d (doublet), t (triplet), hept (heptet), m (multiplet).

2.2.2 Electrospray Ionization Mass Spectrometry (ESI-MS)

Mass spectra were acquired using a *Bruker Daltronic* HCT mass spectrometer (injection speed 240 µL/h). For the measurements, the solutions of the samples were diluted to approx. $2 \cdot 10^{-4}$ mmol/mL. Depending on the nature of the sample spectra were either acquired in the positive or in the negative ion mode using different capillary voltages. Measurements were partwise supported by M. Sc Lorenz Schiegerl, M. Sc. Kerstin Mayer or M. Sc. Christina Fischer. Evaluation of the data occurred with the *Bruker* Compass Data Analysis 4.0 SP 5 program. Spectra were plotted using OriginPro 2016G (*OriginLab*).

2.2.3 Powder X-Ray Diffraction (PXRD)

Powder X-ray diffractograms were acquired on a STADI P (STOE Darmstadt, Cu-K_α radiation, Ge monochromator) diffractometer. The diffractometer is equipped with an DECTRIS Mythen 1K detector. The air- and moisture sensitive samples were finely grounded and filled into glass capillaries (Hilgenberg, diameter 0.3-0.5 mm, wall strength 0.01 mm) under argon atmosphere in a glovebox which were sealed with wax. Measurements occurred in the Debye-Scherrer geometry. Evaluation of the acquired data (diffraction patterns) was done by comparison to theoretical powder patterns (calculated from single crystal data) using the *WinXPOW* package.[6]

2.2.4 Single Crystal X-Ray Diffraction (SC-XRD)

Data collection occurred at different diffractometers at TUM (STOE StadiVari diffractometer equipped with a DECTRIS PILATUS 300K detector; Oxford Diffraction Xcalibur3 diffractometer equipped with a Sapphire 3 detector; Bruker AXS D8 equipped with a APEX II detector; all MoK_α radiation [λ = 0.71073 Å]), University of California, Berkeley (Bruker APEX II QUAZAR (MoK_α radiation) equipped with a APEX II detector) or the Lawrence Berkeley National Laboratory (beamline 11.3.1 of the Advanced Light Source using a PHOTON100 CMOS detector running shutterless using radiation with a wavelength of 0.7288 Å selected by a Si(111) monochromator and focused to 200 μm^2 with a toroidal mirror). The crystal structures were solved by direct methods (SHELXS-97 or SHELXS-2014) and refined by full-matrix least-squares calculations against F^2 (SHELXL-97 or SHELXL-2014).[7-9] The positions of the hydrogen atoms were calculated and refined using a riding model. Unless stated otherwise, all non-hydrogen atoms were treated with anisotropic displacement parameters. In special cases the electron density of disordered solvent molecules was taken care of by the PLATON squeeze function.[10] The supplementary crystallographic data for the structures reported in this thesis have been deposited with the Cambridge Structural database and are available free of charge *via* www.ccdc.cam.ac.uk/data_request/cif.

Preparation of Single Crystals under Inert Gas Atmosphere at Low Temperature

Due to the air and moisture sensitivity of all crystals characterized during this work, the crystals were prepared for measurement under inert gas atmosphere. Since all samples were stored in freezers at temperatures between -32 °C and -70 °C for crystallization, the preparation of the single crystals was carried out using a cooling table setup according to *Kottke* and *Stalke*.[11] The setup of the cooling table with labelling is presented in Scheme 2.1. Regarding single crystals from NH_3(l) solution, containing co-crystallized ammonia molecules, this method is essential for the preparation of intact samples, since decomposition of the crystals starts to occur above temperatures of -30 °C. The crystalline samples were scoped out of the mother liquor at -78 °C under an argon stream and were transferred into perfluorinated ether (Galden®, *Solvay Solexis*), which had previously been cooled below -30 °C. The sample as well as the perfluorinated ether were cooled from below by a liquid nitrogen filled dewar and from above by a cold N_2 gas stream (generated by pumping nitrogen gas through a liquid nitrogen cooled copper cooling coil). Finally, the single crystals were fixed on a glass capillary and positioned in a cold N_2 gas stream (between 100 K and 150 K; *Oxford Cryosystems*) at the respective diffractometer, using the crystal cap system.

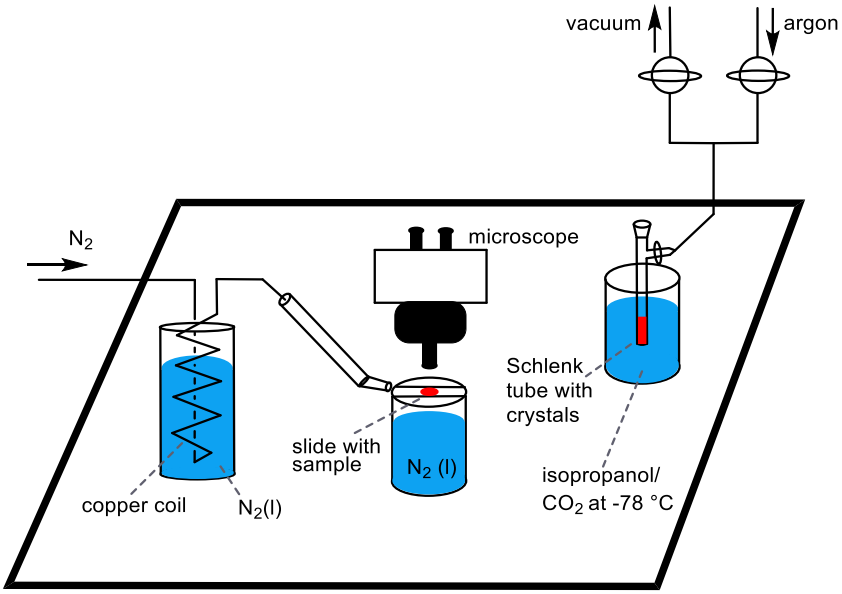

Scheme 2.1: Labelled setup of the cooling table for preparation of single crystals at low temperature according to *Kottke* and *Stalke*.[11] This method is essential for the preparation of single crystals containing NH_3(l) as co-crystallized solvent.

2.2.5 Energy Dispersive X-Ray Analysis (EDX)

Energy dispersive X-ray (EDX) examinations with single crystals were carried out with a *Hitachi* TM-1000 tabletop microscope device. Data evaluation occurred using the SWIFT-ED-TM (*Oxford Instruments*: INCA System Software) program. EDX measurements were carried out by Maria Müller (Fässler group; TUM).

2.2.6 Infrared Spectroscopy (IR)

FT-IR spectra were recorded on a Bruker Alpha FT-IR spectrometer with an ATR geometry, using a Diamond ATR unit (Roland Fischer group; TUM). Sample preparation as well as measurements were carried out in the glovebox under argon atmosphere. Measurements were supported by M. Sc. David Mayer (Roland Fischer group; TUM).

2.2.7 Electron Paramagnetic Resonance (EPR)

EPR spectra were recorded on a JEOL JES-FA 200 spectrometer at X-band frequency (approx. 9 GHz). The thf solutions of the samples were frozen with N_2(l) and the measurements were carried out at 130 K. The g-factors were calculated relative to a Mn^{2+}/MgO standard. EPR measurements were carried out by Dr. Oksana Storcheva.

2.2.8 Elemental Analysis

Elemental analyses were carried out in the microanalytical laboratory of the Chemistry Department of Technische Universität München or in the College of Chemistry microanalytical laboratory at the University of California, Berkeley. Analyses of C, H, N were performed in a combustion analyzer (elementar vario EL, *Bruker*).

2.2.9 Quantum Chemical Calculations

Computational analyses were performed using the Gaussian09 program package,[12] with exchange correlation hybrid functional after Perdew, Burke and Ernzerhof (PBE0)[13, 14] and def2-TZVPP basis sets for all considered elements (H, C, N, P, Si, Cu, Ge).[15, 16] Structure parameters for single point calculations were taken from respective single crystal structures and the compensation of positive charges occurred using a solvation model (polarizable continuum model, PCM).[17] Calculations were done by M. Sc. Jasmin Dums (Fässler group; TUM).

2.3 Literature

[1] S. Ponou, T. F. Fässler, *Z. Anorg. Allg. Chem.* **2007**, *633*, 393.

[2] C. Hoch, M. Wendorff, C. Röhr, *J. Alloys Compd.* **2003**, *361*, 206.

[3] C. Hoch, M. Wendorff, C. Röhr, *Acta Cryst. Sect. C* **2002**, *58*, i45.

[4] A. F. Holleman, E. Wiberg, N. Wiberg, *Lehrbuch der Anorganischen Chemie*, Walter de Gruyter, **2007**.

[5] G. R. Fulmer, A. J. M. Miller, N. H. Sherden, H. E. Gottlieb, A. Nudelman, B. M. Stoltz, J. E. Bercaw, K. I. Goldberg, *Organometallics* **2010**, *29*, 2176.

[6] *WinXPow*, *STOE & Cie GmbH*, Version 2.08., **2003**.

[7] G. M. Sheldrick, *SHELXL-97*, Program for Crystal Structure Refinement, Göttingen, **1997**.

[8] G. M. Sheldrick, *Acta Cryst. Sect. A* **2008**, 64, 112.

[9] G. M. Sheldrick, *Acta Cryst. Sect. C* **2015**, *71*, 3.

[10] A. Spek, *Acta Cryst. Sect. D* **2009**, *65*, 148.

[11] T. Kottke, D. Stalke, *J. Appl. Cryst.* **1993**, *26*, 615.

[12] M. J. Frisch, G. W. Trucks, H. B. Schlegel, G. E. Scuseria, M. A. Robb, J. R. Cheeseman, G. Scalmani, V. Barone, B. Mennucci, G. A. Petersson, H. Nakatsuji, M. Caricato, X. Li, H. P. Hratchian, A. F. Izmaylov, J. Bloino, G. Zheng, J. L. Sonnenberg, M. Hada, M. Ehara, K. Toyota, R. Fukuda, J. Hasegawa, M. Ishida, T. Nakajima, Y. Honda, O. Kitao, H. Nakai, T. Vreven, J. A. Montgomery, Jr., J. E. Peralta, F. Ogliaro, M. Bearpark, J. J. Heyd, E. Brothers, K. N. Kudin, V. N. Staroverov, R. Kobayashi, J. Normand, K. Raghavachari, A. Rendell, J. C. Burant, S. S. Iyengar, J. Tomasi, M. Cossi, N. Rega, J. M. Millam, M. Klene, J. E. Knox, J. B. Cross, V. Bakken, C. Adamo, J. Jaramillo, R. Gomperts, R. E. Stratmann, O. Yazyev, A. J. Austin, R. Cammi, C. Pomelli, J. W. Ochterski, R. L. Martin, K. Morokuma, V. G. Zakrzewski, G. A. Voth, P. Salvador, J. J. Dannenberg, S. Dapprich, A. D. Daniels, Ö. Farkas, J. B. Foresman, J. V. Cioslowski, D. J. Fox, *Gaussian 09*, *Gaussian, Inc.: Wallingford CT*, **2009**.

[13] J. P. Perdew, K. Burke, M. Ernzerhof, *Phys. Rev. Lett.* **1996**, *77*, 3865.

[14] C. Adamo, V. Barone, *J. Chem. Phys.* **1999**, *110*, 6158.

[15] F. L. Hirshfeld, *Theor. Chim. Acta* **1977**, *44*, 129.

[16] F. Weigend, M. Häser, H. Patzelt, R. Ahlrichs, *Chem. Phys. Lett.* **1998**, *294*, 143.

[17] V. Barone, M. Cossi, *J. Phys. Chem. A* **1998**, *102*, 1995.

3 Results and Discussion

3.1 Stabilization and Linkage of Nine-Atomic Group 14 Element *Zintl* Clusters with Transition Metal Moieties

3.1.1 Review of Relevant Literature

Solid state *Zintl* phases of the compositions A_4E_9 (*A*: alkali metal; *E*: Ge-Pb) and $A_{12}Si_{17}$ (*A*: alkali metal) are valuable precursors for well-defined nine-atomic Group 14 element *Zintl* clusters in solution. However, the high negative charge of the clusters, resulting in low-solubility and a highly reductive nature is a drawback in this context. This is especially true for the silicide cluster chemistry, in which phases of the composition $A_{12}Si_{17}$ (*A*: alkali metal) are the only source for $[Si_9]$ clusters.[1, 2] Due to the co-presence of $[Si_4]^{4-}$ cages with the desired $[Si_9]^{4-}$ clusters, these phases reveal very poor solubility and an increased reductive nature when compared to the A_4E_9 (*A*: alkali metal; *E*: Ge-Pb) phases of the heavier congeners. Therefore, the silicide cluster chemistry is mainly limited to NH_3(l) to date, and reactions with other reactants mostly led to redox reactions, yielding partially oxidized silicide clusters.[3-5]
However, reactions of the silicide phases with certain transition metal complexes allowed for the attachment of organometallic moieties to the silicide clusters, yielding $[PhZn(\eta^4\text{-}Si_9)]^{3-}$,[6] $[Ni(CO)_2(\mu\text{-}Si_9)_2]^{8-}$ [7] and $[(MesCu)_2(\eta^3,\eta^3\text{-}Si_4)]^{4-}$,[8] which represent the only examples for the successful decoration of silicide clusters with any substituent prior to this work. By contrast, in case of the heavier homologues of silicon (Ge-Pb), reactions of the nine-atomic clusters with transition metal complexes led to a plethora of different product species, comprising transition metal fragment coordinated $[E_9]^{4-}$ (*E*: Ge-Pb) clusters such as $[PhZn(\eta^4\text{-}E_9)]^{3-}$ (*E*: Ge-Pb),[6] transition metal bridged cluster species like $[(\eta^4\text{-}Ge_9)Cu(\eta^1\text{-}Ge_9)]^{7-}$,[9] or endohedral species in which the transition metal cation or (transition metal) is incorporated into the nine-atomic cluster core such as $[Cu@Sn_9]^{3-}$.[10] Moreover, partial oxidation of the $[E_9]^{4-}$ (Ge-Pb) clusters led to larger intermetalloid aggregates such as $[Au_3Ge_{45}]^{4-}$,[11] and allowed for the incorporation of further metal cations of heavier transition metals in enlarged cluster cores as observed in $[Ir@Sn_{12}]^{3-}$.[12] In general, mainly late and electron-rich transition metal complexes (Group 10-Group 12) have been considered for reactions with the negatively charged Group 14 element *Zintl* clusters, and there is only a limited number of reports on reactions of these clusters with organometallic complexes of Group 6-Group 9 metals.[13-20] This can be explained by the reductive power of the negatively charged clusters, which can also easily undergo redox reactions with their reaction partners. However, recently it was shown by the isolation of $[Cp_2Ti(NH_3)(\eta^1\text{-}Sn_9)]^{3-}$, that also early transition metal complexes (Group 4) can be successfully reacted with the negatively charged Group 14 element clusters.[21] The reactivity of transition metal complexes towards bare nine-atomic Group 14 element *Zintl* clusters is

reviewed in more detail in the introductory part of this work (chapter 1.3.2.1 and chapter 1.3.2.2).

Regarding germanide cluster chemistry in solution, recently methods which allow for the attachment of several silyl groups at the [Ge_9] core have been found. The resulting species [Ge_9{Si*R*$_3$}$_3$]$^-$ (*R*: silyl, alkyl, aryl) and [Ge_9{Si(TMS)$_3$}$_2$]$^{2-}$ reveal a decreased charge, which results in an enhanced solubility in standard solvents (MeCN or thf) and a decreased reductive nature (chapter 1.3.2.2). Despite the attached groups, these decorated [Ge_9] clusters still comprise reactive sites and can undergo subsequent reactions with organometallic complexes, resulting in transition metal bridged [Ge_9] cluster dimers such as [Au(η^3-Ge_9{Si(TMS)$_3$}$_3$)$_2$]$^-$ or transition metal fragment coordinated anionic or neutral cluster species like [(CO)$_5$Cr(η^1-Ge_9{Si(TMS)$_3$}$_3$)]$^-$ or [Cp*Zn(η^3-Ge_9{Si(TMS)$_3$}$_3$)].[22-24] The reactivity of transition metal complexes towards silylated [Ge_9] clusters is reviewed in more detail in chapter 1.3.2.3.

The scope of this work was the stabilization, functionalization and linkage of nine-atomic Group 14 element *Zintl* clusters in solution. Therefore, we were especially interested in the attachment of positively charged transition metal fragments at [*E*$_9$]$^{4-}$ (*E*: Si, Sn) cages and silylated [Ge_9] clusters to obtain transition metal complexes of the *Zintl* clusters with decreased charge and enhanced solubility and stability. Moreover, we wanted to gather deeper insights into the linkage of the nine-atomic Group 14 element cages through transition metal cations or transition metal fragments. In this context transition metal complexes, which can undergo salt metathesis reactions with the negatively charged clusters (attachment of positively charged transition metal fragment under cleavage of the respective potassium salt) and bear relatively bulky and stable organic ligands (steric shielding of the cluster core and enhanced solubility in organic solvents) are promising precursors. Such complexes were found in the coinage metal NHC complexes NHC-*M*-Cl (*M*: Cu, Ag, Au) bearing robust (redox stable) NHC ligands with superb σ-donor capability,[25, 26] and the Ti(III) complex [$Cp_2TiCl]_2$ bearing stable Cp ligands. Moreover, the controlled cleavage of the NHC- or Cp-ligand(s) is possible (NHC: application of silver-NHC complexes as transmetalation agents;[27] Cp: reductive cleavage of Cp ligands),[28] which might allow for the step-by-step linkage of the [*E*$_9$] (*E*: Si, Ge, Sn) clusters.

The reactivity of nine-atomic Group 14 element *Zintl* clusters towards coinage metal NHC complexes is discussed in chapter 3.1.2, which is divided in chapters 3.1.2.1 (reactivity of bare [*E*$_9$]$^{4-}$ (*E*: Si, Sn) clusters towards coinage metal NHC complexes) and 3.1.2.2 (reactivity of [Ge_9{Si*R*$_3$}$_3$]$^-$ (*R*: TMS, ^{i}Bu, ^{i}Pr) and [Ge_9{Si(TMS)$_3$}$_2$]$^{2-}$ towards coinage metal NHC complexes). Moreover, the reactivity of [Ge_9{Si(TMS)$_3$}$_n$]$^{(4-n)-}$ (*n*: 2, 3) towards the early transition metal complex [$Cp_2TiCl]_2$ is reported in chapter 3.1.3.

3.1.2 Reactions of Nine-Atomic Group 14 Element *Zintl* Clusters with Coinage Metal NHC Complexes

In the previous chapter it has already been pointed out that coinage metal NHC complexes NHC-*M*-Cl (*M*: Cu, Ag, Au) are promising precursors for the attachment of positively charged [*M*-NHC]$^+$ fragments at nine-atomic Group 14 element *Zintl* clusters, yielding organometallic fragment coordinated *Zintl* clusters with decreased charge and enhanced stability and solubility. In the course of this work, mainly coinage metal complexes of the sterically demanding NHC^{Dipp} [bis(2,6-di-isopropylphenyl)imidazolylidene] ligand have been applied. Additionally, complexes bearing other NHC ligands with smaller wingtip substituents (NHC^{Mes} and NHC$^{i\text{Pr}}$) were considered in reactions with the $A_{12}Si_{17}$ (*A*: alkali metal) phases.

Investigations on the reactivity of coinage metal NHC complexes NHC-*M*-Cl (*M*: Cu, Ag, Au) towards $A_{12}Si_{17}$ (*A*: alkali metal) and K_4Sn_9 containing bare $[Si_9]^{4-}$ or $[Sn_9]^{4-}$ clusters were carried out at low temperature in NH_3(l) (chapter 3.1.2.1). By contrast, reactions of the coinage metal NHC complexes with silylated $[Ge_9]$ clusters $[Ge_9\{SiR_3\}_3]^-$ (*R*: TMS, ^{i}Bu, ^{i}Pr) and $[Ge_9\{Si(TMS)_3\}_2]^{2-}$ were conducted at room temperature in acetonitrile or thf solution. The latter investigations targeted the synthesis of completely neutral $[Ge_9]$ cluster compounds (chapter 3.1.2.2).

3.1.2.1 Reactions of $[E_9]^{4-}$ (*E*: Si, Sn) Clusters with Coinage Metal NHC Complexes

see chapter 5.1	F. S. Geitner, T. F. Fässler, *Chem. Commun.* **2017**, *53*, 12974.
see chapter 5.2	F. S. Geitner, W. Klein, T. F. Fässler, *Dalton Trans.* **2017**, *46*, 5796.

This chapter deals with the reactivity of the silicide phases $A_{12}Si_{17}$ (*A*: alkali metal) or the stannide phase K_4Sn_9 towards the coinage metal NHC complexes NHC-*M*-Cl (*M*: Cu, Ag, Au) at low temperature in NH_3(l).

The respective examinations resulted in the isolation of $[NHC^{Dipp}Cu(\eta^4\text{-}Si_9)]^{3-}$, which represents only the third example of a transition metal fragment coordinated $[Si_9]^{4-}$ cluster, and a series of $[M\text{-}NHC^{Dipp}]^{+}$ coordinated $[Sn_9]^{4-}$ clusters $[NHC^{Dipp}M(\eta^4\text{-}Sn_9)]^{3-}$ (*M*: Cu, Ag, Au). Moreover, the synthesis of the large intermetalloid species $[(\eta^4\text{-}Sn_9)Ag(\eta^1\text{-}Sn_9)]^{7-}$, comprising varying coordination of the $[Sn_9]^{4-}$ clusters to the bridging Ag^+ cation, was achieved. All species obtained by reaction of $A_{12}Si_{17}$ (*A*: alkali metal) or K_4Sn_9 with the coinage metal NHC complexes NHC-*M*-Cl (*M*: Cu, Ag, Au) are summarized in Scheme 3.1.

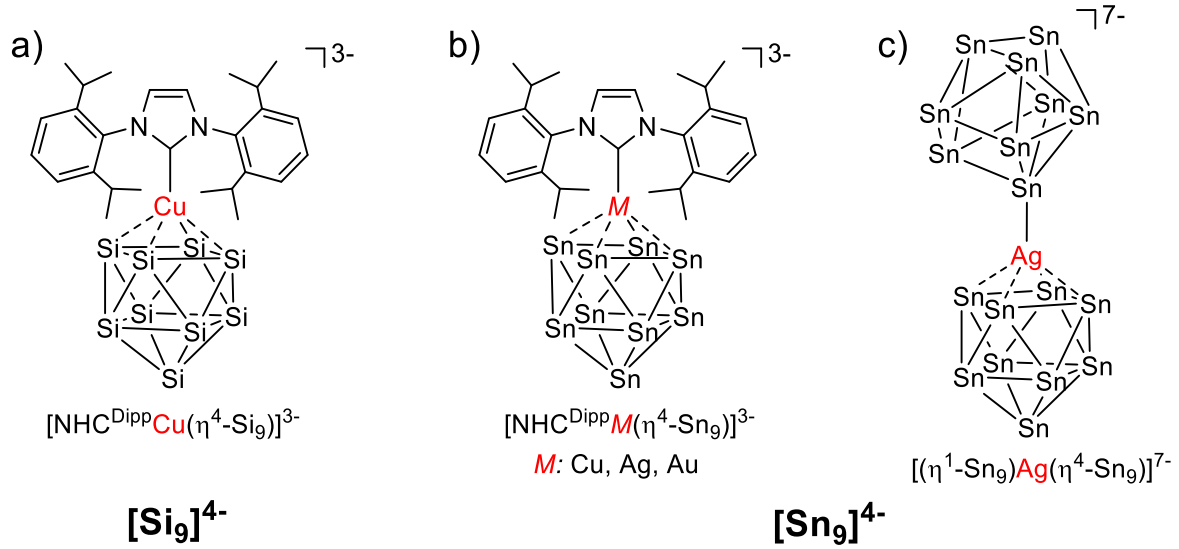

Scheme 3.1: Overview on products obtained from reactions of $[E_9]^{4-}$ (*E*: Si, Sn) clusters with coinage metal NHC complexes in NH_3(l). a) The silicide cluster complex $[NHC^{Dipp}Cu(\eta^4\text{-}Si_9)]^{3-}$, b) the stannide cluster complexes $[NHC^{Dipp}M(\eta^4\text{-}Sn_9)]^{3-}$ (*M*: Cu, Ag, Au), c) the large intermetalloid species $[(\eta^4\text{-}Sn_9)Ag(\eta^1\text{-}Sn_9)]^{7-}$.

Reactions of $A_{12}Si_{17}$ (*A*: alkali metal) with NHC-*M*-Cl (*M*: Cu, Ag, Au)

The synthesis of $[NHC^{Dipp}Cu(\eta^4\text{-}Si_9)]^{3-}$ was achieved by reaction of equimolar amounts of $A_{12}Si_{17}$ (*A*: K, K/Rb, Rb) and $NHC^{Dipp}CuCl$ in NH_3(l) at -70 °C in the presence of [2.2.2]-cryptand (1.86 equiv.; sequestering agent which enhances both solubility of the *Zintl* phases and crystallization of potentially formed products). The product species crystallized as red single crystals of the composition $A_3[A(2.2.2\text{-crypt})]_3[NHC^{Dipp}Cu(\eta^4\text{-}Si_9)]_2$ (*A*: K, K/Rb, Rb) from the reaction mixture and was characterized by single crystal X-ray diffraction. In $[NHC^{Dipp}Cu(\eta^4\text{-}Si_9)]^{3-}$, the $[NHC^{Dipp}Cu]^+$ moiety coordinates $[Si_9]^{4-}$ (square antiprismatic shape; C_{4v} symmetry) *via* its open square plane in a η^4-coordination mode, which is in accordance with the transition metal silicide cluster interactions observed in the previously isolated species $[PhZn(\eta^4\text{-}Si_9)]^{3-}$ (Figure 3.1).[6]

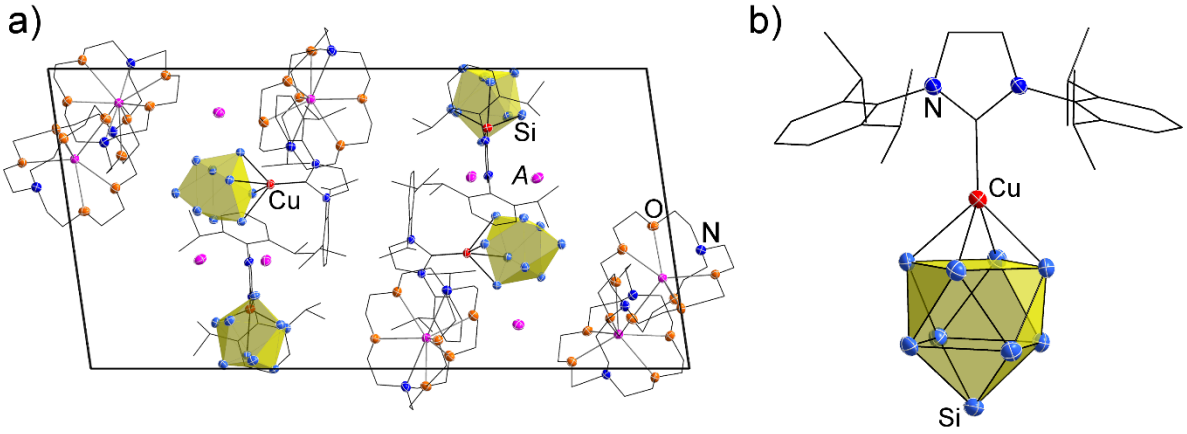

Figure 3.1: a) Unit cell of $A_3[A(2.2.2\text{-crypt})]_3[NHC^{Dipp}Cu(\eta^4\text{-}Si_9)]_2$ (*A*: K, K/Rb, Rb) with half of the cations being sequestered by [2.2.2]-cryptand. b) Molecular structure of $[NHC^{Dipp}Cu(\eta^4\text{-}Si_9)]^{3-}$ with the $[NHC^{Dipp}Cu]^+$ group coordinating the open square plane of the $[Si_9]^{4-}$ cluster. All ellipsoids are shown at a 50 % probability level and carbon atoms are represented as black wire sticks. For clarity, co-crystallized solvent molecules were omitted in a) and co-crystallized solvents molecules as well as cations were omitted in b). Colour code: Si (bright blue), Cu (red), N (dark blue), C (black), O (orange), alkali metal cations (purple).

Comparison of $[NHC^{Dipp}Cu(\eta^4\text{-}Si_9)]^{3-}$ to the previously isolated complex $[(MesCu)_2(\eta^3,\eta^3\text{-}Si_4)]^{4-}$ (obtained by reaction of $A_{12}Si_{17}$ with mesitylcopper in liquid ammonia) reveals a varying affinity of the organometallic Cu^+ complexes towards the $[Si_9]^{4-}$ and $[Si_4]^{4-}$ clusters contained in the $A_{12}Si_{17}$ (*A*: alkali metal) precursor phases (Scheme 3.2).[8]

Whereas the attachment of further $[Cu\text{-}NHC]^+$ fragments (with NHC ligands bearing different wingtip substituents; NHC^{Mes} and NHC^{iPr}) at $[Si_9]^{4-}$ was also achieved, reactions of the silicide phases with the silver- and gold-NHC complexes $NHC^{Dipp}MCl$ (*M*: Ag, Au) resulted in the partial oxidation of the $[Si_9]^{4-}$ clusters without attachment of $[NHC^{Dipp}M]^+$ (*M*: Ag, Au) moieties to the clusters (in accordance with the trend in redox potential; Scheme 3.2).

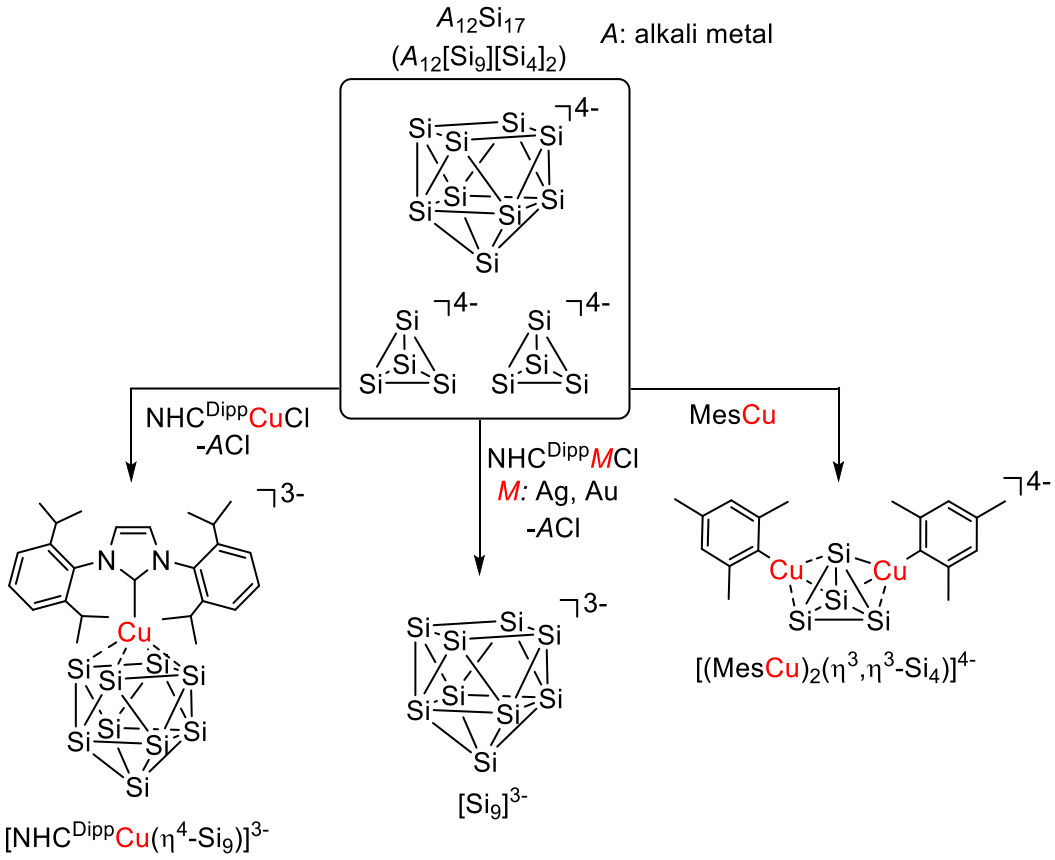

Scheme 3.2: Reactivity of the silicide phases $A_{12}Si_{17}$ (*A*: alkali metal) towards different organometallic coinage metal complexes in NH_3(l). Reactions with NHC^{Dipp}*M*Cl (*M*: Cu, Ag, Au) were carried out in the course of this thesis, whereas investigations on the reactivity of the silicide phases towards mesitylcopper have previously been reported.[8]

In further investigations it was shown that intact [NHC^{Dipp}Cu(η^4-Si$_9$)]$^{3-}$ clusters can be transferred to solvents different from NH_3(l), which is of interest with respect to potential applications. In these studies, liquid ammonia was evaporated-off from reaction mixtures, in which single crystals containing [NHC^{Dipp}Cu(η^4-Si$_9$)]$^{3-}$ had been found. The resulting residues were treated with pyridine or acetonitrile and the obtained deep red extracts were investigated by ESI-MS and NMR spectroscopy. In ESI-MS examinations the molecule peak of [NHC^{Dipp}Cu(η^4-Si$_9$)]$^{3-}$ with two attached protons was monitored at *m/z* 705.1 {[NHC^{Dipp}Cu(η^4-Si$_9$)]$^{3-}$ + 2H$^+$} and in ^{1}H NMR examinations carried out in acetonitrile-d_3 diagnostic signals of the attached [NHC^{Dipp}Cu]$^+$ moiety were detected. NMR spectroscopy also revealed that [NHC^{Dipp}Cu(η^4-Si$_9$)]$^{3-}$ is stable at low temperature, however, at room temperature the cleavage of the Cu-NHC bond under release of the free carbene was observed within two days.

Reactions of K_4Sn_9 with NHC^{Dipp}-*M*-Cl (*M*: Cu, Ag, Au)

The syntheses of $[NHC^{Dipp}M(\eta^4\text{-}Sn_9)]^{3-}$ (*M*: Cu, Ag, Au) were achieved by reactions of equimolar amounts of K_4Sn_9 with $NHC^{Dipp}MCl$ (*M*: Cu, Ag, Au) at -70 °C in NH_3(l) in the presence of [2.2.2]-cryptand (1.86 equiv.). The product species crystallized as black single crystals of the composition $[K(2.2.2\text{-crypt})]_3[NHC^{Dipp}M(\eta^4\text{-}Sn_9)]$ (*M*: Cu, Ag, Au) from the reaction mixtures after two to four months and were characterized by single crystal X-ray diffraction. In analogy to the Cu-Si interactions observed in $[NHC^{Dipp}Cu(\eta^4\text{-}Si_9)]^{3-}$, the coinage metal NHC fragments $[NHC^{Dipp}M]^+$ coordinate the $[Sn_9]^{4-}$ cages *via* their open square plane in a η^4-coordination mode. Regarding reactions of K_4Sn_9 with $NHC^{Dipp}AgCl$ also single crystals of the composition $K_3[K(2.2.2\text{-crypt})]_4[(\eta^4\text{-}Sn_9)Ag(\eta^1\text{-}Sn_9)]$, comprising the large intermetalloid anion $[(\eta^4\text{-}Sn_9)Ag(\eta^1\text{-}Sn_9)]^{7-}$ were found alongside $[K(2.2.2\text{-crypt})]_3[NHC^{Dipp}Ag(\eta^4\text{-}Sn_9)]$. The isolation of both species from the same reaction mixture indicates the stepwise formation of $[(\eta^4\text{-}Sn_9)Ag(\eta^1\text{-}Sn_9)]^{7-}$ with the formation of $[NHC^{Dipp}Ag(\eta^4\text{-}Sn_9)]^{3-}$ being the first reaction step, which is followed by the nucleophilic attack of a second $[Sn_9]^{4-}$ cluster at Ag^+, resulting in the cleavage of the Ag-NHC bond. Interestingly, the two $[Sn_9]^{4-}$ clusters coordinate Ag^+ in different coordination modes, as the second $[Sn_9]^{4-}$ cage approaches Ag^+ with the lone-pair situated at a tin vertex atom (η^1-coordination mode; Figure 3.2). This phenomenon is rather rare and has previously only been observed for a few examples in germanide cluster chemistry such as $[(\eta^4\text{-}Ge_9)Cu(\eta^1\text{-}Ge_9)]^{7-}$,[9] ${}^1_\infty\{Zn[(\eta^4\text{:}\eta^1\text{-}Ge_9)]\}^{2-}$ and $[(\eta^4\text{-}Ge_9)Zn\text{-}(\eta^1,\eta^1\text{-}Ge_9)\text{-}Zn(\eta^4\text{-}Ge_9)]^{8-}$.[17] The different reactivity of $[NHC^{Dipp}Ag(\eta^4\text{-}Sn_9)]^{3-}$ compared to $[NHC^{Dipp}M(\eta^4\text{-}Sn_9)]^{3-}$ (*M*: Cu, Au) can be explained by the relative lability of the Ag-NHC bond (Scheme 3.3).[29]

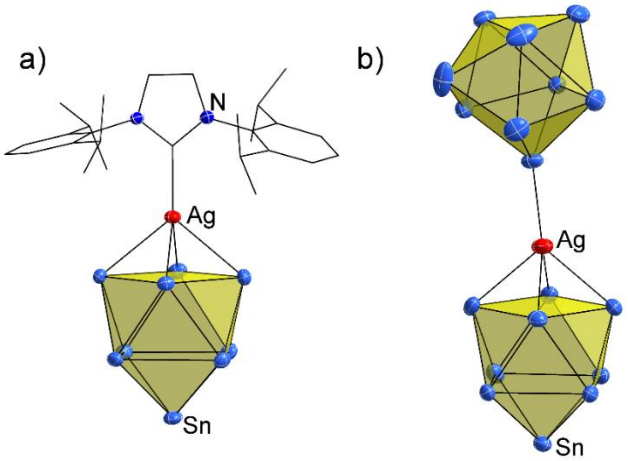

Figure 3.2: Molecular structures of $[NHC^{Dipp}Ag(\eta^4\text{-}Sn_9)]^{3-}$ (a) and the large intermetalloid anion $[(\eta^4\text{-}Sn_9)Ag(\eta^1\text{-}Sn_9)]^{7-}$ (b). All ellipsoids are shown at a 50 % probability level. For clarity, carbon atoms are represented as black wire sticks and cations, as well as co-crystallized solvent molecules are omitted. Both species were isolated from the same NH_3(l) reaction mixture at -70 °C. The structures of $[NHC^{Dipp}M(\eta^4\text{-}Sn_9)]^{3-}$ (*M*: Cu, Au) are analogous to (a). Colour code: Sn (bright blue), Ag (red), N (dark blue), C (black).

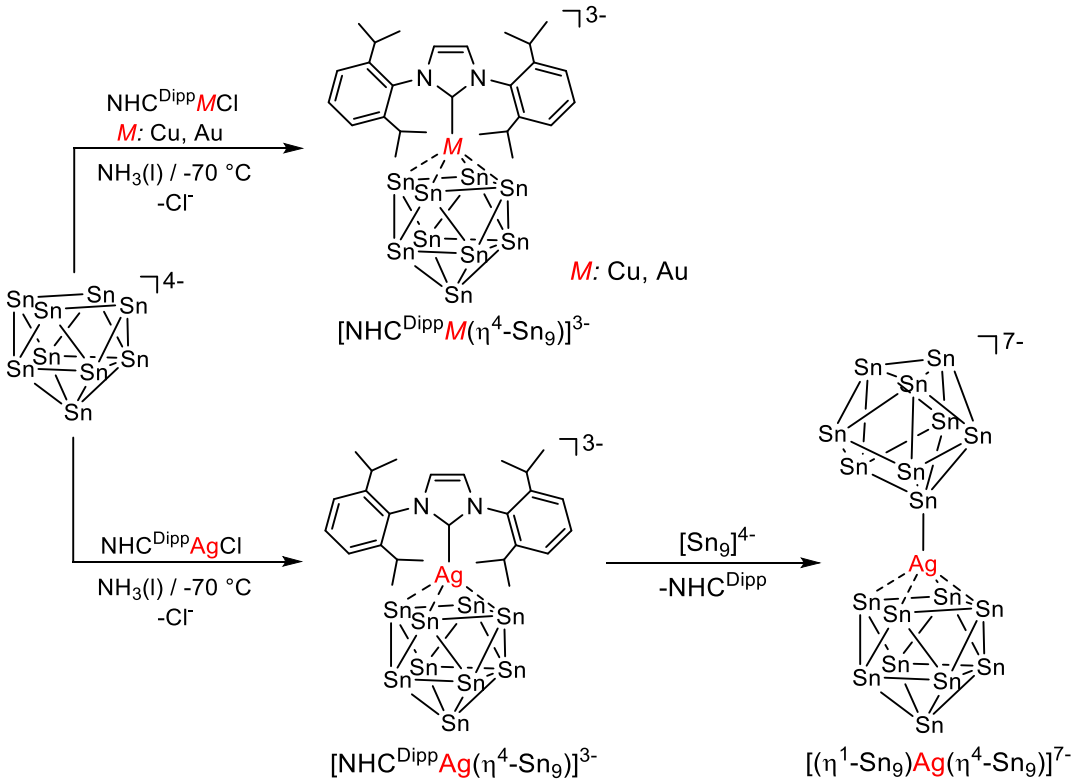

Scheme 3.3: Reactivity of $[Sn_9]^{4-}$ clusters towards $NHC^{Dipp}MCl$ (*M*: Cu, Ag, Au) at low temperature in $NH_3(l)$. Exclusively for $[NHC^{Dipp}Ag(\eta^4\text{-}Sn_9)]^{3-}$ a cleavage of the *M*-NHC bond occurs under formation of the large intermetalloid species $[(\eta^4\text{-}Sn_9)Ag(\eta^1\text{-}Sn_9)]^{7-}$. By contrast, the respective copper- and gold-NHC coordinated species $[NHC^{Dipp}M(\eta^4\text{-}Sn_9)]^{3-}$ (*M*: Cu, Au) are stable at low temperature.

Comparing the polyanions isolated within this work to previously reported intermetalloids $[Cu@Sn_9]^{3-}$ and $[Ag(Sn_9\text{-}Sn_9)]^{5-}$, consisting of $[Sn_9]$ clusters and coinage metal cations, shows the impact of low temperature synthesis and the application of coinage metal NHC complexes as organometallic precursors.[10, 30, 31] $[Cu@Sn_9]^{3-}$ was obtained by reaction of K_4Sn_9 or $K_{12}Sn_{17}$ with mesitylcopper (CuMes) at room temperature or at -70 °C, which reveals the lability of the Cu-Mes bond.[10, 30] By contrast, the more stable Cu-NHC bond allows for the isolation of $[NHC^{Dipp}Cu(\eta^4\text{-}Sn_9)]^{3-}$, which might represent a potential intermediate species on the way to $[Cu@Sn_9]^{3-}$ by cleavage of the Cu-NHC bond and migration of the Cu^+ cation into the $[Sn_9]^{4-}$ core. Moreover, the Ag^+ stabilized $[Sn_9]^{3-}$ dimer $[Ag(Sn_9\text{-}Sn_9)]^{5-}$ (originally obtained by reaction of K_4Sn_9 with mesitylsilver in ethylenediamine) might be obtained by partial oxidation of $[(\eta^4\text{-}Sn_9)Ag(\eta^1\text{-}Sn_9)]^{7-}$ containing $[Sn_9]^{4-}$ clusters.[31] Therefore, the species isolated within this work might contribute to the better understanding of the relations between different intermetalloid species containing $[Sn_9]$ clusters. Relations and potential relations between intermetalloids obtained by reactions of K_4Sn_9 with various transition metal complexes in solution are summarized in Scheme 3.4.

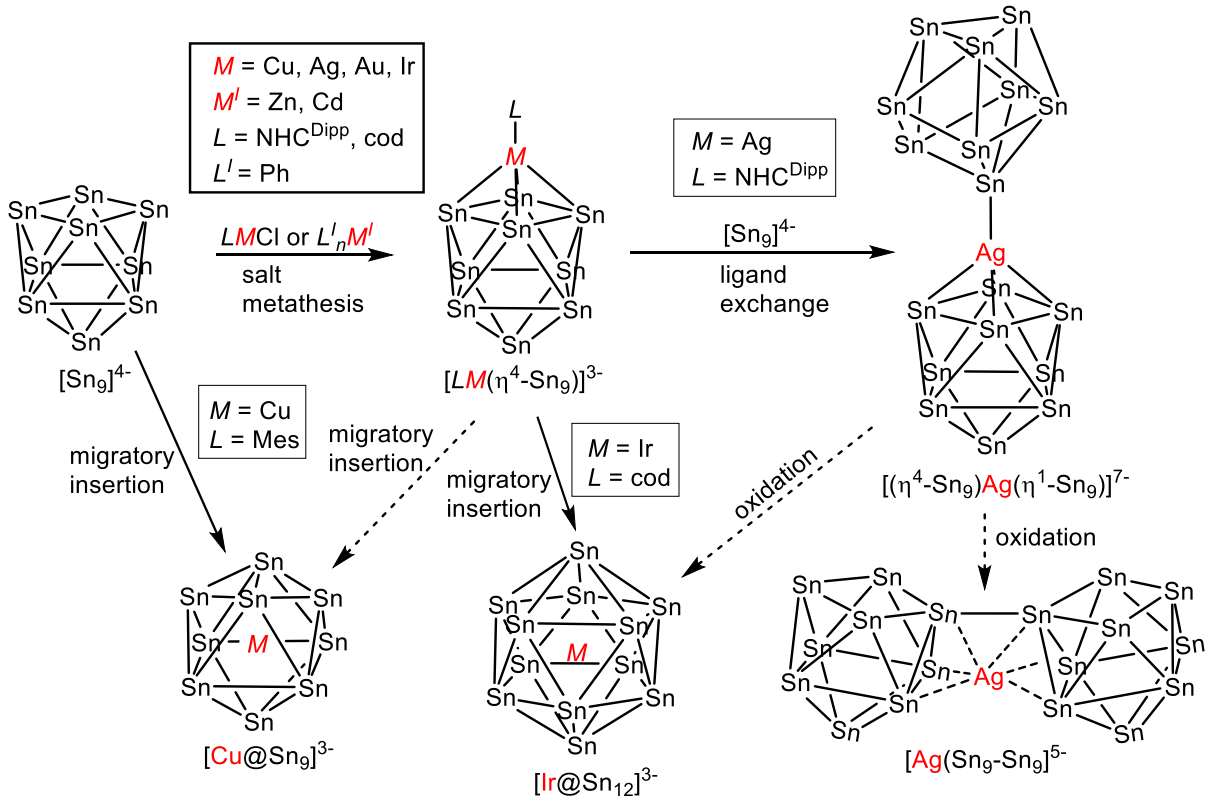

Scheme 3.4: Relation between different intermetalloid anions containing stannide *Zintl* clusters. $[NHC^{Dipp}M(\eta^4\text{-}Sn_9)]^{3-}$ (*M*: Cu, Ag, Au) and $[(\eta^4\text{-}Sn_9)Ag(\eta^1\text{-}Sn_9)]^{7-}$ were isolated in the course of this thesis, whereas the other species have been previously reported. $[(cod)Ir(\eta^4\text{-}Sn_9)]^{3-}$,[12, 32] $[Ph\text{-}M(\eta^4\text{-}Sn_9)]^{3-}$ (*M*: Zn, Cd),[6, 33] $[Cu@Sn_9]^{3-}$,[10, 30] $[Ir@Sn_{12}]^{3-}$ [12] and $[Ag(Sn_9\text{-}Sn_9)]^{5-}$.[31] Dashed arrows represent feasible reaction paths, which are however not experimentally proven yet.

Summary

The investigations on the reactivity of $A_{12}Si_{17}$ (*A*: alkali metal) and K_4Sn_9 towards the coinage metal NHC complexes NHC-*M*-Cl have proven that the latter are suitable precursors for the introduction of positively charged $[NHC^{Dipp}M]^+$ (*M*: Cu, Ag, Au) fragments to the $[E_9]^{4-}$ (*E*: Si, Sn) clusters. The coinage metal NHC fragments coordinate the $[E_9]^{4-}$ (*E*: Si, Sn) clusters *via* their open square plane in a η^4-coordination mode. In this context, the synthesis of the novel silicide complex $[NHC^{Dipp}Cu(\eta^4\text{-}Si_9)]^{3-}$ is especially interesting, since it represents only the third example for a transition metal coordinated $[Si_9]^{4-}$ cluster. The novel species was successfully transferred to solvents different from $NH_3(l)$ (due to enhanced solubility), however it is not stable at room temperature.

Moreover, the stannide complexes $[NHC^{Dipp}M(\eta^4\text{-}Sn_9)]^{3-}$ (*M*: Cu, Ag, Au) might represent intermediate species on the way to novel intermetalloids, and the isolation of $[NHC^{Dipp}Ag(\eta^4\text{-}Sn_9)]^{3-}$ and $[(\eta^4\text{-}Sn_9)Ag(\eta^1\text{-}Sn_9)]^{7-}$ from the same reaction mixture already gave insights into the step-by-step formation of large intermetalloids in solution.

3.1.2.2 Reactions of $[Ge_9\{Si\mathit{R}_3\}_3]^-$ (*R*: TMS, ^{i}Bu, ^{i}Pr) and $[Ge_9\{Si(TMS)_3\}_2]^{2-}$ Clusters with Coinage Metal NHC Complexes

see chapter 5.3	F. S. Geitner, T. F. Fässler, *Eur. J. Inorg. Chem.* **2016**, 2688.
see chapter 5.4	L. S. Schiegerl, F. S. Geitner, C. Fischer, W. Klein, T. F. Fässler, *Z. Anorg. Allg. Chem.* **2016**, *642*, 1419.
see chapter 5.5	F. S. Geitner, M. A. Giebel, A. Pöthig, T. F. Fässler, *Molecules* **2017**, *22*, 1204.

Besides the reactions of bare $[E_9]^{4-}$ (*E*: Si, Sn) clusters with NHC-*M*-Cl (*M*: Cu, Ag, Au) in NH_3(l), which have been discussed in chapter 3.1.2.1, we also conducted investigations on the reactivity of the coinage metal NHC complexes towards silylated $[Ge_9]$ clusters, aiming for the synthesis of neutral $[Ge_9]$ cluster compounds. In contrast to the reactions with the bare $[E_9]^{4-}$ (*E*: Si, Sn) clusters, these reactions were carried out in acetonitrile or thf solution at room temperature.

Reactions of the tris-silylated $[Ge_9]$ clusters $[Ge_9\{Si\mathit{R}_3\}_3]^-$ (*R*: TMS, ^{i}Bu, ^{i}Pr) or the bis-silylated species $[Ge_9\{Si(TMS)_3\}_2]^{2-}$ with the coinage metal NHC complexes $NHC^{Dipp}\mathit{M}Cl$ (*M*: Cu, Ag, Au) yielded a series of neutral $[Ge_9]$ cluster coinage metal NHC compounds $[NHC^{Dipp}\mathit{M}(\eta^3\text{-}Ge_9\{Si(TMS)_3\}_3)]$ (*M*: Cu, Ag, Au), $[NHC^{Dipp}Cu(\eta^3\text{-}Ge_9\{Si\mathit{R}_3\}_3)]$ (*R*: ^{i}Bu, ^{i}Pr) or $[(NHC^{Dipp}\mathit{M})_2(\eta^3,\eta^3\text{-}Ge_9\{Si(TMS)_3\}_2)]$ (*M*: Cu, Ag, Au). The reactivity of the coinage metal NHC complexes towards the variously silylated $[Ge_9]$ clusters is summarized in Table 3.1 and Scheme 3.5.

Table 3.1: Overview on reactivity of $NHC^{Dipp}\mathit{M}Cl$ (*M*: Cu, Ag, Au) towards variously siylated $[Ge_9]$ clusters.

	$NHC^{Dipp}CuCl$	$NHC^{Dipp}AgCl$	$NHC^{Dipp}AuCl$
$[Ge_9\{Si(TMS)_3\}_3]^-$	$[NHC^{Dipp}Cu(Ge_9\mathit{R}_3)]$	$[NHC^{Dipp}Ag(Ge_9\mathit{R}_3)]$	$[NHC^{Dipp}Au(Ge_9\mathit{R}_3)]$
$[Ge_9\{Si(^i Bu)_3\}_3]^-$	$[NHC^{Dipp}Cu(Ge_9\mathit{R}_3)]$	decomposition	decomposition
$[Ge_9\{Si(^i Pr)_3\}_3]^-$	$[NHC^{Dipp}Cu(Ge_9\mathit{R}_3)]$	decomposition	decomposition
$[Ge_9\{Si(TMS)_3\}_2]^{2-}$	$[(NHC^{Dipp}Cu)_2(Ge_9\mathit{R}_2)]$	$[(NHC^{Dipp}Ag)_2(Ge_9\mathit{R}_2)]$	$[(NHC^{Dipp}Au)_2(Ge_9\mathit{R}_2)]$

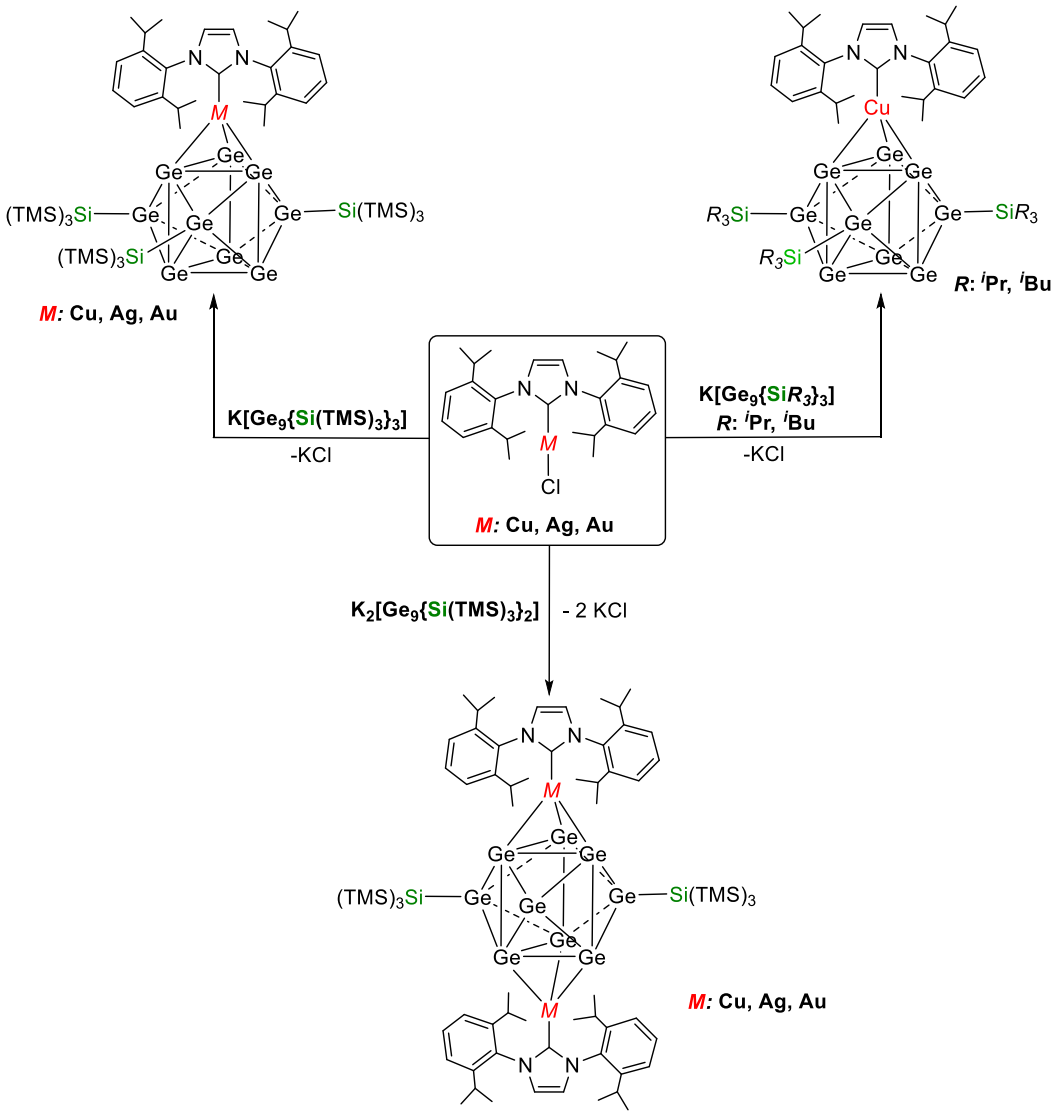

Scheme 3.5: Overview on reactivity of NHC^{Dipp}*M*Cl (*M*: Cu, Ag, Au) towards variously silylated [Ge$_9$] clusters.

Reactions of [Ge$_9${Si*R*$_3$}$_3$]$^-$ (*R*: TMS, ^{i}Bu, ^{i}Pr) with NHC^{Dipp}*M*Cl (*M*: Cu, Ag, Au)

Reactions between the tris-silylated [Ge$_9$] clusters and the coinage metal NHC complexes NHC^{Dipp}*M*Cl (*M*: Cu, Ag, Au; Dipp: 2,6-di-isopropylphenyl) were conducted by dropwise addition of acetonitrile solutions of the respective coinage metal NHC complexes to deep red solutions of [Ge$_9${Si*R*$_3$}$_3$]$^-$ (*R*: TMS, ^{i}Bu, ^{i}Pr) in acetonitrile. In most cases this procedure led to the immediate precipitation of the neutral product species (yellow or orange solids) from the reaction mixtures. In the case of [Ge$_9${Si(TMS)$_3$}$_3$]$^-$, reactions with all coinage metal NHC complexes were successful yielding [NHC^{Dipp}*M*(η^3-Ge$_9${Si(TMS)$_3$}$_3$)] (*M*: Cu, Ag, Au). By contrast, for [Ge$_9${Si*R*$_3$}$_3$]$^-$ (*R*: ^{i}Pr, ^{i}Bu), bearing smaller silyl groups at the [Ge$_9$] core, exclusively reactions with the respective copper NHC complex yielded the desired product compounds [NHC^{Dipp}Cu(η^3-Ge$_9${Si*R*$_3$}$_3$)] (*R*: ^{i}Bu, ^{i}Pr), whereas reactions with NHC^{Dipp}*M*Cl (*M*: Ag, Au) resulted in the decomposition of the [Ge$_9$] cluster species. This observation can be explained by the decreased shielding of the [Ge$_9$] cluster core through the silyl substituents, resulting in

enhanced lability of the [Ge_9] cluster species. Moreover, the smaller silyl substituents can easily dissociate from the [Ge_9] core, which also affects the stability of these species.[24]

The purification of the obtained neutral [Ge_9] cluster coinage metal NHC complexes occurred by re-crystallization from toluene solution at -40 °C and the isolated products were characterized by means of NMR spectroscopy, electrospray ionization mass spectrometry, elemental analysis and single crystal X-ray diffraction.

The [Ge_9] cluster cores in the isolated species reveal the shape of tricapped trigonal prims, with the silyl groups being attached at the capping Ge atoms. The positively charged coinage metal NHC fragments [$NHC^{Dipp}M$]$^+$ coordinate the tris-silylated clusters [Ge_9{SiR_3}$_3$]$^-$ (*R*: TMS, ^{i}Bu, ^{i}Pr) through one of the trigonal bases of the prism in a η^3-cooridnation mode, which is in accordance to previously reported interactions between coinage metal cations or fragments of coinage metal complexes and silylated [Ge_9] cluster (Figure 3.3).[22, 24, 34-37]

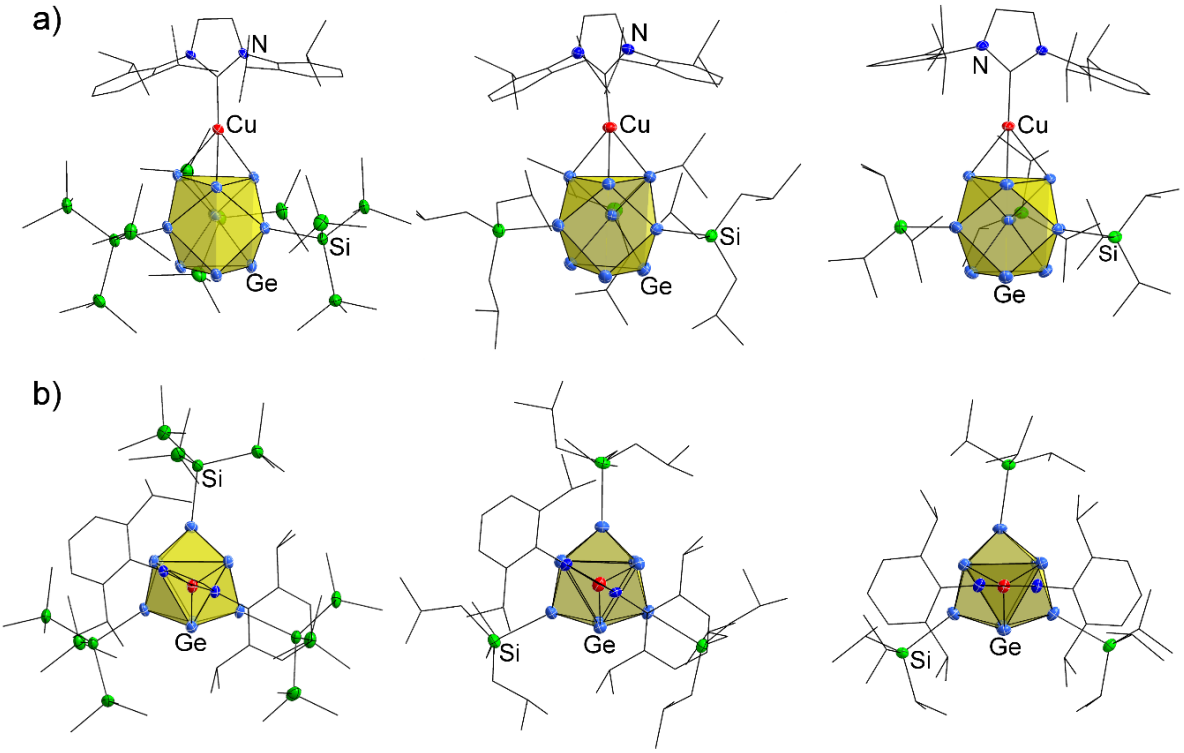

Figure 3.3: Molecular structures of the neutral [Ge_9] cluster copper NHC complexes [$NHC^{Dipp}Cu(\eta^3$-Ge_9{SiR_3}$_3$)] (*R*: TMS, left; ^{i}Bu, middle; ^{i}Pr, right). All ellipsoids are shown at a 50 % probability level. For clarity, carbon atoms are represented as black wire sticks and protons as well as co-crystallized solvent molecules are omitted. a) Coordination of the [Ge_9] clusters by [$NHC^{Dipp}Cu$]$^+$ through trigonal prism bases in a η^3-coordination mode. b) Variation in the orientation of the NHC^{Dipp} ligands towards the silyl groups of the [Ge_9] clusters. Colour code: Ge (bright blue), Si (green), Cu (red), N (dark blue), C (black).

The orientation of the NHC^{Dipp} ligands towards the silyl groups of the [Ge_9] clusters slightly differs in [$NHC^{Dipp}Cu(\eta^3\text{-}Ge_9\{SiR_3\}_3)$] [*R*: TMS (**A**), ^{i}Bu (**B**), ^{i}Pr (**C**)] which might be induced by the different bulkiness of the silyl groups (Figure 3.3). The Cu-Ge distances in all three neutral [Ge_9] cluster copper NHC compounds are similar, adapting mean values of d_{mean}(Cu-Ge): 2.5263(9) Å (**A**), d_{mean}(Cu-Ge): 2.5146(6) Å (**B**) or d_{mean}(Cu-Ge): 2.5328(9) Å (**C**). However, the observed distances are elongated in comparison to the respective Cu-Ge distances occurring in the $[^iPr_3PCu]^+$ or $[Ph_3PCu]^+$ fragment coordinated $[Ge_9\{Si(TMS)_3\}_3]^-$ species $[^iPr_3PCu(\eta^3\text{-}Ge_9\{Si(TMS)_3\}_3)]$ (**D**) and $[Cu(\eta^3\text{-}Ge_9\{Si(TMS)_3\}_3)_2\text{-}CuPPh_3]$ (**E**), revealing mean Cu-Ge distances of d_{mean}(Cu-Ge): 2.484(1) Å (**D**) and d_{mean}(Cu-Ge): 2.399(1) Å (**E**), respectively.[24, 37] Due to the significant difference between the Cu-Ge distances in the $[R_3PCu]^+$ (*R*: Ph, *i*Pr) coordinated [Ge_9] cluster species it is not completely clear whether electronic or steric factors are responsible for the observed variation of the Cu-Ge distances. The Cu-Ge bonding distances in compounds **A**-**E** are summarized in Table 3.2.

Table 3.2: Summary of Cu-Ge distances observed in neutral compounds **A**-**E**.

distance [Å]	**A**	**B**	**C**	**D**[24]	**E**[37]
d_1(Cu-Ge)	2.4943(9)	2.4911(6)	2.4914(8)	2.461(1)	2.365(1)
d_2(Cu-Ge)	2.5188(9)	2.4933(6)	2.541(1)	2.488(1)	2.409(1)
d_3(Cu-Ge)	2.5660(9)	2.5594(6)	2.5661(8)	2.503(1)	2.424(1)
d_{mean}(Cu-Ge)	2.5263(9)	2.5146(6)	2.5328(9)	2.484(1)	2.399(1)

Furthermore, the stability of the synthesized neutral [Ge_9] cluster coinage metal NHC complexes in solution was investigated by carrying out time dependent NMR examinations in thf-d_8. Whereas $[NHC^{Dipp}M(\eta^3\text{-}Ge_9\{Si(TMS)_3\}_3)]$ (*M*: Cu, Au) and $[NHC^{Dipp}Cu(\eta^3\text{-}Ge_9\{SiR_3\}_3)]$ (*R*: ^{i}Bu, ^{i}Pr) were stable for two weeks, in experiments conducted with $[NHC^{Dipp}Ag(\eta^3\text{-}Ge_9\{Si(TMS)_3\}_3)]$, Ag-NHC bond cleavage was observed (in accordance with the relative lability of the Ag-NHC bond), resulting in the complete consumption of the original species after one week.[29] The formed species was identified as $[(NHC^{Dipp})_2Ag]^+[Ag(\eta^3\text{-}Ge_9\{Si(TMS)_3\}_3)_2]^-$, consisting of a cationic silver bis-NHC moiety and an anionic Ag^+ bridged [Ge_9] cluster dimer. Potential reaction paths towards the obtained species are presented in Scheme 3.6. The dimeric Ag^+ bridged [Ge_9] cluster anion had previously been obtained by reaction of $[Ge_9\{Si(TMS)_3\}_3]^-$ with $[Ag\{Al(OC_4F_9)_4\}]$.[34] In contrast to the varying coordination of the two $[Sn_9]^{4-}$ cages to Ag^+ in $[(\eta^4\text{-}Sn_9)Ag(\eta^1\text{-}Sn_9)]^{7-}$ (chapter 3.1.2.1), in $[Ag(\eta^3\text{-}Ge_9\{Si(TMS)_3\}_3)_2]^-$ both *Zintl* clusters coordinate to Ag^+ with triangular Ge faces.

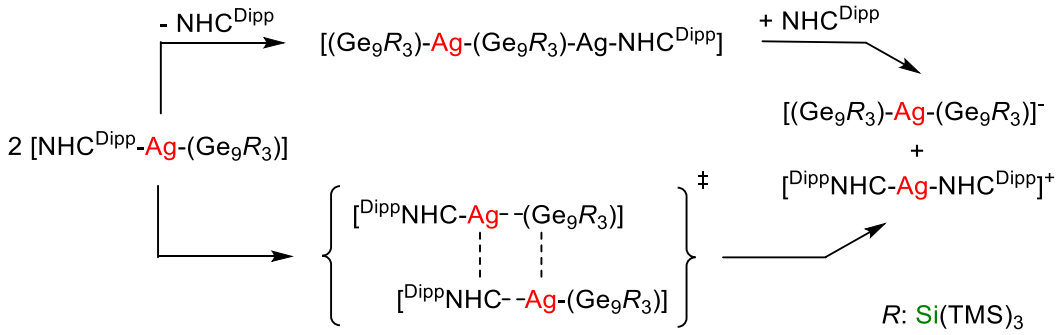

Scheme 3.6: Potential pathways for the rearrangement of $[NHC^{Dipp}Ag(\eta^3\text{-}Ge_9\{Si(TMS)_3\}_3)]$ to $[(NHC^{Dipp})_2Ag]^+[Ag(\eta^3\text{-}Ge_9\{Si(TMS)_3\}_3)_2]^-$ in thf solution at room temperature.

Reactions of $[Ge_9\{Si(TMS)_3\}_2]^{2-}$ with $NHC^{Dipp}MCl$ (*M*: Cu, Ag, Au)

Reactions of the bis-silylated [Ge_9] cluster and $NHC^{Dipp}MCl$ (*M*: Cu, Ag, Au) were carried out by dropwise addition of acetonitrile solutions of the respective coinage metal complex (2 equiv.) to deep red solutions of $[Ge_9\{Si(TMS)_3\}_2]^{2-}$ (1 equiv.) in acetonitrile, resulting in the immediate precipitation of the neutral product species $[(NHC^{Dipp}M)_2(\eta^3,\eta^3\text{-}Ge_9\{Si(TMS)_3\}_2)]$ (*M*: Cu, Ag, Au) as brown solids from the reaction mixtures. The novel compounds were characterized by means of NMR spectroscopy and ESI-MS. Moreover, re-crystallization of $[(NHC^{Dipp}Cu)_2(\eta^3,\eta^3\text{-}Ge_9\{Si(TMS)_3\}_2)]$ from toluene solution gave crystals suitable for single crystal X-ray diffraction. In $[(NHC^{Dipp}Cu)_2(\eta^3,\eta^3\text{-}Ge_9\{Si(TMS)_3\}_2)]$ the two $[NHC^{Dipp}Cu]^+$ moieties coordinate the [Ge_9] cluster (distorted tricapped trigonal prism; C_{2v} symmetry) *via* the two trigonal prism bases in a η^3-coordination mode, and the mean Cu-Ge distances adapt values of d_{mean}(Cu-Ge): 2.513 Å and 2.509 Å (Figure 3.4). Therefore, the observed coordination mode and bond lengths are in accordance with the interactions found in the respective coinage metal complexes of $[Ge_9\{SiR_3\}_3]^-$ (*R*: TMS, ^{i}Bu, ^{i}Pr; Table 3.2). The NHC^{Dipp} ligands adopt eclipsing orientations and are staggered with respect to the silyl groups of the [Ge_9] cluster (Figure 3.4). The isolated species $[(NHC^{Dipp}M)_2(\eta^3,\eta^3\text{-}Ge_9\{Si(TMS)_3\}_2)]$ (*M*: Cu, Ag, Au) represent the first transition metal complexes of $[Ge_9\{Si(TMS)_3\}_2]^{2-}$ and can also be regarded as the first dinuclear coinage metal complexes comprising a bridging [Ge_9] cluster moiety. Further dinuclear Cu^+-complexes with bridging Group 14 element *Zintl* clusters had previously been found in $[(MesCu)_3(\eta^3,\eta^3\text{-}E_4)]^{4-}$ (*E*: Si,[8] Ge,[38] Si/Ge[39]).

Interestingly, the attachment of only one $[NHC^{Dipp}M]^+$ (*M*: Cu, Ag, Au) moiety at the bis-silylated [Ge_9] cluster is not easily achievable. *In-situ* ^{1}H NMR monitoring of reactions of equimolar amounts of the coinage metal NHC complexes and the bis-silylated [Ge_9] cluster in thf-d_8 revealed exclusively the formation of the twofold $[NHC^{Dipp}M]^+$ (*M*: Cu, Ag, Au) coordinated [Ge_9] species besides unreacted $[Ge_9\{Si(TMS)_3\}_2]^{2-}$.

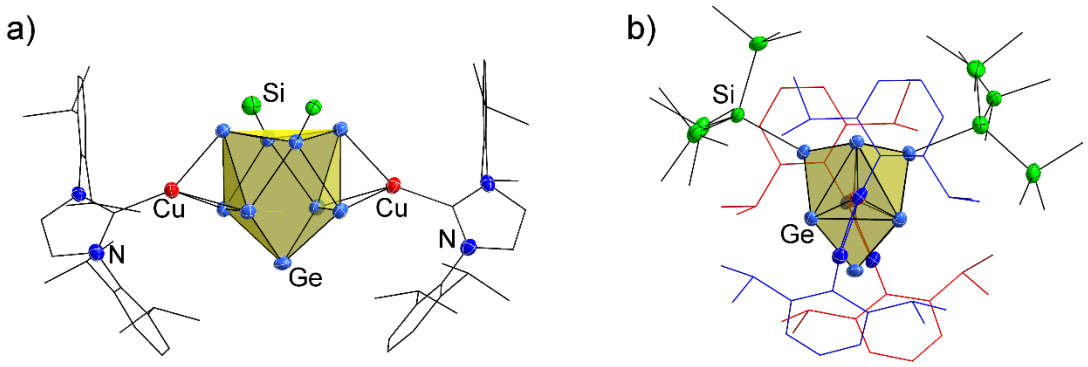

Figure 3.4: Molecular structure of the neutral [Ge_9] cluster copper NHC compound [$(NHC^{Dipp}Cu)_2(\eta^3,\eta^3\text{-}Ge_9\{Si(TMS)_3\}_2)$]. All ellipsoids are shown at a 50 % probability level. For clarity, carbon atoms are represented as black wire sticks and protons as well as co-crystallized solvent molecules are omitted. a) The coordination of the two [$NHC^{Dipp}Cu]^+$ fragments to opposite trigonal faces of [Ge_9] in a η^3-coordination mode. For clarity, TMS groups of the silyl substituents are omitted. b) Top view on the structure revealing the orientation of the two NHC^{Dipp} ligands towards each other and the silyl groups of the [Ge_9] cluster. NHC^{Dipp} ligand in the front is shown in blue whereas the NHC^{Dipp} ligand in the back is presented in red. Colour code: Ge (bright blue), Si (green), Cu (red), N (dark blue).

Summary

Investigations on the reactivity of silylated [Ge_9] clusters towards the coinage metal NHC complexes NHC^{Dipp}*M*Cl (*M*: Cu, Ag, Au) revealed that the latter complexes are also suitable precursors for the attachment of [$NHC^{Dipp}M]^+$ (*M*: Cu, Ag, Au) moieties at [$Ge_9\{SiR_3\}_3]^-$ (*R*: TMS, ^{i}Bu, ^{i}Pr) or [$Ge_9\{Si(TMS)_3\}_2]^{2-}$. In the resulting neutral compounds interactions between [$NHC^{Dipp}M]^+$ (*M*: Cu, Ag, Au) and triangular Ge faces occur (η^3-coordination mode). The [Ge_9] cluster coinage metal NHC compounds are soluble in standard solvents and are long time stable in solution (two weeks). However, for the silver compound [$NHC^{Dipp}Ag(\eta^3\text{-}Ge_9\{Si(TMS)_3\}_3)$] a transformation reaction under cleavage of the Ag-NHC bond was observed, yielding the Ag^+ bridged dimeric species [$Ag(\eta^3\text{-}Ge_9\{Si(TMS)_3\}_3)_2]^-$. In contrast to the Ag^+ bridged stannide dimer [$(\eta^4\text{-}Sn_9)Ag(\eta^1\text{-}Sn_9)]^{7-}$ (varying coordination; chapter 3.1.2.1), in this dimeric species both [Ge_9] clusters coordinate Ag^+ with triangular cluster faces. Moreover, the twofold [$NHC^{Dipp}M]^+$ coordinated species [$(NHC^{Dipp}M)_2(\eta^3,\eta^3\text{-}Ge_9\{Si(TMS)_3\}_2)$] (*M*: Cu, Ag, Au) represent the first examples of dinuclear coinage metal complexes comprising a bridging [Ge_9] cluster moiety.

3.1.3 Reactions of $[Ge_9\{Si(TMS)_3\}_n]^{(4-n)-}$ (*n*: 2, 3) with the Early Transition Metal Complex $[Cp_2TiCl]_2$

see chapter 5.6

F. S. Geitner, W. Klein, O. Storcheva, T. Don Tilley, T. F. Fässler, manuscript for publication.

In previous investigations on the reactivity of $[Ge_9\{Si(TMS)_3\}_n]^{(4-n)-}$ (*n*: 2, 3) towards organometallics mainly complexes of late transition metals (Group 10-Group 12) have been considered.[22, 24, 34-37] Moreover, there were sporadic reports in which Group 6 or Group 7 metal complexes were successfully applied.[23, 36, 40] However, the reactivity of earlier transition metal complexes towards the silylated $[Ge_9]$ clusters has not been investigated yet. Generally, reports on successful reactions of the negatively charged Group 14 element *Zintl* clusters with early transition metal complexes are rare. However, the recent isolation of $[Cp_2Ti(NH_3)(\eta^4\text{-}Sn_9)]^{3-}$ from reaction mixtures of K_4Sn_9 and $[Cp_2TiCl]_2$ in NH_3(l) revealed that positively charged $[Cp_2Ti]^+$ fragments can be attached at the nine-atomic Group 14 element *Zintl* clusters.[21] This triggered us to conduct examinations on the reactivity of $[Cp_2TiCl]_2$ towards $[Ge_9\{Si(TMS)_3\}_n]^{(4-n)-}$ (*n*: 2, 3) in order to gather further insights into the reactivity of Group 14 element *Zintl* clusters towards early transition metal complexes. These studies were carried out in the laboratories of Prof. T. Don Tilley at the University of California, Berkeley.

Investigations on the reactivity of $[Ge_9\{Si(TMS)_3\}_n]^{(4-n)-}$ (*n*: 2, 3) towards $[Cp_2TiCl]_2$ yielded the neutral compound $[Cp_2Ti(MeCN)(\eta^1\text{-}Ge_9\{Si(TMS)_3\}_3)]$ and the dimeric species $K_3[Cp_2Ti(\eta^1\text{-}Ge_9\{Si(TMS)_3\}_2)_2]$. In the latter, the two $[Ge_9\{Si(TMS)_3\}_2]^{2-}$ clusters are bridged by the $[Cp_2Ti]^+$ moiety. The reactivity of $[Cp_2TiCl]_2$ towards silylated $[Ge_9]$ clusters is summarized in Scheme 3.7. The two novel Ti(III)-germanide compounds are the first examples for early transition metal complexes of $[Ge_9\{Si(TMS)_3\}_n]^{(4-n)-}$ (*n*: 2, 3) and represent rare examples for molecular complexes comprising Ti-Ge interactions (to date only four further species comprising such interactions have been crystallographically characterized).[41-43] The attachment of the $[Cp_2Ti]^+$ fragments at the $[Ge_9]$ clusters occurs through donor-acceptor interaction between electron lone-pairs situated at Ge vertex atoms and Ti(III) (η^1-coordination mode), which contrasts the typically observed interactions between transition metal fragments or transition metal cations and silylated $[Ge_9]$ clusters (η^3-coordination mode).[22, 24, 34-37] However, this coordination mode is in accordance to the Ti-Sn interactions observed in $[Cp_2Ti(NH_3)(\eta^4\text{-}Sn_9)]^{3-}$.[21] Moreover, similar donor-acceptor interactions occur between the $[Cr(CO)_5]$ fragment and $[Ge_9\{Si(TMS)_3\}_3]^-$ in $[(CO)_5Cr(\eta^1\text{-}Ge_9\{Si(TMS)_3\}_3)]^-$.[23]

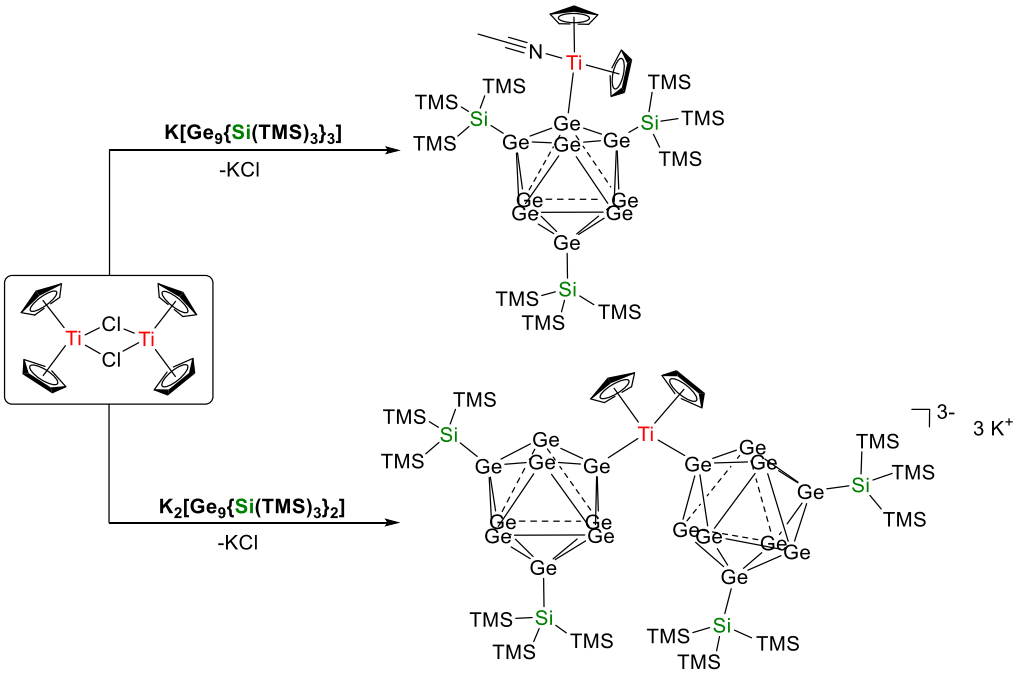

Scheme 3.7: Overview on reactivity of $[Cp_2TiCl]_2$ towards $[Ge_9\{Si(TMS)_3\}_n]^{(4-n)-}$ (*n*: 2, 3).

Synthesis of $[Cp_2Ti(MeCN)(\eta^1\text{-}Ge_9\{Si(TMS)_3\}_3)]$

The synthesis of the neutral compound $[Cp_2Ti(MeCN)(\eta^1\text{-}Ge_9\{Si(TMS)_3\}_3)]$ was achieved by reaction of $K[Ge_9\{Si(TMS)_3\}_3]$ with $[Cp_2TiCl]_2$ in toluene solution at room temperature. The product species was isolated by re-crystallization from toluene solution, yielding dark orange crystals suitable for single crystal X-ray diffraction. In $[Cp_2Ti(MeCN)(\eta^1\text{-}Ge_9\{Si(TMS)_3\}_3)]$, the $[Ge_9]$ cluster reveals the shape of a distorted tricapped trigonal prism (silyl groups are attached at capping Ge atoms) and coordinates the $[Cp_2Ti(MeCN)]^+$ fragment through an electron lone-pair situated at a Ge atom in one of its trigonal bases under formation of donor-acceptor interactions (Figure 3.5). This results in a heavily distorted tetrahedral coordination of Ti(III) by its four ligands. The analytical purity of $[Cp_2Ti(MeCN)(\eta^1\text{-}Ge_9\{Si(TMS)_3\}_3)]$ was proven by elemental analysis and in EPR spectroscopic examinations its g-factor was determined to be g_{iso} = 1.967.

Synthesis of $K_3[Cp_2Ti(\eta^1\text{-}Ge_9\{Si(TMS)_3\}_2)_2]$

The synthesis of the dimeric species $K_3[Cp_2Ti(\eta^1\text{-}Ge_9\{Si(TMS)_3\}_2)_2]$ was achieved by reacting $K_2[Ge_9\{Si(TMS)_3\}_2]$ with $[Cp_2TiCl]_2$ in thf solution at room temperature. Recrystallization from toluene solution yielded dark-green crystals of the product compound suitable for single crystal X-ray diffraction. The tri-anion $[Cp_2Ti(\eta^1\text{-}Ge_9\{Si(TMS)_3\}_2)_2]^{3-}$ consists of a $[Cp_2Ti]^+$ fragment which is coordinated by two $[Ge_9\{Si(TMS)_3\}_2]^{2-}$ clusters (distorted tricapped trigonal prisms with silyl groups attached at two of the capping atoms) with their third capping Ge atom under

formation of donor-acceptor interactions between the electron lone-pairs situated at the Ge atoms and Ti(III) (Figure 3.5). Therefore, the tri-anion can either be described as Ti(III) complex bearing two germanide cluster ligands [with heavily distorted tetrahedral coordination sphere of Ti(III)] or as $[Cp_2Ti]^+$ bridged $[Ge_9\{Si(TMS)_3\}_2]^{2-}$ dimer. The analytical purity of $K_3[Cp_2Ti(\eta^1\text{-}Ge_9\{Si(TMS)_3\}_2)_2]$ was proven by elemental analysis and in EPR spectroscopic examinations its g-factor was determined to be g_{iso} = 1.968.

Summary

The isolations of $[Cp_2Ti(MeCN)(\eta^1\text{-}Ge_9\{Si(TMS)_3\}_3)]$ and $K_3[Cp_2Ti(\eta^1\text{-}Ge_9\{Si(TMS)_3\}_2)_2]$ reveal that the early transition metal complex $[Cp_2TiCl]_2$ is a suitable precursor for the attachment of positively charged $[Cp_2Ti]^+$ fragments at silylated $[Ge_9]$ clusters. The $[Ge_9]$ clusters approach Ti(III) with single Ge vertex atoms under formation of donor-acceptor interactions (η^1-coordination mode), which contrasts the typically observed interactions between transition metal fragments and silylated $[Ge_9]$ clusters (η^3-coordination mode). This bonding mode allows for the linkage of two $[Ge_9]$ clusters without cleavage of a Cp ligand in $[Cp_2Ti(\eta^1\text{-}Ge_9\{Si(TMS)_3\}_2)_2]^{3-}$. The substitution of the Cp ligands in this species by $[Ge_9]$ clusters might allow for the formation of a three-dimensional network.

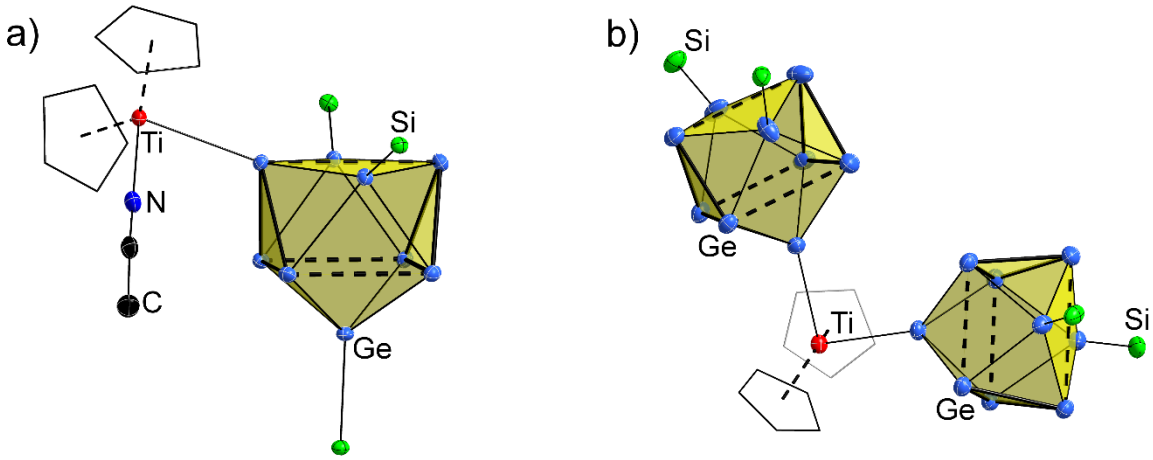

Figure 3.5: Molecular structures of $[Cp_2Ti(MeCN)(\eta^1\text{-}Ge_9\{Si(TMS)_3\}_3)]$ (a) and $[Cp_2Ti(\eta^1\text{-}Ge_9\{Si(TMS)_3\}_2)_2]^{3-}$ (b). Ellipsoids are shown at a 50 % probability level. The trigonal prism bases of the $[Ge_9]$ clusters are emphasized by thick bonds and prism heights are indicated by dashed lines. For clarity, TMS groups of hypersilyl substituents are omitted and carbon atoms (except the MeCN molecule) are presented as black or grey wire sticks. Colour code: Ge (bright blue), Si (green), Ti (red), N (dark blue), C (black or grey).

3.2 Stabilization and Functionalization of Nine-Atomic Germanide *Zintl* Clusters with Main-Group Element Moieties

3.2.1 Review of Relevant Literature

Besides the decoration of $[E_9]^{4-}$ (*E*: Si, Ge, Sn) clusters with organometallic fragments by reaction with the respective transition metal precursors, the attachment of main-group element moieties at the nine-atomic Group 14 element clusters represents another interesting approach with respect to the stabilization, functionalization and linkage of the cages.

The first successful attachment of a main-group element moiety at $[Ge_9]^{4-}$ was achieved by Sevov *et al*. upon reaction of $BiPh_3$ with K_4Ge_9 in ethylenediamine, yielding the twofold substituted $[Ge_9]$ cluster $[Ph_2Bi\text{-}Ge_9\text{-}BiPh_2]^{2-}$.[44] The isolation of this species was followed by reports on the successful introduction of a series of Group-14-element-based substituents (e.g. in $[Ph_3E\text{-}Ge_9\text{-}EPh_3]^{2-}$, *E*: Ge, Sn),[45] In-based moieties (e.g. in $[Ph_3In\text{-}Ge_9\text{-}InPh_3]^{4-}$)[46] or Sb-based groups (e.g. in $[Ph\text{-}Ge_9\text{-}SbPh_2]^{2-}$) to the $[Ge_9]^{4-}$ clusters.[47] In these species interactions between the $[Ge_9]$ clusters and the main-group element substituents mainly occur *via* single *exo* bonds between Ge vertex atoms and the respective main-group element moieties (in the case of stannyl substituents sometimes interactions of the Sn atom with more than one Ge atom were observed, which can be described as multi-centre-2-electron bonds).[48] However, the number of main-group element moieties attached to $[Ge_9]^{4-}$ was limited to two substituents. The first threefold main-group element decorated $[Ge_9]$ cluster $[Ge_9\{Si(TMS)_3\}_3]^-$ was initially obtained by co-condensation techniques, reacting metastable Ge^I-halides and $Li\{Si(TMS)_3\}$.[49] Subsequently, the synthesis of this species was also achieved by heterogenous reactions of solid K_4Ge_9 with $(TMS)_3SiCl$ in acetonitrile, yielding $[Ge_9\{Si(TMS)_3\}_3]^-$ in reasonable yield.[50] In the meantime, a broad range of threefold silyl substituted $[Ge_9]$ clusters $[Ge_9\{SiR_3\}_3]^-$ (*R*: silyl, aryl, alkyl) has been reported,[24, 51-53] and the threefold stannyl group decoration of $[Ge_9]$ was achieved by heterogenous reactions of K_4Ge_9 with R_3SnCl (*R*: ^{i}Pr, Cy).[54, 55] Furthermore, an approach towards the bis-silylated $[Ge_9]$ cluster species $[Ge_9\{Si(TMS)_3\}_2]^{2-}$ was found.[56]

In subsequent reactions of $[Ge_9\{Si(TMS)_3\}_n]^{(4-n)-}$ (*n*: 2, 3) with main-group element compounds or organic reagents the synthesis of neutral species $[Ge_9\{Si(TMS)_3\}_3SnR_3]$ (*R*: Me, Ph, ^{n}Bu),[57, 58] $[Ge_9\{Si(TMS)_3\}_3R]$ (*R*: Et, $CH{=}CH_2$, $(CH_2)_3CH{=}CH_2$),[58, 59] and $[Ge_9\{Si(TMS)_3\}_3C(O)R]$ (*R*: alkyl, aryl),[60] or the mixed-substituted anionic clusters $[Ge_9\{Si(TMS)_3\}_2SiR_2R^I]^-$ (*R*: TMS, R^I: $SiPh_3$; *R*: Ph, R^I: $CH{=}CH_2$ or $(CH_2)_3CH{=}CH_2$) was achieved.[56, 61] However, despite the plethora of reports on the attachment of Group 14 element substituents at $[Ge_9]$, the introduction of further main-group element substituents (from other

main-groups than Group 14) to $[Ge_9]^{4-}$ or $[Ge_9\{Si(TMS)_3\}_2]^{2-}$ by these novel methods has not been reported, yet.

The reactivity of bare $[E_9]^{4-}$ (*E*: Ge, Sn) clusters and silylated $[Ge_9]$ cages towards heavier main-group element compounds and organic reagents is reviewed in more detail in the introductory part of this thesis (chapters 1.3.2.2 and 1.3.2.3).

Within this work we investigated the reactivity of the Group 13 element complexes R_2EBr (*E*: B, Al; *R*: alkyl, aryl, aminoaryl; chapter 3.2.2) and the chlorophosphines RR^{I}PCl (*R*; R^{I}: alkyl, alkenyl, aryl, aminoalkyl; chapter 3.2.3) towards $[Ge_9\{Si(TMS)_3\}_n]^{(4-n)-}$ (*n*: 2, 3) and $[Ge_9]^{4-}$, aiming for novel methods for the stabilization and functionalization of nine-atomic Group 14 element *Zintl* clusters.

3.2.2 Reactions of [Ge$_9$] *Zintl* Clusters with Group 13 Element Compounds

see chapter 5.7

F. S. Geitner, T. F. Fässler, manuscript for publication.

This chapter deals with investigations on the reactivity of [Ge$_9$] *Zintl* clusters towards Group 13 element compounds, which were carried out with respect to the attachment of stabilizing main-group element moieties at [Ge$_9$] clusters. In this context, cyclic diazaborolidines (**A**) or diazaboroles (**B**) are interesting candidates (Scheme 3.8), since these species have previously been applied for the stabilization of a series of In clusters [In$_4$(boryl)$_4$]$^{2-}$, [In$_{19}$(boryl)$_6$] and [In$_{68}$(boryl)$_{12}$] (clusters were obtained by bottom-up synthesis from smaller precursor molecules).[62, 63] Moreover, they are also capable to stabilize further low valent Group 14 element compounds such as acyclic silylenes, germylenes and stannylenes.[64, 65] Therefore, we tested the diazaborolidine [BrBN(Mes)-CH$_2$-CH$_2$-N(Mes)] (**A**), the diazaborole [BrBN(Dipp)-CH=CH-N(Dipp)] (**B**), as well as [Mes$_2$BBr] (**C**) and [^{t}Bu$_2$AlBr]$_2$ (**D**) for their suitability as precursors for the introduction of stabilizing Group 13 element moieties at silylated [Ge$_9$] clusters [Ge$_9${Si(TMS)$_3$}$_n$]$^{(4-n)-}$ (*n*: 2, 3) or at bare [Ge$_9$]$^{4-}$ cages.

Investigations on the reactivity of [Ge$_9${Si(TMS)$_3$}$_2$]$^{2-}$ towards the Group 13 element compounds **A**-**D** yielded a series of anionic mixed-substituted [Ge$_9$] clusters [Ge$_9${Si(TMS)$_3$}$_2$*ER*$_2$]$^-$ (*E*: B, Al; *R*: substituent; **1a**-**4a**), which are summarized in Scheme 3.8.

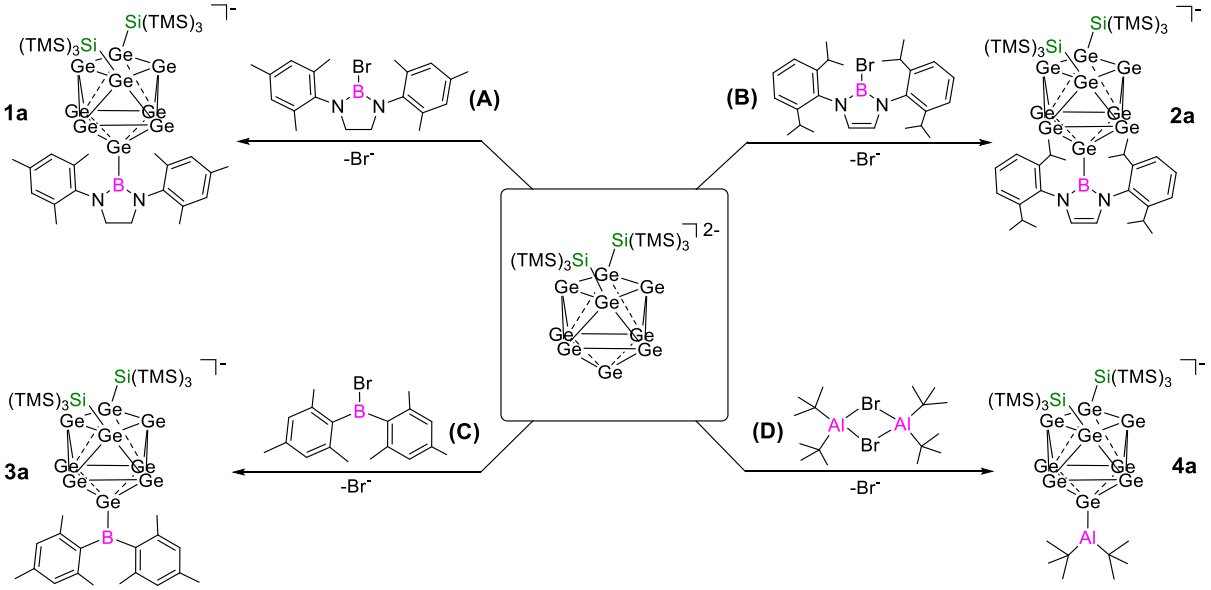

Scheme 3.8: Overview on reactivity of [Ge$_9${Si(TMS)$_3$}$_2$]$^{2-}$ towards Group 13 element compounds **A**-**D**, yielding the mixed-substituted [Ge$_9$] anions **1a**-**4a**. Since **1a**-**4a** could not be crystallographically characterized to date, their structures were proposed to be analogous to similar mixed-substituted [Ge$_9$] cluster species bearing main-group element substituents.[56]

Reactions of $[Ge_9\{Si(TMS)_3\}_n]^{(4-n)-}$ (*n*: 2, 3) with Group 13 Element Compounds

The synthesis of the anions **1a**, **3a** and **4a** (Scheme 3.8) was achieved by stirring mixtures of the reactants in thf solution at room temperature. By contrast, the synthesis of **2a** could not be achieved in thf solution (no reaction at room temperature and formation of $[Ge_9\{Si(TMS)_3\}_3]^-$ as side product at elevated temperature). Therefore, the synthesis of **2a** was conducted in acetonitrile solution at 40 °C. The anions **1a**-**4a** were characterized by means of NMR spectroscopy and electrospray ionization mass spectrometry (ESI-MS), however, crystallographic characterization has not been achieved to date.
By contrast, the syntheses of neutral species in the reactions of **A**-**D** with $[Ge_9\{Si(TMS)_3\}_3]^-$ could not be achieved. Whereas compounds **A**-**C** did not react with the tris-silylated $[Ge_9]$ cluster $[Ge_9\{Si(TMS)_3\}_3]^-$ (probably due to steric crowding), for compound **D** the conversion of the reactants to unknown products was observed.

Reactions of $[Ge_9]^{4-}$ with Group 13 Element Compounds

Investigations on the reactivity of $[Ge_9]^{4-}$ towards compounds **A-D** were carried out by treating solid K_4Ge_9 with an acetonitrile or thf solution of the respective Group 13 element compounds (heterogenous reaction). In ESI-MS investigations of reaction mixtures of compounds **A** or **B** and K_4Ge_9 in acetonitrile, signals that can be assigned to multiple borane-substituted $[Ge_9]$ cluster species were observed (two or three attached groups). However, NMR investigations of the reaction mixtures revealed the presence of several different products in solution. Hence, to date it is not completely clear whether the observed species are also present in solution or if they are formed during the ionization process in the mass spectrometer. By contrast, reactions of K_4Ge_9 with compounds **C** and **D** resulted in the formation of unknown products.

Summary

The Group 13 element compounds **A**-**D** can be applied as precursors for the introduction of main-group element substituents to the bis-silylated $[Ge_9]$ cluster, yielding mixed-substituted species $[Ge_9\{Si(TMS)_3\}_2ER_2]^-$ (*E*: B, Al; *R*: substituent; **1a**-**4a**). However, the exact structure of the obtained anions could not be determined to date. By contrast, the synthesis of neutral $[Ge_9]$ cluster species in reactions of **A**-**D** with $[Ge_9\{Si(TMS)_3\}_3]^-$ could not be achieved (probably due to steric crowding). Regarding reactions with bare $[Ge_9]^{4-}$ clusters, ESI-MS examinations carried out with reaction mixtures of K_4Ge_9 and compounds **A** and **B** indicated the presence of multiple borane-decorated $[Ge_9]$ clusters in the gas phase. However, the respective reaction mixtures contain several different species in low amounts according to NMR spectroscopic investigations.

3.2.3 Phosphine-Functionalization of [Ge_9] *Zintl* Clusters

The attachment of Group 15 element substituents to [Ge_9] clusters is especially interesting with respect to the functionalization of the nonagermanide clusters, since the pentel element moieties can interact with Lewis acidic molecules through their electron lone-pair. In previous investigations the decoration of $[Ge_9]^{4-}$ clusters with Group 15 element moieties has been achieved for the heavy congeners antimony and bismuth by reaction of K_4Ge_9 with EPh_3 (*E*: Sb, Bi) in ethylenediamine, yielding $[Ph_2Sb\text{-}Ge_9\text{-}SbPh_2]^{2-}$, $[Ph_2Sb\text{-}Ge_9\text{-}Ph]^{2-}$, $[Ph_2Sb\text{-}Ge_9\text{-}Ge_9\text{-}SbPh_2]^{4-}$ or $[Ph_2Bi\text{-}Ge_9\text{-}BiPh_2]^{2-}$.[44, 47] By contrast, analogous attempts to attach the respective arsine or phosphine moieties to the [Ge_9] clusters were not successful and the reactions resulted in the partial oxidation of the $[Ge_9]^{4-}$ clusters under formation of oligomeric germanide cluster chains.[47] In general, there are several reports on molecular compounds with Ge-P bonds, comprising [P_4] or $[P_7]^-$ units bearing Ge-based substituents.[66, 67]

Within this work the reactivity of a series of chlorophosphines RR^IPCl (*R*, R^I: alkyl, alkenyl, aryl, aminoalkyl) towards silylated [Ge_9] clusters $[Ge_9\{Si(TMS)_3\}_n]^{(4-n)-}$ (*n*: 2, 3) and bare $[Ge_9]^{4-}$ cages was investigated, aiming for the functionalization of the [Ge_9] clusters with $[PRR^I]^+$ moieties.

3.2.3.1 Phosphine-Functionalization of $[Ge_9\{Si(TMS)_3\}_n]^{(4-n)-}$ (*n*: 2, 3) Clusters

see chapter 5.8	F. S. Geitner, J. V. Dums, T. F. Fässler, *J. Am. Chem. Soc.* **2017**, *139*, 11933.
see chapter 5.9	F. S. Geitner, C. Wallach, T. F. Fässler, *Chem. Eur. J.* **2018**, *24*, 4103.
see chapter 5.10	C. Wallach, F. S. Geitner, T. F. Fässler, manuscript for publication.

Investigations on the reactivity of several chlorophosphines (**A**-**N** in Scheme 3.9 c) towards $[Ge_9\{Si(TMS)_3\}_n]^{(4-n)-}$ (*n*: 2, 3) yielded a broad range of neutral $[Ge_9\{Si(TMS)_3\}_3PRR^I]$ (**1**: *R* = *R*^{I}: ^{i}Pr; **2**: *R* = *R*^{I}: Cy; **3**: *R*: ^{t}Bu, *R*^{I}: $(CH_2)_3CH{=}CH_2$) or anionic $[Ge_9\{Si(TMS)_3\}_2PRR^I]^-$ (**4a**: *R*: ^{t}Bu, *R*^{I}: $(CH_2)_3CH{=}CH_2$; **5a**: *R*: ^{i}Pr, *R*^{I}: ^{t}Bu; **6a**: *R*: ^{t}Bu, *R*^{I}: NEt_2; **7a**: *R* = *R*^{I}: ^{t}Bu; **8a**: *R* = *R*^{I}: 1,1-dimethylpropyl; **9a**: *R* = *R*^{I}: 1-adamantyl; **10a**: *R*: ^{i}Pr, *R*^{I}: N^iPr_2; **11a**: *R*: ^{t}Bu, *R*^{I}: N^iPr_2; **12a**: *R* = *R*^{I}: N^iPr_2; **13a**: *R*: ^{t}Bu, *R*^{I}: Mes; **14a**: *R* = *R*^{I}: *o*-tolyl; **15a**: *R* = *R*^{I}: Mes) mixed-functionalized [Ge_9] clusters (Scheme 3.9 a, b and Scheme 3.10 c). The principle of phosphine-functionalization of [Ge_9] was validated for a series of anionic mixed-functionalized [Ge_9] clusters bearing medium-sized phosphanyl groups (determined by the Tolman cone angle)[68-70] by subsequent reactions with the coinage metal NHC complex $NHC^{Dipp}CuCl$, yielding zwitterionic compounds $[(Ge_9\{Si(TMS)_3\}_2)RR^IP]CuNHC^{Dipp}$ (**4a-CuNHC^{Dipp}**-**9a-CuNHC^{Dipp}**). These species comprise P-Cu interactions between the phosphine moiety attached to [Ge_9] and the Lewis acidic $[NHC^{Dipp}Cu]^+$ fragment (Scheme 3.10 a). By contrast, similar reactions with anionic mixed-functionalized [Ge_9] clusters bearing sterically more demanding phosphanyl groups resulted in [Ge_9] cluster coinage metal NHC complexes $[NHC^{Dipp}Cu(\eta^3\text{-}Ge_9\{Si(TMS)_3\}_2PRR^I)]$ (**10a-CuNHC^{Dipp}**-**15a-CuNHC^{Dipp}**; Scheme 3.10 b). In this case Ge-Cu interactions occur, which reveals the crucial impact of the steric demand of the phosphanyl substituents on the reactivity of the mixed phosphine-functionalized anions **4a**-**15a**. In the latter compounds (**10a-CuNHC^{Dipp}**-**15a-CuNHC^{Dipp}**) the $[NHC^{Dipp}Cu]^+$ fragments bind to the [Ge_9] clusters *via* triangular Ge faces (η^3-cooridination mode), which is in analogy to the Ge-Cu interactions observed in $[NHC^{Dipp}Cu(\eta^3\text{-}Ge_9\{Si(TMS)_3\}_3)]$ (chapter 3.1.2.2).

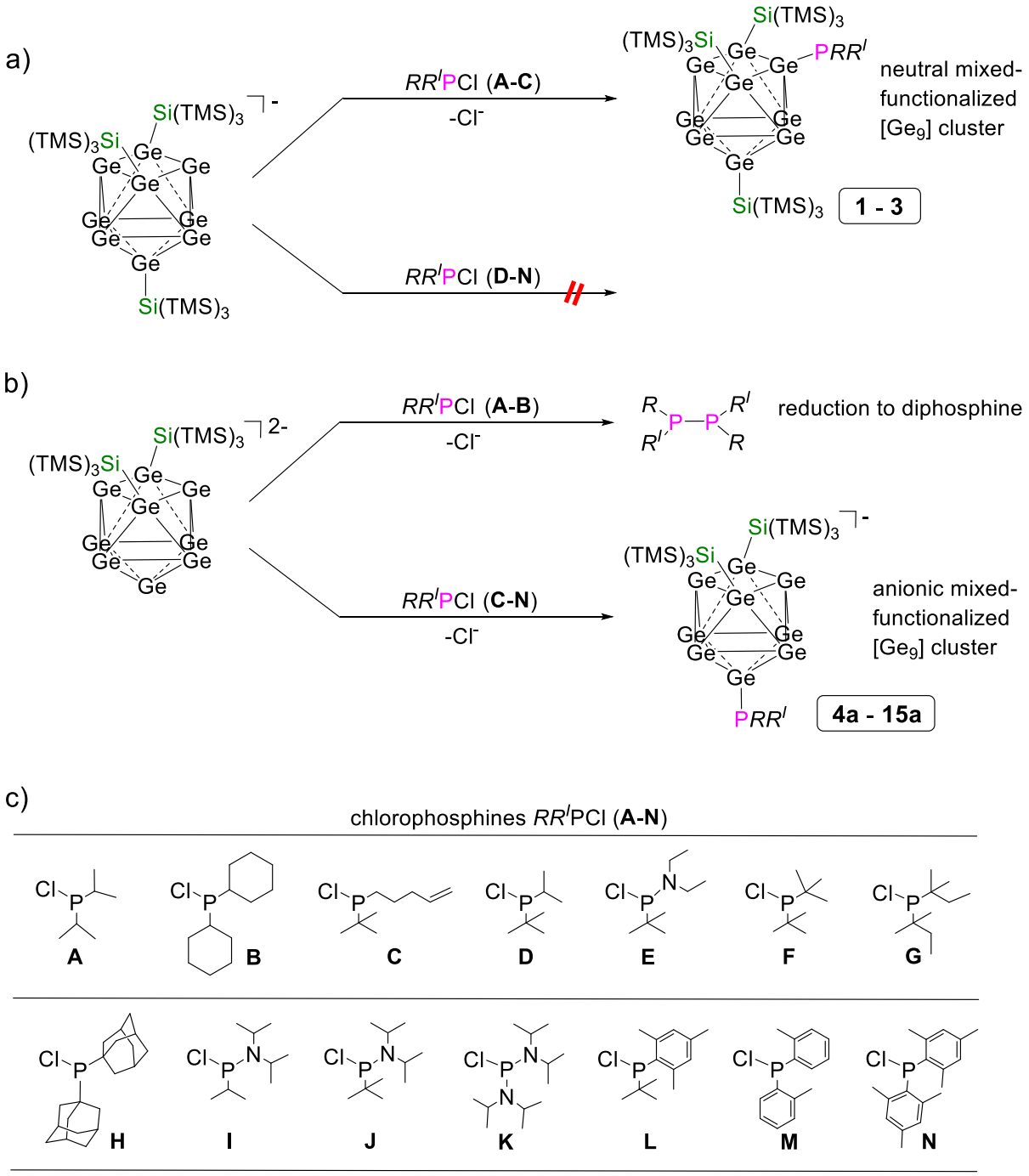

Scheme 3.9: Overview on reactivity of chlorophosphines **A**-**N** towards $[Ge_9\{Si(TMS)_3\}_n]^{(4-n)-}$ (*n*: 2, 3). a) Reactivity of $[Ge_9\{Si(TMS)_3\}_3]^-$ towards chlorophosphines **A**-**N**. b) Reactivity of $[Ge_9\{Si(TMS)_3\}_2]^{2-}$ towards chlorophosphines **A**-**N**. c) List of chlorophosphines **A**-**N**. The chlorophosphines are ordered according to increasing steric impact with **A** being the smallest congener and **N** being the bulkiest homologue (according to the Tolman cone angle).[68-70]

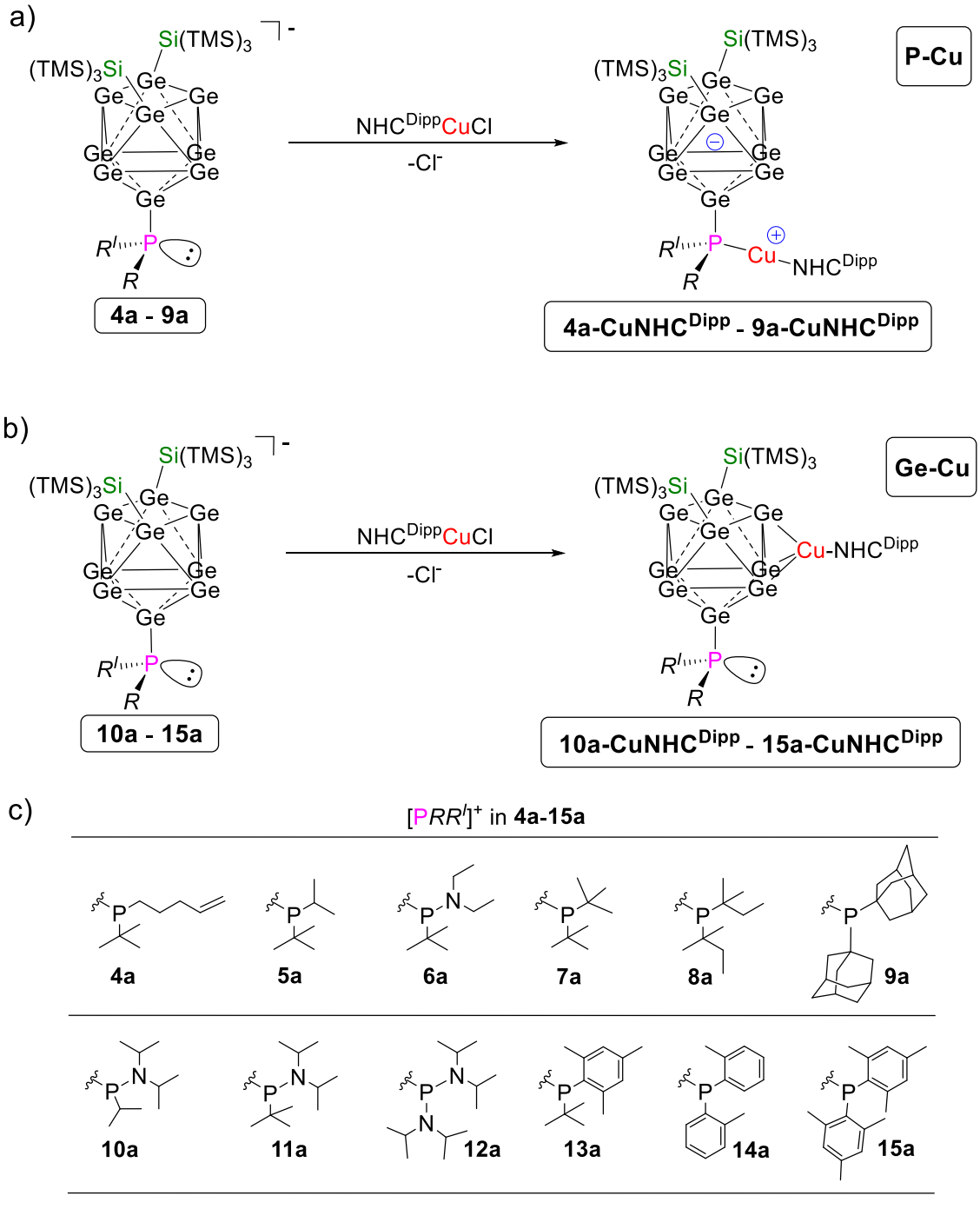

Scheme 3.10: Reactivity of anionic mixed-functionalized [Ge_9] clusters **4a**-**15a** towards $NHC^{Dipp}CuCl$. These investigations were carried out in order to test if the electron lone-pair at the [P*RR*]$^+$ groups attached to [Ge_9] is available for interactions with the Lewis acidic [$NHC^{Dipp}Cu$]$^+$ fragment. a) The formation of the zwitterionic species **4a-CuNHC^{Dipp}-9a-CuNHC^{Dipp}** comprising P-Cu interactions proves the principle of phosphine-functionalization of [Ge_9] with [P*RR*]$^+$ groups of medium steric impact. b) The isolation of [Ge_9] cluster coinage metal NHC complexes **10a-CuNHC^{Dipp}-15a-CuNHC^{Dipp}** comprising Ge-Cu interactions reveals that the steric impact of the phosphanyl substituents has crucial impact on the reactivity of these anions towards $NHC^{Dipp}CuCl$. c) List of [P*RR*]$^+$ substituents attached at the mixed-functionalized clusters **4a**-**15a**.

Reactions of $[Ge_9\{Si(TMS)_3\}_3]^-$ with Chlorophosphines RR^lPCl

Investigations on the reactivity of the tris-silylated [Ge_9] cluster $[Ge_9\{Si(TMS)_3\}_3]^-$ towards the chlorophosphines **A**-**N** (Scheme 3.9 c) were carried out in toluene or C_6D_6 solution at room temperature. Whereas in reactions with the smaller chlorophosphines **A**-**C** the formation of the neutral mixed-substituted compounds **1**-**3** readily occurred, no reactions were observed between the bulkier chlorophosphines **D**-**N** and $[Ge_9\{Si(TMS)_3\}_3]^-$. The latter can be explained by steric crowding at the silyl group shielded [Ge_9] core (Scheme 3.9 a).

In the case of compounds **2** and **3**, re-crystallization from toluene solutions at low temperature gave analytically pure material and crystals suitable for single crystal X-ray diffraction. The [Ge_9] cluster cores in **2** and **3** reveal the shapes of tricapped trigonal prisms and the silyl groups are attached at the three capping Ge atoms. The attachment of the $[PRR^l]^+$ [R = R^l: Cy (**2**); R: ^{t}Bu, R^l: $(CH_2)_3$-CH=CH_2 (**3**)] fragments at [Ge_9] occurs at single Ge vertex atoms in one of the trigonal bases of the prisms under formation of 2-centre-2-electron *exo* bonds (Figure 3.6). The observed interactions are in accordance to the Ge-C bonding mode observed in $[Ge_9\{Si(TMS)_3\}_3Et]$, however, they contrast the multi-centre-2-electron bonds observed between Ge atoms of the clusters and the Sn atom of the substituents in $[Ge_9\{Si(TMS)_3\}SnR_3]$ (R: Ph, ^{n}Bu).[57, 58]

In general, the attachment of small $[PRR^l]^+$ moieties to [Ge_9] provides an easy access to neutral [Ge_9] clusters bearing exclusively transition-metal-free substituents. Moreover, the introduction of alkenyl group substituted phosphine moieties to [Ge_9] (compound **3**) is an interesting approach with respect to the introduction of exposed alkenyl anchor groups, which might allow for interactions of the germanium-rich clusters with nanoparticles or surfaces.

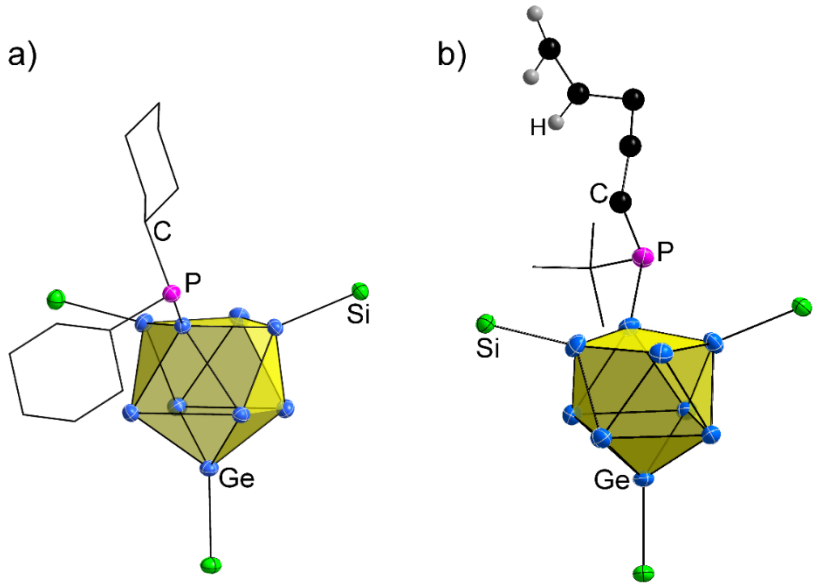

Figure 3.6: Molecular structures of compounds **2** (a) and **3** (b). All ellipsoids are shown at a 50 % probability level. For clarity, TMS groups of hypersilyl substituents and protons (except alkenyl protons) are omitted. Moreover, carbon atoms are shown as black wire sticks or black spheres. Colour code: Ge (bright blue), Si (green), P (purple), C (black), H (grey).

Reactions of $[Ge_9\{Si(TMS)_3\}_2]^{2-}$ with Chlorophosphines RR^iPCl

Examinations on the reactivity of the bis-silylated [Ge_9] cluster $[Ge_9\{Si(TMS)_3\}_2]^{2-}$ towards chlorophosphines **A**-**N** (Scheme 3.9 c) were conducted in thf or acetonitrile solution at room temperature. Whereas reactions of $[Ge_9\{Si(TMS)_3\}_2]^{2-}$ with the small chlorophosphines **A** and **B** led to redox reactions, yielding the respective diphosphines $R_2P\text{-}PR_2$ (*R*: ^{i}Pr, Cy; identified using NMR spectroscopy),[71, 72] reactions with bulkier chlorophosphines **C**-**N** resulted in the formation of a series of anionic mixed-functionalized [Ge_9] clusters **4a**-**15a** (Scheme 3.9 b). The characterization of the obtained anions occurred by means of NMR spectroscopy (^{1}H, ^{31}P, ^{29}Si, ^{13}C) and ESI-MS (monitoring of the respective molecule peaks of **4a**-**15a**). The crystallographic characterization of the anionic species **4a**-**15a** has not been achieved to date (no suitable single crystals were obtained). However, several products obtained in subsequent reactions of **4a**-**15a** with $NHC^{Dipp}CuCl$ (in order to validate phosphine-functionalization of [Ge_9]; see below) could be successfully re-crystallized and characterized by means of single crystal X-ray diffraction.

Reactivity of Neutral and Anionic Mixed-Functionalized [Ge_9] Clusters towards $NHC^{Dipp}CuCl$

Investigations on the reactivity of neutral mixed-functionalized [Ge_9] clusters **1**-**3** and anionic mixed-functionalized [Ge_9] clusters **4a**-**15a** towards $NHC^{Dipp}CuCl$ were carried out in order to prove the principle of phosphine-functionalization of [Ge_9] (in terms of proving that the electron lone-pair at the P atom of the attached $[PRR^i]^+$ group can interact with Lewis acids).
Reactions between the phosphine-functionalized [Ge_9] clusters and $NHC^{Dipp}CuCl$ were conducted in thf (**1**-**3**) or MeCN (**4a**-**15a**) solvent. Whereas in case of the neutral compounds **1**-**3** no reaction with $NHC^{Dipp}CuCl$ was observed, the anionic species **4a**-**15a** readily reacted with the copper NHC complex under formation of charge neutral compounds **4a-CuNHC^{Dipp}**-**15a**-**CuNHC^{Dipp}**, which immediately precipitated as coloured solids (yellow to brown) from the reaction mixtures (Scheme 3.10 a, b). The neutral compounds **4a**-**CuNHC^{Dipp}**-**15a**-**CuNHC^{Dipp}** were characterized by means of NMR spectroscopy (^{1}H, ^{31}P, ^{29}Si, ^{13}C). The diagnostic NMR shift of the hypersilyl groups' proton signal, which is very sensitive towards the number of substituents directly bound to the [Ge_9] core, revealed the occurrence of different interactions (P-Cu or Ge-Cu) between the phosphine-functionalized [Ge_9] clusters **4a**-**15a** and the $[NHC^{Dipp}Cu]^+$ fragments, in dependence of the steric impact of the attached phosphanyl group. In compounds **4a**-**CuNHC^{Dipp}**-**9a**-**CuNHC^{Dipp}** interactions between the attached phosphanyl moiety and the $[NHC^{Dipp}Cu]^+$ fragment occur (no shift of the silyl groups' proton signal since the number of substituents directly bound to [Ge_9] core does not change), validating the principle of phosphine-functionalization of [Ge_9]. Interestingly, the obtained species reveal zwitterionic nature with the negative charge being distributed over the [Ge_9] cluster core and the positive charge at Cu^+. These findings were confirmed by quantum

chemical calculations carried out by M. Sc. Jasmin Dums. The respective molecular structure of the zwitterionic compound **7a-CuNHC^{Dipp}** is presented in Figure 3.7 a. Therefore, the respective mixed phosphine-functionalized anions **4a**-**9a** are suitable precursors for the straightforward synthesis of zwitterionic compounds upon coordination of a cationic transition metal fragment with their phosphanyl moiety, which might be interesting with respect to catalytic applications. By contrast, in compounds **10a**-**CuNHC^{Dipp}**-**15a**-**CuNHC^{Dipp}** the larger phosphanyl substituents prohibit interactions of the [NHC^{Dipp}Cu]$^+$ fragment with the phosphanyl moiety, so instead the organometallic [NHC-Cu]$^+$ fragment coordinates to a triangular face of the [Ge_9] core (resulting in a highfield shift of the silyl groups' proton signal since the number of substituents directly bound to the [Ge_9] core changes). The respective molecular structure of compound **15a-CuNHC^{Dipp}** is presented in Figure 3.7 b. The mean Ge-Cu distance [d_{mean}(Ge-Cu): 2.510(1) Å] observed in **15a-CuNHC^{Dipp}** is in the range of the respective value in [NHC^{Dipp}Cu(η^3-Ge_9{Si(TMS)$_3$}$_3$)] [d_{mean}(Ge-Cu): 2.5263(9) Å; chapter 3.1.2.2] comprising similar Ge-Cu interactions. After all, these studies show that the steric impact of the phosphanyl group's substituents in **4a**-**15a** is decisive for which interactions occur with the [NHC^{Dipp}Cu]$^+$ fragment.

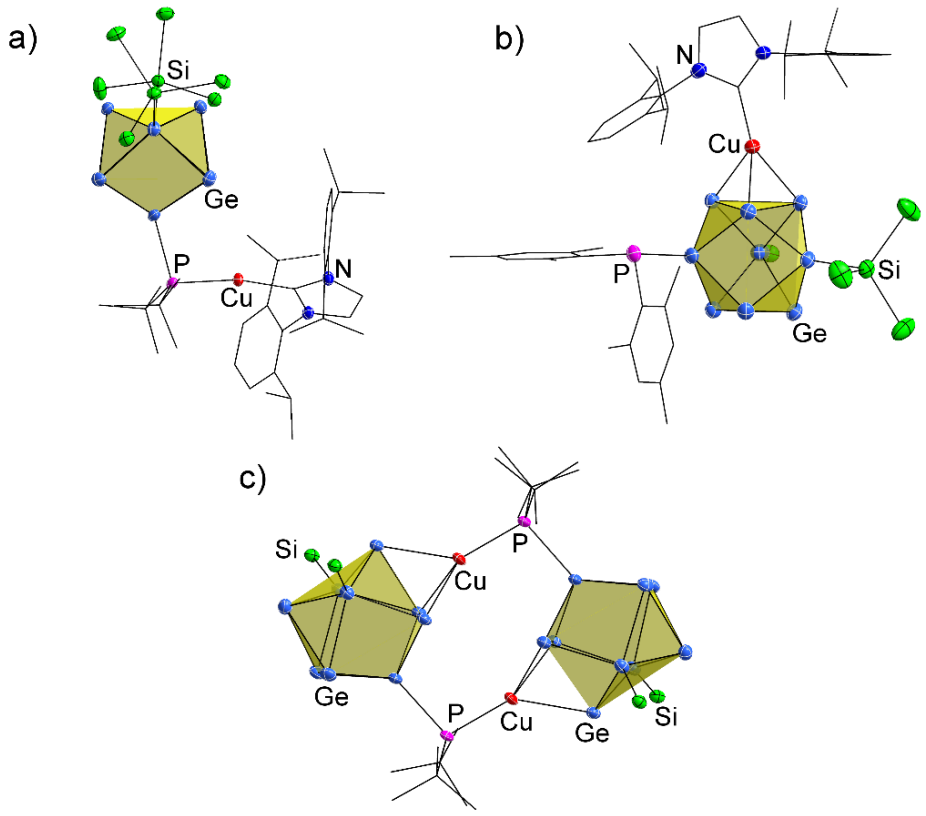

Figure 3.7: Molecular structures of the zwitterionic compound **7a-CuNHC^{Dipp}** (a), the neutral [Ge_9] cluster Cu-NHC compound **15a-CuNHC^{Dipp}** (b) and the dimeric species [{Si(TMS)$_3$}$_2$$Ge_9${(^{t}Bu)$_2$PCu}$_2$$Ge_9${Si(TMS)$_3$}$_2$] (c). All ellipsoids are shown at a 50 % probability level. For clarity, methyl groups (a, b) or TMS groups (c) of hypersilyl substituents as well as protons and co-crystallized solvent molecules are omitted. Moreover, carbon atoms are represented as black wire sticks. Colour code: Ge (bright blue), Si (green), Cu (red), P (purple), C (black), N (dark blue).

In another experiment we could show that the phosphanyl moieties attached to [Ge_9] can also participate in the linkage of [Ge_9] clusters by the formation of the dimeric species [{Si(TMS)$_3$}$_2$$Ge_9${(^{t}Bu)$_2$PCu}$_2$$Ge_9${Si(TMS)$_3$}$_2$] in reactions of **7a** with Cy_3PCuCl (bearing a more labile phosphine substituent; Figure 3.7 c).

Summary

Within this work the phosphine-functionalization of silylated [Ge_9] clusters was achieved by reaction of [Ge_9{Si(TMS)$_3$}$_n$]$^{(4-n)-}$ (*n*: 2, 3) with a series of chlorophosphines *RR'*PCl (**A**-**N**), yielding neutral compounds **1**-**3** and anionic species **4a**-**15a**. Species **1**-**3** represent examples of neutral [Ge_9] cluster compounds comprising exclusively transition-metal-free substituents. Moreover, subsequent reactions of the anionic species **4a**-**9a** with NHC^{Dipp}CuCl yielded a number of charge neutral zwitterionic compounds **4a**-**CuNHC^{Dipp}**-**9a**-**CuNHC^{Dipp}** comprising P-Cu interactions, validating the principle of phosphine-functionalization of [Ge_9]. Therefore, these anionic mixed phosphine-functionalized [Ge_9] clusters are suitable ligands for the straightforward synthesis of zwitterionic compounds, which might be of interest with respect to catalytic applications (e.g. cycloaddition reactions or hydrosilylation).[73, 74] However, the isolation of the neutral [Ge_9] cluster Cu-NHC complexes **10a**-**CuNHC^{Dipp}**-**15a**-**CuNHC^{Dipp}**, in which the [NHC^{Dipp}Cu]$^+$ fragment coordinates to the [Ge_9] core (Ge-Cu interactions), revealed that the steric demand of the phosphanyl substituents has a crucial impact on the reactivity of the mixed phosphine-functionalized anions. Finally, the isolation of the dimeric species [{Si(TMS)$_3$}$_2$$Ge_9${(^{t}Bu)$_2$PCu}$_2$$Ge_9${Si(TMS)$_3$}$_2$] showed that the attached phosphanyl moieties can also participate in the linkage of [Ge_9] cages.

3.2.3.2 Phosphine-Functionalization of $[Ge_9]^{4-}$ Clusters

see chapter 5.11

F. S. Geitner, W. Klein, T. F. Fässler, *Angew. Chem. Int. Ed.* **2018**, *57*, 14509.

Having achieved the synthesis of mixed-functionalized [Ge$_9$] clusters by reaction of [Ge$_9${Si(TMS)$_3$}$_n$]$^{(4-n)-}$ (*n*: 2, 3) with chlorophosphines *RR*^{I}PCl (*R*, *R*^{I}: alkyl, alkenyl, aryl, aminoalkyl), the next step targeted the synthesis of multiple phosphine-functionalized [Ge$_9$] clusters, which was accomplished by reactions of solid K$_4$Ge$_9$ with acetonitrile solutions of (^{i}Pr$_2$N)$_2$PCl or ^{t}Bu(^{i}Pr$_2$N)PCl, yielding the threefold phosphine-functionalized anions [Ge$_9${P*RR*^{I}}$_3$]$^{-}$ (*R*: N^{i}Pr$_2$, *R*^{I}: N^{i}Pr$_2$ or ^{t}Bu; Scheme 3.11 a).

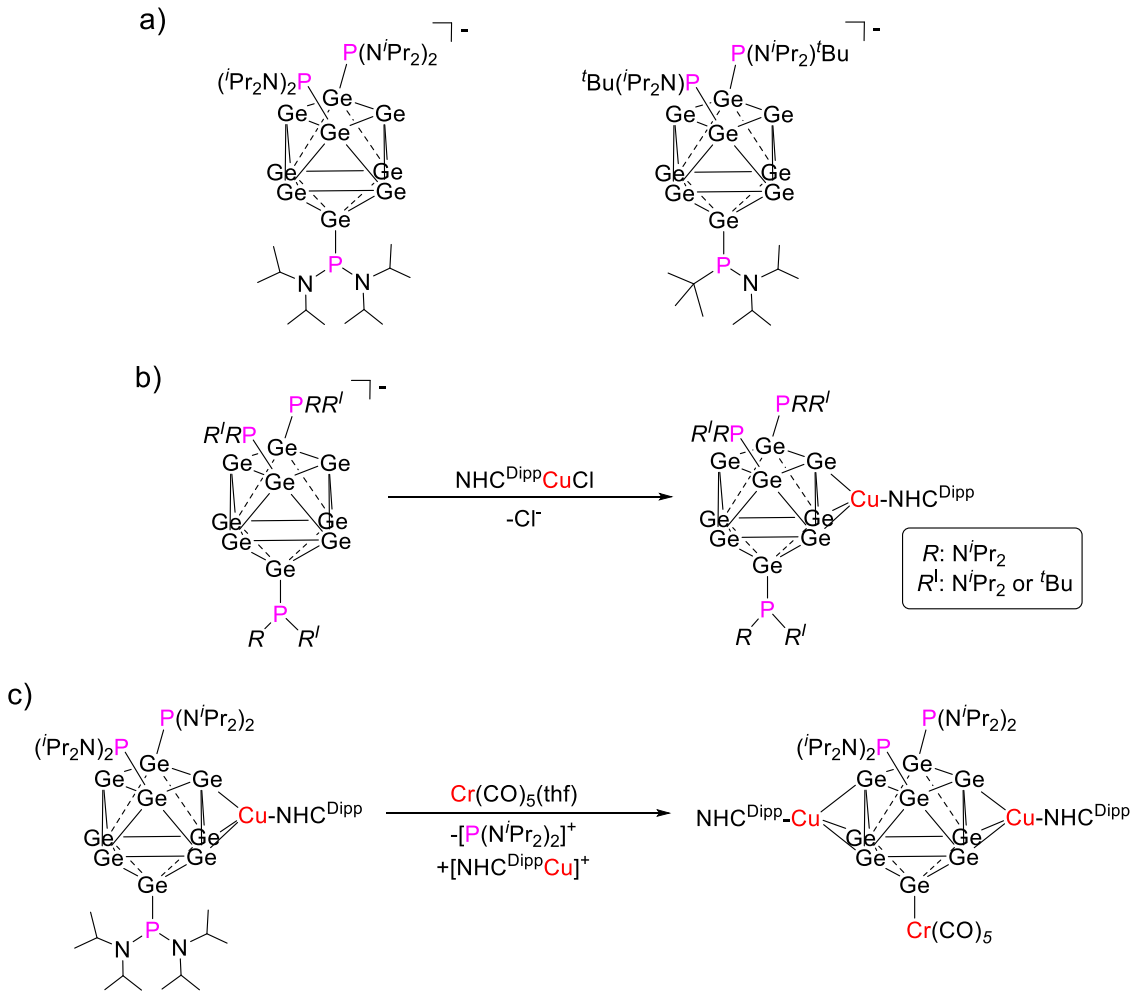

Scheme 3.11: Overview on multiple phosphine-functionalized [Ge$_9$] clusters synthesized within this work and their reactivity towards NHC^{Dipp}CuCl and Cr(CO)$_5$(thf). a) The multiple phosphine-functionalized [Ge$_9$] clusters [Ge$_9${P*RR*^{I}}$_3$]$^{-}$ (*R*: N^{i}Pr$_2$, *R*^{I}: N^{i}Pr$_2$ or ^{t}Bu). b) Reactivity of the anionic multiple phosphine-functionalized [Ge$_9$] clusters towards NHC^{Dipp}CuCl. c) Reactivity of the neutral compound [NHC^{Dipp}Cu(η^3-Ge$_9${P(N^{i}Pr$_2$)$_2$}$_3$)] towards Cr(CO)$_5$(thf).

In investigations on the reactivity of $[Ge_9\{PRR^I\}_3]^-$ (*R*: N^iPr_2, *R*^{I}: N^iPr_2 or ^{t}Bu) towards $NHC^{Dipp}CuCl$, which were conducted in order to test the availability of the attached phosphanyl groups for interactions with the Lewis acidic $[NHC^{Dipp}Cu]^+$ fragment, the neutral compounds $[NHC^{Dipp}Cu(\eta^3\text{-}Ge_9\{PRR^I\}_3)]$ (*R*: N^iPr_2, *R*^{I}: N^iPr_2 or ^{t}Bu), comprising Ge-Cu interactions were obtained (Scheme 3.11 b). Moreover, subsequent reactions of the neutral species $[NHC^{Dipp}Cu(\eta^3\text{-}Ge_9\{P(N^iPr_2)_2\}_3)]$ with $Cr(CO)_5(thf)$ resulted in the first fivefold coordinated neutral $[Ge_9]$ cluster compound $[(NHC^{Dipp}Cu)_2(\eta^3,\eta^3\text{-}Ge_9\{P(N^iPr_2)_2\}_2Cr(CO)_5)]$ *via* a ligand exchange reaction at the $[Ge_9]$ core (Scheme 3.11 c).

Synthesis of Multiple Phosphine-Functionalized $[Ge_9]$ Clusters

The synthesis of multiple phosphine-functionalized $[Ge_9]$ clusters $[Ge_9\{PRR^I\}_3]^-$ (*R*: N^iPr_2, *R*^{I}: N^iPr_2 or ^{t}Bu) was achieved by the heterogenous reaction of solid K_4Ge_9 with the respective chlorophosphines in acetonitrile. By contrast, similar reactions with sterically less demanding chlorophosphines R_2PCl (*R*: ^{i}Pr, Cy) resulted in redox reactions, yielding the respective diphosphines $R_2P\text{-}PR_2$ (*R*: ^{i}Pr, Cy; monitored by NMR),[71, 72] and in experiments with larger chlorophosphines such as Mes_2PCl no reaction occurred at all. Interestingly, the synthesis of $[Ge_9\{PRR^I\}_3]^-$ (*R*: N^iPr_2, *R*^{I}: N^iPr_2 or ^{t}Bu) does not work in thf, and the reduction of the applied chlorophosphines is observed instead.[72] The multiple phosphine-functionalized anions $[Ge_9\{PRR^I\}_3]^-$ (*R*: N^iPr_2, *R*^{I}: N^iPr_2 or ^{t}Bu) were characterized by means of NMR spectroscopy and ESI-MS (monitoring the respective molecule peaks). The crystallographic characterization of the anionic species was not achieved yet (no suitable single crystals were obtained), however, product species formed in subsequent reactions with $NHC^{Dipp}CuCl$ and $Cr(CO)_5(thf)$ were successfully re-crystallized and could be characterized by means of single crystal X-ray diffraction (see below).

Reactions of $[Ge_9\{PRR^I\}_3]^-$ (*R*: N^iPr_2, *R*^{I}: N^iPr_2 or ^{t}Bu) with $NHC^{Dipp}CuCl$ and $Cr(CO)_5(thf)$

Investigations on the reactivity of $[Ge_9\{PRR^I\}_3]^-$ (*R*: N^iPr_2, *R*^{I}: N^iPr_2 or ^{t}Bu) towards $NHC^{Dipp}CuCl$ were carried out by adding acetonitrile solutions of the Cu-NHC complex to deep red solutions of the freshly prepared threefold phosphine-functionalized $[Ge_9]$ clusters in acetonitrile, which instantly led to the precipitation of the crude products $[NHC^{Dipp}Cu(\eta^3\text{-}Ge_9\{PRR^I\}_3)]$ (*R*: N^iPr_2, *R*^{I}: N^iPr_2 or ^{t}Bu) as brown solids from the reactions mixtures. Both species were characterized by means of NMR spectroscopy (signal ratio of phosphine groups and NHC ligand) and ESI-MS (monitoring the molecule peaks with additionally attached $[NHC^{Dipp}Cu]^+$ moieties). Moreover, $[NHC^{Dipp}Cu(\eta^3\text{-}Ge_9\{P(N^iPr_2)_2\}_3)]$ was successfully re-crystallized from toluene solution at low temperature, yielding an analytically pure sample and single crystals suitable for single crystal X-ray diffraction. In $[NHC^{Dipp}Cu(\eta^3\text{-}Ge_9\{P(N^iPr_2)_2\}_3)]$, the $[Ge_9]$ cluster core can be described as a distorted tricapped trigonal prism with the phosphanyl moieties being

attached at the capping Ge atoms (in analogy to the attachment of the silyl groups at [Ge_9] in [$Ge_9\{Si(TMS)_3\}_3]^-$, chapter 1.3.2.2). All of the phosphanyl groups are disordered in the solid state (Figure 3.8 a). The [$NHC^{Dipp}Cu]^+$ moiety coordinates one of the trigonal prism bases of the [Ge_9] cage in a η^3-coordination mode [d_{mean}(Ge-Cu): 2.5119(6) Å] (Figure 3.8 a). Therefore, the structure of [$NHC^{Dipp}Cu(\eta^3\text{-}Ge_9\{P(N^iPr_2)_2\}_3)$] is very similar to the analogous [Ge_9] cluster Cu-NHC compound of the tris-silylated [Ge_9] cluster [$NHC^{Dipp}Cu(\eta^3\text{-}Ge_9\{Si(TMS)_3\}_3)$] [$d_{mean}$(Ge-Cu): 2.5263(9) Å, chapter 3.1.2.2]. The formation of Ge-Cu interactions is also in accordance to the observations made for the mixed-functionalized [Ge_9] cluster bearing the respective $[P(N^iPr_2)_2]^+$ group $[Ge_9\{Si(TMS)_3\}_2P(N^iPr_2)_2]^-$, which undergoes similar Ge-Cu interactions with $[NHC^{Dipp}Cu]^+$ (chapter 3.2.3.1).

Interestingly, the subsequent reaction of [$NHC^{Dipp}Cu(\eta^3\text{-}Ge_9\{P(N^iPr_2)_2\}_3)$] with $Cr(CO)_5$(thf) in thf solution at room temperature led to a rare ligand exchange reaction at the [Ge_9] core. Thereby, one of the $[P(N^iPr_2)_2]^+$ moieties is replaced by the neutral [$Cr(CO)_5$] fragment, yielding a negatively charged intermediate, which is subsequently coordinated by a second $[NHC^{Dipp}Cu]^+$ moiety resulting in [$(NHC^{Dipp}Cu)_2(\eta^3,\eta^3\text{-}Ge_9\{P(N^iPr_2)_2\}_2Cr(CO)_5)$]. This compound readily crystallizes from solution, whereas all other formed species remain in solution (Figure 3.8 b). The novel species is the first example for a neutral fivefold coordinated [Ge_9] cluster compound (all Ge atoms bind to a ligand) and its structure resembles the shape of [$(NHC^{Dipp}Cu)_2(\eta^3,\eta^3\text{-}Ge_9\{Si(TMS)_3\}_2)$] (chapter 3.1.2.2), which was obtained by reaction of $[Ge_9\{Si(TMS)_3\}_2]^{2-}$ with $NHC^{Dipp}CuCl$. However, the latter comprises one “naked” uncoordinated Ge vertex atom.

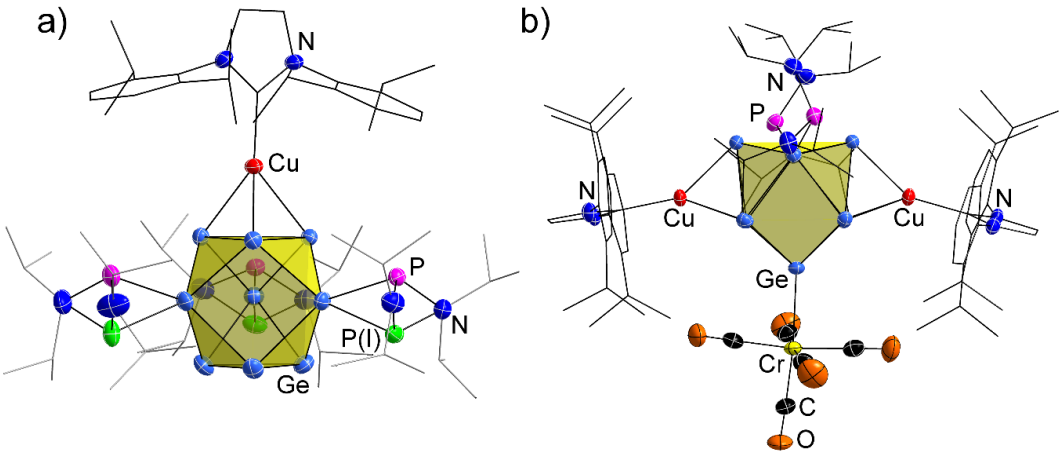

Figure 3.8: Molecular structures of multiple phosphine-functionalized [Ge_9] clusters. All ellipsoids are shown at a 50 % probability level. a) Neutral compound [$NHC^{Dipp}Cu(\eta^3\text{-}Ge_9\{P(N^iPr_2)_2\}_3)$] with positional disorder of all phosphine groups. Major individuals (P) are represented in purple and minor individuals P(I) are shown in green. For clarity reasons carbon atoms are presented as black or grey wire sticks. b) Neutral compound [$(NHC^{Dipp}Cu)_2(\eta^3,\eta^3\text{-}Ge_9\{P(N^iPr_2)_2\}_2Cr(CO)_5)$] obtained by reaction of [$NHC^{Dipp}Cu(\eta^3\text{-}Ge_9\{P(N^iPr_2)_2\}_3)$] with $Cr(CO)_5$(thf) *via* ligand exchange reaction at [Ge_9]. For clarity, carbon atoms (except carbonyl groups) are presented as black wire sticks. Moreover, co-crystallized solvent molecules are omitted in a) and b).

Moreover, we also tested the reactivity of the anionic species $[Ge_9\{PRR^l\}_3]^-$ (*R*: N^iPr_2, R^l: N^iPr_2 or ^{t}Bu) towards Group 6 element carbonyl complexes $[M(CO)_5(thf)]$ (*M*: Cr, Mo, W) at low temperature in thf solution, which resulted in the formation of $[M(CO)_5]$ (*M*: Cr, Mo, W) adducts of $[Ge_9\{P(N^iPr_2)^tBu\}_3]^-$ with up to three coordinated Group 6 complex fragments. However, NMR investigations indicated the formation of product mixtures during these reactions and crystallization of potential product species has not been achieved to date. Therefore, it is not completely clear, whether the Group 6 element fragments interact with the phosphanyl moieties (P-*M* bonds) attached at the $[Ge_9]$ cluster or with the $[Ge_9]$ core itself (Ge-*M* bonds; Scheme 3.12).

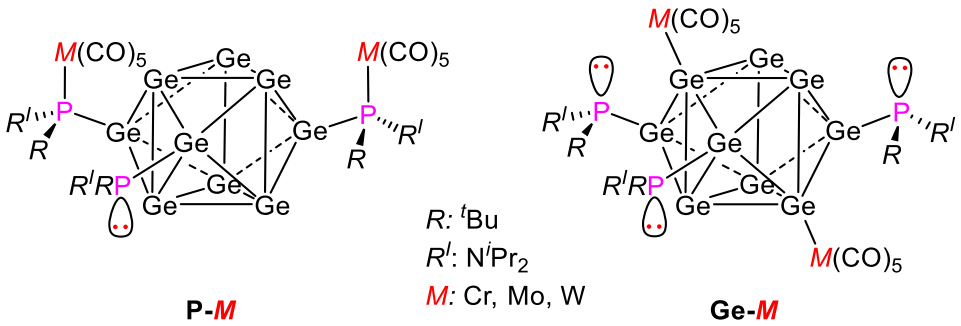

Scheme 3.12: Potential interactions of $[M(CO)_5]$ (*M*: Cr, Mo, W) fragments with $[Ge_9\{P(N^iPr_2)^tBu\}_3]^-$. Respective species have been monitored in ESI-MS examinations of thf reaction mixtures. Lone-pairs at P are symbolized in schematic orbitals.

Summary

Multiple phosphine-functionalized $[Ge_9]$ clusters $[Ge_9\{PRR^l\}_3]^-$ (*R*: N^iPr_2; R^l: N^iPr_2 or ^{t}Bu) were obtained in the heterogenous reactions of solid K_4Ge_9 with acetonitrile solutions of $(^iPr_2N)_2PCl$ or $(^iPr_2N)^tBuPCl$. Attempts to attach sterically less demanding or bulkier phosphanyl groups to $[Ge_9]^{4-}$ were not successful and therefore the number of threefold phosphine-functionalized $[Ge_9]$ species is limited to the two examples mentioned above. Subsequent reactions with $NHC^{Dipp}CuCl$ yielded the neutral compounds $[NHC^{Dipp}Cu(\eta^3\text{-}Ge_9\{PRR^l\}_3)]$ (*R*: N^iPr_2, R^l: N^iPr_2 or ^{t}Bu), which allowed for the crystallization and the structural characterization of the novel multiple phosphine-functionalized species. This revealed the structures of $[Ge_9\{PRR^l\}_3]^-$ (*R*: N^iPr_2; R^l: N^iPr_2 or ^{t}Bu) to be analogous to the tris-silylated cluster $[Ge_9\{Si(TMS)_3\}_3]^-$. Moreover, reactions of $[NHC^{Dipp}Cu(\eta^3\text{-}Ge_9\{P(N^iPr_2)_2\}_3)]$ with $Cr(CO)_5(thf)$ resulted in a ligand exchange reaction at the $[Ge_9]$ cluster core under formation of the fivefold coordinated $[Ge_9]$ cluster $[(NHC^{Dipp}Cu)_2(\eta^3,\eta^3\text{-}Ge_9\{P(N^iPr_2)_2\}_2Cr(CO)_5)]$. Finally, investigations on the reactivity of $[Ge_9\{P(N^iPr_2)^tBu\}_3]^-$ towards $M(CO)_5(thf)$ (*M*: Cr, Mo, W) yielded multiple $[M(CO)_5]$ fragment coordinated $[Ge_9]$ cluster species according to ESI-MS examinations. However, the nature of the interactions (Ge-*M* or P-*M*) is not completely clear to date. Therefore, it cannot be finally

proven yet, if the phosphanyl groups of the multiple phosphine-functionalized [Ge_9] clusters can also undergo interactions with Lewis acidic transition metal fragments.

3.3 Literature

[1] C. Hoch, M. Wendorff, C. Röhr, *J. Alloys Compd.* **2003**, *361*, 206.
[2] V. Quéneau, E. Todorov, S. C. Sevov, *J. Am. Chem. Soc.* **1998**, *120*, 3263.
[3] T. F. Fässler, *Zintl Ions: Principles and Recent Developments, Struc. Bond 139*, Springer, Heidelberg, **2011**.
[4] C. B. Benda, T. Henneberger, W. Klein, T. F. Fässler, *Z. Anorg. Allg. Chem.* **2017**, *643*, 146.
[5] T. Henneberger, W. Klein, T. F. Fässler, *Z. Anorg. Allg. Chem.* **2018**, *644*, 1018.
[6] J. M. Goicoechea, S. C. Sevov, *Organometallics* **2006**, *25*, 4530.
[7] S. Joseph, M. Hamberger, F. Mutzbauer, O. Härtl, M. Meier, N. Korber, *Angew. Chem. Int. Ed.* **2009**, *48*, 8770.
[8] M. Waibel, F. Kraus, S. Scharfe, B. Wahl, T. F. Fässler, *Angew. Chem. Int. Ed.* **2010**, *49*, 6611.
[9] S. Scharfe, T. F. Fässler, *Eur. J. Inorg. Chem.* **2010**, 1207.
[10] S. Scharfe, T. F. Fässler, S. Stegmaier, S. D. Hoffmann, K. Ruhland, *Chem. Eur. J.* **2008**, *14*, 4479.
[11] A. Spiekermann, S. D. Hoffmann, T. F. Fässler, I. Krossing, U. Preiss, *Angew. Chem. Int. Ed.* **2007**, *46*, 5310.
[12] J.-Q. Wang, S. Stegmaier, B. Wahl, T. F. Fässler, *Chem. Eur. J.* **2010**, *16*, 1793.
[13] J. D. Corbett, *Chem. Rev.* **1985**, *85*, 383.
[14] T. F. Fässler, S. D. Hoffmann, *Angew. Chem. Int. Ed.* **2004**, *43*, 6242.
[15] S. C. Sevov, J. M. Goicoechea, *Organometallics* **2006**, *25*, 5678.
[16] S. Scharfe, F. Kraus, S. Stegmaier, A. Schier, T. F. Fässler, *Angew. Chem. Int. Ed.* **2011**, *50*, 3630.
[17] K. Mayer, L.-A. Jantke, S. Schulz, T. F. Fässler, *Angew. Chem. Int. Ed.* **2017**, *56*, 2350.
[18] C. Liu, L.-J. Li, X. Jin, J. E. McGrady, Z.-M. Sun, *Inorg. Chem.* **2018**, *57*, 3025.
[19] L. Wang, Y. Wang, Z. Li, H. Ruan, L. Xu, *Dalton Trans.* **2017**, *46*, 6839.
[20] G. Espinoza-Quintero, J. C. A. Duckworth, W. K. Myers, J. E. McGrady, J. M. Goicoechea, *J. Am. Chem. Soc.* **2014**, *136*, 1210.
[21] C. B. Benda, M. Waibel, T. F. Fässler, *Angew. Chem. Int. Ed.* **2015**, *54*, 522.
[22] C. Schenk, A. Schnepf, *Angew. Chem. Int. Ed.* **2007**, *46*, 5314.
[23] C. Schenk, A. Schnepf, *Chem. Commun.* **2009**, 3208.
[24] K. Mayer, L. J. Schiegerl, T. F. Fässler, *Chem. Eur. J.* **2016**, *22*, 18794.
[25] D. Bourissou, O. Guerret, F. P. Gabbaï, G. Bertrand, *Chem. Rev.* **2000**, *100*, 39.
[26] T. Droge, F. Glorius, *Angew. Chem. Int. Ed.* **2010**, *49*, 6940.
[27] J. C. Garrison, W. J. Youngs, *Chem. Rev.* **2005**, *105*, 3978.
[28] K. Jonas, *Angew. Chem.* **1985**, *97*, 292.
[29] C. Boehme, G. Frenking, *Organometallics* **1998**, *17*, 5801.
[30] C. B. Benda, M. Waibel, T. Köchner, T. F. Fässler, *Chem. Eur. J.* **2014**, *20*, 16738.
[31] J.-Q. Wang, B. Wahl, T. F. Fässler, *Angew. Chem. Int. Ed.* **2010**, *49*, 6592.
[32] D. O. Downing, P. Zavalij, B. W. Eichhorn, *Eur. J. Inorg. Chem.* **2010**, 890.
[33] B. Zhou, M. S. Denning, T. Chapman, J. M. Goicoechea, *Inorg. Chem.* **2009**, *48*, 2899.
[34] C. Schenk, F. Henke, G. Santiso-Quinones, I. Krossing, A. Schnepf, *Dalton Trans.* **2008**, 4436.
[35] F. Henke, C. Schenk, A. Schnepf, *Dalton Trans.* **2009**, 9141.
[36] O. Kysliak, C. Schrenk, A. Schnepf, *Chem. Eur. J.* **2016**, *22*, 18787.
[37] F. Li, S. C. Sevov, *Inorg. Chem.* **2015**, *54*, 8121.

[38] S. Stegmaier, M. Waibel, A. Henze, L.-A. Jantke, A. J. Karttunen, T. F. Fässler, *J. Am. Chem. Soc.* **2012**, *134*, 14450.
[39] M. Waibel, G. Raudaschl-Sieber, T. F. Fässler, *Chem. Eur. J.* **2011**, *17*, 13391.
[40] F. Henke, C. Schenk, A. Schnepf, *Dalton Trans.* **2011**, *40*, 6704.
[41] J. Hlina, J. Baumgartner, C. Marschner, P. Zark, T. Müller, *Organometallics* **2013**, *32*, 3300.
[42] R. E. Marsh, *Acta Cryst. Sect. B* **1997**, *53*, 317.
[43] J. F. Harrod, A. Malek, F. D. Rochon, R. Melanson, *Organometallics* **1987**, *6*, 2117.
[44] A. Ugrinov, S. C. Sevov, *J. Am. Chem. Soc.* **2002**, *124*, 2442.
[45] A. Ugrinov, S. C. Sevov, *Chem. Eur. J.* **2004**, *10*, 3727.
[46] D. F. Hansen, B. Zhou, J. M. Goicoechea, *J. Organomet. Chem.* **2012**, *721*, 53.
[47] A. Ugrinov, S. C. Sevov, *J. Am. Chem. Soc.* **2003**, *125*, 14059.
[48] A. Ugrinov, S. C. Sevov, *Chem. Eur. J.* **2004**, *10*, 3727.
[49] A. Schnepf, *Angew. Chem. Int. Ed.* **2003**, *42*, 2624.
[50] F. Li, S. C. Sevov, *Inorg. Chem.* **2012**, *51*, 2706.
[51] L. J. Schiegerl, F. S. Geitner, C. Fischer, W. Klein, T. F. Fässler, *Z. Anorg. Allg. Chem.* **2016**, *642*, 1419.
[52] O. Kysliak, T. Kunz, A. Schnepf, *Eur. J. Inorg. Chem.* **2017**, 805.
[53] O. Kysliak, C. Schrenk, A. Schnepf, *Inorg. Chem.* **2015**, *54*, 7083.
[54] L. G. Perla, S. C. Sevov, *J. Am. Chem. Soc.* **2016**, *138*, 9795.
[55] L. G. Perla, A. Muñoz-Castro, S. C. Sevov, *J. Am. Chem. Soc.* **2017**, *139*, 15176.
[56] O. Kysliak, A. Schnepf, *Dalton Trans.* **2016**, *45*, 2404.
[57] F. Li, A. Muñoz-Castro, S. C. Sevov, *Angew. Chem. Int. Ed.* **2012**, *51*, 8581.
[58] F. Li, S. C. Sevov, *J. Am. Chem. Soc.* **2014**, *136*, 12056.
[59] S. Frischhut, T. F. Fässler, *Dalton Trans.* **2018**, *47*, 3223.
[60] S. Frischhut, W. Klein, M. Drees, T. F. Fässler, *Chem. Eur. J.* **2018**, *24*, 9009.
[61] K. Mayer, L. J. Schiegerl, T. Kratky, S. Günther, T. F. Fässler, *Chem. Commun.* **2017**, *53*, 11798.
[62] A. V. Protchenko, D. Dange, M. P. Blake, A. D. Schwarz, C. Jones, P. Mountford, S. Aldridge, *J. Am. Chem. Soc.* **2014**, *136*, 10902.
[63] A. V. Protchenko, J. Urbano, J. A. B. Abdalla, J. Campos, D. Vidovic, A. D. Schwarz, M. P. Blake, P. Mountford, C. Jones, S. Aldridge, *Angew. Chem. Int. Ed.* **2017**, *56*, 15098.
[64] A. V. Protchenko, K. H. Birjkumar, D. Dange, A. D. Schwarz, D. Vidovic, C. Jones, N. Kaltsoyannis, P. Mountford, S. Aldridge, *J. Am. Chem. Soc.* **2012**, *134*, 6500.
[65] A. V. Protchenko, M. P. Blake, A. D. Schwarz, C. Jones, P. Mountford, S. Aldridge, *Organometallics* **2015**, *34*, 2126.
[66] J. W. Dube, C. M. E. Graham, C. L. B. Macdonald, Z. D. Brown, P. P. Power, P. J. Ragogna, *Chem. Eur. J.* **2014**, *20*, 6739.
[67] G. E. Quintero, I. Paterson, N. Rees, J. M. Goicoechea, *Dalton Trans.* **2016**, *45*, 1930.
[68] H. Clavier, S. P. Nolan, *Chem. Commun.* **2010**, *46*, 841.
[69] C. A. Tolman, *Chem. Rev.* **1977**, *77*, 313.
[70] B. P. Carrow, L. Chen, *Synlett* **2017**, *28*, 280.
[71] M. Baudler, A. Zarkadas, *Chem. Ber.* **1972**, *105*, 3844.
[72] R. Grubba, A. Wisniewska, K. Baranowska, E. Matern, J. Pikies, *Dalton Trans.* **2011**, *40*, 2017.
[73] F. Lazreg, A. M. Z. Slawin, C. S. J. Cazin, *Organometallics* **2012**, *31*, 7969.
[74] S. Diez-González, E. D. Stevens, N. M. Scott, J. L. Petersen S. P. Nolan *Chem. Eur. J.* **2008**, *14*, 158.

4 Summary and Conclusion

The Group 14 element semiconductors silicon and germanium are interesting materials for a broad range of applications (electronics, photovoltaics and anode materials for lithium ion batteries) and they play a key role in the power revolution process from fossil fuels to renewable energies. In this context nanoparticles or nanostructured materials are of special interest with respect to their unique morphologies and tuneable properties, which makes Group 14 element clusters interesting building blocks. Binary intermetallic compounds of the compositions A_4E_9 (*A*: alkali metal, *E*: Ge-Pb) and $A_{12}E_{17}$ (*A*: alkali metal, *E*: Si-Sn) contain well-defined, nine-atomic $[E_9]^{4-}$ (*E*: Si-Pb) clusters and are accessible in macroscopic yield. Therefore, these *Zintl* phases represent interesting precursors for the solution-based fabrication of nanostructured materials. However, the fourfold negative charge of the $[E_9]^{4-}$ (*E*: Si-Pb) clusters results in poor solubility and a strongly reductive nature, which is a drawback in this context. This is especially true for the silicide cluster chemistry, since $[Si_9]^{4-}$ clusters are exclusively contained in phases of the compositions $A_{12}Si_{17}$ (*A*: alkali metal), which also include $[Si_4]^{4-}$ clusters.

Therefore, the focus of this work was to find novel methods for the stabilization, functionalization and linkage of nine-atomic Group 14 element *Zintl* clusters in solution in order to make the $[E_9]$ (*E*: Si, Ge, Sn) clusters available for future applications.

In this context the reactivity of bare $[E_9]^{4-}$ (*E*: Si, Ge, Sn) cages and silylated $[Ge_9]$ clusters towards transition metal complexes and main-group element compounds was investigated.

Stabilization and Linkage of Nine-Atomic Group 14 Element *Zintl* Clusters with Transition Metal Moieties

Regarding the stabilization and linkage of nine-atomic Group 14 element *Zintl* clusters with transition metal moieties, coinage metal NHC complexes NHC-*M*-Cl (*M*: Cu, Ag, Au; NHC: *N*-heterocyclic carbene) and the early transition metal complex $[Cp_2TiCl]_2$ were applied as precursors.

Investigations on the reactivity of the *Zintl* phases $K_{12}Si_{17}$ and K_4Sn_9 towards the coinage metal NHC complexes were carried out in NH_3(l) at low temperature. These examinations revealed that $NHC^{Dipp}MCl$ (*M*: Cu, Ag, Au) complexes are suitable precursors for the attachment of positively charged $[NHC^{Dipp}M]^+$ fragments at bare $[Si_9]^{4-}$ and $[Sn_9]^{4-}$ clusters, resulting in the silicide complex $[NHC^{Dipp}Cu(\eta^4\text{-}Si_9)]^{3-}$ (Scheme 4.1 a) and the stannide complexes $[NHC^{Dipp}M(\eta^4\text{-}Sn_9)]^{3-}$ (*M*: Cu, Ag, Au). In all these species the coinage metal NHC fragments coordinate the nine-atomic clusters *via* their open square plane in a η^4-coordination mode.

The synthesis of $[NHC^{Dipp}Cu(\eta^4\text{-}Si_9)]^{3-}$ is especially interesting since this species is only the third example of a transition metal fragment coordinated $[Si_9]^{4-}$ cluster. Moreover, it could be shown that intact $[NHC^{Dipp}Cu(\eta^4\text{-}Si_9)]^{3-}$ clusters can be dissolved in solvents different from NH_3(l), such as pyridine or MeCN, which is of importance with respect to potential future

applications of the stabilized silicide clusters. However, it was found that $[NHC^{Dipp}Cu(\eta^4\text{-}Si_9)]^{3-}$ is not stable at room temperature and a cleavage of the Cu-NHC bond occurs. Therefore, further investigations (NMR, ESI-MS) on the degradation or transformation processes and products of $[NHC^{Dipp}Cu(\eta^4\text{-}Si_9)]^{3-}$ in solution are necessary.

The respective stannide cluster complexes $[NHC^{Dipp}M(\eta^4\text{-}Sn_9)]^{3-}$ (*M*: Cu, Ag, Au) are of interest since they can be regarded as intermediates on the way to novel intermetalloid species. In the case of $[NHC^{Dipp}Ag(\eta^4\text{-}Sn_9)]^{3-}$, the cleavage of the Ag-NHC bond is already observed at low temperature, yielding the large intermetalloid $[(\eta^4\text{-}Sn_9)Ag(\eta^1\text{-}Sn_9)]^{7-}$ (Scheme 4.1 b). Interestingly, the two $[Sn_9]^{4-}$ clusters in $[(\eta^4\text{-}Sn_9)Ag(\eta^1\text{-}Sn_9)]^{7-}$ bind to Ag^+ in different coordination modes, which is a rare phenomenon and has also been observed in germanide cluster chemistry.

Further investigations on the reactivity of the coinage metal NHC complexes $NHC^{Dipp}MCl$ (*M*: Cu, Ag, Au) towards silylated $[Ge_9]$ cluster species $[Ge_9\{SiR_3\}_3]^-$ (*R*: TMS, ^{i}Bu, ^{i}Pr) and $[Ge_9\{Si(TMS)_3\}_2]^{2-}$ revealed that $[NHC^{Dipp}M]^+$ (*M*: Cu, Ag, Au) fragments can also be attached to these $[Ge_9]$ cages. In the obtained charge neutral compounds $[NHC^{Dipp}M(\eta^3\text{-}Ge_9\{Si(TMS)_3\}_3)]$ (*M*: Cu, Ag, Au; Scheme 4.1 c), $[NHC^{Dipp}Cu(\eta^3\text{-}Ge_9\{SiR_3\}_3)]$ (*R*: ^{i}Pr, ^{i}Bu) and $[(NHC^{Dipp}M)_2(\eta^3,\eta^3\text{-}Ge_9\{Si(TMS)_3\}_2)]$ (*M*: Cu, Ag, Au; Scheme 4.1 d), the $[NHC^{Dipp}M]^+$ (*M*: Cu, Ag, Au) moieties interact with the $[Ge_9]$ cluster cores in a η^3-coordination mode. Moreover, the latter species represent the first examples for dinuclear coinage metal complexes with a bridging $[Ge_9]$ moiety. The neutral compounds are stable in solution at room temperature except for $[NHC^{Dipp}Ag(\eta^3\text{-}Ge_9\{Si(TMS)_3\}_3)]$, which undergoes a rearrangement reaction yielding the Ag^+ bridged dimer $[Ag(\eta^3\text{-}Ge_9\{Si(TMS)_3\}_3)_2]^-$. In this species both $[Ge_9]$ cages approach Ag^+ with triangular faces in a η^3-coordination mode, which contrasts the varying coordination of Ag^+ by the two $[Sn_9]^{4-}$ clusters in $[(\eta^4\text{-}Sn_9)Ag(\eta^1\text{-}Sn_9)]^{7-}$.

Finally, the reactivity of the early transition metal complex $[Cp_2TiCl]_2$ towards silylated $[Ge_9]$ clusters $[Ge_9\{Si(TMS)_3\}_n]^{(4-n)-}$ (*n*: 2, 3) was investigated. Generally, successful reactions of nine-atomic Group 14 element *Zintl* clusters with early transition metal complexes are rare, however, the isolation of the neutral compound $[Cp_2Ti(MeCN)(\eta^1\text{-}Ge_9\{Si(TMS)_3\}_3)]$ (Scheme 4.1 e) and the dimeric species $K_3[Cp_2Ti(\eta^1\text{-}Ge_9\{Si(TMS)_3\}_2)_2]$ (Scheme 4.1 f) prove that $[Cp_2Ti]^+$ fragments can be attached at silylated $[Ge_9]$ clusters. In both species Ti(III) is approached by the $[Ge_9]$ clusters with single Ge vertex atoms under formation of donor-acceptor interactions (η^1-coordination mode). The formation of $[Cp_2Ti(\eta^1\text{-}Ge_9\{Si(TMS)_3\}_2)_2]^{3-}$ reveals that $[Cp_2Ti]^+$ fragments can connect $[Ge_9]$ clusters even without cleavage of their Cp ligands. Therefore, $[Cp_2Ti(\eta^1\text{-}Ge_9\{Si(TMS)_3\}_2)_2]^{3-}$ might be an interesting starting point for the synthesis of three-dimensional networks by replacement of the Cp ligands through $[Ge_9]$ clusters in future investigations. A representative selection of the species obtained by reactions of nine-atomic

Group 14 element *Zintl* clusters with transition metal complexes within this work is provided in Scheme 4.1.

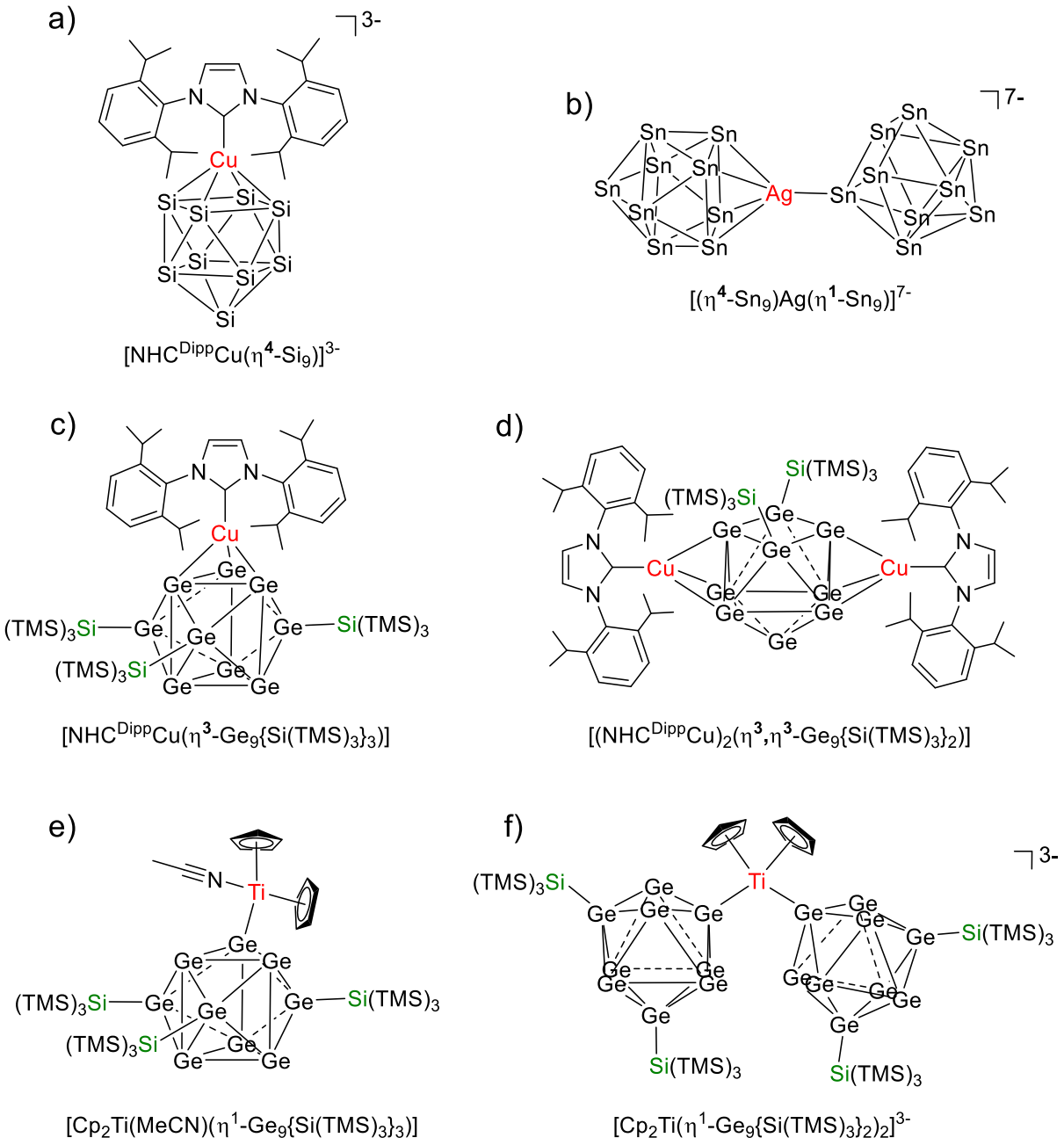

Scheme 4.1: Representative selection of species obtained by reaction of bare $[E_9]^{4-}$ (*E*: Si, Sn) clusters and silylated [Ge9] cages $[Ge_9\{SiR_3\}_3]^-$ (*R*: TMS, ^{i}Bu, ^{i}Pr) or $[Ge_9\{Si(TMS)_3\}_2]^{2-}$ with transition metal complexes within this work.

Stabilization and Functionalization of [Ge_9] Clusters with Main-Group Element Moieties

Regarding the stabilization and functionalization of [Ge_9] cluster species with main-group element moieties, the reactivity of bare [Ge_9]$^{4-}$ clusters and silylated [Ge_9{Si(TMS)$_3$}$_n$]$^{(4-n)-}$ (*n*: 2, 3) cages towards several Group 13 element compounds R_2E-Br (*E*: B, Al; *R*: substituent) and a series of chlorophosphines RR^IPCl (*R*, R^I: alkyl, alkenyl, aryl, aminoalkyl) was investigated.

Hereby, it was found that the Group 13 element compounds [BrBN(Mes)-CH_2-CH_2-N(Mes)] (diazaborolidine), [BrBN(Dipp)-CH=CH-N(Dipp)] (diazaborole), Mes_2BBr and [^{t}Bu$_2$AlBr]$_2$ are suitable precursors for the introduction of additional [ER_2]$^+$ (*E*: B, Al; *R*: substituent) fragments to the bis-silylated [Ge_9] cluster species [Ge_9{Si(TMS)$_3$}$_2$]$^{2-}$, yielding the mixed-substituted anions [Ge_9{Si(TMS)$_3$}$_2$$ER_2$]$^-$ (*E*: B, Al; *R*: substituent; Scheme 4.2 a). By contrast, the attachment of these [ER_2]$^+$ moieties as fourth ligands to [Ge_9{Si(TMS)$_3$}$_3$]$^-$, aiming for charge neutral [Ge_9] cluster compounds, was not possible (probably due to steric crowding). Moreover, reactions of the Group 13 element precursor complexes with K_4Ge_9 resulted either in the decomposition of the reactants or unselective reactions, yielding several product species. Therefore, further investigations on suitable Group 13 element precursor compounds are necessary, which might be found in species with electron-rich substituents of medium bulkiness such as $(Me_2N)_2$BCl or cyclic diazaborols and diazaborolidines with smaller wingtip substituents (e.g. tolyl or ^{i}Pr).

The synthesis of neutral [Ge_9{Si(TMS)$_3$}$_3$PRR^I] (*R*, R^I: small alkyl or alkenyl; Scheme 4.2 b) and anionic [Ge_9{Si(TMS)$_3$}$_2$PRR^I]$^-$ (*R*, R^I: medium or large alkyl, alkenyl, aryl, aminoalkyl; Scheme 4.2 c) mixed phosphine-functionalized [Ge_9] clusters was achieved by reaction of [Ge_9{Si(TMS)$_3$}$_n$]$^{(4-n)-}$ (*n*: 2, 3) with the chlorophosphines RR^IPCl (*R*, R^I: alkyl, alkenyl, aryl, aminoalkyl). The phosphanyl moieties are attached at the [Ge_9] clusters *via* single *exo* Ge-P bonds. The introduction of [PRR^I]$^+$ (*R*, R^I: small alkyl or alkenyl) groups as fourth ligands to [Ge_9{Si(TMS)$_3$}$_3$]$^-$ provides an easy access to neutral [Ge_9] cluster compounds bearing exclusively transition-metal-free substituents. Moreover, the principle of phosphine-functionalization of [Ge_9] was validated for a series of anionic mixed-functionalized [Ge_9] clusters with medium-sized phosphanyl groups by subsequent reactions with the coinage metal NHC complex NHC^{Dipp}CuCl. These examinations yielded a series of charge neutral zwitterionic compounds [(Ge_9{Si(TMS)$_3$}$_2$)R_2P]CuNHC^{Dipp} (*R*: medium-sized substituent; Scheme 4.2 d) comprising P-Cu interactions. The zwitterionic nature of the obtained compounds with the negative charge being distributed over the [Ge_9] core and the positive charge at Cu was confirmed by quantum chemical calculations. Therefore, these phosphine-functionalized [Ge_9] cluster anions can also be regarded as suitable ligands for the straightforward synthesis of zwitterionic compounds upon coordination of a cationic transition-metal fragment with their phosphanyl moiety. However, it was found that the

reactivity of these phosphine-functionalized [Ge_9] clusters depends on the steric impact of the attached phosphanyl substituents, as reactions of mixed phosphine-functionalized [Ge_9] clusters with larger phosphanyl moieties yielded [Ge_9] cluster coinage metal NHC complexes [$NHC^{Dipp}Cu(\eta^3\text{-}Ge_9\{Si(TMS)_3\}_2PR_2)$] (*R*: large substituent) with Ge-Cu instead of P-Cu interactions. Additionally, the attached phosphanyl groups can also participate in the linkage of [Ge_9] clusters, which was shown by the isolation of the dimeric species [$\{Si(TMS)_3\}_2Ge_9\{(^tBu)_2PCu\}_2Ge_9\{Si(TMS)_3\}_2$].

Finally, the synthesis of the multiple-phosphine functionalized [Ge_9] clusters [$Ge_9\{PRR^I\}_3]^-$ (*R*: N^iPr_2, R^I: N^iPr_2 or ^{t}Bu; Scheme 4.2 e) was achieved by heterogenous reaction of K_4Ge_9 with $(^iPr_2N)_2PCl$ or $^tBu(^iPr_2N)PCl$. The respective investigations indicated that multiple phosphine-functionalized [Ge_9] clusters are exclusively accessible with a few medium-sized phosphanyl groups since reactions of K_4Ge_9 with chlorophosphines bearing smaller substituents (reduction to diphosphines) or larger substituents (no reaction) were not successful. Subsequent reactions of the multiple phosphine-functionalized [Ge_9] clusters with $NHC^{Dipp}CuCl$ yielded neutral species [$NHC^{Dipp}Cu(\eta^3\text{-}Ge_9\{P(N^iPr_2)_2\}_3)$] or [$NHC^{Dipp}Cu(\eta^3\text{-}Ge_9\{P(N^iPr_2)^tBu\}_3)$], which allowed for the crystallization and crystallographic characterization of the threefold phosphanyl decorated [Ge_9] cages, and their structure could be determined to be analogous to the respective tris-silylated [Ge_9] cluster $[Ge_9\{Si(TMS)_3\}_3]^-$ (chapter 1.3.2.2). Investigations on the reactivity of [$NHC^{Dipp}Cu(\eta^3\text{-}Ge_9\{P(N^iPr_2)_2\}_3)$] towards $Cr(CO)_5$(thf) yielded the first neutral fivefold coordinated [Ge_9] cluster compound [$(NHC^{Dipp}Cu)_2(\eta^3,\eta^3\text{-}Ge_9\{P(N^iPr_2)_2\}_2Cr(CO)_5)$] and revealed that the multiple phosphine-functionalized [Ge_9] clusters can undergo ligand exchange reactions at the [Ge_9] core. This property might be of interest with respect to the introduction of novel substituents to the [Ge_9] core, which cannot be directly attached to bare $[Ge_9]^{4-}$ clusters. Moreover, reactions of the multiple-phosphine functionalized [Ge_9] cluster anion $[Ge_9\{P(N^iPr_2)^tBu\}_3]^-$ with Group 6 element carbonyl complexes $M(CO)_5$(thf) (*M*: Cr, Mo, W) yielded multiple [$M(CO)_5$] fragments coordinated [Ge_9] cluster species according to ESI-MS examinations. However, it is not completely clear yet, whether the [$M(CO)_5$] fragments interact with the attached phosphanyl groups (P-*M* bonds) or directly with the [Ge_9] cluster core (Ge-*M* bonds). Therefore, further investigations are necessary to unambiguously prove that the phosphanyl moieties of the multiple phosphine-functionalized [Ge_9] clusters can also be approached by Lewis acidic transition metal fragments. Scheme 4.2 provides a representative selection of species obtained by reactions of [Ge_9] clusters with main-group element compounds (and subsequent reaction with $NHC^{Dipp}CuCl$ in case of d) within this work.

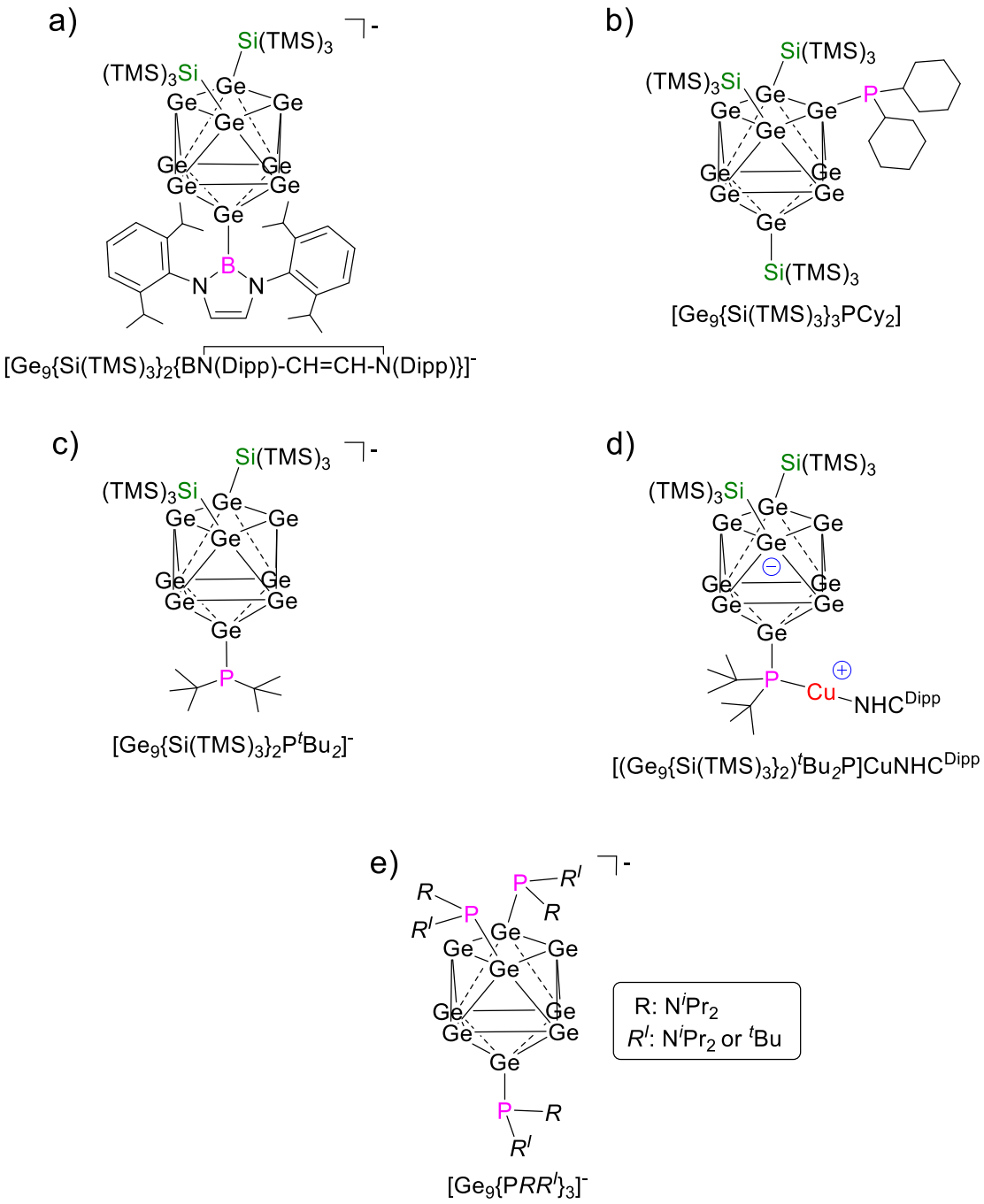

Scheme 4.2: Representative selection of species obtained by reaction of $[Ge_9\{Si(TMS)_3\}_n]^{(4-n)-}$ (*n*: 2, 3) cages or bare $[Ge_9]^{4-}$ clusters with main-group element compounds (and subsequent reaction with $NHC^{Dipp}CuCl$ for d) within this work.

Conclusion

Coinage metal NHC complexes NHC-*M*-Cl (*M*: Cu, Ag, Au) were identified as suitable precursors for the introduction of [NHC-*M*]$^+$ (*M*: Cu, Ag, Au) moieties at bare [*E*$_9$]$^{4-}$ (*E*: Si, Sn) and silylated [Ge$_9$] clusters. The synthesis of [NHC^{Dipp}Cu(η^4-Si$_9$)]$^{3-}$ and its transfer to solvents different from NH$_3$(l) is of special interest with respect to an extension of the silicide cluster chemistry. Moreover, the cleavage of the Cu-NHC bond, which is observed at room temperature, might lead to novel endohedral [Si$_9$] cluster anions or polymeric coinage metal linked [Si$_9$] cluster chains. The respective species could be candidates for the fabrication of core-shell nanoparticles or nanostructured silicon-based materials.

The step-by-step formation of larger intermetalloids consisting of coinage metal cation bridged [Sn$_9$]$^{4-}$ clusters, which has been achieved within this work for [(η^4-Sn$_9$)Ag(η^1-Sn$_9$)]$^{7-}$, might lead to new alloy-like materials or quantum dots. Regarding heavier elements such materials might be of interest for thermoelectric applications.

Moreover, the isolation of two novel Ti(III)-germanide complexes gave further insights into the reactivity of negatively charged Group 14 element *Zintl* clusters towards early transition metal complexes and the obtained species might be used as starting point for the formation of nanostructured, semiconducting three-dimensional networks.

Furthermore, the syntheses of [Ge$_9${Si(TMS)$_3$}$_2$*ER*$_2$]$^-$ (*E*: B, Al; *R*: substituent) indicated that Group 13 element complexes *R*$_2$*E*-Br (*E*: B, Al; *R*: substituent) are potential precursors for the attachment of stabilizing [*ER*$_2$]$^+$ groups at [Ge$_9$]. The resulting species might be interesting with respect to the formation of frustrated Lewis pairs in combination with bulky Lewis bases (e.g. phosphines). In this context, the introduction of both groups [*ER*$_2$]$^+$ (*E*: B, Al) and [P*R*$_2$]$^+$ (*R*: bulky substituent) at [Ge$_9$] might yield intramolecular frustrated Lewis pairs. In general, frustrated Lewis pairs are interesting with respect to small molecule activation and catalysis. Finally, the phosphine-functionalization of silylated [Ge$_9$] clusters and bare [Ge$_9$]$^{4-}$ cages paves the path for a completely new subsequent chemistry of the [Ge$_9$] clusters through the attached *exo* ligand(s). The novel mixed phosphine-functionalized [Ge$_9$] cages represent an interesting novel class of bulky phosphine ligands. Besides being strong σ-donors, these species are also suitable for the straightforward synthesis of zwitterionic organometallic complexes upon coordination to a transition metal cation. Therefore, the resulting compounds are potential candidates for catalytic applications. Moreover, multiple phosphine-functionalized [Ge$_9$] clusters might be applied as building blocks for organometallic frameworks due to their potential capability to bind several transition metal fragements *via* their phosphine moieties. Such frameworks might be of interest with respect to gas storage (e.g. methane or hydrogen) or catalytic applications (in analogy to zeolites). However, further investigations on the availability of the attached phosphanyl groups for interactions with Lewis acids are necessary.

5 Publications and Manuscripts

5.1 Low oxidation state silicon clusters – synthesis and structure of $[NHC^{Dipp}Cu(\eta^4\text{-}Si_9)]^{3-}$

F. S. Geitner, T. F. Fässler*

published in

Chem. Commun. **2017**, *53*, 12974.

Content and Contributions

The scope of this work was the evaluation of the reactivity of the silicide phases $A_{12}Si_{17}$ (*A*: alkali metal) towards coinage metal NHC complexes $NHC^{Dipp}MCl$ (*M*: Cu, Ag, Au), with the aim to introduce $[NHC^{Dipp}M]^+$ moieties at the $[Si_9]^{4-}$ clusters in order to enhance their stability and solubility. Reactions of the *Zintl* phases $K_{12}Si_{17}$, $K_6Rb_6Si_{17}$ or $Rb_{12}Si_{17}$ with NHC-*M*-Cl (*M*: Cu, Ag, Au) were carried out at -70 °C in NH_3(l) in the presence of [2.2.2]-cryptand. In reactions of the silicide phases with the respective Ag-NHC or Au-NHC compounds, oxidation of the $[Si_9]^{4-}$ clusters to $[Si_9]^{3-}$ occurred, manifested by the isolation of single crystals of the composition $[A(2.2.2\text{-crypt})]_3[Si_9]$ (*A*: alkali metal). By contrast, reactions of the silicide *Zintl* phases with $NHC^{Dipp}CuCl$ exclusively yielded single crystals of the composition $A_3[A(2.2.2\text{-crypt})]_3[NHC^{Dipp}Cu(\eta^4\text{-}Si_9)]_2$ (*A*: alkali metal). The $[NHC^{Dipp}Cu]^+$ fragments are attached to the $[Si_9]$ clusters *via* their open *pseudo* square face. $[NHC^{Dipp}Cu(\eta^4\text{-}Si_9)]^{3-}$ can be transferred to pyridine or acetonitrile solution, which is manifested by ESI-MS studies and NMR examinations. However, NMR examinations indicate that $[NHC^{Dipp}Cu(\eta^4\text{-}Si_9)]^{3-}$ is not stable in solution at room temperature and the cleavage of the Cu-NHC bond occurs. Reactions of $K_{12}Si_{17}$ with further Cu-NHC complexes $NHC^{Mes}CuCl$ and $NHC^{iPr}CuCl$ (bearing NHC ligands with different wingtip substituents) revealed that the introduction of various $[Cu\text{-}NHC]^+$ fragments to $[Si_9]^{4-}$ is possible. However, the resulting species were not crystallized to date and could exclusively be monitored in ESI-MS examinations, yet. The publication was written in course of this thesis.

ChemComm

COMMUNICATION

View Article Online
View Journal | View Issue

Cite this: *Chem. Commun.*, 2017, 53, 12974

Received 16th October 2017,
Accepted 11th November 2017

DOI: 10.1039/c7cc07995h

rsc.li/chemcomm

Low oxidation state silicon clusters – synthesis and structure of $[NHC^{Dipp}Cu(\eta^4\text{-}Si_9)]^{3-}$†

Felix S. Geitner[a] and Thomas F. Fässler *[b]

The reaction of $NHC^{Dipp}CuCl$ with the silicide phases $A_{12}Si_{17}$ (A: K, K/Rb, Rb) in NH_3(l) yields $[NHC^{Dipp}Cu(\eta^4\text{-}Si_9)]^{3-}$ (1) as only the third example of a substituted $[Si_9]$ cluster. The corresponding salts $A_3[A(2.2.2\text{-crypt})]_3[NHC^{Dipp}Cu(\eta^4\text{-}Si_9)]_2{\cdot}26NH_3$ (A: K (1a), K/Rb (1b), Rb (1c)) crystallize isostructurally in the space group $P\bar{1}$ and have been characterized by single crystal structure determination. ESI-MS and NMR experiments reveal that the anion $[NHC^{Dipp}Cu(\eta^4\text{-}Si_9)]^{3-}$ can also be transferred to pyridine or acetonitrile solutions at low temperature. However, at room temperature dissociation under the release of the NHC ligand occurs. Variation of the NHC ligand in the $[Cu{-}NHC]^+$-substituted silicide clusters is possible, whereas the reactions of $K_{12}Si_{17}$ with the corresponding $NHC^{Dipp}MCl$ (M: Ag, Au) complexes result in a partial oxidation of the silicide clusters, without attachment of $[M{-}NHC]^+$, yielding $[Si_9]^{3-}$ species.

Nowadays silicon is a key component in almost every electronic device of our daily life, and since silicon is an abundant, inexpensive and nontoxic semiconducting material, the field of application of silicon-based materials is growing continuously. Thereby, nanoparticles or nanostructured materials with unique morphologies are of particular interest. Due to their modified properties, these materials could cover a broad range of applications such as microelectronics, anode materials, solar cells or optoelectronics.[1–5] In this context, the synthesis of silicon cluster compounds as tailor-made nano-scale silicon building blocks might play an important role in the future. A series of such silicon cluster compounds, comprising the so called siliconoid clusters,[6] which are neutral silicon clusters with unsaturated silicon atoms, or a [20]silafullerane with a Si_{20}-core,[7] has been reported.[6–15] However, the synthesis of such compounds often requires multi-step reactions.[16] By contrast, *Zintl* phases of alkali metals, which already contain preformed polyatomic silicon clusters, can be obtained in quantitative yield *via* a solid state reaction from the elements.[17,18] To date, silicide phases of the compositions A_4Si_4 (A: alkali metal; containing $[Si_4]^{4-}$ clusters) and $A_{12}Si_{17}$ (containing $[Si_4]^{4-}$ and $[Si_9]^{4-}$ clusters) are known, whereas the respective A_4E_9 phase (A: alkali metal, E: tetrel element), which is accessible for the heavier tetrel homologues Ge–Pb, has not been obtained for silicon yet. In comparison to the A_4Si_4 phases which are sparingly soluble in any solvent, the $A_{12}Si_{17}$ phases are sufficiently soluble in NH_3(l), as shown by the isolation of a number of solvate structures from this solvent, consisting of polyatomic silicon clusters with exclusively unsubstituted vertices.[19–21] Because of their high negative charges, these silicide clusters are poorly soluble in common solvents and also reveal a high lability towards air or moisture. In order to overcome these problems, the charge of the clusters has to be decreased, which can be achieved by the introduction of positively charged substituents. However, in contrast to the heavier congeners Ge–Pb, for which a broad range of substitution reactions has been published,[22,23] only three examples have been reported for silicide clusters to our knowledge, namely $[PhZn(\eta^4\text{-}Si_9)]^{3-}$,[24] $[Ni(CO)_2(\mu\text{-}Si_9)_2]^{3-}$[8,25,26] and $[(MesCu)_2(\eta^3\text{-}Si_4)]^{4-}$.[27] The isolation of these species has shown that both silicide clusters ($[Si_9]$ and $[Si_4]$) can be functionalized with organometallic fragments. Moreover, the identification of $[Si_4]$ cluster units in ^{29}Si NMR examinations of ammonia solutions of the precursor phase $K_6Rb_6Si_{17}$,[28] as well as the isolation of the solvate compounds $K_8[Si_4][Si_9]{\cdot}14NH_3$[21] and $Rb_{1.2}K_{2.8}[Si_4]{\cdot}7NH_3$[29] have unambiguously revealed the presence of both silicide cluster species in solution.

Recently, we were able to attach $[M{-}NHC]^+$ (M: Cu, Ag, Au) fragments to bare $[Sn_9]^{4-}$ cluster units and to a series of silylated $[Ge_9]$ *Zintl* anions. In contrast to neutral metal–ligand fragments (*e.g.* CuMes) attached to *Zintl* clusters, the introduction of $[M{-}NHC]^+$ fragments yields products with decreased charge (increased stability and solubility). In consequence we expect better solubility in less polar solvents allowing for a larger

[a] *WACKER-Institute for Silicon Chemistry and Department of Chemistry, Technische Universität München, Lichtenbergstraße 4, 85747 Garching, Germany*
[b] *Department of Chemistry, Technische Universität München, Lichtenbergstraße 4, 85747 Garching, Germany. E-mail: thomas.faessler@lrz.tum.de*

† Electronic supplementary information (ESI) available: Detailed synthetic procedures and crystallographic data for compounds **1a** and **1b**. CCDC 1566679 and 1566680. For ESI and crystallographic data in CIF or other electronic format see DOI: 10.1039/c7cc07995h

variety of following-up reactions. Furthermore, the strong coinage metal NHC bond allows for the formation of stable *Zintl* ion complexes.[30–33] In continuation of these studies, we investigated the reactivity of coinage metal carbene complexes towards the silicide phases $A_{12}Si_{17}$ (A: alkali metal).

The reactions of the silicides $K_{12}Si_{17}$, $K_6Rb_6Si_{17}$ and $Rb_{12}Si_{17}$ with $NHC^{Dipp}MCl$ (M: Cu, Ag, Au) were carried out in NH_3(l) in the presence of [2.2.2-crypt]. In a typical procedure, ammonia was condensed onto the mixtures of the reactants, instantly leading to the formation of deep red suspensions. The storage of these suspensions at −70 °C resulted in the formation of single crystals suitable for single crystal X-ray diffraction within three months. Single crystal X-ray diffraction examination revealed that the reactions of the silicide phases with $NHC^{Dipp}MCl$ (M: Ag, Au) led, in accordance with the trend in redox potentials, to a partial oxidation of the cluster units (without the attachment of a coinage metal NHC moiety) and the formation of $[A(2.2.2\text{-crypt})]_3[Si_9]$, containing bare $[Si_9]^{3-}$ clusters.[19] By contrast, similar reactions of the silicide phases with $NHC^{Dipp}CuCl$ exclusively yielded red block-shaped single crystals containing the novel anion $[NHC^{Dipp}Cu(\eta^4\text{-}Si_9)]^{3-}$ (Scheme 1). The obtained salts crystallize isostructurally as $A_3[A(2.2.2\text{-crypt})]_3[NHC^{Dipp}Cu(\eta^4\text{-}Si_9)]_2{\cdot}26NH_3$ with A = K (**1a**), K/Rb (**1b**), and Rb (**1c**) in the space group $P\bar{1}$. Each unit cell contains two crystallographically independent $[NHC^{Dipp}Cu(\eta^4\text{-}Si_9)]^{3-}$ clusters (**A** and **B**, Fig. 1a). However, for compound **1c** only rather small crystals were obtained, which in fact allowed for the determination of the unit cell volume, but the refinement of the X-ray data resulted only in a crude structure model which, nevertheless, revealed the structural similarity to **1a** and **1b**. As expected, the unit cell volume increases with increasing mass of the alkali metal cations (V_{cell}(**1a**) < V_{cell}(**1b**) < V_{cell}(**1c**); ESI†). The $[Si_9]^{4-}$ clusters in **1a** and **1b** show almost perfect C_{4v}-symmetry and coordinate the $[Cu\text{–}NHC^{Dipp}]^+$ fragments *via* their open square faces in a η^4-bonding mode, with mean Cu–Si distances of 2.4235(9) Å (**1a-A**), 2.4394(9) Å (**1a-B**), 2.424(1) Å (**1b-A**), and 2.439(1) Å (**1b-B**) (Fig. 1). The observed Cu–Si distances are in the range of respective bond lengths in $[(MesCu)_2(\eta^3\text{-}Si_4)]^{4-}$ (Cu–Si distances between 2.351 Å and 2.548 Å) and other previously reported data.[27,34,35] The Si–Si distances range between 2.412(1) Å (Si3–Si7) and 2.664(1) Å (Si2–Si3) in **1a**, and between 2.408(2) Å (Si13–Si16) and 2.663(2) Å (Si2–Si3) in **1b**, and are in the range of previously reported data for $[Si_9]$ clusters (ESI†).[16–18] The two crystallographically independent $[NHC^{Dipp}Cu(\eta^4\text{-}Si_9)]^{3-}$ (**1**) clusters, which reveal a different

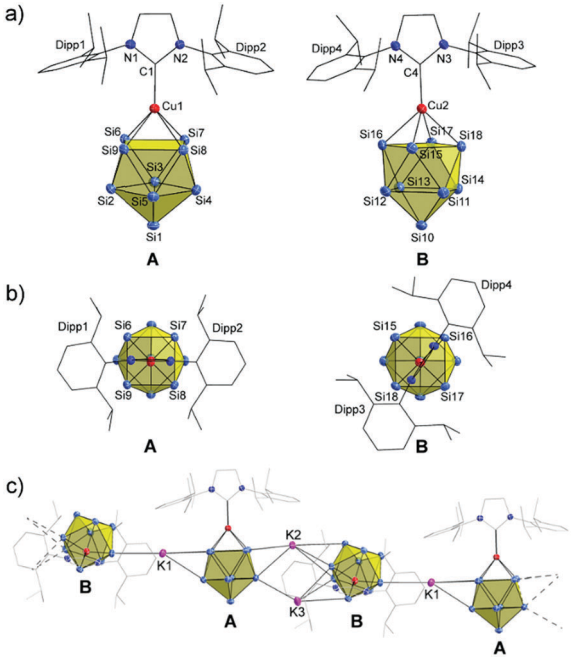

Fig. 1 (a) The molecular structures of the two crystallographically independent $[NHC^{Dipp}Cu(\eta^4\text{-}Si_9)]^{3-}$ clusters **A** and **B** in **1a**. (b) The two different orientations of the $[Cu\text{-}NHC^{Dipp}]^+$ moieties with respect to the $[Si_9]^{4-}$ core in clusters **A** and **B**. (c) Linear strands of K^+-connected $[NHC^{Dipp}Cu(\eta^4\text{-}Si_9)]^{3-}$ clusters **A** and **B** in **1a**. K–Si distances range between 3.4017(1) Å (K2–Si7) and 3.6500(1) Å (K1–Si9). All ellipsoids are shown at a 50% probability level. For clarity reasons, protons and solvent molecules are omitted, and carbon atoms are pictured as grey wires and sticks. Selected bond lengths and angles, and respective pictures for compound **1b**, as well as full ellipsoid molecular structures of **1a** and **1b** are provided in the ESI.†

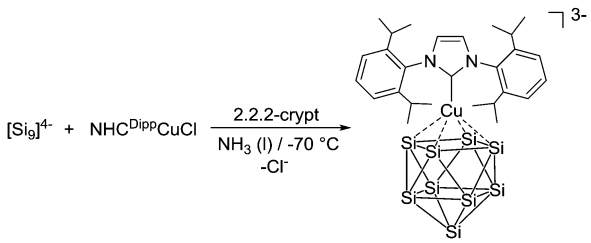

Scheme 1 The reaction of $[Si_9]^{4-}$ with $NHC^{Dipp}CuCl$ in the presence of [2.2.2-crypt] in NH_3(l) yielding $[NHC^{Dipp}Cu(\eta^4\text{-}Si_9)]^{3-}$.

orientation of the NHC^{Dipp} moiety with respect to the $[Si_9]$ core, are interconnected to linear strands by alkali metal cation bridges (Fig. 1b and c).

Note that in compound **1b**, which contains two different cations (K^+ and Rb^+), the cluster species are bridged exclusively by the Rb^+ cations, whereas the K^+ cations are sequestered by [2.2.2-crypt] (ESI†).

For further analytics (ESI-MS, NMR) the solvent (ammonia) was removed from reaction mixtures, in which previously single crystals of compound **1a** had been found. Treating the resulting brownish residue with pyridine or acetonitrile, significant amounts (approx. 60%) could be dissolved. In ESI-MS examinations, carried out with pyridine solutions, a signal was detected at m/z = 705.1, which can be assigned to $\{[NHC^{Dipp}CuSi_9]^{3-} + 2H^+\}^-$. A second signal at m/z = 1155.2 corresponds to the species $\{[(NHC^{Dipp}Cu)_2Si_9]^{2-} + H^+\}^-$ which might have formed during the ionization process (Fig. 2).

In ^{1}H NMR experiments carried out with acetonitrile extracts, $[NHC^{Dipp}Cu(\eta^4\text{-}Si_9)]^{3-}$ (**1**) was detected besides free carbene. The proton spectrum of **1** reveals a significant splitting in the shift values of the signals assigned to the methyl protons of the diisopropylphenyl wingtips of the NHC^{Dipp} ligand, which is typical for a $[Cu\text{–}NHC^{Dipp}]^+$ fragment attached to a *Zintl* cluster.[31–33] The monitoring of silicide cluster species in solution *via* attached groups is of special interest, since detection of Si atoms of the

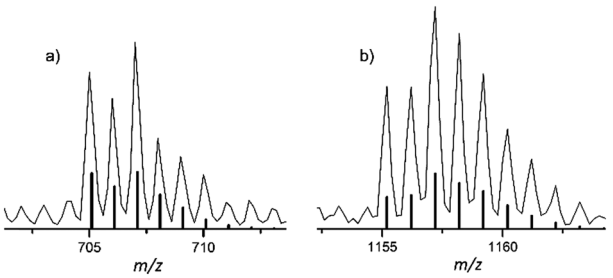

Fig. 2 Selected areas of the ESI-MS spectrum obtained examining a pyridine extract. (a) $\{[NHC^{Dipp}CuSi_9]^{3-} + 2H^+\}^-$ and (b) $\{[(NHC^{Dipp}Cu)_2Si_9]^{2-} + H^+\}^-$. Respective simulated spectra are pictured below as black bars. Spectra were acquired in the negative ion mode (4500 V, 300 °C).

$[Si_9]$ cluster core in solution in ^{29}Si NMR experiments has not been successful to date. The single signal observed in ^{29}Si-NMR experiments of ammonia solutions of $K_6Rb_6Si_{17}$ had been assigned to $[Si_4]$ clusters.[28]

For subsequent ^1H NMR experiments, the sample was washed with toluene prior to the extraction with acetonitrile in order to remove the free carbene NHC^{Dipp}, which then led to a spectrum of almost pure **1** (ESI†). However, the signals assigned to **1** disappear within 46 h at room temperature, and simultaneously signals assigned to free carbene NHC^{Dipp} arise. The red colour indicative of the presence of *Zintl* clusters in solution is retained during this process. Storing the sample at low temperature (−32 °C), this degradation can be retarded and **1** can be monitored besides free carbene after 1 week.

Analogous reactions were carried out with different NHC ligands (NHC^{Mes} (mes = mesityl) and NHC^{iPr} (^{i}Pr = isopropyl)), but did not lead to crystalline materials yet. However, the pyridine-soluble parts of the remaining residues after the removal of ammonia revealed the characteristic ESI-MS signals of the corresponding products (*m*/*z* 621.1 $\{[NHC^{Mes}Cu(\eta^4\text{-}Si_9)]^{3-} + 2H^+\}^-$ or *m*/*z* 469.1 $\{[NHC^{iPr}Cu(\eta^4\text{-}Si_9)]^{3-} + 2H^+\}^-$; ESI†).

It is noteworthy that within this work we exclusively observed products of the reaction between the organometallic $[Cu–NHC]^+$ moieties and $[Si_9]^{4-}$, whereas in previous studies, the reaction of equimolar amounts of $K_6Rb_6Si_{17}$ with mesitylcopper (MesCu) in NH_3(l) solely yielded di(mesitylcopper)-stabilized tetrasilicide tetraanions $[(MesCu)_2(\eta^3\text{-}Si_4)]^{4-}$.[27] The formation of different products from the reaction of the silicide phases $A_{12}Si_{17}$ (A: alkali metal) with these two different types of organometallic Cu^+ complexes can be rationalized as follows: the reaction between the silicide clusters and MesCu corresponds to a coordination of a neutral MesCu fragment to the silicide cluster which, however, might be a reversible process. Hence, interactions between the $[Si_9]$ units and MesCu might also take place in solution, but only the two-fold MesCu-coordinated $[Si_4]$ clusters crystallize from ammonia solution. By contrast, the reaction of $NHC^{Dipp}CuCl$ with the silicide clusters occurs *via* a salt metathesis reaction under the formation of potassium chloride, which prevents such a reversibility. Furthermore, the increased steric impact of an NHC ligand compared to a mesityl ligand might favor an interaction of this unit with the larger $[Si_9]^{4-}$ clusters.

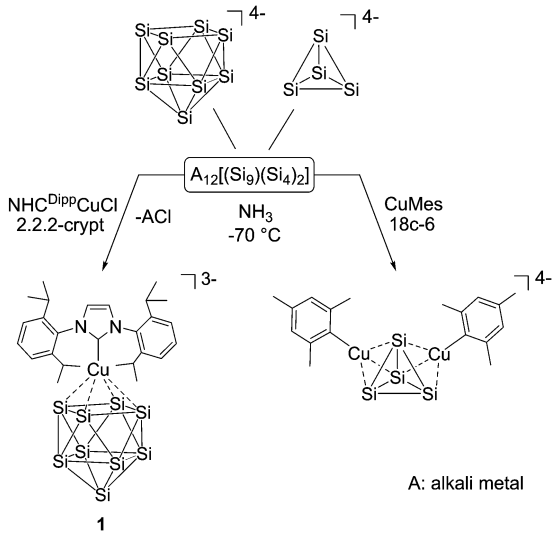

Scheme 2 Different products obtained from the reaction of varying organometallic Cu^+ complexes with the silicide phases $A_{12}Si_{17}$ (A: alkali metal) in NH_3(l).[27]

In summary, within this work we describe the reaction between $[Si_9]^{4-}$ clusters and $[Cu\text{-}NHC^{Dipp}]^+$ units obtaining the three-fold negatively charged species $[NHC^{Dipp}Cu(\eta^4\text{-}Si_9)]^{3-}$ using $A_{12}Si_{17}$ (A: K, K/Rb, Rb) and $NHC^{Dipp}CuCl$ as starting materials. The salts crystallize isostructurally as $A_3[A(2.2.2\text{-crypt})]_3[NHC^{Dipp}Cu(\eta^4\text{-}Si_9)]_2$ with A: K (**1a**), K/Rb (**1b**) and Rb (**1c**). The anionic unit **1** can be transferred to other solvents than NH_3(l) such as pyridine or MeCN, which allows for its further characterization *via* ESI-MS and NMR experiments. $[NHC^{Dipp}Cu(\eta^4\text{-}Si_9)]^{3-}$ is quite stable in solution at low temperatures, whereas at room temperature a rapid cleavage of the Cu–NHC bond is observed. Furthermore, the attachment of different $[Cu–NHC]^+$ fragments at the $[Si_9]$ unit was achieved, whereas, analogous reactions of the silicide phases with the respective $NHC^{Dipp}MCl$ (M: Ag, Au) complexes led to an oxidation of the cluster units without attachment of an $[M\text{-}NHC]^+$ moiety. Moreover, the isolation of the novel compounds **1a–1c** reveals different reactivity patterns for varying organometallic Cu^+-complexes towards the silicide phases $A_{12}Si_{17}$ (Scheme 2).

This work was financially supported by WACKER Chemie AG. F. G. thanks MSc Lorenz Schiegerl for measurements of the ESI-MS spectra, Dr Wilhelm Klein for help with crystallographic issues and TUM graduate school for support.

Conflicts of interest

There are no conflicts to declare.

References

1 M. Ashuri, Q. He and L. L. Shaw, *Nanoscale*, 2016, **8**, 74.
2 M. G. Kanatzidis, *Adv. Mater.*, 2007, **19**, 1165.
3 R. A. Bley and S. M. Kauzlarich, *J. Am. Chem. Soc.*, 1996, **118**, 12461.
4 C. Eun-Chel, P. Sangwook, H. Xiaojing, S. Dengyuan, C. Gavin, P. Sang-Cheol and A. G. Martin, *Nanotechnology*, 2008, **19**, 245201.
5 L. T. Canham, *Appl. Phys. Lett.*, 1990, **57**, 1046.
6 P. Willmes, K. Leszczyńska, Y. Heider, K. Abersfelder, M. Zimmer, V. Huch and D. Scheschkewitz, *Angew. Chem., Int. Ed.*, 2016, **55**, 2907.

7 J. Tillmann, J. H. Wender, U. Bahr, M. Bolte, H.-W. Lerner, M. C. Holthausen and M. Wagner, *Angew. Chem., Int. Ed.*, 2015, **54**, 5429–5433.
8 D. Scheschkewitz, *Angew. Chem., Int. Ed.*, 2005, **44**, 2954.
9 K. Abersfelder, A. J. P. White, H. S. Rzepa and D. Scheschkewitz, *Science*, 2010, **327**, 564–566.
10 K. Abersfelder, A. J. P. White, R. J. F. Berger, H. S. Rzepa and D. Scheschkewitz, *Angew. Chem., Int. Ed.*, 2011, **50**, 7936.
11 K. Abersfelder, A. Russell, H. S. Rzepa, A. J. P. White, P. R. Haycock and D. Scheschkewitz, *J. Am. Chem. Soc.*, 2012, **134**, 16008.
12 J. Jeck, I. Bejan, A. J. P. White, D. Nied, F. Breher and D. Scheschkewitz, *J. Am. Chem. Soc.*, 2010, **132**, 17306.
13 G. Fischer, V. Huch, P. Mayer, S. K. Vasisht, M. Veith and N. Wiberg, *Angew. Chem., Int. Ed.*, 2005, **44**, 7884.
14 A. Tsurusaki, C. Iizuka, K. Otsuka and S. Kyushin, *J. Am. Chem. Soc.*, 2013, **135**, 16340.
15 A. Tsurusaki, J. Kamiyama and S. Kyushin, *J. Am. Chem. Soc.*, 2014, **136**, 12896.
16 C. Präseng and D. Scheschkewitz, in *Functional Molecular Silicon Compounds II*, Struc Bond 155, ed. D. Scheschkewitz, Springer, Berlin, 2014, pp. 1–47.
17 *Zintl Phases: Principles and Recent Developments*, Struc Bond 139, ed. T. F. Fässler, Springer, Heidelberg, 2011.
18 T. F. Fässler in *Zintl Ions: Principles and Recent Developments*, Struc Bond 139, ed. T. F. Fässler, Springer, Heidelberg, 2011, pp. 91–132.
19 J. M. Goicoechea and S. C. Sevov, *J. Am. Chem. Soc.*, 2004, **126**, 6860.
20 S. Joseph, C. Suchentrunk, F. Kraus and N. Korber, *Eur. J. Inorg. Chem.*, 2009, 4641.
21 C. B. Benda, T. Henneberger, W. Klein and T. F. Fässler, *Z. Anorg. Allg. Chem.*, 2017, **643**, 146.
22 S. Scharfe, F. Kraus, S. Stegmaier, A. Schier and T. F. Fässler, *Angew. Chem., Int. Ed.*, 2011, **50**, 3630.
23 S. C. Sevov and J. M. Goicoechea, *Organometallics*, 2006, **25**, 5678.
24 J. M. Goicoechea and S. C. Sevov, *Organometallics*, 2006, **25**, 4530.
25 S. Joseph, M. Hamberger, F. Mutzbauer, O. Härtl, M. Meier and N. Korber, *Angew. Chem., Int. Ed.*, 2009, **48**, 8770.
26 S. Gärtner, M. Hamberger and N. Korber, *Crystals*, 2015, **5**, 275.
27 M. Waibel, F. Kraus, S. Scharfe, B. Wahl and T. F. Fässler, *Angew. Chem., Int. Ed.*, 2010, **49**, 6611.
28 M. Neumeier, F. Fendt, S. Gärtner, C. Koch, T. Gärtner, N. Korber and R. M. Gschwind, *Angew. Chem., Int. Ed.*, 2013, **52**, 4483.
29 C. Lorenz, S. Gärtner and N. Korber, *Z. Anorg. Allg. Chem.*, 2017, **643**, 141.
30 F. S. Geitner, W. Klein and T. F. Fassler, *Dalton Trans.*, 2017, **46**, 5796.
31 F. S. Geitner and T. F. Fässler, *Eur. J. Inorg. Chem.*, 2016, 2688.
32 L. J. Schiegerl, F. S. Geitner, C. Fischer, W. Klein and T. F. Fässler, *Z. Anorg. Allg. Chem.*, 2016, **642**, 1419.
33 F. S. Geitner, M. A. Giebel, A. Pöthig and T. F. Fässler, *Molecules*, 2017, **22**, 1204.
34 K. W. Klinkhammer, J. Klett, Y. Xiong and S. Yao, *Eur. J. Inorg. Chem.*, 2003, 3417.
35 G. Tan, B. Blom, D. Gallego, E. Irran and M. Driess, *Chem. – Eur. J.*, 2017, **20**, 9400.

Low Oxidation State Silicon Clusters – Synthesis and Structure of $[NHC^{Dipp}Cu(\eta^4\text{-}Si_9)]^{3-}$

Felix. S. Geitner,[a] Thomas. F. Fässler*[b]

[*b] Prof. Dr. Thomas. F. Fässler, Department of Chemistry, Technische Universität München Lichtenbergstraße 4, 85747 Garching/München, Germany

[a] Felix S. Geitner, WACKER Institute for Silicon Chemistry and Departement of Chemistry, Technische Universität München Lichtenbergstraße 4, 85747 Garching/München, Germany

Content

1. Experimental Section

1.1 General:

All manipulations were carried out under a purified argon atmosphere using standard Schlenk and glove box techniques. $K_{12}Si_{17}$, $K_6Rb_6Si_{17}$ and $Rb_{12}Si_{17}$ were prepared by fusion of stoichiometric amounts of the elements in sealed tantalum ampoules and stored under argon atmosphere. Imidazolium salts and NHC*M*Cl (*M*: Cu, Ag, Au; NHC: NHC^{Dipp}, NHC^{Mes} and NHC^{iPr}) were prepared according to modified literature procedures.[1-4] [2.2.2-crypt] was dried *in vacuo* overnight. Liquid ammonia was dried and stored over sodium metal. Anhydrous pyridine (VWR) was stored over molecular sieves prior to usage. All other solvents were obtained from a MBraun Grubbs apparatus.

1.2 Syntheses

1a: $K_{12}Si_{17}$ (71 mg, 0.075 mmol, 1 eq.), $NHC^{Dipp}CuCl$ (36.5 mg, 0.075 mmol, 1 eq.) and [2.2.2-crypt] (52 mg, 0.135 mmol, 1.86 eq.) were weighted into a Schlenk tube. Addition of ammonia (approximately 2 mL) led to the formation of a deep red suspension. The samples were stored in a freezer at -70 °C. Compound **1a** crystallizes as red block-shaped crystals in approx. 35 % yield (estimated by the amount of red crystalline material found in the sample).

1b: $K_6Rb_6Si_{17}$ (92 mg, 0.075 mmol, 1 eq.), $NHC^{Dipp}CuCl$ (36.5 mg, 0.075 mmol, 1 eq.) and [2.2.2-crypt] (52 mg, 0.135 mmol, 1.86 eq.) were weighted into a Schlenk tube. Addition of ammonia (approximately 2 mL) led to the formation of a deep red suspension. The samples were stored in a freezer at -70 °C. Compound **1b** crystallizes as red block-shaped crystals in approx. 30 % yield (estimated by the amount of red crystalline material found in the sample).

1c: $Rb_{12}Si_{17}$ (113 mg, 0.075 mmol, 1 eq.), $NHC^{Dipp}CuCl$ (36.5 mg, 0.075 mmol, 1 eq.) and [2.2.2-crypt] (52 mg, 0.135 mmol, 1.86 eq.) were weighted into a Schlenk tube. Addition of ammonia (approximately 2 mL) led to the formation of a deep red suspension. The samples were stored in a freezer at -70 °C. Compound **1c** crystallizes as red block-shaped crystals in approx. 30 % yield (estimated by the amount of red crystalline material found in the sample).

Reactions of $K_{12}Si_{17}$ with NHC^{Dipp}*M*Cl (*M*: Ag, Au)

$K_{12}Si_{17}$ (71 mg, 0.075 mmol, 1 eq.), NHC^{Dipp}*M*Cl (40.0 mg (*M*: Ag); 46.5 mg (*M*: Au), 0.075 mmol, 1 eq.) and [2.2.2-crypt] (52 mg, 0.135 mmol, 1.86 eq.) were weighted into a Schlenk tube. Addition of ammonia (approximately 2 mL) led to the formation of deep red suspensions. The samples were stored in a freezer at -70 °C. After 3 months, bright orange block-shaped were found, which were identified as $[K(2.2.2\text{-crypt})]_3[Si_9]$ by SC-XRD.[5]

Reactions of $K_{12}Si_{17}$ with NHC-CuCl (NHC: NHC^{Mes}, NHC^{iPr})

$K_{12}Si_{17}$ (71 mg, 0.075 mmol, 1 eq.), NHC-CuCl (30.3 mg (NHC: NHC^{Mes}); 18.0 mg (NHC: NHC^{iPr}), 0.075 mmol, 1 eq.) and [2.2.2-crypt] (52 mg, 0.135 mmol, 1.86 eq.) were weighted into a Schlenk tube. Addition of ammonia (approximately 2 mL) led to the formation of deep red suspensions. The samples were stored in a freezer at -70 °C overnight. Subsequently, ammonia was removed and the obtained solids were extracted with pyridine, yielding deep red suspensions. ESI-MS examinations of these solids revealed the attachment of the respective $[Cu\text{-}NHC]^+$ moieties to the $[Si_9]$ clusters. Selected areas of the acquired ESI-MS spectra are pictured in Figure SI 10.

1.3 Single Crystal Structure Determination

Crystal structure determination: The thermally very unstable, air and moisture sensitive crystals of **1a**-**1c** were transferred from the mother liquor into cooled perfluoroalkylether oil under a cold N_2 gas stream. For single crystal data collection, the single crystals were fixed on a glass capillary and positioned in a 120 K cold N_2 gas stream using the crystal cap system. Single crystal data collection was performed at an Oxford-Diffraction Xcalibur3 diffractometer ($Mo_{K\alpha}$ radiation). Structures were solved by Direct Methods (SHELXS-2014) and refined by full-matrix least-squares calculations against F^2 (SHELXL-2014).[6] Supplementary crystallographic data for this paper has been deposited with the Cambridge Structural database and are available free of charge via www.ccdc.cam.ac.uk/data_request/cif. In compound **1b** free refinement of the K and Rb postions gave a K/Rb ratio of 3.15/2.85. Furthermore, one Rb^+ cation (Rb1) is disordered and has been refined on split positions. Regarding compound **1c** only small crystals, which did not diffract very good were obtained. Hence, for **1c** only the unit cell volume and a crude structural model, confirming its similarity to compounds **1a** and **1b**, could be determined.

Table SI 1: Crystallographic data for compounds **1a** and **1b**.

Compound	**1a**	**1b**
formula	$Si_{18}Cu_2C_{108}H_{258}N_{10}O_{18}K_6 \cdot 26NH_3$	$Si_{18}Cu_2C_{108}H_{258}N_{10}O_{18}K_{3.15}Rb_{2.85} \cdot 26NH_3$
crystal size	0.5 x 0.45 x 0.35	0.35 x 0.30 x 0.15
fw (g·mol^{-1})	3216.79	3348.94
space group	$P\bar{1}$	$P\bar{1}$
***a* (Å)**	17.1066(3)	17.1296(4)
***b* (Å)**	18.1573(3)	18.1554(3)
***c* (Å)**	30.8056(5)	30.7960(5)
α (deg)	87.076(1)	86.899(1)
β (deg)	81.339(2)	81.149(2)
γ (deg)	65.383(2)	65.729(2)
***V* (Å^3)**	8598.9(3)	8626.5(3)
Z	2	2
***T* (K)**	120(2)	120(2)
λ (Å)	0.71073	0.71073
ρ_{calcd} (g·cm^{-3})	1.242	1.289
μ (mm^{-1})	0.580	1.308
collected reflections	238725	205952
independent reflections	33153	33838
R_{int} / R_δ	0.0780 / 0.0861	0.0943 / 0.1597
parameters / restraints	1709 / 30	1726 / 61
***R_1* [*I* > 2 σ(*I*) / all data]**	0.0418 / 0.0766	0.0443 / 0.1068
w*R_2* [*I* > 2 σ(*I*) / all data]	0.0962 / 0.1036	0.0967 / 0.1074
goodness of fit	0.900	0.823
max./min. diff. el. density (e / Å^{-3})	0.99/ -0.59	1.38/-0.78
CCDC	1566679	1566680

Table SI 2: Cell parameters and cell volume of compound **1c**.

Compound	**1c**
***a* (Å)**	17.139(3)
***b* (Å)**	18.180(4)
***c* (Å)**	30.822(6)
***α* (deg)**	87.02(3)
***β* (deg)**	81.27(3)
***γ* (deg)**	65.86(3)
***V* (Å^3)**	8661(4)

Table SI 3: Selected bond lengths of cluster **A** in compounds **1a** and **1b**:

1a-A		**1b-A**	
Bond	**Distance in [Å]**	**Bond**	**Distance in [Å]**
Cu1-Si6	2.4195(9)	Cu1-Si6	2.425(1)
Cu1-Si7	2.4186(9)	Cu1-Si7	2.417(1)
Cu1-Si8	2.4238(8)	Cu1-Si8	2.419(1)
Cu1-Si9	2.4321(9)	Cu1-Si9	2.436(1)
Cu1-C1	1.925(3)	Cu1-C1	1.931(4)
Si1-Si2	2.420(1)	Si1-Si2	2.422(2)
Si1-Si3	2.445(1)	Si1-Si3	2.446(2)
Si1-Si4	2.422(1)	Si1-Si4	2.416(2)
Si1-Si5	2.464(1)	Si1-Si5	2.460(2)
Si2-Si3	2.664(1)	Si2-Si3	2.663(2)
Si2-Si5	2.624(1)	Si2-Si5	2.622(2)
Si2-Si6	2.420(1)	Si2-Si6	2.421(2)
Si2-Si9	2.418(1)	Si2-Si9	2.420(2)
Si3-Si4	2.651(1)	Si3-Si4	2.644(2)
Si3-Si6	2.423(1)	Si3-Si6	2.422(2)
Si3-Si7	2.412(1)	Si3-Si7	2.412(2)
Si4-Si5	2.592(1)	Si4-Si5	2.595(2)
Si4-Si7	2.428(1)	Si4-Si7	2.425(2)
Si4-Si8	2.414(1)	Si4-Si8	2.410(2)
Si5-Si8	2.422(1)	Si5-Si8	2.416(2)
Si5-Si9	2.426(1)	Si5-Si9	2.426(2)
Si6-Si7	2.560(1)	Si6-Si7	2.545(2)
Si6-Si9	2.587(1)	Si6-Si9	2.585(2)
Si7-Si8	2.606(1)	Si7-Si8	2.614(2)
Si8-Si9	2.569(1)	Si8-Si9	2.568(2)

Table SI 4: Selected bond lengths of cluster **B** in compounds **1a** and **1b**:

1a-B		**1b-B**	
Bond	**Distance in [Å]**	**Bond**	**Distance in [Å]**
Cu2-Si15	2.4459(9)	Cu2-Si15	2.456(1)
Cu2-Si16	2.4243(9)	Cu2-Si16	2.415(1)
Cu2-Si17	2.4590(9)	Cu2-Si17	2.461(1)
Cu2-Si18	2.4283(9)	Cu2-Si18	2.424(1)
Cu2-C4	1.953(3)	Cu2-C4	1.943(4)
Si10-Si11	2.444(1)	Si10-Si11	2.442(2)
Si10-Si12	2.433(1)	Si10-Si12	2.434(2)
Si10-Si13	2.445(1)	Si10-Si13	2.451(2)
Si10-Si14	2.427(1)	Si10-Si14	2.428(2)
Si11-Si12	2.638(1)	Si11-Si12	2.645(2)
Si11-Si14	2.647(1)	Si11-Si14	2.644(2)
Si11-Si15	2.433(1)	Si11-Si15	2.427(2)
Si11-Si18	2.436(1)	Si11-Si18	2.432(2)
Si12-Si13	2.642(1)	Si12-Si13	2.635(2)
Si12-Si15	2.437(1)	Si12-Si15	2.438(2)
Si12-Si16	2.418(1)	Si12-Si16	2.415(2)
Si13-Si14	2.652(1)	Si13-Si14	2.657(2)
Si13-Si16	2.412(1)	Si13-Si16	2.408(2)
Si13-Si17	2.427(1)	Si13-Si17	2.425(2)
Si14-Si17	2.425(1)	Si14-Si17	2.425(2)
Si14-Si18	2.418(1)	Si14-Si18	2.424(2)
Si15-Si16	2.574(1)	Si15-Si16	2.568(2)
Si15-Si18	2.560(1)	Si15-Si18	2.545(2)
Si16-Si17	2.557(1)	Si16-Si17	2.553(2)
Si17-Si18	2.575(1)	Si17-Si18	2.574(2)

Table SI 5: Comparison of bond lengths and angles in compounds **1a** and **1b**:

Compound	**1a**		**1b**	
Cluster	**1a-A**	**1a-B**	**1b-A**	**1b-B**
d(Si-Si); shortest [Å]	2.412(1)	2.412(1)	2.410(2)	2.408(2)
d(Si-Si); longest [Å]	2.664(1)	2.652(1)	2.663(2)	2.657(2)
d(Cu-Si); mean [Å]	2.4235(9)	2.4394(9)	2.424(1)	2.439(1)
d(Cu-$C_{carbene}$) [Å][a]	1.925(3)	1.953(3)	1.931(4)	1.943(4)
csp-Cu-$C_{carbene}$ [°][b]	178.54(2)	176.82(4)	178.02(3)	175.96(8)
torsion angle α [°][c]	179.80(2)	179.90(2)	179.98(2)	179.70(2)
d2/d1[d]	1.00	1.02	1.00	1.02

[a] d(Cu-$C_{Carbene}$): Distance between Cu^+ and the respective carbene carbon atoms C1 or C4. [b] csp: centre of gravity of the square open plane of [Si_9], which coordinates to the [Cu-NHC]$^+$ fragment. [c] For clusters **A**: Si6-Si7-Si8-Si9; for clusters **B**: Si15-Si16-Si17-Si18. [d] Relation of the diagonal lengths of the square open plane of the [Si_9] clusters coordinating to [Cu-NHC]$^+$.

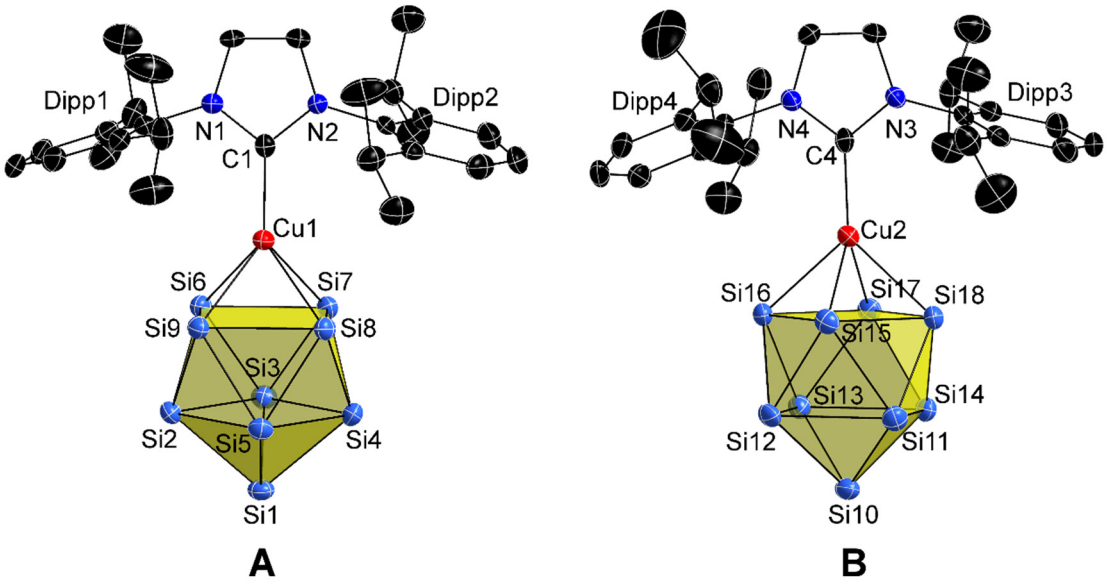

Figure SI 1: Full ellipsoid molecular structures of the two crystallographically different [$NHC^{Dipp}Cu(\eta^4\text{-}Si_9)$]$^{3-}$ clusters in compound **1a**. Ellipsoids are shown at a 50 % probability level. Hydrogen atoms and solvent molecules are omitted for clarity.

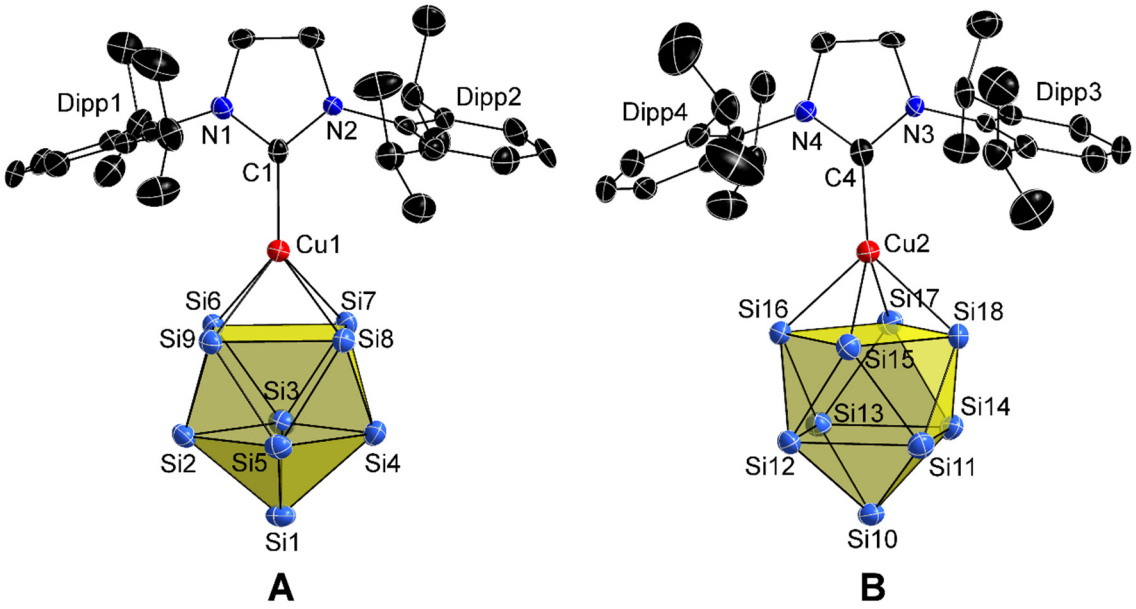

Figure SI 2: Full ellipsoid molecular structures of the two crystallographically different $[NHC^{Dipp}Cu(\eta^4\text{-}Si_9)]^{3-}$ clusters in compound **1b**. Ellipsoids are shown at a 50 % probability level. Hydrogen atoms and solvent molecules are omitted for clarity.

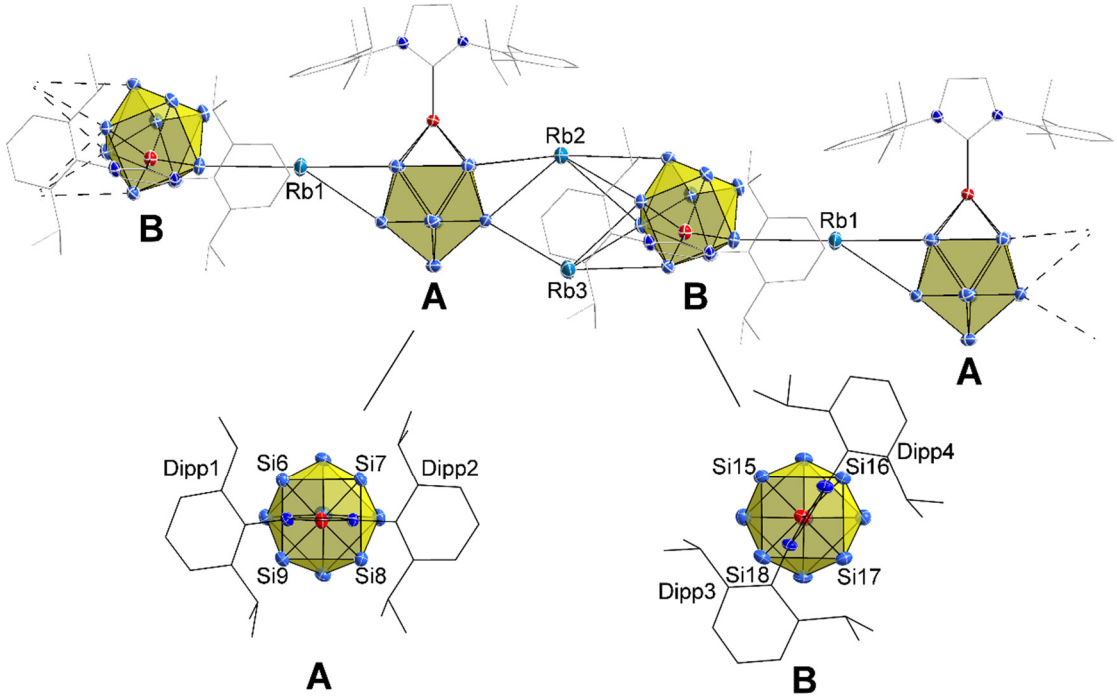

Figure SI 3: Top: Linear strands of Rb^+ connected $[NHC^{Dipp}Cu(\eta^4\text{-}Si_9)]^{3-}$ clusters **A** and **B** in **1b**. Rb-Si distances range between 3.467(1) Å (Rb1-Si2) and 3.872(1) Å (Rb3-Si12). Ellipsoids are shown at a 50 % probability level. For clarity protons and solvent molecules are omitted and carbon atoms are pictured as grey wire sticks. Bottom: Different orientations of $[Cu\text{-}NHC^{Dipp}]^+$ moieties towards the $[Si_9]^{4-}$ core in **A** and **B**.

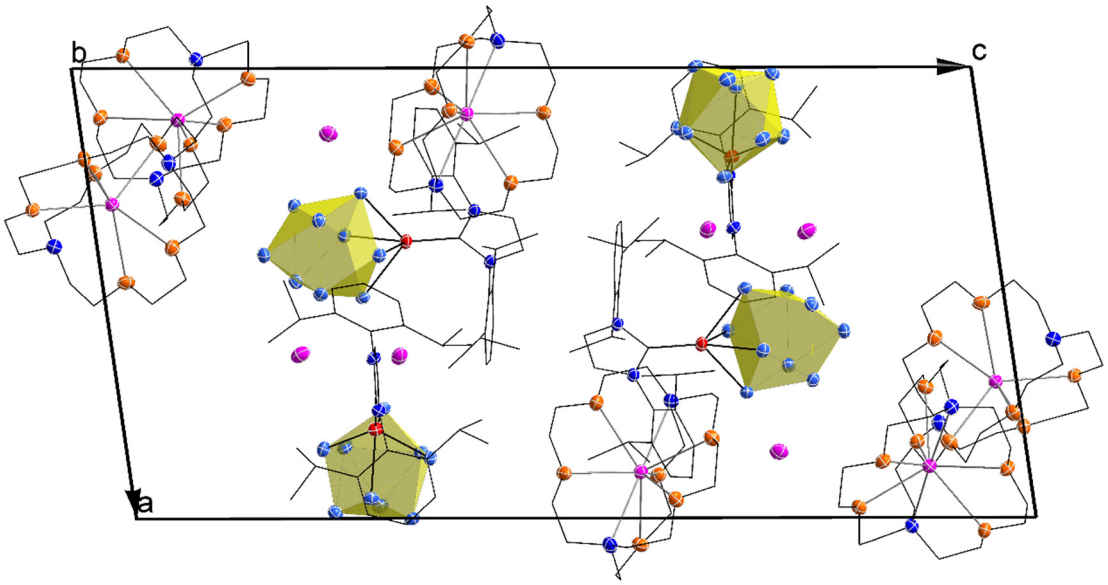

Figure SI 4 Unit cell of compound **1a**. Ellipsoids are shown at a 50 % probability. For clarity protons and solvent molecules are omitted and carbon atoms are pictured as grey wire sticks. Si atoms (bright blue), Cu atoms (red), K atoms (pink) N atoms (dark blue), O atoms (orange).

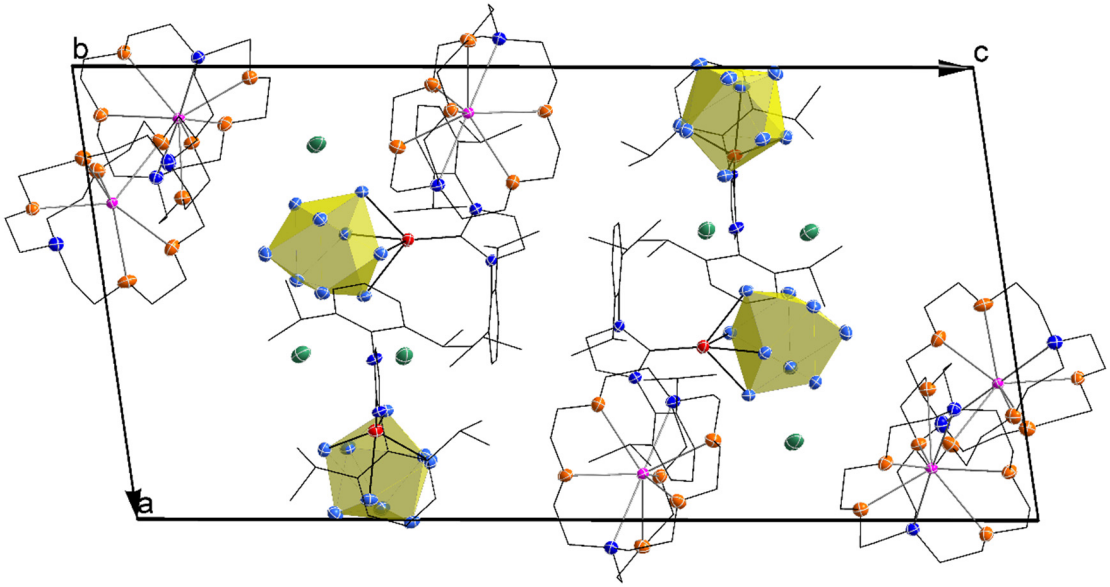

Figure SI 5 Unit cell of compound **1b**. Ellipsoids are shown at a 50 % probability. For clarity protons and solvent molecules are omitted and carbon atoms are pictured as grey wire sticks. Si atoms (bright blue), Cu atoms (red), Rb atoms (green), K atoms (pink), N atoms (dark blue), O atoms (orange).

1.4 NMR Spectroscopy

Subsequent to removal of NH_3 (l) from the reaction mixture, the orange-brownish residue was extracted with acetonitrile-d_3 and filtered to remove remaining solids. NMR spectra were acquired on a Bruker Avance Ultrashield 400 MHz spectrometer. The ^{1}H NMR spectra were calibrated using the residual proton signal of the used deuterated solvents. Chemical shifts are reported in parts per million (ppm) relative to TMS, with the residual solvent peak serving as internal reference.[7] Abbreviations for signal multiplicities are: doublet (d), heptet (h) or multiplet (m). For the time dependent studies, the sample was either stored at room-temperature or at -32 °C. In case of the low temperature examinations the J-Young tube was placed in an Argon-filled Schlenk tube in a freezer in between the single measurements.

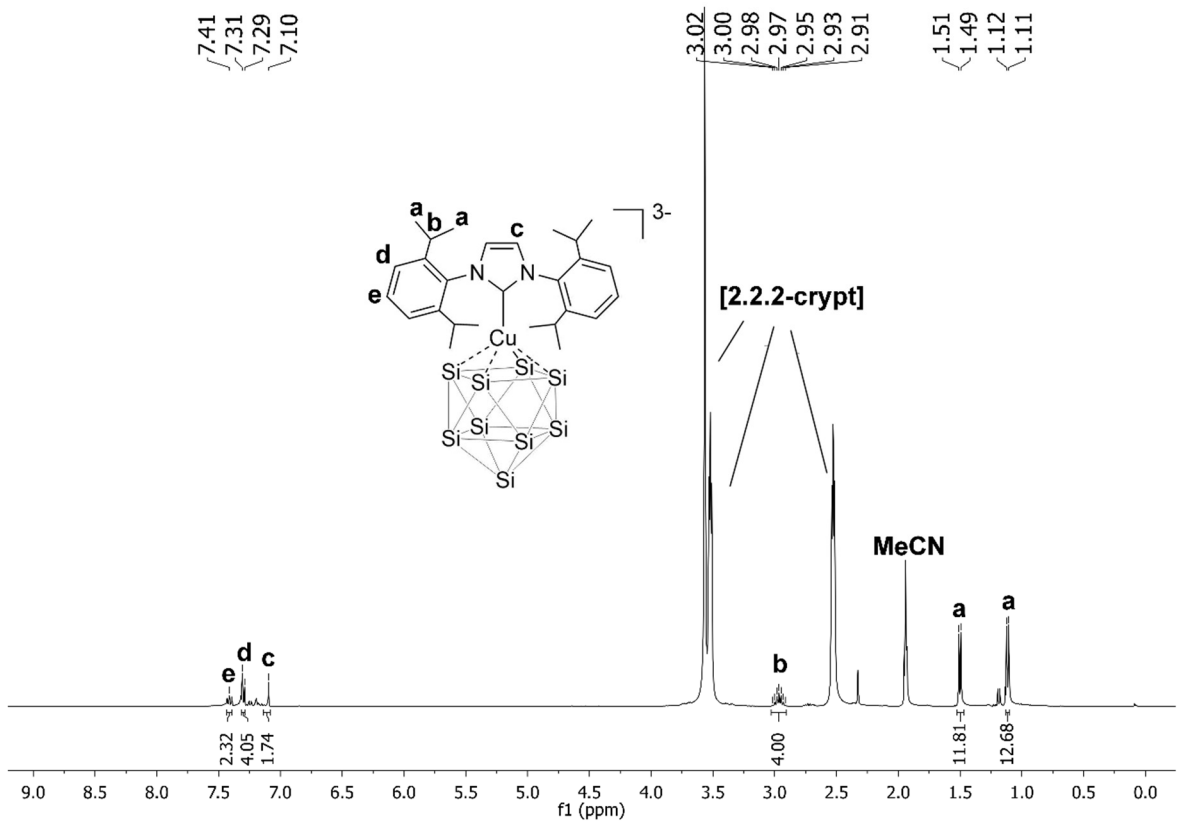

Figure SI 6 ^{1}H NMR spectrum of $[NHC^{Dipp}Cu(\eta^4\text{-}Si_9)]^{3-}$ (**1**) in MeCN-d_3.

^{1}H NMR (400 MHz, 298 K, MeCN-d_3): δ [ppm] = 7.43-7.39 (m, 2H, $CH_{Ph(p)}$), 7.32-7.29 (m, 4H, $CH_{Ph(m)}$), 7.10 (s, 2H, CH_{Im}), 2.97 (h, $^3J_{HH}$ = 6.8 Hz, 4H, $CH_{i\text{Pr}}$), 1.49 (d, $^3J_{HH}$ = 6.8 Hz, 12H, $Me_{i\text{Pr}}$), 1.11 (d, $^3J_{HH}$ = 6.8 Hz, 12H, $Me_{i\text{Pr}}$). The intensity of the doublet at 1.11 ppm is slightly increased, due to an overlap of this signal with one of the respective signals of free carbene NHC^{Dipp}, which was present in small amounts in the sample.

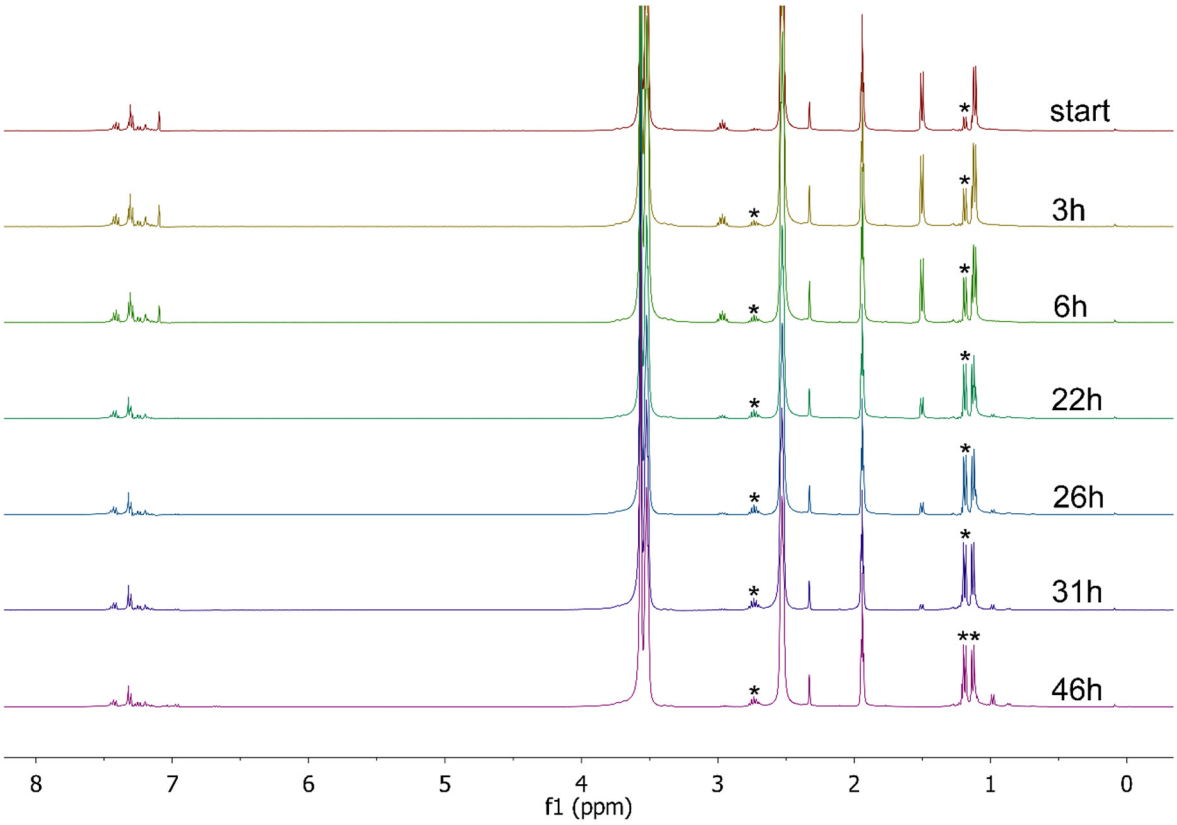

Figure SI 7 Time dependant ^{1}H NMR examination of [NHC^{Dipp}Cu(η^4-Si$_9$)]$^{3-}$ (**1**) in MeCN-d$_3$ at room temperature, revealing the complete degradation of **1** within 46 h. Characteristic signals of the free carbene are marked with (*).

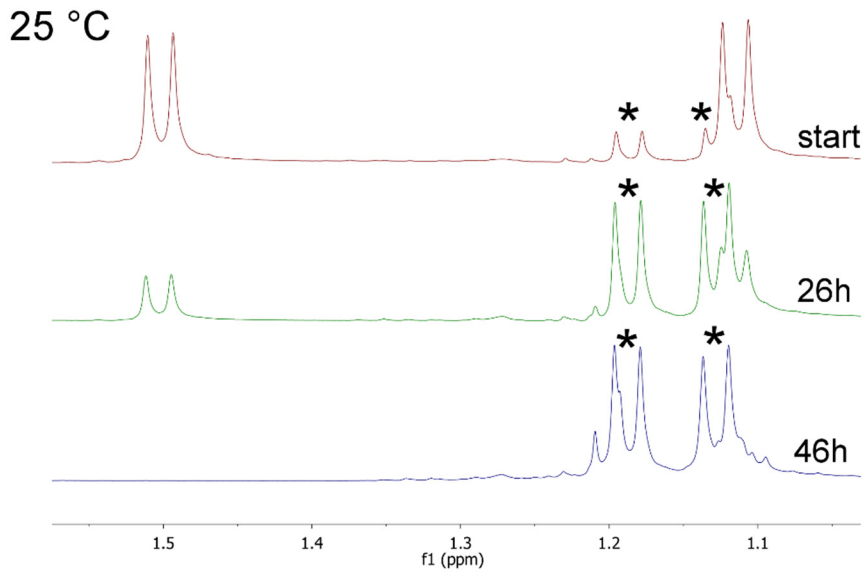

Figure SI 8 Selected area of time dependant ^{1}H NMR examination of [NHC^{Dipp}Cu(η^4-Si$_9$)]$^{3-}$ (**1**) in MeCN-d$_3$ at room temperature, revealing the complete degradation of **1** within 46 h. Characteristic signals of the free carbene are marked with (*).

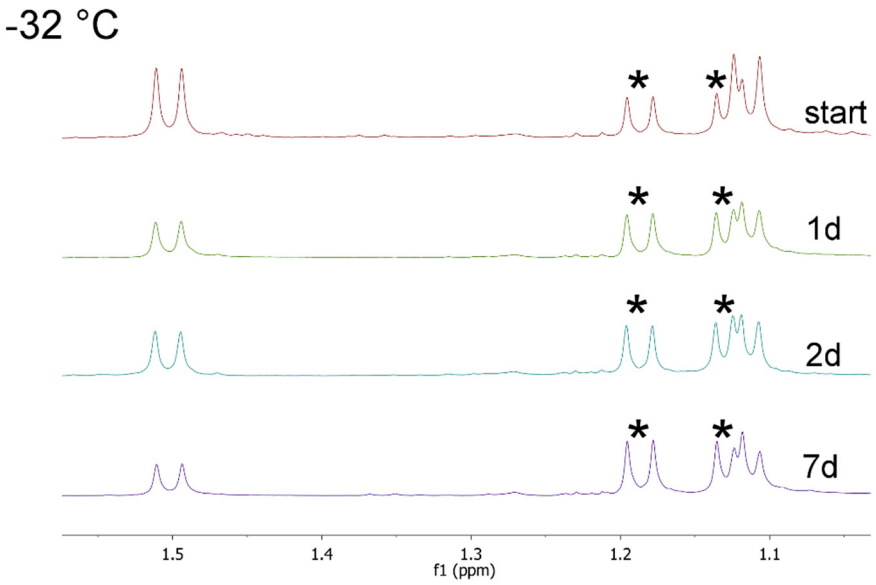

Figure SI 9 Selected area of time dependant ^{1}H NMR examination of [NHC^{Dipp}Cu(η^4-Si$_9$)]$^{3-}$ (**1**) in MeCN-d$_3$ at -32 °C, revealing the stability of **1** at low temperature. Slow progress of the reaction can be assigned to the short exposure to room temperature during the measurements. Characteristic signals of the free carbene are marked with (*).

1.5 Electron Spray Ionization Mass Spectrometry (ESI-MS)

Subsequent to removal of NH_3 (l) from the reaction mixture, the orange-brownish residue was dissolved in pyridine and filtered to remove remaining solids. Aliquots of this solution were diluted with pyridine to obtain suitable concentration for ESI-MS examinations. The measurements were performed on a HCT (*Bruker Corp.*). Analysis of the data occurred using the program Bruker Compass Data Analysis 4.0 SP 5 (*Bruker Corp.*). The dry gas temperature was adjusted to 300°C and the injection speed to 240 µL/s. Visualization of the spectra occurred with the programs OriginPro 2016G (*Origin Lab Corp.*) and Excel 2016 (*Microsoft Corp.*).

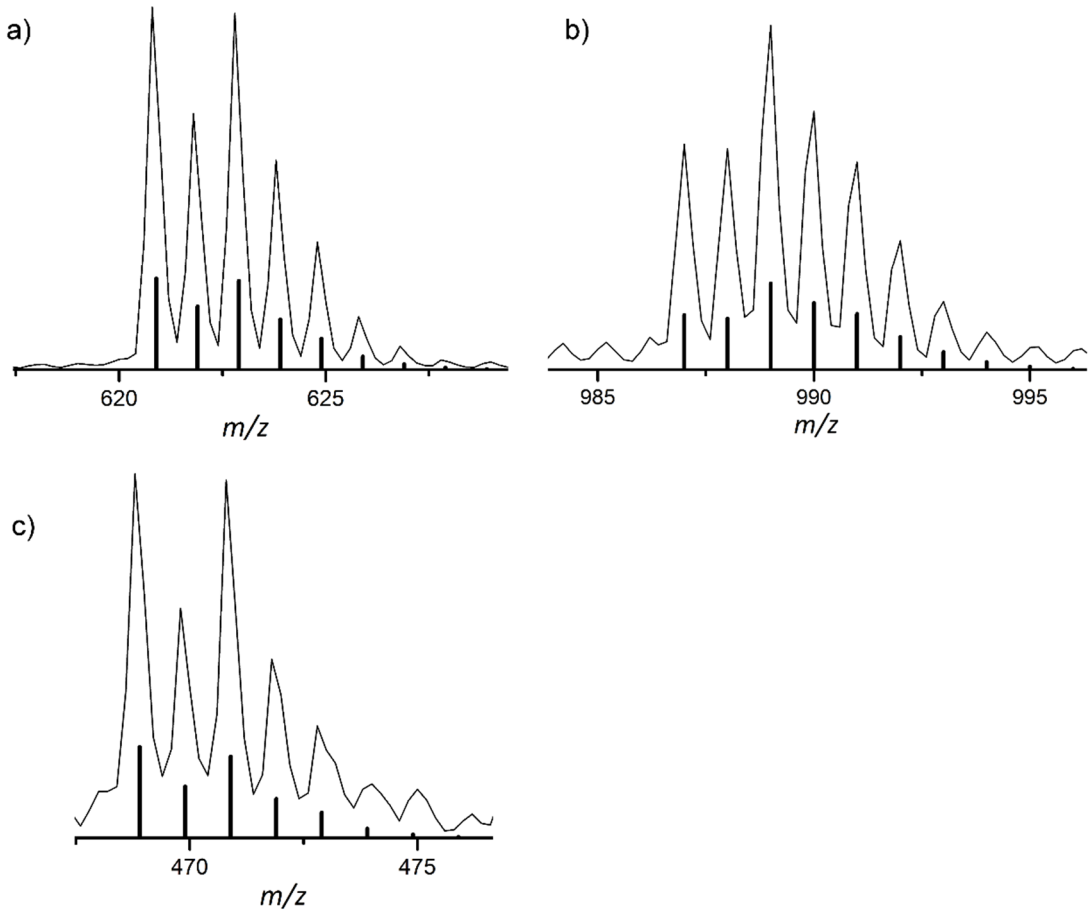

Figure SI 10 ESI-MS spectra of a) $\{[NHC^{Mes}CuSi_9]^{3-} + 2H^+\}^-$, b) $\{[(NHC^{Mes}Cu)_2Si_9]^{2-} + H^+\}^-$ and c) $\{[NHC^{iPr}Cu\text{-}Si_9]^{3-} + 2H^+\}$. All spectra were acquired in negative ion mode; a), b) (4500 V, 300 °C) and c) (3500 V, 300 °C).

Furthermore, MS-MS fragmentation experiments were carried out for $[NHC^{Dipp}Cu(\eta^4\text{-}Si_9)]^{3-}$ (**1**), resulting in the cleavage of the Cu-NHC^{Dipp} bonds for both originally monitored species at *m/z* 705.0 $\{[NHC^{Dipp}CuSi_9)]^{3-} + 2H^+\}^-$ (Figure SI 11) and *m/z* 1155.2 $\{[(NHC^{Dipp}Cu)_2Si_9]^{2-} + H^+\}^-$ (Figure SI 12). By contrast the Cu-Si bonds and the $[Si_9]$ cages stayed intact in these examinations.

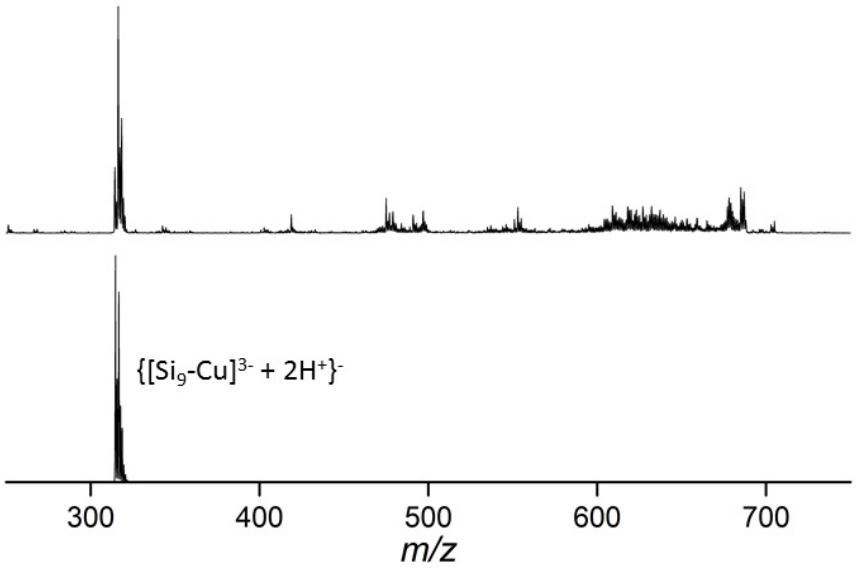

Figure SI 11: MS-MS fragmentation spectrum of $\{[NHC^{Dipp}CuSi_9)]^{3-} + 2H^+\}^-$ (top) and calculated reference spectrum of $\{[Si_9\text{-}Cu]^{3-} + 2H^+\}^-$ (bottom).

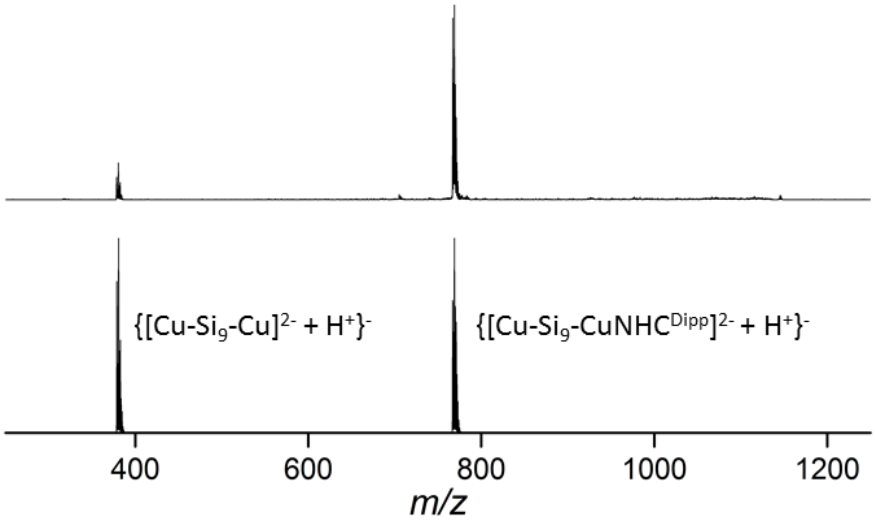

Figure SI 12: MS-MS fragmentation spectrum of $\{[(NHC^{Dipp}Cu)_2Si_9]^{2-} + H^+\}^-$ (top) and calculated reference spectra of $\{[Cu\text{-}Si_9\text{-}Cu]^{2-} + H^+\}^-$ and $\{[Cu\text{-}Si_9\text{-}CuNHC^{Dipp}]^{2-} + H^+\}^-$ (bottom).

References

1. L. Hintermann, *Beilstein J. Org. Chem.*, 2007, **3**, 22.
2. O. Santoro, A. Collado, A. M. Z. Slawin, S. P. Nolan and C. S. J. Cazin, *Chem. Commun.*, 2013, **49**, 10483.
3. P. de Frémont, N. M. Scott, E. D. Stevens, T. Ramnial, O. C. Lightbody, C. L. B. Macdonald, J. A. C. Clyburne, C. D. Abernethy and S. P. Nolan, *Organometallics*, 2005, **24**, 6301.
4. A. Collado, A. Gomez-Suarez, A. R. Martin, A. M. Z. Slawin and S. P. Nolan, *Chem. Commun.*, 2013, **49**, 5541.
5. J. M. Goicoechea and S. C. Sevov, *Journal of the American Chemical Society*, 2004, **126**, 6860.
6. G. Sheldrick, *Acta Cryst. Sect. C*, 2015, **71**, 3.
7. G. R. Fulmer, A. J. M. Miller, N. H. Sherden, H. E. Gottlieb, A. Nudelman, B. M. Stoltz, J. E. Bercaw and K. I. Goldberg, *Organometallics*, 2010, **29**, 2176.

5.2 Formation of the intermetalloid cluster $[AgSn_{18}]^{7-}$ – the reactivity of coinage metal NHC compounds towards $[Sn_9]^{4-}$

F. S. Geitner, W. Klein, T. F. Fässler*

published in

Dalton Trans. **2017**, *46*, 5796.

Content and Contributions

The scope of this paper was to test the reactivity of coinage metal NHC complexes $NHC^{Dipp}MCl$ (*M*: Cu, Ag, Au) towards the *Zintl* phase K_4Sn_9, containing bare $[Sn_9]^{4-}$ clusters, aiming for the synthesis of enlarged intermetalloid species. Reactions were carried out at low temperature (-70 °C) in liquid ammonia in presence of [2.2.2]-cryptand as sequestering agent. Reactions of K_4Sn_9 with the respective Cu-NHC and Au-NHC compounds led to the addition of $[NHC^{Dipp}M]^+$ (*M*: Cu, Au) fragments to the $[Sn_9]^{4-}$ clusters *via* the open *pseudo* square plane of the tin polyanions, resulting in $[NHC^{Dipp}M(\eta^4\text{-}Sn_9)]^{3-}$ (*M*: Cu, Au). By contrast, similar reactions of $[Sn_9]^{4-}$ with respective Ag-NHC compound $NHC^{Dipp}AgCl$ resulted in the formation of two different species. The first species $[NHC^{Dipp}Ag(\eta^4\text{-}Sn_9)]^{3-}$ was similar to the products obtained in analogous reactions with the Cu-NHC and Au-NHC complexes, whereas the second species (main fraction) was identified to be the larger intermetalloid anion $[AgSn_{18}]^{7-}$, comprising two $[Sn_9]^{4-}$ clusters bridged by Ag^+. The formation of the novel anion can be rationalized by the nucleophilic attack of a second $[Sn_9]^{4-}$ cluster at the initially formed $[NHC^{Dipp}Ag(\eta^4\text{-}Sn_9)]^{3-}$, under cleavage of the Ag-NHC bond. The different reactivity can be explained by the relative lability of the Ag-NHC bond. Interestingly, the two $[Sn_9]^{4-}$ clusters in $[AgSn_{18}]^{7-}$ reveal different coordination modes towards Ag^+. Whereas one of the clusters coordinates the metal cation with its open square plane, as also observed in $[NHC^{Dipp}M(\eta^4\text{-}Sn_9)]^{3-}$ (*M*: Cu, Ag, Au), the second cluster is bound to Ag^+ *via* a single exo bond. Thus, the sum formula of the novel anion can also be written as $[(\eta^4\text{-}Sn_9)Ag(\eta^1\text{-}Sn_9)]^{7-}$. The isolation of different species from one reaction solution allows for closer insights into the growing process of larger intermetalloid cage compounds in solution. All novel compounds were characterized by means of single crystal X-ray diffraction. The crystal structure refinement for crystals containing $[AgSn_{18}]^{7-}$ (especially the modelling of a partially disordered $[Sn_9]$ cage) was assisted by Dr. Wilhelm Klein. This publication was written in the course of this thesis.

Dalton Transactions

COMMUNICATION

View Article Online
View Journal | View Issue

Cite this: *Dalton Trans.*, 2017, **46**, 5796

Received 1st March 2017,
Accepted 22nd March 2017

DOI: 10.1039/c7dt00754j

rsc.li/dalton

Formation of the intermetalloid cluster $[AgSn_{18}]^{7-}$ – the reactivity of coinage metal NHC compounds towards $[Sn_9]^{4-}$†

F. S. Geitner,[a] W. Klein[b] and T. F. Fässler *[b]

In recent years the formation of intermetalloid clusters by reacting homoatomic tetrel cluster anions with transition metal complexes has become a promising synthetic route. Nevertheless a better understanding of the processes occurring in solution is necessary. Here we present a series of novel polyanionic coinage metal NHC *Zintl* clusters $[NHC^{Dipp}M(\eta^4\text{-}Sn_9)]^{3-}$ (M: Cu, Ag, Au; Dipp: diisopropylphenyl) which are obtained at low temperatures from the reaction of K_4Sn_9 with $NHC^{Dipp}MCl$ (M: Cu–Au) in liquid ammonia. For M = Ag a larger intermetalloid Ag^I-bridged nonastannide dimer $[(\eta^4\text{-}Sn_9)Ag(\eta^1\text{-}Sn_9)]^{7-}$ is also formed. The stepwise formation of the intermetalloid cluster $[AgSn_{18}]^{7-}$ is discussed and compared with that of previously reported intermetalloid stannides.

Intermetalloid clusters are molecules or molecular ions that consist of several metals and/or semimetals. The atoms in such clusters reveal coordination numbers, which are in the range of those observed in intermetallic compounds.[1] Even though in many cases there are striking differences in the coordination spheres of the atoms, the non-classical bonding in intermetalloid clusters approaches the complexity of the bonding situation observed in intermetallic phases. Besides the extraction of intermetalloid moieties from intermetallic phases, the reaction of polyhedral *Zintl* ions with organometallic compounds has become a fruitful approach toward the controlled formation of larger clusters.[2,3] Thereby, a plethora of novel materials comprising transition metal bridged empty *Zintl* cages and also transition metal filled endohedral *Zintl* clusters, resulting from the embedment of the transition metal into the cluster core, have been synthesized.[4,5] Even though many intermetalloid clusters obtained by the reaction of *Zintl* phases with organometallic compounds do not have direct intermetallic structural analogues, molecular structures with similar structural motifs can be observed. For example $[Co@Sn_9]^{4-}$ (ref. 6) shows a similar structure to the $CoSn_8$ units in $Mg_2Co_3Sn_{10+x}$,[7] and a shell-type structure analogous to $[As@Ni_{12}@As_{20}]^{3-}$ (ref. 8) or $[Sb@Pd_{12}@Sb_{20}]^{n-}$ (ref. 9) is found in the $Cu_{12}Sn_{21}$ unit of the ternary phase $Na_{12}Cu_{12}Sn_{21}$.[10]

Intermetalloid clusters are interesting materials concerning the formation of nano-dots or the synthesis of nanostructured materials for catalytic applications.[11,12] Despite the plethora of intermetalloid clusters obtained by reacting *Zintl* ions with organometallic compounds, detailed studies on their formation mechanisms are rare. However, such examinations providing a deeper insight into the reactivity of *Zintl* clusters in solution are necessary with respect to the reproducibility, selectivity and tuneability of the synthesis of novel intermetalloid compounds using *Zintl* polyanions as starting materials. Recently, Dehnen *et al.* reported a detailed study on multimetallic cluster growth comprising mixed Ge/As clusters and the incorporation of Ta for obtaining larger clusters.[2] Concerning group 14 *Zintl* clusters, the synthesis of $[Ir@Sn_{12}]^{3-}$ from $[(\eta^4\text{-}Sn_9)Ir(cod)]^{3-}$ by partial oxidation-induced cluster fragmentation, and the formation of $[(\eta^4\text{-}Ge_9)CuP(iPr)_3]^{3-}$ and $[(\eta^4\text{-}Ge_9)Cu(\eta^1\text{-}Ge_9)]^{7-}$ indicate the stepwise reaction of *Zintl* anions with transition metal complexes in solution.[3,13] Oxidative cluster growth of $[Ge_9]$ clusters had been observed for bare $[Ge_9]$ clusters resulting in a $[Ge_{45}]^{9-}$ unit[14] or ligand-stabilized clusters $[Ge_9R_3]^-$ (R = $Si(TMS)_3$) leading to $[Ge_{18}R_6]$.[15] Additionally, the recently observed formation of the cluster polyanion $[Ti(Sn_8)Cp]^{3-}$ in liquid ammonia at −70 °C provided a deeper insight into the processes occurring in solution, since the intermetalloid $[TiSn_8]$ unit adopts the shape of an icosahedral $[Sn_{12}]$ fragment.[16] In this context it becomes obvious that reactivity studies at low temperatures are a valuable tool for "freezing" metastable intermediate structures, allowing for a better understanding of the processes occurring during the formation of intermetalloid clusters. Furthermore, the selection of suitable organometallic precursors is decisive for such

[a]*WACKER-Institute for Silicon Chemistry and Department of Chemistry, Technische Universität München Lichtenbergstraße 4, 85747 Garching/München, Germany*
[b]*Department of Chemistry, Technische Universität München Lichtenbergstraße 4, 85747 Garching/München, Germany. E-mail: thomas.faessler@lrz.tum.de; Fax: (+49)89-289-13186*

†Electronic supplementary information (ESI) available: Detailed synthetic procedures and crystallographic data for all described compounds. CCDC 1530025–1530028. For ESI and crystallographic data in CIF or other electronic format see DOI: 10.1039/c7dt00754j

examinations. In previous studies we had already examined the reactivity of coinage metal NHC complexes $NHC^{Dipp}MCl$ (M: Cu, Ag, Au) towards the tris-silylated cluster $[Ge_9R_3]^-$ (R: {Si(TMS)$_3$}) leading to $[(\eta^3\text{-}Ge_9R_3)M(NHC^{Dipp})]$ (M: Cu–Au).[17] The resulting neutral compounds are stable in solution for M = Cu and Au. In contrast for M = Ag a transformation occurs, yielding the silver bridged dimeric *Zintl* cluster species $[Ag(\eta^3\text{-}Ge_9R_3)_2][Ag(NHC^{Dipp})_2]$.[17–19] This observation revealed both the stability of the coinage metal NHC bond (especially for M = Cu and Au) and the potential formation of larger coinage metal-bridged cluster adducts upon cleavage of the M–NHC bond.

Within this work we examined the reactivity of $NHC^{Dipp}MCl$ (M: Cu, Ag, Au) towards K_4Sn_9. The reactions were carried out in the presence of [2.2.2-crypt] in liquid ammonia. When ammonia was condensed onto a mixture of solids, deep red suspensions were formed immediately. After storage in a freezer at −70 °C for several months, black block-shaped crystals were obtained, which were examined by single crystal X-ray diffraction. Reactions of $NHC^{Dipp}MCl$ (M: Cu, Au) with K_4Sn_9 yielded crystals of the composition $[NHC^{Dipp}M(\eta^4\text{-}Sn_9)][K(2.2.2\text{-crypt})]_3$ {Cu (**1**), Au (**3**)}, containing the *Zintl* cluster coinage metal carbene anions $[NHC^{Dipp}M(\eta^4\text{-}Sn_9)]^{3-}$ [Cu (**1a**), Au (**3a**)], with approximately 30% yield. In contrast the reaction of $NHC^{Dipp}AgCl$ with K_4Sn_9 under the same reaction conditions yielded crystals of varying composition. Besides $[K(2.2.2\text{-crypt})]_3[NHC^{Dipp}Ag(\eta^4\text{-}Sn_9)]$ (**2**), which was obtained as a minor component, $K_3[K(2.2.2\text{-crypt})]_4[(\eta^4\text{-}Sn_9)Ag(\eta^1\text{-}Sn_9)]$ (**4**), containing the intermetalloid Ag^I-bridged dimeric $[Sn_9]^{4-}$ cluster $[AgSn_{18}]^{7-}$ (**4a**), was isolated as a major product in a ratio of about 9 : 1 (Fig. 1). The formation of the *Zintl* cluster coinage metal NHC units **1a–3a** proves the addition of the $[M\text{–}NHC]^+$ fragment to $[Sn_9]^{4-}$ in a salt metathesis reaction, and simultaneous formation of KCl, to be the first reaction step occurring in solution. However, whereas **1a** and **3a** are stable at −70 °C, polyanionic **2a** undergoes a subsequent reaction by a nucleophilic attack of a second $[Sn_9]^{4-}$ unit at the electrophilic Ag^I center under release of the NHC^{Dipp} ligand. Besides the isolation of the polyanions **2a** and **4a** from the same reaction solution, the required release of NHC^{Dipp} is manifested by ^{1}H NMR investigations of the residue of the reaction mixture. After removal of NH_3 (l) only the presence of free carbene and the absence of $[Ag(NHC^{Dipp})_2]^+$ were observed. The latter cation was however observed upon the formation of the previously reported Ag^I bridged tris-silylated cluster dimer $[Ag(\eta^3\text{-}Ge_9R_3)_2]^-$.[17]

The varying reactivity of **1a–3a** at −70 °C can be assigned to the lability of the Ag–NHC bond compared to that of the corresponding M–NHC units of copper and gold.[20] Compounds **1–3** crystallize in the monoclinic space group *C*2/*c* and contain three [2.2.2-crypt] sequestered potassium cations as counter ions. The $[Sn_9]^{4-}$ clusters coordinate to the transition metals of the $[M\text{–}NHC^{Dipp}]^+$ fragments with their open square planes. The M–Sn distances {2.7368 Å (**1a**), 2.8579(6) Å (**2a**) and 2.8180(4) Å (**3a**)} follow the trend observed for other coinage metal complexes with a significantly smaller Au^I compared to Ag^I ions.[21,22] The $[Sn_9]^{4-}$ polyanions **1a–3a** reveal

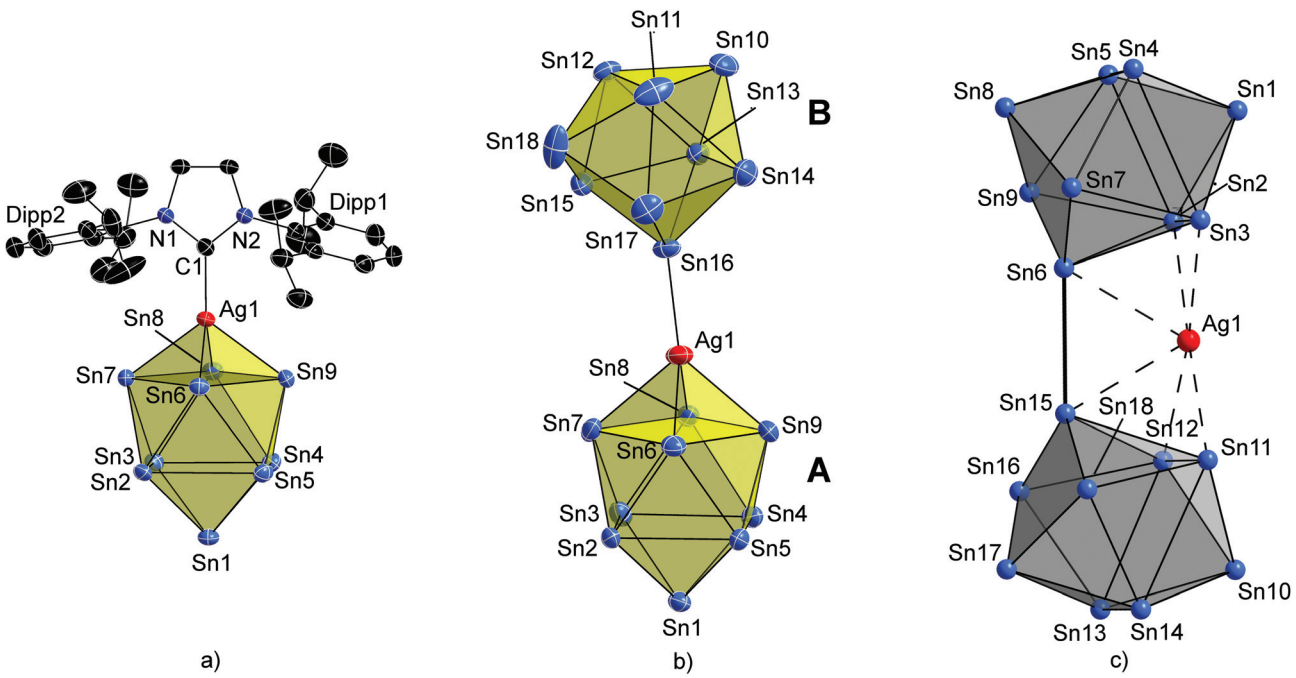

Fig. 1 Molecular structures of (a) **2a** and (b) **4a**. Displacement ellipsoids are shown at a 50% probability level. For clarity hydrogen atoms, counter ions and co-crystallized NH_3 molecules are omitted. Diisopropylphenyl-wingtip substituents are abbreviated as Dipp1 and Dipp2. Atom labelling for **1a** and **3a** occurred analogously to that of **2a**. (c) The Ag^I stabilized dimer $[Ag(Sn_9\text{–}Sn_9)]^{5-}$.[24] Molecular structures of **1a** and **3a** as well as selected bond lengths and angles for **1–4** are presented in the ESI.†

nearly perfect C_{4v}-symmetry as manifested by the dihedral angles α of their open squares (Sn6–Sn9) {178.90(2)° (**1a**), 178.87(2)° (**2a**) and 178.88(1)° (**3a**)} and the ratio of their open square plane diameters D2(Sn6–Sn8)/D1(Sn7–Sn9) = 1.01 (**1a**, **3a**) and 1.00 (**2a**) (values for perfect C_{4v}-symmetry are α = 180° and D2/D1 = 1). All Sn–Sn distances are in the range of 2.9210(6) Å to 3.3104(7) Å and thus similar to those in bare $[Sn_9]^{4-}$.[23]

The larger intermetalloid cluster polyanion $[AgSn_{18}]^{7-}$ (**4a**) crystallizes with three bare and four sequestered potassium counter ions. Interestingly, the two $[Sn_9]^{4-}$ clusters are attached to the Ag^I cation in different coordination modes. Whereas one cluster (**A**) coordinates to Ag^I with its open square, the other $[Sn_9]^{4-}$ unit (**B**) binds through the lone pair of a Sn atom of its square open plane forming a Sn–Ag *exo* bond according to $[(\eta^4\text{-}Sn_9)Ag(\eta^1\text{-}Sn_9)]^{7-}$ (**4a**) (Fig. 1). Thereby, the Ag–Sn *exo* bond with a distance of 2.7130(8) Å (Ag1–Sn16) is significantly shorter than the mean Ag–Sn distance of 2.8886(9) Å to the four Sn atoms (Sn6–Sn9) of cluster **A**. This variation in the coordination mode of the nine-atom tetrel clusters is a very rare example and has not yet been observed for stannides. However, quite recently the coordination through a lone pair of the cluster has been established for nona-germanides in $[Ge_9Zn\text{-}Ge_9\text{-}ZnGe_9]$,[25] $^1_\infty\{Zn[(\eta^4\text{:}\eta^1\text{-}Ge_9)]\}^{2-}$ [25] and $[(\eta^4\text{-}Ge_9)Cu(\eta^1\text{-}Ge_9)]$,[13] the latter being analogous to **4a**. In **4a**, the fourfold coordinating cluster **A** reveals nearly perfect C_{4v}-symmetry, whereas cluster **B**, coordinating to Ag^I with only one Sn atom, is slightly more distorted and shows an orientational disorder.[26] The Sn–Sn distances within the $[Sn_9]^{4-}$ clusters adopt the typical values between 2.913(3) Å and 3.2572(7) Å.[23] The non-sequestered potassium cations in **4** are arranged in a triangle around the Ag–Sn16 bond and coordinate to the Sn atoms of clusters **A** and **B** with K–Sn distances between 3.665(4) Å (K3–Sn14) and 3.966(3) Å (K1–Sn15) (ESI†). A comparison of the isolated cluster polyanions **1a–4a** with already known intermetalloid compounds consisting of $[Sn_9]$ cages and coinage metal cations, namely $[Cu@Sn_9]^{3-}$ [27,28]

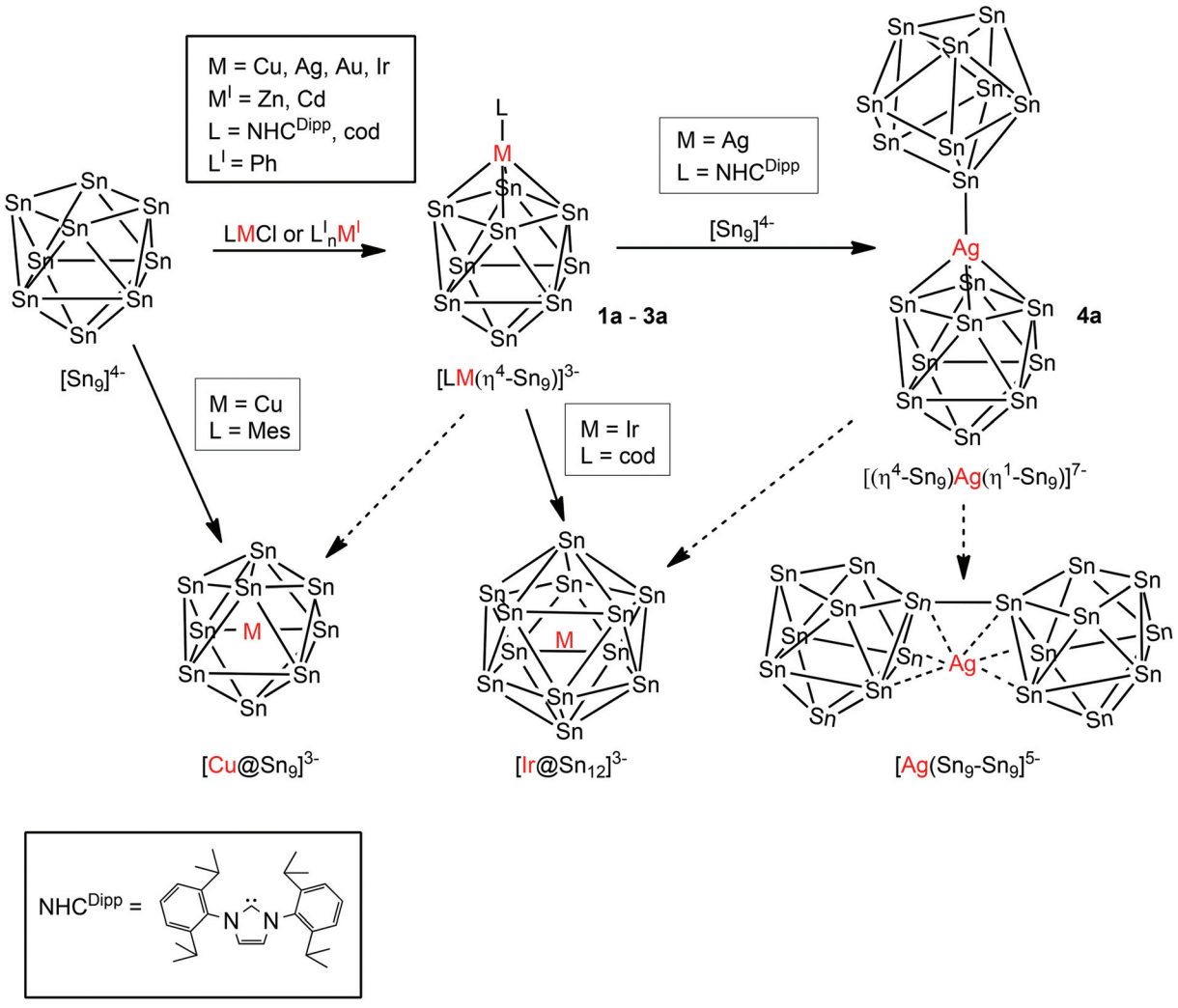

Scheme 1 Relationship between compounds obtained from reactions of K_4Sn_9 with various organometallic complexes and subsequent reactions: $[(cod)Ir(\eta^4\text{-}Sn_9)]^{3-}$,[3,32] $[Ph\text{-}M(\eta^4\text{-}Sn_9)]^{3-}$ (Zn,[33] Cd[34]), $[Cu@Sn_9]^{3-}$,[27,28] $[Ir@Sn_{12}]^{3-}$,[3] and $[Ag(Sn_9\text{–}Sn_9)]^{5-}$.[24] Dashed arrows: feasible reactions, however not proven yet.

and $[Ag(Sn_9–Sn_9)]^{5-}$ (Fig. 1c),[24] reveals the impact of low temperature synthesis and the application of semi-labile, ligand-stabilized coinage metal precursors. The endohedrally filled cluster $[Cu@Sn_9]^{3-}$ [27,28] is obtained by reacting K_4Sn_9 or $K_{12}Sn_{17}$ with mesityl copper at room temperature or at −70 °C and indicates the lability of the Cu–Mes bond.[27,28] In contrast, the Cu–NHC^{Dipp} bond is more stable, allowing for the isolation of compound **1**, which is also a feasible intermediate species on the way to Cu-filled endohedral stannides by ligand release and embedment of the metal cation into the cluster (Scheme 1). Ligand release in the presence of excessive $[Sn_9]^{4-}$ clusters allows for a ligand exchange reaction as it has been observed for **2a** in the formation of $[(\eta^4\text{-}Sn_9)Ag(\eta^1\text{-}Sn_9)]^{7}$ (**4a**). Thereby, the NHC^{Dipp} moiety is replaced by a $[Sn_9]^{4-}$ cluster acting as a two-electron donor (Scheme 1). A similar study of the reactivity of the organometallic [Ir-cod] fragment (cod = cyclooctadiene) towards $[Sn_9]^{4-}$ had previously revealed the formation of the π-complex $[(cod)Ir(\eta^4\text{-}Sn_9)]^{3-}$, in full analogy to the formation of **2a**, in the first reaction step. However, attempts to exchange the cod ligand by diphenylphosphinoethane resulted in a partial oxidation of the cluster units and fragmentation of the cages followed by disproportionation, yielding the Ir-filled dodecahedral stannide species $[Ir@Sn_{12}]^{3-}$.[3] Concerning species **1a–4a** a partial oxidation might lead to similar reaction cascades. Especially for **4a** with two $[Sn_9]^{4-}$ clusters in close vicinity to each other, oxidation might lead to the formation of the Ag^{I}-stabilized, *exo* bond-connected $[Sn_9]^{3-}$ dimer $[Ag(Sn_9–Sn_9)]^{5-}$, which has been obtained for the first time from the reaction of mesityl silver with $[Sn_9]^{4-}$ at room temperature in ethylenediamine.[24] Therefore, the present study provides valuable information allowing, in combination with previous studies, for a better understanding of the relationship between different stannide clusters (Scheme 1). It becomes obvious that the strength of the interaction between the organic ligand and the transition metal, as well as the reaction temperature and the availability of *Zintl* clusters in solution are decisive parameters concerning the reactivity of K_4Sn_9 towards organometallic compounds. Furthermore, the size of the transition metal cation seems to be essential for the probability to migrate into the cluster core upon release of the organic ligand. Concerning bare $[Sn_9]$ cages, to date only the enclosure of Ni^0 in $[Ni@Sn_9]^{3-}$ [29] has been reported besides the already mentioned embedment of Cu^{I}. In contrast the encapsulation of larger transition metal cations requires a partial oxidation-induced cluster growth as observed for $[Ir@Sn_{12}]^{3-}$.[3] Further examples of enlarged tin clusters embedding Pd or Pt are $[Pd_2@Sn_{18}]^{4-}$ [30] or $[Pt_2@Sn_{17}]^{4-}$.[31]

In summary, the anions **1a–3a**, which were isolated in this work, represent important intermediate structures on the way to the formation of larger intermetalloid clusters. Besides providing missing link structures for already known intermetalloids, such as $[Cu@Sn_9]^{3-}$, a plethora of further subsequent reactions of **1a–3a** yielding novel intermetalloid compounds is feasible. Concerning **2a**, this property of the novel *Zintl* clusters has already been proven by the isolation of $[AgSn_{18}]^{7-}$ (**4a**).

This work was financially supported by Wacker Chemie AG. F.G. thanks Dr Alexander Pöthig and the SC-XRD Laboratory of the Catalysis Research Center for measurement of **1**, T. Henneberger and Dr A. Schier for helpful discussions and TUM Graduate School for support.

References

1 T. F. Fässler and S. D. Hoffmann, *Angew. Chem., Int. Ed.*, 2004, **43**, 6242.
2 S. Mitzinger, L. Broeckaert, W. Massa, F. Weigend and S. Dehnen, *Nat. Commun.*, 2016, **7**, 10480.
3 J.-Q. Wang, S. Stegmaier, B. Wahl and T. F. Fässler, *Chem. – Eur. J.*, 2010, **16**, 1793.
4 S. Scharfe, F. Kraus, S. Stegmaier, A. Schier and T. F. Fässler, *Angew. Chem., Int. Ed.*, 2011, **50**, 3630.
5 S. C. Sevov and J. M. Goicoechea, *Organometallics*, 2006, **25**, 5678.
6 H. He, W. Klein, L.-A. Jantke and T. F. Fässler, *Z. Anorg. Allg. Chem.*, 2014, **640**, 2864.
7 M. Schreyer, G. Kraus and T. F. Fässler, *Z. Anorg. Allg. Chem.*, 2004, **630**, 2520.
8 M. J. Moses, J. C. Fettinger and B. W. Eichhorn, *Science*, 2003, **300**, 778.
9 Y. Wang, M. Moses-DeBusk, L. Stevens, J. Hu, P. Zavalij, K. Bowen, B. I. Dunlap, E. R. Glaser and B. Eichhorn, *J. Am. Chem. Soc.*, 2017, **139**, 619.
10 S. Stegmaier and T. F. Fässler, *J. Am. Chem. Soc.*, 2011, **133**, 19758.
11 N. Korber, *Angew. Chem., Int. Ed.*, 2009, **48**, 3216.
12 S. Zhou, K. McIlwrath, G. Jackson and B. Eichhorn, *J. Am. Chem. Soc.*, 2006, **128**, 1780.
13 S. Scharfe and T. F. Fässler, *Eur. J. Inorg. Chem.*, 2010, 1207.
14 A. Spiekermann, S. D. Hoffmann, T. F. Fässler, I. Krossing and U. Preiss, *Angew. Chem., Int. Ed.*, 2007, **46**, 5310.
15 O. Kysliak, C. Schrenk and A. Schnepf, *Angew. Chem., Int. Ed.*, 2016, **55**, 3216.
16 C. B. Benda, M. Waibel and T. F. Fässler, *Angew. Chem., Int. Ed.*, 2015, **54**, 522.
17 F. S. Geitner and T. F. Fässler, *Eur. J. Inorg. Chem.*, 2016, 2688.
18 C. Schenk and A. Schnepf, *Angew. Chem., Int. Ed.*, 2007, **46**, 5314.
19 C. Schenk, F. Henke, G. Santiso-Quinones, I. Krossing and A. Schnepf, *Dalton Trans.*, 2008, 4436.
20 C. Boehme and G. Frenking, *Organometallics*, 1998, **17**, 5801.
21 M. A. Omary, M. A. Rawashdeh-Omary, M. W. A. Gonser, O. Elbjeirami, T. Grimes, T. R. Cundari, H. V. K. Diyabalanage, C. S. P. Gamage and H. V. R. Dias, *Inorg. Chem.*, 2005, **44**, 8200.
22 A. Bayler, A. Schier, G. A. Bowmaker and H. Schmidbaur, *J. Am. Chem. Soc.*, 1996, **118**, 7006.
23 C. Hoch, M. Wendorff and C. Röhr, *Acta Crystallogr., Sect. C: Cryst. Struct. Commun.*, 2002, **58**, i45.

24 J.-Q. Wang, B. Wahl and T. F. Fässler, *Angew. Chem., Int. Ed.*, 2010, **49**, 6592.
25 K. Mayer, L. A. Jantke, S. Schulz and T. F. Fässler, *Angew. Chem., Int. Ed.*, 2017, **56**, 2350.
26 Dihedral angles of the open square planes: **A** (Sn6–Sn9): 179.57° and **B** (Sn15–Sn18): 177.18°. Diameter ratios of the open square planes: **A** D2(Sn7–Sn9)/D1(Sn6–Sn8) = 1.00 and **B** D2(Sn15–Sn17)/D1(Sn16–Sn18) = 1.09.
27 S. Scharfe, T. F. Fässler, S. Stegmaier, S. D. Hoffmann and K. Ruhland, *Chem. – Eur. J.*, 2008, **14**, 4479.
28 C. B. Benda, M. Waibel, T. Köchner and T. F. Fässler, *Chem. – Eur. J.*, 2014, **20**, 16738.
29 D. Rios, M. M. Gillett-Kunnath, J. D. Taylor, A. G. Oliver and S. C. Sevov, *Inorg. Chem.*, 2011, **50**, 2373.
30 F. S. Kocak, P. Zavalij, Y.-F. Lam and B. W. Eichhorn, *Inorg. Chem.*, 2008, **47**, 3515.
31 B. Kesanli, J. E. Halsig, P. Zavalij, J. C. Fettinger, Y.-F. Lam and B. W. Eichhorn, *J. Am. Chem. Soc.*, 2007, **129**, 4567.
32 D. O. Downing, P. Zavalij and B. W. Eichhorn, *Eur. J. Inorg. Chem.*, 2010, 890.
33 J. M. Goicoechea and S. C. Sevov, *Organometallics*, 2006, **25**, 4530.
34 B. Zhou, M. S. Denning, T. A. D. Chapman and J. M. Goicoechea, *Inorg. Chem.*, 2009, **48**, 2899.

Electronic Supplementary Material (ESI) for Dalton Transactions.

On the Formation of the Intermetalloid Cluster $[AgSn_{18}]^{7-}$ - The Reactivity of Coinage Metal NHC Compounds towards $[Sn_9]^{4-}$

F. S. Geitner,[a] W. Klein,[b] T. F. Fässler*[b]

[*b] Prof. Dr. T. F. Fässler, Department of Chemistry, Technische Universität München Lichtenbergstraße 4, 85747 Garching/München, Germany

[a] Felix S. Geitner, WACKER Institute for Silicon Chemistry and Departement of Chemistry, Technische Universität München Lichtenbergstraße 4, 85747 Garching/München, Germany

Inhalt

Experimental Section

All manipulations were carried out under a purified argon atmosphere using standard Schlenk and glove box techniques. K_4Sn_9 was prepared by fusion of stoichiometric amounts of the elements in sealed steel autoclaves and stored under argon atmosphere. 1,3-Bis(2,6-diisopropylphenyl)imidazolium chloride and $NHC^{Dipp}MCl$ (M: Cu, Ag, Au) were prepared according to modified literature procedures.[1-4] [2.2.2-Crypt] was dried in vacuo overnight. Liquid ammonia was dried and stored over sodium metal.

Syntheses:

1: K_4Sn_9 (62 mg, 0.050 mmol, 1 eq.), $NHC^{Dipp}CuCl$ (24.5 mg, 0.05 mmol, 1 eq.) and [2.2.2-crypt] (35 mg, 0.090 mmol, 1.86 eq.) were weighted into a Schlenk tube. Addition of ammonia (approximately 2 mL) led to the formation of a deep red suspension. The reaction mixture was homogenized by shaking the Schlenk tube several times and subsequently stored in a freezer at -70 °C. Compound **1** crystallizes as black block-shaped crystals. Since the crystals cannot be isolated from the reaction solution (decomposition due to loss of ammonia), the yield of approximately 30 % can only be estimated from the amount of crystalline material found in the reaction mixture.

2 and **4**: K_4Sn_9 (44 mg, 0.036 mmol, 1 eq.), $NHC^{Dipp}AgCl$ (19 mg, 0.036 mmol, 1 eq.) and [2.2.2-crypt] (54 mg, 0.144 mmol, 4 eq.) were weighted into a Schlenk tube. Addition of ammonia (approximately 1 mL) led to the formation of a deep red suspension. The reaction mixture was homogenized by shaking the Schlenk tube several times and subsequently stored in a freezer at -70 °C. After several months black block-shaped crystals had formed. Single crystal X-ray diffraction examination revealed a ratio of crystals of compound **4** to those of compound **2** of 9:1. Since the crystals cannot be isolated from the reaction solution (decomposition due to loss of ammonia), the yield of approximately 25 % (with respect to amount of Zintl phases used) can only be estimated from the amount of crystalline material found in the reaction mixture.

3: K_4Sn_9 (44 mg, 0.036 mmol, 1 eq.), $NHC^{Dipp}AuCl$ (22 mg, 0.036 mmol, 1 eq.) and [2.2.2-crypt] (25 mg, 0.067 mmol, 1.86 eq.) were weighted into a Schlenk tube. Addition of ammonia (approximately 1 mL) led to the formation of a deep red suspension. The reaction mixture was homogenized by shaking the Schlenk tube several times and subsequently stored in a freezer at -70 °C. Compound **3** crystallizes as black block-shaped crystals. Since the crystals cannot be isolated from the reaction solution (decomposition due to loss of ammonia), the yield of approximately 30 % can only be estimated from the amount of crystalline material found in the reaction mixture.

NMR experiments:

NMR spectra were measured on a Bruker Avance Ultrashield 400 MHz spectrometer. After evaporation of NH_3 (l) the residue was dissolved in MeCN to give a deep red solution. An aliquot sample of this solution was transferred to an NMR inner tube which was sealed with a plastic cap and positioned in a $CDCl_3$ filled standard NMR tube. The NMR spectrum was calibrated on the residual proton signal of $CDCl_3$.

Crystal Structure Determinations

The thermally very unstable, air and moisture sensitive crystals of **1**-**4** were transferred from the mother liquor into cooled perfluoroalkylether oil under a cold N_2 gas stream. For single crystal data collection, the single crystals were fixed on a glass capillary and positioned in a 100 K (**1**) or 120 K (**2**-**4**) cold N_2 gas stream using the crystal cap system. Single crystal data collection was either performed at an Oxford-Diffraction Xcalibur3 diffractometer ($Mo_{K\alpha}$ radiation) (**2**-**4**) or a Bruker AXS D8 diffractometer (**1**). Structures were solved by Direct Methods (SHELXS-2014) and refined by full-matrix least-squares calculations against F^2 (SHELXL-2014).[5] The positions of the hydrogen atoms were calculated and refined using a riding model. Unless otherwise stated, all non-hydrogen atoms were treated with anisotropic displacement parameters. The supplementary crystallographic data for this paper have been deposited with the Cambridge Structural database and are available free of charge via www.ccdc.cam.ac.uk/data_request/cif.

Crystal structure determination discussion:

The crystallographic data for compounds **1**-**4** are summarized in Table SI 1 and Table SI 2. In compounds **1**-**3** one of the ammonia molecules reveals only 50 % occupancy. In compound **2** some N atoms of ammonia molecules could not be refined anisotropically. For several different crystals of compound **4**, after structure refinement large residual electron density remained in the vicinity of atoms Sn11, Sn14, and Sn18, which have been included as additional Sn atoms (Sn19, Sn20, Sn21) and were refined as split atoms with a common occupancy factor. The two resulting individuals of the Sn_9 cluster are shown in Fig. SI 2. Furthermore, one of the $[K(2.2.2\text{-crypt})]^+$ units in **4** is disordered and was refined on split positions.

Table SI 1: Crystallographic data for compounds **1**-**3**.

Compound	**1**	**2**	**3**
formula	$Sn_9CuC_{81}H_{216}N_{32}O_{18}K_3$*	$Sn_9AgC_{81}H_{216}N_{32}O_{18}K_3$*	$Sn_9AuC_{81}H_{216}N_{32}O_{18}K_3$*
fw (g·mol^{-1})	3175.90	3220.23	3309.32
space group (no)	*C*2/*c*	*C*2/*c*	*C*2/*c*
***a* (Å)**	58.988(13)	57.925(2)	58.0663(14)
***b* (Å)**	16.921(4)	16.7406(3)	16.7942(3)
***c* (Å)**	31.528(7)	31.1204(8)	31.1263(7)
α (deg)	90	90	90
β (deg)	116.24(10)	115.003(3)	115.319(3)
γ (deg)	90	90	90
***V* (Å^3)**	28225(11)	27349.6(1.3)	27437.9(1.2)
Z	8	8	8
***T* (K)**	100(2)	120(2)	120(2)
λ (Å)	Mo *Kα*	Mo *Kα*	Mo *Kα*
ρ_{calcd} (g·cm^{-3})	1.495	1.564	1.602
μ (mm^{-1})	1.859	1.907	2.826
collected reflections	73013	147792	375392
independent reflections	24209	26868	26937
R_{int} / R_δ	0.0404/0.0463	0.0830/0.1113	0.1486/0.0708
parameters / restraints	1310/12	1290/30	1290/42
R_1 [$I > 2\sigma(I)$ / all data]	0.0300/0.0428	0.0363/0.0811	0.0361/0.0613
wR_2 [$I > 2\sigma(I)$ / all data]	0.0658/0.0716	0.0698/0.0759	0.0805/0.0848
goodness of fit	1.008	0.826	0.952
max./min. diff. el. density (e / Å^{-3})	0.93/-0.66	1.45/-0.64	1.34/-0.76
CCDC	1530025	1530026	1530027

[*]: 23.5 NH_3 cocrystallized molecules per formula unit are included in the sum formulae.

Table SI 2: Crystallographic data for compound **4**.

Compound	**4**
formula	$Sn_{18}Ag_1C_{72}H_{213}N_{31}O_{24}K_7$*
fw (g·mol^{-1})	4415.71
space group (no)	$P\bar{1}$
***a* (Å)**	17.3360(2)
***b* (Å)**	17.5287(2)
***c* (Å)**	27.4117(3)
***α* (deg)**	78.650(1)
***β* (deg)**	85.741(1)
***γ* (deg)**	71.589(1)
***V* (Å^3)**	7748.2(2)
Z	2
***T* (K)**	120(2)
***λ* (Å)**	Mo *Kα*
ρ_{calcd} (g·cm^{-3})	1.893
***μ* (mm^{-1})**	3.212
collected reflections	289154
independent reflections	29513
R_{int}* / *R_δ	0.0878/0.0455
parameters / restraints	1547/176
***R_1* [*I* > 2 *σ*(*I*) / all data]**	0.0462/0.0667
w*R_2* [*I* > 2 *σ*(*I*) / all data]	0.1242/0.1325
goodness of fit	1.077
max./min. diff. el. density (e / Å^{-3})	2.67/-1.63
CCDC	1530028

[*]: 23 NH_3 cocrystallized molecules per formula unit are included in sum formula.

Molecular Structures

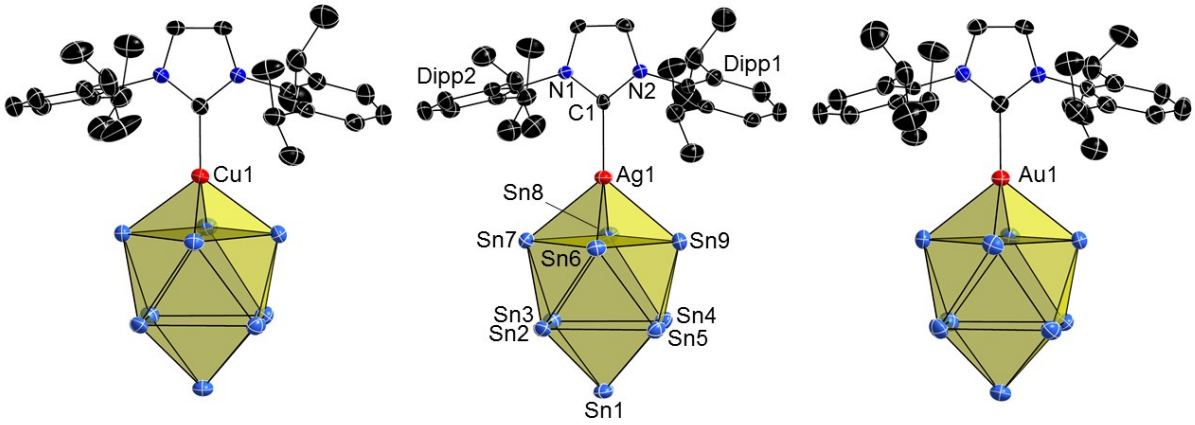

Figure SI 1: Molecular structures of **1a** (left) **2a** (middle) **3a** (right). Displacement ellipsoids are shown at a 50% probability level. For clarity hydrogen atoms, counterions and cocrystallized NH_3 molecules are omitted. Diisopropylphenyl-wingtips of NHC ligand are abbreviated as Dipp1 and Dipp2. **1a** and **3a** are labelled analogously to **2a**.

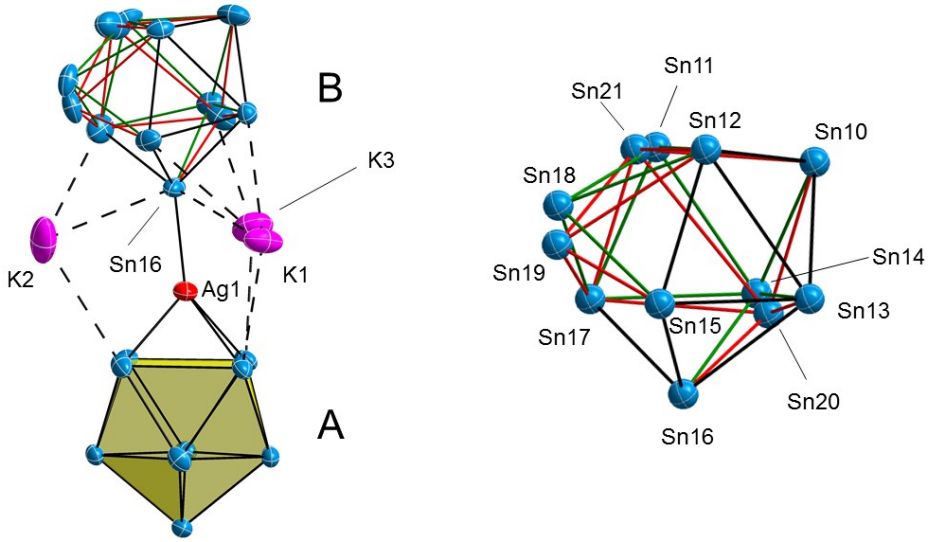

Figure SI 2: The dimeric cluster anion in compound **4**, exhibiting the two orientations of the disordered cluster B, with occupancies of 80.1 % (green) and 19.9 % (red). Also shown is the arrangement of "naked" potassium cations around the Sn-Ag-Sn bonding axis, which coordinate to both Sn_9^{4-} clusters with K-Sn distances below 4 Å (left). Displacement ellipsoids are shown at a 50% probability level. Moreover, a detailed view on the two orientations of disordered cluster B is given (right). For clarity atoms are here shown in ball and stick style.

Selected Distances and Angles

Table SI 3: Selected bond lengths [Å] and angles [°] in polyanions **1a**-**4a**.

	$[NHC^{Dipp}M(\eta^4\text{-}Sn_9)]^{3-}$			$[(\eta^1\text{-}Sn_9)M(\eta^4\text{-}Sn_9)]^{7-}$	
	1a	**2a**	**3a**	**4a (A)**	**4a (B)**
d(M-Sn6)	2.7216(7)	2.8527(6)	2.8149(4)	2.9111(8)	-
d(M-Sn7)	2.7376(8)	2.8698(6)	2.8310(4)	2.8785(8)	-
d(M-Sn8)	2.7491(7)	2.8670(6)	2.8206(4)	2.8749(9)	-
d(M-Sn9)	2.7391(6)	2.8419(5)	2.8055(4)	2.8884(8)	-
d(M-L)[a]	1.979(3)	2.181(5)	2.092(4)	2.7126(8)	-
d_{min}(Sn-Sn)	2.9458(6) (Sn1-Sn5)	2.9210(6) (Sn2-Sn6)	2.9307(5) (Sn1-Sn5)	2.9165(8) (Sn4-Sn9)	2.913(3) (Sn10-Sn14)
d_{max}(Sn-Sn)	3.3104(7) (Sn2-Sn5)	3.2737(5) (Sn2-Sn5)	3.2648(5) (Sn2-Sn5)	3.2572(7) (Sn3-Sn4)	3.2499(7) (Sn12-Sn13)
D2/D1[b]	1.01	1.00	1.01	1.00	1.08
∢(csp-M-L)[a][c]	179.83(2)	178.48(3)	179.18(2)	172.86(2)	-
torsion angle α[d]	178.90(2)	178.87(2)	178.88(1)	179.41(1)	177.24(2)

[a] L: NHC^{Dipp} for **1a**-**3a** and η^1-Sn_9 for **4a (A)**.

[b] D2/D1: diameter ratio of the square open plane with D2 (Sn7-Sn9) and D1 (Sn6-Sn8) for **1a**-**4a (A)** and D2 (Sn15-Sn17) and D1 (Sn16-Sn18) for **4a (B)**.

[c] csp: center of gravity of the atoms of the open square of the Sn_9^{4-} cluster.

[d] α: torsion angle of the open square (Sn6-Sn7-Sn8-Sn9).

Table SI 4: M-Sn and Sn-Sn distances [Å] in compounds **1** (left), **2** (middle), and **3** (right).

bond	**distance [M = Cu]**	**distance [M = Ag]**	**distance [M = Au]**
M-Sn6	2.7216(7)	2.8527(6)	2.8149(4)
M-Sn7	2.7376(8)	2.8698(6)	2.8310(4)
M-Sn8	2.7491(7)	2.8670(6)	2.8206(4)
M-Sn9	2.7391(6)	2.8419(5)	2.8055(4)
M-C1	1.979(3)	2.181(5)	2.092(4)
Sn1-Sn2	2.9939(7)	2.9428(5)	2.9471(5)
Sn1-Sn3	2.9773(7)	2.9540(6)	2.9612(5)
Sn1-Sn4	2.9868(7)	2.9564(6)	2.9643(5)
Sn1-Sn5	2.9458(6)	2.9261(6)	2.9307(5)
Sn2-Sn3	3.1938(6)	3.1681(6)	3.1539(5)
Sn3-Sn4	3.2284(7)	3.1923(6)	3.1864(5)
Sn4-Sn5	3.1959(7)	3.1792(6)	3.1646(5)
Sn5-Sn2	3.3104(7)	3.2737(5)	3.2648(5)
Sn2-Sn6	2.9529(7)	2.9210(6)	2.9319(4)
Sn2-Sn7	2.9771(6)	2.9500(5)	2.9573(5)
Sn3-Sn7	3.0122(8)	2.9664(5)	2.9730(5)
Sn3-Sn8	2.9965(8)	2.9672(6)	2.9761(5)
Sn4-Sn8	3.0039(6)	2.9592(5)	2.9707(5)
Sn4-Sn9	2.9965(7)	2.9637(6)	2.9708(5)
Sn5-Sn9	2.9614(6)	2.9294(6)	2.9396(5)
Sn5-Sn6	3.0199(7)	2.9700(5)	2.9762(5)
Sn6-Sn7	3.0868(7)	3.1005(5)	3.1231(5)
Sn7-Sn8	3.1049(6)	3.0849(5)	3.1033(5)
Sn8-Sn9	3.0938(7)	3.1189(6)	3.1414(5)
Sn9-Sn6	3.1151(6)	3.1029(5)	3.1219(5)
Sn6-Sn8	4.3647(8)	4.3734(5)	4.3977(5)
Sn7-Sn9	4.4037(8)	4.3996(5)	4.4336(5)

Table SI 5: Ag-Sn and Sn-Sn distances in **4**.

bond	**distance in [Å]**	**bond**	**distance in [Å]**
Ag-Sn6	2.9118(9)	Sn11-Sn12	3.186(2)
Ag-Sn7	2.8785(8)	Sn11-Sn14	3.184(4)
Ag-Sn8	2.8749(9)	Sn11-Sn17	2.933(3)
Ag-Sn9	2.8884(8)	Sn11-Sn18	2.946(4)
Sn1-Sn2	2.9523(7)	Sn12-Sn13	3.2499(7)
Sn1-Sn3	2.9280(7)	Sn12-Sn15	2.9439(8)
Sn1-Sn4	2.9458(7)	Sn12-Sn18	2.924(3)
Sn1-Sn5	2.9541(7)	Sn13-Sn15	2.9767(8)
Sn2-Sn3	3.2366(7)	Sn13-Sn16	2.9702(7)
Sn3-Sn4	3.2572(7)	Sn14-Sn16	3.005(3)
Sn4-Sn5	3.1633(7)	Sn14-Sn17	2.945(3)
Sn5-Sn2	3.1870(7)	Sn15-Sn16	2.9276(8)
Sn2-Sn6	2.9499(7)	Sn16-Sn17	2.9321(8)
Sn2-Sn7	2.9683(7)	Sn17-Sn18	3.034(2)
Sn3-Sn7	2.9252(8)	Sn15-Sn18	3.013(3)
Sn3-Sn8	2.9237(7)	Sn15-Sn17	4.3645(8)
Sn4-Sn8	2.9607(7)	Sn16-Sn18	4.046(1)
Sn4-Sn9	2.9165(8)	Sn10-Sn20	3.03(1)
Sn5-Sn9	2.9773(7)	Sn10-Sn21	3.23(2)
Sn5-Sn6	2.9527(7)	Sn12-Sn19	3.220(8)
Sn6-Sn7	3.0902(8)	Sn12-Sn21	3.16(1)
Sn6-Sn8	4.3896(8)	Sn13-Sn20	2.95(1)
Sn7-Sn9	4.3833(7)	Sn15-Sn19	2.65(1)
Sn8-Sn9	3.0892(8)	Sn16-Sn19	3.53(2)
Ag-Sn16	2.7126(8)	Sn17-Sn19	2.79(1)
Sn10-Sn11	2.922(4)	Sn17-Sn20	3.15(2)
Sn10-Sn12	2.9514(9)	Sn17-Sn21	2.79(1)
Sn10-Sn13	2.9203(8)	Sn19-Sn21	3.01(2)
Sn10-Sn14	2.913(3)		

References

1. L. Hintermann, *Beilstein J. Org. Chem.*, 2007, **3**, 22.
2. O. Santoro, A. Collado, A. M. Z. Slawin, S. P. Nolan and C. S. J. Cazin, *Chem. Commun.*, 2013, **49**, 10483-10485.
3. P. de Frémont, N. M. Scott, E. D. Stevens, T. Ramnial, O. C. Lightbody, C. L. B. Macdonald, J. A. C. Clyburne, C. D. Abernethy and S. P. Nolan, *Organometallics*, 2005, **24**, 6301-6309.
4. A. Collado, A. Gomez-Suarez, A. R. Martin, A. M. Z. Slawin and S. P. Nolan, *Chem. Commun.*, 2013, **49**, 5541-5543.
5. G. Sheldrick, *Acta Crystallographica Section C*, 2015, **71**, 3-8.

5.3 Introducing Tetrel Zintl Ions to *N*-heterocyclic Carbenes – Synthesis of Coinage Metal NHC Complexes of $[Ge_9\{Si(SiMe_3)_3\}_3]^-$

F. S. Geitner, T. F. Fässler*

published in

Eur. J. Inorg. Chem. **2016**, 2688.

Content and Contributions

The scope of this work was to test the reactivity of coinage metal NHC complexes towards the tris-silylated [Ge_9] cluster [$Ge_9\{Si(TMS)_3\}_3]^-$, aiming for the synthesis of coinage metal NHC fragment coordinated [Ge_9] clusters. Therefore, the coinage metal NHC complexes NHC^{Dipp}*M*Cl (*M*: Cu, Ag, Au) were reacted with $[Ge_9\{Si(TMS)_3\}_3]^-$ in acetonitrile, which resulted in the formation of neutral [Ge_9] cluster coinage metal NHC compounds [NHC^{Dipp}*M*(η^3-$Ge_9\{Si(TMS)_3\}_3$)] (*M*: Cu, Ag, Au) through addition of $[NHC^{Dipp}M]^+$ fragments to one of the triangular bases of the tricapped trigonal prismatic [Ge_9] clusters in salt metathesis reactions. The product compounds were characterized by means of NMR, elemental analysis and single crystal X-ray diffraction. Whereas for (*M*: Cu, Au) the obtained neutral compounds are remarkably stable in solution (up to two weeks), for the respective Ag^+ compound a rearrangement reaction in solution occurs within one week, which was monitored by NMR. The resulting novel species was identified as $[Ag(\eta^3\text{-}Ge_9\{Si(TMS)_3\}_3)_2]^-[AgNHC^{Dipp}{}_2]^+$ by single crystal X-ray diffraction and NMR spectroscopy. The evaluation of the single crystal data of this compound was assisted by Dr. Wilhelm Klein. The differing reactivity of the Ag^+ compound can be explained by the increased lability of the Ag-NHC bond if compared to analogous Cu^+ or Au^+ species. The publication was written in the course of this thesis.

ChemPubSoc Europe

DOI: 10.1002/ejic.201600258

EurJIC European Journal of Inorganic Chemistry

Communication

Zintl Ion Ligands

Introducing Tetrel Zintl Ions to *N*-Heterocyclic Carbenes – Synthesis of Coinage Metal NHC Complexes of $[Ge_9\{Si(SiMe_3)_3\}_3]^-$

Felix S. Geitner[a] and Thomas F. Fässler*[b]

Abstract: Reaction of the functionalized tetrel cluster $[Ge_9R_3]^-$ {R = $Si(SiMe_3)_3$} with coinage metal *N*-heterocyclic carbene (NHC) complexes affords the first Zintl cluster transition metal complexes coordinated by NHC molecules. In $[(\eta^3\text{-}Ge_9R_3)\text{-}M(NHC^{Dipp})]$, the D_{3d}-symmetric cluster polyhedron coordinates with a triangular Ge_3 face to the coinage metals M = Cu, Ag, Au, which themselves also bind to the NHC. The role of fine tuning of electronic properties by using an NHC ligand is discussed for the transformation reaction of $[(\eta^3\text{-}Ge_9R_3)\text{-}Ag(NHC^{Dipp})]$ to yield $[Ag(\eta^3\text{-}Ge_9R_3)_2][Ag(NHC^{Dipp})_2]$. All complexes are fully characterized including single-crystal X-ray structure analyses.

Introduction

Metalloid and intermetalloid clusters of the tetrel elements have been intensively studied in recent years, resulting in the successful synthesis of a large number of novel substances.[1] In the last decade, the potential of Zintl tetrel clusters to act as precursors for semiconducting materials or novel element allotropes has been put in the focus of research efforts.[2] In addition to compounds containing ligand-free nine-atom group 14 clusters or ligand-free intermetalloid clusters, the chemistry of functionalized clusters of the form $[Ge_9R_3]^-$ {R = $Si(SiMe_3)_3$},[3] which has also been obtained by other methods,[4] and $[Ge_9R^I{}_2]^{2-}$ (R^I = C_2H_3),[5] obtained from the reaction of Zintl ions with alkynes, starts to establish a very promising field to extend the chemistry of main-group element-rich compounds. Recently, also the first connection between two Zintl clusters by an electronically unsaturated C_4 bridge has been realized in Zintl triads.[6] A big advantage of such functionalized species over bare Zintl ions is their enhanced stability and their solubility in less polar solvents such as tetrahydrofuran or acetonitrile, while the fourfold negatively charged Zintl clusters afford aprotic and highly polar solvents e.g. ethylenediamine, dimethylformamide, or liquid ammonia. $[Ge_9R_3]^-$, which consists of a Ge_9 core with the shape of a tricapped trigonal prism and three silyl substituents bound to the three capping atoms by *exo*-bonds can be easily synthesized in a heterogeneous reaction of K_4Ge_9 and $Si(SiMe_3)_3Cl$ in acetonitrile.[3]

Up to now there is a rather limited number of reports on the successful reaction of $[Ge_9R_3]^-$ with organic ligands,[7] main-group metal organyls,[7,8] and transition metal complexes of groups 6, 10, 11, and 12.[9]

In $[(CO)_3M(\eta^5\text{-}Ge_9R_3)]^-$ (M = Cr, Mo, W),[9b] the group 6 metal is incorporated into the cluster core, in analogy to the structure of the bare stannides $[(CO)_3M(\eta^5\text{-}Sn_9)]$ (Cr, Mo, W)[10] and the plumbide $[(CO)_3Mo(\eta^5\text{-}Pb_9)]$,[11] leading to a cluster enlargement.[9a,9b] For $[(CO)_5Cr(Ge_9R_3)]^-$, the cluster coordinates to the chromium atom through one Ge atom in the triangular base of the prism.[9a] Regarding group 10, 11, and 12 metals, only metal-bridged dimeric species $[M(\eta^3\text{-}Ge_9R_3)_2]$[9c–9f] have been published, except the recently published Cu-bridged dimer, which, in addition, coordinates to $Cu(PPh_3)$ at the free triangular base of one of the clusters.[9c]

In functionalized or bare Zintl ions, the addition of transition metals has been achieved with precursors bearing alkyl (*i*Pr), alkenyl (cod), alkynyl (phenylacetylenide), arene (phenyl, mesityl, cyclopentadienyl), carbonyl, phosphine [PPh_3, PCy_3, $P(iPr)_3$], and amine (ethylendiamine) ligands.[1b,12] However, *N*-heterocyclic carbene ligands (NHCs), which are chemically very robust and have diverse electronic properties,[13] have not been considered in Zintl ion chemistry yet. Due to their superb σ-donor properties, NHC complexes of transition metals are used in many homogeneous catalyst systems.[14] Fine-tuning the electronic properties with NHCs and similar heterocyclic carbenes such as cyclic alkyl(amino) carbenes (CAACs) recently opened fantastic possibilities to stabilize rather unusual molecules and complexes.[15] In comparison with phosphine ligands, NHCs do not tend to ligand dissociation, and NHC complexes are more stable towards oxygen and moisture.[14]

Results and Discussion

In this context, we started to examine the reactivity of coinage metal NHC complexes towards $[Ge_9R_3]^-$.

The reaction of $K[Ge_9R_3]$ {R = $Si(SiMe_3)_3$} with one equivalent of coinage metal NHC halides $NHC^{Dipp}MX$ [NHC^{Dipp}: 1,3-bis(2,6-diisopropylphenyl)-2,3-dihydroimidazol-2-ide; M: Cu, Ag, Au; X:

[a] *Institute for Silicon Chemistry and Department of Chemistry, Technische Universität München, Lichtenbergstraße 4, 85747 Garching/München, Germany*

[b] *Department of Chemistry, Technische Universität München, Lichtenbergstraße 4, 85747 Garching/München, Germany*
E-mail: thomas.faessler@lrz.tum.de
http://www.ch.tum.de/faessler/

Supporting information for this article is available on the WWW under http://dx.doi.org/10.1002/ejic.201600258.

Cl, Br] in acetonitrile at room temperature afforded cluster compounds [NHC^{Dipp}M(η^3-Ge_9R_3)] {M: Cu (**1**), Ag (**2**), and Au (**3**)} (Scheme 1). The complexes precipitate from the reaction solution as orange (**1**, **3**) or yellow to brownish (**2**) solids in good yields.

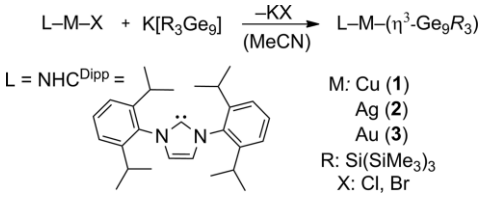

Scheme 1. Reaction of $[Ge_9R_3]^-$ with coinage metal NHC complexes.

Neutral complexes **1**–**3** are not soluble in acetonitrile but readily dissolve in thf and toluene. Recrystallization from toluene at –40 °C delivers analytically pure samples in 30–60 % yield that have been characterized by ^{1}H, ^{13}C, and ^{29}Si-INEPT NMR spectroscopy (Table 1 and spectra in the Supporting Information), as well as suitable block-like single crystals for X-ray diffraction (orange for **2** and red for **1** and **3**).

Table 1. NMR shifts [ppm] of TMS groups in compounds **1**–**3**. All spectra were recorded in [D$_8$]thf.

Complex	δ (^{1}H NMR)	δ (^{13}C NMR)	δ (^{29}Si NMR)
1	0.22	3.57	–9.60
2	0.20	3.44	–9.43
3	0.22	3.64	–9.31

The ^{1}H NMR signals appear at shifts of approximately δ = 0.2 ppm. Comparison of the intensities of the TMS groups to the signals of the NHC ligand shows, as expected, a relation of 1:1 between $[Ge_9R_3]^-$ and the NHC^{Dipp} ligand. In addition to the signals assigned to the intermetalloid NHC compounds in the spectrum of compound **2**, a second signal set with very low intensity (TMS shift at δ = 0.33 ppm) is detected. Furthermore, ESI-MS measurements were carried out with a thf solution of compound **1**, resulting in signals at *m/z* relations of 1396.6 ($[Ge_9R_3]^-$) and 1570.6 {[Cu(η^3-Ge_9R_3)K]$^-$ + thf} in the negative-ion mode, implying the cleavage of the cluster and the NHC ligand from the compound, respectively, under ionization conditions (Supporting Information). Single-crystal X-ray structure determinations of **1**–**3** confirm the compositions expected from the spectroscopic data. The intermetalloid NHC complexes crystallize in the triclinic space group $P\bar{1}$. As a representative example, the molecular structure of **3** is depicted in Figure 1 (the structures of **1** and **2** are shown in the Supporting Information).

In compounds **1**–**3**, the shape of the $[Ge_9R_3]^-$ unit can be described as a tricapped triangular prism with silyl groups on the capping atoms. Being situated over one of the triangular bases of the cluster, the coinage-metal–NHC fragment binds to three Ge atoms (Ge1, Ge2, and Ge3), forming a η^3-bond, as already observed for transition-metal-bridged dimers.[9c–9f] The mean Ge–M bond length increases in the order 2.5263(9) (**1**), 2.637(1) (**3**), and 2.7440(4) Å (**2**) and correlates with the increasing covalent radii of two-coordinate M^+ [r(Cu$^+$) = 1.11 Å; r(Au$^+$) = 1.25 Å; r(Ag$^+$) = 1.34 Å] (Table 2).[16] This observation is also true for the coinage-metal–NHC bonds.

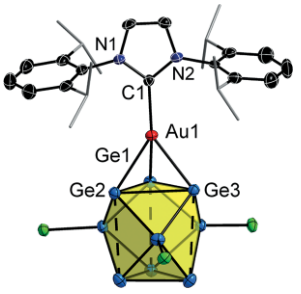

Figure 1. Molecular structure of **3**. Displacement ellipsoids are shown at a 50 % probability level. For clarity, TMS groups at the cluster and the cocrystallized toluene molecule are omitted and isopropyl groups of the NHC^{Dipp} ligand are pictured as gray-colored wires. Selected bond lengths and angles are listed in Table 2.

Table 2. Selected bond lengths [Å] and angles [°] of complexes **1**–**3**.

NHC^{Dipp}M-(η^3-Ge_9R_3)	**1**	**2**	**3**
Distances			
M–Ge1	2.4943(9)	2.734(1)	2.6184(4)
M–Ge2	2.5188(9)	2.758(1)	2.6621(4)
M–Ge3	2.5660(9)	2.740(1)	2.6318(4)
M–C1	1.957(5)	2.174(7)	2.072(3)
Angles			
ctp–M1–C1[a]	173.59(1)	178.1(2)	178.00(6)
C1–N1–C101	122.8(4)	127.4(6)	127.9(3)
C1–N2–C201	126.2(4)	127.2(6)	127.3(3)
Plane A/plane B[b]	11.4(2)	18.4(3)	28.62(7)

[a] ctp: center of gravity of the atoms of the triangular plane Ge1–Ge2–Ge3. [b] Dihedral angle of plane A through atoms N1–C1–N2 (imidazolium ring) and plane B M–ctp–Ge4 (for **1** and **3**) and Ag–ctp–Ge5 (for **2**). The smallest possible angles with respect to the three Ge atoms were chosen.

The coordination of the two ligands to the coinage metals, which are at the center of gravity of atoms Ge1 to Ge3 and the C1 atom of the NHC ligand, is nearly linear in **2** and **3** (178°) and more bent in **1** (174°). This parameter correlates with the conformation of the NHC ligand with respect to the $[Ge_9R_3]^-$ cluster and is best illustrated by a top view of the triangular plane coordinating to the transition-metal–NHC fragments, where Ge1 is the atom with the shortest Ge–M distance (Figure 2). The orientation of the mean plane of the imidazolium ring of the NHC ligands in **1**–**3** with respect to the Ge_9 core and, as a consequence, the interaction of the wingtip substituents of the NHC ligands with the silyl groups of the Ge_9 cluster differ. In **2** and **3**, both of the diisopropylphenyl (Dipp) groups of the NHC ligand slightly overlap with a silyl group on the Ge_9 cluster. However, regarding Cu complex **1**, one of the Dipp groups fully overlaps with a cluster silyl group while the other NHC substituent lies between the two other silyl groups. The special conformation of copper compound **1** can be explained by looking at the bonding angle between the imidazolium ring and the Dipp groups (C1–N1–C101 and C1–N2–C201) (Table 2). In complexes **2** and **3**, the bonding angles are similar for the two aryl rings (127°); however, in **1**, the angles are significantly different [122.8(4)° and 126.2(4)°]. Therefore, the Dipp group closer to the $[Ge_9R_3]^-$ unit (the smaller angle) is located between two silyl groups, resulting in a stronger overlap and a larger angle

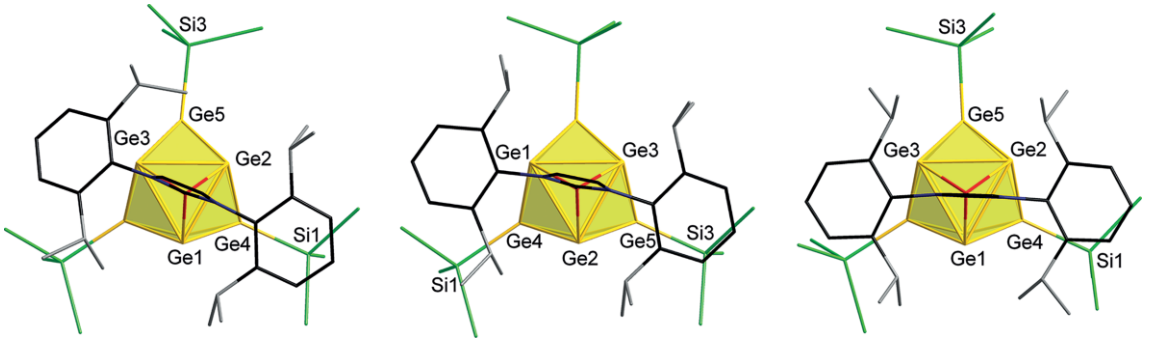

Figure 2. Front view of structures **1** (left) to **3** (right). Structures are pictured in wire-and-stick style. Methyl groups of TMS functions are omitted and isopropyl groups of NHC^{Dipp} are pictured in gray for clarity.

over the other aryl group with the remaining silyl group. In consequence, a more distinct deviation from linear coordination for compound **1** lowers the steric interaction between the overlapping Dipp group and silyl substituent. Furthermore, Figure 2 reveals that the Ge5–Si3 bond is bent away from the di-*i*Pr group in **1**.

During the preparation of compound **2**, small orange crystalline needles of the side product, which had been detected by ^{1}H NMR spectroscopy, were isolated by slow diffusion of diethyl ether vapor into a C_6D_6 solution of the product mixture. Even though the crystals did not diffract very well, it was possible to indubitably determine all heavy atoms.

$[AgGe_{18}R_6][Ag(NHC^{Dipp})_2]$ (**4**) consists of the anionic coinage-metal-bridged Ge_9 dimer $[(\eta^3\text{-}Ge_9R_3)Ag(\eta^3\text{-}Ge_9R_3)]^-$ (**4a**) and the cationic bis(NHC) species $[Ag(NHC^{Dipp})_2]^+$ (**4b**) (Figure 3).

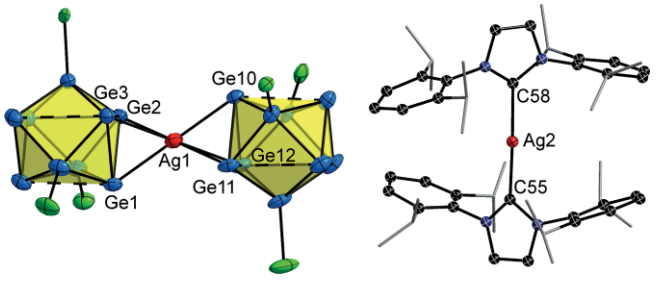

Figure 3. Molecular structure of **4**. Cocrystallized toluene molecules are omitted for clarity. In anion **4a**, TMS groups at the clusters are omitted for clarity. Cation **4b** is pictured in ball-and-stick style, and its isopropyl groups are presented in gray color in wire-and-stick style for clarity. All displacement ellipsoids are shown at a 50 % probability level.

A continuous rearrangement of compound **2** to compound **4** within approximately one week according to Scheme 2 was monitored by ^{1}H NMR spectroscopy in $[D_8]$thf (Figure 4).

Similar experiments with compounds **1** and **3** revealed no rearrangement of the copper and the gold compounds within two weeks. We assign the formation of **4** to the weaker NHC–Ag bond relative to the Cu–NHC and Au–NHC bonds.[17] Compound **4** forms either by means of a concerted metathesis reaction by ligand exchange or by NHC–Ag bond cleavage and formation of an intermediate of the type $[L\text{–}Ag\{(\eta^3\text{:}\eta^3)\text{-}Ge_9R_3\}Ag(\eta^3\text{-}Ge_9R_3)]$ (**5**). The formation of the latter can easily be rationalized by a nucleophilic attack of a $[L\text{–}Ag(\eta^3\text{-}Ge_9R_3)]$ molecule with the free triangular cluster side at the electrophilic

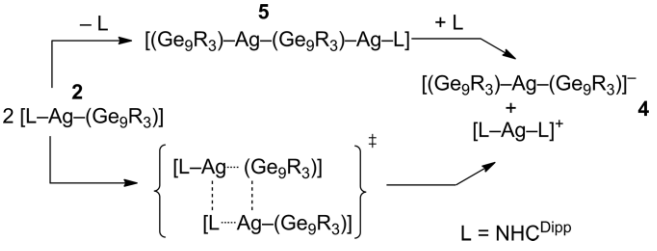

Scheme 2. Rearrangement reaction of compound **2** to give compound **4**.

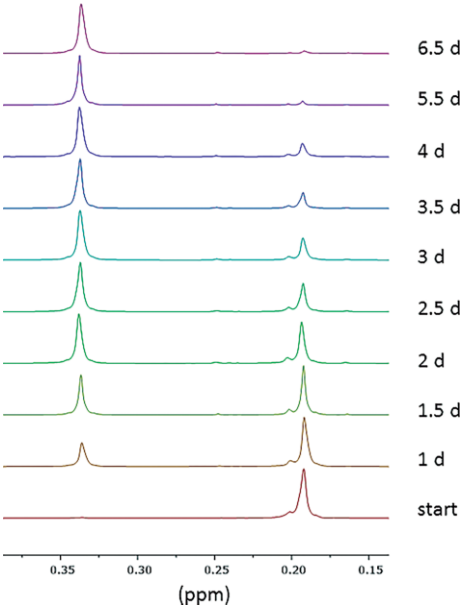

Figure 4. ^{1}H NMR spectroscopic study of the rearrangement of compound **2** (δ = 0.20 ppm) to dimeric species **4** (δ = 0.33 ppm).[9e] The corresponding signals are caused by methyl protons of TMS groups.

Ag atom of a second $[L\text{–}Ag(\eta^3\text{-}Ge_9R_3)]$ molecule followed by cleavage of the NHC moiety. An intermediate structure similar to **5** was recently observed for M = Cu and L = PPh_3 by the group of Sevov.[9c] Both mechanisms afford the cleavage of the M–NHC bond, which is more likely for M = Ag than M = Cu or Au, and therefore no rearrangement is observed in compounds **1** and **3**.[17]

The structure of **4a** is similar to the coinage-metal-bridged dimers published by Schnepf: the $[Ge_9R_3]^-$ units coordinate the transition metal in staggered configuration via three germanium atoms forming a η^3-bond each.[9d,9e] Comparing the M–Ge bond lengths in the intermetalloid NHC species **1**–**3** to those of the known coinage-metal-bridged dimeric cluster compounds and compound **4**, the bonding distances are, as expected, shorter due to the lower coordination number of the central metal in NHC complexes **1**–**3** {e.g. for [NHC^{Dipp}-Cu(η^3-Ge_9R_3)]: Cu–Ge 2.5263(9) Å; for $[CuGe_{18}R_6]^-$: Cu–Ge 2.622(1) Å}.[9e]

The coexistence of compound **2** and **4** can be compared to the formation of the ligand-free Zintl complexes [L–Cu(η^4-Ge_9)]$^{3-}$ (L = PR_3, R = *i*Pr, Cy) (**6**) and the Cu-bridged complex [(η^4-Ge_9)–Cu–(η^1-Ge_9)]$^{7-}$ (**7**), which were obtained from NH_3 (l) solutions. The isolation of the two products, however, only indirectly suggests the stepwise release of the ligands in R_3PCuCl upon reaction with $[Ge_9]^{4-}$.[18]

Conclusions

Neutral Zintl cluster transition metal NHC complexes **1**–**3** [(η^3-Ge_9R_3)M(NHC^{Dipp})] can be synthesized for M = Cu, Ag, and Au in good yields. These compounds are highly stable and soluble in standard solvents, and they were fully characterized.

^{1}H NMR spectroscopic investigations confirm the stability of complexes **1** and **3** in solution, while for compound **2** a rearrangement to dimeric species **4** can been monitored. Therefore, we are convinced that coordination of transition metal NHC fragments to Zintl clusters provides a means of closer exploration of tetrel clusters in solution and leads to more straightforward synthesis procedures for intermetalloid compounds.

Acknowledgments

This work was financially supported by Wacker Chemie AG. F. S. G. thanks the Technische Universität München Graduate School for support.

Keywords: Zintl anions · Cluster compounds · NHC complexes · Coinage metals

[1] a) S. C. Sevov, J. M. Goicoechea, *Organometallics* **2006**, *25*, 5678–5692; b) S. Scharfe, F. Kraus, S. Stegmaier, A. Schier, T. F. Fässler, *Angew. Chem. Int. Ed.* **2011**, *50*, 3630–3670; *Angew. Chem.* **2011**, *123*, 3712.
[2] a) A. M. Guloy, R. Ramlau, Z. Tang, W. Schnelle, M. Baitinger, Y. Grin, *Nature* **2006**, *443*, 320–323; b) G. S. Armatas, M. G. Kanatzidis, *Science* **2006**, *313*, 817–820; c) D. Sun, A. E. Riley, A. J. Cadby, E. K. Richman, S. D. Korlann, S. H. Tolbert, *Nature* **2006**, *441*, 1126–1130; d) M. M. Bentlohner, M. Waibel, P. Zeller, K. Sarkar, P. Müller-Buschbaum, D. Fattakhova-Rohlfing, T. F. Fässler, *Angew. Chem. Int. Ed.* **2016**, *55*, 2441–2445; *Angew. Chem.* **2016**, *128*, 2487–2491.
[3] F. Li, S. C. Sevov, *Inorg. Chem.* **2012**, *51*, 2706–2708.
[4] A. Schnepf, *Angew. Chem. Int. Ed.* **2003**, *42*, 2624–2625; *Angew. Chem.* **2003**, *115*, 2728.
[5] a) M. W. Hull, S. C. Sevov, *Inorg. Chem.* **2007**, *46*, 10953–10955; b) C. B. Benda, J.-Q. Wang, B. Wahl, T. F. Fässler, *Eur. J. Inorg. Chem.* **2011**, 4262–4269.
[6] M. M. Bentlohner, W. Klein, Z. H. Fard, L.-A. Jantke, T. F. Fässler, *Angew. Chem. Int. Ed.* **2015**, *54*, 3748–3753; *Angew. Chem.* **2015**, *127*, 3819.
[7] F. Li, S. C. Sevov, *J. Am. Chem. Soc.* **2014**, *136*, 12056–12063.
[8] F. Li, A. Munoz-Castro, S. C. Sevov, *Angew. Chem. Int. Ed.* **2012**, *51*, 8581–8584; *Angew. Chem.* **2012**, *124*, 8709.
[9] a) C. Schenk, A. Schnepf, *Chem. Commun.* **2009**, 3208; b) F. Henke, C. Schenk, A. Schnepf, *Dalton Trans.* **2011**, *40*, 6704; c) F. Li, S. C. Sevov, *Inorg. Chem.* **2015**, *54*, 8121–8125; d) C. Schenk, A. Schnepf, *Angew. Chem. Int. Ed.* **2007**, *46*, 5314–5316; *Angew. Chem.* **2007**, *119*, 5408; e) C. Schenk, F. Henke, G. Santiso-Quinones, I. Krossing, A. Schnepf, *Dalton Trans.* **2008**, 4436–4441; f) F. Henke, C. Schenk, A. Schnepf, *Dalton Trans.* **2009**, 9141–9145.
[10] B. Kesanli, J. Fettinger, B. Eichhorn, *Chem. Eur. J.* **2001**, *7*, 5277–5285.
[11] L. Yong, S. D. Hoffmann, T. F. Fässler, *Eur. J. Inorg. Chem.* **2005**, 3663–3669.
[12] a) J. M. Goicoechea, S. C. Sevov, *J. Am. Chem. Soc.* **2006**, *128*, 4155–4161; b) B. Zhou, M. S. Denning, C. Jones, J. M. Goicoechea, *Dalton Trans.* **2009**, 1571–1578.
[13] T. Droge, F. Glorius, *Angew. Chem. Int. Ed.* **2010**, *49*, 6940–6952; *Angew. Chem.* **2010**, *122*, 7094.
[14] a) E. A. B. Kantchev, C. J. O'Brien, M. G. Organ, *Angew. Chem. Int. Ed.* **2007**, *46*, 2768–2813; *Angew. Chem.* **2007**, *119*, 2824; b) W. A. Herrmann, M. Elison, J. Fischer, C. Köcher, G. R. J. Artus, *Angew. Chem. Int. Ed. Engl.* **1995**, *34*, 2371–2374; *Angew. Chem.* **1995**, *107*, 2602.
[15] a) H. Tanaka, M. Ichinohe, A. Sekiguchi, *J. Am. Chem. Soc.* **2012**, *134*, 5540–5543; b) R. S. Ghadwal, H. W. Roesky, S. Merkel, J. Henn, D. Stalke, *Angew. Chem. Int. Ed.* **2009**, *48*, 5683–5686; *Angew. Chem.* **2009**, *121*, 5793; c) D. S. Weinberger, M. Melaimi, C. E. Moore, A. L. Rheingold, G. Frenking, P. Jerabek, G. Bertrand, *Angew. Chem. Int. Ed.* **2013**, *52*, 8964–8967; *Angew. Chem.* **2013**, *125*, 9134.
[16] M. A. Omary, M. A. Rawashdeh-Omary, M. W. A. Gonser, O. Elbjeirami, T. Grimes, T. R. Cundari, H. V. K. Diyabalanage, C. S. P. Gamage, H. V. R. Dias, *Inorg. Chem.* **2005**, *44*, 8200–8210.
[17] C. Boehme, G. Frenking, *Organometallics* **1998**, *17*, 5801–5809.
[18] S. Scharfe, T. F. Fässler, *Eur. J. Inorg. Chem.* **2010**, 1207–1213.

Received: March 8, 2016
Published Online: April 19, 2016

Eur. J. Inorg. Chem. **2016** · ISSN 1099–0682

SUPPORTING INFORMATION

DOI: 10.1002/ejic.201600258
Title: Introducing Tetrel Zintl Ions to *N*-Heterocyclic Carbenes – Synthesis of Coinage Metal NHC Complexes of $[Ge_9\{Si(CH_3)_3\}_3]^-$
Author(s): Felix S. Geitner, Thomas F. Fässler*

Contents:

General Information

All manipulations were performed under oxygen free, dry conditions under argon atmosphere using standard Schlenk or glovebox techniques. Glassware was dried prior to use by heating it *in vacuo*. The solvents used were obtained from a MBraun Grubbs apparatus. All other commercially available chemicals were used without further purification. K_4Ge_9 was prepared by fusion of stoichiometric amounts of the elements in stainless steel tubes at 650 °C. 1,3-bis(2,6-diisopropylphenyl)imidazolium chloride, the corresponding coinage metal halide complexes and $K[Ge_9R_3]$ (R: $Si(SiMe_3)_3$) were synthesized according to modified literature procedures.[1-5] NMR spectra were acquired on a Bruker Avance Ultrashield 400 MHz and a Bruker DPX 400 MHz spectrometer. All chemical shifts are reported in parts per million (ppm) relative to TMS, with the residual solvent peak serving as internal reference.[6] Abbreviations for signal multiplicities are: singulett (s), dublett (d), triplett (t), heptett (h). ESI-MS analysis was performed on a Bruker Daltronic HCT mass spectrometer. Crystallographic data was collected with an Oxford Diffraction Xcalibur3 diffractometer, MoKα radiation (λ = 0.71073 Å). The structures were solved by direct methods (SHELXS-97) and refined by full-matrix least-squares calculations on $\sum \omega(F_0^2\text{-}F_c^2)^2$ (SHELXL-97).[7] Unless otherwise stated all non-hydrogen atoms were refined with anisotropic displacement parameters. All hydrogen atoms were placed in calculated positions and refined by using a riding model. Elemental analyses were conducted by the micro-analytical laboratory of the TUM.

Synthetic Procedure

*[Dipp-Cu(η^3-Ge_9R_3)] (**1**)*

Cu-Dipp-Br (53 mg, 0.1 mmol, 1 eq.) was dissolved in MeCN (1 mL). Dropwise addition of a deep red solution of $K[Ge_9R_3]$ {R: $Si(SiMe_3)_3$} (140 mg, 0.1 mmol, 1 eq.) in MeCN (1.5 mL) to the coinage metal NHC solution instantly led to formation of an orange precipitate. The reaction mixture was stirred at room temperature for 15 min. Subsequently, the colourless supernatant solution was filtered off, the precipitate was washed with 1 mL of MeCN and dried *in vacuo* to afford an orange solid. The crude product was dissolved in toluene, filtered and placed in a freezer at -40 °C for recrystallization, obtaining analytically pure red crystals (40 mg, 48 %).

^{1}H NMR: (400 MHz, 298 K, thf-d_8): δ [ppm] = 7.48-7.42 (d, $^3J_{HH}$ = 7.7 Hz, 2H, $CH_{Ph(p)}$), 7.38-7.33 (t, $^3J_{HH}$ = 7.7 Hz, 4H, $CH_{Ph(m)}$), 7.30 (s, 2H, CH_{Im}), 2.88 (hept, $^3J_{HH}$ = 7.6 Hz, 4H, CH_{iPr}), 1.51 (d, $^3J_{HH}$ = 6.9 Hz, 12H, Me_{iPr}), 1.17 (d, $^3J_{HH}$ = 6.9 Hz, 12H, Me_{iPr}), 0.22 (s, 81H, Me_{TMS}).

^{13}C NMR: (101 MHz, 298 K, thf-d_8): δ [ppm] 146.24 (s, $C_{Ph(iPr)}$), 136.69 (s, $C_{Ph}N$), 131.41 (s, $CH_{Ph(p)}$), 125,69 (s, $CH_{Ph(m)}$), 124.95(s, CH_{Im}), 29.79 (s, CH_{iPr}), 26.15 (s, Me_{iPr}), 3.57 (s, Me_{TMS}).

^{29}Si-INEPT NMR: (79 MHz, 298 K, thf-d_8): δ [ppm] = -9.60 (s, Si_{TMS}), -102.14 (s, Si_{Ge9}).

ESI-MS: *m/z* 1396.7 ($[Ge_9R_3]^-$), 1570.6 ($[Cu(\eta^3\text{-}Ge_9R_3)K]^-$ + thf)

Elemental analysis: Anal. Calcd. for $C_{54}H_{117}CuGe_9N_2Si_{12}$: C, 35.1; H, 6.4; N, 1.5. Found: C, 35.4 H, 6.0; N, 1.8.

[Dipp-Ag(η^3-Ge_9R_3)] (***2***)

Ag-Dipp-Cl (37 mg, 0.07 mmol, 1 eq.) was dissolved in MeCN (1 mL). Dropwise addition of a deep red solution of K[Ge_9R_3] {R: $Si(SiMe_3)_3$} (100 mg, 0.07 mmol, 1 eq.) in MeCN (1 mL) to the coinage metal NHC solution instantly led to formation of a yellow precipitate. The reaction mixture was stirred at room temperature for 15 min. Subsequently, the colourless supernatant solution was filtered off, the precipitate was washed with 1 mL of MeCN and dried *in vacuo* to afford a yellow solid. The crude product was dissolved in toluene, filtered and placed in a freezer at -40 °C for recrystallization, obtaining analytically pure orange crystals (40 mg, 30 %). Due to the light sensitivity of the silver compound the reaction was carried out under exclusion of light.

^{1}H NMR: (400 MHz, 298 K, thf-*d_8*): δ [ppm] = 7.49-7.44 (m, 4H, $CH_{Ph(p)}$ + CH_{Im}), 7.38-7.34 (m, 4H, $CH_{Ph(m)}$), 2.83 (hept, $^3J_{HH}$ = 7.6 Hz, 4H, CH_{iPr}), 1.48 (d, $^3J_{HH}$ = 6.9 Hz, 12H, Me_{iPr}), 1.20 (d, $^3J_{HH}$ = 6.9 Hz, 12H, Me_{iPr}), 0.20 (s, 81H, Me_{TMS}).

^{13}C NMR: (101 MHz, 298 K, thf-*d_8*): δ [ppm] = 146.41(s, $C_{Ph(iPr)}$), 136.70 (s, $C_{Ph}N$), 131.43 (s, $C_{Ph(p)}$), 125.53 (s, $C_{Ph(m)}$), 125.36 (s, CH_{Im}), 29.79 (s, CH_{iPr}), 26.33 (s, Me_{iPr}), 24.86 (s, Me_{iPr}), 3.44 (s, Me_{TMS}).

^{29}Si-INEPT NMR: (79 MHz, 298 K, thf-d_8): δ [ppm] = -9.43 (s, Si_{TMS}), -103.96 (s, Si_{Ge9}).

Elemental analysis: Anal. Calcd. for $C_{54}H_{117}AgGe_9N_2Si_{12}$: C, 34.2; H, 6.2; N, 1,5. Found: C, 34.0; H, 6.2; N, 1.5.

[Dipp-Au(η^3-Ge_9R_3)] (***3***)

Au-Dipp-Cl (30 mg, 0.05 mmol, 1 eq.) was dissolved in MeCN (1 mL). Dropwise addition of a deep red solution of K[Ge_9R_3] {R: $Si(SiMe_3)_3$} (68 mg, 0.05 mmol, 1 eq.) in MeCN (1 mL) to the coinage metal NHC solution instantly led to formation of an orange precipitate. The reaction mixture was stirred at room temperature for 15 min. Subsequently, the colourless supernatant solution was filtered off, the precipitate was washed with 1 mL of MeCN and dried *in vacuo* to afford an orange solid. The crude product was dissolved in toluene, filtered and placed in a freezer at -40 °C for recrystallization, obtaining analytically pure red crystals (60 mg, 60 %).

^{1}H NMR: (400 MHz, 298 K, thf-*d_8*): δ [ppm] = 7.49-7.43 (d, $^3J_{HH}$ = 7.7 Hz, 2H, $CH_{Ph(p)}$), 7.40 (s, 2H, CH_{Im}), 7.38-7.32 (t, $^3J_{HH}$ = 7.7 Hz, 4H, $CH_{Ph(m)}$), 2.85 (hept, $^3J_{HH}$ = 7.6 Hz, 4H, CH_{iPr}), 1.51 (d, $^3J_{HH}$ = 6.9 Hz, 12H, Me_{iPr}), 1.16 (d, $^3J_{HH}$ = 6.9 Hz, 12H, Me_{iPr}), 0.22 (s, 81H, Me_{TMS}).

^{13}C NMR: (101 MHz, 298 K, thf-*d_8*): δ [ppm] = 146.18 (s, $C_{Ph(iPr)}$), 136.25 (s, $C_{Ph}N$), 131.51 (s, $CH_{Ph(p)}$), 125.60 (s, $CH_{Ph(m)}$), 125.13 (s, CH_{Im}), 29.62 (s, CH_{iPr}), 3.64 (s, Me_{TMS}).

^{29}Si-INEPT NMR: (79 MHz, 298 K, thf-d_8): δ [ppm] = -9.31 (s, Si_{TMS}), -103.37 (s, Si_{Ge9}).

Elemental analysis: Anal. Calcd. for $C_{54}H_{117}AuGe_9N_2Si_{12}$: C, 32.7; H, 5.95; N, 1.4. Found: C, 32.2; H, 6.0; N, 1.5.

Crystallographic Data

General: Crystallographic data are summarized in Tables S1 and S2. X-ray diffraction measurements were performed on single crystals coated in perfluorated polyether (Galden®; *Solvay Solexis*). Crystals were picked at a cooling table in a cooled nitrogen gas stream. Single crystal data were collected on an Oxford Diffraction Xcalibur3 diffractometer, $Mo_{K\alpha}$ radiation (λ = 0.71073 Å). The structures were solved by direct methods (SHELXS-97).[7] Unless otherwise stated all non-hydrogen atoms were refined with anisotropic displacement parameters, all hydrogen atoms were placed in calculated positions and refined using a riding model. Full-matrix least-squares refinements were carried out by minimizing $\sum \omega(F_0^2\text{-}F_c^2)^2$ with SHELXL-97 weighting scheme.[7] All structures were checked for possible problems using Platon. Images of the crystal structures were generated by Diamond 3.0. Crystallographic data (excluding structure factors) for **1**-**4** have been deposited with the Cambridge Structural database and are available free of charge.

Further explanations:

In complexes **2** and **3**, the ellipsoids of four respectively one carbon atom had to be restrained by an ISOR-instruction. Concerning compound **4** the measured needle-like crystal has been very small and therefore, reflection intensities are low leading to higher quality factors. Furthermore, several atoms in **4** could not be refined anisotropic. To date no better crystal of **4** could be isolated.

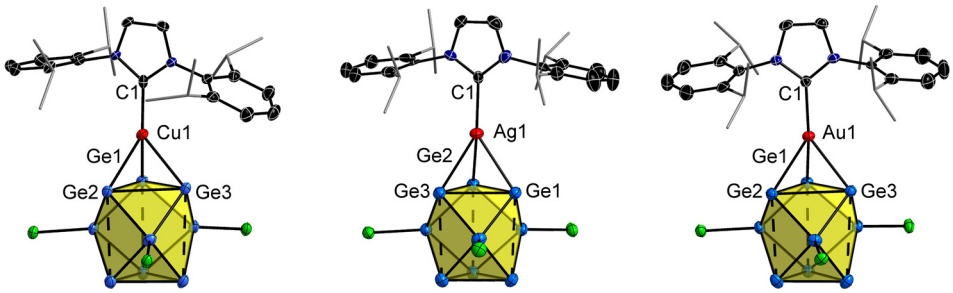

Figure S1: Molecular structures of compounds **1**-**3**. Displacement ellipsoids are shown at a 50% probability level. For clarity TMS groups at the clusters and cocrystallized toluene molecules in compounds **2** and **3** are omitted. Isopropyl groups of NHC ligands are pictured as grey colored wire and stick model.

Table S1: Crystallographic data for Compounds **1**-**3**.

Compound name	**1**	**2**	**3**
formula	$C_{54}H_{117}CuGe_9N_2Si_{12}$	$C_{54}H_{117}AgGe_9N_2Si_{12}$*1.5 tol	$C_{54}H_{117}AuGe_9N_2Si_{12}$*tol
CCDC number	1438677	1438678	1438679
M (g/mol)	1848.43	2030.45	2073.99
Crystal description	red block	orange block	red block
Crystal dimensions (mm)	0.3x0.3x0.1	0.4x0.2x0.2	0.6x0.4x0.6
Temperature (K)	121(2)	121(2)	121(2)
Crystal system	triclinic	triclinic	triclinic
Space group	$P\bar{1}$	$P\bar{1}$	$P\bar{1}$
a [Å]	13.3598(6)	13.9165(8)	13.5500(2)
b [Å]	14.6625(6)	14.4481(7)	15.8449(3)
c [Å]	22.4421(10)	25.9410(13)	23.9783(5)
α [°]	85.080(4)	75.215(4)	79.965(2)
β [°]	89.339(4)	84.931(4)	79.709(2)
γ [°]	76.935(4)	75.031(4)	68.575(2)
V [$Å^3$]	4266.3(3)	4870.6(4)	4681.75(15)
Z	2	2	2
ρ_{calc} [g/cm^3]	1.439	1.384	1.471
F_{000}	1880	2065	2080
μ [mm^{-1}]	3.565	3.111	4.591
Θ ranges	2.94-26.00	3.02-25.50	3.01-26.00
Measured reflections	47582	44230	79353
Independent reflections (all data)	16571	18095	18370
R_{int}/R_σ	0.0756/0.1249	0.0845/0.1695	0.0770/0.0665
Unique reflections ($I_0>2\sigma(I_0)$)	9515	8910	13645
Data/restraints/parameters	16751/0/738	18095/6/839	18370/24/803
GoF (on F^2)	0.827	0.865	0.966
R_1/wR_2 ($I_0>2\sigma(I_0)$)	0.0450/0.0957	0.0607/0.1378	0.0320/0.0637
R_1/wR_2 (all data)	0.0818/0.1013	0.1168/0.1481	0.0479/0.0656
Max./Min. residual electron density [e. $Å^{-3}$]	1.428/ -0.783	2.372/ -1.004	1.195/ -0.916

Compounds **2** and **3** cocrystallize with 1.5, respectively 1 toluene molecule.

Table S2: Crystallographic data for compounds **4**.

Compound name	**4**
formula	$C_{108}H_{234}Ag_2Ge_{18}N_4Si_{24}$* 2 tol
CCDC number	1438680
M (g/mol)	3969.78
Crystal description	orange needle
Crystal dimensions (mm)	0.4x0.1x0.05
Temperature (K)	121(2)
Crystal system	monoclinic
Space group	$P2_1/c$
a [Å]	18.417(4)
b [Å]	26.377(5)
c [Å]	38.982(8)
α [°]	90
β [°]	91.58(3)
γ [°]	90
V [Å^3]	18929(7)
Z	4
d_{calc} [g/cm^3]	1.393
F_{000}	8064
μ [mm^{-1}]	3.200
Θ ranges	2.85-26.00
Measured reflections	234022
Independent reflections (all data)	37164
R_{int}/R_σ	0.2755/0.4845
Unique reflections ($I_0>2\sigma(I_0)$)	8694
Data/restraints/parameters	37164/0/1283
GoF (on F^2)	0.791
R_1/wR_2 ($I_0>2\sigma(I_0)$)	0.0987/0.1882
R_1/wR_2 (all data)	0.2933/0.2312
Max./Min. residual electron density [e. Å^{-3}]	1.767/ -0.895

Compound **4** cocrystallizes with 2 toluene molecules.

NMR Spectra

General: All NMR spectra were acquired on a Bruker Avance Ultrashield 400 MHz and a Bruker DPX 400 MHz spectrometer. All of the spectra were recorded in thf-d_8 at 298 K.

In the ^{13}C NMR spectra of the samples the signals of the diisopropylphenyl methyl groups partly or fully interfere with the residual solvent signal and therefore no shifts could be appointed. Furthermore, in all of the ^{13}C NMR spectra the signals of the carbene carbon atom could not be observed. Therefore, the attached ^{13}C spectra are just presented to a shift of 150 ppm. The signals marked with a* in the ^{1}H and ^{13}C NMR spectra of **2** (Figures 5 and 6) are caused by the dimeric species $[Ag(\eta^3\text{-}Ge_9R_3)_2][Ag(NHC^{Dipp})_2]$ which starts to form upon dissolution of **2** in thf-d_8.

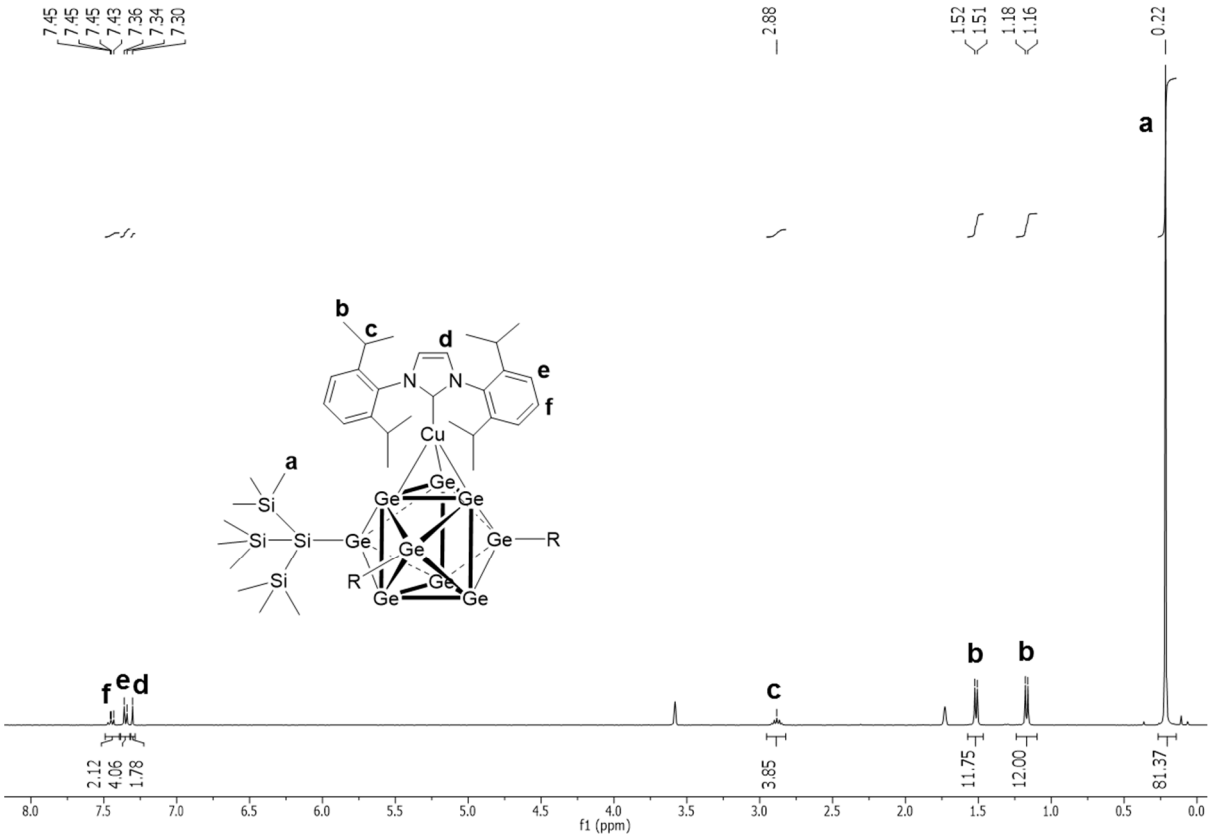

Figure 2: ^{1}H NMR spectrum of **1**.

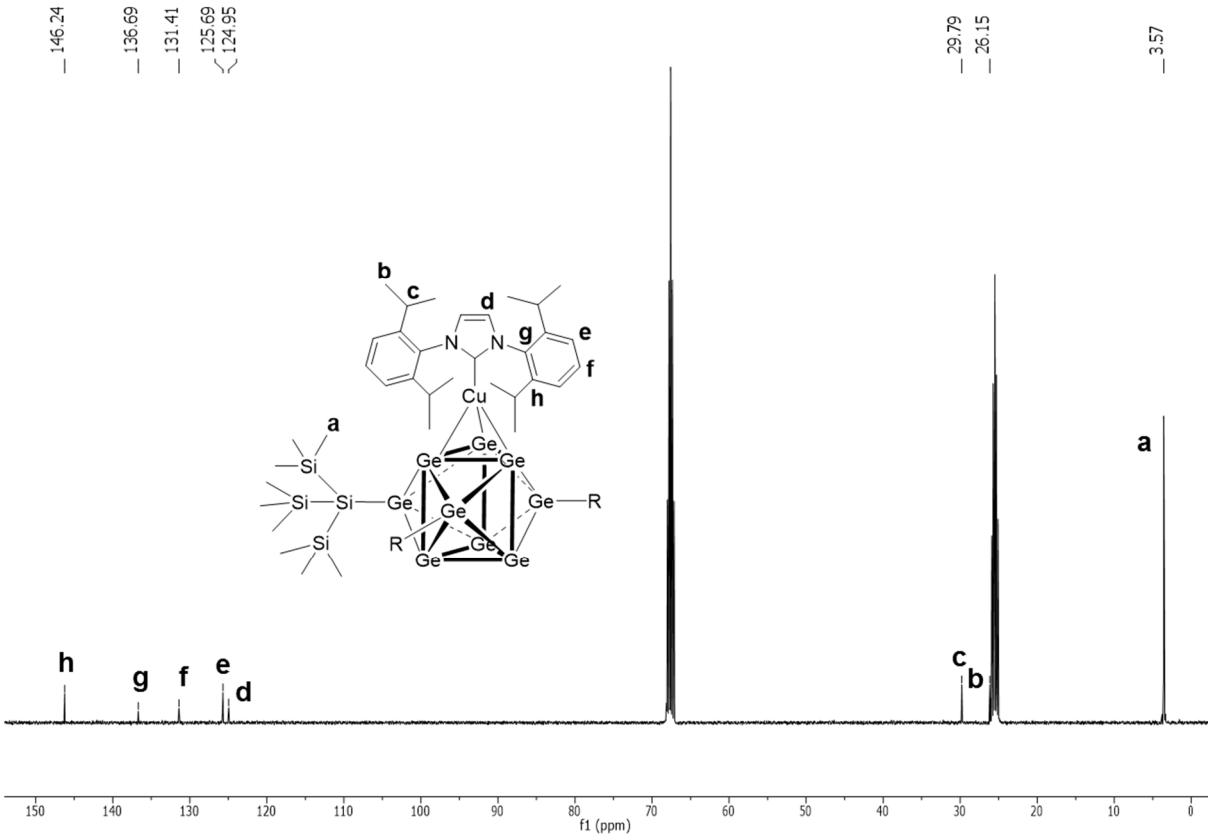

Figure S3: ^{13}C NMR spectrum of **1**.

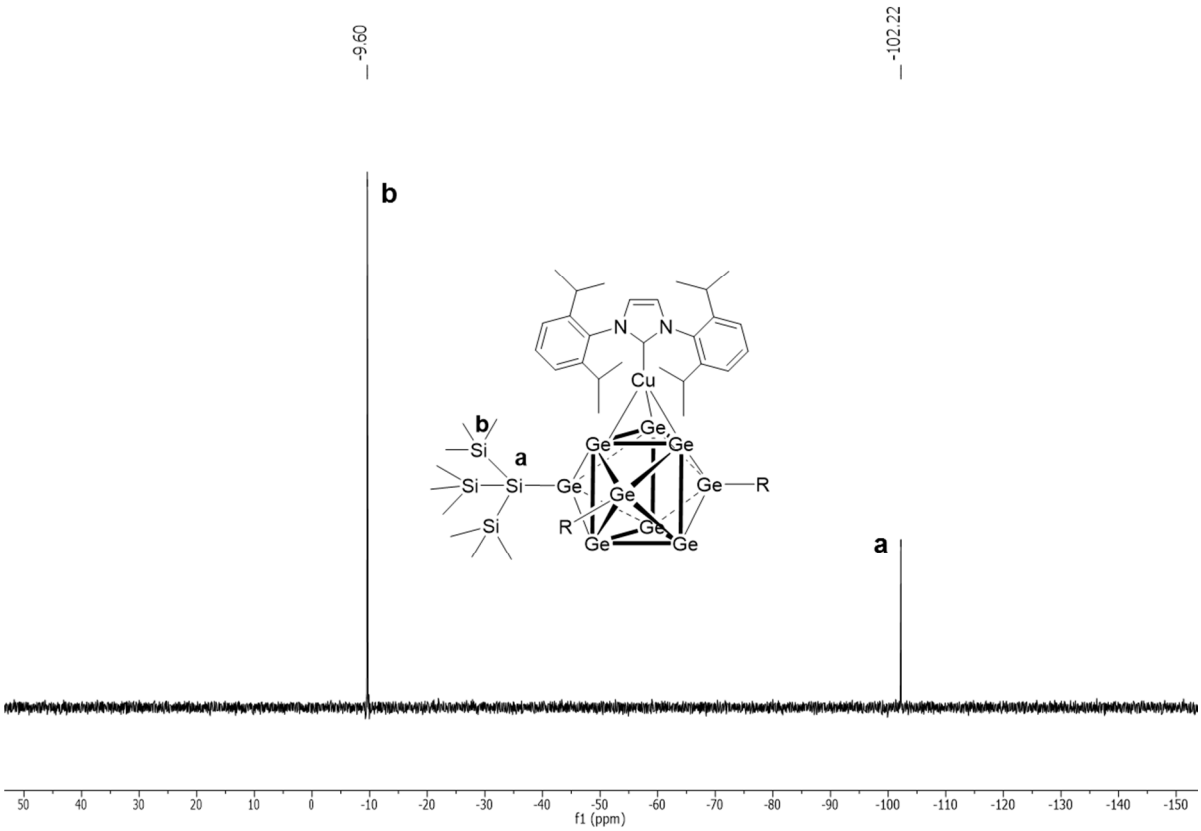

Figure S4: ^{29}Si-INEPT NMR spectrum of **1**.

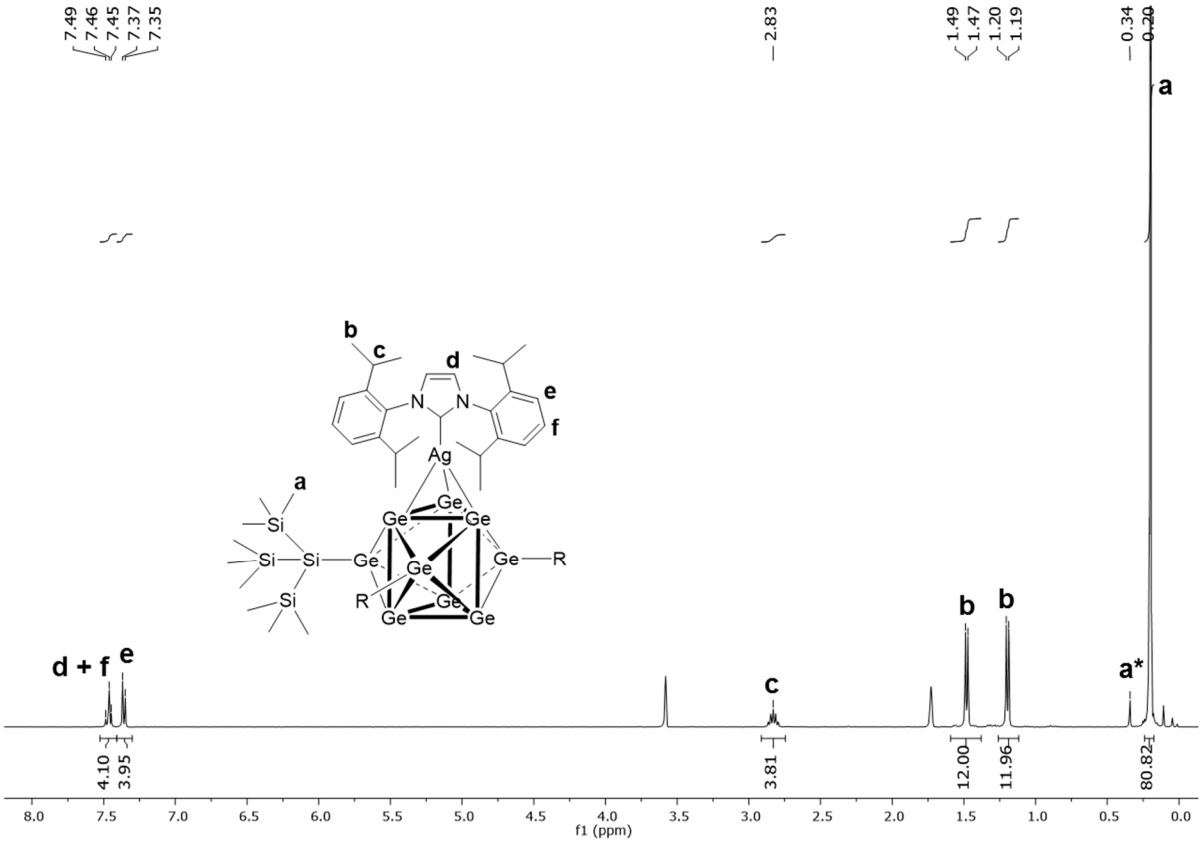

Figure S5: ^{1}H NMR spectrum of **2**.

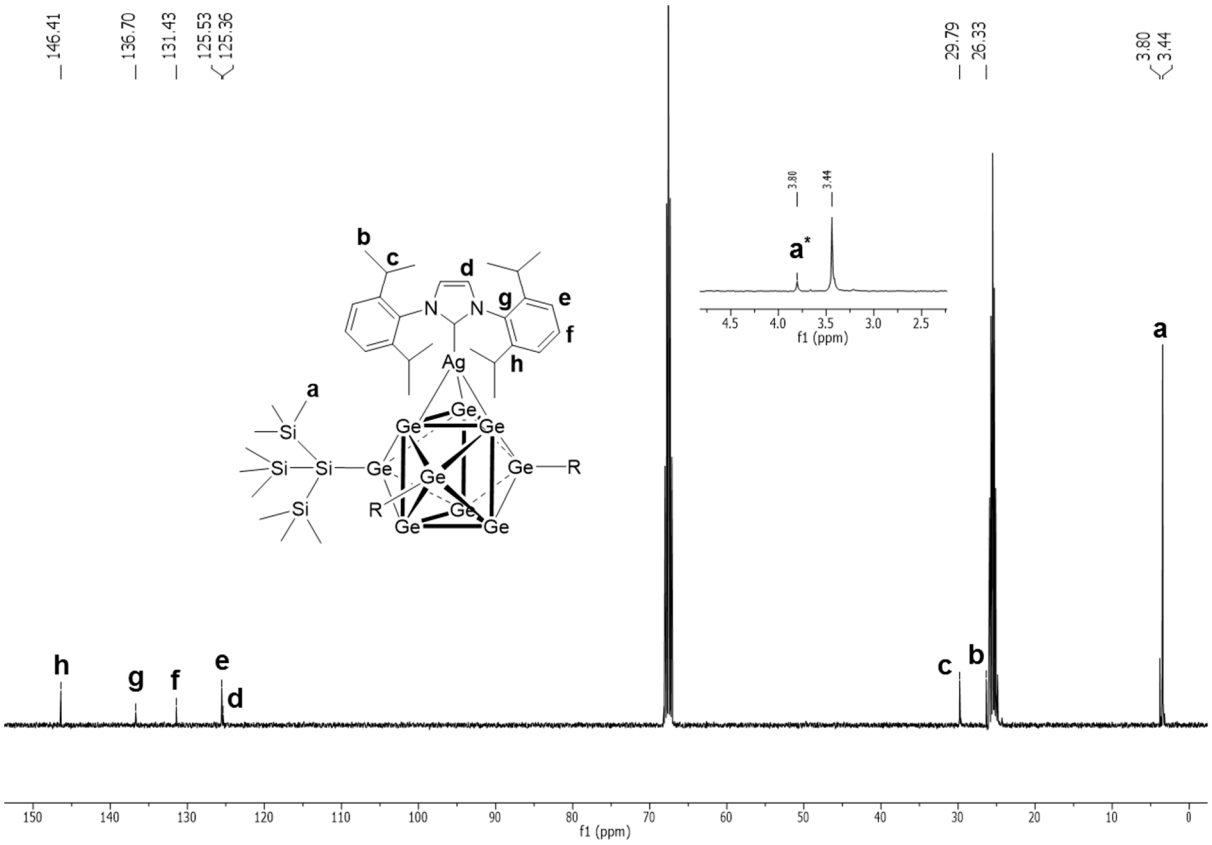

Figure S6: ^{13}C NMR spectrum of **2**.

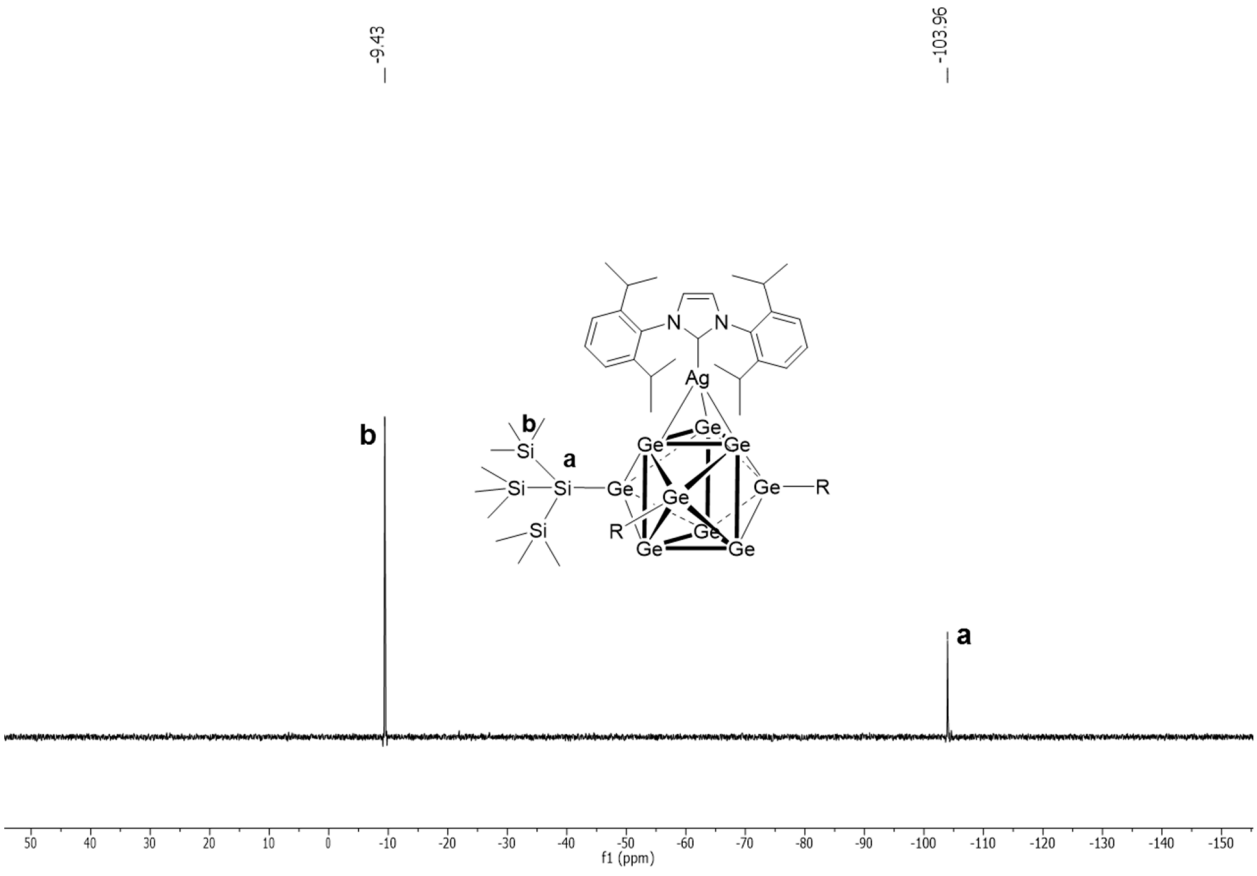

Figure S7: ^{29}Si-INEPT NMR spectrum of **2**.

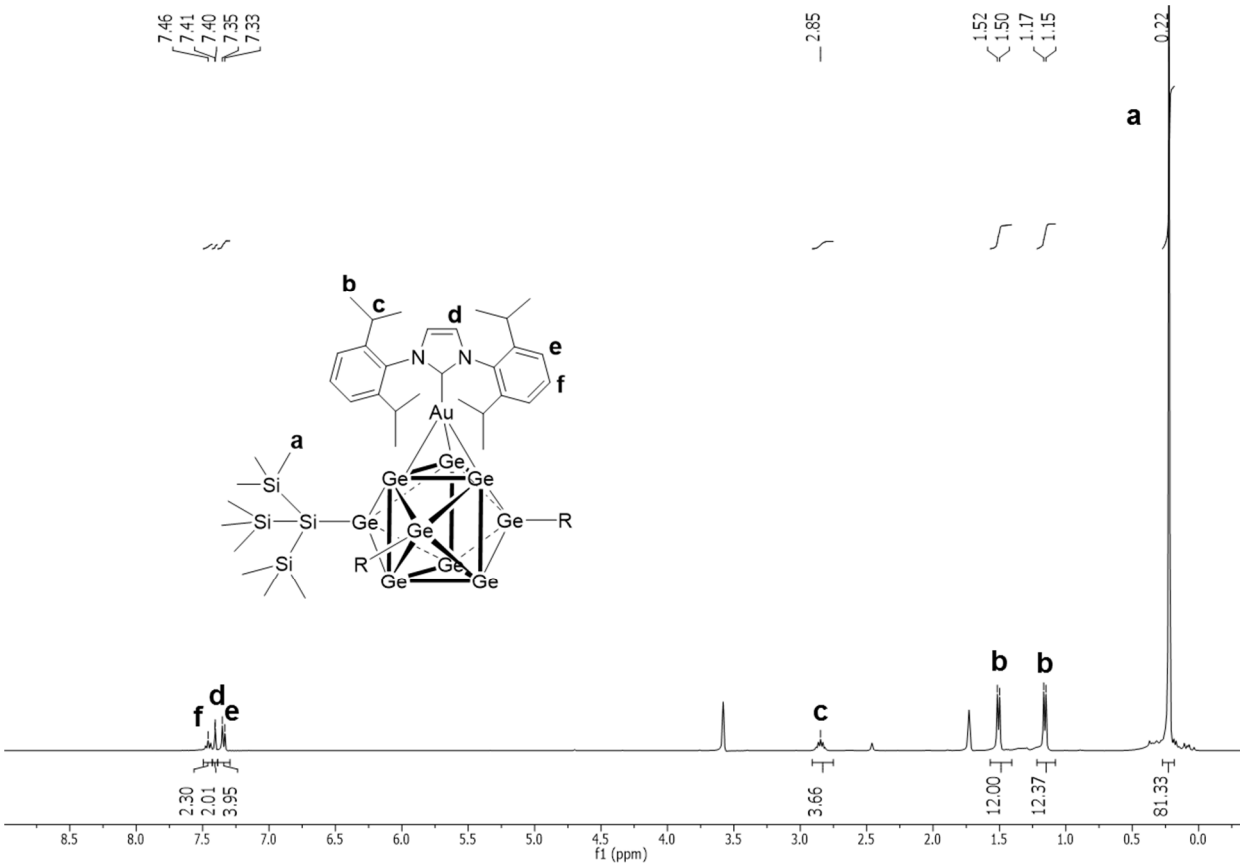

Figure S8: ^{1}H NMR spectrum of **3**.

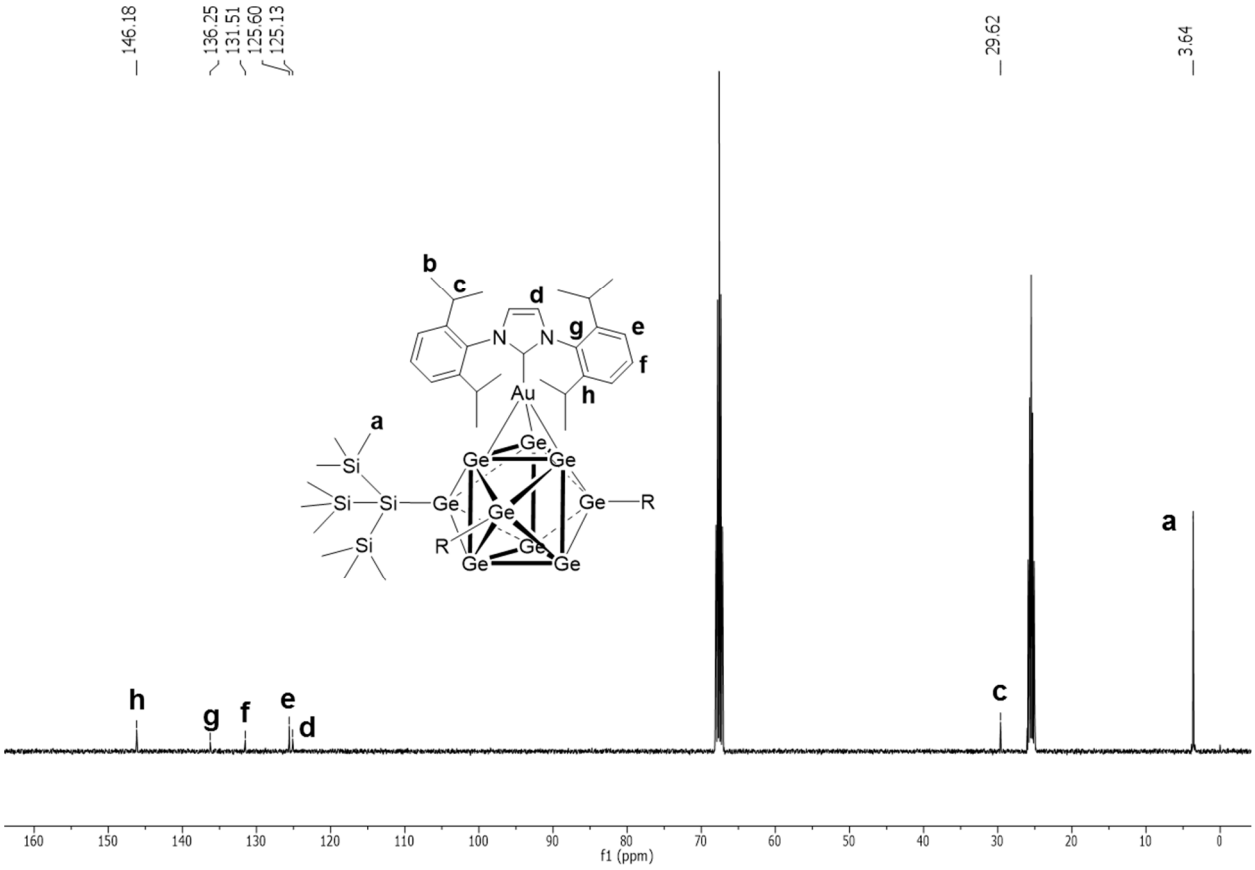

Figure S9: ^{13}C NMR spectrum of **3**.

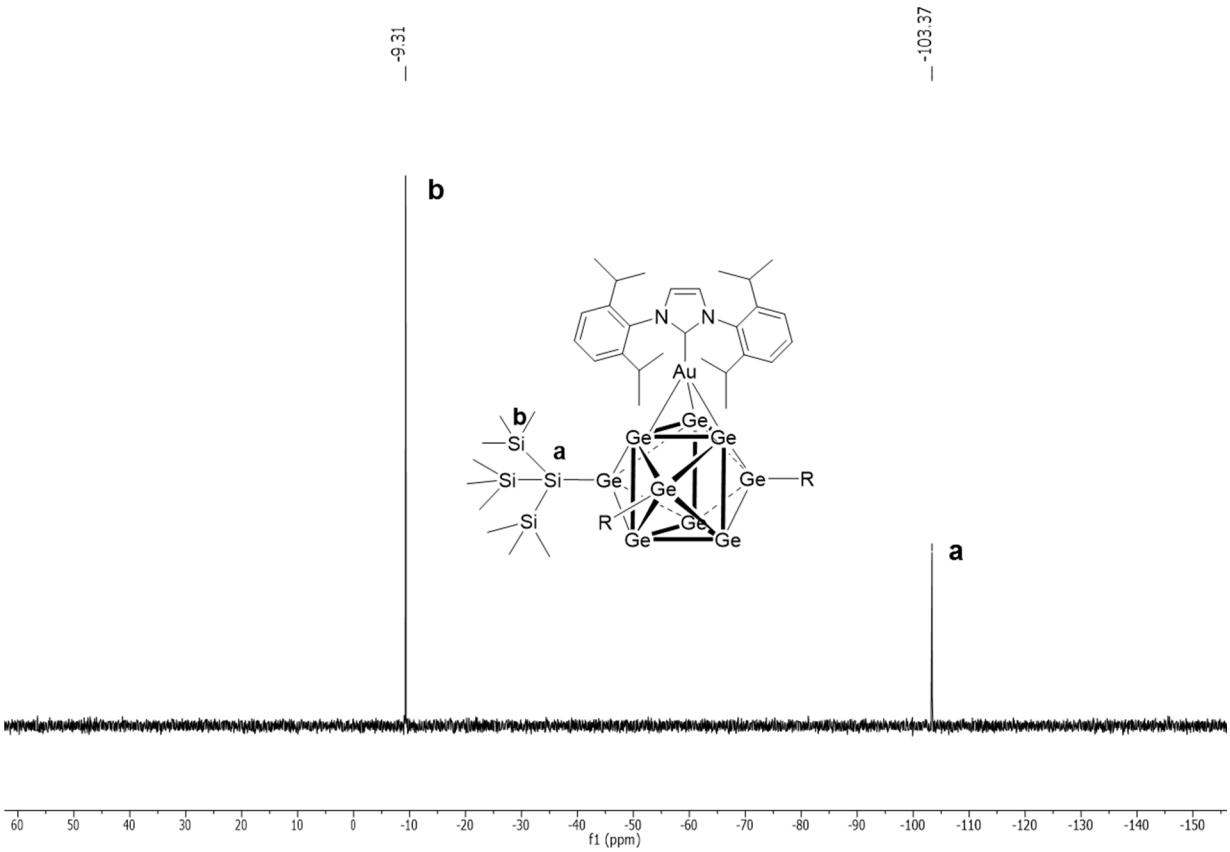

Figure S10: ^{29}Si-INEPT NMR spectrum of **3**.

ESI-Mass Spectra

General: ESI-mass spectrometry was performed on Bruker Daltronic mass spectrometry device. For the measurement the crude product of **1** was dissolved in thf and the resulting solution was filtered through a syringe filter. Subsequently, the sample was introduced by direct infusion with a syringe pump at 240 µL/h. Measurement data is summarized in Table 3.

Table S3: ESI-Mass Spectra measurement data.

	negative ion mode	positive ion mode
capillary voltage [kV]	4.5	-4
capillary exit [V]	-196	220
drying gas temperature [°C]	125	300

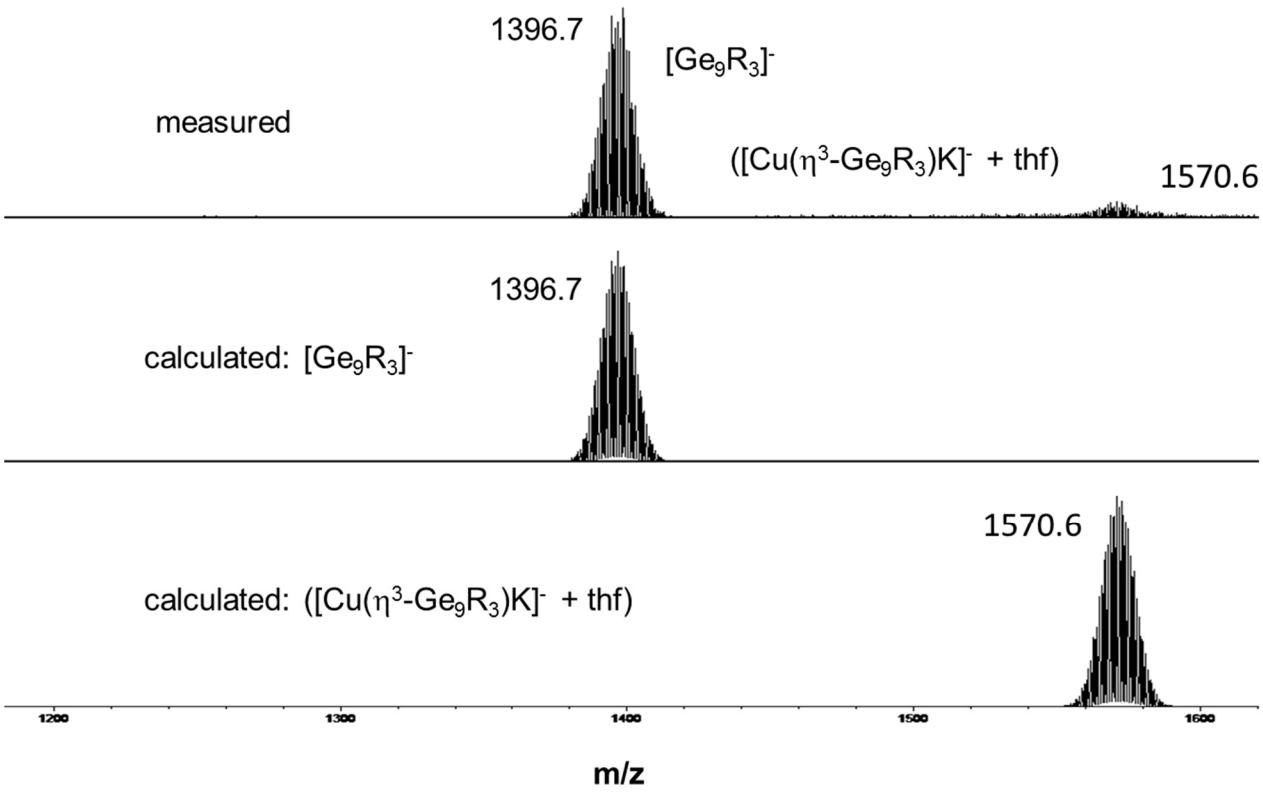

Figure S11: Measured and calculated ESI-MS spectra of compound **1** in negative ion mode.

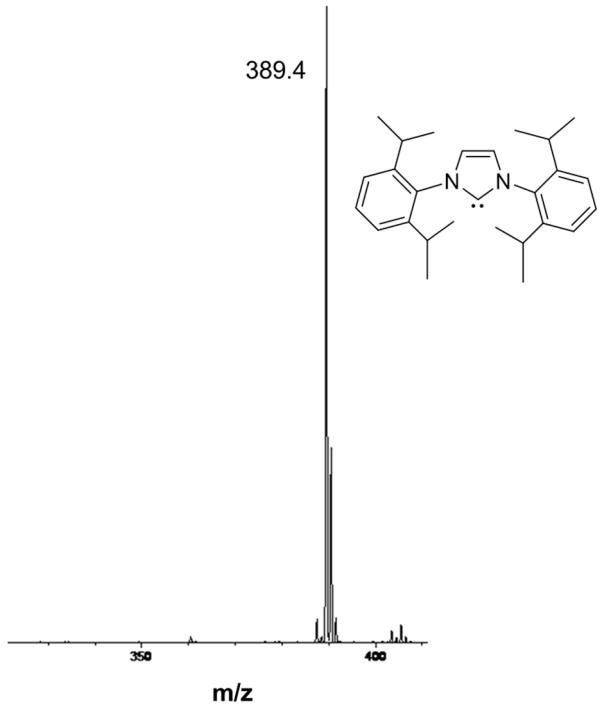

Figure S12: Measured l ESI-MS spectrum of compound **1** in positive ion mode.

References

1. L. Hintermann, *Beilstein J. Org. Chem.*, 2007, **3**, 22.
2. O. Santoro, A. Collado, A. M. Z. Slawin, S. P. Nolan and C. S. J. Cazin, *Chem. Commun.*, 2013, **49**, 10483-10485.
3. P. de Frémont, N. M. Scott, E. D. Stevens, T. Ramnial, O. C. Lightbody, C. L. B. Macdonald, J. A. C. Clyburne, C. D. Abernethy and S. P. Nolan, *Organometallics*, 2005, **24**, 6301-6309.
4. A. Collado, A. Gomez-Suarez, A. R. Martin, A. M. Z. Slawin and S. P. Nolan, *Chem. Commun.*, 2013, **49**, 5541-5543.
5. F. Li and S. C. Sevov, *Inorg. Chem.*, 2012, **51**, 2706-2708.
6. G. R. Fulmer, A. J. M. Miller, N. H. Sherden, H. E. Gottlieb, A. Nudelman, B. M. Stoltz, J. E. Bercaw and K. I. Goldberg, *Organometallics*, 2010, **29**, 2176-2179.
7. G. M. Sheldrick, *Acta Cryst.*, 2008, **64**, 112-122.

5.4 Functionalization of [Ge_9] with Small Silanes: [$Ge_9(SiR_3)_3$]$^-$ (R: *i*Bu, *i*Pr, Et) and the Structures of (CuNHC^{Dipp})[Ge_9{Si(*i*Bu)$_3$}$_3$], (K-18c6)Au[Ge_9{Si(*i*Bu)$_3$}$_3$]$_2$, and (K-18c6)$_2$[Ge_9{Si(*i*Bu)$_3$}$_2$]

L. J. Schiegerl,‡ F. S. Geitner,‡ C. Fischer, W. Klein, T. F. Fässler*

[‡] authors contributed equally to this work.

published in

Z. Anorg. Allg. Chem. **2016**, *642*, 1419.

Content and Contributions

The aim of this work was the introduction of small silane substituents to [Ge_9] clusters and to test the stability and reactivity of the obtained species in subsequent reactions. The introduction of small silanes to [Ge_9] was achieved by heterogenous reaction of acetonitrile solutions of the chloro trialkylsilanes R_3SiCl (*R*: ^{i}Bu, ^{i}Pr, Et) with solid K_4Ge_9. These studies were carried out by M. Sc. Lorenz Schiegerl. Subsequently, the stability of the resulting clusters in solution, as well as their reactivity towards transition metal complexes was tested. Reaction of $[Ge_9\{Si(^iBu)_3\}_3]^-$ with the copper NHC complex $NHC^{Dipp}CuCl$ resulted in the attachment of a $[NHC^{Dipp}Cu]^+$ unit to the [Ge_9] cluster core, yielding the neutral [Ge_9] cluster copper NHC compound $[NHC^{Dipp}Cu(\eta^3\text{-}Ge_9\{Si(^iBu)_3\}_3)]$, which was characterized by means of NMR, elemental analysis, single crystal X-ray diffraction and ESI-MS. Additional reactions of $[Ge_9\{Si(^iBu)_3\}_3]^-$ with $Au(PPh_3)Cl$, bearing a more labile phosphine ligand, led to the first Au^+ bridged cluster species of this novel [Ge_9] cluster anion. Moreover, attempts to crystallize the bare threefold-silylated cluster $[Ge_9\{Si(^iBu)_3\}_3]^-$ in presence of the sequestering agent [18]crown-6 solely led to crystals of the bis-silylated species $[Ge_9\{Si(^iBu)_3\}_2]^{2-}$, which indicated an increased lability of the smaller silyl substituents. Investigations on the reactivity of $[Ge_9\{Si(^iBu)_3\}_3]^-$ towards the Au-phosphine complex and attempts to crystallize bare $[Ge_9\{Si(^iBu)_3\}_3]^-$ species were carried out by M. Sc. Lorenz Schiegerl. Evaluation of the diffraction data for the latter two compounds was assisted by Dr. Wilhelm Klein and Christina Fischer helped with the acquisition of ESI-MS spectra. The publication was written in the course of this thesis.

Journal of Inorganic and General Chemistry
ZAAC
Zeitschrift für anorganische und allgemeine Chemie
www.zaac.wiley-vch.de
ARTICLE

DOI: 10.1002/zaac.201600295

Functionalization of [Ge_9] with Small Silanes: $[Ge_9(SiR_3)_3]^-$ (R = *i*Bu, *i*Pr, Et) and the Structures of $(CuNHC^{Dipp})[Ge_9\{Si(iBu)_3\}_3]$, $(K\text{-}18c6)Au[Ge_9\{Si(iBu)_3\}_3]_2$, and $(K\text{-}18c6)_2[Ge_9\{Si(iBu)_3\}_2]$

Lorenz J. Schiegerl,[a][‡] Felix S. Geitner,[b][‡] Christina Fischer,[a] Wilhelm Klein,[a] and Thomas F. Fässler*[a]

Keywords: Germanium; Silanes; Functionalization; Coinage Metals; *Zintl* clusters

Abstract. Novel silylation reactions at [Ge_9] *Zintl* clusters starting from the chlorosilanes SiR_3Cl (R = *i*Bu, *i*Pr, Et) and the *Zintl* phase K_4Ge_9 are reported. The formation of the tris-silylated anions $[Ge_9(SiR_3)_3]^-$ [R = *i*Bu (**1a**), *i*Pr (**1b**), Et (**1c**)] by heterogeneous reactions in acetonitrile was monitored by ESI-MS measurements. For R = *i*Bu ^1H, ^{13}C and ^{29}Si NMR experiments confirmed the exclusive formation of **1a**. Subsequent reactions of **1a** with $CuNHC^{Dipp}Cl$ and $Au(PPh_3)Cl$ result in formation of the neutral metal complex $(CuNHC^{Dipp})[Ge_9\{Si(iBu)_3\}_3]\cdot 0.5$ tol (**2**·0.5 tol) and the metal bridged dimeric unit $\{Au[Ge_9\{Si(iBu)_3\}_3]_2\}^-$ (**3a**), isolated as a $(K\text{-}18c6)^+$ salt in $(K\text{-}18c6)Au[Ge_9\{Si(iBu)_3\}_3]_2\cdot$tol (**3**·tol), respectively. Finally, from a toluene/hexane solution of **1a** in presence of 18-crown-6, crystals of the compound $(K\text{-}18c6)_2[Ge_9\{Si(iBu)_3\}_2]\cdot$tol (**4**·tol), containing the bis-silylated cluster anion $[Ge_9(Si(iBu)_3)_2]^{2-}$ (**4a**), were obtained. The compounds **2**·0.5 tol, **3**·tol and **4**·tol were characterized by single-crystal structure determination.

Introduction

Within the last decades the research field of soluble *Zintl* clusters has grown rapidly, yielding a broad range of novel compounds. Reacting *Zintl* clusters with organometallics and organic substances in solution, new compounds which are not accessible by pure solution or solid state chemistry, were obtained. In this context *Zintl* phases of the form A_4E_9 (A: alkali metal; E: tetrel element) containing nine-atomic clusters $[E_9]^{4-}$ (E: Ge – Pb) are often applied as soluble *Zintl* cluster precursors.[1] Reactions of *Zintl* clusters in highly polar, protic solvents such as ethylenediamine or liquid ammonia with transition metal compounds yielded numerous intermetalloid clusters with $[Sn_9Cr(CO)_3]^{4-}$[2] being the first one and $[Au_3Ge_{45}]^{9-}$[3] the largest one obtained by this route so far. Further, numerous [Ge_9] clusters with one or two *exo*-bonded main-group fragments[4] as well as the phenyl-substituted $[Ph\text{-}Ge_9\text{-}SbPh_2]^{2-}$[4a] and alkyl-substituted $[t\text{Bu-}Ge_9\text{-}Ge_9\text{-}t\text{Bu}]^{4-}$[5] clusters were obtained.

Recently, functionalization of *Zintl* clusters with organic substituents[6] was put in the research focus by the explorations of $[Ge_9(CH{=}CH_2)_2]^{2-}$ and $[Ge_9\{Si(SiMe_3)_3\}_3]^-$. The bis-vinylated anion $[Ge_9(CH{=}CH_2)_2]^{2-}$ [7] is obtained by reacting K_4Ge_9 with bistrimethylsilylacetylene (btmsa) in ethylenediamine. In a similar reaction procedure the linkage of two [Ge_9] clusters was achieved to obtain the *Zintl* triad $[RGe_9\text{-}CH{=}CH\text{-}CH{=}CH\text{-}Ge_9R]^{4-}$.[8] In contrast, $[Ge_9\{Si(SiMe_3)_3\}_3]^-$ was at first synthesized in small amounts starting from GeBr by the group of *Schnepf*,[9] a reasonable synthesis procedure allowing the large scale synthesis of $[Ge_9\{Si(SiMe_3)_3\}_3]^-$ by heterogeneous reaction of acetonitrile solutions of $Si(SiMe_3)_3Cl$ with solid K_4Ge_9 was reported subsequently by the group of *Sevov*.[10]

Because of its low charge and the steric shielding of the [Ge_9] core by the bulky $[Si(SiMe_3)_3]$ groups, tris-silylated cluster anion $[Ge_9\{Si(SiMe_3)_3\}_3]^-$ and its compounds are comparably stable and reveal solubility in standard solvents such as acetonitrile, tetrahydrofuran or toluene. Recently, a broad range of subsequent reactions of $[Ge_9\{Si(SiMe_3)_3\}_3]^-$ with organic substances and organometallic complexes has been reported in literature, such as dimeric $M[Ge_9\{Si(SiMe_3)_3\}_3]_2$ compounds (M = Zn, Cd, Hg),[11] obtained by reactions with the respective MCl_2 salts, and the coinage metal bridged dimeric anions $\{M[Ge_9\{Si(SiMe_3)_3\}_3]_2\}^-$ (M = Cu, Ag, Au).[12] Furthermore, the neutral dimeric compound $Cu_2(PPh_3)[Ge_9\{Si(SiMe_3)_3\}_3]_2$ was obtained by reaction with $Cu(PPh_3)_3Br$ and conversion with $Pd(PPh_3)_4$ yielded the Pd^0 bridged dimeric anion $\{Pd[Ge_9\{Si(SiMe_3)_3\}_3]_2\}^{2-}$.[13] Lately, the first penta-functionalized deltahedral cluster

* Prof. Dr. T. F. Fässler
E-Mail: thomas.faessler@lrz.tum.de
[a] Department of Chemistry
Technische Universität München
Lichtenbergstraße 4
85747 Garching, Germany
[b] WACKER Institute for Silicon Chemistry and Department of Chemistry
Technische Universität München
Lichtenbergstraße 4
85748 Garching, Germany
[‡] authors contributed equally to this work.
Supporting information for this article is available on the WWW under http://dx.doi.org/10.1002/zaac.201600295 or from the author.

$[Ge_9\{Si(SiMe_3)_3\}_3]Pd(PPh_3)Et$, in which a Pd atom is incorporated into the $[Ge_9]$ cluster yielding a $[Ge_9Pd]$ cluster core, was reported.[14] Additionally, neutral *Zintl* cluster coinage metal NHC compounds (*M*–NHC)$[Ge_9\{Si(SiMe_3)_3\}_3]$[15] were obtained reacting $[Ge_9\{Si(SiMe_3)_3\}_3]^-$ and *M*NHC^{Dipp}Cl[16] (NHC: N-heterocyclic carbene; *M*: Cu, Ag, Au), being the first compounds combining *Zintl* cluster- and NHC chemistry. Furthermore, the introduction of a Cu-phosphine residue in $(CuPiPr_3)[Ge_9\{Si(SiMe_3)_3\}_3]$ and a Zn-Cp* moiety in $(ZnCp^*)[Ge_9\{Si(SiMe_3)_3\}_3]$ reveal the ability of $[Ge_9\{Si(SiMe_3)_3\}_3]^-$ to act as ligand in versatile metalorganic compounds.[17]

Further examinations focusing on the variation of the number of silyl groups at the $[Ge_9]$ cluster revealed that the bis-silylated species $[Ge_9\{Si(SiMe_3)_3\}_2]^{2-}$, characterized as $(K–2.2.2–crypt)_2[Ge_9\{Si(SiMe_3)_3\}_2]$, is easily accessible by addition of solid K_4Ge_9 to acetonitrile solutions of $[Ge_9\{Si(SiMe_3)_3\}_3]^-$.[18] Moreover, novel silyl groups with varying steric demand were introduced at $[Ge_9]$ clusters, yielding $[Ge_9\{Si(SiMe_3)_2(SiPh_3)\}_3]^-$ [19] and $[Ge_9(SiPh_3)_3]^-$ [17]. The reactivity of $[Ge_9\{Si(SiMe_3)_2(SiPh_3)\}_3]^-$ is quite similar to that of $[Ge_9\{Si(SiMe_3)_3\}_3]^-$ which can be derived from formation of the dimeric Hg compounds of both tris-silylated clusters.[12] In contrast, $[Ge_9(SiPh_3)_3]^-$ shows a significantly different behavior. Therefore, reaction with $Cu(PiPr_3)Cl$ does not yield a neutral compound bearing a Cu-phosphine moiety, as it was observed for $[Ge_9\{Si(SiMe_3)_3\}_3]^-$, but $(CuPiPr_3)_4[Ge_9(SiPh_3)_2]_2$ is formed, where two bis-silylated $[Ge_9(SiPh_3)_2]^{2-}$ cluster units are bridged by two $[CuPiPr_3]^+$ groups.[17] These observations of different reactivity of the tris-silylated clusters induced by different silyl groups with varying steric demand triggered us to investigate the introduction of further sterically less bulky organo-silanes at $[Ge_9]$ and the reactivity of the resulting clusters in subsequent reactions.

Results and Discussion

Reacting K_4Ge_9 with $Si(iBu)_3Cl$ (3 equiv.) in a heterogeneous reaction according to the *Zintl* route yields, after stirring at room temperature overnight and subsequent filtration, a red solution. ESI-MS examination of the obtained solution revealed the formation of the novel tris-silylated tetrel cluster anion $[Ge_9\{Si(iBu)_3\}_3]^-$ (**1a**) (*m*/*z* = 1253; Figure 1, a). After removal of the solvent in vacuo the residual brownish solid was analyzed by ^1H, ^{13}C and ^{29}Si NMR spectroscopy. In all NMR spectra (^1H, ^{13}C, ^{29}Si) the observed signals can be assigned to one single species (further NMR discussion in the Supporting Information). Evaluation of both, NMR and ESI-MS data, manifests that exclusively the tris-silylated species **1a** is formed. Thus, functionalization of $[Ge_9]^{4-}$ clusters with sterically less demanding $[Si(iBu)_3]^+$ groups than $[Si(SiMe_3)_3]^+$ yields stable, tris-silylated clusters.

Analogously, the reactivity of K_4Ge_9 towards the chlorosilanes SiR_3Cl (R = *i*Pr, Et) was examined. ESI-MS examinations of the resulting red solutions in acetonitrile indicate the formation of the respective tris-silylated anions **1b** (Figure 1, b; *m*/*z* = 1126) and **1c** (Figure 1, c; *m*/*z* = 999). These observations manifest that silylation of $[Ge_9]$ is possible with a broad range of alkylsilanes SiR_3Cl (R = *i*Bu, *i*Pr and Et) bearing less bulky organic groups, besides the recently reported silylation reaction with $SiPh_3Cl$.[17] Thus, the introduction of silyl groups of varying steric demand is possible and probably opens up a path for a plethora of novel compounds such as recently reported $(CuPiPr_3)_4[Ge_9(SiPh_3)_2]_2$, which was obtained by reaction of $[Ge_9(SiPh_3)_3]^-$ with $Cu(PiPr_3)Cl$ with substitution of silyl groups by cationic metalorganic Cu-phosphine fragments, revealing different reactivity of the clusters induced by variation of the silyl groups.

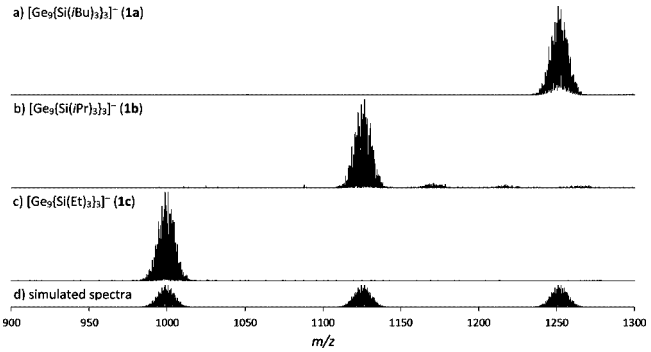

Figure 1. ESI-MS spectra of the tris-silylated species in acetonitrile. a) $[Ge_9\{Si(iBu)_3\}_3]^-$ (**1a**) (*m*/*z* = 1253); b) $[Ge_9\{Si(iPr)_3\}_3]^-$ (**1b**) (*m*/*z* = 1126); c) $[Ge_9\{Si(Et)_3\}_3]^-$ (**1c**) (*m*/*z* = 999); d) simulated spectra of the anions (an overview and a detailed view on the spectra are shown in the Supporting Information).

We examined the reactivity of **1a** towards the organometallic compound CuNHC^{Dipp}Cl, which, as recently reported by our group, forms stable neutral tetrel cluster copper NHC compounds of the form (CuNHC^{Dipp})$[Ge_9\{Si(SiMe_3)_3\}_3]$[15] upon reaction with $[Ge_9\{Si(SiMe_3)_3\}_3]^-$. Following a similar synthesis procedure, an acetonitrile solution of **1a** was added dropwise to a solution of CuNHC^{Dipp}Cl in acetonitrile yielding an orange-brownish precipitate. Subsequent isolation and purification by recrystallization from toluene at –40 °C yielded analytically pure red crystals in good yield, which were characterized by NMR spectroscopy (^1H, ^{13}C, ^{29}Si), ESI-MS, elemental analysis and single-crystal X-ray diffraction. The ^1H NMR spectrum reveals the ratio of the signals caused by the silyl substituents and the NHC^{Dipp} group to be 1:1, which was also confirmed by elemental analysis for the elements C, H and N (further NMR discussion in Supporting Information). The molecular structure of (CuNHC^{Dipp})$[Ge_9\{Si(iBu)_3\}_3]$ (**2**), which crystallizes with 0.5 toluene molecules per formula unit, is represented in Figure 2. In **2**, the $[Ge_9]$ cluster adapts the shape of a distorted tricapped trigonal prism with two elongated prism heights (C_{2v} symmetry) and the capping Ge atoms bearing the $[Si(iBu)_3]^+$ groups. As observed in other *M*-NHC complexes (*M* = Cu, Ag, Au), the Cu atom coordinates to a deltahedral face of the $[Ge_9]$ core. The Ge-Cu distances of 2.4911(6)–2.5594(6) Å are in the range of the known Cu-NHC complex (CuNHC^{Dipp})$[Ge_9\{Si(SiMe_3)_3\}_3]$ (average 2.53 Å).[15] The NHC ligand is staggered with respect to the three silyl ligands as expected from the steric demands of the

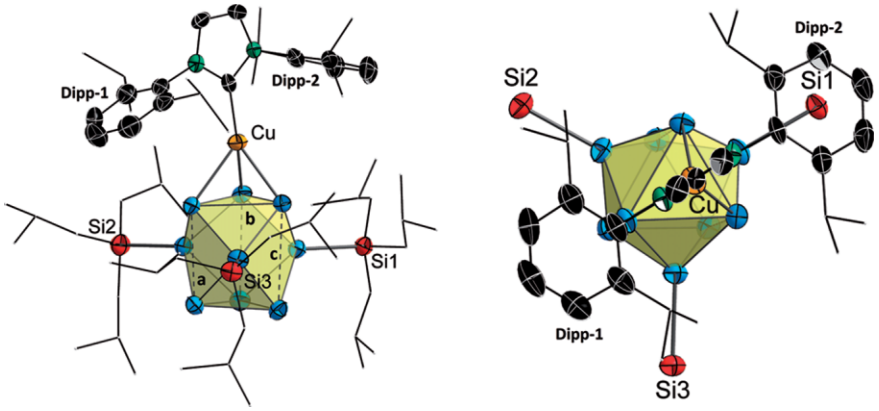

Figure 2. Molecular structure of monomeric compound (CuNHC^{Dipp})[Ge$_9${Si(*i*Bu)$_3$}$_3$)] (**2**) (left) and a detail view from the ligand side (right) on the arrangement of the groups at the [Ge$_9$] cluster. The lengths of the prismatic heights **a**, **b** and **c** are shown in Table 1. Atoms are shown as ellipsoids with 70 % probability (Ge atoms blue; Si atoms red, Cu atoms orange, N atoms green and C atoms black or shown as wire/sticks for the *i*Bu (not shown on the right) and *i*Pr (NHC^{Dipp}) groups; H atoms are omitted for reasons of clarity).

ligands. A similar arrangement was found for the respective compound (CuNHC^{Dipp})[Ge$_9${Si(SiMe$_3$)$_3$}$_3$].

The distortion of the [Ge$_9$] cluster from D_{3h} towards C_{2v} symmetry is best described by the three heights of the underlying trigonal prism (Table 1). Whereas two of the heights are rather similar (3.4235(5) Å and 3.3918(5) Å given as *c* and *b* in Figure 2, respectively), the third height *a* is remarkably shorter (3.1947(5) Å), as has been found to be a frequent motif of distortion in [Ge$_9${Si(SiMe$_3$)$_3$}$_3$]$^-$ cluster anions.[20] Coordination of the [CuNHC^{Dipp}]$^+$ fragment at the tris-silylated [Ge$_9$] cluster occurs via one of the trigonal faces of the cluster with formation of a η^3-coordination. Thereby, the longest Ge–Cu distance (2.5596(7) Å) is observed towards the Ge atom in the shortest prismatic height. The two remaining Ge–Cu bonds are clearly shorter with lengths of 2.4907(7) Å and 2.4930(7) Å and located at the side of the cluster where the Dipp-2 group overlaps with a silyl group (Figure 2). In contrast, the Dipp-1 group is positioned between the two remaining silyl groups in a sterically more favorable environment. The stronger repulsion is further supported by the tilt (C–Cu–Ge angle) of the NHC^{Dipp} group towards the side of Dipp-1 (with the shorter prismatic height *a*) with 131.20(1)°. This C–Cu–Ge angle is significantly smaller than at the side of Dipp-2 (with the longer prismatic heights *b* and *c*) (143.42(1)° and 141.69(1)°).

Table 1. Selected interatomic Ge–Ge distances in Å within the tris-silylated [Ge$_9$] clusters.

compound	within prismatic base 1	within prismatic base 2	prismatic heights
2	2.6304(6)	2.7771(5) *(η^3-Cu$^+$)*	3.4235(5) *(c,* Figure 2*)*
	2.6748(6)	2.8914(6) *(η^3-Cu$^+$)*	3.3918(5) *(b,* Figure 2*)*
	2.6771(5)	2.9143(5) *(η^3-Cu$^+$)*	3.1947(5) *(a,* Figure 2*)*
3	2.6407(13) *(η^3-K$^+$)*	2.9572(12) *(η^3-Au$^+$)*	3.3651(13)
	2.6711(13) *(η^3-K$^+$)*	2.9842(13) *(η^3-Au$^+$)*	3.4238(13)
	2.6459(14) *(η^3-K$^+$)*	2.9214(13) *(η^3-Au$^+$)*	3.2870(13)

In ESI-MS experiments, carried out with a tetrahydrofuran solution of the isolated red crystals, mainly the two species {(CuNHC^{Dipp})$_2$[Ge$_9${Si(*i*Bu)$_3$}$_3$]}$^+$ (*m*/*z* = 2155) (**2a**) and {(CuNHC^{Dipp})[Ge$_9${Si(*i*Bu)$_3$}$_2$]·3thf}$^+$ (*m*/*z* = 1719) (**2b**) were detected (spectra are shown in Supporting Information). Since the presence of both observed species can be excluded in the isolated crystals (elemental analysis, single X-ray diffraction) and in solution (NMR), their formation occurs unambiguously during the ionization process. Thereby, **2a** is formed upon coordination of a second Cu-NHC fragment to the free trigonal face of **2**, while species **2b** results from cleavage of a [Si(*i*Bu$_3$)$_3$]$^+$ group. The observation of **2a** is a further hint that it is possible to add more than one metalorganic fragment to tris-silylated clusters, which is also observed for the recently reported compound (CuP*i*Pr$_3$)[Ge$_9${Si(SiMe$_3$)$_3$}$_3$],[17] whereby [(CuP*i*Pr$_3$)$_2$[Ge$_9${Si(SiMe$_3$)$_3$}$_3$]$^+$ was detected in ESI-MS measurements. The appearance of **2b** indicates the lability of one [Si(*i*Bu$_3$)$_3$]$^+$ group at [Ge$_9$] with formation of the bis-silylated species.

Moreover, the reactivity of **1a** towards gold(I) phosphine complex Au(PPh$_3$)Cl was investigated. We have successfully used this ligand before for reactions with bare [Ge$_9$]$^{4-}$ clusters.[21] Addition of 1 equiv. of Au(PPh$_3$)Cl to a red acetonitrile solution of **1a** immediately led to a color change with formation of a brownish precipitate. After stirring the reaction solution overnight and purification of the precipitate, the solvent was removed in vacuo. Subsequently, the brownish residue was dissolved in toluene and filtered in order to remove potassium chloride, yielding a brown solution. After removal of toluene in vacuo, NMR experiments (^{1}H, ^{13}C, ^{29}Si, ^{31}P), indicating the formation of a dominating signal group of one silylated [Ge$_9$] species and a second silylated species in decisively smaller amount (further NMR discussion in the Supporting Information). Furthermore, the presence of free PPh$_3$ indicates the cleavage of the Au-PPh$_3$. In order to obtain closer information about the observed species, the residue was dissolved

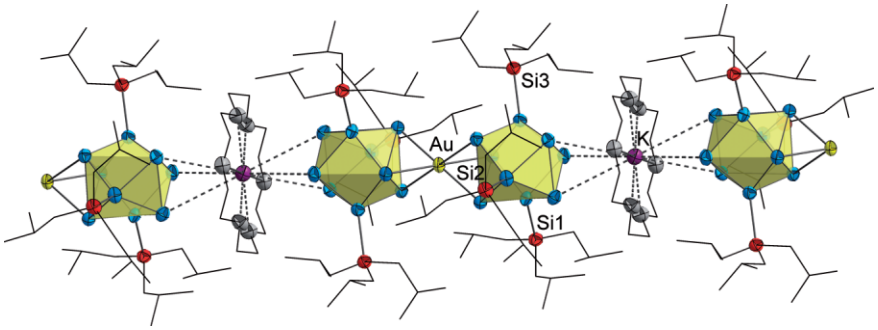

Figure 3. Molecular structure of (K-18c6)Au[Ge_9{Si(iBu)$_3$}$_3$]$_2$ (**3**) showing the linear polymeric arrangement of the clusters. Atoms are shown as ellipsoids with 70% probability (Ge atoms blue; Si atoms red, Au atoms yellow, O atoms gray and K atoms purple; C atoms are shown as wire/sticks; H atoms are omitted for reasons of clarity).

in toluene and layered with 18-crown-6 in hexane yielding red, block shaped single crystals after 5 days. Single crystal X-ray diffraction revealed the red crystals to consist of coinage metal bridged dimeric complex (K-18c6)Au[Ge_9{Si(iBu)$_3$}$_3$]$_2$·tol (**3**·tol) (Figure 3).

In the molecular structure of **3**, shown in Figure 3, the central Au^+ cation coordinates to two tris-silylated [Ge_9{Si(iBu)$_3$}$_3$]$^-$ (**1a**) anions, via one of their triangular faces formed by Ge atoms that are not connected to ligands. The two η^3–coordinated cluster faces have a staggered arrangement around the Au atom. The overall negative charge of the Au^+ bridged dimer is compensated by an 18-crown-6 sequestered potassium cation, which coordinates itself to two of the opposing triangular faces of the tris-silylated clusters, resulting in a linear polymeric arrangement (Figure 3). The Ge–Ge distances within the trigonal prism bases coordinating Au^+ are significantly elongated due to the metal coordination (2.9214(13)–2.9842(13) Å) (an overview to the Ge-Ge distances within the prismatic bases is shown in Table 1). This observation is in accordance with the literature-known anion {Au[Ge_9{Si(SiMe$_3$)$_3$}$_3$]$_2$}$^-$,[22] for which an average Ge–Ge distance of 2.96 Å is reported. In contrast, the Ge–Ge distances of the trigonal face, that coordinates to the cation of the [K-18c6]$^+$ unit, are remarkably shorter [2.6407(13)–2.6711(13) Å], confirming a weaker interaction of the potassium cation. The Ge–Au distances are in a range of 2.6485(10)–2.6651(9) Å and comparable to those in {Au[Ge_9{Si(SiMe$_3$)$_3$}$_3$]$_2$}$^-$ (average 2.69 Å). This observation shows that there is no decisively influence on the η^3-coordination of Au^+ by the lower steric demand of the silyl groups in **3**. However, the Ge–Au bonding distances in **3** are significantly longer if compared to the η^1-coordination of Au^+ with bare [Ge_9] clusters in [$Ge_9Au_3Ge_9$]$^{5-}$ (average value of 2.45 Å).[21]

In **3**, the [Ge_9] cluster shape is best described by a tricapped trigonal prism (D_{3h} symmetry) with the capping Ge atoms bearing the [Si(iBu)$_3$]$^+$ groups. In contrast to **2**, the prismatic heights in **3** are in a closer range [3.2870(13)–3.4238(13) Å] resulting in a clearly lower deviation of the [Ge_9] cores from D_{3h} towards C_{2v} symmetry compared to **2** (Table 1). Thus, the steric demands of the ligands and the coordinated transition metal fragments might be the origin of the weaker distortion of the [Ge_9] clusters (Figure 4).

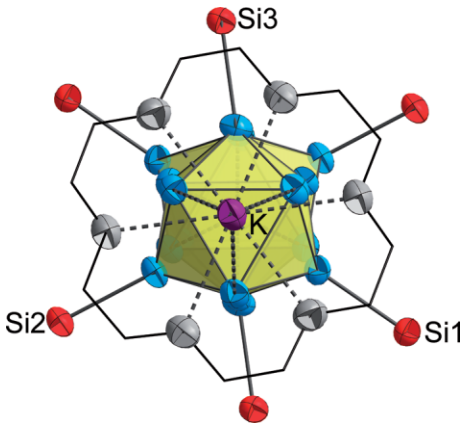

Figure 4. Detail view from the [K-18c6]$^+$ side on the arrangement of the groups at the [Ge_9] cluster in **3**. Atoms are shown as ellipsoids with 70% probability (Ge atoms blue; Si atoms red, O atoms gray, K atoms purple and C atoms as wire/sticks; the iBu groups and H atoms are omitted for reasons of clarity).

ESI-MS examinations, carried out with aliquots from the reaction solution diluted in tetrahydrofuran, revealed the presence of Au^+ bridged dimeric species {Au[Ge_9{Si(iBu)$_3$}$_3$]$_2$}$^-$ (**3a**) (m/z = 2701) besides free tris-silylated cluster [Ge_9{Si(iBu)$_3$}$_3$]$^-$; (**1a**) (m/z = 1053). The spectra are shown in the Supporting Information. This observation shows the presence of the dimer **3a** in the reaction solution as well as its stability in the gas phase.

Further, dissolution of the potassium salt of **1a** in toluene and subsequent layering with 18-crown-6 in hexane yielded yellow needle-shaped crystals, which were identified as (K-18c6)$_2$[Ge_9{Si(iBu)$_3$}$_2$]·tol (**4**·tol) by single crystal X-ray diffraction. In **4**, the [Ge_9] cluster is covalently linked to two [Si(iBu$_3$)$_3$]$^+$ groups and its twofold negative charge is compensated by two 18-crown-6 sequestered potassium atoms (Figure 5). Regarding the molecular structure of **4**, the [Ge_9] cluster possesses crystallographic C_{2v} symmetry with the C_2 axis aligned through the capping Ge5 atom and the center of the four atoms Ge, Ge', Ge2, and Ge2'. The shape is described as

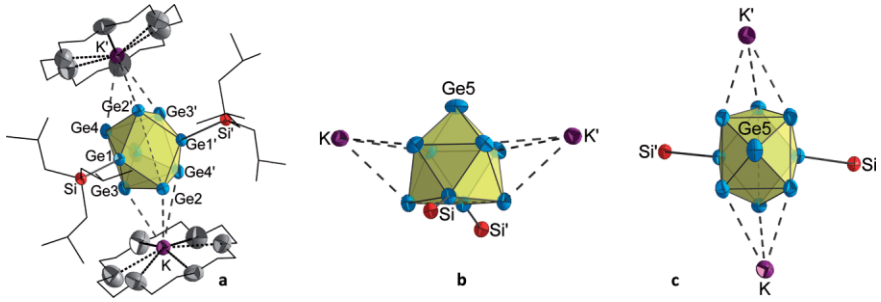

Figure 5. Molecular structure of the bis-silylated compound **4**. a) Complete molecular structure view on the square open face of the mono-capped square-antiprism [Ge_9] cluster with C_{2v} symmetry; b) Detailed side view on the square faces; c) Detailed top view on the Ge5-capped square face. Atoms are shown as ellipsoids with 70 % probability (Ge atoms blue; Si atoms red, K atoms purple and O atoms gray; C atoms are shown as wire/sticks; *i*Bu and 18-crown-6 groups are not shown in the detail views; H atoms are omitted for reasons of clarity; symmetry operation: (') $-x+1, y, -z+1.5$).

distorted mono-capped square antiprism with the two ligands connected to opposing vertex atoms of the open rectangle. This observation is in accordance to known bis-functionalized clusters such as $[Ge_9(CHCH_2)_2]^{2-}$,[7] $[RGe_9\text{-}CH{=}CH\text{-}CH{=}CH\text{-}Ge_9R]^{4-}$,[8] and $[Ge_9\{Si(SiMe_3)_3\}_2]^{2-}$ [18] as well as in the bis-silylated compound $(CuP\mathit{i}Pr_3)_4[Ge_9(SiPh_3)_2]_2$.[17] However, the symmetry is significantly different to the tris-silylated anion $[Ge_9\{Si(SiMe_3)_3\}_3]^-$, where the [$Ge_9$] core reveals D_{3h} symmetry and can hence be described as tricapped trigonal prism with the three capping Ge atoms bearing the silyl groups. In compound **4**, the lengths of the diagonals of the rectangular open face significantly differ ($d_2/d_1 = 1.23$) with a distance between the two silyl bonding Ge atoms of 3.1844(8) Å and the distance between the ligand-free Ge atoms of 3.9326(6) Å. However, the Ge–Ge bond lengths within the non-capped rectangle are in the narrow range of 2.5228(6)–2.5403(6) Å, whereas the Ge-Ge distances in the Ge-capped square are significantly longer [2.7396(6)–2.8659(7) Å] forming a nearly perfect square [Ge-Ge-Ge angles are 89.411(2)° and 90.589(2)°]. The $[Si(\mathit{i}Bu_3)_3]^+$ groups coordinate at the cluster with Ge–Si bond lengths of 2.3806(1) Å, which are slightly shorter than those reported for the bis-silylated species $[Ge_9(SiPh_3)_2]_2(CuP\mathit{i}Pr_3)_4$ and $[Ge_9\{Si(SiMe_3)_3\}_2]^{2-}$ (average 2.41 Å each).

In **4**, two K cations coordinate to two opposing deltahedral faces of the cluster with K-Ge distances in the range of 3.475(1) Å to 3.825(1) Å (Figure 5). The two symmetry dependent K cations additionally coordinate to an 18-crown-6 molecule.

For ^{1}H NMR and ESI-MS investigations the crystals were dissolved in CD_3CN and acetonitrile, respectively, resulting in yellow solutions. In ESI-MS examinations, the pristine bis-silylated anion $[Ge_9\{Si(\mathit{i}Bu)_3\}_2]^-$ (m/z = 1053) as well as $\{(K\text{-}18c6)[Ge_9\{Si(\mathit{i}Bu)_3\}_3]\}^-$ (m/z = 1354) bearing one $[K\text{-}18c6]^+$ group were monitored. The latter species is also detected in ^{1}H NMR measurements according to the observed signal ratio. Further ^{1}H NMR examinations of the same sample revealed that the bis-silylated species is not stable in the more polar solvent CD_3CN for several days (further discussion and information in Supporting Information). It can be concluded that **4** is formed from the tris-silylated species **1** in the solvent mixture of toluene and hexane in presence of 18-crown-6 as sequestering agent. One $[Si(\mathit{i}Bu_3)_3]^+$ group splits from the [Ge_9] core and the more polar bis-silylated cluster arises, which crystallizes in the non-polar solvent mixture.

Conclusion

The influence on the reactivity of silylated cluster compounds by decreasing the steric demand of the silyl groups at $[Ge_9(SiR_3)]^-$ clusters has been investigated for the organic ligands R = *i*Bu, *i*Pr and Et. ESI-MS investigations confirm the existence of the respective tris-silylated clusters in solution. Reaction of $[Ge_9\{Si(\mathit{i}Bu)_3\}_3]^-$ (**1a**) with $CuNHC^{Dipp}Cl$ yielded the tris-silylated cluster in compound $(CuNHC^{Dipp})[Ge_9\{Si(\mathit{i}Bu)_3\}_3]$ (**2**), which is similar to recently reported *Zintl* cluster copper NHC compound $(CuNHC^{Dipp})[Ge_9\{Si(SiMe_3)_3\}_3]$.[15] However, ESI-MS measurements indicate the lability of the $[Si(\mathit{i}Bu)_3]^+$ group by detection of the bis-silylated species $\{(CuNHC^{Dipp})[Ge_9\{Si(\mathit{i}Bu)_3\}_2)]\cdot 3thf\}^+$ as one of the main signals. Dimeric compound **3**, which is obtained by conversion of **1** with $Au(PPh_3)Cl$, consists of two Au^+ bridged tris-silylated [Ge_9] clusters. The different distortions of the underlying trigonal prisms in the [Ge_9] clusters cores correspond to the steric demands of the ligands and those of the coordinated transition metal fragments. The cleavage of a $[Si(\mathit{i}Bu)_3]^+$ group from $[Ge_9\{Si(\mathit{i}Bu)_3\}_3]^-$ (**1a**) in non-polar solution, yielding the respective bis-silylated cluster in compound **4**, reveals an increased lability of the $Si(\mathit{i}Bu)_3$ ligand compared to $Si(SiMe_3)_3$ groups. This observation is in good accordance to recently reported isolation of bis-silylated species $(CuP\mathit{i}Pr_3)_4[Ge_9(SiPh_3)_2]_2$, resulting from the substitution of $[SiPh_3]^+$ groups by Cu^+-phosphine fragments.[17]

The isolation of bis-silylated as well as tris-silylated compounds within this work proves that on the one hand $[Si(\mathit{i}Bu)_3]^+$ seems to be more labile than respective $[Si(SiMe_3)_3]^+$ groups, however on the other hand the isolation of two coinage metal complexes of tris-silylated cluster **1a** indicate higher stability of $[Si(\mathit{i}Bu)_3]^+$ compared to $[SiPh_3]^+$. Further investigations on the reactivity of the herein reported tris-silylated clusters bearing sterically less bulky $[Si(\mathit{i}Pr)_3]^+$

and $[Si(Et)_3]^+$ groups can provide deeper insights into the relation between steric shielding of the clusters and their reactivity.

Experimental Section

General. All reactions and manipulations were performed under a purified argon atmosphere using standard Schlenk and glove box techniques. The *Zintl* compound of the nominal composition K_4Ge_9 was synthesized by heating (2 K min^{-1}) of a stoichiometric mixture of both elements K and Ge (99.999 % Chempur) at 650 °C in a stainless steel autoclave for 46 h and slow cooling (1 K min^{-1}) to room temperature. Dry solvents were obtained from solvent purifiers (MBraun) and subsequently stored over dried molecular sieves. 18-crown-6 was purified by sublimation in vacuo at 80 °C. $Au(PPh_3)Cl$ was synthesized according to known procedures[23] from $HAuCl_4$ and PPh_3 and dried in vacuo for 8 h. $CuNHC^{Dipp}Cl$ was synthesized according to a description in literature.[24] All other chemicals were purchased commercially and used as received.

Single Crystal Structure Determination. The air and moisture sensitive single crystals of **2** and **4** were transferred from the mother liquor into a perfluoropolyalkyl ether oil at 213 K under a cold N_2 stream and subsequently fixed on a glass capillary and positioned in a 120 K cold N_2 gas stream using the crystal cap system. Single crystals of **3** were prepared analogously without crystal cooling in a glove box. The single-crystal X-ray diffraction data were collected using an Oxford Diffraction Xcalibur3 diffractometer (Mo K_α radiation). The structures were solved by Direct Methods and refined by full-matrix least-squares calculations against F^2 using SHELX-2014.[25] Non-hydrogen atoms were treated with anisotropic displacement parameters. Positions of the hydrogen atoms were calculated and refined using a riding model. In $(CuNHC^{Dipp})[Ge_9\{Si(i\text{Bu})_3\}_3]\cdot 0.5$ tol (**2**·0.5 tol) one *i*Bu group attached to Si1 is disordered and has been refined at two split positions, for presentation the carbon atoms with the lower occupation (C12A, C13A, C14A and C15A) are deleted. The amount of solvent molecules was determined by using the squeeze function. The toluene molecules in $(K\text{-}18c6)Au[Ge_9\{Si(i\text{Bu})_3\}_3]_2\cdot$tol (**3**·tol) and $(K\text{-}18c6)_2[Ge_9\{Si(i\text{Bu})_3\}_2]\cdot$tol (**4**·tol) are found in two superposing orientations, respectively, therefore the respective atoms have been refined at split positions with half occupation. Crystallographic details are given in Table 2. Further information about the crystal structure investigations may be obtained from the Cambridge Crystallographic Data Centre via www.ccdc.cam.ac.uk/data_request/cif, on quoting the depository numbers CCDC-1499454 (**2**), CCDC -1499455 (**3**), CCDC-1499456 (**4**). The crystal structures have been visualized with Diamond.[26]

Electron Dispersive X-ray (EDX) Analysis: Single crystals of all compounds were analyzed with a scanning electron microscope (JEOL 5900LV) equipped with an energy dispersive X-ray analyzer (Oxford Instruments).

NMR Spectroscopy. The ^1H, ^{13}C and ^{29}Si NMR spectra were recorded on a Bruker AvanceIII400 FT system or on a Bruker AV 500c (*Bruker Corp.*) at 300 K. The signals of the ^1H and ^{13}C spectra were calibrated on the rest proton signal of the used deuterated solvents C_6D_6, CD_3CN or C_4D_8O. Chemical shifts are given in δ values by parts per million (ppm). The coupling constants J are stated in Hz. Signal multiplicities are abbreviated as follows: s - singlet, d - doublet, t - triplet, h - heptet and m - multiplet. The spectra were evaluated with MestReNova.[27]

Electrospray Ionization Mass Spectrometry (ESI-MS). The preparation of the samples was performed in a glovebox. The measurements were performed on a HCT (*Bruker Corp.*). Analysis of the data was evaluated using the program Bruker Compass Data Analysis 4.0 SP 5 (*Bruker Corp.*). The dry gas temperature was adjusted to 125 or 300 °C and the injection speed to 240 µL s^{-1}. Visualization of the spectra was done with the programs OriginPro 2016G (*Origin Lab Corp.*) and Excel 2016 (*Microsoft Corp.*).

Elemental Analysis. Elemental analyses were performed by the microanalytical laboratory at the Department of Chemistry of the Technische Universität München. The elements C, H and N were determined with a combustion analyzer (elementar vario EL, *Bruker Corp.*).

Table 2. Selected crystallographic data of the crystal structures of **2**, **3** and **4**.

Compound	**2**·0.5 tol	**3**·tol	**4**·tol
formula	$C_{63}H_{117}CuGe_9N_2Si_3$	$C_{91}H_{194}Au_1Ge_{18}K_1O_6Si_6$	$C_{55}H_{110}Ge_9K_2O_{12}Si_2$
fw /g·mol^{-1}	1703.70	3095.68	1751.11
space group (no)	$P2_1/n$ (14)	$P\bar{1}$ (2)	$C2/c$ (15)
a /Å	13.2540(4)	13.4037(4)	16.3651(4)
b /Å	46.196(13)	15.7894(5)	28.4911(7)
c /Å	13.5183(4)	18.1041(6)	17.1371(4)
α /°	90	69.111(3)	90
β /°	102.286(3)	71.815(3)	105.108(3)
γ /°	90	65.983(3)	90
V /Å^3	8087.5(4)	3206.6(2)	7714.2(3)
Z	4	1	4
T /K	120(2)	120(2)	120(2)
ρ_{calc} /g·cm^{-3}	1.399	1.603	1.508
μ /mm^{-1}	3.629	5.414	3.642
measured reflections	197984	166666	128438
independent reflections	15005	12609	7574
R_{int} / R_σ	0.0589 / 0.0660	0.2070 / 0.0980	0.0627 / 0.0446
reflections $> 2\sigma$	9888	8323	5176
parameters / restraints	756 / 18	561 / 8	382 / 0
R_1 [$I > 2\ \sigma(I)$ / all data]	0.0307 / 0.0559	0.0549 / 0.0815	0.0385 / 0.0597
wR_2 [$I > 2\ \sigma(I)$ / all data]	0.0688 / 0.0743	0.1627 / 0.1677	0.1019 / 0.1066
goodness of fit	0.913	1.050	0.985
largest difference peak/hole /e Å^{-3}	0.757 / –0.738	5.663 / –2.059	1.401 / –0.451
CCDC number	1499454	1499455	1499456

$[Ge_9\{Si(iBu)_3\}_3]^-$ (1a) and $(K\text{-}18c6)_2[Ge_9\{Si(iBu)_3\}_2]\cdot tol$ (4·tol). K_4Ge_9 (162 mg, 0.20 mmol, 1 equiv.) was added to a solution of $Si(iBu)_3Cl$ (141 mg, 0.60 mmol, 3 equiv.) in acetonitrile (4 mL). The reaction mixture was stirred overnight and filtered. Removal of the solvent in vacuo yielded a brownish solid revealing the formation of **1a** (40 %; based on the assumption of the potassium salt). For crystallization the brownish solid was dissolved in toluene (4 mL) and filtered obtaining a brown solution. Subsequent layering of this solution with hexane containing 18-crown-6 (79.3 mg, 0.30 mmol, 3 equiv.) in hexane yielded yellow, needle-shaped crystals (19 %) after storing at –32 °C for 5 months.

$[Ge_9\{Si(iBu)_3\}_3]^-$ (1a). ^{1}H NMR (400 MHz, CD_3CN, 25 °C): δ = 2.05 (m, 3 H, CH_{iBu}), 0.93 (d, J = 6.6 Hz, 18 H, $CH_{3(iBu)}$), 0.79 (d, J = 6.7 Hz, 6 H, $CH_{2(iBu)}$). **^{13}C NMR** (101 MHz, CD_3CN, 25 °C): δ = 32.05 (CH_{iBu}), 27.36 ($CH_{3(iBu)}$), 27.24 ($CH_{2(iBu)}$). **^{29}Si NMR** (99 MHz, CD_3CN, 25 °C): δ = 22.09. **ESI-MS** (negative mode, 4000 V, 125 °C): m/z = 1253 $[Ge_9\{Si(iBu)_3\}_3]^-$.

$(K\text{-}18c6)_2[Ge_9\{Si(iBu)_3\}_2]\cdot tol$ (4·tol). ^{1}H NMR (400 MHz, CD_3CN, 25 °C): δ = 3.56 (s, 24 H, $C_{12}H_{24}O_6$), 0.94 (m, 2 H, CH_{iBu}), 0.85 (d, J = 6.6 Hz, 12 H, $CH_{3(iBu)}$), 0.50 (d, J = 6.6 Hz, 4 H, $CH_{2(iBu)}$). **ESI-MS** (negative mode, 4000 V, 125 °C): m/z = 1053 $[Ge_9\{Si(iBu)_3\}_2]^-$. **ESI-MS** (negative mode, 4000 V, 125 °C): m/z = 1354 $\{[Ge_9\{Si(iBu)_3\}_3]K\text{-}18c6\}^-$; qualitative EDX analysis of crystals of **4**·tol revealed the presence of Si, Ge and K: Si 17.51 (calcd. 15.4); Ge 61.57 (calcd. 69.2); K 20.92 (calcd. 15.4) %.

$[Ge_9\{Si(Et)_3\}_3]^-$ (1b) and $[Ge_9\{Si(iPr)_3\}_3]^-$ (1c). To a solution of SiR_3Cl (R = *i*Pr: 116 mg, 0.60 mmol, 3 equiv.; R = Et: 90.4 mg, 0.60 mmol, 3 equiv.) in acetonitrile (4 mL) K_4Ge_9 (162 mg, 0.20 mmol, 1 equiv.) was added. The reaction mixture was stirred overnight and filtered yielding brownish solutions. For ESI-MS examinations the reaction solutions were diluted with acetonitrile until a suitable concentration was obtained. ESI-MS measurements revealed the formation of the tris-silylated species **1b** (34 %; based on the assumption of the potassium salt) and **1c** (37 %; based on the assumption of the potassium salt). **ESI-MS** (negative mode, 4500 V, 125 °C): m/z 1126 (**1b**). **ESI-MS** (negative mode, 4500 V, 125 °C): m/z = 999 (**1c**).

$(CuNHC^{Dipp})[Ge_9\{Si(iBu)_3\}_3]\cdot 0.5$ tol (2·0.5 tol). An acetonitrile solution (2 mL) of $Si(iBu)_3Cl$ (70.0 mg, 0.30 mmol, 3 equiv.) was added to K_4Ge_9 (81.0 mg, 0.10 mmol, 1 equiv.). The reaction mixture was stirred overnight and subsequently filtered to obtain a red solution. Dropwise addition of this solution to an acetonitrile solution (2 mL) of $CuNHC^{Dipp}Cl$ (48.0 mg, 0.10 mmol, 1 equiv.) instantly led to formation of an orange-brownish precipitate. After stirring the reaction mixture for 30 min, the precipitate was allowed so settle down and the colorless supernatant solution was filtered off. The precipitate was washed with acetonitrile (1 mL) and dried in vacuo yielding a brownish solid. Purification by recrystallization from toluene at –40 °C yielded red block-shaped crystals (41 %) after two weeks.**^{1}H NMR** (400 MHz, C_6D_6, 25 °C): δ = 7.42 (t, J = 7.8 Hz, 2 H, $CH_{Ph(p)}$), 7.29 (d, J = 7.8 Hz, 4 H, $CH_{Ph(m)}$), 6.29 (s, 2 H, CH_{Im}), 2.75 (h, J = 6.8 Hz, 4 H, CH_{iPr}), 2.18 (m, 9 H, CH_{iBu}), 1.66 (d, J = 6.8 Hz, 12 H, $CH_{3(iPr)}$), 1.12 (m, 66 H, $CH_{3(iPr)}$ + $CH_{3(iBu)}$), 1.03 (d, 18 H, J = 6.8 Hz, $CH_{2(iBu)}$). **^{1}H NMR** (400 MHz, C_4D_8O, 25 °C): δ = 7.49 (t, J = 7.8 Hz, 2 H, $CH_{Ph(p)}$), 7.43 (s, 2 H, CH_{Im}), 7.37 (d, J = 7.8 Hz, 4 H, $CH_{Ph(m)}$), 2.78 (h, J = 6.8 Hz, 4 H, CH_{iPr}), 1.96 (m, 9 H, CH_{iBu}), 1.55 (d, J = 6.8 Hz, 12 H, $CH_{3(iPr)}$), 1.22 (d, J = 6.8 Hz, 12 H, $CH_{3(iPr)}$), 0.94 (d, J = 6.6 Hz, 54 H, $CH_{3(iBu)}$), 0.81 (d, 18 H, J = 6.8 Hz, $CH_{2(iBu)}$). **^{13}C NMR** (101 MHz, C_6D_6, 25 °C): δ = 145.89 ($C_{Ph(iPr)}$), 135.16 ($C_{Ph}N$), 130.81 ($CH_{Ph(p)}$), 124.45 ($CH_{Ph(m)}$), 121.60 (CH_{Im}), 30.94 (CH_{iBu}), 29.14 (CH_{iPr}), 27.33 ($CH_{3(iBu)}$), 26.99 ($CH_{2(iBu)}$), 25.78 ($CH_{3(iPr)}$), 24.77 ($CH_{3(iPr)}$). **^{29}Si NMR** (79 MHz, C_6D_6, 25 °C): δ = 22.17. **ESI-MS** (positive mode, 3500 V, 300 °C): m/z = 2155 $\{(CuNHC^{Dipp})_2[Ge_9\{Si(iBu)_3\}_3]\}^+$. **ESI-MS** (positive mode, 4000 V, 300 °C): m/z = 1719 $\{(CuNHC^{Dipp})[Ge_9\{Si(iBu)_3\}_2]\cdot 3thf\}^+$; Elemental analysis of **2**: C 44.6 (calcd. 44.4); H 7.1 (calcd. 6.9); N 1.7 (calcd. 1.6) %

$(K\text{-}18c6)Au[Ge_9\{Si(iBu)_3\}_3]_2\cdot tol$ (3·tol). K_4Ge_9 (162 mg, 0.20 mmol, 1 equiv.) was added to a solution of $Si(iBu)_3Cl$ (141 mg, 0.60 mmol, 3 equiv.) in acetonitrile (4 mL). After stirring overnight, the reaction mixture was filtered, yielding a red solution. Addition of $Au(PPh_3)Cl$ (98.9 mg, 0.20 mmol, 1 equiv.) immediately led to the formation of a brown precipitate. The reaction mixture was stirred at r. t. overnight. Subsequent filtration, washing with acetonitrile and removal of the solvent in in vacuo yielded a brown solid, which was extracted with toluene (2 mL). Layering with a hexane solution of 18-crown-6 (106 mg, 0.40 mmol, 2 equiv.) after filtration yielded red, block-shaped crystals (26 %) after 5 days. Single crystal X-ray diffraction confirmed formation of **3** and EDX measurements the presence of the elements Si, Ge, K and Au in the single crystals. **^{1}H NMR** (400 MHz, C_6D_6, 25 °C): δ = 1.97 (m, 3 H, CH_{iBu}), 1.07 (d, J = 6.6 Hz, 18 H, $CH_{3(iBu)}$), 0.76 (d, J = 6.8 Hz, 6 H, $CH_{2(iBu)}$). **^{13}C NMR** (101 MHz, C_6D_6, 25 °C): δ = 28.47 (CH_{iBu}), 26.91($CH_{3(iBu)}$), 24.63 ($CH_{2(iBu)}$). **^{29}Si NMR** (79 MHz, C_6D_6, 25 °C): δ = 4.67 ppm. **ESI-MS** (negative mode, 4000 V, 300 °C): m/z = 2701 $\{Au[Ge_9\{Si(iBu)_3\}_3]_2\}^-$; qualitative EDX analysis of crystals of **3**·tol revealed the presence of Si, Ge, K and Au with approximate atomic ratios: Si 25.47 (calcd. 23.1); Ge 64.42 (calcd. 69.2); K 4.2 (calcd. 3.85); Au 5.92 (calcd. 3.85) %.

Supporting Information (see footnote on the first page of this article): ^{1}H, ^{13}C, and ^{29}Si NMR spectra as well as ESI-MS spectra of compounds **1**–**4**, additional details of the crystal structures.

Acknowledgments

This work was supported by the research network "Solar Technologies go Hybrid" (State of Bavaria), the Deutsche Forschungsgemeinschaft (DFG) (FA 198/14-1) and Wacker Chemie AG. Furthermore, the authors thank Kerstin Mayer and TUM Graduate School.

References

[1] a) S. Scharfe, F. Kraus, S. Stegmaier, A. Schier, T. F. Fässler, *Angew. Chem.* **2011**, *123*, 3712; *Angew. Chem. Int. Ed.* **2011**, *50*, 3630; b) T. F. Fässler, *Coord. Chem. Rev.* **2001**, *215*, 347; c) J. D. Corbett, *Chem. Rev.* **1985**, *85*, 383; d) S. C. Sevov, J. M. Goicoechea, *Organometallics* **2006**, *25*, 5678.
[2] B. W. Eichhorn, R. C. Haushalter, W. T. Pennington, *J. Am. Chem. Soc.* **1988**, *110*, 8704.
[3] A. Spiekermann, S. D. Hoffmann, T. F. Fässler, I. Krossing, U. Preiss, *Angew. Chem.* **2007**, *119*, 5404; *Angew. Chem. Int. Ed.* **2007**, *46*, 5310.
[4] a) A. Ugrinov, S. C. Sevov, *J. Am. Chem. Soc.* **2003**, *125*, 14059; b) A. Ugrinov, S. C. Sevov, *Chem. Eur. J.* **2004**, *10*, 3727.
[5] M. W. Hull, A. Ugrinov, I. Petrov, S. C. Sevov, *Inorg. Chem.* **2007**, *46*, 2704.
[6] a) C. B. Benda, H. He, W. Klein, M. Somer, T. F. Fässler, *Z. Anorg. Allg. Chem.* **2015**, *641*, 1080; b) M. W. Hull, S. C. Sevov, *J. Am. Chem. Soc.* **2009**, *131*, 9026.
[7] a) M. W. Hull, S. C. Sevov, *Inorg. Chem.* **2007**, *46*, 10953; b) C. B. Benda, J.-Q. Wang, B. Wahl, T. F. Fässler, *Eur. J. Inorg. Chem.* **2011**, 4262.
[8] M. M. Bentlohner, W. Klein, Z. H. Fard, L.-A. Jantke, T. F. Fässler, *Angew. Chem.* **2015**, *127*, 3819; *Angew. Chem. Int. Ed.* **2015**, *54*, 3748.

[9] A. Schnepf, *Angew. Chem.* **2003**, *115*, 2728; *Angew. Chem. Int. Ed.* **2003**, *42*, 2624.
[10] F. Li, S. C. Sevov, *Inorg. Chem.* **2012**, *51*, 2706.
[11] F. Henke, C. Schenk, A. Schnepf, *Dalton Trans.* **2009**, 9141.
[12] C. Schenk, F. Henke, G. Santiso-Quinones, I. Krossing, A. Schnepf, *Dalton Trans.* **2008**, 4436.
[13] F. Li, S. C. Sevov, *Inorg. Chem.* **2015**, *54*, 8121.
[14] F. Li, A. Muñoz-Castro, S. C. Sevov, *Angew. Chem.* **2016**, *128*, 8772–8775; *Angew. Chem. Int. Ed.* **2016**, *55*, 8630.
[15] F. S. Geitner, T. F. Fässler, *Eur. J. Inorg. Chem.* **2016**, 2688.
[16] Dipp = 1,3-bis(2,6-diisopropylphenyl-)imidazol-2-ylidene.
[17] K. Mayer, L. J. Schiegerl, T. F. Fässler, *Chem. Eur. J.* **2016**, published online, DOI: 10.1002/chem.201603475.
[18] O. Kysliak, A. Schnepf, *Dalton Trans.* **2016**, *45*, 2404.
[19] O. Kysliak, C. Schrenk, A. Schnepf, *Inorg. Chem.* **2015**, *54*, 7083.
[20] C. Fischer, W. Klein, L.-A. Jantke, L. J. Schiegerl, T. F. Fässler, *Z. Anorg. Allg. Chem.* **2016**, published online, DOI: 10.1002/zaac.201600296.
[21] A. Spiekermann, S. D. Hoffmann, F. Kraus, T. F. Fässler, *Angew. Chem.* **2007**, *119*, 1663; *Angew. Chem. Int. Ed.* **2007**, *46*, 1638.
[22] C. Schenk, A. Schnepf, *Angew. Chem.* **2007**, *119*, 5408; *Angew. Chem. Int. Ed.* **2007**, *46*, 5314.
[23] S. Ahrland, K. Dreisch, B. Norén, Å. Oskarsson, *Mater. Chem. Phys.* **1993**, *35*, 281.
[24] H. Kaur, F. K. Zinn, E. D. Stevens, S. P. Nolan, *Organometallics* **2004**, *23*, 1157.
[25] C. B. Hübschle, G. M. Sheldrick, B. Dittrich, *J. Appl. Crystallogr.* **2011**, *44*, 1281.
[26] H. Putz, K. Brandenburg, *DIAMOND - Crystal and Molecular Structure Visualization*, Version 3.2k **2014**, Bonn, Germany.
[27] MestrelabResearch, *MestReNova v9.1.0–14011*, **2014**.

Received: August 19, 2016
Published Online: November 15, 2016

Z. Anorg. Allg. Chem. **2016** · ISSN 0044–2313

SUPPORTING INFORMATION

Title: Functionalization of $[Ge_9]$ with Small Silanes: $[Ge_9(SiR_3)_3]^-$ (R = *i*Bu, *i*Pr, Et) and the Structures of $(CuNHC^{Dipp})[Ge_9\{Si(iBu)_3\}_3]$, $(K\text{-}18c6)Au[Ge_9\{Si(iBu)_3\}_3]_2$, and $(K\text{-}18c6)_2[Ge_9\{Si(iBu)_3\}_2]$

Author(s): L. J. Schiegerl, F. S. Geitner, C. Fischer, W. Klein, T. F. Fässler*

Ref. No.: z201600295

Supporting Information

for

Functionalization of [Ge_9] with Small Silanes: [$Ge_9(SiR_3)_3]^-$ (R = *i*Bu, *i*Pr, Et) and the Structures of ($CuNHC^{Dipp}$)[Ge_9{$Si(iBu)_3$}$_3$], (K-18c6)Au[Ge_9{$Si(iBu)_3$}$_3$]$_2$, and (K-18c6)$_2$[Ge_9{$Si(iBu)_3$}$_2$]

Lorenz J. Schiegerl,[‡[a]] Felix S. Geitner,[‡ [b]] Christina Fischer,[[a]] Wilhelm Klein,[[a]]

and Thomas F. Fässler*[[a]]

[a] Department of Chemistry, Technische Universität München

Lichtenbergstraße 4, 85747 Garching, Germany

E-Mail: thomas.faessler@lrz.tum.de

[b] WACKER Institute for Silicon Chemistry and Department of Chemistry, Technische Universität München

Lichtenbergstraße 4, 85748 Garching, Germany

[‡]authors contributed equally to this work

Content

1 NMR data of **1a** and the compounds **2 – 4**

[Ge_9{Si(*i*Bu)$_3$}$_3$]$^-$ (**1a**):

The ^{1}H NMR spectrum shows three proton signals (2.05, 0.93, and 0.79 ppm) of the *i*Bu groups in [Ge_9{Si(*i*Bu)$_3$}$_3$]$^-$ (**1a**) with the expected signal ratio of 1:6:2 (reactant Si(*i*Bu)$_3$Cl in CD_3CN: 1.91, 0.98, and 0.88 ppm). The ^{13}C NMR spectrum also shows three signals for the three different carbon atoms in **1a** (Si(*i*Bu)$_3$Cl in CD_3CN: 28.41, 26.40, and 25.24 ppm). In the ^{29}Si NMR spectrum one signal is observed at 22.09 ppm (Si(*i*Bu)$_3$Cl in CD_3CN: 31.08 ppm).

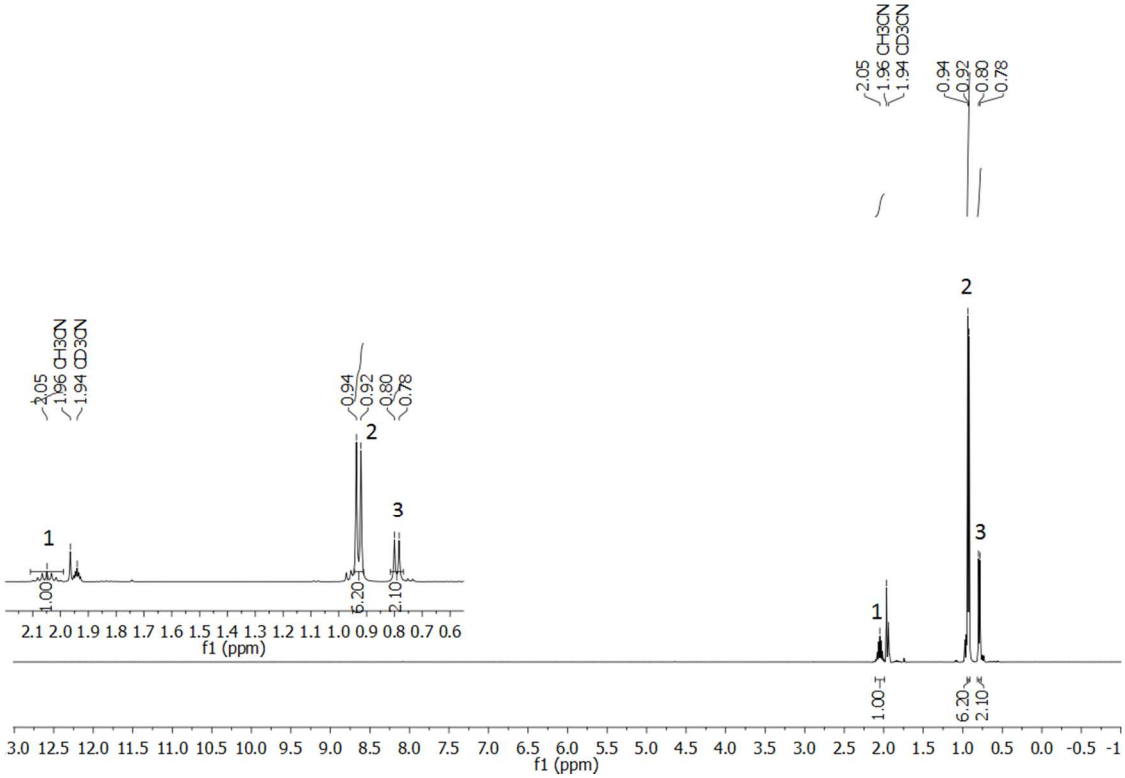

Figure SI 1: ^{1}H NMR spectrum of [Ge_9{Si(*i*Bu)$_3$}$_3$]$^-$ (**1a**) in CD_3CN.

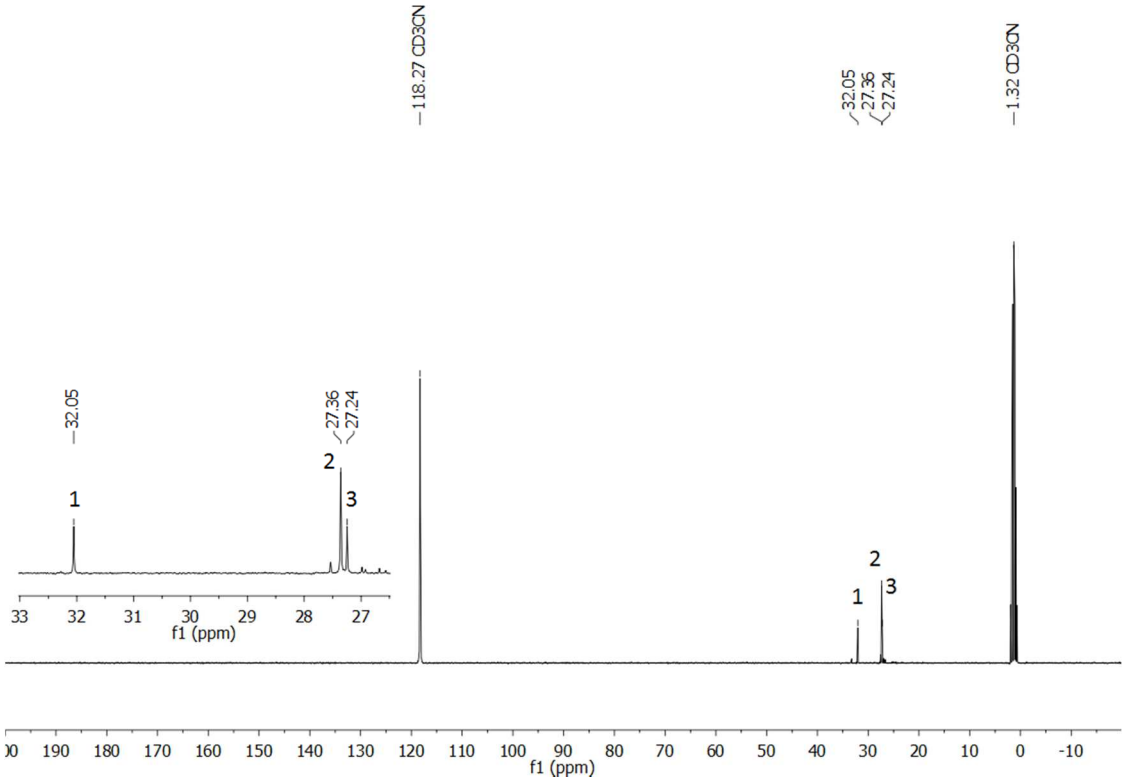

Figure SI 2: ^{13}C NMR spectrum of $[Ge_9\{Si(iBu)_3\}_3]^-$ (**1a**) in CD_3CN.

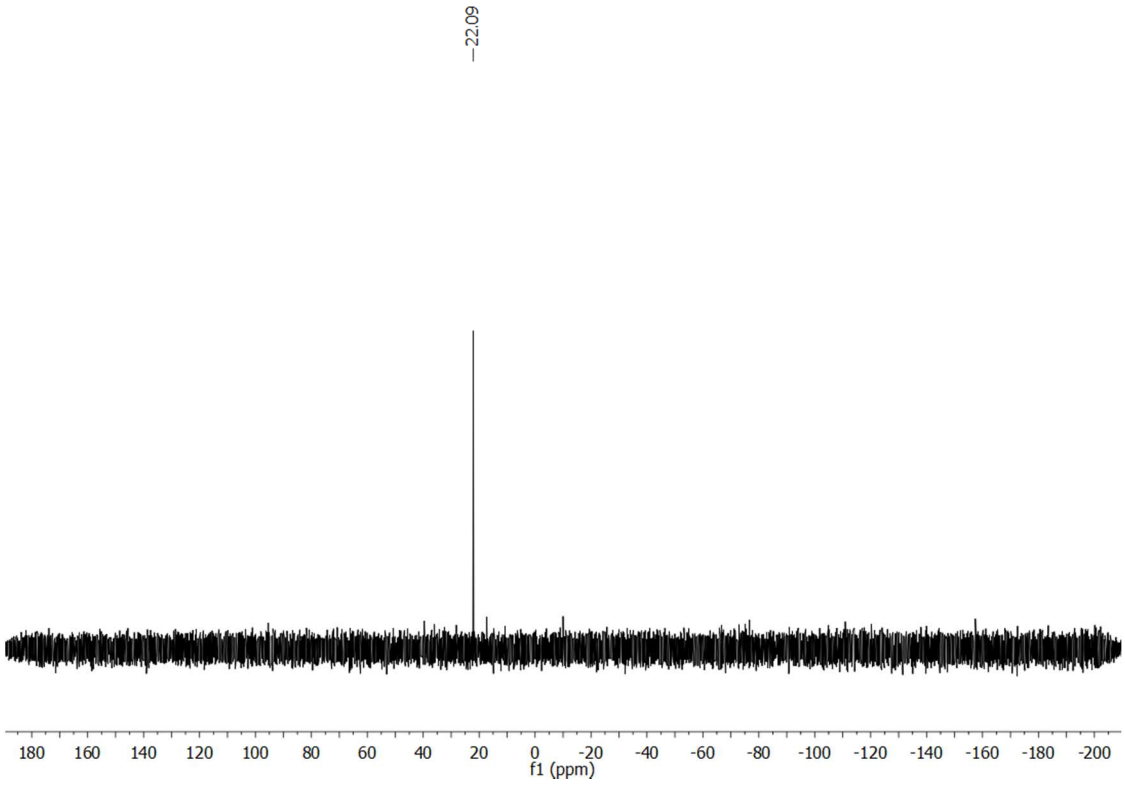

Figure SI 3: ^{29}Si NMR spectrum of $[Ge_9\{Si(iBu)_3\}_3]^-$ (**1a**) in CD_3CN.

(CuNHC^{Dipp})[Ge$_9${Si(*i*Bu)$_3$}$_3$] (**2**):

The ^{1}H NMR spectrum measured in C_6D_6 consists of eight proton signals with a ratio of 2:4:2:4:9:12:66:18. Since the signals caused by the methyl groups of the silyl residues (54 H) overlap with those of two Dipp groups (12 H) of the NHC (d at 1.12 ppm), a second ^{1}H NMR spectrum in C_4D_8O is provided, where no signal overlapping occurs. The ^{13}C NMR spectrum consists of eleven signals, in the ^{29}Si NMR spectrum one signal is observed at 22.17 ppm.

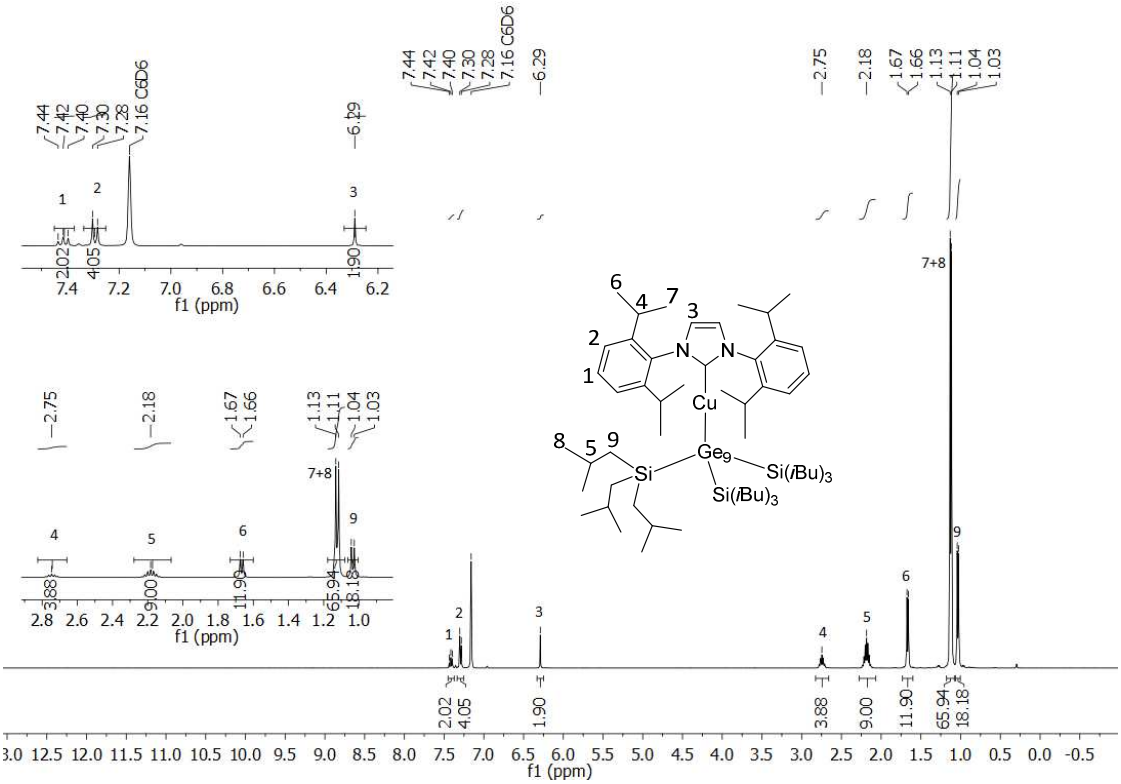

Figure SI 4: ^{1}H NMR spectrum of (CuNHC^{Dipp})[Ge$_9${Si(*i*Bu)$_3$}$_3$] (**2**) in C_6D_6.

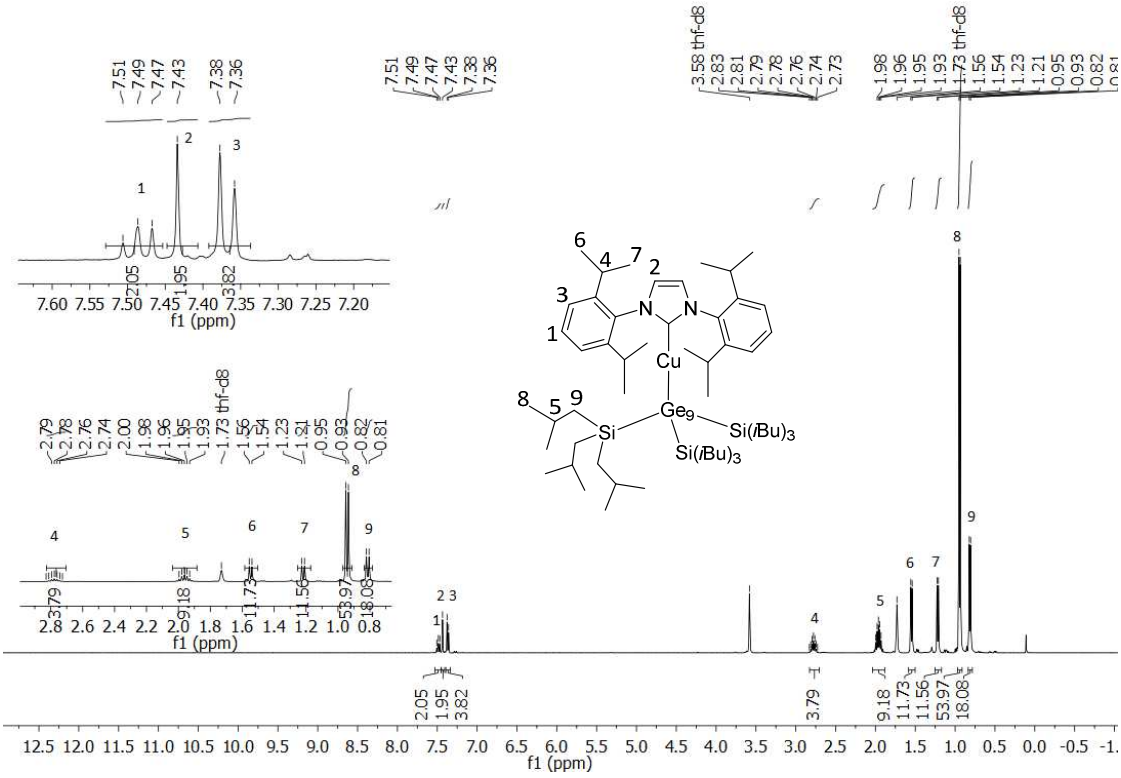

Figure SI 5: ^{1}H NMR spectrum of (CuNHC^{Dipp})[Ge$_9${Si(*i*Bu)$_3$}$_3$] (**2**) in C_4D_8O.

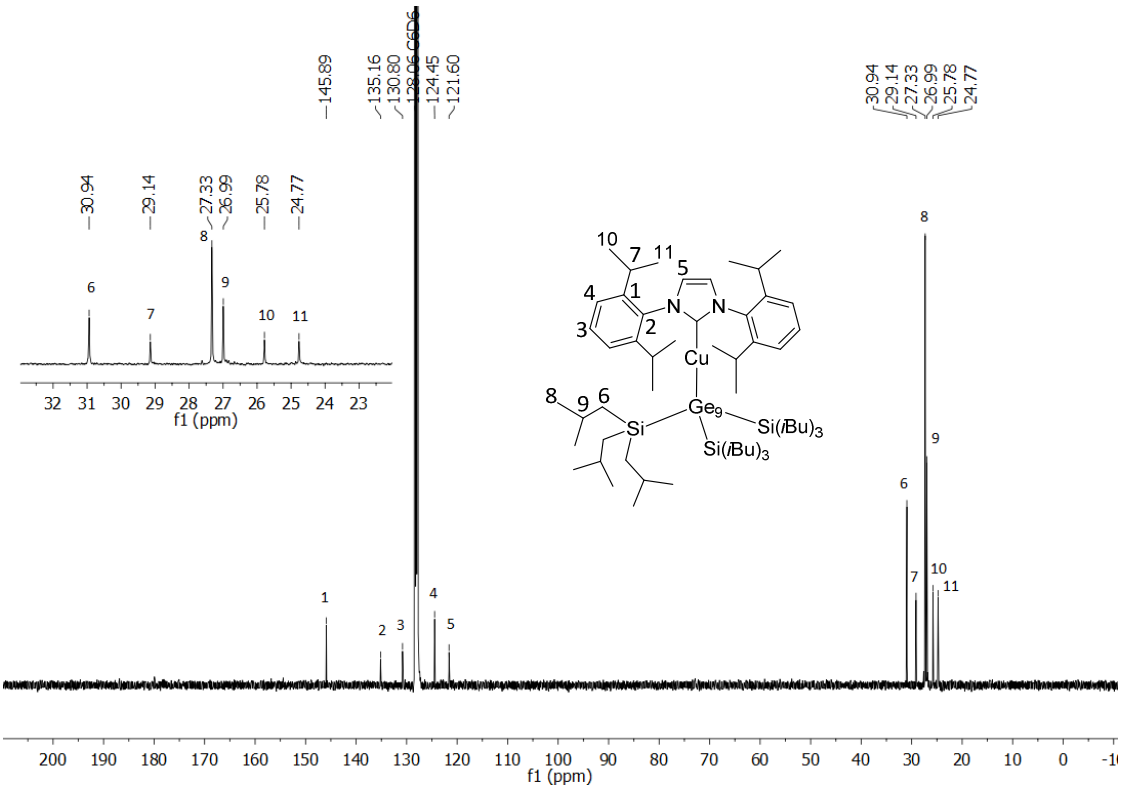

Figure SI 6: ^{13}C NMR spectrum of (CuNHC^{Dipp})[Ge$_9${Si(*i*Bu)$_3$}$_3$] (**2**) in C_6D_6.

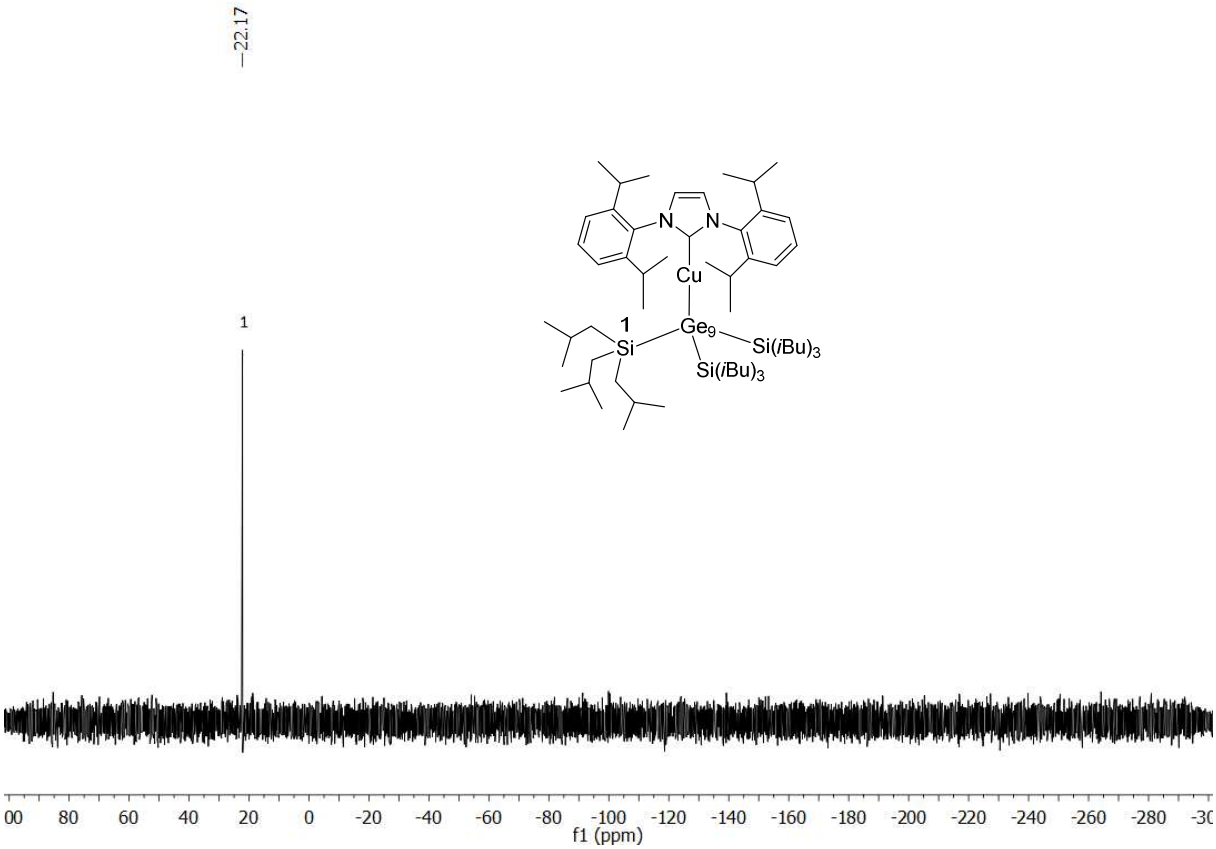

Figure SI 7: ^{29}Si NMR spectrum of (CuNHC^{Dipp})[Ge$_9${Si(*i*Bu)$_3$}$_3$] (**2**)in C_6D_6.

(K-18c6)Au[Ge$_9${Si(*i*Bu)$_3$}$_3$]$_2$ (**3**):

In the ^{1}H NMR spectrum the main signals (1.97 (C*H*$_{i\text{Bu}}$), 1.07 (C*H*$_{3(i\text{Bu})}$), and 0.76 ppm (C*H*$_{2(i\text{Bu})}$)) originate from the [Si(*i*Bu)$_3$]$^+$ groups of one silylated species with the expected signal ratio of 1:6:2. Another silylated species can be assigned in clearly smaller amount to the signals 1.64, 0.86, and 0.54 ppm with the same expected signal ratio. Verification of the existence of the two signal groups further derives from 2D COSY experiments. The signals between 7.0 and 7.5 ppm can be assigned to free PPh_3. The ^{13}C NMR spectrum confirms the presence of the three species by showing mainly three signal groups (28.47 (*C*H$_{i\text{Bu}}$), 26.91 (*C*H$_{3(i\text{Bu})}$), and 24.63 ppm (*C*H$_{2(i\text{Bu})}$)) for the three different carbon atoms of the [Si(*i*Bu)$_3$]$^+$ groups of the silylated species, the smaller amount of a second silylated species is confirmed by the smaller signals at 26.49, 24.74, and 23.99 ppm. The carbon signals for PPh_3 appear between 128 and 138 ppm, doublet splitting originates from phosphorous coupling. Further evidence for the presence of two silylated species in different amounts provides the ^{29}Si NMR spectrum. A dominating signal appears at 4.67 ppm and a decisively smaller signal at 2.04 ppm. The ^{31}P NMR spectrum exclusively shows the signal of free PPh_3 at 5.33 ppm. The corresponding ESI-MS spectra are shown in Figure SI 19 and 20 and show the presence of [Ge$_9${Si(*i*Bu)$_3$}$_3$]$^-$ (**1a**) and {Au[Ge$_9${Si(*i*Bu)$_3$}$_3$]$_2$}$^-$ (**3a**) under measurement conditions.

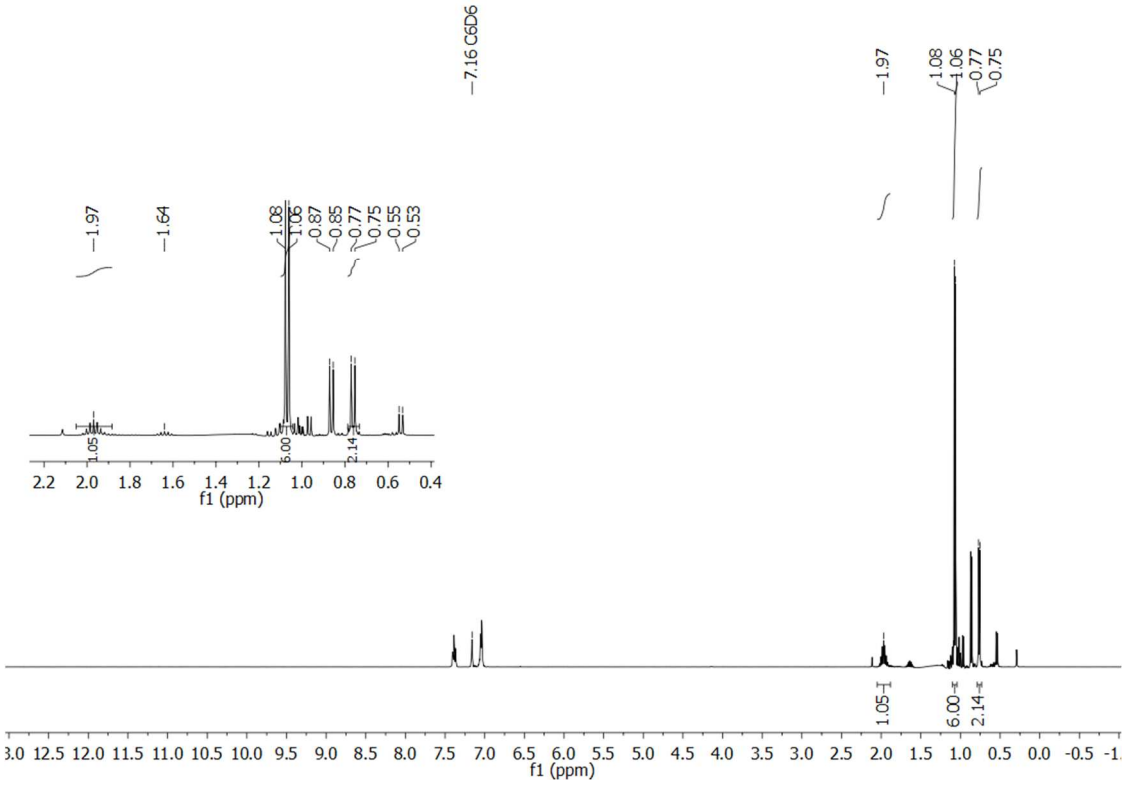

Figure SI 8: ^{1}H NMR spectrum of $\{Au[Ge_9\{Si(iBu)_3\}_3]_2\}^-$ (**3a**) in C_6D_6.

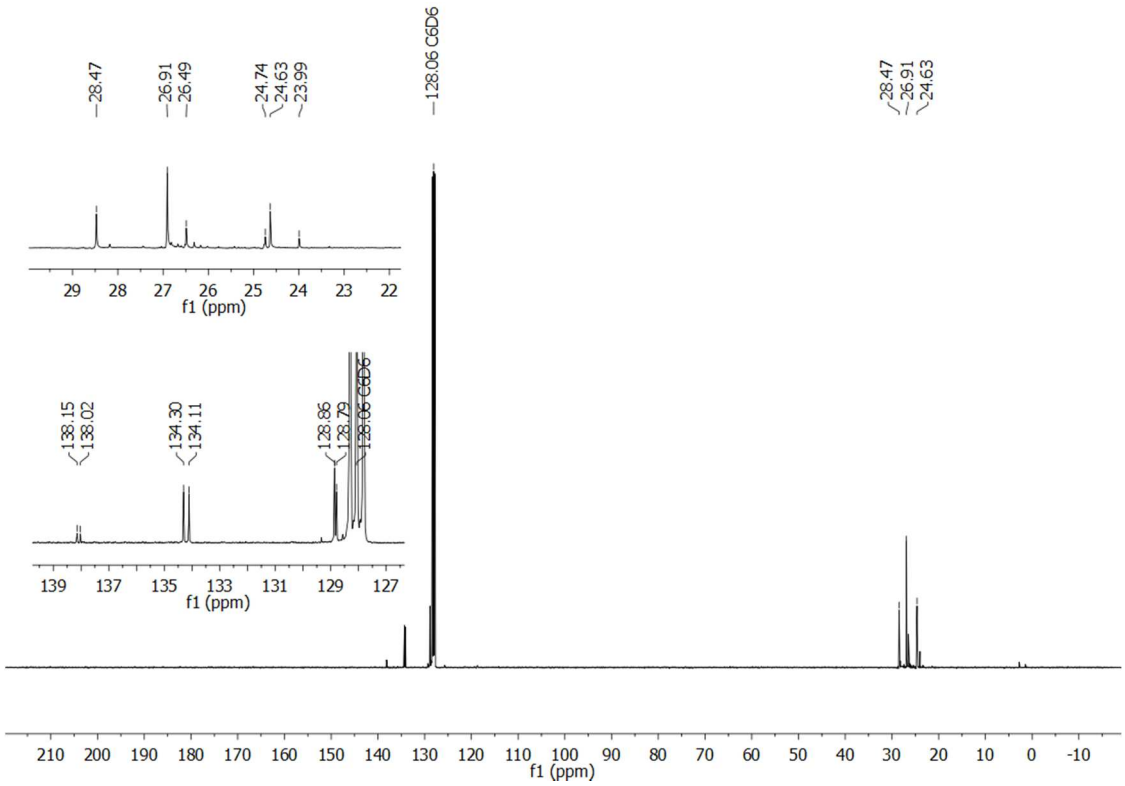

Figure SI 9: ^{13}C NMR spectrum of $\{Au[Ge_9\{Si(iBu)_3\}_3]_2\}^-$ (**3a**) in C_6D_6.

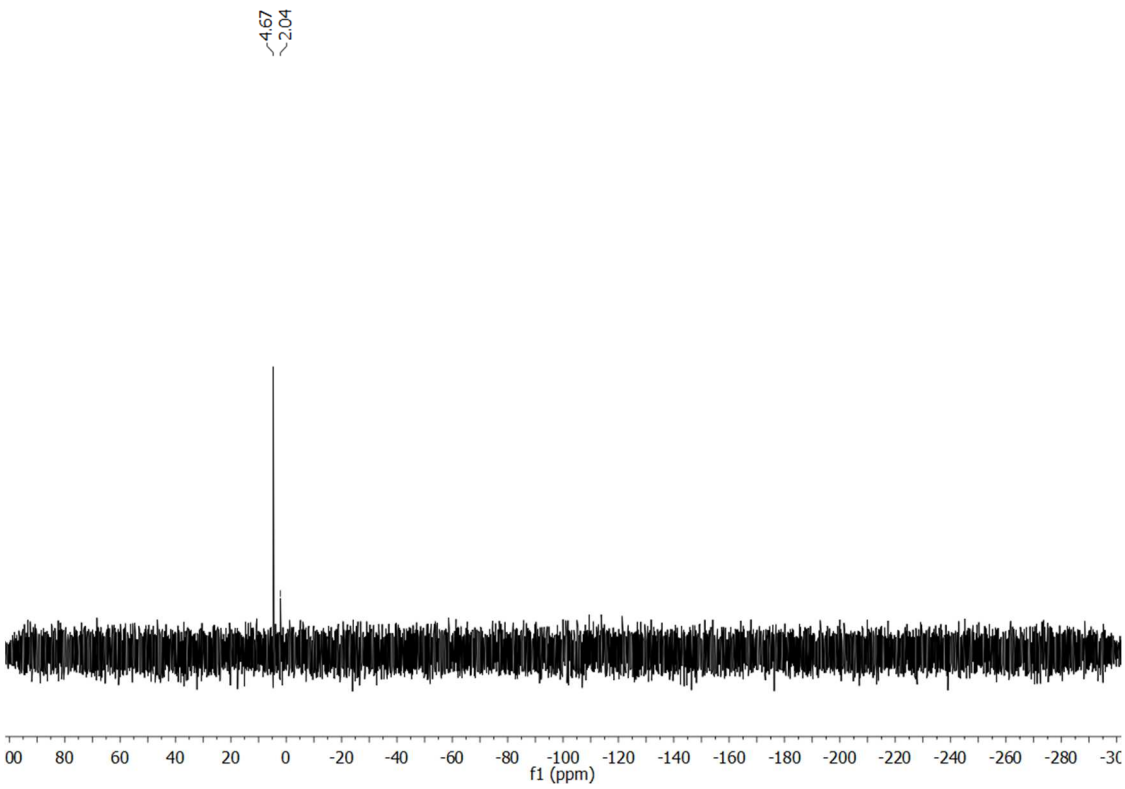

Figure SI 10: ^{29}Si NMR spectrum of $\{Au[Ge_9\{Si(i\text{Bu})_3\}_3]_2\}^-$ (**3a**) in C_6D_6.

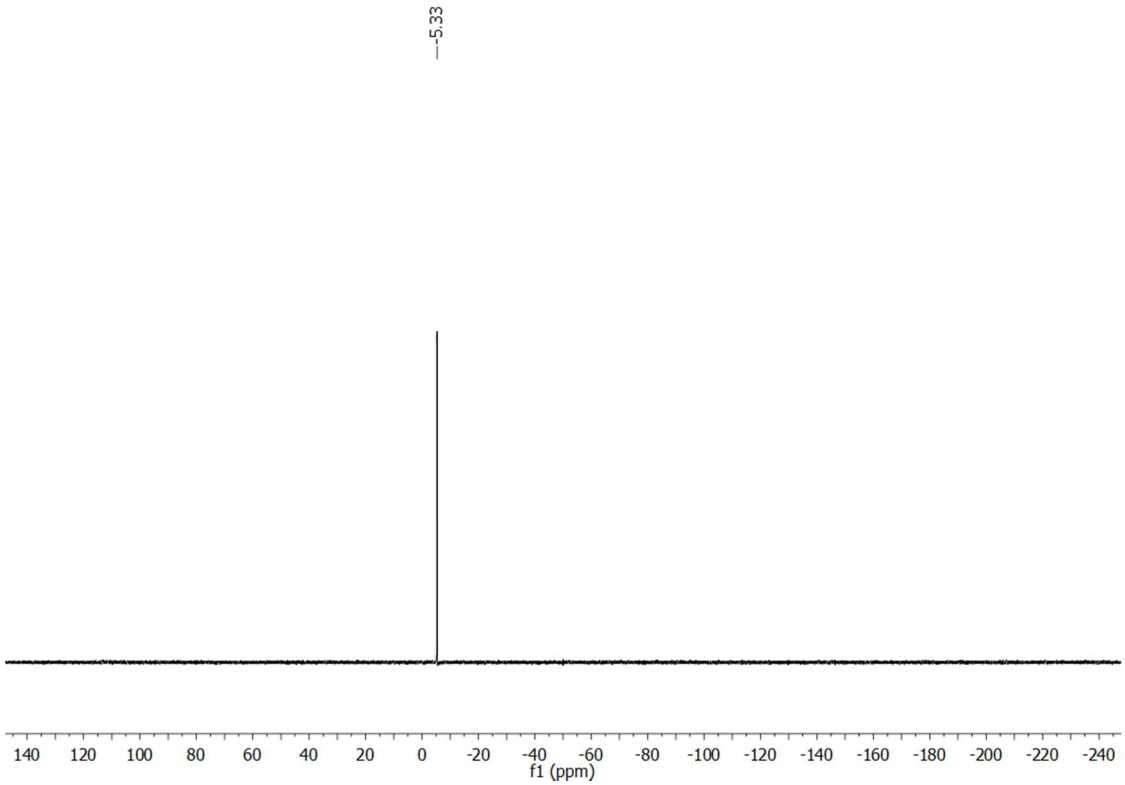

Figure SI 11: ^{31}P NMR spectrum of $\{Au[Ge_9\{Si(i\text{Bu})_3\}_3]_2\}^-$ (**3a**) in C_6D_6.

$(K\text{-}18c6)_2[Ge_9\{Si(i\text{Bu})_3\}_2]$ (**4**):

The ^{1}H NMR spectrum consists of four signals with an integral ratio of 24:2:12:4 for the bis-silylated compound. The bis-silylated anion $[Ge_9\{Si(i\text{Bu})_3\}_2]^{2-}$ (**4a**), obtained from hexane/toluene solution, is observed to be unstable in the more polar solvent CD_3CN over several days and its decomposition can be monitored by time dependent ^{1}H NMR investigation (Figure SI 12b).

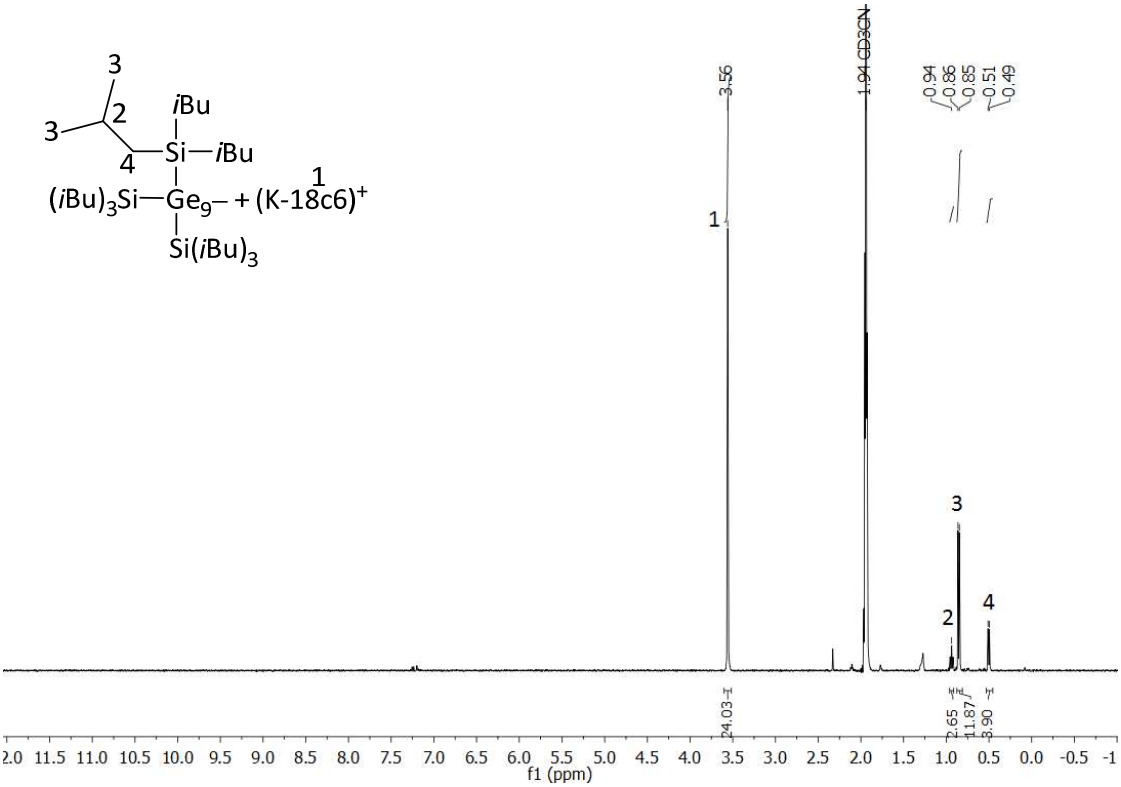

Figure SI 12a: ^{1}H NMR spectrum of $(K\text{-}18c6)_2[Ge_9\{Si(i\text{Bu})_3\}_2]$ (**4**) in CD_3CN.

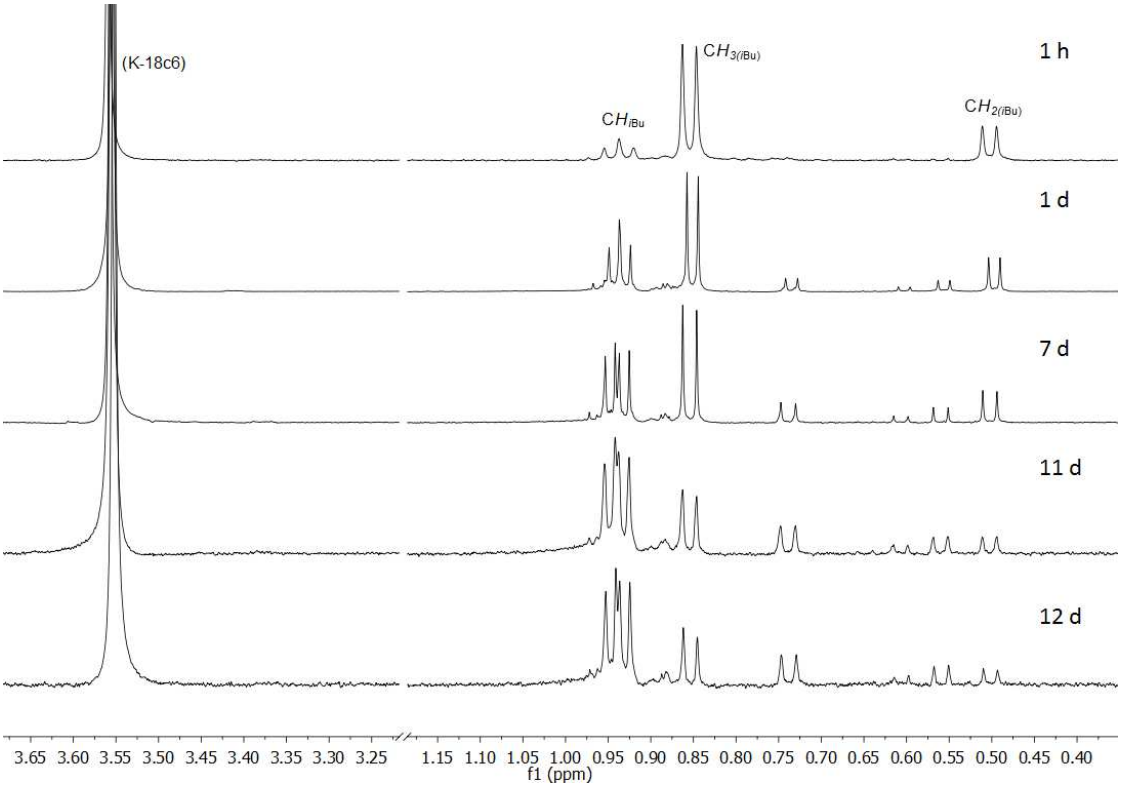

Figure SI 12b: Time-depending ^{1}H NMR spectra of (K-18c6)$_2$[Ge$_9${Si(*i*Bu)$_3$}$_2$] (**4**) in CD_3CN.

2 ESI-MS data of **1a**, **1b**, **1c** and the compounds **2 – 4**

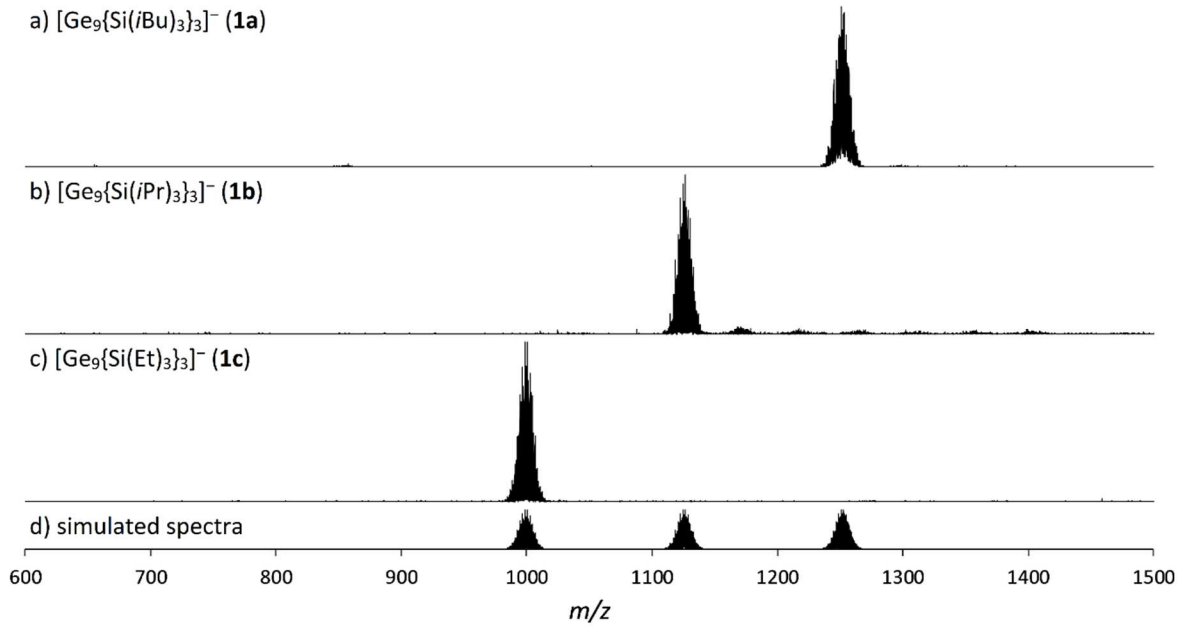

Figure SI 13. Overview on the ESI-MS spectra of the tris-silylated species in acetonitrile. a) $[Ge_9\{Si(i\text{Bu})_3\}_3]^-$ (**1a**) (*m/z* = 1253); b) $[Ge_9\{Si(i\text{Pr})_3\}_3]^-$ (**1b**) (*m/z* = 1126); c) $[Ge_9\{Si(\text{Et})_3\}_3]^-$ (**1c**) (*m/z* = 999); d) simulated spectra of the anions.

$[Ge_9\{Si(i\text{Bu})_3\}_3]^-$ (**1a**):

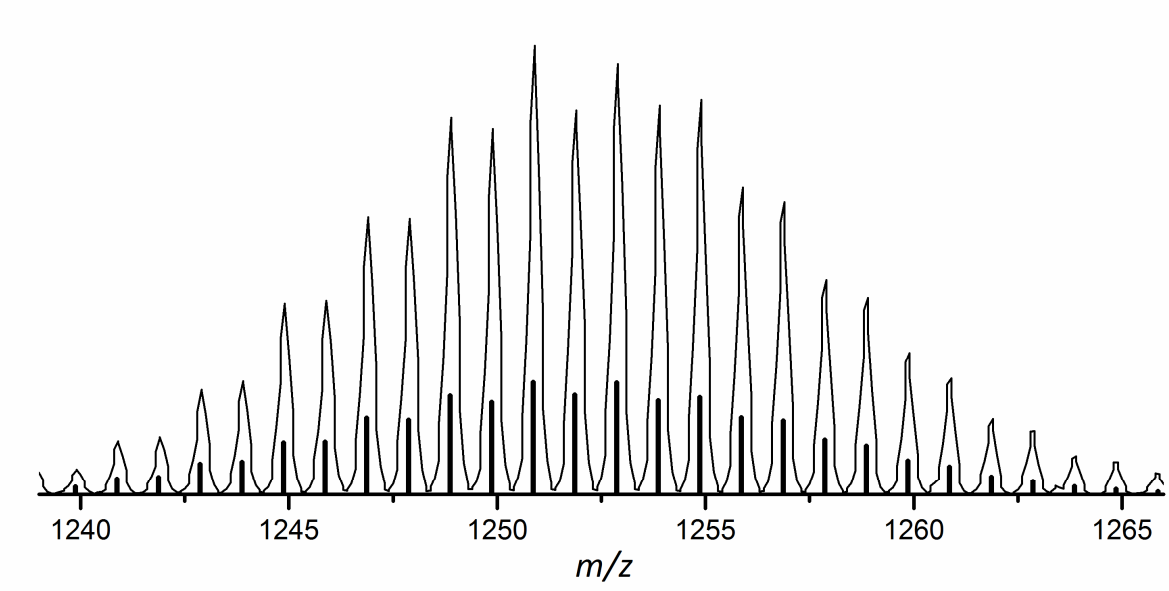

Figure SI 14. ESI-MS spectrum of $[Ge_9\{Si(i\text{Bu})_3\}_3]^-$ (**1a**) (*m/z* = 1253); line: simulated mass spectrum, bars: calculated mass spectrum.

$[Ge_9\{Si(i\text{Pr})_3\}_3]^-$ (**1b**):

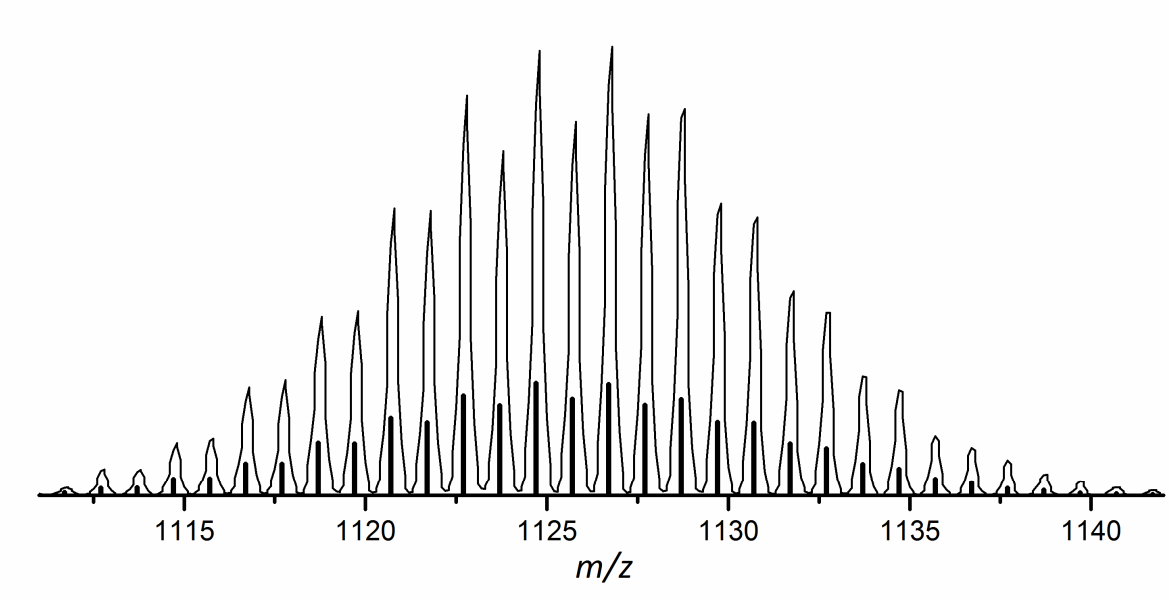

Figure SI 15. ESI-MS spectrum of $[Ge_9\{Si(i\text{Pr})_3\}_3]^-$ (**1b**) (*m/z* = 1126) line: measured mass spectrum, bars: simulated mass spectrum.

$[Ge_9\{Si(Et)_3\}_3]^-$ (**1c**):

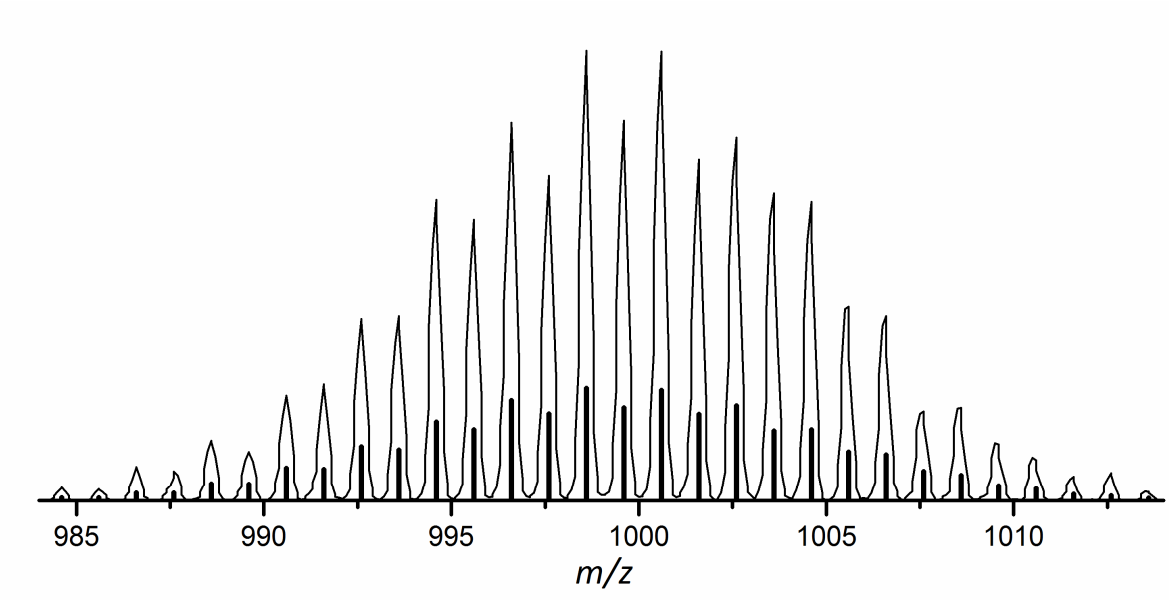

Figure SI 16. ESI-MS spectrum of $[Ge_9\{Si(Et)_3\}_3]^-$ (**1c**) (*m/z* = 999) line: measured mass spectrum, bars: simulated mass spectrum.

(CuNHC^{Dipp})[Ge$_9${Si(*i*Bu)$_3$}$_3$] (**2**):

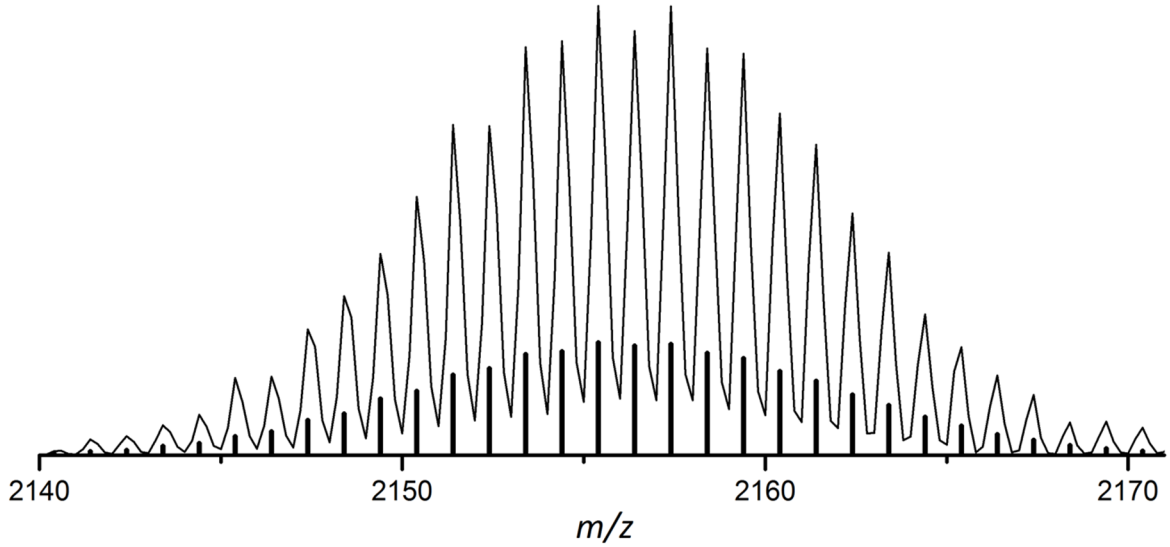

Figure SI 17. ESI-MS spectrum of {(CuNHC^{Dipp})$_2$[Ge$_9${Si(*i*Bu)$_3$}$_3$]}$^+$ (*m/z* = 2155); line: measured mass spectrum, bars: simulated mass spectrum.

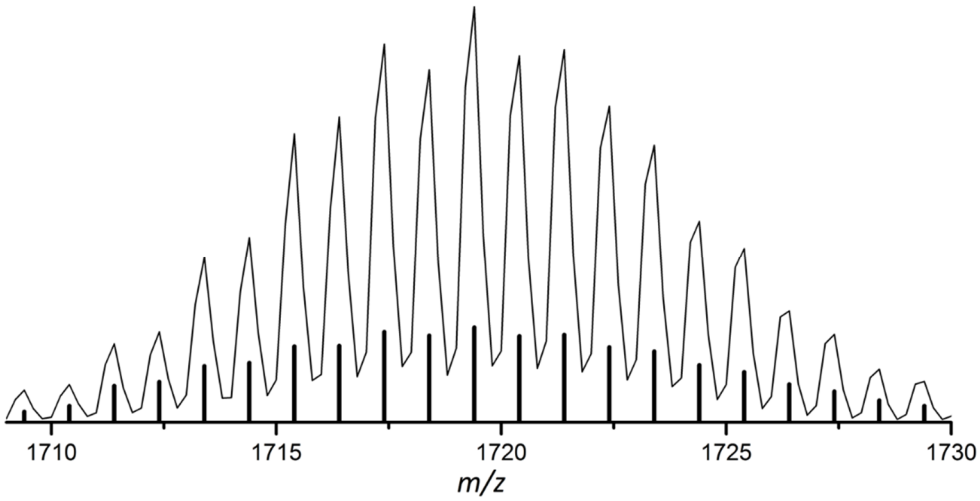

Figure SI 18. ESI-MS spectrum of {(CuNHC^{Dipp})[Ge$_9${Si(*i*Bu)$_3$}$_2$]·3thf}$^+$ (*m/z* = 1719); line: measured mass spectrum, bars: simulated mass spectrum.

(K-18c6)Au[Ge_9{Si(*i*Bu)$_3$}$_3$]$_2$ (**3**):

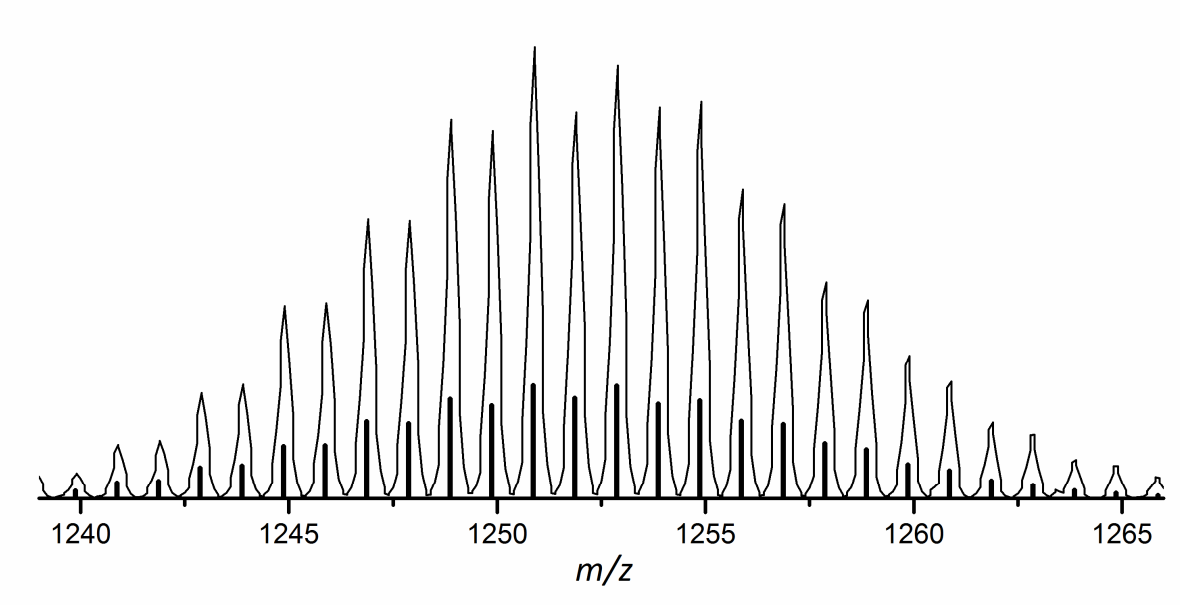

Figure SI 19. ESI-MS spectrum of [Ge_9{Si(*i*Bu)$_3$}$_3$]$^-$ (**1a**) (*m/z* = 1252); line: measured mass spectrum, bars: simulated mass spectrum.

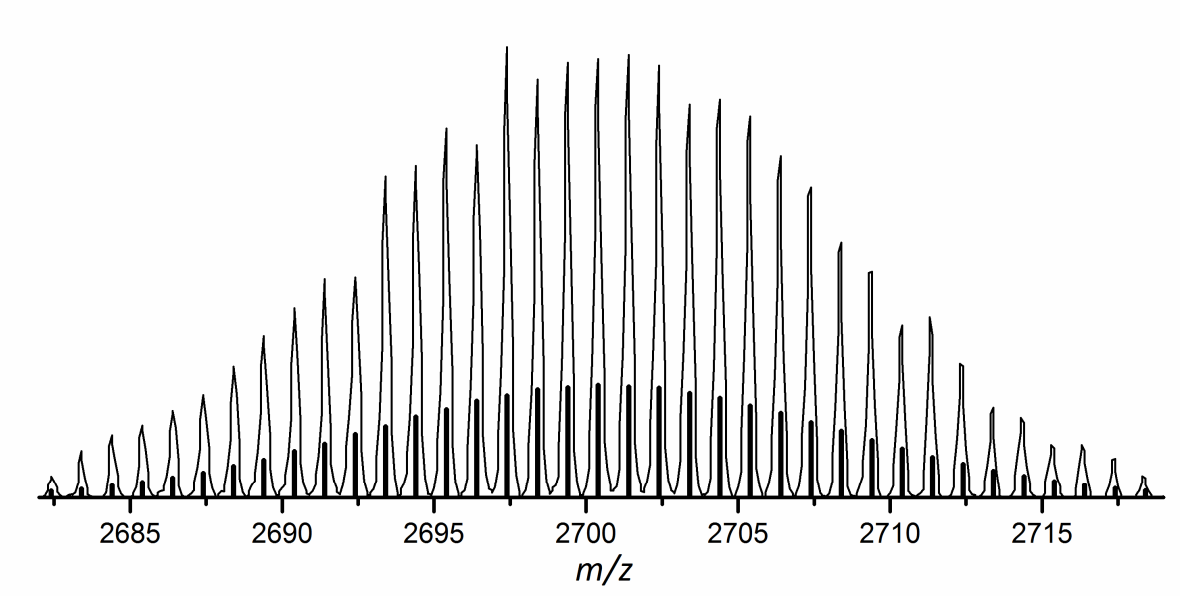

Figure SI 20. ESI-MS spectrum of {Au[Ge_9{Si(*i*Bu)$_3$}$_3$]$_2$}$^-$ (**3a**) (*m/z* = 2701) line: measured mass spectrum, bars: simulated mass spectrum.

(K-18c6)$_2$[Ge$_9${Si(*i*Bu)$_3$}$_2$] (**4**):

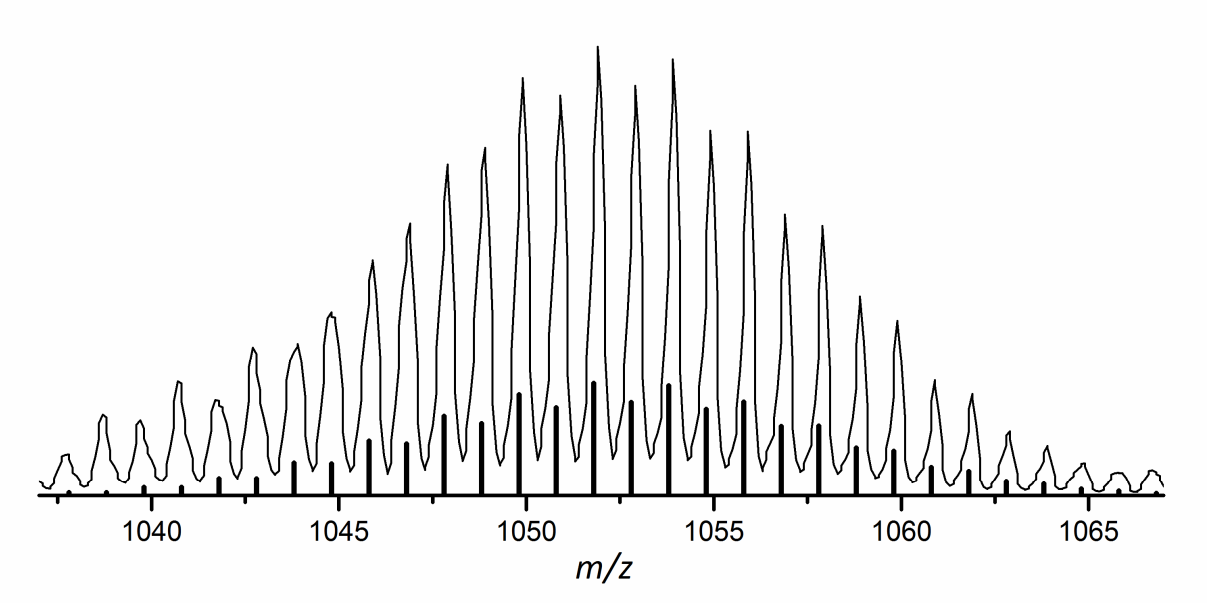

Figure SI 21. ESI-MS spectrum of [Ge$_9${Si(*i*Bu)$_3$}$_2$]$^-$ (**4a**) (*m/z* = 1053; negative mode, 4000 V, 125 °C); line: measured mass spectrum, bars: simulated mass spectrum.

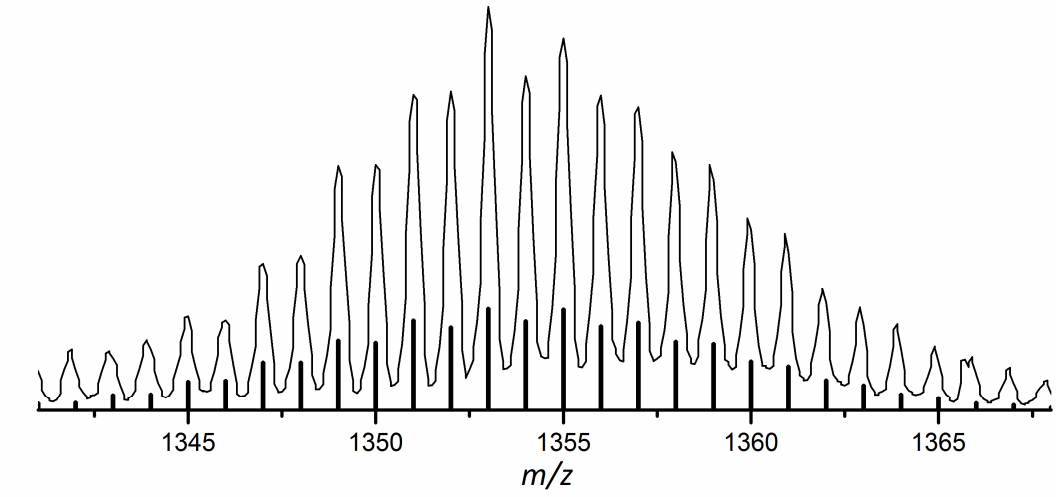

Figure SI 22. ESI-MS spectrum of {(K-18c6)[Ge$_9${Si(*i*Bu)$_3$}$_2$]}$^-$ (*m/z* = 1354); line: measured mass spectrum, bars: simulated mass spectrum.

3 Crystallographic details of the compounds **2 – 4**

Unit cells:

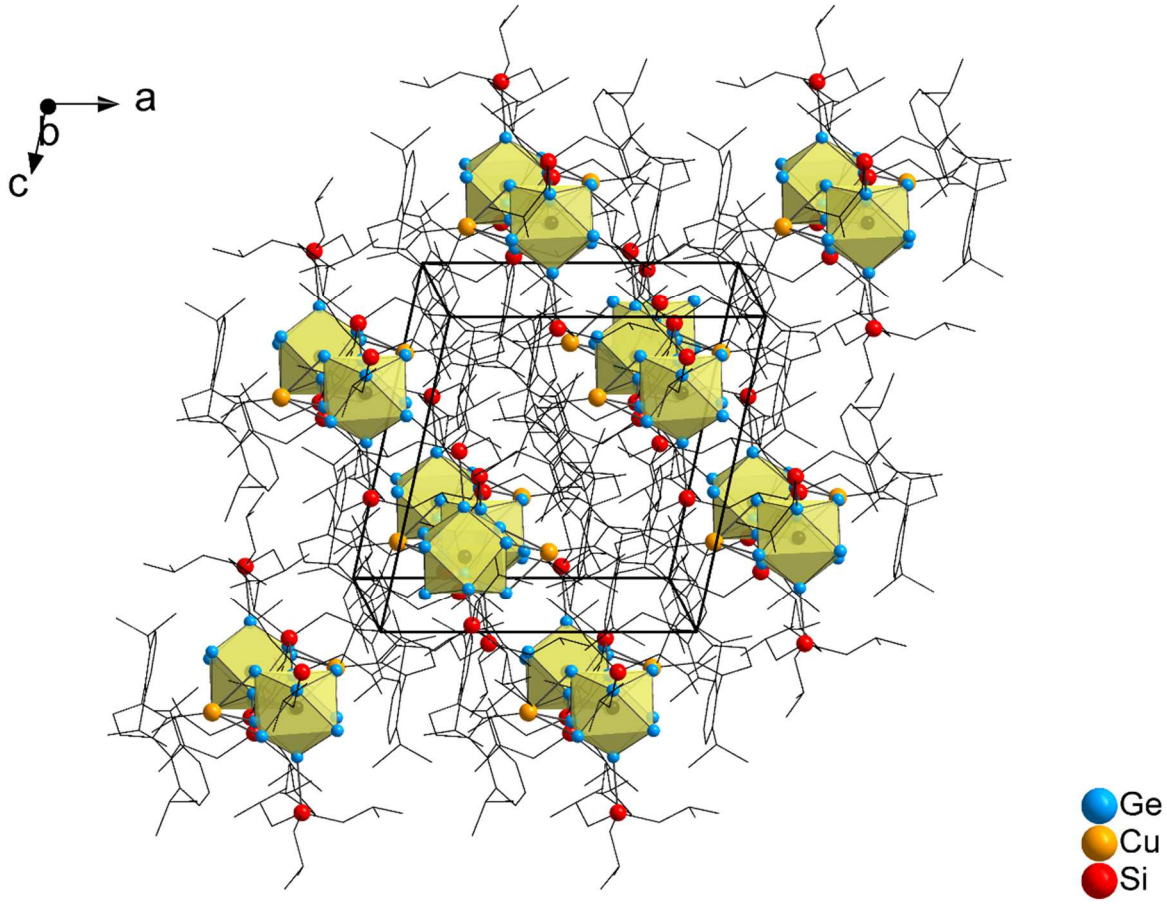

Figure SI 23: Unit cell of compound **2**. Ge atoms are blue, Si atoms red, and Cu atoms orange. The clusters are shown as polyhedra, whereas for reasons of clarity C and N atoms are represented as wire/sticks and H atoms are omitted.

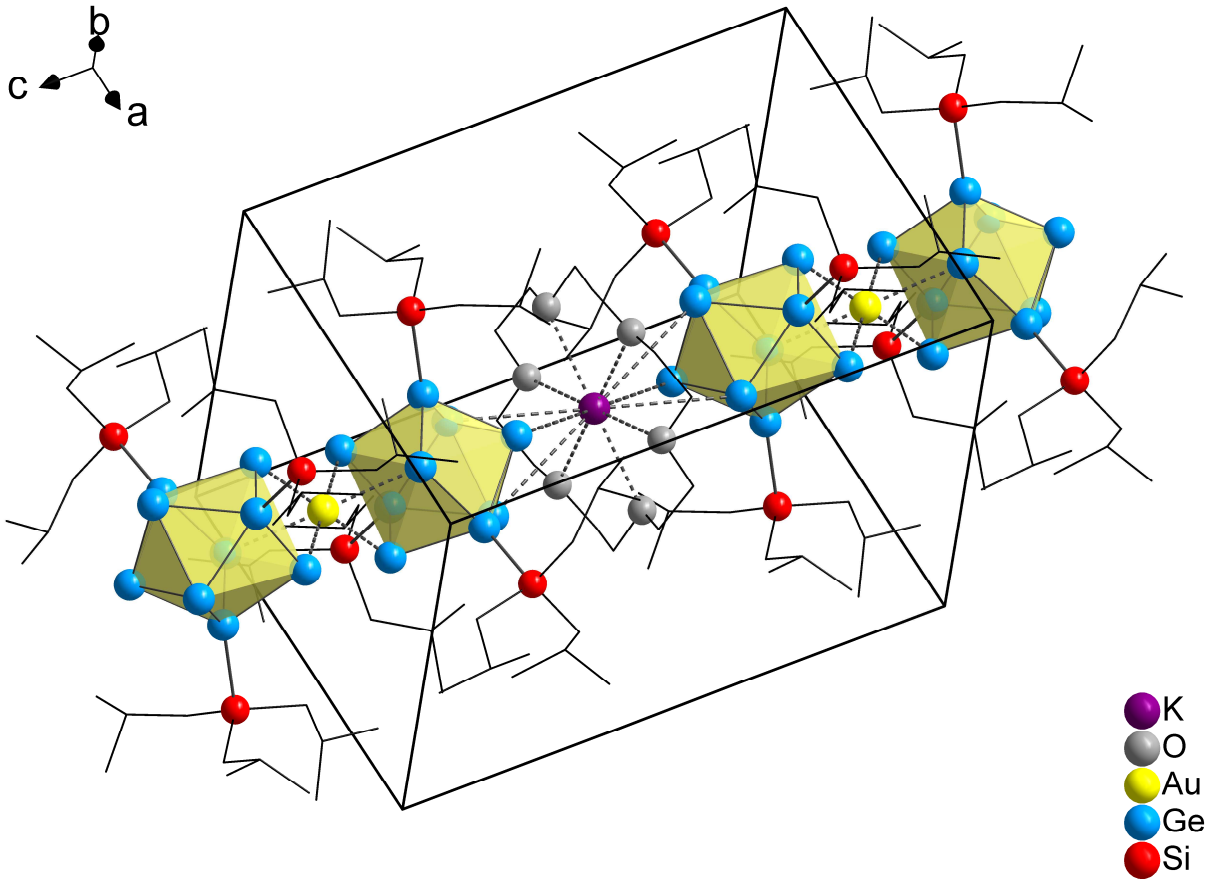

Figure SI 24: Unit cell of compound **3**. Ge atoms are blue, Si atoms red, Au atoms yellow, and K atoms purple. The clusters are shown as polyhedra, whereas for reasons of clarity C atoms are represented as wire/sticks and H atoms are omitted.

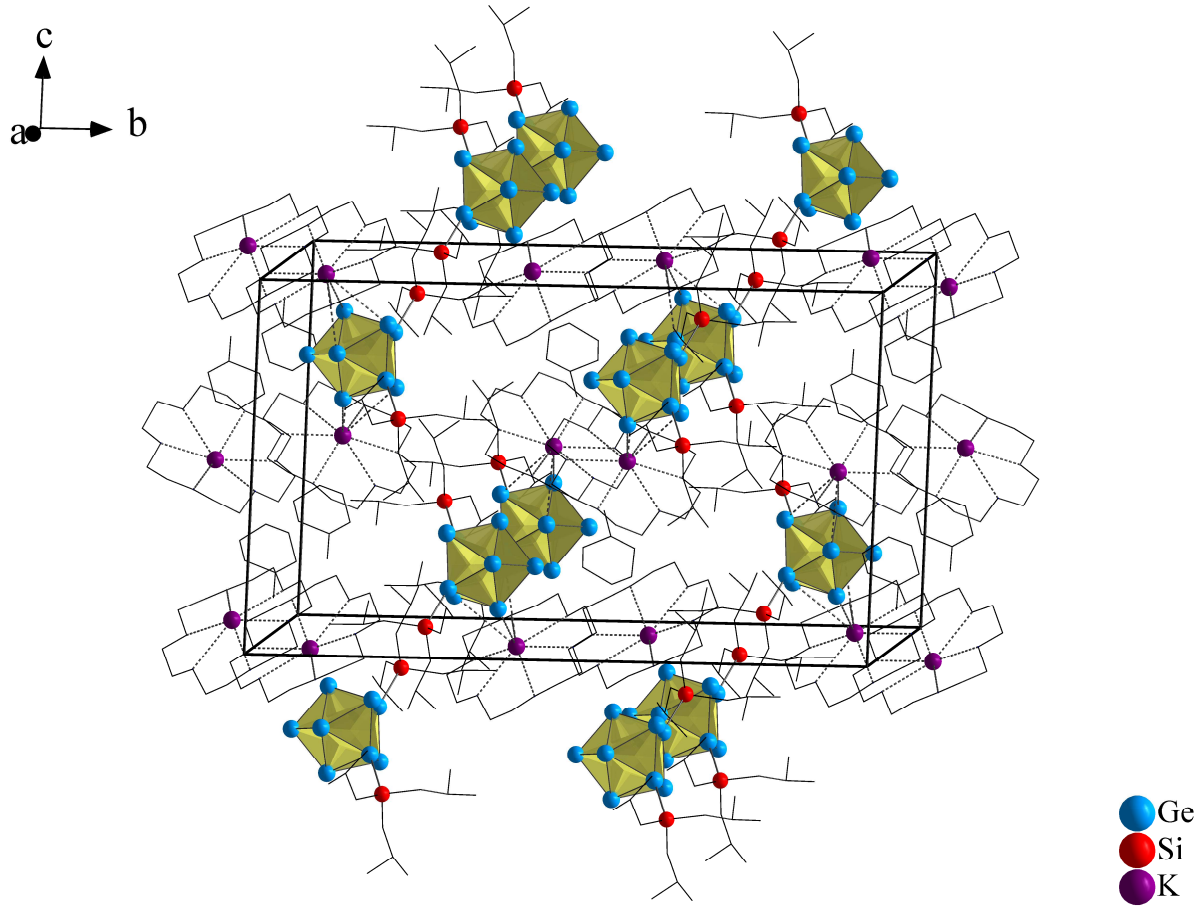

Figure SI 25: Unit cell of compound **4**. Ge atoms are blue, Si atoms red, and K atoms purple. The clusters are shown as polyhedra, whereas for reasons of clarity C and O atoms are represented as wire/sticks and H atoms are omitted.

Selected bond lengths of the compounds **2 – 4**: The molecular structures, including selected atom names, are shown for further clarification.

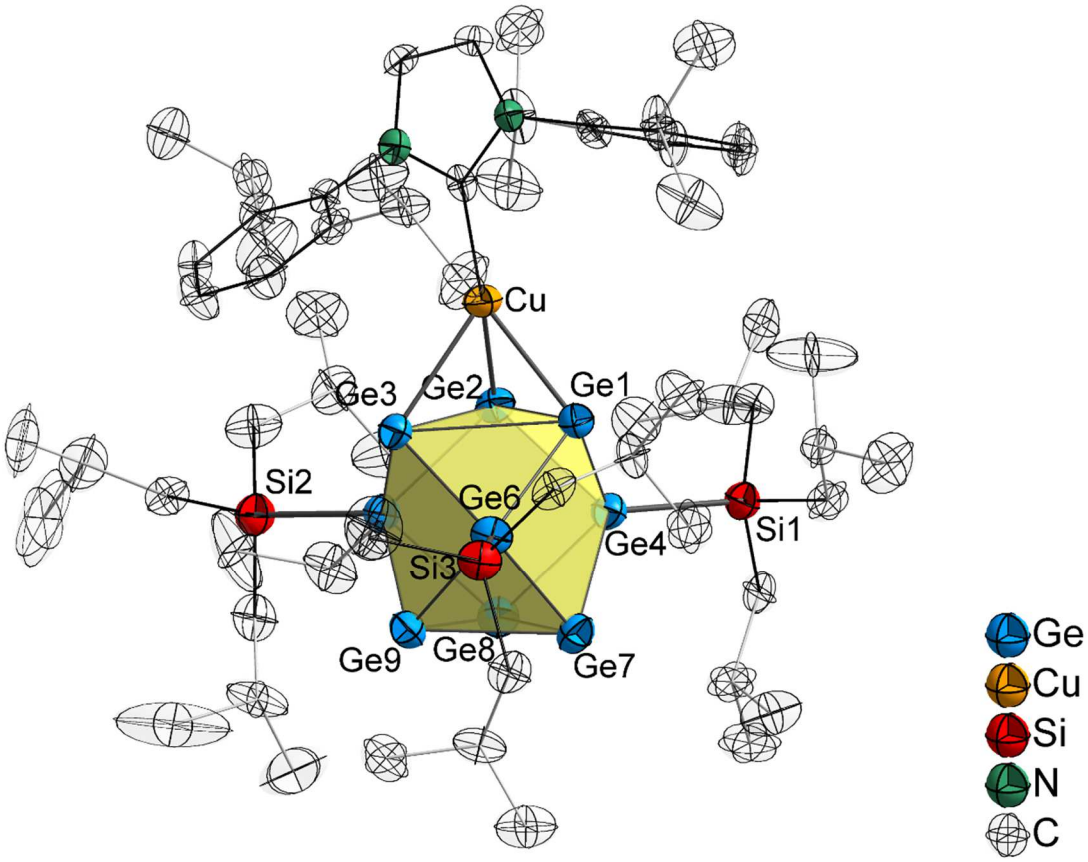

Figure SI 26. Molecular structure **2**. Atoms are shown as ellipsoids with 70 %, H atoms are omitted.

Table SI 1. Selected bond lengths (Å) in **2**.

atom 1	atom 2	distance	atom 1	atom 2	distance
Ge4	Si1	2.3849(11)	Ge1	Ge4	2.5118(5)
Ge5	Si2	2.3826(12)	Ge1	Ge6	2.5023(5)
Ge6	Si3	2.3854(10)	Ge2	Ge4	2.5080(6)
Ge1	Cu1	2.4911(6)	Ge2	Ge5	2.5016(6)
Ge2	Cu1	2.4933(6)	Ge3	Ge5	2.5112(5)
Ge3	Cu1	2.5594(6)	Ge3	Ge6	2.5163(6)
Cu1	C1	1.943(3)	Ge4	Ge7	2.5577(5)
Ge1	Ge2	2.7771(5)	Ge4	Ge8	2.5554(6)
Ge1	Ge3	2.8914(6)	Ge5	Ge8	2.5533(6)
Ge2	Ge3	2.9143(5)	Ge5	Ge9	2.5520(5)
Ge7	Ge8	2.6304(6)	Ge6	Ge7	2.5493(5)
Ge7	Ge9	2.6748(6)	Ge6	Ge9	2.5482(5)
Ge8	Ge9	2.6771(5)			

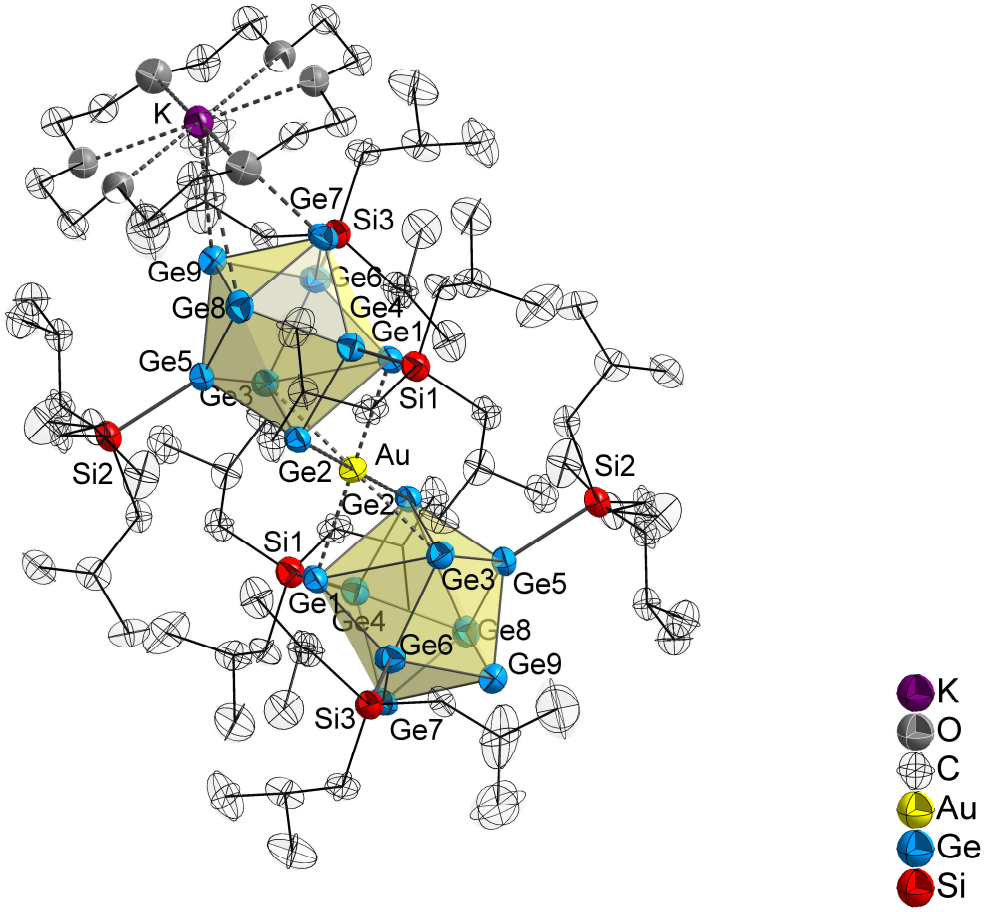

Figure SI 27. Molecular structure **3**. Atoms are shown as ellipsoids with 70 %, H atoms are omitted.

Table SI 2. Selected bond lengths (Å) in **3**.

atom 1	atom 2	distance	atom 1	atom 2	distance
Ge4	Si1	2.391(3)	Ge1	Ge4	2.5110(14)
Ge5	Si2	2.381(2)	Ge1	Ge6	2.5036(12)
Ge6	Si3	2.377(3)	Ge2	Ge4	2.4986(12)
Ge1	Au	2.6651(9)	Ge2	Ge5	2.4981(13)
Ge2	Au	2.6592(9)	Ge3	Ge5	2.4965(12)
Ge3	Au	2.6485(10)	Ge3	Ge6	2.4991(13)
Ge1	Ge2	2.9572(12)	Ge4	Ge7	2.5781(14)
Ge1	Ge3	2.9842(13)	Ge4	Ge8	2.5742(13)
Ge2	Ge3	2.9214(13)	Ge5	Ge8	2.5589(13)
Ge7	Ge8	2.6407(13)	Ge5	Ge9	2.5657(13)
Ge7	Ge9	2.6711(13)	Ge6	Ge7	2.5563(13)
Ge8	Ge9	2.6459(14)	Ge6	Ge9	2.5592(13)

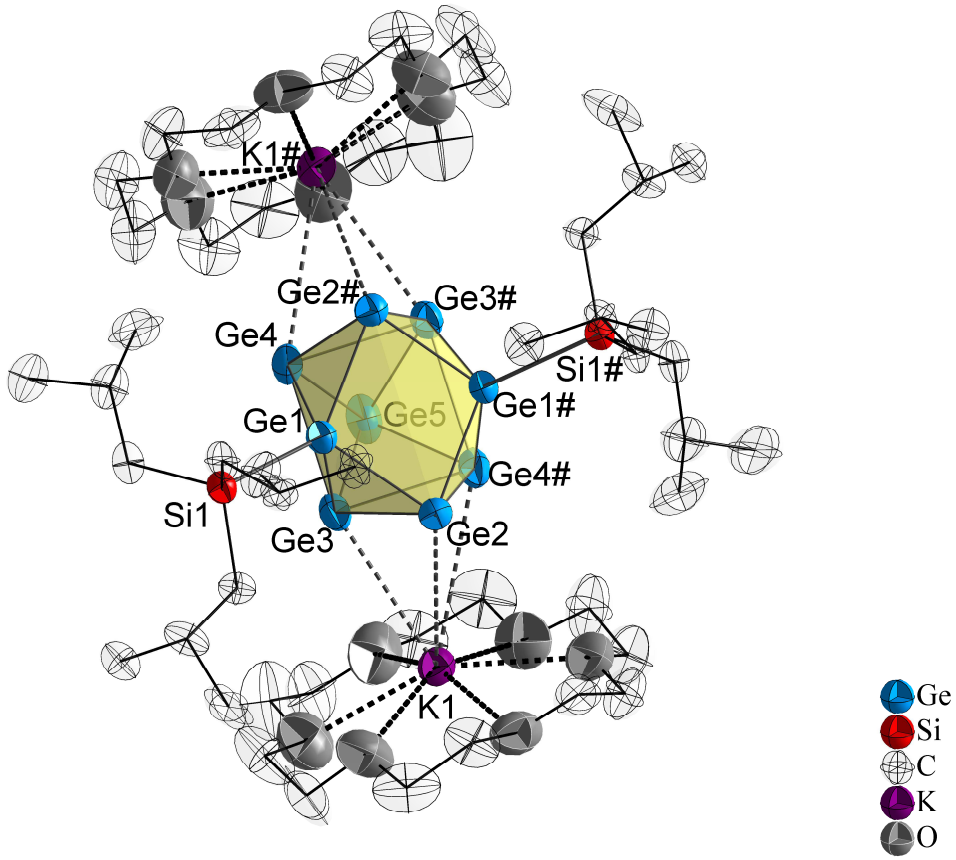

Figure SI 28. Molecular structure **4**. Atoms are shown as ellipsoids with 70 % probability, H atoms are omitted. Symmetry operation: (#) −x+1, y, −z+1.5).

Table SI 3. Selected bond lengths (Å) in **4**.

atom 1	atom 2	distance
Ge1	Si1	2.3807(12)
Ge2	K1	3.8253(11)
Ge3	K1	3.4750(11)
Ge4	K1	3.7259(11)
Ge1	Ge2	2.5228(6)
Ge1#	Ge2#	2.5403(6)
Ge1	Ge3	2.5762(6)
Ge1	Ge4	2.5748(6)
Ge2	Ge3	2.6511(6)
Ge2	Ge4	2.6656(6)
Ge3	Ge4#	2.7396(6)
Ge3	Ge4	2.8659(7)
Ge3	Ge5	2.5745(6)
Ge4	Ge5	2.5847(6)

5.5 *N*-Heterocyclic Carbene Coinage Metal Complexes of the Germanium-Rich Metalloid Clusters $[Ge_9R_3]^-$ and $[Ge_9R^I_2]^{2-}$ with $R = Si(^iPr)_3$ and $R^I = Si(TMS)_3$

F. S. Geitner,[‡] M. A. Giebel,[‡] A. Pöthig, T. F. Fässler*

[‡] authors contributed equally to this work.

published in

Molecules **2017**, *22*, 1204.

Content and Contributions

The scope of this work was the examination of the silylation reaction of the *Zintl* phase $K_{12}Ge_{17}$ containing nine-atomic [Ge_9] clusters and four atomic [Ge_4] tetrahedrons, as well as the evaluation of the reactivity of variously silylated [Ge_9] cluster compounds towards coinage metal NHC complexes NHC^{Dipp}*M*Cl (*M*: Cu, Ag, Au). Reactions of $K_{12}Ge_{17}$ with $(TMS)_3SiCl$ were carried out heterogeneously by treating the solid *Zintl* phase with acetonitrile solutions of the chlorosilane (in analogy to similar reactions with K_4Ge_9), which resulted in the formation of deep red reaction mixtures. The synthesis of $K_{12}Ge_{17}$, as well as the reactions with $(TMS)_3SiCl$ were carried out by M. Sc. Michael Giebel. Subsequently, acetonitrile solutions of the coinage metal NHC complexes NHC^{Dipp}*M*Cl (*M*: Cu, Ag, Au) were added, which resulted in the formation of [$(NHC^{Dipp}M)_2(\eta^3,\eta^3\text{-}Ge_9\{Si(TMS)_3\}_2)$] (*M*: Cu, Ag, Au), representing a new class of neutral dinuclear [Ge_9] cluster coinage metal NHC compounds. The same species can also directly be obtained by reaction of the bis-silylated [Ge_9] cluster $[Ge_9\{Si(TMS)_3\}_2]^{2-}$ with the respective coinage metal NHC complexes in acetonitrile. All of these novel compounds were characterized by means of NMR and ESI-MS and for $[(NHC^{Dipp}Cu)_2(\eta^3,\eta^3\text{-}Ge_9\{Si(TMS)_3\}_2)]$ single crystals were obtained from toluene solution at -40 °C, revealing the attachment of the $[Cu\text{-}NHC^{Dipp}]^+$ moieties at the two opposite triangular bases of the distorted tricapped trigonal prismatic [Ge_9] cluster core (C_{2v} symmetry). Isolation of the single crystals and evaluation of the single crystal X-ray data was done by Dr. Alexander Pöthig. Moreover, within this work reactions of the tris-silylated [Ge_9] cluster $[Ge_9\{Si(^iPr)_3\}_3]^-$ with $NHC^{Dipp}CuCl$ were carried out, resulting in the neutral compound $[NHC^{Dipp}Cu(\eta^3\text{-}Ge_9\{Si(^iPr)_3\}_3)]$. Single crystals of $[NHC^{Dipp}Cu(\eta^3\text{-}Ge_9\{Si(^iPr)_3\}_3)]$ were obtained from toluene solution at low temperature and single crystal X-ray diffraction revealed the similar structure of the novel compound to its analogues bearing larger silyl groups $[Si(^iBu)_3]^+$ or $[Si(TMS)_3]^+$ at the [Ge_9] core. However, the decreased steric impact of the silyl groups attached to [Ge_9] leads to a slightly different orientation of the NHC^{Dipp} moiety towards the silyl groups of the [Ge_9] cluster. The publication was written in the course of this thesis.

molecules

MDPI

Article

N-Heterocyclic Carbene Coinage Metal Complexes of the Germanium-Rich Metalloid Clusters $[Ge_9R_3]^-$ and $[Ge_9R^I_2]^{2-}$ with R = Si(^{i}Pr)$_3$ and R^I = Si(TMS)$_3$

Felix S. Geitner [1,†], Michael A. Giebel [2,†], Alexander Pöthig [3] and Thomas F. Fässler [2,*]

1 Wacker Institute for Silicon Chemistry and Department of Chemistry, Technische Universität München, Lichtenbergstraße 4, 85747 Garching, Germany; felix.geitner@mytum.de
2 Department of Chemistry, Technische Universität München, Lichtenbergstraße 4, 85747 Garching, Germany; michael.giebel@tum.de
3 TUM Catalysis Research Center (CRC), Ernst-Otto-Fischer Straße 1, 85747 Garching, Germany; alexander.poethig@tum.de
* Correspondence: thomas.faessler@lrz.tu-muenchen.de; Tel.: +49-289-13186
† These authors contributed equally to this work.

Received: 18 June 2017; Accepted: 15 July 2017; Published: 19 July 2017

Abstract: We report on the synthesis of novel coinage metal NHC (*N*-heterocyclic carbene) compounds of the germanium-rich metalloid clusters $[Ge_9R_3]^-$ and $[Ge_9R^I_2]^{2-}$ with R = Si(^{i}Pr)$_3$ and R^I = Si(TMS)$_3$. NHC^{Dipp}Cu{η^3-Ge_9R_3} with R = Si(^{i}Pr)$_3$ (**1**) represents a less bulky silyl group-substituted derivative of the known analogous compounds with R = Si(^{i}Bu)$_3$ or Si(TMS)$_3$. The coordination of the [NHC^{Dipp}Cu]$^+$ moiety to the cluster unit occurs via one triangular face of the tri-capped trigonal prismatic [Ge_9] cluster. Furthermore, a series of novel *Zintl* cluster coinage metal NHC compounds of the type (NHC*M*)$_2${η^3-$Ge_9R^I_2$} (R^I = Si(TMS)$_3$ *M* = Cu, Ag and Au; NHC = NHC^{Dipp} or NHC^{Mes}) is presented. These novel compounds represent a new class of neutral dinuclear *Zintl* cluster coinage metal NHC compounds, which are obtained either by the stepwise reaction of a suspension of $K_{12}Ge_{17}$ with Si(TMS)$_3$Cl and the coinage metal carbene complexes NHC*M*Cl (*M* = Cu, Ag, Au), or via a homogenous reaction using the preformed bis-silylated cluster $K_2[Ge_9(Si(TMS)_3)_2]$ and the corresponding NHC*M*Cl (*M* = Cu, Ag, Au) complex. The molecular structures of NHC^{Dipp}Cu{η^3-Ge_9(Si(^{i}Pr)$_3$)$_3$} (**1**) and (NHC^{Dipp}Cu)$_2${η^3-Ge_9(Si(TMS)$_3$)$_2$} (**2**) were determined by single crystal X-ray diffraction methods. In **2**, the coordination of the [NHC^{Dipp}Cu]$^+$ moieties to the cluster unit takes place via both open triangular faces of the [Ge_9] entity. Furthermore, all compounds were characterized by means of NMR spectroscopy (^{1}H, ^{13}C, ^{29}Si) and ESI-MS.

Keywords: coinage metal; NHC compounds; *Zintl* clusters; binuclear compounds

1. Introduction

Polyatomic *Zintl* clusters $[E_9]^{4-}$ or $[E_4]^{4-}$ (E: tetrel element) can be extracted from the neat solids of their alkali metal salts with the compositions A_4E_9 and $A_{12}E_{17}$ (A = alkali metal, E = Si-Pb) and are then accessible for further reactions. The first synthesis of an organometallic *Zintl* cluster species, $[Sn_9Cr(CO)_3]^{4-}$, was achieved in 1988 by treatment of the *Zintl* phase K_4Sn_9 with Cr(CO)$_3$Mes (Mes = mesitylene) [1]. Since then, a large number of transition metal compounds containing *Zintl* cluster ligands have been reported. In various studies, precursors, especially of the late transition metals (groups 10, 11 and 12), have successfully been treated with these anionic *Zintl* clusters [2,3]. However, the addition of early transition metal fragments to *Zintl* clusters has been recently achieved [4].

Reactions of *Zintl* clusters with coinage metal precursor complexes and Zn organyls revealed that the addition of a metal atom to the bare clusters can also initiate cluster growth under

formation of larger intermetalloid clusters. For example the reaction of the *Zintl* phase K_4Ge_9 with R_3PCuCl (R = alkyl, aryl) at first leads to $[(R_3P)Cu(\eta^4\text{-}Ge_9)]^{3-}$, but the subsequent substitution of the PR_3 group by a second $[Ge_9]$ cluster unit results in the coinage metal-bridged dimeric species $[(\eta^4\text{-}Ge_9)Cu(\eta^1\text{-}Ge_9)]^{7-}$ [5]. Furthermore, reactions of tetrel clusters with Ph_2Zn yield compounds of the shape $[E_9ZnPh]^{3-}$ (E: Si-Pb) [6], and similar reactions with Cp_2Zn afford heteroatomic *closo*-clusters $[Ge_9Zn]^{2-}$, which, due to their electron donor and acceptor capabilities, allow for inter-cluster growth to form $^1_\infty[\{Zn[(\eta^4\text{:}\eta^1\text{-}Ge_9)]\}^{2-}]$ polymers [7]. In the case of the clusters of the heavier homologues Sn and Pb, the migration of Cu^+ into the polyhedral clusters under the loss of the original ligand sphere and formation of the endohedrally filled $[Cu@E_9]^{3-}$ (E = Sn, Pb) clusters was observed for CuMes [8]. By contrast, the reaction of CuMes with the smaller tetrahedral *Zintl* clusters $[E_4]^{4-}$ leads to the mesitylcopper complexes $[(MesCu)_2(\eta^3\text{-}E_4)]^{4-}$ (E = Si, Ge) [9,10]. Additionally, larger intermetalloids $[Au_3Ge_{18}]^{5-}$ and $[Au_3Ge_{45}]^{4-}$ were obtained in the reaction of bare $[Ge_9]^{4-}$ clusters with $(PPh_3)AuCl$ [11,12]. In recent studies, we introduced *N*-heterocyclic carbene ligands (NHCs) into the *Zintl* cluster chemistry by treating coinage metal carbene compounds $NHC^{Dipp}MCl$ (*M* = Cu, Ag, Au) with bare or silylated *Zintl* clusters. The reaction of $NHC^{Dipp}MCl$ (*M* = Cu, Ag, Au) with $[Sn_9]^{4-}$ in NH_3 (l) yielded a series of anionic *Zintl* cluster coinage metal NHC compounds $[NHC^{Dipp}M(\eta^4\text{-}Sn_9)]^{3-}$ (*M* = Cu, Ag, Au). For $[NHC^{Dipp}Ag(\eta^4\text{-}Sn_9)]^{3-}$ a subsequent reaction takes already place at −70 °C, giving $[(\eta^4\text{-}Sn_9)Ag(\eta^1\text{-}Sn_9)]^{7-}$ via a nucleophilic attack of a second $[Sn_9]^{4-}$ cluster unit at the Ag^+ center, under cleavage of the Ag-NHC bond [13]. Thus, the obtained species can be regarded as low-temperature intermediates on the way to larger intermetalloid compounds. These products show that bare tetrel *Zintl* clusters can act as ligands in organometallic complexes, and that subsequent reactions of such species can lead to larger intermetalloids. However, in some cases, unforeseen oxidation reactions of the bare *Zintl* clusters can also occur, and it should be mentioned that, due to their highly negative charges, homogenous reactions of bare *Zintl* clusters usually require highly polar solvents (ethylendiamine, dmf, NH_3(l)).

Much less reactive germanide *Zintl* clusters can be obtained by silyl substitution of the $[Ge_9]^{4-}$ clusters. The resulting bis- and tris-silylated cluster species $[Ge_9R_2]^{2-}$ (R = $Si(TMS)_3$) [14] and $[Ge_9R_3]^{-}$ (R: various silyl groups) [15–20] are, due to their lower charge, soluble in common solvents (acetonitrile, thf, toluene). Subsequent reactions of the tris-silylated cluster $[Ge_9R_3]^{-}$ (R: $Si(TMS)_3$) with coinage metal complexes, in most cases coinage metal phosphine complexes, commonly yield coinage metal-bridged cluster dimers, under the loss of the original ligand sphere of the transition metal [19,21,22]. However, there are also a few reports in which the Cu-phosphine bond is retained [18,23]. The reaction of coinage metal NHC complexes such as $NHC^{Dipp}MCl$ (*M* = Cu, Ag, Au) with tris-silylated clusters $[Ge_9R_3]^{-}$ (R = $Si(TMS)_3$, $Si(^iBu)_3$) leads to $NHC^{Dipp}M\{\eta^3\text{-}Ge_9(Si(TMS)_3)_3\}$ (*M* = Cu, Ag, Au) [24] or $NHC^{Dipp}Cu\{\eta^3\text{-}Ge_9(Si(^iBu)_3)_3\}$ [19]. These uncharged complexes readily dissolve in rather non-polar solvents such as thf or toluene. Furthermore, these species are stable at room temperature, except for $NHC^{Dipp}Ag\{\eta^3\text{-}Ge_9(Si(TMS)_3)_3\}$, for which a transformation reaction in thf solution under formation of $[Ag\{\eta^3\text{-}Ge_9(Si(TMS)_3)_3\}_2][Ag(NHC^{Dipp})_2]$ is observed within seven days [24].

In continuation of our work, we examined the reactivity of coinage metal carbene compounds towards silylated *Zintl* clusters and studied the impact of a tris-silylated cluster ligand, bearing the sterically less bulky silyl group $[Si(^iPr)_3]^+$ on the structure of the resulting Cu-NHC complex. Furthermore, we investigated the reactivity of coinage metal carbene compounds towards solutions obtained from the silylation of the *Zintl* phase $K_{12}Ge_{17}$ instead of the previously used phase K_4Ge_9. Finally, we studied the reactivity of NHC*M*Cl (*M* = Cu, Ag, Au) complexes towards the bis-silylated cluster compound $[Ge_9\{Si(TMS)_3\}_2]^{2-}$.

2. Results and Discussion

In analogy to the synthesis of $NHC^{Dipp}Cu\{\eta^3\text{-}Ge_9R_3\}$, comprising the bulky silyl groups $[Si(^iBu)_3]^+$ or $[Si(TMS)_3]^+$, we prepared the novel *Zintl* cluster coinage metal NHC complex with the less bulky

silyl group $[Si(^{i}Pr)_3]^+$ (**1**) by reacting the respective silylated cluster species $[Ge_9\{Si(^{i}Pr)_3\}_3]^-$ with $NHC^{Dipp}CuCl$ in acetonitrile (Scheme 1). ^{1}H-NMR studies reveal a signal ratio of 3:1 for the signals assigned to the ^{i}Pr substituents (silyl groups) and the NHC^{Dipp} ligand. Remarkably, the proton signals of the isopropyl groups (CH_3 and CH) have identical chemical shift values (*pseudo*-singlet), independent of the applied solvent (C_6D_6, thf-d_8), as also confirmed by 2D-NMR investigations (HSQC), in which the protons can be assigned to the carbon atom they are bound to (in the ^{13}C-NMR spectrum the signals of the CH_3 and the CH groups of the isopropyl units are split; Supporting Information; Figure SI 2 and Figure SI 3).

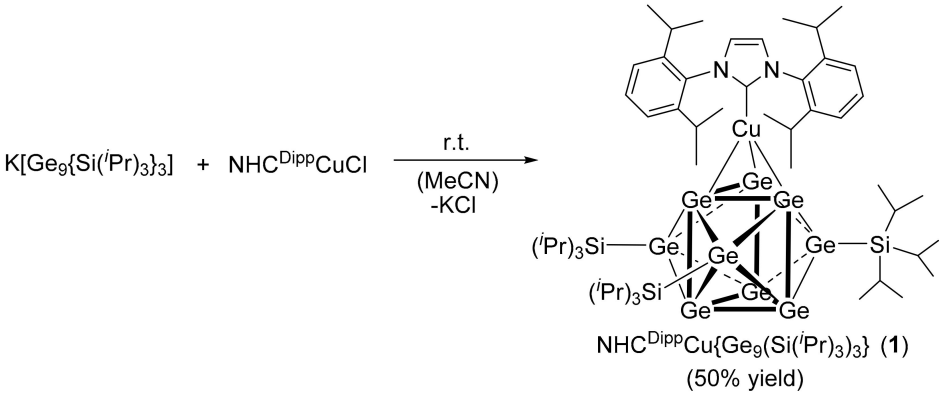

Scheme 1. Synthesis of compound **1** from $K[Ge_9\{Si(^{i}Pr)_3\}_3]$ and $NHC^{Dipp}CuCl$.

In the ESI-MS experiment carried out with athf solution of **1**, a signal is detected at m/z 2029.3 $[(NHC^{Dipp}Cu)_2\{\eta^3\text{-}Ge_9(Si(^{i}Pr)_3)_3\}]^+$ in the positive ion mode, matching the mass obtained by the addition of a second $[Cu\text{-}NHC^{Dipp}]^+$ fragment to **1** (Figure 1).

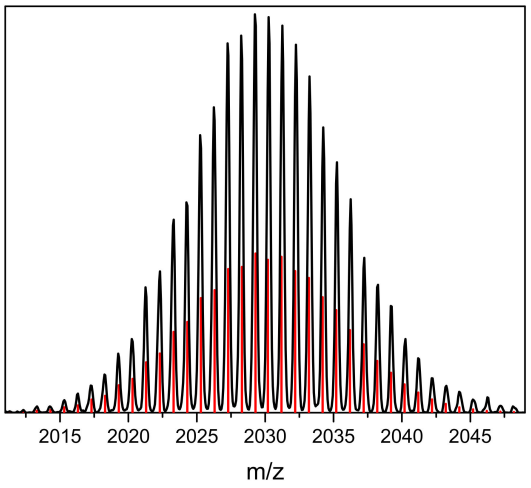

Figure 1. Selected area of the ESI-MS spectrum obtained by examination of a thf solution of compound **1**. The mass spectrum was acquired in positive ion mode (4500 V, 300 °C), monitoring **1** with an additionally attached $[Cu\text{-}NHC]^+$ moiety at m/z 2029.3 $[(NHC^{Dipp}Cu)_2\{\eta^3\text{-}Ge_9(Si(^{i}Pr)_3)_3\}]^+$. The calculated pattern with the characteristic isotope distribution is shown below as red bars.

Recrystallization of **1** from toluene at −40 °C resulted in red crystals, suitable for single crystal X-ray diffraction. The purity of the sample was confirmed by elemental analysis of the red solid obtained by grinding the crystals. In **1**, the $[NHC^{Dipp}Cu]^+$ moiety is coordinated to the tri-capped trigonal prismatic $[Ge_9\{Si(^{i}Pr)_3\}_3]^-$ cluster via one of the triangular faces in a η^3-fashion with a mean Cu-Ge distance of 2.5328(9) Å (Figure 2; bond lengths are summarized in Table 1).

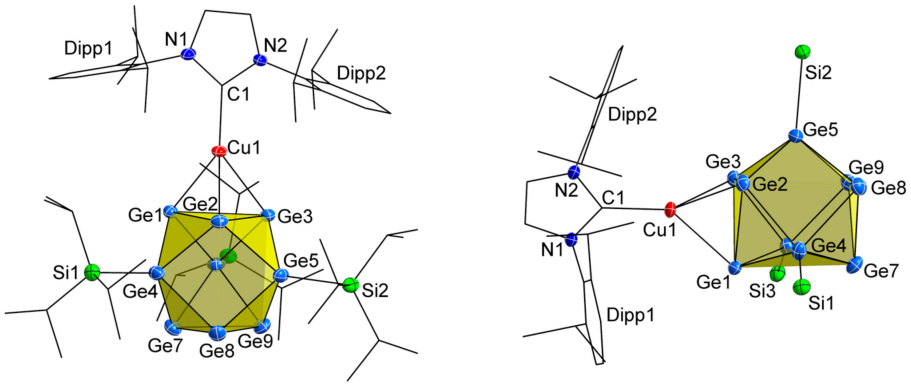

Figure 2. Two perspective views of the molecular structure of compound **1**. Displacement ellipsoids are shown at a 50% probability level. For clarity, hydrogen atoms and co-crystallized toluene molecules are omitted. To the right: Side view of **1**, revealing a nearly linear coordination of Cu^+ by NHC^{Dipp} and the center of one triangular plane of $[Ge_9\{Si(^iPr)_3\}_3]^-$. Isopropyl groups of the silyl substituents of the cluster are omitted. Selected bond lengths and angles are summarized in Table 1 and the Supporting Information (Table SI 1).

The Cu^+ center is linearly coordinated by the NHC and *Zintl* cluster ligands (177.7°; Table 1), and the Cu-C1 (C1: carbene carbon) bond length of 1.951(3) Å is in the range of previously reported data [24]. However, the orientation of the NHC^{Dipp} ligand at Cu^+ with respect to the silyl substituents of the *Zintl* cluster in **1** differs from that in $NHC^{Dipp}Cu\{\eta^3\text{-}Ge_9R_3\}$ with the bulkier ligands $[Si(^iBu)_3]^+$ or $[Si(TMS)_3]^+$ (Figure 3b,c). In **1**, the NHC^{Dipp} ligand shows a more ecliptic arrangement towards two of the $[Si(^iPr)_3]^+$ groups attached to the $[Ge_9]$ unit (Figure 3a), whereas in the analogous compounds with the larger silyl groups one di-isopropyl (Dipp) wingtip of the NHC ligand shows a staggered arrangement towards two of silyl groups, and consequently the other wingtip is situated directly above the third silyl substituent (Figure 3b,c). As a result, the coordination of Cu^+ by NHC^{Dipp} ligand and silylated cluster deviates less from linearity in **1,** than in $NHC^{Dipp}Cu\{\eta^3\text{-}Ge_9R_3\}$ with R = $Si(^iBu)_3$ or $Si(TMS)_3$.

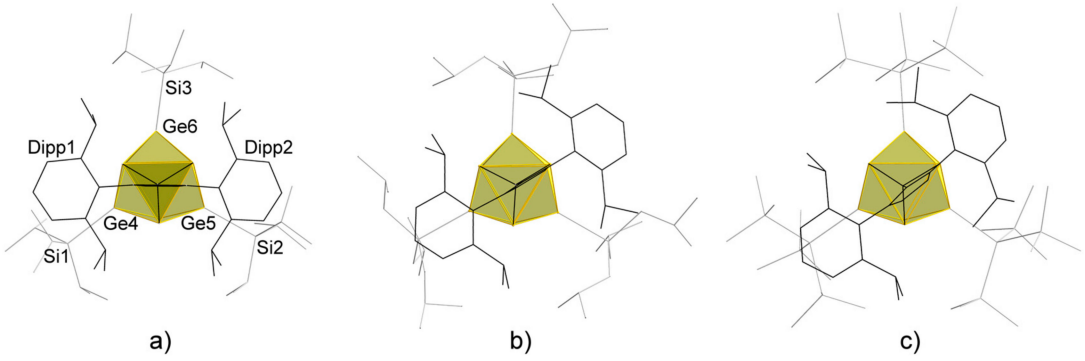

Figure 3. Top views of $NHC^{Dipp}Cu\{\eta^3\text{-}Ge_9R_3\}$. The silyl groups connected to the cluster are shown as grey wire frames. (**a**) R = $Si(^iPr)_3$, **1**; (**b**) R = $Si(^iBu)_3$ [19] and (**c**) R = $Si(TMS)_3$ [24].

In order to explore other sources for germanium clusters, we investigated the synthesis of silylated clusters by using the *Zintl* phase $K_{12}Ge_{17}$ as cluster source. This phase contains $[Ge_9]^{4-}$ clusters as well as tetrahedral $[Ge_4]^{4-}$ units. Therefore, analogous reactions might lead to the extraction of other silylated cluster species. In a previous study, we were able to isolate $[Si_4]^{4-}$ clusters as MesCu complexes from a starting material of the composition $K_{12}Si_{17}$, carrying out reactions in NH_3 (l) [9]. In the current study, we found that the heterogenous reaction of $K_{12}Ge_{17}$ with 6 eq. of $Si(TMS)_3Cl$

in acetonitrile also leads to a deep red suspension upon stirring over night at room temperature, in analogy to the silylation reaction of K_4Ge_9 [16].

Table 1. Selected distances and angles in compound **1** and its analogues $NHC^{Dipp}Cu\{\eta^3\text{-}Ge_9R_3\}$ ($R = Si(^iBu)_3$, $Si(TMS)_3$).

Distances [Å]	1	R = Si(^{i}Bu)$_3$ [19]	R = Si(TMS)$_3$ [24]
d_1(Cu-Ge1)	2.4914(8)	2.4911(6)	2.4943(9)
d_2(Cu-Ge2)	2.541(1)	2.4933(6)	2.5188(9)
d_3(Cu-Ge3)	2.5661(8)	2.5594(6)	2.5660(9)
d_{mean}(Cu-Ge) [a]	2.5328(9)	2.5146(6)	2.5263(9)
d(Cu-C1) [b]	1.951(3)	1.943(3)	1.957(5)
angles [deg.]			
ctp-Cu-C1 [c]	177.67(4)	172.77(2)	173.59(1)

[a] The average Cu-Ge distances are given as d_{mean}(Cu-Ge). [b] Distances between Cu^+ and carbene carbon atoms are given as d(Cu-C1). [c] ctp: center of gravity of the coordinating atoms of the triangular face of the [Ge_9] cluster.

After filtration, the addition of a solution of $NHC^{Dipp}CuCl$ in acetonitrile to this deep red filtrate immediately led to the formation of a brownish precipitate, which was isolated by filtering off the supernatant solution. The solid was then dissolved in toluene, and the mixture was filtered to remove KCl formed during the reaction. Subsequently, the solvent was removed in vacuo yielding the crude product as a brown solid. ^{1}H-NMR measurements indicated the attachment of $[NHC^{Dipp}Cu]^+$ to [Ge_9] by a significant divergence of the doublets assigned to the methyl groups of the diisopropylphenyl wingtips of the NHC ligand, which had previously been observed upon similar reactions [19,24]. Furthermore, the 1:1 signal ratio of the signals assigned to the protons of the hypersilyl groups and those of the NHC^{Dipp} ligand, as well as the poor solubility of the product in acetonitrile and its good solubility in non-polar solvents such as thf and toluene suggested the presence of an uncharged species according to a composition of $(NHC^{Dipp}Cu)_2\{\eta^3\text{-}Ge_9(Si(TMS)_3)_2\}$ (**2**).

In ESI-MS examination of an acetonitrile solution of the product, signals were detected at m/z 1600.8 in the negative ion mode and at m/z 2092.8 in the positive ion mode, corresponding to $[NHC^{Dipp}Cu\{Ge_9(Si(TMS)_3)_2\}]^-$ or $[(NHC^{Dipp}Cu)_2\{Ge_9(Si(TMS)_3)_2\}K]^+$, respectively (Figure 4). In combination with the characteristic isotope distribution, these observations were a strong indication for the existence of **2**.

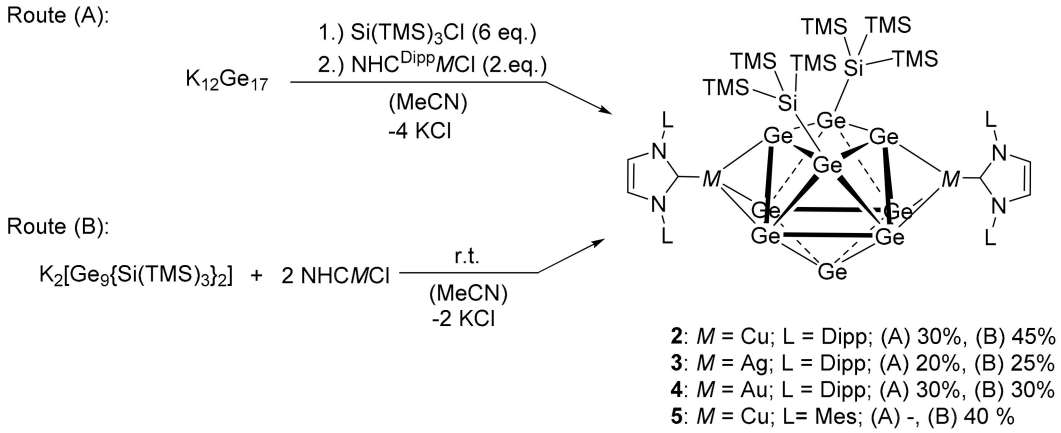

Scheme 2. Syntheses of binuclear *Zintl* cluster coinage metal NHC compounds **2**–**5** via different routes (A or B). Wingtip substituents (L) of the NHC ligands are abbreviated as Dipp = diisopropylphenyl or Mes = mesityl. The product yields obtained by the different synthesis methods are given as (A) (product yield of route A) or (B) (product yield of route B).

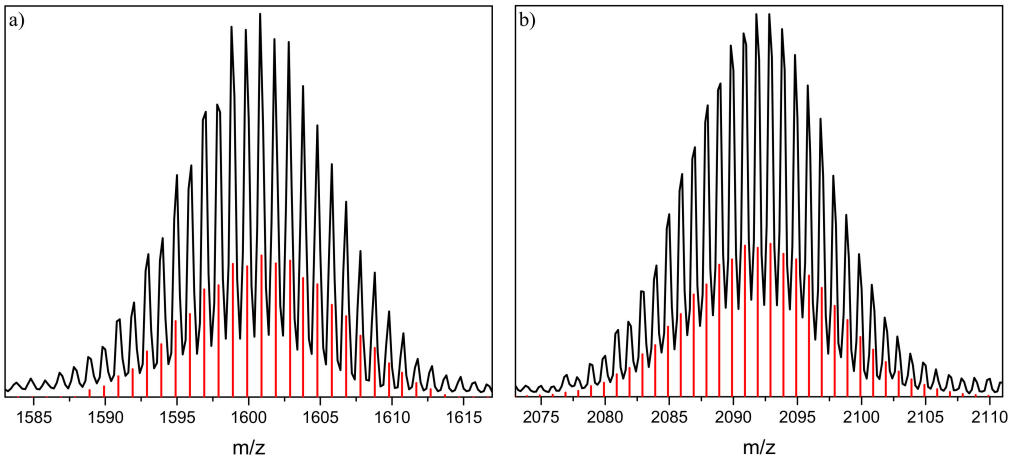

Figure 4. Selected areas of the ESI-MS spectrum obtained by examination of an acetonitrile solution of compound **2**. (**a**) Negative ion mode (4500 V, 300 °C), monitoring **2** with a cleaved $[Cu\text{-}NHC]^+$ moiety at m/z 1600.8 $[NHC^{Dipp}Cu\{Ge_9(Si(TMS)_3)_2\}]^-$ and (**b**) positive ion mode (6000 V, 300 °C), monitoring **2** with an attached potassium cation at m/z 2092.8 $[(NHC^{Dipp}Cu)_2\{Ge_9(Si(TMS)_3)_2\}K]^+$. The simulated mass spectra with the corresponding isotope distribution are shown below as red bars.

Single crystals of **2** suitable for an X-ray diffraction structure determination were obtained by recrystallization from toluene at −40 °C. The analysis of the obtained diffraction data confirmed the assumptions derived from the NMR and ESI-MS experiments, and revealed the first dinuclear *Zintl* cluster coinage metal NHC complex $(NHC^{Dipp}Cu)_2\{\eta^3\text{-}Ge_9R^I_2\}$ (R^I = Si(TMS)$_3$) (**2**). The central [Ge$_9$] unit adopts the shape of a distorted, C_{2v}-symmetric, monocapped square antiprism, in which two opposite Ge atoms (Ge6 and Ge8) of the open square (Ge6-Ge7-Ge8-Ge9) carry the silyl groups. The deviation from C_{4v}-symmetry is expressed by the ratio of the diagonal lengths of the open square d(Ge7-Ge9)/d(Ge6-Ge8) = 1.11 (with $d2/d1 = 1$ for a perfect C_{4v}-symmetry), and the deviation from D_{3h}-symmetry of a tri-capped trigonal prism is revealed by the significantly different three prism heights h(Ge2-Ge3) = 2.9003(3) Å, h(Ge4-Ge5) = 2.9054(3) Å and h(Ge7-Ge9) = 3.6969(4) Å, which are supposed to be of equal length for perfect D_{3h}-symmetry.

The two $[NHC^{Dipp}Cu]^+$ moieties coordinate in a η^3-fashion to the two opposed trigonal faces of the [Ge$_9$] unit adjacent to the uncapped rectangle (Ge6-Ge7-Ge8-Ge9) and include the germanium atoms (Ge7 or Ge9), which do not bind to a silyl group (Figure 5). Hence, the interaction between the bis-silylated [Ge$_9$] cluster and the two $[NHC^{Dipp}Cu]^+$ moieties (**A** and **B**; Figure 5a) in **2** mirrors the coordination mode, which has previously been observed in *Zintl* cluster coinage metal NHC compounds of tris-silylated [Ge$_9$] cluster species. The mean Cu-Ge distances d_{mean}(Cu-Ge) in **2** (2.513(1) Å for **A** and 2.509(1) Å for **B**; Figure 5a), as well as the Cu-$C_{Carbene}$ distances (1.941(5) Å for **A** and 1.913(5) Å for **B**), are in good agreement with those observed in **1** and in $[NHC^{Dipp}Cu\{\eta^3\text{-}Ge_9R_3\}]$ (R = Si(^{i}Bu)$_3$, Si(TMS)$_3$) [19,24]. However, the coordination of Cu1 and Cu2 by NHC and *Zintl* cluster deviates more from linearity (162.88(2)° for **A** and 163.92(2)° for **B**; Table 2) than that in **1** (Table 1). Furthermore, the two NHC^{Dipp} moieties show a staggered orientation towards themselves and the silyl groups (Figure 5b). Both of these observations can be explained by interactions between the TMS groups of the hypersilyl ligands with the Dipp wingtips of the NHC ligands.

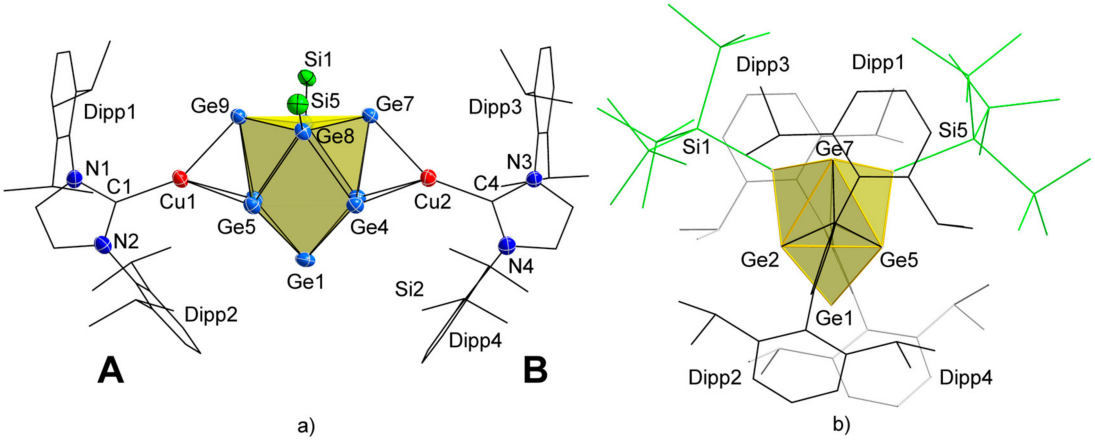

Figure 5. Two perspectives of the molecular structure of compound **2**. (**a**) Front view of **2** revealing the C_{2v}-symmetry of the cluster. Displacement ellipsoids are shown at a 50 % probability level. For clarity, hydrogen atoms, co-crystallized toluene molecules, and the TMS groups are omitted. The two $[NHC^{Dipp}Cu]^+$ moieties are labelled as **A** and **B**; (**b**) View along the Cu1–Cu2 vector showing the orientation of the two NHC^{Dipp} moieties and the silyl substituents of the $[Ge_9]$ cluster. All ligands are pictured as wire frames. For clarity, the NHC^{Dipp} ligand in the background is pictured in grey and the silyl groups are shown in green. Selected bond lengths and angles are summarized in Table 2 and in the Supporting Information (Table SI 2).

An investigation of the deep red solution, obtained by silylation of $K_{12}Ge_{17}$ ($K_{12}[Ge_9][Ge_4]_2$) with 6 eq. $Si(TMS)_3Cl$ prior to the addition of $NHC^{Dipp}CuCl$ by means of ^1H and ^{29}Si NMR spectroscopy revealed, that the bis-silylated cluster $[Ge_9\{Si(TMS)_3\}_2]^{2-}$ is formed as the main product, despite the excess of $Si(TMS)_3Cl$ used (assuming that only nine-atomic germanide clusters would react with $Si(TMS)_3Cl$). For K_4Ge_9, this reaction would exclusively yield the tris-silylated cluster $[Ge_9\{Si(TMS)_3\}_3]^-$. Thus, we assume that the $[Ge_4]^{4-}$ clusters also partially react with $Si(TMS)_3Cl$, which leads to side products, as is obvious from ^1H and ^{29}Si-INEPT NMR experiments (Supporting Information; Figure SI 19 and Figure SI 20).

Table 2. Selected distances and angles in compound **2**.

Distances [Å]	2	
	A	B
d_1(Cu-Ge)	2.601(1)	2.532(1)
d_2(Cu-Ge)	2.532(1)	2.582(1)
d_3(Cu-Ge)	2.405(1)	2.413(1)
d_{mean}(Cu-Ge) [a]	2.513(1)	2.509(1)
d(Cu-$C_{carbene}$)	1.941(5)	1.913(5)
angles [deg.]		
ctp-Cu-$C_{carbene}$ [b]	162.88(2)	163.92(2)

The copper-germanium distances d(Cu-Ge) are defined as follows: **A**: d_1(Cu1-Ge2), $d2$(Cu1-Ge5), $d3$(Cu1-Ge9); **B:** $d1$(Cu2-Ge3), $d2$(Cu2-Ge4), $d3$(Cu2-Ge7). Labelling is given in in Figure 2. [a] The average Cu-Ge distances are given as d_{mean}(Cu-Ge). [b] ctp: center of gravity of the coordinating atoms of the triangular faces of the $[Ge_9]$ cluster.

Compound **2** can also be prepared, using the bis-silylated cluster $[Ge_9\{Si(TMS)_3\}_2]^{2-}$ [14] as a starting material. The addition of an acetonitrile solution of $NHC^{Dipp}CuCl$ (2 eq.) to a solution of $[Ge_9\{Si(TMS)_3\}_2]^{2-}$ in acetonitrile gives analytically pure **2** in good yield (45%, Scheme 2). Further experiments with $NHC^{Dipp}MCl$ (M = Ag, Au) yielded similar products $(NHC^{Dipp}M)_2\{\eta^3\text{-}Ge_9R_2\}$ (M = Ag (**3**), Au (**4**)) according to NMR data. Furthermore, adducts of compounds **3** and **4** were detected in ESI-MS experiments (Figure 6).

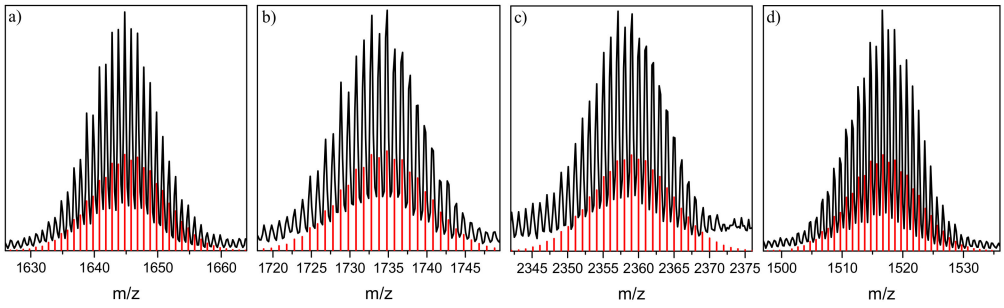

Figure 6. Selected areas of the ESI-MS spectra obtained by examination of a solution of (**a**) compound **3** in acetonitrile, (**b**,**c**) compound **4** in thf and (**d**) compound **5** in acetonitrile. (**a**) Negative ion mode (4500 V, 300 °C) monitoring **3** with a cleaved $[Ag\text{-}NHC]^+$ moiety at m/z 1644.8 $[NHC^{Dipp}Ag\{Ge_9(Si(TMS)_3)_2\}]^-$. (**b**) Negative ion mode (4500 V, 300 °C), monitoring **4** with a cleaved $[Au\text{-}NHC]^+$ moiety at m/z 1734.8 $[NHC^{Dipp}Au\{Ge_9(Si(TMS)_3)_2\}]^-$ and (**c**) positive ion mode (6000 V, 300 °C), monitoring **4** with an attached potassium cation at m/z 2359.0 $[(NHC^{Dipp}Au)_2\{Ge_9(Si(TMS)_3)_2\}K]^+$. (**d**) Negative ion mode (4500 V, 300 °C) monitoring **5** with a cleaved $[Cu\text{-}NHC]^+$ moiety at m/z 1516.6 $[NHC^{Mes}Cu\{Ge_9(Si(TMS)_3)_2\}]^-$. The simulated mass spectra with the corresponding isotope distribution are shown below as red bars.

The possibility to also introduce other NHC ligands by this method is shown by the reaction of the bis-silylated cluster $[Ge_9\{Si(TMS)_3\}_2]^{2-}$ with $NHC^{Mes}CuCl$, bearing slightly smaller mesityl wingtip substituents. The obtained product $(NHC^{Mes}Cu)_2\{\eta^3\text{-}Ge_9(Si(TMS)_3)_2\}$ (**5**) was characterized by NMR spectroscopy and ESI-MS (adduct with a cleaved $[Cu\text{-}NHC]^+$ moiety was detected; Figure 6). Interestingly, the reaction of equimolar amounts of $[Ge_9\{Si(TMS)_3\}]^{2-}$ and $NHC^{Dipp}CuCl$ always yielded mixtures of **2** and unreacted $[Ge_9\{Si(TMS)_3\}]^{2-}$. Thus, the introduction of only one $[NHC^{Dipp}Cu]^+$ moiety remains an open challenge.

3. Materials and Methods

3.1. General

All manipulations were performed under oxygen-free, dry conditions in an argon atmosphere using standard Schlenk or glove box techniques. Glassware was dried prior to use by heating it in vacuo. The solvents used were obtained from an MBraun Grubbs apparatus. All other commercially available chemicals were used without further purification. K_4Ge_9 was prepared by fusion of stoichiometric amounts of the elements in stainless-steel tubes at 650 °C, and $K_{12}Ge_{17}$ was synthesized by fusion of stoichiometric amounts of the elements in tantalum containers at 800 °C. 1,3-Bis(2,6-diisopropylphenyl)imidazolium chloride, 1,3-dimesitylimidazolium chloride and the corresponding coinage metal halide complexes as well as $K_2[Ge_9R^I{}_2]$ (R^I = $Si(TMS)_3$) and $K[Ge_9R_3]$ (R = $Si(^iPr)_3$) were synthesized according to modified literature procedures [14,16,25–28]. All filtrations performed within this work were carried out using Whatman filter papers.

3.2. Single Crystal Structure Determination

The air- and moisture-sensitive crystals of **1** and **2** were transferred from the mother liquor into cooled perfluoroalkylether oil under a cold stream of N_2 gas. For diffraction data collection, the single crystals were fixed on a glass capillary and positioned in a 150 K (**1**) or 100 K (**2**) cold N_2 gas stream using the crystal cap system. Data collection was performed with a Bruker AXS D8 diffractometer (Mo-*Kα* radiation) (**2**) or a STOE StadiVari (Mo-*Kα* radiation) diffractometer equipped with a DECTRIS PILATUS 300K detector (**1**). Structures were solved by Direct Methods (SHELXS-2014) and refined by full-matrix least-squares calculations against F^2 (SHELXL-2014) [29]. The positions of the hydrogen atoms were calculated and refined using a riding model. Unless stated otherwise, all non-hydrogen

atoms were treated with anisotropic displacement parameters. The supplementary crystallographic data for this paper have been deposited with the Cambridge Structural database and are available free of charge via www.ccdc.cam.ac.uk/data_request/cif. The crystallographic data for compounds **1** and **2** are summarized in Table 3. In compound **1**, the electron density of a disordered toluene molecule was taken care of by the PLATON squeeze function [30]. Furthermore, some reflections were affected by the beamstop, and therefore they were excluded for refinement. In compound **2** one of the hypersilyl substituents is disordered and was refined on split positions. Furthermore, the electron density of a disordered toluene molecule was taken care of by the PLATON squeeze function [30].

Table 3. Crystallographic data for compounds **1** and **2**.

Compound	**1**	**2**
formula	$C_{54}H_{99}Ge_9Cu_1N_2Si_3 \cdot 2$ tol	$C_{72}H_{128}Ge_9Cu_2N_4Si_8 \cdot 4$ tol.
fw ($g \cdot mol^{-1}$)	1761.73	2423.42
space group (no.)	$P\bar{1}$ (2)	$P\bar{1}$ (2)
a (Å)	12.377(3)	15.102(2)
b (Å)	13.387(3)	16.831(3)
c (Å)	26.468(5)	25.659(5)
α (deg.)	77.69(3)	108.951(9)
β (deg.)	78.76(3)	101.847(8)
γ (deg.)	77.58(3)	90.837(8)
V ($Å^3$)	4133.0(2)	6013.8(2)
Z	2	2
T (K)	150(2)	100(2)
λ (Å)	Mo-$K\alpha$	Mo-$K\alpha$
ρ_{calcd} ($g \cdot cm^{-3}$)	1.416	1.338
μ (mm^{-1})	3.553	2.680
collected reflections	62327	90837
independent reflections	14985	21064
R_{int}/R_{δ}	0.0263/0.0187	0.0914/0.0943
parameters/restraints	776/0	1273/366
R_1 ($I > 2\,\sigma(I)$/all data)	0.0330/0.0414	0.0468/0.0985
wR_2 ($I > 2\,\sigma(I)$/all data)	0.0801/0.0854	0.0953/0.1126
goodness of fit	1.084	0.998
max./min. diff. el. density ($e \cdot Å^{-3}$)	0.710/−0.757	0.827/–0.653
CCDC	1553930	1553929

3.3. NMR Spectroscopy

Sample preparation was performed in a glove box. NMR spectra were measured on a Bruker Avance Ultrashield 400 MHz spectrometer. The ^{1}H- and ^{13}C-NMR spectra were calibrated using the residual proton signal of the used deuterated solvents [31]. Chemical shifts are reported in parts per million (ppm) relative to TMS, with the residual solvent peak serving as internal reference. Abbreviations for signal multiplicities are: singlet (s), doublet (d), triplet (t), heptet (hept), multiplet (m). The evaluation of the spectra was carried out using the MestReNova program.

3.4. Electron Spray Ionization Mass Spectrometry (ESI-MS)

The sample preparation for the ESI-MS experiments was done in a glove box. ESI MS analyses were performed on a Bruker Daltronic HCT mass spectrometer (dry gas temperature: 300 °C; injection speed 240 µL/s), and the data evaluation was carried out using the Bruker Compass Data Analysis 4.0 SP 5 program (Bruker, Bremen, Germany). Spectra were plotted using OriginPro2016G (Origin Lab) and Excel 2016 (Microsoft).

3.5. Elemental Analyses (EA)

Elemental analyses were carried out in the micro-analytical laboratory of the Chemistry Department of Technische Universität München. Analyses of C, H, N were performed in a combustion analyzer (elementar vario EL, Bruker).

3.6. Syntheses

$NHC^{Dipp}Cu\{\eta^3\text{-}Ge_9(Si(^iPr)_3)_3\}$ (**1**)

K_4Ge_9 (121 mg, 0.150 mmol) was treated with an acetonitrile solution (3 mL) of $Si(^iPr)_3Cl$ (87 mg, 0.450 mmol). A deep red reaction mixture was obtained after stirring at r.t. over night. The suspension was filtered to remove remaining solids, and a solution of $NHC^{Dipp}CuCl$ (73 mg, 0.150 mmol, 1 eq.) in acetonitrile (1.5 mL) was added, which led to the immediate formation of an orange precipitate. The supernatant solution (slightly orange) was filtered off, and the residue was washed with acetonitrile (2 mL). After removal of the solvent in vacuo, the solids were dissolved in toluene (1 mL) and filtered to remove KCl formed upon the reactions. The sample was stored in a freezer at −40 °C for crystallization yielding the pure product as red block-shaped crystals (116 mg, 50%), suitable for single crystal X-ray diffraction.

^{1}H-NMR (400 MHz, 298 K, C_6D_6): δ[ppm] = 7.33–7.27 (m, 2H, $CH_{Ph(p)}$), 7.18 (m, 4H, $CH_{Ph(m)}$)*, 6.26 (s, 2H, CH_{Im}), 2.76 (hept, $^3J_{HH}$ = 6.4 Hz, 4H, CH_{iPr}), 1.58 (d, $^3J_{HH}$ = 6.9 Hz, 12H, Me_{iPr}), 1.27 (*pseudo*-s, 63H, $Me_{iPr(silyl)}$ + $CH_{iPr(silyl)}$), 1.07 (d, $^3J_{HH}$ = 6.9 Hz, 12H, Me_{iPr}).

^{13}C-NMR (101 MHz, 298 K, C_6D_6): δ[ppm] = 145.67 (s, $C_{Ph(iPr)}$), 135.27 (s, $C_{Ph}N$), 130.61 (s, $CH_{Ph(p)}$), 124.36 (s, $CH_{Ph(m)}$), 122.01 (s, CH_{Im}), 29.08 (s, CH_{iPr}), 25.15 (s, Me_{iPr}), 24.82 (s, Me_{iPr}), 20.97 (s, $Me_{iPr(silyl)}$), 15.76 (s, $CH_{iPr(silyl)}$).

^{29}Si-INEPT NMR: (79 MHz, 298 K, C_6D_6): δ[ppm] = 38.62 (s, Si_{Ge9}).
ESI-MS (positive mode, 4500 V, 300 °C): 2029.3 $[(NHC^{Dipp}Cu)_2\{\eta^3\text{-}Ge_9(Si(^iPr)_3)_3\}]^+$.
Elemental analysis: Anal. calcd. for $C_{54}H_{99}Ge_9Cu_1N_2Si_3$: C, 41.1; H, 6.3; N, 1.8; found: C, 40.7; H, 6.2; N, 1.8.
[*] Signal overlaps with the residual solvent signal of C_6D_6. Therefore, no multiplicity of the signal or a certain area for a multiplet could be determined. The integral of the signal is assumed to be 4, according to the 4 protons in *meta*-position at the phenyl ring causing this signal.

$(NHC^{Dipp}Cu)_2\{\eta^3\text{-}Ge_9(Si(TMS)_3)_2\}$ (**2**)

Route A:
$K_{12}Ge_{17}$ (204.5 mg, 0.120 mmol) was treated with $Si(TMS)_3Cl$ (204.0 mg, 0.720 mmol) in a heterogeneous reaction in acetonitrile (2 mL) to form a deep red solution upon stirring at r.t. over night. The mixture was filtered, and a solution of $NHC^{Dipp}CuCl$ (117 mg, 0.240 mmol) in acetonitrile (2 mL) was added, instantly leading to the formation of a brown precipitate. The mixture was stirred for 15 min at r.t. to assure complete conversion of the reactants. After filtering off the supernatant solution (deep red) and removal of the solvent in vacuo, a brown solid was obtained. The solid was dissolved in toluene (3 mL) and filtered to remove KCl formed during the reaction. The toluene solution was concentrated to half of its original volume and placed in a freezer at −40 °C for crystallization, yielding red plate-shaped crystals of the product (74 mg, 30%), suitable for single crystal X-ray diffraction.

Route B:
A solution of $K_2[Ge_9R_2]$ (R: $Si(TMS)_3$) (92 mg, 0.075 mmol) in acetonitrile (1 mL) was treated with an acetonitrile solution (1.5 mL) of $NHC^{Dipp}CuCl$ (73 mg, 0.150 mmol), instantly leading to the formation of a brownish precipitate. The mixture was stirred for 15 min at r.t. to assure complete conversion of the reactants. Subsequently, the supernatant solution (slightly red) was filtered off, and the residue was dried in vacuo. The residue was dissolved in toluene (2 mL) and filtered to remove KCl formed

during the reaction, and then the solution was concentrated to half of its original volume. The sample was stored in a freezer at -40 °C for recrystallization, yielding red crystals (69 mg, 45%) of the product.

^{1}H-NMR (400 MHz, 298 K, thf-d_8): δ[ppm] = 7.47–7.42 (m, 4H, $CH_{Ph(p)}$), 7.32 (d, $^{3}J_{HH}$ = 7.8 Hz, 8H, $CH_{Ph(m)}$), 7.23 (s, 4H, CH_{Im}), 2.77 (hept, $^{3}J_{HH}$ = 6.8 Hz, 8H, CH_{iPr}), 1.46 (d, $^{3}J_{HH}$ = 6.9 Hz, 24H, Me_{iPr}), 1.09 (d, $^{3}J_{HH}$ = 6.9 Hz, 24H, Me_{iPr}), 0.05 (s, 54H, Me_{TMS}).

^{1}H-NMR (400 MHz, 298 K, C_6D_6): δ[ppm] = 7.35–7.30 (m, 4H, $CH_{Ph(p)}$), 7.23 (d, $^{3}J_{HH}$ = 7.8 Hz, 8H, $CH_{Ph(m)}$), 6.22 (s, 4H, CH_{Im}), 2.79 (hept, $^{3}J_{HH}$ = 6.8 Hz, 8H, CH_{iPr}), 1.63 (d, $^{3}J_{HH}$ = 6.9 Hz, 24H, Me_{iPr}), 1.01 (d, $^{3}J_{HH}$ = 6.9 Hz, 24H, Me_{iPr}), 0.41 (s, 54H, Me_{TMS}).

^{13}C-NMR (101 MHz, 298 K, thf-d_8): δ[ppm] = 146.12 (s, $C_{Ph(iPr)}$), 136.68 (s, $C_{Ph}N$), 130.83 (s, $CH_{Ph(p)}$), 125.13 (s, $CH_{Ph(m)}$), 124.01 (s, CH_{Im}), 29.51 (s, CH_{iPr}), 25.83 (s, Me_{iPr}), 3.40 (s, Me_{TMS}).

^{29}Si-INEPT NMR: (79 MHz, 298 K, thf-d_8): δ[ppm] = −10.63 (s, Si_{TMS}), −105.36 (s, Si_{Ge9}).
ESI-MS: *m*/*z* 1600.8 $[NHC^{Dipp}Cu\{Ge_9(Si(TMS)_3)_2\}]^-$, 2092.8 $[(NHC^{Dipp}Cu)_2\{Ge_9(Si(TMS)_3)_2\}K]^+$.
Elemental analysis: Anal. Calcd. for $C_{72}H_{128}Ge_9Cu_2N_4Si_8$: C, 42.1; H, 6.2; N, 2.7; found: C, 42.0; H, 6.3; N, 2.7.

$(NHC^{Dipp}Ag)_2\{\eta^3\text{-}Ge_9(Si(TMS)_3)_2\}$ (**3**)

Route A:
$K_{12}Ge_{17}$ (204.5 mg, 0.120 mmol) was treated with $Si(TMS)_3Cl$ (204.0 mg, 0.720 mmol) in a heterogeneous reaction in acetonitrile (2 mL) to form a deep red solution upon stirring at r.t. over night. The mixture was filtered, and a solution of $NHC^{Dipp}AgCl$ (128 mg, 0.240 mmol) in acetonitrile (2 mL) was added, instantly leading to the formation of a brown precipitate. Filtering off the supernatant solution (deep red) and removal of the solvent in vacuo led to a brown solid which was dissolved in toluene (3 mL) and filtered to remove KCl formed during the reaction. The toluene solution was concentrated to half of its original volume and placed in a freezer at −40 °C for crystallization. However, crystals suitable for single crystal X-ray diffraction could not be obtained yet. The crude product was obtained as a brownish solid after removal of toluene (51 mg, 20%).

Route B:
A solution of $K_2[Ge_9R_2]$ (R: $Si(TMS)_3$) (92 mg, 0.075 mmol) in acetonitrile (1 mL) was treated with an acetonitrile solution (1.5 mL) of $NHC^{Dipp}AgCl$ (80 mg, 0.150 mmol), instantly leading to the formation of a brownish precipitate. The mixture was stirred for 15 min at r.t. to assure complete conversion of the reactants. The supernatant solution (slightly red) was filtered off, and the residue was dried in vacuo. The residue was dissolved in toluene (2 mL) and filtered to remove KCl formed during the reaction, and the solution was concentrated to half of its original volume. The sample was stored in a freezer at −40 °C. However, crystals suitable for single crystal X-ray diffraction could not be obtained yet. The crude product was obtained as a brownish solid after removal of toluene (40 mg, 25%).

^{1}H-NMR (400 MHz, 298 K, thf-d_8): δ[ppm] = 7.46–7.42 (m, 4H, $CH_{Ph(p)}$), 7.40 (s, 4H, CH_{Im}), 7.30 (d, $^{3}J_{HH}$ = 7.8 Hz, 8H, $CH_{Ph(m)}$), 2.70 (hept, $^{3}J_{HH}$ = 6.8 Hz, 4H, CH_{iPr}), 1.43 (d, $^{3}J_{HH}$ = 6.9 Hz, 24H, Me_{iPr}), 1.14 (d, $^{3}J_{HH}$ = 6.9 Hz, 24H, Me_{iPr}), 0.01 (s, 54H, Me_{TMS}).

^{13}C-NMR (101 MHz, 298 K, thf-d_8): δ[ppm] = 146.31 (s, $C_{Ph(iPr)}$), 136.56 (s, $C_{Ph}N$), 130.97 (s, $CH_{Ph(p)}$), 125.04 (s, $CH_{Ph(m)}$), 124.29 (s, CH_{Im}), 29.56 (s, CH_{iPr}), 26.28 (s, Me_{iPr}), 24.67 (s, Me_{iPr}), 3.36 (s, Me_{TMS}).

^{29}Si-INEPT NMR: (79 MHz, 298 K, thf-d_8): δ[ppm] = −10.38 (s, Si_{TMS}), −105,75 (s, Si_{Ge9}).
ESI-MS: *m*/*z* 1644.8 $[NHC^{Dipp}Ag\{Ge_9(Si(TMS)_3)_2\}]^-$.

$(NHC^{Dipp}Au)_2\{\eta^3\text{-}Ge_9(Si(TMS)_3)_2\}$ (**4**)

Route A:
$K_{12}Ge_{17}$ (204.5 mg, 0.120 mmol) was treated with $Si(TMS)_3Cl$ (204.0 mg, 0.720 mmol) in a heterogeneous reaction in acetonitrile (2 mL) to form a deep red solution upon stirring at r.t. over night. The mixture was filtered, and a solution of $NHC^{Dipp}AuCl$ (149 mg, 0.240 mmol) in acetonitrile (3 mL) was added, instantly leading to the formation of a brown precipitate. Filtering off the supernatant solution (deep red), and removal of the solvent in vacuo led to a brown solid which was dissolved in toluene (3 mL) and filtered to remove KCl formed during the reaction. The toluene solution was concentrated to half of its original volume and placed in a freezer at −40 °C for crystallization. However, crystals suitable for single crystal X-ray diffraction could not be obtained yet. The crude product was obtained as a brownish solid after removal of toluene (83 mg, 30%).

Route B:
A solution of $K_2[Ge_9R_2]$ (R: $Si(TMS)_3$) (92 mg, 0.075 mmol) in acetonitrile (1 mL) was treated with an acetonitrile solution (2 mL) of $NHC^{Dipp}AuCl$ (93 mg, 0.150 mmol), instantly leading to the formation of a brownish precipitate. The mixture was stirred for 15 min at r.t. to assure complete conversion of the reactants. The supernatant solution (light red) was filtered off, and the residue was dried in vacuo. The residue was dissolved in toluene (2 mL) and filtered to remove KCl formed during the reaction, and the solution was concentrated to half of its original volume. The sample was stored in a freezer at −40 °C. However, crystals suitable for single crystal X-ray diffraction could not be obtained yet. The crude product was obtained as a brownish solid after removal of toluene (52 mg, 30%).

^{1}H-NMR (400 MHz, 298 K, C_6D_6): δ[ppm] = 7.32–7.28 (m, 4H, $CH_{Ph(p)}$), 7.20 (d, $^3J_{HH}$ = 7.7 Hz, 8H, $CH_{Ph(m)}$), 6.28 (s, 4H, CH_{Im}), 2.73 (hept, $^3J_{HH}$ = 6.6 Hz, 8H, CH_{iPr}), 1.61 (d, $^3J_{HH}$ = 6.9 Hz, 24H, Me_{iPr}), 1.04 (d, $^3J_{HH}$ = 6.9 Hz, 24H, Me_{iPr}), 0.43 (s, 54H, Me_{TMS}).

^{1}H-NMR (400 MHz, 298 K, thf-d_8): δ[ppm] = 7.45-7.38 (m, 8H, $CH_{Ph(p)}$ + CH_{Im}), 7.27 (d, $^3J_{HH}$ = 7.7 Hz, 8H, $CH_{Ph(m)}$), 2.74 (hept, $^3J_{HH}$ = 6.6 Hz, 8H, CH_{iPr}), 1.43 (d, $^3J_{HH}$ = 6.9 Hz, 24H, Me_{iPr}), 1.13 (d, $^3J_{HH}$ = 6.9 Hz, 24H, Me_{iPr}), 0.09 (s, 54H, Me_{TMS}).

^{13}C-NMR (101 MHz, 298 K, C_6D_6): δ[ppm] = 145.43 (s, $C_{Ph(iPr)}$), 135.16 (s, $C_{Ph}N$), 130.84 (s, $CH_{Ph(p)}$), 124.75 (s, $CH_{Ph(m)}$), 122.38 (s, CH_{Im}), 28.92 (s, CH_{iPr}), 25.52 (s, Me_{iPr}), 24.63 (s, Me_{iPr}), 3.45 (s, Me_{TMS}).

^{29}Si-INEPT NMR (79 MHz, 298 K, C_6D_6): δ[ppm] = −9.72 (s, Si_{TMS}), −105.49 (s, Si_{Ge9}).
ESI-MS: *m/z* 1734.8 $[NHC^{Dipp}Au\{Ge_9(Si(TMS)_3)_2\}]^-$, 2359.0 $[(NHC^{Dipp}Au)_2\{Ge_9(Si(TMS)_3)_2\}K]^+$.

$(NHC^{Mes}Cu)_2\{\eta^3\text{-}Ge_9(Si(TMS)_3)_2\}$ (**5**)

A solution of $K_2[Ge_9R_2]$ (R: $Si(TMS)_3$) (92 mg, 0.075 mmol) in acetonitrile (1 mL) was treated with an acetonitrile solution (2 mL) of $NHC^{Mes}CuCl$ (60.5 mg, 0.150 mmol), instantly leading to the formation of a brownish precipitate. The mixture was stirred for 15 min at r.t. to assure complete conversion of the reactants. The supernatant solution (light red) was filtered off, and the residue was dried in vacuo. The residue was dissolved in toluene (2 mL) and filtered to remove KCl formed during the reaction. The sample was stored in a freezer at −40 °C. However, crystals suitable for single crystal X-ray diffraction could not be obtained yet. The crude product was obtained as a brownish solid after removal of toluene (59 mg, 40%).

^{1}H-NMR (400 MHz, 298 K, thf-d_8): δ[ppm] = 7.13 (s, 4H, CH_{Im}), 7.01 (s, 8H, CH_{Ph}), 2.42 (s, 12H, Me_p), 2.10 (s, 24H, Me_o), 0.08 (s, 54H, Me_{TMS}).

^{13}C-NMR (101 MHz, 298 K, thf-d_8): δ[ppm] = 139.35 (s, $C_{Ph(Me(p))}$), 136.57 (s, $C_{Ph}N$), 135.69 (s, $C_{Ph(Me(o))}$) 130.54 (s, CH_{Ph}), 121.98 (s, CH_{Im}), 21.72 (s, $CH_{Me(p)}$), 18.69 (s, $Me_{Me(o)}$), 3.18 (s, Me_{TMS}).

^{29}Si-INEPT NMR (79 MHz, 298 K, thf-d_8): δ[ppm] = −10.24 (s, Si_{TMS}), −108.84 (s, Si_{Ge9}).
ESI-MS: *m/z* 1516.6 $[NHC^{Mes}Cu\{Ge_9(Si(TMS)_3)_2\}]^-$.

4. Conclusions

Within this work, we studied the silylation reaction of $K_{12}Ge_{17}$ and the reactivity of bis- and tris-silylated [Ge_9] clusters towards coinage metal carbene complexes $NHC^{Dipp}MCl$ (*M*: Cu, Ag, Au). The reaction of $K_{12}Ge_{17}$ with 6 eq. of $Si(TMS)_3Cl$ yielded the bis-silylated cluster $[Ge_9\{Si(TMS)_3\}_2]^{2-}$ as the main product in solution, contrasting the analogue reaction of K_4Ge_9, which exclusively results in the formation of $[Ge_9\{Si(TMS)_3\}_3]^-$. The subsequent reaction of the obtained solutions, as well as the reaction of pure $[Ge_9\{Si(TMS)_3\}_2]^{2-}$ with $NHC^{Dipp}MCl$, yielded the novel neutral dinuclear *Zintl* cluster coinage metal NHC compounds $(NHCM)_2\{\eta^3\text{-}Ge_9R^I_2\}$ (*M* = Cu, Ag, Au; NHC = NHC^{Dipp}, NHC^{Mes} and R^I = $Si(TMS)_3$) (**2**–**5**). Furthermore, the reaction of $[Ge_9\{Si(^iPr)_3\}_3]^-$ with $NHC^{Dipp}CuCl$ gave the neutral compound $NHC^{Dipp}Cu\{Ge_9R_3\}$ (R = $Si(^iPr)_3$) (**1**), which showed different structural features compared to its analogues bearing the larger silyl groups $[Si(^iBu)_3]^+$ and $[Si(TMS)_3]^+$.

Supplementary Materials: The following material is available online, Tables SI1–SI3: Selected bond lengths and angles of compounds **1** and **2**, as well as comparison of cluster shapes of both compounds to previously reported similar compounds. Figure SI 1: Full ellipsoid pictures of compounds **1** and **2**. Figure S I2–SI 20: NMR spectra of compounds **1**–**5**.

Acknowledgments: This work was financially supported by Wacker Chemie AG. The authors thank M. Sc. Lorenz Schiegerl and M. Sc. Christina Fischer for the ESI MS measurements. Furthermore, F.S.G. thanks TUM Graduate School for support, and M.A.G. thanks IGSSE for support.

Author Contributions: Examinations on the reactivity of the silylated [Ge_9] clusters towards coinage metal carbene compounds as well as purification, crystal growth, isolation of a single domain crystal species and evaluation of the diffraction data (compound **1**) was performed by Felix S. Geitner. Investigations on the silylation of $K_{12}Ge_{17}$ with $Si(TMS)_3Cl$ and sample preparation for ESI MS were carried out by Michael A. Giebel. Isolation of a single domain crystal species and evaluation of the diffraction data of compound **2** was done by Alexander Pöthig. Thomas Fässler is principal investigator.

Conflicts of Interest: The authors declare no conflict of interest.

References

1. Eichhorn, B.W.; Haushalter, R.C.; Pennington, W.T. Synthesis and Structure of *closo*-$Sn_9Cr(CO)_3^{4-}$: The First Member in a New Class of Polyhedral Clusters. *J. Am. Chem. Soc.* **1988**, *110*, 8704. [CrossRef]
2. Scharfe, S.; Kraus, F.; Stegmaier, S.; Schier, A.; Fässler, T.F. Zintl Ions, Cage Compounds, and Intermetalloid Clusters of Group 14 and Group 15 Elements. *Angew. Chem. Int. Ed.* **2011**, *50*, 3630. [CrossRef] [PubMed]
3. Sevov, S.C.; Goicoechea, J.M. Chemistry of Deltahedral Zintl Clusters. *Organometallics* **2006**, *25*, 5678. [CrossRef]
4. Benda, C.B.; Waibel, M.; Fässler, T.F. On the Formation of Intermetalloid Clusters: Titanocene(III)diammine as a Versatile Reactant Toward Nonostannide Clusters. *Angew. Chem. Int. Ed.* **2015**, *54*, 522. [CrossRef]
5. Scharfe, S.; Fässler, T.F. Varying Bonding Modes of the Zintl Ion $[Ge_9]^{4-}$ in Cu^I Complexes: Syntheses and Structures of $[Cu(\eta^4\text{-}Ge_9)(PR_3)]^{3-}$ (R: *i*Pr, Cy) and $[Cu(\eta^4\text{-}Ge_9)(\eta^1\text{-}Ge_9)]^{7-}$. *Eur. J. Inorg. Chem.* **2010**, 1207. [CrossRef]
6. Goichechea, J.M.; Sevov, S.C. Organozinc Derivatives of Delthedral Zintl Ions: Synthesis and Characterization of *closo*-$[E_9Zn(C_6H_5)]^{3-}$ (E: Si, Ge, Sn, Pb). *Organometallics* **2006**, *25*, 4530. [CrossRef]
7. Mayer, K.; Jantke, L.-A.; Schulz, S.; Fässler, T.F. Retention of the Zn-Zn bond in $[Ge_9Zn\text{-}ZnGe_9]^{6-}$ and Formation of $[(Ge_9Zn)\text{-}(Ge_9)\text{-}(ZnGe_9)]^{8-}$ and Polymeric $^1_\infty[-(Ge_9Zn)^{2-}-]$. *Angew Chem. Int. Ed.* **2017**, *56*, 2350. [CrossRef] [PubMed]
8. Scharfe, S.; Fässler, T.F.; Stegmaier, S.; Hoffmann, S.D.; Ruhland, K. $[Cu@Sn_9]^{3-}$ and $[Cu@Pb_9]^{3-}$: Intermetalloid Clusters with Endohedral Cu Atoms in Spherical Environments. *Chem. Eur. J.* **2008**, *14*, 4479. [CrossRef] [PubMed]
9. Waibel, M.; Kraus, F.; Scharfe, S.; Wahl, B.; Fässler, T.F. $[(MesCu)_2(\eta^3\text{-}Si_4)]^{4-}$: A Mesitylcopper Stabilized Tetrasilicide Tetraanion. *Angew. Chem. Int. Ed.* **2010**, *49*, 6611. [CrossRef] [PubMed]
10. Stegmaier, S.; Waibel, M.; Henze, A.; Jantke, L.-A.; Karttunen, A.J.; Fässler, T.F. Soluble Zintl Phases $A_{14}ZnGe_{16}$ (A: K, Rb) Featuring $[(\eta^3\text{-}Ge_4)Zn(\eta^2\text{-}Ge_4)]^{6-}$ and $[Ge_4]^{4-}$ Clusters and the Isolation of $[(MesCu)_2(\eta^3,\eta^3\text{-}Ge_4)]^{4-}$: The Missing Link in the Solution Chemistry of Tetrahedral Group 14 Element Zintl Clusters. *J. Am. Chem. Soc.* **2012**, *134*, 14450. [CrossRef] [PubMed]

11. Spiekermann, A.; Hoffmann, S.D.; Kraus, F.; Fässler, T.F. $[Au_3Ge_{18}]^{5-}$: A Gold-Germanium Cluster with Remarkable Au-Au Interactions. *Angew. Chem. Int. Ed.* **2007**, *46*, 1638. [CrossRef] [PubMed]
12. Spiekermann, A.; Hoffmann, S.D.; Fässler, T.F.; Krossing, I.; Preiss, U. $[Au_3Ge_{45}]^{5-}$-A Binary Anion Containing a $\{Ge_{45}\}$ Cluster. *Angew. Chem. Int. Ed.* **2007**, *46*, 5310. [CrossRef] [PubMed]
13. Geitner, F.S.; Klein, W.; Fässler, T.F. On the Formation of the Intermetalloid Cluster $[AgSn_{18}]^{7-}$—The Reactivity of Coinage Metal NHC Compounds towards $[Sn_9]^{4-}$. *Dalton Trans.* **2017**, *46*, 5796. [CrossRef] [PubMed]
14. Kysliak, O.; Schnepf, A. $\{Ge_9[Si(SiMe_3)_3]_2\}^-$: A Starting Point for Mixed Substituted Metalloid Germanium Clusters. *Dalton Trans.* **2016**, *45*, 2404. [CrossRef] [PubMed]
15. Schnepf, A. $\{Ge_9[Si(SiMe_3)_3]_3\}^-$: A Soluble Polyhedral Ge_9 Cluster Stabilized by only Three Silyl Groups. *Angew Chem. Int. Ed.* **2003**, *42*, 2624. [CrossRef] [PubMed]
16. Li, F.; Sevov, S.C. Rational Synthesis of $\{Ge_9[Si(SiMe_3)_3]_3\}^-$ From Its Parent Zintl Ion Ge_9^{4-}. *Inorg. Chem.* **2012**, *51*, 2706. [CrossRef] [PubMed]
17. Kysliak, O.; Kunz, T.; Schnepf, A. Metalloid $Ge_9R_3^-$ Clusters with Various Silyl Substituents: From Shielded to Open Cluster Cores. *Eur. J. Inorg. Chem.* **2017**, 805. [CrossRef]
18. Mayer, K.; Schiegerl, L.J.; Fässler, T.F. On the Reactivity of Silyated Ge_9 Clusters: Synthesis and Characterization of $[ZnCp^*(Ge_9\{Si(SiMe_3)_3\}_3]$, $[CuPiPr_3(Ge_9\{Si(SiMe_3)_3\}_3]$, and $[(CuiPr_3)_4\{Ge_9(SiPh_3)_2\}_2]$. *Chem. Eur. J.* **2016**, *22*, 18794. [CrossRef] [PubMed]
19. Schiegerl, L.J.; Geitner, F.S.; Fischer, C.; Klein, W.; Fässler, T.F. Functionalization of $[Ge_9]$ with Small Silanes: $[Ge_9(SiR_3)_3]^-$ (R: *i*Bu, *i*Pr, Et) and the Structures of $(CuNHC^{Dipp})[Ge_9\{Si(iBu)_3\}_3]$, (K-18c6)Au$[Ge_9\{Si(iBu)_3\}_3]_2$ and $(K\text{-}18c6)_2[Ge_9\{Si(iBu)_3\}_2]$. *Z. Anorg. Allg. Chem.* **2016**, *642*, 1419. [CrossRef]
20. Kysliak, O.; Schrenk, C.; Schnepf, A. $\{Ge_9[Si(SiMe_3)_2(SiPh_3)]_3\}^-$: Ligand Modification in Metalloid Germanium Cluster Chemistry. *Inorg. Chem.* **2015**, *54*, 7083. [CrossRef] [PubMed]
21. Schenk, C.; Schnepf, A. $[AuGe_{18}\{Si(SiMe_3)_3\}_6]^-$: A Soluble Au-Ge Cluster on the Way to a Molecular Cable? *Angew. Chem. Int. Ed.* **2007**, *46*, 5314–5316. [CrossRef] [PubMed]
22. Schenk, C.; Henke, F.; Santiso-Quinones, G.; Krossing, I.; Schnepf, A. $[Si(SiMe_3)_3]_6Ge_{18}M$ (M: Cu, Ag, Au): Metalloid Cluster Compounds as Unusual Buliding Blocks for a Supramolecular Chemistry. *Dalton Trans.* **2008**, 4436. [CrossRef] [PubMed]
23. Li, F.; Sevov, S.C. Coordination of Tri-Substituted Nona-Germanium Clusters to Cu(I) and Pd(0). *Inorg. Chem.* **2015**, *54*, 8121. [CrossRef] [PubMed]
24. Geitner, F.S.; Fässler, T.F. Introducing Tetrel Zintl Ions to *N*-Heterocyclic Carbenes— Synthesis of Coinage Metal NHC Complexes of $[Ge_9\{Si(SiMe_3)_3\}_3]^-$. *Eur. J. Inorg. Chem.* **2016**, 2688. [CrossRef]
25. Hintermann, L. Expedient Syntheses of the N-Heterocyclic Carbene Precursor Imidazolium Salts IPr·HCl, IMes·HCl and IXy·HCl. *Beilstein J. Org. Chem.* **2007**, *3*, 22. [CrossRef] [PubMed]
26. Santoro, O.; Collado, A.; Slawin, A.M.Z.; Nolan, S.P.; Cazin, C.S.J. A General Synthesis Route to [Cu(X)(NHC)] (NHC = *N*-Heterocyclic Carbene, X = Cl, Br, I) Complexes. *Chem. Commun.* **2013**, *49*, 10483. [CrossRef] [PubMed]
27. De Frémont, P.; Scott, N.M.; Stevens, E.D.; Ramnial, T.; Lightbody, O.C.; Macdonald, C.L.B.; Clyburne, J.A.C.; Abernethy, C.D.; Nolan, S.P. Synthesis of Well-Defined *N*-Heterocyclic Carbene Silver(I) Complexes. *Organometallics* **2005**, *24*, 6301. [CrossRef]
28. Collado, A.; Gomez-Suarez, A.; Martin, A.R.; Slawin, A.M.Z.; Nolan, S.P. Straightforward Synthesis of [Au(NHC)(X)] (NHC = *N*-Heterocyclic Carbene, X = Cl, Br, I) Complexes. *Chem. Commun.* **2013**, *49*, 5541. [CrossRef] [PubMed]
29. Sheldrick, G. Crystal Structure Refinement with SHELXL. *Acta Cryst. Sect. C* **2015**, *71*, 3. [CrossRef] [PubMed]
30. Spek, A. Single Crystal Structure Validation with the Programm PLATON. *J. Appl. Cryst.* **2003**, *36*, 7. [CrossRef]
31. Fulmer, G.R.; Miller, A.J.M.; Sherden, N.H.; Gottlieb, H.E.; Nudelman, A.; Stoltz, B.M.; Bercaw, J.E.; Goldberg, K.I. NMR Chemical Shifts of Trace Impurities: Common Laboratory Solvents, Organics, and Gases in Deuterated Solvents Relevant to the Organometallic Chemist. *Organometallics* **2010**, *29*, 2176. [CrossRef]

Sample Availability: Samples of all compounds are not available from the authors.

Supporting Information

Coinage Metal NHC Compounds of Germanium-Rich Metalloid Clusters $[Ge_9R_3]^-$ and $[Ge_9R^I_2]^{2-}$ with $R = Si(^iPr)_3$ and $R^I = Si(TMS)_3$

Felix S. Geitner [1#], Michael A. Giebel [2#], Alexander Pöthig [3] and Thomas F. Fässler [2,*]

[1] Felix S. Geitner, WACKER Institute for Silicon Chemistry and Department of Chemistry, Technische Universität München, Lichtenbergstraße 4, 85747 Garching, Germany.

[2] Michael A. Giebel, Department of Chemistry, Technische Universität München, Lichtenbergstraße 4, 85747 Garching, Germany.

[2,*] Prof. Dr. T. F. Fässler, Department of Chemistry, Technische Universität München, Lichtenbergstraße 4, 85747 Garching, Germany.

[3] Dr. Alexander Pöthig, TUM Catalysis Research Center (CRC), Ernst-Otto-Fischer Straße 1, 85747 Garching, Germany.

[#] Authors contributed equally to this work

Content

Selected Distances and Angles

Table SI 1: Selected bond lengths and angles of compound **1**.

bond	distance [Å]
Ge1-Ge2	2.8393(9)
Ge1-Ge3	2.8797(9)
Ge1-Ge4	2.5065(9)
Ge1-Ge6	2.5059(8)
Ge2-Ge3	2.834(1)
Ge2-Ge4	2.5189(8)
Ge2-Ge5	2.5205(8)
Ge3-Ge5	2.5211(9)
Ge3-Ge6	2.5261(8)
Ge4-Ge7	2.5473(9)
Ge4-Ge8	2.5631(8)
Ge5-Ge8	2.5578(9)
Ge5-Ge9	2.5401(8)
Ge6-Ge7	2.5547(9)
Ge6-Ge9	2.5572(8)
Ge7-Ge8	2.6421(9)
Ge8-Ge9	2.651(1)
Ge1-Ge7	3.4392(9)
Ge2-Ge8	3.3338(8)
Ge3-Ge9	3.2900(8)
Ge4-Si1	2.383(1)
Ge5-Si2	2.406(1)
Ge6-Si3	2.383(1)
Cu1-Ge1	2.4914(8)
Cu1-Ge2	2.5407(9)
Cu1-Ge3	2.5661(8)
Cu1-C1	1.951(3)
atoms	angle [°]
C1-Cu1-ctp1	177.67(4)

Table SI 2: Selected bond lengths and angles of compound **2**.

bond	distance [Å]
Ge1-Ge2	2.5909(9)
Ge1-Ge3	2.595(1)
Ge1-Ge4	2.591(1)
Ge1-Ge5	2.5781(9)
Ge2-Ge3	2.900(1)
Ge2-Ge5	2.7804(9)
Ge2-Ge6	2.5774(9)
Ge2-Ge9	2.8269(9)
Ge3-Ge4	2.805(1)
Ge3-Ge6	2.5521(8)
Ge3-Ge7	2.8189(9)
Ge4-Ge5	2.906(1)
Ge4-Ge7	2.8333(9)
Ge4-Ge8	2.5651(8)
Ge5-Ge8	2.5638(9)
Ge5-Ge9	2.8102(9)
Ge6-Ge7	2.5132(8)
Ge6-Ge9	2.5047(9)
Ge7-Ge8	2.5147(9)
Ge8-Ge9	2.505(1)
Ge2-Ge3	2.9003(3)
Ge4-Ge5	2.9054(3)
Ge7-Ge9	3.6969(4)
Ge6-Si1	2.388(2)
Ge8-Si5	2.43(1)
Cu1-Ge2	2.601(1)
Cu1-Ge5	2.532(1)
Cu1-Ge9	2.405(1)
Cu2-Ge3	2.532(1)
Cu2-Ge4	2.582(1)
Cu2-Ge7	2.413(1)
Cu1-C1	1.941(5)
Cu2-C4	1.913(5)
atoms	angle [°]
C1-Cu1-ctp1	162.88(2)
C4-Cu2-ctp2	163.93(2)

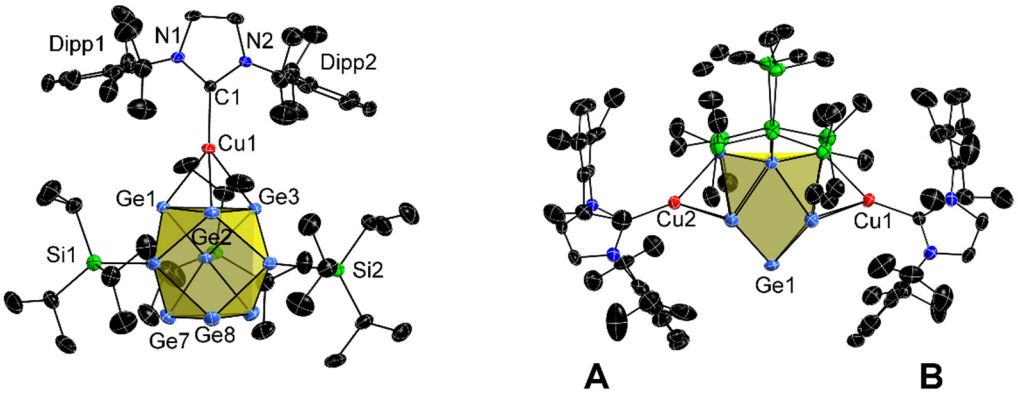

Figure SI 1. Molecular structure of compound **1** (left) and compound **2** (right). Displacement ellipsoids are shown at a 50 % probability level. For clarity, hydrogen atoms and co-crystallized toluene molecules are omitted. For **2**, the two $[NHC^{Dipp}Cu]^+$ moieties are labelled as **A** and **B**. Selected bond lengths and angles are summarized in Table SI 1 (**1**) and Table SI 2 (**2**).

Table SI 3: Comparison of the *Zintl* cluster shape in compounds **1**, **2** and $[NHC^{Dipp}Cu\{\eta^3\text{-}Ge_9R_3\}]$ ($R = Si(^iBu)_3$, $Si(TMS)_3$).

distances [Å]	**1**	**2**	$R = Si(^iBu)_3$	$R = Si(TMS)_3$
h_1	3.4392(9)	2.9003(3)	3.4235(1)	3.3253(8)
h_2	3.3338(8)	2.9054(3)	3.3918(1)	3.3029(8)
h_3	3.2900(8)	3.6969(4)	3.1947(1)	3.4028(8)
maximum difference	0.1492(9)	0.7966(3)	0.2288(1)	0.0999(8)

Heights of the trigonal prism in compound **2** are defined as: h1 (Ge2-Ge3), h2 (Ge4-Ge5) and h3 (Ge7-Ge9). For all other compounds heights are defined as: h1 (Ge1-Ge7), h2 (Ge2-Ge8) h3 (Ge3-Ge9).

In *Zintl* cluster coinage metal NHC compounds, the contained silylated *Zintl* cluster ligands reveal either D_{3h}- or C_{2v}-symmetry. Assuming D_{3h}-symmetry the clusters can be described as tricapped trigonal prisms with the capping atoms bearing the silyl groups. In case of perfect D_{3h}-symmetry the heights of the trigonal prism (h) would all be equal. Regarding the data summarized in Table SI 3 it becomes obvious, that the clusters reveal most perfect D_{3h}-symmetry in $NHC^{Dipp}Cu\{\eta^3\text{-}Ge_9(Si(TMS)_3)_3\}$ (smallest difference between minimum and maximum height of the trigonal prism). In compound **1** and $NHC^{Dipp}Cu\{\eta^3\text{-}Ge_9(Si(^iBu)_3)_3\}$ the trigonal prisms within the clusters are slightly more distorted. By contrast for novel compound **2** one of the heights is significantly longer than the others, which manifests the C_{2v}-symmetry of the $[Ge_9]$ cluster in **2**.

NMR data

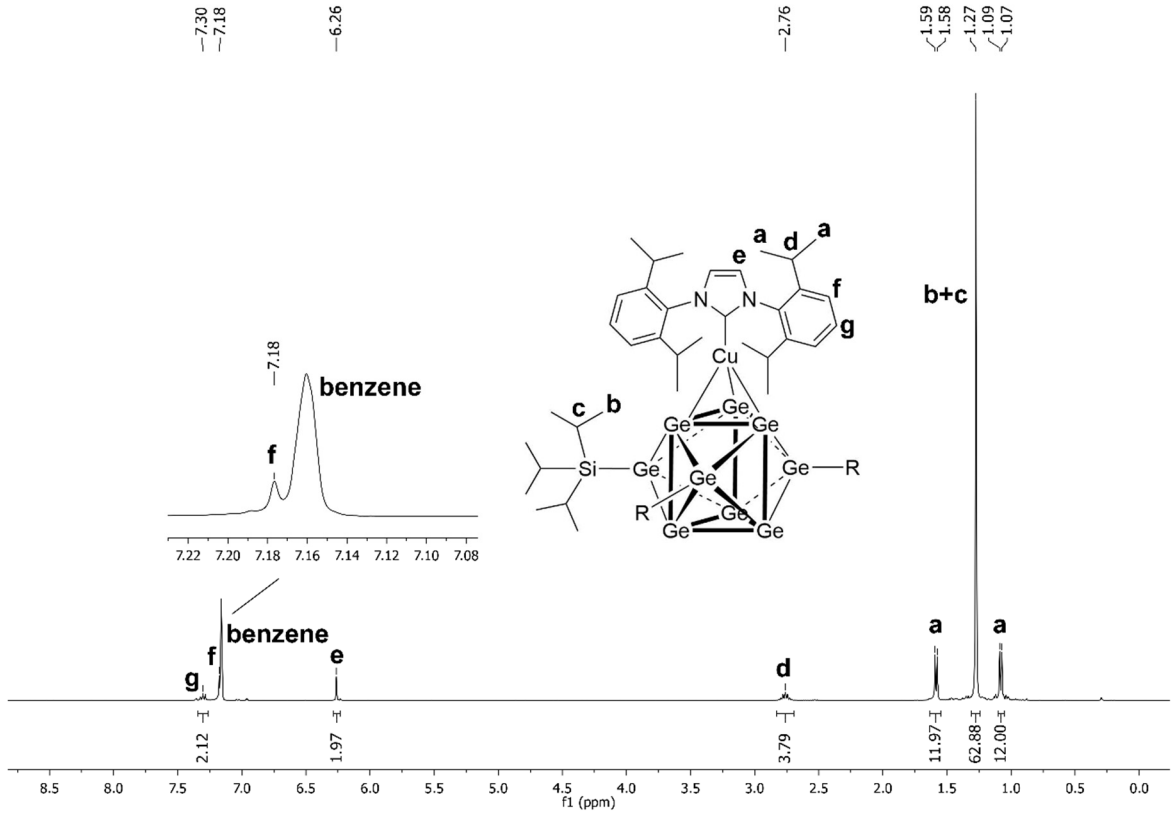

Figure SI 2: ^{1}H NMR of compound **1** in C_6D_6.

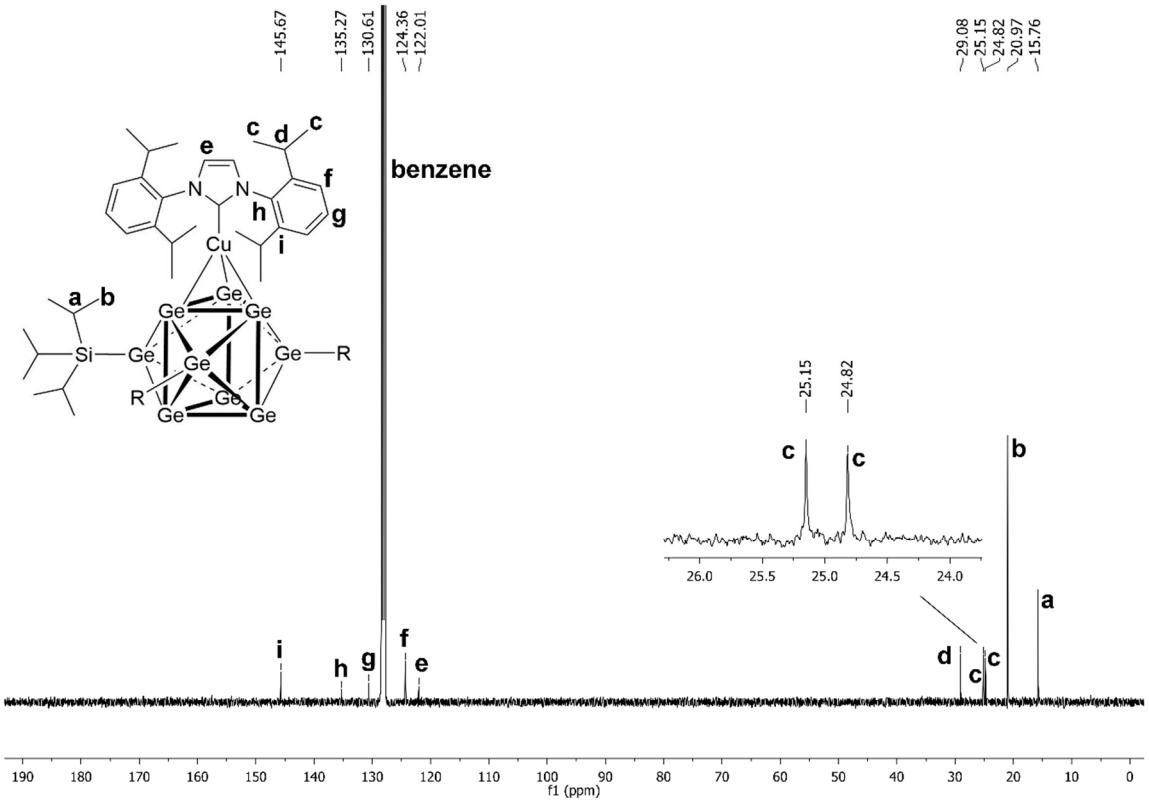

Figure SI 3: ^{13}C NMR of compound **1** in C_6D_6.

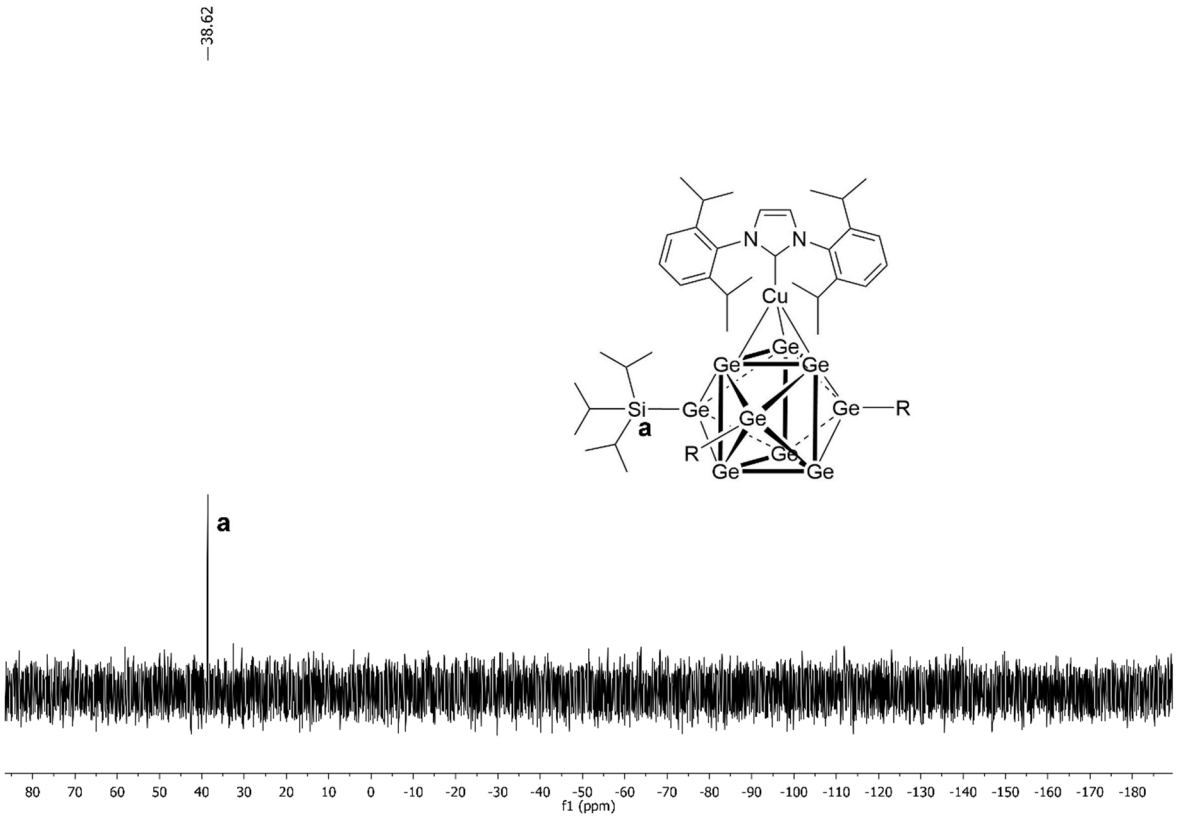

Figure SI 4: ^{29}Si-INEPT NMR of compound **1** in C_6D_6.

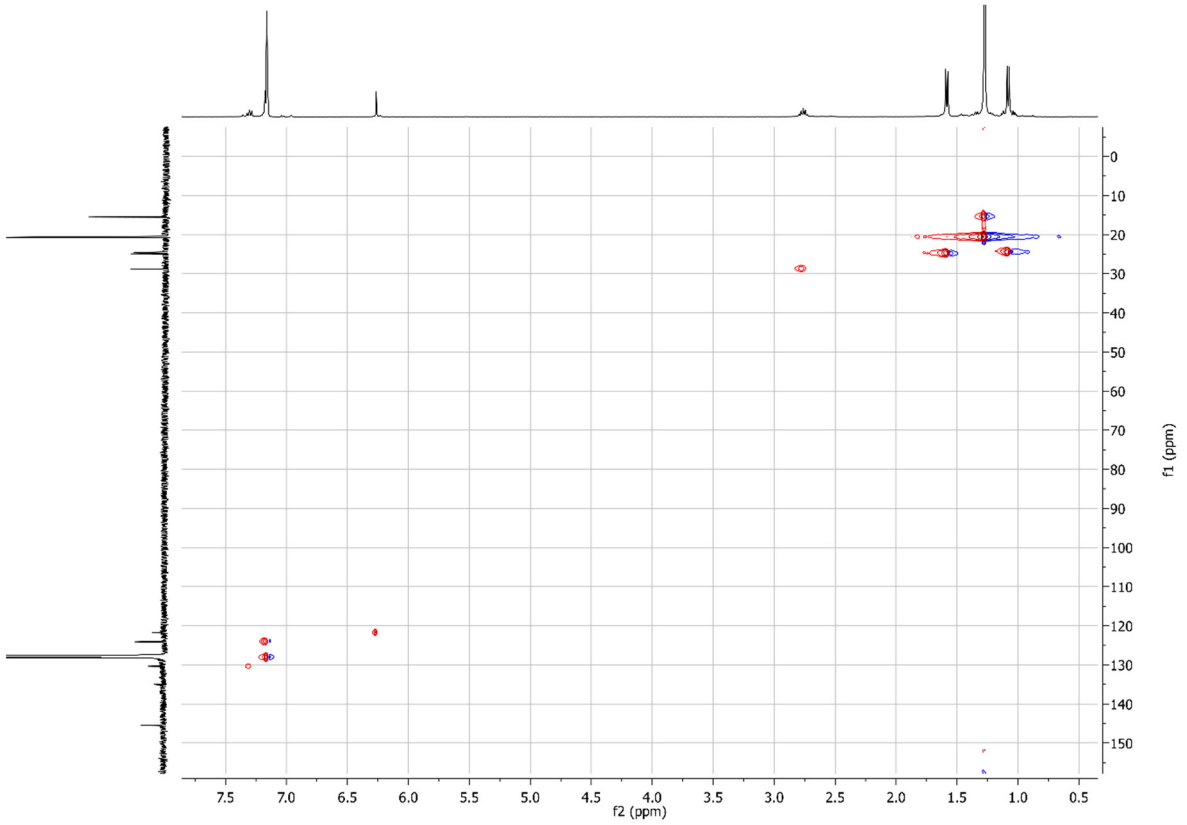

Figure SI 5: 2D-HSQC NMR of compound **1** in C_6D_6 revealing $Me_{iPr(silyl)}$ and $CH_{iPr(silyl)}$ to appear as one signal (pseudo singlet) in the ^1H NMR spectrum.

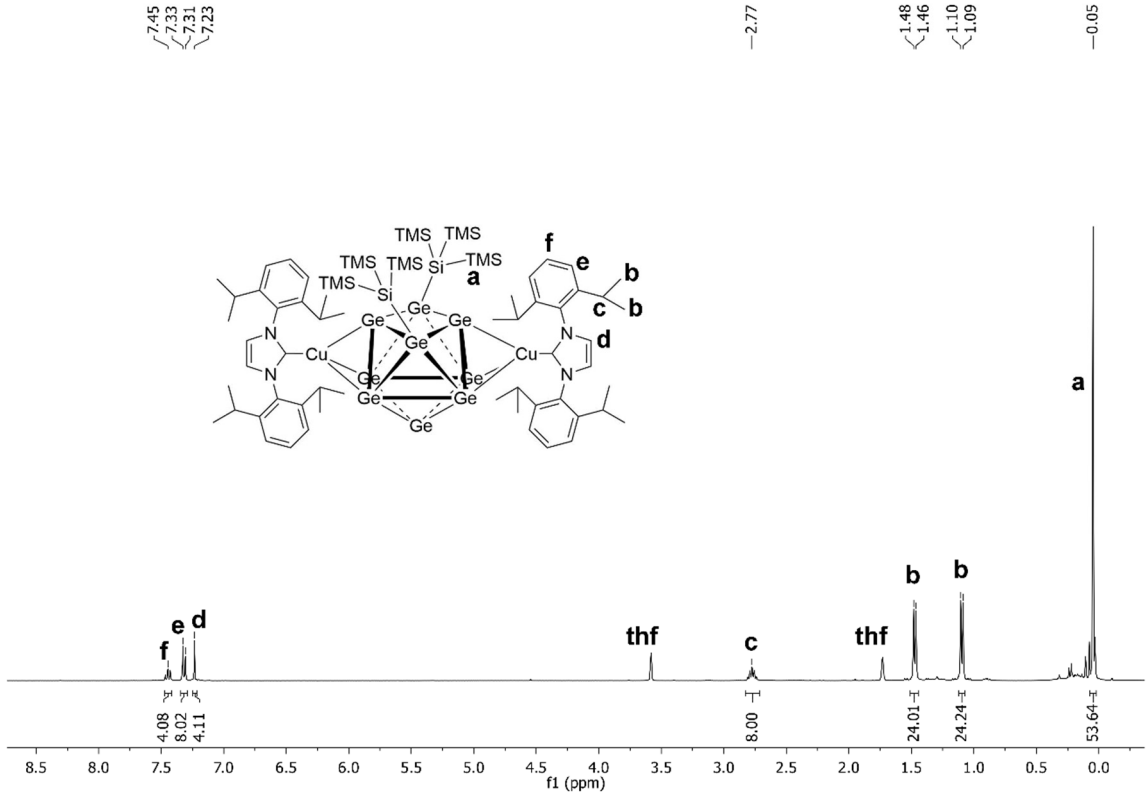

Figure SI 6: ^1H NMR of compound **2** in thf-d_8.

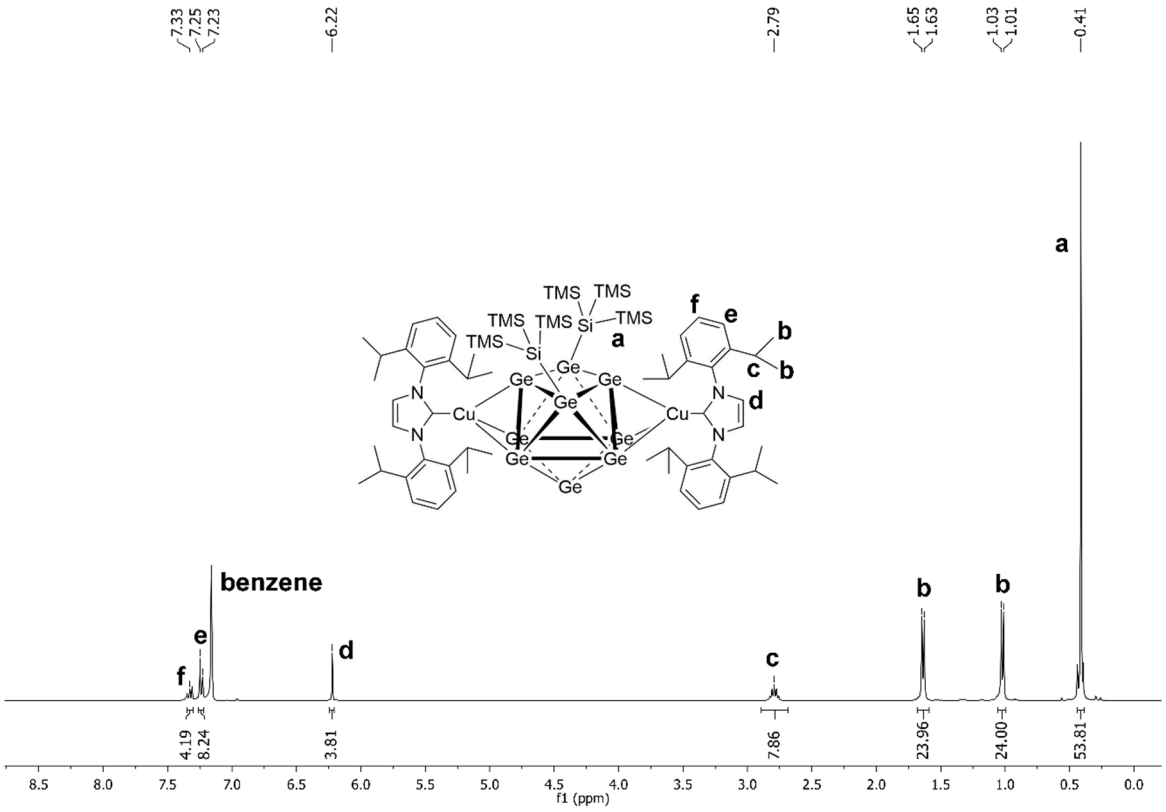

Figure SI 7: ^{1}H NMR of compound **2** in C_6D_6.

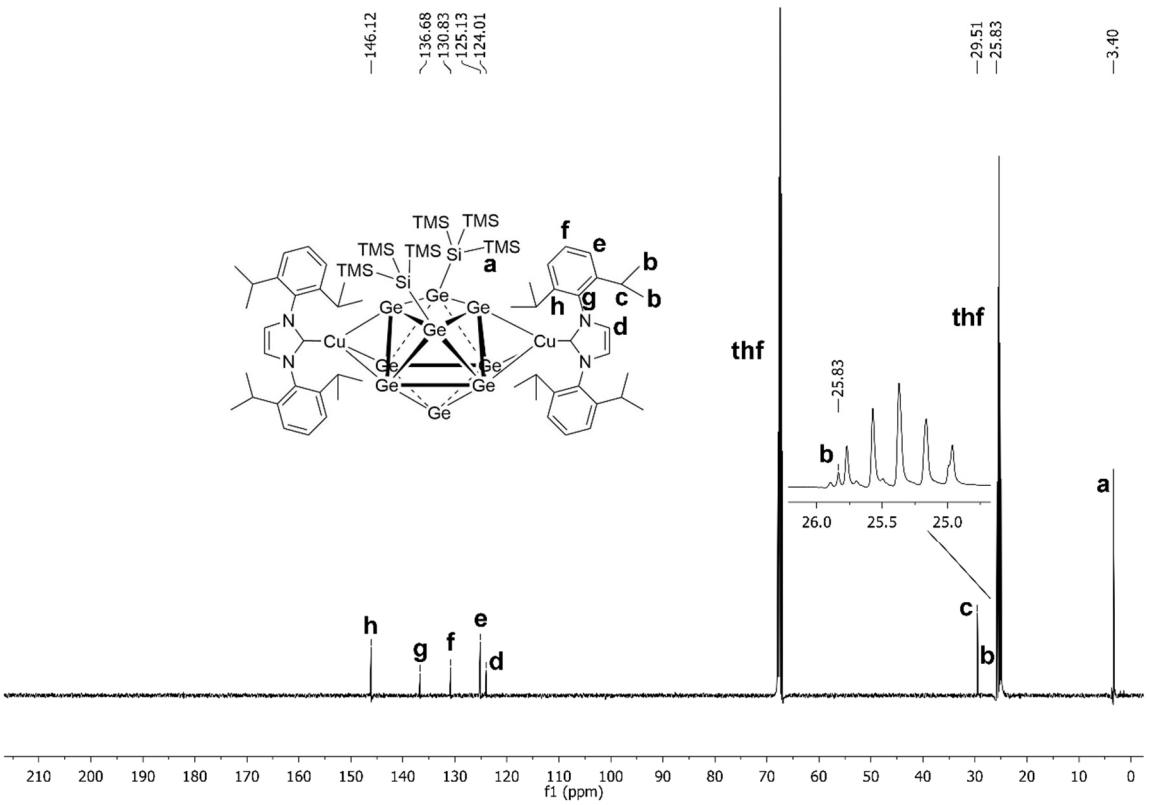

Figure SI 8: ^{13}C NMR of compound **2** in thf-d_8.

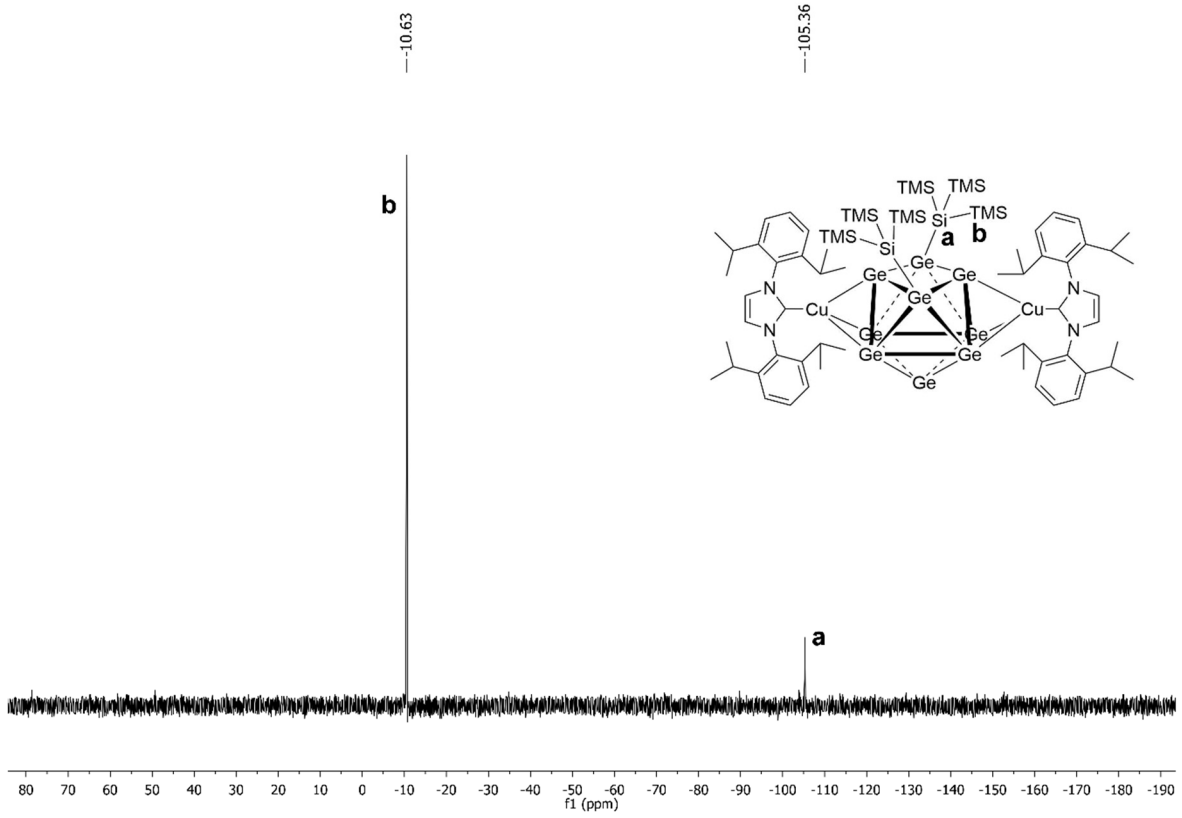

Figure SI 9: ^{29}Si-INEPT NMR of compound **2** in thf-d_8.

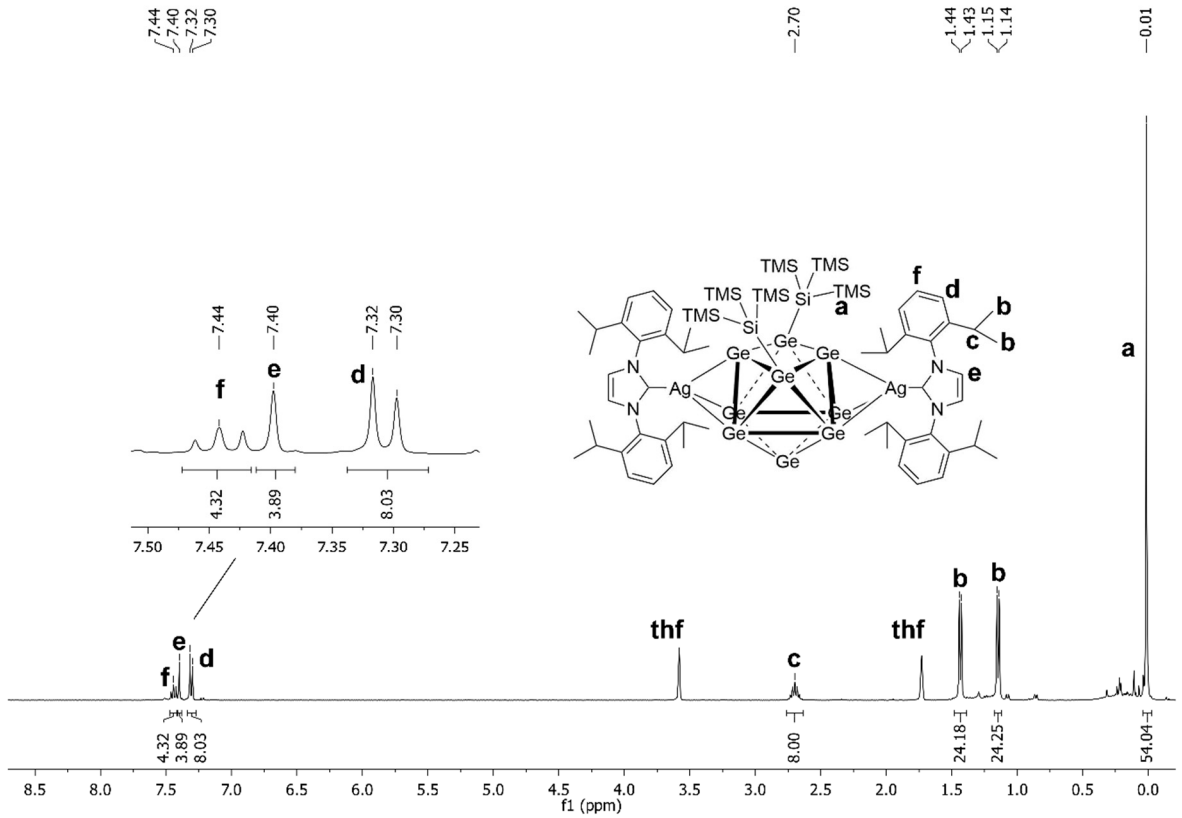

Figure SI 10: ^{1}H NMR of compound **3** in thf-d_8.

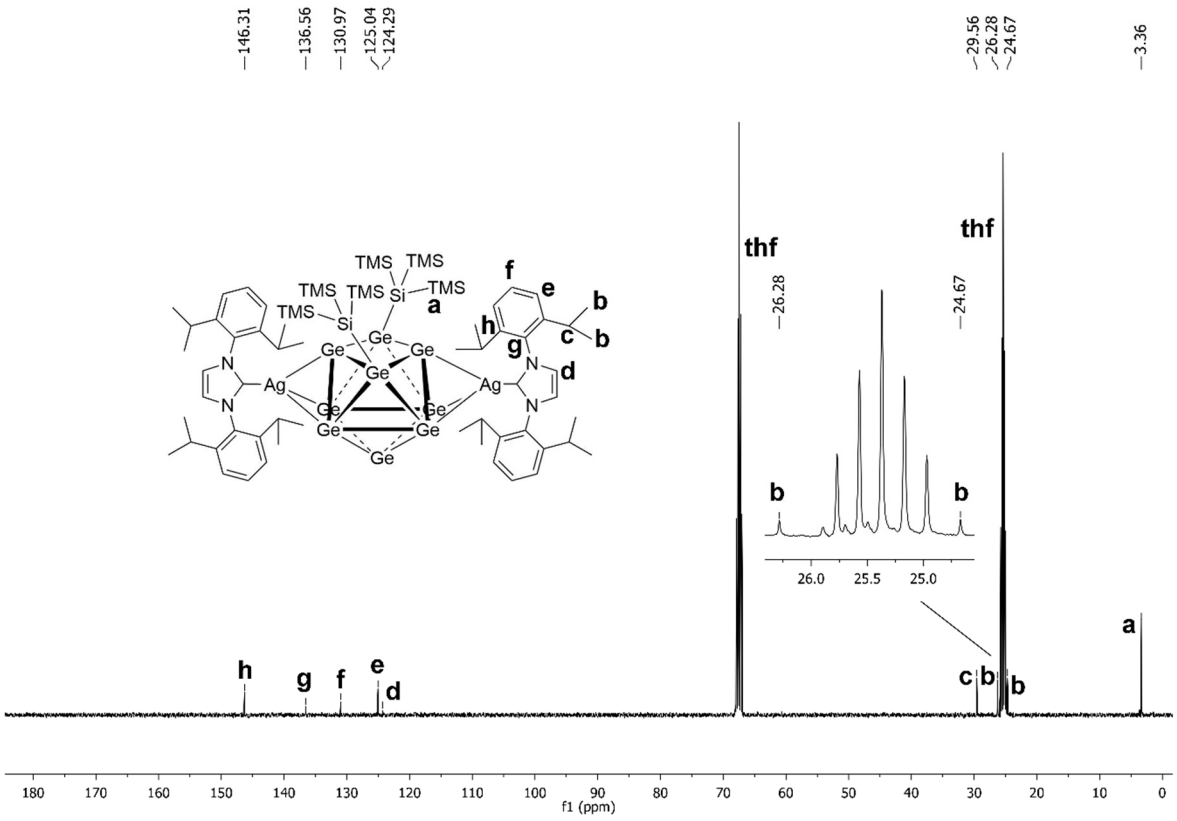

Figure SI 11: ^{13}C NMR of compound **3** in thf-d_8.

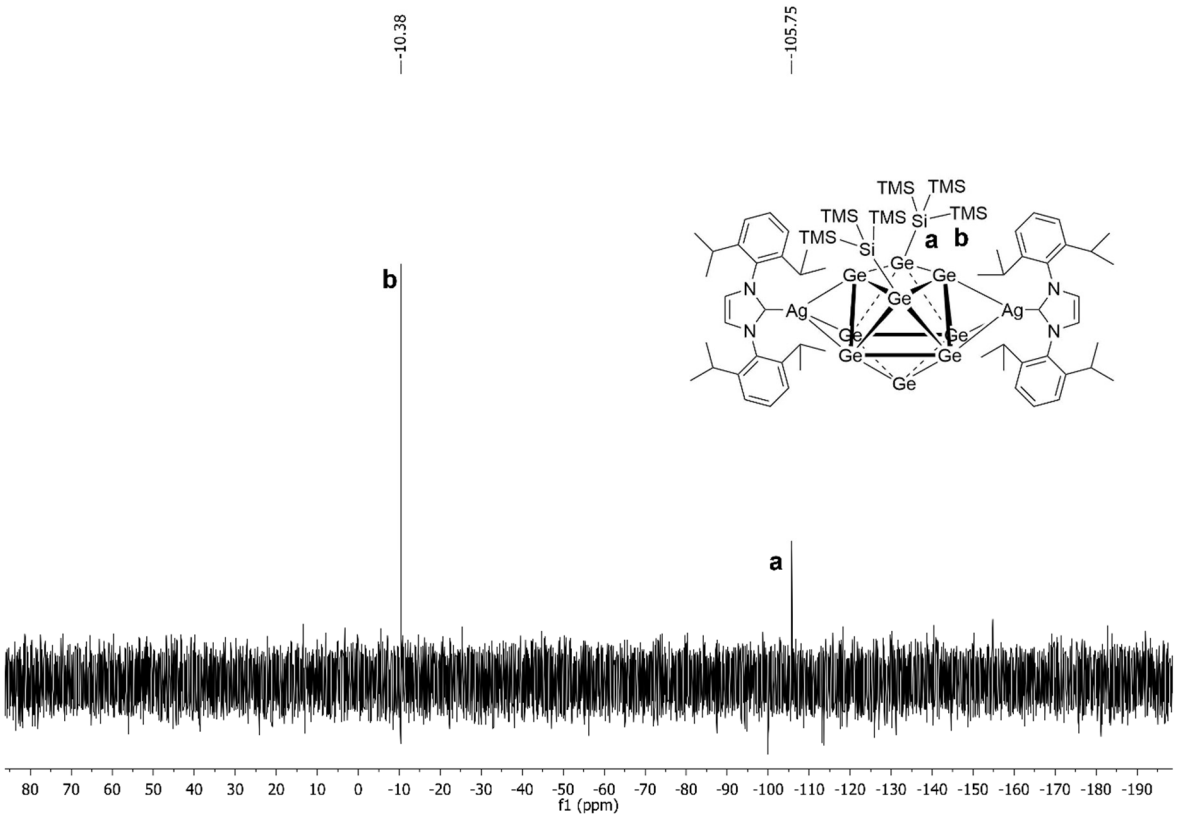

Figure SI 12: ^{29}Si-INEPT NMR of compound **3** in thf-d_8.

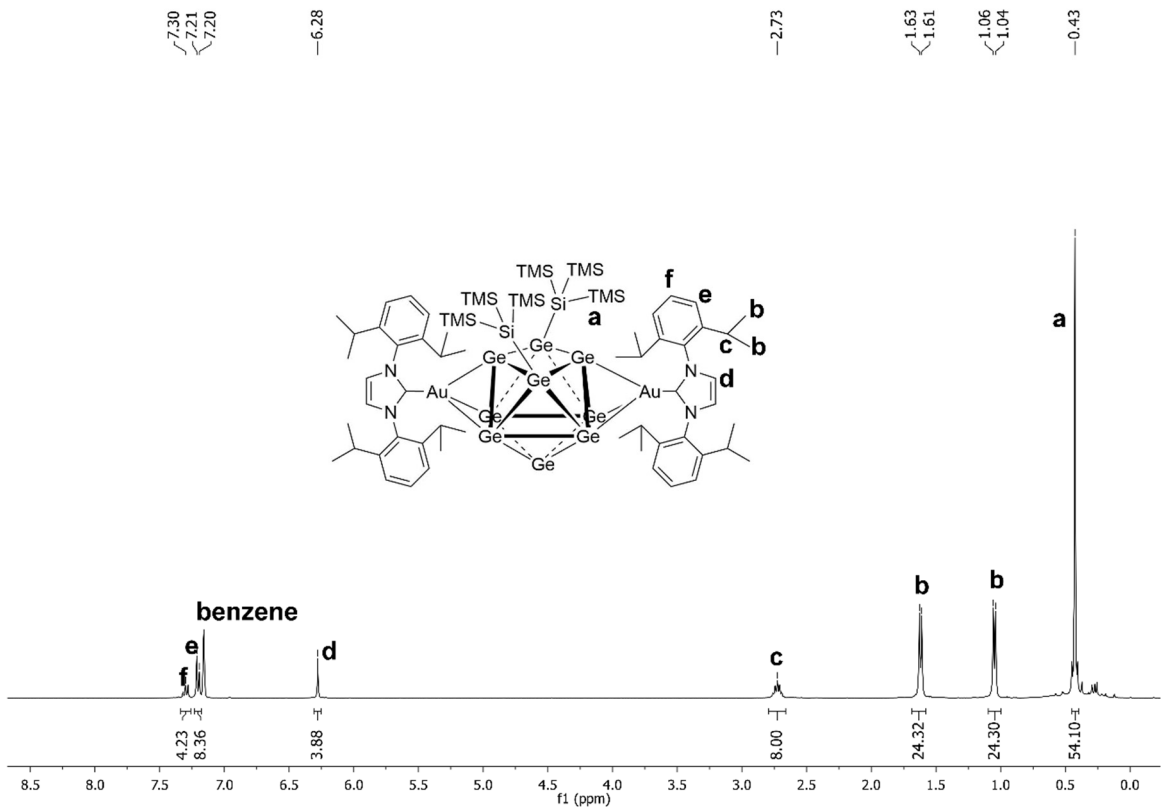

Figure SI 13: ^{1}H NMR of compound **4** in C_6D_6.

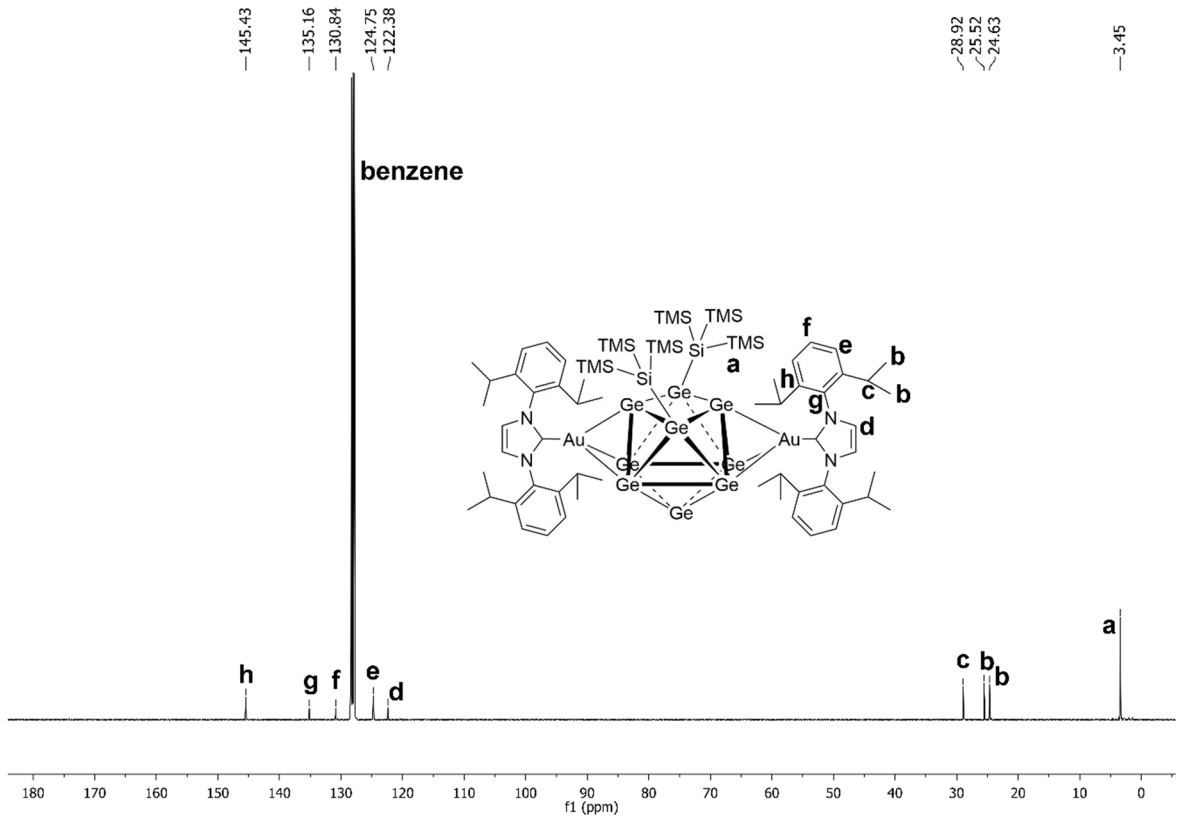

Figure SI 14: ^{13}C NMR of compound **4** in C_6D_6.

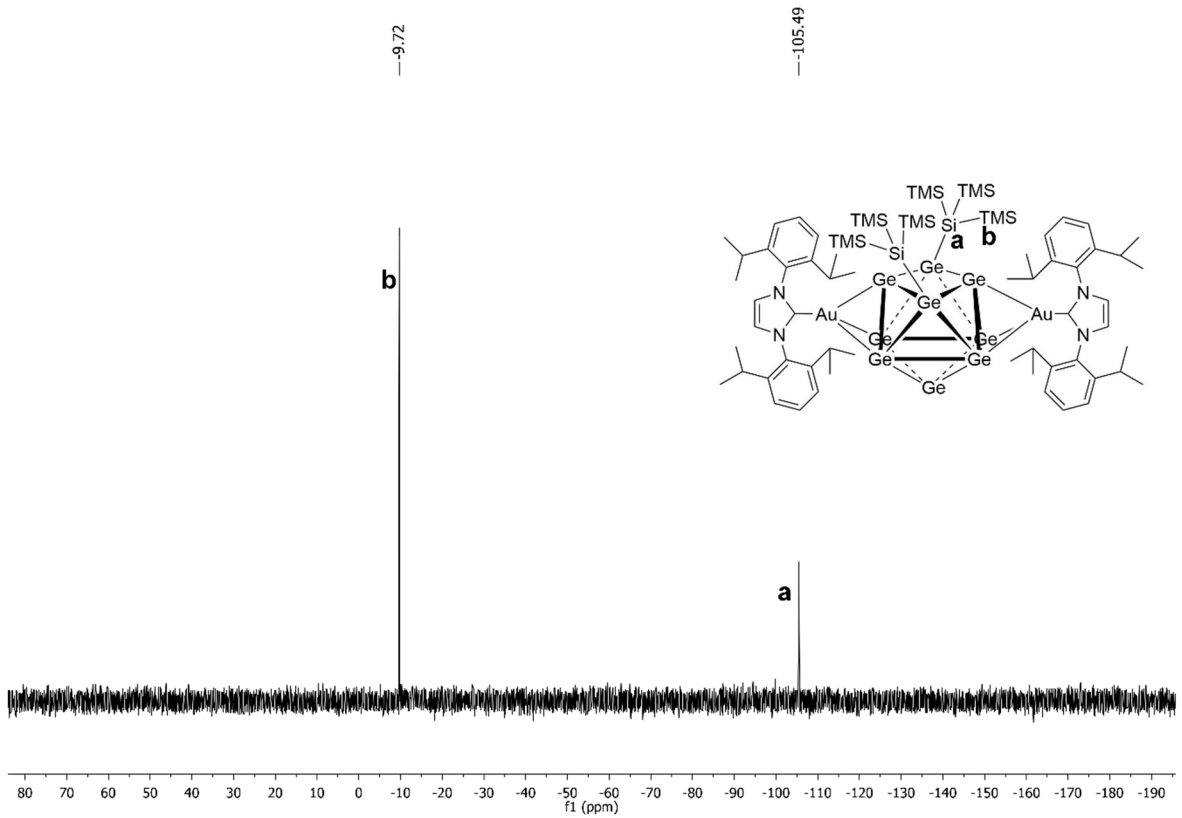

Figure SI 15: ^{29}Si-INEPT NMR of compound **4** in C_6D_6.

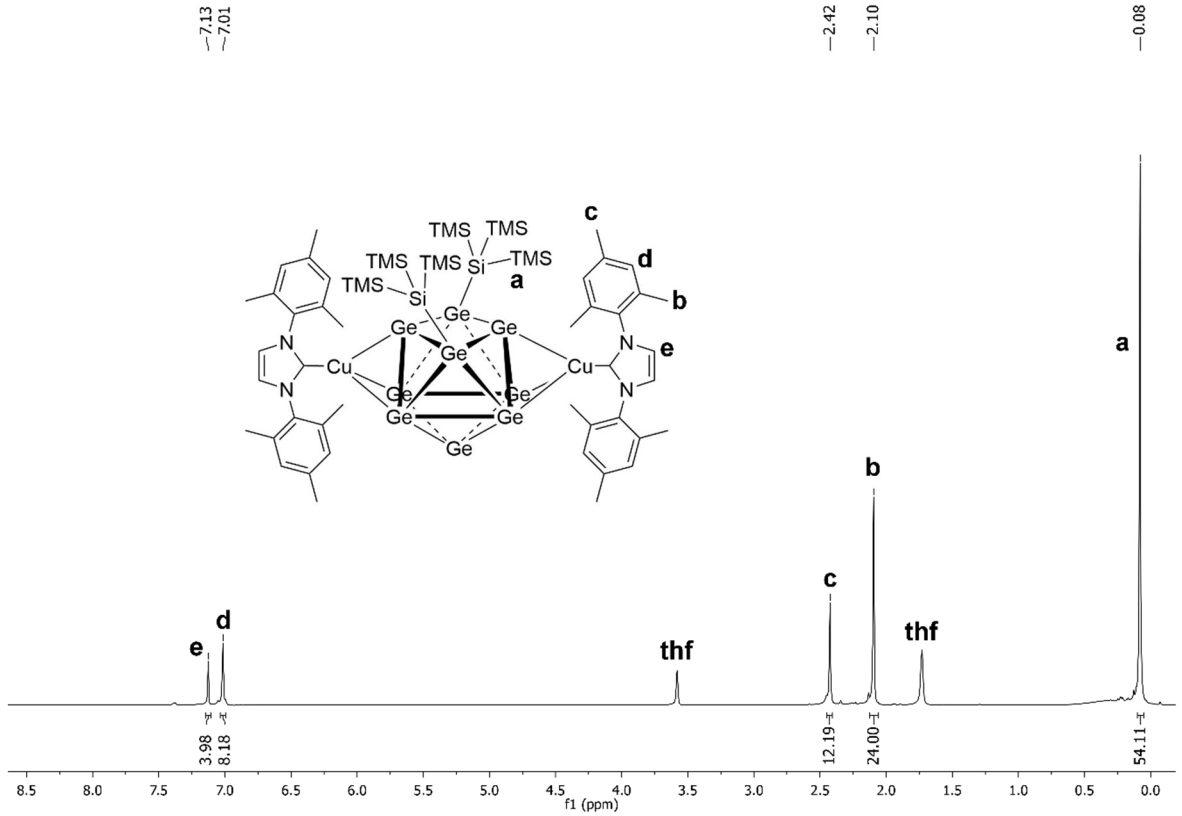

Figure SI 16: ^{1}H NMR of compound **5** in thf-d_8.

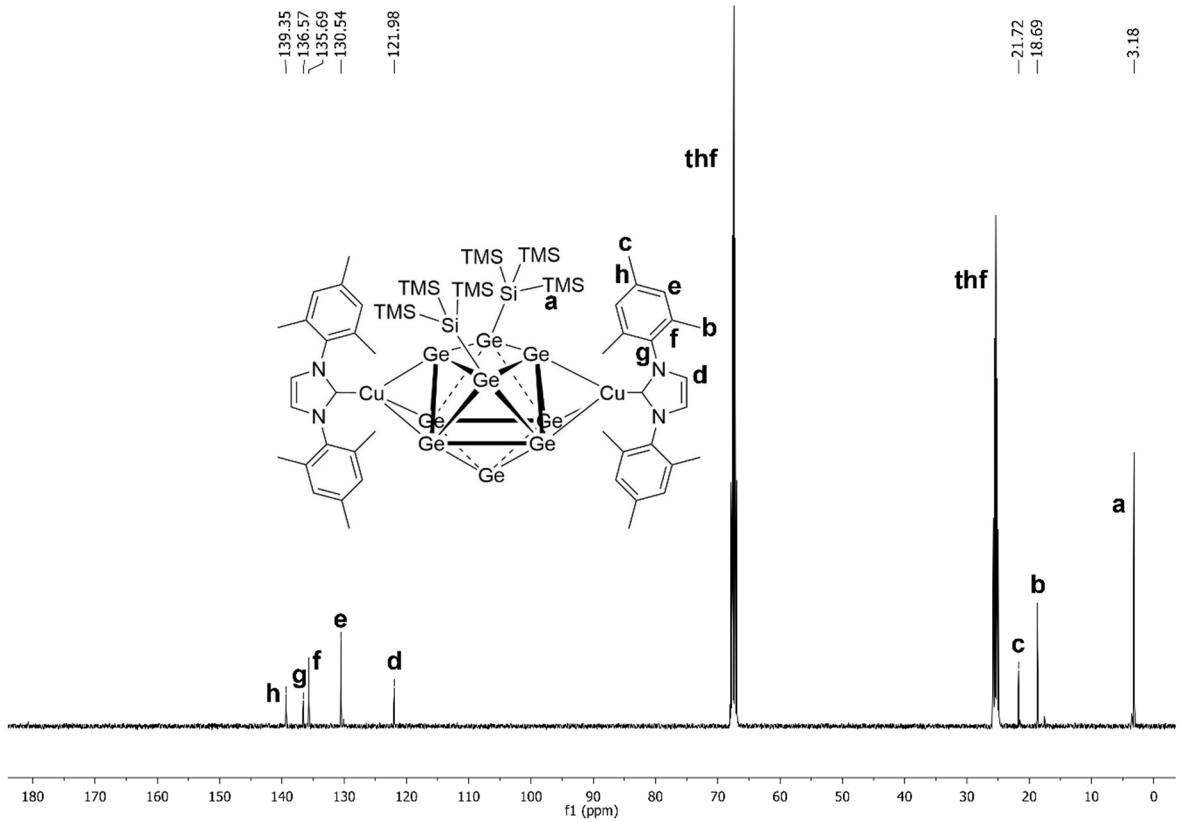

Figure SI 17: ^{13}C NMR of compound **5** in thf-d_8.

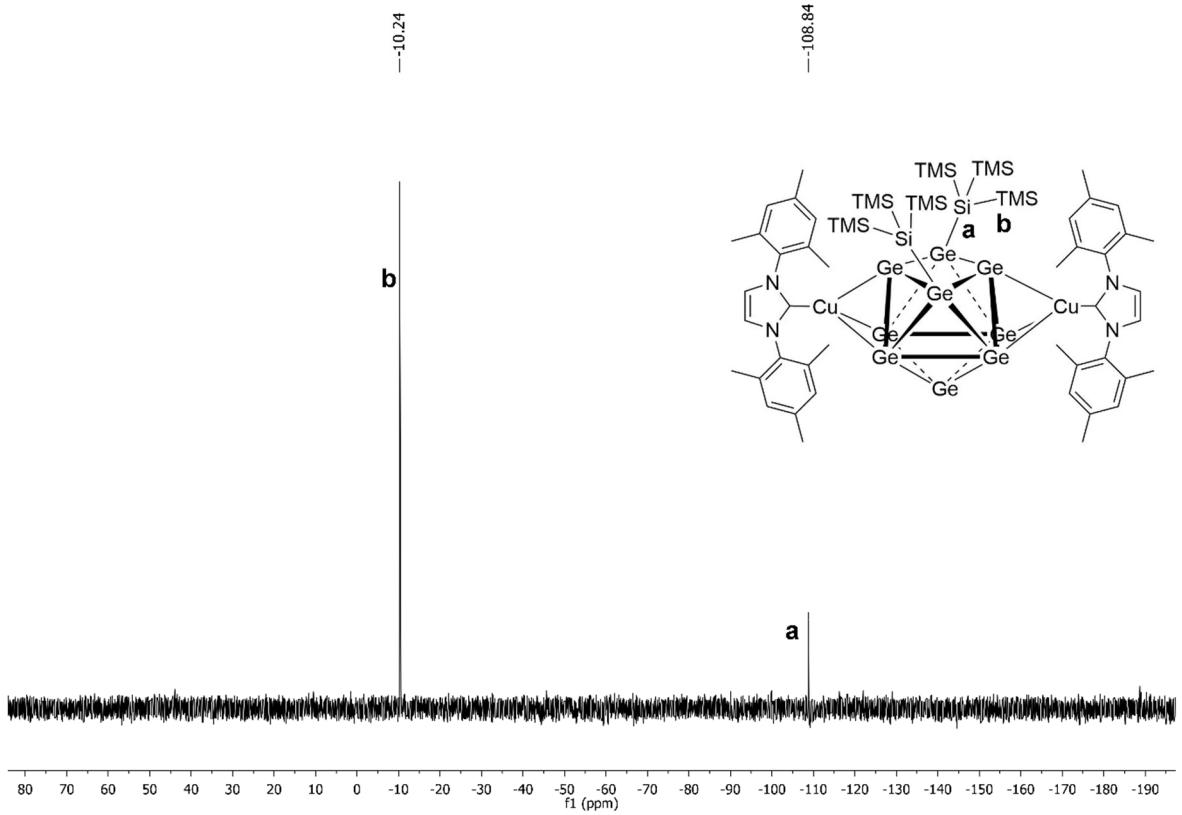

Figure SI 18: ^{29}Si-INEPT NMR of compound **5** in thf-d_8

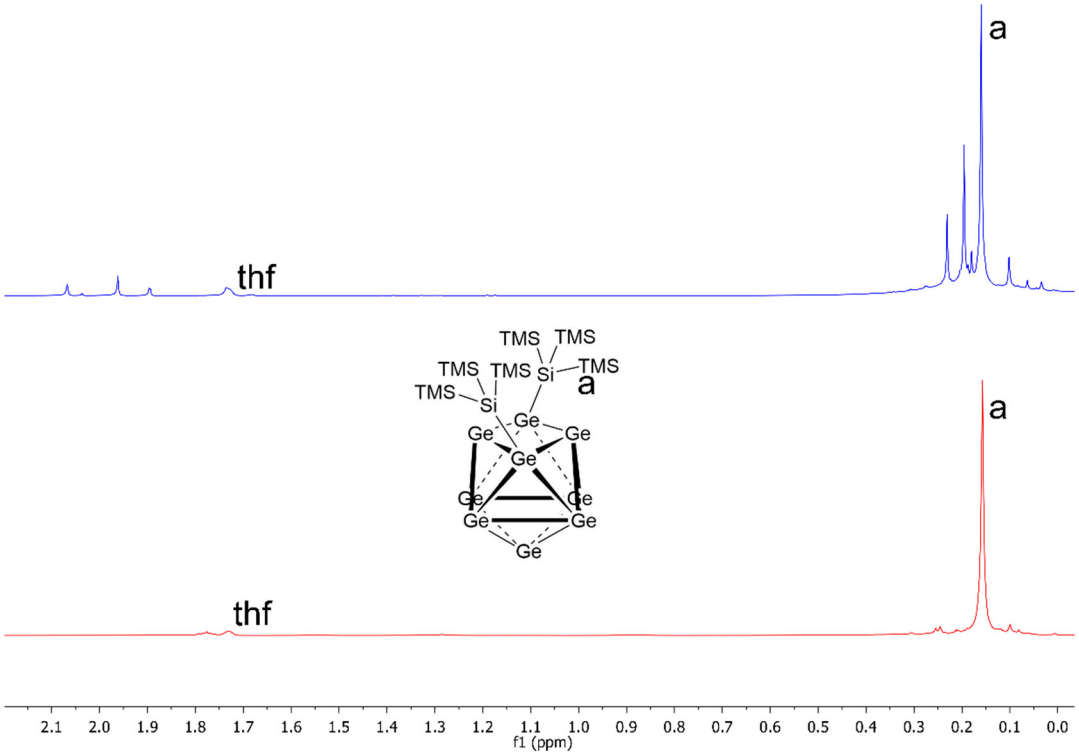

Figure SI 19: Comparison of ^{1}H NMR spectra of worked-up product of silylation of $K_{12}Ge_{17}$ with $Si(TMS)_3Cl$ (6 eq.) (blue/top) and $[Ge\{Si(TMS)_3\}]^{2-}$ (red/bottom) in thf-d_8.

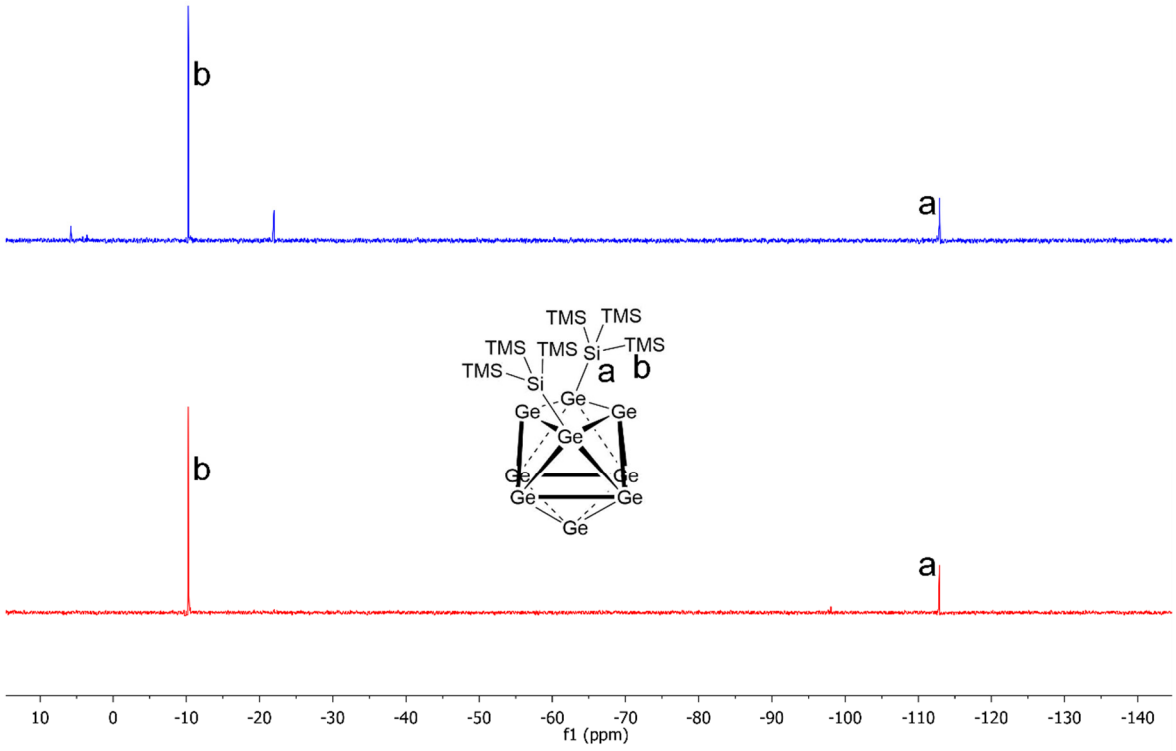

Figure SI 20: Comparison of ^{29}Si-INEPT NMR spectra of worked-up product of silylation of $K_{12}Ge_{17}$ with $Si(TMS)_3Cl$ (6 eq.) (blue/top) and $[Ge\{Si(TMS)_3\}]^{2-}$ (red/bottom) in thf-d_8.

5.6 Early Transition Metal Complexes of $[Ge_9\{Si(TMS)_3\}_n]^{(4-n)-}$ (*n*: 2, 3) – Synthesis and Characterization of $[Cp_2Ti(MeCN)(\eta^1\text{-}Ge_9\{Si(TMS)_3\}_3)]$ and $K_3[Cp_2Ti(\eta^1\text{-}Ge_9\{Si(TMS)_3\}_2)_2]$

F. S. Geitner, W. Klein, O. Storcheva, T. Don Tilley, T. F. Fässler*

Manuscript for publication

Content and Contributions

The scope of this work was the investigation of the reactivity of silylated [Ge_9] clusters towards the Ti(III) complex [$Cp_2TiCl]_2$, aiming for the synthesis of novel Ti(III)-germanide complexes. These reactivity studies were carried out in the laboratories of Prof. T. Don Tilley at the University of California, Berkeley. Reactions of the tris-silylated [Ge_9] cluster [$Ge_9\{Si(TMS)_3\}_3]^-$ with [$Cp_2TiCl]_2$ were carried out in toluene solution at room temperature. Subsequent re-crystallization at low temperature gave crystals of the neutral compound [$Cp_2Ti(MeCN)(\eta^1\text{-}Ge_9\{Si(TMS)_3\}_3)$]. Moreover, investigations on the reactivity of the bis-silylated [Ge_9] cluster [$Ge_9\{Si(TMS)_3\}_2]^{2-}$ towards [$Cp_2TiCl]_2$ were carried out in thf solution at room temperature. Subsequent recrystallization from toluene solution at low temperature gave crystals of $K_3[Cp_2Ti(\eta^1\text{-}Ge_9\{Si(TMS)_3\}_2)_2]$, comprising the novel tri-anion $[Cp_2Ti(\eta^1\text{-}Ge_9\{Si(TMS)_3\}_2)_2]^{3-}$, in which Ti(III) is coordinated by two $[Ge_9\{Si(TMS)_3\}_2]^{2-}$ clusters. This novel anion can either be described as $[Cp_2Ti]^+$ fragment bridged [Ge_9] dimer or as Ti(III) complex bearing two germanide cluster ligands. The refinement of the crystal structure of $K_3[Cp_2Ti(\eta^1\text{-}Ge_9\{Si(TMS)_3\}_2)_2]$, especially the modelling of some severely disordered silyl groups and co-crystallized toluene molecules, was done by Dr. Wilhelm Klein. The formation of single *exo* Ge-Ti bonds in both novel species manifests this bonding mode to be favoured for interactions of Group 14 element *Zintl* clusters with Ti(III) fragments. Besides single crystal X-ray diffraction the novel Ti(III)-germanide complexes were characterized by means of elemental analysis and EPR spectroscopy. The EPR measurements were carried out by Dr. Oksana Storcheva. This manuscript for publication was written in the course of this thesis.

Early Transition Metal Complexes of $[Ge_9\{Si(TMS)_3\}_n]^{(4-n)-}$ (*n*: 2, 3) – Synthesis and Characterization of $[Cp_2Ti(MeCN)(\eta^1\text{-}Ge_9\{Si(TMS)_3\}_3)]$ and $K_3[Cp_2Ti(\eta^1\text{-}Ge_9\{Si(TMS)_3\}_2)_2]$

Felix S. Geitner,[a] Wilhelm Klein,[b] Oksana Storcheva,[b] T. Don Tilley[c] and Thomas F. Fässler[b*]

[a] Department Chemie, Technische Universität München, Lichtenbergstraße 4, 85747 Garching b. München and WACKER Institute for Silicon Chemistry.

[b] Department Chemie, Technische Universität München, Lichtenbergstraße 4, 85747 Garching b. München.

[c] Department of Chemistry, University of California, Berkeley, CA 94720-1460 Berkeley

Abstract

Anionic clusters with homoatomic $[Ge_9]$ core represent interesting examples for molecules with Ge atoms in low oxidation state. In this study their behaviour towards early transition metal complexes was investigated. Herein we report the syntheses of Ti(III) complexes of silylated $[Ge_9]$ *Zintl* clusters, which represent rare examples for molecular complexes comprising Ti-Ge interactions. The neutral species $[Cp_2Ti(MeCN)(\eta^1\text{-}Ge_9\{Si(TMS)_3\}_3)]$ (**1**) was obtained by reaction of $K[Ge_9\{Si(TMS)_3\}_3]$ with $[Cp_2TiCl]_2$ in toluene and following re-crystallization, yielding the product species as dark-orange crystals. By contrast, reactions of $K_2[Ge_9\{Si(TMS)_3\}_2]$ with $[Cp_2TiCl]_2$ in thf and subsequent re-crystallization from toluene solution resulted in the formation of dark green crystals of $K_3[Cp_2Ti(\eta^1\text{-}Ge_9\{Si(TMS)_3\}_2)_2]$ (**2**). Compound **2** comprises the tri-anion $[Cp_2Ti(\eta^1\text{-}Ge_9\{Si(TMS)_3\}_2)_2]^{3-}$ (**2a**), which can be described as $[Cp_2Ti]^+$ bridged $[Ge_9\{Si(TMS)_3\}_2]^{2-}$ dimer or as a heavily distorted tetrahedral Ti(III)-complex bearing two germanide cluster ligands. In both novel compounds donor-acceptor interactions between single Ge vertex atoms of the $[Ge_9]$ clusters and Ti(III) occur. Compounds **1** and **2** were characterized by means of single crystal X-ray diffraction, EPR spectroscopy and elemental analysis.

Introduction

Homoatomic *Zintl* clusters $[E_9]^{4-}$ (*E*: Si-Pb) can be extracted from solid state *Zintl* phases of the compositions A_4E_9 (*A*: alkali metal; *E*: Ge-Pb) and $A_{12}E_{17}$ (*A*: alkali metal; *E*: Si-Sn) and are subsequently available for further reactions. In the meantime, reactions of *Zintl* clusters with organometallics, main-group element compounds and organic reagents have led to a plethora of different *Zintl* cluster compounds.[1-4] Regarding reactions of *Zintl* clusters with organometallics, mainly complexes of late transition metals have been considered. In the resulting transition metal *Zintl* cluster complexes, the organometallic fragments typically

interact with the $[E_9]^{4-}$ (*E*: Si-Pb) clusters *via* their open square planes in a η^4-coordination mode as for example observed in $[PhZn(\eta^4\text{-}E_9)]^{3-}$ (*E*: Si–Pb)[5] or $[(CO)_3M(\eta^4\text{-}E_9)]^{4-}$ (*M*: Cr, Mo, W; *E*: Sn, Pb).[6-9] However, organometallic fragments can also interact with the electron lone-pairs situated at the clusters' vertex atoms, which was shown by the isolations of $[(\eta^4\text{-}Ge_9)Cu(\eta^1\text{-}Ge_9)]^{7-}$,[10] $[(\eta^4\text{-}Ge_9)Zn\text{-}(\eta^1,\eta^1\text{-}Ge_9)\text{-}Zn(\eta^4\text{-}Ge_9)]^{8-}$ and $^1_\infty\{Zn[(\eta^4\text{:}\eta^1\text{-}Ge_9)]\}^{2-}$.[11] Generally, examples for successful reactions of tetrel element *Zintl* clusters with early transition metal complexes are rare. This can be explained by the highly reductive nature of the polyanionic *Zintl* clusters (due to their high negative charge), which can also easily undergo redox reactions with their reaction partners. Recently, the incorporation of lanthanoid cations in less negatively charged bimetallic (Group 14-Group 15 element) *Zintl* anions was achieved,[12] and the isolation of $[Cp_2Ti(NH_3)(\eta^1\text{-}Sn_9)]^{3-}$ from mixtures of K_4Sn_9 and $[Cp_2TiCl]_2$ in NH_3(l) at low temperature revealed that the attachment of early transition metal fragments to homoatomic $[E_9]^{4-}$ tetrel element *Zintl* clusters is also possible.[13] Interestingly, the attachment of the $[Cp_2Ti(NH_3)]^+$ fragment at $[Sn_9]^{4-}$ occurs *via* donor-acceptor interactions between an electron lone-pair situated at a tin vertex atom of the cluster and Ti(III). Alongside $[Cp_2Ti(NH_3)(\eta^1\text{-}Sn_9)]^{3-}$ further species comprising Ti-Sn interactions were found in $[Ti(Sn_8)Cp]^{3-}$ and $[Ti_4Sn_{15}Cp_5]^{n-}$ (*n*: 4 or 5), resulting from the fragmentation of the $[Sn_9]^{4-}$ clusters upon reaction with $[Cp_2TiCl]_2$.[13] By contrast, in the case of $[Ge_9]^{4-}$, the introduction of fragments of early transition metal complexes has not been achieved, yet. However, recently methods to decorate the $[Ge_9]$ clusters with several silyl groups were found. Despite the attached silyl moieties, which decrease the charge of the $[Ge_9]$ clusters and enhance their solubility and stability, the silylated species $[Ge_9\{Si(TMS)_3\}_n]^{(4-n)-}$ (*n*: 2, 3) still comprise uncoordinated Ge vertex atoms, which can interact with further reaction partners.[14-16] Subsequent reactions of $[Ge_9\{Si(TMS)_3\}_3]^-$ with transition metal complexes yielded a series of transition metal bridged dimers $[M(\eta^3\text{-}Ge_9\{Si(TMS)_3\}_3)_2]^{n-}$ (*M*: Mn,[17] Cu-Au,[18, 19] Pd,[20] Zn-Hg;[21] *n*: 0, -1, -2), and further fourfold coordinated $[Ge_9]$ clusters $[NHC^{Dipp}M(\eta^3\text{-}Ge_9\{Si(TMS)_3\}_3)]$ (*M*: Cu, Ag, Au),[22] $[^iPr_3PCu(\eta^3\text{-}Ge_9\{Si(TMS)_3\}_3)]$,[23] $[dppeNi(\eta^3\text{-}Ge_9\{Si(TMS)_3\}_3)]$[17] or $[Cp^*Zn(\eta^3\text{-}Ge_9\{Si(TMS)_3\}_3)]$ were obtained.[23] In all these species the organometallic fragments are attached at triangular Ge faces of the $[Ge_9]$ clusters in a η^3-coordination mode. Moreover, similar $[Ge_9]$ cluster transition metal interactions were observed in $[(NHC^{Dipp}M)_2(\eta^3,\eta^3\text{-}Ge_9\{Si(TMS)_3\}_2)]$ (*M*: Cu, Ag, Au), in which the bis-silylated $[Ge_9]$ cluster bridges two $[NHC^{Dipp}M]^+$ (*M*: Cu, Ag, Au) moieties.[24] Different coordination modes were observed between Group 6 carbonyl fragments and $[Ge_9\{Si(TMS)_3\}_3]^-$. In $[(CO)_3M(\eta^5\text{-}Ge_9\{Si(TMS)_3\}_3)]^-$ (*M*: Cr, Mo, W), interactions between the Group 6 atom and five Ge vertices of the $[Ge_9]$ core occur and the Cr atom is integrated in the cluster skeleton.[25, 26] By contrast, donor-acceptor interactions between an electron lone-pair situated at a Ge vertex atom and the $[Cr(CO)_5]$ fragment were observed in $[(CO)_5Cr(\eta^1\text{-}Ge_9\{Si(TMS)_3\}_3)]^-$, which revealed that the lone-pairs situated at uncoordinated Ge

vertices of the silylated [Ge_9] cluster species are still accessible for Lewis acidic transition metal fragments.[25] In combination with the previous isolation of [$Cp_2Ti(NH_3)(\eta^1\text{-}Sn_9)$]$^{3-}$, comprising analogous Ti-Sn interactions,[13] this triggered us to investigate the reactivity of the more stable [$Ge_9\{Si(TMS)_3\}_n$]$^{(4-n)-}$ (*n*: 2, 3) clusters towards the early transition metal complex [$Cp_2TiCl]_2$, aiming for the introduction of [$Cp_2Ti]^+$ fragments at the [Ge_9] core.

Results and Discussion

Reactions of K[$Ge_9\{Si(TMS)_3\}_3$] with the bis(cyclopentadienyl)titanium(III)chloride dimer [$Cp_2TiCl]_2$ were conducted by addition of green toluene solutions of the Ti(III)-complex (0.5 equiv.) to orange suspensions of K[$Ge_9\{Si(TMS)_3\}_3$] (1.0 equiv.) in toluene, which resulted in deep red reaction mixtures. Stirring at room temperature overnight and subsequent evaporation of the solvent *in vacuo* yielded a brown solid, which was washed with pentane and re-dissolved in toluene. The resulting deep red solution was layered with pentane and placed in a freezer at -35 °C, yielding dark orange block-shaped crystals, suitable for single crystal X-ray diffraction, after two days. The novel species was identified as [$Cp_2Ti(MeCN)(\eta^1\text{-}Ge_9\{Si(TMS)_3\}_3)$] (**1**), which crystallizes in the monoclinic space group $P2_1/c$ with one solvent molecule (pentane/toluene) per formula unit. The acetonitrile molecule coordinating to Ti(III) originates from residual solvent in the reactant K[$Ge_9\{Si(TMS)_3\}_3$].
In compound **1** the shape of the [Ge_9] cluster can be described as distorted tricapped trigonal prism [triangular prism bases: Ge1-Ge5-Ge8 and Ge3-Ge6-Ge7; prism heights: d(Ge1-Ge3): 3.812(3) Å, d(Ge5-Ge6): 3.077(3) Å, d(Ge7-Ge8): 3.053(3) Å], in which one prism height is significantly elongated resulting in C_{2v} symmetry (Figure 1; Table 1). The silyl groups are bound to the capping Ge atoms (Ge2, Ge4 and Ge9) with distances between 2.371(2) Å (Ge9-Si3) and 2.413(2) Å (Ge4-Si2). Within the [Ge_9] core, the shortest distances are observed between Ge atoms of the triangular bases of the prism and capping Ge atoms [d(Ge8-Ge9): 2.512(1) Å], and the longest distances occur between Ge atoms within the triangular bases of the prism [d(Ge6-Ge7) 2.854(2) Å]. The observed Ge-Ge and Ge-Si distances are in the range of previously reported data.[22, 25] The [Ge_9] cluster binds to Ti(III) with a single Ge vertex atom in one of its trigonal bases [d(Ge1-Ti): 2.767(2) Å] under formation of donor-acceptor interactions between the electron lone-pair situated at the Ge atom and the Lewis acidic Ti(III). The Ti-Ct (Ct: centroid of Cp ring) distances of 2.049(1) Å (Ti-Ct1) or 2.045(1) Å (Ti-Ct2) and the Ti-N distance of 2.164(6) Å are in accordance with previously reported data for similar Ti(III) complexes.[13, 27, 28] The four ligands (2 · cyclopentadienyl, [Ge_9] cluster and acetonitrile) coordinate Ti(III) in heavily distorted tetrahedral manner, which is expressed by the Ct1-Ti-Ct2 (Ct: centroid of Cp ring): 135.34(5)° and the Ge1-Ti-N: 84.59(3)° angles.

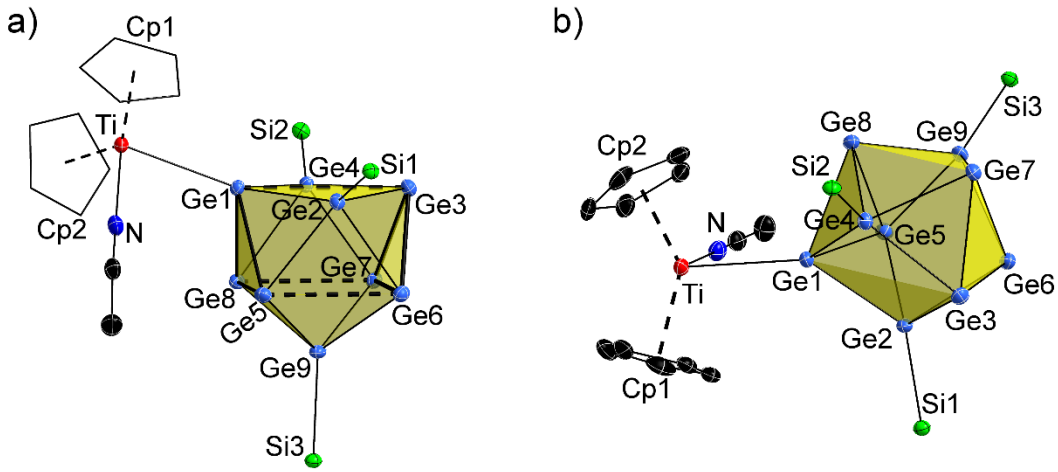

Figure 1: Two perspectives of the labelled molecular structure of compound **1**. All displacement ellipsoids are shown at a 50 % probability level. a) C_{2v} symmetric shape of the [Ge_9] cluster with the hypersilyl groups being bound to the capping Ge atoms (Ge2, Ge4 and Ge9) of the tricapped trigonal prism, and the [$Cp_2Ti(MeCN)]^+$ moiety coordinating to Ge1 in one of the trigonal bases of the prism. The trigonal bases of the prism are emphasized by thick bonds and prism heights are indicated by dashed lines. b) Distorted tetrahedral coordination of Ti(III) by its four ligands. For clarity, TMS groups of the hypersilyl ligands of [Ge_9], as well as protons and solvent molecules are omitted in both pictures. Selected bond lengths and angles of **1** are summarized in Table 2 and in Table S2 in the Supporting information.

The analytical purity of **1** was confirmed by elemental analysis and in EPR spectroscopic investigations carried out at 130 K with a frozen thf solution of **1**, its g-factor was determined to be g_{iso} = 1.967 (anisotropic values and respective spectrum are presented in the Supporting information). In ESI-MS examinations carried out with thf solutions of dissolved crystals of compound **1**, exclusively $[Ge_9\{Si(TMS)_3\}_3]^-$ (*m/z* 1396.8) was monitored, which is formed upon cleavage of the $[Cp_2Ti(MeCN)]^+$ moiety from **1** during the ionization process in the mass spectrometer.

Reactions between $K_2[Ge_9\{Si(TMS)_3\}_2]$ and $[Cp_2TiCl]_2$ were carried out by adding green thf solutions of $[Cp_2TiCl]_2$ (0.5 equiv.) to deep red solutions of $[Ge_9\{Si(TMS)_3\}_2]^{2-}$ (1.0 equiv.) in thf, resulting in the formation of brown/green reaction mixtures. Stirring at room temperature for 3 h and subsequent evaporation of the solvent *in vacuo*, yielded a brown solid. The residue was washed with pentane, before it was dissolved in toluene and filtered to remove remaining solids. The resulting deep red filtrate was placed in a freezer at -35 °C for recrystallization. Overnight, dark-green block-shaped crystals were obtained, which were suitable for single crystal X-ray diffraction. The crystals were identified as $K_3[Cp_2Ti(\eta^1\text{-}Ge_9\{Si(TMS)_3\}_2)_2]$ (**2**) comprising the tri-anion $[Cp_2Ti(\eta^1\text{-}Ge_9\{Si(TMS)_3\}_2)_2]^{3-}$ (**2a**). Compound **2** crystallizes in the monoclinic space group $P2_1/c$ with the unit cell containing two crystallographically independent dimeric cluster anions (**2a-I** and **2a-II**) and six co-crystallized toluene molecules (some of the toluene molecules coordinate to the K^+ cations) per formula unit. In all of the tested crystals some of the silyl groups at the [Ge_9] clusters revealed rotational disorder and were therefore

refined on split position. The shape of the [Ge_9] clusters [**A** (Ge1-Ge9) and **B** (Ge10-Ge18) in **2a-I**, and **C** (Ge19-Ge27) and **D** (Ge28-Ge36) in **2a-II**)] can be best described as heavily distorted tricapped trigonal prims [**A**: triangular prism bases: Ge2-Ge3-Ge7 and Ge4-Ge5-Ge9; prism heights: d(Ge2-Ge5): 3.018(1) Å, d(Ge3-Ge4): 3.069(1) Å, d(Ge7-Ge9): 3.788(1) Å; **B**: triangular prism bases: Ge11-Ge12-Ge16 and Ge13-Ge14-Ge18; prism heights: d(Ge11-Ge14): 3.467(1) Å, d(Ge12-Ge13): 2.967(1) Å, d(Ge16-Ge18): 3.576(1) Å; **C**: triangular prism bases: Ge20-Ge21-Ge25 and Ge22-Ge23-Ge27; prims heights: d(Ge20-Ge23): 3.486(1) Å, d(Ge21-Ge22): 2.981(1) Å, d(Ge25-Ge27): 3.558(1) Å; **D**: triangular prism bases: Ge29-Ge30-Ge34 and Ge31-Ge32-Ge36; prism heights: d(Ge29-Ge32): 3.042(1) Å, d(Ge30-Ge31): 3.019(1) Å, d(Ge34-Ge36): 3.797(1) Å]. In [Ge_9] clusters **A-D** the distortion mainly results from significant elongation or shortening of one of the prism heights (Figure 2). However, since all three prism heights adapt significantly different values in **A-D**, these [Ge_9] cages rather reveal C_S symmetry. The prism heights occurring in the [Ge_9] cores of **1** and **2** (clusters **A**-**D**) are summarized in Table 1.

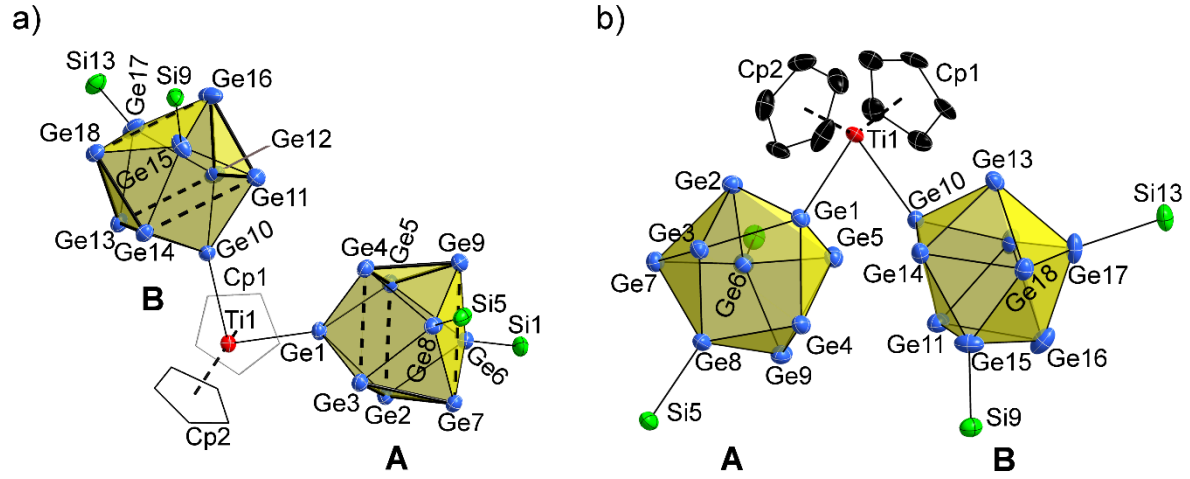

Figure 2: Two perspectives of the labelled molecular structure of **2a-I**. Labelling for **2a**-**II** occurred analogously to **2a**-**I** starting from Ge19. The molecular structure of **2a-II** is shown in the Supporting information. All displacement ellipsoids are shown at a 50 % probability level. a) C_S symmetric shape of the [Ge_9] clusters and coordination of [Ge_9] by the two silyl groups and the $[Cp_2Ti]^+$ fragment *via* the three capping Ge atoms (Ge1, Ge6, Ge8 or Ge10, Ge15, Ge17) of the trigonal prism. The trigonal bases of the prism are emphasized by thick bonds and prism heights are indicated by dashed lines. For clarity, carbon atoms of the cyclopentadienyl rings are represented as grey or black wire sticks. b) Distorted tetrahedral coordination of Ti(III) by its four ligands. In a) and b) protons, solvent toluene molecules and TMS groups of the hypersilyl substituents are omitted and only the major species of disordered silyl groups are shown. Selected bond lengths and angles of **2a-I** and **2a-II** are summarized in Table 2 and in Tables S3 and S4 in the Supporting information.

Table 1: Trigonal prism heights in the [Ge_9] clusters in compound **1** and the anions **2a-I** and **2a-II**. Labelling with h_1-h_3 occurred according to increasing prism height.

prism heights [Å]	**1**	**2a-I**		**2a-II**	
		A	**B**	**C**	**D**
h_1	3.053(3)	3.018(1)	2.967(1)	2.981(1)	3.019(1)
h_2	3.077(3)	3.069(1)	3.467(1)	3.486(1)	3.042(1)
h_3	3.812(3)	3.788(1)	3.576(1)	3.558(1)	3.797(1)

The shortest Ge-Ge interactions within the [Ge_9] cores in **2** occur between Ge atoms of the trigonal prims bases and capping Ge atoms [d(Ge34-Ge35): 2.517(1) Å], and the longest distances are observed within the triangular Ge bases [d(Ge31-Ge32): 2.746(1) Å]. The silyl groups are bound to two of the capping Ge atoms with Ge-Si distances (of non-disordered silyl groups) between 2.382(3) Å (Ge15-Si9) and 2.395(3) Å (Ge33-Si33). Therefore, the Ge-Ge, as well as the Ge-Si distances are in accordance with the respective values in compound **1** and with previously reported data.[22, 25] The two $[Ge_9\{Si(TMS)_3\}_2]^{2-}$ clusters bind to the $[Cp_2Ti]^+$ fragment *via* donor-acceptor interactions between the electron lone-pairs situated at the Ge vertices and the Lewis acidic Ti(III). The anionic species **2a** can either be described as $[Cp_2Ti]^+$ bridged $[Ge_9\{Si(TMS)_3\}_2]^{2-}$ dimer or as tetrahedral Ti(III) complex bearing two germanide cluster ligands. The Ge-Ti distances in **2a** adapt values between 2.714(2) Å (Ge1-Ti1) and 2.738(2) Å (Ge10-Ti1), which are in the range of the Ge-Ti distance observed in compound **1** [d(Ge1-Ti): 2.767(2) Å] and the Ti-Ct (Ct: centroid of Cp ligand) distances between 2.049(1) Å (Ti2-Ct3; **2a-II**) and 2.063 Å (Ti2-Ct4; **2a-II**) are also in accordance with the values observed in compound **1** and in further previously reported Ti(III) complexes (Figure 2; Table 2).[13, 27, 28] The coordination of Ti(III) by its four ligands occurs again in distorted tetrahedral manner, which is expressed by the Ct1-Ti1-Ct2: 134.01(2)° and Ge1-Ti1-Ge10: 83.83(2)° angles in **2a-I** and the Ct3-Ti2-Ct4: 133.94(2)° and Ge19-Ti2-Ge28: 83.51(2)° angles in molecule **2a-II**.

The analytical purity of compound **2** was confirmed by elemental analysis and in EPR spectroscopic investigations carried out at 130 K with a frozen thf solution of **2**, its g-factor was determined to be g_{iso} = 1.968 (anisotropic components and EPR spectrum are presented in the Supporting information). In ESI-MS examinations carried out with thf solutions of dissolved crystals of **2**, the molecule peak of **2a** could not be monitored. However, a signal which can be assigned to $\{[Cp_2Ti(Ge_9\{Si(TMS)_3\}_2)]\}^-$ was monitored at m/z 1326.5 (Supporting information). The observed species is formed upon cleavage of $[Ge_9\{Si(TMS)_3\}_2]^{2-}$ from **2a** during the ionization process in the mass spectrometer.

Table 2: Selected bond lengths and angles in **1** and **2a**. The crystallographically independent cluster anions are labelled as **2a-I** and **2a-II**.

distances [Å]	**1**	**2a-I**	**2a-II**
Ge-Ti	2.767(2) (Ge1-Ti)	2.714(2) (Ge1-Ti1)	2.732(2) (Ge19-Ti2)
	-	2.738(2) (Ge10-Ti1)	2.725(2) (Ge28-Ti2)
Ge-Ct*	2.049(1) (Ti-Ct1)	2.051(2) (Ti1-Ct1)	2.049(1) (Ti2-Ct3)
	2.045(1) (Ti-Ct2)	2.055(1) (Ti1-Ct2)	2.063(1) (Ti2-Ct4)
Ti-N	2.164(6) (Ti-N)	-	-
angles [°]	**1**	**2a-I**	**2a-II**
Ct-Ti-Ct*	135.34(5) (Ct1-Ti-Ct2)	134.01(2) (Ct1-Ti1-Ct2)	133.94(2) (Ct3-Ti2-Ct4)
Ge-Ti-N	84.59(3) (Ge1-Ti1-N)	-	-
Ge-Ti-Ge	-	83.83(2) (Ge1-Ti1-Ge10)	83.51(2) (Ge19-Ti2-Ge28)

*Ct: centroids of Cp ligands.

Compounds **1** and **2** represent rare examples for molecular complexes comprising Ti-Ge interactions (to date only four of such complexes have been crystallographically characterized).[29-31] Moreover, the formation of donor-acceptor interactions between Ti(III) and electron lone-pairs situated at Ge vertex atoms in compounds **1** and **2** contrasts the typical interactions between transition metal fragments and $[Ge_9\{Si(TMS)_3\}_n]^{(4-n)-}$ (*n*: 2, 3), which usually occur by coordination of the transition metals to triangular faces of the $[Ge_9]$ clusters in a η^3-coordination mode.[17-24] In the case of $[Ge_9\{Si(TMS)_3\}_n]^{(4-n)-}$ (*n*: 2, 3), similar donor-acceptor interactions have previously only been observed in $[(CO)_5Cr(\eta^1\text{-}Ge_9\{Si(TMS)_3\}_3)]^-$. However, the nature of the Ti-Ge bonds in **1** and **2** is in accordance with the Ti-Sn coordination mode observed in the previously found anion $[Cp_2Ti(NH_3)(\eta^1\text{-}Sn_9)]^{3-}$, which manifests this bonding mode to be favoured for interactions of $[Cp_2Ti]^+$ fragments with nine-atomic tetrel element *Zintl* clusters.[13]

In summary, within this work the synthesis of the first Ti(III)-complexes of $[Ge_9]$ *Zintl* clusters was achieved. The neutral compound $[Cp_2Ti(MeCN)(\eta^1\text{-}Ge_9\{Si(TMS)_3\}_3)]$ (**1**) and the tri-anion $[Cp_2Ti(\eta^1\text{-}Ge_9\{Si(TMS)_3\}_2)_2]^{3-}$ (**2a**) are rare examples for molecular complexes comprising Ti-Ge interactions. The occurrence of donor-acceptor interactions between the electron lone-pairs situated at Ge vertex atoms of $[Ge_9]$ and the Lewis acidic Ti(III) manifests that this bonding mode is favoured for interactions between Ti(III) and nine-atomic tetrel element *Zintl* clusters.

Acknowledgement

The authors acknowledge the National Institutes of Health (NIH) for funding UC Berkeley CheXray X-ray-crystallographic facility under grant no. S10-RR027172 and the Beamline 11.3.1 of the Advanced Light Source, which is a DOE Office of Science User Facility under contract no. DE-AC02-05CH11231. F. S. G. thanks Irene Cai and Rex Handford for help with the single crystal measurements and Amélie Nicolay for helpful discussions. Moreover, F. S. G. thanks TUM Graduate School for support.

Literature

[1] J. D. Corbett, *Chem. Rev.* **1985**, *85*, 383.
[2] T. F. Fässler, S. D. Hoffmann, *Angew. Chem. Int. Ed.* **2004**, *43*, 6242.
[3] S. C. Sevov, J. M. Goicoechea, *Organometallics* **2006**, *25*, 5678.
[4] S. Scharfe, F. Kraus, S. Stegmaier, A. Schier, T. F. Fässler, *Angew. Chem. Int. Ed.* **2011**, *50*, 3630.
[5] J. M. Goicoechea, S. C. Sevov, *Organometallics* **2006**, *25*, 4530.
[6] B. W. Eichhorn, R. C. Haushalter, W. T. Pennington, *J. Am. Chem. Soc.* **1988**, *110*, 8704.
[7] B. W. Eichhorn, R. C. Haushalter, *Chem. Commun.* **1990**, 937.
[8] J. Campbell, H. P. A. Mercier, H. Franke, D. P. Santry, D. A. Dixon, G. J. Schrobilgen, *Inorg. Chem.* **2002**, *41*, 86.
[9] B. Kesanli, J. Fettinger, B. Eichhorn, *Chem. Eur. J.* **2001**, *7*, 5277.
[10] S. Scharfe, T. F. Fässler, *Eur. J. Inorg. Chem.* **2010**, 1207.
[11] K. Mayer, L.-A. Jantke, S. Schulz, T. F. Fässler, *Angew. Chem. Int. Ed.* **2017**, *56*, 2350.
[12] F. Lips, M. Hołyńska, R. Clérac, U. Linne, I. Schellenberg, R. Pöttgen, F. Weigend, S. Dehnen, *J. Am. Chem. Soc.* **2012**, *134*, 1181.
[13] C. B Benda, M. Waibel, T. F. Fässler, *Angew. Chem. Int. Ed.* **2015**, *54*, 522.
[14] A. Schnepf, *Angew. Chem. Int. Ed.* **2003**, *42*, 2624.
[15] F. Li, S. C. Sevov, *Inorg. Chem.* **2012**, *51*, 2706.
[16] O. Kysliak, A. Schnepf, *Dalton Trans.* **2016**, *45*, 2404.
[17] O. Kysliak, C. Schrenk, A. Schnepf, *Chem. Eur. J.* **2016**, *22*, 18787.
[18] C. Schenk, A. Schnepf, *Angew. Chem. Int. Ed.* **2007**, *46*, 5314.
[19] C. Schenk, F. Henke, G. Santiso-Quinones, I. Krossing, A. Schnepf, *Dalton Trans.* **2008**, 4436.
[20] F. Li, S. C. Sevov, *Inorg. Chem.* **2015**, *54*, 8121.
[21] F. Henke, C. Schenk, A. Schnepf, *Dalton Trans.* **2009**, 9141.
[22] F. S. Geitner, T. F. Fässler, *Eur. J. Inorg. Chem.* **2016**, 2688.
[23] K. Mayer, L. J. Schiegerl, T. F. Fässler, *Chem. Eur. J.* **2016**, *22*, 18794.
[24] F. S. Geitner, M. A. Giebel, A. Pöthig, T. F. Fässler, *Molecules* **2017**, *22*, 1204.
[25] C. Schenk, A. Schnepf, *Chem. Commun.* **2009**, 3208.
[26] F. Henke, C. Schenk, A. Schnepf, *Dalton Trans.* **2011**, *40*, 6704.
[27] Y. A. Wasslen, E. Tois, S. Haukka, K. A. Kreisel, G. P. A. Yap, M. D. Halls, S. T. Barry, *Inorg. Chem.* **2010**, *49*, 1976.
[28] D. Sekutowski, G. D. Stucky, *J. Am. Chem. Soc.* **1976**, *98*, 1376.
[29] J. Hlina, J. Baumgartner, C. Marschner, P. Zark, T. Müller, *Organometallics* **2013**, *32*, 3300.

[30] J. F. Harrod, A. Malek, F. D. Rochon, R. Melanson, *Organometallics* **1987**, *6*, 2117.
[31] R. E. Marsh, *Acta Cryst. Sect. B* **1997**, *53*, 317.

Supporting Information

Early Transition Metal Complexes of $[Ge_9\{Si(TMS)_3\}_n]^{(4-n)-}$ (*n*: 2, 3) – Synthesis and Characterization of $[Cp_2Ti(MeCN)(\eta^1\text{-}Ge_9\{Si(TMS)_3\}_3)]$ and $K_3[Cp_2Ti(\eta^1\text{-}Ge_9\{Si(TMS)_3\}_2)_2]$

Felix S. Geitner,[a] Wilhelm Klein,[b] Oksana Storcheva,[b] T. Don Tilley[c] and Thomas F. Fässler[b*]

[a] Department Chemie, Technische Universität München, Lichtenbergstraße 4, 85747 Garching b. München and WACKER Institute for Silicon Chemistry.

[b] Department Chemie, Technische Universität München, Lichtenbergstraße 4, 85747 Garching b. München.

[c] Department of Chemistry, University of California, Berkeley, CA 94720-1460 Berkeley

General Information

All manipulations were performed under oxygen-free, dry conditions under nitrogen or argon atmosphere using standard Schlenk or glove box techniques. Glassware was dried prior to usage by heating it *in vacuo*. Pentane (HPLC grade) and toluene (ACS grade) were purchased from Fisher Scientific. Thf was purchased from Macron Fine Chemicals. The solvents were dried using a JC Meyers Phoenix SDS solvent purification system and subsequently stored over molecular sieves 3 Å. All other commercially available chemicals were used without further purification. K_4Ge_9 was prepared by fusion of stoichiometric amounts of the elements in stainless-steel tubes at 650 °C. The silylated [Ge_9] clusters K[Ge_9{$Si(TMS)_3$}$_3$] and K_2[Ge_9{$Si(TMS)_3$}$_2$], as well as the bis(cyclopentadienyl)titanium(III)chloride dimer [$Cp_2TiCl]_2$ were synthesized according to modified literature procedures.[1-3]

Single Crystal Structure Determination

The air- and moisture-sensitive crystals of **1** and **2** were transferred from the mother liquor into perfluoroalkyl ether oil in a nitrogen filled glovebox. For diffraction data collection, the single crystals were fixed on a glass capillary and positioned in a 100 K cold N_2 gas stream. Data collection occured at a Bruker APEX II QUAZAR diffractometer (MoK_α radiation) equipped with a APEX II detector (University of California, Berkeley; compound **2**) or the beamline 11.3.1 of the Advanced Light Source using a PHOTON100 CMOS detector running shutterless using radiation with a wavelength of 0.7288 Å selected by a Si(111) monochromator and focused to 200 μm^2 with a toroidal mirror (Lawrence Berkeley National Laboratory; compound **1**). Structures were solved by Direct Methods (SHELXS-2014) and refined by full-matrix least-squares calculations against F^2 (SHELXL-2014).[4] The positions of the hydrogen atoms were calculated and refined using a riding model. Unless stated otherwise, all non-hydrogen atoms were treated with anisotropic displacement parameters. The supplementary crystallographic data for this paper has been deposited with the Cambridge Structural database and are available free of charge *via* www.ccdc.cam.ac.uk/data_request/cif. The crystallographic data for compounds **1** and **2** is summarized in Table S1. In compound **1** the co-crystallized solvent molecule was refined on split positions pentane (70 %) and toluene (30 %). In compound **2** some of the hypersilyl groups at the [Ge_9] clusters reveal a rotational disorder and were refined on split positions.

EPR Spectroscopy

EPR measurements were carried out using a JEOL JES-FA 200 spectrometer at X-band frequency (approx. 9.05 GHz, centre field: 336 mT, field width: 50 mT, modulation frequency: 100 kHz, modulation width: 0.4 mT, power: 5.0 mW, measurement temperature 130 K). The g-values were determined using Mn^{2+} (nuclear spin I = 5/2) embedded in MgO as standard (4^{th} line g = 1.981). Sample preparation occurred in an argon filled glovebox and samples were frozen in N_2(l) prior to the measurements.

Elemental Analyses (EA)

Elemental analyses were performed by the Microanalytical Laboratory in the College of Chemistry at the University of California, Berkeley.

Electrospray Ionization Mass Spectrometry (ESI-MS)

ESI-MS analyses were performed on a Bruker Daltronic HCT mass spectrometer (injection speed: 240 µL/h). Sample preparation occurred in an argon filled glovebox and the data evaluation was carried out using the Bruker Compass Data Analysis 4.0 SP 5 program (*Bruker*). Spectra were plotted using OriginPro2016G (*OriginLab*).

Synthetic Procedures

[$Cp_2Ti(MeCN)(\eta^1$-$Ge_9\{Si(TMS)_3\}_3$)] (1): K[$Ge_9\{Si(TMS)_3\}_3$] (108 mg, 0.075 mmol, 1 equiv.) was suspended in toluene (1 mL) and a toluene solution (2 mL) of $[Cp_2TiCl]_2$ (16 mg, 0.037 mmol, 0.5 equiv.) was added, resulting in the formation of a deep red solution after 5 min. The reaction mixture was stirred over night at room temperature before the solvent was removed *in vacuo* and the obtained solid was washed with pentane (3 mL). Subsequently, the solid was dissolved in toluene (1.5 mL), filtered to remove remaining solids, layered with pentane (2.5 mL) and stored in a freezer at -35 °C, yielding dark orange block-shaped crystals (24 mg, 20 %) after 2 d. **Elemental analysis**: anal. calcd. for $C_{39}H_{94}Ti_1Ge_9Si_{12}N$·0.3 tol·0.7 pent: C, 31.8; H, 6.1; N, 0.8; found: C, 31.4; H, 5.7 N; 0.7. Sum formula for elemental analysis was determined according to composition of the crystals. The acetonitrile molecule originates from residual solvent in the reactant K[$Ge_9\{Si(TMS)_3\}_3$].

$K_3[Cp_2Ti(\eta^1\text{-}Ge_9\{Si(TMS)_3\}_2)_2]$ (2): $K_2[Ge_9\{Si(TMS)_3\}_2]$ (91 mg, 0.075 mmol, 1 equiv.) was dissolved in thf (1 mL) and a thf solution of $[Cp_2TiCl]_2$ (16 mg, 0.037 mmol, 0.5 equiv.) was added to obtain a green/brown reaction mixture, which was stirred at room temperature before the solvent was removed *in vacuo* and the remaining brown solid was washed with pentane (3 mL). Subsequently, the solid was extracted with toluene (3 mL), filtered to remove insoluble materials and stored in a freezer at -35 °C, yielding dark green block-shaped crystals (40 mg, 20 %) overnight. **Elemental analysis**: anal. calcd. for $C_{46}H_{118}Ti_1Ge_{18}Si_{16}K_3$: C, 21.3; H, 4.6; found: C, 21.3; H, 4.6.

Crystallographic Data

Table S1: Crystallographic data of compounds **1** and **2**.

compound	**1**	**2**
formula	$Ge_9Si_{12}TiC_{39}H_{94}N\cdot0.3tol\cdot0.7pent$	$(K_3Ge_{18}Si_{16}TiC_{46}H_{118}\cdot6tol)_2$
fw [g·mol^{-1}]	1686.57	3145.25
space group	*P2$_1$/c*	*P2$_1$/c*
a [Å]	15.458(1)	42.249(1)
b [Å]	22.460(2)	36.427(1)
c [Å]	22.268(2)	18.0896(5)
α [°]	90	90
β [°]	95.176(6)	100.638(2)
γ [°]	90	90
V [Å^3]	7700(11)	27362(1)
Z	4	2
T [K]	100(2)	100(2)
λ [Å]	0.7288	MoK_α
ρ_{calcd} [g·cm^{-3}]	1.455	1.527
μ [mm^{-1}]	3.771	4.208
collected reflections	119727	219866
independent reflections	17236	50264
R_{int} / R_δ	0.0771/0.0481	0.0497/0.0449
parameters / restraints	664/0	2727/1056
R_1 [$I > 2\,\sigma(I)$ / all data]	0.0288/0.0426	0.0718/0.0894
wR_2 [$I > 2\,\sigma(I)$ / all data]	0.0568/0.0622	0.1406/0.1463
goodness of fit	1.011	1.212
max./min. diff. el. density [e / Å^{-3}]	0.51/-0.40	2.37/-1.30

Table S2: Selected bond lengths and angles in compound **1**.

bond	distance [Å]
Ge1-Ge2	2.527(1)
Ge1-Ge4	2.527(1)
Ge1-Ge5	2.633(2)
Ge1-Ge8	2.651(2)
Ge2-Ge3	2.557(2)
Ge2-Ge5	2.598(1)
Ge2-Ge6	2.566(1)
Ge3-Ge4	2.567(1)
Ge3-Ge6	2.616(2)
Ge3-Ge7	2.657(2)
Ge4-Ge7	2.568(2)
Ge4-Ge8	2.615(1)
Ge5-Ge8	2.852(2)
Ge5-Ge9	2.514(1)
Ge6-Ge7	2.854(2)
Ge6-Ge9	2.518(2)
Ge7-Ge9	2.525(1)
Ge8-Ge9	2.512(1)
Ge2-Si1	2.405(2)
Ge4-Si2	2.413(2)
Ge9-Si3	2.371(2)
Ge1-Ti	2.767(2)
Ti-Ct1*	2.049(1)
Ti-Ct2*	2.045(1)
atoms	angle [°]
Ct1-Ti-Ct2*	135.34(5)
Ge1-Ti-N	84.59(3)

*Ct: centroids of Cp rings; Ct1: C1-C5; Ct2: C6-C10

Table S3: Selected bond lengths and angles in **2a-l**.

bond	distance [Å]	bond	distance [Å]
Ge1-Ge2	2.583(1)	Ge10-Ge11	2.584(1)
Ge1-Ge4	2.561(1)	Ge10-Ge12	2.577(1)
Ge1-Ge5	2.546(2)	Ge10-Ge13	2.577(1)
Ge1-Ge8	2.651(2)	Ge10-Ge14	2.583(1)
Ge2-Ge3	2.716(2)	Ge11-Ge12	2.666(1)
Ge2-Ge6	2.595(1)	Ge11-Ge15	2.544(1)
Ge2-Ge7	2.641(1)	Ge11-Ge16	2.591(1)
Ge3-Ge7	2.672(1)	Ge12-Ge16	2.715(1)
Ge3-Ge8	2.553(2)	Ge12-Ge17	2.536(1)
Ge4-Ge7	2.657(2)	Ge13-Ge14	2.672(1)
Ge4-Ge8	2.560(2)	Ge13-Ge17	2.551(1)
Ge4-Ge9	2.638(1)	Ge13-Ge18	2.728(1)
Ge5-Ge6	2.546(2)	Ge14-Ge15	2.545(1)
Ge5-Ge9	2.683(1)	Ge14-Ge18	2.599(1)
Ge6-Ge7	2.531(2)	Ge15-Ge16	2.574(1)
Ge6-Ge9	2.529(2)	Ge15-Ge18	2.542(1)
Ge7-Ge8	2.523(1)	Ge16-Ge17	2.534(2)
Ge8-Ge9	2.539(1)	Ge17-Ge18	2.498(1)
Ge6-Si1	2.387(3)	Ge15-Si9	2.382(3)
Ge8-Si5	2.386(3)	Ge17-Si13 / Ge17-Si17	2.312(6) / 2.488(8)
Ge1-Ti1	2.714(2)	Ge10-Ti1	2.738(2)
Ti1-Ct1*	2.051(2)	Ti1-Ct2*	2.055(1)
atoms	angle [°]	atoms	angle [°]
Ct1-Ti1-Ct2*	134.01(2)	Ge1-Ti1-Ge10	83.83(2)

*Ct: centroids of Cp rings; Ct1: C1-C5; Ct2: C6-C10

Table S4: Selected bond lengths and angles in **2a-II**.

bond	distance [Å]	bond	distance [Å]
Ge19-Ge20	2.576(1)	Ge28-Ge29	2.556(1)
Ge19-Ge21	2.585(1)	Ge28-Ge30	2.573(1)
Ge19-Ge22	2.579(1)	Ge28-Ge31	2.548(1)
Ge19-Ge23	2.585(1)	Ge28-Ge32	2.572(1)
Ge20-Ge21	2.670(1)	Ge29-Ge30	2.730(1)
Ge20-Ge24	2.544(1)	Ge29-Ge33	2.559(1)
Ge20-Ge25	2.596(2)	Ge29-Ge34	2.687(1)
Ge21-Ge25	2.709(1)	Ge30-Ge34	2.646(1)
Ge21-Ge26	2.539(1)	Ge30-Ge35	2.586(1)
Ge22-Ge23	2.660(1)	Ge31-Ge32	2.746(1)
Ge22-Ge26	2.554(1)	Ge31-Ge35	2.546(1)
Ge22-Ge27	2.735(1)	Ge31-Ge36	2.673(1)
Ge23-Ge24	2.550(1)	Ge32-Ge33	2.567(1)
Ge23-Ge27	2.592(1)	Ge32-Ge36	2.626(1)
Ge24-Ge25	2.583(1)	Ge33-Ge34	2.567(1)
Ge24-Ge27	2.545(1)	Ge33-Ge36	2.552(1)
Ge25-Ge26	2.539(1)	Ge34-Ge35	2.517(1)
Ge26-Ge27	2.492(1)	Ge35-Ge36	2.540(1)
Ge24-Si21	2.385(3)	Ge33-Si33	2.395(3)
Ge26-Si25 / Ge26-Si29	2.423(9) / 2.357(8)	Ge35-Si37 / Ge35-Si41	2.474(8) / 2.289(9)
Ge19-Ti2	2.732(2)	Ge28-Ti2	2.725(2)
Ti2-Ct3*	2.049(1)	Ti2-Ct4*	2.063(1)
atoms	angle [°]	atoms	angle [°]
Ct3-Ti2-Ct4*	133.94(2)	Ge19-Ti2-Ge28	83.51(2)

*Ct: centroids of Cp rings; Ct1: C56-C60; Ct2: C61-C65

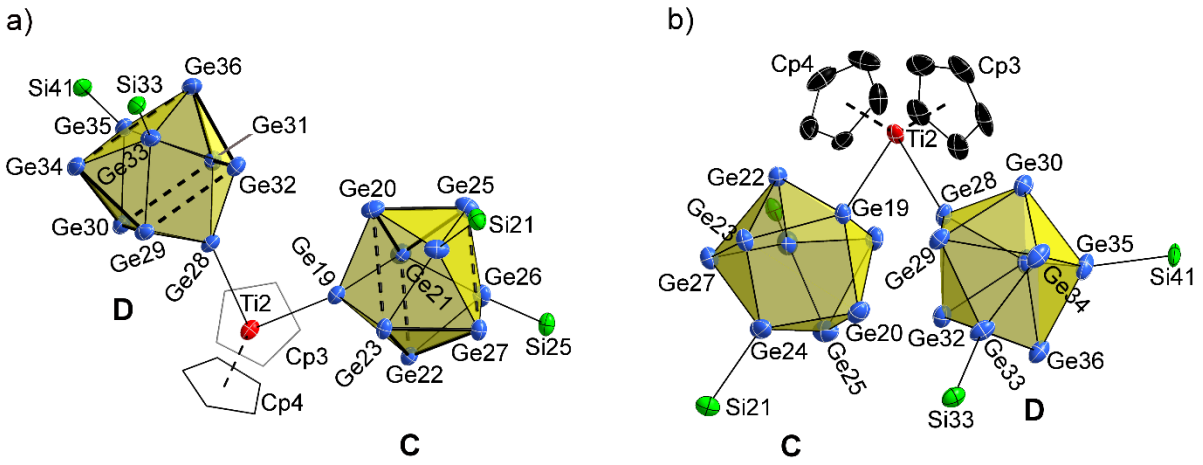

Figure S1: Two perspectives of the labelled molecular structure of **2a-II**. All displacement ellipsoids are shown at a 50 % probability level. a) C_S symmetric shape of the [Ge_9] clusters and coordination of [Ge_9] by the two silyl groups and the [Cp_2Ti]$^+$ moiety *via* the three capping atoms (Ge19, Ge24, Ge26 or Ge28, Ge33, Ge35) of the trigonal prism. For clarity, carbon atoms of the cyclopentadienyl rings are represented as grey or black wire sticks. b) Distorted tetrahedral coordination of Ti(III) by its four ligands. In a) and b) protons, solvent toluene molecules and TMS groups of the hypersilyl ligands are omitted and only the major species of disordered silyl groups are shown. Selected bond lengths and angles of **2a-II** are summarized in Table 2 in the manuscript and in Tables S3 and S4 in the Supporting information. The molecular structure of **2a-I** is presented in the manuscript.

EPR Data

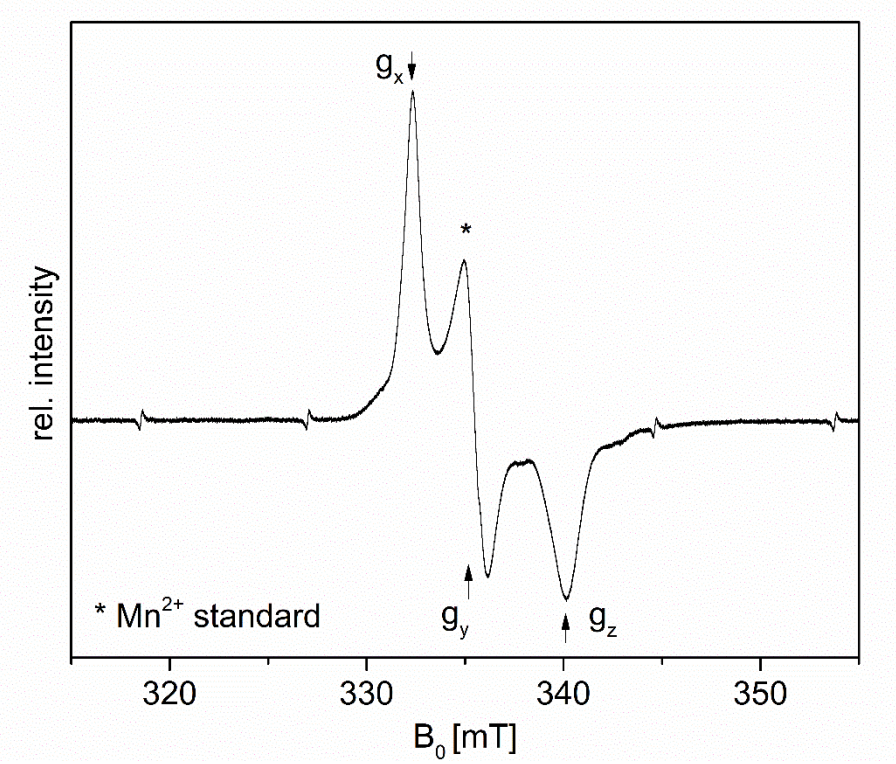

Figure S2: EPR spectrum of compound **1** in frozen thf solution at 130 K. The values for the anisotropic g-factors g_x: 1.993; g_y: 1.974 and g_z: 1.933 were determined in relation to a Mn^{2+} standard (phase inverted, labelled with *) and the isotropic g-factor was calculated to be g_{iso}: 1.967.

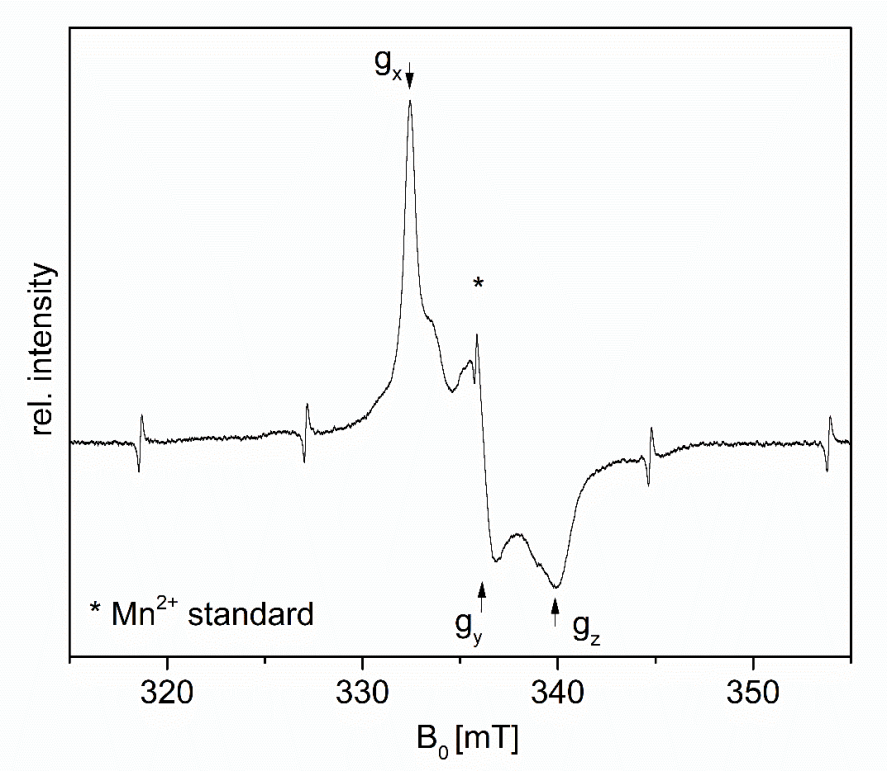

Figure S3: EPR spectrum of compound **2** in frozen thf solution at 130 K. The values for the anisotropic g-factors g_x: 1.992; g_y: 1.970 and g_z: 1.942 were determined in relation to a Mn^{2+} standard (phase inverted, labelled with *) and the isotropic g-factor was calculated to be g_{iso}: 1.968.

ESI-MS Data

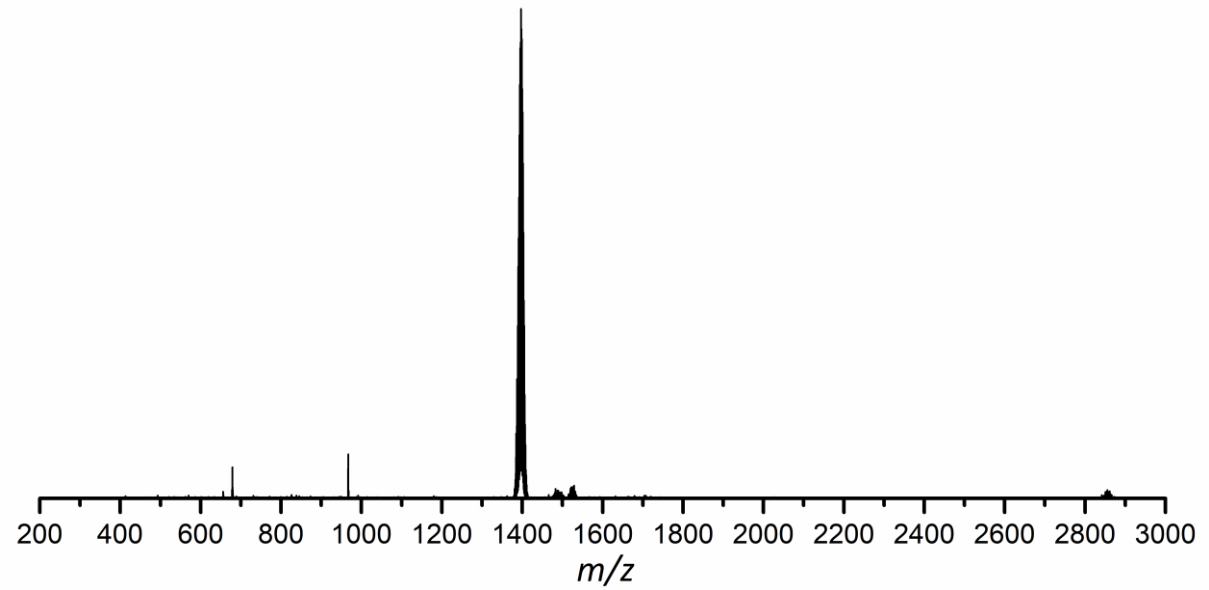

Figure S4: ESI-MS spectrum obtained upon examination of an aliquot sample of a thf solution of diluted crystals of **1**. The signal at *m/z* 1396.8 can be assigned to $\{[Ge_9\{Si(TMS)_3\}_3]\}^-$, being formed upon cleavage of the $[Cp_2Ti(MeCN)]^+$ moiety from **1** during the ionization process.

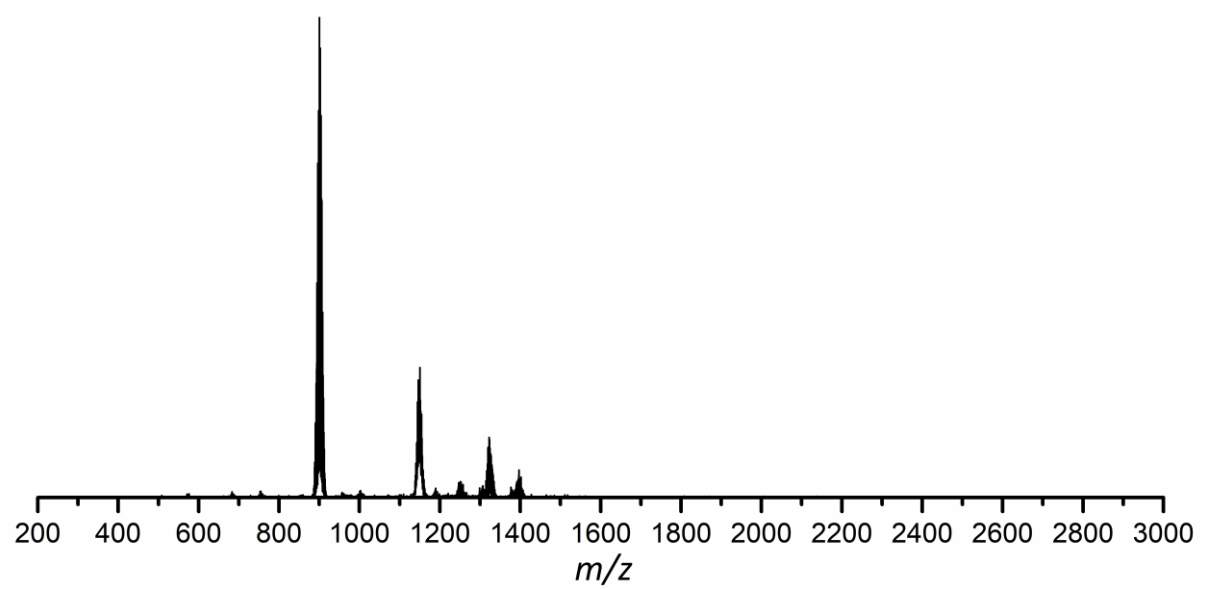

Figure S5: ESI-MS spectrum obtained upon examination of an aliquot sample of a thf solution of diluted crystals of compound **2**. The signal at *m/z* 1326.5 can be assigned to $\{[Cp_2Ti(Ge_9\{Si(TMS)_3\}_2)]\}^-$, which is formed upon cleavage of one bis-silylated [Ge_9] cluster ligand from **2a**. Besides the signal assigned to the Ge_9-Ti compound signals at *m/z* 900.4 and *m/z* 1147.4 were monitored. These signals can be assigned to [Ge_9] clusters $\{[Ge_9\{Si(TMS)_3\}_3]\}^-$ or $\{[Ge_9\{Si(TMS)_3\}_2]\}^-$ which probably result from further fragmentation of $\{[Cp_2Ti(Ge_9\{Si(TMS)_3\}_2)]\}^-$ during the ionization process.

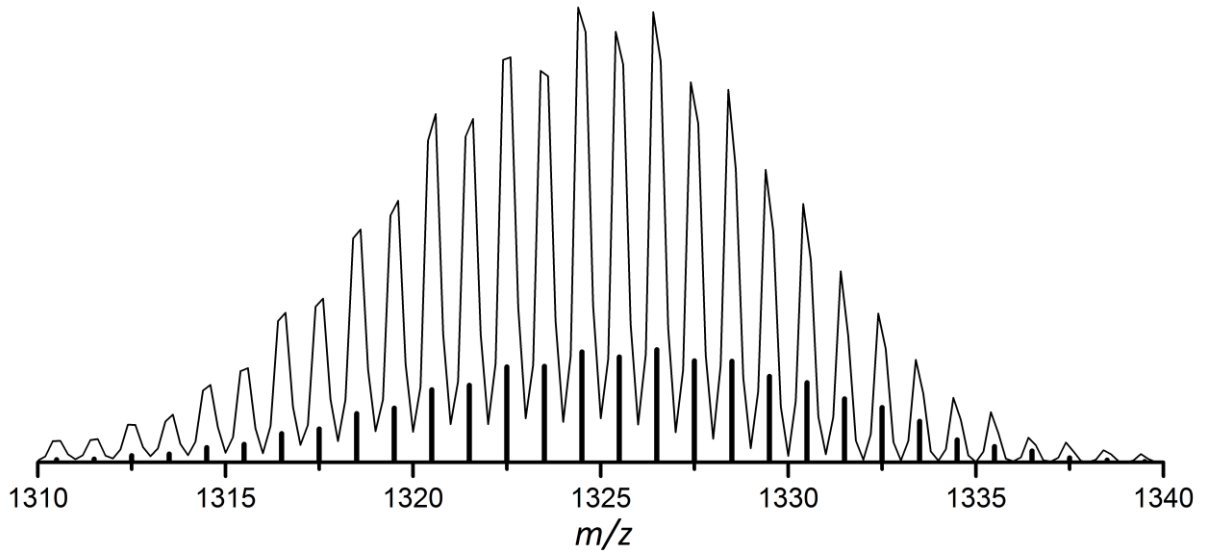

Figure S6: Detail view on ESI-MS signal at *m/z* 1326.5, which can be assigned to $\{[Cp_2Ti(Ge_9\{Si(TMS)_3\}_2)]\}^-$. The signal was monitored upon measurement of an aliquot sample of a diluted thf solution of crystals of compound **2**.

Literature

[1] F. Li, S. C. Sevov, *Inorg. Chem.* **2012**, *51*, 2706.
[2] O. Kysliak, A. Schnepf, *Dalton Trans.* **2016**, *45*, 2404.
[3] C. B. Benda, M. Waibel, T. F. Fässler, *Angew. Chem. Int. Ed.* **2015**, *54*, 522.
[4] G. M. Sheldrick, *Acta Cryst. Sect. C* **2015**, *71*, 3.

5.7 Probing the Reactivity of [Ge_9] *Zintl* Clusters towards Group 13 and Group 15 Element Compounds

F. S. Geitner, T. F. Fässler*

Manuscript for publication

Content and Contributions

The scope of this work was the probing of the reactivity of [Ge_9] *Zintl* clusters towards Group 13 and Group 15 element compounds, aiming for novel potent tetrel cluster stabilization and functionalization methods. Reactions of the cyclic diazaborolidine [BrBN(Mes)-CH_2-CH_2-N(Mes)] or diazaborole [BrBN(Dipp)-CH=CH-N(Dipp)], as well as Mes_2BBr and [^{t}$Bu_2AlBr]_2$ with the tris-silylated [Ge_9] cluster [Ge_9{$Si(TMS)_3$}$_3$]$^-$ did not result in a conversion of the reactants. By contrast, the bis-silylated [Ge_9] cluster [Ge_9{$Si(TMS)_3$}$_2$]$^{2-}$ readily reacted with [BrBN(Mes)-CH_2-CH_2-N(Mes)], Mes_2BBr and [^{t}$Bu_2AlBr]_2$ in thf solution, yielding the mixed-substituted [Ge_9] cluster anions [Ge_9{$Si(TMS)_3$}$_3$*E*R_2]$^-$ (*E*: B, Al; *R*: substituents). In the case of [BrBN(Dipp)-CH=CH-N(Dipp)] reactions in thf were not successful, however, an alternative route was found by carrying out the reaction in acetonitrile at 40 °C, yielding the analogous product species. All of the mixed-substituted [Ge_9] cluster anions were characterized by means of NMR and ESI-MS. Moreover, the reactivity of the Group 13 element compounds towards bare [Ge_9]$^{4-}$ clusters was tested by treating solid K_4Ge_9 with thf or acetonitrile solutions of the main-group element compounds. Whereas reactions of K_4Ge_9 with Mes_2BBr or [^{t}$Bu_2AlBr]_2$ led to unkown products, ESI-MS examinations carried out with reaction mixtures of K_4Ge_9 and [BrBN(Mes)-CH_2-CH_2-N(Mes)] or [BrBN(Dipp)-CH=CH-N(Dipp)], indicated the presence of multiple borane-substituted [Ge_9] clusters in the gas phase. However, NMR examinations revealed the formation of product mixtures containing several species in low amounts. Moreover, reactions of ^{t}Bu_2SbCl with [Ge_9{$Si(TMS)_3$}$_3$]$^-$ led to the formation of the neutral species [Ge_9{$Si(TMS)_3$}$_3$Sb^tBu_2]. By contrast, reactions of ^{t}Bu_2SbCl with [Ge_9{$Si(TMS)_3$}$_2$]$^{2-}$ and [Ge_9]$^{4-}$ resulted in the reduction of the stibane compound yielding $Sb_4^{t}Bu_4$. This manuscript for publication was written in course of this thesis.

Probing the Reactivity of [Ge_9] *Zintl* Clusters towards Group 13 and Group 15 Element Compounds

Felix S. Geitner,[a] and Thomas F. Fässler[b*]

[a] Department Chemie, Technische Universität München, Lichtenbergstraße 4, 85747 Garching b. München and WACKER Institute for Silicon Chemistry.

[b] Department Chemie, Technische Universität München, Lichtenbergstraße 4, 85747 Garching b. München.

Abstract

Herein we report on the reactivity of [Ge_9] *Zintl* clusters towards various Group 13 and Group 15 element compounds, aiming for the introduction of novel main-group substituents to [Ge_9]. Reactions of the twofold silylated cluster $[Ge_9\{Si(TMS)_3\}_2]^{2-}$ with the diazaborolidine [BrBN(Mes)-CH_2-CH_2-N(Mes)] (**A**) or the diazaborole [BrBN(Dipp)-CH=CH-N(Dipp)] (**B**) led to the formation of the mixed-substituted anions $[Ge_9\{Si(TMS)_3\}_2\{BN(Mes)\text{-}CH_2\text{-}CH_2\text{-}N(Mes)\}]^-$ (**1a**) or $[Ge_9\{Si(TMS)_3\}_2\{BN(Dipp)\text{-}CH{=}CH\text{-}N(Dipp)\}]^-$ (**2a**), respectively. Analogous reactions of $[Ge_9\{Si(TMS)_3\}_2]^{2-}$ with Mes_2BBr (**C**) and $[^tBu_2AlBr]_2$ (**D**) yielded $[Ge_9\{Si(TMS)_3\}_2ER_2]^-$ [*E*: B, *R*: Mes (**3a**); *E*: Al, *R*: ^{t}Bu (**4a**)]. The anions **1a**-**4a** are the first examples for borane- or alane-substituted [Ge_9] clusters. Moreover, the neutral compound $[Ge_9\{Si(TMS)_3\}_3Sb^tBu_2]$ (**5**) was obtained by reaction of the tris-silylated cluster $[Ge_9\{Si(TMS)_3\}_3]^-$ with $^tBu_2SbCl$ (**E**). **1a**-**4a** were characterized by means of NMR spectroscopy and electrospray ionization mass spectrometry (ESI-MS) and the neutral compound **5** was characterized by NMR spectroscopy. In additional studies on the reactivity of **A** and **B** towards $[Ge_9]^{4-}$, ESI-MS investigations indicated the formation of multiple borane-substituted [Ge_9] cluster species.

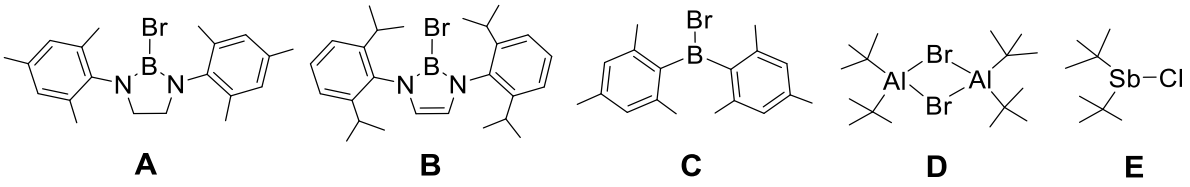

Figure 1: Group 13 and Group 15 element compounds applied as precursors for the introduction of novel main-group element substituents to [Ge_9] within this work.

Introduction

Solid state reactions of stoichiometric amounts of potassium and germanium at elevated temperatures yield *Zintl* phases of the compositions K_4Ge_9 or $K_{12}Ge_{17}$ in quantitative yield. Treatment of these phases with highly polar solvents such as NH_3(l), ethylenediamine or dmf, allows for the dissolution of the contained $[Ge_9]^{4-}$ clusters, and subsequent reactions with organometallics, main group element compounds or organic reagents in solution led to a broad range of novel compounds.[1-4] The high negative charge of the clusters causing insolubility in non-polar solvents and high reactivity/sensitivity prohibited a further extension of their chemistry for a long time. However, especially the dissolution of the nine-atomic clusters from these solid state phases is of interest with respect to the synthesis of nanostructured materials and provides an elegant alternative to the bottom-up synthesis of similar metalloid clusters in solution (these methods sometimes comprise multi-step reactions and yield the polyatomic clusters in rather low yield).[5-8] In order to make the $[Ge_9]$ clusters available for a broader application spectrum, the solubility and stability of the fourfold negatively charged $[Ge_9]$ clusters needs to be enhanced, which can both be achieved by the introduction of multiple positively charged substituents to the $[Ge_9]$ core. Suitable methods for the introduction of such groups to the $[Ge_9]$ clusters in one-step reactions were found in the vinylation reaction of $[Ge_9]^{4-}$, yielding the bis-vinylated cluster $[Ge_9\{CH{=}CH_2\}_2]^{2-}$,[9, 10] or the silylation reaction of $[Ge_9]^{4-}$ yielding the tris-silylated cluster $[Ge_9\{Si(TMS)_3\}_3]^-$ (Figure 2 **I**).[5, 11] The obtained species are soluble in standard solvents (e. g. MeCN) and still comprise ligand free Ge vertices which are only connected to other Ge atoms. In case of the tris-silylated cluster $[Ge_9\{Si(TMS)_3\}_3]^-$ these properties led to the evolution of a prosperous subsequent chemistry. Reacting $[Ge_9\{Si(TMS)_3\}_3]^-$ with organometallics, main-group element compounds or organic reagents, a series of novel $[Ge_9]$ cluster species was obtained comprising various transition metal bridged $[Ge_9]$ cluster dimers (Figure 2 **II**),[12-16] the first tetra-substituted neutral $[Ge_9]$ cluster compounds,[17-22] as well as $[Ge_9]$ cluster compounds bearing alkenyl anchor groups, which might allow for the attachment of the germanium-rich cluster species to nanoparticles or other surfaces (Figure 2 **III**).[23] Additionally, the oxidation of $[Ge_9\{Si(TMS)_3\}_3]^-$ led to the larger metalloid aggregate $[Ge_{18}\{Si(TMS)_3\}_6]$.[24] In further studies different silyl groups were introduced at $[Ge_9]$,[20, 21, 25, 26] a reasonable route towards the bis-silylated $[Ge_9]$ cluster $[Ge_9\{Si(TMS)_3\}_2]^{2-}$ was found,[27] and threefold stannyl decoration of $[Ge_9]$ was achieved.[28, 29] Moreover, phosphine-functionalization of silylated $[Ge_9]$ clusters was accomplished, yielding neutral compounds $[Ge_9\{Si(TMS)_3\}_3PR_2]$ (*R*: ^{i}Pr, Cy) or anionic species $[Ge_9\{Si(TMS)_3\}_2PR_2]^-$ (*R*: ^{t}Bu, Mes, N^{i}Pr$_2$; Figure 2 **IV**).

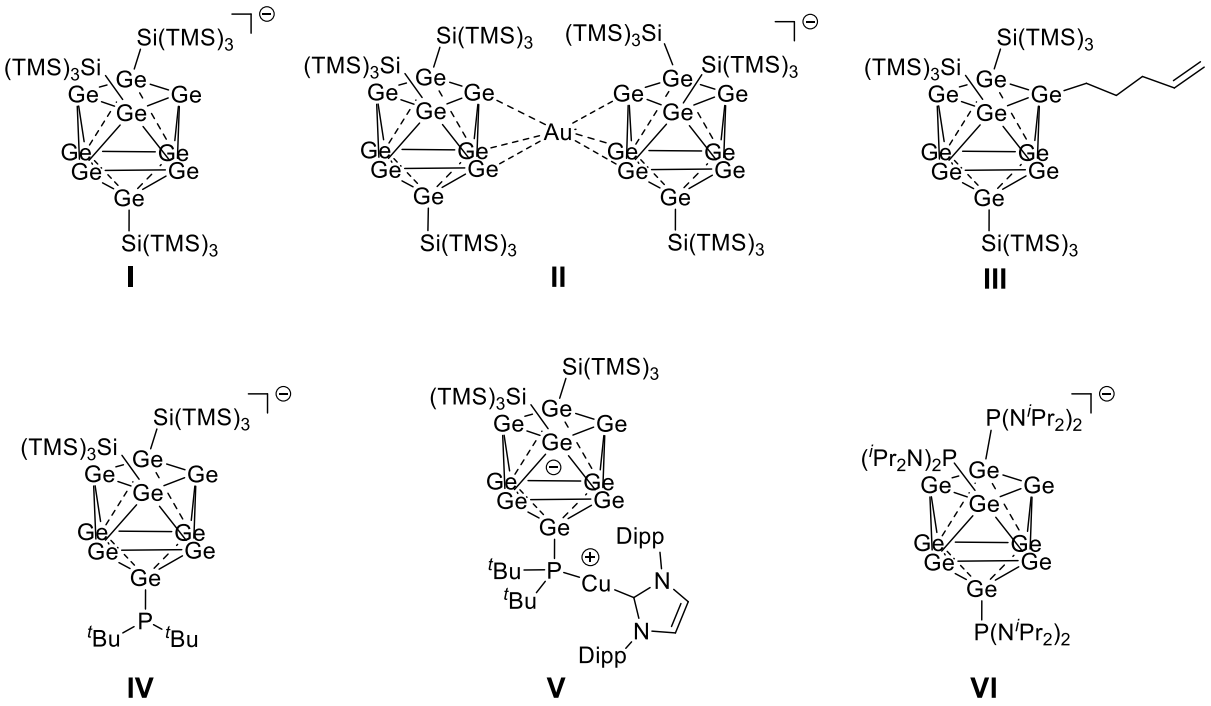

Figure 2: Examples for main-group element-substituted [Ge_9] clusters and species resulting from their reactions with organic reagents or transition metal complexes. **I**: $[Ge_9\{Si(TMS)_3\}_3]^-$,[11] **II**: $[Au(\eta^3\text{-}Ge_9\{Si(TMS)_3\}_3)_2]$,[12] **III**: $[Ge_9\{Si(TMS)_3\}_3(CH_2)_3CH{=}CH_2]$,[23] **IV**: $[Ge_9\{Si(TMS)_3\}_2P^tBu_2]^-$,[22] **V**: $[(Ge_9\{Si(TMS)_3\}_2)^tBu_2P]CuNHC^{Dipp}$,[22] **VI**: $[Ge_9\{P(N^iPr_2)_2\}_3]^-$.[31]

The latter species is able to interact with Lewis acids either *via* the attached phosphanyl moiety forming zwitterionic compounds $[(Ge_9\{Si(TMS)_3\}_2)^tBu_2P]M(NHC^{Dipp})$ (*M*: Cu, Ag, Au) (Figure 2 **V**), or with the [Ge_9] cluster core forming [Ge_9] cluster Cu-NHC compounds $[NHC^{Dipp}Cu(\eta^3\text{-}Ge_9\{Si(TMS)_3\}_2PR_2)]$ (*R*: Mes, N^iPr_2).[22, 30] Recently, the threefold phosphine-functionalization of [Ge_9] was also achieved by the isolations of $[Ge_9\{PRR^I\}_3]^-$ (*R*: N^iPr_2, R^I: N^iPr_2 or ^{t}Bu; Figure 2 **VI**), and the obtained anions were successfully reacted with $NHC^{Dipp}CuCl$ and $Cr(CO)_5(thf)$.[31] The prosperous subsequent chemistry of the silylated [Ge_9] clusters revealed the large potential of such stabilized nonagermanide clusters. This triggered us to investigate the suitability of further main-group element compounds as precursors for the introduction of positively charged substituents to the [Ge_9] clusters. Within this work we investigated the reactivity of [BrBN(Mes)-CH_2-CH_2-N(Mes)] (**A**), [BrBN(Dipp)-CH=CH-N(Dipp)] (**B**) (with varying backbone of the central heterocycle and wingtip substituents of different steric demand), the diarylbromoborane Mes_2BBr (**C**), as well as the bromoalane $[^tBu_2AlBr]_2$ (**D**) and the chlorostibane $^tBu_2SbCl$ (**E**) towards silylated [Ge_9] species $[Ge_9\{Si(TMS)_3\}_n]^{(4\text{-}n)\text{-}}$ (*n*: 2, 3) and bare $[Ge_9]^{4-}$ clusters (Figure 1 and Scheme 1).

Results and Discussion

Reactions of Group 13 Element Compounds with $[Ge_9\{Si(TMS)_3\}_n]^{(4-n)-}$ (*n*: 2, 3)

Reactions of the diazaborolidine **A** with $[Ge_9\{Si(TMS)_3\}_2]^{2-}$ were carried out in thf solution at room temperature. The reaction mixtures were stirred for 3 h, before they were filtered to remove insoluble materials and the solvent was evaporated *in vacuo*, yielding brown solids. ^{1}H NMR examinations revealed the attachment of the cyclic borolidine moiety to the $[Ge_9]$ cluster core forming $[Ge_9\{Si(TMS)_3\}_2\{BN(Mes)\text{-}CH_2\text{-}CH_2\text{-}N(Mes)\}]^-$ (**1a**), which can be monitored by the downfield shift of the silyl groups' proton signal (0.16 ppm → 0.25 ppm; thf-d_8) and the observed signal ratio (Supporting information). Furthermore, in ESI-MS examinations a signal which can be assigned to the anion **1a** with an attached thf molecule was monitored at *m/z* 1526.8 $\{[Ge_9\{Si(TMS)_3\}_2\{BN(Mes)\text{-}CH_2\text{-}CH_2\text{-}N(Mes)\}]^- + thf\}^-$ (**1a-thf**) proving its presence in solution (Figure 3). Due to the straightforward formation of **1a** we also conducted reactions of the diazaborole **B** with $[Ge_9\{Si(TMS)_3\}_2]^{2-}$. In comparison to **A**, **B** comprises an unsaturated backbone of the central heterocycle (less flexible) and sterically more demanding 2,6-di-isopropylphenyl wingtip substituents. In contrast to the synthesis of **1a**, no reaction between **B** and $[Ge_9\{Si(TMS)_3\}_2]^{2-}$ occurred in thf solution at room temperature. Upon elevation of the temperature a reaction between the reactants commenced, however, significant amounts of the tris-silylated $[Ge_9]$ cluster $[Ge_9\{Si(TMS)_3\}_3]^-$ were formed as side product. Finally, the synthesis of $[Ge_9\{Si(TMS)_3\}_2\{BN(Dipp)\text{-}CH{=}CH\text{-}N(Dipp)\}]^-$ (**2a**) was achieved by conducting the reaction in acetonitrile solution at 40 °C (full conversion of the reactants was observed after 3 d). The anion **2a** was characterized by NMR spectroscopy and the molecule peak of **2a** with an attached MeCN molecule was monitored in ESI-MS examinations at *m/z* 1581.0 $\{[Ge_9\{Si(TMS)_3\}_2\{BN(Dipp)\text{-}CH{=}CH\text{-}N(Dipp)\}]^- + MeCN\}^-$ (**2a-MeCN**; Figure 3). By contrast, no reactions occur between **A** or **B** and the tris-silylated $[Ge_9]$ cluster $[Ge_9\{Si(TMS)_3\}_3]^-$. We assume that the increased steric shielding of the $[Ge_9]$ cluster core is the reason for this observation.

In further examinations, the diarylbromoborane Mes_2BBr (**C**) was reacted with $[Ge_9\{Si(TMS)_3\}_2]^{2-}$ in thf solution, yielding a brown solid after work-up (filtration to remove remaining solids and evaporation of solvent *in vacuo*). ^{1}H NMR examinations revealed the formation of $[Ge_9\{Si(TMS)_3\}_2BMes_2]^-$ (**3a**) by the shift of the silyl groups' proton signal and the observed signal ratio of the $[Ge_9]$ cluster's substituents (silyl groups / borane). Additionally, the molecule peak of **3a** was monitored with an attached thf molecule at *m/z* 1470.8 $\{[Ge_9\{Si(TMS)_3\}_2(BMes_2)]^- + thf\}^-$ (**3a-thf**, Figure 3) in ESI-MS examinations. As already observed for species **A** and **B**, compound **C** does not react with $[Ge_9\{Si(TMS)_3\}_3]^-$ (probably due to steric crowding).

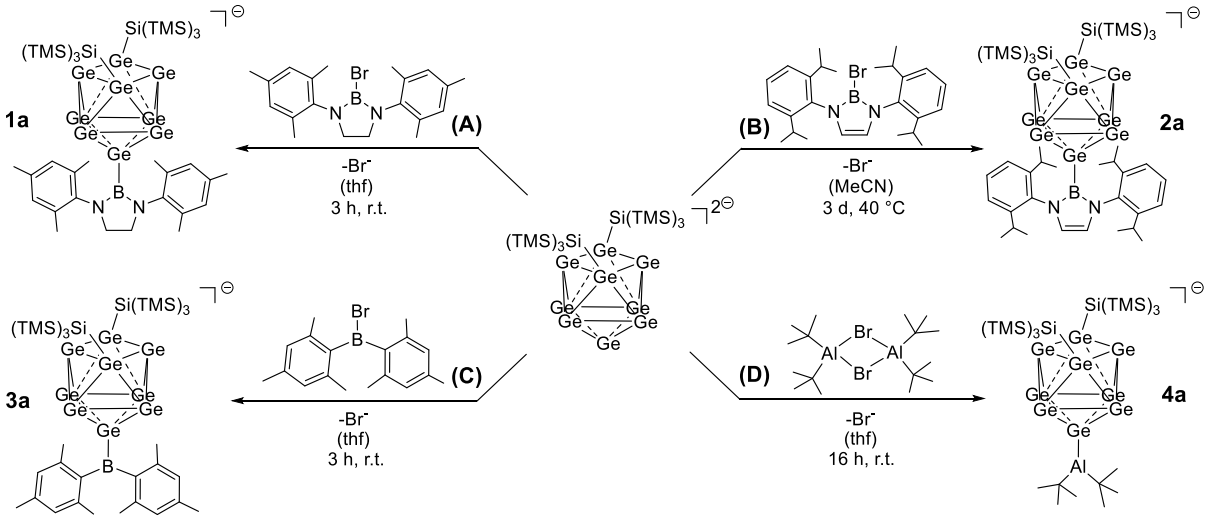

Scheme 1: Reactions of $[Ge_9\{Si(TMS)_3\}_2]^{2-}$ with Group 13 element compounds **A**-**D**, yielding mixed-substituted $[Ge_9]$ clusters **1a**-**4a**. Since anions **1a**-**4a** could not be crystallographically characterized to date, their structures were proposed to be similar to analogous species with other main-group element substituents bound to $[Ge_9]$.[22, 27, 30]

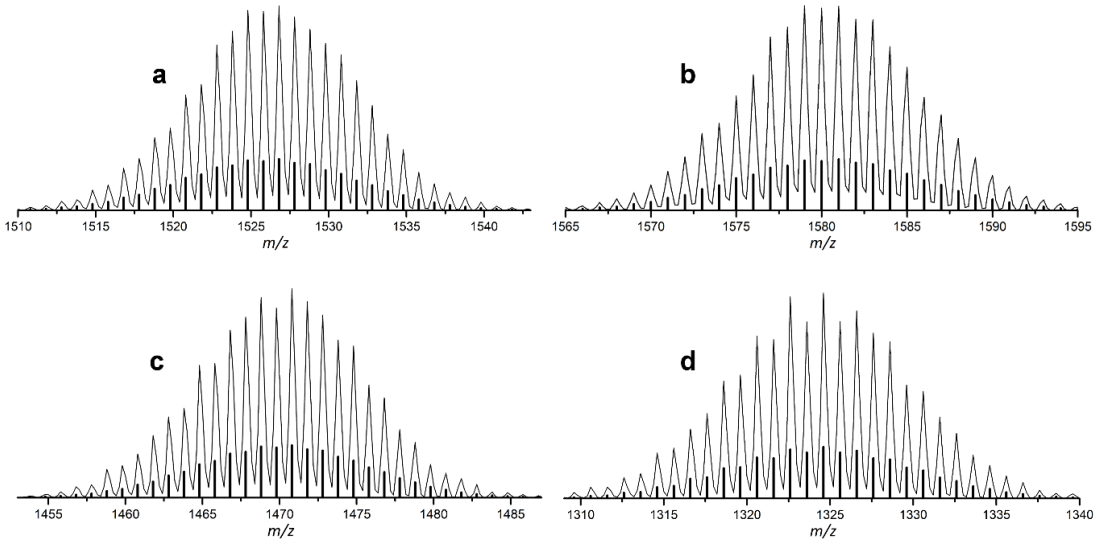

Figure 3: Selected areas of ESI-MS spectra of the mixed-substituted $[Ge_9]$ cluster anions **1a**-**4a**. a) *m/z* 1526.8 $\{[Ge_9\{Si(TMS)_3\}_2\{BN(Mes)\text{-}CH_2\text{-}CH_2\text{-}N(Mes)\}]^-$ + thf$\}^-$ (**1a-thf**); b) *m/z* 1581.0 $\{[Ge_9\{Si(TMS)_3\}_2\{BN(Dipp)\text{-}CH{=}CH\text{-}N(Dipp)\}]^-$ + MeCN$\}^-$ (**2a-MeCN**); c) *m/z* 1470.8 $\{[Ge_9\{Si(TMS)_3\}_2(BMes_2)]^-$ + thf$\}^-$ (**3a-thf**); d) *m/z* 1324.6 $\{[Ge_9\{Si(TMS)_3\}_2(Al^tBu_2)]^-$ + Cl$\}^-$ (**4a-Cl**). Calculated patterns are represented as black bars. Overview spectra of the ESI-MS measurements are provided in the Supporting information. Proposed structures for **1a**-**4a** are presented in Scheme 1.

Moreover, the reactivity of $[^tBu_2AlBr]_2$ (**D**) towards $[Ge_9\{Si(TMS)_3\}_n]^{(4-n)-}$ (*n*: 2, 3) was investigated. In analogy to the reactivity of the boron-based compounds (**A-C**), $[^tBu_2AlBr]_2$ (**D**) readily reacted with $[Ge_9\{Si(TMS)_3\}_2]^{2-}$ under formation of $[Ge_9\{Si(TMS)_3\}_2(Al^tBu_2)]^-$ (**4a**). Anion **4a** was characterized by NMR spectroscopy (^1H, ^{13}C, ^{29}Si), and in ESI-MS examinations a signal that can be assigned to **4a** with an attached chloride was detected at *m/z* 1324.6 $\{[Ge_9\{Si(TMS)_3\}_2(Al^tBu_2)] + Cl\}^-$ (**4-Cl**, Figure 3). By contrast, reactions of **D** with $[Ge_9\{Si(TMS)_3\}_3]^-$ resulted in the conversion of the reactants to unknown products.

Reactions of $^tBu_2SbCl$ with $[Ge_9\{Si(TMS)_3\}_n]^{(4-n)-}$ (*n*: 2, 3)

Reactions of $^tBu_2SbCl$ with $[Ge_9\{Si(TMS)_3\}_2]^{2-}$ resulted in the reduction of the chlorostibane to the antimony tetra-cycle $Sb_4(^tBu)_4$ and unknown oxidation product(s) of the $[Ge_9]$ cluster species (broad ^1H NMR signal in silyl group area).[32, 33] By contrast, $^tBu_2SbCl$ readily reacted with $[Ge_9\{Si(TMS)_3\}_3]^-$ under formation of the neutral compound $[Ge_9\{Si(TMS)_3\}_3Sb^tBu_2]$ (**5**) (Scheme 2). Compound **5** was characterized by means of NMR spectroscopy (^1H, ^{13}C, ^{29}Si).

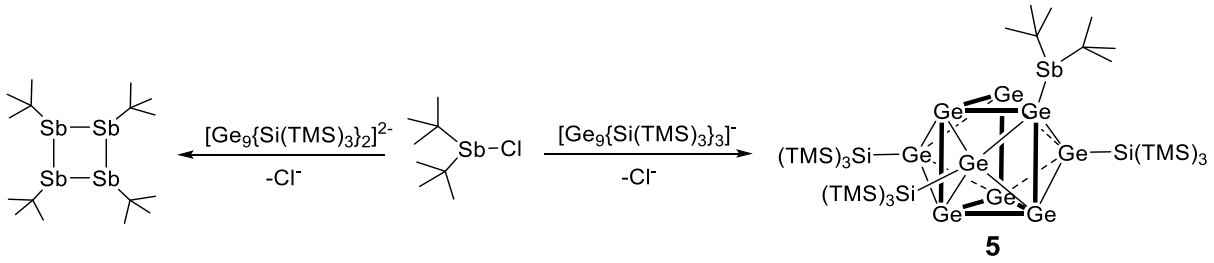

Scheme 2: Reactivity of $^tBu_2SbCl$ towards $[Ge_9\{Si(TMS)_3\}_n]^{(4-n)-}$ (*n*: 2, 3). Since compound **5** could not be crystallographically characterized to date its structure was proposed to be analogous to previously reported neutral compounds bearing $[PR_2]^+$ (*R*: alkyl) moieties as fourth substituents.[22] However, it is also possible that the stibane group is situated above a Ge_3 face and interacts with more than one Ge vertex atom (2-electron-multi-center bond). Such interactions have previously been observed for stannyl groups bound to $[Ge_9\{Si(TMS)_3\}_3]^-$ as a fourth ligand.[17, 18]

Investigations on the Reactivity of Compounds **A-E** towards $[Ge_9]^{4-}$

In analogy to the synthesis of $[Ge_9\{Si(TMS)_3\}_n]^{(4-n)-}$ (*n*: 2, 3) from K_4Ge_9 and $(TMS)_3SiCl$,[11] acetonitrile or thf solutions of the main-group element compounds **A**-**E** were reacted with solid K_4Ge_9 (heterogenous reaction). The resulting reaction mixtures were stirred at room temperature. Subsequently, the mixtures were filtered to remove all solids and the obtained solutions were examined by means of NMR spectroscopy and ESI-MS.

Regarding reactions of compounds **A** or **B** with K_4Ge_9, ESI-MS examinations indicated the presence of multiple borane-substituted $[Ge_9]$ clusters in the gas phase. In reactions carried out with compound **A**, the major signal was monitored at *m/z* 1345.9 and could be assigned to a twofold borane-substituted $[Ge_9]$ species with two attached acetonitrile molecules $\{[Ge_9\{BN(Mes)\text{-}CH_2\text{-}CH_2\text{-}N(Mes)\}_2]^- + 2\ MeCN\}^-$ (Figure 4). By contrast, in investigations of

reaction solutions containing **B**, the main signal was detected at *m/z* 1937.2 and could be assigned to a threefold borane-substituted [Ge_9] cluster with three attached acetonitrile molecules {[Ge_9{BN(Dipp)-CH=CH-N(Dipp)}$_3$]$^-$ + 3 MeCN}$^-$ (Figure 4). However, NMR examinations carried out with the respective reaction solutions revealed the presence of product mixtures consisting of several species. Therefore, it is not completely clear to date, whether the monitored species are present in solution or if they are formed during the ionization process in the mass spectrometer. Furthermore, analogous reactions of K_4Ge_9 with compounds **C** and **D** resulted in unknown products, and compound **E** was reduced to the antimony tetra-cycle $Sb_4{}^tBu_4$ (as already observed in reactions of **E** with [Ge_9{Si(TMS)$_3$}$_2$]$^{2-}$).[32, 33]

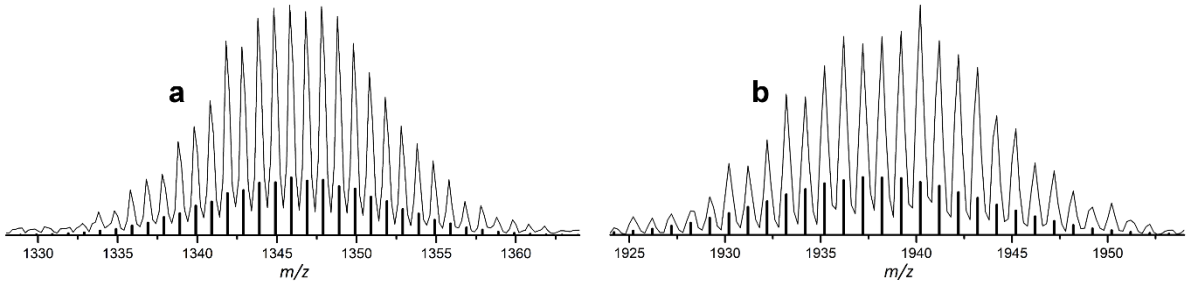

Figure 4: Selected areas of ESI-MS spectra of the multiple borane substituted [Ge_9] clusters. a) *m/z* 1345.9 {[Ge_9{BN(Mes)-CH$_2$-CH$_2$-N(Mes)}$_2$]$^-$+ 2 MeCN}$^-$; b) *m/z* 1937.2 {[Ge_9{BN(Dipp)-CH=CH-N(Dipp)}$_3$]$^-$ + 3 MeCN}$^-$. Calculated patterns are shown as black bars. The number of solvent molecules attached to the [Ge_9] cluster species in ESI-MS examinations correlates with the number of borane substituents. Overview spectra of the ESI-MS measurements are provided in the Supporting information.

Conclusion

Within this work, a series of mixed-substituted [Ge_9] cluster anions **1a**-**4a** was obtained by reaction of Group 13 element compounds **A**-**D** with [Ge_9{Si(TMS)$_3$}$_2$]$^{2-}$. Moreover, reaction of the chlorostibane **E** with [Ge_9{Si(TMS)$_3$}$_3$]$^-$ yielded neutral compound **5**. All these species were characterized by means of NMR spectroscopy and the anions **1a**-**4a** were additionally monitored in ESI-MS examinations. Unfortunately, crystallographic characterization was not achieved to date, therefore, the structures of the anions **1a**-**4a** and the neutral compound **5** can only be proposed referring to known structures. Moreover, ESI-MS examinations indicated the formation of multiple borane-substituted [Ge_9] clusters upon heterogenous reactions of acetonitrile solutions of **A** and **B** with K_4Ge_9. However, it is not completely clear yet, whether the monitored species are formed during the ionization process in the mass spectrometer or if they are already present in solution.

Experimental Section

General Information

All manipulations were performed under oxygen-free, dry conditions under argon atmosphere using standard Schlenk or glove box techniques. Glassware was dried prior to usage by heating it *in vacuo*. The solvents used were obtained from an *MBraun* Grubbs apparatus. All other commercially available chemicals were used without further purification. K_4Ge_9 was prepared by fusion of stoichiometric amounts of the elements in stainless-steel tubes at 650 °C. The silylated clusters $K[Ge_9\{Si(TMS)_3\}_3]$,[11] $K_2[Ge_9\{Si(TMS)_3\}_2]$,[27] the diazaborolidine [BrBN(Mes)-CH_2-CH_2-N(Mes)] (**A**),[34] the diazaborole [BrBN(Dipp)-CH=CH-N(Dipp)] (**B**),[34] the diarylbromoborane Mes_2BBr (**C**; donated by Dr. Daniel Franz; Inoue group TUM),[35] as well as the dialkylbromoalane $[^tBu_2AlBr]_2$ [36] (**D**) and the dialkylchlorostibane $^tBu_2SbCl$ (**E**)[37] were prepared according to modified literature procedures.

NMR Spectroscopy

NMR spectra were measured on a Bruker Avance Ultrashield 400 MHz spectrometer. The ^1H NMR spectra were calibrated using the residual proton signal of the used deuterated solvents. Chemical shifts are reported in parts per million (ppm) relative to TMS, with the solvent peaks serving as internal reference.[38] Abbreviations for signal multiplicities are: singlet (s), doublet (d), triplet (t), heptet (hept), broad signal (brs). In ^{11}B NMR examination of **3a** the respective signal could not be detected and in the ^{13}C NMR spectrum of **4a** the carbon signal of C_{tBu} could not be monitored. All recorded NMR spectra are provided in the Supporting information.

Electrospray Ionization Mass Spectrometry (ESI-MS)

ESI-MS analyses were performed on a Bruker Daltronic HCT mass spectrometer (injection speed: 240 µL/h), and the data evaluation was carried out using the Bruker Compass Data Analysis 4.0 SP 5 program (*Bruker*). Spectra were plotted using OriginPro2016G (*OriginLab*). All recorded ESI-MS spectra are provided in the Supporting information.

Syntheses

$K[Ge_9\{Si(TMS)_3\}_2\{BN(Mes)\text{-}CH_2\text{-}CH_2\text{-}N(Mes)\}]$ (1)

$K_2[Ge_9\{Si(TMS)_3\}_2]$ (123 mg, 0.100 mmol, 1 equiv.) and $[BrBN(Mes)\text{-}CH_2\text{-}CH_2\text{-}N(Mes)]$ (39 mg, 0.100 mmol, 1 equiv.) were weighted in into a Schlenk tube and dissolved in thf (2.5 mL) to obtain a deep red reaction solution. The reaction mixture was stirred for 3 h at r. t. and subsequently filtered to remove solid materials. After removal of the solvent *in vacuo* the crude product was obtained as brownish solid (101 mg, 68 %). **^{1}H NMR** (400 MHz, 298 K, thf-d_8): δ [ppm] = 6.84 (s, 4H, CH_{Ph}), 3.42 (s, 4H, $CH_{2(Bb)}$), 2.30 (s, 12H, Me_o), 2.23 (s, 6H Me_p), 0.24 (s, 54H, Me_{TMS}). **^{13}C NMR** (101 MHz, 298 K, thf-d_8): δ [ppm] 140.99 (s, $C_{Ph(N)}$), 137.10 (s, $C_{Ph(o)}$), 134.91 (s, $C_{Ph(p)}$), 129.65 (s, CH_{Ph}), 49.34(s, $CH_{2(Bb)}$), 21.37 (s, Me_p), 18.75 (s, Me_o), 3.24 (s, Me_{TMS}). **^{29}Si-INEPT NMR** (79 MHz, 298 K, thf-d_8): δ [ppm] = -9.51 (s, Si_{TMS}), -108.54 (s, Si_{Ge9}). **^{11}B NMR** (128 MHz, 298 K, thf-d_8): δ [ppm] = 23.25 (brs, B_{Ge9}). **ESI-MS** (negative ion mode, 4500 V, 300 °C): *m/z* 1526.8 $\{[Ge_9\{Si(TMS)_3\}_2\{BN(Mes)\text{-}CH_2\text{-}CH_2\text{-}N(Mes)\}]^- + thf\}^-$.

$K[Ge_9\{Si(TMS)_3\}_2\{BN(Dipp)\text{-}CH{=}CH\text{-}N(Dipp)\}]$ (2)

$K_2[Ge_9\{Si(TMS)_3\}_2]$ (92 mg, 0.075 mmol, 1 equiv.) and $[BrBN(Dipp)\text{-}CH{=}CH\text{-}N(Dipp)]$ (35 mg, 0.075 mmol, 1 equiv.) were weighted in into a Schlenk tube and dissolved in MeCN (2.5 mL) to obtain a deep red reaction solution. The reaction mixture was stirred at 40 °C for 3 d until NMR monitoring revealed full conversion of the reactants. Subsequently, the mixture was filtered to remove solid materials and the solvent was evaporated *in vacuo* to obtain the crude product as brown solid (71 mg, 60 %). **^{1}H NMR** (400 MHz, 298 K, MeCN-d_3): δ [ppm] = 7.23-7.19 (m, 2H, $CH_{Ph(p)}$), 7.16-7.12 (m, 4H,$CH_{Ph(m)}$), 6.04 (s, 2H, $CH_{(Bb)}$), 3.15 (hept, $^3J_{HH}$ = 6.8 Hz, 4H, CH_{iPr}), 1.20 (d, 12H, $^3J_{HH}$ = 6.8 Hz, Me_{iPr}), 1.12 (d, 12H, $^3J_{HH}$ = 6.8 Hz, Me_{iPr}), 0.20 (s, 54H, Me_{TMS}).**^{13}C NMR** (101 MHz, 298 K, MeCN-d_3): δ [ppm] 147.29 (s, $C_{Ph(iPr)}$), 139.58 (s, $C_{Ph(N)}$), 127.80 (s, $CH_{Ph(p)}$), 124.21 (s, $CH_{Ph(m)}$), 118.92 (s, $CH_{(Bb)}$), 28.87 (s, CH_{iPr}), 25.27 (s, Me_{iPr}), 24.78 (s, Me_{iPr}), 2.93 (s, Me_{TMS}). **^{29}Si-INEPT NMR** (79 MHz, 298 K, MeCN-d_3): δ [ppm] = -9.26 (s, Si_{TMS}), -106.96 (s, Si_{Ge9}). **^{11}B NMR** (128 MHz, 298 K, MeCN-d_3): δ [ppm] = 22.60 (brs, B_{Ge9}). **ESI-MS** (negative ion mode, 4000 V, 300 °C): *m/z* 1581.0 $\{[Ge_9\{Si(TMS)_3\}_2\{BN(Dipp)\text{-}CH{=}CH\text{-}N(Dipp)\}]^- + MeCN\}^-$.

K[Ge$_9${Si(TMS)$_3$}$_2$(BMes$_2$)] (3)

$K_2[Ge_9\{Si(TMS)_3\}_2]$ (92 mg, 0.075 mmol, 1 equiv.) and Mes_2BBr (25 mg, 0.075 mmol, 1 equiv.) were weighted in into a Schlenk tube and dissolved in thf (2 mL) to obtain a deep red reaction solution. The reaction mixture was stirred for 3 h at r. t. and subsequently filtered to remove solid materials. After removal of the solvent *in vacuo* the crude product was obtained as brownish solid (59 mg, 55 %). **^{1}H NMR** (400 MHz, 298 K, thf-d_8): δ [ppm] = 6.71 (brs, 8H, CH_{Ph}), 2.21 (brs, 18H, $Me_{Ph(o)+(p)}$), 0.24 (s, 54H, Me_{TMS}). **^{13}C NMR** (101 MHz, 298 K, thf-d_8): δ [ppm] 141.51 (s, $C_{Ph(B)}$), 139.62 (s, $C_{Ph(p)}$), 138.51 (s, $C_{Ph(o)}$), 128.86 (brs, CH_{Ph}), 23.08 (brs, Me_p), 21.35 (s, Me_o), 3.22 (s, Me_{TMS}). **^{29}Si-INEPT NMR** (79 MHz, 298 K, thf-d_8): δ [ppm] = -9.52 (s, Si_{TMS}), -108.59 (s, Si_{Ge9}). **ESI-MS** (negative ion mode, 3500 V, 300 °C): *m/z* 1470.8 $\{[Ge_9\{Si(TMS)_3\}_2(BMes_2)]^- + thf\}^-$. In ^{11}B NMR examinations no signal was detected for **3a**, which might either result from low concentration of the sample in solution or from signal broadening (in the respective ^{1}H NMR spectrum the observed signals were also broadened).

K[Ge$_9${Si(TMS)$_3$}$_2$(Al^{t}Bu$_2$)] (4)

$K_2[Ge_9\{Si(TMS)_3\}_2]$ (92 mg, 0.075 mmol, 1 equiv.) and $[^tBu_2AlBr]_2$ (16.6 mg, 0.036 mmol, 0.5 equiv.) were weighted in into a Schlenk tube and dissolved in thf (2.5 mL) to obtain a deep red reaction solution. The reaction mixture was stirred at r. t. for 16 h and subsequently filtered to remove solid materials. After removal of the solvent *in vacuo* the crude product was obtained as brownish solid (57 mg, 57 %). **^{1}H NMR** (400 MHz, 298 K, thf-d_8): δ [ppm] = 0.89 (s, 18H, ^{t}Bu), 0.23 (s, 54H, Me_{TMS}). **^{13}C NMR** (101 MHz, 298 K, thf-d_8): δ [ppm] = 31.41 (s, Me_{tBu}) 3.23 (s, Me_{TMS}). **^{29}Si-INEPT NMR** (79 MHz, 298 K, thf-d_8): δ [ppm] = -9.53 (s, Si_{TMS}), -108.61 (s, Si_{Ge9}). **ESI-MS** (negative ion mode, 400 V, 300 °C): *m/z* 1324.6 $\{[Ge_9\{Si(TMS)_3\}_2(Al^tBu_2)]^- + Cl\}^-$. In ^{13}C NMR measurement the signal of the central carbon atom of the ^{t}Bu group (C_{tBu}) was not monitored.

[Ge$_9${Si(TMS)$_3$}$_3$(Sb^{t}Bu$_2$)] (5)

$K[Ge_9\{Si(TMS)_3\}_3]$ (143 mg, 0.100 mmol, 1 equiv.) was weighted in into a Schlenk tube and a toluene solution (3 mL) of $^tBu_2SbCl$ (27 mg, 0.100 mmol, 1 equiv.) was added to obtain a deep red reaction solution. The reaction mixture was stirred for 1.5 h at r. t. and subsequently filtered to remove solid materials. After removal of the solvent *in vacuo* the crude product was obtained as brown oily solid (79 mg, 47%). **^{1}H NMR** (400 MHz, 298 K, C_6D_6): δ [ppm] = 1.66 (s, 18H, ^{t}Bu), 0.47 (s, 81H, Me_{TMS}). **^{13}C NMR** (101 MHz, 298 K, C_6D_6): δ [ppm] = 35.18 (s, Me_{tBu}), 34.97 (s, Me_{tBu}), 30.87 (s, C_{tBu}), 3.10 (s, Me_{TMS}). **^{29}Si-INEPT NMR** (79 MHz, 298 K, C_6D_6): δ [ppm] = -8.46 (s, Si_{TMS}), -101.65 (s, Si_{Ge9}).

Reactions of K_4Ge_9 with [BrBN(Mes)-CH_2-CH_2-N(Mes)]

K_4Ge_9 (61 mg, 0.075 mmol, 1 equiv.) was treated with an acetonitrile solution (4 mL) of [BrBN(Mes)-CH_2-CH_2-N(Mes)] (87 mg, 0.225 mmol, 3 equiv.) and the resulting suspension was stirred at room temperature for 5 d, yielding a deep red suspension. The mixture was filtered to remove remaining solids and ESI-MS examinations were carried out with aliquots of the sample monitoring a signal at m/z 1345.9 which can be assigned to the twofold borane substituted [Ge_9] cluster species {[Ge_9{BN(Mes)-CH_2-CH_2-N(Mes)}$_2$]$^-$+ 2 MeCN}$^-$. However, NMR examinations carried out with the same sample revealed low selectivity of the reaction as several different species were observed.

Reactions of K_4Ge_9 with [BrBN(Dipp)-CH=CH-N(Dipp)]

K_4Ge_9 (61 mg, 0.075 mmol, 1 equiv.) was treated with an acetonitrile solution (4 mL) of [BrBN(Dipp)-CH=CH-N(Dipp)] (105 mg, 0.225 mmol, 3 equiv.) and the resulting suspension was stirred at room temperature for 7 d yielding a deep red suspension. The mixture was filtered to remove remaining solids and ESI-MS examinations were carried out with aliquots of the sample monitoring a signal at m/z 1937.2 which can be assigned to the threefold borane-substituted [Ge_9] cluster species {[Ge_9{BN(Dipp)-CH=CH-N(Dipp)}$_3$]$^-$ + 3 MeCN}$^-$. However, NMR examinations carried out with the same sample revealed low selectivity of the reaction as several different species were observed.

Acknowledgment

F. S. G. thanks M. Sc. Lorenz Schiegerl for ESI-MS measurements and Dr. Daniel Franz (Inoue group, Technical University of Munich) for supply with Mes_2BBr and fruitful discussions. Furthermore, F. S. G. thanks TUM Graduate School for support.

Literature

[1] J. D. Corbett, *Chem. Rev.* **1985**, *85*, 383.
[2] T. F. Fässler, S. D. Hoffmann, *Angew. Chem. Int. Ed.* **2004**, *43*, 6242.
[3] S. C. Sevov, J. M. Goicoechea, *Organometallics* **2006**, *25*, 5678.
[4] S. Scharfe, F. Kraus, S. Stegmaier, A. Schier, T. F. Fässler, *Angew. Chem. Int. Ed.* **2011**, *50*, 3630.
[5] A. Schnepf, *Angew. Chem. Int. Ed.* **2003**, *42*, 2624.
[6] A. F. Richards, H. Hope, P. P. Power, *Angew. Chem.* **2003**, *115*, 4205.
[7] A. F. Richards, M. Brynda, M. M. Olmstead, P. P. Power, *Organometallics* **2004**, *23*, 2841.
[8] A. Sekiguchi, Y. Ishida, Y. Kabe, M. Ichinohe, *J. Am. Chem. Soc.* **2002**, *124*, 8776.
[9] M. W. Hull, S. C. Sevov, *Inorg. Chem.* **2007**, *46*, 10953.
[10] C. B. Benda, J.-Q. Wang, B. Wahl, T. F. Fässler, *Eur. J. Inorg. Chem.* **2011**, 4262.
[11] F. Li, S. C. Sevov, *Inorg. Chem.* **2012**, *51*, 2706.
[12] C. Schenk, A. Schnepf, *Angew. Chem. Int. Ed.* **2007**, *46*, 5314.
[13] C. Schenk, F. Henke, G. Santiso-Quinones, I. Krossing, A. Schnepf, *Dalton Trans.* **2008**, 4436.
[14] F. Henke, C. Schenk, A. Schnepf, *Dalton Trans.* **2009**, 9141.
[15] O. Kysliak, C. Schrenk, A. Schnepf, *Chem. Eur. J.* **2016**, *22*, 18787.
[16] F. Li, S. C. Sevov, *Inorg. Chem.* **2015**, *54*, 8121.
[17] F. Li, A. Muñoz-Castro, S. C. Sevov, *Angew. Chem. Int. Ed.* **2012**, *51*, 8581.
[18] F. Li, S. C. Sevov, *J. Am. Chem. Soc.* **2014**, *136*, 12056.
[19] F. S. Geitner, T. F. Fässler, *Eur. J. Inorg. Chem.* **2016**, 2688.
[20] L. J. Schiegerl, F. S. Geitner, C. Fischer, W. Klein, T. F. Fässler, *Z. Anorg. Allg. Chem.* **2016**, *642*, 1419.
[21] K. Mayer, L. J. Schiegerl, T. F. Fässler, *Chem. Eur. J.* **2016**, *22*, 18794.
[22] F. S. Geitner, J. V. Dums, T. F. Fässler, *J. Am. Chem. Soc.* **2017**, *139*, 11933.
[23] S. Frischhut, T. F. Fässler, *Dalton Trans.* **2018**, *47*, 3223.
[24] O. Kysliak, C. Schrenk, A. Schnepf, *Angew. Chem. Int. Ed.* **2016**, *55*, 3216.
[25] O. Kysliak, C. Schrenk, A. Schnepf, *Inorg. Chem.* **2015**, *54*, 7083.
[26] O. Kysliak, T. Kunz, A. Schnepf, *Eur. J. Inorg. Chem.* **2017**, 805.
[27] O. Kysliak, A. Schnepf, *Dalton Trans.* **2016**, *45*, 2404.
[28] L. G. Perla, S. C. Sevov, *J. Am. Chem. Soc.* **2016**, *138*, 9795.
[29] L. G. Perla, A. Muñoz-Castro, S. C. Sevov, *J. Am. Chem. Soc.* **2017**, *139*, 15176.
[30] F. S. Geitner, C. Wallach, T. F. Fässler, *Chem. Eur. J.* **2018**, *24*, 4103.
[31] F. S. Geitner, W. Klein, T. F. Fässler, *Angew. Chem. Int. Ed.* **2018**, *57*, 14509.
[32] H. J. Breunig, *Z. Naturforsch.* B **1978**, *33*, 242.
[33] H. J. Breunig, H. Kischkel, *Z. Anorg. Allg. Chem.* **1983**, *502*, 175.
[34] Y. Segawa, Y. Suzuki, M. Yamashita, K. Nozaki, *J. Am. Chem. Soc.* **2008**, *130*, 16069.
[35] A. Sundararaman, F. Jäkle, *J. Organomet. Chem.* **2003**, *681*, 134.
[36] I. N. Krossing, H. Nöth, S. Staude, *Z. Naturforsch. B* **2008**, *63*, 1045.
[37] K. Issleib, B. Hamann, L. Schmidt, *Z. Anorg. Allg. Chem.* **1965**, *339*, 298.
[38] G. R. Fulmer, A. J. M. Miller, N. H. Sherden, H. E. Gottlieb, A. Nudelman, B. M. Stoltz, J. E. Bercaw, K. I. Goldberg, *Organometallics* **2010**, *29*, 2176.

Supporting Information

Probing the Reactivity of [Ge_9] *Zintl* Clusters towards Group 13 and Group 15 Element Compounds

Felix S. Geitner,[a] and Thomas F. Fässler[b*]

[a] Department Chemie, Technische Universität München, Lichtenbergstraße 4, 85747 Garching b. München and WACKER Institute for Silicon Chemistry.

[b] Department Chemie, Technische Universität München, Lichtenbergstraße 4, 85747 Garching b. München.

NMR Spectra

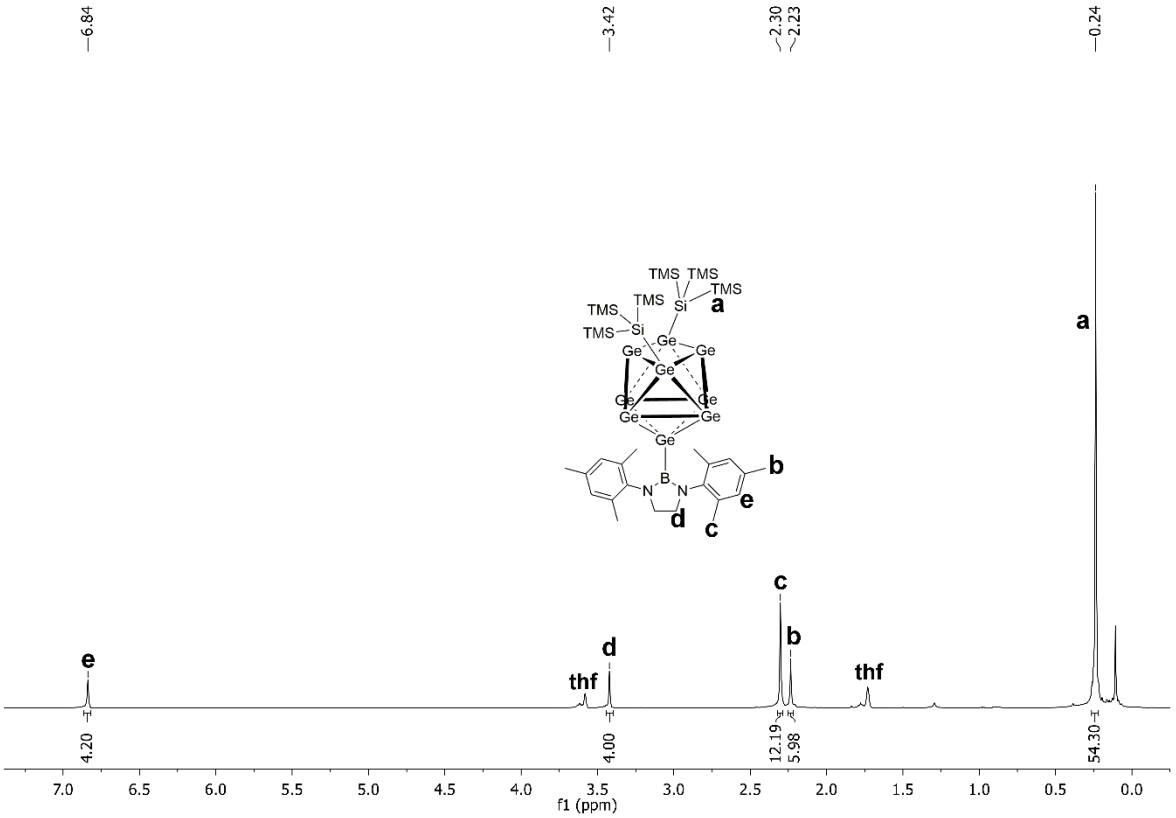

Figure S1: ^{1}H NMR spectrum of **1a** in thf-d_8.

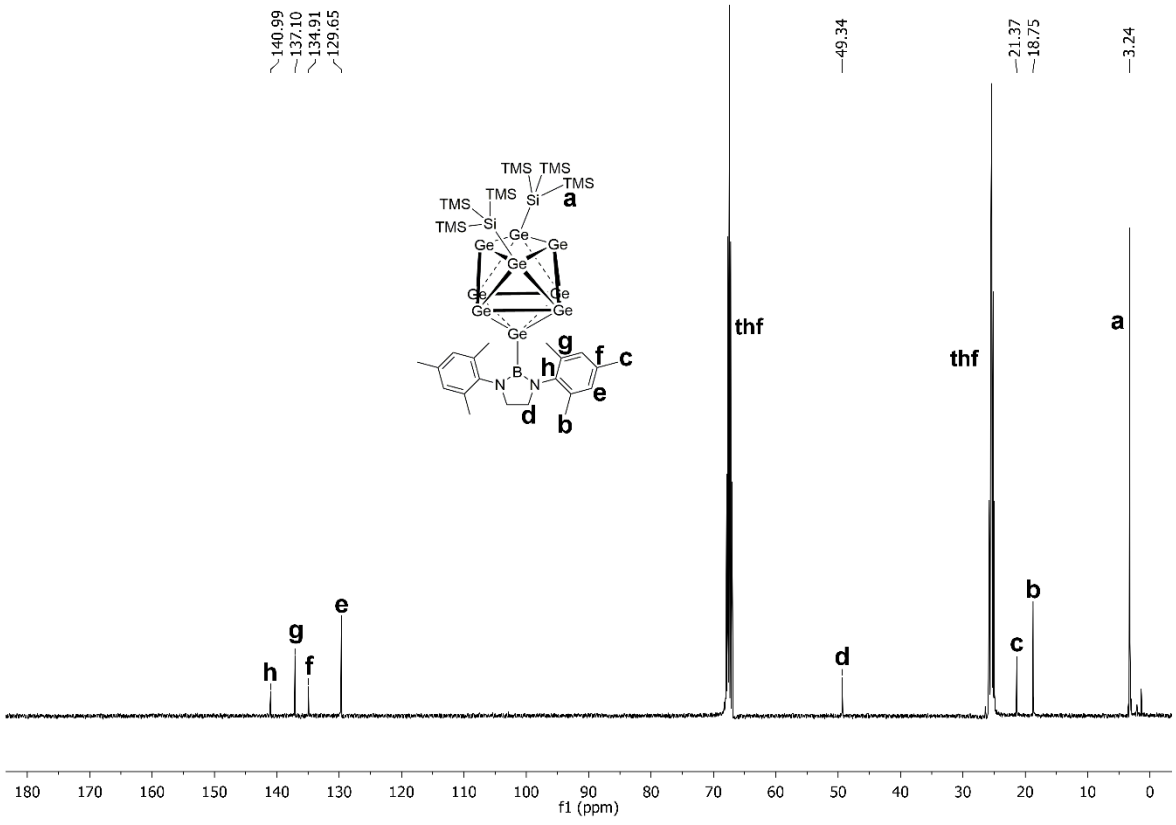

Figure S2: ^{13}C NMR spectrum of **1a** in thf-d_8.

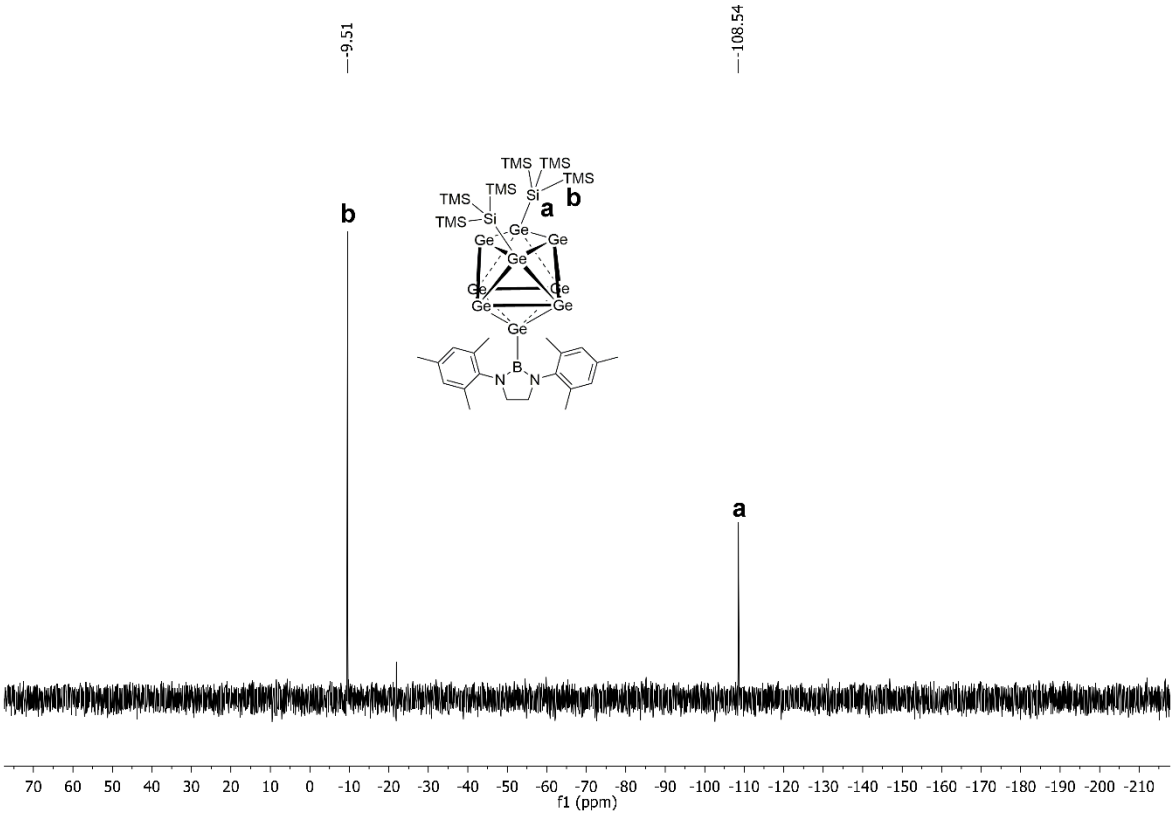

Figure S3: ^{29}Si-INEPT NMR spectrum of **1a** in thf-d_8.

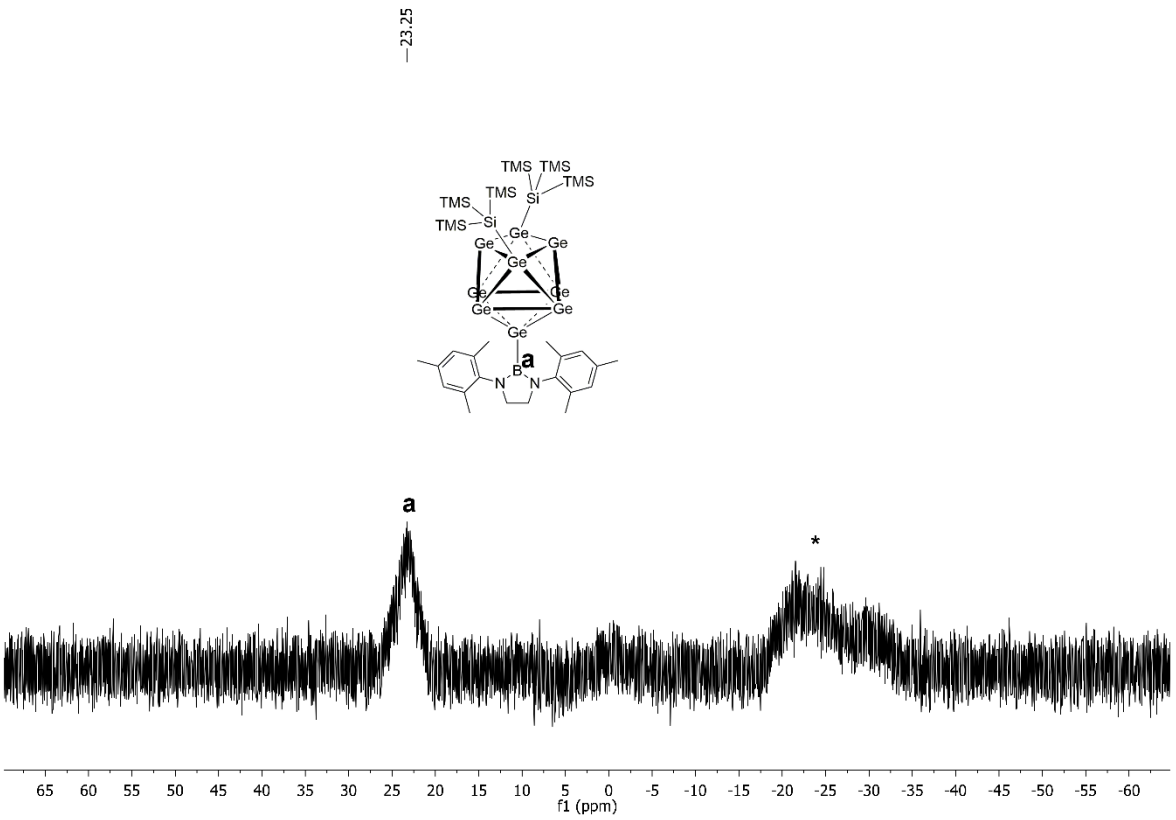

Figure S4: ^{11}B NMR spectrum of **1a** in thf-d_8. Asterisked broad signal is caused by NMR tube.

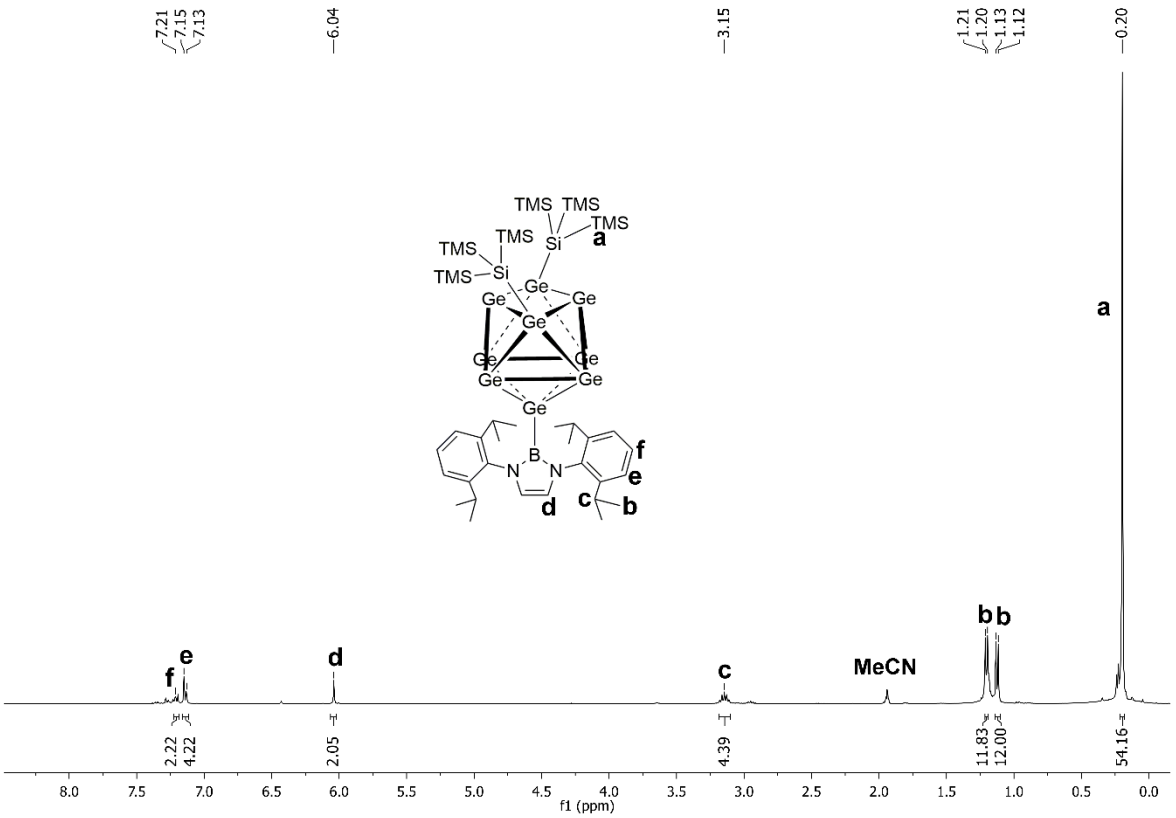

Figure S5: ^{1}H NMR spectrum of **2a** in MeCN-d_3.

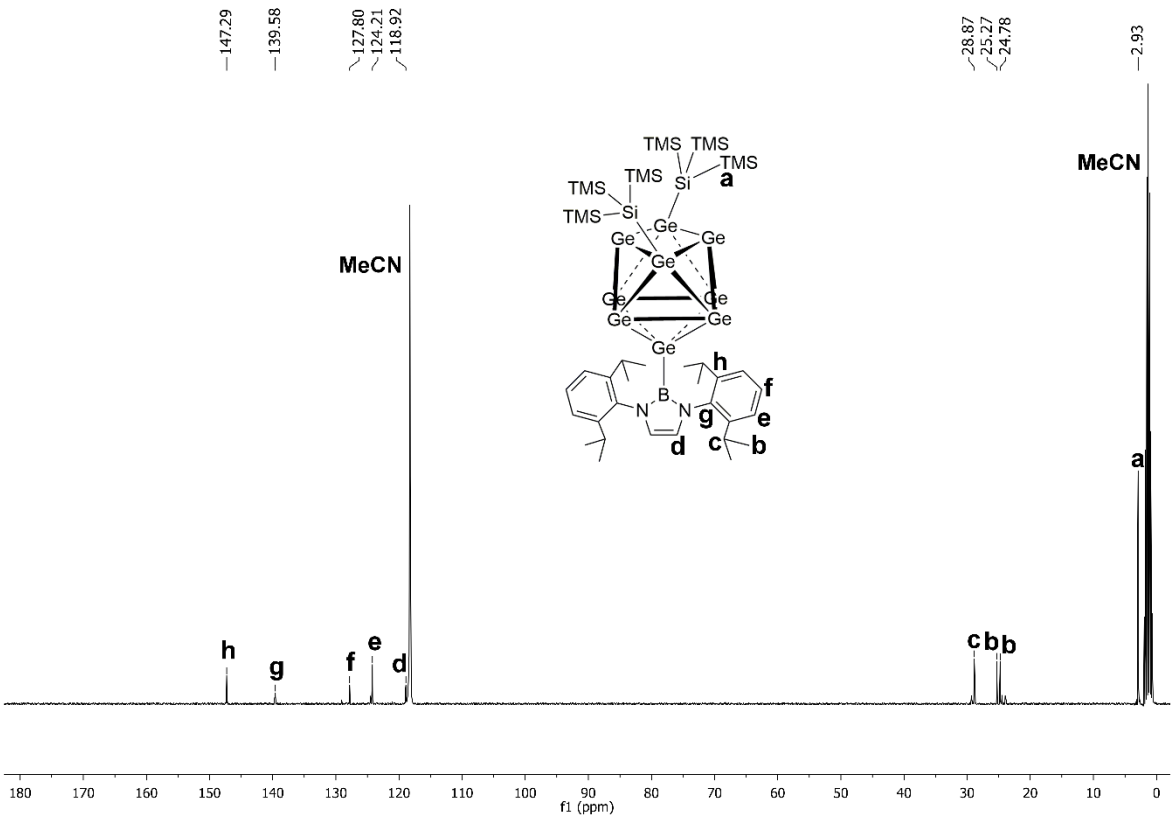

Figure S6: ^{13}C NMR spectrum of **2a** in MeCN-d_3.

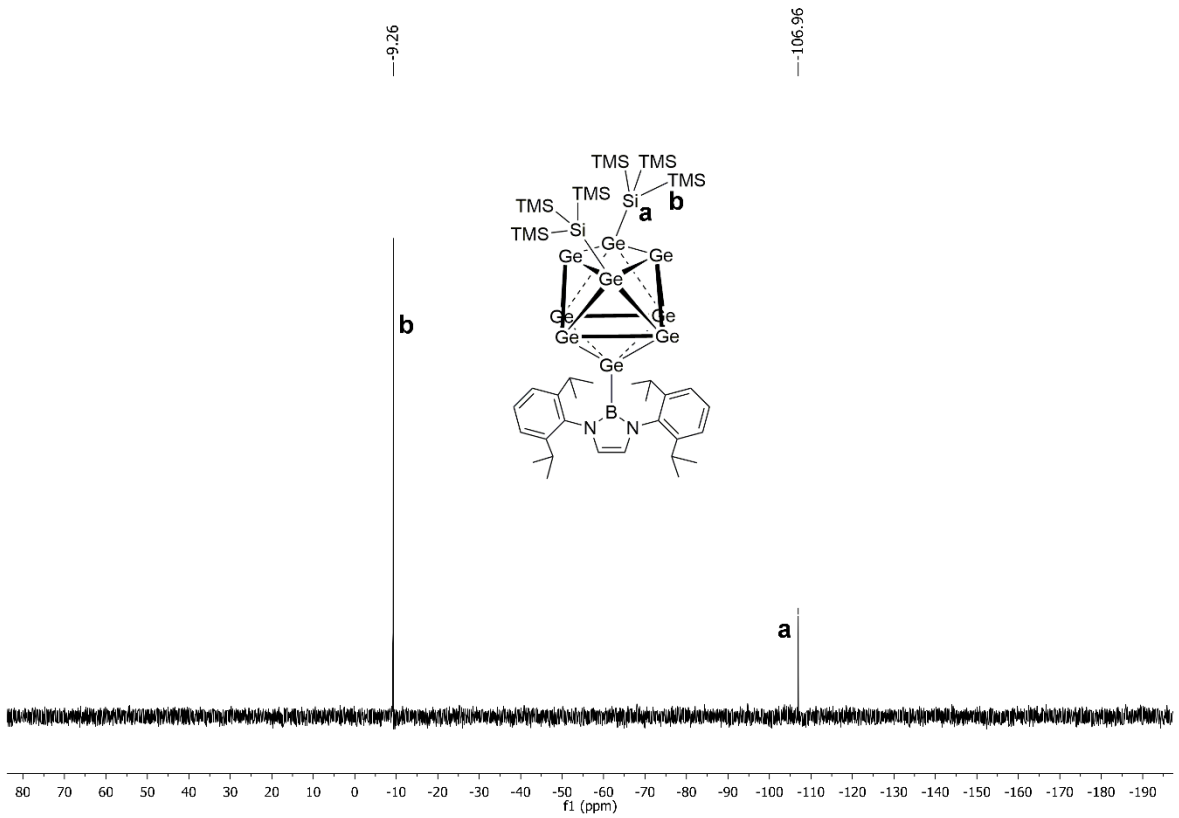

Figure S7: ^{29}Si-INEPT NMR spectrum of **2a** in MeCN-d_3.

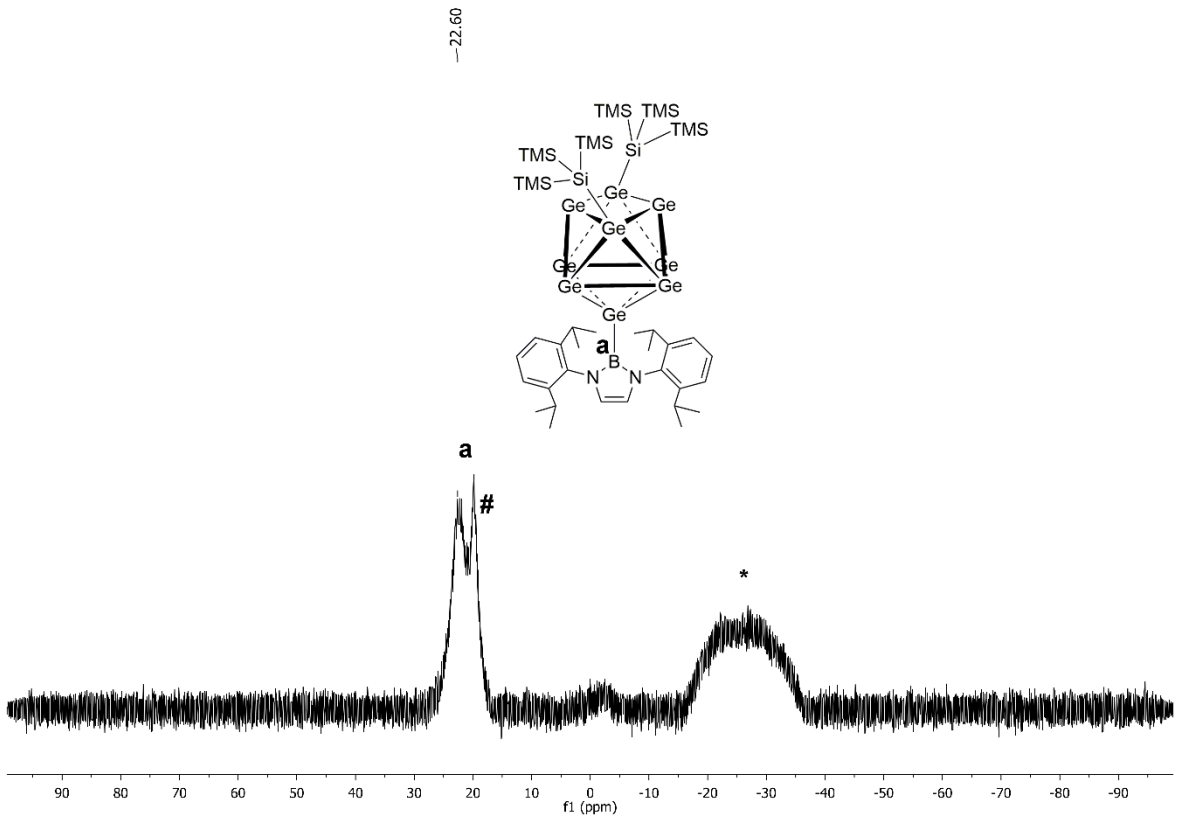

Figure S8: ^{11}B NMR spectrum of **2a** in MeCN-d_3. Asterisked broad signal is caused by NMR tube. Signal marked with # belongs to unknown impurity.

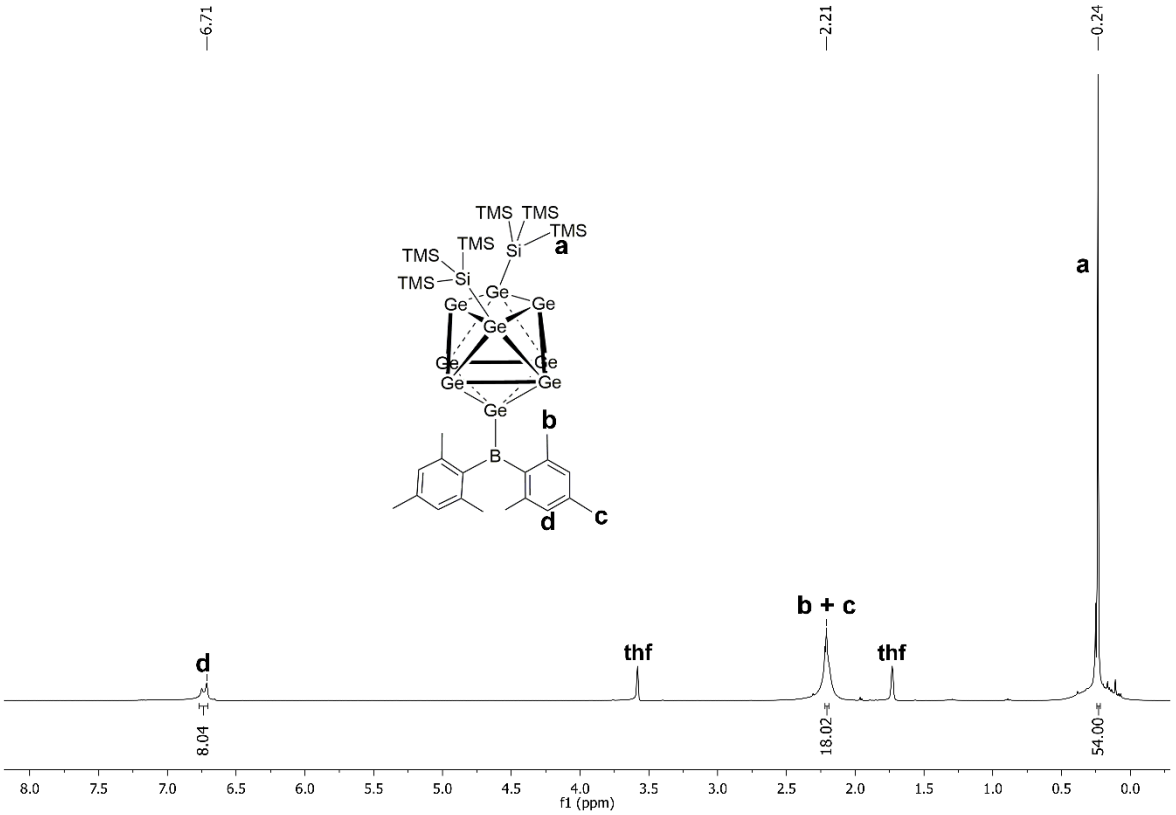

Figure S9: ^{1}H NMR spectrum of **3a** in thf-d_8.

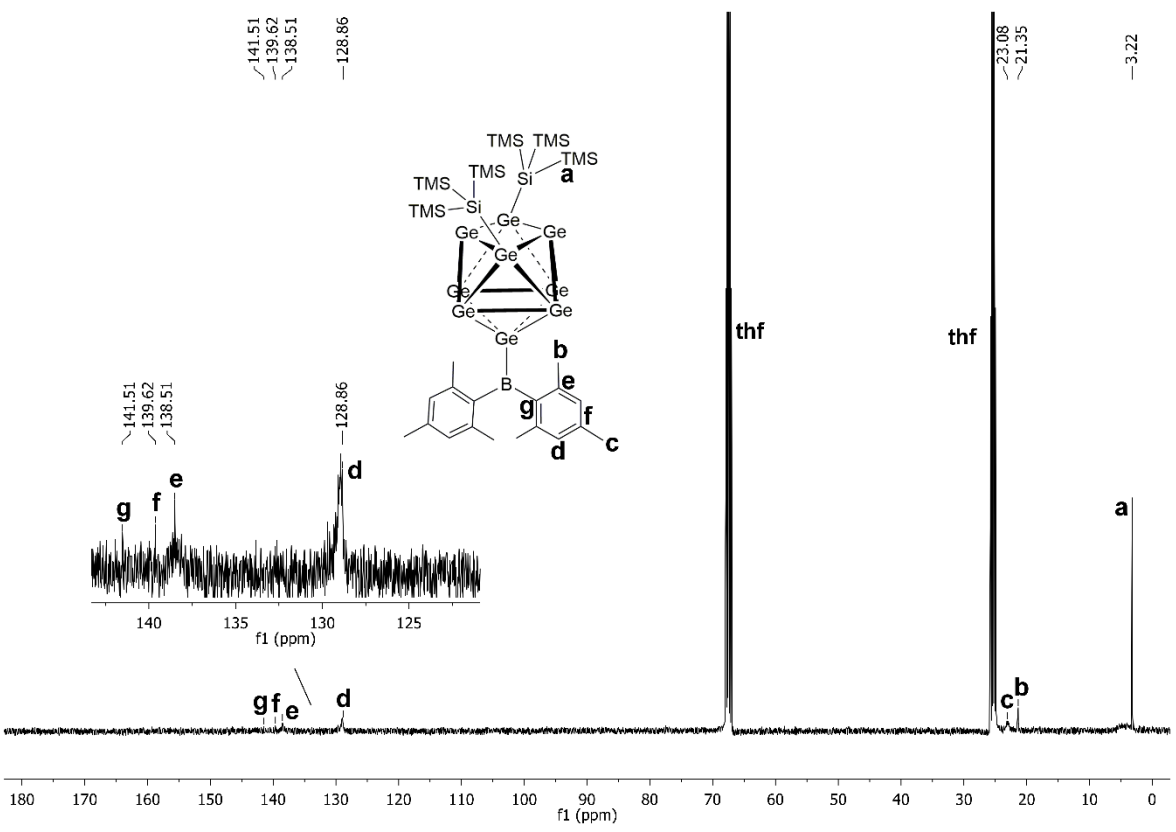

Figure S10: ^{13}C NMR spectrum of **3a** in thf-d_8.

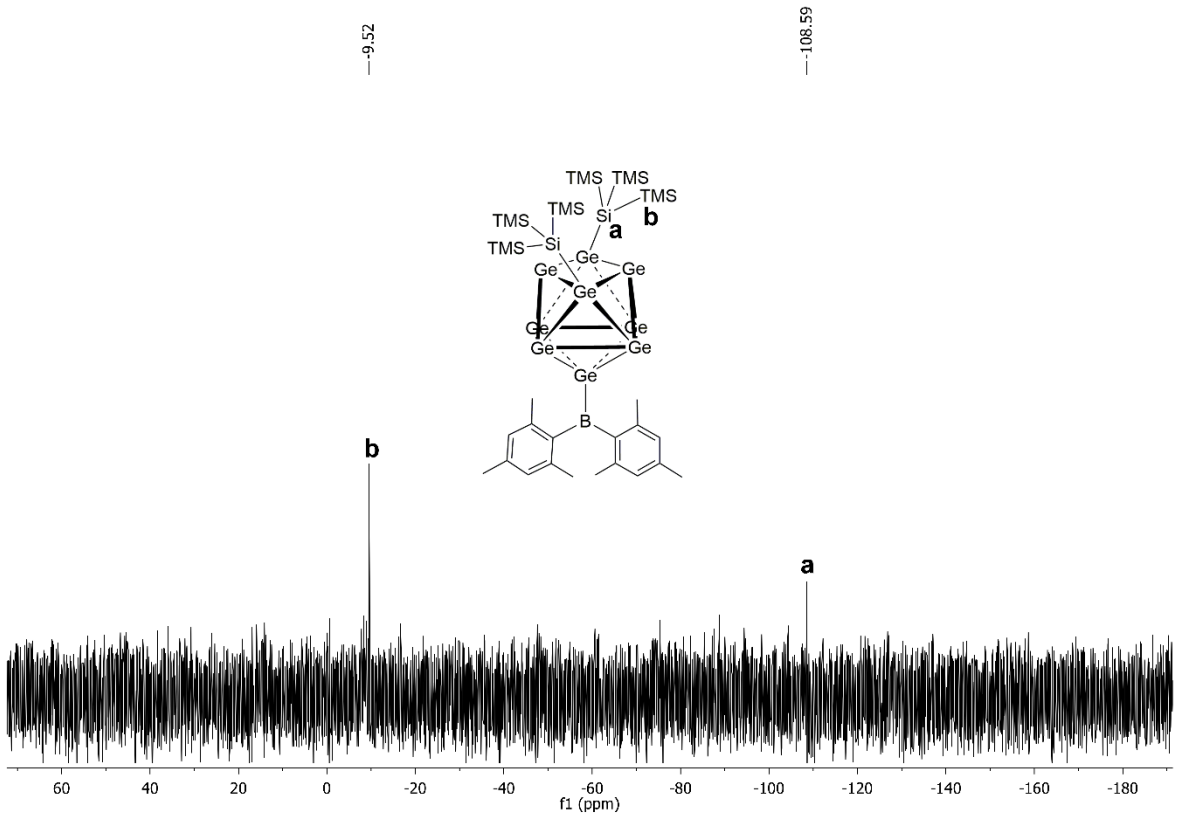

Figure S11: ^{29}Si-INEPT NMR spectrum of **3a** in thf-d_8.

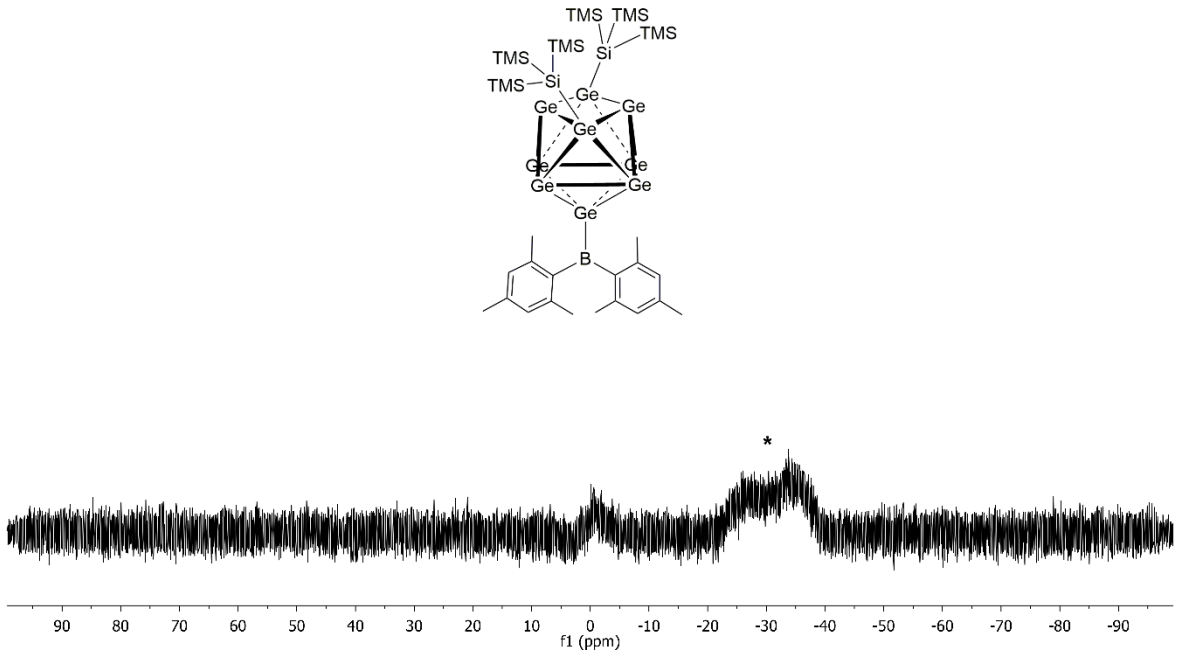

Figure S12: ^{11}B NMR spectrum of **3a** in thf-d_8. No signal which can be assigned to **3** could be monitored for unknown reason. Asterisked broad signal is caused by NMR tube.

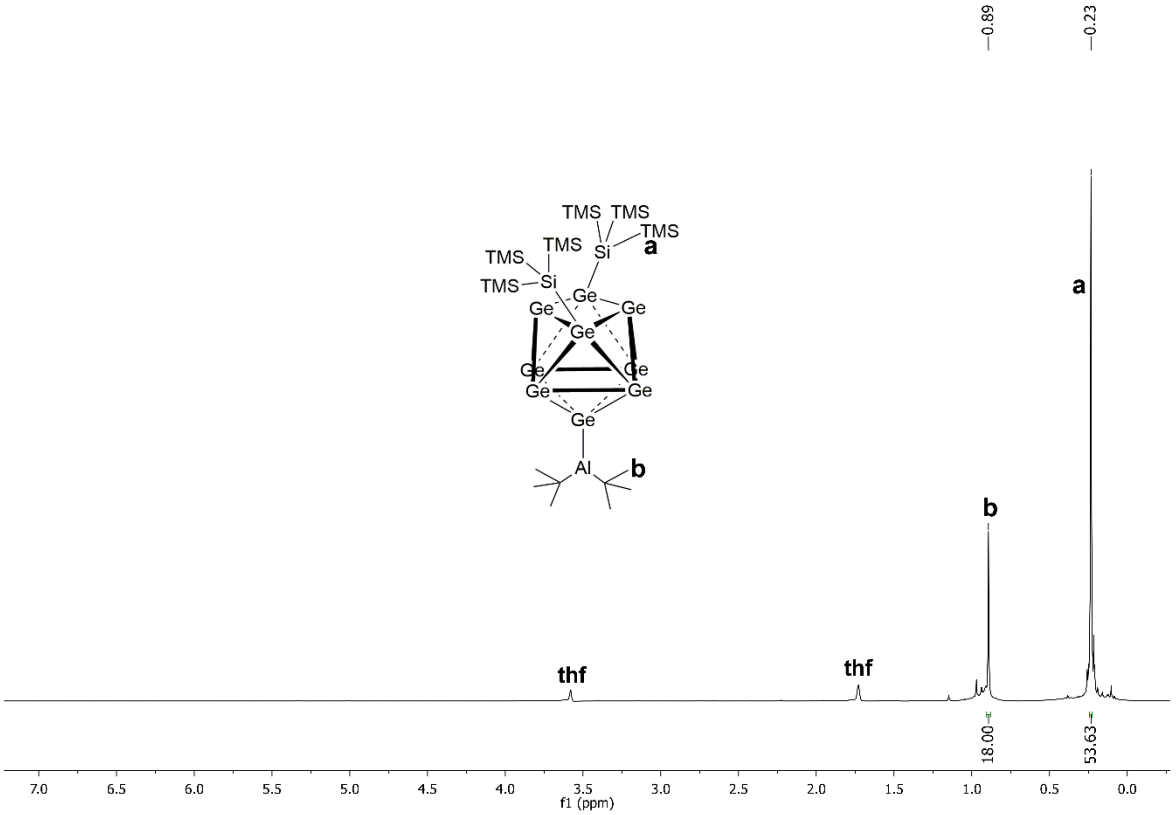

Figure S13: ^{1}H NMR spectrum of **4a** in thf-d_8.

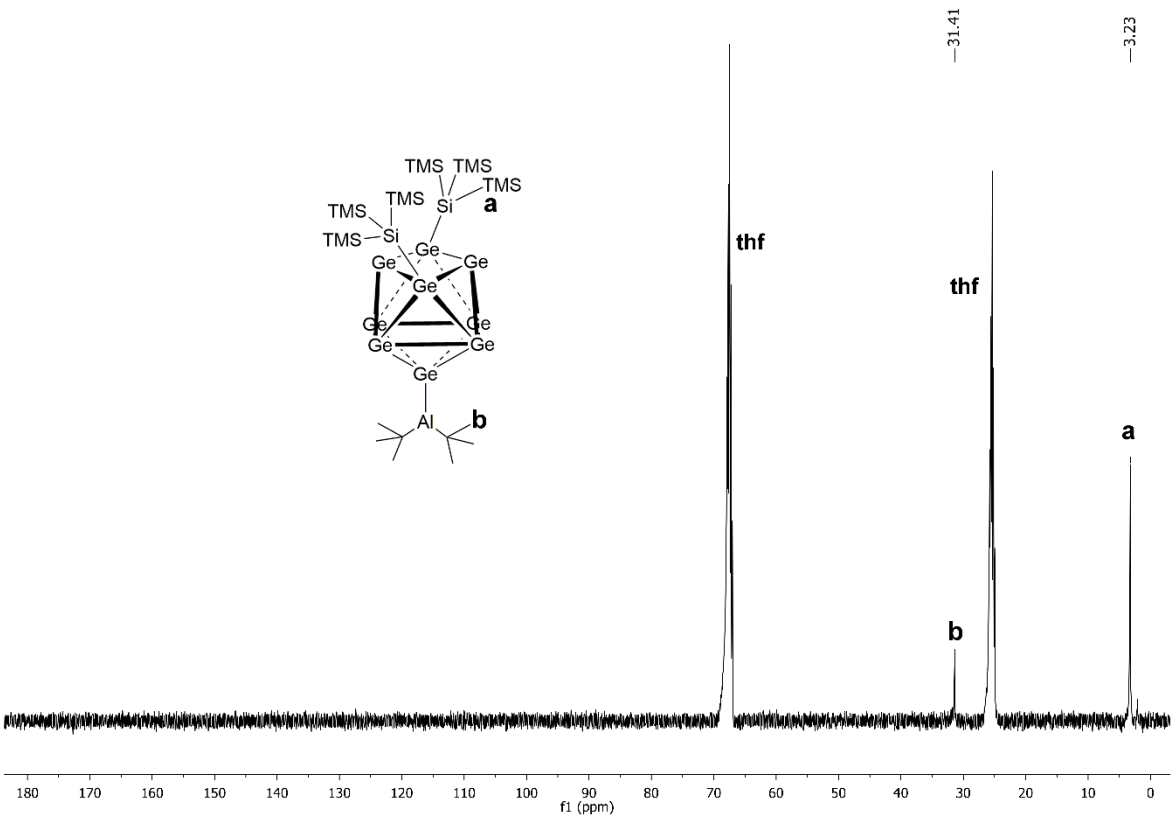

Figure S14: ^{13}C NMR spectrum of **4a** in thf-d_8. The signal of C_{tBu} could not be monitored for unknown reason.

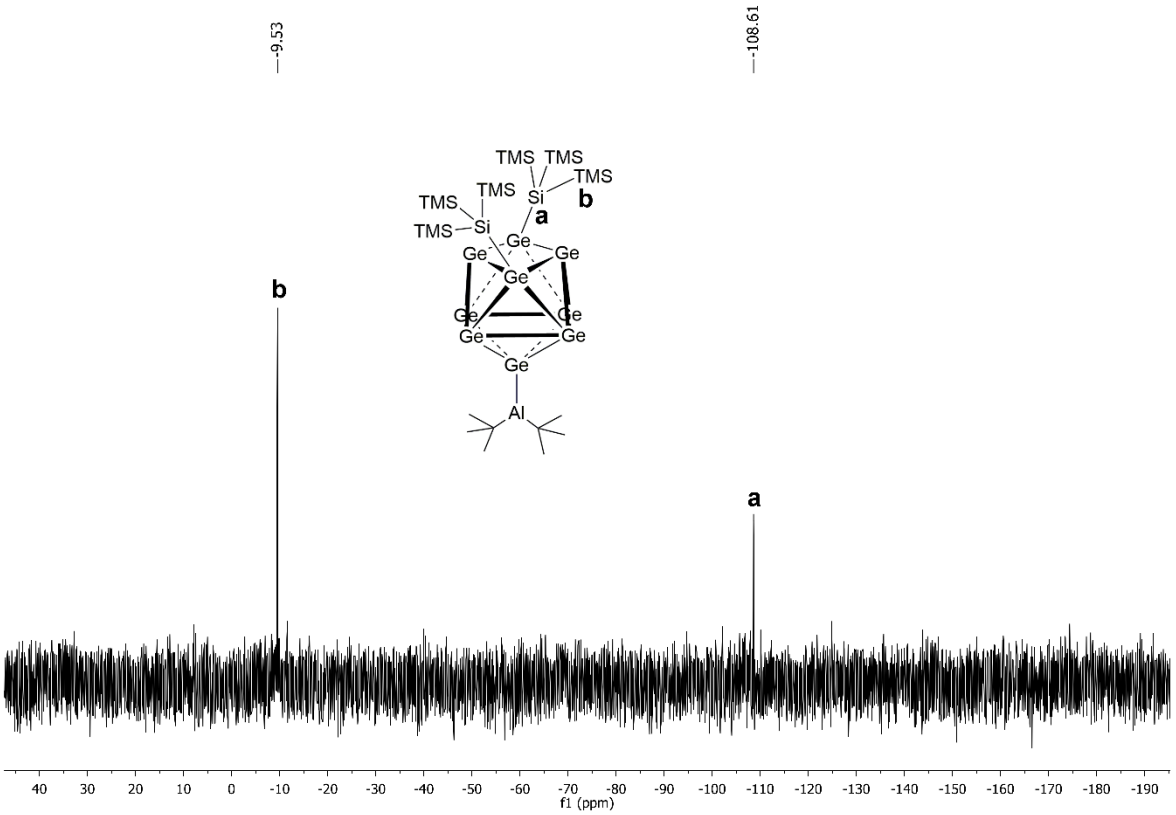

Figure S15: ^{29}Si-INEPT NMR spectrum of **4a** in thf-d_8.

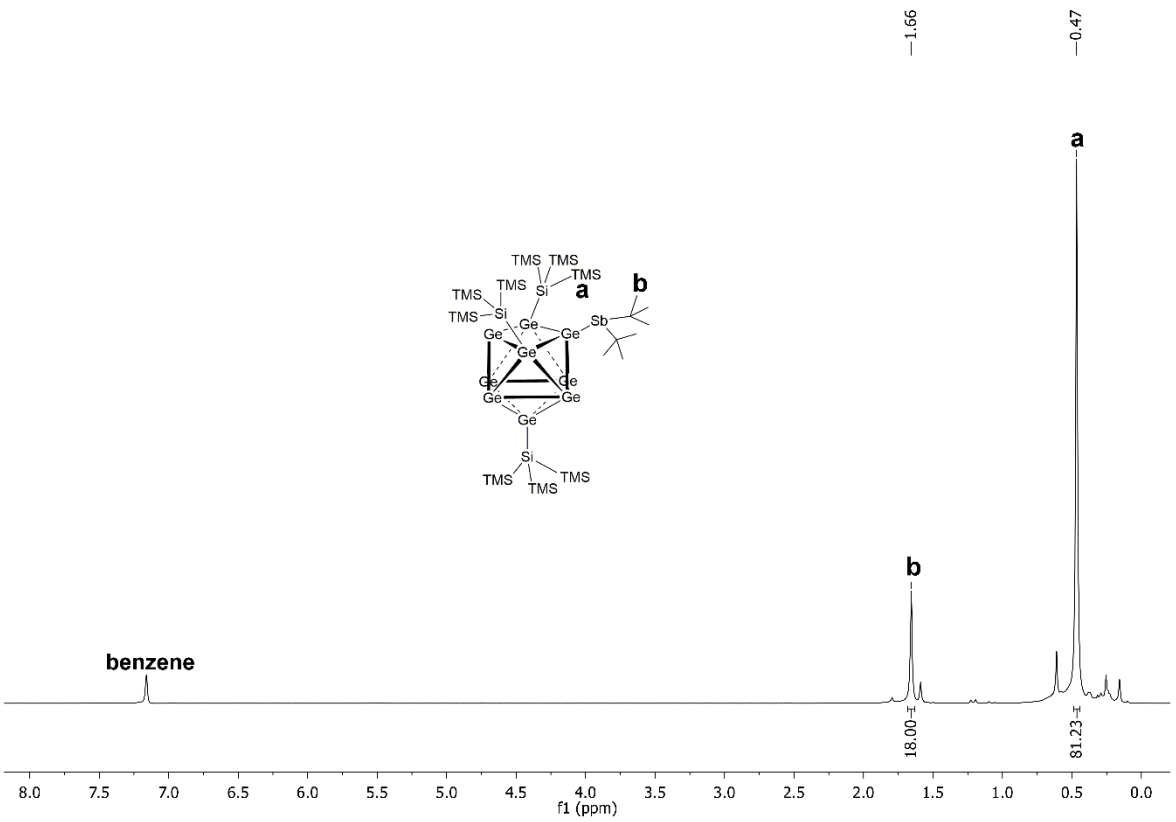

Figure S16: ^{1}H NMR spectrum of compound **5** in C_6D_6.

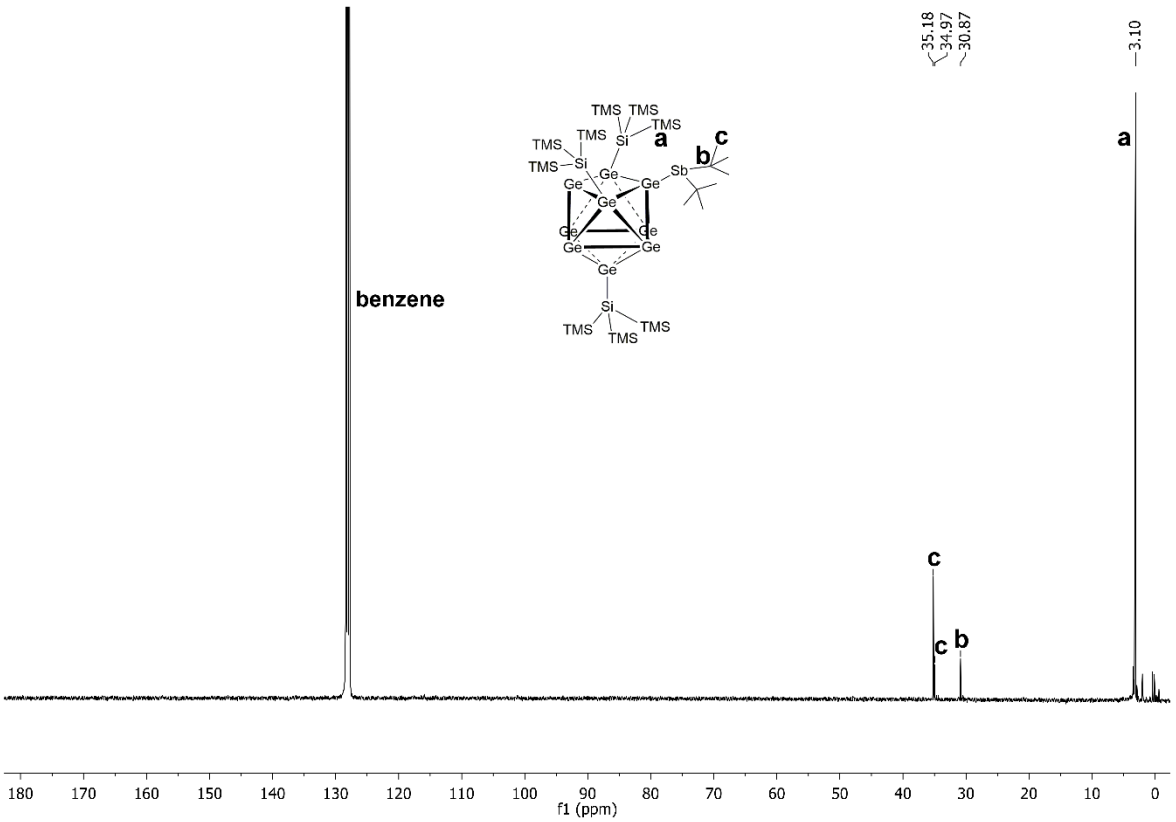

Figure S17: ^{13}C NMR spectrum of compound **5** in C_6D_6.

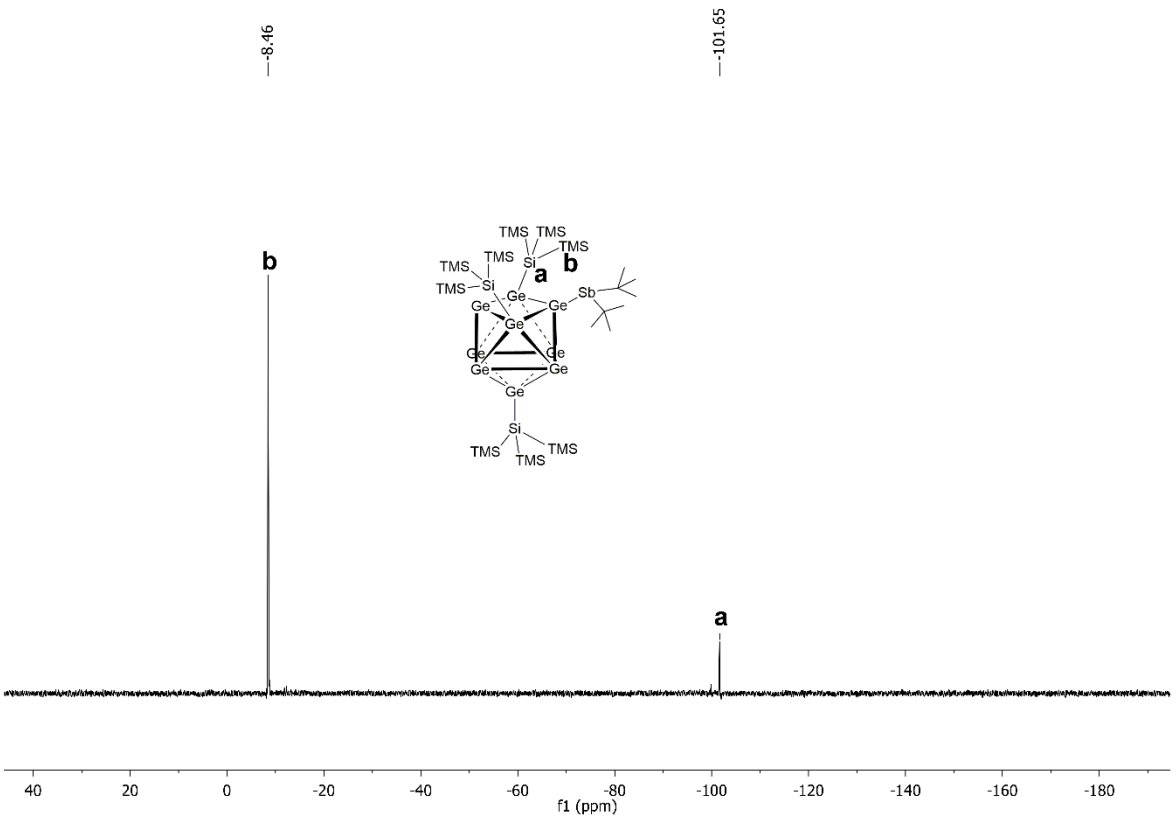

Figure S18: ^{29}Si-INEPT NMR spectrum of compound **5** in C_6D_6.

ESI-MS Spectra

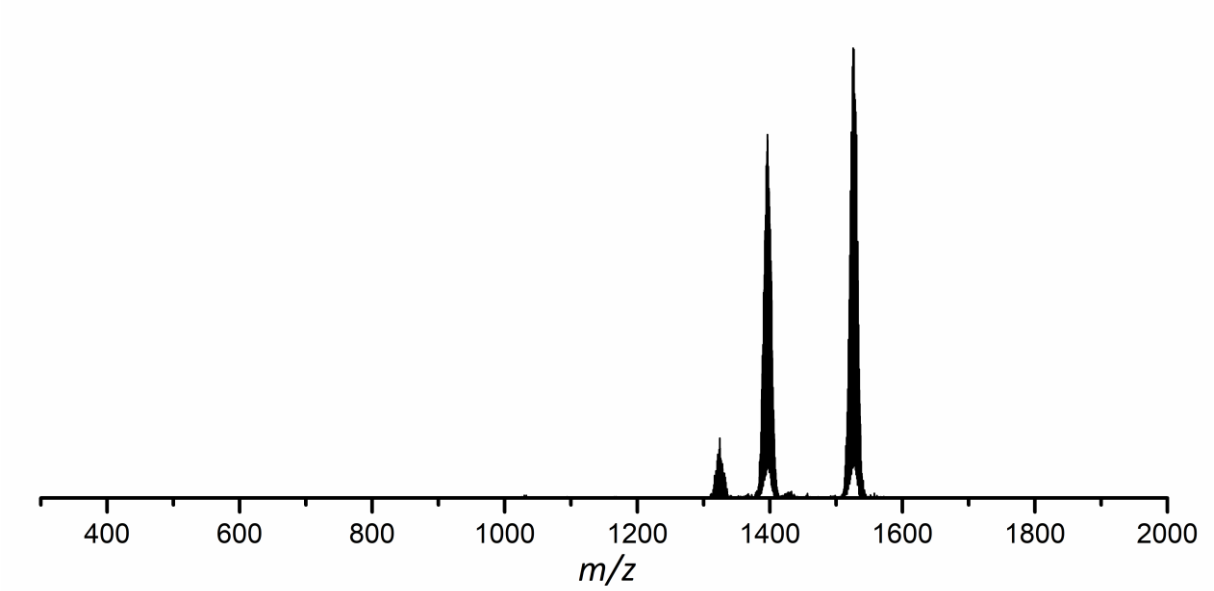

Figure S19: ESI-MS spectrum (negative mode, 4500 V, 300 °C) obtained upon examination of a thf solution of $[Ge_9\{Si(TMS)_3\}_2\{BN(Mes)\text{-}CH_2\text{-}CH_2\text{-}N(Mes)\}]^-$ (**1a**). Besides the signal at *m/z* 1526.8 $\{[Ge_9\{Si(TMS)_3\}_2\{BN(Mes)\text{-}CH_2\text{-}CH_2\text{-}N(Mes)\}]^- + thf\}^-$ (**1a-thf**), a further signal at *m/z* 1396.4 ($[Ge_9\{Si(TMS)_3\}_3]^-$) was detected. The tris-silylated species $[Ge_9\{Si(TMS)_3\}_3]^-$ is formed during the ionization process, since in NMR studies its absence in solution is proven (Figures S1-S3). A detailed view of the signal of **1a-thf** is provided in Figure 1 in the manuscript.

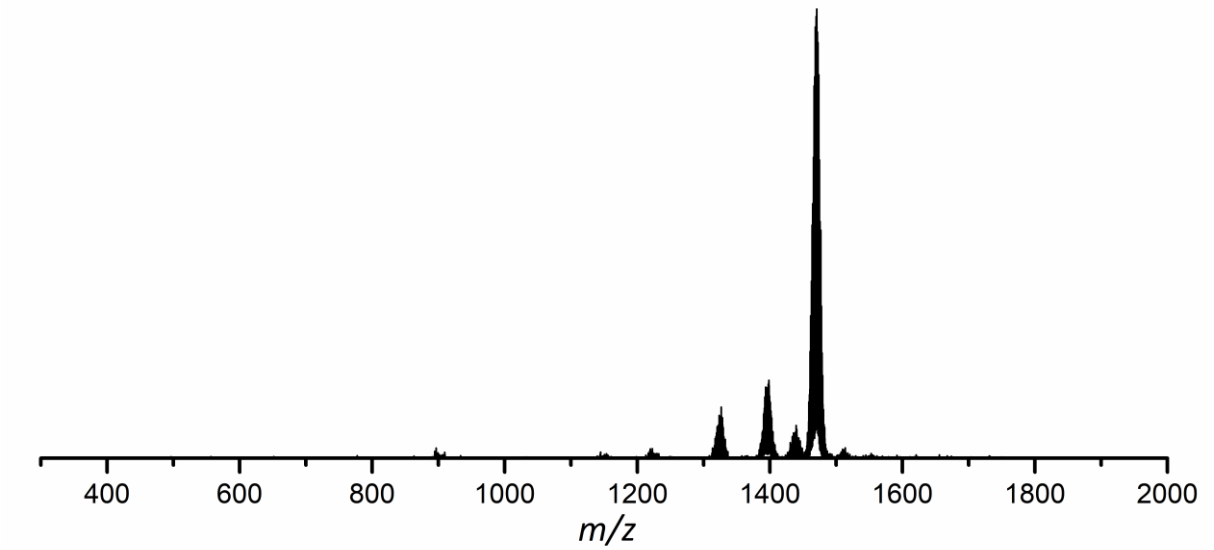

Figure S20: ESI-MS spectrum (negative mode, 3500 V, 300 °C) obtained upon examination of a thf solution of $[Ge_9\{Si(TMS)_3\}_2(BMes_2)]^-$ (**3a**). Besides the signal at *m/z* 1450.8 $\{[Ge_9\{Si(TMS)_3\}_2(BMes_2)]^- + thf\}^-$ (**3a-thf**), a further signal at *m/z* 1396.4 ($[Ge_9\{Si(TMS)_3\}_3]^-$) was detected. The tris-silylated species $[Ge_9\{Si(TMS)_3\}_3]^-$ is formed during the ionization process, since in NMR studies its absence in solution is proven (Figures S9-S11). A detailed view of the signal of **3a-thf** is provided in Figure 1 in the manuscript.

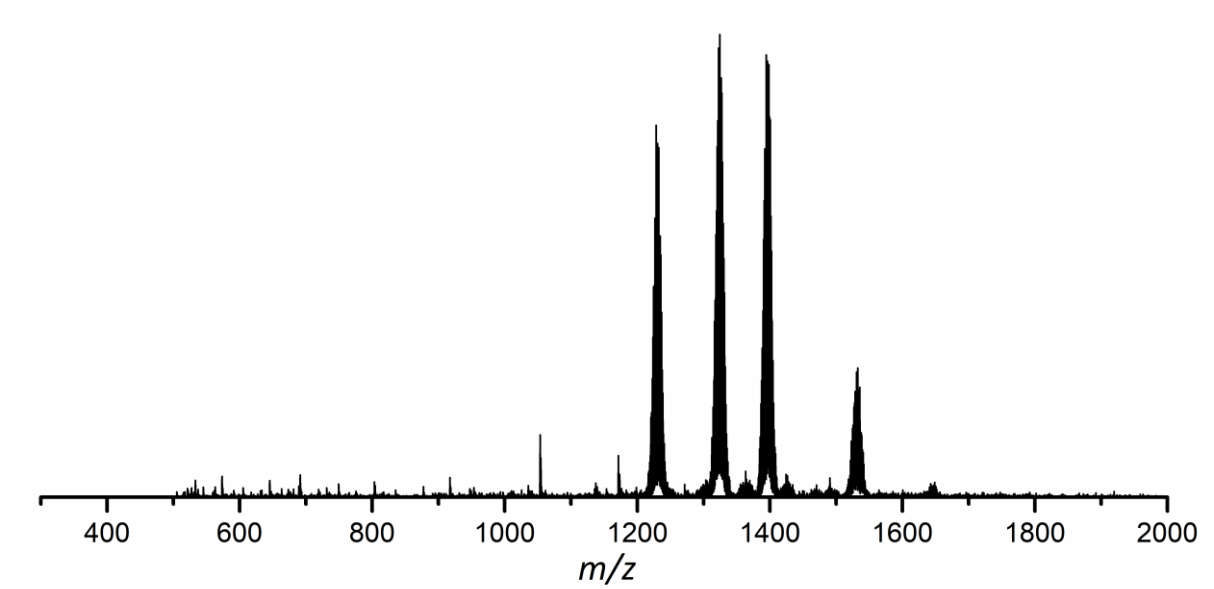

Figure S21: ESI-MS spectrum (negative mode, 4000 V, 300 °C) obtained upon examination of a thf solution of $[Ge_9\{Si(TMS)_3\}_2(Al^tBu_2)]^-$ (**4a**). Besides the signal at *m/z* 1324.6 $\{[Ge_9\{Si(TMS)_3\}_2(Al^tBu_2)]^- + Cl\}^-$ (**4a-Cl**), further signals at *m/z* 1396.4 ($[Ge_9\{Si(TMS)_3\}_3]^-$), *m/z* 1230.6 and at *m/z* 1531.8 (the two latter species could not be assigned to any species yet) were detected. The tris-silylated species $[Ge_9\{Si(TMS)_3\}_3]^-$ is formed during the ionization process, since in NMR studies its absence in solution is proven (Figures S16-S18). A detailed view of the signal of **4a-Cl** is provided in Figure 1 in the manuscript.

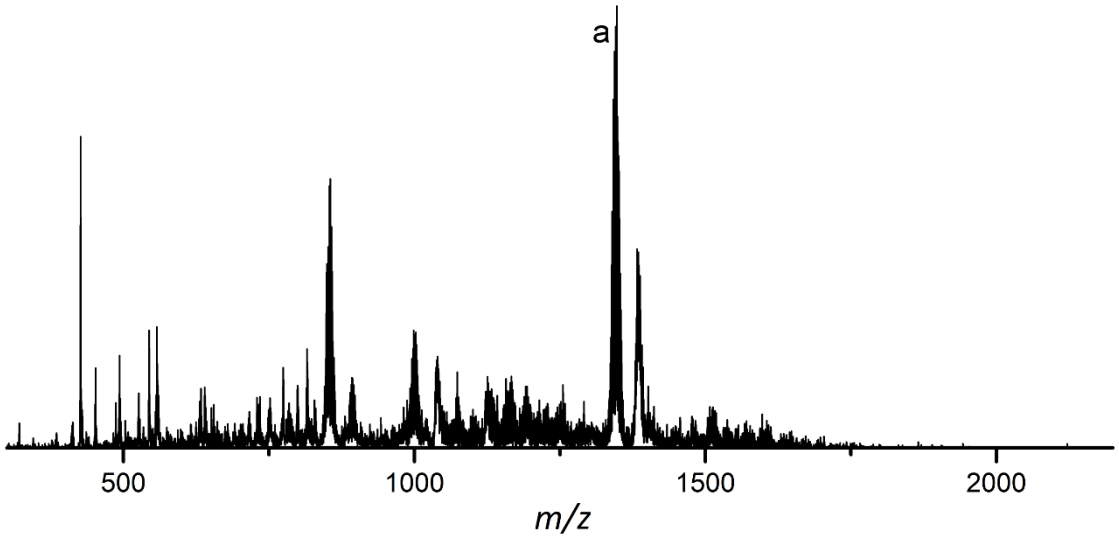

Figure S22: ESI-MS spectrum (negative mode, 4000 V, 300 °C) obtained upon examination of an acetonitrile reaction mixture of K_4Ge_9 and [BrBN(Mes)-CH_2-CH_2-N(Mes)] (3 equiv.) revealing a signal at *m/z* 1345.9 (marked with a), which can be assigned to $\{[Ge_9\{BN(Mes)\text{-}CH_2\text{-}CH_2\text{-}N(Mes)\}_2]^- + 2\ MeCN\}^-$. NMR examination of the respective reaction solution revealed low selectivity of the reaction as several products were monitored. A detailed view of the respective signal (a) is provided in Figure 2 in the manuscript.

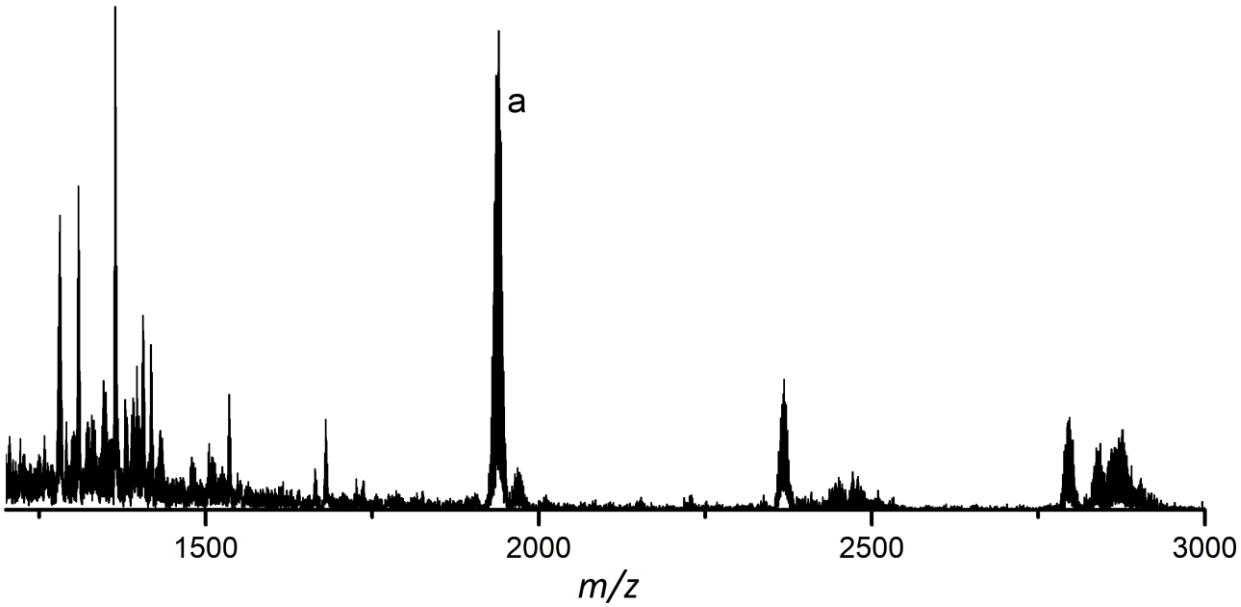

Figure S23: ESI-MS spectrum (negative mode, 3500 V, 300 °C) obtained upon examination of an acetonitrile reaction solution of K_4Ge_9 and [BrBN(Dipp)-CH=CH-N(Dipp)] (3 eq.) revealing a signal at *m/z* 1937.2 (marked with a), which can be assigned to $\{[Ge_9\{BN(Dipp)\text{-}CH{=}CH\text{-}N(Dipp)\}_3]^- + 3\ MeCN\}^-$. NMR examination of the respective reaction solution revealed low selectivity of the reaction as several products were monitored. A detailed view of the respective signal (a) is provided in Figure 2 in the manuscript.

5.8 Derivatization of Phosphine Ligands with Bulky Deltahedral Zintl Clusters – Synthesis of Charge Neutral Zwitterionic Tetrel Cluster Compounds $[(Ge_9\{Si(TMS)_3\}_2)^tBu_2P]M(NHC^{Dipp})$ (M: Cu, Ag, Au)

F. S. Geitner, J. V. Dums, T. F. Fässler*

reprinted with permission from

F. S. Geitner, J. V. Dums, T. F. Fässler, *J. Am. Chem. Soc.* **2017**, *139*, 11933.

Content and Contributions

The scope of this work was the evaluation of the reactivity of the bis-silylated cluster $[Ge_9\{Si(TMS)_3\}_2]^{2-}$ and the tris-silylated cluster $[Ge_9\{Si(TMS)_3\}_3]^-$ towards chlorophosphines R_2PCl (*R*: alkyl), with the intention to introduce $[PR_2]^+$ (*R*: alkyl) groups, comprising an electron lone-pair at the P atom which can potentially interact with Lewis acids, at the $[Ge_9]$ cluster core. Reactions of the tris-silylated $[Ge_9]$ cluster with small chlorophosphines R_2PCl (*R*: ^{i}Pr, Cy) led to the formation of neutral mixed-functionalized clusters $[Ge_9\{Si(TMS)_3\}_3PR_2]$ (*R*: ^{i}Pr, Cy). The novel compounds were characterized by means of NMR, single crystal X-ray diffraction (*R*: Cy) and elemental analysis (*R*: Cy). By contrast, the larger chlorophosphine ^{t}Bu$_2$PCl did not react with $[Ge_9\{Si(TMS)_3\}_3]^-$, even at elevated temperatures. However, reactions with the bis-silylated $[Ge_9]$ cluster resulted in the formation of the anionic mixed-functionalized $[Ge_9]$ cluster $[Ge_9\{Si(TMS)_3\}_2{}^tBu_2P]^-$. Subsequent reactions of the novel mixed-functionalized anion with coinage metal NHC complexes $NHC^{Dipp}MCl$ (*M*: Cu, Ag, Au) led to the formation of zwitterionic compounds $[(Ge_9\{Si(TMS)_3\}_2)^tBu_2P]M(NHC^{Dipp})$ (*M*: Cu, Ag, Au), comprising P-*M* interactions. Hence, $[Ge_9\{Si(TMS)_3\}_2{}^tBu_2P]^-$ can rather be described as a phosphine which is derivatized by a bulky deltahedral *Zintl* cluster. The characterization of the zwitterionic species occurred by means of NMR, single crystal X-ray diffraction (*M*: Cu) and elemental analysis (*M*: Cu). Besides being the first zwitterionic compounds comprising nine-atomic tetrel *Zintl* clusters, these novel species are also the first overall neutral threefold substituted $[Ge_9]$ clusters. The zwitterionic nature of $[(Ge_9\{Si(TMS)_3\}_2)^tBu_2P]M(NHC^{Dipp})$ (*M*: Cu, Ag, Au) was manifested by quantum chemical calculations revealing a delocalization of the negative charge over the $[Ge_9]$ cluster core, whereas the positive charge is situated at Cu. The quantum chemical calculations were carried out by M. Sc. Jasmin Dums. The publication was written in course of this thesis.

JACS
JOURNAL OF THE AMERICAN CHEMICAL SOCIETY
Article
pubs.acs.org/JACS

Derivatization of Phosphine Ligands with Bulky Deltahedral *Zintl* Clusters—Synthesis of Charge Neutral Zwitterionic Tetrel Cluster Compounds $[(Ge_9\{Si(TMS)_3\}_2)^tBu_2P]M(NHC^{Dipp})$ (M: Cu, Ag, Au)

Felix S. Geitner,[†,‡] Jasmin V. Dums,[†] and Thomas F. Fässler*[,†]

[†]Department of Chemistry, Technical University of Munich, Lichtenbergstraße 4, 85747 Garching, Germany
[‡]WACKER Institute for Silicon Chemistry, Lichtenbergstraße 4, 85747 Garching, Germany

Supporting Information

ABSTRACT: Reactions of silylated clusters $[Ge_9\{Si(TMS)_3\}_3]^-$ or $[Ge_9\{Si(TMS)_3\}_2]^{2-}$ with dialkylhalophosphines R_2PCl (Cy, ^{i}Pr, ^{t}Bu) at ambient temperature yield the first tetrel *Zintl* cluster compounds bearing phosphine moieties. Varying reactivity of the dialkylhalophosphines toward the silylated clusters is observed depending on the bulkiness of the phosphine's alkyl substituents and on the number of hypersilyl groups at the tetrel cluster. Reactions between phosphines with small cyclohexyl- (Cy) or isopropyl- (^{i}Pr) groups and the tris-silylated cluster $[Ge_9\{Si(TMS)_3\}_3]^-$ yield the novel neutral cluster compounds $[Ge_9\{Si(TMS)_3\}_3PR_2]$ (R: Cy (**1**), ^{i}Pr (**2**)) with discrete Ge−P *exo* bonds. By contrast, the bulkier phosphine $^tBu_2PCl$ does not react with $[Ge_9\{Si(TMS)_3\}_3]^-$ due to steric crowding. However, the reaction with the bis-silylated cluster $[Ge_9\{Si(TMS)_3\}_2]^{2-}$ yields the novel cluster compound $[Ge_9\{Si(TMS)_3\}_2P^tBu_2]^-$ (**3**). Subsequent reactions of compound **3** with $NHC^{Dipp}MCl$ (M: Cu, Ag, Au) yield the charge neutral zwitterionic compounds $[(Ge_9\{Si(TMS)_3\}_2)^tBu_2P]M(NHC^{Dipp})$ (M: Cu, Ag, Au) (**4**–**6**), in which compound **3** acts as a phosphine ligand bearing a bulky tetrel *Zintl* cluster moiety. Compounds **4**–**6** also represent the first uncharged examples for 3-fold substituted tetrel *Zintl* clusters.

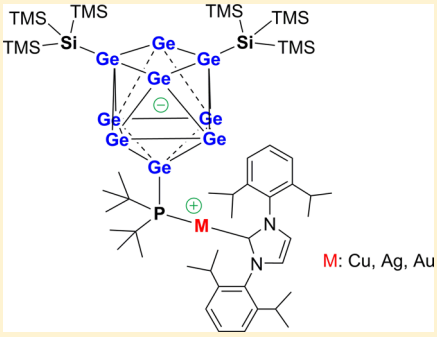

INTRODUCTION

The chemistry of *Zintl* clusters in solution has been extensively studied over the last decades, yielding a broad range of novel compounds.[1,2] In the beginning research was focused on the isolation of bare tetrel *Zintl* cages or on the reactivity of such clusters toward transition metal complexes. These reactions yielded either endohedrally filled clusters or intermetalloid compounds of increased cluster size.[1,2] However, with the isolation of the first dimeric,[3] oligomeric[4−7] or polymeric[8,9] *Zintl* cluster compounds as intermediates, examinations on the reactivity of main group element compounds toward *Zintl* clusters came into research focus. The introduction of main group element moieties at tetrel *Zintl* clusters upon reaction in solution was achieved and led to the isolation of the first $[Ge_9]$ cluster with two diphenylbismuth ligands $[Ph_2Bi-Ge_9-BiPh_2]^{2-}$, which was obtained by the reaction of K_4Ge_9 with $BiPh_3$ in ethylenediamine[10] (the isolation of $[TlSn_9]^{3-}$ was not considered since this compound was crystallized from an ethylenediamine solution of a preformed KTlSn alloy).[11] In subsequent studies on the reactivity of K_4Ge_9 toward main group element compounds, ER_3 (E: In, Ge, Sn; R: alkyl) and ER_2 (E: Sb; R: alkyl) moieties were introduced by the reaction of the respective *Zintl* phase with ER_4, R_3ECl, ER_3^- (E: Ge, Sn), or ER_3 (E: In, Sb) in ethylenediamine,[12−14] and a series of different cluster compounds comprising $[R_2E-Ge_9-ER_2]^{2-}$, $[R-Ge_9-SbR_2]^{2-}$, $[R_2Sb-Ge_9-Ge_9-SbR_2]^{4-}$ (E: Sb, Bi; R: alkyl)[10,12] and $[Ge_9-SnR_3]^{3-}$, $[R_3E-Ge_9-ER_3]^{2-}$, $[R_3Sn-Ge_9-Ge_9-SnR_3]^{4-}$ (E: In, Ge, Sn; R: alkyl) was obtained.[13,14]

In contrast to transition metal fragments, which usually interact with the open squares of the *Zintl* clusters, the attachment of the main group element moieties at the *Zintl* clusters mainly occurs via a discrete exo bond between one Ge atom of the cluster and the respective main group element. Exclusively in $[Ge_9-SnR_3]^{3-}$, an interaction of the tin atom with a second Ge atom of the cluster was observed (for R = Ph symmetric bridging is observed, whereas for R = Me one of the Ge−Sn distances is remarkably longer; "semi-bridging").[13] Regarding the mechanisms leading to the formation of the aforementioned compounds, a nucleophilic interaction of the main group element fragments with the Ge_9^{n-} (*n*: 2, 3, 4) clusters was established for the introduction of Sb-, Bi-, Ge-, and Sn-based groups, whereas for the introduction of respective In-based moieties an acid−base interaction between In^{3+} and $[Ge_9]$ was proposed.[10,12,13] Additionally, main group metal-bridged $[Ge_9]$ dimers $[In(Ge_9)_2]^{5-}$,[14] $[Sn(Ge_9)_2]^{4-}$[15] and $[(Ge_9)_2InPh]^{4-}$,[14] the latter with a Ge−Ge bond, were obtained by the reaction of $InPh_3$ or $SnPh_2Cl_2$ with K_4Ge_9 in

Received: June 6, 2017
Published: July 26, 2017

DOI: 10.1021/jacs.7b05834
J. Am. Chem. Soc. 2017, 139, 11933−11940

ethylenediamine. Furthermore, a main group element moiety was also attached to $[Sn_9]$ clusters ($[Sn_9SnCy_3]^{3-}$)[16,17] by reacting K_4Sn_9 with Cy_3SnCl (in addition, $[Sn_9\{Si(TMS)_3\}_2]^{2-}$ was obtained by other methods from the reaction of Sn(I)Cl with $LiSi(TMS)_3$).[18]

In all these compounds, the maximum number of substituents attached to the $[Ge_9]$ or $[Sn_9]$ core was limited to two ligands. The first tris-substituted cluster bearing three hypersilyl groups, $[Ge_9\{Si(TMS)_3\}_3]^-$, has initially been obtained in small yield by the reaction of Ge(I) halides with $LiSi(TMS)_3$.[19] However, recently a rational synthesis route for $[Ge_9\{Si(TMS)_3\}_3]^-$ was reported, yielding the tris-silylated cluster in a large scale by the heterogeneous reaction of K_4Ge_9 with $Si(TMS)_3Cl$ in acetonitrile or thf.[20] This novel route has led to a prosperous subsequent chemistry of $[Ge_9\{Si(TMS)_3\}_3]^-$, obtaining a series of transition metal-bridged cluster dimers $[M(Ge_9R_3)_2]^{n-}$ (R: $Si(TMS)_3$),[21−27] and 4-fold substituted clusters bearing transition metal organyl fragments as fourth group attached to the cluster $[R_xM(Ge_9R_3)]^{n-}$.[24−26,28,29] Additionally, reactions of $[Ge_9\{Si(TMS)_3\}_3]^-$ with main group element compounds resulted in the introduction of $[SnR_3]^+$ (R: Ph, Me, ^{n}Bu) groups,[30,31] or in the formation of an additional Tl^+ vertex, and an ethyl group was introduced by reacting the tris-silylated cluster with bromoethane.[31] Furthermore, other silyl groups were introduced at $[Ge_9]$ affording the silylated clusters $[Ge_9R_3]^-$ (R: $Si(TMS)_2(SiPh_3)$, $SiPh_3$, $Si(^iBu)_3$, $Si(^iPr)_3$, $SiEt_3$, SiH^tBu_2),[26,32−34] and a similar stannyl decorated cluster (R: $Sn(^iPr)_3$) was obtained analogously.[35] Recently, a reasonable synthesis for the bis-silylated cluster $[Ge_9\{Si(TMS)_3\}_2]^{2-}$ has been discovered, paving the path for the synthesis of mixed functionalized clusters such as $[Ge_9\{Si(TMS)_3\}_2\{Si(TMS)_2(SiPh_3)\}]^-$.[36] Almost all group IV elements have been introduced as main group element ligands (Si, Ge, Sn) or organic groups (C) at *Zintl* clusters, under formation of group-IV-element cluster bonds.[12,13,17,20,30,31] By contrast, for the neighboring pnictogenes, only reactions of compounds of the heavier congeners Sb and Bi with tetrel *Zintl* clusters have been successful although in rather moderate yields, whereas attempts to introduce respective arsenic or phosphorus species have failed so far.[10,12] However, especially the introduction of phosphine substituents would be interesting regarding the extension of the *Zintl* cluster chemistry, since in contrast to the known silyl- (SiR_3) and stannyl- (SnR_3) ligands, the PR_2 groups possess a free electron pair allowing for further reaction with Lewis acids. Hence such compounds can be regarded as a novel class of bulky phosphine ligands with a *Zintl* cluster moiety as the third substituent (PR_2R^I; R: alkyl, R^I: *Zintl* cluster) similarly to carboranyl phosphines.[37] Variously substituted phosphine ligands have already been applied in organometallic chemistry to modify the electronic and steric properties of catalytically active metal centers, and *Zintl* cluster-substituted phosphine ligands are of interest because of the special electronic situation at the cluster units.[37−40]

Here we report on the first introduction of phosphine moieties to tetrel *Zintl* clusters, using dialkylhalophosphines and silylated $[Ge_9]$ cluster anions as starting materials, and the dependence of the reactivity of the applied reactants on steric issues is discussed.[41] Furthermore, the ability of the novel compounds to act as *Zintl*-cluster-substituted phosphine ligands in organometallic complexes is revealed by their reaction with $NHC^{Dipp}MCl$ (M: Cu, Ag, Au), yielding the charge neutral zwitterionic compounds $[(Ge_9\{Si(TMS)_3\}_2)^tBu_2P]M(NHC^{Dipp})$ (M: Cu, Ag, Au).

RESULTS AND DISCUSSION

Solid $K[Ge_9\{Si(TMS)_3\}_3]$ was treated with toluene solutions of equimolar amounts of the phosphines R_2PCl (R: Cy, ^{i}Pr, ^{t}Bu) at ambient temperature, leading to deep red solutions. After a reaction time of 3 h at room temperature, the mixtures were filtered to remove all solids and subsequently dried in vacuo. NMR examinations carried out with the dark brown solid residues revealed the conversion of the reactants to a novel product species for the reactions of $K[Ge_9\{Si(TMS)_3\}_3]$ with R_2PCl (R: Cy, ^{i}Pr), whereas in case of the sterically more demanding phosphine $^tBu_2PCl$ no reaction was observed. Further experiments to react $^tBu_2PCl$ with $K[Ge_9\{Si(TMS)_3\}_3]$ under varying reaction conditions were also not successful, proving that a reaction of the bulky $^tBu_2PCl$ with tris-silylated $[Ge_9]$ is not possible.

According to the ratio of the ^{1}H NMR signals, the reactions of $[Ge_9\{Si(TMS)_3\}_3]^-$ with R_2PCl (R: Cy, ^{i}Pr) resulted, as expected, in the introduction of one $[R_2P]^+$ (R = Cy, ^{i}Pr) group at the tris-silylated $[Ge_9]$ cluster under formation of $[Ge_9\{Si(TMS)_3\}_3PR_2]$ (R = Cy (**1**), ^{i}Pr (**2**)). The neutral cluster species **1** and **2** reveal excellent solubility in thf, toluene, and hexane. Compound **1** can be recrystallized from toluene at −40 °C, yielding crystals suitable for single crystal X-ray diffraction in 30% yield. Unfortunately, attempts to recrystallize compound **2** in order to obtain single crystals has not been successful yet. Compound **1** crystallizes as red plate-shaped crystals in the monoclinic space group $P2_1/c$ with a unit cell containing three crystallographically independent cluster units (all revealing a similar interaction between the $[Ge_9]$ core and the phosphine substituent) and one cocrystallized toluene molecule per cluster. The $[Ge_9]$ cages possess distorted C_{2v}-symmetry. Thus, the $[Ge_9]$ clusters in **1** can either be described as distorted, capped square antiprisms or as distorted tricapped trigonal prisms. Considering the shape of the $[Ge_9]$ clusters in **1** as a square antiprism, two opposite Ge atoms of the open square are bearing a silyl group each, and the third silyl group is located at the capping Ge atom of the other square. However, describing the $[Ge_9]$ cluster core as tricapped trigonal prism, as it was done in previous publications, the silyl groups are located at the three capping Ge atoms (Figure 1). For a better comparability to previously reported cluster species, we will stick to the description of the $[Ge_9]$ cores as distorted tricapped trigonal prisms in the following discussion. Hence, the $[Cy_2P]^+$ fragments are attached to the clusters at one of the two open triangular faces, forming Ge−P *exo* bonds with a mean Ge−P distance of 2.345(2) Å, which is in the range of previously reported Ge−P single bonds.[42−45] In all three crystallographically independent clusters (I−III) of **1**, the Ge−P bond is tilted away from the triangular Ge plane, resulting in a mean angle of 155.1(2)° between the respective edge of the trigonal prism and the Ge−P bond (Ge7−Ge9−P1 in Figure 1), which is indicative of a discrete 2-center-2-electron bond between the phosphine ligand and the cluster unit.

Comparing the Ge−P bond in **1** to the Ge−Sn interaction in similar cluster compounds $[Ge_9\{Si(TMS)_3\}_3SnR_3]$ (R: Ph, ^{n}Bu), it becomes evident that the interactions are different. However, the $[SnR_3]^+$ (R: Ph, ^{n}Bu) fragments also interact with one of the triangular faces of the $[Ge_9]$ cluster, in contrast to the Ge−P interaction in **1** (the bonds point radially away from

DOI: 10.1021/jacs.7b05834
J. Am. Chem. Soc. 2017, 139, 11933−11940

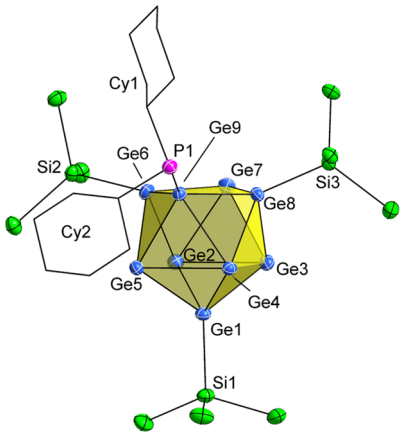

Figure 1. Molecular structure of compound **1** (cluster I). Displacement ellipsoids are shown at a 50% probability level. For clarity methyl groups of the hypersilyl moieties, hydrogen atoms and cocrystallized toluene molecules are omitted. The unit cell of compound **1** contains three crystallographically independent clusters. Atom labeling for clusters II and III occurred analogously to cluster I, starting from Ge10 and Ge19, respectively. Selected bond lengths are summarized in the Supporting Information (Tables SI 1 and SI 2).

the cluster), the Ge−Sn bonds are tilted toward the triangular Ge face.

The Sn atom is not only attached to one single Ge atom, but interacts with two or even three Ge atoms of the triangular Ge plane (this situation has been described as 2-electron-multicenter bond).[30,31]

Therefore, the spatial orientation of the Ge−P bond in **1** can rather be compared to the one of the Ge−Si interaction between the $[Ge_9]$ cluster and the $[Si(TMS)_3]^+$ groups or the Ge−C bond observed upon introduction of an organic ethyl moiety to $[Ge_9\{Si(TMS)_3\}_3]^-$ yielding $[Ge_9\{Si(TMS)_3\}_3Et]$.[19,20,31] Furthermore, the observed bonding mode in **1** is in accordance with the situation for the Ge-E (E: In, Ge, Sn, Sb, Bi) interactions between bare $[Ge_9]$ clusters and respective main group elements E.[10,12−14] The occurrence of only one sharp signal for the TMS groups in ^{1}H NMR spectrum suggests that the interaction between the $[Ge_9]$ core and the $[PR_2]^+$ (Cy, ^{i}Pr) unit is not static. The most likely reason for this fluctional behavior is a migration of the $[PR_2]^+$ (Cy, ^{i}Pr) moieties between the Ge atoms of the triangular Ge plane faster than the NMR time scale. Such a mechanism had previously been described for $[Ge_9\{Si(TMS)_3\}_3SnR_3]$ (R: Ph, ^{n}Bu), where the $[SnR_3]^+$ groups show a similar behavior.[30,31] A comparison of the mean vertical prismatic heights (3.0172(7) Å, 3.0191(8) Å and 3.7052(8) Å) of the three crystallographically independent clusters in **1** reveals an elongation of one edge in association with the formation of the Ge−P *exo* bond. The Ge−Si distances in **1** range between 2.374(2) Å (Ge10−Si13) and 2.408(2) Å (Ge6−Si2) and are also in agreement with the values observed in previously reported similar clusters.[19,20] The Ge−Ge bonds within the $[Ge_9]$ clusters adapt typical values between 2.473(1) Å (Ge17−Ge18) and 2.9187(9) Å (Ge13−Ge14). The shortest distances are observed between the Ge atom carrying the phosphine moiety and one of the three capping Ge atoms bearing a silyl group, whereas the longest bonds occur in the triangular plane comprising the Ge atom with the phosphine moiety.

Since ^{t}Bu$_2$PCl did not react with $[Ge_9\{Si(TMS)_3\}_3]^-$ we investigated its reaction with the sterically less crowded bis-silylated cluster $[Ge_9\{Si(TMS)_3\}_2]^{2-}$. A solution of ^{t}Bu$_2$PCl in thf-$d_8$ was added to equimolar amounts of the solid bis-silylated cluster $K_2[Ge_9\{Si(TMS)_3\}_2]$ in an airtight J-Young NMR tube, yielding a deep red solution.

The first ^{1}H NMR spectrum taken after 30 min revealed already full conversion of the reactants. The ratio of the signals indicates the attachment of a $[^tBu_2P]^+$ moiety to the bis-silylated cluster. Besides the detected ratio, the downfield shift of the proton signal of the TMS groups from 0.16 to 0.25 ppm reveals the attachment of a third substituent to the $[Ge_9]$ cluster. In a larger scale, the reaction mixture was stirred for 30 min at room temperature before it was filtered and dried in vacuo to obtain $K[Ge_9\{Si(TMS)_3\}_2P^tBu_2]$ (**3**) as a dark brownish solid.

Compound **3** was characterized by NMR experiments (^{1}H, ^{13}C, ^{31}P, and ^{29}Si) and ESI−MS examinations, where **3** was detected at *m*/*z* 1294.6 $\{[Ge_9\{Si(TMS)_3\}_2P^tBu_2]^-\}$ (Figure 2).

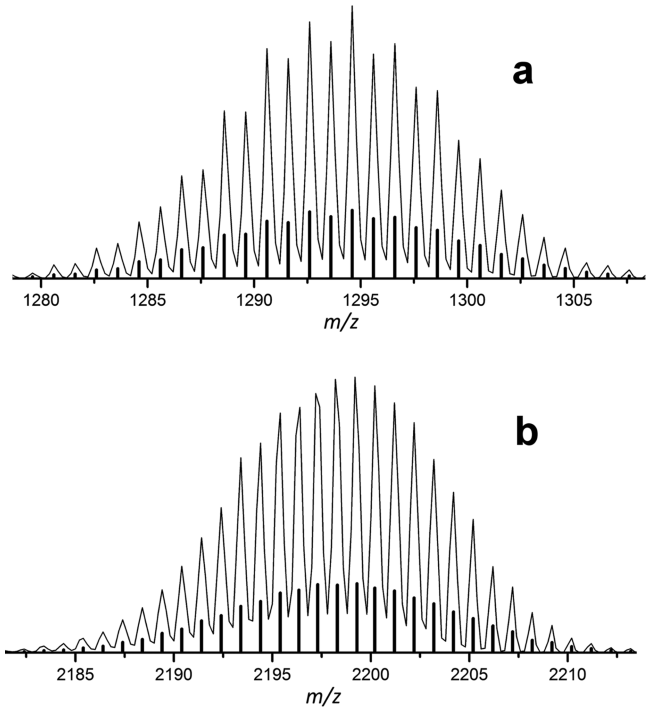

Figure 2. ESI−MS spectra of compounds **3** (a) and **4** (b). Mass spectrum **a** was acquired in negative ion mode (4000 V, 300 °C) monitoring the molecule peak of **3** at *m*/*z* 1294.6 $\{[Ge_9\{Si(TMS)_3\}_2{}^tBu_2P]^-\}$. Mass spectrum **b** was acquired in positive ion mode (4000 V, 300 °C) monitoring **4** with an additionally attached $[Cu-NHC]^+$ moiety at *m*/*z* 2199.3 $\{[(NHC^{Dipp}Cu)[(Ge_9\{Si(TMS)_3\}_2)^tBu_2P]M(NHC^{Dipp})]^+\}$. Calculated spectra are pictured as black bars.

Compound **3** readily dissolves in a broad range of organic solvents (acetonitrile to hexane), but unfortunately, we have not been able to crystallize or isolate **3** in its pure form to date.

In order to show the possibility that novel compound **3**, which can be regarded as bulky *Zintl*-type cluster functionalized phosphine, can act as a ligand to a transition metal, we investigated its reactivity toward the coinage metal carbene complexes $NHC^{Dipp}MCl$ (M: Cu, Ag, Au). Reactions of these organometallics with tris-silylated cluster $[Ge_9R_3]^-$ have yielded neutral complexes $NHC^{Dipp}M[(\eta^3\text{-}Ge_9R_3)]$ (R: $Si(TMS)_3$; M: Cu, Ag, Au) before.[25]

DOI: 10.1021/jacs.7b05834
J. Am. Chem. Soc. 2017, 139, 11933−11940

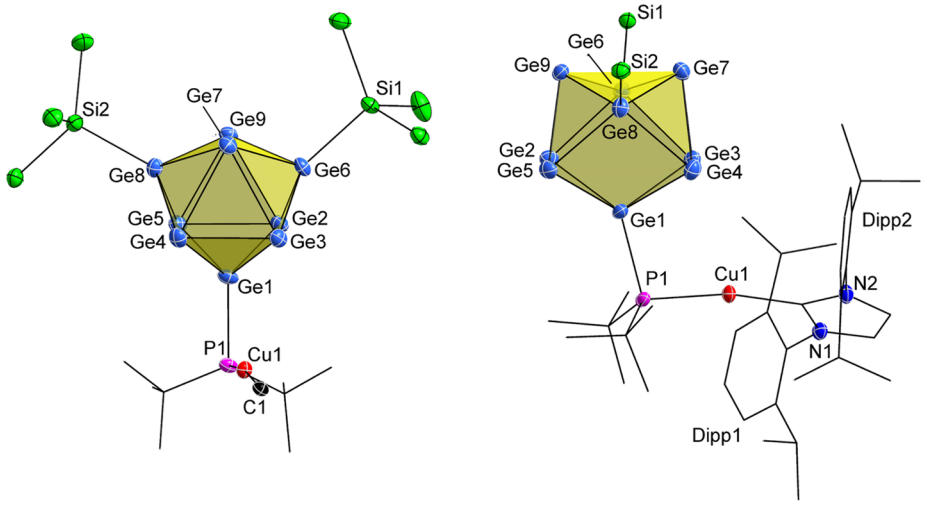

Figure 3. Molecular structure of compound **4**. Displacement ellipsoids are shown at a 50% probability level. For clarity hydrogen atoms and cocrystallized toluene molecules are omitted, and carbon atoms are pictured in wire and stick style. Left: Coordination of the three substituents to the C_{2v}-symmetric [Ge_9] core. Methyl groups of the hypersilyl moieties and the NHC^{Dipp} ligand are omitted for clarity. Right: Coordination of the [$Cu{-}NHC^{Dipp}$]$^+$ moiety to the phosphine substituent of the [Ge_9] core. TMS groups of the hypersilyl substituents are omitted. Selected bond lengths are summarized in Table SI 3.

We carried out NMR-scale experiments adding an equimolar amount of $NHC^{Dipp}CuCl$ to a solution of **3** in thf-d_8. The first ^{1}H NMR spectrum obtained after 30 min revealed the complete conversion of the two reactants to a novel compound with an attached [$Cu{-}NHC^{Dipp}$]$^+$ moiety according to the ratio of the proton signals. In the ^{1}H NMR spectrum of the new compound the protons of the *tert*-butyl groups are shifted from 1.25 ppm (**3**) to 0.89 ppm, indicative of an interaction of the [$Cu{-}NHC^{Dipp}$]$^+$ moiety with the electron lone pair of the [^{t}Bu$_2$P]$^+$ substituent of the cluster in a compound of the composition [(Ge_9{Si(TMS)$_3$}$_2$)^{t}Bu$_2$P]Cu(NHC^{Dipp}) (**4**). However, further NMR experiments (^{13}C, ^{29}Si, and ^{31}P) did not reveal any significant signal shifts that would give closer hints at the nature of the formed compound. An improvement of the synthetic procedure was achieved using acetonitrile as solvent, since the addition of an acetonitrile solution of $NHC^{Dipp}CuCl$ to the deep red solution of **3** in acetonitrile instantly leads to the precipitation of the product species as a brownish solid. Excessive reactants can directly be removed by filtering of the pale-yellow supernatant solution followed by washing of the remaining solid with acetonitrile. Subsequently, the solid was dissolved in toluene and filtered to remove KCl formed during the reaction. Concentration of the toluene extract and storage at −30 °C led to the formation of orange plate-shaped single crystals suitable for single crystal X-ray diffraction. Evaluation of the obtained data manifested the assumption (derived from the NMR experiments) of an attached [$Cu{-}NHC^{Dipp}$]$^+$ moiety at the cluster's phosphine substituent and formation of the neutral compound [(Ge_9{Si(TMS)$_3$}$_2$)^{t}Bu$_2$P]Cu(NHC^{Dipp}) (**4**) (Figure 3). Elemental analysis carried out with the homogeneous orange solid of **4** confirmed its purity. In ESI−MS examinations carried out with thf solutions of **4**, a signal was detected at m/z 2199.3 in the positive ion mode, which can be assigned to {[(NHC^{Dipp}Cu)[Ge_9{Si(TMS)$_3$}$_2$)^{t}Bu$_2$P)]Cu(NHC^{Dipp})]$^+$} formed by the addition of a further [$Cu{-}NHC^{Dipp}$]$^+$ fragment to the cluster during the ionization process (Figure 2).

Compound **4** is the first example of an overall neutral, 3-fold substituted tetrel *Zintl* cluster and the first zwitterionic tetrel *Zintl* cluster compound with a positive charge at the Cu$^+$ center and a negative charge delocalized over the [Ge_9] core, which is a 22-skeletal-electron *nido* cluster (Scheme 1). This consideration is confirmed by quantum-chemical calculations at a DFT-PBE0/def2-TZVPP level of theory.[46−48] The single point calculation of **4**, using the geometry of its crystal structure, shows a significant HOMO−LUMO gap of 3.26 eV, proving its kinetic stability. The calculation of Hirshfeld[49] and natural charges[50] reveals, that the positive charge situated at the Cu$^+$ center in **4** is similar as in cationic compound [^{t}Bu$_3$PCu(NHC^{Dipp})]$^+$.[51] Furthermore, a significantly negative overall charge of the [Ge_9] cluster is found, manifesting the zwitterionic nature of **4** (Table SI 4). Moreover, the calculations reveal a decrease of the positive charge situated at P upon formal replacement of an alkyl group in [^{t}Bu$_3$PCu(NHC^{Dipp})]$^+$ by the [Ge_9] unit, which can also be rationalized by the lower Pauling electronegativity of Ge (2.0) compared to C (2.5).[52] The Electron Localization Function (ELF) of compound **4** and cationic complex [^{t}Bu$_3$PCu(NHC^{Dipp})]$^+$ reveals for both cases strong covalent

Scheme 1. Zwitterionic Nature of the Charge-Neutral Compounds [Ge_9{Si(TMS)$_3$}$_2$^{t}Bu$_2$P]M(NHC^{Dipp}) (M: Cu, Ag, Au; 4−6)

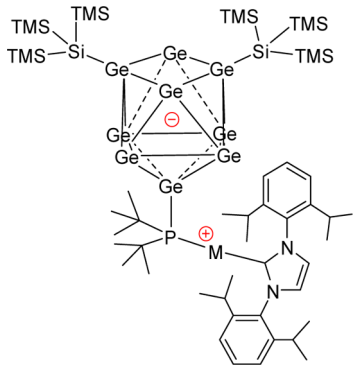

DOI: 10.1021/jacs.7b05834
J. Am. Chem. Soc. 2017, 139, 11933−11940

bonds between Cu^+ and P as well as P and Ge or C, respectively (Figure 4).[53,54]

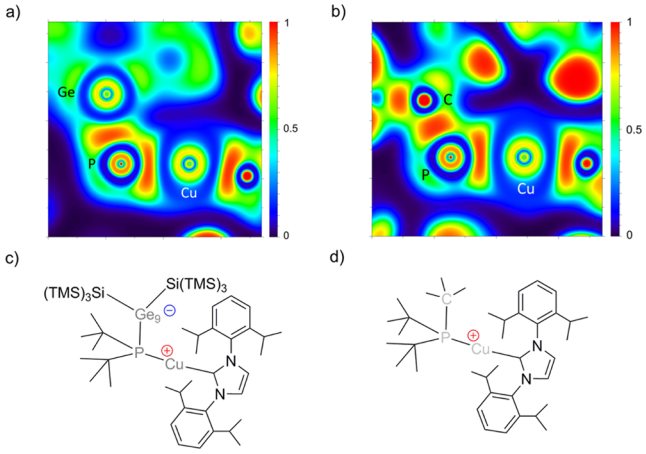

Figure 4. Color-filled maps of ELF representations (a) and (b) and corresponding Lewis structures of zwitterion **4** (c) and $[^tBu_3PCu(NHC^{Dipp})]^+$ (d), respectively. a) ELF through the plane of Ge, P, and Cu atoms of **4** as indicated by gray atoms in Figure 4c. b) ELF of $[^tBu_3PCu(NHC^{Dipp})]^+$ through the plane of C, P, and Cu atoms as indicated by gray atoms in Figure 4d.[56]

The zwitterionic nature of **4** is also in good agreement with its poor solubility in hexane (by contrast, the neutral compounds **1** and **2** dissolve readily in hexane). A similar zwitterionic species comprising a main group element cluster has been reported for a Pt^{IV} complex bearing a stanna-*closo*-dodecaborate moiety, in which the positive charge is also located at the transition metal, whereas the negative charge is distributed over the cluster unit.[55]

Somehow the formation of **4** is not surprising since coordinative bonds between phosphines and transition metals are very common (phosphines are good ligands), whereas Cu−Ge bonds are rather rare. The observed reactivity also proves the ability of compound **3** to act as a *Zintl* cluster-substituted phosphine ligand in organometallic chemistry. This is of special interest since such units are both, sterically demanding phosphine ligands and suitable ligands for the synthesis of zwitterionic compounds (due to the negative charge of the tetrel *Zintl* cluster); the latter property is shown by the synthesis of compound **4**.

Both attributes (steric impact of the ligand and formation of zwitterionic compounds upon coordination to a metal cation) of this novel class of ligands have already been revealed to be favorable for catalytic applications.[37−39]

Furthermore, the conversion of **3** to **4** is a very rare example of a reaction occurring at an *exo*-bonded main group substituent bound to a tetrel *Zintl* cluster. This has previously only been observed for the transformation of $[Pd@Sn_9{-}SnCy_3]^{3-}$ to $[Pd@Sn_9{-}PdSnCy_3]^{3-}$ by oxidative insertion of Pd^0 into the $Sn_9{-}SnCy_3$ bond[17] (certainly a series of ligand exchange reactions at transition metal organyl fragments bound to *Zintl* clusters has been reported).[57−59]

Compound **4** crystallizes in the triclinic space group $P\bar{1}$ with 0.5 toluene molecules per formula unit. The $[Ge_9]$ core can either be described as a distorted, capped square antiprism or as a distorted, tricapped trigonal prism with C_{2v}-symmetry (Figure 3). For a better comparability to already reported cluster species we stick to the latter description in the following discussion. The two silyl substituents and the phosphine substituent are bound to the capping Ge atoms. The Ge−P distance of 2.316(1) Å (Ge1−P1) is slightly shorter than the respective distances in compound **1**, but is also in the range of a Ge−P single bond.[42−45] Concerning the Ge−Ge bonds, distances between 2.530(1) Å (Ge1−Ge3) and 2.737(1) Å (Ge3−Ge7) are observed, with the shortest bond between the capping Ge atom with the phosphine moiety and one of the triangular bases, and the longest distance is observed within one of the triangular bases. Comparison of the heights of the trigonal prism reveals one significantly shorter edge Ge7−Ge9 (3.070(1) Å) and two longer edges Ge2−Ge3 (3.620(1) Å) and Ge4−Ge5 (3.658(1) Å).

Therefore, the arrangement of the $[Ge_9]$ cluster in **4** lies somewhere in between the shape of the bis-silylated cluster $[Ge_9\{Si(TMS)_3\}_2]^{2-}$ (capped square antiprism) and the mixed silyl group-functionalized cluster $[Ge_9\{Si(TMS)_3\}_2\{Si(TMS)_2(SiPh_3)\}]^-$ (nearly perfect trigonal prismatic configuration of $[Ge_9]$).[36] The Ge−Si distances in **4** range between 2.371(1) Å (Ge8−Si2) and 2.380(1) Å (Ge6−Si1) and thus correspond to the values observed in **1** and previously reported similar cluster compounds.[19,20] The attachment of the $[Cu{-}NHC^{Dipp}]^+$ moiety occurs via a coordinative bond through interaction of the lone pair located at the phosphorus atom and the Lewis-acidic Cu^+. Hence compound **3** acts as *Zintl* cluster substituted phosphine ligand upon formation of **4**, resulting in a distorted tetrahedral coordination of the phosphorus atom. The coordination of Cu^+ by NHC^{Dipp} and the *Zintl* cluster-substituted phosphine slightly deviates from linearity (167°), since the $Cu{-}NHC^{Dipp}$ bond is bent away from the bulky $[Ge_9]$ cluster moiety of the phosphine group.

After complete characterization of compound **4**, we tested the reactivity of compound **3** toward further coinage metal NHC compounds $NHC^{Dipp}MCl$ (M: Ag, Au) and obtained similar products $[(Ge_9\{Si(TMS)_3\}_2)^tBu_2P]M(NHC^{Dipp})$ (M: Ag (**5**), Au (**6**)) according to NMR data. Thus, compound **3** reacts as a *Zintl* cluster-substituted phosphine ligand and paves the path for a completely new reaction branch of tetrel *Zintl* cluster chemistry in solution, in which the tetrel *Zintl* clusters can rather be described as bulky substituents of a phosphine ligand.

CONCLUSIONS

Within this work, we achieved the introduction of phosphine moieties at tetrel *Zintl* clusters for the first time and synthesized a series of novel mixed-functionalized cluster compounds bearing phosphine substituents (**1**−**3**). Depending on steric factors, a varying reactivity between the dialkylhalophosphines and the tetrel clusters was observed. Compounds **1**−**3** are potential phosphine ligands PR_2R^I (R: alkyl, R^I: *Zintl* cluster) with a bulky tetrel *Zintl* cluster as the third substituent. This property of the novel compounds could be demonstrated by subsequent reaction of compound **3** with coinage metal carbene complexes yielding compounds **4**−**6**. Besides providing a novel class of bulky phosphine ligands, compound **3** is a suitable ligand for the synthesis of zwitterionic compounds upon attachment to a metal cation, as it has been shown within this work by the synthesis of charge neutral zwitterionic compounds **4**−**6**. Both attributes have previously been revealed to be favorable regarding catalytic applications of respective compounds.[37−40] Quantum chemical calculations reveal the

DOI: 10.1021/jacs.7b05834
J. Am. Chem. Soc. 2017, 139, 11933−11940

Table 1. Crystallographic Data for Compounds 1 and 4

compound	1	4
formula	$(Ge_9Si_{12}P_1C_{39}H_{103}\cdot tol)_3$	$Ge_9Si_8P_1Cu_1N_2C_{53}H_{108}\cdot 0.5$ tol
fw [g·mol^{-1}]	5057.10	1745.95
space group	$P2_1/c$	$P\bar{1}$
a [Å]	23.694(5)	13.961(3)
b [Å]	25.662(5)	15.006(3)
c [Å]	38.749(8)	23.068(5)
α [°]	90	73.93(3)
β [°]	91.82(3)	84.92(3)
γ [°]	90	62.67(3)
V [Å^3]	23549(8)	4121.3(2)
Z	4	2
T [K]	100(2)	100(2)
λ [Å]	Mo $K\alpha$	Mo $K\alpha$
ρ_{calcd} [g·cm^{-3}]	1.426	1.407
μ [mm^{-1}]	3.626	3.650
collected reflections	556461	111996
independent reflections	46245	16192
R_{int}/R_δ	0.0984/0.0422	0.0511/0.0297
parameters/restraints	1956/6	699/0
R_1 [$I > 2\,\sigma(I)$/all data]	0.0499/0.0807	0.0335/0.0497
wR_2 [$I > 2\,\sigma(I)$/all data]	0.1114/0.1280	0.0778/0.0856
goodness of fit	1.032	1.019
max./min diff. el. density [e/Å^{-3}]	2.70/−0.89	0.79/−0.52
CCDC	1543931	1543932

zwitterionic nature and the kinetic stability of these novel compounds.

EXPERIMENTAL SECTION

General. All manipulations were performed under oxygen-free, dry conditions under argon atmosphere using standard Schlenk or glovebox techniques. Glassware was dried prior to use by heating it in vacuo. The solvents used were obtained from a MBraun Grubbs apparatus. All other commercially available chemicals were used without further purification. K_4Ge_9 was prepared by fusion of stoichiometric amounts of the elements in stainless-steel tubes at 650 °C. 1,3-Bis(2,6-diisopropylphenyl)imidazolium chloride, the corresponding coinage metal halide complexes as well as $K_2[Ge_9R_2]$ and $K[Ge_9R_3]$ (R: $Si(TMS)_3$) were synthesized according to modified literature procedures.[20,36,60−63]

Single Crystal Structure Determination. The air- and moisture-sensitive crystals of **1** and **4** were transferred from the mother liquor into cooled perfluoroalkylether oil under a cold stream of N_2 gas. For diffraction data collection, the single crystals were fixed on a glass capillary and positioned in a 100 K cold N_2 gas stream using the crystal cap system. Data collection was performed with a STOE StadiVari ($Mo_{K\alpha}$ radiation) diffractometer equipped with a DECTRIS PILATUS 300 K detector. Structures were solved by Direct Methods (SHELXS-2014) and refined by full-matrix least-squares calculations against F^2 (SHELXL-2014).[64] The positions of the hydrogen atoms were calculated and refined using a riding model. Unless stated otherwise, all non-hydrogen atoms were treated with anisotropic displacement parameters. The supplementary crystallographic data for this paper have been deposited with the Cambridge Structural database and are available free of charge via www.ccdc.cam.ac.uk/data_request/cif. The crystallographic data for compounds **1** and **4** are summarized in Table 1. In compound **1** a TMS group of a hypersilyl substituent is disordered and was refined on split positions. In compound **4**, the electron density of a disordered toluene molecule was taken care of by the PLATON squeeze function.[65]

NMR Spectroscopy. Sample preparation was performed in a glovebox. NMR spectra were measured on a Bruker Avance Ultrashield 400 MHz spectrometer. The ^{1}H and ^{13}C NMR spectra were calibrated using the residual proton signal of the used deuterated solvents.[66] Chemical shifts are reported in parts per million (ppm) relative to TMS, with the residual solvent peak serving as internal reference. Abbreviations for signal multiplicities are singlet (s), doublet (d), triplet (t), and heptet (h). In the acquired ^{13}C NMR spectra of compounds **4**−**6** the carbene carbon signal could not be monitored.

Electron Spray Ionization Mass Spectrometry (ESI−MS). The sample preparation for ESI−MS examinations was done in a glovebox. ESI−MS analyses were performed on a Bruker Daltronic HCT mass spectrometer (dry gas temperature: 300 °C; injection speed 240 μL/s), and the data evaluation was carried out using the Bruker Compass Data Analysis 4.0 SP 5 program (Bruker). Spectra were plotted using OriginPro2016G (Origin Lab) and Excel 2016 (Microsoft).

Elemental Analyses (EA). Elemental analyses were carried out in the microanalytical laboratory of the Chemistry Department of Technische Universität München. Analyses of C, H, and N were performed in a combustion analyzer (elementar vario EL, Bruker).

Computational Analysis. The computational analysis for **4** and $[^tBu_3PCu(NHC^{Dipp})]^+$ were performed using the Gaussian09 program package,[67] with exchange correlation hybrid functional after Perdew, Burke, and Ernzerhof (PBE0)[46,47] and def2-TZVPP basis sets for all considered elements H, C, N, P, Si, Cu, and Ge.[48,68] The structure parameters for the single point calculation of **4** and $[^tBu_3PCu(NHC^{Dipp})]^+$ were taken from the single crystal structure reported here and from the literature,[51] respectively. For the compensation of the positive charge a solvation model (polarizable continuum model, PCM) was applied.[69]

Syntheses. *$[Ge_9\{Si(TMS)_3\}_3PCy_2]$ (**1**).* $K[Ge_9\{Si(TMS)_3\}_3]$ (143.5 mg, 0.100 mmol, 1 equiv) was treated with a solution of Cy_2PCl (23.3 mg, 0.100 mmol, 1 equiv) in toluene (3.0 mL) to obtain a deep red reaction mixture. After stirring for 1 h at r.t., the mixture was filtered to remove KCl formed upon the reaction. Subsequently, the filtrate was concentrated to half of its original volume in vacuo and stored in a freezer at −40 °C. After 1 week, red plate-shaped crystals of **1** had formed, which were suitable for single crystal X-ray examination. Thereafter, the crystals were isolated by filtering off the supernatant solution, washed with MeCN and homogenized to obtain an analytically pure brown solid (48 mg; 30% yield) after drying in vacuo. **^{1}H NMR** (400 MHz, 298 K, thf-d_8): δ [ppm] = 2.07−1.75 (m,

DOI: 10.1021/jacs.7b05834
J. Am. Chem. Soc. 2017, 139, 11933−11940

10H, $CH_{2(Cy)}$), 1.70−1.63 (m, 2H, CH_{Cy}), 1.55−1.15 (m, 10H, $CH_{2(Cy)}$), 0.37 (s, 81H, Me_{TMS}). **^{13}C NMR** (101 MHz, 298 K, thf-d_8): δ [ppm] = 35.06 (d, $^1J_{CP}$ = 28.3 Hz, CH_{Cy}), 34.44 (d, $^2J_{CP}$ = 11.2 Hz, $CH_{2(Cy)}$), 28.35 (d, $^3J_{CP}$ = 9.1 Hz, $CH_{2(Cy)}$), 27.04 (s, $CH_{2(Cy)}$), 3.25 (s, Me_{TMS}). **^{29}Si-INEPT NMR** (79 MHz, 298 K, thf-d_8): δ [ppm] = −8.16 (s, Si_{TMS}), −101.12 (s, Si_{Ge9}). **^{31}P NMR** (162 MHz, 298 K, thf-d_8): δ [ppm] = 20.96 (m, P_{Ge9}). **EA**: anal. calcd. for $C_{39}H_{103}Ge_9PSi_{12}$·0.75 tol: C, 31.8; H, 6.6; found: C, 31.7 H, 6.6. The following signals in the ^{1}H and ^{13}C NMR spectra are caused by cocrystallized toluene, which was still present in the sample after drying in vacuo. **^{1}H NMR** (400 MHz, 298 K, thf-d_8): δ [ppm] = 7.19−7.13 (m, CH_{Ph}), 2.31 (s, CH_3). **^{13}C NMR** (101 MHz, 298 K, thf-d_8): δ [ppm] = 138.47 (s, CH_{Ph}), 129.70 (s, CH_{Ph}), 128.94 (s, CH_{Ph}), 126.07 (s, CH_{Ph}), 21.53 (s, CH_3).

$[Ge_9\{Si(TMS)_3\}_3P^iPr_2]$ ***(2)***. $K[Ge_9\{Si(TMS)_3\}_3]$ (143.5 mg, 0.100 mmol, 1 equiv) was treated with a solution of $^iPr_2PCl$ (15.3 mg, 0.100 mmol, 1 equiv) in toluene (3.0 mL) to obtain a deep red reaction mixture. After stirring for 1 h at r.t., the mixture was filtered to remove KCl formed upon the reaction. Subsequently, the solvent was removed in vacuo to obtain the crude product as a dark brownish solid (61 mg; 40% yield). Purification by recrystallization from toluene at −40 °C has not been successful. **^{1}H NMR** (400 MHz, 298 K, C_6D_6): δ [ppm] = 2.24 (m, 2H, CH_{iPr}), 1.30 (dd, $^3J_{HP}$ = 13.3 Hz, $^3J_{HH}$ = 6.8 Hz, 12H, Me_{iPr}), 0.46 (s, 81H, Me_{TMS}). **^{13}C NMR** (101 MHz, 298 K, C_6D_6): δ [ppm] = 25.03 (d, $^1J_{CP}$ = 28.3 Hz, CH_{iPr}), 23.50 (d, $^2J_{CP}$ = 13.1 Hz, Me_{iPr}), 3.11 (s, Me_{TMS}). **^{29}Si-INEPT NMR** (79 MHz, 298 K, C_6D_6): δ [ppm] = −8.25 (s, Si_{TMS}), −101.61 (s, Si_{Ge9}). **^{31}P NMR** (162 MHz, 298 K, C_6D_6): δ [ppm] = 28.36 (m, P_{Ge9}).

$K[Ge_9\{Si(TMS)_3\}_2P^tBu_2]$ ***(3)***. $K_2[Ge_9\{Si(TMS)_3\}_2]$ (92 mg, 0.075 mmol, 1 equiv) was treated with a solution of $^tBu_2PCl$ in thf (2.5 mL) to obtain a deep red reaction mixture. After stirring for 30 min at r.t., the mixture was filtered to remove KCl formed upon the reaction, and the filtrate was dried in vacuo to obtain the crude product as a dark brownish solid (49 mg, 50% yield). Purification by recrystallization from several organic solvents (MeCN−hexane) has not been successful, due to the good solubility of **1** in all applied solvents. **^{1}H NMR** (400 MHz, 298 K, thf-d_8): δ [ppm] = 1.25 (d, $^3J_{HP}$ = 10.9 Hz, 18H, Me_{tBu}), 0.25 (s, 54, Me_{TMS}). **^{13}C NMR** (101 MHz, 298 K, thf-d_8): δ [ppm] = 34.04 (d, $^2J_{CP}$ = 14.1 Hz, Me_{tBu}), 32.66 (d, $^1J_{CP}$ = 37.4 Hz, C_{tBu}, 32.00 (d, $^2J_{CP}$ = 13.1 Hz, Me_{tBu}), 26.43 (s, Me_{tBu}), 3.19 (s, Me_{TMS}). **^{29}Si-INEPT NMR** (79 MHz, 298 K, thf-d_8): δ [ppm] = −9.50 (s, Si_{TMS}), −107.88 (s, Si_{Ge9}). **^{31}P NMR** (162 MHz, 298 K, thf-d_8): δ [ppm] = 57.22 (m, P_{Ge9}). **ESI−MS** (negative mode, 4000 V, 300 °C): m/z 1294.6 $\{[Ge_9(Si(TMS)_3\}_2P^tBu_2]^-\}$.

$[(Ge_9\{Si(TMS)_3\}_2)^tBu_2P]Cu(NHC^{Dipp})$ ***(4)***. $K_2[Ge_9\{Si(TMS)_3\}_2]$ (92 mg, 0.075 mmol, 1 equiv) was treated with a solution of $^tBu_2PCl$ (13.5 mg, 0.075 mmol, 1 equiv) in MeCN (2.5 mL) to obtain a deep red reaction mixture. After stirring for 30 min at r.t., a solution of $NHC^{Dipp}CuCl$ (36.5 mg, 0.075 mmol, 1 equiv) in MeCN (1 mL) was added, instantly leading to the formation of a brownish precipitate. The supernatant solution was filtered off, and the solid was washed with MeCN (2 mL). The solid was then dissolved in toluene and filtered. Removal of toluene and washing of the remaining solid with hexane (2.5 mL) yielded compound **4** as a dark orange solid (53 mg; 40% yield). (The reaction can also be carried out in thf. Thereby, compound **4** remains in solution upon the addition of $NHC^{Dipp}CuCl$). **^{1}H NMR** (400 MHz, 298 K, thf-d_8): δ [ppm] = 7.63 (s, 2H, CH_{Im}), 7.56−7.46 (m, 2H, $CH_{Ph(p)}$), 7.43−7.37 (m, 4H, $CH_{Ph(m)}$), 2.89 (hept, $^3J_{HH}$ = 6.8 Hz, 4H, CH_{iPr}), 1.48 (d, $^3J_{HH}$ = 6.8 Hz, 12H, Me_{iPr}), 1.19 (d, $^3J_{HH}$ = 6.8 Hz, 12H, Me_{iPr}), 0.89 (d, $^3J_{HP}$ = 13.9 Hz, 18H, Me_{tBu}), 0.27 (s, 54H, Me_{TMS}). **^{13}C NMR** (101 MHz, 298 K, thf-d_8): δ [ppm] = 146.34 (s, $C_{Ph(iPr)}$), 136.86 (s, $C_{Ph}N$), 131.61 (s, $CH_{Ph(p)}$), 125.69 (s, CH_{Im}), 125.47 (s, $CH_{Ph(m)}$), 34.24 (s, Me_{tBu}), 33.20 (d, $^1J_{CP}$ = 7.0 Hz, C_{tBu}), 29.85 (s, CH_{iPr}), 3.12 (s, Me_{TMS}). **^{29}Si-INEPT NMR** (79 MHz, 298 K, thf-d_8): δ [ppm] = −9.11 (s, Si_{TMS}), −105.50 (s, Si_{Ge9}). **^{31}P NMR** (162 MHz, 298 K, thf-d_8): δ [ppm] = 50.26 (m, P_{Ge9}). **ESI−MS** (positive mode, 4000 V, 300 °C): m/z 2199.3 $\{[(NHC^{Dipp}Cu)[(Ge_9\{Si(TMS)_3\}_2)^tBu_2P]M(NHC^{Dipp})]^+\}$. **EA**: anal. calcd. for $C_{53}H_{108}CuGe_9N_2PSi_8$: C, 36.5; H, 6.2; N, 1.6; found: C, 36.9 H, 6.3; N, 1.5.

$[(Ge_9\{Si(TMS)_3\}_2)^tBu_2P]Ag(NHC^{Dipp})$ ***(5)***. $K_2[Ge_9\{Si(TMS)_3\}_2]$ (92 mg, 0.075 mmol, 1 equiv) was treated with a solution of $^tBu_2PCl$ (13.5 mg, 0.075 mmol, 1 equiv) in MeCN (2.5 mL) to obtain a deep red reaction mixture. After stirring for 30 min at r.t., a solution of $NHC^{Dipp}AgCl$ (40.0 mg, 0.075 mmol, 1 equiv) in MeCN (1 mL) was added and led to the formation of a brownish precipitate. The supernatant solution was filtered off, and the solid was washed with MeCN (2 mL). The solid was then dissolved in toluene and filtered. Removal of toluene and washing with hexane (2.5 mL) yielded compound **5** as a brownish solid (40 mg; 30% yield). In this case the procedure was not convenient to remove all contaminations from the sample, however. **^{1}H NMR** (400 MHz, 298 K, thf-d_8): δ [ppm] = 7.70 (s, 2H, CH_{Im}), 7.56−7.46 (m, 2H, $CH_{Ph(p)}$), 7.43−7.37 (m, 4H, $CH_{Ph(m)}$), 2.79 (hept, $^3J_{HH}$ = 6.8 Hz, 4H, CH_{iPr}), 1.46 (d, $^3J_{HH}$ = 6.8 Hz, 12H, Me_{iPr}), 1.21 (d, $^3J_{HH}$ = 6.8 Hz, 12H, Me_{iPr}), 0.90 (d, $^3J_{HP}$ = 14.3 Hz, 18H, Me_{tBu}), 0.28 (s, 54H, Me_{TMS}). **^{13}C NMR** (101 MHz, 298 K, thf-d_8): δ [ppm] = 146.51 (s, $C_{Ph(iPr)}$), 136.83 (s, $C_{Ph}N$), 131.69 (s, $CH_{Ph(p)}$), 125.57 (s, CH_{Im}), 125.34 (s, $CH_{Ph(m)}$), 34.40 (s, Me_{tBu}), 32.94 (d, $^1J_{CP}$ = 9.7 Hz, C_{tBu}), 29.81 (s, CH_{iPr}), 3.10 (s, Me_{TMS}). **^{29}Si-INEPT NMR** (79 MHz, 298 K, thf-d_8): δ [ppm] = −9.12 (s, Si_{TMS}), −105.64 (s, Si_{Ge9}). **^{31}P NMR** (162 MHz, 298 K, thf-d_8): δ [ppm] = 50.88 (d, $^1J_{PAg}$ = 428 Hz, P_{Ge9}).

$[(Ge_9\{Si(TMS)_3\}_2)^tBu_2P]Au(NHC^{Dipp})$ ***(6)***. $K_2[Ge_9\{Si(TMS)_3\}_2]$ (92 mg, 0.075 mmol, 1 equiv) was treated with a solution of $^tBu_2PCl$ (13.5 mg, 0.075 mmol, 1 equiv) in MeCN (2.5 mL) to obtain a deep red reaction mixture. After stirring for 30 min at r.t., a solution of $NHC^{Dipp}AuCl$ (46.5 mg, 0.075 mmol, 1 equiv) in MeCN (1 mL) was added, leading to the formation of a brownish precipitate. The supernatant solution was filtered off, and the solid was washed with MeCN (2 mL). The solid was then dissolved in toluene and filtered. Removal of toluene and washing of the remaining solid with hexane (2.5 mL) yielded compound **6** as a brownish solid in (45 mg; 25% yield). However, this procedure was not convenient to remove all contaminations from the sample. **^{1}H NMR** (400 MHz, 298 K, thf-d_8): δ [ppm] = 7.75 (s, 2H, CH_{Im}), 7.56−7.46 (m, 2H, $CH_{Ph(p)}$), 7.43−7.37 (m, 4H, $CH_{Ph(m)}$), 2.79 (hept, $^3J_{HH}$ = 6.8 Hz, 4H, CH_{iPr}), 1.49 (d, $^3J_{HH}$ = 6.8 Hz, 12H, Me_{iPr}), 1.21 (d, $^3J_{HH}$ = 6.8 Hz, 12H, Me_{iPr}), 0.91 (d, $^3J_{HP}$ = 14.9 Hz, 18H, Me_{tBu}), 0.28 (s, 54H, Me_{TMS}). **^{13}C NMR** (101 MHz, 298 K, thf-d_8): δ [ppm] = 146.36 (s, $C_{Ph(iPr)}$), 136.11 (s, $C_{Ph}N$), 131.90 (s, $CH_{Ph(p)}$), 126.07 (s, CH_{Im}), 125.43 (s, $CH_{Ph(m)}$), 36.38 (s, Me_{tBu}), 32.91 (d, $^1J_{CP}$ = 5.3 Hz, C_{tBu}), 29.91 (s, CH_{iPr}), 3.09 (s, Me_{TMS}). **^{29}Si-INEPT NMR** (79 MHz, 298 K, thf-d_8): δ [ppm] = −9.13 (s, Si_{TMS}), −106.16 (s, Si_{Ge9}). **^{31}P NMR** (162 MHz, 298 K, thf-d_8): δ [ppm] = 82.49 (m, P_{Ge9}).

■ ASSOCIATED CONTENT

Supporting Information

The Supporting Information is available free of charge on the ACS Publications website at DOI: 10.1021/jacs.7b05834.

Selected bond lengths of compounds **1** and **4**, as well as additional ESI−MS data for compound **4** (PDF)
NMR spectra of compounds **1**−**6** (PDF)
Crystallographic data for compounds **1** and **4** (CIF)

■ AUTHOR INFORMATION

Corresponding Author

*thomas.faessler@lrz.tu-muenchen.de

ORCID

Thomas F. Fässler: 0000-0001-9460-8882

Notes

The authors declare no competing financial interest.

■ ACKNOWLEDGMENTS

This work was financially supported by Wacker Chemie AG. F.S.G. thanks M. Sc. Lorenz Schiegerl, M. Sc. Kerstin Mayer for the ESI−MS measurements, Dr. Wilhelm Klein for help with

DOI: 10.1021/jacs.7b05834
J. Am. Chem. Soc. 2017, 139, 11933−11940

crystallographic issues, and Dr. Annette Schier for reading the manuscript. Furthermore, F.S.G. and J.V.D. thank TUM Graduate School for support.

REFERENCES

(1) Scharfe, S.; Kraus, F.; Stegmaier, S.; Schier, A.; Fässler, T. F. *Angew. Chem., Int. Ed.* **2011**, *50*, 3630.
(2) Sevov, S. C.; Goicoechea, J. M. *Organometallics* **2006**, *25*, 5678.
(3) Xu, L.; Sevov, S. C. *J. Am. Chem. Soc.* **1999**, *121*, 9245.
(4) Ugrinov, A.; Sevov, S. C. *J. Am. Chem. Soc.* **2002**, *124*, 10990.
(5) Yong, L.; Hoffmann, S. D.; Fässler, T. F. *Z. Anorg. Allg. Chem.* **2005**, *631*, 1149.
(6) Ugrinov, A.; Sevov, S. C. *Inorg. Chem.* **2003**, *42*, 5789.
(7) Yong, L.; Hoffmann, S. D.; Fässler, T. F. *Z. Anorg. Allg. Chem.* **2004**, *630*, 1977.
(8) Downie, C.; Mao, J.-G.; Parmar, H.; Guloy, A. M. *Inorg. Chem.* **2004**, *43*, 1992.
(9) Downie, C.; Tang, Z.; Guloy, A. M. *Angew. Chem., Int. Ed.* **2000**, *39*, 337.
(10) Ugrinov, A.; Sevov, S. C. *J. Am. Chem. Soc.* **2002**, *124*, 2442.
(11) Burns, R. C.; Corbett, J. D. *J. Am. Chem. Soc.* **1982**, *104*, 2804.
(12) Ugrinov, A.; Sevov, S. C. *J. Am. Chem. Soc.* **2003**, *125*, 14059.
(13) Ugrinov, A.; Sevov, S. C. *Chem. - Eur. J.* **2004**, *10*, 3727.
(14) Hansen, D. F.; Zhou, B.; Goicoechea, J. M. *J. Organomet. Chem.* **2012**, *721*−*722*, 53.
(15) Bentlohner, M. M.; Jantke, L.-A.; Henneberger, T.; Fischer, C.; Mayer, K.; Klein, W.; Fässler, T. F. *Chem. - Eur. J.* **2016**, *22*, 13946.
(16) Kocak, F. S.; Zavalij, P. Y.; Lam, Y.-F.; Eichhorn, B. W. *Chem. Commun.* **2009**, 4197.
(17) Kocak, F. S.; Zavalij, P.; Eichhorn, B. *Chem. - Eur. J.* **2011**, *17*, 4858.
(18) Schrenk, C.; Winter, F.; Pöttgen, R.; Schnepf, A. *Inorg. Chem.* **2012**, *51*, 8583.
(19) Schnepf, A. *Angew. Chem., Int. Ed.* **2003**, *42*, 2624.
(20) Li, F.; Sevov, S. C. *Inorg. Chem.* **2012**, *51*, 2706.
(21) Schenk, C.; Schnepf, A. *Angew. Chem., Int. Ed.* **2007**, *46*, 5314.
(22) Schenk, C.; Henke, F.; Santiso-Quinones, G.; Krossing, I.; Schnepf, A. *Dalton Trans.* **2008**, 4436.
(23) Henke, F.; Schenk, C.; Schnepf, A. *Dalton Trans.* **2009**, 9141.
(24) Kysliak, O.; Schrenk, C.; Schnepf, A. *Chem. - Eur. J.* **2016**, *22*, 18787.
(25) Geitner, F. S.; Fässler, T. F. *Eur. J. Inorg. Chem.* **2016**, *2016*, 2688.
(26) Mayer, K.; Schiegerl, L. J.; Fässler, T. F. *Chem. - Eur. J.* **2016**, *22*, 18794.
(27) Li, F.; Sevov, S. C. *Inorg. Chem.* **2015**, *54*, 8121.
(28) Schenk, C.; Schnepf, A. *Chem. Commun.* **2009**, 3208.
(29) Henke, F.; Schenk, C.; Schnepf, A. *Dalton Trans.* **2011**, *40*, 6704.
(30) Li, F.; Munoz-Castro, A.; Sevov, S. C. *Angew. Chem., Int. Ed.* **2012**, *51*, 8581.
(31) Li, F.; Sevov, S. C. *J. Am. Chem. Soc.* **2014**, *136*, 12056.
(32) Kysliak, O.; Schrenk, C.; Schnepf, A. *Inorg. Chem.* **2015**, *54*, 7083.
(33) Schiegerl, L. J.; Geitner, F. S.; Fischer, C.; Klein, W.; Fässler, T. F. *Z. Anorg. Allg. Chem.* **2016**, *642*, 1419.
(34) Kysliak, O.; Kunz, T.; Schnepf, A. *Eur. J. Inorg. Chem.* **2017**, *2017*, 805.
(35) Perla, L. G.; Sevov, S. C. *J. Am. Chem. Soc.* **2016**, *138*, 9795.
(36) Kysliak, O.; Schnepf, A. *Dalton Trans.* **2016**, *45*, 2404.
(37) Fey, N.; Haddow, M. F.; Mistry, R.; Norman, N. C.; Orpen, A. G.; Reynolds, T. J.; Pringle, P. G. *Organometallics* **2012**, *31*, 2907.
(38) Liedtke, J.; Rüegger, H.; Loss, S.; Grützmacher, H. *Angew. Chem., Int. Ed.* **2000**, *39*, 2478.
(39) Cipot, J.; McDonald, R.; Stradiotto, M. *Chem. Commun.* **2005**, 4932.
(40) Lu, C. C.; Peters, J. C. *J. Am. Chem. Soc.* **2002**, *124*, 5272.
(41) For *Zintl* clusters such a functinalization is not reported yet. However, the introduction of a phosphino group at an anionic unsaturated Si_6 cluster has previously been achieved. Willmes, P.; Leszczynska, K.; Heider, Y.; Abersfelder, K.; Zimmer, M.; Huch, V.; Scheschkewitz, D. *Angew. Chem., Int. Ed.* **2016**, *55*, 2907.
(42) Izod, K.; Rayner, D. G.; El-Hamruni, S. M.; Harrington, R. W.; Baisch, U. *Angew. Chem., Int. Ed.* **2014**, *53*, 3636.
(43) Dube, J. W.; Graham, C. M. E.; Macdonald, C. L. B.; Brown, Z. D.; Power, P. P.; Ragogna, P. J. *Chem. - Eur. J.* **2014**, *20*, 6739.
(44) Quintero, G. E.; Paterson-Taylor, I.; Rees, N. H.; Goicoechea, J. M. *Dalton Trans.* **2016**, *45*, 1930.
(45) Karsch, H. H.; Baumgartner, G.; Gamper, S. *J. Organomet. Chem.* **1993**, *462*, C3.
(46) Perdew, J. P.; Burke, K.; Ernzerhof, M. *Phys. Rev. Lett.* **1996**, *77*, 3865.
(47) Adamo, C.; Barone, V. *J. Chem. Phys.* **1999**, *110*, 6158.
(48) Weigend, F.; Ahlrichs, R. *Phys. Chem. Chem. Phys.* **2005**, *7*, 3297.
(49) Hirshfeld, F. L. *Theor. Chim. Acta* **1977**, *44*, 129.
(50) Reed, A. E.; Weinstock, R. B.; Weinhold, F. *J. Chem. Phys.* **1985**, *83*, 735.
(51) Lazreg, F.; Slawin, A. M. Z.; Cazin, C. S. J. *Organometallics* **2012**, *31*, 7969.
(52) Pauling, L. *J. Am. Chem. Soc.* **1932**, *54*, 3570.
(53) Becke, A. D.; Edgecombe, K. E. *J. Chem. Phys.* **1990**, *92*, 5397.
(54) Fässler, T. F.; Savin, A. *Chem. Unserer Zeit* **1997**, *31*, 110.
(55) Marx, T.; Wesemann, L.; Dehnen, S. *Organometallics* **2000**, *19*, 4653.
(56) Lu, T.; Chen, F. *J. Comput. Chem.* **2012**, *33*, 580.
(57) Scharfe, S.; Fässler, T. F. *Eur. J. Inorg. Chem.* **2010**, *2010*, 1207.
(58) Zhou, B.; Denning, M. S.; Chapman, T. A. D.; Goicoechea, J. M. *Inorg. Chem.* **2009**, *48*, 2899.
(59) Goicoechea, J. M.; Sevov, S. C. *J. Am. Chem. Soc.* **2006**, *128*, 4155.
(60) Collado, A.; Gomez-Suarez, A.; Martin, A. R.; Slawin, A. M. Z.; Nolan, S. P. *Chem. Commun.* **2013**, *49*, 5541.
(61) de Frémont, P.; Scott, N. M.; Stevens, E. D.; Ramnial, T.; Lightbody, O. C.; Macdonald, C. L. B.; Clyburne, J. A. C.; Abernethy, C. D.; Nolan, S. P. *Organometallics* **2005**, *24*, 6301.
(62) Santoro, O.; Collado, A.; Slawin, A. M. Z.; Nolan, S. P.; Cazin, C. S. J. *Chem. Commun.* **2013**, *49*, 10483.
(63) Hintermann, L. *Beilstein J. Org. Chem.* **2007**, *3*, 22.
(64) Sheldrick, G. *Acta Crystallogr., Sect. C: Struct. Chem.* **2015**, *71*, 3.
(65) Spek, A. *J. Appl. Crystallogr.* **2003**, *36*, 7.
(66) Fulmer, G. R.; Miller, A. J. M.; Sherden, N. H.; Gottlieb, H. E.; Nudelman, A.; Stoltz, B. M.; Bercaw, J. E.; Goldberg, K. I. *Organometallics* **2010**, *29*, 2176.
(67) Frisch, M. J.; Trucks, G. W.; Schlegel, H. B.; Scuseria, G. E.; Robb, M. A.; Cheeseman, J. R.; Scalmani, G.; Barone, V.; Mennucci, B.; Petersson, G. A.; Nakatsuji, H.; Caricato, M.; Li, X.; Hratchian, H. P.; Izmaylov, A. F.; Bloino, J.; Zheng, G.; Sonnenberg, J. L.; Hada, M.; Ehara, M.; Toyota, K.; Fukuda, R.; Hasegawa, J.; Ishida, M.; Nakajima, T.; Honda, Y.; Kitao, O.; Nakai, H.; Vreven, T.; Montgomery, Jr., J. A.; Peralta, J. E.; Ogliaro, F.; Bearpark, M.; Heyd, J. J.; Brothers, E.; Kudin, K. N.; Staroverov, V. N.; Kobayashi, R.; Normand, J.; Raghavachari, K.; Rendell, A.; Burant, J. C.; Iyengar, S. S.; Tomasi, J.; Cossi, M.; Rega, N.; Millam, J. M.; Klene, M.; Knox, J. E.; Cross, J. B.; Bakken, V.; Adamo, C.; Jaramillo, J.; Gomperts, R.; Stratmann, R. E.; Yazyev, O.; Austin, A. J.; Cammi, R.; Pomelli, C.; Ochterski, J. W.; Martin, R. L.; Morokuma, K.; Zakrzewski, V. G.; Voth, G. A.; Salvador, P.; Dannenberg, J. J.; Dapprich, S.; Daniels, A. D.; Farkas, Ö.; Foresman, J. B.; Ortiz, J. V.; Cioslowski, J.; Fox, D. J. *Gaussian 09*; Gaussian, Inc.: Wallingford CT, 2009.
(68) Weigend, F.; Häser, M.; Patzelt, H.; Ahlrichs, R. *Chem. Phys. Lett.* **1998**, *294*, 143.
(69) Barone, V.; Cossi, M. *J. Phys. Chem. A* **1998**, *102*, 1995.

DOI: 10.1021/jacs.7b05834
J. Am. Chem. Soc. 2017, 139, 11933−11940

Derivatization of Phosphine Ligands with Bulky Deltahedral *Zintl* Clusters – Synthesis of Charge Neutral Zwitterionic Tetrel Cluster Compounds $[(Ge_9\{Si(TMS)_3\}_2)^tBu_2P]M(NHC^{Dipp})$ (M: Cu, Ag, Au)

Felix. S. Geitner,[†] Jasmin V. Dums, Thomas. F. Fässler[*]

[†] Felix S. Geitner, WACKER Institute for Silicon Chemistry and Department of Chemistry, Technische Universität München, Lichtenbergstraße 4, 85747 Garching, Germany
Jasmin V. Dums, Department of Chemistry, Technische Universität München, Lichtenbergstraße 4, 85747 Garching, Germany

[*] Prof. Dr. Thomas. F. Fässler, Department of Chemistry, Technische Universität München
Lichtenbergstraße 4, 85747 Garching, Germany

Content

Selected Distances

Table SI 1: Selected bonding distances [Å] in **1** (Cluster I and Cluster II).

bond	**distance**	**bond**	**distance**
Cluster 1		Cluster 2	
Ge1-Ge2	2.5284(9)	Ge10-Ge11	2.5312(9)
Ge1-Ge3	2.5206(9)	Ge10-Ge12	2.5241(9)
Ge1-Ge4	2.5095(8)	Ge10-Ge13	2.5030(8)
Ge1-Ge5	2.512(1)	Ge10-Ge14	2.498(1)
Ge2-Ge3	2.8285(9)	Ge11-Ge12	2.8284(9)
Ge2-Ge6	2.550(1)	Ge11-Ge15	2.559(1)
Ge2-Ge7	2.669(1)	Ge11-Ge16	2.657(1)
Ge3-Ge7	2.6398(9)	Ge12-Ge16	2.6542(9)
Ge3-Ge8	2.5490(9)	Ge12-Ge17	2.5666(9)
Ge4-Ge5	2.9147(9)	Ge13-Ge14	2.9187(9)
Ge4-Ge8	2.631(1)	Ge13-Ge17	2.635(1)
Ge4-Ge9	2.6232(8)	Ge13-Ge18	2.6142(9)
Ge5-Ge6	2.673(1)	Ge14-Ge15	2.676(1)
Ge5-Ge9	2.6090(9)	Ge14-Ge18	2.5858(9)
Ge6-Ge7	2.586(1)	Ge15-Ge16	2.595(1)
Ge6-Ge9	2.4862(8)	Ge15-Ge18	2.4927(9)
Ge7-Ge8	2.5791(9)	Ge16-Ge17	2.5737(9)
Ge8-Ge9	2.4745(9)	Ge17-Ge18	2.473(1)
Ge1-Si1	2.376(2)	Ge10-Si13	2.374(2)
Ge6-Si2	2.408(2)	Ge15-Si14	2.407(2)
Ge8-Si3	2.391(1)	Ge17-Si15	2.398(2)
Ge9-P1	2.343(2)	Ge18-P2	2.336(2)
Ge2-Ge5	3.0006(7)	Ge11-Ge14	3.0042(7)
Ge3-Ge4	3.0687(7)	Ge12-Ge13	3.0300(7)
Ge7-Ge9	3.6920(8)	Ge16-Ge18	3.7057(8)
P1-C101	1.876(5)	P2-C201	1.863(6)
P1-C26	1.871(5)	P2-C207	1.866(6)

Table SI 2: Selected bonding distances [Å] in **1** (Cluster III).

bond	**distance**
Cluster 3	
Ge19-Ge20	2.5213(9)
Ge19-Ge21	2.5264(9)
Ge19-Ge22	2.507(1)
Ge19-Ge23	2.5118(8)
Ge20-Ge21	2.8262(9)
Ge20-Ge24	2.5681(9)
Ge20-Ge25	2.6317(9)
Ge21-Ge25	2.670(1)
Ge21-Ge26	2.5721(9)
Ge22-Ge23	2.9046(9)
Ge22-Ge26	2.665(1)
Ge22-Ge27	2.6247(9)
Ge23-Ge24	2.643(1)
Ge23-Ge27	2.6146(9)
Ge24-Ge25	2.5706(8)
Ge24-Ge27	2.4966(9)
Ge25-Ge26	2.557(1)
Ge26-Ge27	2.4902(8)
Ge19-Si25	2.375(2)
Ge24-Si26	2.404(2)
Ge26-Si27	2.402(2)
Ge27-P3	2.355(2)
Ge20-Ge23	3.0470(8)
Ge21-Ge22	2.9586(8)
Ge25-Ge27	3.7180(9)
P3-C301	1.869(6)
P3-C307	1.870(6)

Table SI 3: Selected bonding distances [Å] in **4**.

bond	**distance**
Ge1-Ge2	2.5407(7)
Ge1-Ge3	2.530(1)
Ge1-Ge4	2.5468(8)
Ge1-Ge5	2.534(1)
Ge2-Ge5	2.633(1)
Ge2-Ge6	2.552(1)
Ge2-Ge9	2.6967(9)
Ge3-Ge4	2.595(1)
Ge3-Ge6	2.5322(8)
Ge3-Ge7	2.737(1)
Ge4-Ge7	2.714(1)
Ge4-Ge8	2.5271(8)
Ge5-Ge8	2.534(1)
Ge5-Ge9	2.704(1)
Ge6-Ge7	2.5548(1)
Ge6-Ge9	2.553(1)
Ge7-Ge8	2.551(1)
Ge8-Ge9	2.5461(7)
Ge6-Si1	2.380(1)
Ge8-Si2	2.371(1)
Ge1-P1	2.316(1)
Ge2-Ge3	3.620(1)
Ge4-Ge5	3.658(1)
Ge7-Ge9	3.070(1)
Cu1-C1	1.923(3)
Cu1-P1	2.218(1)
P1-C22	1.883(4)
P1-C26	1.883(4)

Computational Analysis

Table SI 4: Selected charges from Hirshfeld[1] and Natural Population Analysis[2] for Compound **4** and [^{t}Bu$_3$PCu(NHC^{Dipp})]$^+$.[3]

	Compound 4		**[^{t}Bu$_3$PCu(NHC^{Dipp})]$^+$**	
Atom	Hirshfeld	NPA	Hirshfeld	NPA
P1	0.08	0.41	0.16	0.85
Cu1	0.16	0.42	0.20	0.41
[Ge$_9$] (Ge1-Ge9)	-0.33	-0.91	-	-

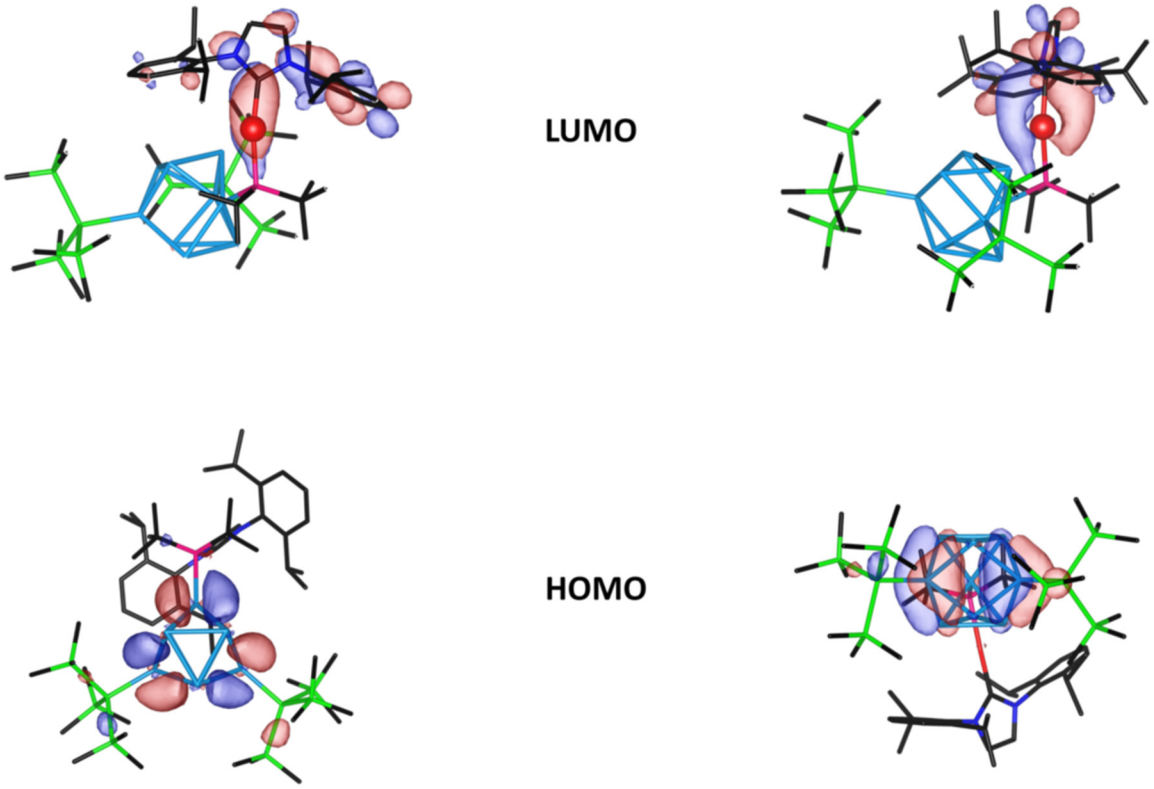

Figure SI 1: HOMO and LUMO orbital of compound **4**. C atoms are shown in black, N atoms in dark blue, P atoms in pink, Si atoms in green, Cu atoms in red and Ge atoms in light blue. Pictures were created using VESTA.[4]

NMR spectra

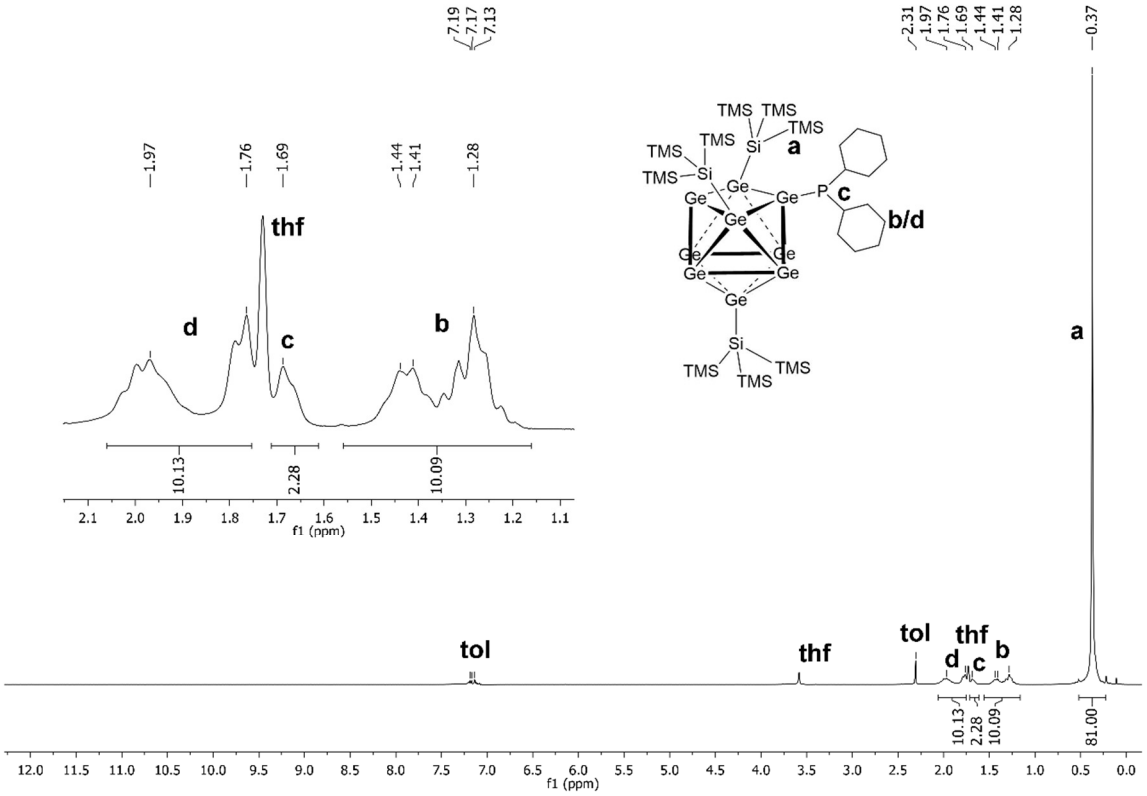

Figure SI 2: ^{1}H NMR spectrum of compound **1** in thf-d_8.

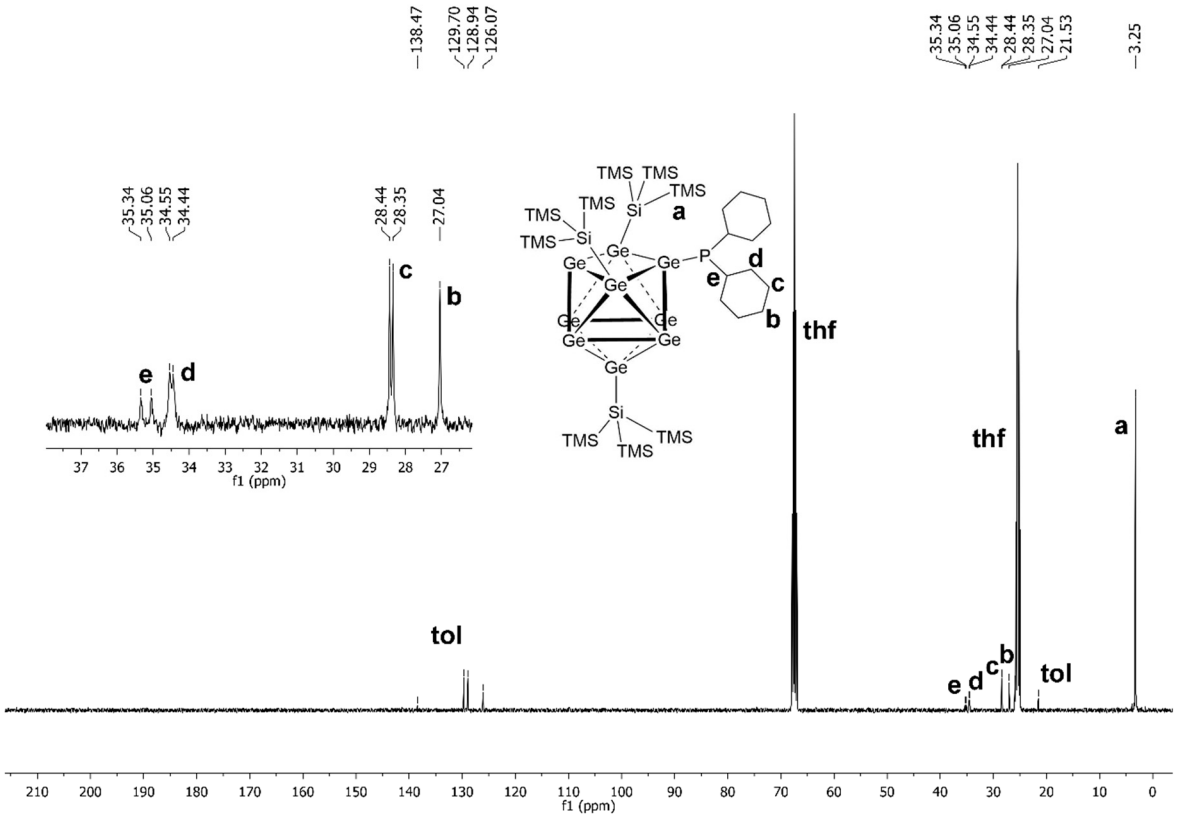

Figure SI 3: ^{13}C NMR spectrum of compound **1** in thf-d_8.

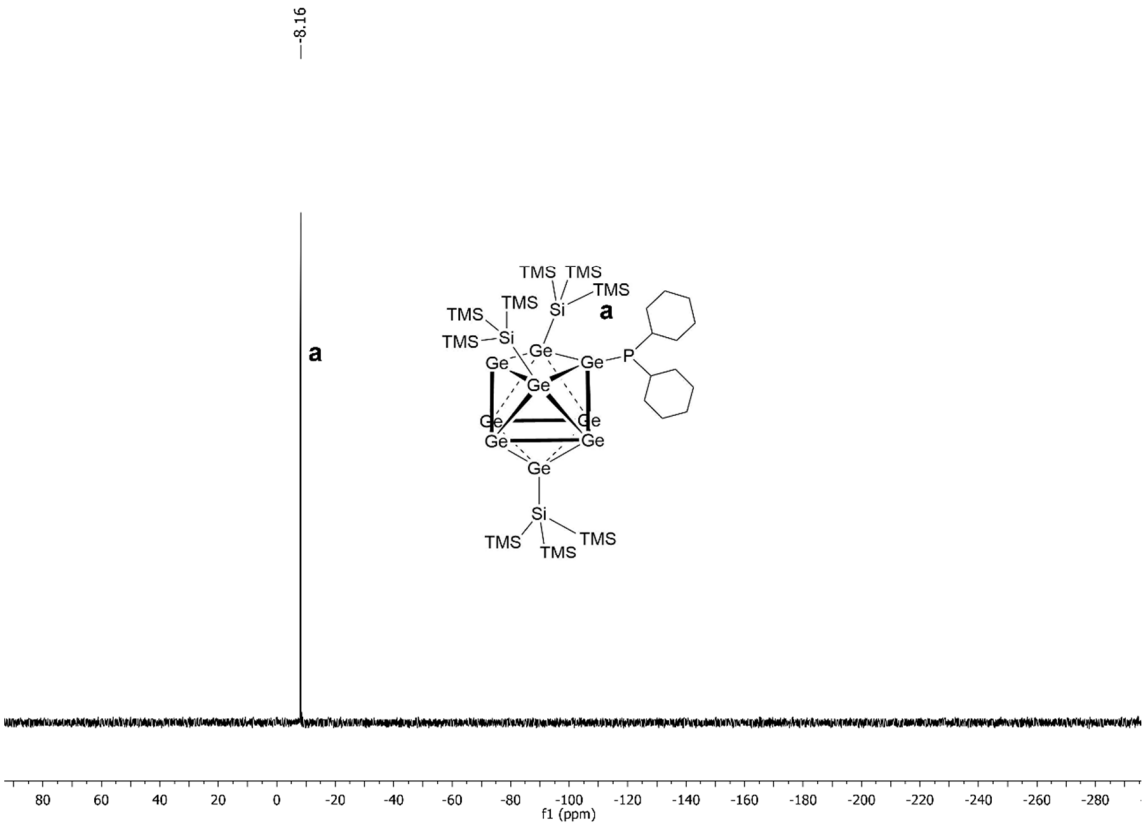

Figure SI 4a: ^{29}Si NMR spectrum of compound **1** in thf-d_8. Measurement was carried out with purified sample and relaxation time of 4s.

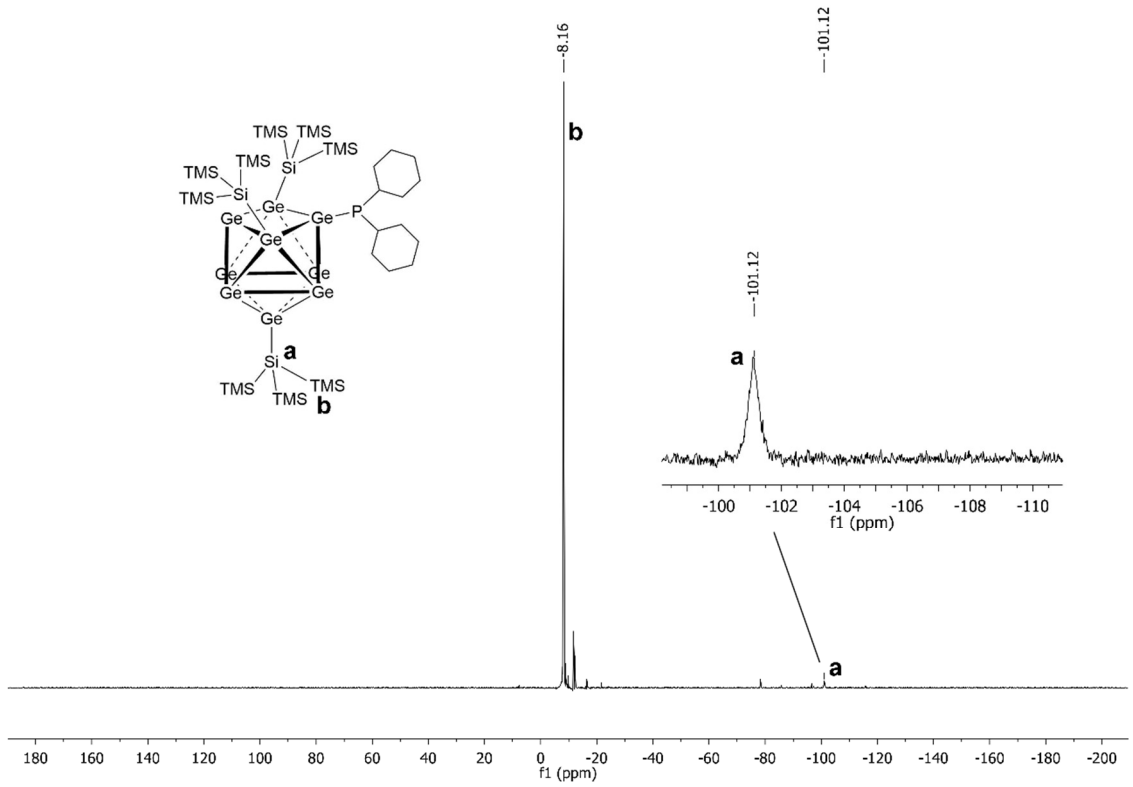

Figure SI 4b: ^{29}Si NMR spectrum of compound **1** in thf-d_8. Measurement was carried out with crude product sample and relaxation time of 15s.

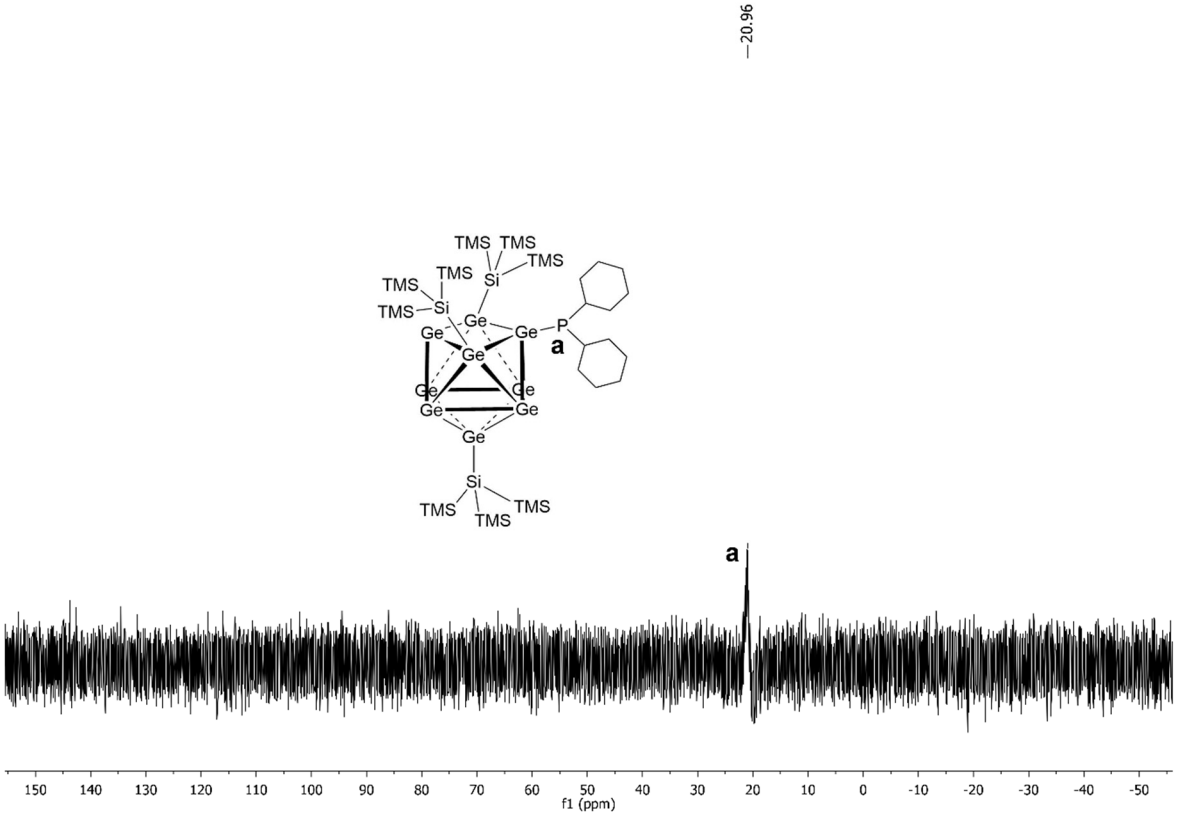

Figure SI 5: ^{31}P NMR spectrum of compound **1** in thf- d_8.

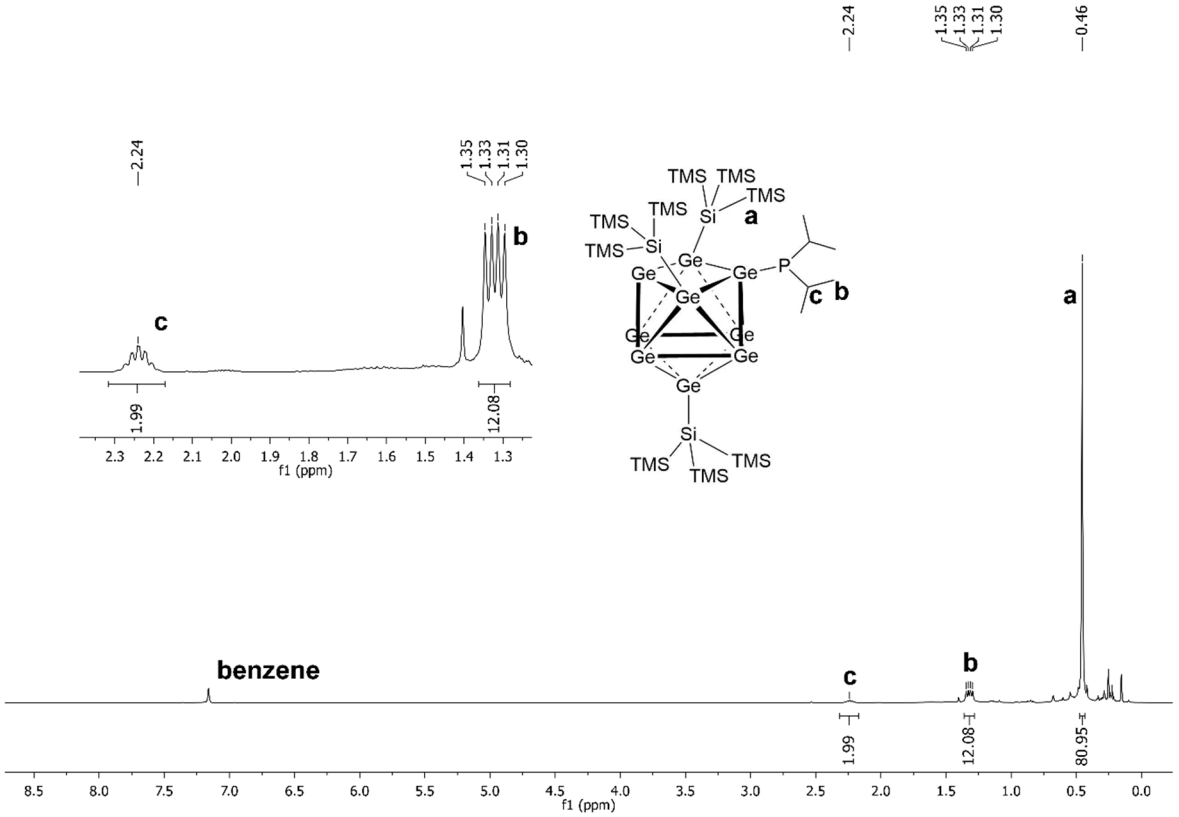

Figure SI 6: ^{1}H NMR spectrum of compound **2** in C_6D_6.

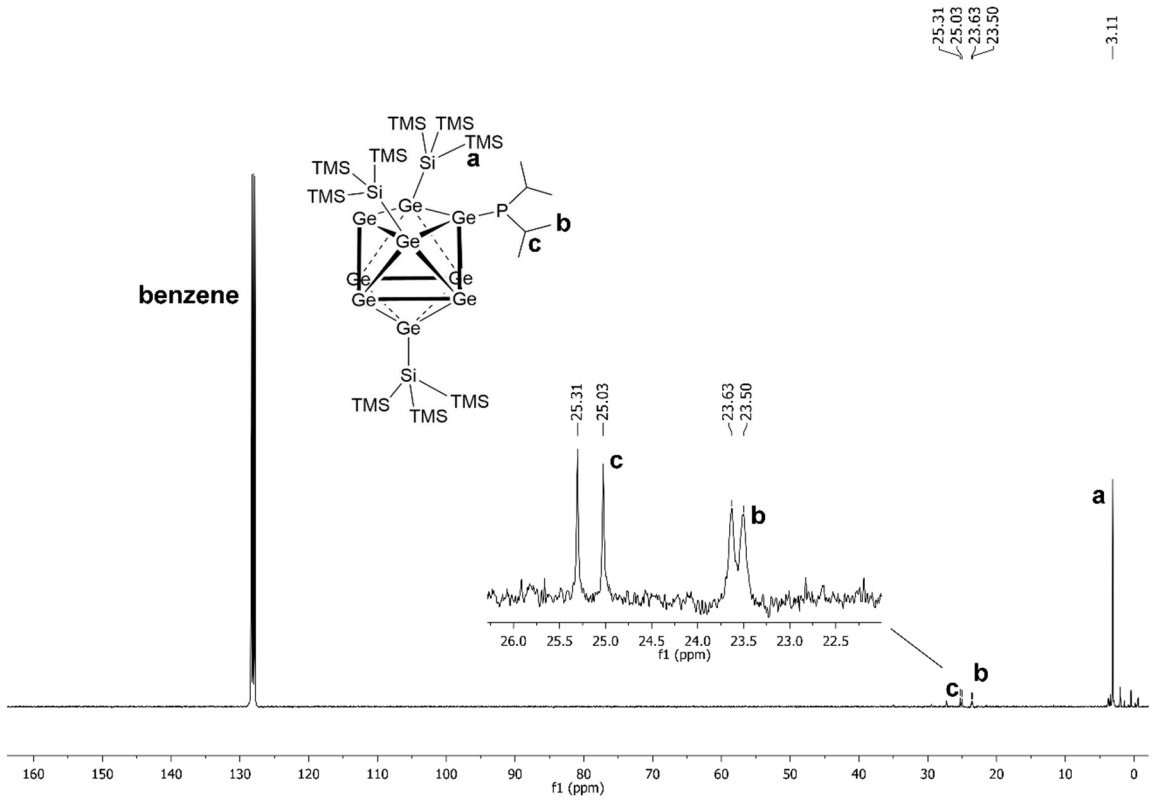

Figure SI 7: ^{13}C NMR spectrum of compound **2** in C_6D_6.

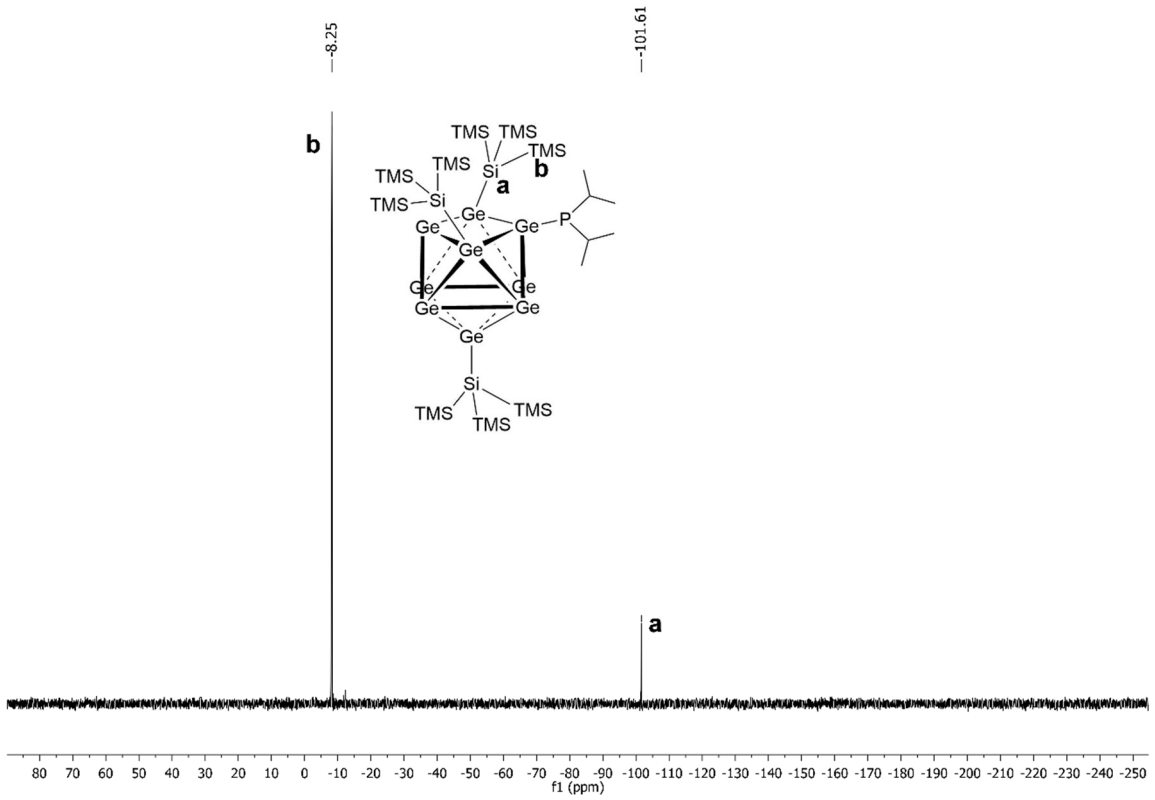

Figure SI 8: ^{29}Si NMR spectrum of compound **2** in C_6D_6.

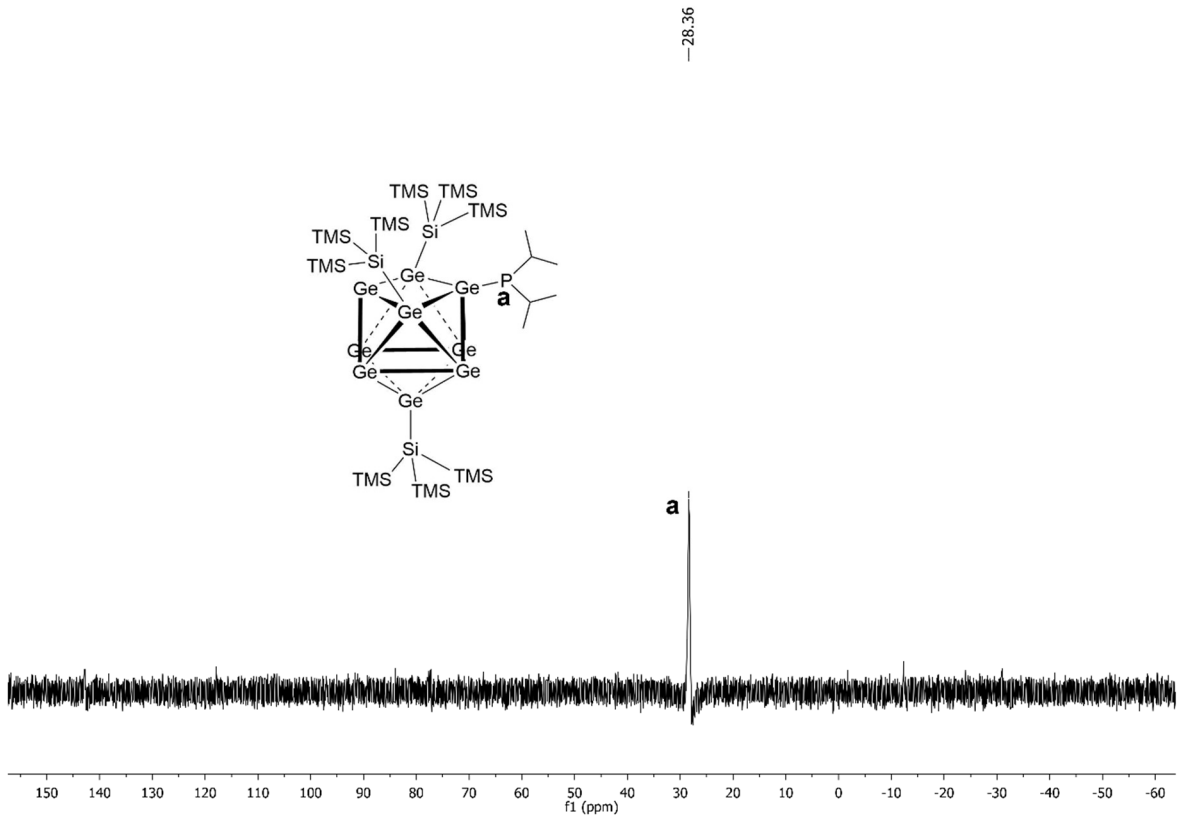

Figure SI 9: ^{31}P NMR spectrum of compound **2** in C_6D_6.

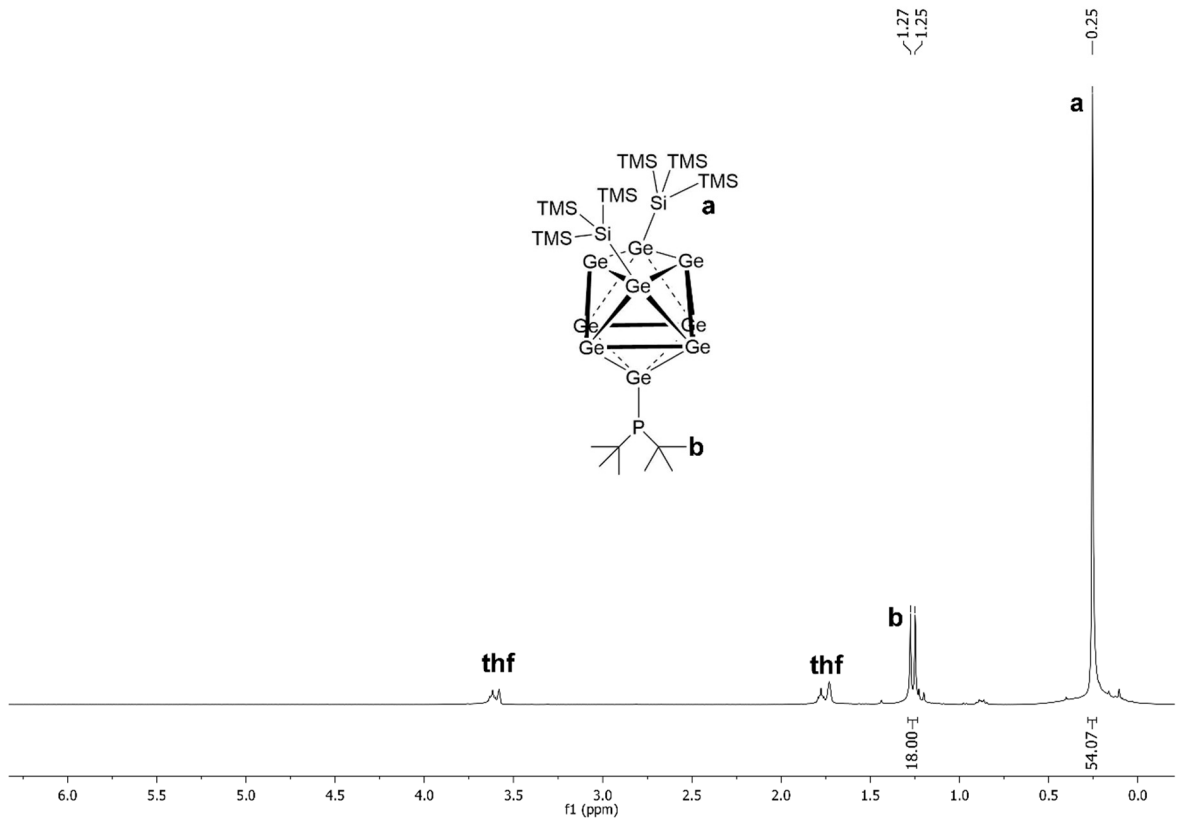

Figure SI 10: ^{1}H NMR spectrum of compound **3** in thf-d_8.

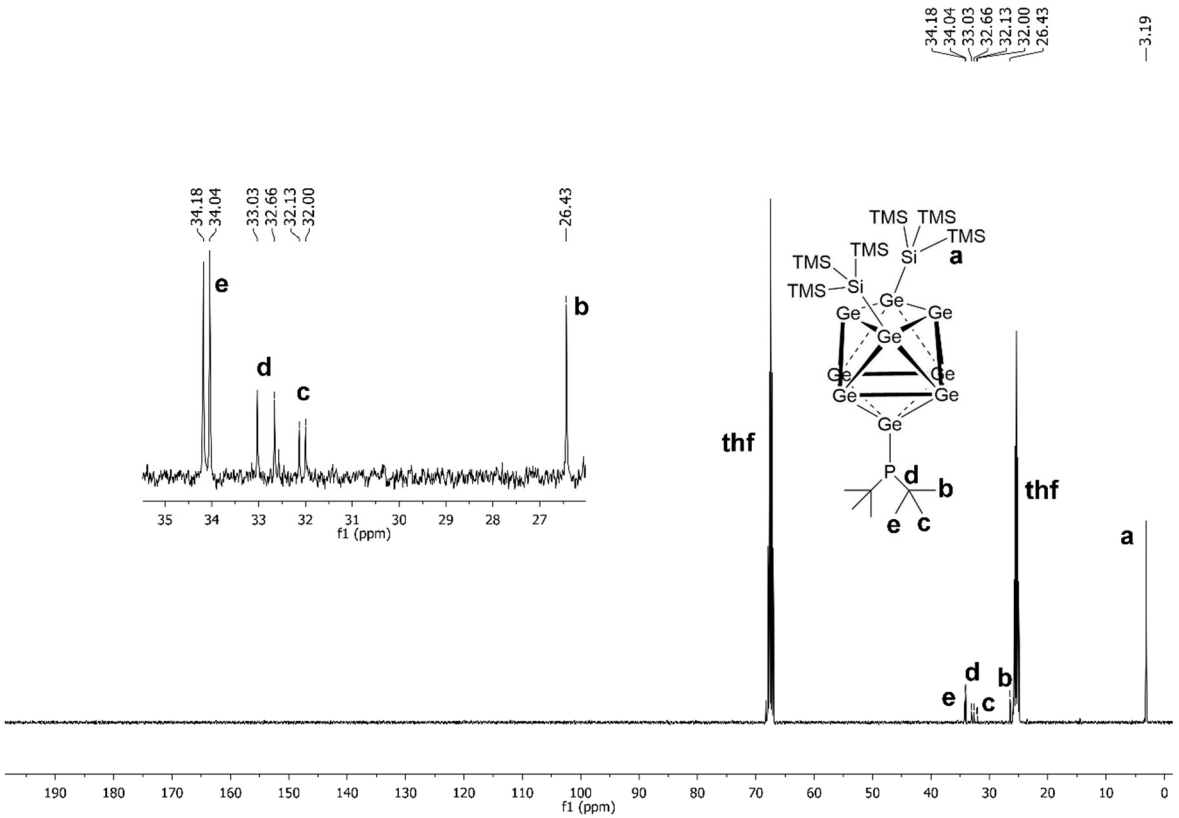

Figure SI 11: ^{13}C NMR spectrum of compound **3** in thf-d_8.

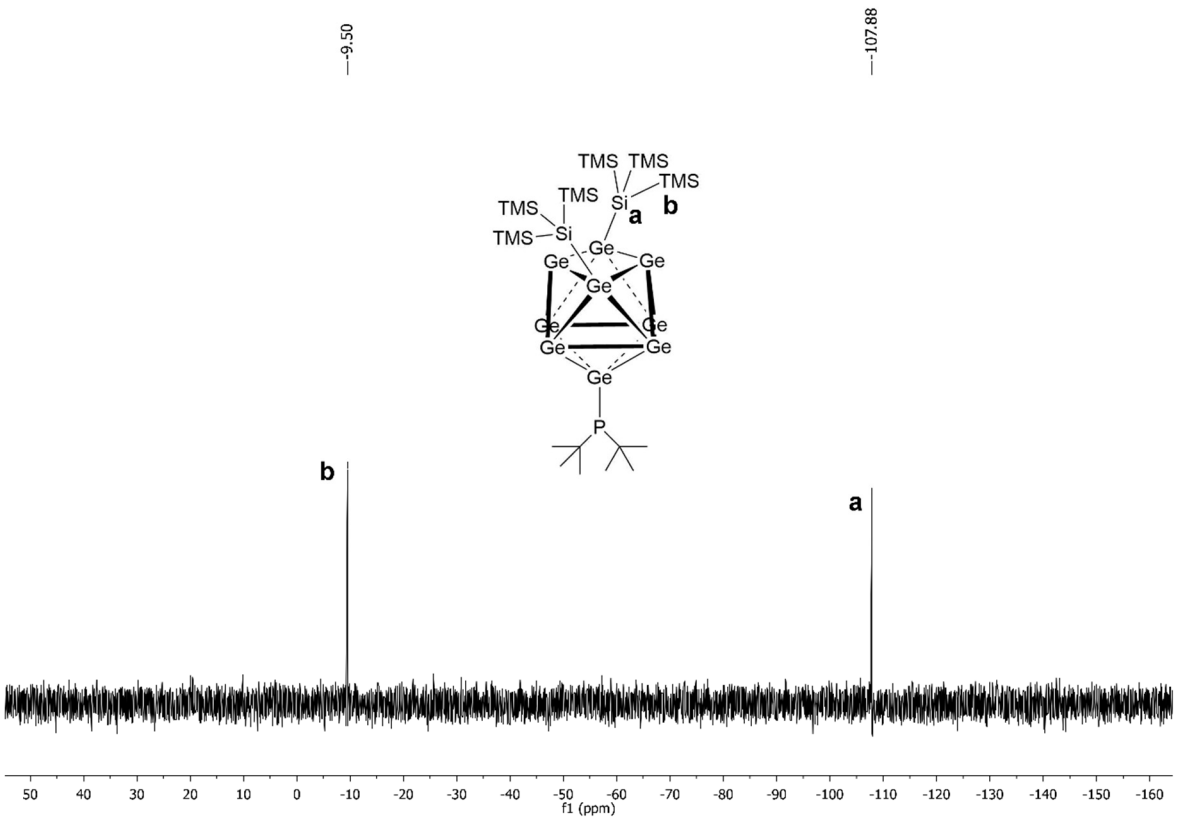

Figure SI 12: ^{29}Si NMR spectrum of compound **3** in thf-d_8.

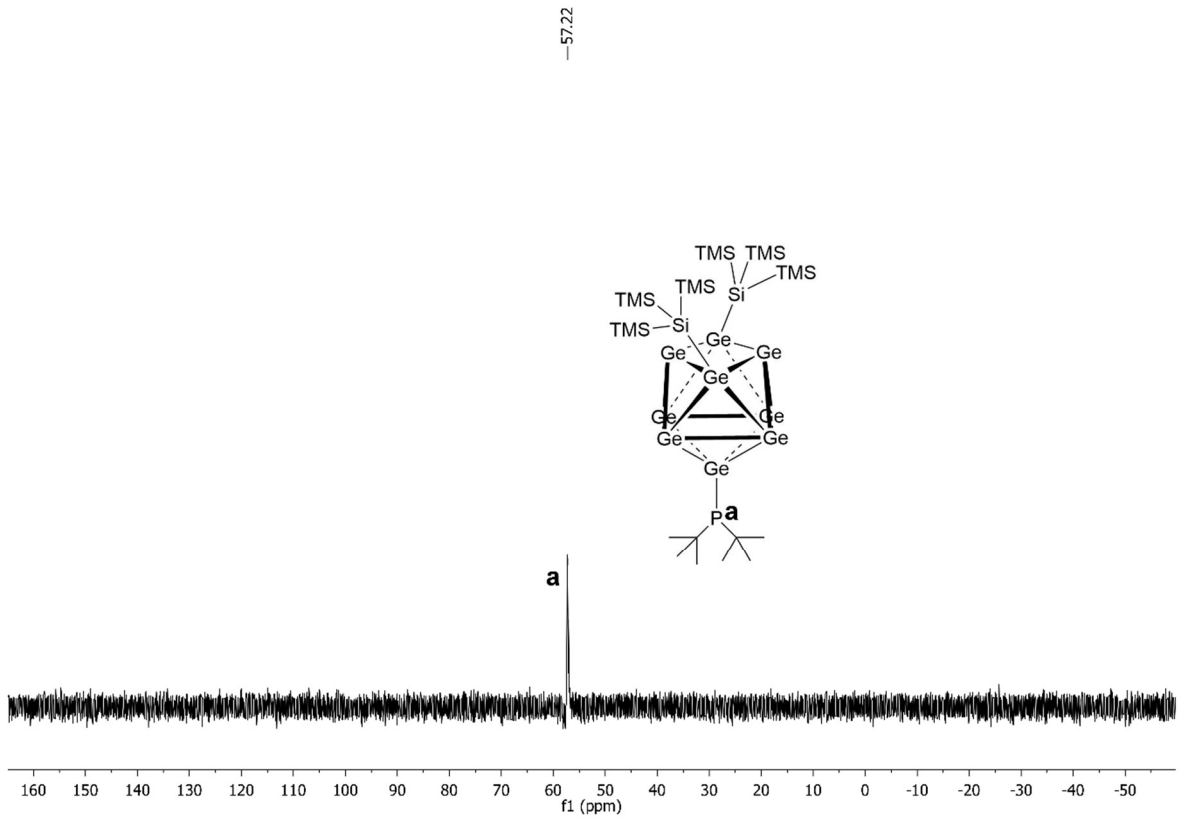

Figure SI 13: ^{31}P NMR spectrum of compound **3** in thf-d_8.

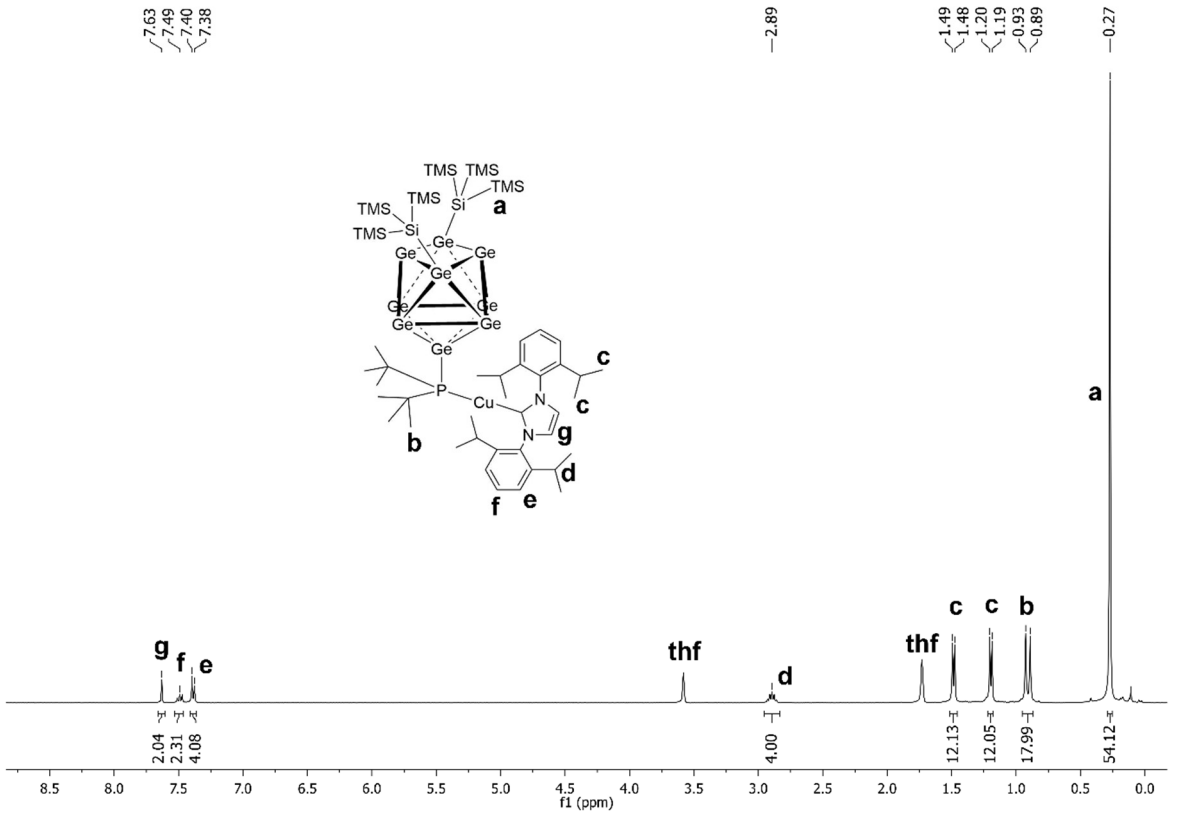

Figure SI 14: ^{1}H NMR spectrum of compound **4** in thf-d_8.

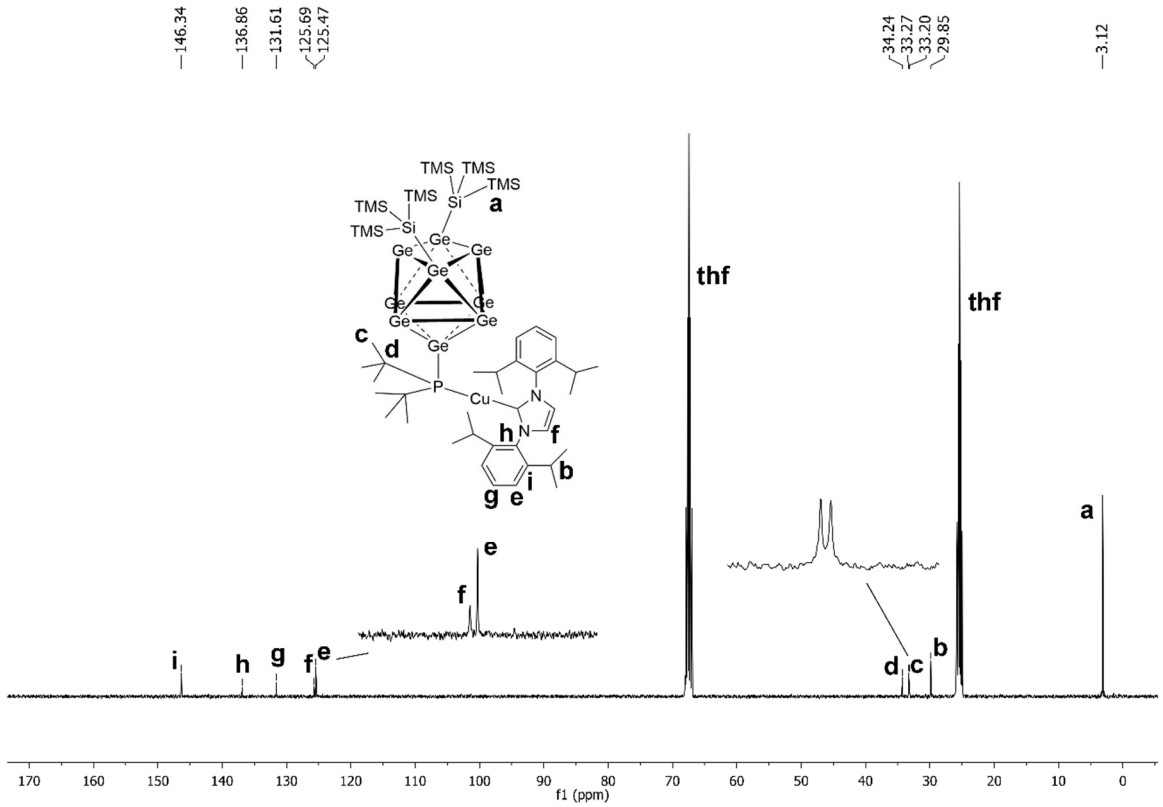

Figure SI 15: ^{13}C NMR spectrum of compound **4** in thf-d_8.

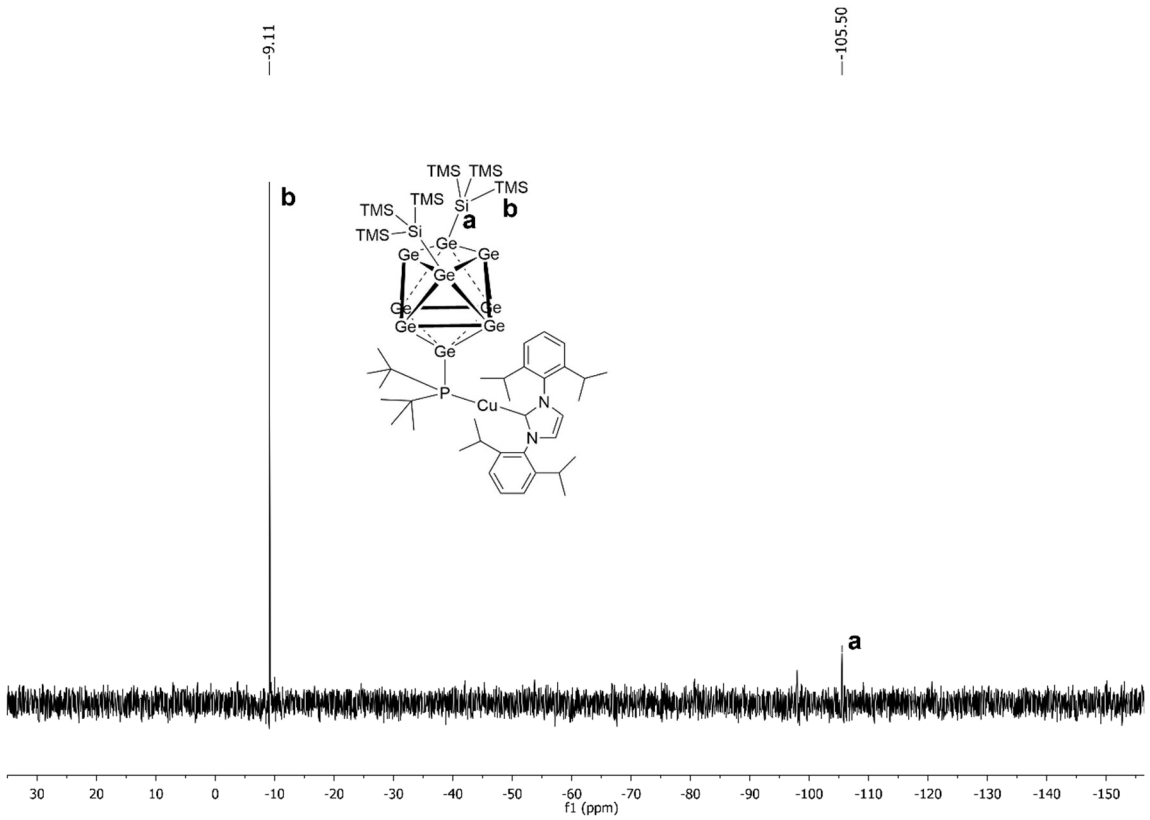

Figure SI 16: ^{29}Si NMR spectrum of compound **4** in thf-d_8.

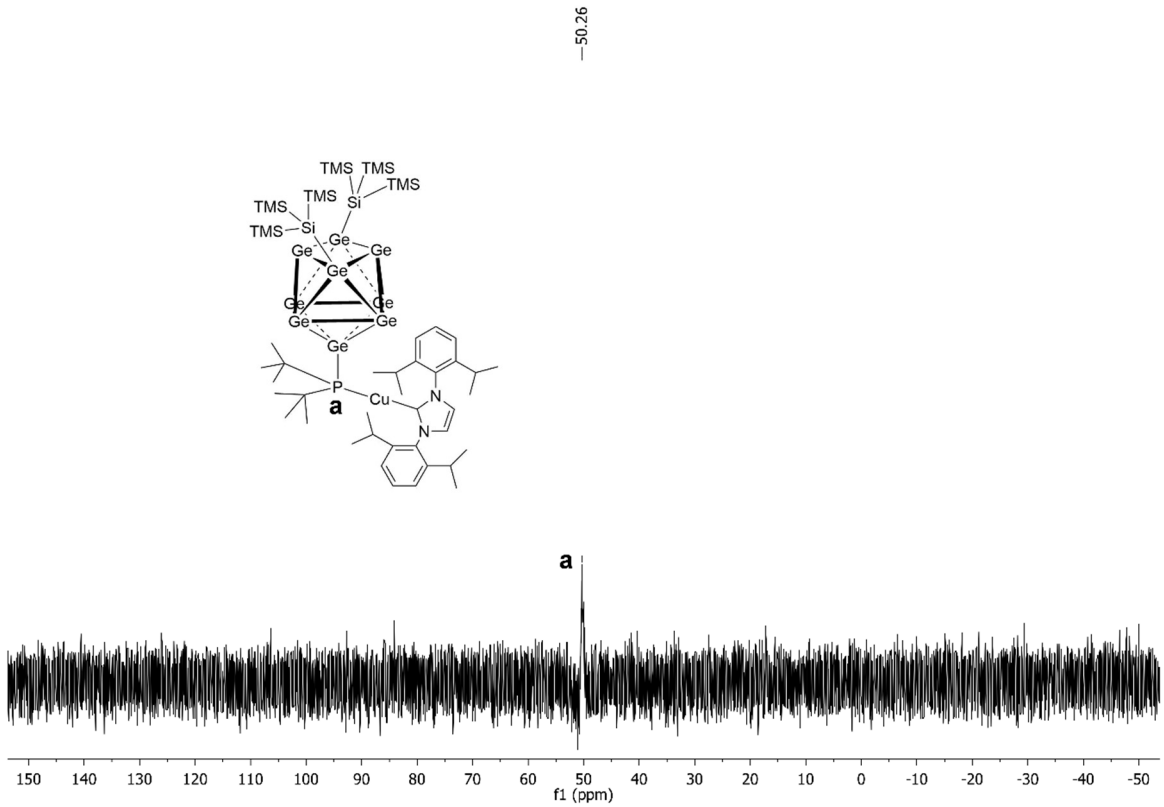

Figure SI 17: ^{31}P NMR spectrum of compound **4** in thf-d_8.

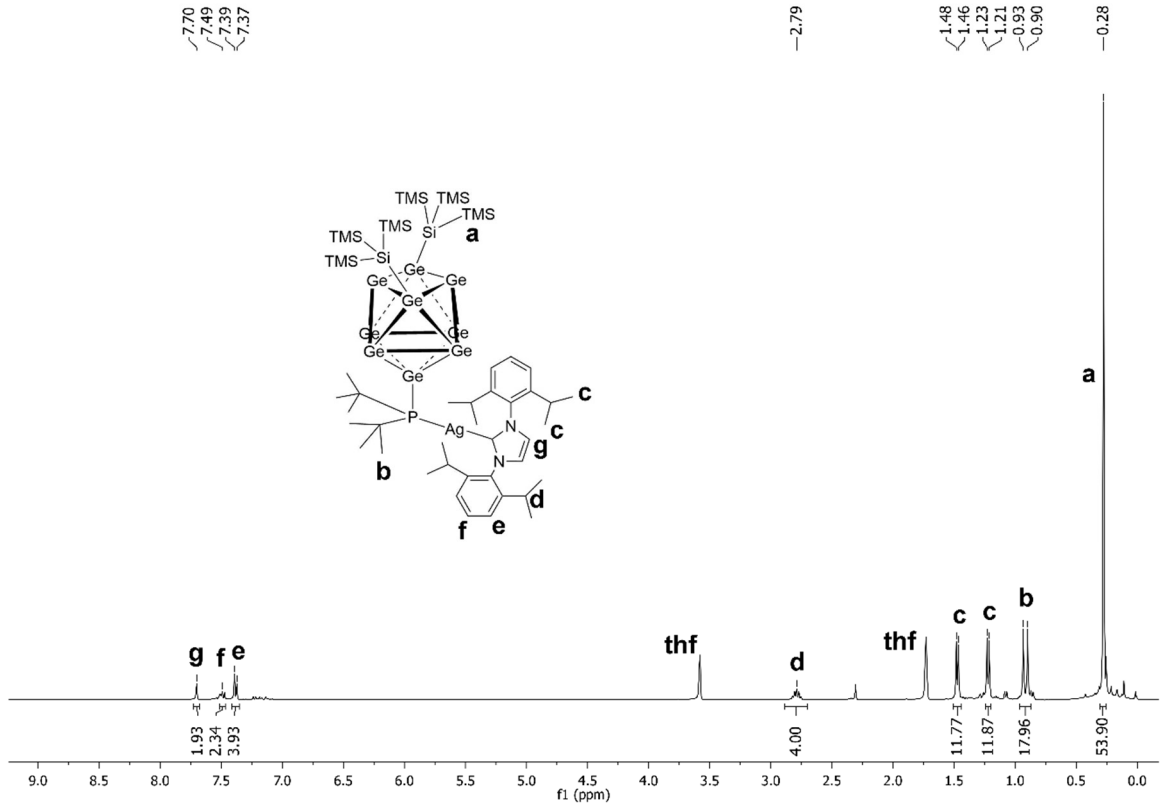

Figure SI 18: ^{1}H NMR spectrum of compound **5** in thf-d_8.

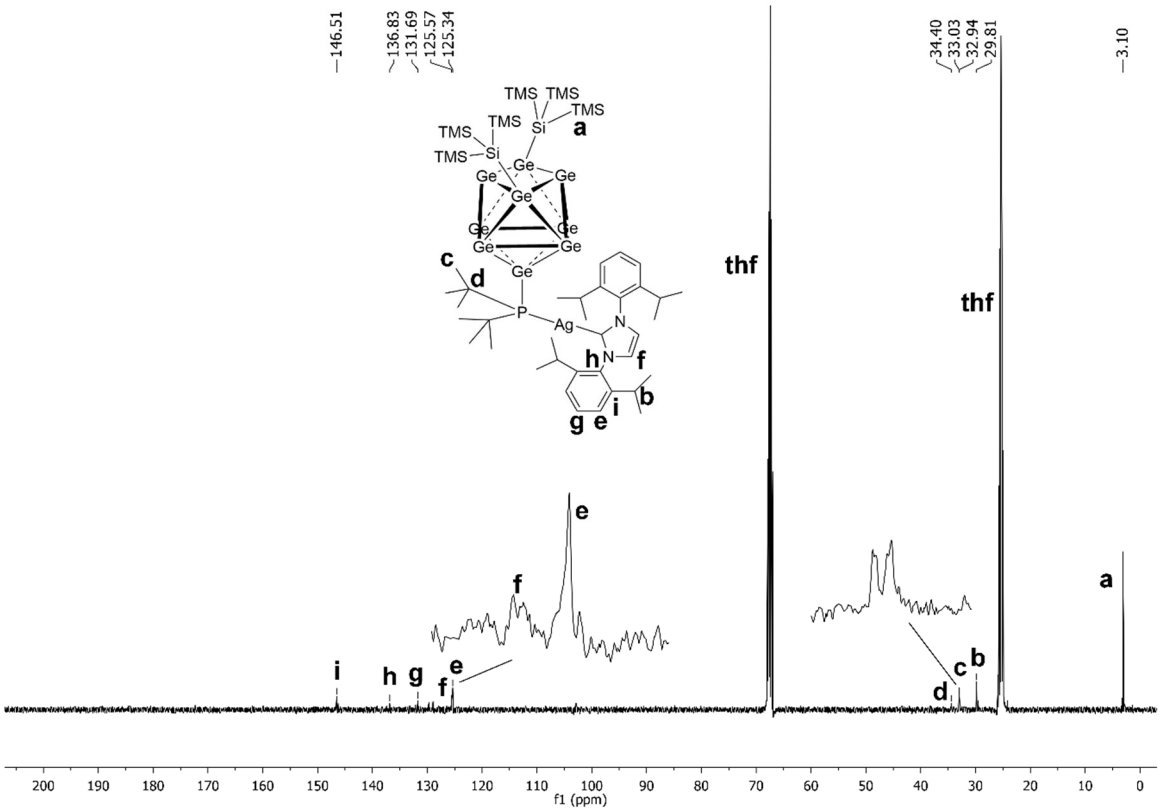

Figure SI 19: ^{13}C NMR spectrum of compound **5** in thf-d_8.

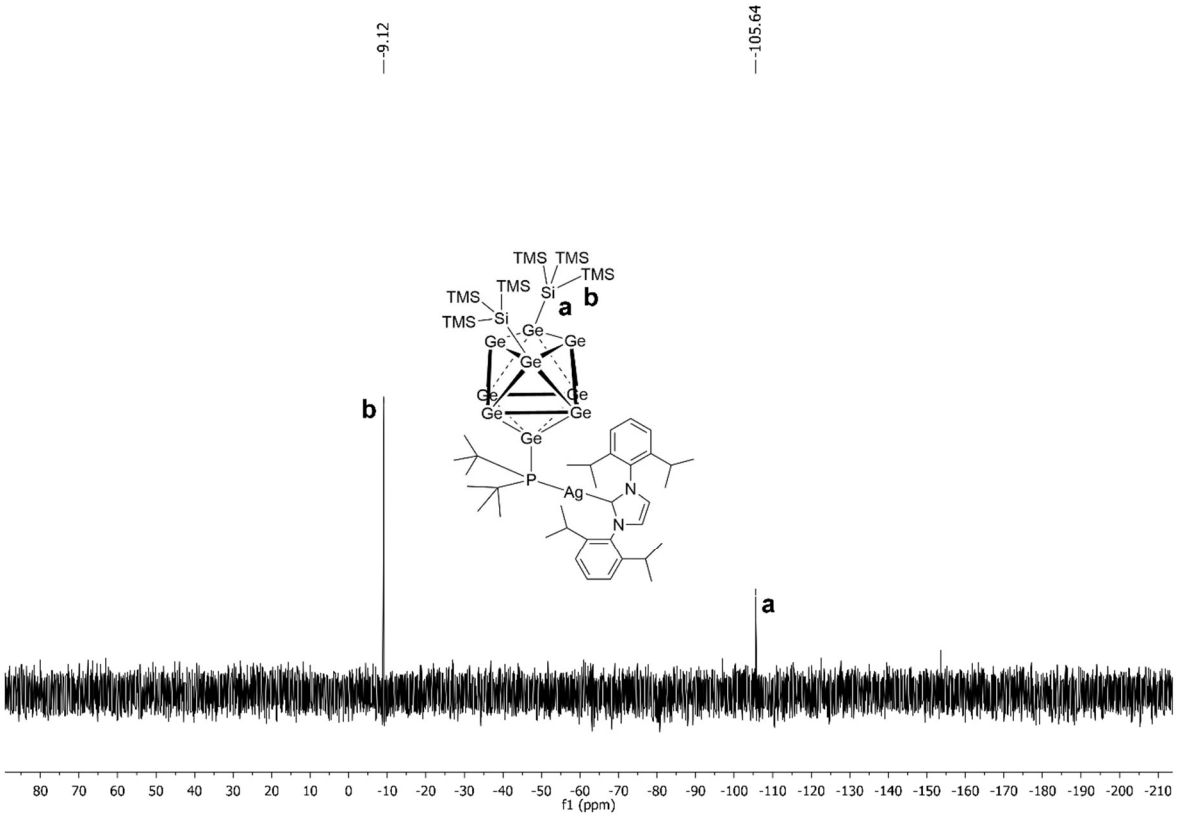

Figure SI 20: ^{29}Si NMR spectrum of compound **5** in thf-d_8.

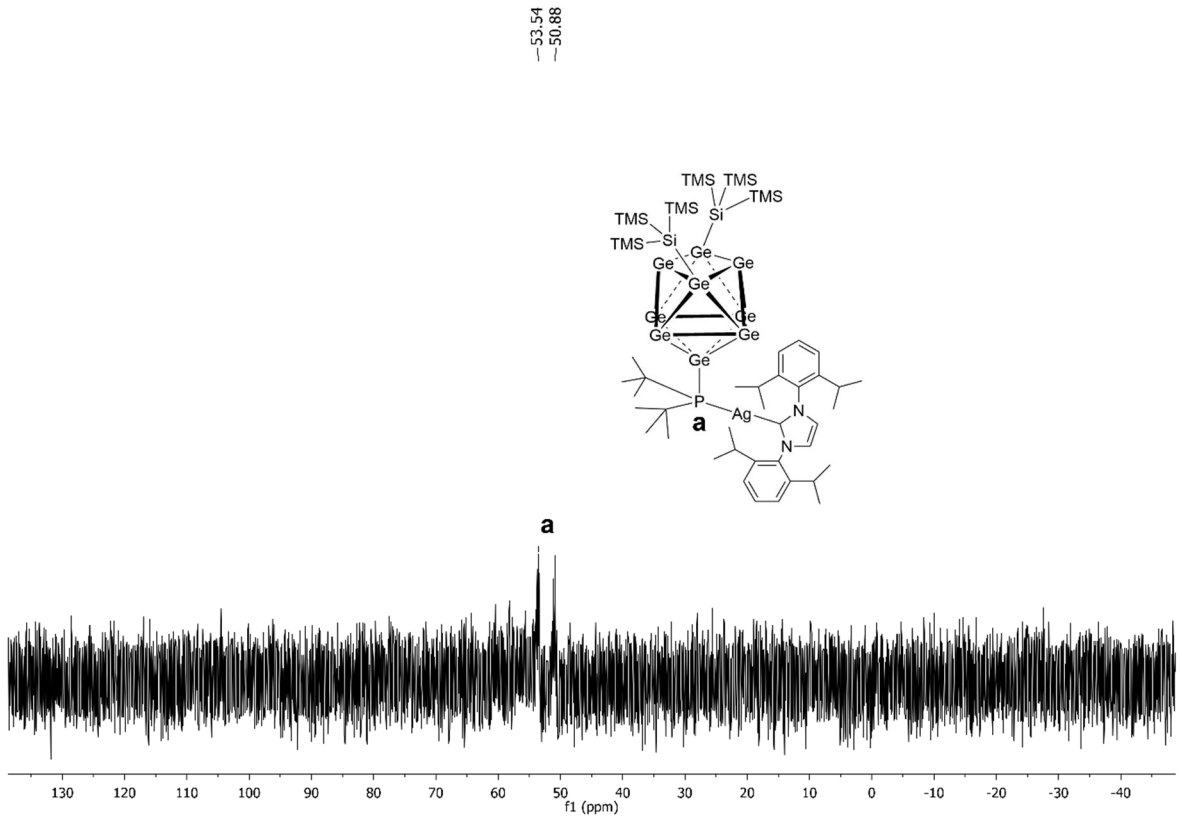

Figure SI 21: ^{31}P NMR spectrum of compound **5** in thf-d_8.

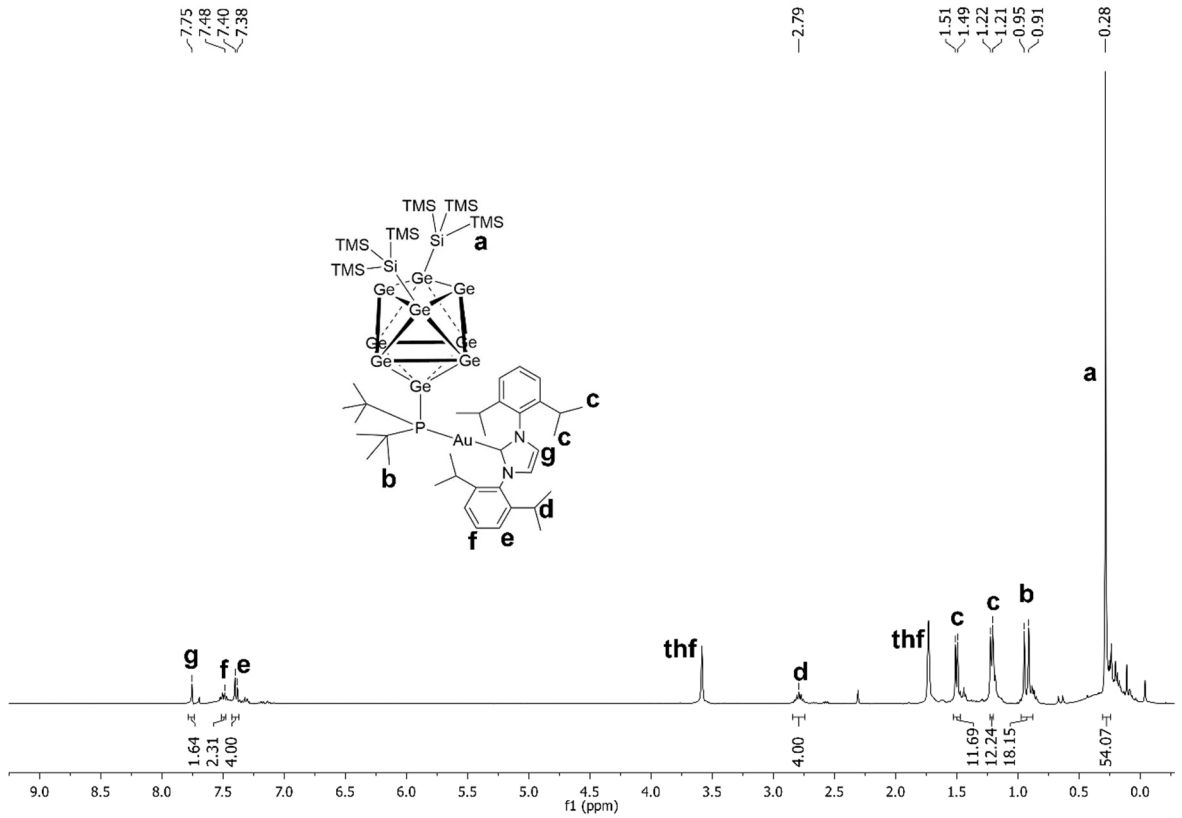

Figure SI 22: ^{1}H NMR spectrum of compound **6** in thf-d_8.

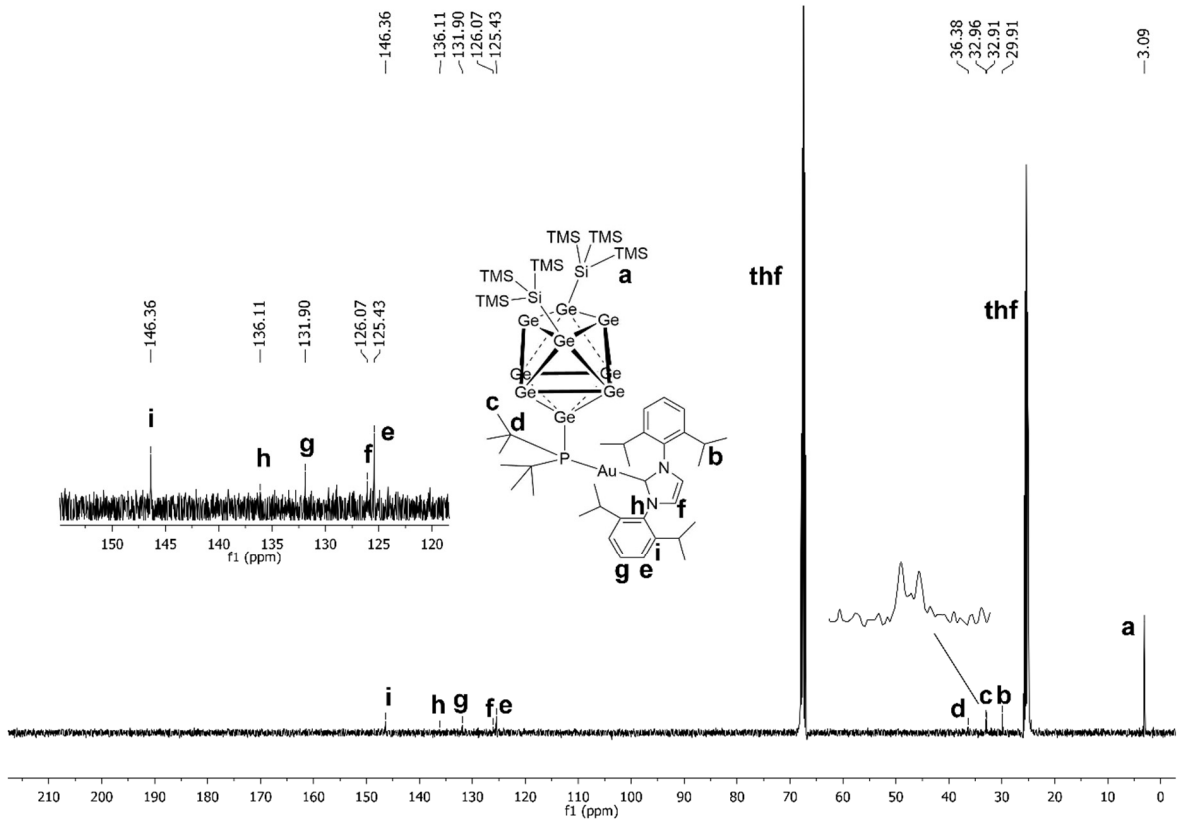

Figure SI 23: ^{13}C NMR spectrum of compound **6** in thf-d_8.

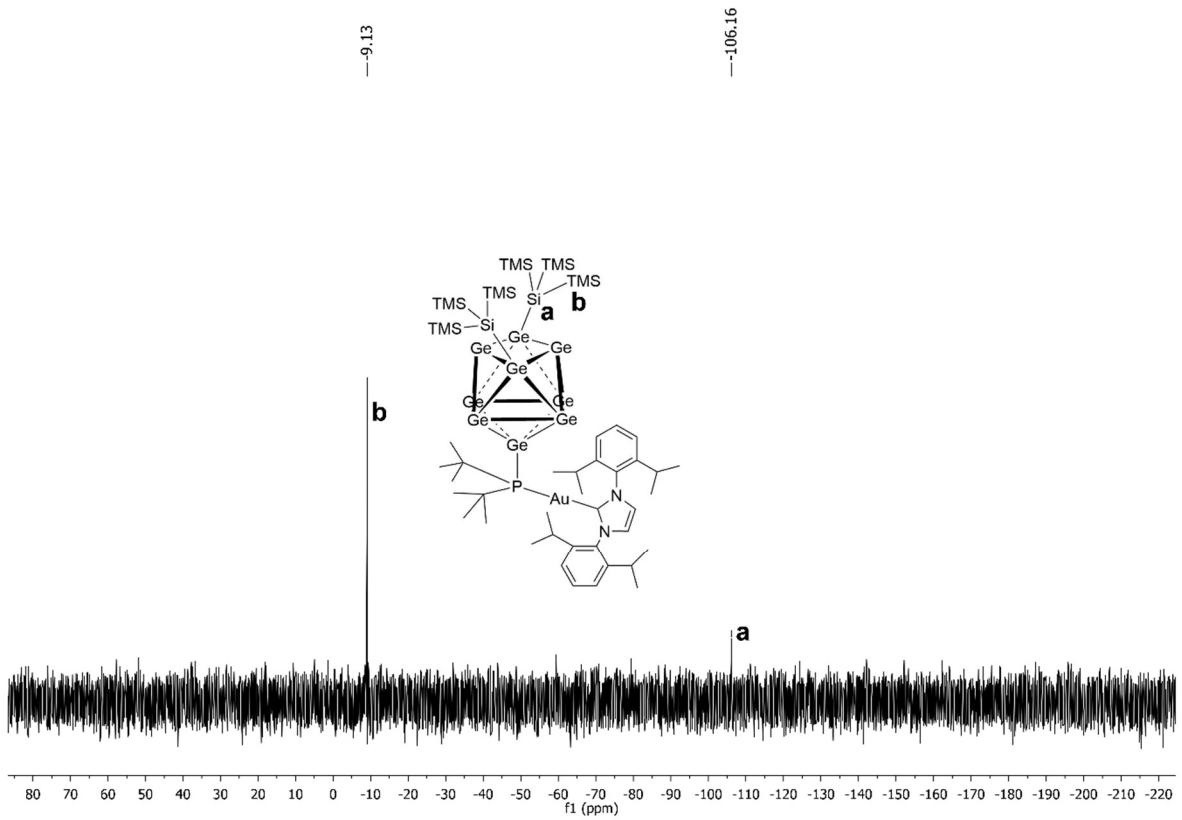

Figure SI 24: ^{29}Si NMR spectrum of compound **6** in thf-d_8.

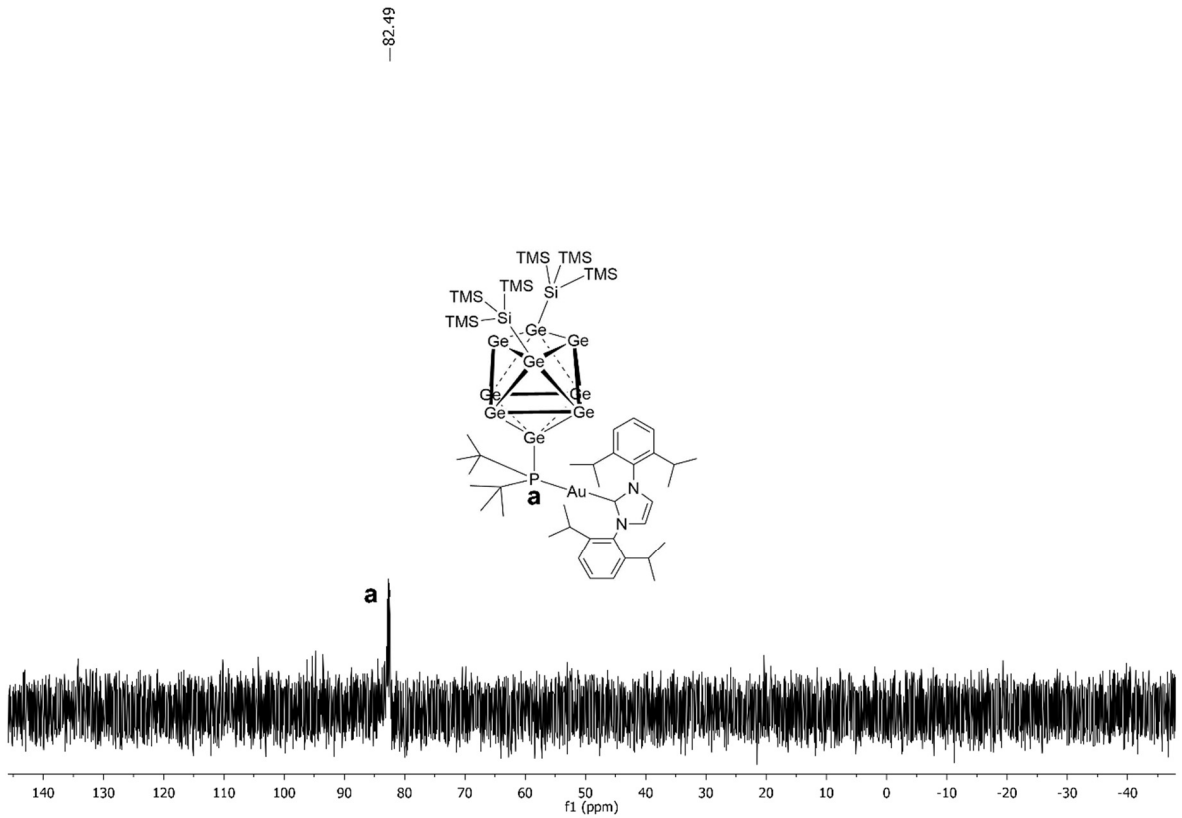

Figure SI 25: ^{31}P NMR spectrum of compound **6** in thf-d_8.

ESI-MS spectra

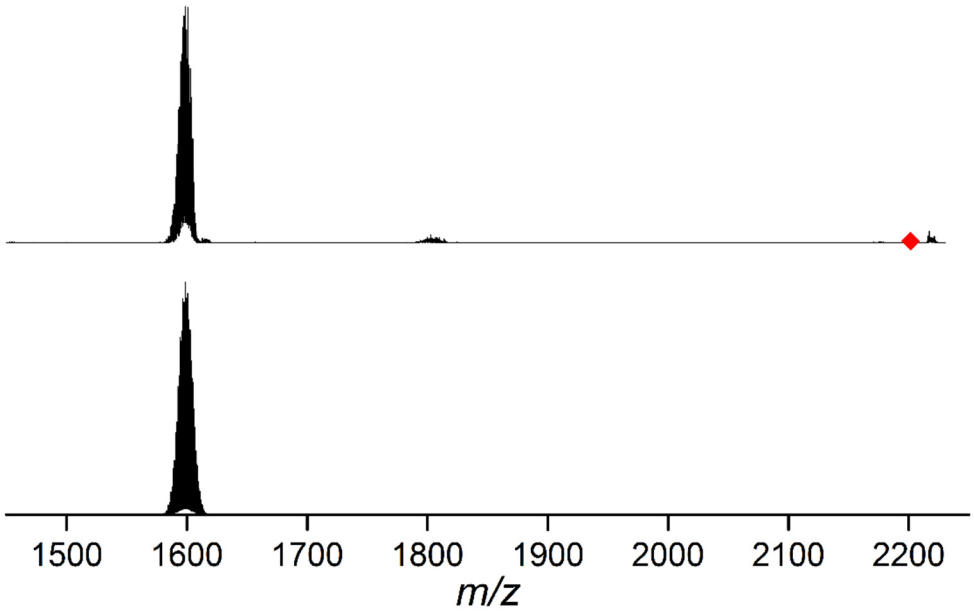

Figure SI 26: MS-MS fragmentation of signal at *m/z* 2199.3 {[(NHC^{Dipp}Cu)[(Ge$_9${Si(TMS)$_3$}$_2$)^{t}Bu$_2$P]Cu(NHC^{Dipp})]$^+$} (red square), yielding signal at *m/z* 1598.7 {[(NHC^{Dipp}Cu)Ge$_9${Si(TMS)$_3$}$_2$]$^+$}, resulting from cleavage of NHC^{Dipp}CuP^{t}Bu$_2$-moiety. Measured spectrum (top) was acquired in positive ion mode (4000 V, 300 °C), calculated spectrum is pictured below.

References

(1) Hirshfeld, F. L. *Theor. Chim. Acta* **1977**, *44*, 129.

(2) Reed, A. E.; Weinstock, R. B.; Weinhold, F. *J. Chem. Phys.* **1985**, *83*, 735.

(3) Lazreg, F.; Slawin, A. M. Z.; Cazin, C. S. J. *Organometallics* **2012**, 31, 7969.

(4) Momma, K.; Izumi, F. *J. Appl. Crystallogr.* **2008**, 41, 653.

5.9 On the Variable Reactivity of Phosphine-Functionalized [Ge_9] Clusters: *Zintl* Cluster-Substituted Phosphines or Phosphine-Substituted *Zintl* Clusters

F. S. Geitner, C. Wallach, T. F. Fässler*

published in

Chem. Eur. J. **2018**, *24*, 4103.

Content and Contributions

The scope of this work was to test the reactivity of the mixed-functionalized [Ge_9] cluster anion [Ge_9{$Si(TMS)_3$}$_2^{t}Bu_2$P]$^-$ towards further Cu^+ organometallics (NHC^{Mes}CuCl and Cy_3PCuCl) and to synthesize further mixed-functionalized [Ge_9] cluster anions [Ge_9{$Si(TMS)_3$}$_2$$R_2$P]$^-$ (*R*: Mes, N^{i}Pr$_2$) with sterically more demanding phosphanyl substituents. Reactions of [Ge_9{$Si(TMS)_3$}$_2^{t}Bu_2$P]$^-$ with NHC^{Mes}CuCl resulted in the zwitterionic species [(Ge_9{$Si(TMS)_3$}$_2$)^tBu_2P]CuNHC^{Mes} in analogy to the respective reactions with NHC^{Dipp}CuCl. By contrast, reactions of this mixed-functionalized anion with Cy_3PCuCl resulted in the formation of the neutral twofold-bridged dimeric species [{$Si(TMS)_3$}$_2$$Ge_9${(^{t}Bu)$_2$PCu}$_2$$Ge_9${$Si(TMS)_3$}$_2$] under cleavage of the complete original ligands sphere of Cu^+. The experiments resulting in the formation of the latter species were carried out by B. Sc. Christoph Wallach. The novel compounds were both characterized by means of NMR, single crystal X-ray diffraction and elemental analysis. The synthesis of sterically more demanding mixed-functionalized anions [Ge_9{$Si(TMS)_3$}$_2$$R_2$P]$^-$ (*R*: Mes, N^{i}Pr$_2$) was achieved by reaction of the bis-silylated [Ge_9] cluster [Ge_9{$Si(TMS)_3$}$_2$]$^{2-}$ with the respective chlorophosphines in thf or MeCN. The cluster anions were characterized by means of NMR and ESI-MS. Subsequent reactions with NHC^{Dipp}CuCl resulted in the attachment of a [NHC^{Dipp}Cu]$^+$ fragment to a triangular Ge face of the [Ge_9] core of both anions, yielding [NHC^{Dipp}Cu(η^3-Ge_9{$Si(TMS)_3$}$_2$PR_2)] (*R*: Mes, N^{i}Pr$_2$). The neutral compounds were again characterized by NMR, single crystal X-ray diffraction (*R*: Mes) and elemental analysis (*R*: Mes). The isolation of these species reveals that the reactivity of mixed-functionalized [Ge_9] clusters towards Lewis acids strongly depends on the bulkiness of the introduced [PR_2]$^+$ group. This publication was written in course of this thesis.

ChemPubSoc Europe

DOI: 10.1002/chem.201705678

CHEMISTRY A European Journal Full Paper

Phosphine Substituents

On the Variable Reactivity of Phosphine-Functionalized [Ge_9] Clusters: *Zintl* Cluster-Substituted Phosphines or Phosphine-Substituted *Zintl* Clusters

Felix S. Geitner,[b] Christoph Wallach,[a] and Thomas F. Fässler*[a]

Dedicated to Professor Hartmut Bärnighausen on the occasion of his 85th birthday

Abstract: The reaction of $[(Ge_9\{Si(TMS)_3\}_2P\mathit{t}Bu_2)]^-$ with $NHC^{Mes}CuCl$ yields $[(Ge_9\{Si(TMS)_3\}_2)(\mathit{t}Bu_2P)]Cu(NHC^{Mes})$ (**1**), which is a new derivative of the recently reported monomeric zwitterionic tetrel cluster compounds $[(Ge_9\{Si(TMS)_3\}_2)(\mathit{t}Bu_2P)]M(NHC^{Dipp})$ (*M*: Cu, Ag, Au). By contrast, the reaction of the same anion $[(Ge_9\{Si(TMS)_3\}_2P\mathit{t}Bu_2)]^-$ with the more labile copper phosphine complex Cy_3PCuCl leads to the formation of $[Ge_9\{Si(TMS)_3\}_2\{(\mathit{t}Bu)_2PCu\}_2Ge_9\{Si(TMS)_3\}_2]$ (**2**), which is a neutral dimeric twofold-bridged [Ge_9] cluster compound, with the *exo*-bonded phosphine substituent being involved in the cluster bridging. In case of the presence of sterically more demanding phosphines in $[Ge_9\{Si(TMS)_3\}_2PR_2]^-$ [R: Mes (**3**) and N*i*Pr_2 (**4**)], reactions with $NHC^{Dipp}CuCl$ yielded the complexes $NHC^{Dipp}Cu[\eta^3\text{-}Ge_9\{Si(TMS)_3\}_2(PR_2)]$ [R: Mes (**5**) and N*i*Pr_2 (**6**)], comprising exclusively Cu–Ge bonds. Compounds **5** and **6** show varying reactivity in dependence of the identity of the phosphine group and represent the first examples of fourfold-substituted [Ge_9] clusters with three different ligands bound to the [Ge_9] cluster core. All compounds were characterized by ^1H, ^{13}C, ^{31}P, and ^{29}Si NMR spectroscopy. Additionally, compounds **3** and **4** were analyzed by ESI-MS, and the structures of compounds **1**, **2**, and **5** were characterized by single-crystal X-ray diffraction.

Introduction

Polyatomic *Zintl* clusters, which can be extracted from the respective *Zintl* phases of the compositions A_4E_9 or $A_{12}E_{17}$ (A: alkali metal, E: tetrel element), can be applied as ligands in organometallic chemistry. These cluster species are especially interesting not only because of their easy accessibility in a one-step solid state reaction, followed by the extraction of the cluster unit in an appropriate solvent, but also because of their electronic properties.[1] The first addition of a *Zintl* cluster moiety to a transition-metal fragment was observed by the group of Eichhorn, yielding $[Sn_9Cr(CO_3)]^{4-}$.[2] Subsequently, a large number of papers with bare *Zintl* clusters serving as ligands for transition metals has been published.[1] However, in most cases the resulting compounds are carrying high negative charges, they are tremendously air- and moisture-sensitive, highly reactive and poorly soluble in standard organic solvents. Furthermore, they were obtained in low yields, which hampered detailed studies and potential applications. A breakthrough was achieved with the introduction of covalently bonded *exo*-ligands to the bare tetrel clusters, which decreases the charge of the cluster species and thus increases their solubility in less polar solvents such as MeCN, THF, or toluene, now allowing for a plethora of follow-up reactions. Examples for such substituted units are the bis-vinylated [Ge_9] cluster $[Ge_9(CH_2{=}CH)_2]^{2-}$[3] or the tris-silylated cluster compound $[Ge_9\{Si(TMS)_3\}_3]^-$,[4] both of which can be isolated in reasonable yields. The bis-vinylated representative has not yet been introduced as a ligand to a transition-metal complex, whereas a series of transition-metal complexes bearing $[Ge_9\{Si(TMS)_3\}_3]^-$ ligands has been obtained, including compounds of the type $[L_xM\{Ge_9R_3\}]^{n-}$ (R: $Si(TMS)_3$; *M*: Cu–Au, Cr–W, Zn)[5] or transition-metal-bridged dimeric [Ge_9] cluster species $[\{R_3Ge_9\}M\{Ge_9R_3\}]^{n-}$ (R: $Si(TMS)_3$; *M*: Cu–Au, Zn–Hg, Mn).[6] The applicability of $[Ge_9\{Si(TMS)_3\}_3]^-$ as a ligand for transition metals has led to subsequent studies, in which a series of different silyl groups were attached to the cluster units, leading to a new group of potential transition-metal ligands, with various shielding of the [Ge_9] core unit.[5b,d,7] Furthermore, a reasonable synthesis route for the bis-silylated cluster $[Ge_9\{Si(TMS)_3\}_2]^{2-}$ has been developed, which allowed for the synthesis of mixed-substituted tris-silylated cluster ligands and led to the monomeric unit $[Ge_9\{Si(TMS)_3\}_2\{Si(TMS)_2(SiPh_3)\}]^-$ and to the dimeric species $[\{Si(TMS)_3\}_2Ge_9\{SiMe_2\text{-}Ph\text{-}SiMe_2\}Ge_9\{Si(TMS)_3\}_2]^{2-}$.[8] The bis-silylated cluster species also react directly with organometallic Cu^I compounds, yielding compounds of the type

[a] C. Wallach, Prof. Dr. T. F. Fässler
Department Chemie, Technische Universität München
Lichtenbergstraße 4, 85747 Garching b. München (Germany)
E-mail: thomas.faessler@lrz.tum.de

[b] F. S. Geitner
WACKER Institute for Silicon Chemistry and Department Chemie
Technische Universität München, Lichtenbergstraße 4
85747 Garching b. München (Germany)

Supporting information and the ORCID number(s) for the author(s) of this article can be found under https://doi.org/10.1002/chem.201705678.

$[(CuP{i}Pr_3)_4\{Ge_9(SiPh_3)_2\}_2]$[5b] or $(NHC\text{-}M)_2[\eta^3\text{-}Ge_9\{Si(TMS)_3\}_2]$ (*M*: Cu, Ag, and Au; NHC: NHC^{Dipp} or NHC^{Mes}).[9]

In addition to the reports on silyl-substituted clusters and their transition-metal complexes, the synthesis of stannyl-decorated clusters $[Ge_9\{SnR_3\}_3]^-$ (R: *i*Pr, Cy) has been reported, which form large $[Ge_{18}Pd_3(SnR)_6]^{2-}$ aggregates upon reaction with $Pd(PPh_3)_4$.[10,11] However, in these silyl- and stannyl- substituted $[Ge_9]$ cluster compounds only the $[Ge_9]$ unit can interact with transition metal complexes, whereas a cluster substitution with *exo*-bonded phosphine groups $[PR_2]^+$ opens alternative reaction pathways due to the electron lone pair located at the phosphorus atom. Recently, we presented the first compounds of this type, namely the neutral clusters $[Ge_9\{Si(TMS)_3\}_3PR_2]$ (R: *i*Pr, Cy) and the anionic cluster unit $[Ge_9\{Si(TMS)_3\}_2P{t}Bu_2]^-$. The latter mixed-functionalized cluster can interact with transition metals through the electron lone pair at the phosphine moiety, leading to the zwitterionic compounds $[(Ge_9\{Si(TMS)_3\}_2){t}Bu_2P]M(NHC^{Dipp})$ (*M*: Cu, Ag, Au) as a proof of the concept stated above.[12] The basic cluster unit $[Ge_9\{Si(TMS)_3\}_2P{t}Bu_2]^-$ can also be described as a negatively charged phosphine ligand, which bears a bulky tetrel *Zintl* cluster as the third substituent, revealing attributes (steric impact and capability to form zwitterionic compounds) which might be of interest regarding catalytic applications.[13]

Here, we describe further investigations of the reactivity of $[Ge_9\{Si(TMS)_3\}_2P{t}Bu_2]^-$ towards Cu^I complexes including a variation of the NHC ligands (slightly smaller mesityl wingtips, compared to $NHC^{Dipp}CuCl$) and a substitution of the NHC group by the phosphine ligand Cy_3P (Cy = cyclohexyl). We also studied the influence of the steric demand of phosphine substituents attached to the $[Ge_9]$ core in $[Ge_9\{Si(TMS)_3\}_2PR_2]^-$ (R = Mes and N*i*Pr$_2$) on the reactivity of the resulting compounds towards $NHC^{Dipp}CuCl$.

Results and Discussion

The addition of solid $NHC^{Mes}CuCl$ to a solution of $[Ge_9\{Si(TMS)_3\}_2P{t}Bu_2]^-$ (obtained by the reaction of solid $K_2[Ge_9\{Si(TMS)_3\}_2]$ with tBu$_2$PCl in acetonitrile)[12] immediately led to the formation of a brownish precipitate. The ratio of the proton signals of the product in the ^{1}H NMR spectrum revealed the attachment of an $[NHC^{Mes}Cu]^+$ moiety to the $[Ge_9\{Si(TMS)_3\}_2P{t}Bu_2]^-$ unit. Furthermore, the significant high-field shift of the proton signal of the phosphine substituent's *tert*-butyl groups from 1.25 to 0.89 ppm indicated that this $[NHC^{Mes}Cu]^+$ group is attached to the phosphorus atom of the $[Ge_9\{Si(TMS)_3\}_2P{t}Bu_2]^-$ unit under formation of $[(Ge_9\{Si(TMS)_3\}_2){t}Bu_2P]Cu(NHC^{Mes})$ (**1**). Additionally, the signals of a second product were detected in several NMR spectra (^{1}H, ^{31}P and ^{29}Si) of the crude product. Orange plate-shaped crystals of **1** suitable for single-crystal X-ray diffraction were obtained from toluene at −32 °C in 40% yield. Analysis of the single crystal data revealed the attachment of the $[NHC^{Mes}Cu]^+$ unit to the phosphorus atom of the $[Ge_9\{Si(TMS)_3\}_2P{t}Bu_2]^-$ cluster under formation of a zwitterionic species in analogy to the previously described compounds $[(Ge_9\{Si(TMS)_3\}_2){t}Bu_2P]M(NHC^{Dipp})$ (*M*: Cu, Ag, Au) (Figure 1).

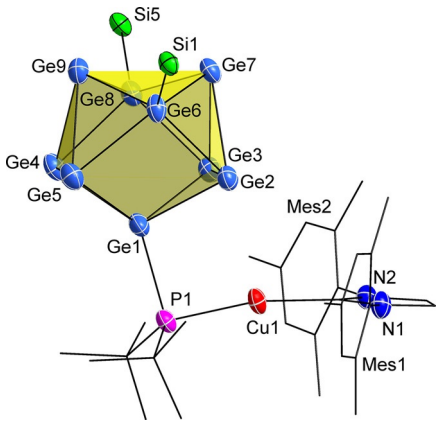

Figure 1. Molecular structure of compound **1** (cluster I) with atom labelling. Ellipsoids are shown at a 50% probability level. For clarity, the TMS groups of the hypersilyl ligands, the hydrogen atoms and the toluene molecules are omitted. All carbon atoms are pictured in the wire and stick style. Labelling of cluster II occurred analogously starting from Ge10. Selected bond lengths and angles are summarized in the Supporting Information (Table SI1).

Compound **1** crystallizes in the monoclinic space group $P2_1/c$, and the unit cell contains two crystallographically independent cluster species. The $[Ge_9]$ cores in **1** show a distorted trigonal prismatic structure with approximate C_{2v} symmetry, as indicated by one significantly shorter height of the trigonal prism (see the Supporting Information). The two silyl substituents and the phosphine ligand are attached to the three capping Ge atoms.

The Ge–Ge distances range between 2.524(1) (Ge2–Ge6) and 2.750(1) Å (Ge3–Ge7), and the Ge–Si distances vary from 2.383(2) (Ge6–Si1) to 2.386(2) Å (Ge17–Si13). The Ge–P distances of 2.316(2) (Ge1–P1) and 2.310(2) Å (Ge10–P2) are in the range of previously reported data.[12] The Cu atoms of the $[NHC^{Mes}Cu]^+$ fragments bind to the phosphorus atom of the phosphine substituent, resulting in a strongly distorted tetrahedral coordination sphere at the P atom [Ge1-P1-Cu1: 94.15(1)° and Ge10-P2-Cu2: 93.10(1)°]. The coordination of Cu^+ by the NHC^{Mes} and phosphine substituents deviates slightly from linearity, with angles of $C9_{NHC}$-Cu1-P1: 168.90(1)° and $C56_{NHC}$-Cu2-P2: 169.56(1)°, because the Cu–NHC^{Mes} bond is tilted away from the $[Ge_9]$ core. Besides compound **1**, a reddish polycrystalline material was found in several samples, when the synthesis of **1** was carried out in acetonitrile, whereas no such side product was obtained with THF as the solvent. However, in THF, excessive reactants and other impurities can hardly be removed because compound **1** does not precipitate from the reaction solution, and all attempts to obtain pure samples of **1** by recrystallization have not been successful so far in this case.

To study the influence of the ligand bound to the Cu^I precursor, we also reacted $[Ge_9\{Si(TMS)_3\}_2P{t}Bu_2]^-$ with Cy_3PCuCl (Cy: cyclohexyl) in acetonitrile and immediately obtained a brownish precipitate. The NMR spectra of the crude product revealed the formation of a novel species, which was similar to the side product we had observed in the previous reaction in acetonitrile.

The presence of large amounts of free PCy_3 detected in the ^1H and ^{31}P NMR spectra and a signal ratio of 108 (silyl group) to 36 protons (phosphine group) in the ^1H NMR spectrum of the product indicated the presence of a dimeric cluster species, $[\{Si(TMS)_3\}_2Ge_9\{(tBu)_2PCu\}_2Ge_9\{Si(TMS)_3\}_2]$ (**2**). After the removal of PCy_3 by washing of the crude product with acetonitrile the product was dissolved in toluene, filtered and stored in a freezer at −32 °C for crystallization, giving red-block shaped crystals (36 mg. 35 %), which were suitable for single-crystal X-ray diffraction.

Compound **2** crystallizes in the triclinic space group $P\bar{1}$. Two $[Ge_9\{Si(TMS)_3\}_2PtBu_2]^-$ units are bridged by two Cu^+ ions which are binding to the phosphorus atom of the phosphine group of one and to a triangular Ge_3 face of the second cluster unit (Figure 2). The $[Ge_9]$ clusters show C_{2v}-symmetry (similar to **1**), and the three *exo*-bonded main group substituents are attached to the three capping Ge atoms. The Ge–Ge distances range between 2.4930(9) (Ge1–Ge4) and 2.934(1) Å (Ge2–Ge3), and the Ge–Si bonds lie between 2.378(2) (Ge6–Si5) and 2.386(2) Å (Ge5–Si1). The Ge–P bonds with distances of 2.327(2) (Ge4–P1) and 2.328(2) Å (Ge13–P2), the mean Ge–Cu distances of 2.508(1) (**A**) and 2.504(1) Å (**B**), as well as the Cu–P bonds of 2.254(2) (Cu1–P2) and 2.245(2) Å (Cu2–P1) are very similar in both clusters and are in the range of previously reported data (Table 1).[5a,b,d,12,14]

The coordination of the two Cu^+ ions by the phosphorus atom and the center of gravity of the Ge_3 triangle is almost linear (ctp(**A**)-Cu1-P2: 176.49(2)°, ctp(**B**)-Cu2-P1: 177.59(2)°; ctp: center of gravity), and the phosphorus atoms are coordinated by their substituents in a slightly distorted tetrahedral manner, as shown by the angles Ge4-P1-Cu2 of 101.52(1)° and Ge13-P2-Cu1 of 101.42(1)° (Table 1). The distance between Cu1 and Cu2 of 4.479(1) Å does not indicate any bonding interaction.

The formation of **2** can be rationalized by a two-step reaction, with the attachment of $[Cy_3PCu]^+$ to the phosphine moiety of $[Ge_9\{Si(TMS)_3\}_2PtBu_2]^-$ in a salt metathesis reaction in the first step (analogously to the formation of compound **1**), followed by the mutual nucleophilic attack of the negatively charged $[Ge_9]$ cluster cores of two intermediate cluster species at the Cu^+ center of the other cluster under cleavage of the labile phosphine ligands and formation of the Cu-Ge η^3-bonds (Scheme 1) as the second step. Obviously, a similar subsequent reaction also occurs for compound **1** in acetonitrile under cleavage of the NHC^{Mes} ligand, yielding compound **2** as a side product, although in this case only to a small extent. Another compound with a bis-silylated $[Ge_9]$ unit and a bridging Cu^+ has been found previously in the neutral dimer $[(CuPiPr_3)_4\{Ge_9(SiPh_3)_2\}_2]$.[5b]

Table 1. Selected distances [Å] and angles [°] in compound **2**.

Parameter	Distance	Parameter	Distance
d(Ge1–Cu1)	2.476(1)	d(Ge10–Cu2)	2.504(1)
d(Ge2–Cu1)	2.518(1)	d(Ge11–Cu2)	2.510(1)
d(Ge3–Cu1)	2.5302(9)	d(Ge12–Cu2)	2.497(1)
P1–Cu2	2.245(2)	P2–Cu1	2.254(2)
Parameter	**Angle**	**Parameter**	**Angle**
ctp(**A**)-Cu1-P2[a]	177.59(1)	ctp(**B**)-Cu2-P1[a]	176.49(1)
Ge4-P1-Cu2	101.52(2)	Ge13-P2-Cu1	101.42(2)

[a] ctp: center of gravity of the triangular Ge_3 plane coordinating to Cu^I. ctp(**A**): Ge1-Ge3; ctp(**B**): Ge10-Ge12.

To further investigate the influence of the steric impact of the $[PR_2]^+$ group on the formation of phosphine-functionalized $[Ge_9]$ clusters, we reacted $K_2[Ge_9\{Si(TMS)_3\}_2]$ with the sterically more demanding chlorophosphines Mes_2PCl (Mes: mesityl) and $(iPr_2N)_2PCl$ in acetonitrile. The NMR spectra of the corresponding crude products revealed the formation of the desired mixed-functionalized cluster anions $[Ge_9\{Si(TMS)_3\}_2PMes_2]^-$ (**3**) and $[Ge_9\{Si(TMS)_3\}_2P(NiPr_2)_2]^-$ (**4**), respectively. The anions were also detected in the ESI-MS experiments of acetonitrile solutions at *m/z* 1418.8 (**3**) or *m/z* 1380.8 (**4**), respectively (Figure 3).

No single crystals of the products have been obtained so far, but the identification of the anions by NMR and ESI-MS experiments was unambiguous, so that further studies regarding the reactivity of these anionic species towards $NHC^{Dipp}CuCl$ were carried out. The addition of acetonitrile solutions of the crude

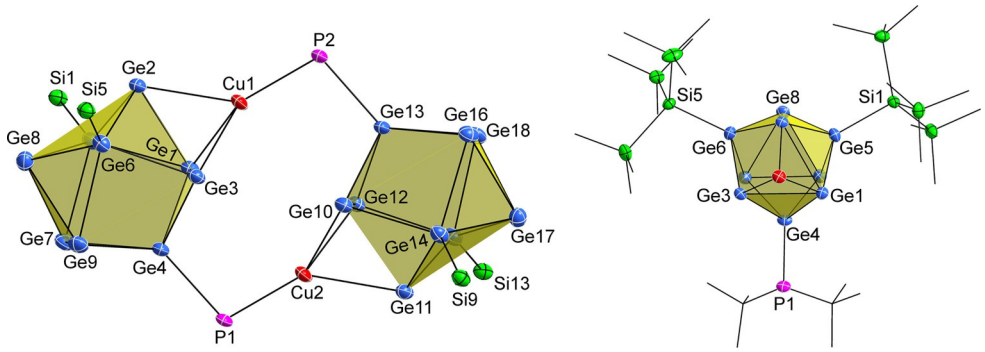

Figure 2. Left: Molecular structure of compound **2** with atom labelling. Ellipsoids are shown at a 50 % probability level. For clarity, all TMS groups of the hypersilyl ligands, the *tert*-butyl groups of the phosphine ligands, the hydrogen atoms, and the toluene molecules are omitted. Right: Detail view of Cluster **A** showing the C_{2v}-symmetric shape and the coordination sphere of the $[Ge_9]$ core. For clarity, all carbon atoms are pictured in the wire and stick style. Selected bond lengths and angles are summarized in Table 1 and in the Supporting information (Table SI 2).

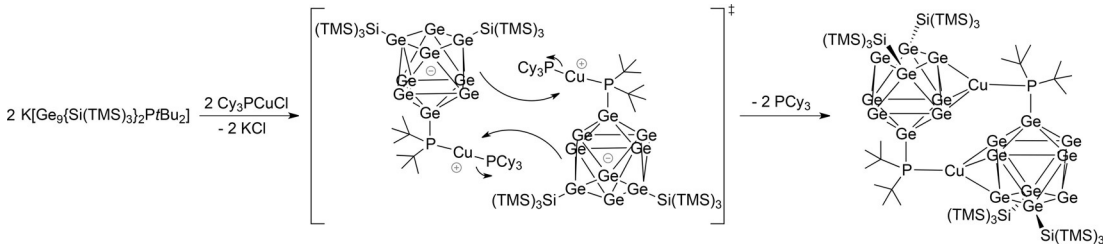

Scheme 1. Formation of compound **2** through a two-step reaction of $[Ge_9\{Si(TMS)_3\}_2PtBu_2]^-$ with Cy_3PCl.

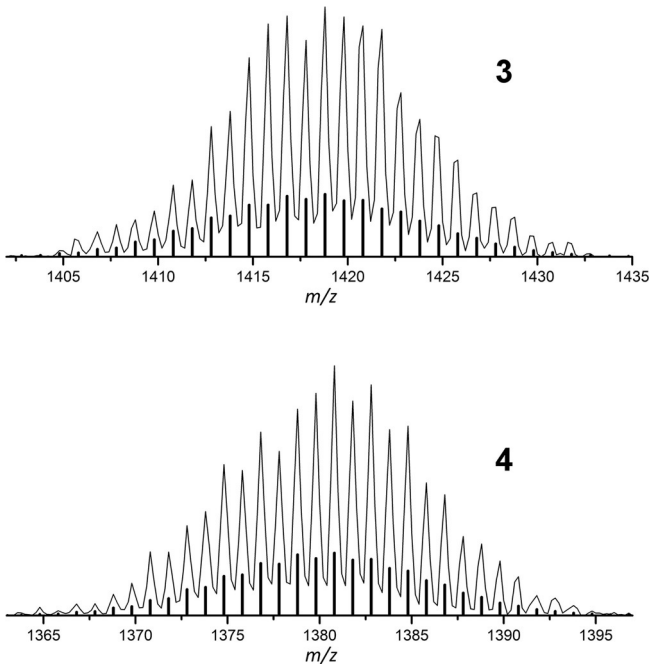

Figure 3. ESI-MS spectra of the anions **3** and **4**. The mixed-functionalized anions were detected from acetonitrile solutions in negative ion mode (4500 V, 300 °C) at *m/z* 1418.8 (**3**) and *m/z* 1380.8 (**4**), respectively.

products to solutions of $NHC^{Dipp}CuCl$ in acetonitrile immediately led to the formation of bright brownish precipitates. The ^1H NMR spectra of the products revealed an attachment of the $[NHC^{Dipp}Cu]^+$ moiety to both cluster anions (**3** and **4**). In both cases the signals assigned to the protons of the silyl substituents at the $[Ge_9]$ cluster showed a significant downfield shift after the reaction with $NHC^{Dipp}CuCl$ (**3**: 0.25→0.16 ppm and **4**: 0.24→0.18 ppm). This is in contrast to the observations made for **1** and $[(Ge_9\{Si(TMS)_3\}_2)(tBu_2P)]M(NHC^{Dipp})$,[12] in which no significant shift of these signals occurred upon the attachment of $[NHC\text{-}M]^+$ (*M*: Cu, Ag, Au) to the phosphine moiety bound to the cluster. However, similar downfield shifts of such protons had previously been observed upon the coordination of $[NHC^{Dipp}M]^+$ (*M*: Cu, Ag, Au) to a triangular Ge_3 face of the trissilylated $[Ge_9]$ cluster $[Ge_9\{Si(TMS)_3\}_3]^-$ under formation of $NHC^{Dipp}M[\eta^3\text{-}Ge_9\{Si(TMS)_3\}_3]$.[5a]

Hence, the NMR experiments indicated the formation of the non-zwitterionic *Zintl* cluster Cu–NHC complexes $NHC^{Dipp}Cu[\eta^3\text{-}Ge_9\{Si(TMS)_3\}_2(PMes_2)]$ (**5**) and $NHC^{Dipp}Cu[\eta^3\text{-}Ge_9\{Si(TMS)_3\}_2\{P(NiPr_2)_2\}]$ (**6**), comprising direct interactions between the $[NHC^{Dipp}Cu]^+$ moieties and the $[Ge_9]$ cluster cores. Recrystallization of the crude products from toluene and cooling to −40 °C led to the formation of red block-shaped crystals of compound **5** (44 mg, 30%) suitable for single-crystals X-ray diffraction analysis, and the diffraction data manifested the assumed nature of **5** (Figure 4). Unfortunately, in case of **6** recrystallization and single crystal growth were not successful so far, but the corresponding NMR data of **6** strongly suggest a similar structure as observed for compound **5**.

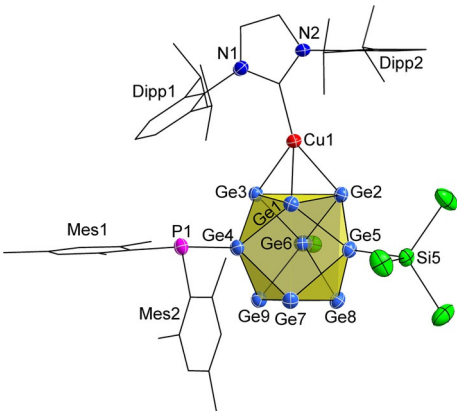

Figure 4. Molecular structure of compound **5** (cluster I) with atom labelling. Ellipsoids are shown at a 50% probability level. For clarity methyl groups of one hypersilyl ligand and TMS groups of the other hypersilyl substituent (background), hydrogen atoms and toluene molecules are omitted, and all carbon atoms are pictured in the wire and stick style. Labelling of cluster II occurred analogously starting from Ge10. Selected bond lengths and angles are summarized in the Supporting Information (Table SI 3).

Compound **5** crystallizes in the triclinic space group $P\bar{1}$, and the unit cell contains two crystallographically different cluster species. The $[Ge_9]$ cluster cores show C_{2v} symmetry, indicated by the different heights of the trigonal prismatic cluster bases (one edge is shorter than the other two; see the Supporting Information). The Ge–Ge distances lie between 2.483(1) (Ge3–Ge4) and 2.885(1) Å (Ge10–Ge11), and the Ge–Si distances range from 2.375(2) (Ge5–Si5) to 2.386(2) Å (Ge15–Si9). The Ge–P distances of 2.330(2) (Ge4–P1) and 2.335(2) Å (Ge13–P2), as well as the mean Cu–Ge distances of 2.513(1) (cluster I-Cu1) or 2.507(1) Å (cluster II-Cu2) are similar to the respective bonds in **1** (Ge–P) and **2** (Ge–P and Ge–Cu). The coordination of Cu^+ by the *Zintl* cluster and the NHC^{Dipp} ligand deviates significantly from linearity (ctp1-Cu1-$C1_{NHC}$: 167.96(4)°, ctp2-Cu2-$C64_{NHC}$:

169.22(4)°; ctp: center of gravity of coordinating Ge triangle). This can be rationalized by the orientation of the mesityl substituents of the $[PMes_2]^+$ group, which are pointing away from the $[Ge_9]$ side with the attached $[NHC^{Dipp}Cu]^+$moiety. Hence, the Cu–NHC bond is tilted in the direction of the phosphine moiety of the cluster, thereby minimizing steric interactions of the NHC ligand with the two silyl ligands of the $[Ge_9]$ core.

In addition to revealing varying reactivity of phosphine-functionalized $[Ge_9]$ cluster anions towards $NHC^{Dipp}CuCl$ in dependence of the bulkiness of the substituents of the phosphine moiety (Scheme 2), compound **5** is the first example of a fourfold-substituted germanide cluster bearing three different substituents (silyl groups, a phosphine ligand and a $[NHC^{Dipp}Cu]^+$ moiety) at the $[Ge_9]$ cluster core. However, it has to be mentioned that the related compound $[(TMS)_3SiEtGe_9Pd(PPh_3)]$ with its Ge_9Pd core, which was described as a penta-substituted cluster, also contains three different ligand groups attached to a Ge_9Pd unit.[15]

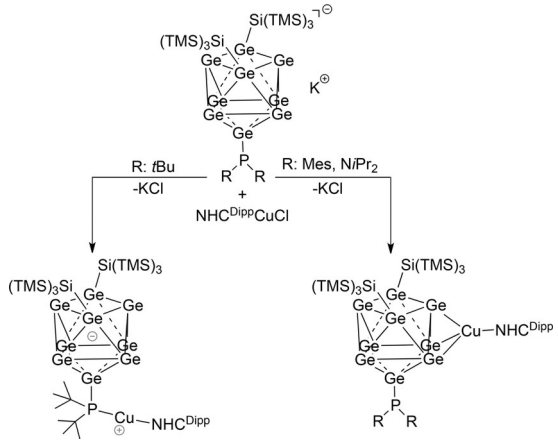

Scheme 2. Different reactivity of mixed-functionalized $[Ge_9\{Si(TMS)_3\}_2PR_2]^-$ (R: *t*Bu, Mes, N*i*Pr$_2$) clusters towards $NHC^{Dipp}CuCl$.

Conclusions

We have shown that the reaction of $[Ge_9\{Si(TMS)_3\}_2PtBu_2]^-$ with $NHC^{Mes}CuCl$ yields the zwitterionic compound $[(Ge_9\{Si(TMS)_3\}_2)tBu_2P]CuNHC^{Mes}$ (**1**), in analogy to our previous results obtained for the reactions of the cluster anion with $NHC^{Dipp}MCl$ (*M*: Cu, Ag, Au). By contrast, the reaction of $[Ge_9\{Si(TMS)_3\}_2PtBu_2]^-$ with Cy_3PCuCl, bearing a more labile phosphine moiety, led to the formation of the Cu^+-bridged dimeric $[Ge_9]$ species $[Ge_9\{Si(TMS)_3\}_2\{(tBu)_2PCu\}_2Ge_9\{Si(TMS)_3\}_2]$ (**2**), in which the *exo*-bonded $[PtBu_2]^+$ group is involved in the cluster bridging. The formation of **2** can be rationalized by a two-step reaction with the formation of a zwitterionic intermediate in the first, and the mutual nucleophilic attack of the $[Ge_9]$ cores of two of such molecules at Cu^+ under cleavage of PCy_3 in the second step.

The introduction of sterically more demanding phosphine substituents to the twofold silylated clusters was achieved in $[Ge_9\{Si(TMS)_3\}_2PR_2]^-$ [R: Mes (**3**), N*i*Pr$_2$ (**4**)]. Subsequent reactions of these units with $NHC^{Dipp}CuCl$ yielded *Zintl* cluster Cu-NHC compounds of the type $NHC^{Dipp}Cu[\eta^3\text{-}Ge_9\{Si(TMS)_3\}_2(PR_2)]$ with R: Mes (**5**) or N*i*Pr$_2$ (**6**), comprising exclusively Cu–Ge interactions. Hence, anions of the type $[Ge_9\{Si(TMS)_3\}_2PR_2]^-$ can act either as *Zintl* cluster-substituted anionic phosphine ligands (**1**), or as phosphine-substituted *Zintl* clusters (**5**, **6**), depending on the bulkiness of the phosphine moiety. In this context, compound **2** comprising both, Cu–P and Cu–Ge interactions, can be regarded as an intermediate species.

Experimental Section

General: All manipulations were performed under oxygen-free, dry conditions under argon atmosphere using standard Schlenk or glove box techniques. Glassware was dried prior to use by heating it in vacuo. The solvents used were obtained from an MBraun Grubbs apparatus. All other commercially available chemicals were used without further purification. K_4Ge_9 was prepared by fusion of stoichiometric amounts of the elements in stainless-steel tubes at 650 °C. The applied imidazolium salts (NHC^{Dipp}·HCl, NHC^{Mes}·HCl), the corresponding Cu–NHC complexes, as well as Cy_3PCuCl and $K_2[Ge_9R_2]$ (R: $Si(TMS)_3$) were synthesized according to modified literature procedures.[4a, 8a, 16]

Single crystal structure determination: The air- and moisture-sensitive crystals of **1**, **2** and **5** were transferred from the mother liquor into cooled perfluoroalkyl ether oil under a cold stream of N_2 gas. For diffraction data collection, the single crystals were fixed on a glass capillary and positioned in a 123 K (**1**, **2**) or 150 K (**5**) cold N_2 gas stream using the crystal cap system. Data collection was performed with a STOE StadiVari ($Mo_{K\alpha}$ radiation) diffractometer equipped with a DECTRIS PILATUS 300 K detector. Structures were solved by Direct Methods (SHELXS-2014) and refined by full-matrix least-squares calculations against F^2 (SHELXL-2014).[17] The positions of the hydrogen atoms were calculated and refined using a riding model. Unless stated otherwise, all non-hydrogen atoms were treated with anisotropic displacement parameters. CCDC 1586546, 1586547 and 1586548 contain the supplementary crystallographic data for this paper. These data are provided free of charge by The Cambridge Crystallographic Data Centre. The crystallographic data for compounds **1**, **2** and **5** are summarized in Table 2. In compound **1** a hypersilyl substituent is disordered and was refined on split positions. In compound **5**, a TMS group of a hypersilyl substituent is disordered and was refined on split positions. In compounds **1**, **2** and **5**, several solvent toluene molecules were disordered, and their electron densities were taken care of by the PLATON squeeze function.[18]

NMR spectroscopy: NMR spectra were measured on a Bruker Avance Ultrashield 400 MHz spectrometer. The ^{1}H spectra were calibrated using the residual proton signal of the used deuterated solvents.[19] Chemical shifts are reported in parts per million (ppm) relative to TMS, with the solvent peaks serving as internal reference. Abbreviations for signal multiplicities are: singlet (s), doublet (d), triplet (t), heptet (h). ^{29}Si NMR spectra were acquired with the ^{29}Si-INEPT-RD method (RD: refocused with decoupling). In the ^{13}C NMR spectra of compounds **1**, **5** and **6** the carbene carbon signal could not be detected.

Electron spray ionization mass spectrometry (ESI-MS): ESI-MS analyses were performed on a Bruker Daltronic HCT mass spectrometer (dry gas temperature: 300 °C; injection speed: 240 $\mu L\,s^{-1}$), and the data evaluation was carried out using the Bruker Compass Data Analysis 4.0 SP 5 program (Bruker). Spectra were plotted using OriginPro2016G (Origin Lab) and Excel 2016 (Microsoft).

Table 2. Crystallographic data for compounds **1**, **2** and **5**.

Compound	**1**	**2**	**5**
Formula	$(Ge_9Si_8P_1Cu_1N_2C_{47}H_{96})_2$	$Ge_{18}Si_{16}P_2Cu_2C_{52}H_{144}$	$(Ge_9Si_8P_1Cu_1N_2C_{63}H_{112})_2$
FW [g mol^{-1}]	1661.79	2714.74	1870.08
Space group	$P2_1/c$	$P\bar{1}$	$P\bar{1}$
a [Å]	30.083(6)	15.417(3)	16.112(3)
b [Å]	19.546(4)	18.141(4)	26.077(5)
c [Å]	31.908(6)	24.232(5)	26.712(5)
α [°]	90	99.44(3)	108.30(3)
β [°]	113.65(3)	95.19(3)	95.46(3)
γ [°]	90	94.41(3)	90.88(3)
V [Å^3]	17186(7)	6629(8)	10594(2)
Z	8	2	4
T [K]	123(2)	123(2)	150(2)
λ [Å]	Mo $K\alpha$	Mo $K\alpha$	Mo $K\alpha$
ρ_{calcd} [g cm^{-3}]	1.285	1.360	1.172
μ [mm^{-1}]	3.497	4.516	2.843
collected rflns	349117	123422	205655
independent rflns	33767	24666	41628
R_{int}/ R_δ	0.0772/0.0317	0.0546/0.0369	0.0998/0.0617
parameters/restraints	1356/21	860/6	1607/12
R_1 [$I > 2\sigma(I)$/ all data]	0.0530/0.0743	0.0413/0.0607	0.0549/0.0873
wR_2 [$I > 2\sigma(I)$/ all data]	0.1204/0.1311	0.0989/0.1099	0.1299/0.1476
GoF	1.113	1.017	1.014
max./min. diff. el. density [e Å^{-3}]	1.02/−0.91	0.80/−0.86	1.18/−1.33
CCDC	1586546	1586547	1586548

Elemental analyses (EA): Elemental analyses were carried out in the micro-analytical laboratory of the Chemistry Department of Technische Universität München. Analyses of C, H, N were performed in a combustion analyzer (elementar vario EL, Bruker).

Syntheses

[(Ge$_9${Si(TMS)$_3$}$_2$)*t*Bu$_2$P]Cu(NHC^{Mes}) (1): $K_2[Ge_9\{Si(TMS)_3\}_2]$ (92 mg, 0.075 mmol, 1 equiv) was treated with a solution of tBu$_2$PCl (13.5 mg, 0.075 mmol, 1 equiv) in thf (2.5 mL), leading to a deep red reaction mixture. After stirring for 20 min at r.t., solid NHC^{Mes}CuCl (30.3 mg, 0.075 mmol, 1 equiv) was added, and the reaction mixture was stirred at room temperature for 1 h. Subsequently, the solvent was removed in vacuo, leaving the crude product as a dark brownish solid. The solid was dissolved in toluene (2 mL) and filtered to remove formed KCl. Thereafter, the solution was concentrated to approximately half of its original volume and stored in a freezer at −32 °C.

Unfortunately, recrystallization has not been successful yet. Alternatively, the reaction can be carried out in acetonitrile. In this case, recrystallization from toluene at −32 °C gave orange plate-shaped crystals (50 mg, 40% yield), but the obtained crystalline sample was contaminated by compound **2**, which occurs as a side product. ^{1}H NMR (400 MHz, 298 K, [D$_8$]THF): $\delta = 7.48$ (s, 2H, CH$_{Im}$), 7.04 (s, 4H, CH$_{Ph}$), 2.34 (s, 6H, Me$_{(p)}$), 2.27 (s, 12H, Me$_{(o)}$), 0.89 (d, $^3J_{HP} = 13.9$ Hz, 18H, Me$_{tBu}$), 0.28 ppm (s, 54H, Me$_{TMS}$); ^{13}C NMR (101 MHz, 298 K, [D$_8$]THF): $\delta = 140.07$ (s, $C_{Ph(Me)}$), 136.78 (s, C$_{Ph}$N), 135.86 (s, CH$_{Ph(Me)}$), 130.60 (s, CH$_{Ph}$), 123.88 (s, CH$_{Im}$), 34.21 (s, Me$_{tBu}$), 32.85 (d, $^1J_{CP} = 7.0$ Hz, C$_{tBu}$), 21.53 (s, Me$_{Ph(p)}$), 19.08 (s, Me$_{Ph(o)}$), 3.10 ppm (s, Me$_{TMS}$); ^{29}Si-INEPT NMR (79 MHz, 298 K, [D$_8$]THF): $\delta = -9.08$ (s, Si$_{TMS}$), −105.39 ppm (s, Si$_{Ge9}$); ^{31}P NMR (162 MHz, 298 K, [D$_8$]THF): $\delta =$ 44.54 ppm (m, P$_{Ge9}$).

[{Si(TMS)$_3$}$_2$Ge$_9${(*t*Bu)$_2$PCu}$_2$Ge$_9${Si(TMS)$_3$}$_2$] (2): $K_2[Ge_9\{Si(TMS)_3\}_2]$ (92 mg, 0.075 mmol, 1 equiv) was treated with a solution of tBu$_2$PCl (13.5 mg, 0.075 mmol, 1 equiv) in MeCN (2.5 mL) leading to a deep red reaction mixture. After stirring for 20 min at r.t., solid Cy$_3$PCuCl (28.5 mg, 0.075 mmol, 1 equiv) was added, instantly giving a brownish precipitate. The mixture was stirred for 20 min at r.t to assure complete conversion of the reactants. Subsequently, the bright orange supernatant solution was filtered off, and the solid was washed with MeCN (10 mL). The solid was dissolved in toluene (3 mL) and filtered to remove formed KCl. Thereafter, the solution was concentrated to approximately half of its original volume and stored in a freezer at −32 °C, yielding red-block shaped crystals (36 mg, 35% yield). ^{1}H NMR (400 MHz, 298 K, C$_6$D$_6$): $\delta = 1.55$ (d, $^3J_{HP} = 14.6$ Hz, 36H, Me$_{tBu}$), 0.46 ppm (s, 54H, Me$_{TMS}$); ^{1}H NMR ([D$_8$]THF): $\delta = 1.55$ (d, $^3J_{HP} = 14.6$ Hz, 36H, Me$_{tBu}$), 0.33 ppm (s, 54H, Me$_{TMS}$); ^{13}C NMR (101 MHz, 298 K, C$_6$D$_6$): δ [ppm] = 35.86 (s, C$_{tBu}$), 33.48 (d, $^2J_{CP} = 6.0$ Hz, Me$_{tBu}$), 2.90 ppm (s, Me$_{TMS}$); ^{29}Si-INEPT NMR (79 MHz, 298 K, C$_6$D$_6$): $\delta = -8.78$ (s, Si$_{TMS}$), −102.39 ppm (s, Si$_{Ge9}$); ^{31}P NMR (162 MHz, 298 K, C$_6$D$_6$): $\delta = 58.65$ ppm (m, P$_{Ge9}$; EA: anal. calcd for $Ge_{18}Si_{16}P_2Cu_2C_{52}H_{144}$: C, 23.0; H, 5.4; found: C, 22.8; H, 5.4.

K[Ge$_9${Si(TMS)$_3$}$_2$PMes$_2$] (3): A solid mixture of of $K_2[Ge_9\{Si(TMS)_3\}_2]$ (92 mg, 0.075 mmol, 1 equiv) and Mes$_2$PCl (22.9 mg, 0.075 mmol, 1 equiv) was treated with acetonitrile (2 mL) yielding a deep red suspension, which was stirred at r.t. for 30 min. Subsequently, the mixture was filtered to remove solid residues and formed KCl. Removal of the solvent yielded the crude product as a dark brownish solid (53 mg, 50%). Unfortunately, purification by recrystallization from several solvents has not been successful so far. ^{1}H NMR (400 MHz, 298 K, [D$_8$]THF): $\delta = 6.80$ (s, 4H, CH$_{Mes}$), 2.23 (s, 12H, Me$_{iPr}$), 2.20 (s, 6H, Me$_{Mes(p)}$), 0.25 ppm (s, 54H, Me$_{TMS}$); ^{13}C NMR (101 MHz, 298 K, [D$_8$]THF): $\delta = 142.80$ (d, $^1J_{CP} = 12.1$ Hz, C$_{Ph}$P), 138.50 (s, $C_{Ph(Me)}$), 135.58 (s, $C_{Ph(Me)}$), 129.82 (s, CH$_{Ph}$), 22.91 (d, $^3J_{CP} = 10.1$ Hz, Me$_{Mes(o)}$), 21.04 (s, Me$_{Mes(p)}$), 3.17 ppm (s, Me$_{TMS}$); ^{29}Si-INEPT NMR (79 MHz, 298 K, [D$_8$]THF): $\delta = -9.36$ (s, Si$_{TMS}$), −108.00 ppm (s, Si$_{Ge9}$); ^{31}P NMR (162 MHz, 298 K, [D$_8$]THF): $\delta = -46.26$ ppm (m, P$_{Ge9}$); ESI-MS (negative mode, 4500 V, 300 °C): *m/z* 1418.8 $[Ge_9\{Si(TMS)_3\}_2PMes_2]^-$.

K[Ge$_9${Si(TMS)$_3$}$_2$P(N*i*Pr$_2$)$_2$] (4): A solid mixture of K$_2$[Ge$_9${Si(TMS)$_3$}$_2$] (92 mg, 0.075 mmol, 1 equiv) and (*i*Pr$_2$N)$_2$PCl (20.0 mg, 0.075 mmol, 1 equiv) was treated with acetonitrile (2 mL) yielding a deep red suspension, which was stirred at r.t. for 30 min. Subsequently, the mixture was filtered to remove solid residues and formed KCl. Removal of the solvent yields the crude product as a dark brownish solid (47 mg, 45%). Unfortunately, purification by recrystallization from several solvents was not successful.[1]H NMR (400 MHz, 298 K, [D$_8$]THF): $\delta = 3.65$ (m, 4H, CH$_{iPr}$), 1.21 (d, $^3J_{HH} = 6.6$ Hz, 12H, Me$_{iPr}$), 1.12 (d, $^3J_{HH} = 6.6$ Hz, 12H, Me$_{iPr}$), 0.24 ppm (s, 54H, Me$_{TMS}$); ^{13}C NMR (101 MHz, 298 K, [D$_8$]THF): $\delta = 51.17$ (d, $^2J_{CP} = 10.0$ Hz, CH$_{iPr}$), 24.85 (m, Me$_{iPr}$), 3.25 ppm (s, Me$_{TMS}$); ^{29}Si-INEPT NMR (79 MHz, 298 K, [D$_8$]THF): $\delta = -11.51$ (s, Si$_{TMS}$), -110.59 ppm (s, Si$_{Ge9}$); ^{31}P NMR (162 MHz, 298 K, [D$_8$]THF): $\delta = 73.82$ ppm (m, P$_{Ge9}$); ESI-MS (negative mode, 4500 V, 300 °C): *m/z* 1380.8 [Ge$_9${Si(TMS)$_3$}$_2$P(N*i*Pr$_2$)$_2$]$^-$.

NHC^{Dipp}Cu[η^3-Ge$_9${Si(TMS)$_3$}$_2$(PMes$_2$)] (5): A solid mixture of K$_2$[Ge$_9${Si(TMS)$_3$}$_2$] (92 mg, 0.075 mmol, 1 equiv) and Mes$_2$PCl (22.9 mg, 0.075 mmol, 1 equiv) was treated with MeCN (1.5 mL) to obtain a deep red reaction mixture. After stirring for 20 min at r.t., a solution of NHC^{Dipp}CuCl (36.5 mg, 0.075 mmol, 1 equiv) in MeCN (1,5 mL) was added, instantly leading to the formation of a brownish precipitate. The mixture was stirred for 20 min at r.t to assure complete conversion of the reactants. Subsequently, the bright orange supernatant solution was filtered off, the solid was washed with MeCN (2 mL) and dissolved in toluene (2 mL). The solution was filtered to remove formed KCl and stored in a freezer at −40 °C, yielding red block-shaped crystals (44 mg, 30% yield). [1]H NMR (400 MHz, 298 K, [D$_8$]THF): $\delta = 7.42$ (s, 2H, CH$_{Im}$), 7.33–7.29 (m, 4H, CH$_{Dipp(m)}$), 7.27–7.23 (m, 2H, CH$_{Dipp(p)}$), 6.68 (s, 4H CH$_{Mes}$), 2.93 (hept, $^3J_{HH} = 6.9$ Hz, 4H, CH$_{iPr}$), 2.34 (s, 12H, Me$_{Mes(o)}$), 2.19 (s, 6H, Me$_{Mes(p)}$), 1.54 (d, $^3J_{HH} = 6.9$ Hz, 12H, Me$_{iPr}$), 1.17 (d, $^3J_{HH} = 6.9$ Hz, 12H, Me$_{iPr}$), 0.16 ppm (s, 54H, Me$_{TMS}$); ^{13}C NMR (101 MHz, 298 K, [D$_8$]THF): $\delta = 146.27$ (s, $C_{Ph(iPr)}$), 142.17 (s, C$_{Ph}$P), 142.03 (s, $C_{Ph(Me)}$), 137.36 (s, $C_{Ph(Me)}$), 136.35 (s, C$_{Ph}$N), 131.14 (s, CH$_{Dipp(p)}$), 130.34 (s, CH$_{Mes}$), 125.22 (s, CH$_{Dipp(m)}$), 124.04 (s, CH$_{Im}$), 29.81 (s, CH$_{iPr}$), 21.04 (s, Me$_{Mes(p)}$), 3.14 ppm (s, Me$_{TMS}$) (signals of Me$_{iPr}$ and Me$_{Mes(o)}$ overlap with residual [D^8]THF signal (25.35 ppm), hence no exact shifts can be determined); ^{29}Si-INEPT NMR (79 MHz, 298 K, [D$_8$]THF): $\delta = -11.19$ (s, Si$_{TMS}$), -106.17 ppm (s, Si$_{Ge9}$); ^{31}P NMR (162 MHz, 298 K, [D$_8$]THF): $\delta = -47.16$ ppm (m, P$_{Ge9}$); EA: anal. calcd for Ge$_9$Si$_8$PCuN$_2$C$_{63}$H$_{112}$: C, 40.4; H, 6.0; N, 1.5; found: C, 39.4; H, 5.7; N, 1.6.

NHC^{Dipp}Cu[η^3-Ge$_9${Si(TMS)$_3$}$_2${P(N*i*Pr$_2$)$_2$}] (6): A solid mixture of K$_2$[Ge$_9${Si(TMS)$_3$}$_2$] (92 mg, 0.075 mmol, 1 equiv) and (*i*Pr$_2$N)$_2$PCl (20.0 mg, 0.075 mmol, 1 equiv) was treated with MeCN (1.5 mL) to obtain a deep red reaction mixture. After stirring for 20 min at r.t., a solution of NHC^{Dipp}CuCl (36.5 mg, 0.075 mmol, 1 equiv) in MeCN (1,5 mL) was added, instantly leading to the formation of a brownish precipitate. The mixture was stirred for 20 min at r.t. to assure complete conversion of the reactants. Subsequently, the bright orange supernatant solution was filtered, the solid was washed with MeCN (2 mL) and dissolved in toluene (2 mL). The solution was filtered to remove formed KCl. After removal of the solvent the crude product was obtained as a dark orange solid (41 mg 30%). Unfortunately, purification by recrystallization from several solvents at low temperature was not successful. [1]H NMR (400 MHz, 298 K, [D$_8$]THF): $\delta = 7.46$–7.41 (m, 2H, CH$_{Ph(p)}$), 7.37–7.34 (m, 6H, CH$_{Ph(m)}$ + CH$_{Im}$), 3.83–3.62 (m, 4H CH$_{iPr(phosphine)}$), 2.91 (hept, $^3J_{HH} = 6.9$ Hz, 4H, CH$_{iPr(NHC)}$), 1.56 (d, $^3J_{HH} = 6.9$ Hz, 12H, Me$_{iPr(NHC)}$), 1.23–1.16 (m, 36H, Me$_{iPr(NHC + phosphine)}$), 0.18 ppm (s, 54H, Me$_{TMS}$); ^{13}C NMR (101 MHz, 298 K, [D$_8$]THF): $\delta = 146.03$ (s, $C_{Ph(iPr)}$), 136.29 (s, C$_{Ph}$N), 130.95 (s, CH$_{Ph(p)}$), 125.16 (s, CH$_{Ph(m)}$), 124.04 (s, CH$_{Im}$), 51.67 (d, $^2J_{CP} = 11.1$ Hz CH$_{iPr(phosphine)}$), 29.62 (s, CH$_{iPr(NHC)}$), 24.39 (d, Me$_{iPr(phosphine)}$), 3.14 ppm (s, Me$_{TMS}$) (signals of Me$_{iPr(NHC)}$ overlap with residual [D^8]THF signal (25.35 ppm), hence no exact shifts can be determined); ^{29}Si-INEPT NMR (79 MHz, 298 K, [D$_8$]THF): $\delta = -11.47$ (s, Si$_{TMS}$), -105.99 ppm (s, Si$_{Ge9}$); ^{31}P NMR (162 MHz, 298 K, [D$_8$]THF): $\delta = 87.71$ ppm (m, P$_{Ge9}$).

Acknowledgements

This work was financially supported by Wacker Chemie AG. F.S.G. thanks M.Sc. Lorenz Schiegerl and M.Sc. Kerstin Mayer for ESI-MS measurements and Dr. Wilhelm Klein for help with crystallographic issues. Furthermore, F.S.G. thanks TUM Graduate School for support.

Conflict of interest

The authors declare no conflict of interest.

Keywords: coinage metal · dimer · N-heterocyclic carbene · phosphine · *zintl* clusters

[1] a) J. D. Corbett, *Chem. Rev.* **1985**, *85*, 383; b) T. F. Fässler, S. D. Hoffmann, *Angew. Chem. Int. Ed.* **2004**, *43*, 6242; *Angew. Chem.* **2004**, *116*, 6400; c) S. C. Sevov, J. M. Goicoechea, *Organometallics* **2006**, *25*, 5678; d) S. Scharfe, F. Kraus, S. Stegmaier, A. Schier, T. F. Fässler, *Angew. Chem. Int. Ed.* **2011**, *50*, 3630; *Angew. Chem.* **2011**, *123*, 3712.

[2] B. W. Eichhorn, R. C. Haushalter, W. T. Pennington, *J. Am. Chem. Soc.* **1988**, *110*, 8704.

[3] a) M. W. Hull, S. C. Sevov, *Inorg. Chem.* **2007**, *46*, 10953; b) C. B. Benda, J.-Q. Wang, B. Wahl, T. F. Fässler, *Eur. J. Inorg. Chem.* **2011**, 4262.

[4] a) F. Li, S. C. Sevov, *Inorg. Chem.* **2012**, *51*, 2706; b) A. Schnepf, *Angew. Chem. Int. Ed.* **2003**, *42*, 2624; *Angew. Chem.* **2003**, *115*, 2728.

[5] a) F. S. Geitner, T. F. Fässler, *Eur. J. Inorg. Chem.* **2016**, 2688; b) K. Mayer, L. J. Schiegerl, T. F. Fässler, *Chem. Eur. J.* **2016**, *22*, 18794; c) C. Schenk, A. Schnepf, *Chem. Commun.* **2009**, 3208; d) L. J. Schiegerl, F. S. Geitner, C. Fischer, W. Klein, T. F. Fässler, *Z. Anorg. Allg. Chem.* **2016**, *642*, 1419; e) F. Henke, C. Schenk, A. Schnepf, *Dalton Trans.* **2011**, *40*, 6704.

[6] a) C. Schenk, A. Schnepf, *Angew. Chem. Int. Ed.* **2007**, *46*, 5314; *Angew. Chem.* **2007**, *119*, 5408; b) C. Schenk, F. Henke, G. Santiso-Quinones, I. Krossing, A. Schnepf, *Dalton Trans.* **2008**, 4436; c) F. Henke, C. Schenk, A. Schnepf, *Dalton Trans.* **2009**, 9141; d) O. Kysliak, C. Schrenk, A. Schnepf, *Chem. Eur. J.* **2016**, *22*, 18787.

[7] O. Kysliak, T. Kunz, A. Schnepf, *Eur. J. Inorg. Chem.* **2017**, 805.

[8] a) O. Kysliak, A. Schnepf, *Dalton Trans.* **2016**, *45*, 2404; b) O. Kysliak, C. Schrenk, A. Schnepf, *Inorg. Chem.* **2017**, *56*, 9693.

[9] F. S. Geitner, M. A. Giebel, A. Pöthig, T. F. Fässler, *Molecules* **2017**, *22*, 1204.

[10] L. G. Perla, S. C. Sevov, *J. Am. Chem. Soc.* **2016**, *138*, 9795.

[11] L. G. Perla, A. Muñoz-Castro, S. C. Sevov, *J. Am. Chem. Soc.* **2017**, *139*, 15176.

[12] F. S. Geitner, J. V. Dums, T. F. Fässler, *J. Am. Chem. Soc.* **2017**, *139*, 11933.

[13] a) N. Fey, M. F. Haddow, R. Mistry, N. C. Norman, A. G. Orpen, T. J. Reynolds, P. G. Pringle, *Organometallics* **2012**, *31*, 2907; b) J. Liedtke, H. Rüegger, S. Loss, H. Grützmacher, *Angew. Chem. Int. Ed.* **2000**, *39*, 2478; *Angew. Chem.* **2000**, *112*, 2596; c) J. Cipot, R. McDonald, M. Stradiotto, *Chem. Commun.* **2005**, 4932; d) C. C. Lu, J. C. Peters, *J. Am. Chem. Soc.* **2002**, *124*, 5272.

[14] S. Scharfe, T. F. Fässler, *Eur. J. Inorg. Chem.* **2010**, 1207.

[15] F. Li, A. Muñoz-Castro, S. C. Sevov, *Angew. Chem. Int. Ed.* **2016**, *55*, 8630; *Angew. Chem.* **2016**, *128*, 8772.

[16] a) L. Hintermann, *Beilstein J. Org. Chem.* **2007**, *3*, 22; b) O. Santoro, A. Collado, A. M. Z. Slawin, S. P. Nolan, C. S. J. Cazin, *Chem. Commun.* **2013**,

49, 10483; c) G. A. Bowmaker, S. E. Boyd, J. V. Hanna, R. D. Hart, P. C. Healy, B. W. Skelton, A. H. White, *Dalton Trans.* **2002**, 2722.
[17] G. Sheldrick, *Acta Crystallogr. Sect. C* **2015**, *71*, 3.
[18] A. Spek, *Acta Crystallogr. Sect. D* **2009**, *65*, 148.
[19] G. R. Fulmer, A. J. M. Miller, N. H. Sherden, H. E. Gottlieb, A. Nudelman, B. M. Stoltz, J. E. Bercaw, K. I. Goldberg, *Organometallics* **2010**, *29*, 2176.

Manuscript received: November 29, 2017
Accepted manuscript online: January 11, 2018
Version of record online: February 16, 2018

CHEMISTRY
A European Journal

Supporting Information

On the Variable Reactivity of Phosphine-Functionalized [Ge_9] Clusters: *Zintl* Cluster-Substituted Phosphines or Phosphine-Substituted *Zintl* Clusters

Felix S. Geitner,[b] Christoph Wallach,[a] and Thomas F. Fässler*[a]

chem_201705678_sm_miscellaneous_information.pdf

Supporting Information

Content

1. Crystal Structure Data

Table SI 1: Selected distances [Å] in compound **1**.

bond	**distance**	**bond**	**distance**
Cluster I		Cluster II	
Ge1-Ge2	2.555(1)	Ge10-Ge11	2.545(1)
Ge1-Ge3	2.5443(9)	Ge10-Ge12	2.5499(9)
Ge1-Ge4	2.537(1)	Ge10-Ge13	2.535(1)
Ge1-Ge5	2.540(1)	Ge10-Ge14	2.532(1)
Ge2-Ge6	2.524(1)	Ge11-Ge15	2.533(1)
Ge2-Ge7	2.716(1)	Ge11-Ge16	2.702(1)
Ge3-Ge7	2.750(1)	Ge12-Ge16	2.732(1)
Ge3-Ge8	2.530(1)	Ge12-Ge17	2.530(1)
Ge4-Ge5	2.639(1)	Ge13-Ge14	2.636(1)
Ge4-Ge8	2.5625(9)	Ge13-Ge17	2.549(1)
Ge4-Ge9	2.7087(9)	Ge13-Ge18	2.7080(9)
Ge5-Ge6	2.549(1)	Ge14-Ge15	2.549(1)
Ge5-Ge9	2.695(1)	Ge14-Ge18	2.706(1)
Ge6-Ge7	2.5561(9)	Ge15-Ge16	2.5535(9)
Ge6-Ge9	2.547(1)	Ge15-Ge18	2.541(1)
Ge7-Ge8	2.5547(9)	Ge16-Ge17	2.5624(9)
Ge8-Ge9	2.550(1)	Ge17-Ge18	2.547(1)
Ge6-Si1	2.383(2)	Ge15-Si9	2.384(2)
Ge8-Si5	2.385(2)	Ge17-Si13	2.386(2)
Ge1-P1	2.316(2)	Ge10-P2	2.310(2)
Cu1-P1	2.200(2)	Cu2-P2	2.211(2)
Cu1-C9	1.915(6)	Cu2-C56	1.902(6)
Ge2-Ge5	3.650(5)	Ge11-Ge14	3.650(2)
Ge3-Ge4	3.621(3)	Ge12-Ge13	3.621(7)
Ge7-Ge9	3.085(9)	Ge16-Ge18	3.094(1)

Table SI 2: Selected distances [Å] in compound **2**.

bond	distance	bond	distance
Ge1-Ge2	2.868(1)	Ge10-Ge11	2.889(1)
Ge1-Ge3	2.875(1)	Ge10-Ge12	2.877(1)
Ge1-Ge4	2.4930(9)	Ge10-Ge13	2.5014(9)
Ge1-Ge5	2.513(1)	Ge10-Ge14	2.515(1)
Ge2-Ge3	2.934(1)	Ge11-Ge12	2.910(1)
Ge2-Ge5	2.503(1)	Ge11-Ge14	2.505(9)
Ge2-Ge6	2.5121(9)	Ge11-Ge15	2.5103(9)
Ge3-Ge4	2.500(1)	Ge12-Ge13	2.493(1)
Ge3-Ge6	2.520(1)	Ge12-Ge15	2.515(1)
Ge4-Ge7	2.562(1)	Ge13-Ge16	2.5677(9)
Ge4-Ge9	2.577(1)	Ge13-Ge18	2.5666(9)
Ge5-Ge7	2.562(1)	Ge14-Ge16	2.586(1)
Ge5-Ge8	2.580(1)	Ge14-Ge17	2.5666(9)
Ge6-Ge8	2.5641(9)	Ge15-Ge17	2.567(1)
Ge6-Ge9	2.580(1)	Ge15-Ge18	2.586(1)
Ge7-Ge8	2.626(1)	Ge16-Ge17	2.647(1)
Ge7-Ge9	2.644(1)	Ge16-Ge18	2.646(1)
Ge8-Ge9	2.689(1)	Ge17-Ge18	2.663(1)
Ge5-Si1	2.386(2)	Ge14-Si9	2.379(2)
Ge6-Si5	2.378(2)	Ge15-Si13	2.380(2)
Ge4-P1	2.327(2)	Ge13-P2	2.328(2)
Ge1-Cu1	2.476(1)	Ge10-Cu2	2.504(1)
Ge2-Cu1	2.518(1)	Ge11-Cu2	2.510(1)
Ge3-Cu1	2.5302(9)	Ge12-Cu2	2.497(1)
Ge1-Ge7	3.563(1)	Ge10-Ge16	3.503(4)
Ge2-Ge8	3.314(6)	Ge11-Ge17	3.315(5)
Ge3-Ge9	3.332(2)	Ge12-Ge18	3.387(6)
P1-Cu2	2.245(6)	P2-Cu1	2.254(2)

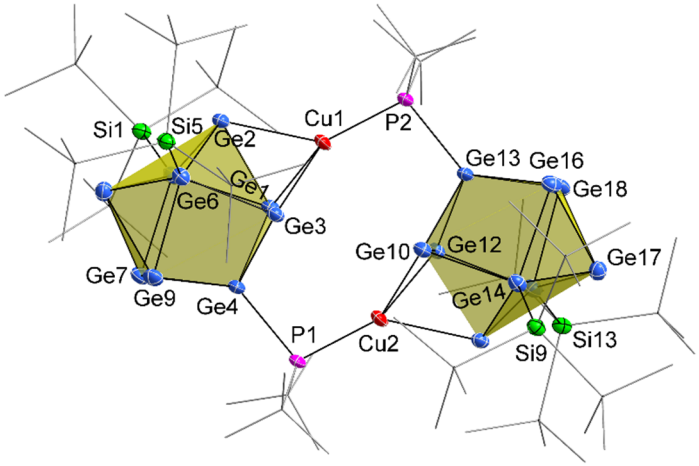

Figure SI 1: Molecular structure of compound **2**. Ellipsoids are shown at a 50 % probability level. For clarity TMS groups of the hypersilyl substituents and the *tert*-butyl groups of the phosphine ligands are pictured as grey wire sticks. Hydrogen atoms and solvent molecules are omitted.

Table SI 3: Selected distances [Å] in compound **5**.

bond	**distance**	**bond**	**distance**
Cluster I		Cluster II	
Ge1-Ge2	2.864(1)	Ge10-Ge11	2.885(1)
Ge1-Ge4	2.524(1)	Ge10-Ge13	2.528(1)
Ge1-Ge5	2.505(1)	Ge10-Ge14	2.501(1)
Ge2-Ge3	2.821(1)	Ge11-Ge12	2.796(1)
Ge2-Ge5	2.512(1)	Ge11-Ge14	2.517(1)
Ge2-Ge6	2.528(1)	Ge11-Ge15	2.535(1)
Ge3-Ge4	2.483(1)	Ge12-Ge13	2.487(1)
Ge3-Ge6	2.514(1)	Ge12-Ge15	2.516(1)
Ge4-Ge7	2.569(1)	Ge13-Ge16	2.573(1)
Ge4-Ge9	2.539(1)	Ge13-Ge18	2.548(1)
Ge5-Ge7	2.577(1)	Ge14-Ge16	2.570(1)
Ge5-Ge8	2.577(1)	Ge14-Ge17	2.544(1)
Ge6-Ge8	2.569(1)	Ge15-Ge17	2.566(1)
Ge6-Ge9	2.574(1)	Ge15-Ge18	2.576(1)
Ge7-Ge8	2.598(1)	Ge16-Ge17	2.696(1)
Ge7-Ge9	2.686(1)	Ge16-Ge18	2.674(1)
Ge8-Ge9	2.667(1)	Ge17-Ge18	2.591(1)
Ge5-Si5	2.375(2)	Ge14-Si13	2.380(2)
Ge6-Si1	2.385(2)	Ge15-Si9	2.386(2)
Ge4-P1	2.330(2)	Ge13-P2	2.335(2)
Ge1-Cu1	2.530(1)	Ge10-Cu2	2.522(1)
Ge2-Cu1	2.519(1)	Ge11-Cu2	2.518(1)
Ge3-Cu1	2.491(1)	Ge12-Cu2	2.482(1)
Ge1-Ge7	3.185(6)	Ge10-Ge16	3.168(3)
Ge2-Ge8	3.479(4)	Ge11-Ge17	3.420(2)
Ge3-Ge9	3.470(3)	Ge12-Ge18	3.543(6)

2. NMR Spectra

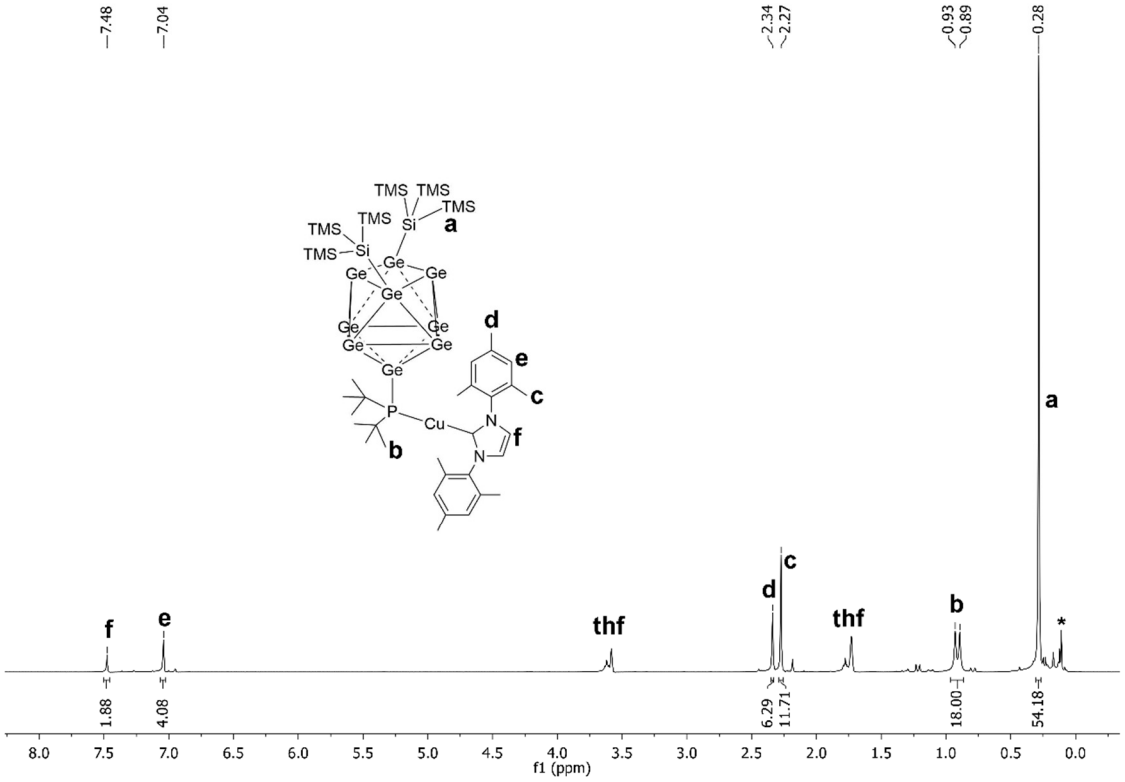

Figure SI 2: ^{1}H NMR of compound **1** (synthesized in thf, signal marked with * is assigned to silicon grease) in thf-d_8.

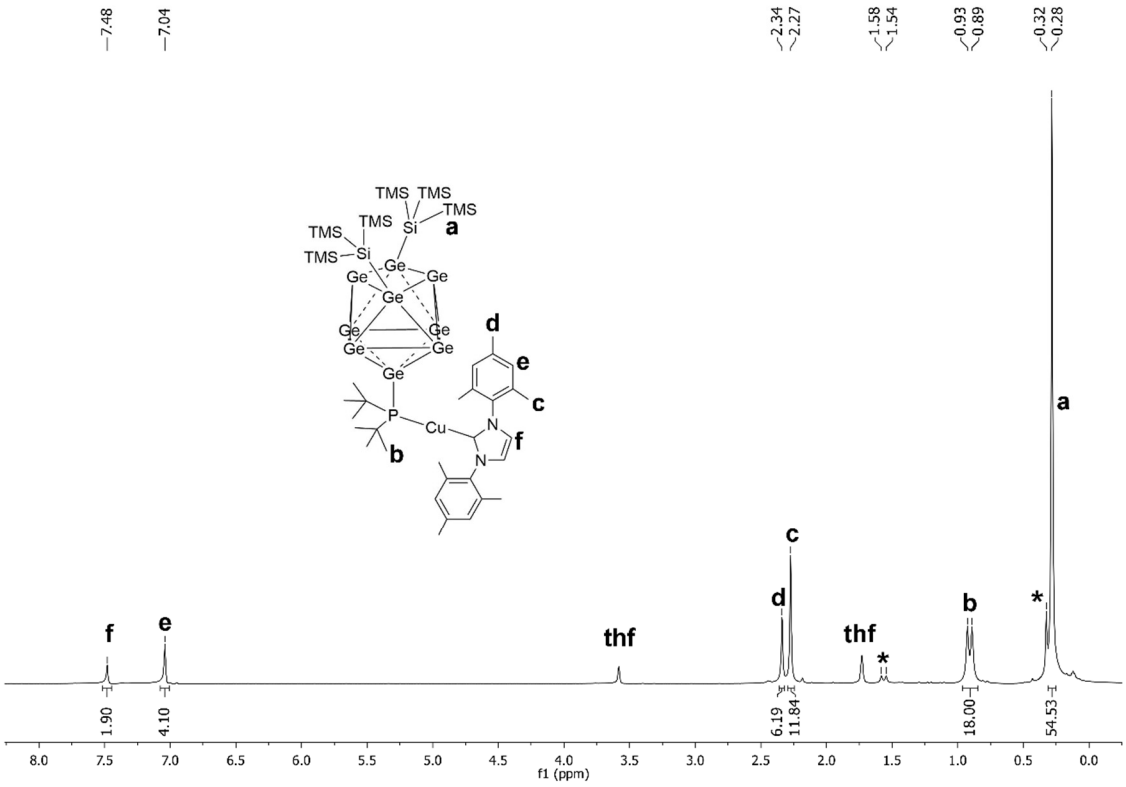

Figure SI 3: ^{1}H NMR of compound **1** (synthesized in MeCN, signals of side phase **2** are marked with *) in thf-d_8.

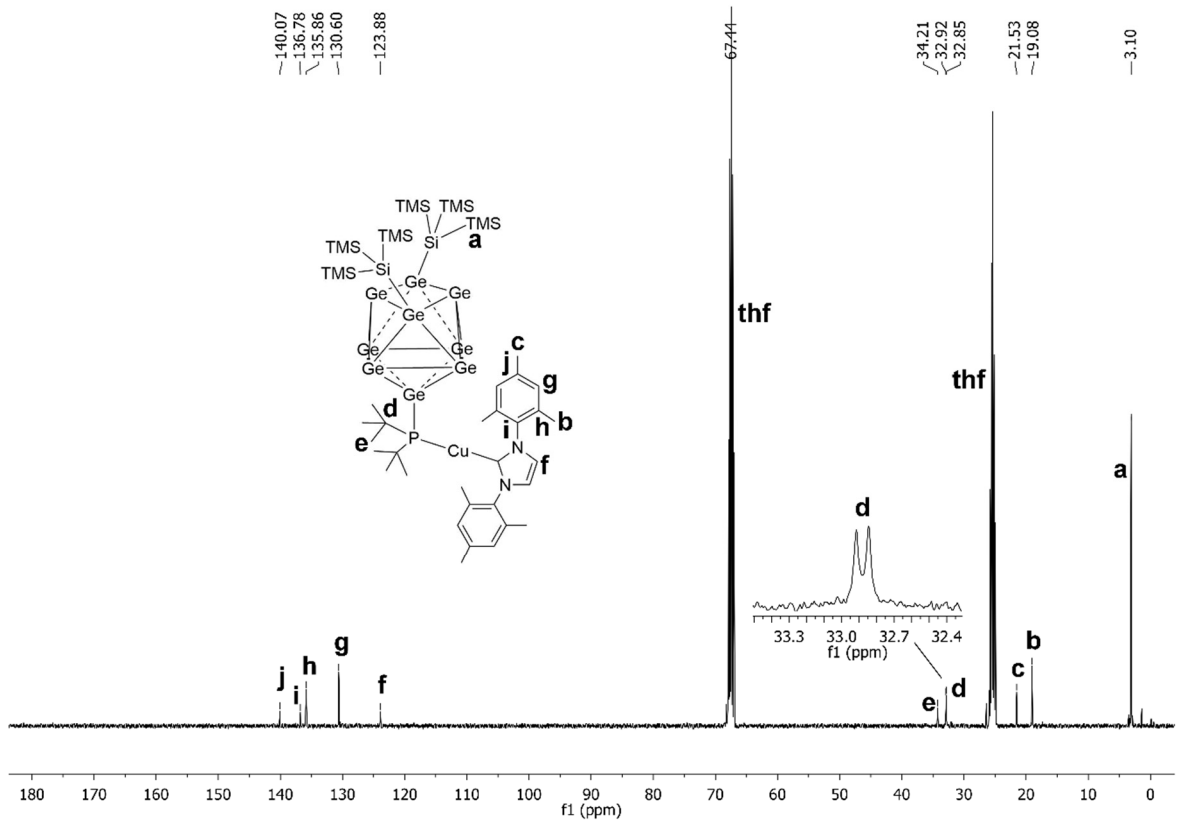

Figure SI 4: ^{13}C NMR of compound **1** (synthesized in thf) in thf-d_8.

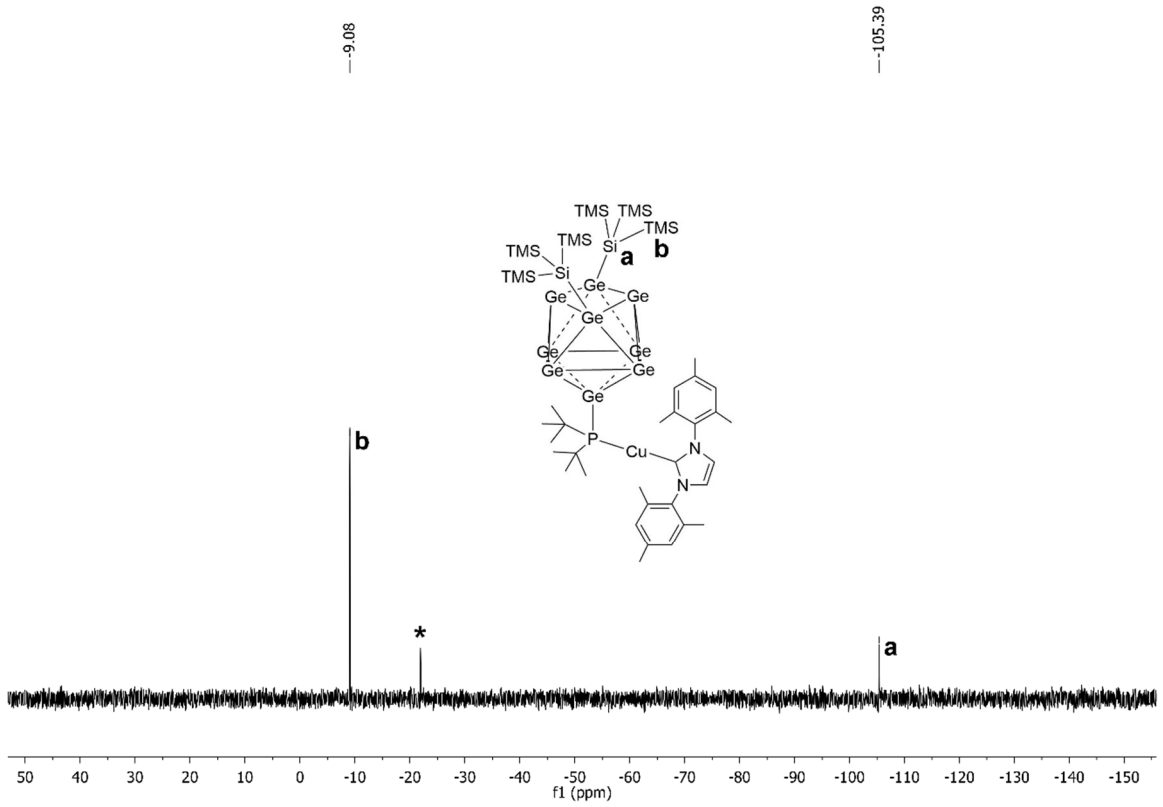

Figure SI 5: ^{29}Si-INEPT-RD NMR of compound **1** (synthesized in thf; signal marked with * is assigned to silicon grease) in thf-d_8.

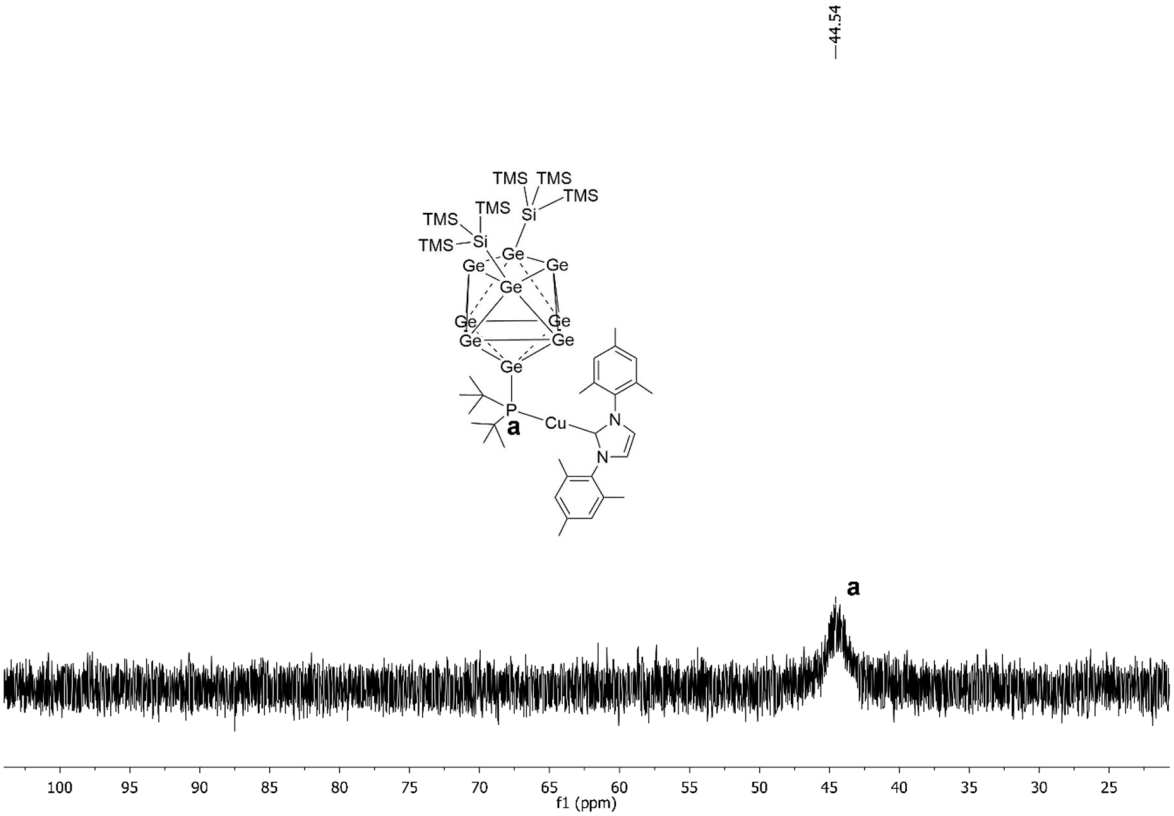

Figure SI 6: ^{31}P NMR of compound **1** (synthesized in thf) in thf-d_8.

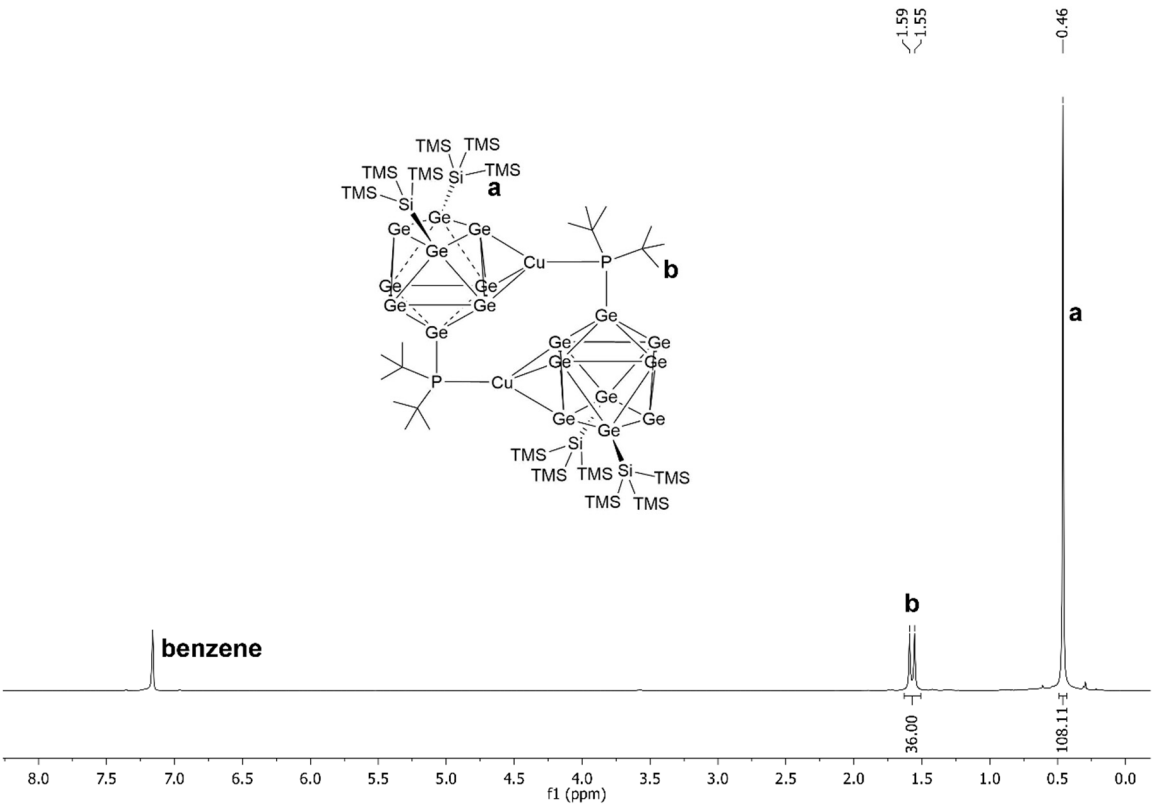

Figure SI 7: ^{1}H NMR of compound **2** in C_6D_6.

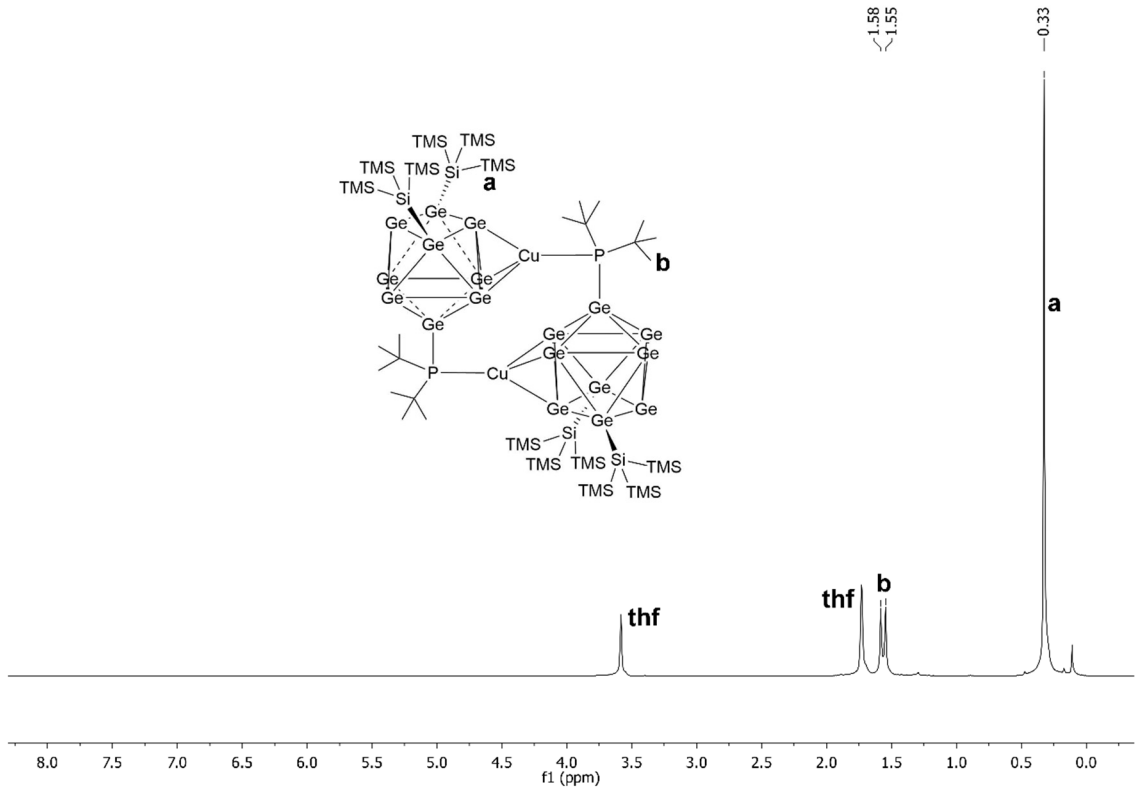

Figure SI 8: ^{1}H NMR of compound **2** in thf-d_8.

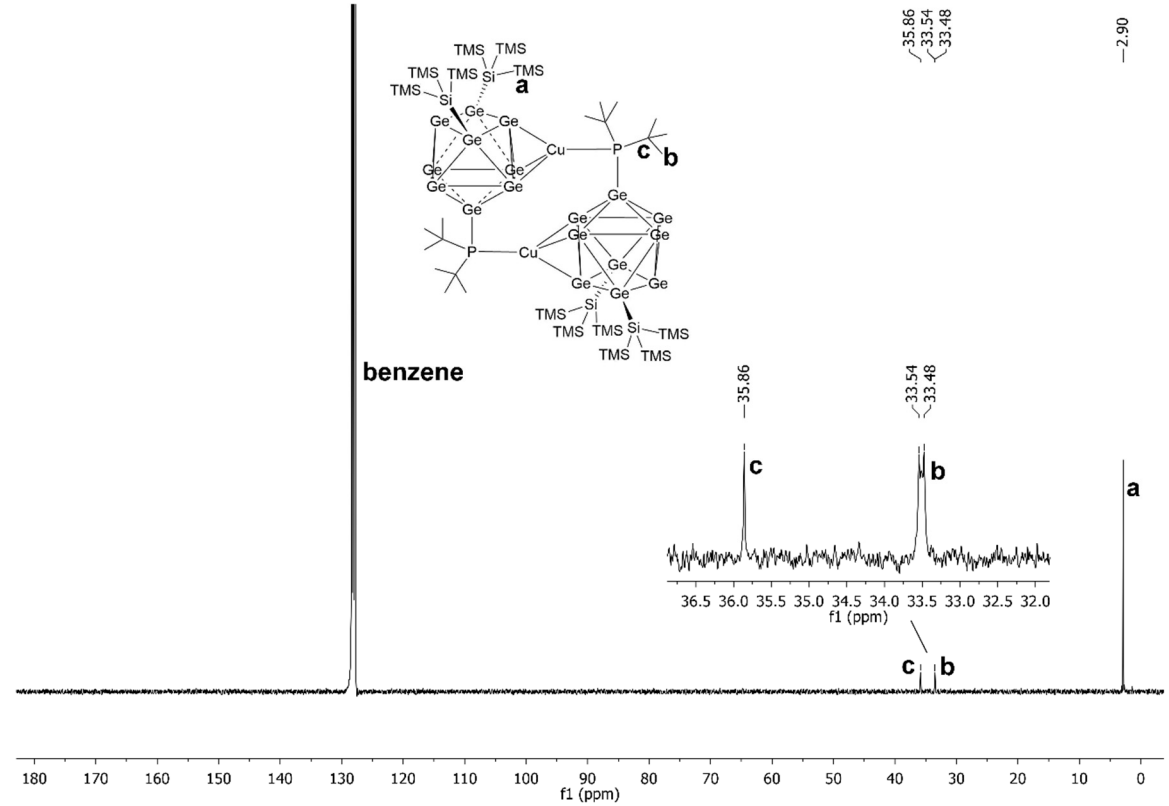

Figure SI 9: ^{13}C NMR of compound **2** in C_6D_6.

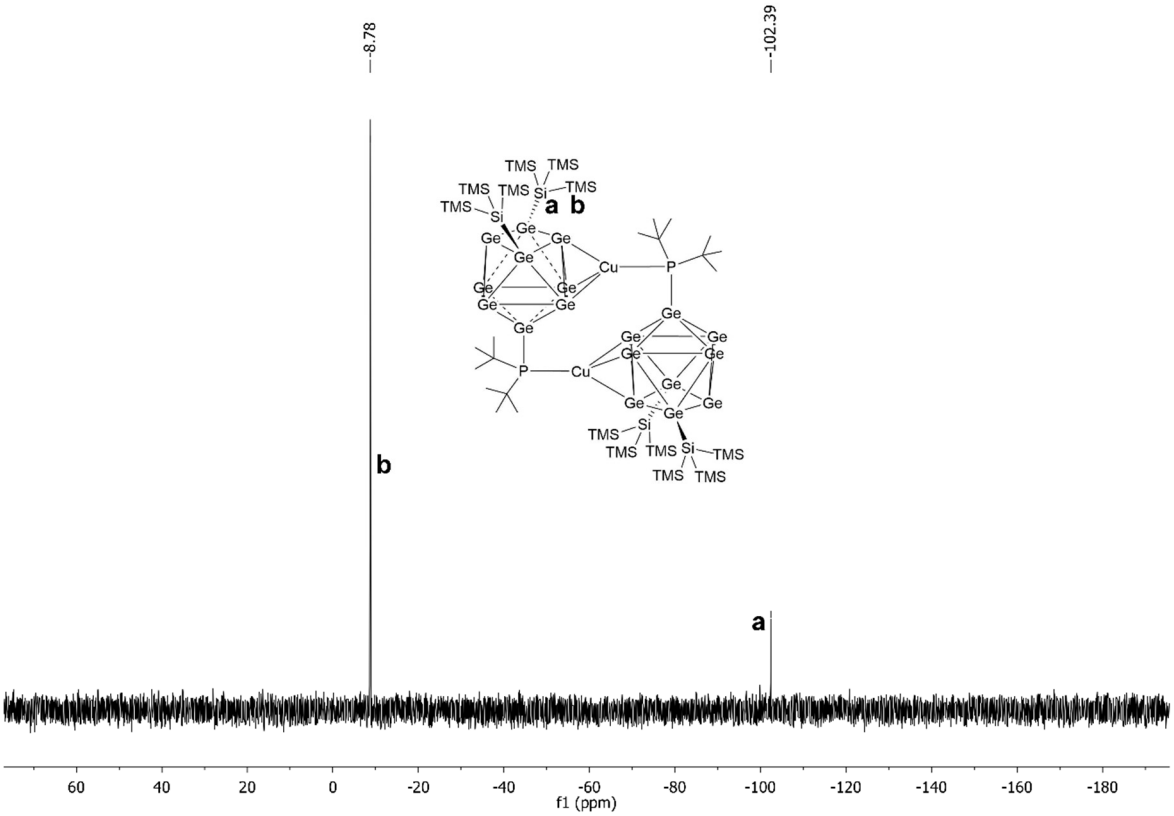

Figure SI 10: ^{29}Si-INEPT-RD NMR of compound **2** in C_6D_6.

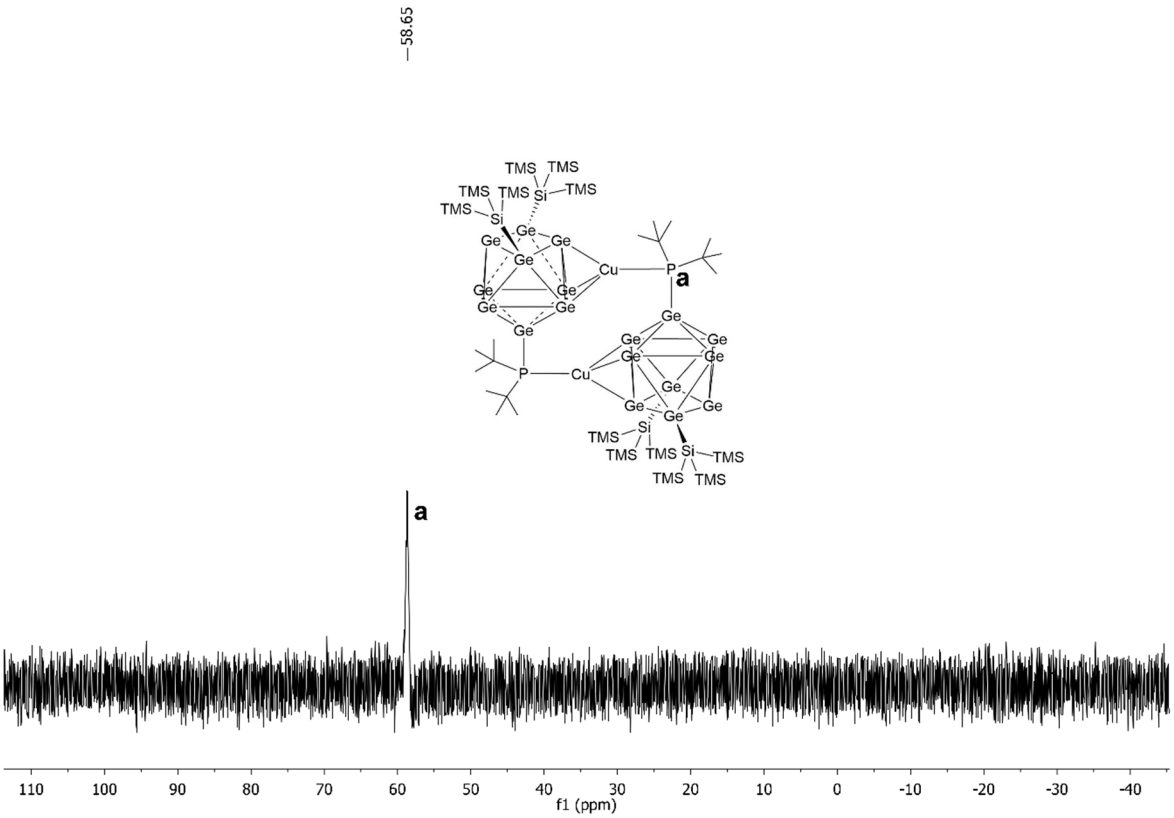

Figure SI 11: ^{31}P-NMR of compound **2** in C_6D_6.

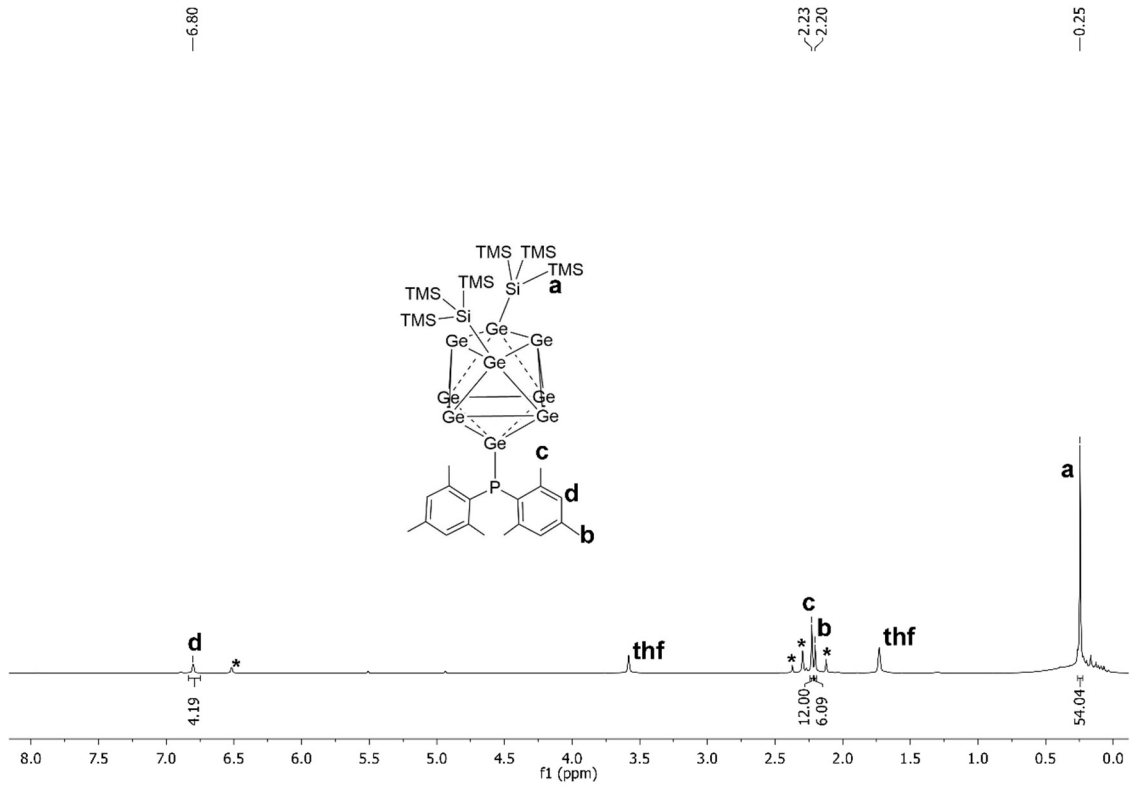

Figure SI 12:[1]H NMR of compound **3** in thf-d_8 (signals marked with * belong to unidentified impurities).

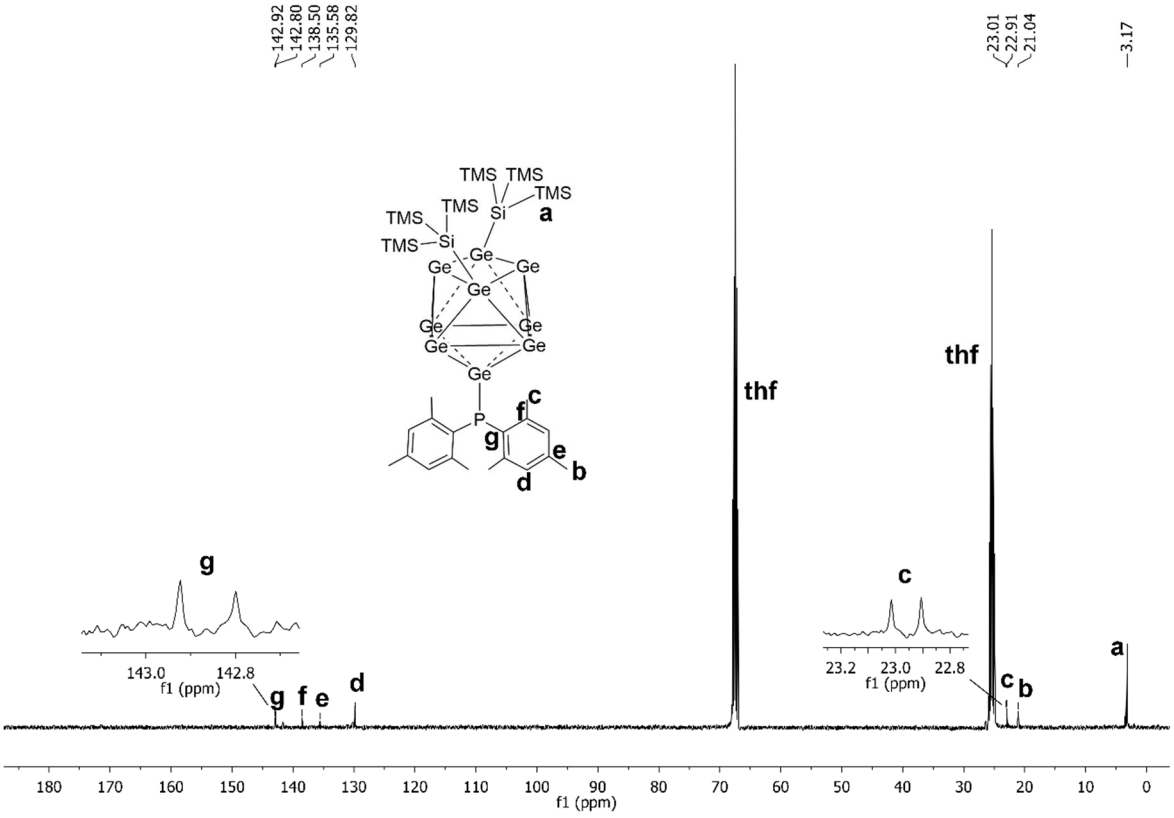

Figure SI 13:[13]C NMR of compound **3** in thf-d_8.

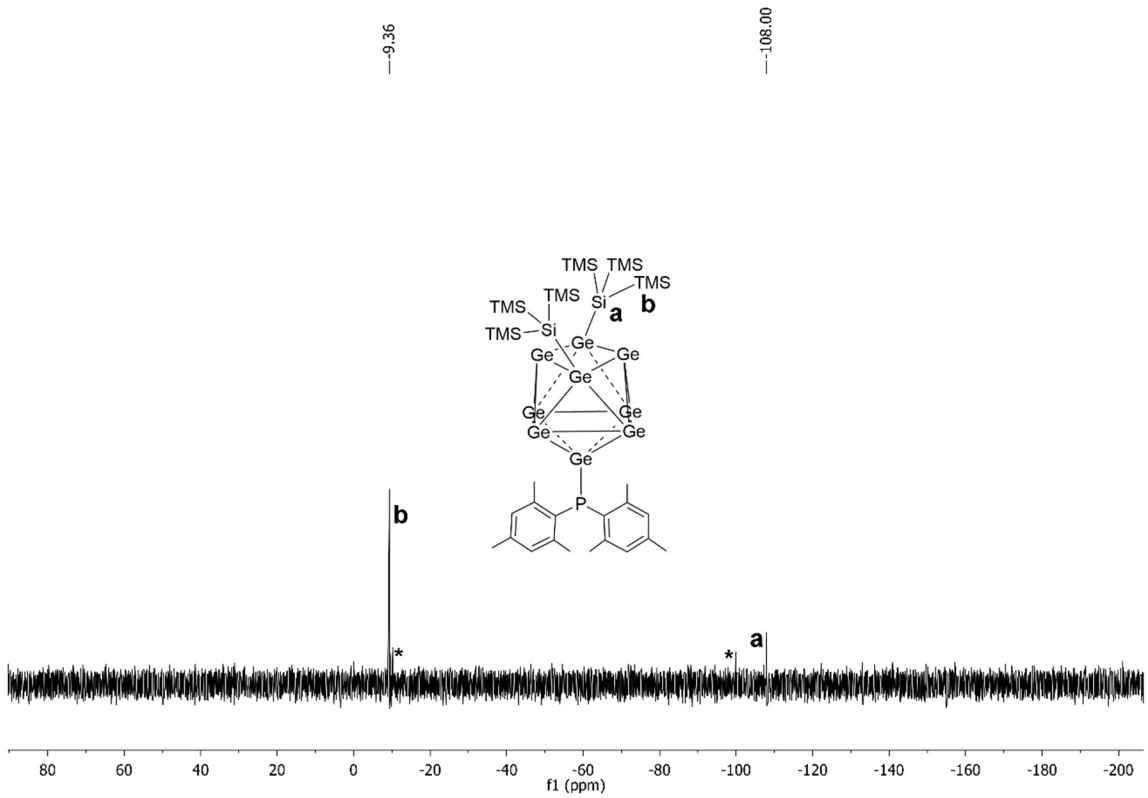

Figure SI 14:[29]Si-INEPT-RD NMR of compound **3** in thf-d_8 (signals marked with * belong to unidentified impurities).

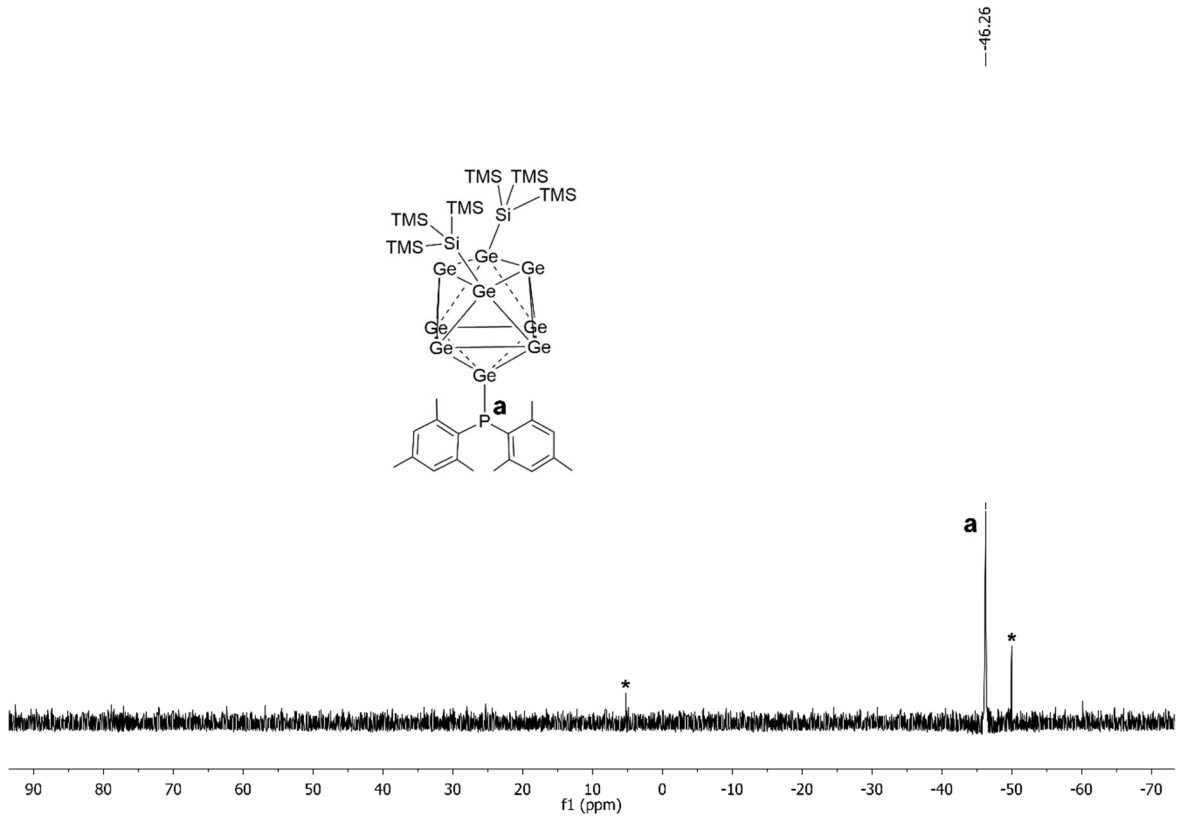

Figure SI 15:[31]P NMR of compound **3** in thf-d_8 (signals marked with * belong to unidentified impurities).

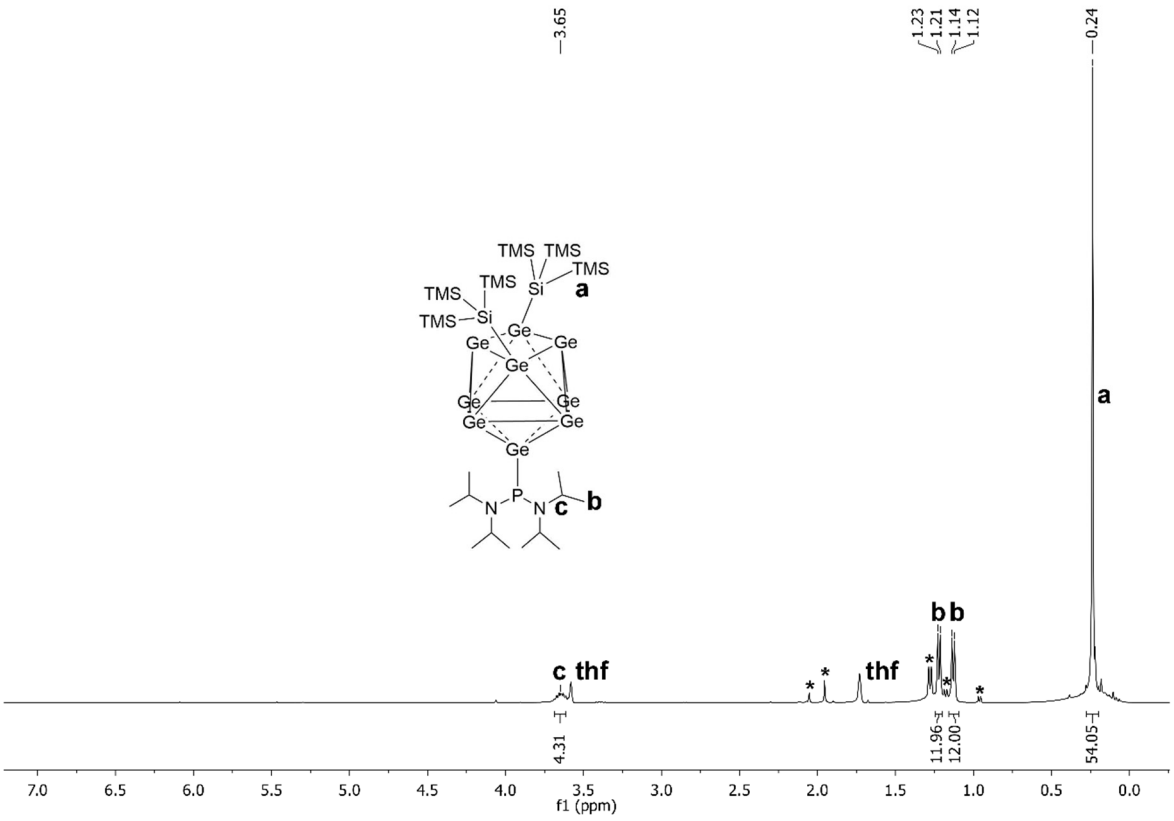

Figure SI 16:[1]H NMR of compound **4** in thf-d_8 (signals marked with * belong to unidentified impurities).

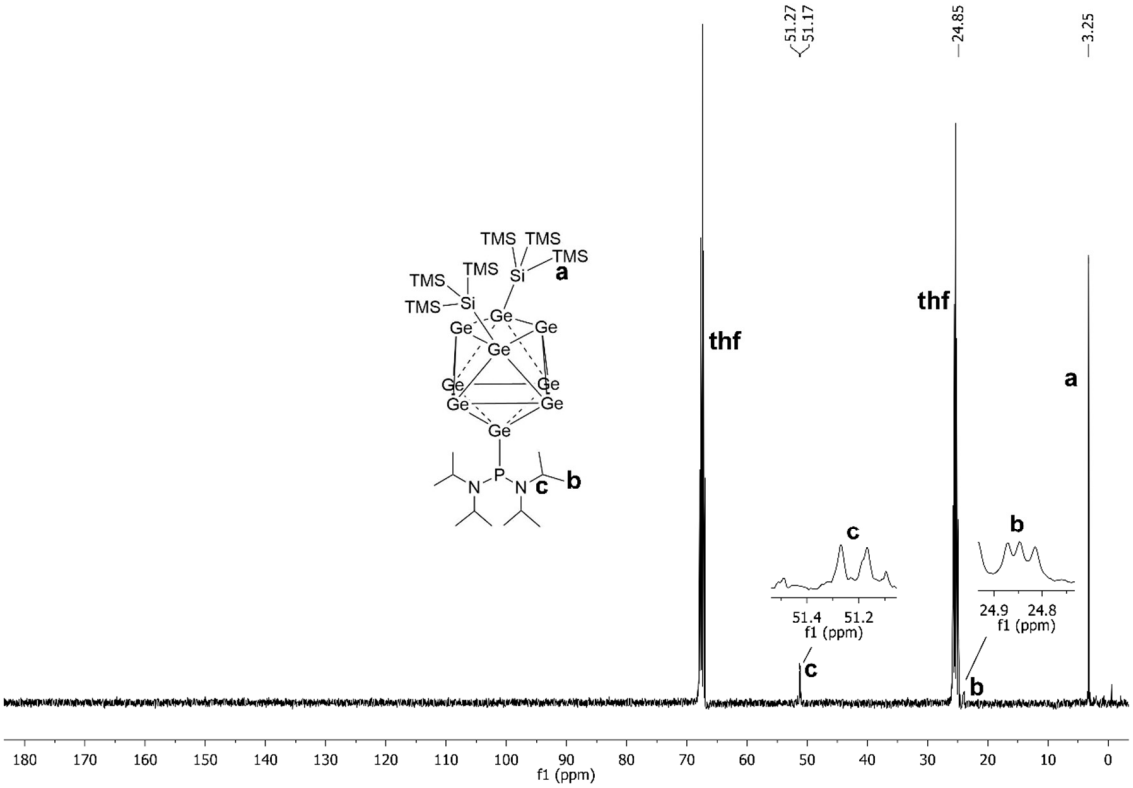

Figure SI 17:[13]C NMR of compound **4** in thf-d_8.

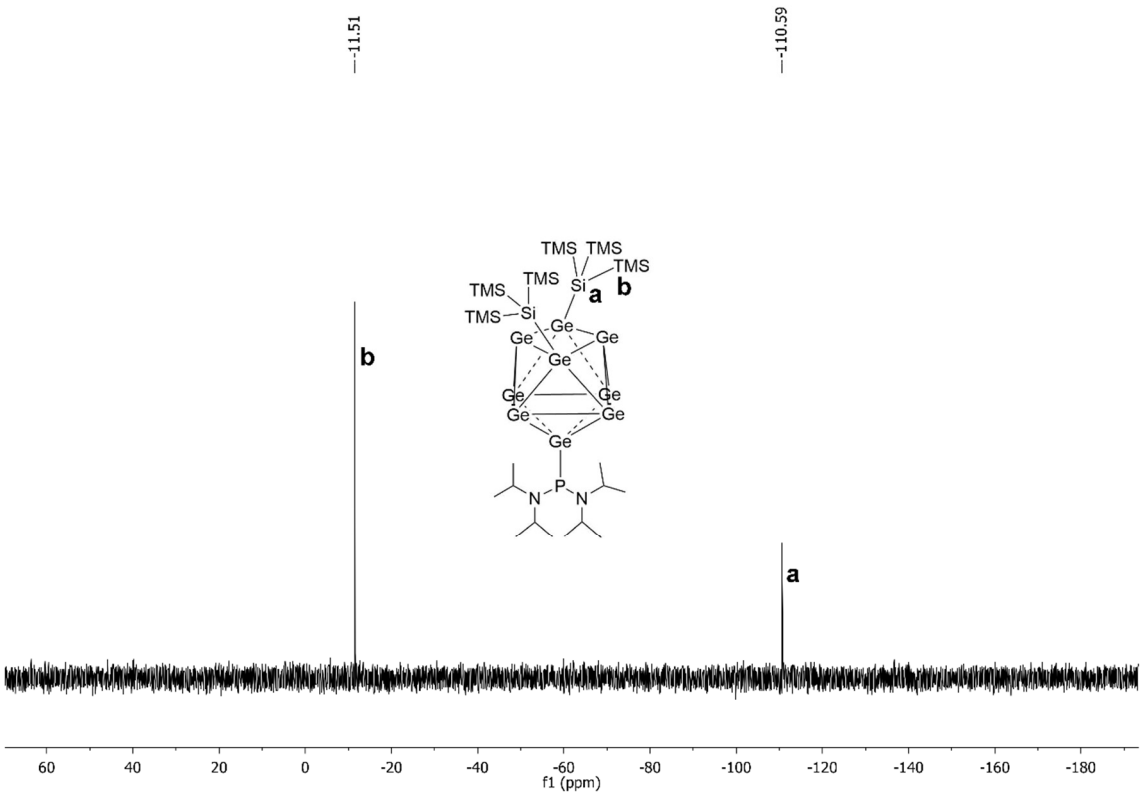

Figure SI 18:[29]Si-INEPT-RD NMR of compound **4** in thf-d_8.

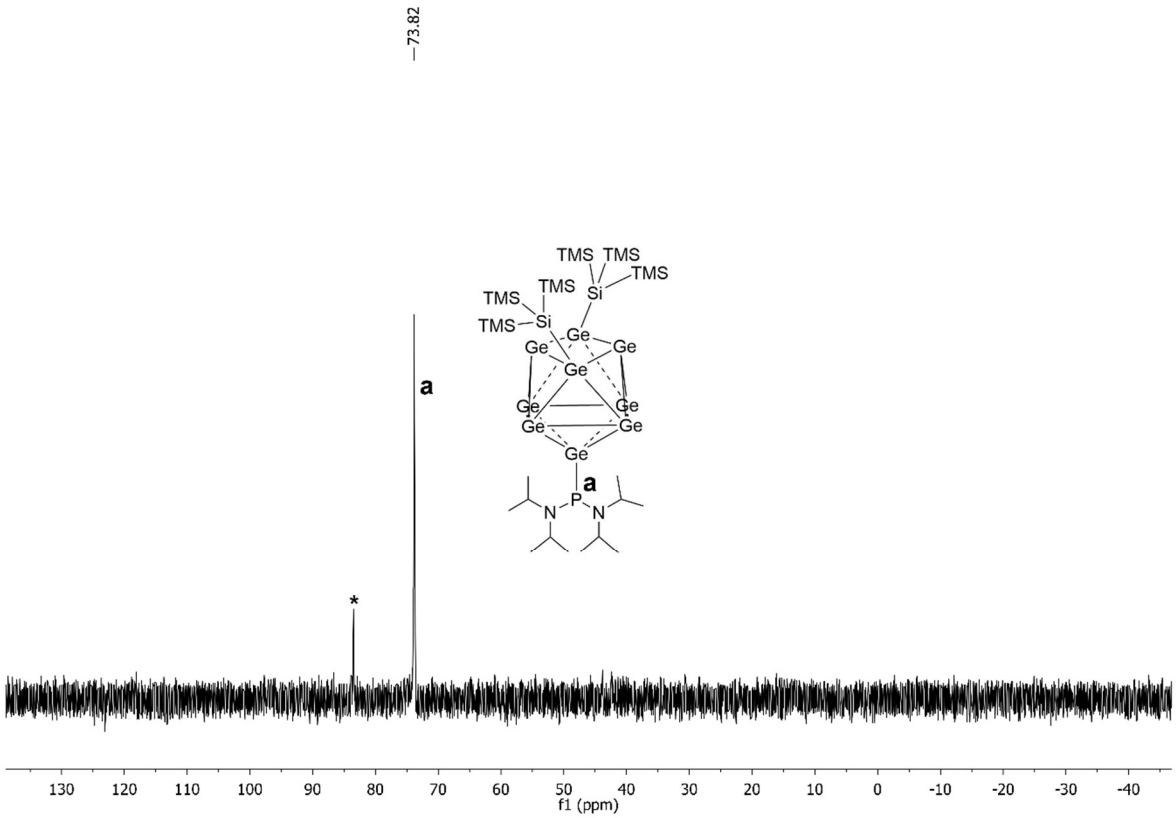

Figure SI 19:[31]P NMR of compound **4** in thf-d_8 (signal marked with * belongs to unidentified impurity).

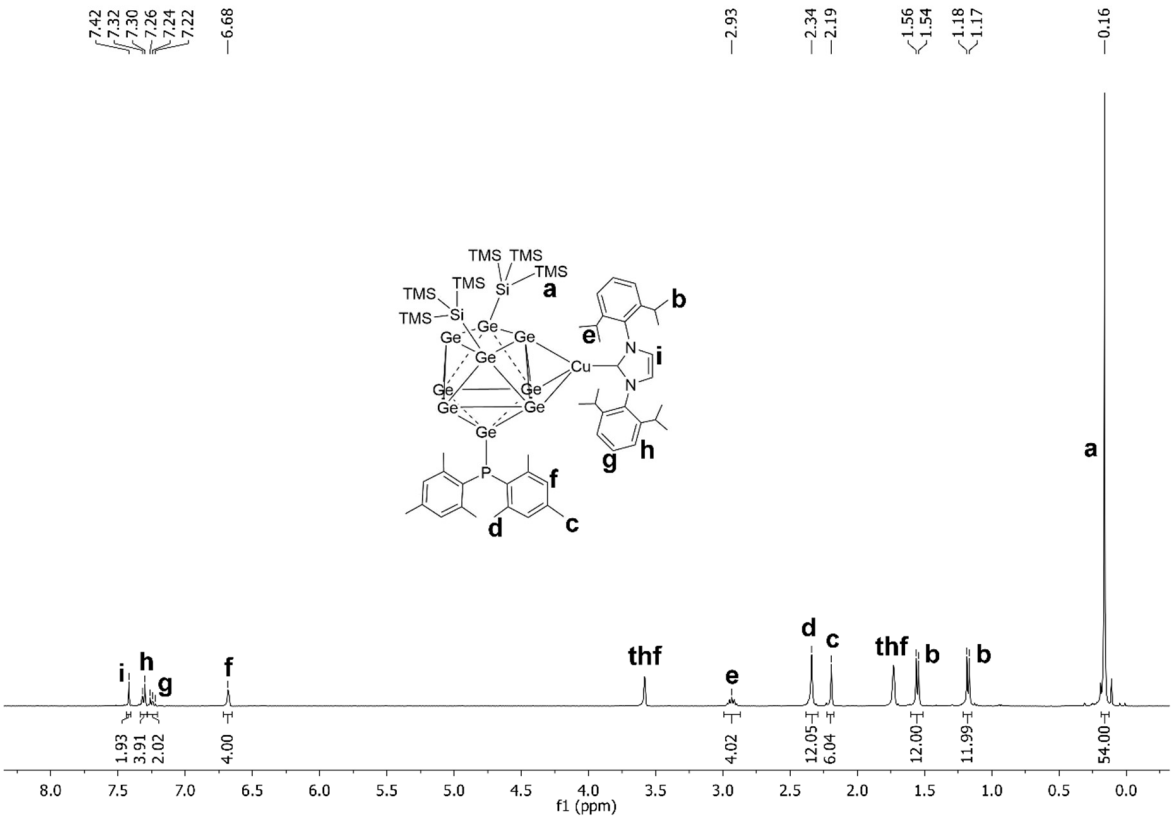

Figure SI 20:[1]H NMR of compound **5** in thf-d_8.

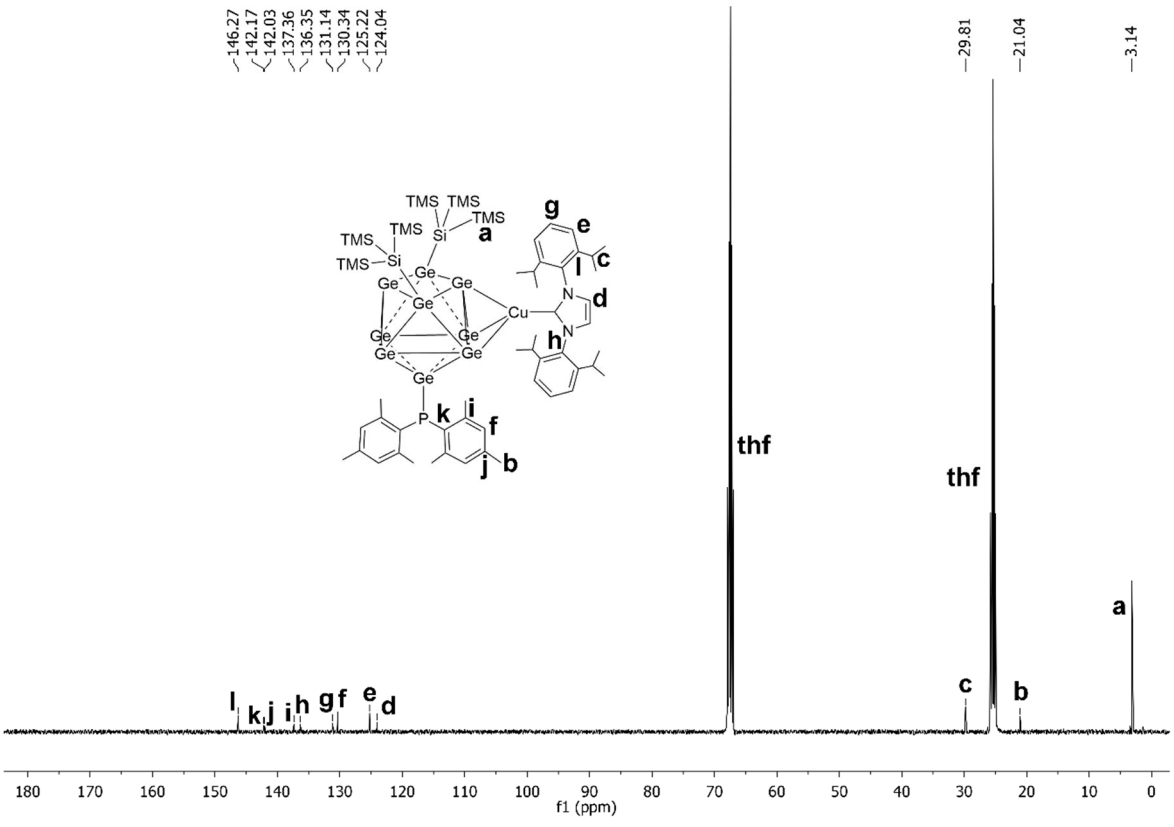

Figure SI 21:[13]C NMR of compound **5** in thf-d_8.

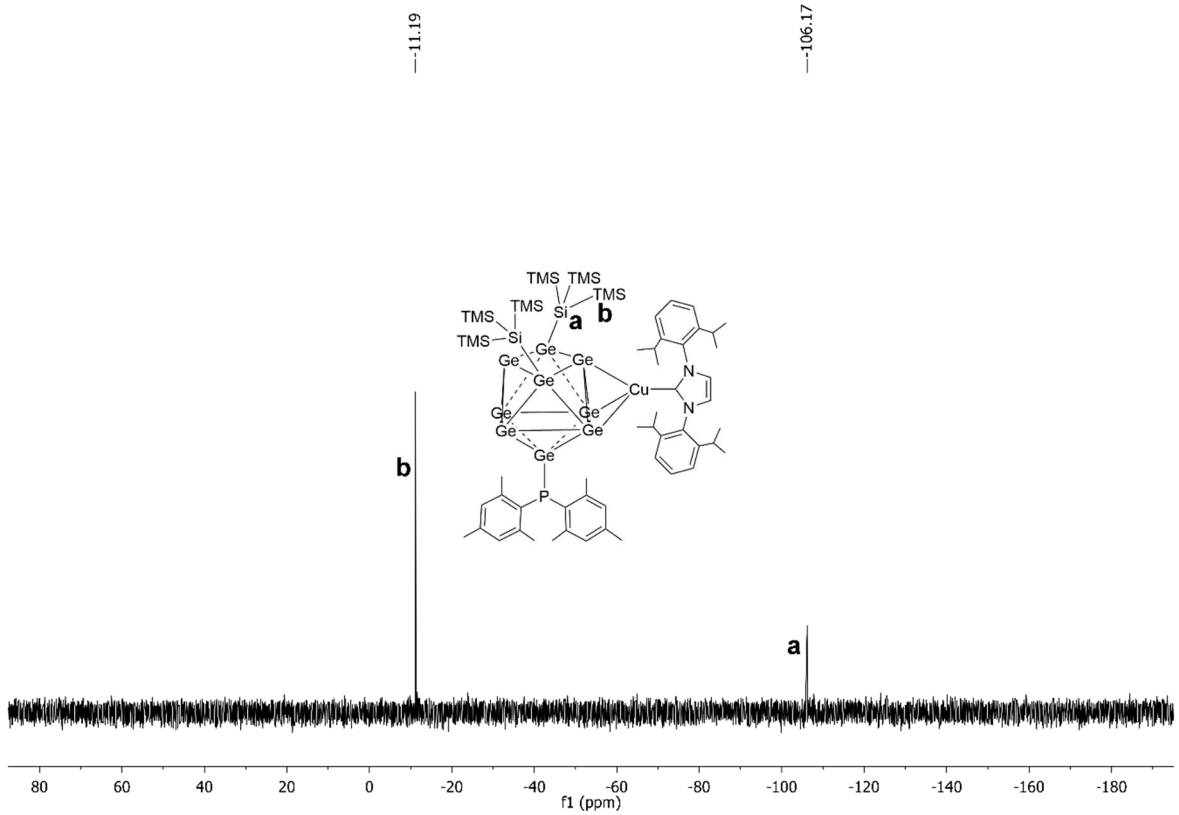

Figure SI 22:[29]Si-INEPT-RD NMR of compound **5** in thf-d_8.

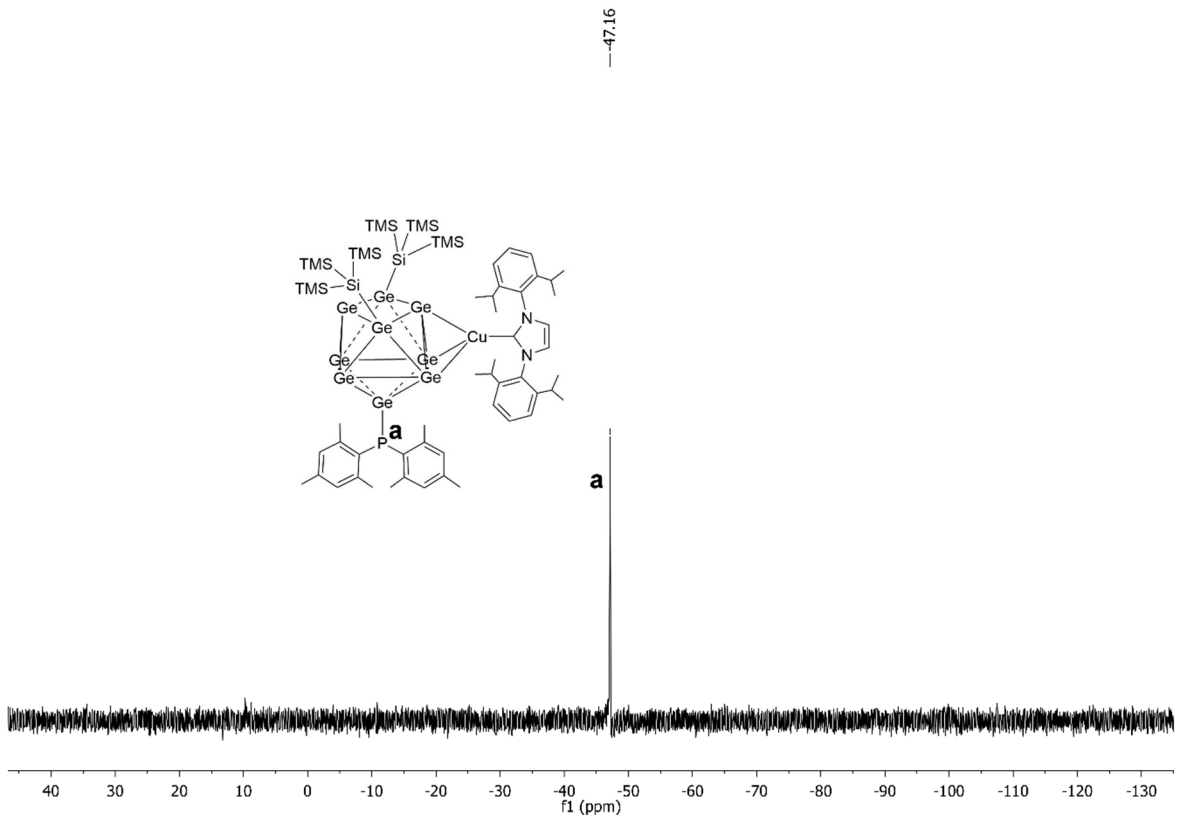

Figure SI 23:[31]P NMR of compound **5** in thf-d_8.

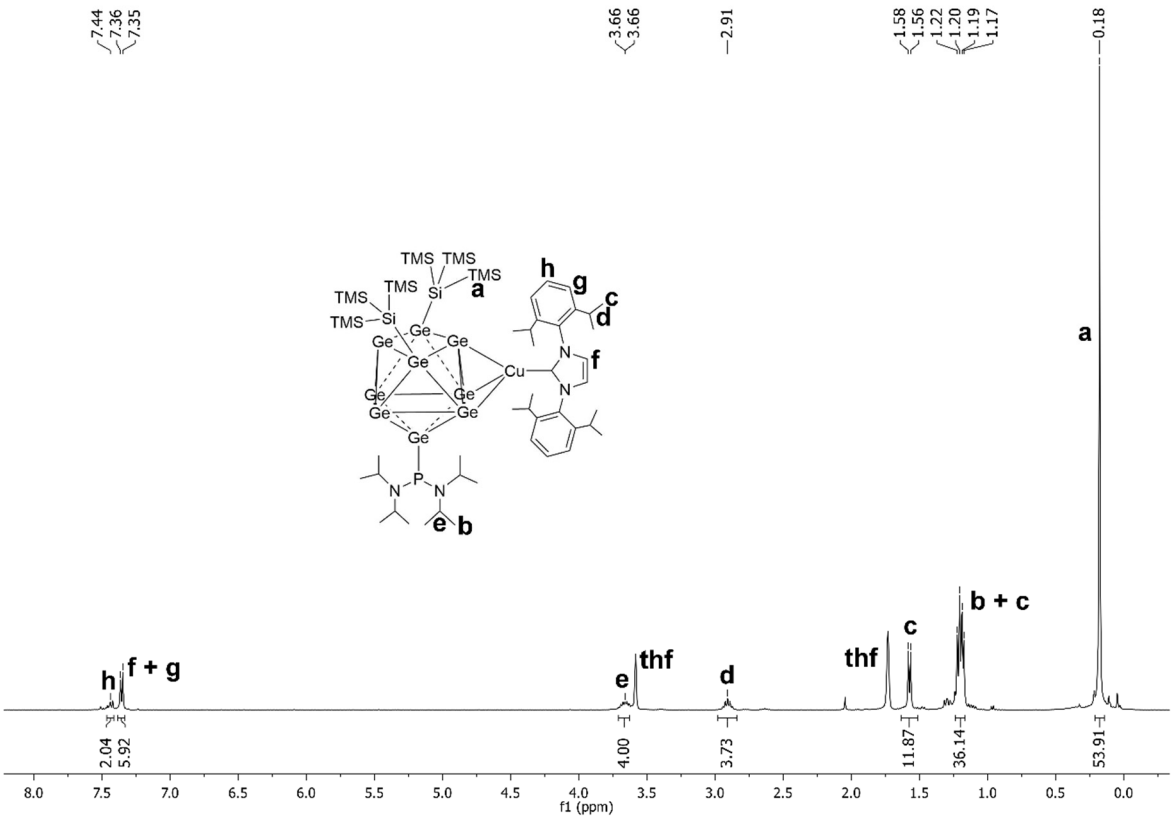

Figure SI 24:[1]H NMR of compound **6** in thf-d_8.

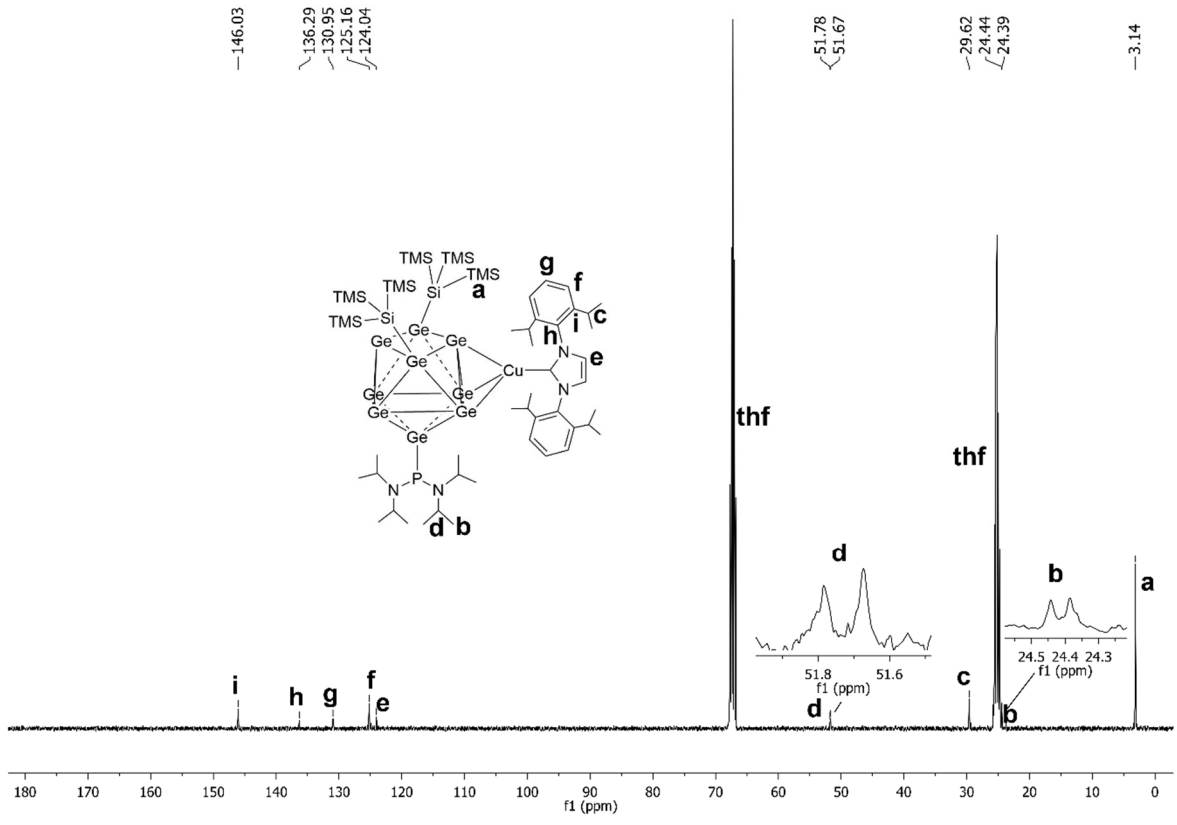

Figure SI 25:[13]C NMR of compound **6** in thf-d_8.

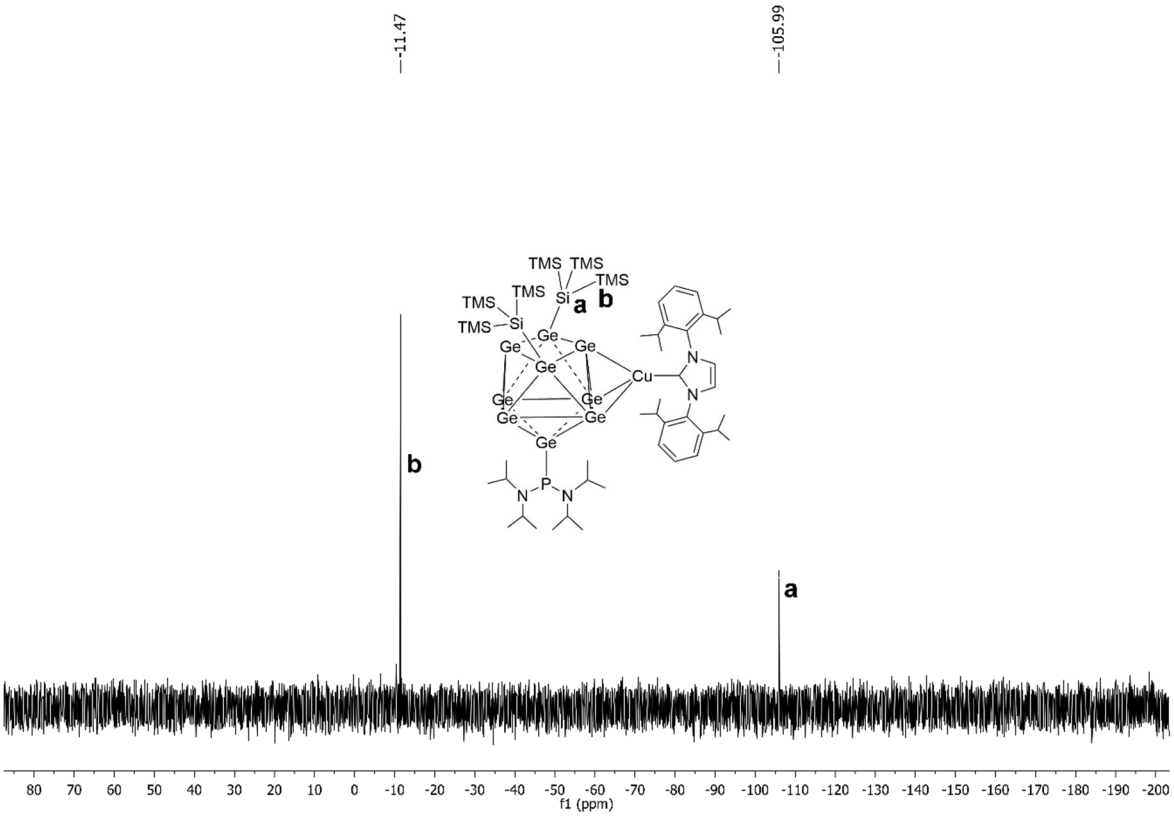

Figure SI 26:[29]Si-INEPT-RD NMR of compound **6** in thf-d_8.

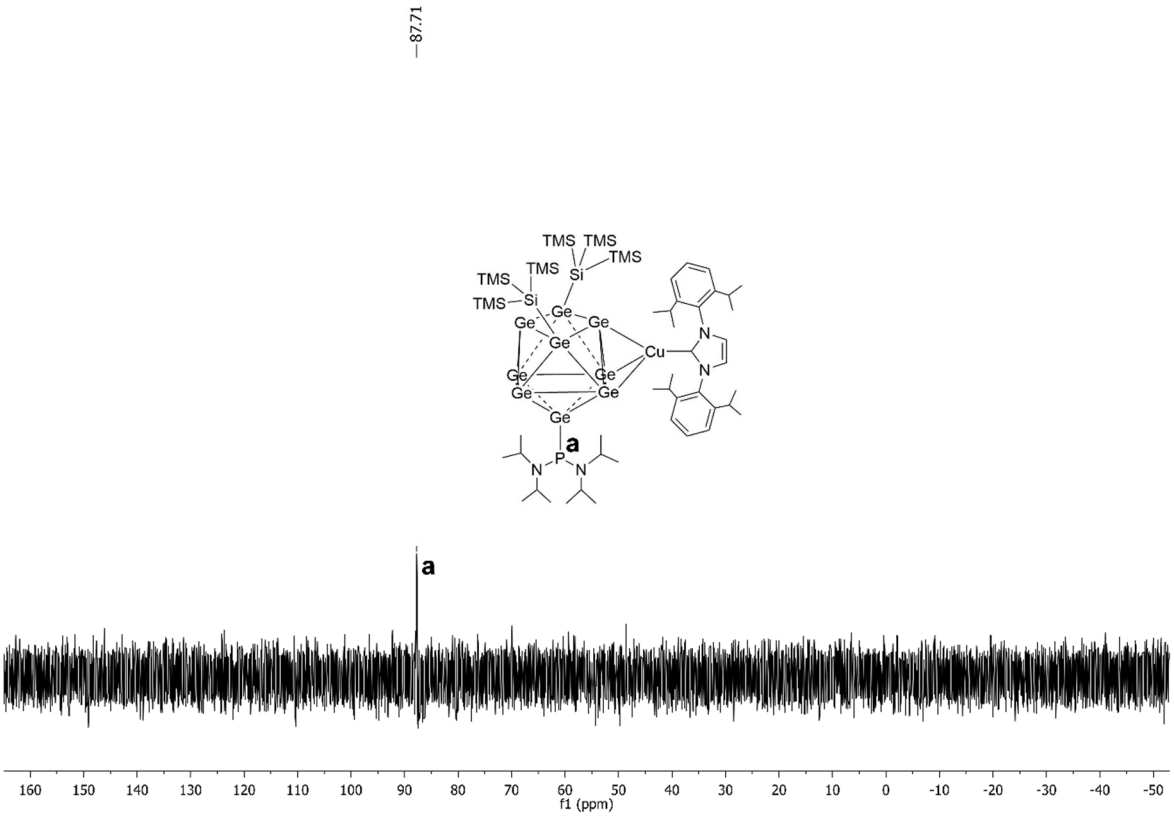

Figure SI 27:[31]P NMR of compound **6** in thf-d_8.

5.10 Enhancing the Variability of [Ge_9] Cluster Chemistry through Phosphine-Functionalization

C. Wallach,[‡] F. S. Geitner,[‡] W. Klein, T. F. Fässler*

[‡] authors contributed equally to this work.

Manuscript for publication

Content and Contributions

The scope of this work was the introduction of phosphanyl moieties with functional pentenyl substituents at the [Ge_9] cluster core, which might be used as anchor groups for the attachment of the germanide clusters at nanoparticles or other surfaces. Moreover, a series of novel mixed-functionalized [Ge_9] cluster anions was synthesized and their suitability to form zwitterionic compounds was tested by reacting them with $NHC^{Dipp}CuCl$. The novel pentenyl-functionalized chlorophosphine $^{t}Bu\{(CH_2)_3CH=CH_2\}PCl$ was synthesized in a Grignard reaction using $^{t}BuPCl_2$ and pentenylmagnesium bromide as starting materials. Subsequent reactions with $[Ge_9\{Si(TMS)_3\}_3]^-$ or $[Ge_9\{Si(TMS)_3\}_2]^{2-}$ resulted in the introduction of the pentenyl-functionalized phosphanyl moiety at both [Ge_9] cluster species, yielding neutral compound $[Ge_9\{Si(TMS)_3\}_3P^{t}Bu\{(CH_2)_3CH=CH_2\}]$ or the anionic species $[Ge_9\{Si(TMS)_3\}_2P^{t}Bu\{(CH_2)_3CH=CH_2\}]^-$. The synthesis of the pentenyl-functionalized chlorophosphine and the subsequent reactions with the silylated [Ge_9] clusters were carried out by M. Sc. Christoph Wallach. In the case of the neutral compound, single crystals and analytically pure samples were obtained by re-crystallization from toluene solution at low temperature and the crystal structure revealed the exposed nature of the alkenyl double bond. The crystal structure refinement, especially the modelling of the disordered phosphanyl group was supported by Dr. Wilhelm Klein. By contrast, the anionic species was characterized by NMR spectroscopy and ESI-MS spectrometry. Additionally, the synthesis of a series of novel mixed-functionalized [Ge_9] cluster anions $[Ge_9\{Si(TMS)_3\}_2RR^{I}P]^-$ (*R*: ^{i}Pr, R^{I}: ^{t}Bu; *R*: ^{t}Bu, R^{I}: NEt_2; *R* = R^{I}: 1,1-dimethylpropyl; *R* = R^{I}: 1-adamantyl; *R*: ^{i}Pr, R^{I}: $N^{i}Pr_2$; *R*: ^{t}Bu, R^{I}: $N^{i}Pr_2$; *R*: ^{t}Bu, R^{I}: Mes; *R* = R^{I} = *o*-tolyl) was achieved by reaction of the bis-silylated [Ge_9] cluster with the respective chlorophosphines and the obtained anions were characterized by means of NMR spectroscopy and ESI-MS. Subsequent reactions with $NHC^{Dipp}CuCl$ and NMR examination of the obtained neutral products allowed for the evaluation, whether the novel mixed-functionalized anions are suitable for the synthesis of zwitterionic compounds (for *R*: ^{i}Pr, R^{I}: ^{t}Bu; *R*: ^{t}Bu, R^{I}: NEt_2; *R* = R^{I}: dimethylpropyl; *R* = R^{I}: 1-adamantyl) or rather direct interactions of $[NHC^{Dipp}Cu]^+$ with the [Ge_9] cluster core occur (for *R*: ^{i}Pr, R^{I}: $N^{i}Pr_2$; *R*: ^{t}Bu, R^{I}: $N^{i}Pr_2$; *R*: ^{t}Bu, R^{I}: Mes; *R* = R^{I} = *o*-tolyl). Besides tremendously increasing the number of mixed-functionalized [Ge_9] clusters suitable for the straightforward synthesis of zwitterionic compounds, these results manifest that the steric impact of the phosphanyl group's substituents is the decisive factor for which interactions (P-Cu or Ge-Cu) occur. The synthesis of the mixed-functionalized [Ge_9] clusters and subsequent reactions with $NHC^{Dipp}CuCl$ were mostly carried out by M. Sc.Christoph Wallach. This publication was written in course of this thesis.

Enhancing the Variability of [Ge_9] Cluster Chemistry through Phosphine-Functionalization

Christoph Wallach,[a]‡ Felix S. Geitner,[b]‡ Wilhelm Klein[a] and Thomas F. Fässler[a]*

[‡] authors contributed equally to this work

[a] Department Chemie, Technische Universität München, Lichtenbergstraße 4, 85747 Garching b. München.

[b] Department Chemie, Technische Universität München, Lichtenbergstraße 4, 85747 Garching b. München and WACKER Institute for Silicon Chemistry.

Abstract

Herein we report the synthesis of a series of mixed-functionalized [Ge_9] clusters [Ge_9{$Si(TMS)_3$}$_3$P*RR*^{l}] (*R*: ^{t}Bu, *R*^{l}: $(CH_2)_3CH{=}CH_2$; **2**) and [Ge_9{$Si(TMS)_3$}$_2$P*RR*^{l}]$^-$ (*R*, *R*^{l}: alkyl, alkenyl, aryl, aminoalkyl; **3a**-**11a**). In **2** and **3a** pentenyl-functionalization of the [Ge_9] clusters was achieved by reaction of the novel chlorophosphine ^{t}Bu{$(CH_2)_3CH{=}CH_2$}PCl (**1**) with silylated [Ge_9] clusters. Furthermore, the reactivity of the cluster anions **3a**-**11a** towards $NHC^{Dipp}CuCl$ showed that in dependency on the phosphine's steric demand zwitterions (**3-CuNHC^{Dipp}-7-CuNHC^{Dipp}**) featuring P-Cu interactions are formed, or Ge-Cu coordination (**8-CuNHC^{Dipp}–11-CuNHC^{Dipp}**) occurs. Besides providing a novel variable method for the introduction of alkenyl moieties to [Ge_9] clusters, this work expands the spectrum of mixed-functionalized [Ge_9] cluster anions, which are suitable ligands for the straightforward synthesis of zwitterionic compounds upon coordinating transition metal cations with their phosphanyl moiety.

Introduction

Zintl phases K_4Ge_9 and $K_{12}Ge_{17}$, containing nine-atomic germanide clusters, are easily accessible from the elements in quantitative yield *via* solid state reactions. With respect to their straightforward synthesis and their interesting electronic properties (fourfold negative charge, however their shape can be explained by the *Wade-Mingos* rules for electron deficient cage compounds), the included [Ge_9] clusters are not only of interest regarding the synthesis of nanostructured materials, but are also interesting ligands with respect to organometallic chemistry.[1-4] In this context especially substituted [Ge_9] cages bearing multiple organic or main-group element substituents are interesting due to their decreased charge, which makes them soluble in standard solvents (MeCN and thf) and decreases their reductive nature at the same time. Examples for such [Ge_9] cages were originally found in the bis-vinylated species

$[Ge_9\{CH=CH_2\}_2]^{2-}$ [5] or the tris-silylated cluster $[Ge_9\{Si(TMS)_3\}_3]^-$,[6-8] however only for the latter species a prosperous subsequent chemistry evolved, introducing the tris-silylated $[Ge_9]$ cluster to organics,[9, 10] main group element compounds[9, 11] or transition metal complexes.[12-21] Subsequently, further silylated $[Ge_9]$ cluster species bearing various silyl substituents were reported[20-23], the number of the silyl substituents was varied (twofold substituted $[Ge_9]$ cluster $[Ge_9\{Si(TMS)_3\}_2]^{2-}$),[24] and tris-stannyl decoration of $[Ge_9]$ was achieved.[25, 26] However, the reactivity of these cluster species was limited to the $[Ge_9]$ cluster core due to the inert nature of the attached silyl or stannyl groups. For further expansion of the $[Ge_9]$ clusters chemistry, the introduction of functional and potentially reactive groups to the $[Ge_9]$ core was necessary. In previous studies we already achieved the attachment of $[PR_2]^+$ (*R*: alkyl, aryl, aminoalkyl) groups at tris- and bis-silylated $[Ge_9]$ clusters obtaining neutral species $[Ge_9\{Si(TMS)_3\}_3PR_2]$ (*R*: ^{i}Pr, Cy) or anionic clusters $[Ge_9\{Si(TMS)_3\}_2PR_2]^-$ (*R*: ^{t}Bu, Mes, N^{i}Pr$_2$), respectively. In subsequent reactions with the Lewis acidic copper NHC complex NHC^{Dipp}CuCl we found that the anionic species can interact with $[NHC^{Dipp}Cu]^+$ either *via* the $[Ge_9]$ cluster core forming $[Ge_9]$ cluster Cu-NHC compounds $[NHC^{Dipp}Cu(\eta^3\text{-}Ge_9\{Si(TMS)_3\}_2PR_2)]$ (*R*: Mes, N^{i}Pr$_2$) or with the electron lone-pair situated at the phosphorous atom under formation of the zwitterionic compound $[(Ge_9\{Si(TMS)_3\}_2)^tBu_2P]CuNHC^{Dipp}$.[27, 28] In this context the steric impact of the phosphanyl group's substituents appears to be the decisive factor for which interactions occur (smaller substituents: P-Cu; larger substituents: Ge-Cu). According to these findings, anionic mixed-functionalized clusters $[Ge_9\{Si(TMS)_3\}_2PR_2]^-$ can either be described as phosphine-substituted *Zintl* clusters (*R*: Mes, N^{i}Pr$_2$) or as *Zintl* cluster-substituted phosphines (*R*: ^{t}Bu). The latter species allows for the straightforward synthesis of zwitterionic compounds upon coordination to a transition metal cation, which might be of interest regarding catalytic applications.

In further approaches to obtain $[Ge_9]$ clusters with functional ligands, silylated $[Ge_9]$ cages were decorated with alkenyl moieties obtaining neutral compounds $[Ge_9\{Si(TMS)_3\}_3\{(CH_2)_n\text{-}CH=CH_2\}]$ (*n*: 1, 3),[10] or alkenyl functionalized silyl groups were introduced at bis-silylated $[Ge_9]$ clusters yielding $[Ge_9\{Si(TMS)_3\}_2\{SiPh_2(CH_2)_n\text{-}CH=CH_2\}]^-$ (*n*: 0, 3) and at bare $[Ge_9]^{4-}$ clusters obtaining $[Ge_9\{SiPh_2(CH_2)_n\text{-}CH=CH_2\}_3]^-$ (*n*: 0, 3).[29] Interesting aspects of the introduction of alkenyl moieties are that they might potentially be used as anchor groups with respect to the attachment of the germanium-rich clusters at nanoparticles and other surfaces or for the linkage of the $[Ge_9]$ clusters in order to build-up nanostructured materials. The requirements for optimal anchor groups are: straightforward introduction at $[Ge_9]$ clusters, variable applicability (e.g. for bis- and tris-silylated cluster compounds) and exposed position of the reactive terminal double bond upon attachment to the $[Ge_9]$ cluster. Alkenyl-functionalized phosphanyl groups fulfil most of the demands for such an anchor group (easy and variable introduction). In order to assure an exposed nature of the

reactive double bond a functionalized chlorophosphine with a long alkenyl chain was needed. However, reports on alkenyl-functionalized chlorophosphines are very rare and the reported molecules were only substituted with short alkenyl chains.[30, 31] Therefore, we investigated the synthesis of a novel chlorophosphine comprising a pentenyl group and examined its reactivity towards variously silylated [Ge_9] clusters. Furthermore, we synthesized a series of novel mixed-functionalized cluster anions [Ge_9{$Si(TMS)_3$}$_2$P*RR*^{I}]$^-$ (*R*, *R*^{I}: alkyl, aryl, aminoalkyl) and tested their suitability as ligands for the straightforward synthesis of zwitterionic compounds upon reaction with NHC^{Dipp}CuCl.

Results and Discussion

The pentenyl-functionalized chlorophosphine ^{t}Bu{$(CH_2)_3CH=CH_2$}PCl (**1**) was obtained by reaction of a freshly prepared 5-bromomagnesiumpentene Grignard solution with ^{t}BuPCl$_2$ in diethylether. In order to assure the mono alkenylation of ^{t}BuPCl$_2$ a slight excess (1.25 eq.) of the dichlorophosphine was used. The purification of **1** occurred *via* vacuum distillation obtaining compound **1** as colourless liquid in medium yield. In the next step we tested the reactivity of **1** towards the tris-silylated cluster [Ge_9{$Si(TMS)_3$}$_3$]$^-$ and the bis-silylated cluster [Ge{$Si(TMS)_3$}$_2$]$^{2-}$. For reactions of **1** with [Ge_9{$Si(TMS)_3$}$_3$]$^-$, the silylated cluster was dissolved in toluene and a toluene solution of **1** was added. The resulting deep red reaction mixture was stirred at r. t. for 1 h before the solvent was removed *in vacuo* and the remaining brownish solid was washed with MeCN to remove excessive reactants. ^{1}H NMR examination of the crude product implicated the attachment of a [^{t}Bu{$(CH_2)_3CH=CH_2$}P]$^+$ moiety to [Ge_9{$Si(TMS)_3$}$_3$]$^-$ according to the observed signal ratio. Subsequently, the solid was dissolved in toluene, filtered to remove insoluble materials and stored in a freezer at -40 °C, yielding orange block-shaped crystals. The single crystal data confirmed the attachment of the pentenyl functionalized phosphanyl moiety at the [Ge_9] cluster under formation of the neutral compound [Ge_9{$Si(TMS)_3$}$_3$P^{t}Bu{$(CH_2)_3CH=CH_2$}] (**2**). Compound **2** crystallizes in the triclinic space group *P*-1, with the unit cell containing two formula units. The shape of the [Ge_9] cluster core can be best described as slightly distorted capped square antiprism (C_{4v} symmetry). The Ge-Ge distances range between 2.4715(6) Å (Ge1-Ge2) and 3.1642(6) Å (Ge5-Ge8) with the shortest distances in the open square plane and the longest distances in the Ge capped square. The hypersilyl groups are attached at two opposite Ge vertices (Ge2 and Ge4) within the open square plane of the cluster and at the capping Ge atom (Ge9) with distances between 2.374 Å (Ge9-Si9) and 2.404 Å (Ge2-Si1), that are in the range of previously reported data.[19, 27, 28] The disordered phosphanyl group is attached to a further Ge vertex within the open square plane of the [Ge_9] cluster and the two individuals reveal Ge-P bonding distances of

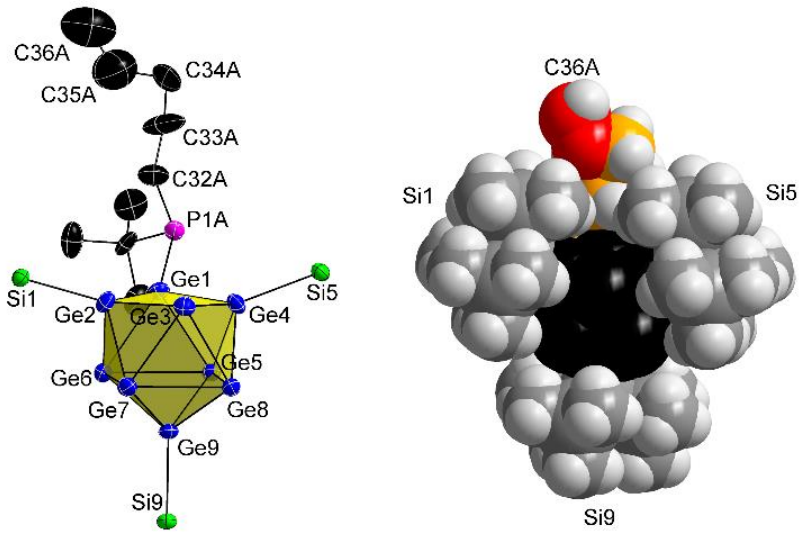

Figure 1. Left: Molecular structure of compound **2**, showing the C_{4v} symmetric shape of the [Ge_9] cluster core and the attachment of all ligands *via* 2-centre-2-electron *exo* bonds. All ellipsoids are shown at a 50 % probability level. For clarity, the TMS groups of the silyl ligands and all protons are omitted. Right: Space filling model of compound **2**, showing the exposed nature of the double bond of the pentenyl group. Hydrocarbon chain is shown in orange and the carbon atoms connected by the double bond (C35A and C36A) are presented in red. For clarity, in both pictures only the major individual of the disordered phosphanyl group is shown. Selected distances of **2** and pictures comprising the minor phosphanyl individual are provided in the Supporting information.

2.362(2) Å (Ge1-P1A) or 2.337(2) Å (Ge1-P1B), which are also in the range of reported Ge-P single bonds (Figure 1).[27, 28, 32] The observed disorder probably results from the pyramidal inversion of the ligands bound to the P atom (P1A: Ge1, C28A, C32A; P1B: Ge1, C28B, C32B). Both individuals of the disordered phosphanyl moiety point radially away from the centre of the [Ge_9] cluster manifested by the angles Ge3-Ge1-P1A: 137.76(5)° and Ge3-Ge1-P1B: 137.61(8)° proving the nature of the Ge-P interaction as a covalent 2-centre-2-electron *exo* bond. The functional pentenyl group reveals an exposed position and is not encumbered by any other ligands (space filling model), which might allow for further reactions at the alkenyl site (Figure 1, Supporting information). Reactions of **1** with the bis-silylated cluster $[Ge_9\{Si(TMS)_3\}_2]^{2-}$ were carried out in MeCN. Addition of a solution of **1** in MeCN to an acetonitrile solution of $[Ge_9\{Si(TMS)_3\}_2]^{2-}$ resulted in a deep red reaction mixture, which was stirred at r. t. for 1 h, before the mixture was filtered to remove all solids and the solvent was removed *in vacuo*. NMR examination of the obtained brownish solid revealed the formation of the mixed-functionalized anion $[Ge_9\{Si(TMS)_3\}_2P^tBu\{(CH_2)_3CH{=}CH_2\}]^-$ (**3a**) according to the observed signal ratio. In ESI-MS examinations the molecule peak of **3a** was monitored at *m/z* 1306.8 (Figure 2). Hence, the pentenyl-functionalized chlorophosphine **1** is a suitable precursor for the introduction of pentenyl anchor groups at variously silylated [Ge_9] clusters comprising varying charge and steric shielding of the [Ge_9] cluster core.

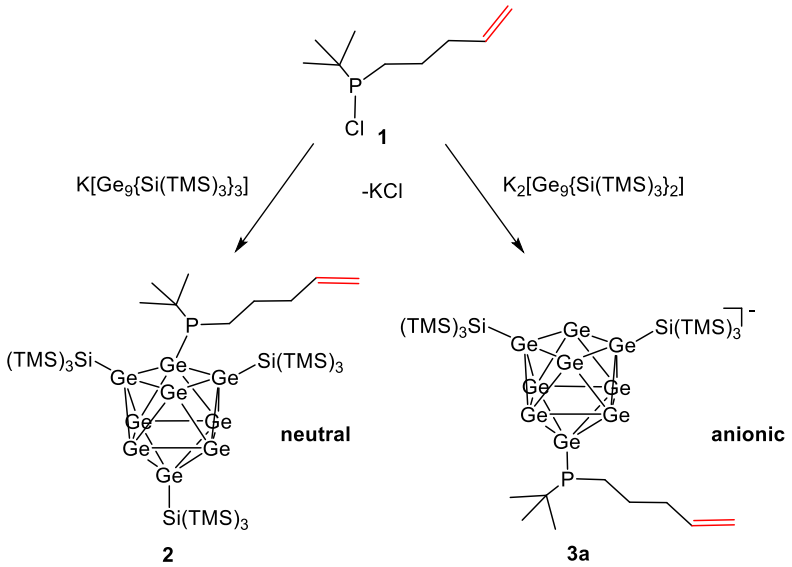

Scheme 1. Reactions of novel pentenyl-functionalized chlorophosphine **1** with tris-silylated cluster $[Ge_9\{Si(TMS)_3\}_3]^-$ (left) or bis-silylated cluster $[Ge_9\{Si(TMS)_3\}_2]^{2-}$ (right) yielding neutral species **2** or anion **3a** comprising a pentenyl anchor group attached at the $[Ge_9]$ cluster *via* the phosphanyl moiety.

In further investigations we synthesized a series of mixed-functionalized $[Ge_9]$ anions $[Ge_9\{Si(TMS)_3\}_2PRR^l]^-$ (**4a**: *R*: ^{i}Pr, *R*^{l}: ^{t}Bu; **5a**: *R*: ^{t}Bu, *R*^{l}: NEt_2; **6a**: *R* = *R*^{l}: 1,1-dimethylpropyl; **7a**: *R* = *R*^{l}: 1-adamantyl; **8a**: *R*: ^{i}Pr, *R*^{l}: N^{i}Pr$_2$; **9a**: *R*: ^{t}Bu, *R*^{l}: N^{i}Pr$_2$; **10a**: *R*: ^{t}Bu, *R*^{l}: Mes; **11a**: *R* = *R*^{l}: *o*-tolyl) and tested their suitability to readily form zwitterionic compounds by reaction with NHC^{Dipp}CuCl and subsequent NMR examination (Table 1). The anionic clusters **4a**-**11a** were obtained by reactions of bis-silylated cluster $[Ge_9\{Si(TMS)_3\}_2]^{2-}$ with the respective chlorophosphines *RR*^{l}PCl in acetronitrile, yielding the crude products as brownish solids in medium to good yield after filtration of the reaction solutions and removal of the solvent *in vacuo* (in analogy to **3a**). The novel anions were characterized by NMR spectroscopy (chemical shift of silyl group signals around 0.25 ppm) and ESI-MS investigations (monitoring of molecule peaks). All NMR and ESI-MS spectra are presented in the Supporting information.

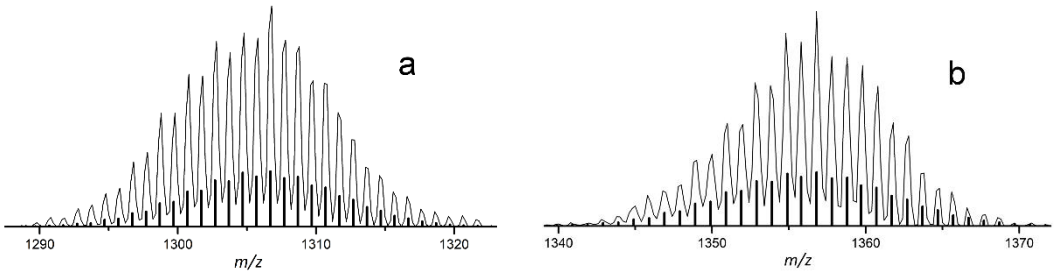

Figure 2. ESI-MS spectra of anions **3a** (a) and **10a** (b). Spectrum a was recorded from thf solution in the negative ion mode (3500 V, 300 °C) monitoring the molecule peak of **3a** at *m/z* 1306.8. Spectrum b was obtained from thf solution in negative ion mode (3500 V, 300 °C) monitoring the molecule peak of **10a** at *m/z* 1356.8. Calculated patterns are presented as black bars. All other ESI-MS spectra are provided in the Supporting information.

Interestingly, reactions of the electron poor chlorophosphine $(C_6F_5)_2PCl$, which is of similar bulkiness as $^tBu_2PCl$, with $[Ge_9\{Si(TMS)_3\}_2]^{2-}$ were not successful and resulted in unknown products. This indicates that a certain basicity of the applied chlorophosphines is mandatory for the successful synthesis of mixed-functionalized [Ge_9] clusters (all other tested chlorophosphines had increased donor strength according to the Tolman electronic parameter).[33] Reactions of **3a**-**11a** with $NHC^{Dipp}CuCl$ were carried out by adding MeCN solutions of $NHC^{Dipp}CuCl$ to freshly prepared solutions of the respective anions **3a**-**11a** in MeCN, which resulted in the immediate formation of brownish precipitates. The supernatant solutions were filtered off, the residues were washed with MeCN and the resulting red to brown solids were examined by NMR spectroscopy proving the attachment of $[NHC^{Dipp}Cu]^+$ moieties to the anions **3a**-**11a** under formation of the neutral compounds **3-CuNHC^{Dipp}**-**11-CuNHC^{Dipp}**. In order to determine whether a zwitterionic compound with P-Cu interactions or a [Ge_9] cluster Cu-NHC compound (Ge-Cu interactions) was formed, the chemical shift of the silyl groups' methyl protons, which is very sensitive with regard to the number of substituents directly bound to the [Ge_9] cluster core, was used. If a zwitterionic compound is formed, the silyl group's proton signal is not significantly shifted since the [Ge_9] core is not directly affected. By contrast, the addition of a $[NHC^{Dipp}Cu]^+$ fragment to the [Ge_9] core increases the number of substituents at the [Ge_9] cluster and the silyl group's proton signal is shifted highfield.[10]

Using this method, the anions **3a**-**7a** could be identified to react as *Zintl* cluster substituted-phosphines (no significant shift of silyl groups' signal upon coordination of $[NHC^{Dipp}Cu]^+$), being suitable ligands for the synthesis of zwitterionic compounds $[(Ge_9\{Si(TMS)_3\}_2)RR^lP]CuNHC^{Dipp}$ **3-CuNHC^{Dipp}**-**7-CuNHC^{Dipp}** comprising P-Cu interactions. By contrast, anions **8a**-**11a** can be described as phosphine-substituted *Zintl* clusters since the [Ge_9] cluster core directly interacts with the $[NHC^{Dipp}Cu]^+$ moiety (indicated by the highfield shift of the silyl groups' proton signal upon coordination of $[NHC^{Dipp}Cu]^+$) under formation of [Ge_9] cluster copper NHC compounds $[NHC^{Dipp}Cu(\eta^3\text{-}Ge_9\{Si(TMS)_3\}_2PRR^l)]$ **8-CuNHC^{Dipp}**-**11-CuNHC^{Dipp}** (Table 1, Figure 3). Hence, mixed-functionalized [Ge_9] cluster anions with phosphanyl groups bearing one *tert*-butyl group and another smaller ligand (**3a**-**5a**), as well as phosphine moieties with slightly larger 1,1-dimethylpropyl (**6a**), or 1-adamanytl groups (**7a**), if compared to $[^tBu_2P]^+$,[33-35] are suitable precursors for the straightforward synthesis of zwitterionic compounds upon coordination to a transition metal cation.

By contrast, more bulky substituents such as N^iPr_2 or Mes do not allow for P-Cu interactions, even with the second substituent at phosphorus being a smaller *tert*-butyl (**9a**, **10a**) or *iso*-propyl group (**8a**). Similar reactivity is observed upon introduction of $[(o\text{-tolyl})_2P]^+$ (**11a**).

Table 1. ^{1}H NMR shifts of the methyl protons of the silyl groups of mixed-functionalized [Ge_9] cluster anions [Ge_9{$Si(TMS)_3$}$_2$P*RR'*]$^-$ (**3a**-**11a**) and respective zwitterionic compounds **3-CuNHC^{Dipp}-7-CuNHC^{Dipp}** (left) or [Ge_9] cluster Cu-NHC compounds **8-CuNHC^{Dipp}-11-CuNHC^{Dipp}** (right). The change of the shift value Δshift upon coordination of [NHC^{Dipp}Cu]$^+$ to the cluster anions allows for the determination of the nature of the interactions.

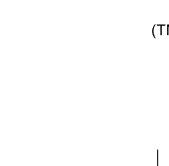

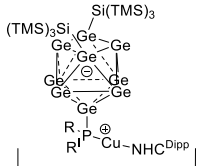

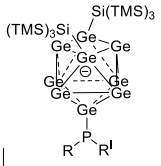

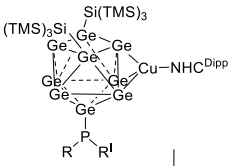

		[ppm]	[ppm]	Δshift		[ppm]	[ppm]	Δshift
3	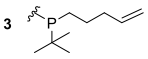	0.26 **3a**	0.25 **3-CuNHC^{Dipp}**	-0.01	8	0.25 **8a**	0.19 **8-CuNHC^{Dipp}**	-0.06
4		0.26 **4a**	0.27 **4-CuNHC^{Dipp}**	0.01	9	0.25 **9a**	0.19 **9-CuNHC^{Dipp}**	-0.06
5	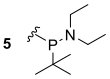	0.25 **5a**	0.23 **5-CuNHC^{Dipp}**	-0.02	10	0.25 **10a**	0.19 **10-CuNHC^{Dipp}**	-0.06
6	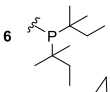	0.25 **6a**	0.27 **6-CuNHC^{Dipp}**	0.02	11	0.27 **11a**	0.19 **11-CuNHC^{Dipp}**	-0.08
7	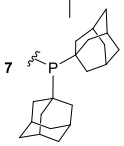	0.26 **7a**	0.28 **7-CuNHC^{Dipp}**	0.02				

These findings confirm that the steric impact of the phosphanyl group's substituents is the decisive factor if mixed-functionalized [Ge_9] clusters are capable to coordinate Cu^+ with their phosphanyl moiety and are thus suitable ligands for the straightforward synthesis of zwitterionic organometallic complexes.

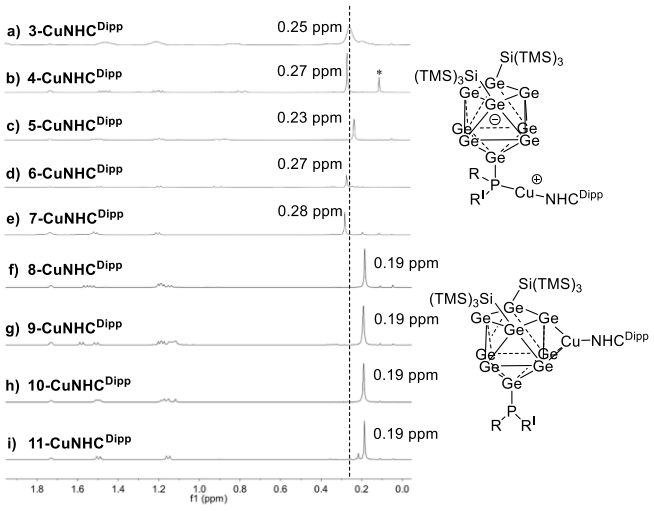

Figure 3. Selected areas of the ^{1}H NMR spectra of compounds **3-CuNHC^{Dipp}-11-CuNHC^{Dipp}** in thf-d_8 allowing for the determination of the interactions (P-Cu or Ge-Cu) between the mixed-functionalized cluster anions **3a**-**11a** and the [NHC^{Dipp}Cu]$^+$ moiety, using the chemical shift of the silyl groups' methyl proton signal as indicator. Dashed line is at chemical shift value of 0.25 ppm. Asterisked signal belongs to silicon grease impurity.

Conclusions

Within this work we achieved the synthesis of a pentenyl-functionalized chlorophosphine (**1**) and provided a novel variable method for the introduction of exposed alkenyl anchor groups at variously silylated [Ge_9] clusters *via* the phosphanyl moiety, yielding neutral compound **2** or the anion **3a**. Moreover, a series of mixed-functionalized anions [Ge_9{$Si(TMS)_3$}$_2$P*RR'*]$^-$ (**4a**-**11a**) was synthesized and the reactivity of the anions **3a**-**11a** towards $NHC^{Dipp}CuCl$ was tested. The novel anions **3a**-**7a** were identified to react as [Ge_9] cluster substituted-phosphines and are suitable ligands for the formation of zwitterionic compounds **3-CuNHC^{Dipp}-7-CuNHC^{Dipp}** (P-Cu interactions). By contrast, anions **8a**-**11a** can be regarded as phosphine-substituted *Zintl* clusters and form neutral [Ge_9] cluster Cu-NHC compounds **8-CuNHC^{Dipp}-11-CuNHC^{Dipp}** (Ge-Cu interactions). Besides expanding the spectrum of mixed-functionalized [Ge_9] clusters suitable for the synthesis of zwitterionic compounds upon coordination of a transition metal cation (**3a**-**7a**), the obtained results confirm that the steric impact of the phosphanyl group's substituents is the decisive factor for the reactivity of the mixed-functionalized [Ge_9] clusters.

Experimental Section

General

All manipulations were performed under oxygen-free, dry conditions under argon atmosphere using standard Schlenk or glove box techniques. Glassware was dried prior to usage by heating it *in vacuo*. The solvents used were obtained from an *MBraun* Grubbs apparatus. All other commercially available chemicals were used without further purification. K_4Ge_9 was prepared by fusion of stoichiometric amounts of the elements in stainless-steel tubes at 650 °C. The silylated cluster compounds K[Ge_9{$Si(TMS)_3$}$_3$] and K_2[Ge_9{$Si(TMS)_3$}$_2$],[7, 24] the chlorophosphines $MesPCl_2$,[36] $^iPr^tBuPCl$,[37] $^tBu(NEt_2)PCl$,[38] (1,1-dimethylpropyl)$_2$PCl,[39] $^iPr(N^iPr_2)PCl$,[40] $^tBu(N^iPr_2)PCl$,[40] $^tBuMesPCl$,[41] $(C_6F_5)_2PCl$,[42] the imidazolium salt NHC^{Dipp}·HCl and the corresponding Cu-NHC complex were synthesized according to modified literature procedures.[7, 23, 24, 43-45]

Single Crystal Structure Determination

The air- and moisture-sensitive crystals of **2** were transferred from the mother liquor into cooled perfluoroalkyl ether oil under a cold stream of N_2 gas. For diffraction data collection, the single crystals were fixed on a glass capillary and positioned in a 150 K cold N_2 gas stream using the crystal cap system. Data collection was performed with a STOE StadiVari (MoK_α radiation) diffractometer equipped with a DECTRIS PILATUS 300K detector. The structure was solved by Direct Methods (SHELXS-2014) and refined by full-matrix least-squares calculations against F^2 (SHELXL-2014).[46] The positions of the hydrogen atoms were calculated and

refined using a riding model. Unless stated otherwise, all non-hydrogen atoms were treated with anisotropic displacement parameters. The supplementary crystallographic data for this paper have been deposited with the Cambridge Structural database and are available free of charge *via* www.ccdc.cam.ac.uk/data_request/cif. The crystallographic data for compound **2** is summarized in Table 2. In compound **2** the phosphanyl group attached at the [Ge_9] cluster is disordered and was refined on split positions. The carbon atoms 32A/B or 36A/B were refined with identical room coordinates and the carbon atoms C28A/B, C32A/B, C34A/B, C36A/B were refined with identical anisotropic vibrational parameters. Furthermore, some of the carbon atoms of the phosphanyl moiety were treated with ISOR restraints (C29A, C35A/B, C36A/B).

NMR Spectroscopy

NMR spectra were measured on a Bruker Avance Ultrashield 400 MHz spectrometer. The ^{1}H NMR spectra were calibrated using the residual proton signal of the used deuterated solvents. Chemical shifts are reported in parts per million (ppm) relative to TMS, with the solvent peaks serving as internal reference.[47] Abbreviations for signal multiplicities are: singlet (s), doublet (d), triplet (t), heptet (hept). ^{29}Si NMR spectra were acquired with the ^{29}Si-INEPT-RD method (RD: refocused with decoupling). In some of the ^{13}C NMR spectra the methyl groups of the Dipp substituents of the NHC ligand overlap with the thf solvent signal and could therefore not be properly assigned. The carbene carbon signals could not be monitored in any of the ^{13}C NMR spectra of compounds **3-NHC^{Dipp}**-**11-NHC^{Dipp}**. In the ^{29}Si-INEPT-RD spectra of compounds **8-CuNHC^{Dipp}** and **9-CuNHC^{Dipp}**, the Si_{Ge9} Signal could not be detected. All recorded NMR spectra are provided in the Supporting information.

Table 2. Crystallographic data of compound **2**.

Compound	**2**
formula	$C_{36}H_{99}Ge_9Si_{12}P$
fw [g·mol^{-1}]	1552.86
space group	*P-1*
a [Å]	9.7899(5)
b [Å]	14.9782(5)
c [Å]	25.002(1)
α [°]	80.934(3)
β [°]	83.629(3)
γ [°]	84.714(3)
V [Å^3]	3587.5(3)
Z	2
T [K]	123
λ [Å]	MoK_α
ρ_{calcd} [g·cm^{-3}]	1.440
μ [mm^{-1}]	3.960
collected reflections	56768
independent reflections	14066
R_{int} / R_δ	0.0568/0.0383
parameters / restraints	618/40
R_1 [$I > 2\,\sigma(I)$ / all data]	0.0397/0.0566
wR_2 [$I > 2\,\sigma(I)$ / all data]	0.0937/0.1041
goodness of fit	1.043
max./min. diff. el. density [e / Å^{-3}]	0.93/-0.74
CCDC	1831874

Electrospray Ionization Mass Spectrometry (ESI-MS)

ESI-MS analyses were performed on a Bruker Daltronic HCT mass spectrometer (dry gas temperature: 300 °C; injection speed: 240 µL/h) and the data evaluation was carried out using the Bruker Compass Data Analysis 4.0 SP 5 program (*Bruker*). Spectra were plotted using OriginPro2016G (*OriginLab*). All acquired ESI-MS spectra are provided in the Supporting information.

Elemental Analyses (EA)

Elemental analyses were carried out in the microanalytical laboratory of the Chemistry Department of Technische Universität München. Analyses of C, H, N were performed in a combustion analyzer (elementar vario EL, *Bruker*).

Syntheses

^{t}Bu{(CH$_2$)$_3$CH=CH$_2$}PCl (1):

5-bromopentene (5.0 g, 33.5 mmol, 1 eq.) was added dropwise to a suspension of magnesium shavings (4.0 g, 164.0 mmol, 4.9 eq.) in Et_2O (50 mL) under constant reflux (two grains of iodine were added for activation). After complete addition of the halide, the mixture was refluxed for further 3.5 h. The concentration of the obtained *Grignard* solution was determined to be 0.6 mol/l by titration of menthol using 1,10-phenanthroline as indicator. Subsequently, the *Grignard* solution (30 mL, 18.1 mmol, 1 eq.) was dropwise added to a solution of $^{t}Bu_2PCl$ (3.60 g, 22.6 mmol, 1.25 eq.) in Et_2O (50 mL) at -78 °C, before the cooling was removed and the reaction solution was allowed to warm-up to room temperature. Addition of hexane (30 mL) led to the formation of a colorless precipitate and the resulting suspension was stirred at r. t. overnight. The mixture was filtered to remove all solids and the solvent was removed *in vacuo* to yield the crude product. Purification occurred by vacuum distillation ($9 \cdot 10^{-3}$ mbar, 41 °C), yielding **1** as colorless liquid (0.90 g, 23 %).**^{1}H NMR** (400 MHz, 298 K, $CDCl_3$): δ [ppm] = 5.84 – 5.75 (m, 1H, CH_{db}), 5.07 – 4.08 (m, 2H, $CH_{2(db)}$), 2.23 – 1.18 (m, 2H, CH_2), 1.87 – 1.56 (m, 4H, CH_2), 1.16 (d, $^{3}J_{HP}$ = 13.0 Hz, 9H, Me_{tBu}). **^{13}C NMR** (101 MHz, 298 K, $CDCl_3$): δ [ppm] = 137.99 (s, CH_{db}), 115.47 (s, $CH_{2(db)}$), 34.83 (m, CH_2), 32.54 (d, $^{1}J_{CP}$ = 28.6 Hz C_{tBu}), 29.57 (d, $^{1}J_{CP}$ = 35.2 Hz, CH_2), 26.10 (d, $^{2}J_{CP}$ = 16.8 Hz, Me_{tBu}), 25.46 (d, $^{2}J_{CP}$ = 16.8 Hz, Me_{tBu}) 24.72 (d, $^{2}J_{CP}$ = 16.0 Hz, CH_2). **^{31}P NMR** (162 MHz, 298 K, $CDCl_3$): δ [ppm] = 128.41 (m, P_{Ge9}).

$[Ge_9\{Si(TMS)_3\}_3P^tBu\{(CH_2)_3CH=CH_2\}]$ (2):

$K[Ge_9\{Si(TMS)_3\}_3]$ (70 mg, 0.049 mmol, 1 eq.) was dissolved in toluene (1 mL) and a toluene solution (1 mL) of $^tBu\{(CH_2)_3CH=CH_2\}PCl$ (10.6 mg, 0.049 mmol, 1 eq.) was added, yielding a deep red reaction mixture. After stirring at r. t. for 1 h, the solvent was removed under reduced pressure and the obtained dark brown solid was washed with acetonitrile (3 x 2 mL). Subsequently, the solid was dissolved in toluene (1 mL), filtered to remove insoluble materials and stored in a freezer at -40 °C, yielding the purified product as orange crystals (25.9 mg, 35 %).**^{1}H NMR** (400 MHz, 298 K, C_6D_6): δ [ppm] = 5.94 – 5.84 (m, 1H, CH_{db}), 5.20 – 5.07 (m, 2H, $CH_{2(db)}$), 2.28 – 2.19 (m, 2H, CH_2), 2.19 – 2.10 (m, 2H, CH_2), 1.95 – 1.82 (m, 2H, CH_2), 1.34 (d, $^3J_{HP}$ = 11.4 Hz, 9H, Me_{tBu}), 0.47 (s, 81H, Me_{TMS}).**^{13}C NMR** (101 MHz, 298 K, C_6D_6): δ [ppm] = 138.38 (s, CH_{db}), 115.53 (s, $CH_{2(db)}$), 36.05 (d, $^1J_{CP}$ = 13.0 Hz, CH_2), 31.46 (d, $^2J_{CP}$ = 13.9 Hz, Me_{tBu}), 30.26 (d, $^3J_{CP}$ = 21.9 Hz, CH_2), 28.78 (d, $^1J_{CP}$ = 30.0 Hz, C_{tBu}), 27.93 (d, $^2J_{CP}$ = 30.1 Hz, CH_2), 3.10 (s, Me_{TMS}). **^{29}Si-INEPT NMR** (79 MHz, 298 K, C_6D_6): δ [ppm] = -8.31 (s, Si_{TMS}), -102.52 (s, Si_{Ge9}).**^{31}P NMR** (162 MHz, 298 K, C_6D_6): δ [ppm] = 19.46 (m, P_{Ge9}). **EA:** anal. calcd. for $Ge_9Si_{12}P_1C_{36}H_{99}$: C, 27.8; H, 6.4; found: C, 27.8; H, 6.4.

General Procedure for Syntheses of $K[Ge_9\{Si(TMS)_3\}_2PRR']$ (3-11)

$K_2[Ge_9\{Si(TMS)_3\}_2]$ was dissolved in MeCN and an acetonitrile solution of the respective chlorophosphine was added. The resulting mixtures were stirred at r. t. for 1 h, before the solutions were filtered to remove all solids and the solvents were removed *in vacuo* to yield the crude products of compounds **3**-**11** as brownish solids.

General Procedure for Syntheses of $[(Ge_9\{Si(TMS)_3\}_2)RR'P]CuNHC^{Dipp}$ (3-$CuNHC^{Dipp}$-7-$CuNHC^{Dipp}$) and $[NHC^{Dipp}Cu(\eta^3\text{-}Ge_9\{Si(TMS)_3\}_2PRR')]$ (8-$CuNHC^{Dipp}$-11-$CuNHC^{Dipp}$)

$K_2[Ge_9\{Si(TMS)_3\}_2]$ was dissolved in MeCN and the respective chlorophosphine dissolved in MeCN was added. The resulting mixtures were stirred at r. t. for 1 h, before a solution of $NHC^{Dipp}CuCl$ in MeCN was dropwise added, resulting in the formation of red to brown precipitates. The supernatant solutions (slightly orange) were filtered-off and the solids were washed with acetonitrile. Subsequently, the solids were dissolved in toluene and filtered to remove insoluble materials, before the solvent was removed *in vacuo* to yield the crude products as red to brown solids.

$K[Ge_9\{Si(TMS)_3\}_2P^tBu\{(CH_2)_3CH=CH_2\}]$ (3):

$K_2[Ge_9\{Si(TMS)_3\}_2]$ (100 mg, 0.082 mmol, 1 eq.) and $^tBu(CH_2)_3CH=CH_2PCl$ (20.5 mg, 0.107 mmol, 1.3 eq.) in MeCN (2 + 1 mL). The crude product was obtained as brown solid (72 mg, 65 %).**^{1}H NMR** (400 MHz, thf-d_8, 298 K): δ [ppm] = 7.26 – 7.07 (m, 1H, CH_{db}),

5.91 – 5.68 (m, 2H, $CH_{2(db)}$), 2.26 – 2.11 (m, 2H, CH_2), 2.10 – 2.01 (m, 2H, CH_2), 1.71 – 1.63 (m, 2H, CH_2), 1.14 (d, $^3J_{HP}$ = 11.4 Hz, 9H, Me_{tBu}), 0.26 (s, 54H, Me_{TMS}). **^{13}C NMR** (101 MHz, thf-d_8, 298 K): δ [ppm] = 139.23 (s, CH_{db}), 115.28 (s, $CH_{2(db)}$), 36.67 (s, CH_2), 36.01 (s, CH_2), 31.07 (s, C_{tBu}), 29.47 (s, Me_{tBu}), 19.24 (d, $^1J_{CP}$, CH_2), 3.20 (s, Me_{TMS}). **^{29}Si-INEPT NMR** (79 MHz, thf-d_8, 298 K): δ [ppm] = -11.32 (s, Si_{TMS}), -109.61 (s, Si_{Ge9}). **^{31}P NMR** (400 MHz, thf-d_8, 298 K): δ [ppm] = 4.11 (m, P_{Ge9}). **ESI-MS:** (negative ion mode, 3500 V, 300 °C): *m/z* 1306.8 $[Ge_9\{Si(TMS)_3\}_2P^tBu(CH_2)_3CH{=}CH_2]^-$.

$[(Ge_9\{Si(TMS)_3\}_2)\{^tBu(CH_2)_3CH{=}CH_2\}P]CuNHC^{Dipp}$ (3-$CuNHC^{Dipp}$):

$K_2[Ge_9\{Si(TMS)_3\}_2]$ (100 mg, 0.082 mmol, 1 eq.) and $\{^tBu(CH_2)_3CH{=}CH_2\}PCl$ (20.5 mg, 0.107 mmol, 1.3 eq.) in MeCN (2 + 1 mL). $NHC^{Dipp}CuCl$ (39.6 mg, 0.082 mmol, 1 eq.) in MeCN (2 mL). The crude product was obtained as dark brown solid (75 mg, 52 %). **^{1}H NMR** (400 MHz, thf-d_8, 298 K): δ [ppm] = 7.56 (s, 2H, CH_{Im}), 7.47 (s, 2H, $CH_{Ph(p)}$), 7.39 (s, 4H, $CH_{Ph(m)}$), 5.74 – 5.57 (m, 1H, CH_{db}), 4.98 – 4.85 (m, 2H, CH_{2db}), 2.87 – 2.72 (m, 4H, CH_{iPr}), 2.01 – 1.87 (m, 6H, CH_2), 1.46 (s, 12H, Me_{iPr}), 1.21 (s, 12H, Me_{iPr}), 0.83 (d, $^3J_{HP}$ = 12.1 Hz, 9H, Me_{tBu}), 0.25 (s, 54H, Me_{TMS}). **^{13}C NMR** (101 MHz, thf-d_8, 298 K): δ [ppm] = 146.34 (s, $C_{Ph(o)}$), 139.09 (s, CH_{db}), 136.30 (s, C_{PhN}), 131.63 (s, $CH_{Ph(p)}$), 125.37 (s, $CH_{Ph(m)}$), 125.08 (s, CH_{Im}), 115.24 (s, CH_{2db}), 36.48 (s, CH_2), 30.18 (s, CH_{iPr}), 29.83 (s, Me_{tBu}), 29.67 (s, CH_2), 29.49 (s, CH_2), 26.19 (s, C_{tBu}), 3.14 (s, Me_{TMS}). **^{29}Si-INEPT NMR** (79 MHz, thf-d_8, 298 K): δ [ppm] = -11.02 (s, Si_{TMS}), -107.01 (s, Si_{Ge9}). **^{31}P NMR** (162 MHz, thf-d_8, 298 K): δ [ppm] = 8.33 (m, P_{Ge9}).

$K[Ge_9\{Si(TMS)_3\}_2P^iPr^tBu]$ (4):

$K_2[Ge_9\{Si(TMS)_3\}_2]$ (36.8 mg, 0.030 mmol, 1 eq.) and $^iPr^tBuPCl$ (7.4 mg, 0.033 mmol, 1.1 eq.) in MeCN (1 + 1 mL). The crude product was obtained as brown solid (29 mg, 74 %). **^{1}H NMR** (400 MHz, 298 K, thf-d_8): δ [ppm] = 2.00 (hept, 1H, CH_{iPr}), 1.24 – 1.07 (m, 6H, Me_{iPr}), 1.20 (d, $^3J_{HP}$ = 11.0 Hz, 9H, Me_{tBu}), 0.26 (s, 54H, Me_{TMS}). **^{13}C NMR** (101 MHz, thf-d_8, 298 K): δ [ppm] = 32.40 (s, CH_{iPr}), 29.89 (s, Me_{tBu}), 27.40 (s, Me_{iPr}), 26.52 (d, $^1J_{CP}$ = 10.8 Hz, C_{tBu}), 3.18 (s, Me_{TMS}). **^{29}Si-INEPT NMR** (79 MHz, thf-d_8, 298 K): δ [ppm] = -11.53 (s, Si_{TMS}), -109.67 (s, Si_{Ge9}). **^{31}P NMR** (162 MHz, 298 K, thf-d_8): δ [ppm] = 35.55 (m, P_{Ge9}). **ESI-MS** (negative ion mode, 3500 V, 300 °C): *m/z* 1280.8 $[Ge_9\{Si(TMS)_3\}_2P^iPr^tBu]^-$.

$[(Ge_9\{Si(TMS)_3\}_2)^iPr^tBuP]CuNHC^{Dipp}$ (4-$CuNHC^{Dipp}$):

$K_2[Ge_9\{Si(TMS)_3\}_2]$ (36.8 mg, 0.030 mmol, 1 eq.) and $^iPr^tBuPCl$ (7.4 mg, 0.033 mmol, 1.1 eq.) in MeCN (1 + 1 mL). $NHC^{Dipp}CuCl$ (14.6 mg, 0.030 mmol, 1 eq.) in MeCN (1 mL). The crude product was obtained as bright brown solid (35.1 mg, 67 %). **^{1}H NMR** (400 MHz, thf-d_8, 298 K): δ [ppm] = 7.59 (s, 2H, CH_{Im}), 7.51 – 7.46 (m, 2H, $CH_{Ph(p)}$), 7.42 – 7.35 (m, 4H, $CH_{Ph(m)}$), 2.86 (hept, $^3J_{HH}$ = 6.9 Hz, 2H, CH_{iPr}), 2.78 (hept, $^3J_{HH}$ = 6.9 Hz, 2H, CH_{iPr}), 1.45 (dd, $^3J_{HH}$ = 6.9 Hz,

12H, Me$_{iPr}$), 1.19 (dd, $^3J_{HH}$ = 6.9 Hz, 12H, Me$_{iPr}$), 0.91 (dd, $^3J_{HH}$ = 6.8 Hz, 6H, Me$_{iPrP}$), 0.79 (d, $^3J_{HP}$ = 6.8 Hz, 9H, Me$_{tBu}$), 0.27 (s, 54H, Me$_{TMS}$). **^{13}C NMR** (101 MHz, thf-d_8, 298 K): δ [ppm] = 146.43 (s, C$_{Ph(m)}$), 136.66 (s, C$_{PhN}$), 131.58 (s, CH$_{Ph(p)}$), 125.48 (s, CH$_{Ph(o)}$), 125.36 (s, CH$_{Im}$), 31.47 (s, Me$_{iPr}$), 31.40 (Me$_{tBu}$), 3.12 (Me$_{TMS}$).**^{29}Si-INEPT NMR** (79 MHz, thf-d_8, 298 K): δ [ppm] = -9.14 (s, Si$_{TMS}$), -105.28 (s, Si$_{Ge9}$). **^{31}P NMR** (162 MHz, thf-d_8, 298 K): δ [ppm] = 32.97 (m, P$_{Ge9}$).

K[Ge$_9${Si(TMS)$_3$}$_2$P^{t}Bu(NEt$_2$)] (5):

K$_2$[Ge$_9${Si(TMS)$_3$}$_2$] (44.2 mg, 0.036 mmol, 1 eq.) and ^{t}Bu(NEt$_2$)PCl (6.8 mg, 0.047 mmol, 1.3 eq.) in MeCN (1 + 1 mL). the crude product was obtained as brown solid (24 mg, 50 %).**^{1}H NMR** (400 MHz, thf-d_8, 298 K): δ [ppm] = 3.05 – 2.94 (m, 2H, CH$_{2(NEt2)}$), 2.93 – 2.82 (m, 2H, CH$_{2(NEt2)}$), 1.14 (d, $^3J_{HP}$ = 13.0 Hz, 9H, Me$_{tBu}$), 0.97 (t, $^3J_{HH}$ = 7.1 Hz, 6H, Me$_{(NEt2)}$), 0.25 (s, 54H, Me$_{TMS}$). **^{13}C NMR** (101 MHz, thf-d_8, 298 K): δ [ppm] = 50.58 (s, CH$_{2(NEt2)}$), 34.97 (d, $^1J_{CP}$ = 30.9 Hz, C$_{tBu}$), 30.05 (s, Me$_{tBu}$), 15.39 (s, Me$_{(NEt2)}$), 3.22 (s, Me$_{TMS}$). **^{29}Si-INEPT NMR** (79 MHz, thf-d_8, 298 K): δ [ppm] = -11.38 (s, Si$_{TMS}$), -109.96 (s, Si$_{Ge9}$).**^{31}P NMR** (162 MHz, thf-d_8, 298 K): δ [ppm] = 110.04 (m, P$_{Ge9}$). **ESI-MS** (negative ion mode, 4000 V, 300 °C): *m/z* 1309.7 [Ge$_9${Si(TMS)$_3$}$_2$P^{t}Bu(NEt$_2$)]$^-$.

[(Ge$_9${Si(TMS)$_3$}$_2$)^{t}Bu(NEt$_2$)P]CuNHC^{Dipp} (5-CuNHC^{Dipp}):

K$_2$[Ge$_9${Si(TMS)$_3$}$_2$] (44.2 mg, 0.036 mmol, 1 eq.) and ^{t}Bu(NEt$_2$)PCl (6.8 mg, 0.047 mmol, 1.3 eq.) in MeCN (1 + 1 mL). NHC^{Dipp}CuCl (17.5 mg, 0.036 mmol, 1 eq.) in MeCN (1 mL). The crude product was obtained as red solid (23.1 mg, 36 %). **^{1}H NMR** (400 MHz, thf-d_8, 298 K): δ [ppm] = 7.51 (s, 2H, CH$_{Im}$), 7.48 – 7.44 (m, 2H, CH$_{Ph(p)}$), 7.40 – 7.50 (m, 4H, CH$_{Ph(m)}$), 2.89 (hept, $^3J_{HH}$ = 6.8 Hz, 4H, CH$_{iPr}$), 2.82 – 2.72 (m, 4H, CH$_{2(NEt2)}$), 1.50 (dd, $^3J_{HH}$ = 6.8 Hz, 12H, Me$_{iPr}$), 1.19 (dd, $^3J_{HH}$ = 6.8 Hz, 12H, Me$_{iPr}$), 0.91 (s, 6H, Me$_{(NEt2)}$), 0.89 – 0.84 (m, 9H, Me$_{tBu}$), 0.23 (s, 54H, CH$_{3\ TMS}$). **^{13}C NMR** (101 MHz, thf-d_8, 298 K): δ [ppm] = 146.33 (s, C$_{Ph(o)}$), 136.56 (s, CH$_{Ph(p)}$), 131.38 (s, C$_{PhN}$), 125.34 (s, CH$_{Ph(m)}$), 125.01 (s, CH$_{Im}$), 49.05 (s, CH$_{2(NEt2)}$), 36.98 (s, C$_{tBu}$), 29.80 (s, CH$_{iPr}$), 29.47 (s, Me$_{tBu}$), 14.60 (s, Me$_{(NEt2)}$), 3.19 (s, Me$_{TMS}$). **^{29}Si-INEPT NMR** (79 MHz, thf-d_8, 298 K): δ [ppm] = -11.13 (s, Si$_{TMS}$), -106.74 (s, Si$_{Ge9}$).**^{31}P NMR** (162 MHz, thf-d_8, 298 K): δ [ppm] = 108.78 (m, P$_{Ge9}$).

K[Ge$_9${Si(TMS)$_3$}$_2$P(1,1-dimethylpropyl)$_2$] (6):

K$_2$[Ge$_9${Si(TMS)$_3$}$_2$] (61.3 mg, 0.050 mmol, 1 eq.) and (1,1-dimethylpropyl)$_2$PCl (12.0 mg, 0.050 mmol, 1 eq.) in MeCN (1 + 1 mL). The crude product was obtained as brown solid (32 mg, 47 %). **^{1}H NMR** (400 MHz, thf-d_8, 298 K): δ [ppm] = 1.91 – 1.83 (m, 2H, CH$_{amyl}$), 1.59 – 1.45 (m, 4H, CH$_{2(Amyl)}$), 1.26 (d, $^3J_{HP}$ = 4.5 Hz, 6H, Me$_{amyl\text{-}sidechain}$), 1.23 (d, $^3J_{HP}$ = 4.5 Hz, 6H, Me$_{amyl\text{-}sidechain}$), 0.83 (t, $^3J_{HH}$ = 7.4 Hz, 6H, Me$_{amyl}$), 0.25 (s, 54H, Me$_{TMS}$). **^{13}C NMR** (101 MHz,

thf-d_8, 298 K): δ [ppm] = 38.17 (s, $CH_{2(Amyl)}$), 36.12 (d, $^1J_{CP}$ = 38.9 Hz, C_{amyl}), 31.00 (s, Me_{amyl}), 29.93 (s, Me_{amyl}), 9.60 (s, $Me_{amyl\text{-}sidechain}$), 3.19 ($Me_{TMS}$).**^{29}Si-INEPT** (79 MHz, thf-d_8, 298 K): δ [ppm] = -9.50 (s, Si_{TMS}), -108.11 (s, Si_{Ge9}). **^{31}P NMR** (162 MHz, thf-d_8, 298 K): δ [ppm] = 52.93 (m, P_{Ge9}). **ESI-MS:** (negative ion mode, 3000 V, 300 °C): *m/z* 1322.8 $[Ge_9\{Si(TMS)_3\}_2P(1.1\text{-dimethylpropyl})_2]^-$.

[(Ge_9{Si(TMS)$_3$}$_2$)(1,1-dimethylpropyl)$_2$P]CuNHC^{Dipp} (6-CuNHC^{Dipp}):

$K_2[Ge_9\{Si(TMS)_3\}_2]$ (61.3 mg, 0.050 mmol, 1 eq.) and (1,1-dimethylpropyl)$_2$PCl (12.0 mg, 0.050 mmol, 1 eq.) in MeCN (1 + 1 mL). $NHC^{Dipp}CuCl$ (24.3 mg, 0.050 mmol, 1 eq.) in MeCN (1 mL). The crude product was obtained as brown solid (27.3 mg, 32 %). **^{1}H-NMR** (400 MHz, thf-d_8, 298 K): δ [ppm] = 7.61 (s, 2H, CH_{Im}), 7.51 – 7.47 (m, 2H, $CH_{Ph(p)}$), 7.40 – 7.38 (m, 4H, $CH_{Ph(m)}$), 2.89 (hept, $^3J_{HH}$ = 6.8 Hz, 4H, CH_{iPr}), 1.49 (d, $^3J_{HH}$ = 6.8 Hz, 12H, Me_{iPr}), 1.36 (m, 10H, $CH_{2(Amyl)}$/Me_{amyl}), 1.19 (d, $^3J_{HH}$ = 6.8 Hz, 12H, Me_{iPr}), 0.90 (d, $^3J_{HP}$ = 14.5 Hz, 12H, $Me_{amyl\text{-}sidechain}$), 0.27 (s, 54H, Me_{TMS}). **^{13}C-NMR** (101 MHz, thf-d_8, 298 K): δ [ppm] = 146.34 (s, $C_{Ph(o)}$), 136.77 (s, C_{PhN}), 131.56 (s, $CH_{Ph(p)}$), 125.62 (s, CH_{Im}), 125.40 (s, $CH_{Ph(m)}$), 37.93 (s, Me_{amyl}), 36.83 (s, $CH_{2(Amyl)}$), 29.86 (s, CH_{iPr}), 28.56 ($Me_{amyl\text{-}sidechain}$), 3.12 ($Me_{TMS}$). **^{29}Si-INEPT** (79 MHz, thf-d_8, 298 K): δ [ppm] = -11.00 (s, Si_{TMS}), -107.54 (s, Si_{Ge9}).**^{31}P-NMR** (162 MHz, thf-d_8, 298 K): δ [ppm] = 60.18 (m, P_{Ge9}).

K[Ge_9{Si(TMS)$_3$}$_2$P(1-adamantyl)$_2$] (7):

$K_2[Ge_9\{Si(TMS)_3\}_2]$ (61.3 mg, 0.050 mmol, 1 eq.) and (1-adamantyl)$_2$PCl (16.9 mg, 0.050 mmol, 1 eq.) in MeCN (1 + 1 mL). The crude product was obtained as brown solid (58 mg, 78 %) **^{1}H NMR** (400 MHz, thf-d_8, 298 K): δ [ppm] = 2.17 – 1.88 (m, 20H, CH/$CH_{2(adamantyl)}$), 1.69 (s, 4H, CH/$CH_{2(adamantyl)}$), 1.61 – 1.54 (m, 6H, CH/$CH_{2(adamantyl)}$), 0.26 (s, 54H, Me_{TMS}). **^{13}C NMR** (101 MHz, thf-d_8, 298 K): δ [ppm] = 45.05, 37.97, 37.76, 37.62, 37.57, 37.39 (s, CH_2/$CH_{adamantyl}$), 3.16 (s, Me_{TMS}). **^{31}P NMR** (162 MHz, thf-d_8, 298 K): δ [ppm] = 57.32 (m, P_{Ge9}). **^{29}Si-INEPT NMR** (79 MHz, thf-d_8, 298 K): δ [ppm] = -11.53 (s, Si_{TMS}), -110.03 (s, Si_{Ge9}). **ESI-MS:** (negative ion mode, 4000 V, 300 °C): *m/z* 1450.8 $[Ge_9\{Si(TMS)_3\}_2P(1\text{-adamantyl})_2]^-$.

[(Ge_9{Si(TMS)$_3$}$_2$)(1-adamantyl)$_2$P]CuNHC^{Dipp} (7-CuNHC^{Dipp}):

$K_2[Ge_9\{Si(TMS)_3\}_2]$ (61.3 mg, 0.050 mmol, 1 eq.) and (1-adamantyl)$_2$PCl (16.9 mg, 0.050 mmol, 1 eq.) in MeCN (1 + 1 mL). $NHC^{Dipp}CuCl$ (24.3 mg, 0.050 mmol, 1 eq.) in MeCN (1 mL). The crude product was obtained as bright brown solid (62 mg, 66 %). **^{1}H NMR** (400 MHz, thf-d_8, 298 K): δ [ppm] = 7.59 (s, 2H, CH_{Im}), 7.52 – 7.48 (m, 2H, $CH_{Ph(p)}$), 7.43 – 7.39 (m, 4H, $CH_{Ph(m)}$), 2.91 (hept, $^3J_{HH}$ = 6.8 Hz, 4H, CH_{iPr}), 2.02 – 1.44 (m, 30H, CH/$CH_{2(adamantyl)}$), 1.51 (d, $^3J_{HH}$ = 6.8 Hz, 12H, Me_{iPr}), 1.20 (d, $^3J_{HH}$ = 6.8 Hz, 12H, Me_{iPr}), 0.28 (s, 54H, Me_{TMS}).

^{13}C NMR (101 MHz, thf-d_8, 298 K): δ [ppm] = 146.43 (s, $C_{Ph(o)}$), 137.04 (s, C_{PhN}), 131.68 (s, $CH_{Ph(p)}$), 125.95 (s, CH_{Im}), 125.52 (s, $CH_{Ph(m)}$), 44.49, 38.79, 37.68, 37.15 (C/CH/$CH_{2(adamantyl)}$), 30.02 (CH_{iPr}), 29.93 ($CH_{2(adamantyl)}$), 3.39 (Me_{TMS}). **^{29}Si-INEPT NMR** (79 MHz, thf-d_8, 298 K): δ [ppm] = -10.99 (s, Si_{TMS}), -107.74 (s, Si_{Ge9}). **^{31}P NMR** (162 MHz, thf-d_8, 298 K): δ [ppm] = 48.76 (m, P_{Ge9}).

K[Ge$_9${Si(TMS)$_3$}$_2$P^{i}Pr(N^{i}Pr$_2$)] (8):

K_2[Ge$_9${Si(TMS)$_3$}$_2$] (73.6 mg, 0.060 mmol, 1 eq.) and ^{i}Pr(N^{i}Pr$_2$)PCl (13.6 mg, 0.066 mmol, 1.1 eq.) in MeCN (1.5 + 1 mL). The crude product was obtained as brown solid (54 mg, 60 %). **^{1}H NMR** (400 MHz, thf-d_8, 298 K): δ [ppm] = 3.56 – 3.36 (m, 2H, CH_{NiPr}), 2.09 – 2.01 (m, 1H, CH_{PiPr}), 1.18 (d, $^3J_{HH}$ = 6.8 Hz, 6H, Me_{NiPr}), 1.12 (d, $^3J_{HH}$ = 6.9 Hz, 3H, Me_{PiPr}), 1.06 (d, $^3J_{HH}$ = 6.9 Hz, 3H, Me_{PiPr}), 1.02 (d, $^3J_{HH}$ = 6.8 Hz, 6H, Me_{NiPr}), 0.25 (s, 54H, Me_{TMS}). **^{13}C NMR** (101 MHz, thf-d_8, 298 K): δ [ppm] = 32.24 (d, $^1J_{CP}$ = 24.1 CH_{iPr}), 22.76 (d, $^2J_{CP}$ = 14.7 Hz, Me_{iPr}), 21.87 (d, $^3J_{CP}$ = 28.9 Hz, Me_{NiPr2}), 3.22 (s, Me_{TMS}). **^{29}Si-INEPT** (79 MHz, thf-d_8, 298 K): δ [ppm] = -9.57 (s, Si_{TMS}), -108.08 (s, Si_{Ge9}). **^{31}P NMR** (162 MHz, thf-d_8, 298 K): δ [ppm] = 69.83 (m, P_{Ge9}). **ESI-MS:** (negative ion mode, 3500 V, 300 °C): *m/z* 1323.8. [Ge$_9${Si(TMS)$_3$}$_2$P^{i}Pr(N^{i}Pr$_2$)]$^-$

[NHC^{Dipp}Cu{η^3-Ge$_9${Si(TMS)$_3$}$_2$P^{i}Pr(N^{i}Pr$_2$)}] (8-CuNHC^{Dipp}):

K_2[Ge$_9${Si(TMS)$_3$}$_2$] (73.6 mg, 0.060 mmol, 1 eq.) and ^{i}Pr(N^{i}Pr$_2$)PCl (13.6 mg, 0.066 mmol, 1.1 eq.) in MeCN (1.5 + 1 mL). NHC^{Dipp}CuCl (29.2 mg, 0.060 mmol, 1 eq.) in MeCN (1.5 mL). The crude product was obtained as orange solid (57.0 mg, 53 %).**^{1}H NMR** (400 MHz, thf-d_8, 298 K): δ [ppm] = 7.48 – 7.44 (m, 2H, $CH_{Ph(p)}$), 7.39 (s, 2H, CH_{Im}), 7.38 – 7.34 (m, 4H, $CH_{Ph(m)}$), 3.52 – 3.38 (m, 2H, CH_{NiPr2}), 2.95 – 2.85 (m, 4H, $CH_{NHC(iPr)}$), 2.28 – 2.17 (m, 1H, CH_{PiPr}), 1.54 (dd, $^3J_{HH}$ = 6.8 Hz, 12H, $Me_{NHC(iPr)}$), 1.22 – 1.16 (m, 24H, $Me_{NHC(iPr)/NiPr2}$), 1.14 (d, 6H, Me_{PiPr}), 0.19 (s, 54H, Me_{TMS}). **^{13}C NMR** (101 MHz, thf-d_8, 298 K): δ [ppm] = 146.29 (s, $C_{Ph(o)}$), 136.41 (s, $CH_{Ph(p)}$), 131.21 (s, C_{PhN}), 125.23 (s, $C_{Ph(m)}$), 124.16 (s, CH_{Im}), 29.81 (s, $CH_{NHC(iPr)}$), 22.60 (s, Me_{PiPr}), 3.25 (Me_{TMS}). **^{29}Si-INEPT NMR** (79 MHz, thf-d_8, 298 K): δ [ppm] = -9.49 (s, Si_{TMS}).**^{31}P NMR** (162 MHz, thf-d_8, 298 K): δ [ppm] = 76.49 (m, P_{Ge9}).

K[Ge$_9${Si(TMS)$_3$}$_2$P^{t}Bu(N^{i}Pr$_2$)] (9):

K_2[Ge$_9${Si(TMS)$_3$}$_2$] (44.2 mg, 0.036 mmol, 1 eq.) and ^{t}Bu(N^{i}Pr$_2$)PCl (8.8 mg, 0.040 mmol, 1.1 eq.) in MeCN (1 + 1 mL). The crude product was obtained as brown solid (39 mg, 78 %). **^{1}H NMR** (400 MHz, thf-d_8, 298 K): δ [ppm] = 3.09 (brs, 1H, CH_{iPr}), 1.18 – 1.02 (m, 12H, Me_{iPr}), 1.12 (d, $^3J_{HP}$ = 13.3 Hz, 9H, Me_{tBu}), 0.25 (s, 54H, Me_{TMS}). **^{13}C NMR** (101 MHz, thf-d_8, 298 K): δ [ppm] = 35.15 (d, $^1J_{CP}$ = 32.4 Hz, C_{tBu}), 30.86 (d, $^2J_{CP}$ = 17.4 Hz, Me_{tBu}), 30.68 (s, Me_{NiPr2}), 3.22 (s, Me_{TMS}). **^{29}Si-INEPT NMR** (79 MHz, thf-d_8, 298 K): δ [ppm] = -9.59 (s, Si_{TMS}), -108.11

(s, Ge_9). **^{31}P NMR** (162 MHz, thf-d_8, 298 K): δ [ppm] = 83.12 (m, P_{Ge9}). **ESI-MS:** (negative ion mode, 3000 V, 300 °C): *m/z* 1337.8 $[Ge_9\{Si(TMS)_3\}_2P^tBu(N^iPr_2)]^-$.

$[NHC^{Dipp}Cu\{\eta^3\text{-}Ge_9\{Si(TMS)_3\}_2P^tBu(N^iPr_2)\}]$ (9-CuNHC^{Dipp}):

$K_2[Ge_9\{Si(TMS)_3\}_2]$ (44.2 mg, 0.036 mmol, 1 eq.) and ^{t}Bu(N^iPr$_2$)PCl (8.8 mg, 0.040 mmol, 1.1 eq.) in MeCN (1 + 1 mL). NHC^{Dipp}CuCl (17.5 mg, 0.036 mmol, 1 eq.) in MeCN (1 mL). The crude product was obtained as red solid (42.9 mg, 67 %).**^{1}H NMR** (400 MHz, thf-d_8, 298 K): δ [ppm] = 7.46 – 7.42 (m, 2H, $CH_{Ph(p)}$), 7.38 (s, 2H, CH_{Im}), 7.37 – 7.34 (m, 4H, $CH_{Ph(m)}$), 2.91 (hept, $^3J_{HH}$ = 6.8 Hz, 4H, $CH_{NHC(iPr)}$), 1.57 (d, $^3J_{HH}$ = 6.8 Hz, 6H, $Me_{NHC(iPr)}$), 1.50 (d, $^3J_{HH}$ = 6.8 Hz, 6H, $Me_{NHC(iPr)}$), 1.19 (dd, $^3J_{HH}$ = 6.8 Hz, 12H, $Me_{NHC(iPr)}$), 1.15 – 1.11 (m, 21H, $Me_{NiPr/tBu}$), 0.19 (s, 54H, Me_{TMS}). **^{13}C NMR** (101 MHz, thf-d_8, 298 K): δ [ppm] = 146.34 (s, $C_{Ph(o)}$), 136.95 (s, $CH_{Ph(p)}$), 131.23 (s, C_{PhN}), 125.36 (s, $CH_{Ph(m)}$), 124.35 (s, CH_{Im}), 30.77 (s $CH_{NHC(iPr)}$), 29.82 (Me_{tBu}), 3.31 (Me_{TMS}). **^{29}Si-INEPT NMR** (79 MHz, thf-d_8, 298 K): δ [ppm] = -9.52 (s, Si_{TMS}).**^{31}P NMR** (162 MHz, thf-d_8, 298 K): δ [ppm] = 88.11 (m, P_{Ge9}).

$K[Ge_9\{Si(TMS)_3\}_2P^tBu(Mes)]$ (10):

$K_2[Ge_9\{Si(TMS)_3\}_2]$ (44.2 mg, 0.036 mmol, 1 eq.) and ^{t}Bu(Mes)PCl (14.3 mg, 0.054 mmol, 1.5 eq.) in MeCN (1 + 1 mL). The crude product was obtained as brown solid (35 mg, 69 %). **^{1}H-NMR** (400 MHz, thf-d_8, 298 K): δ [ppm] = 6.73 (m, 2H, CH_{Mes}), 2.56 – 2.46 (m, 6H, Me_{Mes}), 2.15 (s, 3H, Me_{Mes}), 1.07 (d, $^3J_{HP}$ = 12.5 Hz, 9H, Me_{tBu}), 0.25 (s, 54H, Me_{TMS}). **^{13}C-NMR** (101 MHz, thf-d_8, 298 K): *δ* [ppm] = 145.95 (s, $C_{Ph(P)}$, 137.34 (s, $C_{Ph(o)}$), 134.35 (s, $C_{Ph(p)}$), 130.06 (s, CH_{Ph}), 33.39 (s, C_{tBu}), 32.27 (s, Me_{tBu}), 31.22 (s, $Me_{(o)}$), 21.09 (s, $Me_{(p)}$), 3.20 (s, Me_{TMS}). **^{29}Si-INEPT** (79 MHz, thf-d_8, 298 K): δ [ppm] = -11.31 (s, Si_{TMS}), -109.41 (s, Si_{Ge9}). **^{31}P-NMR** (162 MHz, thf-d_8, 298 K): δ [ppm] = -19.40 (m, P_{Ge9}). **ESI-MS:** (negative ion mode, 3500 V, 300 °C): *m/z* 1356.8 $[Ge_9\{Si(TMS)_3\}_2P^tBu(Mes)]^-$.

$[NHC^{Dipp}Cu\{\eta^3\text{-}Ge_9\{Si(TMS)_3\}_2P^tBu(Mes)\}]$ (10-CuNHC^{Dipp}):

$K_2[Ge_9\{Si(TMS)_3\}_2]$ (44.2 mg, 0.036 mmol, 1 eq.) and ^{t}Bu(Mes)PCl (14.3 mg, 0.054 mmol, 1.5 eq.) in MeCN (1 + 1 mL). NHC^{Dipp}CuCl (17.5 mg, 0.036 mmol, 1 eq.) in MeCN (1 mL). The crude product was obtained as bright red solid (41.0 mg, 61 %). **^{1}H NMR** (400 MHz, thf-d_8, 298 K): δ [ppm] = 7.42 – 7.37 (m, 4H, $CH_{Ph(m)}$), 7.37 – 7.32 (m, 2H, CH_{Im}), 7.29 – 7.21 (m, 2H, $CH_{Ph(p)}$), 6.92 – 6.85 (m, 2H, CH_{Mes}), 2.89 (hept, $^3J_{HH}$ = 6.8 Hz, 4H, CH_{iPr}), 2.76 – 2.64 (m, 6H, Me_{Mes}), 2.23 (s, 3H, Me_{Mes}), 1.50 (d, $^3J_{HH}$ = 6.8 Hz, 12H, Me_{iPr}), 1.19 (s, 3H, Me_{tBu}), 1.16 (d, $^3J_{HH}$ = 6.8 Hz, 12H, Me_{iPr}), 1.09 – 1.14 (brs, 6H, Me_{tBu}), 0.19 (s, 54H, Me_{TMS}). **^{13}C NMR** (101 MHz, thf-d_8, 298 K): δ [ppm] = 146.19 (s, $C_{Ph(o)}$), 138.84 (s, C_{PhN}), 136.38 (s, $C_{Mes(o)}$), 131.23 (s, $CH_{Ph(p)}$), 130.46 (s, CH_{Mes}), 129.63 (s, C_{MesP}), 129.50 (s, $C_{Mes(p)}$), 125.31 (s, CH_{Im}), 124.19 (s, $CH_{Ph(m)}$), 34.50 (s, C_{tBu}), 32.09 (Me_{tBu}), 29.80 (CH_{iPr}), 21.05 (s, $Me_{Mes(o)}$), 3.28

(Me_{TMS}). **^{29}Si-INEPT** (79 MHz, thf-d_8, 298 K): δ [ppm] = -11.22 (s Si_{TMS}), -105.12 (s, Si_{Ge9}).**^{31}P NMR** (162 MHz, thf-d_8, 298 K): δ [ppm] = -14.77 (m, P_{Ge9}).

K[Ge$_9${Si(TMS)$_3$}$_2$P(*o*-tolyl)$_2$] (11):

$K_2[Ge_9\{Si(TMS)_3\}_2]$ (73.6 mg, 0.060 mmol, 1 eq.) and (*o*-tolyl)$_2$PCl (14.9 mg, 0.060 mmol, 1 eq.) in MeCN (1.5 + 1 mL). The crude product was obtained as brown solid (38 mg, 45 %). **^{1}H NMR** (400 MHz, thf-d_8, 298 K): δ [ppm] = 6.94 – 6.87 (m, 8H, $CH_{o\text{-tolyl}}$), 2.20 (s, 6H, $Me_{o\text{-tolyl}}$), 0.27 (s, 54H, Me_{TMS}). **^{13}C NMR** (101 MHz, thf-d_8, 298 K): δ [ppm] = 143.05, 141.35, 136.45, 129.62, 127.24, 125.77 (s, C_{Ph}/CH_{Ph}), 22.54 (d,$^3J_{CP}$ =19.9 Hz, Me_{Ph}), 3.18 (s, Me_{TMS}). **^{29}Si-INEPT** (79 MHz, thf-d_8, 298 K): δ [ppm] = -9.29 (s Si_{TMS}), -107.67 (s, Si_{Ge9}). **^{31}P NMR** (162 MHz, thf-d_8, 298 K): δ [ppm] = -41.66 (m, P_{Ge9}). **ESI-MS:** (negative ion mode, 4000 V, 300 °C): *m/z* 1362.8 $[Ge_9\{Si(TMS)_3\}_2P(o\text{-tolyl})_2]^-$.

[NHC^{Dipp}Cu{η^3-Ge$_9${Si(TMS)$_3$}$_2$P(*o*-tolyl)$_2$}] (11-CuNHC^{Dipp}):

$K_2[Ge_9\{Si(TMS)_3\}_2]$ (73.6 mg, 0.060 mmol, 1 eq.) and (*o*-tolyl)$_2$PCl (14.9 mg, 0.060 mmol, 1 eq.) in MeCN (1.5 + 1 mL). $NHC^{Dipp}CuCl$ (29.2 mg, 0.060 mmol, 1 eq.) in MeCN (1.5 mL) The crude product was obtained as brown solid (40.1 mg, 37 %). **^{1}H NMR** (400 MHz, thf-d_8, 298 K): δ [ppm] = 7.61 – 7.56 (m, 2H, $CH_{Ph(m)}$), 7.41 (s, 2H, CH_{Im}), 7.27 (s, 2H, $CH_{o\text{-tolyl}(p)}$), 7.25 (s, 2H, $CH_{o\text{-tolyl}(m)}$), 7.16 – 7.05 (m, 6H, $CH_{Ph(m)/o\text{-tolyl}(o)/o\text{-tolyl}(m)}$), 6.99 – 6.94 (m, 2H, $CH_{Ph(p)}$), 2.88 (hept, $^3J_{HH}$ = 6.8 Hz, 4H, CH_{iPr}), 2.39 (s, 6H, $Me_{o\text{-tolyl}}$), 1.50 (d, $^3J_{HH}$ = 6.8 Hz, 12H, Me_{iPr}), 1.15 (d, $^3J_{HH}$ = 6.8 Hz, 12H, Me_{iPr}), 0.19 (s, 54H, Me_{TMS}). **^{13}C NMR** (101 MHz, thf-d_8, 298 K): δ [ppm] = 146.16 (s, C_{PhN}), 142.01 (s, $C_{o\text{-tolyl}(P)}$), 140.51 (s, $C_{o\text{-tolyl}(o)}$), 136.49 (s, $CH_{Ph(m)}$), 131.16 (s, $CH_{o\text{-tolyl}(m)}$), 130.37 (s, $CH_{o\text{-tolyl}(o)}$), 128.54 (s, $CH_{Ph(m)}$), 126.34 (s, $CH_{Ph(p)}$), 125.19 (s, $CH_{o\text{-tolyl}(p/m)}$), 123.90 (s, CH_{Im}), 29.77 (s, CH_{iPr}), 22.65 (s, $Me_{o\text{-tolyl}}$), 3.15 (Me_{TMS}). **^{29}Si-INEPT NMR** (79 MHz, thf-d_8, 298 K): δ [ppm] = -9.28 (s, Si_{TMS}), -104.48 (s, Si_{Ge9}).**^{31}P NMR** (162 MHz, thf-d_8, 298 K): δ [ppm] = -37.15 (m, P_{Ge9}).

Acknowledgements

This work was financially supported by Wacker Chemie AG. C. W. and F. S. G. thank M. Sc. Kerstin Mayer for support with ESI-MS measurements. Furthermore, F. S. G. thanks TUM Graduate School for support.

Keywords: Phosphine • Mixed Functionalization • Alkenyl • Zwitterion • Anchor Group

Literature

[1] J. D. Corbett, *Chem. Rev.* **1985**, *85*, 383.
[2] T. F. Fässler, S. D. Hoffmann, *Angew. Chem. Int. Ed.* **2004**, *43*, 6242.
[3] S. C. Sevov, J. M. Goicoechea, *Organometallics* **2006**, *25*, 5678.
[4] S. Scharfe, F. Kraus, S. Stegmaier, A. Schier, T. F. Fässler, *Angew. Chem.* **2011**, *50*, 3630.
[5] M. W. Hull, S. C. Sevov, *Inorg. Chem.* **2007**, *46*, 10953.
[6] A. Schnepf, *Angew. Chem. Int. Ed.* **2003**, *42*, 2624.
[7] F. Li, S. C. Sevov, *Inorg. Chem.* **2012**, *51*, 2706.
[8] C. B. Benda, J.-Q. Wang, B. Wahl, T. F. Fässler, *Eur. J. Inorg. Chem.* **2011**, 4262.
[9] F. Li, S. C. Sevov, *J. Am. Chem. Soc.* **2014**, *136*, 12056.
[10] S. Frischhut, T. F. Fässler, *Dalton Trans.* **2018**, *47*, 3223.
[11] F. Li, A. Muñoz-Castro, S. C. Sevov, *Angew. Chem. Int. Ed.* **2012**, *51*, 8581.
[12] C. Schenk, A. Schnepf, *Angew. Chem. Int. Ed.* **2007**, *46*, 5314.
[13] C. Schenk, F. Henke, G. Santiso-Quinones, I. Krossing, A. Schnepf, *Dalton Trans.* **2008**, 4436.
[14] F. Henke, C. Schenk, A. Schnepf, *Dalton Trans.* **2009**, 9141.
[15] C. Schenk, A. Schnepf, *Chem. Commun.* **2009**, 3208.
[16] F. Henke, C. Schenk, A. Schnepf, *Dalton Trans.* **2011**, *40*, 6704.
[17] O. Kysliak, C. Schrenk, A. Schnepf, *Chem. Eur. J.* **2016**, *22*, 18787.
[18] F. Li, S. C. Sevov, *Inorg. Chem.* **2015**, *54*, 8121.
[19] F. S. Geitner, T. F. Fässler, *Eur. J. Inorg. Chem.* **2016**, 2688.
[20] K. Mayer, L. J. Schiegerl, T. F. Fässler, *Chem. Eur. J.* **2016**, *22*, 18794.
[21] L. J. Schiegerl, F. S. Geitner, C. Fischer, W. Klein, T. F. Fässler, *Z. Anorg. Allg. Chem.* **2016**, *642*, 1419.
[22] O. Kysliak, C. Schrenk, A. Schnepf, *Inorg. Chem.* **2015**, *54*, 7083.
[23] O. Kysliak, T. Kunz, A. Schnepf, *Eur. J. Inorg. Chem.* **2017**, 805.
[24] O. Kysliak, A. Schnepf, *Dalton Trans.* **2016**, *45*, 2404.
[25] L. G. Perla, S. C. Sevov, *J. Am. Chem. Soc.* **2016**, *138*, 9795.
[26] L. G. Perla, A. Muñoz-Castro, S. C. Sevov, *J. Am. Chem. Soc.* **2017**, *139*, 15176.
[27] F. S. Geitner, J. V. Dums, T. F. Fässler, *J. Am. Chem. Soc.* **2017**, *139*, 11933.
[28] F. S. Geitner, C. Wallach, T. F. Fässler, *Chem. Eur J.* **2018**, *24*, 4103.
[29] K. Mayer, L. J. Schiegerl, T. Kratky, S. Günther, T. F. Fässler, *Chem. Commun.* **2017**, *53*, 11798.
[30] S. Haber, P. Le Floch, F. Mathey, *Chem. Commun.* **1992**, 1799.
[31] F. Mercier, C. Hugel-Le Goff, F. Mathey, *Organometallics* **1988**, *7*, 955.
[32] K. Izod, D. G. Rayner, S. M. El-Hamruni, R. W. Harrington, U. Baisch, *Angew. Chem. Int. Ed.* **2014**, *53*, 3636.
[33] C. A. Tolman, *Chem. Rev.* **1977**, *77*, 313.
[34] H. Clavier, S. P. Nolan, *Chem. Commun.* **2010**, *46*, 841.
[35] M. Neumeier, F. Fendt, S. Gärtner, C. Koch, T. Gärtner, N. Korber, R. M. Gschwind, *Angew. Chem. Int. Ed.* **2013**, *52*, 4483.
[36] S. T. Liddle, K. Izod, *Organometallics* **2004**, *23*, 5550.
[37] A. J. Rucklidge, G. E. Morris, A. M. Z. Slawin, D. J. Cole-Hamilton, *Helv. Chim. Acta* **2006**, *89*, 1783.
[38] O. J. Scherer, W. Gick, *Chem. Ber.* **1970**, *103*, 71.
[39] P. C. Crofts, D. M. Parker, *J. Chem. Soc.* **1970**, 2529.

[40] B. Wrackmeyer, C. Köhler, W. Milius, J. M. Grevy, Z. García-Hernández, R. Contreras, *Heteroat. Chem.* **2002**, *13*, 667.
[41] W. McFarlane, C. T. Regius, *Polyhedron* **1997**, *16*, 1855.
[42] S. Joseph, M. Hamberger, F. Mutzbauer, O. Härtl, M. Meier, N. Korber, *Angew. Chem. Int. Ed.* **2009**, *48*, 8770.
[43] L. Hintermann, *Beilstein J. Org. Chem.* **2007**, *3*, 22.
[44] O. Santoro, A. Collado, A. M. Z. Slawin, S. P. Nolan, C. S. J. Cazin, *Chem. Commun.* **2013**, *49*, 10483.
[45] G. A. Bowmaker, S. E. Boyd, J. V. Hanna, R. D. Hart, P. C. Healy, B. W. Skelton, A. H. White, *Dalton Trans.* **2002**, 2722.
[46] G. M. Sheldrick, *Acta Cryst. Sect. C* **2015**, *71*, 3.
[47] G. R. Fulmer, A. J. M. Miller, N. H. Sherden, H. E. Gottlieb, A. Nudelman, B. M. Stoltz, J. E. Bercaw, K. I. Goldberg, *Organometallics* **2010**, *29*, 2176.

Supporting Information

Enhancing the Variability of [Ge_9] Cluster Chemistry through Phosphine-Functionalization

C. Wallach,[a]‡ F. S. Geitner,[b]‡ W. Klein[a] and T. F. Fässler[a]*

[‡] authors contributed equally to this work

[a] Department Chemie Technische Universität München, Lichtenbergstraße 4, 85747 Garching b. München.

[b] Department Chemie Technische Universität München, Lichtenbergstraße 4, 85747 Garching b. München and WACKER Institute for Silicon Chemistry.

Crystallographic Data

Table S1. Selected distances in compound **2**.

bonds	distance [Å]	bonds	distance [Å]
Ge1-Ge2	2.4715(6)	Ge1-P1A	2.362(2)
Ge1-Ge4	2.4760(6)	P1A-C32A	1.788(6)
Ge1-Ge5	2.6043(5)	P1A-C28A	1.86(2)
Ge1-Ge6	2.6059(6)	C28A-C29A	1.49(3)
Ge1-Ge3	3.6324(6)	C28A-C30A	1.59(3)
Ge2-Ge7	2.5307(6)	C28A-C31A	1.50(1)
Ge2-Ge3	2.5908(6)	C32A-C33A	1.521(8)
Ge2-Ge6	2.6832(6)	C33A-C34A	1.536(9)
Ge2-Ge4	3.5112(6)	C34A-C35A	1.501(9)
Ge3-Ge4	2.5799(6)	C35A-C36A	1.328(9)
Ge3-Ge8	2.6458(6)		
Ge3-Ge7	2.6645(6)	Ge1-P1B	2.337(2)
Ge4-Ge8	2.5305(6)	P1B-C32B	1.827(6)
Ge4-Ge5	2.6713(6)	P1B-C28B	1.87(3)
Ge5-Ge9	2.5048(6)	C28B-C30B	1.45(5)
Ge5-Ge6	2.9186(6)	C28B-C31B	1.57(2)
Ge5-Ge8	3.1642(6)	C28B-C32B	1.51(4)
Ge6-Ge9	2.5220(6)	C32B-C33B	1.485(8)
Ge6-Ge7	3.0469(6)	C33B-C34B	1.52(1)
Ge7-Ge9	2.5354(6)	C34B-C35B	1.52(1)
Ge7-Ge8	2.7862(6)	C35B-C36B	1.339(9)
Ge8-Ge9	2.5339(6)		
Ge2-Si1	2.404(1)		
Ge4-Si5	2.390(1)		
Ge9-Si9	2.374(1)		

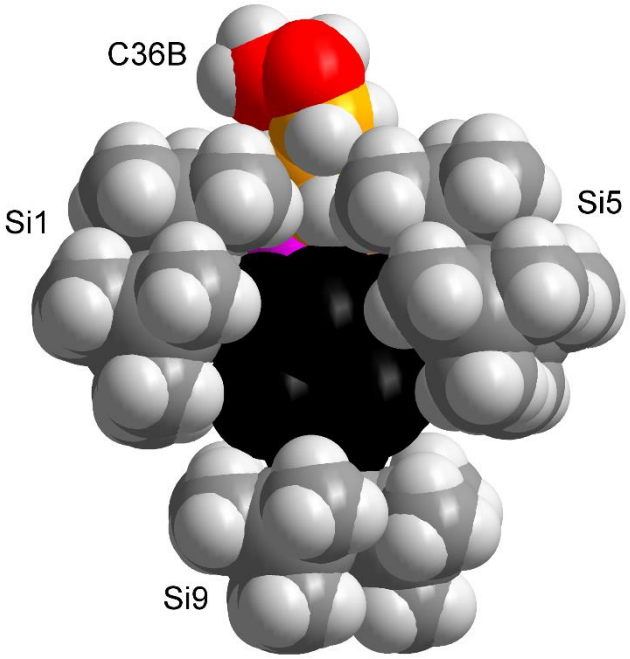

Figure S1. Space filling model of compound **2** (with minor phosphine individual), showing the exposed nature of the double bond of the pentenyl group. Hydrocarbon chain is shown in orange and the carbon atoms connected by the double bond (C35B and C36B) are presented in red. The respective picture comprising the major individual is provided in the manuscript.

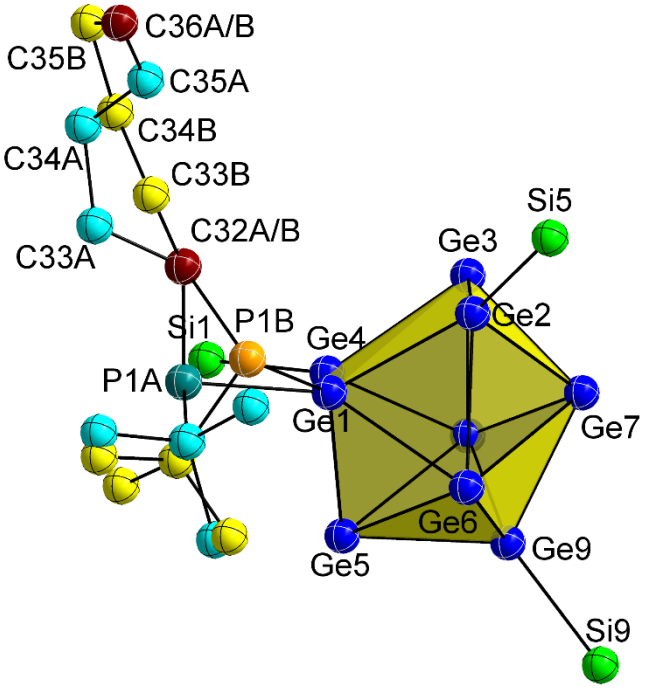

Figure S2. Crystal structure of compound **2** with two individuals of the disordered phosphine ligand. Major individual (P1A dark green, carbon atoms turquoise) and minor individual (P1B orange, carbon atoms yellow). For clarity, all atoms are presented isotropically and TMS groups of the hypersilyl groups as well as all protons are omitted.

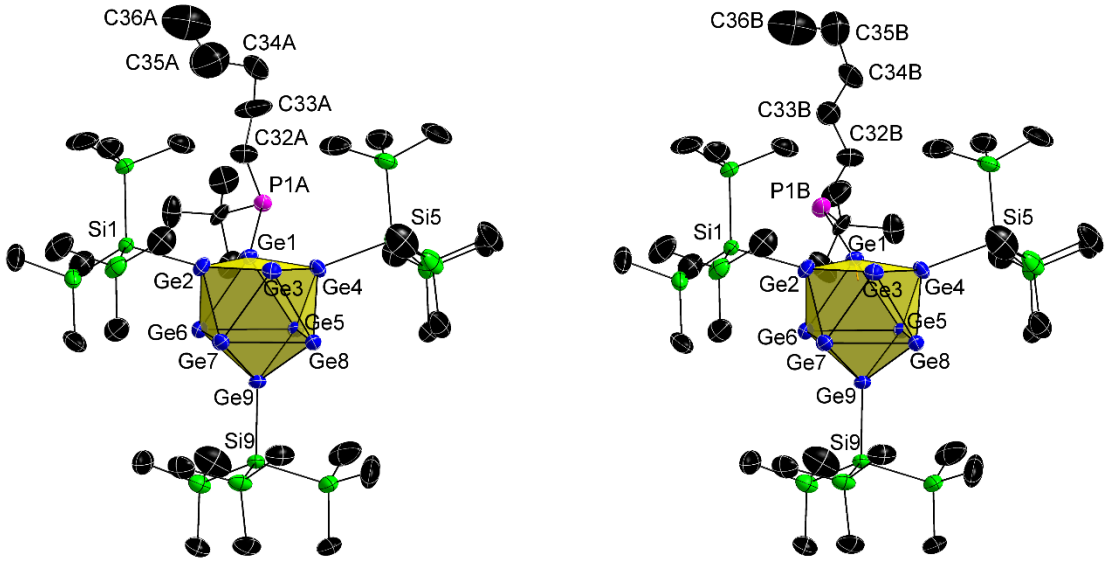

Figure S3. Full ellipsoid plots of compound **2**. Ellipsoids are shown at a 50 % probability level. Compound **2** with major individual of disordered phosphine group (left) and with minor individual of the phosphine group (right). For clarity, all protons are omitted.

NMR Spectra

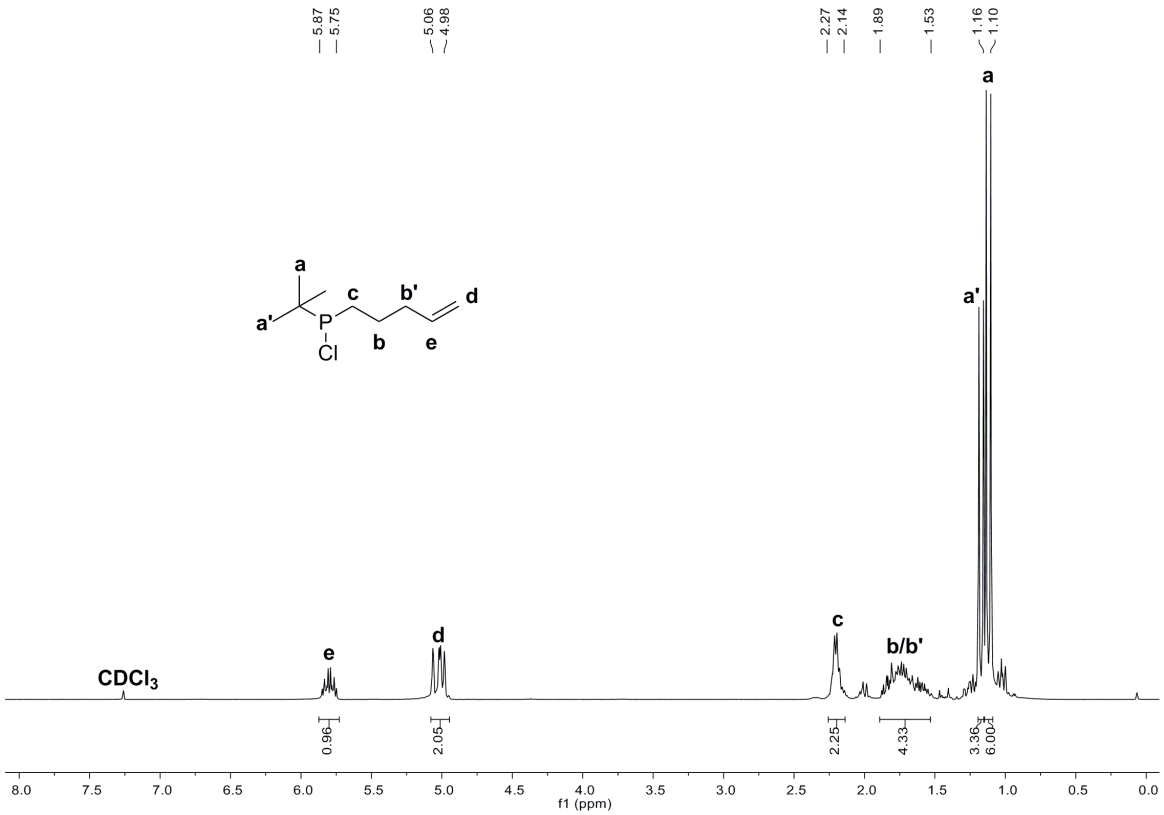

Figure S4. ^{1}H NMR spectrum of compound **1** in $CDCl_3$.

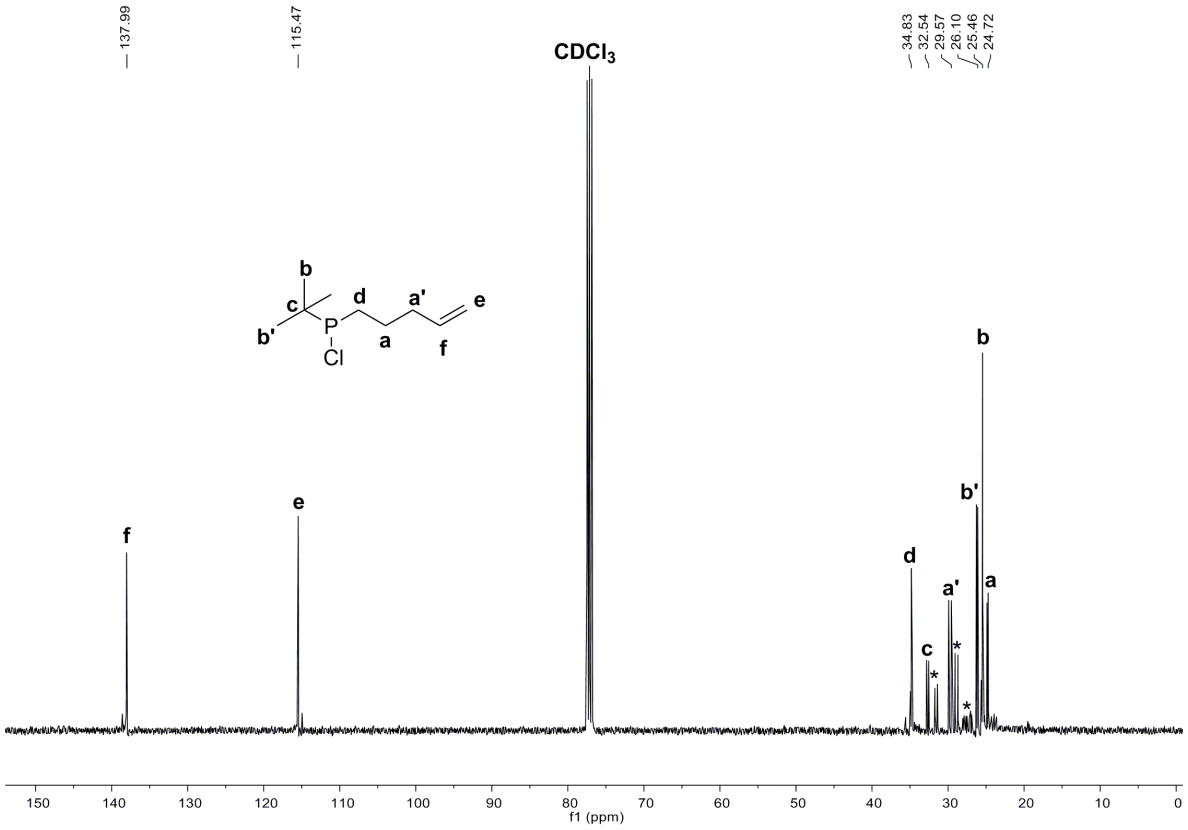

Figure S5. ^{13}C NMR spectrum of compound **1** in $CDCl_3$ (signals marked with * belong to unknown impurities).

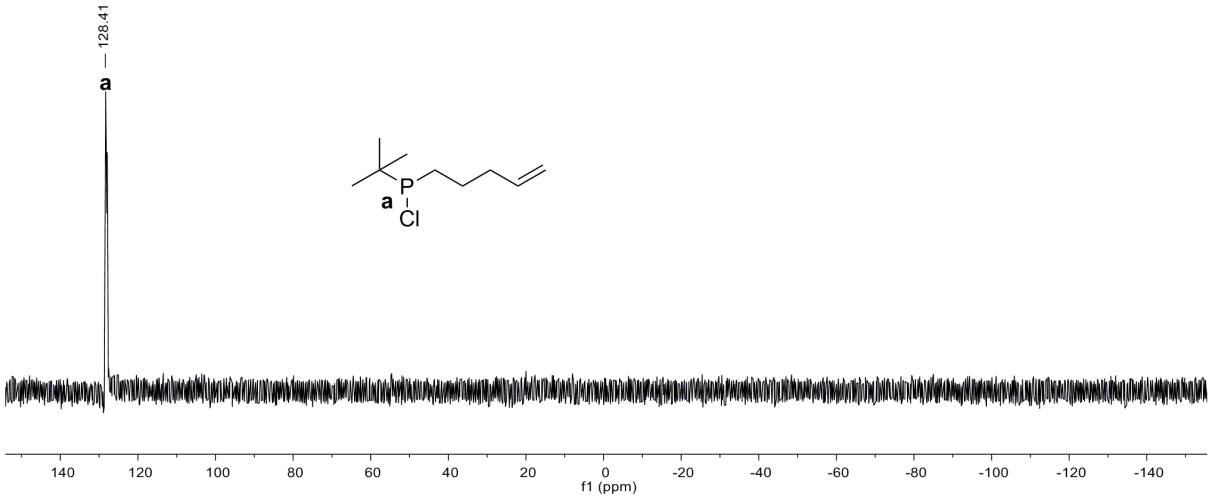

Figure S6. ^{31}P NMR spectrum of compound **1** in $CDCl_3$.

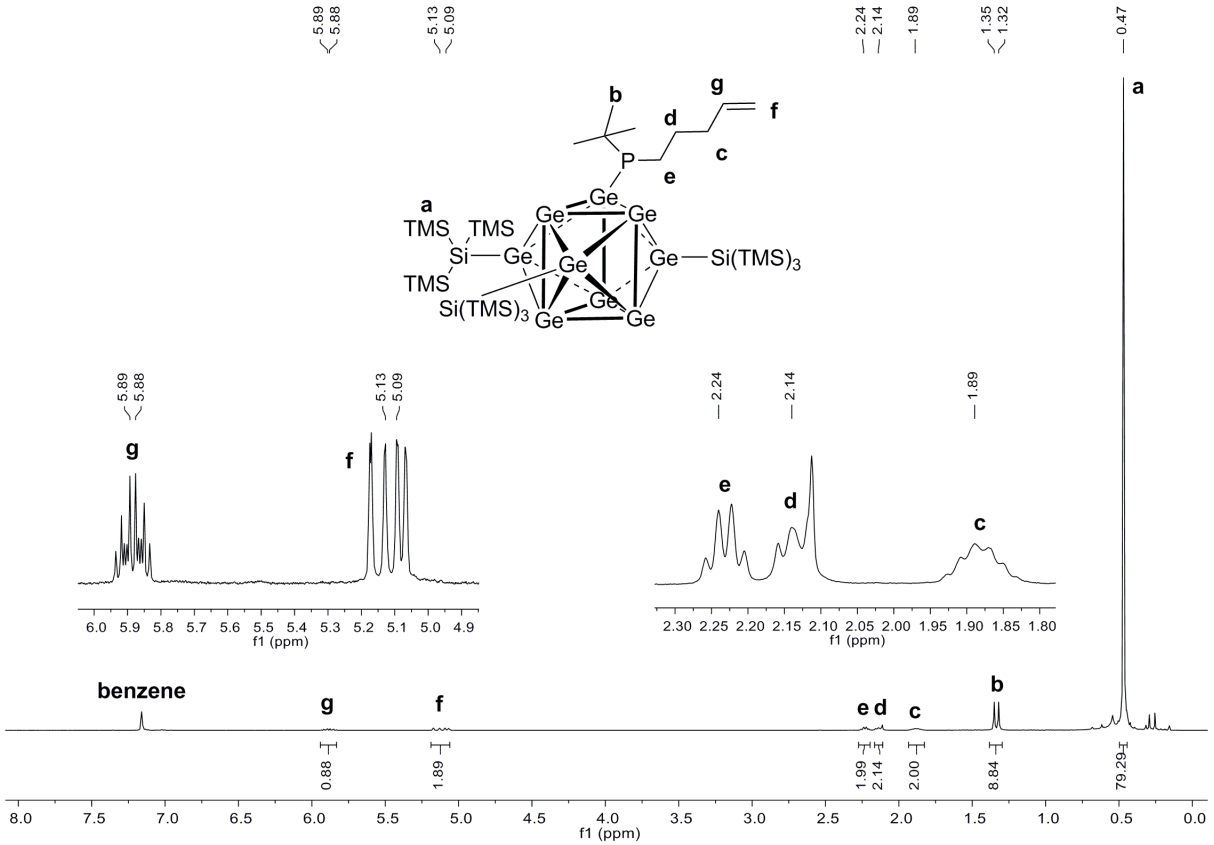

Figure S7. ^{1}H NMR spectrum of compound **2** in C_6D_6.

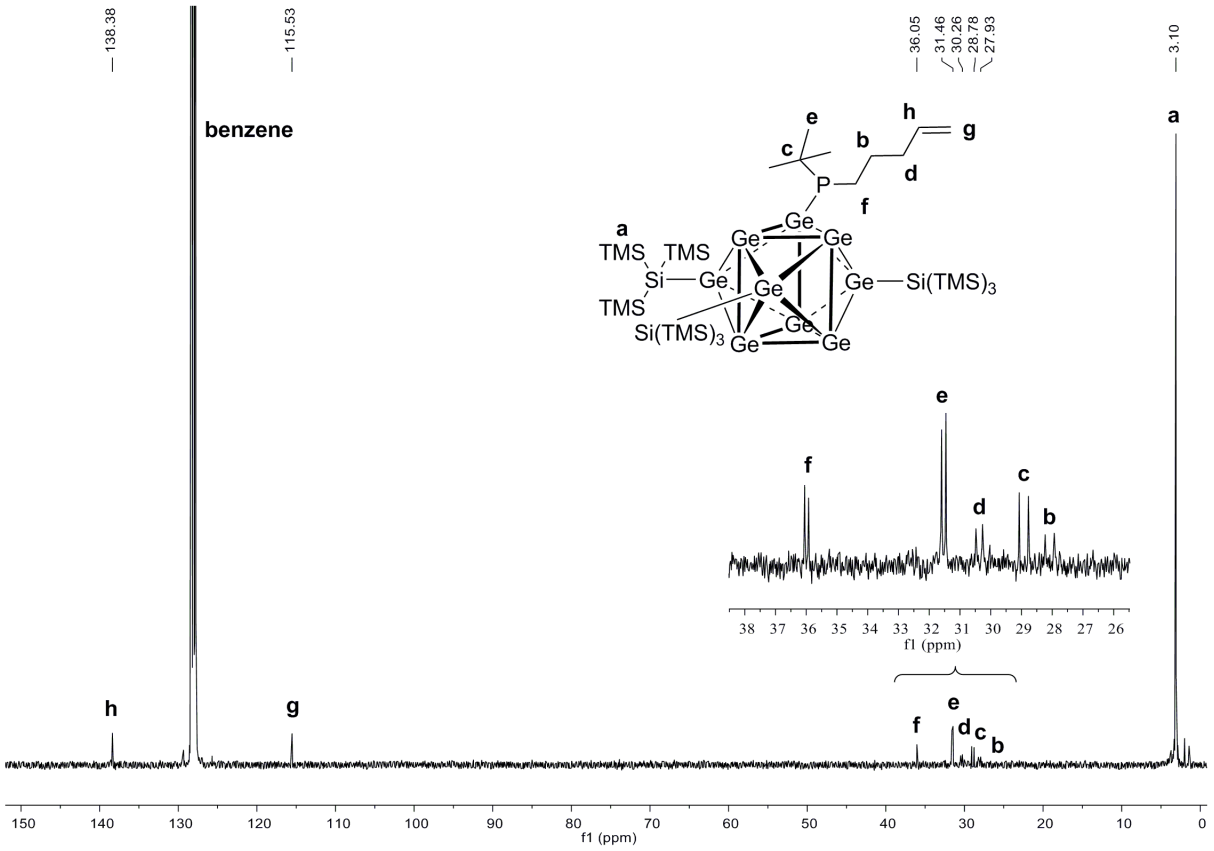

Figure S8. ^{13}C spectrum NMR of compound **2** in C_6D_6.

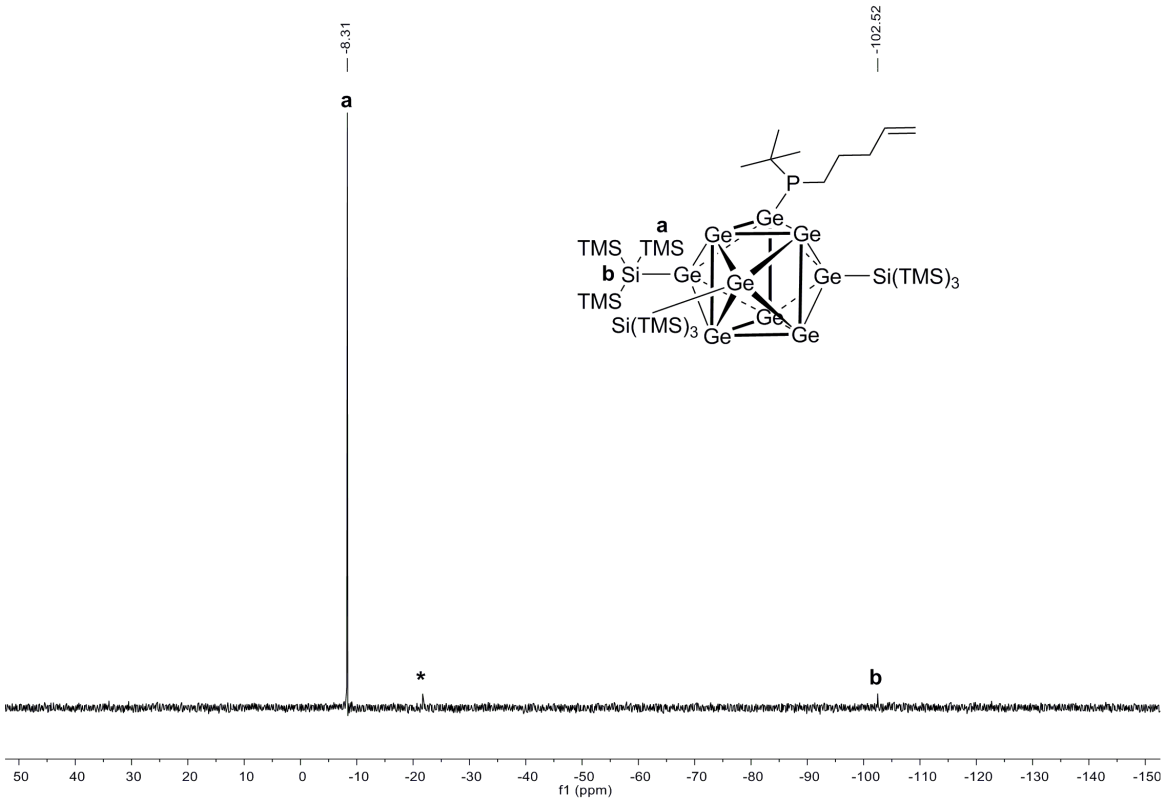

Figure S9. ^{29}Si-INEPT-RD NMR spectrum of compound **2** in in C_6D_6 (signal marked with * belongs to unknown impurity).

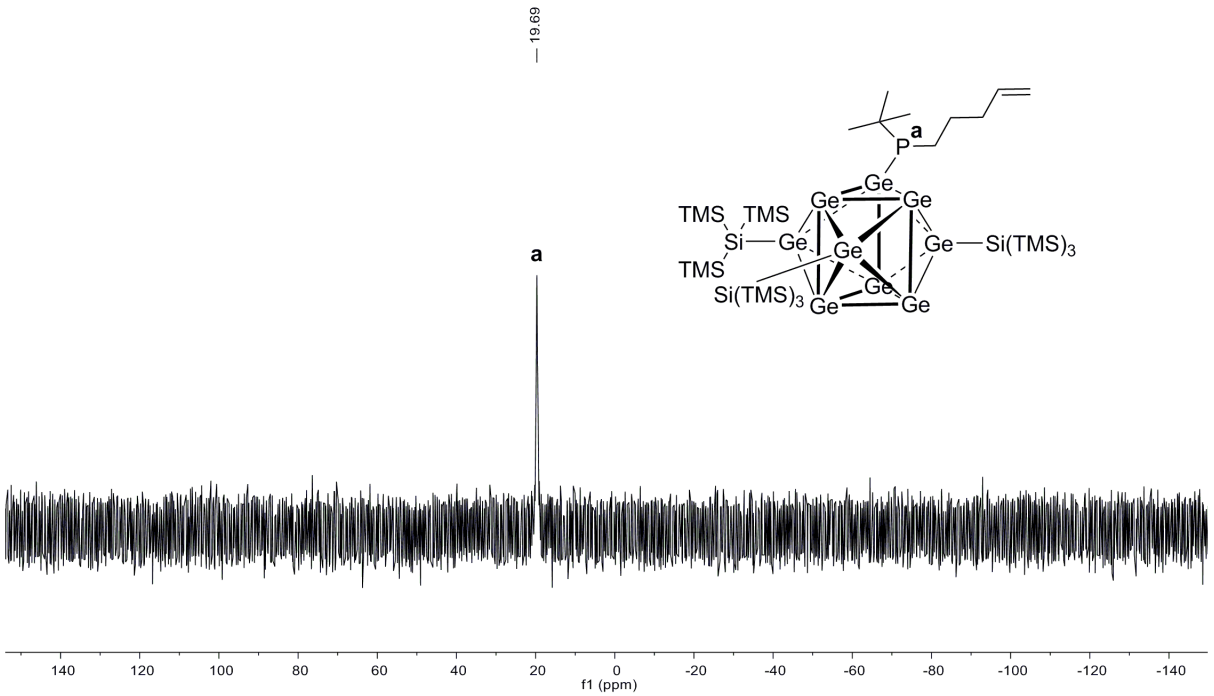

Figure S10. ^{31}P NMR spectrum of compound **2** in C_6D_6.

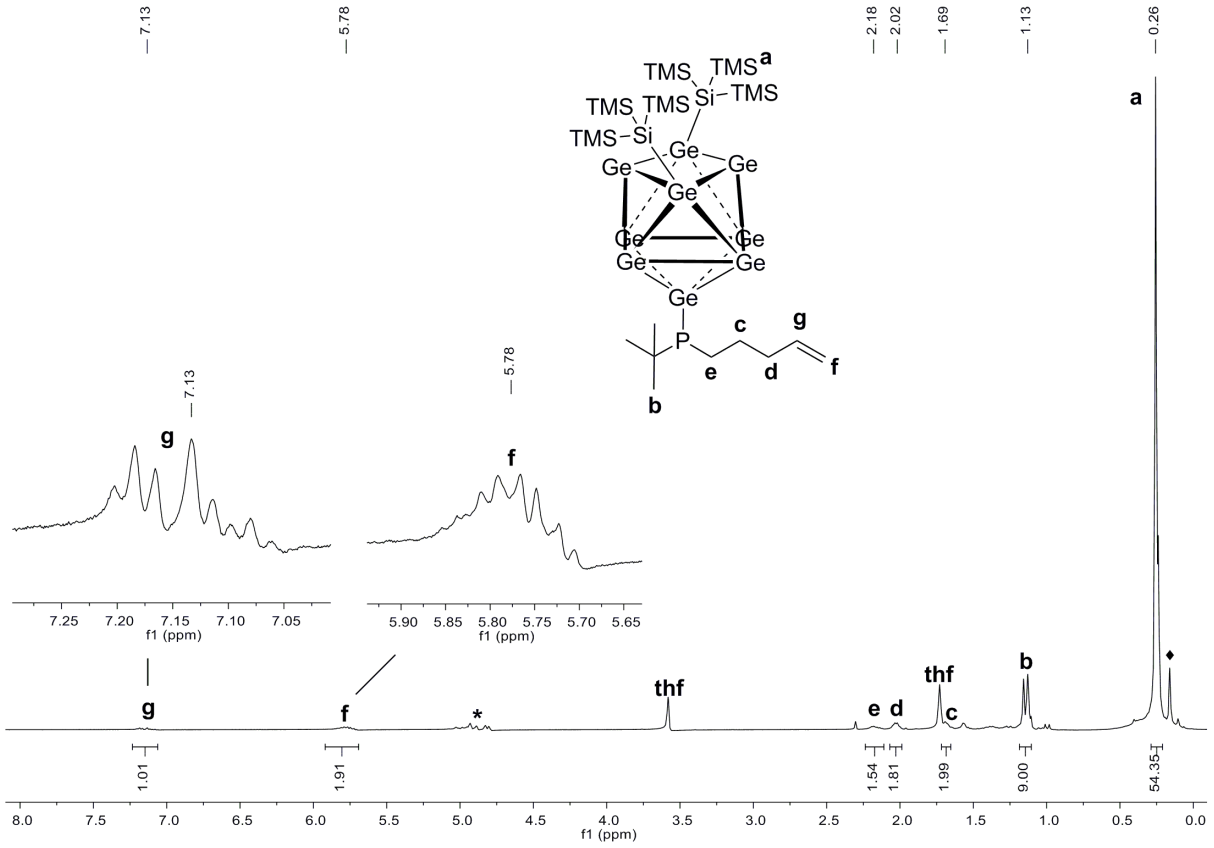

Figure S11. ^{1}H NMR spectrum of compound **3a** in thf-d_8 (signal marked with * belongs to unknown impurity, signal marked with ♦ belongs to silicon grease).

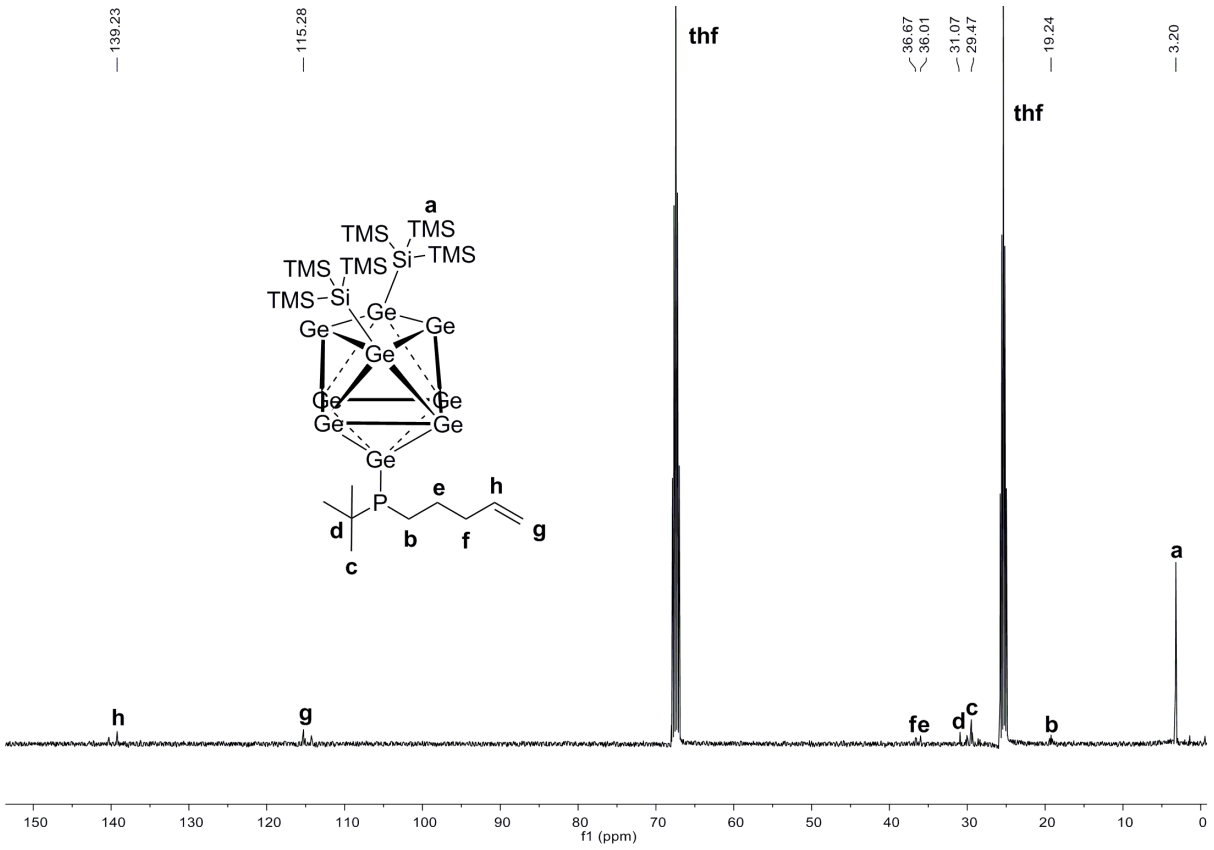

Figure S12. ^{13}C NMR spectrum of compound **3a** in thf-d_8.

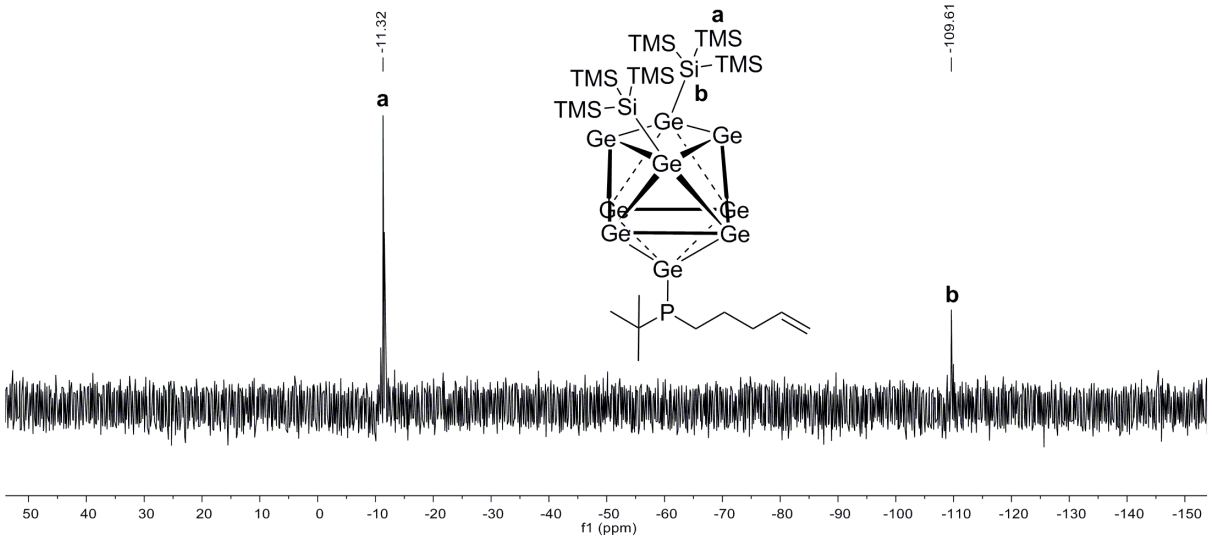

Figure S13. ^{29}Si-INEPT-RD NMR spectrum of compound **3a** in thf-d_8.

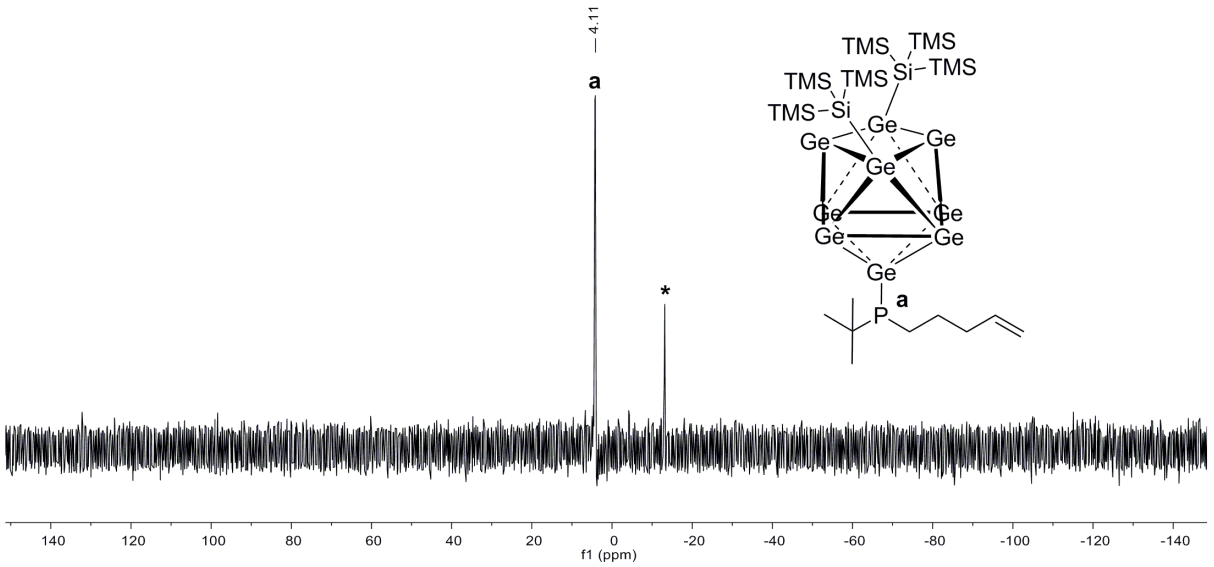

Figure S14. ^{31}P NMR spectrum of compound **3a** in thf-d_8 (signal marked with * belongs to unknown impurity).

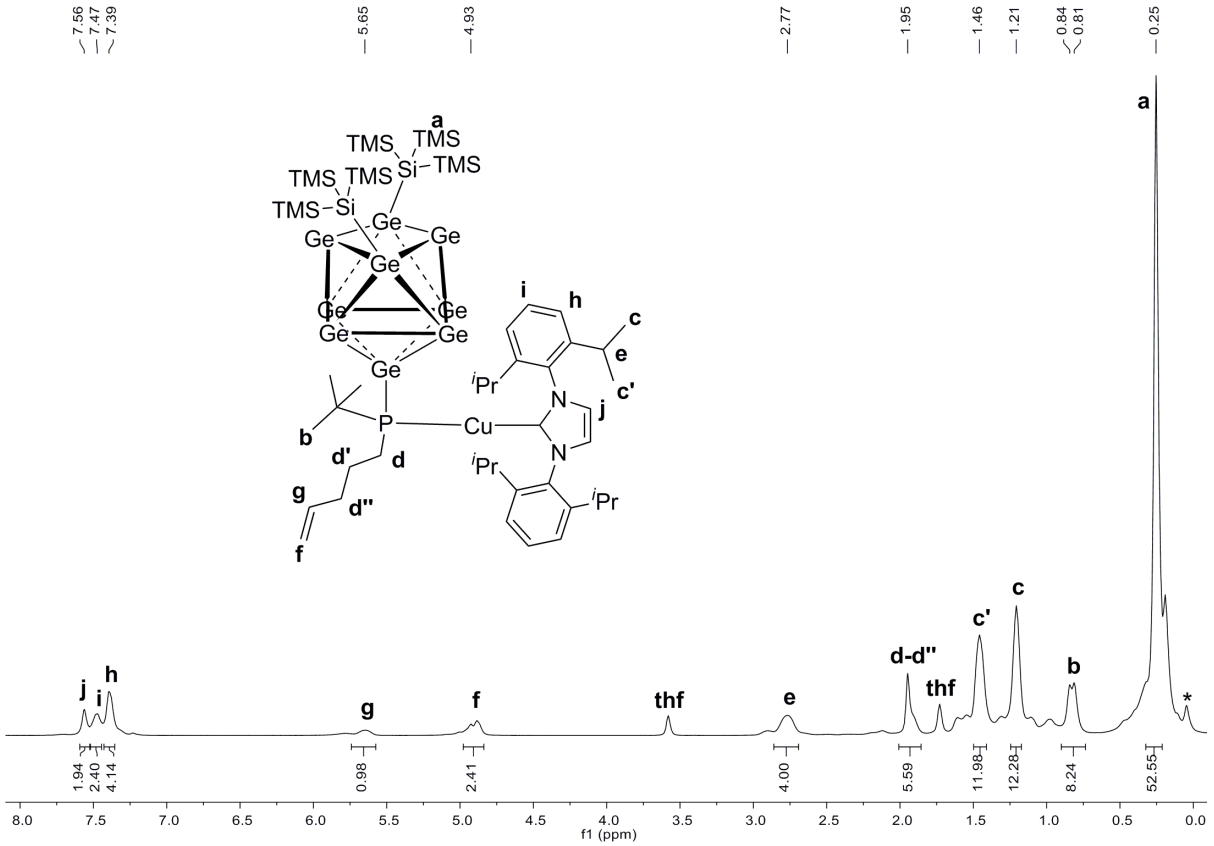

Figure S15. ^{1}H NMR spectrum of compound **3-CuNHC^{Dipp}** in thf-d_8 (signal marked with * belongs to silicon grease).

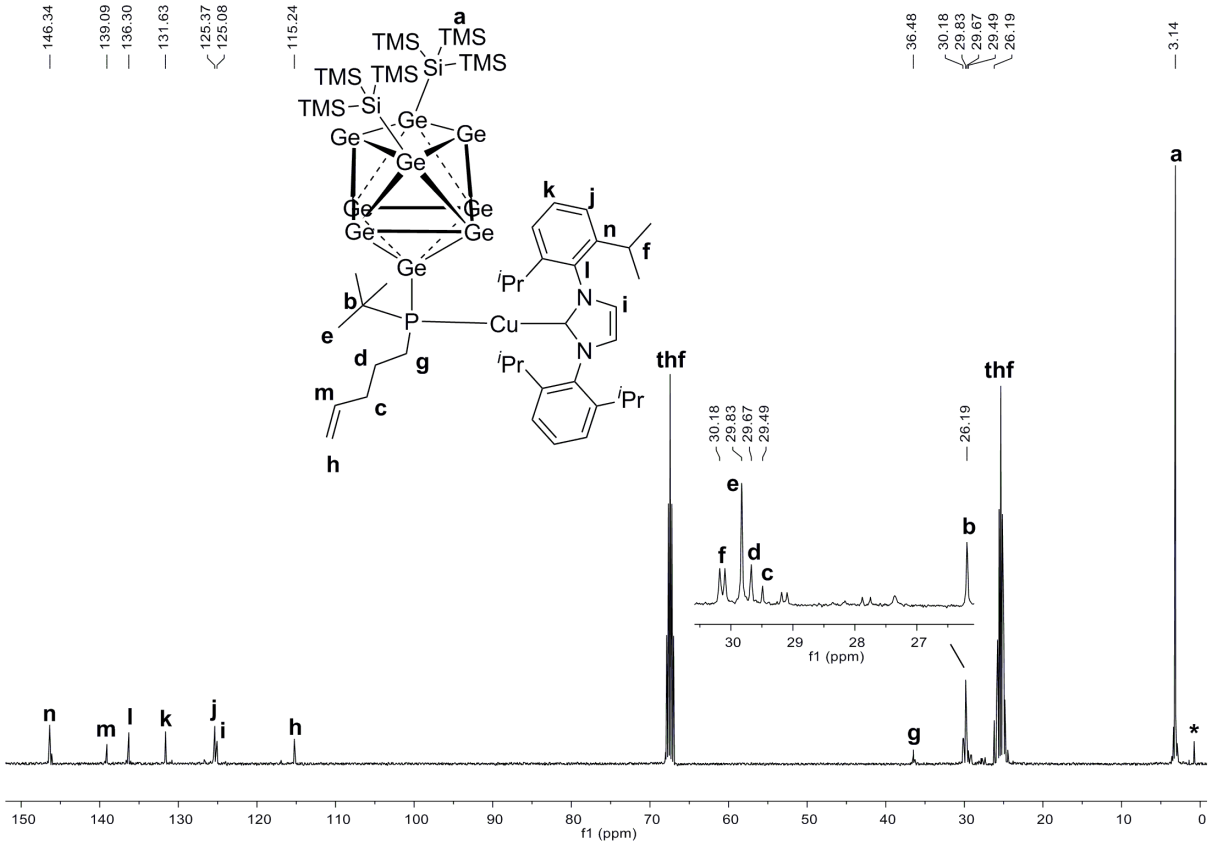

Figure S16. ^{13}C NMR spectrum of compound **3-CuNHC^{Dipp}** in thf-d_8 (signal marked with * belongs to silicon grease).

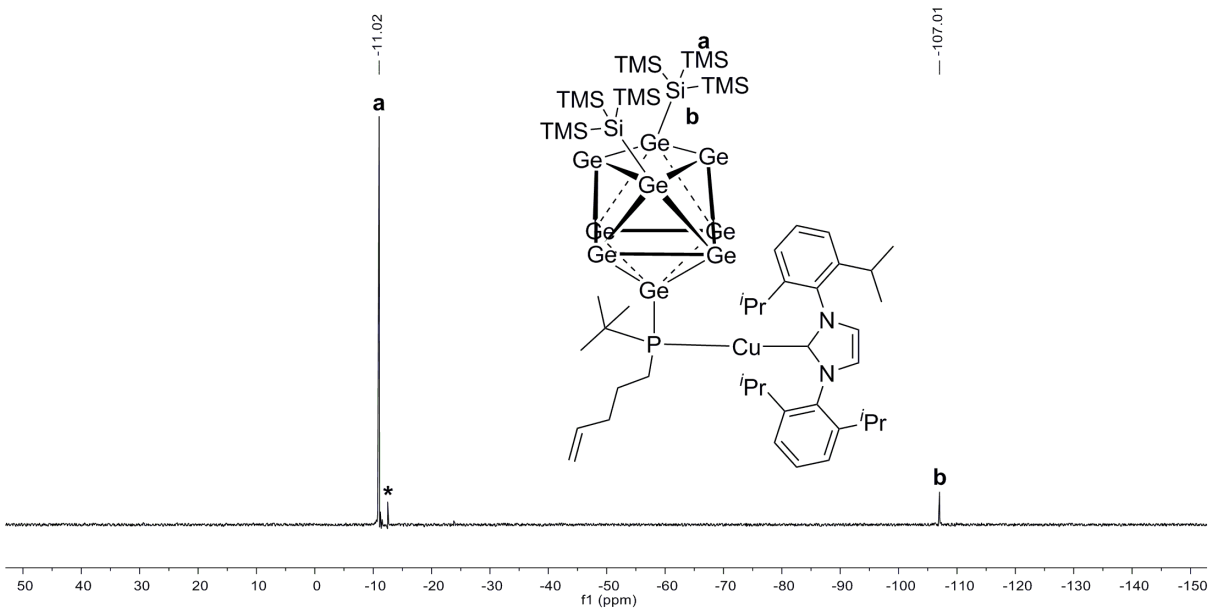

Figure S17. ^{29}Si-INEPT-RD NMR spectrum of compound **3-CuNHC^{Dipp}** in thf-d_8 (signal marked with * belongs to unknown impurity).

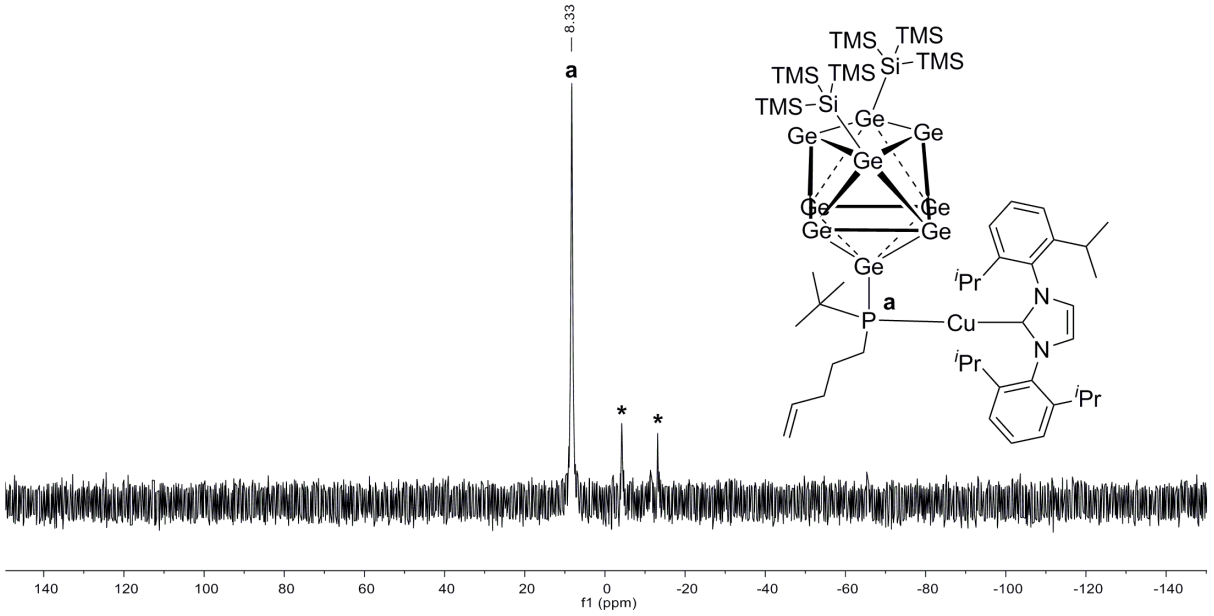

Figure S18. ^{31}P NMR spectrum of compound **3-CuNHC^{Dipp}** in thf-d_8 (signals marked with * belong to unknown impurities).

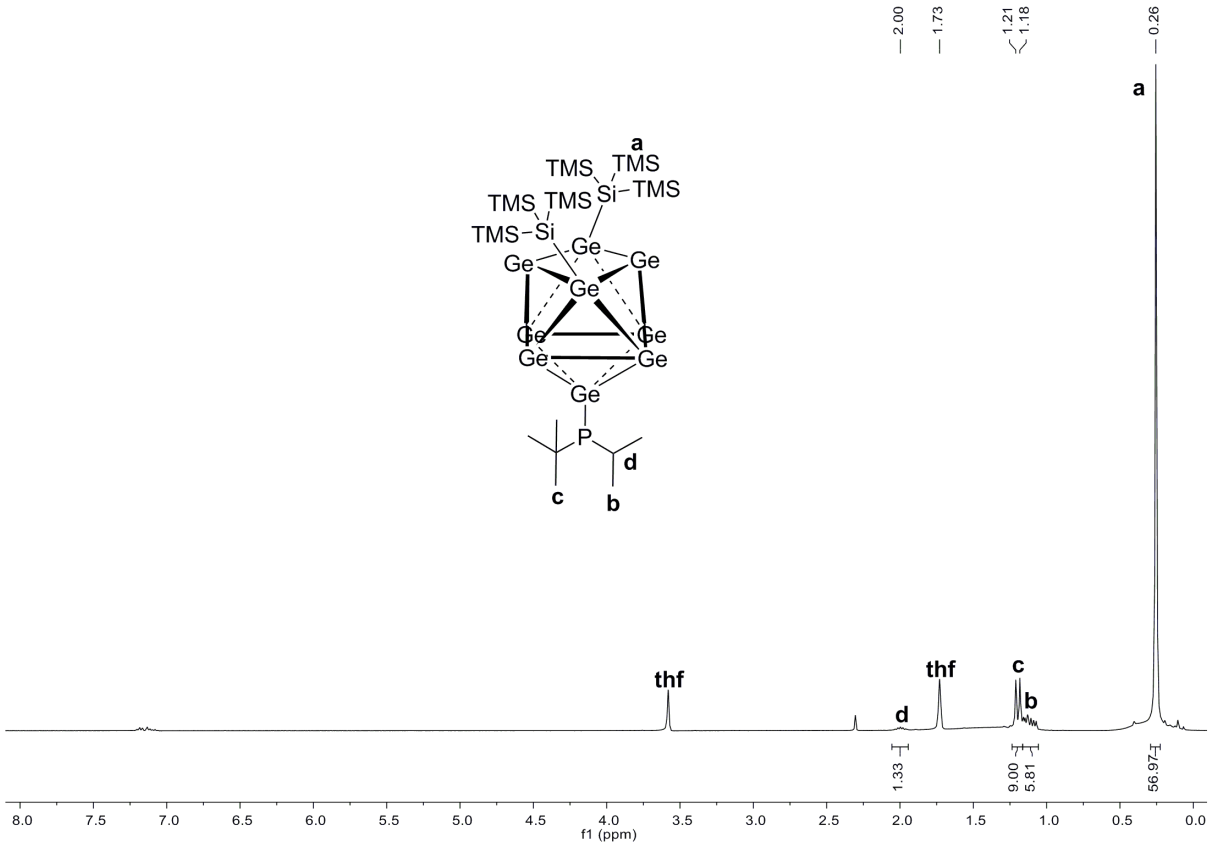

Figure S19. ^{1}H NMR spectrum of compound **4a** in thf-d_8.

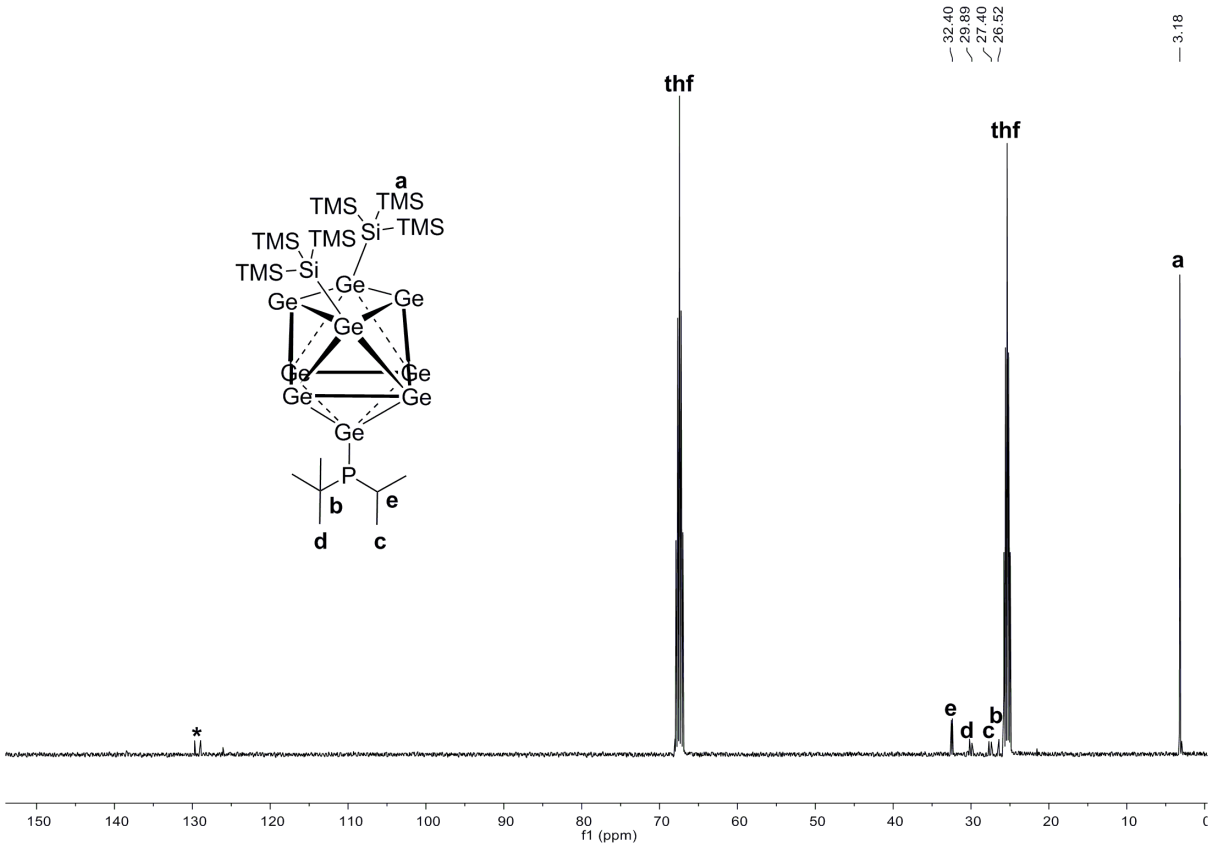

Figure S20. ^{13}C NMR spectrum of compound **4a** in thf-d_8.

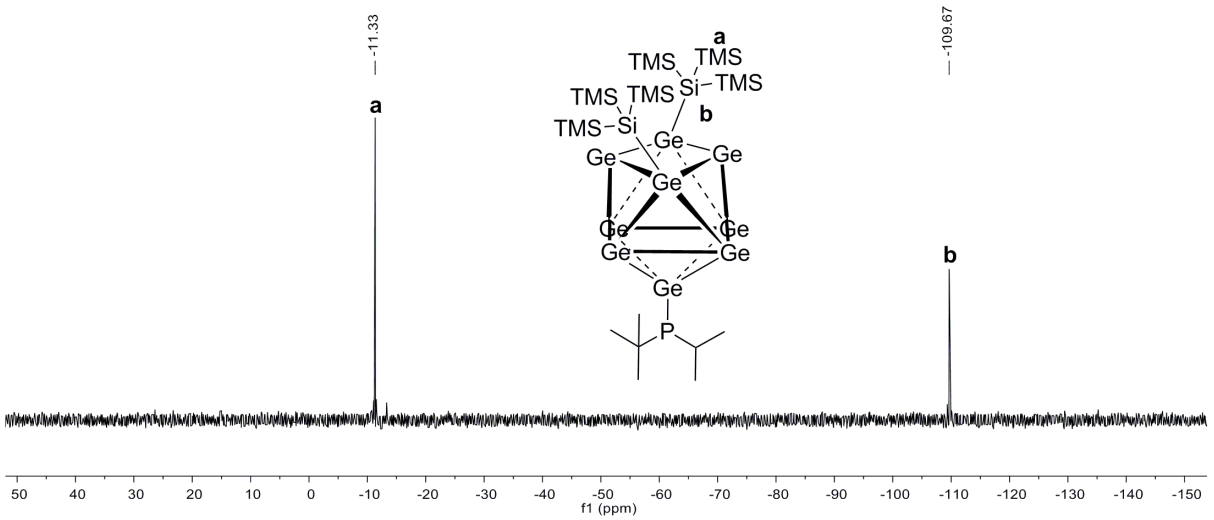

Figure S21. ^{29}Si-INEPT-RD NMR spectrum of compound **4a** in thf-d_8.

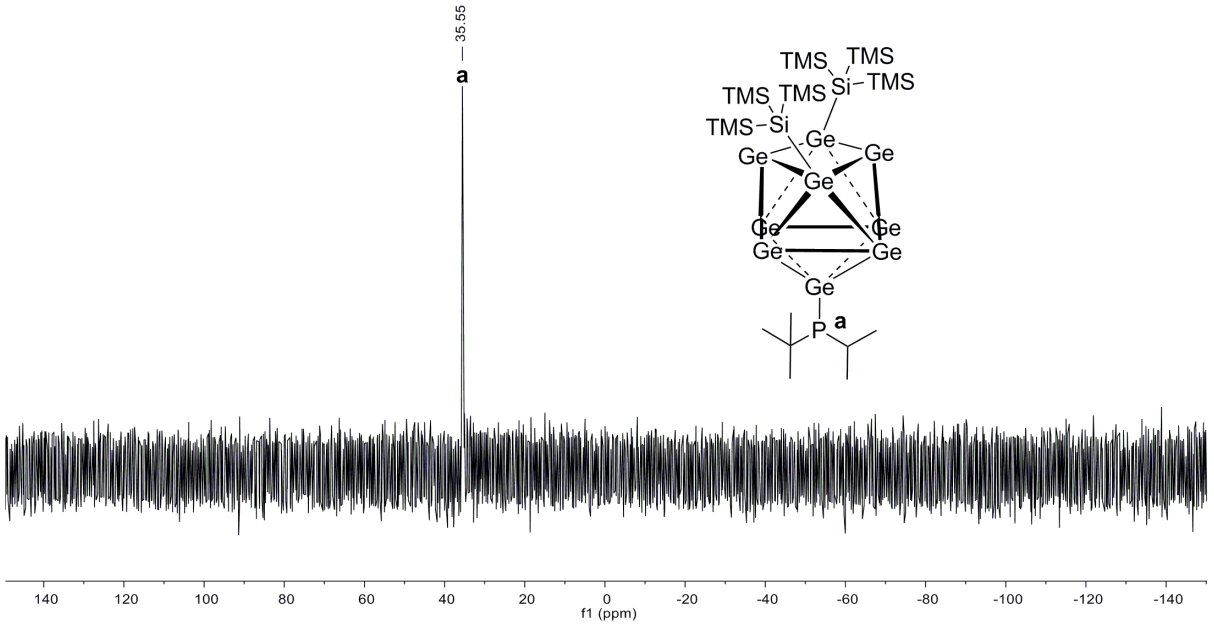

Figure S22. ^{31}P NMR spectrum of compound **4a** in thf-d_8.

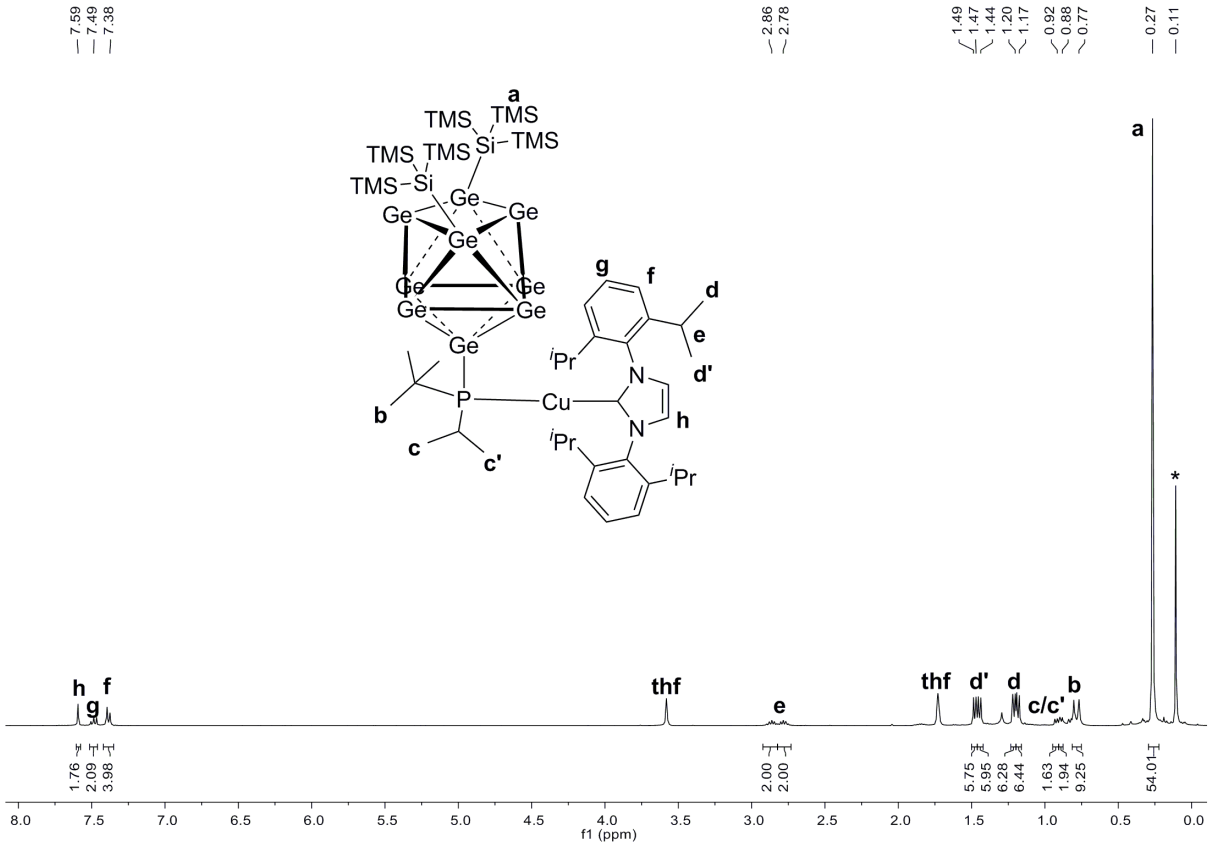

Figure S23. ^{1}H NMR spectrum of compound **4-CuNHC^{Dipp}** in thf-d_8 (signal marked with * belongs to silicon grease).

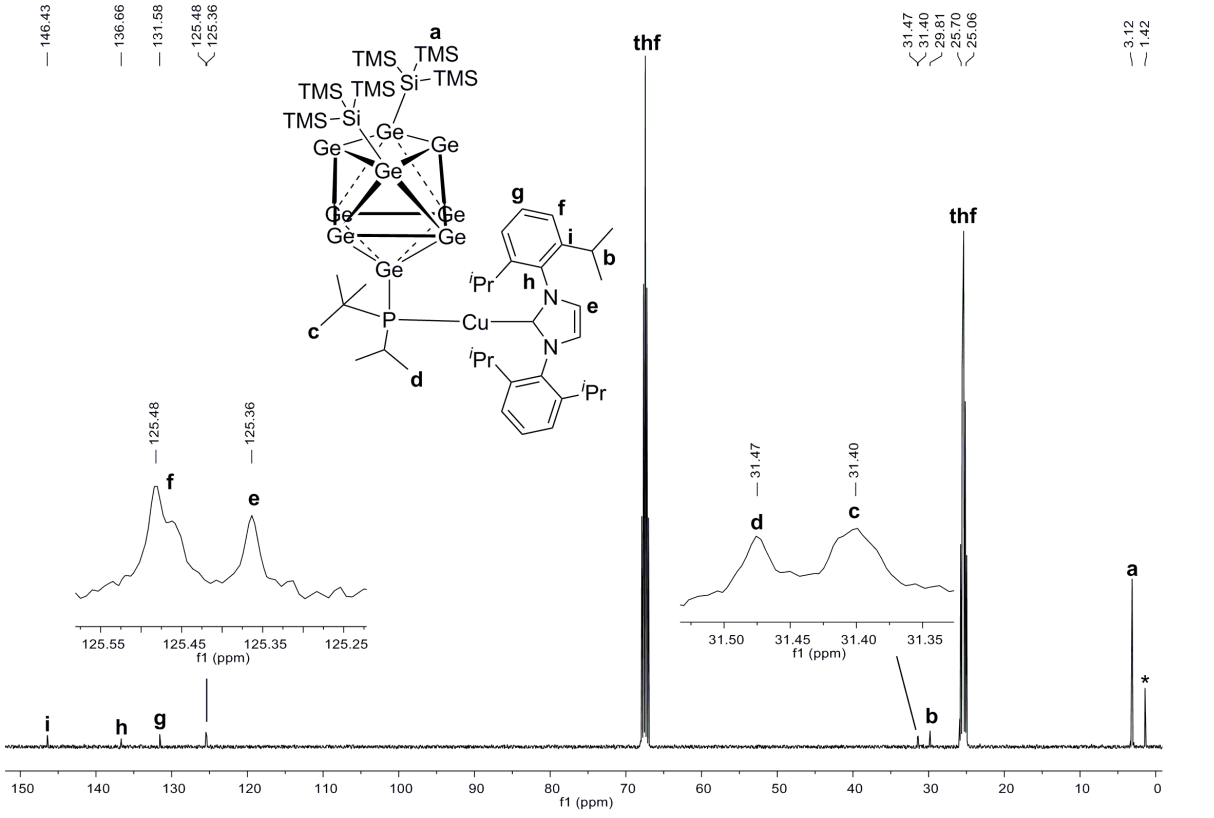

Figure S24. ^{13}C NMR spectrum of compound **4-CuNHC^{Dipp}** in thf-d_8 (signal marked with * belongs to silicon grease).

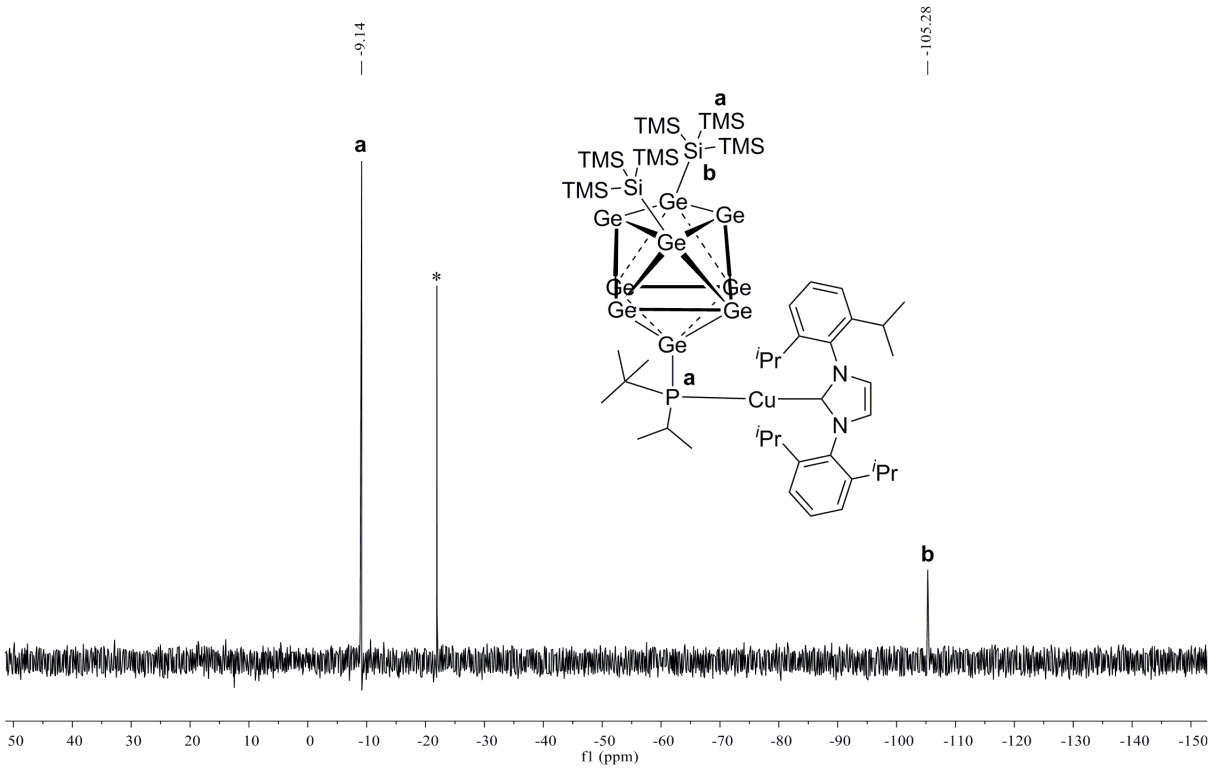

Figure S25. ^{29}Si-INEPT-RD NMR spectrum of compound **4-CuNHC^{Dipp}** in thf-d_8 (signal marked with * belongs to silicon grease).

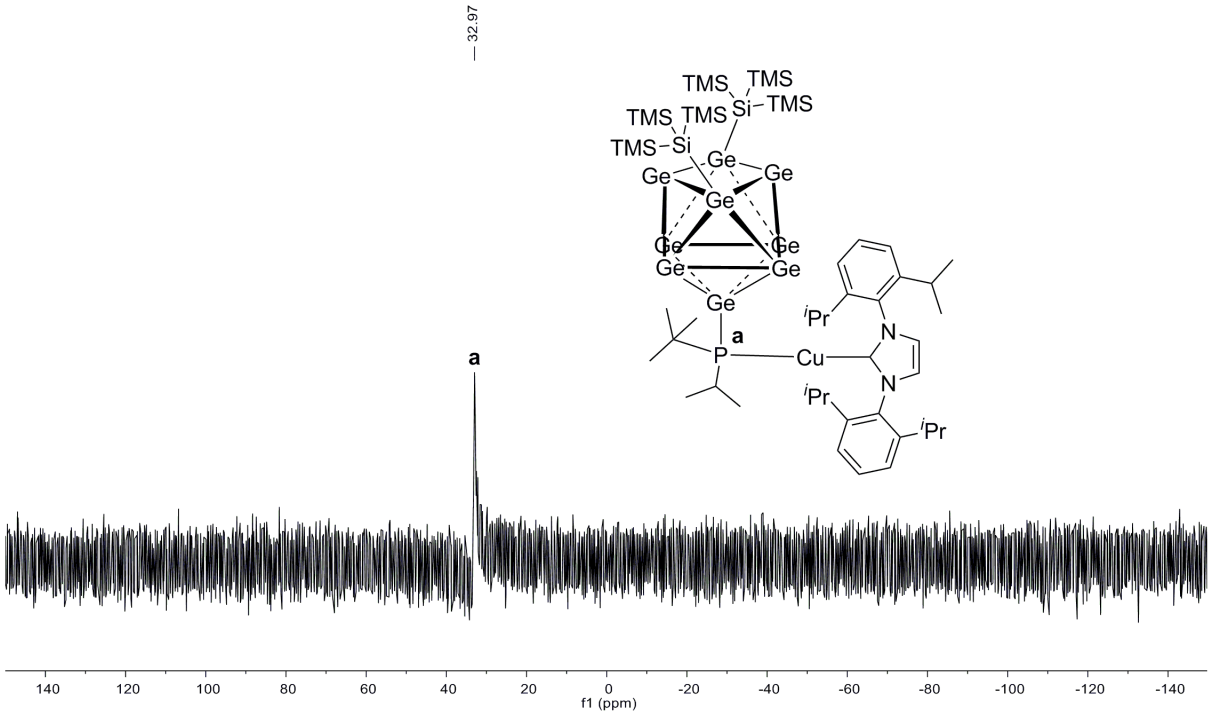

Figure S26. ^{31}P NMR spectrum of compound **4-CuNHC^{Dipp}** in thf-d_8.

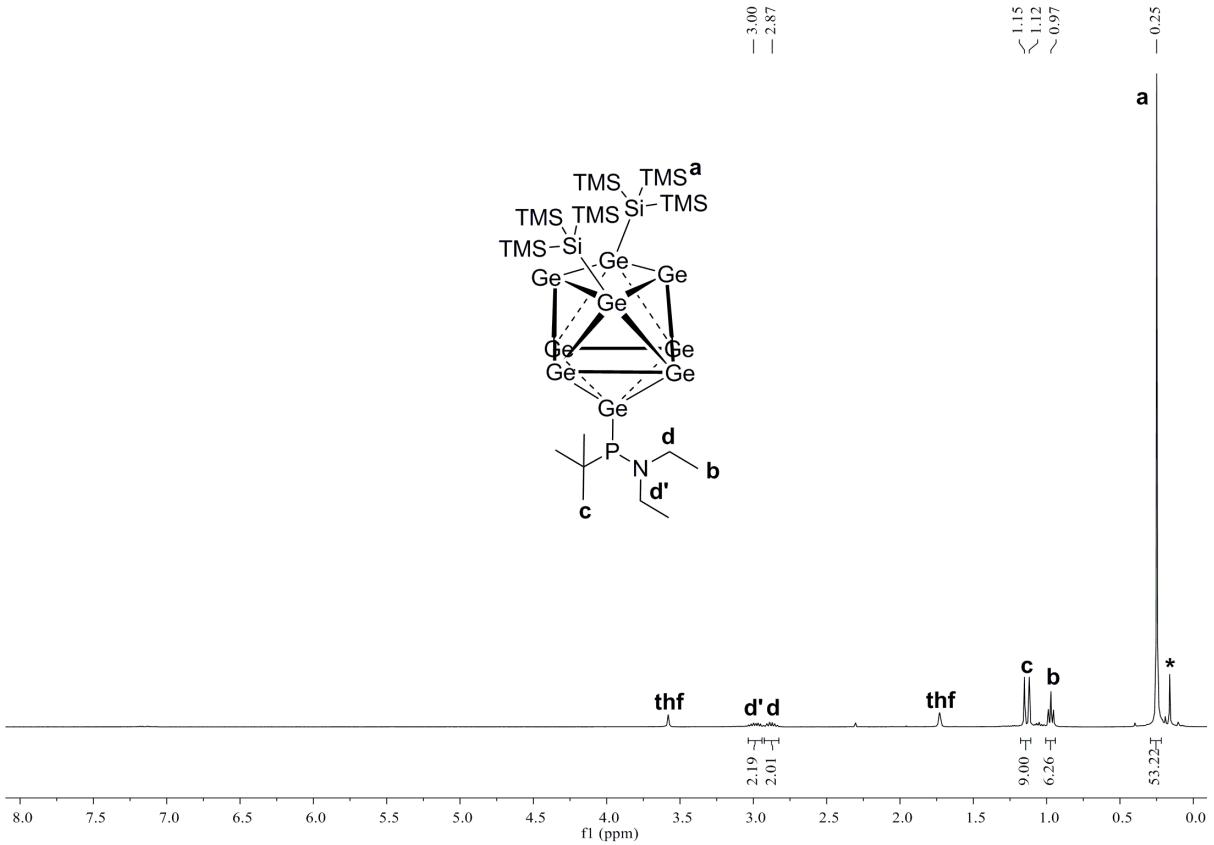

Figure S27. ^{1}H NMR spectrum of compound **5a** in thf-d_8 (signal marked with * belongs to unknown impurity).

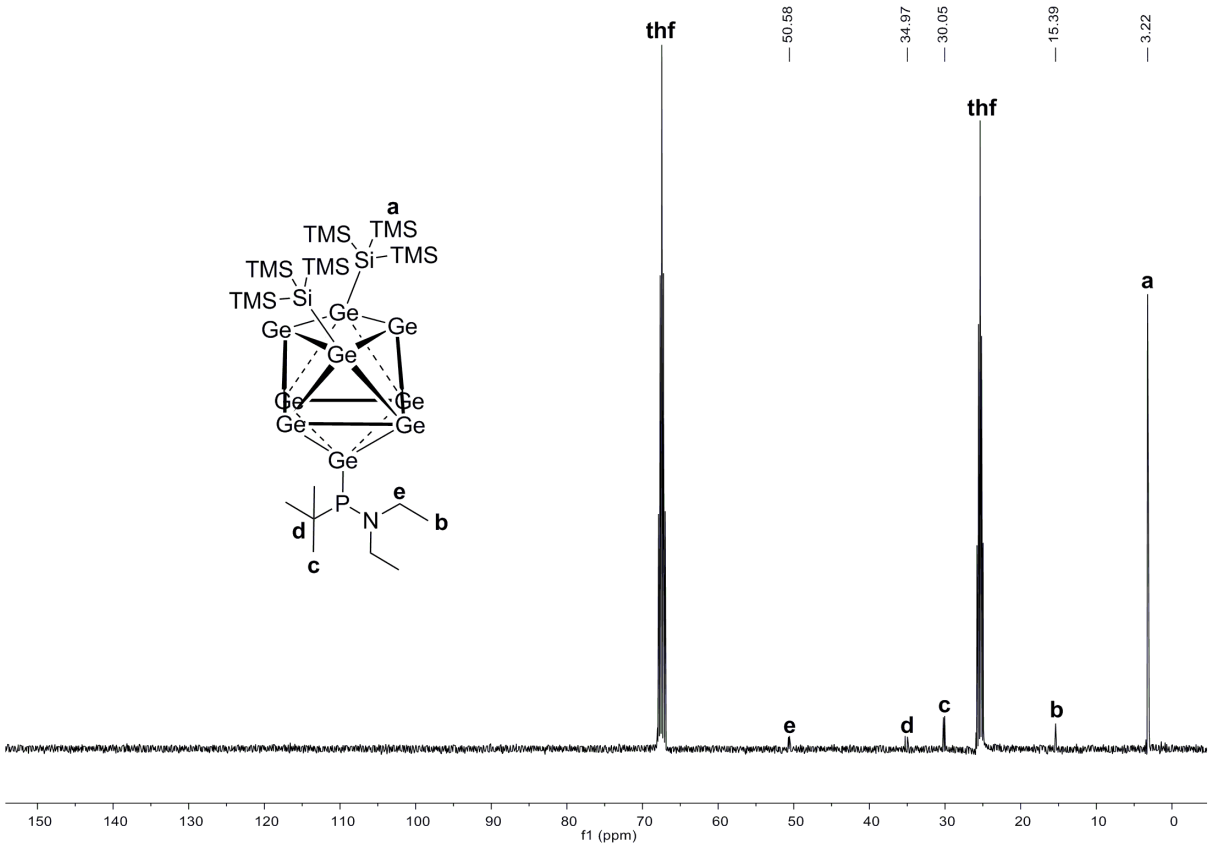

Figure S28. ^{13}C NMR spectrum of compound **5a** in thf-d_8.

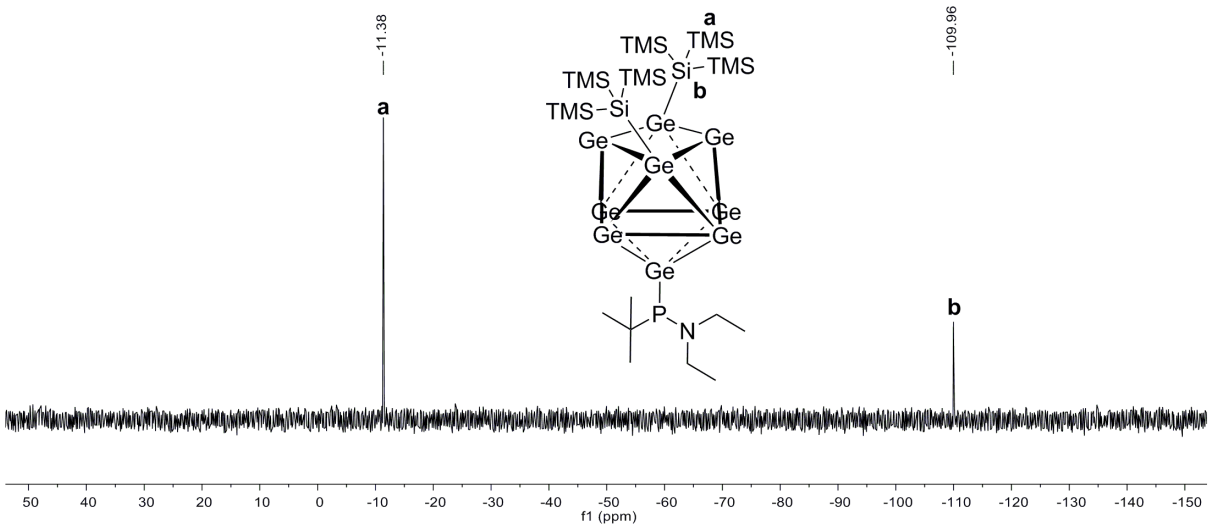

Figure S29. ^{29}Si-INEPT-RD NMR spectrum of compound **5a** in thf-d_8.

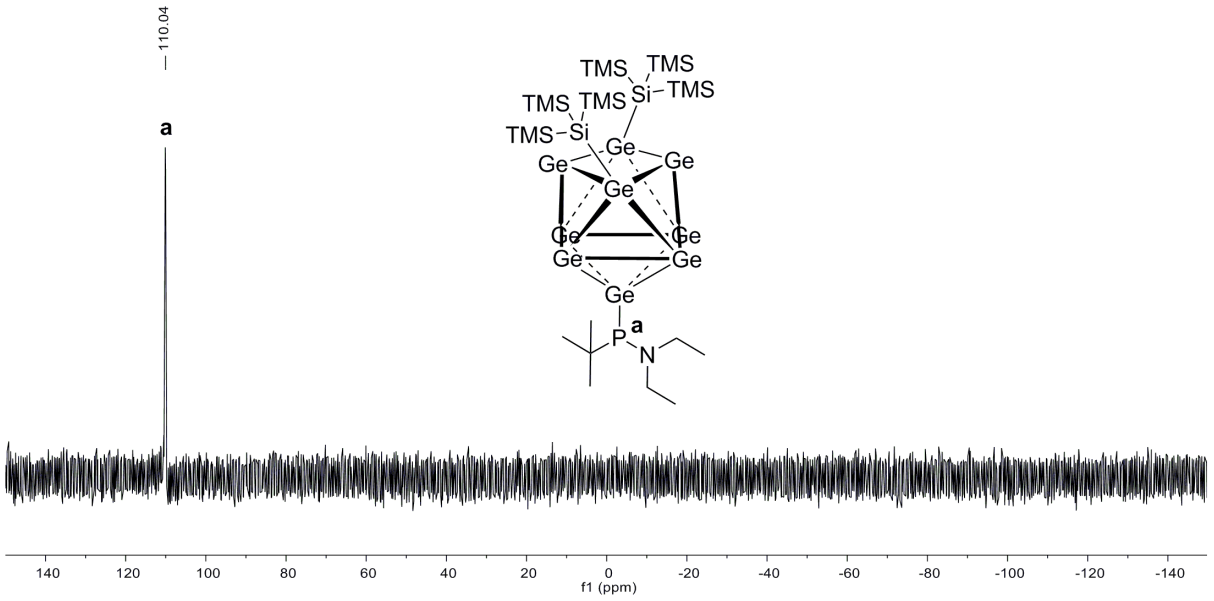

Figure S30. ^{31}P NMR spectrum of compound **5a** in thf-d_8.

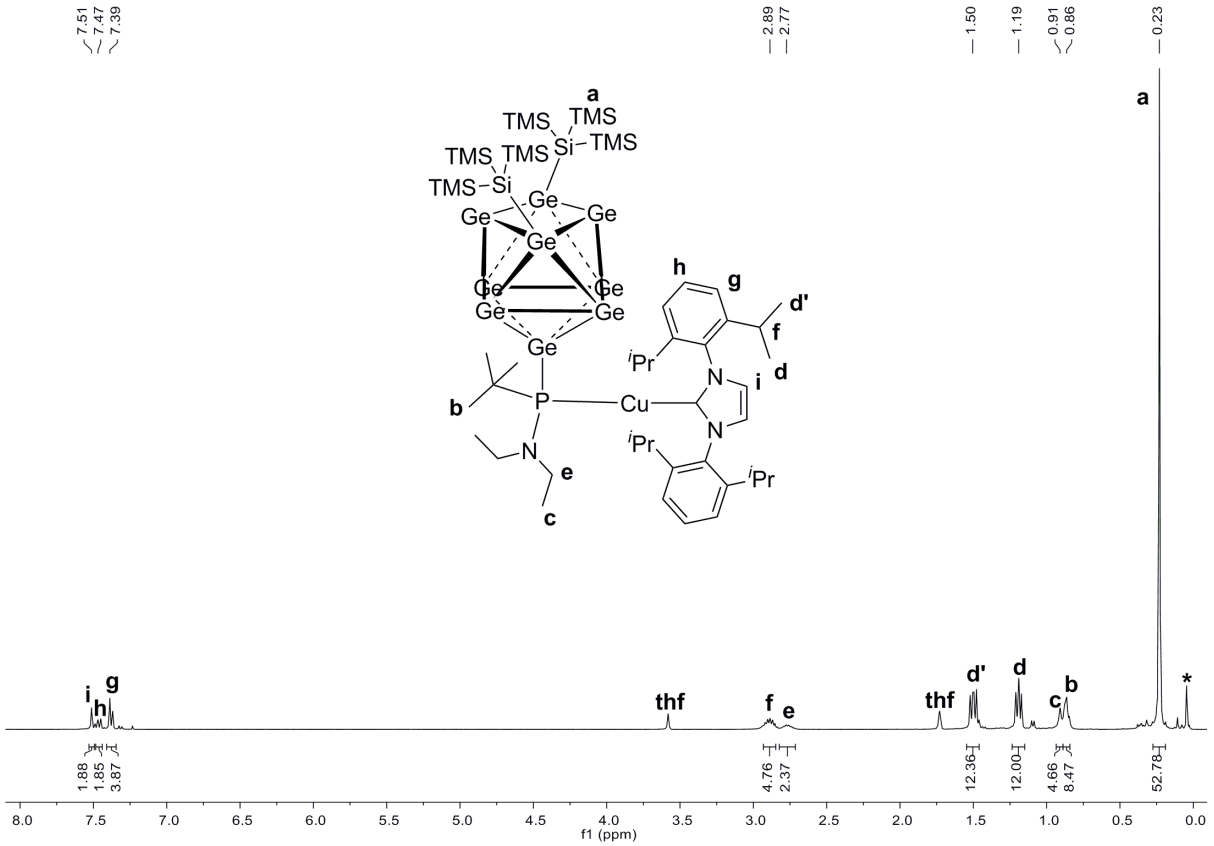

Figure S31. ^{1}H NMR spectrum of compound **5-CuNHC^{Dipp}** in thf-d_8 (signal marked with * belongs to unknown impurity).

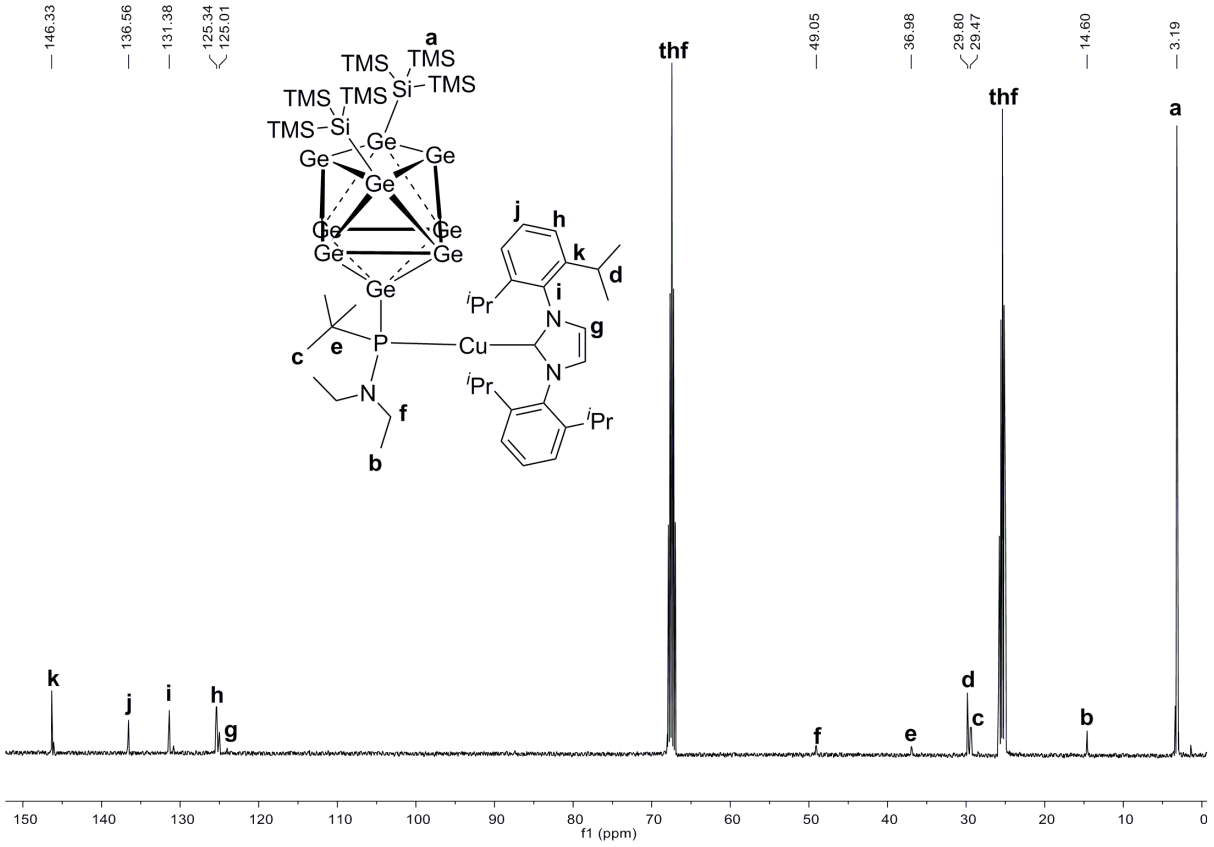

Figure S32. ^{13}C NMR spectrum of compound **5-CuNHC^{Dipp}** in thf-d_8.

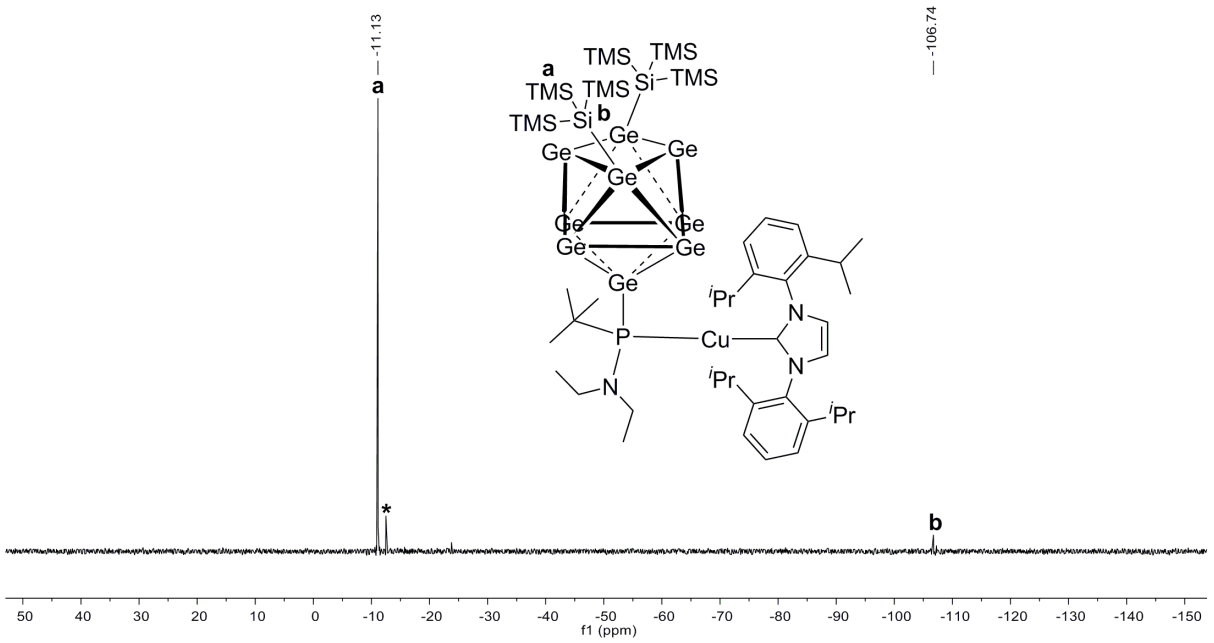

Figure S33. ^{29}Si-INEPT-RD NMR spectrum of compound **5-CuNHC^{Dipp}** in thf-*d*$_8$ (signal marked with * belongs to unknown impurity).

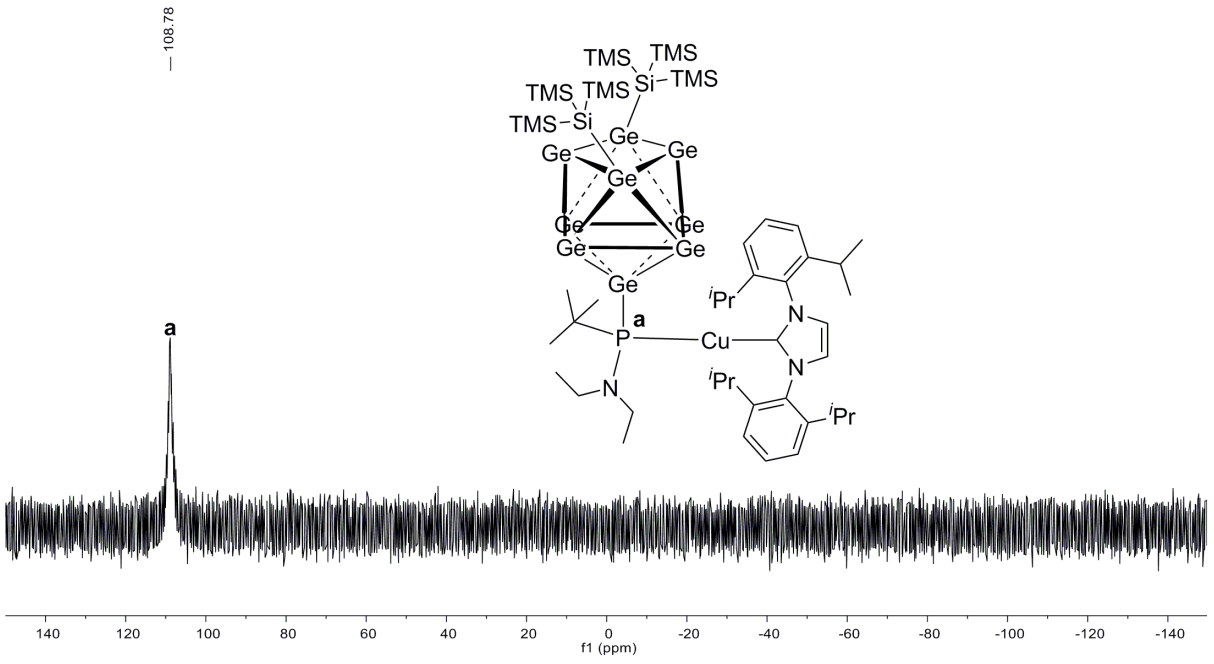

Figure S34. ^{31}P NMR spectrum of compound **5-CuNHC^{Dipp}** in thf-*d*$_8$.

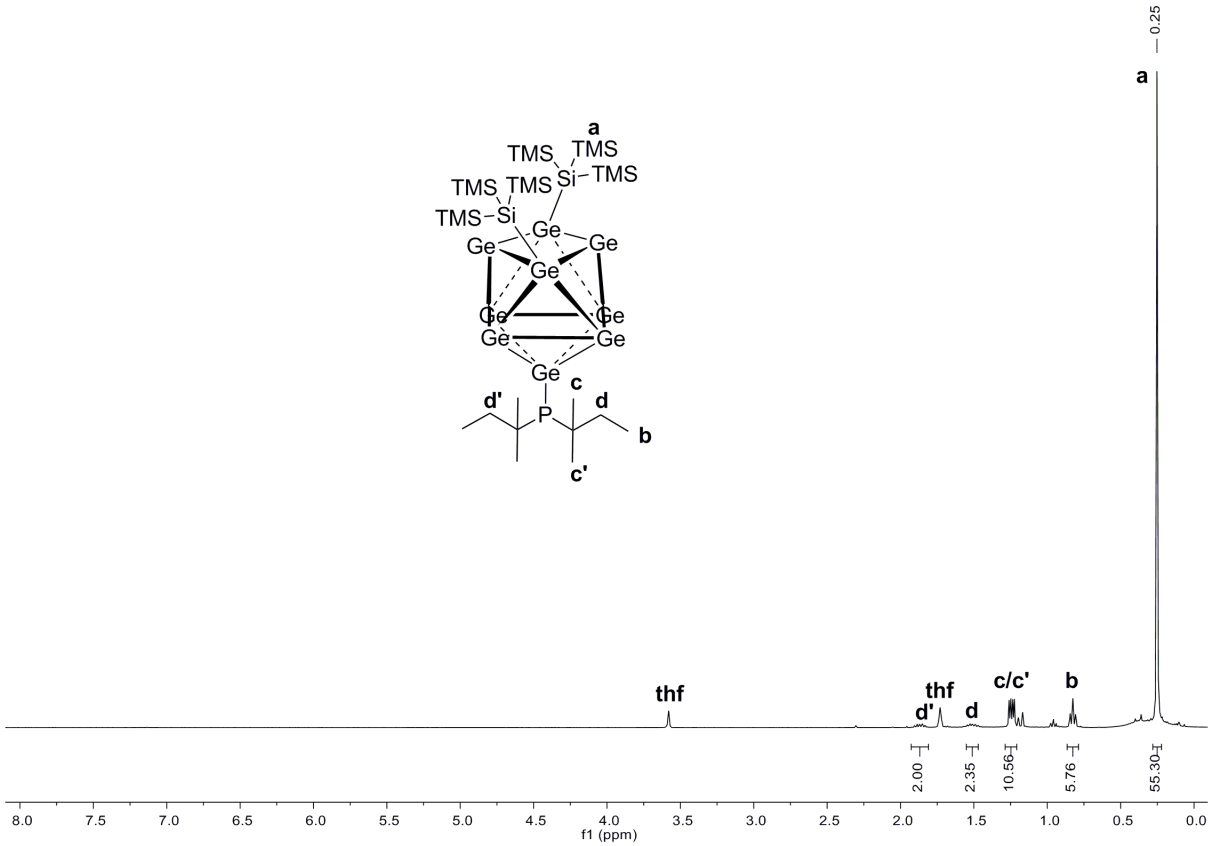

Figure S35. ^{1}H NMR spectrum of compound **6a** in thf-d_8.

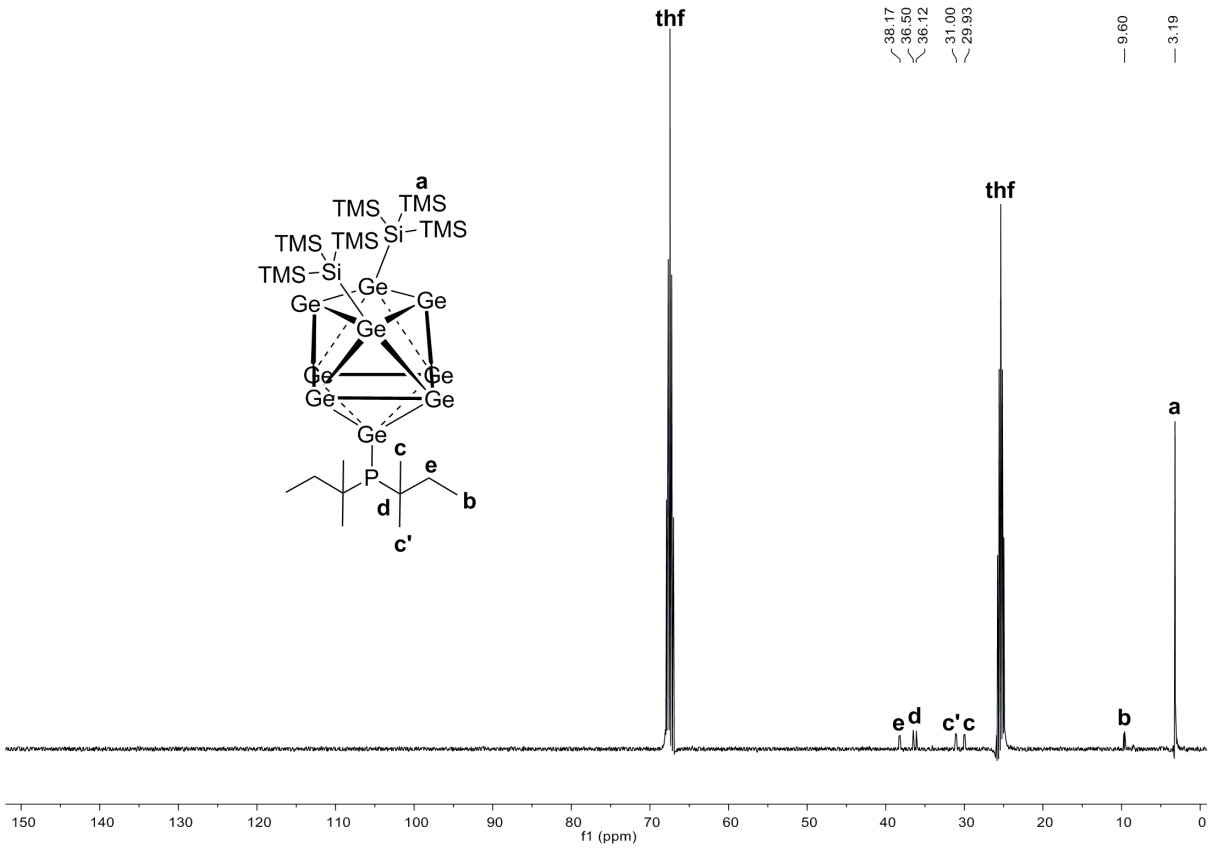

Figure S36. ^{13}C NMR spectrum of compound **6a** in thf-d_8.

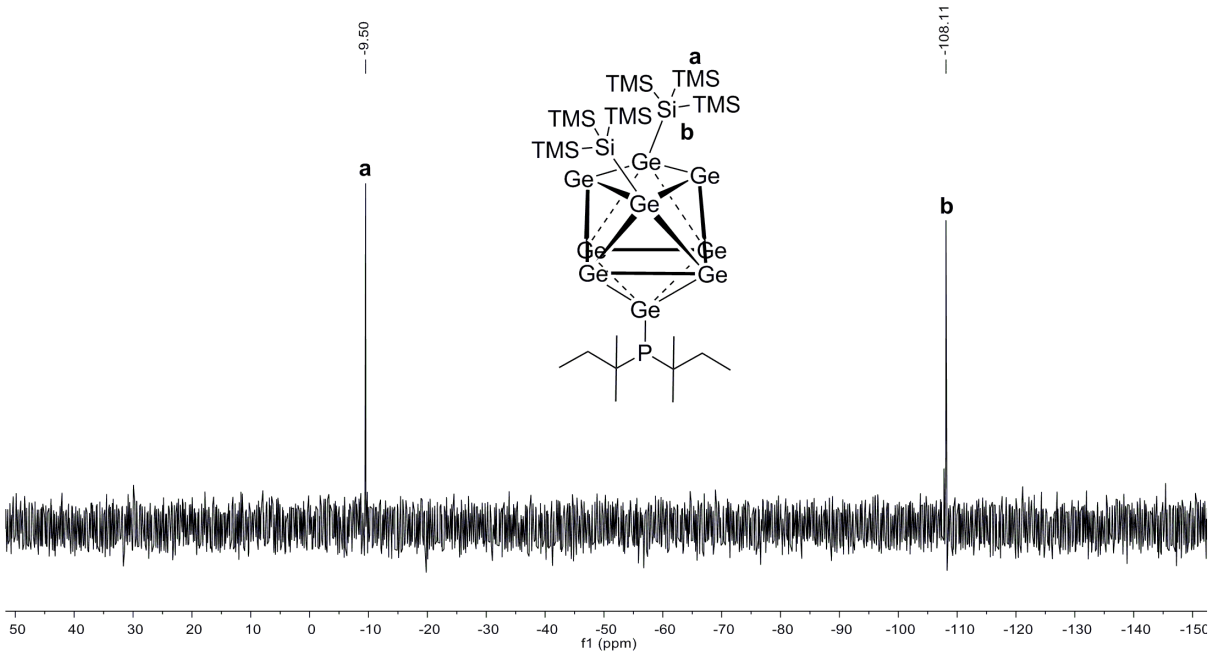

Figure S37. ^{29}Si-INEPT-RD NMR spectrum of compound **6a** in thf-d_8.

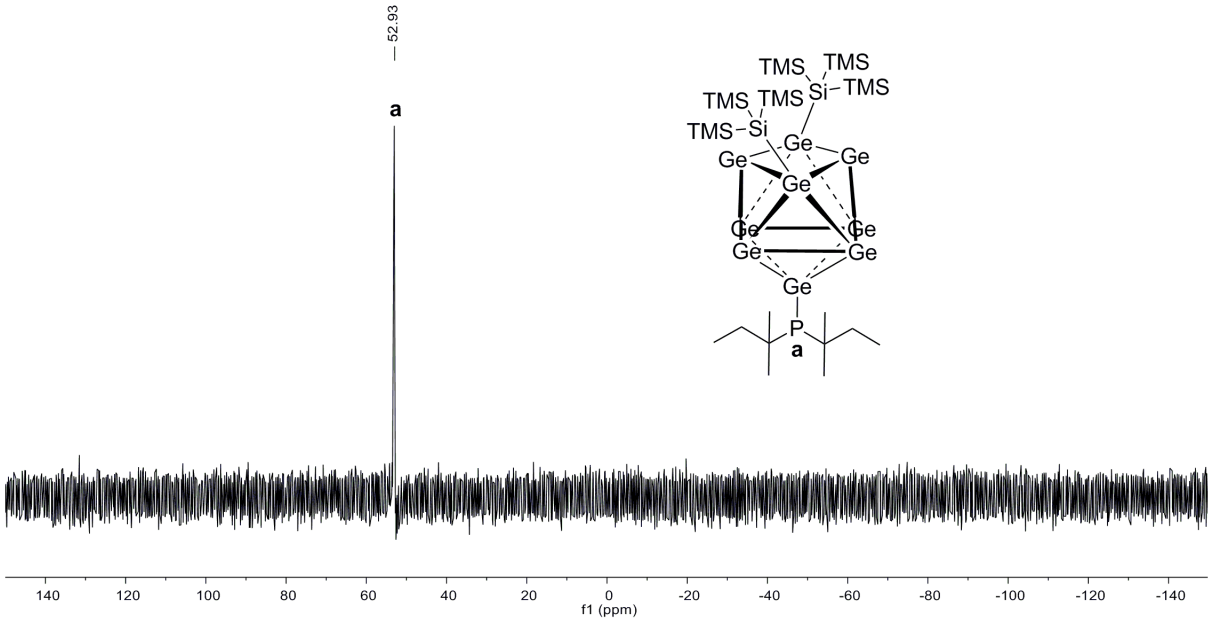

Figure S38. ^{31}P NMR spectrum of compound **6a** in thf-d_8

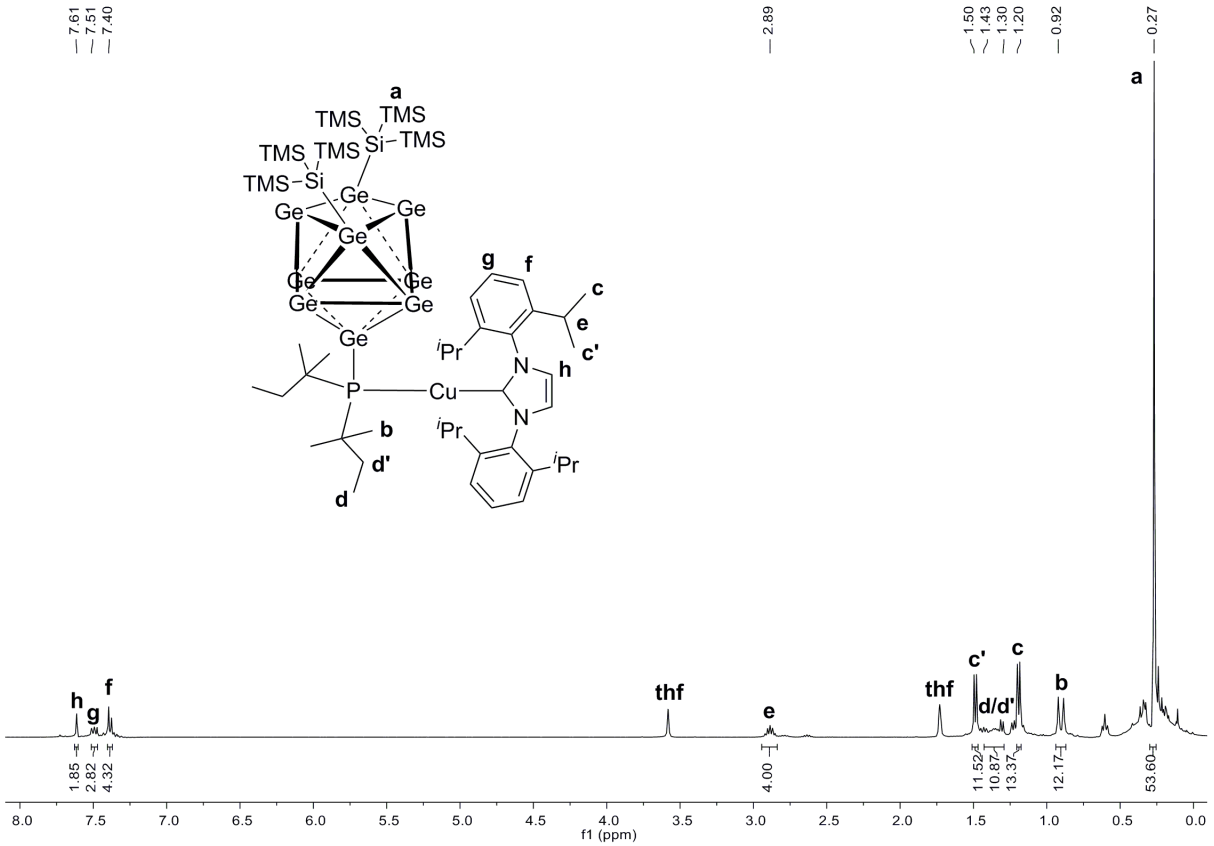

Figure S39. ^{1}H NMR spectrum of compound **6-CuNHC^{Dipp}** in thf-d_8.

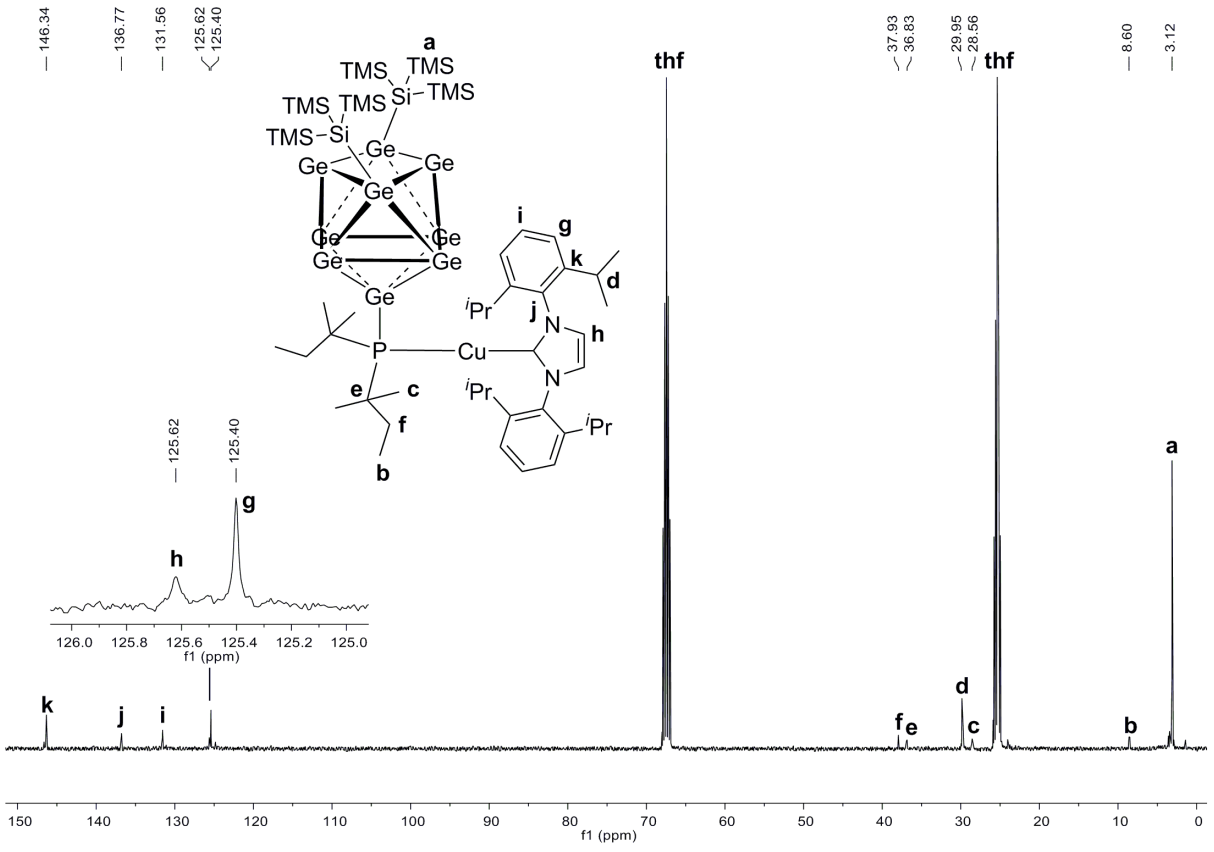

Figure S40. ^{13}C NMR spectrum of compound **6-CuNHC^{Dipp}** in thf-d_8.

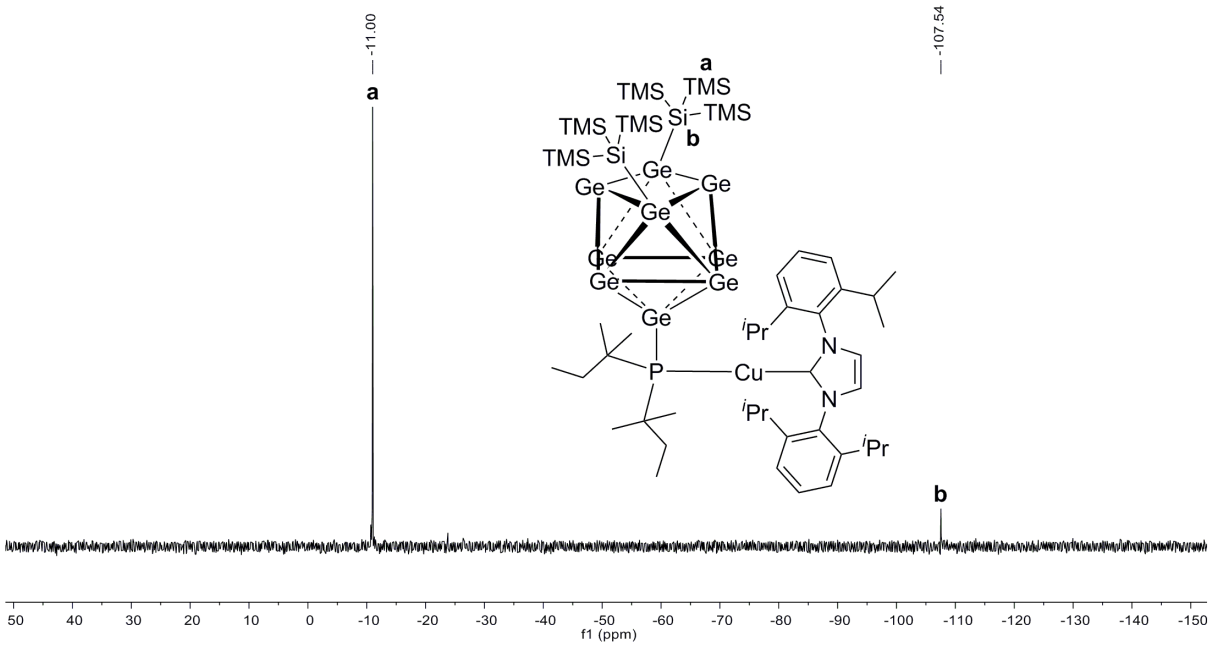

Figure S41. ^{29}Si-INEPT-RD NMR spectrum of compound **6-CuNHC^{Dipp}** in thf-d_8.

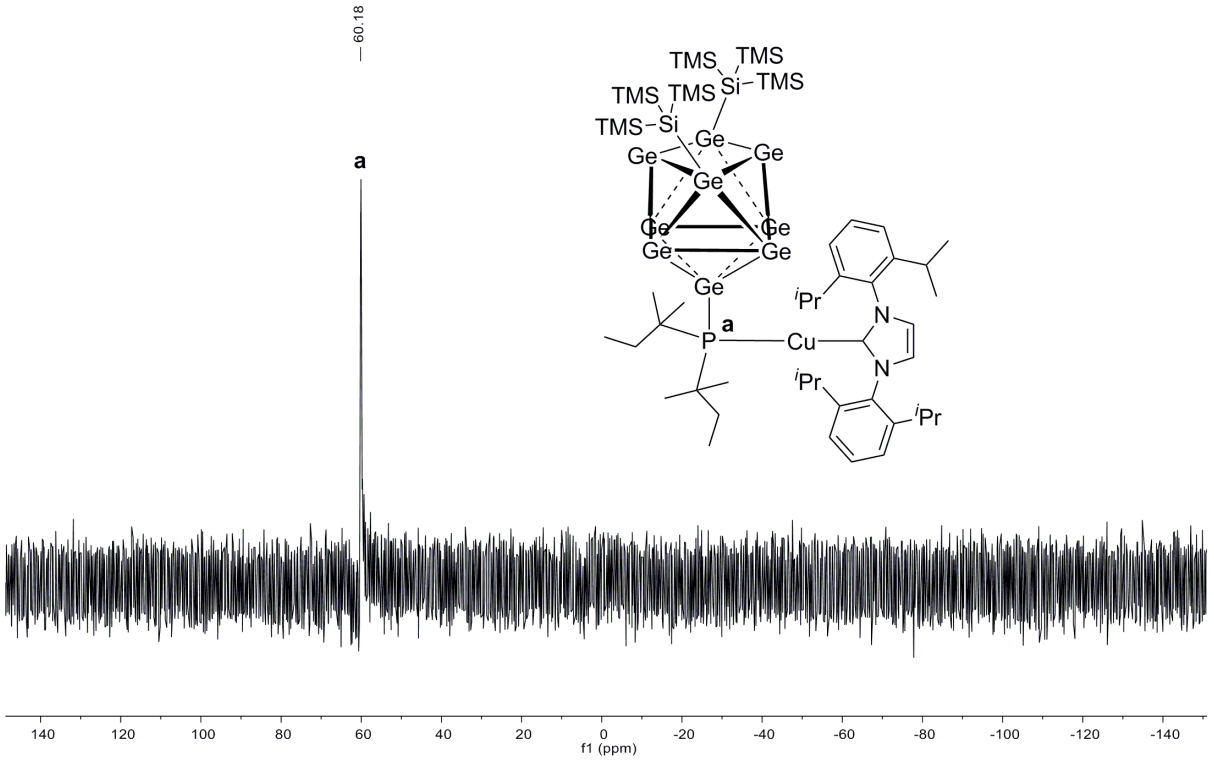

Figure S42. ^{31}P NMR spectrum of compound **6-CuNHC^{Dipp}** in thf-d_8.

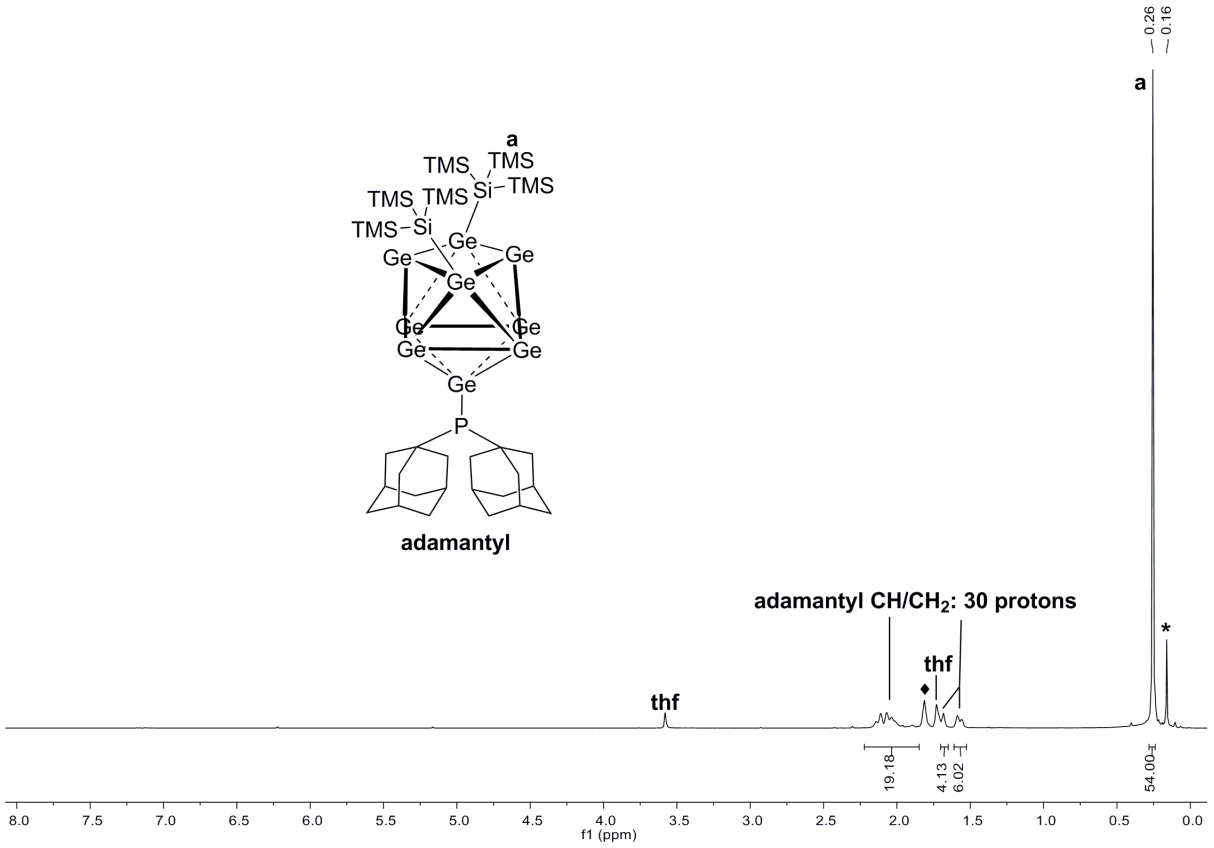

Figure S43. ^{1}H NMR spectrum of compound **7a** in thf-d_8 (signal marked with * belongs to bis-silylated cluster $[Ge_9\{Si(TMS)_3\}_2]^{2-}$, signal marked with ♦ belongs to an unknown impurity).

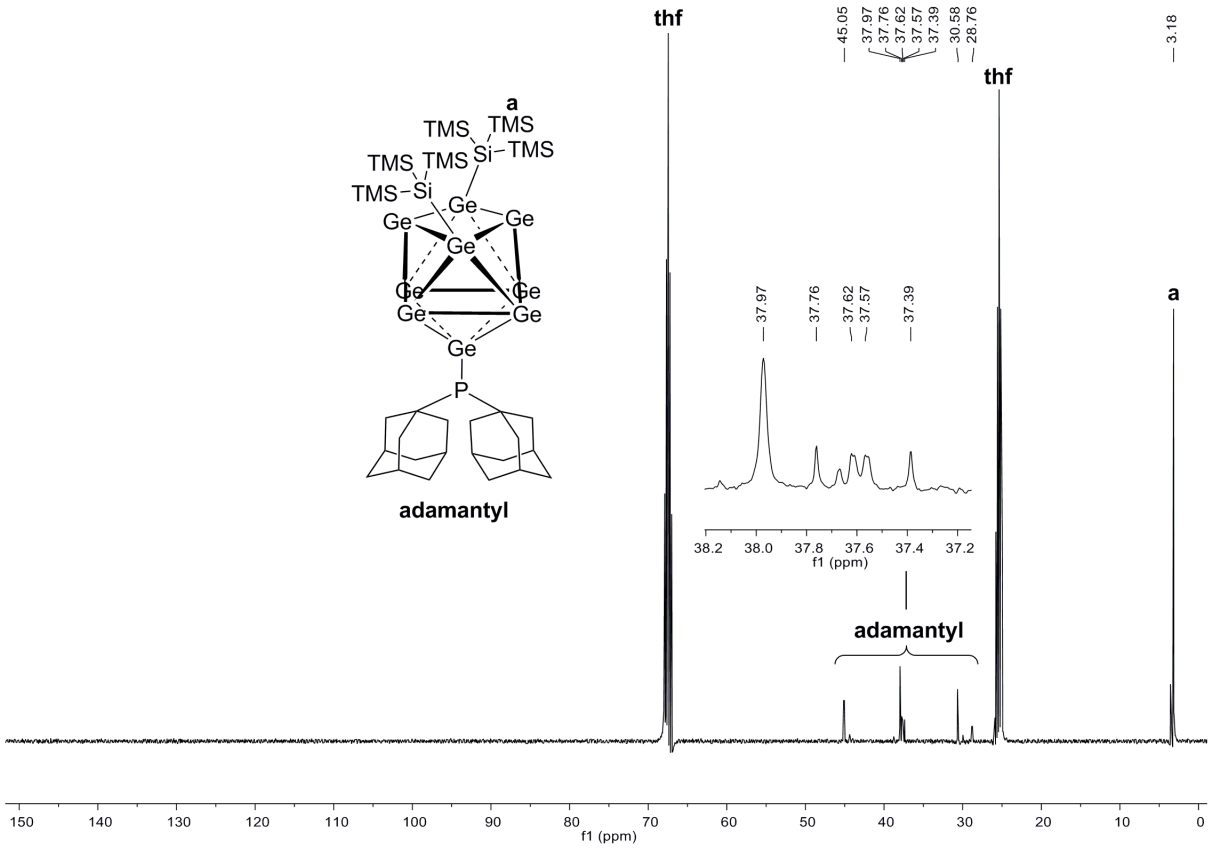

Figure S44. ^{13}C NMR spectrum of compound **7a** in thf-d_8.

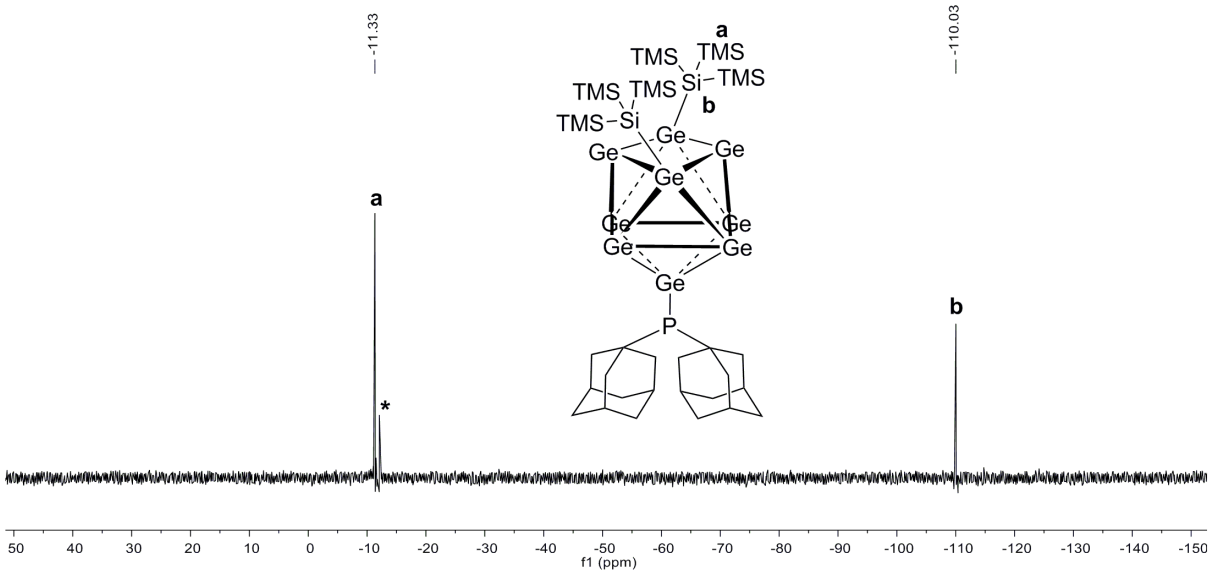

Figure S45. ^{29}Si-INEPT-RD NMR spectrum of compound **7a** in thf-d_8 (signal marked with * belongs to unknown impurity).

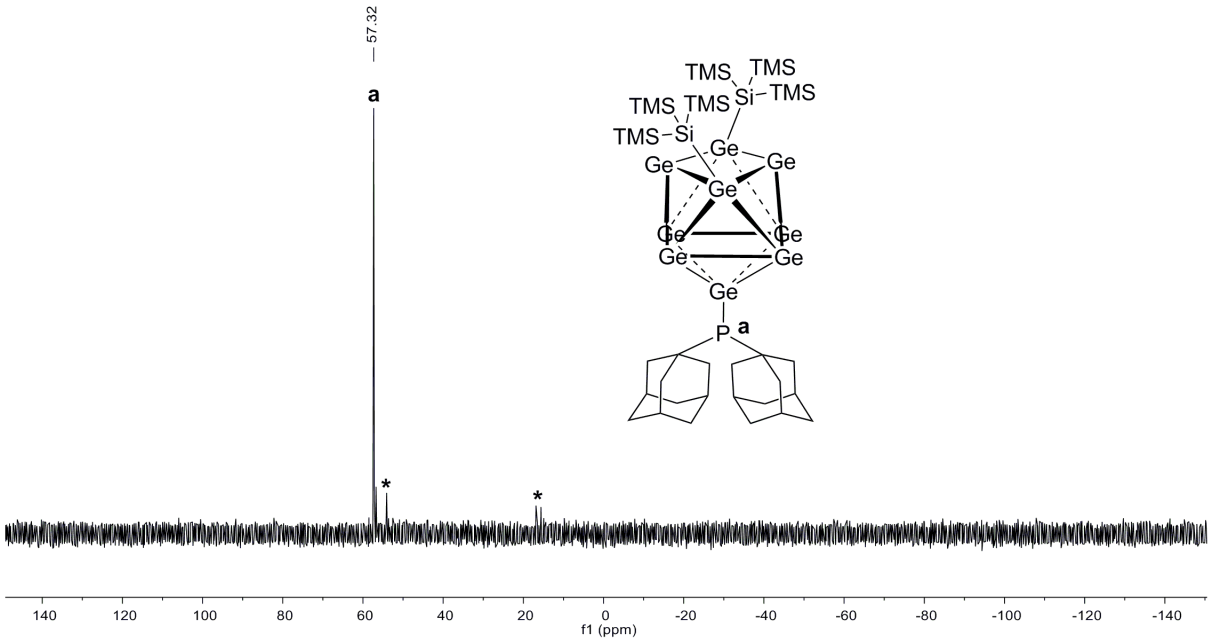

Figure S46. ^{31}P NMR spectrum of compound **7a** in thf-d_8 (signals marked with * belong to unknown impurities).

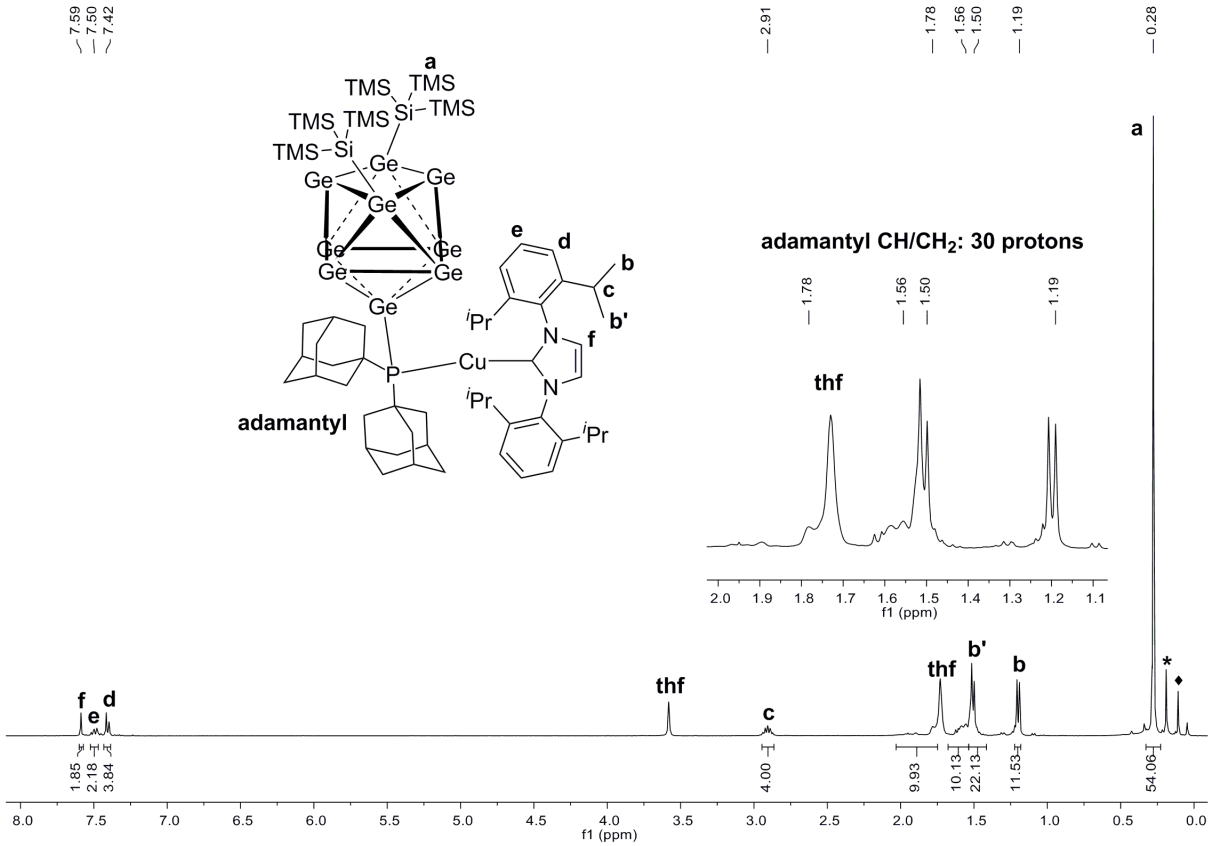

Figure S47. ^{1}H NMR spectrum of compound **7-CuNHC^{Dipp}** in thf-d_8 (signal marked with * belongs to unknown impurity, signal marked with ♦ belongs to silicon grease).

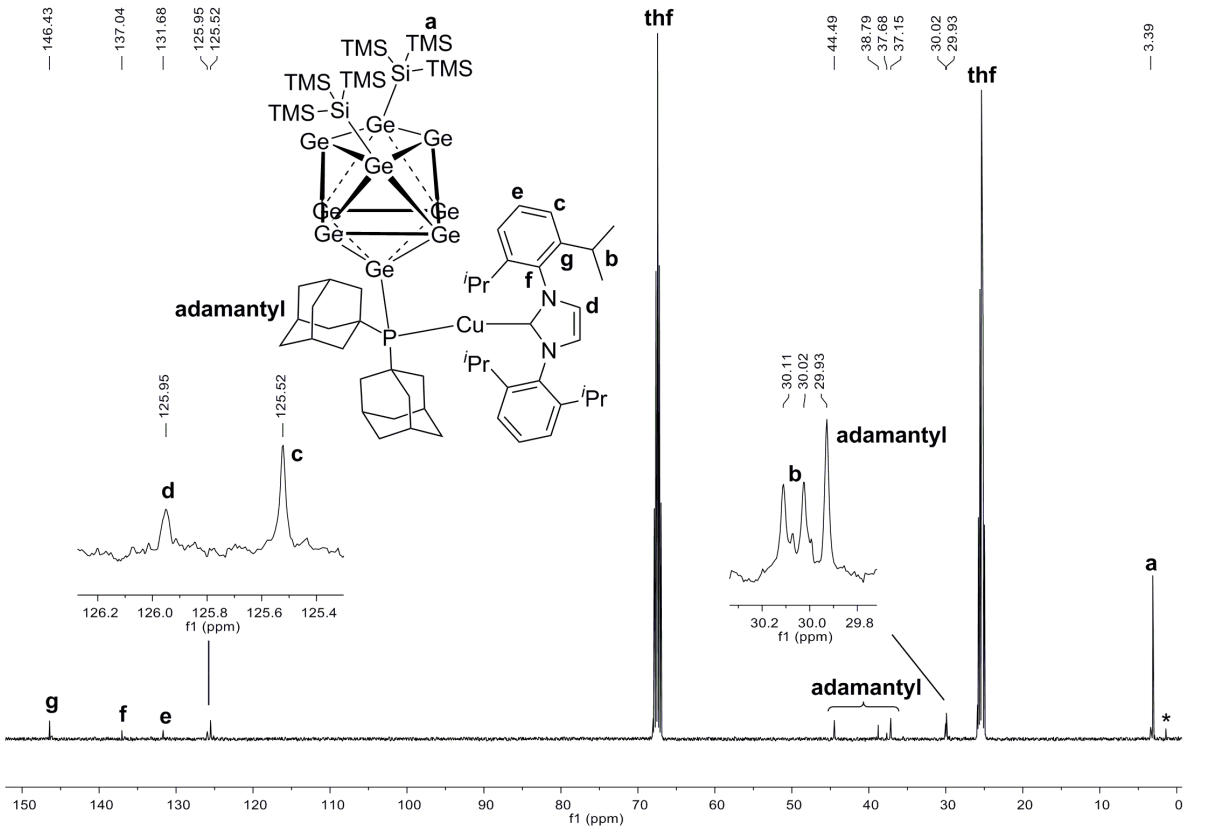

Figure S48. ^{13}C NMR spectrum of compound **7-CuNHC^{Dipp}** in thf-d_8 (signal marked with * belongs to silicon grease).

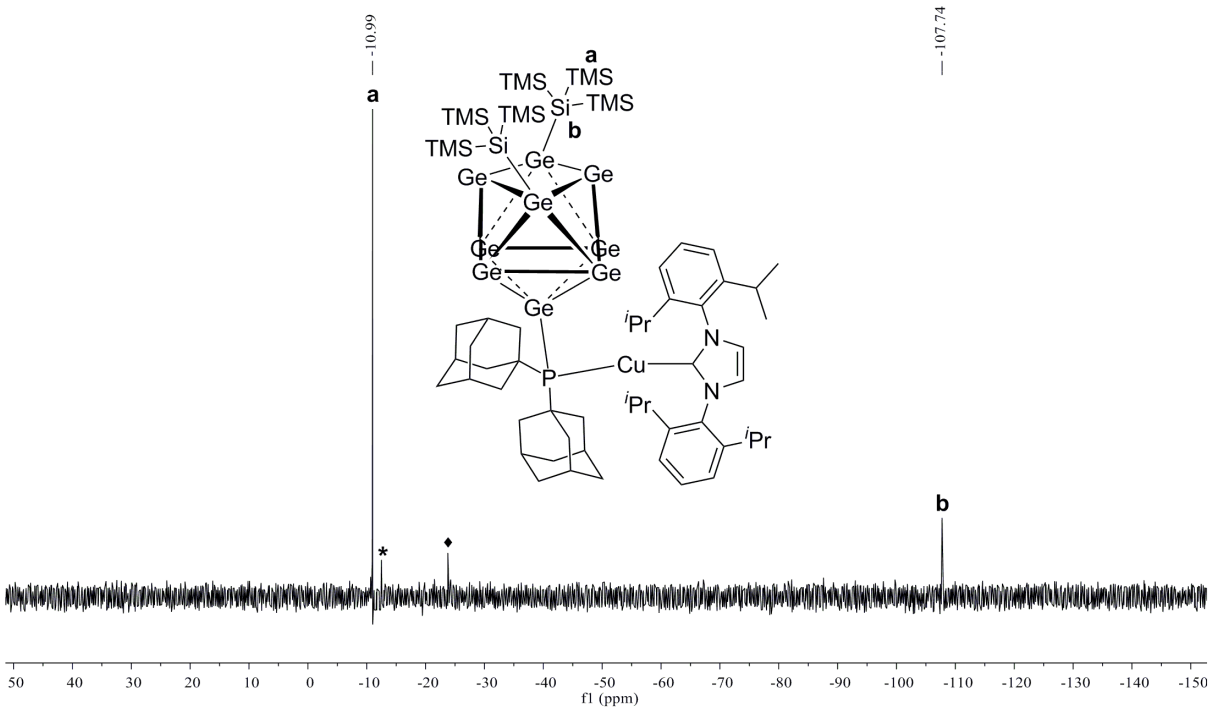

Figure S49. ^{29}Si-INEPT-RD NMR spectrum of compound **7-CuNHC^{Dipp}** in thf-d_8 (signal marked with * belongs to unknown impurity, signal marked with ♦ belongs to silicon grease).

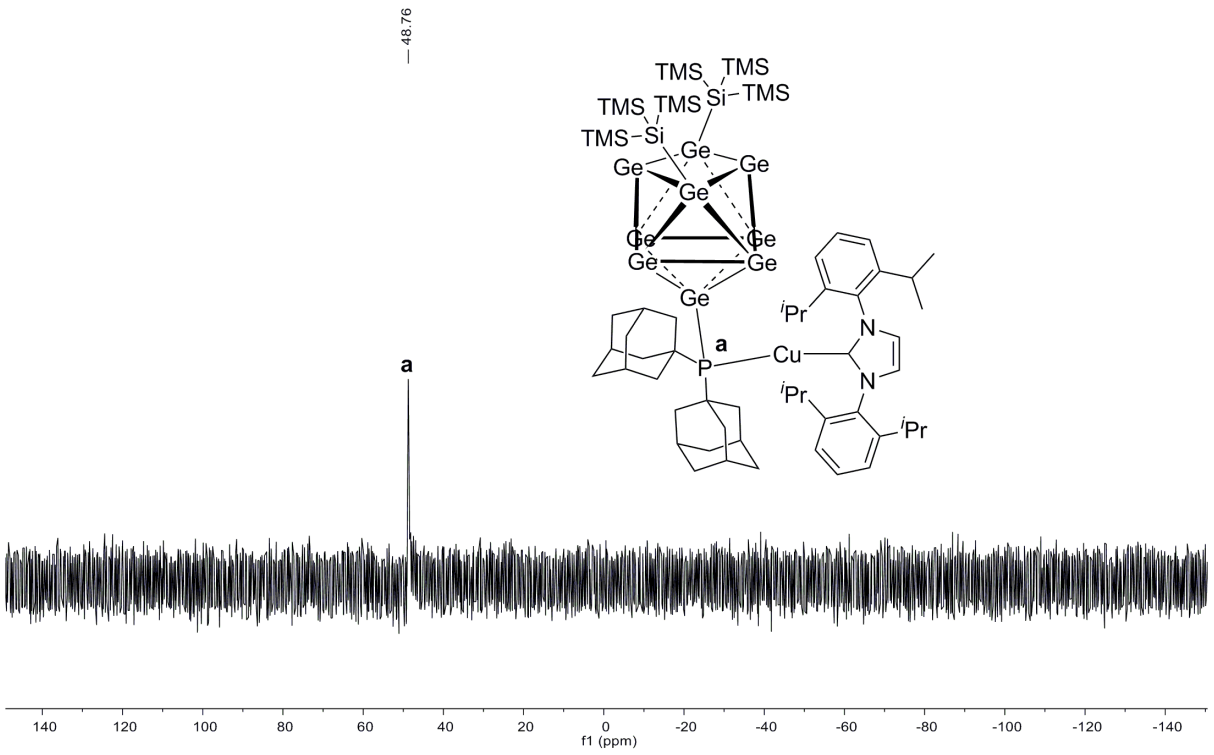

Figure S50. ^{31}P NMR spectrum of compound **7-CuNHC^{Dipp}** in thf-d_8.

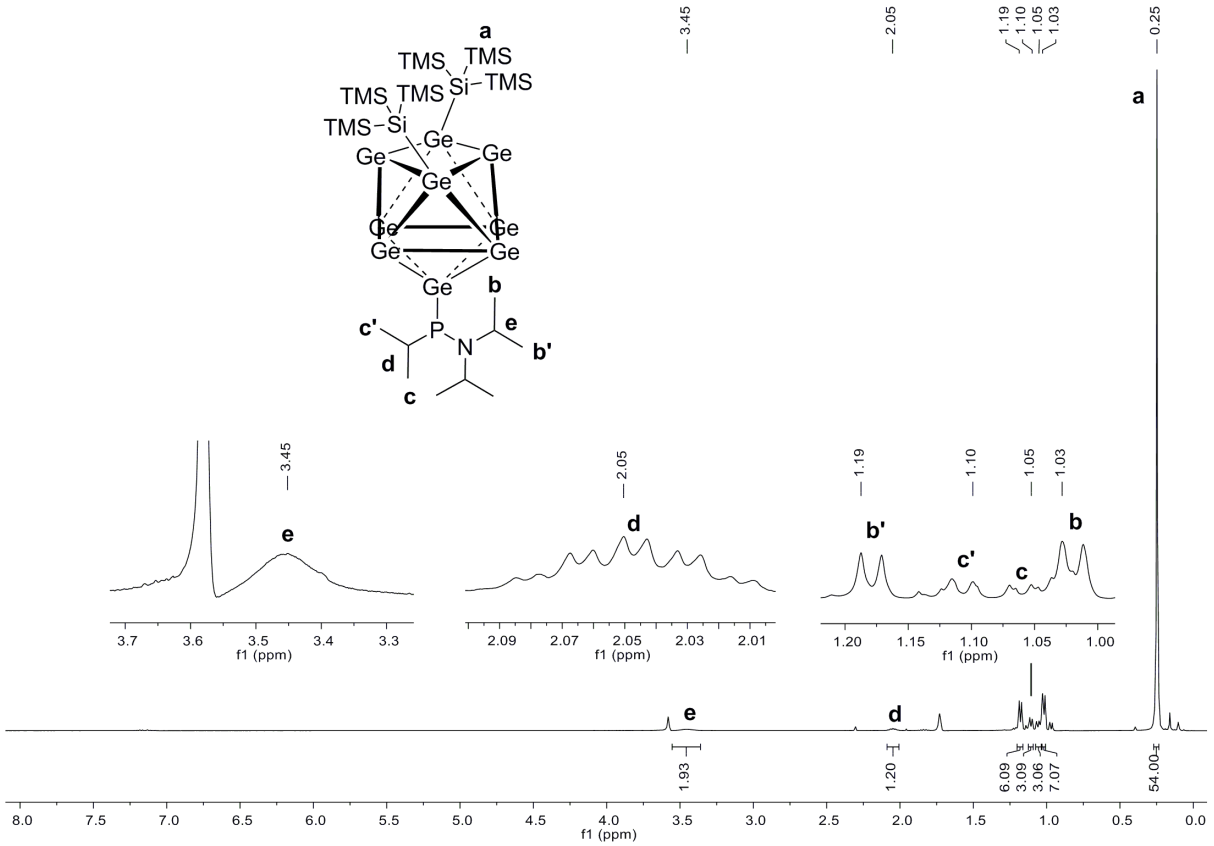

Figure S51. ^{1}H NMR spectrum of compound **8a** in thf-d_8.

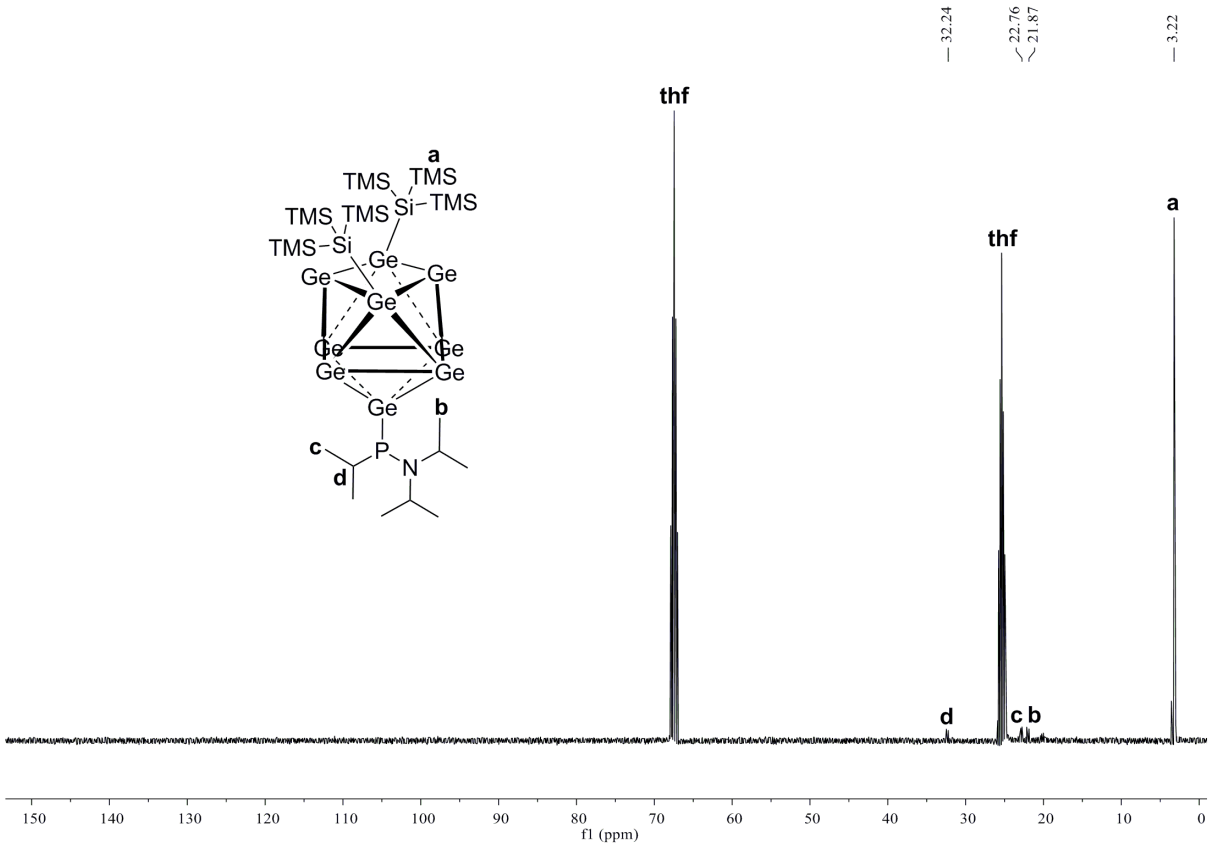

Figure S52. ^{13}C NMR spectrum of compound **8a** in thf-d_8.

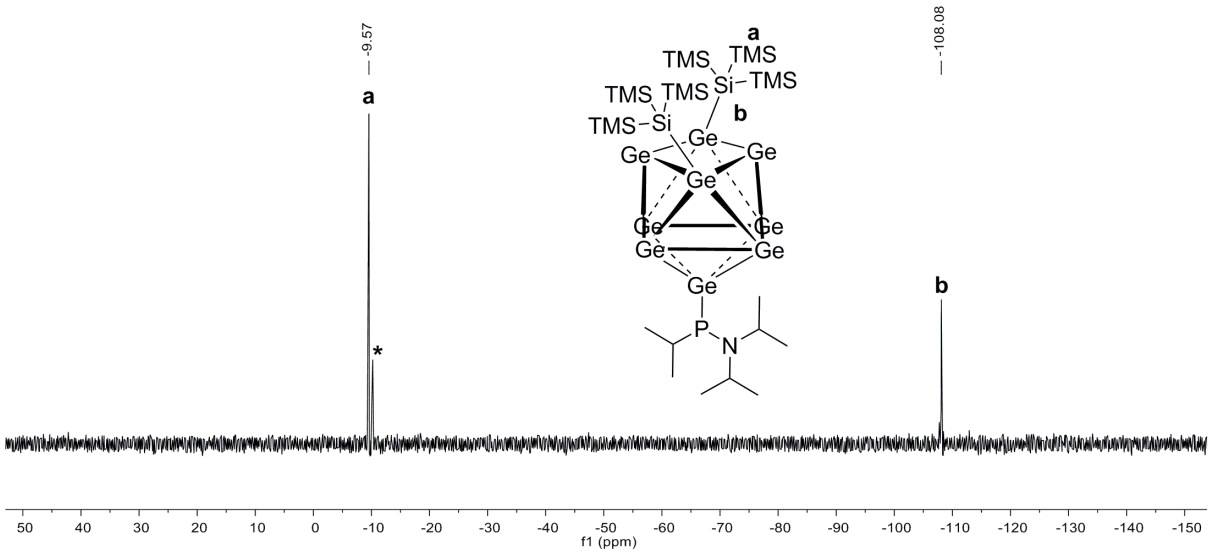

Figure S53. ^{29}Si-INEPT-RD NMR spectrum of compound **8a** in thf-d_8 (signal marked with * belongs to unknown impurity).

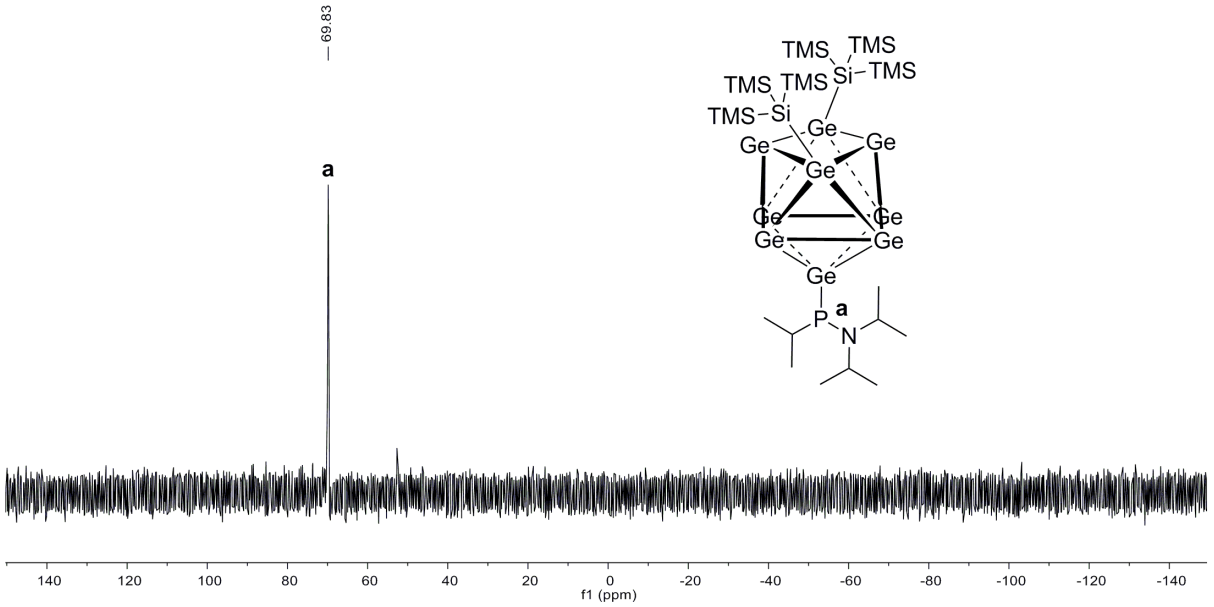

Figure S54. ^{31}P NMR spectrum of compound **8a** in thf-d_8.

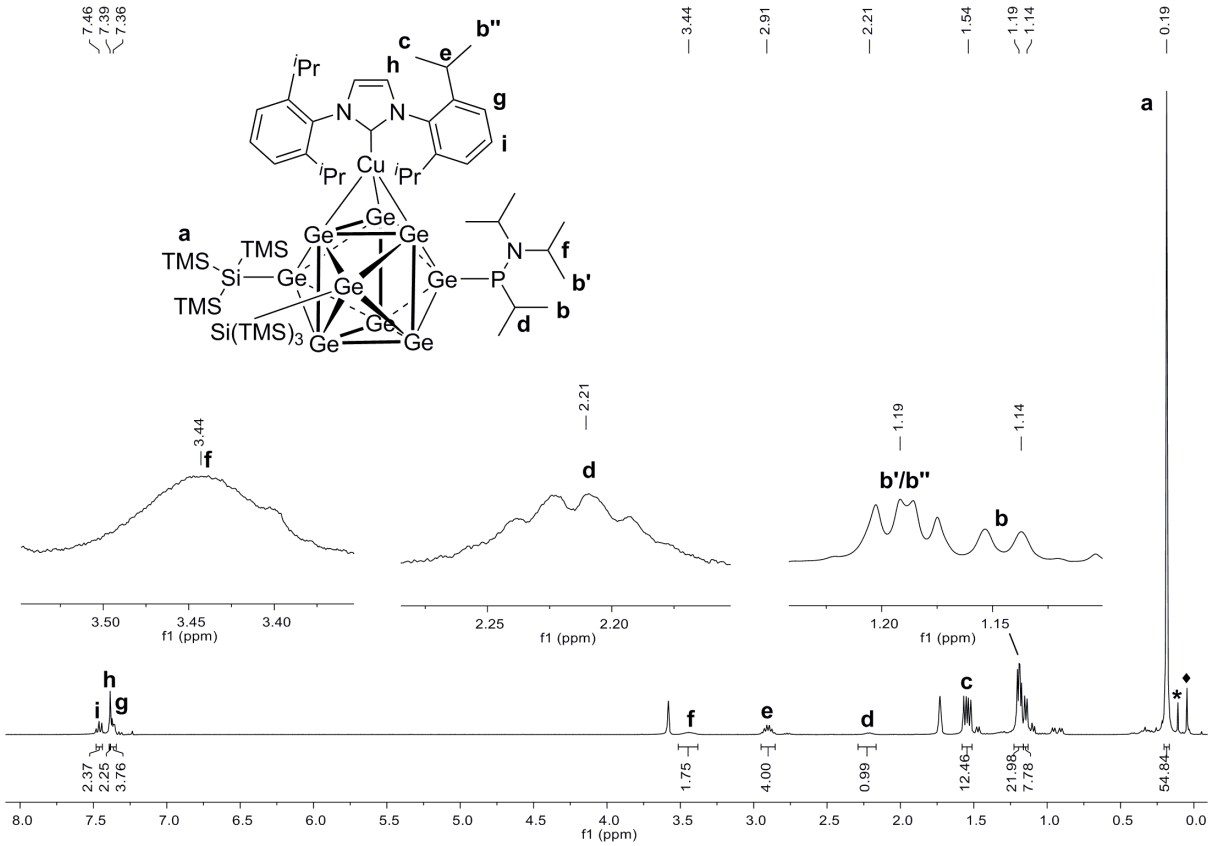

Figure S55. ^{1}H NMR spectrum of compound **8-CuNHC^{Dipp}** in thf-d_8 (signal marked with * belongs to unknown impurity, signal marked with ♦ belongs to silicon grease).

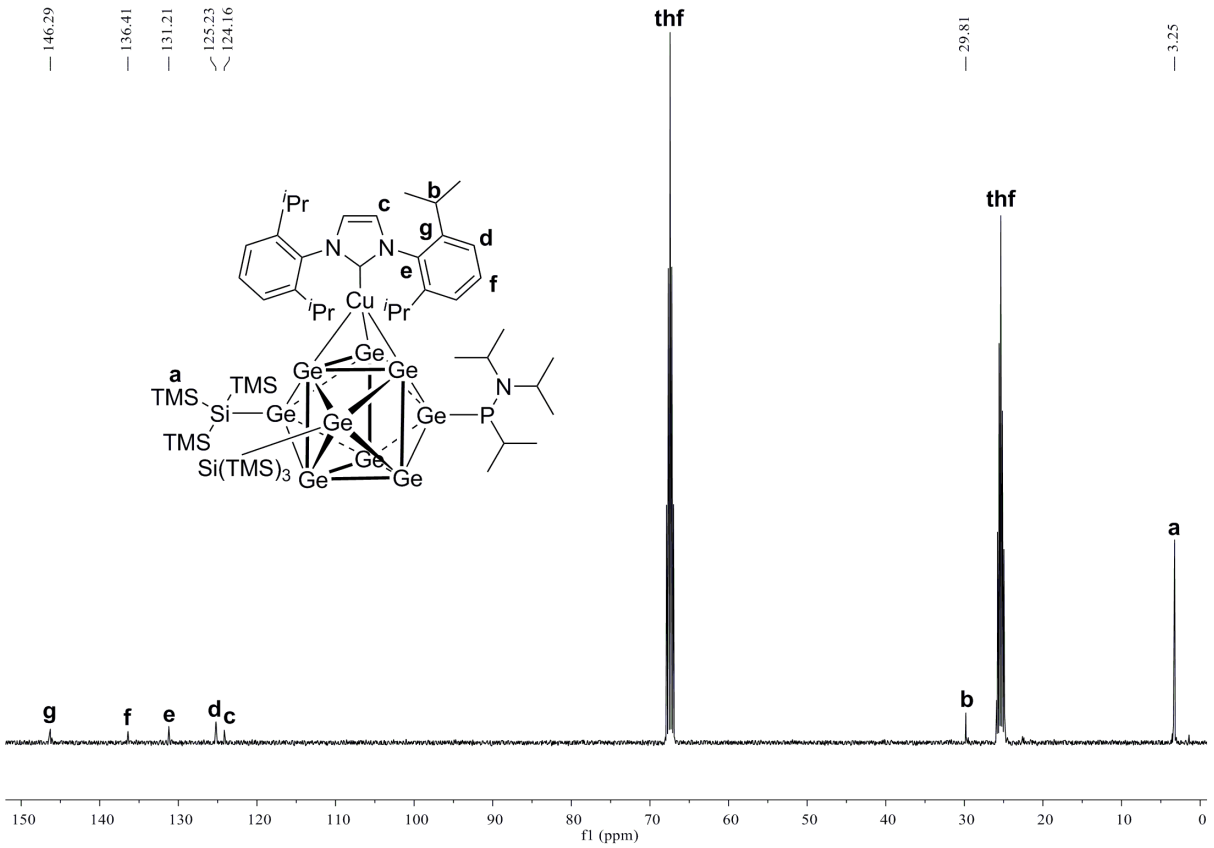

Figure S56. ^{13}C NMR spectrum of compound **8-CuNHC^{Dipp}** in thf-d_8.

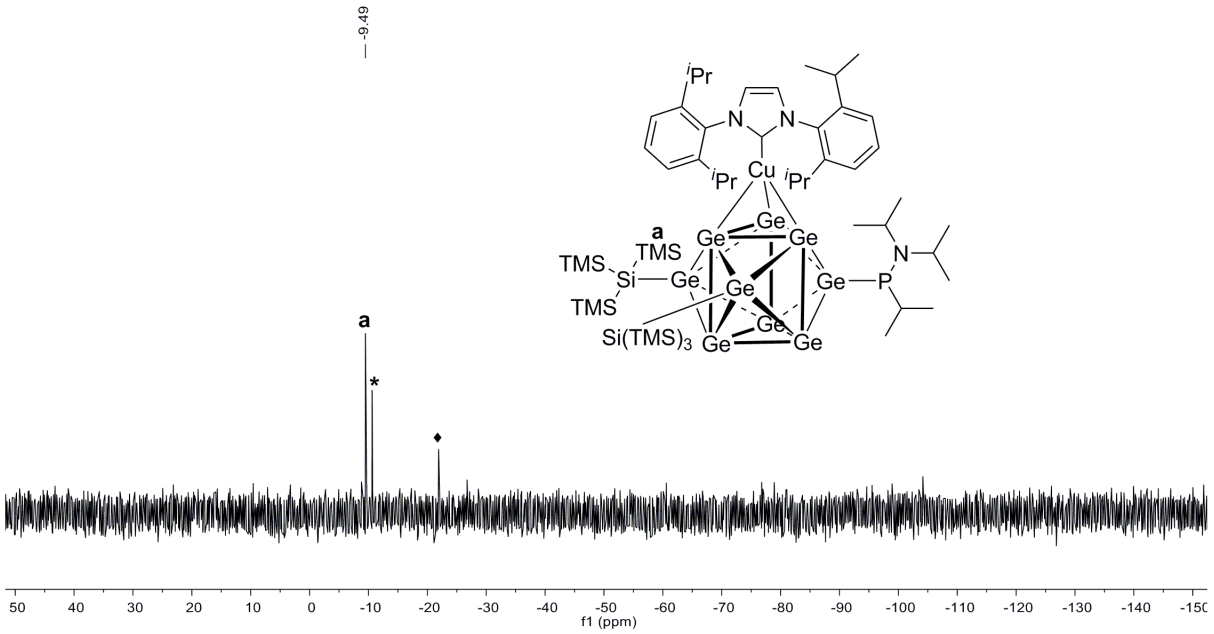

Figure S57. ^{29}Si-INEPT-RD NMR spectrum of compound **8-CuNHC^{Dipp}** in thf-d_8 (signal marked with * belongs to unknown impurity, signal marked with ♦ belongs to silicon grease). Signal of Si_{Ge9} could not be detected for unknown reason.

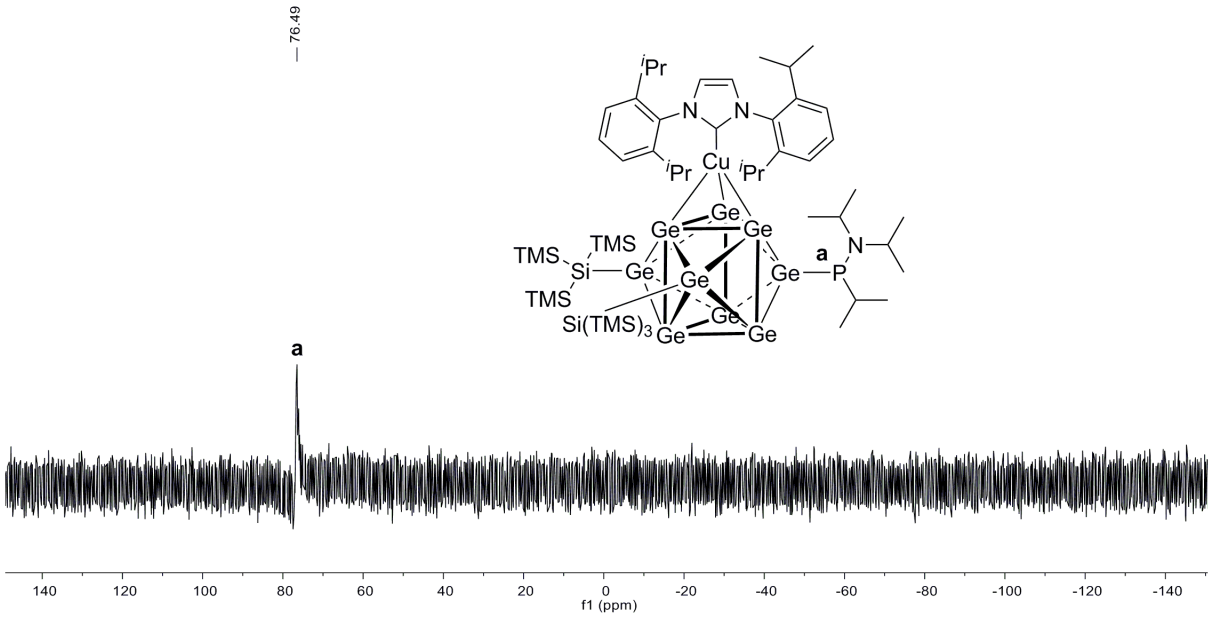

Figure S58. ^{31}P NMR spectrum of compound **8-CuNHC^{Dipp}** in thf-d_8.

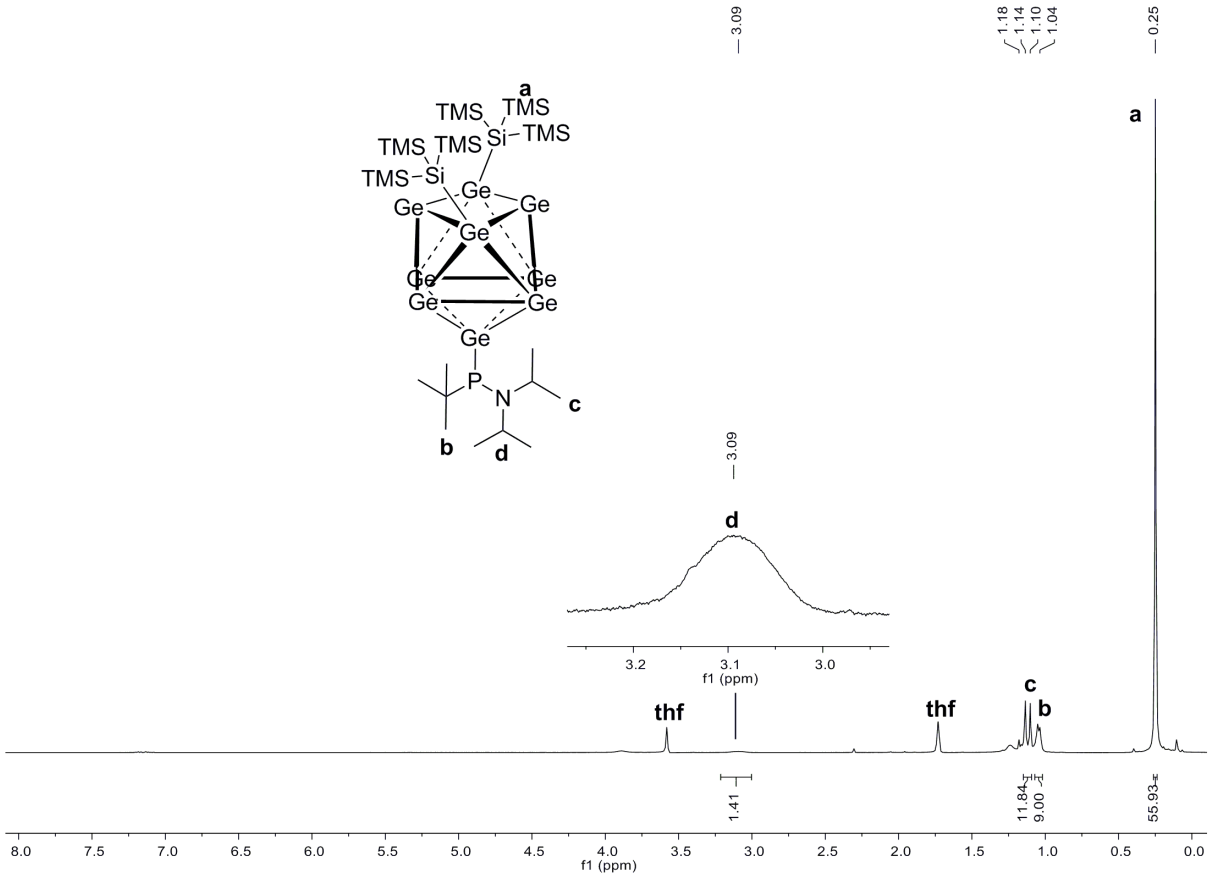

Figure S59. ^{1}H NMR spectrum of compound **9a** in thf-d_8.

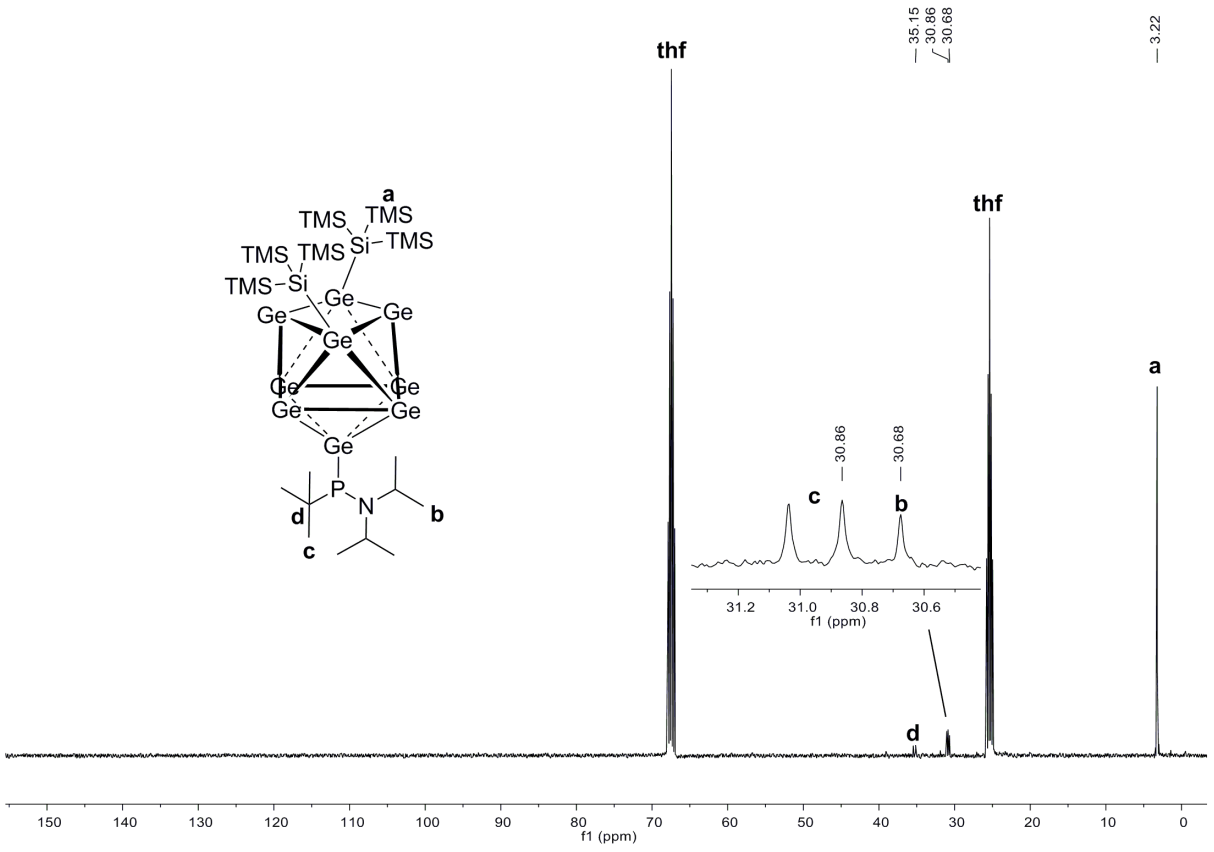

Figure S60. ^{13}C NMR spectrum of compound **9a** in thf-d_8.

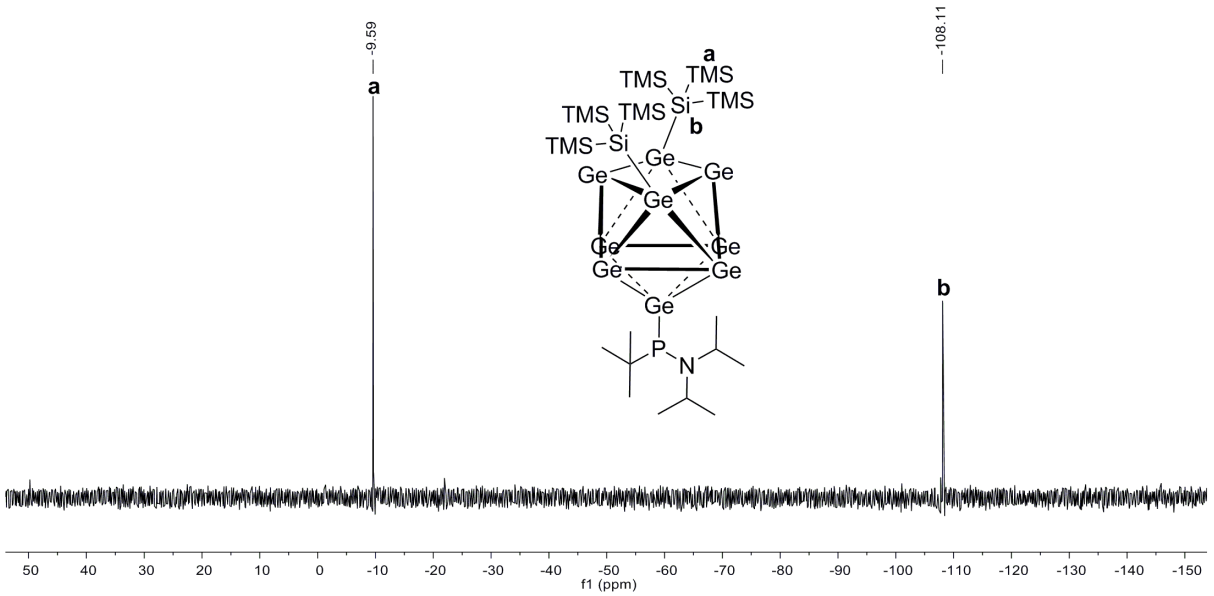

Figure S61. ^{29}Si-INEPT-RD NMR spectrum of compound **9a** in thf-d_8.

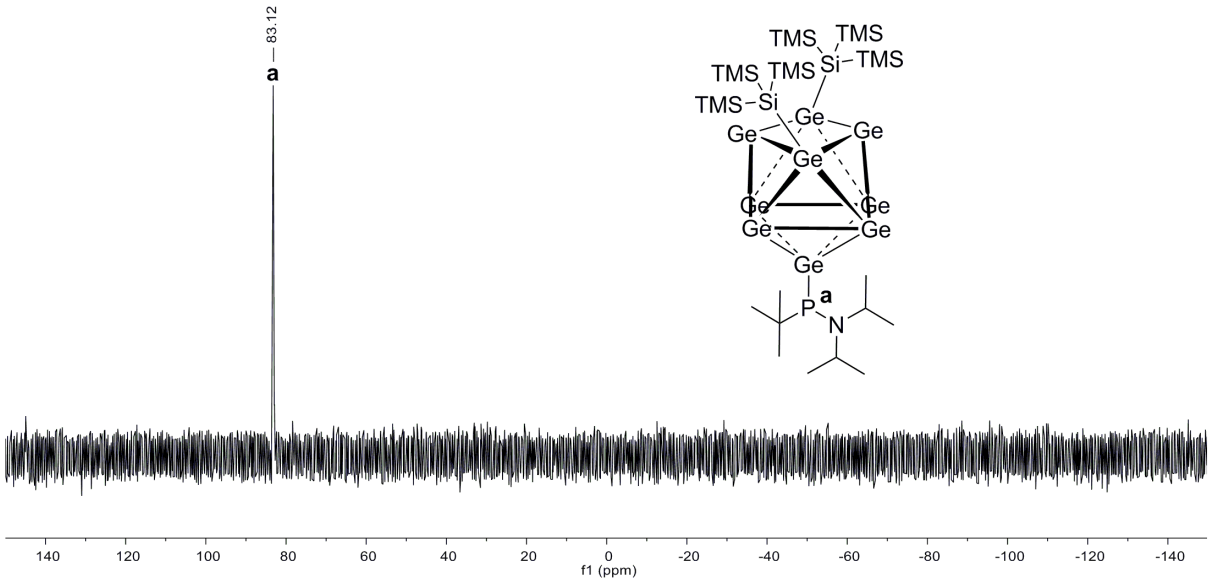

Figure S62. ^{31}P NMR spectrum of compound **9a** in thf-d_8.

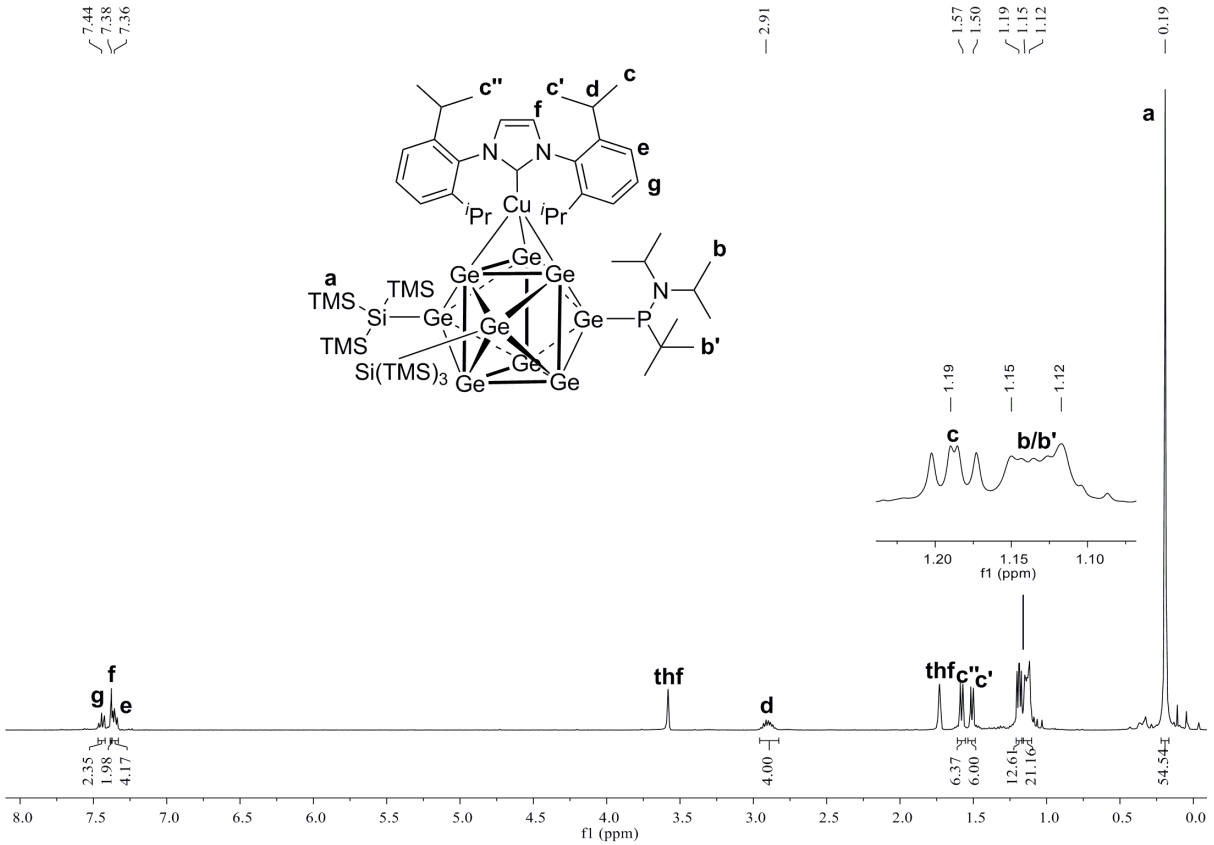

Figure S63. ^{1}H NMR spectrum of compound **9-CuNHC^{Dipp}** in thf-d_8.

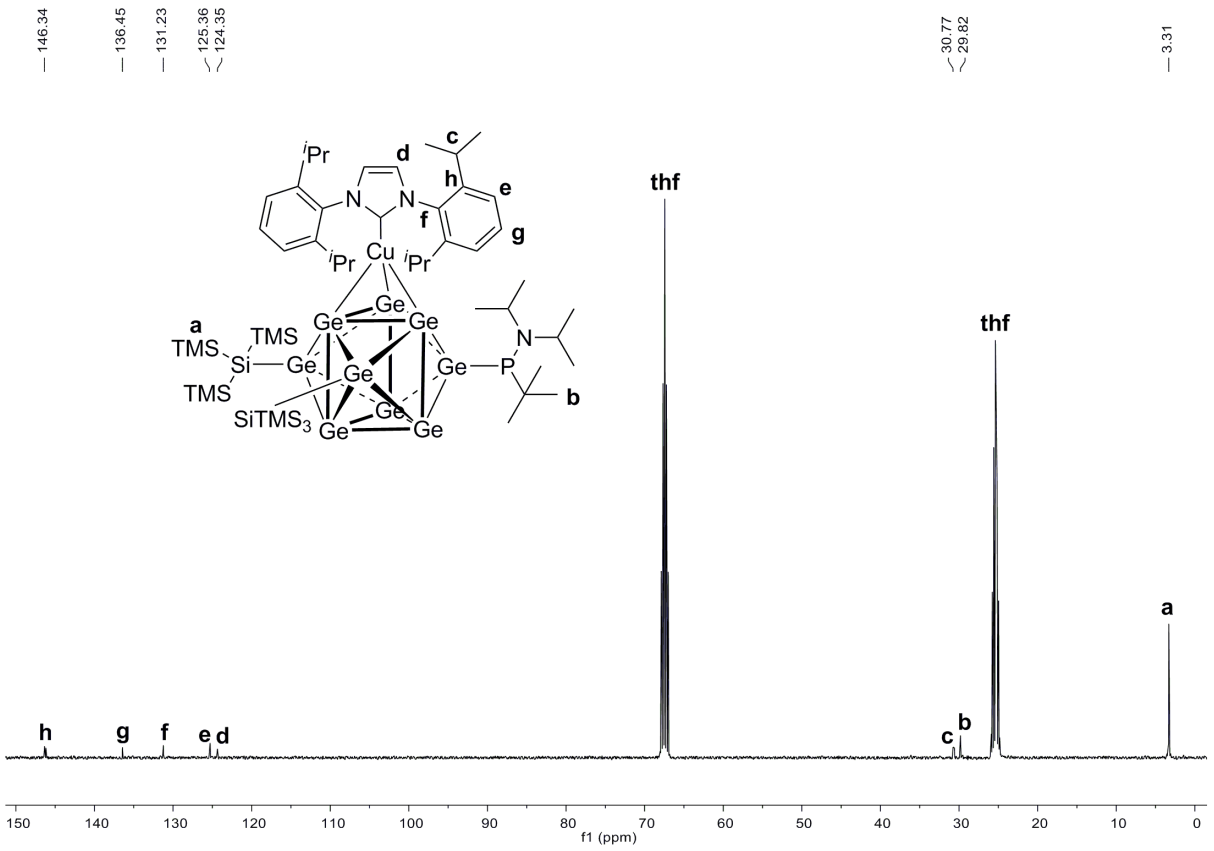

Figure S64. ^{13}C NMR spectrum of compound **9-CuNHC^{Dipp}** in thf-d_8.

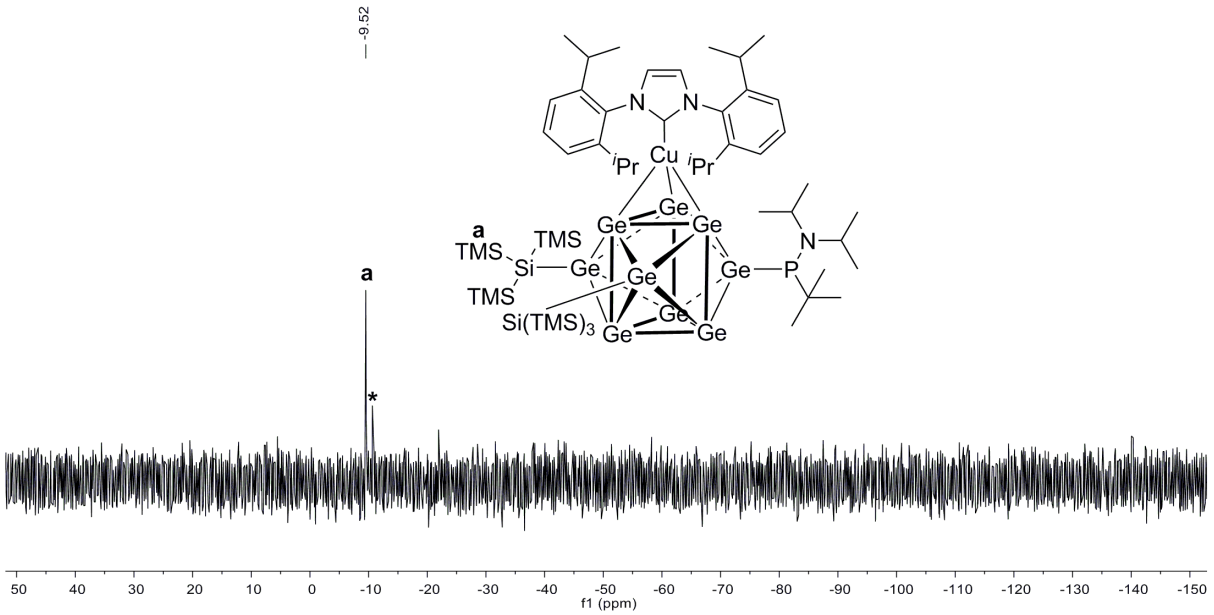

Figure S65. ^{29}Si-INEPT-RD NMR spectrum of compound **9-CuNHC^{Dipp}** in thf-d_8 (signal marked with * belongs to unknown impurity). Signal of Si_{Ge9} could not be detected for unknown reason.

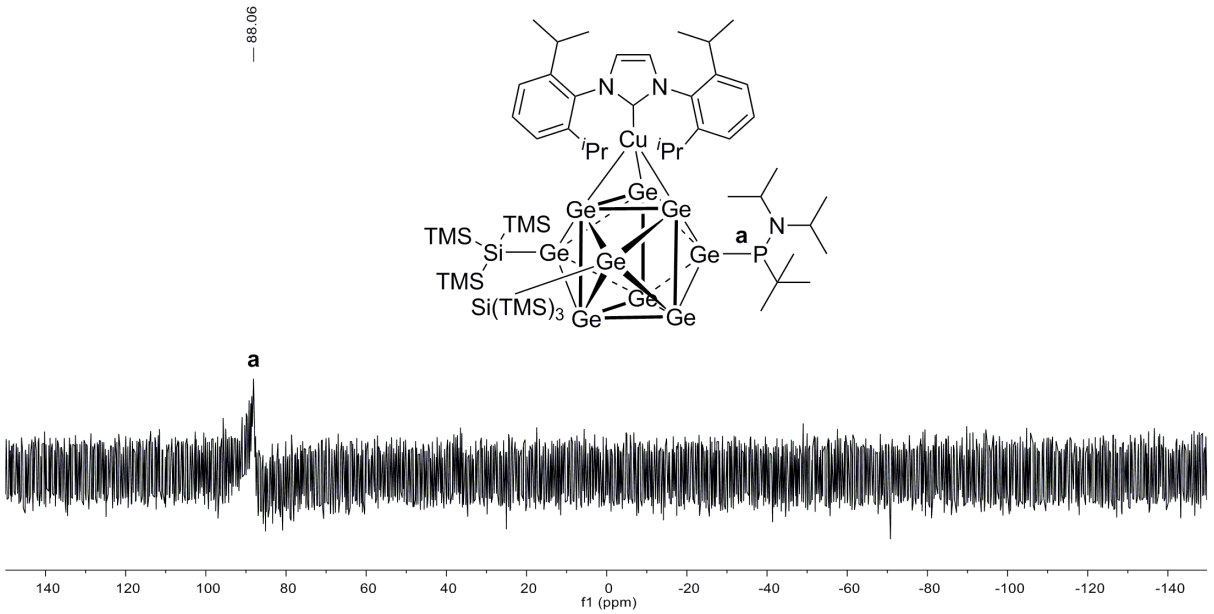

Figure S66. ^{31}P NMR spectrum of compound **9-CuNHC^{Dipp}** in thf-d_8.

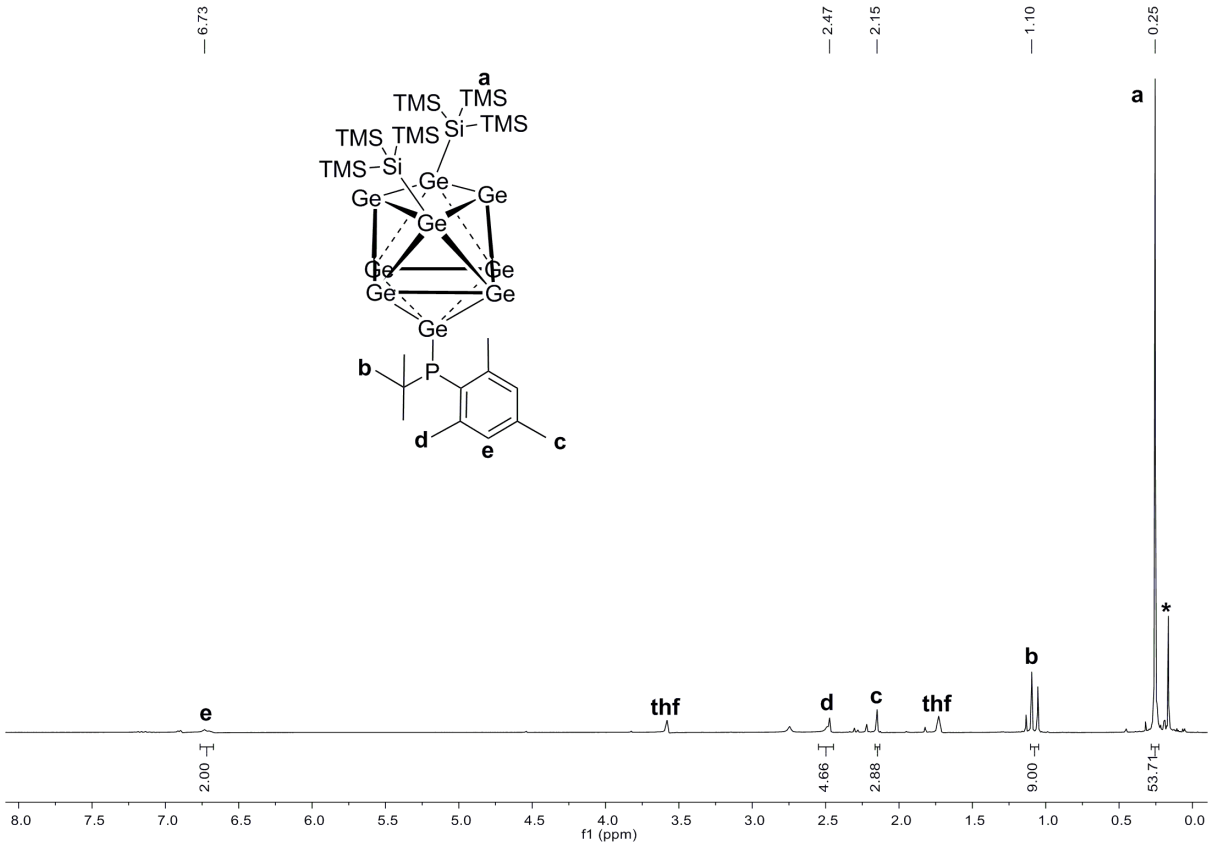

Figure S67. ^{1}H NMR spectrum of compound **10a** in thf-d_8 (signal marked with * belongs to unknown impurity).

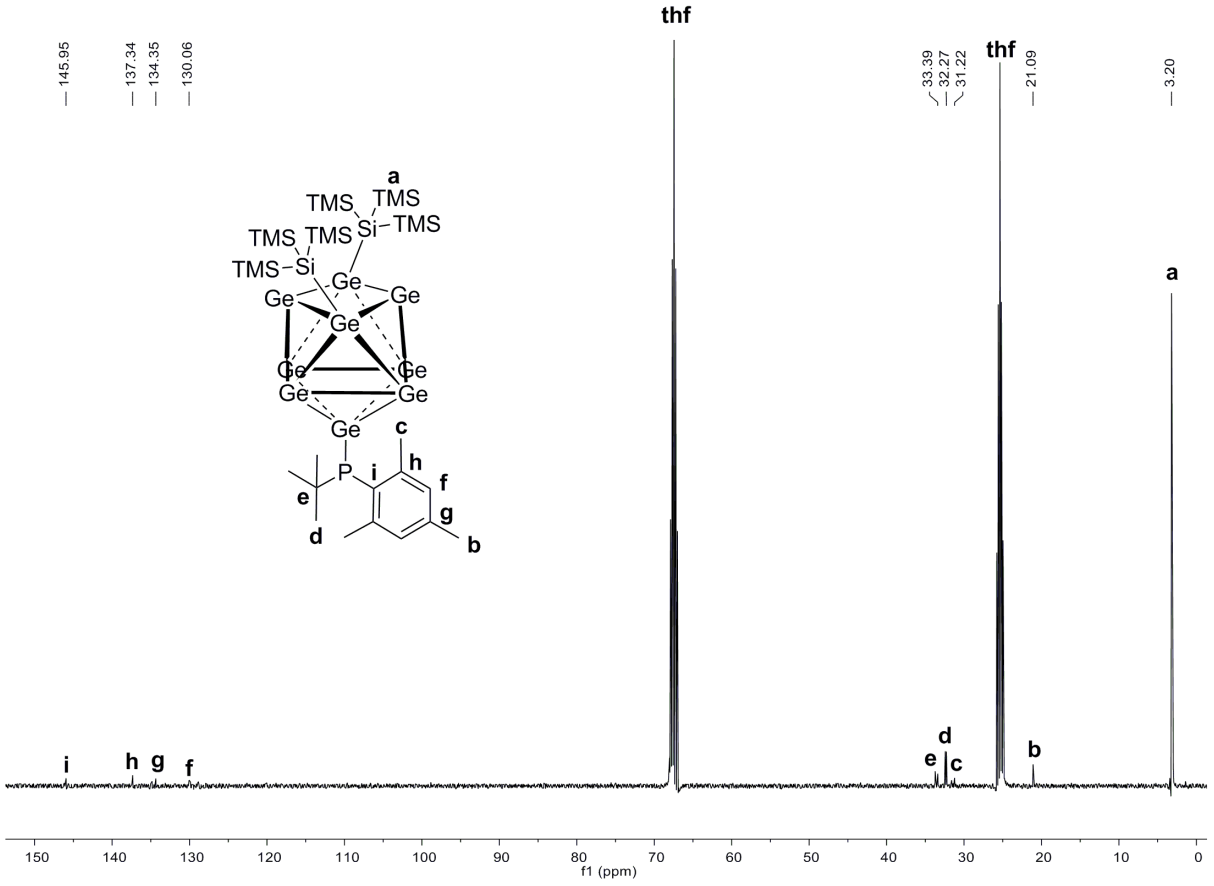

Figure S68. ^{13}C NMR spectrum of compound **10a** in thf-d_8.

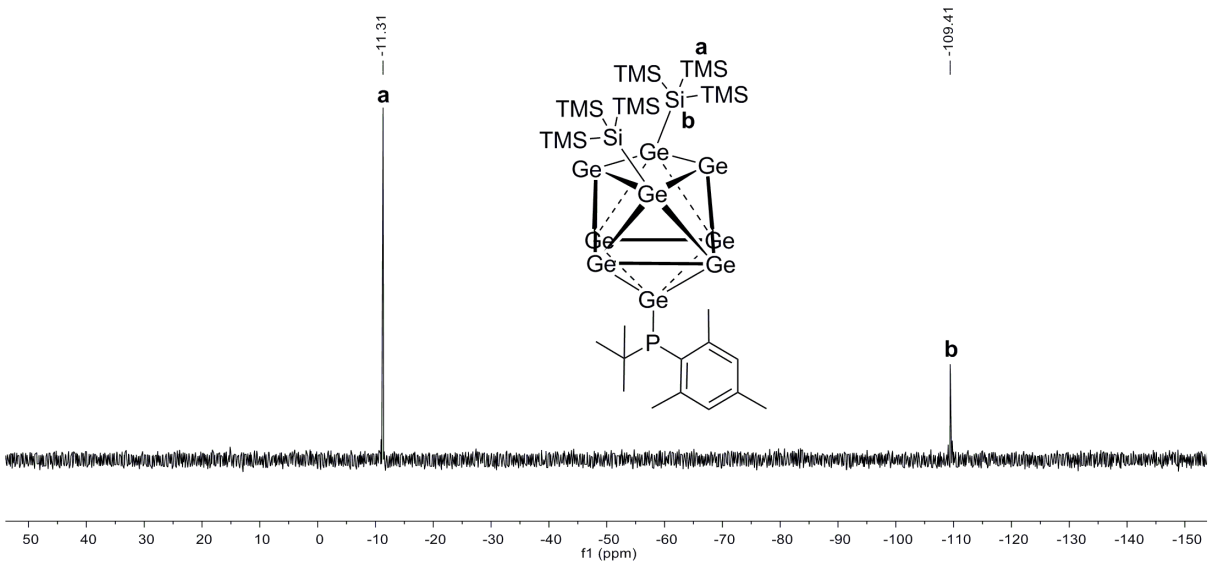

Figure S69. ^{29}Si-INEPT-RD NMR spectrum of compound **10a** in thf-d_8.

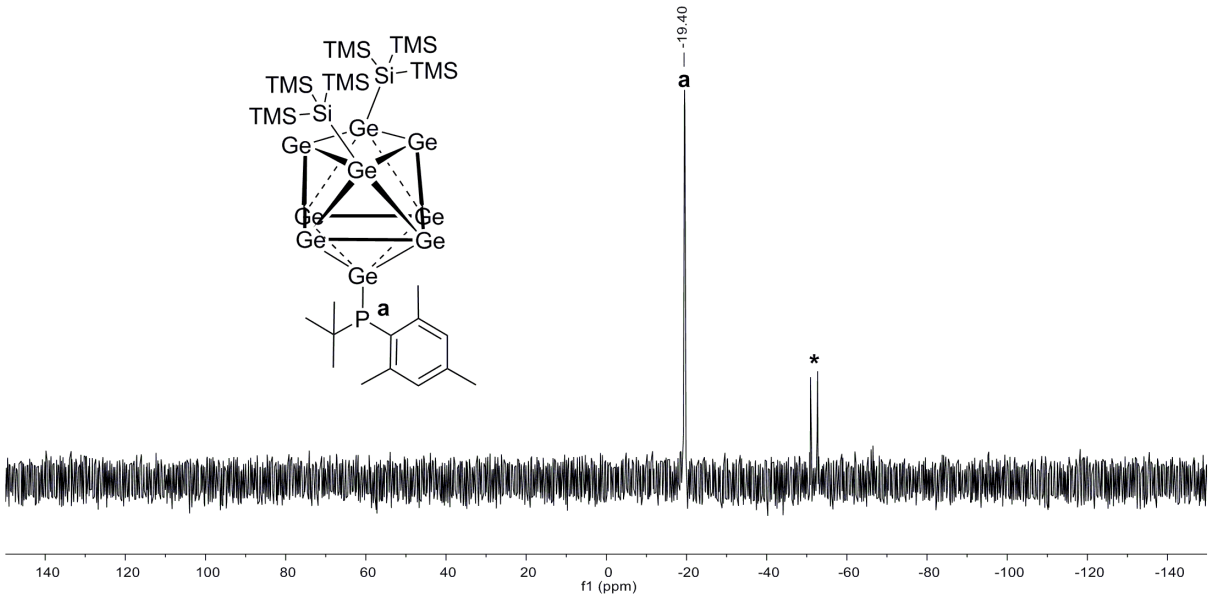

Figure S70. ^{31}P NMR spectrum of compound **10a** in thf-d_8 (signals marked with * belong to unknown impurities).

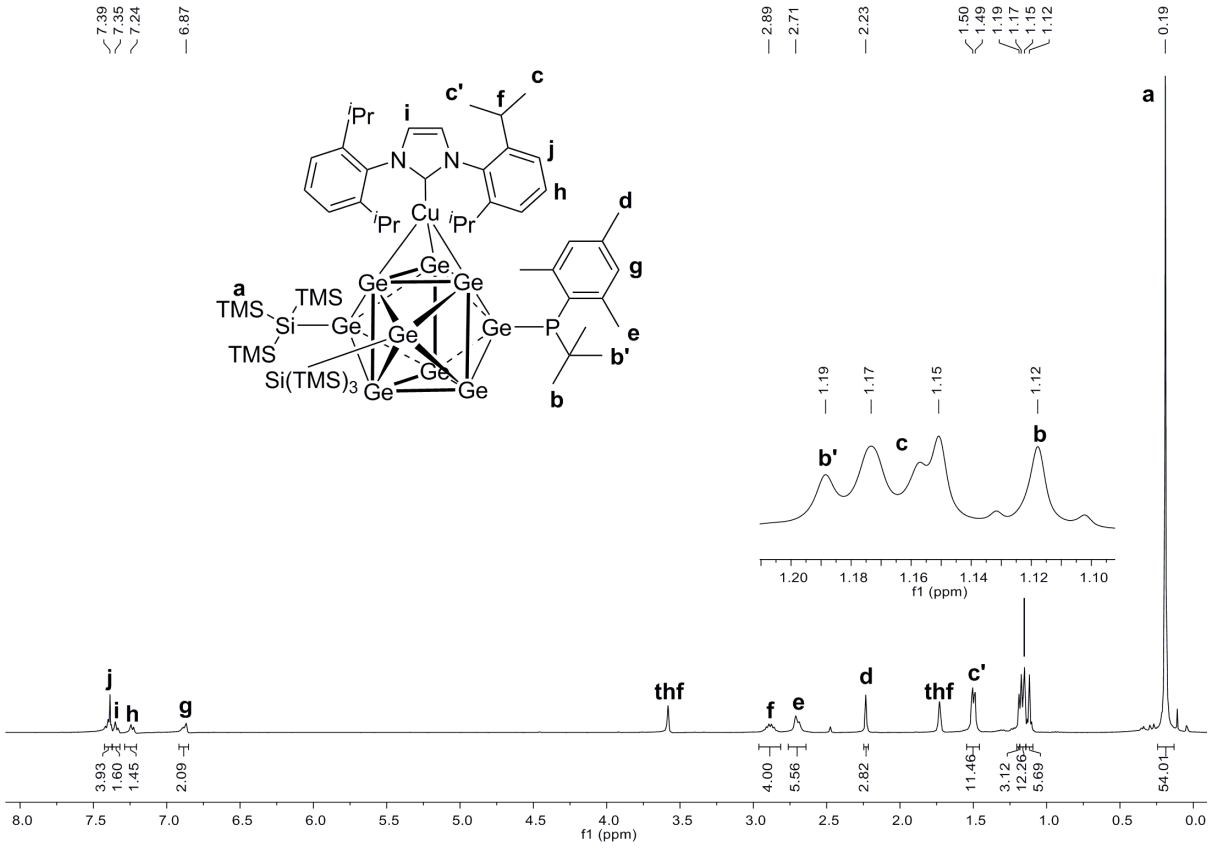

Figure S71. ^{1}H NMR spectrum of compound **10-CuNHC^{Dipp}** in thf-d_8.

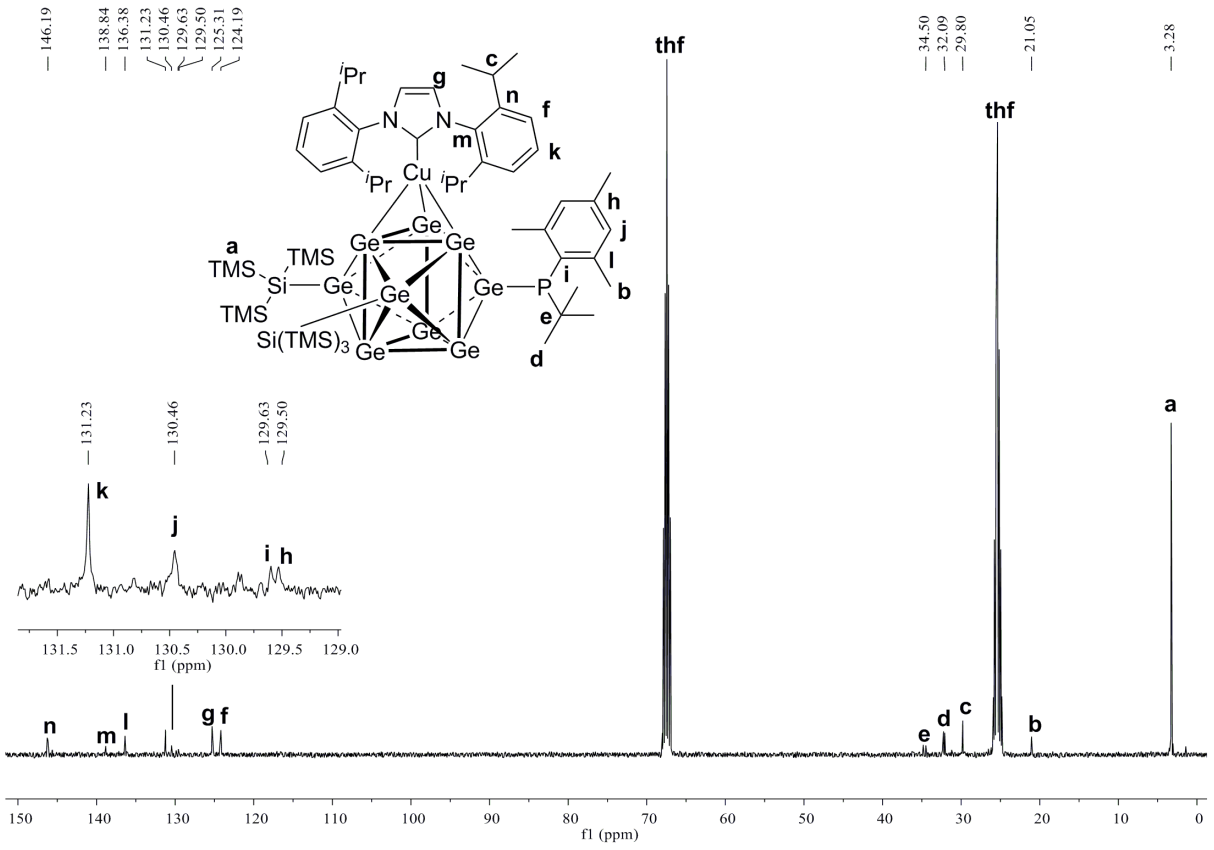

Figure S72. ^{13}C NMR spectrum of compound **10-CuNHC^{Dipp}** in thf-d_8.

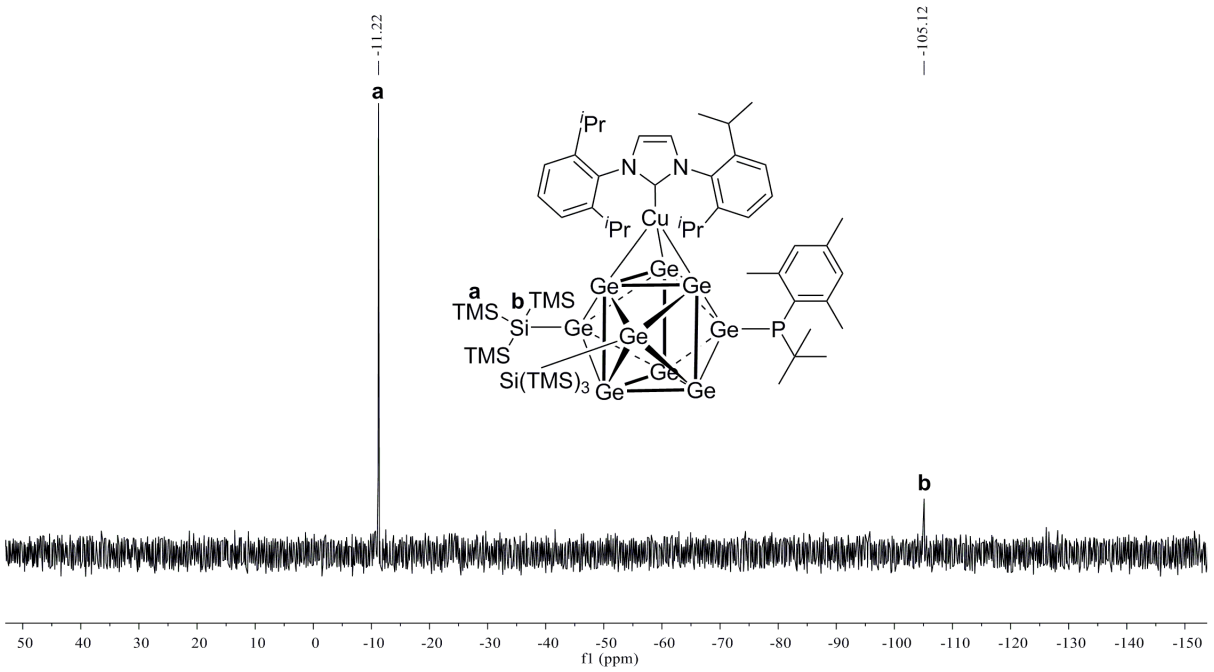

Figure S73. ^{29}Si-INEPT-RD NMR spectrum of compound **10-CuNHC^{Dipp}** in thf-*d*$_8$.

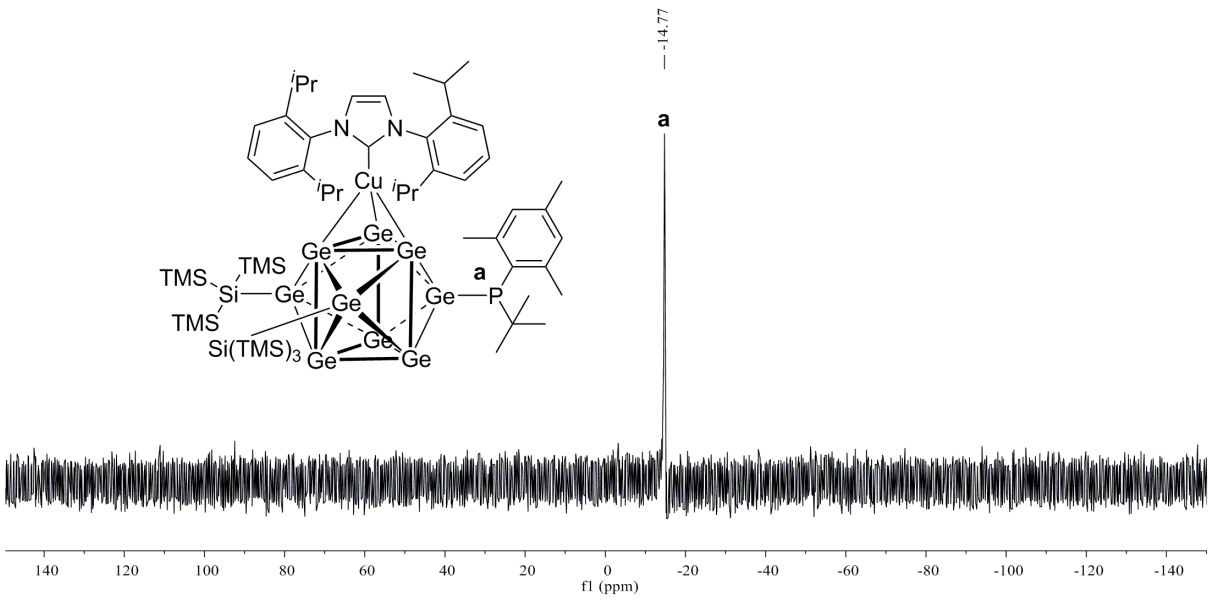

Figure S74. ^{31}P NMR spectrum of compound **10-CuNHC^{Dipp}** in thf-*d*$_8$.

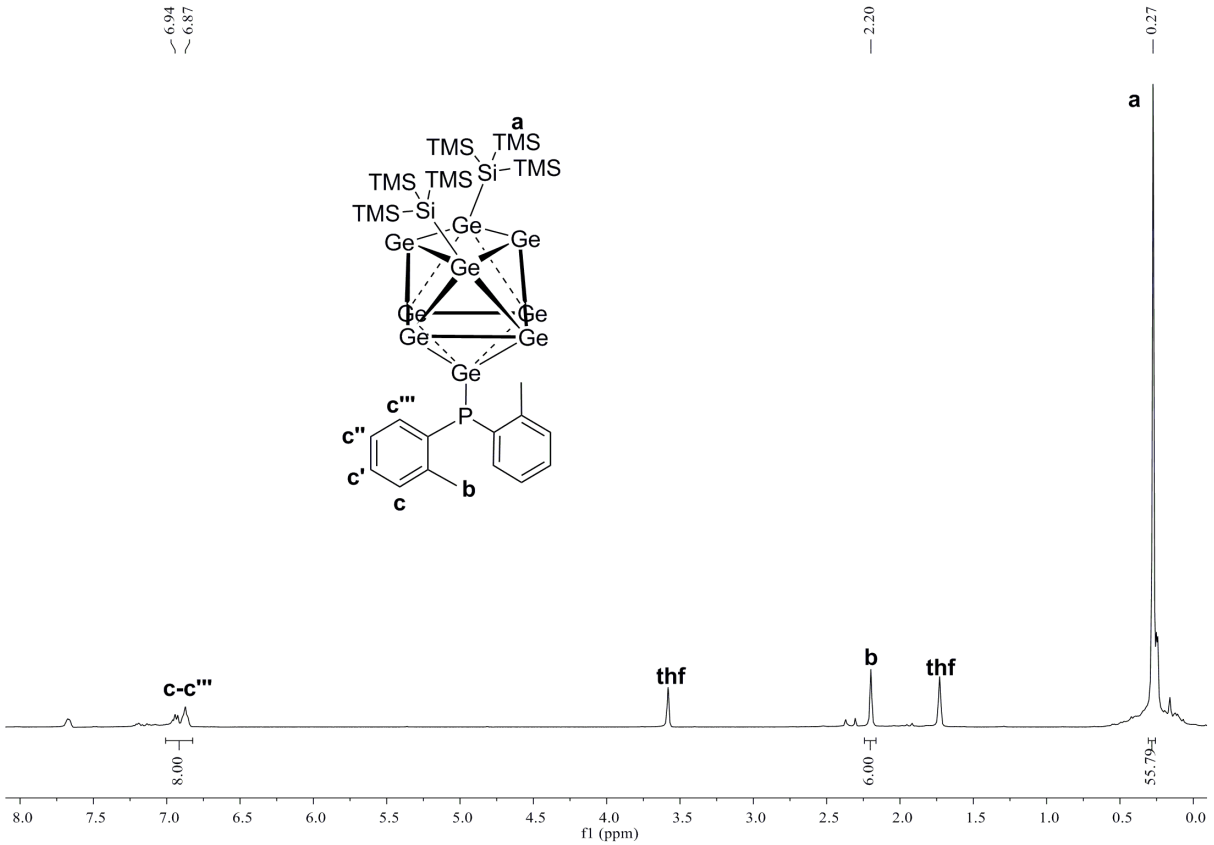

Figure S75. ^{1}H NMR spectrum of compound **11a** in thf-d_8.

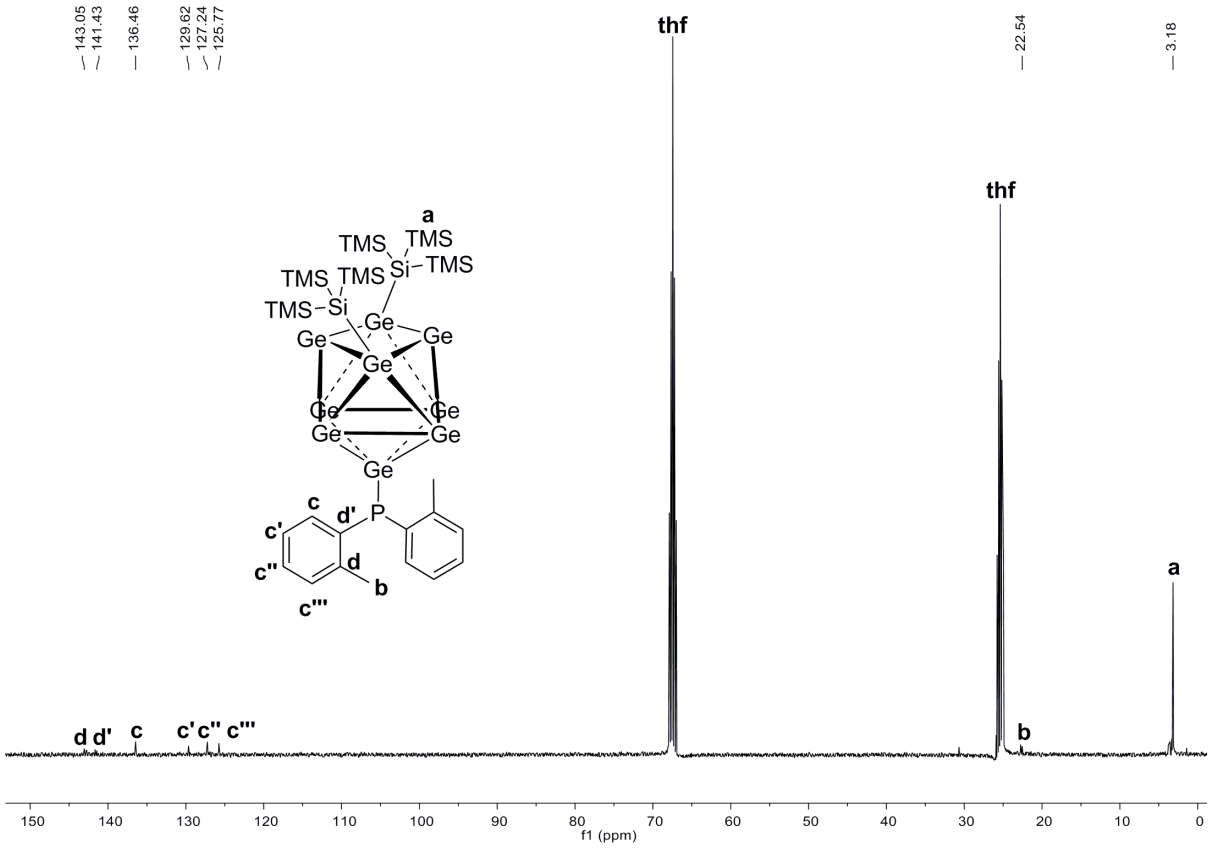

Figure S76. ^{13}C NMR spectrum of compound **11a** in thf-d_8.

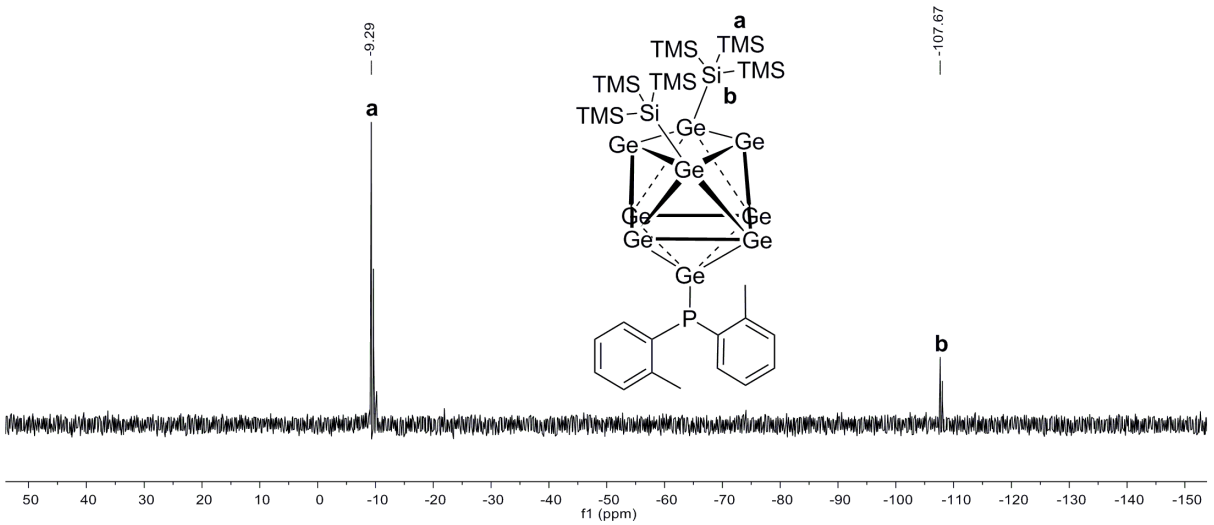

Figure S77. ^{29}Si-INEPT-RD NMR spectrum of compound **11a** in thf-d_8.

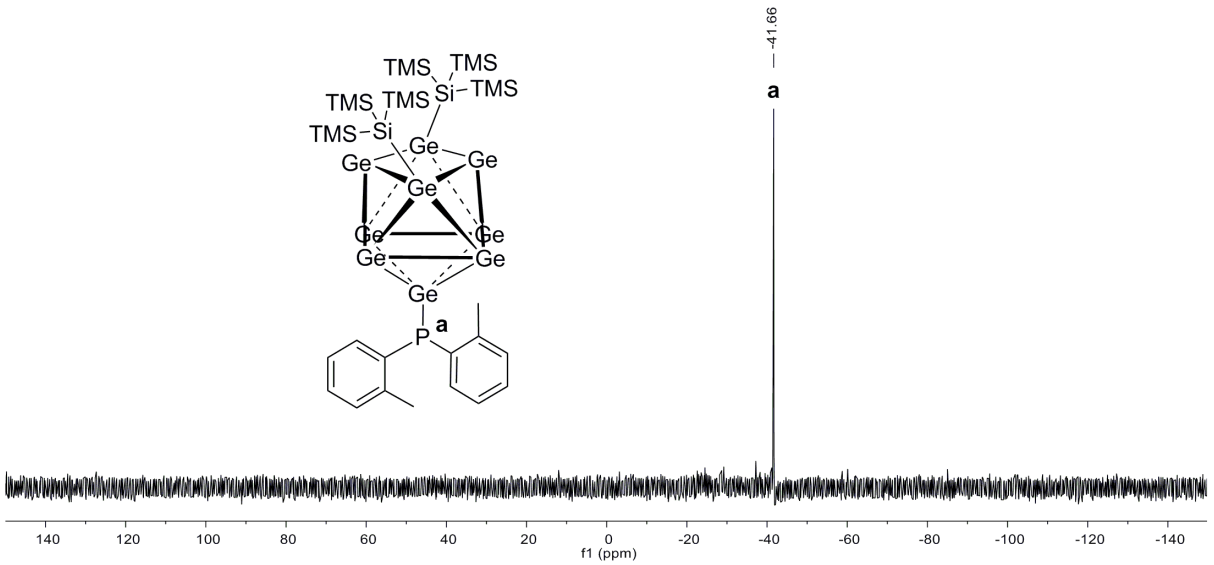

Figure S78. ^{31}P NMR spectrum of compound **11a** in thf-d_8.

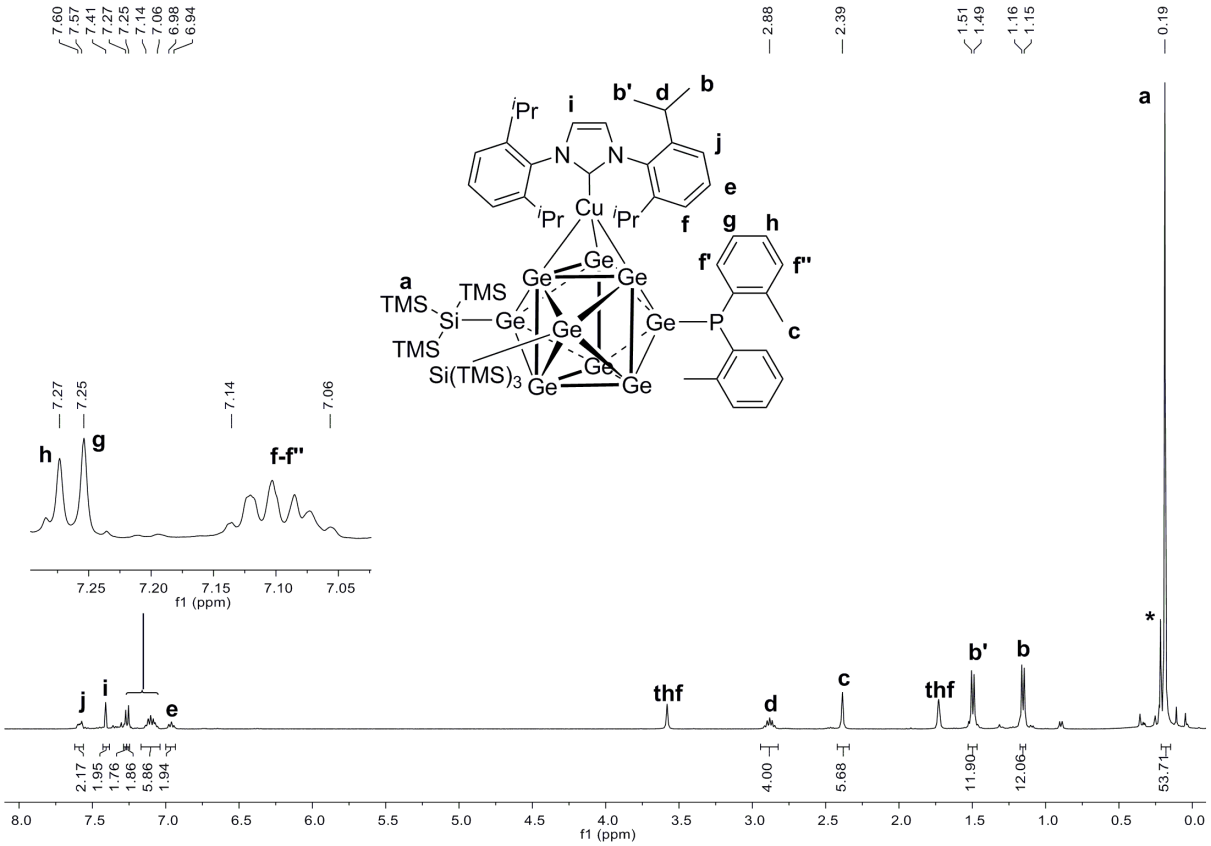

Figure S79. ^{1}H NMR spectrum of compound **11-CuNHC^{Dipp}** in thf-*d*$_8$ (signal marked with * belongs to unknown impurity).

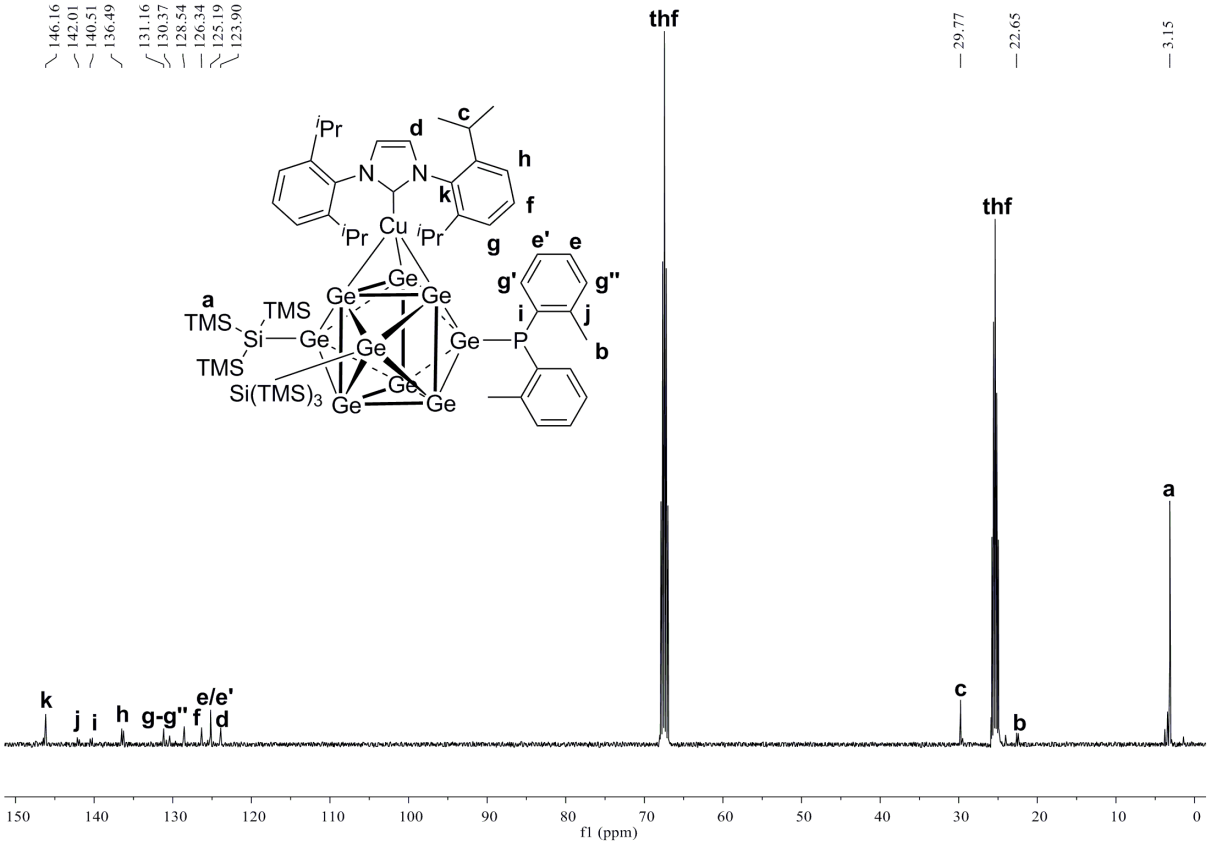

Figure S80. ^{13}C NMR spectrum of compound **11-CuNHC^{Dipp}** in thf-*d*$_8$.

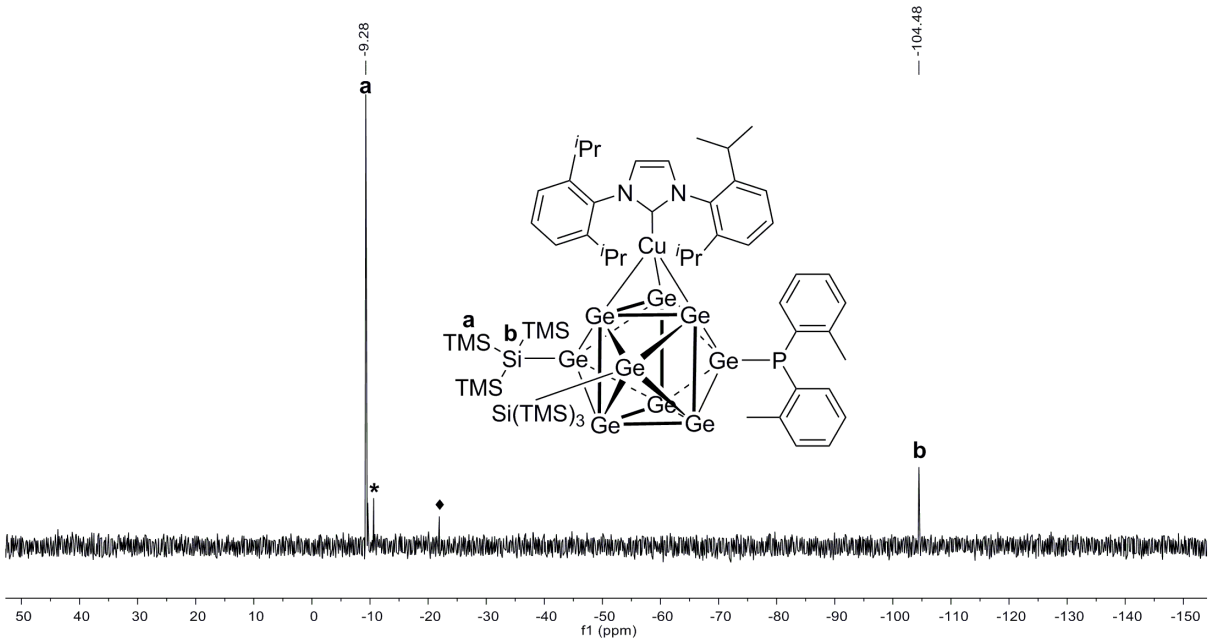

Figure S81. ^{29}Si-INEPT-RD NMR spectrum of compound **11-CuNHC^{Dipp}** in thf-d_8 (signal marked with * belongs to unknown impurity, signal marked with ♦ belongs to silicon grease).

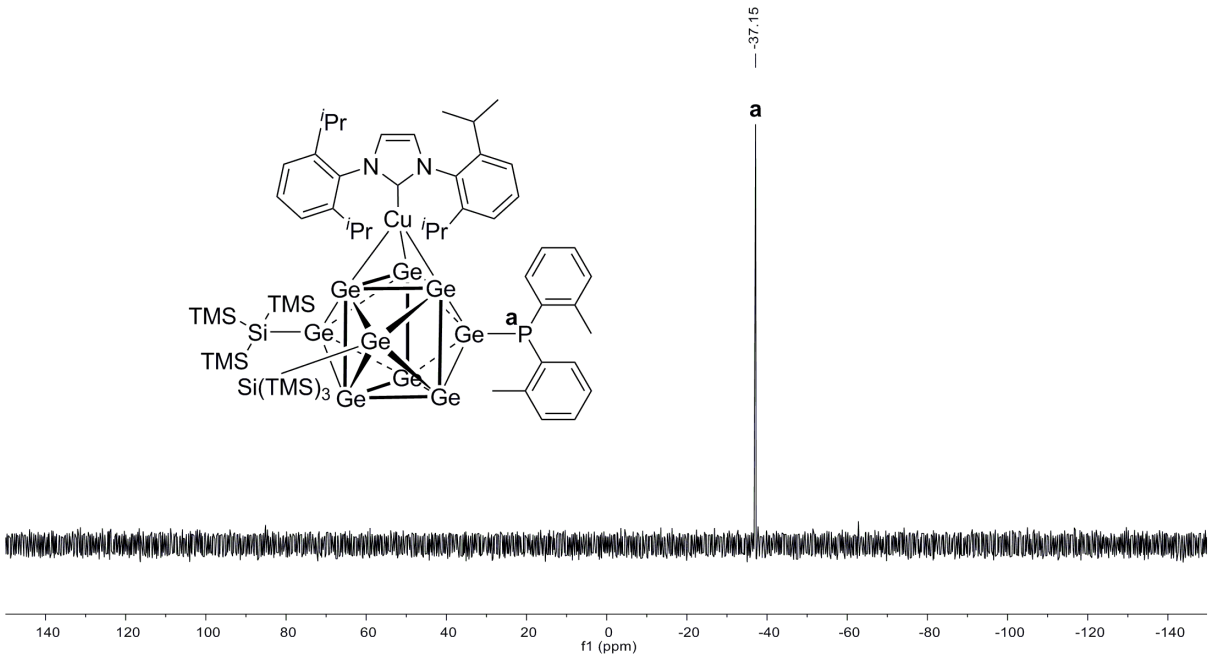

Figure S82. ^{31}P NMR spectrum of compound **11-CuNHC^{Dipp}** in thf-d_8.

ESI-MS Spectra

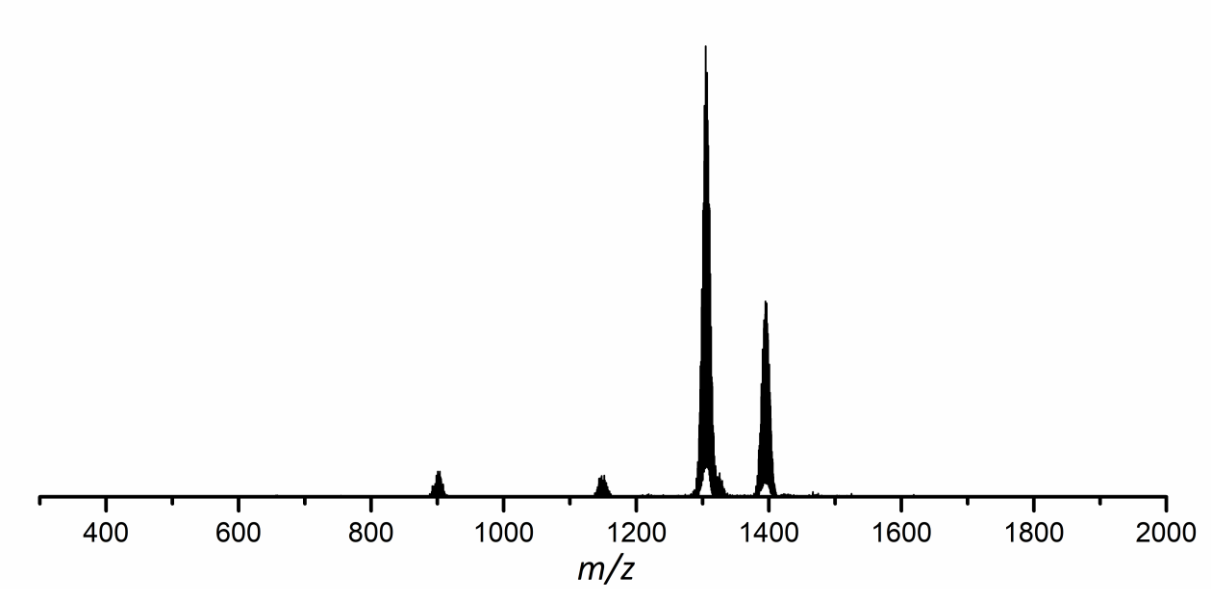

Figure S83. Overview spectrum of ESI-MS measurement (negative ion mode, 3500 V, 300 °C) of a thf solution of compound **3a**, monitoring the molecule peak at *m/z* 1306.8 $[Ge_9\{Si(TMS)_3\}_2P^tBu(CH_2)_3CH{=}CH_2]^-$. Besides the molecule peak a signal at *m/z* 1396.4 is monitored, which can be assigned to tris-silylated cluster $[Ge_9\{Si(TMS)_3\}_3]^-$, which is formed during the ionization process (species is not present in NMR spectra of **3a**). Detail view of signal of anion **3a** is provided in the manuscript.

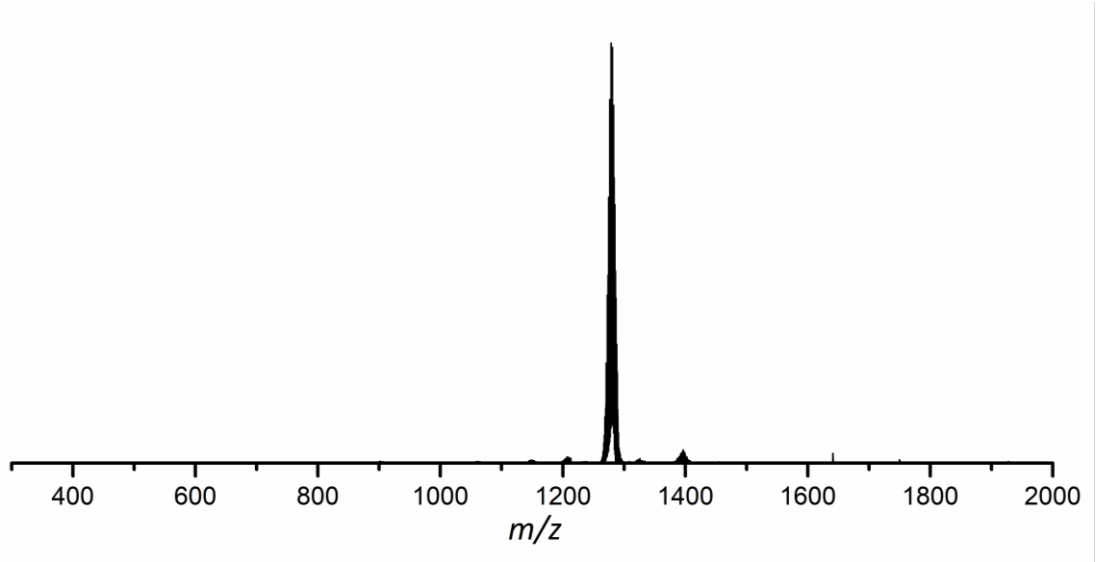

Figure S84. Overview spectrum of ESI-MS measurement (negative ion mode, 3500 V, 300 °C) of a thf solution of compound **4a**, monitoring the molecule peak at *m/z* 1280.8 $[Ge_9\{Si(TMS)_3\}_2P^iPr^tBu]^-$.

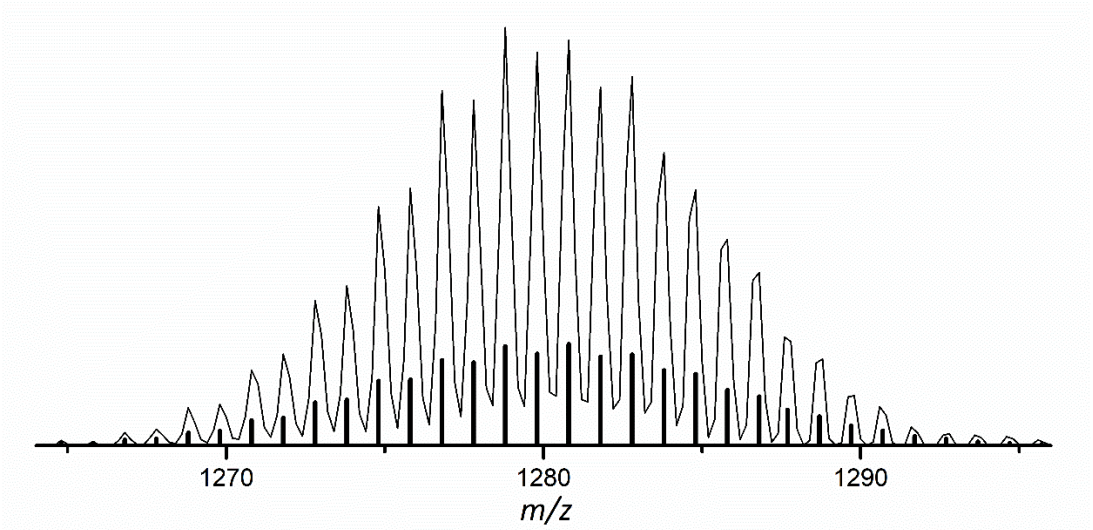

Figure S85. Detail view of ESI-MS signal (negative ion mode, 3500 V, 300 °C) of $[Ge_9\{Si(TMS)_3\}_2P^iPr^tBu]^-$ (**4a**) at *m/z* 1280.8 monitored from thf solution. Calculated pattern is represented as black bars.

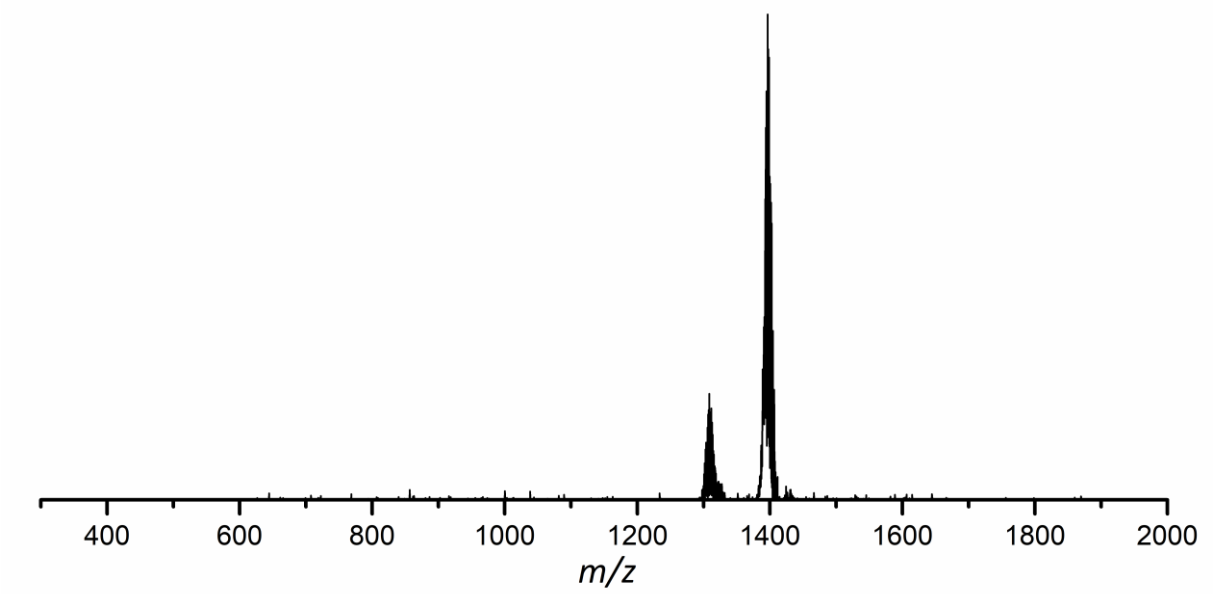

Figure S86. Overview spectrum of ESI-MS measurement (negative ion mode, 4000 V, 300 °C) of a thf solution of compound **5a**, monitoring the molecule peak at *m/z* 1309.7 $[Ge_9\{Si(TMS)_3\}_2P^tBu(NEt_2)]^-$. Besides the molecule peak a signal at *m/z* 1396.4 is monitored, which can be assigned to tris-silylated cluster $[Ge_9\{Si(TMS)_3\}_3]^-$, which is formed during the ionization process (species is not present in NMR spectra of **5a**).

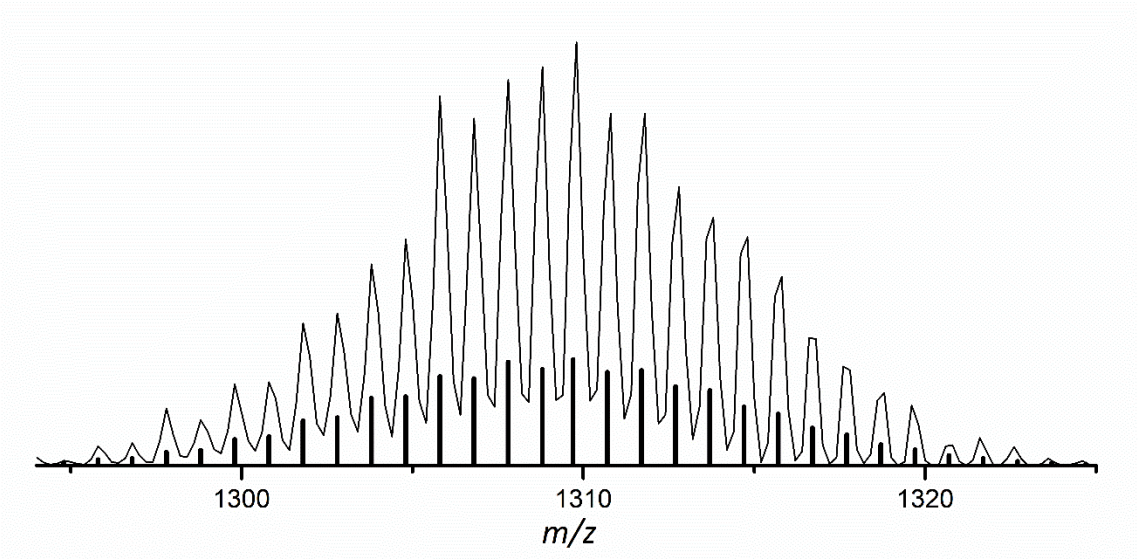

Figure S87. Detail view of ESI-MS signal (negative ion mode, 4000 V, 300 °C) of $[Ge_9\{Si(TMS)_3\}_2P^tBu(NEt_2)]^-$ (**5a**) at *m/z* 1309.7 monitored from thf solution. Calculated pattern is represented as black bars.

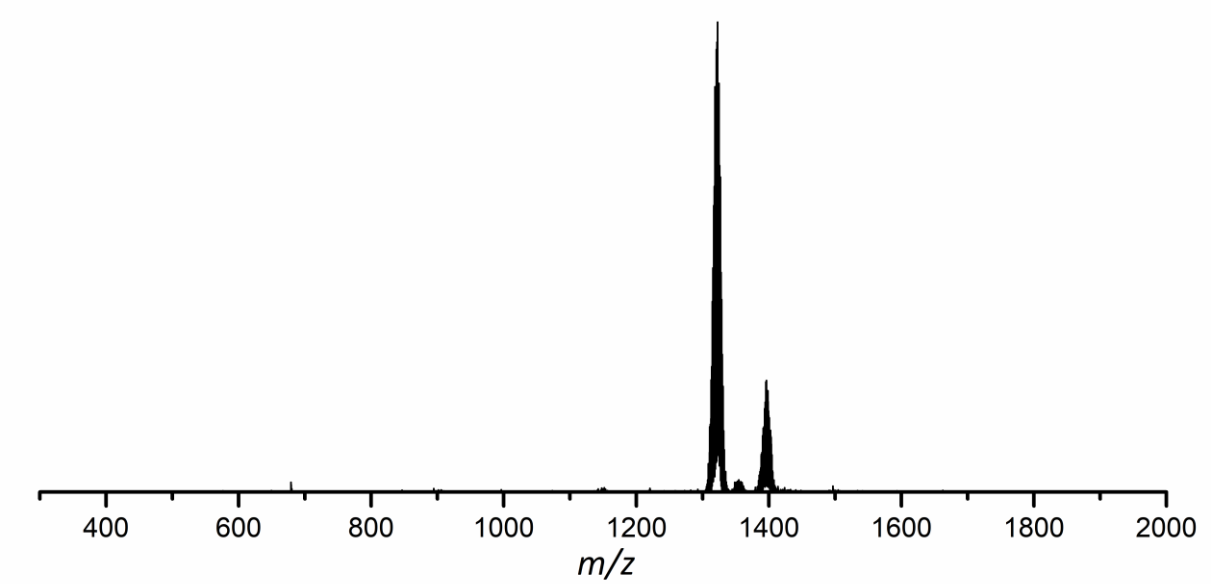

Figure S88. Overview spectrum of ESI-MS measurement (negative ion mode, 3000 V, 300 °C) of a thf solution of compound **6a**, monitoring the molecule peak at *m/z* 1322.8 $[Ge_9\{Si(TMS)_3\}_2P(1,1\text{-dimethylpropyl})_2]^-$. Besides the molecule peak a signal at *m/z* 1396.4 is monitored, which can be assigned to tris-silylated cluster $[Ge_9\{Si(TMS)_3\}_3]^-$, which is formed during the ionization process (species is not present in NMR spectra of **6a**).

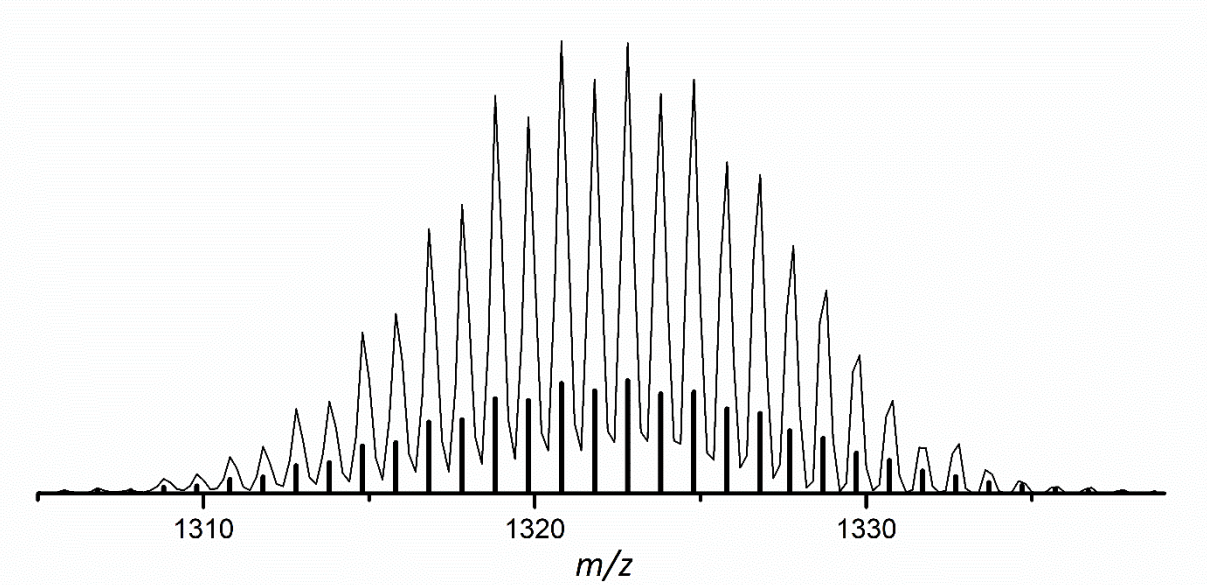

Figure S89. Detail view of ESI-MS signal (negative ion mode, 3000 V, 300 °C) of $[Ge_9\{Si(TMS)_3\}_2P(1,1\text{-dimethylpropyl})_2]^-$ (**6a**) at *m/z* 1322.8 monitored from thf solution. Calculated pattern is represented as black bars.

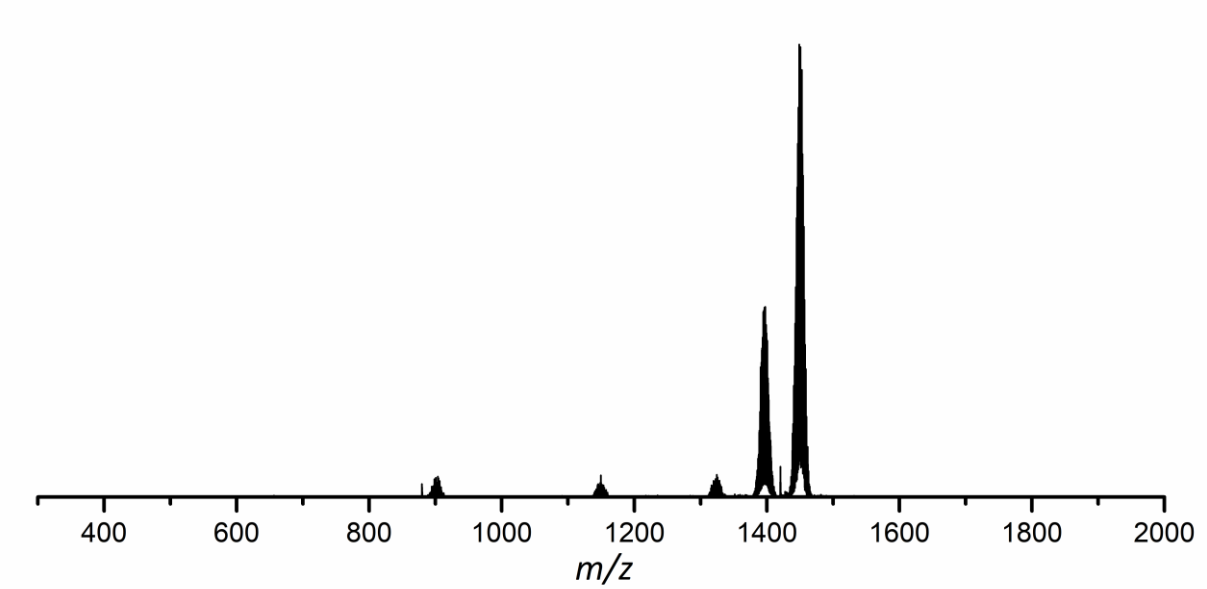

Figure S90. Overview spectrum of ESI-MS measurement (negative ion mode, 4000 V, 300 °C) of a thf solution of compound **7a**, monitoring the molecule peak at *m/z* 1450.8 $[Ge_9\{Si(TMS)_3\}_2P(1\text{-adamantyl})_2]^-$. Besides the molecule peak a signal at *m/z* 1396.4 is monitored, which can be assigned to tris-silylated cluster $[Ge_9\{Si(TMS)_3\}_3]^-$, which is formed during the ionization process (species is not present in NMR spectra of **7a**).

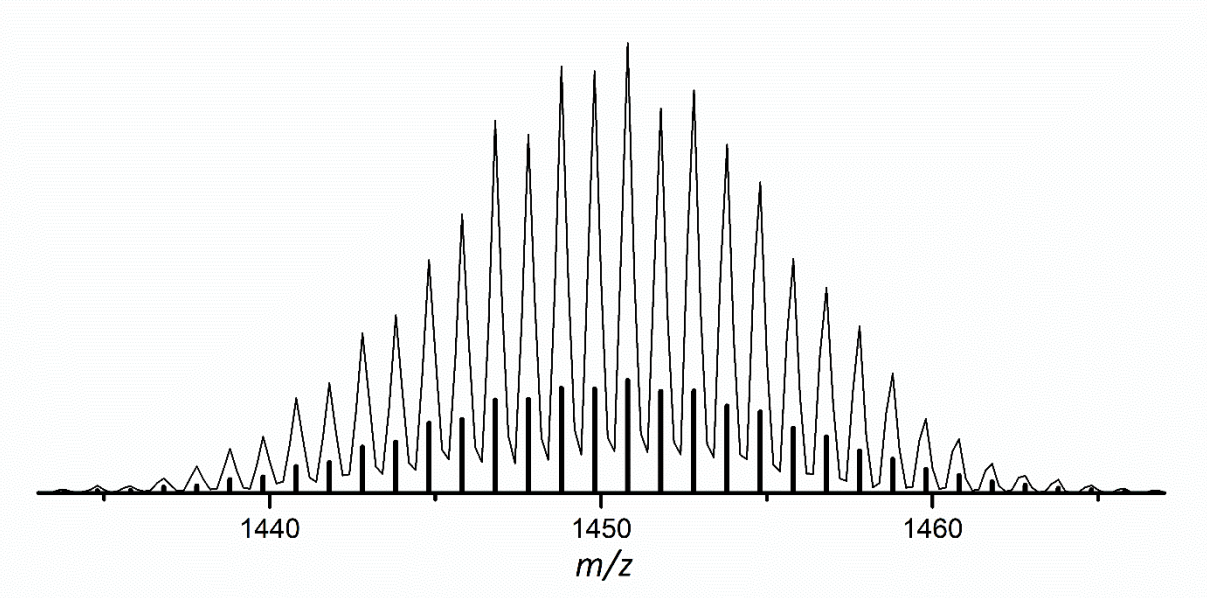

Figure S91. Detail view of ESI-MS signal (negative ion mode, 4000 V, 300 °C) of $[Ge_9\{Si(TMS)_3\}_2P(1\text{-adamantyl})_2]^-$ (**7a**) at *m/z* 1450.8 monitored from thf solution. Calculated pattern is represented as black bars.

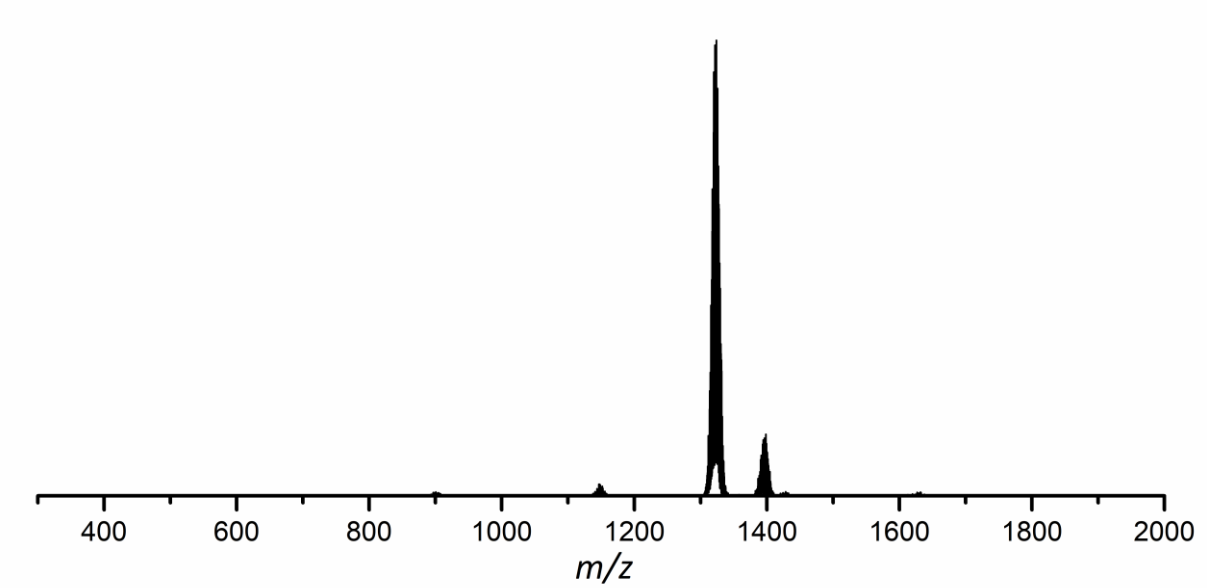

Figure S92. Overview spectrum of ESI-MS measurement (negative ion mode, 3500 V, 300 °C) of a thf solution of compound **8a**, monitoring the molecule peak at *m/z* 1323.8 $[Ge_9\{Si(TMS)_3\}_2P^iPr(N^iPr_2)]^-$. Besides the molecule peak a signal at *m/z* 1396.4 is monitored, which can be assigned to tris-silylated cluster $[Ge_9\{Si(TMS)_3\}_3]^-$, which is formed during the ionization process (species is not present in NMR spectra of **8a**).

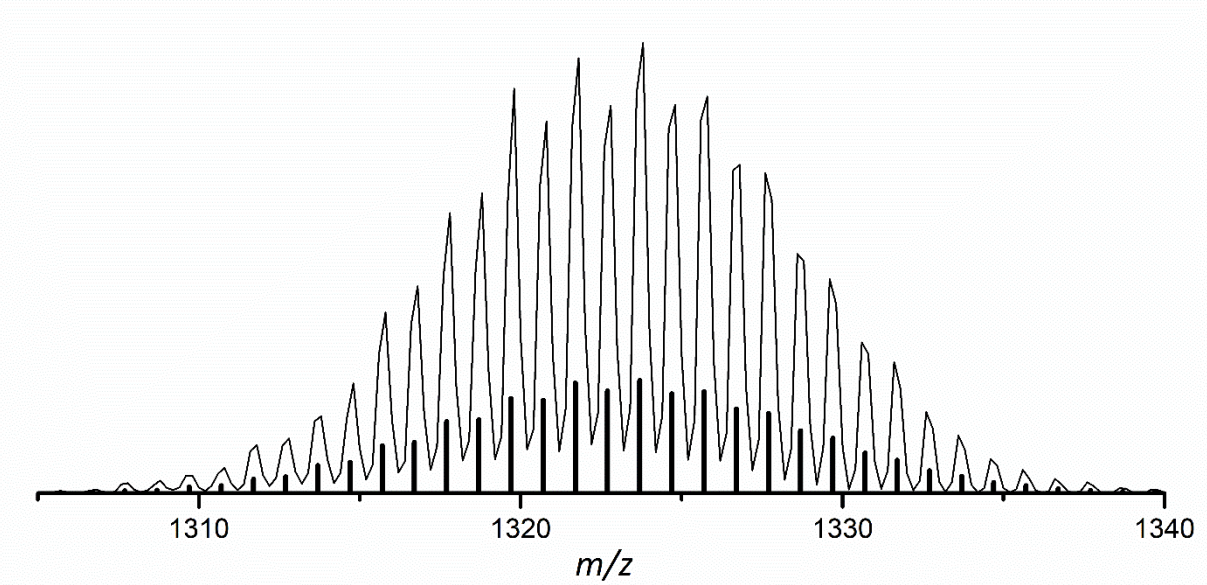

Figure S93. Detail view of ESI-MS signal (negative ion mode, 3500 V, 300 °C) of $[Ge_9\{Si(TMS)_3\}_2P^iPr(N^iPr_2)]^-$ (**8a**) at *m/z* 1323.8 monitored from thf solution. Calculated pattern is represented as black bars.

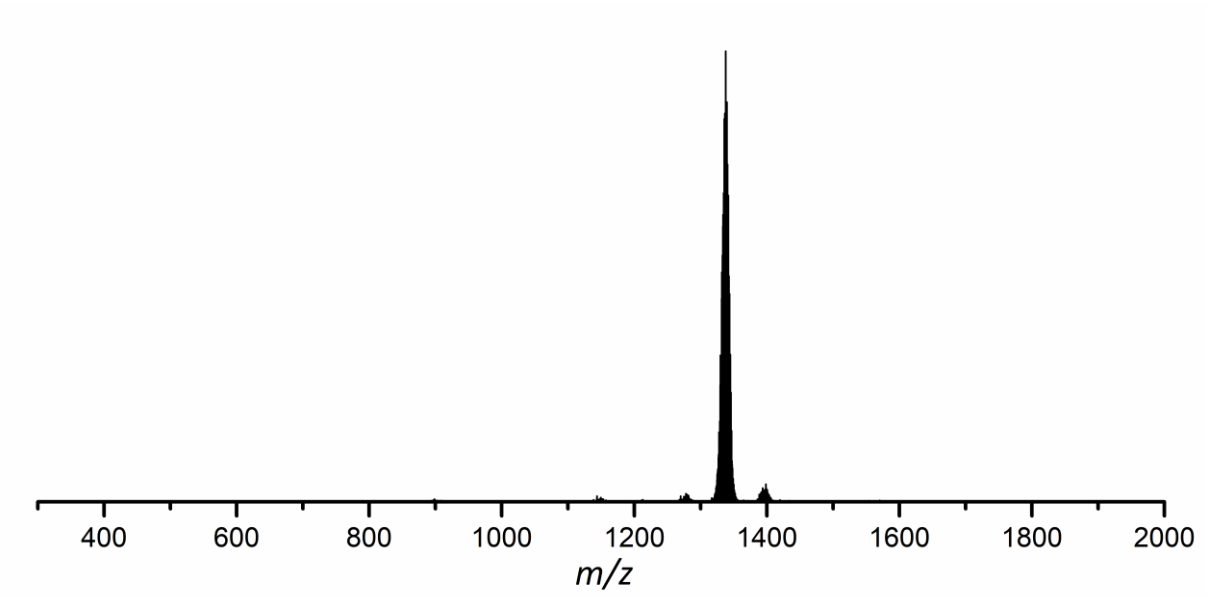

Figure S94. Overview spectrum of ESI-MS measurement (negative ion mode, 3000 V, 300 °C) of a thf solution of compound **9a**, monitoring the molecule peak at *m/z* 1337.8 $[Ge_9\{Si(TMS)_3\}_2P^tBu(N^iPr_2)]^-$.

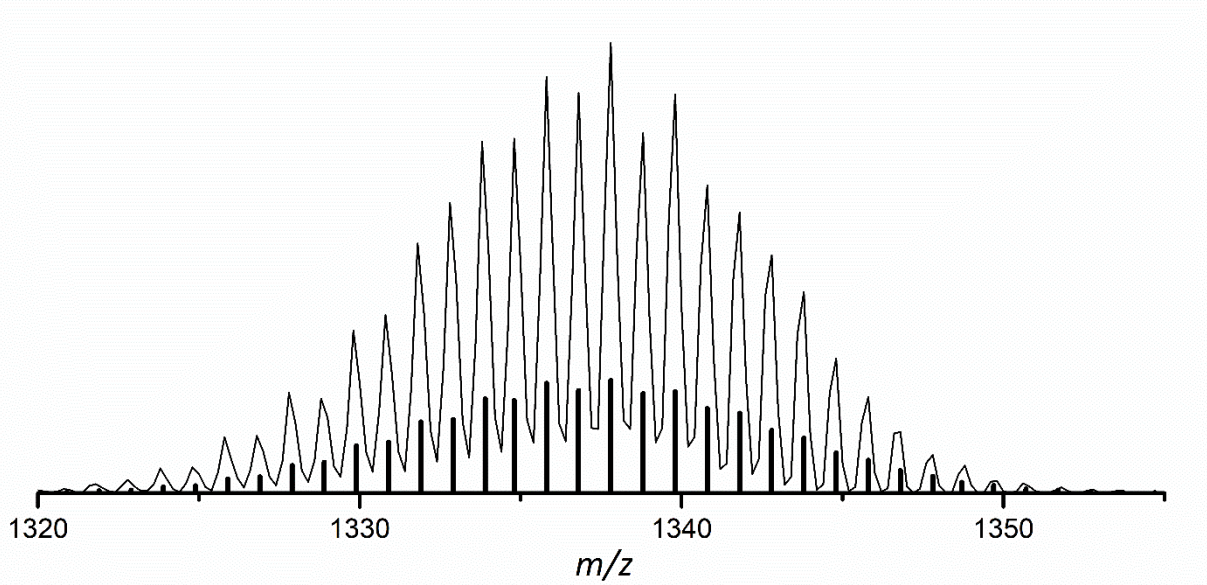

Figure S95. Detail view of ESI-MS signal (negative ion mode, 3000 V, 300 °C) of $[Ge_9\{Si(TMS)_3\}_2P^tBu(N^iPr_2)]^-$ (**9a**) at *m/z* 1337.8 monitored from thf solution. Calculated pattern is represented as black bars.

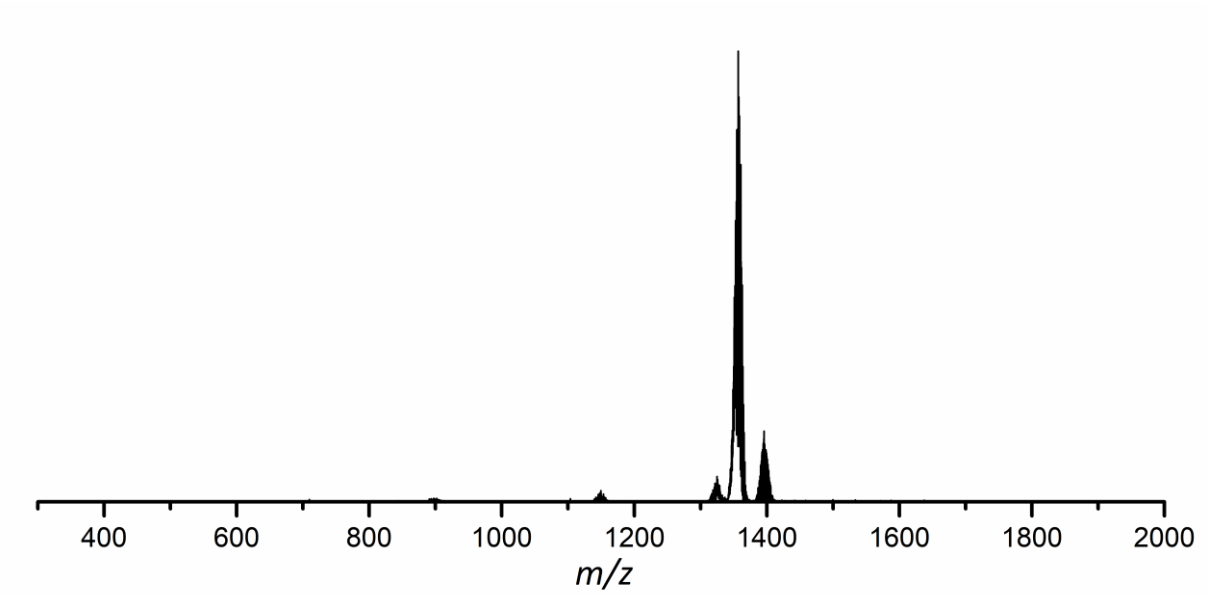

Figure S96. Overview spectrum of ESI-MS measurement (negative ion mode, 3500 V, 300 °C) of a thf solution of compound **10a**, monitoring the molecule peak at *m/z* 1356.8 $[Ge_9\{Si(TMS)_3\}_2P^tBu(Mes)]^-$. Besides the molecule peak a signal at *m/z* 1396.4 is monitored, which can be assigned to tris-silylated cluster $[Ge_9\{Si(TMS)_3\}_3]^-$, which is formed during the ionization process (species is not present in NMR spectra of **10a**). Detail view of the mixed functionalized cluster´s signal is provided in the manuscript.

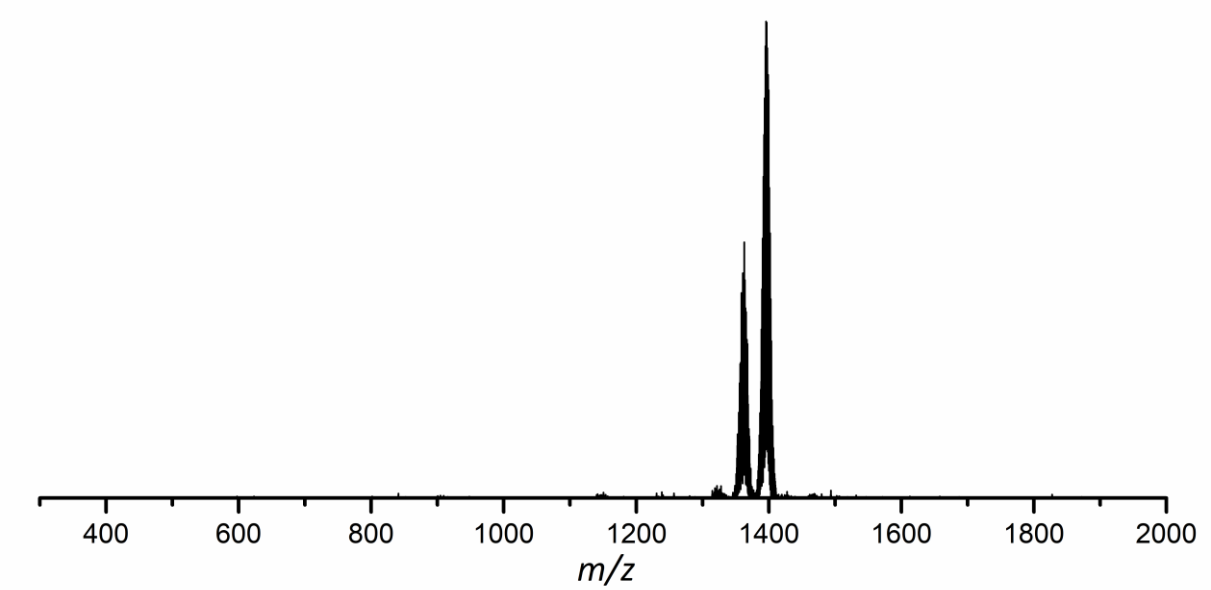

Figure S97. Overview spectrum of ESI-MS measurement (negative ion mode, 4000 V, 300 °C) of a thf solution of compound **11a**, monitoring the molecule peak at *m/z* 1362.8 $[Ge_9\{Si(TMS)_3\}_2P(o\text{-tolyl})_2]^-$. Besides the molecule peak a signal at *m/z* 1396.4 is monitored, which can be assigned to tris-silylated cluster $[Ge_9\{Si(TMS)_3\}_3]^-$, which is formed during the ionization process (species is not present in NMR spectra of **11a**).

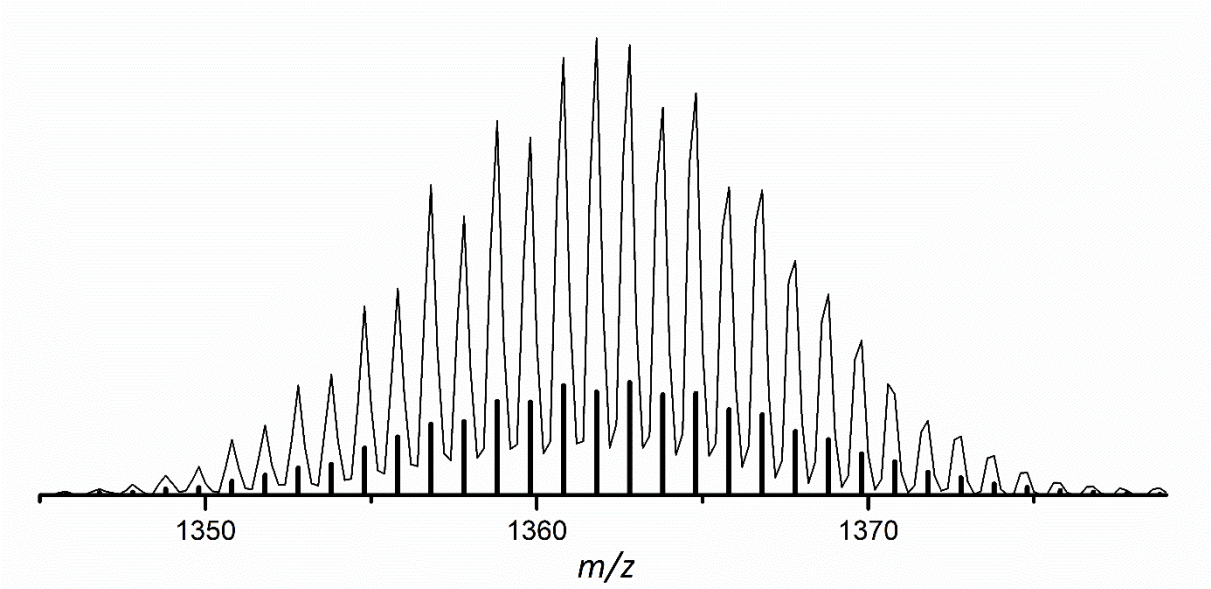

Figure S98. Detail view of ESI-MS signal (negative ion mode, 4000 V, 300 °C) of $[Ge_9\{Si(TMS)_3\}_2P(o\text{-tolyl})_2]^-$ (**11a**) at *m/z* 1362.8 monitored from thf solution. Calculated pattern is represented as black bars.

5.11 Synthesis and Reactivity of Multiple Phosphine-Functionalized Nonagermanide Clusters

F. S. Geitner, W. Klein, T. F. Fässler*

published in

Angew. Chem. Int. Ed. **2018**, *57*, 14509; *Angew. Chem.* **2018**, *130*, 14717.

Content and Contributions

The scope of this work was the synthesis of multiple phosphine-functionalized [Ge_9] clusters and to test their reactivity towards various organometallics. The synthesis of multiple phosphine-functionalized [Ge_9] clusters was achieved by heterogenous reactions of solid K_4Ge_9 with acetonitrile solutions of the chlorophosphines (^{i}Pr$_2$N)$_2$PCl or (^{i}Pr$_2$N)^{t}BuPCl. The resulting threefold phosphine-functionalized [Ge_9] clusters [Ge_9{P*RR*^{I}}$_3$]$^-$ (*R*: N^{i}Pr$_2$, *R*^{I}: N^{i}Pr$_2$ or ^{t}Bu) were characterized by means of NMR and ESI-MS. Subsequent reactions with NHC^{Dipp}CuCl resulted in neutral compounds [NHC^{Dipp}Cu(η^3-Ge_9{P*RR*^{I}}$_3$)] (*R*: N^{i}Pr$_2$, *R*^{I}: N^{i}Pr$_2$ or ^{t}Bu), which were characterized by means of NMR, single crystal X-ray diffraction (*R*^{I}: N^{i}Pr$_2$) and elemental analysis (*R*^{I}: N^{i}Pr$_2$). In the crystal structure of [NHC^{Dipp}Cu(η^3-Ge_9{P(N^{i}Pr$_2$)$_2$}$_3$)] all phosphanyl groups are disordered. The crystal structure refinement of this structure, especially the modelling of the disordered phosphanyl groups, was done by Dr. Wilhelm Klein. Reactions of [Ge_9{P(N^{i}Pr$_2$)^{t}Bu}$_3$]$^-$ with Group 6 carbonyl complexes *M*(CO)$_5$(thf) (*M*: Cr, Mo, W) resulted in the attachment of multiple [*M*(CO)$_5$] fragments to the cluster anions according to ESI-MS studies. Moreover, the reaction of [NHC^{Dipp}Cu(η^3-Ge_9{P(N^{i}Pr$_2$)$_2$}$_3$)] with Cr(CO)$_5$(thf) yielded the first neutral fivefold-coordinated [Ge_9] cluster [(NHC^{Dipp}Cu)$_2$(η^3,η^3-Ge_9{P(N^{i}Pr$_2$)$_2$}$_2$Cr(CO)$_5$)], in which every Ge atom of the cluster core is approached by a ligand. The novel species was characterized by means of NMR, single crystal X-ray diffraction, IR spectroscopy and elemental analysis. The crystal structure refinement was assisted by Dr. Wilhelm Klein. The formation of this novel compound occurs *via* ligand exchange reaction at [Ge_9], in which one of the [P(N^{i}Pr$_2$)$_2$]$^+$ ligands is substituted by the neutral Cr(CO)$_5$ fragment. This reactivity of the multiple phosphine-functionalized [Ge_9] clusters might also be interesting with respect to the introduction of novel substituents, which cannot directly be introduced at bare [Ge_9]$^{4-}$ clusters. This publication was written in course of this thesis.

Cage Molecules

International Edition: DOI: 10.1002/anie.201803476
German Edition: DOI: 10.1002/ange.201803476

Synthesis and Reactivity of Multiple Phosphine-Functionalized Nonagermanide Clusters

*Felix S. Geitner, Wilhelm Klein, and Thomas F. Fässler**

Dedicated to Professor Dr. Dietmar Stalke on the occasion of his 60th birthday

Abstract: *Herein we report on the synthesis of the first multiple phosphine-substituted nonagermanide clusters in a one-step reaction from K_4Ge_9. Their reactions towards various transition metal complexes show a large variety of reactive sites. The novel threefold phosphine-functionalized $[Ge_9]$ clusters $[Ge_9\{PRR^I\}_3]^-$ {R: N^iPr_2; R^I: N^iPr_2 (**1a**) or ^{t}Bu (**2a**)} are obtained by reaction of pristine $[Ge_9]^{4-}$ clusters with the respective chlorophosphines. Subsequent reactions with $NHC^{Dipp}CuCl$ yield neutral compounds $(NHC^{Dipp}Cu)[Ge_9\{P(N^iPr_2)_2\}_3]$ (**3**) and $(NHC^{Dipp}Cu)[Ge_9\{P(N^iPr_2)^tBu\}_3]$ (**4**), respectively. The reaction of neutral compound **3** with $Cr(CO)_5(thf)$ yields the first uncharged fivefold substituted $[Ge_9]$ cluster $(NHC^{Dipp}Cu)_2[Ge_9\{P(N^iPr_2)_2\}_2Cr(CO)_5]$ (**5**) via a ligand exchange reaction at the $[Ge_9]$ cluster core. Compounds **3** and **5** are characterized by single crystal structure determination.*

Pristine homoatomic clusters are extraordinary building units for low-valent main-group element compounds. The reactivity of anionic clusters of the heavier tetrel elements (Zintl clusters) has been well developed within the last decades. Starting from reactions with transition metal complexes, the field has quickly expanded, and nowadays a broad range of Zintl cluster based compounds comprising cluster polymers (dimers and oligomers included), main group element cluster adducts or Zintl clusters bearing organic ligands, is known.[1] However, for a long time the relatively high charge restricted investigations to a rather limited number of highly polar aprotic solvents. Therefore, derivatization for stabilizing the clusters and at the same time increasing their solubility should allow for a broader range of follow-up reactions. Such methods were found in the silylation of nonagermanide clusters yielding threefold substituted clusters $[Ge_9\{SiR_3\}_3]^-$ (R: various groups; first example was $[Ge_9\{Si(TMS)_3\}_3]^-$),[2] or twofold silylated species $[Ge_9\{Si(TMS)_3\}_2]^{2-}$.[3] These molecular anions still contain Ge atoms in low oxidation state which are exclusively connected to other Ge atoms and therefore offer good possibilities for subsequent reactions with organometallics,[4] organics,[5] or main group element compounds.[5a,6] Furthermore, the introduction of stannyl groups at $[Ge_9]$ was achieved and subsequent reactions of the obtained tris-stannylated species with $Pd(PPh_3)_4$ led to the larger aggregates $[Ge_{18}Pd_3(SnR_3)_6]^{2-}$ (R: ^{i}Pr, Cy).[7] However, the threefold derivatization of $[Ge_9]$ clusters with covalently bound ligands was limited to group IV substituents, and the resulting cluster compounds were, despite their prosperous subsequent chemistry, only capable to interact with Lewis acids via the not substituted Ge atoms of the cluster core. In a previous work we have shown that it is also possible to introduce one phosphine moiety to bis-silylated or tris-silylated $[Ge_9]$ clusters yielding the uncharged molecules $[Ge_9\{Si(TMS)_3\}_3PR_2]$ (R: ^{i}Pr, Cy) or anionic species $[Ge_9\{Si(TMS)_3\}PR_2]^-$ (R: ^{t}Bu, Mes, N^iPr_2). The latter are able to bind to $[NHC^{Dipp}Cu]^+$ either via the cluster core (R: Mes, N^iPr_2), or via the P atom of the phosphine ligand (R: ^{t}Bu).[8] Thus, the introduction of phosphine moieties to $[Ge_9]$ results in a multifarious coordination behavior of the resulting clusters. However, the multi-step synthesis through presilylated clusters hindered downstream chemistry and triggered us to develop an approach for the introduction of multiple phosphine moieties to $[Ge_9]$ in order to avoid a multi-step synthesis. Here we report on one-step reactions of K_4Ge_9 with different chlorophosphines R_2PCl (R: alkyl, aryl, aminoalkyl) in acetonitrile or thf and some subsequent reactions.

We found that the steric impact of the phosphines as well as the applied solvent have a crucial impact on the reactivity. Reactions carried out in thf either resulted in no reaction at all (R: Mes) or in reductive coupling of the chlorophosphines yielding $R_2P\text{-}PR_2$ species (R: ^{i}Pr, Cy, ^{t}Bu, N^iPr).[9] In analogous reactions in acetonitrile, similar reactivities were observed for phosphines with small (R: ^{i}Pr, Cy; reductive coupling) or large ligands (R: Mes, no reaction). By contrast heterogenous reactions of K_4Ge_9 with $(^iPr_2N)_2PCl$ or $(^iPr_2N)^tBuPCl$ led to the formation of deep red solutions containing threefold phosphine-functionalized nonagermanide clusters, which can be detected in ESI-MS examinations (negative ion mode) at m/z 1347.1 $[Ge_9\{P(N^iPr_2)_2\}_3]^-$ (**1a**) or m/z 1218.5 $[Ge_9\{P(N^iPr_2)^tBu\}_3]^-$ (**2a**), respectively (Figure 1). Removal of the solvent after filtration yields dark brown solids **1** and **2** in medium yield. NMR examinations carried out with the isolated solids reveal the presence of the products, but in the ^{1}H NMR and ^{31}P NMR spectra also the signals of impurities are detected. The purity of compounds **1** and **2** can be increased by performing the reactions with

[*] M. Sc. F. S. Geitner, Dr. W. Klein, Prof. Dr. T. F. Fässler
Department Chemie Technische Universität München
Lichtenbergstraße 4, 85747 Garching b. München (Germany)
E-mail: thomas.faessler@lrz.tum.de
M. Sc. F. S. Geitner
WACKER Institute for Silicon Chemistry (Germany)
Supporting information and the ORCID identification number(s) for the author(s) of this article can be found under: https://doi.org/10.1002/anie.201803476.

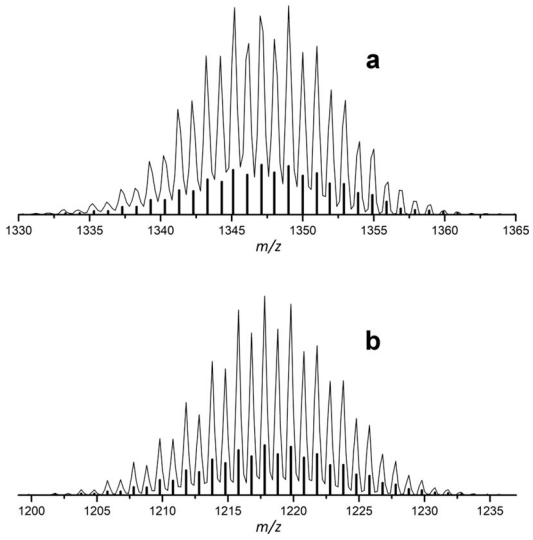

Figure 1. Selected areas of ESI-MS spectra of anions **1a** (a) and **2a** (b) Spectrum a) was recorded in acetonitrile in negative ion mode (3500 V, 300 °C), monitoring the molecule peak of **1a** $[Ge_9\{P(N^iPr_2)_2\}_3]^-$ at *m/z* 1347.1. Spectrum b) was acquired in acetonitrile in negative ion mode (3500 V, 300 °C), detecting the molecule peak of **2a** $[Ge_9\{P(N^iPr_2)^tBu\}_3]^-$ at *m/z* 1218.5. Calculated spectra are represented as black bars. The spectra of all ESI-MS examinations are provided in the Supporting information.

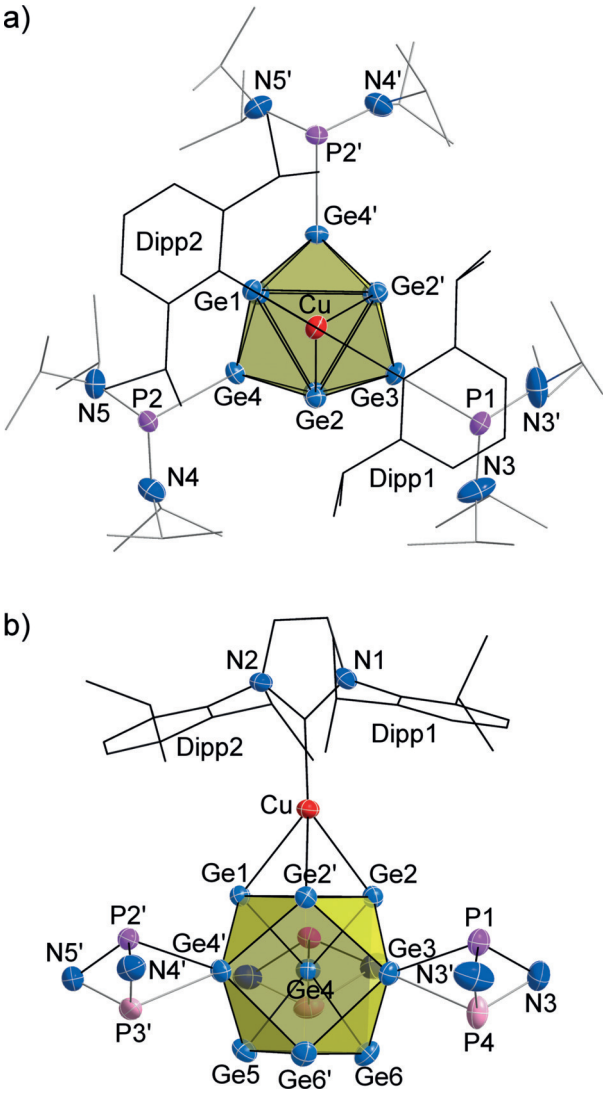

Figure 2. Two views of the molecular structure of compound **3** (atoms labelled with a dash correspond to symmetry generated atoms). Ellipsoids are shown at a 50% probability level. a) View on the $[NHC^{Dipp}Cu]^+$ coordinated trigonal face of the $[Ge_9]$ cluster revealing the attachment of the three phosphine substituents at the capping Ge atoms of the trigonal prism. b) Disorder of the phosphine groups (caused by phosphine inversion) and attachment of the $[NHC^{Dipp}Cu]^+$ fragment to one of the triangular faces of the $[Ge_9]$ cluster. For clarity the isopropyl groups of the phosphine substituents are omitted. Major phosphine moieties (P1, P2 and P2^I) are represented in purple, minor moieties (P3, P4, P4^I) are shown in pink. In both pictures all protons as well as the solvent toluene molecule are omitted, and carbon atoms are presented as black or grey wire sticks. The crystallographic data of **3**, selected bond lengths and full ellipsoid plots are provided in the Supporting information.

only two equivalents of the respective chlorophosphine. In order to test the reactivity of the novel threefold phosphine-functionalized clusters, $NHC^{Dipp}CuCl$ was added to acetonitrile solutions of **1** or **2**, leading to the formation of brownish precipitates, which were separated by filtration and washed with acetonitrile. NMR investigations carried out with the crude materials revealed the attachment of a $[NHC^{Dipp}Cu]^+$ unit to **1a** or **2a**, yielding neutral compounds $NHC^{Dipp}Cu[Ge_9\{P(N^iPr_2)_2\}_3]$ (**3**) or $NHC^{Dipp}Cu[Ge_9\{P(N^iPr_2)^tBu\}_3]$ (**4**), respectively. In the case of compound **4** the NMR spectra were recorded at increased temperature (333 K) since at room temperature a significant signal broadening was observed. The crude solids of **3** and **4** were then dissolved in toluene, filtered to remove remaining solids and stored in a freezer at −40 °C. Whereas, no crystals could be obtained for compound **4** yet, red crystals of compound **3**, suitable for single crystal X-ray diffraction, were isolated in 30% yield.

Compound **3** crystallizes in the orthorhombic space group *Pnma*, with one cocrystallized toluene molecule per formula unit. The $[Ge_9]$ cluster core has the shape of a slightly distorted tricapped trigonal prism (C_{2v} symmetry) with Ge-Ge distances between 2.5025(5) Å (Ge2-Ge3) and 2.8669(5) Å (Ge1-Ge2), which are in the range of previously reported data (Figure 2).[4h,i,8] The phosphine moieties $[P(N^iPr_2)_2]^+$ are attached to the cluster via the three capping Ge atoms (Ge3, Ge4 and Ge4^I). Several examined single crystals of **3** all showed a disorder of all three phosphine substituents at temperatures of 100 K or 150 K, resulting from the pyramidal inversion of the substituents bound to the P atoms (e.g. for P1: Ge3, N3, N3^I), which is frozen in the crystal structure (Figure 2). The individuals with larger occupancy (95.4% P1 or 69.5% P2) point towards the triangular cluster face carrying the $[NHC^{Dipp}Cu]^+$ moiety (Figure 2). Interestingly, for the phosphine moiety (P1) situated in an ecliptic position towards the NHC^{Dipp} ligand, this orientation seems to be more favorable (larger occupancy) than for the other two phosphine groups that are positioned in a staggered manner. The Ge-P bonding distances range between 2.352(1) Å (Ge3-P1) and 2.380(1) Å (Ge4-P2), and are therefore in the range of the Ge-P distances observed in mixed substituted clusters bearing

silyl and phosphine moieties.[8] Furthermore, the Ge-Cu distances of 2.5441(7) Å (Ge1-Cu) and 2.4958(5) Å (Ge2-Cu=Ge2^{I}-Cu) are also similar to previously reported data.[4g,i]

ESI-MS experiments carried out with thf solutions of compounds **3** and **4** showed signals at *m*/*z* 2251.4, which can be assigned to $\{(NHC^{Dipp}Cu)_2[Ge_9\{P(N^iPr_2)_2\}_3]\}^+$ (**3-CuNHC^{Dipp}**) or *m*/*z* 2122.3, belonging to $\{(NHC^{Dipp}Cu)_2[Ge_9\{P(N^iPr_2)^tBu\}_3]\}^+$ (**4-CuNHC^{Dipp}**), in the positive ion mode. The attachment of the second $[NHC^{Dipp}Cu]^+$ unit to **3** or **4** most probably occurs during the evaporation process in the mass spectrometer.

In order to further investigate the reactivity of the anions **1a** and **2a**, and of the neutral compounds **3** and **4**, they were reacted with the group-6 carbonyl complexes $M(CO)_5$(thf) (M: Cr, Mo, W).[10] In previous reports $M(CO)_5$ units had been attached to [Ge$_9$] clusters (Ge–Cr bond),[4d,1g] or to phosphines such as $(CO)_5$Cr-P(GeMe$_3$)$_3$] (Ge–P bond).[11] Upon the addition of thf solutions of $M(CO)_5$(thf) (*M*: Cr, Mo, W; 4 equiv. based on $M(CO)_6$) to thf solutions of **1a** or **2a** at −78 °C, red solutions are formed, which were then allowed to warm to room temperature under stirring overnight. A subsequent investigation of the reaction solutions by ESI-MS, NMR, and IR indicated the decomposition of the [Ge$_9$] clusters for reactions carried out with **1a**. By contrast for reactions with **2a**, the ESI-MS experiments revealed signals, that can be assigned to the twofold $M(CO)_5$ (*M*: Cr, Mo, W) coordinated cluster species $\{[Ge_9\{P(N^iPr_2)^tBu\}_3]\{M(CO)_5\}_2\}^-$ at *m*/*z* 1601.5 (*M*: Cr), 1689.5 (*M*: Mo) or 1865.5 (*M*: W) in the negative ion mode. Additionally for the reaction of **2a** with $Cr(CO)_5$(thf) also a signal corresponding to a threefold $Cr(CO)_5$ coordinated species $\{[Ge_9\{P(N^iPr_2)^tBu\}_3]\{Cr(CO)_5\}_3\}^-$ was detected at *m*/*z* 1793.5 (Supporting Information). The latter species might be formed during the ionization process, however at least the detection of this signal reveals the potential formation of such molecules in the gas phase. The attachment of two $M(CO)_5$ moieties at **2a** can occur either at the PR$_2$ moieties bound to the [Ge$_9$] core or via the formation of Ge-*M* *exo* bonds at the two open triangular faces of the [Ge$_9$] cluster core (one Ge atom in each triangular face; Figure 3). However, the observation of the threefold $Cr(CO)_5$ coordinated multiple phosphine-substituted cluster might rather hint at P-*M* interactions. IR spectra of the respective mixtures showed broad signals in the region of CO stretching vibrations with very low intensity, which is probably caused by the presence of several different products and solvent effects.

Attempts to obtain better IR spectra in less polar non-coordinating solvents and with solid materials were not successful.

These results reveal a significant difference in the reactivity of **2a**, compared to the tris-silylated cluster $[Ge_9\{Si(TMS)_3\}_3]^-$ which only accepts one $Cr(CO)_5$ moiety via Ge-Cr interactions.[4d]

The reaction of uncharged compound **3** with $Cr(CO)_5$(thf) yielded a deep red solution, which was stirred at RT overnight, before the solvent was removed in vacuo, resulting in a brown solid. The solid was extracted with toluene, and from the resulting deep red solution black block-shaped crystals suitable for single crystal structure analysis were obtained at

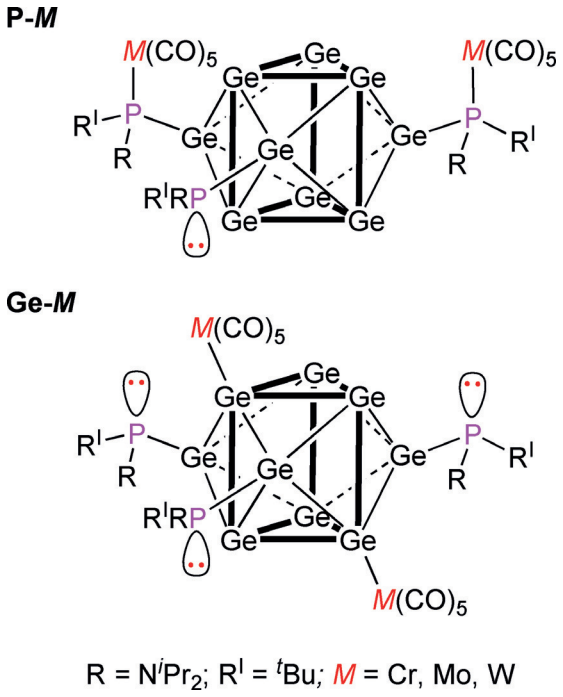

Figure 3. Potential binding sites for $M(CO)_5$ fragments at the multiple phosphine functionalized [Ge$_9$] clusters. Interactions can either occur via P-*M* bonds (top) or Ge-*M* bonds (bottom).

−40 °C after one-week in 20% yield. The X-ray structure determination reveals the formation of the first neutral, monomeric cluster $(NHC^{Dipp}Cu)_2[Ge_9\{P(N^iPr_2)_2\}_2Cr(CO)_5]$ (**5**), in which each Ge vertex is involved in *exo*-cluster bonds. A similarly crowded [Ge$_9$Pd] cluster core has been recently reported by Sevov et al. in which four Ge atoms form covalent *exo*-bonds, five Ge atoms have no external bond, and a phosphine group coordinates to the Pd atom.[12] Furthermore, **5** is the first [Ge$_9$] cluster bearing two different transition metal ligands.

Compound **5** crystallizes in the triclinic space group $P\bar{1}$, with 4.5 cocrystallized toluene molecules per formula unit. The [Ge$_9$] cluster core is best described as a heavily distorted tricapped trigonal prism, in which one prism height [*d*(Ge1-Ge7): 3.5710(5) Å] is significantly longer than the two others [*d*(Ge2-Ge8): 3.0257(5) Å and *d*(Ge3-Ge9): 3.1080(5) Å]. The Ge-Ge distances range between 2.3362(4) Å (Ge1-Ge4) and 2.8871(5) Å (Ge2-Ge3). The shortest Ge-Ge bonds are found between capping Ge atoms and Ge atoms within the triangular faces of the cluster, whereas the longest bonds are situated within the triangular faces of the cluster coordinated by Cu$^+$. The two phosphine moieties as well as the $Cr(CO)_5$ ligand bind to the capping Ge atoms of the trigonal prism by covalent bonds (Ge-P) or donor-acceptor interactions (Ge-Cr), respectively. The Ge-P distances of *d*(Ge4-P1): 2.3721(9) Å and *d*(Ge5-P2): 2.3756(9) Å are in the range of those observed in compound **3** and in previous work.[8] The $Cr(CO)_5$ moiety binds to the third capping Ge atom at a distance of 2.5140(6) Å (Cr1-Ge6), which is also in accordance to previously reported data, resulting in a distorted octahedral coordination sphere of the Cr atom [$\sphericalangle$(Ge6-Cr1-C81) = 174.4(1)°].[4d]

The two $[NHC^{Dipp}Cu]^+$ moieties coordinate to the triangular faces of the $[Ge_9]$ core. Cu2 coordinates to Ge7 to Ge9 with nearly similar Cu-Ge distances between 2.4241(5) Å (Ge1-Cu1) and 2.5654(5) Å (Ge9-Cu2), which are in the range of known values,[4g,i,k,8b] whereas Cu1 coordinates the opposite triangular face with significantly shorter and longer distances of 2.3674(5) Å (Ge3-Cu1) to 2.6873(6) Å (Ge2-Cu1). As a result the coordination of Cu1 and Cu2 by the NHC ligands and the centres of gravity of the Ge_3 faces significantly deviates from linearity [∡(ctp1-Cu1-C1) = 166.6(1)° or ∡(ctp2-Cu2-C28) = 170.4(1)° with ctp1: centre of gravity of Ge1 to Ge3 and ctp2: centre of gravity of Ge7 to Ge9] and the NHC^{Dipp} ligands are tilted toward the $Cr(CO)_5$ coordinated site of the cluster. A top view on one of the triangular $[NHC^{Dipp}Cu]^+$ coordinated faces of the clusters, reveals a staggered arrangement of the NHC^{Dipp} moieties towards the two phosphine groups and the $Cr(CO)_5$ moiety, and the NHC ligands show an ecliptic arrangement with respect to each other (Figure 4 and the Supporting Information). Crystals of **5** were also characterized by NMR, IR spectroscopy, and elemental analysis, confirming the purity of the obtained material (Supporting Information). In the IR spectrum of **5** four signals 2028 (s), 1911 (vs.), 1877 (sh), 1860 (s) were observed in the carbonyl region in accordance with related complexes such as $[Ge_9\{Si(TMS)_3\}_3Cr(CO)_5]^-$ or $[Ge_6\{Cr(CO)_5\}_6]^{2-}$.[4d,13]

The formation of compound **5** can be rationalized by replacement of one formally positively charged $[P(N^iPr_2)_2]^+$ group in **3** by the neutral $Cr(CO)_5$ fragment, resulting in a fourfold coordinated negatively charged cluster in the first step (**3** is stable in solution in absence of the Cr^0 complex). Subsequently, a second $[NHC^{Dipp}Cu]^+$ unit is added yielding the uncharged compound **5**, which in contrast to the other products of the reaction, crystallizes readily from toluene solution. Further investigations (NMR, ESI-MS, IR) of the mother liquor carried out in order to characterize the side products of this reaction did not yield unambiguous results, however, no other cluster species were detected in ESI-MS studies. A product similar to **5** but without phosphine ligands has previously been obtained by the reaction of the bis-silylated cluster $[Ge_9\{Si(TMS)_3\}_2]^{2-}$ with $NHC^{Dipp}CuCl$, yielding $(NHC^{Dipp}Cu)_2[Ge_9\{Si(TMS)_3\}_2]$.[4k] However, the formation of **5** under replacement of a phosphine moiety by $Cr(CO)_5$ is a rare example of a ligand exchange reaction occurring at a Zintl cluster and indicates a more variable reactivity of the phosphine-functionalized cluster species if compared to that of the silylated clusters.

Within this work the manifold reactivity of multiple phosphine functionalized $[Ge_9]$ clusters (**1a**, **2a**), which are obtained in a one-step synthesis starting from K_4Ge_9, is presented. Reactions with $NHC^{Dipp}CuCl$ led to the formation of neutral species **3** and **4** allowing for the first crystallographic characterization of a multiple phosphine-functionalized cluster. Furthermore according to ESI-MS reactions of **2a** with $M(CO)_5$(thf) (M: Cr, Mo, W) yield multiple $M(CO)_5$-coordinated species $\{[Ge_9\{P(N^iPr_2)^tBu\}_3]\{M(CO)_5\}_n\}^-$ ($n = 2$, 3). The reaction of compound **3** with $Cr(CO)_5$(thf) leads to a ligand exchange, upon which a phosphine moiety is replaced by the $Cr(CO)_5$ fragment, under formation of a fivefold coordinated, neutral $[Ge_9]$ cluster compound $(NHC^{Dipp}Cu)_2[Ge_9\{P(N^iPr_2)_2\}_2Cr(CO)_5]$ (**5**). Hence, besides providing several functional groups at the $[Ge_9]$ core, the increased lability of the phosphine moieties at $[Ge_9]$ makes these species suitable precursors for the synthesis of variable coordinated $[Ge_9]$ clusters.

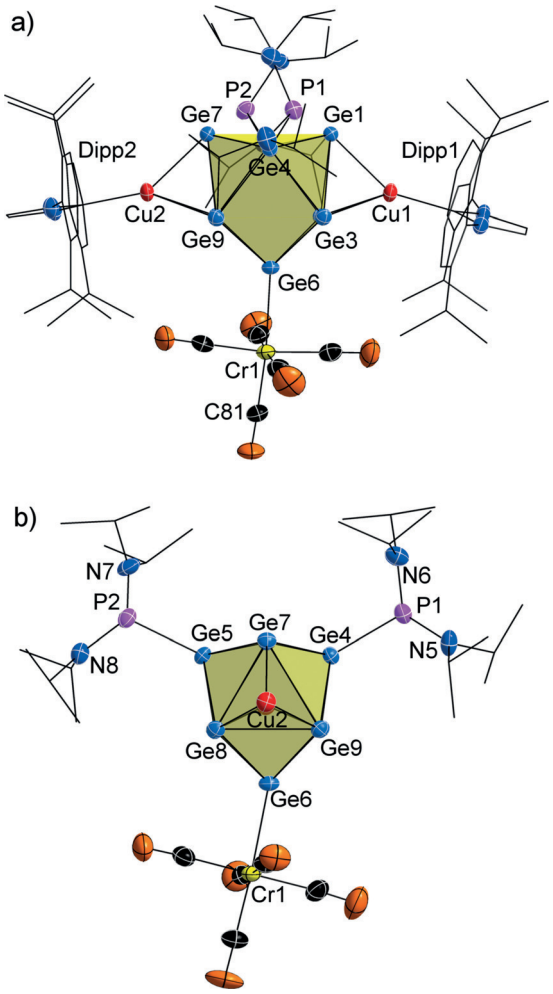

Figure 4. Two views of the molecular structure of compound **5** with labelling. Ellipsoids are shown at a 50% probability level. a) Side view on compound **5** showing the different coordination of the five ligands to the $[Ge_9]$ core. For clarity carbon atoms (except CO ligands) are represented as black wire sticks. b) View on one of the $[NHC^{Dipp}Cu]^+$ coordinated trigonal faces of the $[Ge_9]$ cluster showing the attachment of the two phosphine substituents and the $Cr(CO)_5$ ligand at the capping Ge atoms of the trigonal prism. For clarity the NHC^{Dipp} ligands are omitted, and the isopropyl groups of the phosphine moieties are represented as black wire sticks. In both pictures all protons and co-crystallized toluene molecules are omitted. The crystallographic data of **5**, selected bond lengths and angles, as well as a full ellipsoid picture are provided in the Supporting information.

Acknowledgements

This work was financially supported by Wacker Chemie AG. F.S.G. thanks M. Sc. David Mayer for IR measurements and Dr. Annette Schier for reading the manuscript. Furthermore, F.S.G. thanks TUM Graduate School for support.

Conflict of interest

The authors declare no conflict of interest.

Keywords: cage molecules · cluster · germanium · phosphorus · reactivity

How to cite: *Angew. Chem. Int. Ed.* **2018**, *57*, 14509–14513
Angew. Chem. **2018**, *130*, 14717–14721

[1] a) J. D. Corbett, *Chem. Rev.* **1985**, *85*, 383; b) T. F. Fässler, S. D. Hoffmann, *Angew. Chem. Int. Ed.* **2004**, *43*, 6242; *Angew. Chem.* **2004**, *116*, 6400; c) S. C. Sevov, J. M. Goicoechea, *Organometallics* **2006**, *25*, 5678; d) S. Scharfe, F. Kraus, S. Stegmaier, A. Schier, T. F. Fässler, *Angew. Chem. Int. Ed.* **2011**, *50*, 3630; *Angew. Chem.* **2011**, *123*, 3712; e) C. B. Benda, M. Waibel, T. Köchner, T. F. Fässler, *Chem. Eur. J.* **2014**, *20*, 16738; f) M. M. Bentlohner, L. A. Jantke, T. Henneberger, C. Fischer, K. Mayer, W. Klein, T. F. Fässler, *Chem. Eur. J.* **2016**, *22*, 13946; g) L. Wang, Y. Wang, Z. Li, H. Ruan, C. Xu, *Dalton Trans.* **2017**, *46*, 6839; h) L. Liu, L. J. Li, X. Jin, J. E. McGrady, Z. M. Sun, *Inorg. Chem.* **2018**, *57*, 3025.

[2] a) A. Schnepf, *Angew. Chem. Int. Ed.* **2003**, *42*, 2624; *Angew. Chem.* **2003**, *115*, 2728; b) F. Li, S. C. Sevov, *Inorg. Chem.* **2012**, *51*, 2706.

[3] O. Kysliak, A. Schnepf, *Dalton Trans.* **2016**, *45*, 2404.

[4] a) C. Schenk, A. Schnepf, *Angew. Chem. Int. Ed.* **2007**, *46*, 5314; *Angew. Chem.* **2007**, *119*, 5408; b) C. Schenk, F. Henke, G. Santiso-Quinones, I. Krossing, A. Schnepf, *Dalton Trans.* **2008**, 4436; c) F. Henke, C. Schenk, A. Schnepf, *Dalton Trans.* **2009**, 9141; d) C. Schenk, A. Schnepf, *Chem. Commun.* **2009**, 3208; e) F. Henke, C. Schenk, A. Schnepf, *Dalton Trans.* **2011**, *40*, 6704; f) F. Li, S. C. Sevov, *Inorg. Chem.* **2015**, *54*, 8121; g) F. S. Geitner, T. F. Fässler, *Eur. J. Inorg. Chem.* **2016**, 2688; h) K. Mayer, L. J. Schiegerl, T. F. Fässler, *Chem. Eur. J.* **2016**, *22*, 18794; i) L. J. Schiegerl, F. S. Geitner, C. Fischer, W. Klein, T. F. Fässler, *Z. Anorg. Allg. Chem.* **2016**, *642*, 1419; j) O. Kysliak, C. Schrenk, A. Schnepf, *Chem. Eur. J.* **2016**, *22*, 18787; k) F. S. Geitner, M. A. Giebel, A. Pöthig, T. F. Fässler, *Molecules* **2017**, *22*, 1204.

[5] a) F. Li, S. C. Sevov, *J. Am. Chem. Soc.* **2014**, *136*, 12056; b) S. Frischhut, T. F. Fässler, *Dalton Trans.* **2018**, *47*, 3223.

[6] F. Li, A. Munoz-Castro, S. C. Sevov, *Angew. Chem. Int. Ed.* **2012**, *51*, 8581; *Angew. Chem.* **2012**, *124*, 8709.

[7] a) L. G. Perla, S. C. Sevov, *J. Am. Chem. Soc.* **2016**, *138*, 9795; b) L. G. Perla, A. Muñoz-Castro, S. C. Sevov, *J. Am. Chem. Soc.* **2017**, *139*, 15176.

[8] a) F. S. Geitner, J. V. Dums, T. F. Fässler, *J. Am. Chem. Soc.* **2017**, *139*, 11933; b) F. S. Geitner, C. Wallach, T. F. Fässler, *Chem. Eur. J.* **2018**, *24*, 4103.

[9] a) M. Baudler, A. Zarkadas, *Chem. Ber.* **1972**, *105*, 3844; b) D. L. Dodds, M. F. Haddow, A. G. Orpen, P. G. Pringle, G. Woodward, *Organometallics* **2006**, *25*, 5937; c) R. Grubba, A. Wisniewska, K. Baranowska, E. Matern, J. Pikies, *Dalton Trans.* **2011**, *40*, 2017.

[10] V. C. Gibson, N. J. Long, A. J. P. White, C. K. Williams, D. J. Williams, M. Fontani, P. Zanello, *Dalton Trans.* **2002**, 3280.

[11] H. Schumann, L. Rösch, H. J. Kroth, J. Pickardt, H. Neumann, B. Neudert, *Z. Anorg. Allg. Chem.* **1977**, *430*, 51.

[12] F. Li, A. Munoz-Castro, S. C. Sevov, *Angew. Chem. Int. Ed.* **2016**, *55*, 8630; *Angew. Chem.* **2016**, *128*, 8772.

[13] P. Kircher, G. Huttner, K. Heinze, G. Renner, *Angew. Chem. Int. Ed.* **1998**, *37*, 1664; *Angew. Chem.* **1998**, *110*, 1754.

Manuscript received: March 22, 2018
Revised manuscript received: June 19, 2018
Accepted manuscript online: July 12, 2018
Version of record online: August 6, 2018

Communications

Cage Molecules

F. S. Geitner, W. Klein,
T. F. Fässler* _____ ■■■■–■■■■

Synthesis and Reactivity of Multiple Phosphine-Functionalized Nonagermanide Clusters

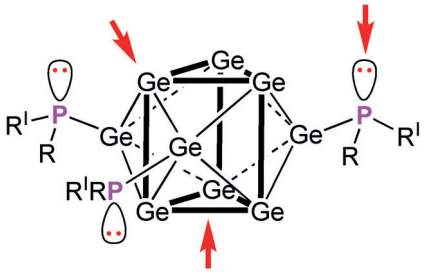

R: N^{i}Pr$_2$; R^I: N^{i}Pr$_2$, ^{t}Bu

Multifunctional Cluster Compounds: Threefold phosphine-functionalized clusters are easily accessible via one-step synthesis from the Zintl phase K_4Ge_9. The novel species reveal various reactive sites that can be approached by Lewis acids, comprising the lone pairs at P, single Ge atoms or Ge_3 triangular clusters faces (red arrows).

Angewandte Chemie
Eine Zeitschrift der Gesellschaft Deutscher Chemiker

Supporting Information

Synthesis and Reactivity of Multiple Phosphine-Functionalized Nonagermanide Clusters

*Felix S. Geitner, Wilhelm Klein, and Thomas F. Fässler**

anie_201803476_sm_miscellaneous_information.pdf

Supporting Information

69451 Weinheim, Germany

Abstract: Herein we report on the synthesis of the first multiple phosphine-substituted nonagermanide clusters in a one-step reaction from K_4Ge_9. Their reactions towards various transition metal complexes show a large variety of reactive sites. The novel threefold phosphine-functionalized [Ge_9] clusters $[Ge_9\{PRR^I\}_3]^-$ {R: N^{i}Pr$_2$; R^I: N^{i}Pr$_2$ (**1a**) or ^{t}Bu (**2a**)} are obtained by reaction of pristine $[Ge_9]^{4-}$ clusters with the respective chlorophosphines. Subsequent reactions with NHC^{Dipp}CuCl yield neutral compounds (NHC^{Dipp}Cu)[$Ge_9\{P(N^iPr_2)_2\}_3$] (**3**) and (NHC^{Dipp}Cu)[$Ge_9\{P(N^iPr_2)^tBu\}_3$] (**4**), respectively. The reaction of neutral compound **3** with $Cr(CO)_5$(thf) yields the first uncharged fivefold substituted [Ge_9] cluster (NHC^{Dipp}Cu)$_2$[$Ge_9\{P(N^iPr_2)_2\}_2$]$_2$Cr(CO)$_5$] (**5**) via a ligand exchange reaction at the [Ge_9] cluster core. Compounds **3** and **5** are characterized by single crystal structure determination.

SUPPORTING INFORMATION

Table of Contents

Experimental Procedures

General

All manipulations were performed under oxygen-free, dry conditions under argon atmosphere using standard Schlenk or glove box techniques. Glassware was dried prior to use by heating it *in vacuo*. The solvents used were obtained from an MBraun Grubbs apparatus. All other commercially available chemicals were used without further purification. K_4Ge_9 was prepared by fusion of stoichiometric amounts of the elements in stainless-steel tubes at 650 °C. The chlorophosphine (N^iPr_2)^{t}BuPCl,[1] the imidazolium salt NHC^{Dipp}·HCl,[2] and the respective copper carbene $NHC^{Dipp}CuCl$[3] were prepared according to modified literature procedures. The carbonyl complexes $M(CO)_5$(thf) (*M*: Cr, Mo, W) were freshly prepared by radiation of $M(CO)_6$ with an UV lamp before each reaction.

Single Crystal Structure Determination

The air- and moisture-sensitive crystals of **3** and **6** were transferred from the mother liquor into cooled perfluoroalkyl ether oil under a cold stream of N_2 gas. For diffraction data collection, the single crystals were fixed on a glass capillary and positioned in a 150 K cold N_2 gas stream using the crystal cap system. Data collection was performed with a STOE StadiVari ($Mo_{K\alpha}$ radiation) diffractometer equipped with a DECTRIS PILATUS 300K detector. Structures were solved by Direct Methods (SHELXS-2014) and refined by full-matrix least-squares calculations against F^2 (SHELXL-2014).[4] The positions of the hydrogen atoms were calculated and refined using a riding model. Unless stated otherwise, all non-hydrogen atoms were treated with anisotropic displacement parameters. The supplementary crystallographic data for this paper have been deposited with the Cambridge Structural database and are available free of charge *via* www.ccdc.cam.ac.uk/data_request/cif. The crystallographic data for compounds **3** and **6** are summarized in Table S1. In compound **3** all phosphine substituents are disordered and were refined on split positions. Some carbon atoms within the distorted groups had to be treated with ISOR restraints. Furthermore, the solvent toluene molecule´s methyl group is also disordered. For compound **6** some carbon atoms of the cocrystallized toluene molecules were treated with ISOR restraints.

NMR Spectroscopy

NMR spectra were measured on a Bruker Avance Ultrashield 400 MHz spectrometer. The ^{1}H NMR spectra were calibrated using the residual proton signal of the used deuterated solvents. Chemical shifts are reported in parts per million (ppm) relative to TMS, with the solvent peaks serving as internal reference.[5] Abbreviations for signal multiplicities are: singlet (s), doublet (d), triplet (t), heptet (hept), broad signal (brs).

Electron Spray Ionization Mass Spectrometry (ESI-MS)

ESI-MS analyses were performed on a Bruker Daltronic HCT mass spectrometer (injection speed: 240 µL/s), and the data evaluation was carried out using the Bruker Compass Data Analysis 4.0 SP 5 program (Bruker). Spectra were plotted using OriginPro2016G (Origin Lab) and Excel 2016 (Microsoft).

IR Spectroscopy

FT-IR spectra were recorded on a Bruker Alpha FT-IR spectrometer with an ATR geometry, using a diamond ATR unit under argon atmosphere.

Energy Dispersive X-Ray Analysis

Energy dispersive X-ray (EDX) examinations with single crystals were carried out with a *Hitachi* TM-1000 tabletop microscope device. Data evaluation occurred using the SWIFT-ED-TM (*Oxford Instruments*: INCA System Software) program.

Elemental Analyses (EA)

Elemental analyses were carried out in the micro-analytical laboratory of the Chemistry Department of Technische Universität München. Analyses of C, H, N were performed in a combustion analyzer (elementar vario EL, Bruker).

Syntheses

K[Ge$_9${P(N^{i}Pr$_2$)$_2$}$_3$] (1): Solid K_4Ge_9 (250 mg, 0.308 mmol, 1 eq.) was treated with an acetonitrile solution (8 mL) of (^{i}Pr$_2$N)$_2$PCl (165 mg, 0.616 mmol, 2 eq.). After stirring for 3h at r.t, remaining solids were removed by filtration and the obtained deep red solution was dried in vacuo, yielding crude K[Ge$_9${P(N^{i}Pr$_2$)$_2$}$_3$] (98 mg, 35 %) as brownish solid. **^{1}H NMR** (400 MHz, 298 K, MeCN-d_3): δ [ppm] = 3.60 (m, 12H, $CH_{(PN^iPr)}$), 1.16 (d, $^3J_{HH}$ = 6.6 Hz, 36H, $Me_{(PN^iPr)}$), 1.11 (d, $^3J_{HH}$ = 6.6 Hz, 36H, $Me_{(PN^iPr)}$). **^{13}C NMR** (101 MHz, 298 K, MeCN-d_3): δ [ppm] = 51.17 (d, $^2J_{CP}$ = 9.6 Hz, $CH_{(PN^iPr)}$), 24.95 (d, $^3J_{CP}$ = 8.4 Hz, $Me_{(PN^iPr)}$), 24.59 (d,$^3J_{CP}$ = 5.7 Hz, $Me_{(PN^iPr)}$), **^{31}P NMR** (162 MHz, 298 K, MeCN-d_3): δ [ppm] = 75.97 (m, P_{Ge9}). **ESI-MS** (negative ion mode, 3500 V, 300 °C): *m/z* 1347.1 [Ge$_9${P(N^{i}Pr$_2$)$_2$}$_3$]$^-$.

K[Ge$_9${P(N^{i}Pr$_2$)^{t}Bu}$_3$] (2): Solid K_4Ge_9 (250 mg, 0.308 mmol, 1 eq.) was treated with an acetonitrile solution (8 mL) of (^{i}Pr$_2$N)^{t}BuPCl (138 mg, 0.616 mmol, 2 eq.). After stirring for 3h at r.t, remaining solids were removed by filtration and the obtained deep red solution was dried in vacuo, yielding crude K[Ge$_9${P(N^{i}Pr$_2$)^{t}Bu}$_3$] (116 mg, 45 %) as brownish solid. **^{1}H NMR** (400 MHz, 298 K, MeCN-d_3): δ [ppm] = 3.74 (brs, 3H, $CH_{(PN^iPr)}$), 3.13 (brs, 3H, $CH_{(PN^iPr)}$), 1.10 (d, $^4J_{HP}$ = 13.7 Hz, 36H, $Me_{(PN^iPr)}$), 1.04 (brs, 27H, $Me_{(P^tBu)}$). **^{13}C NMR** (101 MHz, 298 K, MeCN-d_3): δ [ppm] = 56.99 (brs, $CH_{(PN^iPr)}$), 45.72 (d, $^2J_{CP}$ = 35.8 Hz, $CH_{(PN^iPr)}$), 35.23 (d, $^1J_{CP}$ = 31.2 Hz, $C_{^tBu}$), 30.48 (d, $^3J_{CP}$ = 17.3 Hz, $Me_{(PN^iPr)}$), 28.65 (d, $^2J_{CP}$ = 16.7 Hz, $Me_{^tBu}$), 26.08 (brs, $Me_{^tBu}$). **^{31}P NMR** (162 MHz, 298 K, MeCN-d_3): δ [ppm] = 84.42 (m, P_{Ge9}). **ESI-MS** (negative ion mode, 3500 V, 300 °C): *m/z* 1218.5 [Ge$_9${P(N^{i}Pr$_2$)^{t}Bu}$_3$]$^-$.

NHC^{Dipp}Cu[Ge$_9${P(N^{i}Pr$_2$)$_2$}$_3$] (3): Solid K_4Ge_9 (250 mg, 0.308 mmol, 1 eq.) was treated with an acetonitrile solution (8 mL) of (^{i}Pr$_2$N)$_2$PCl (165 mg, 0.616 mmol, 2 eq.). After stirring for 3h at r.t, remaining solids were removed by filtration, obtaining a deep red solution. Dropwise addition of an acetonitrile solution (4 mL) of NHC^{Dipp}CuCl (150 mg, 0.308 mmol, 1 eq.) led to the formation of a bright brownish precipitate. The reaction mixture was stirred for 15 min at room temperature. Subsequently, the orange supernatant solution was filtered off and the solid was washed with acetonitrile (2 x 4 mL) before it was dried in vacuo. The solid was extracted with toluene (8 mL), filtered to remove remaining solids and concentrated to half of its original volume before it was placed in a freezer at -40 °C for crystallization. After one-week pure NHC^{Dipp}Cu[Ge$_9${P(N^{i}Pr$_2$)$_2$}$_3$] (111 mg, 30 %) was obtained as red crystals. **^{1}H NMR** (400 MHz, 298 K, thf-d_8): δ [ppm] = 7.46-7.42 (m, 4H, CH_{Im} + $CH_{Ph(p)}$), 7.38-7.36 (m, 4H, $CH_{Ph(m)}$), 3.52-3.40 (m, 12H, $CH_{(PN^iPr)}$), 2.91 (hept, $^3J_{HH}$ = 7.2 Hz, 4H, $CH_{^iPr(NHC)}$), 1.64 (d, $^3J_{HH}$ = 6.9 Hz, 12H, $Me_{^iPr(NHC)}$), 1.24 (d, $^3J_{HH}$ = 6.9 Hz, 12H, $Me_{^iPr(NHC)}$), 1.14 (d, $^3J_{HH}$ = 6.6 Hz, 36H, $Me_{(PN^iPr)}$), 1.06 (d, $^3J_{HH}$ = 6.6 Hz, 36H, $CH_{(PN^iPr)}$). **^{13}C NMR** (101 MHz, 298 K, thf-d_8): δ [ppm] = 146.64 (s, $C_{Ph(^iPr)}$), 136.34 (s, $C_{Ph}N$), 130.92 (s, $CH_{Ph(p)}$), 124.97 (s, $CH_{Ph(m)}$), 123.31 (s, CH_{Im}), 52.02 (d, $^2J_{CP}$ = 10.6 Hz, $CH_{(PN^iPr)}$), 29.89 (s, $CH_{^iPr(NHC)}$), 24.64 (d, $^3J_{CP}$ = 6.0 Hz, $Me_{(PN^iPr)}$). **^{31}P NMR** (162 MHz, 298 K, thf-d_8): δ [ppm] = 87.99 (m, P_{Ge9}). In ^{13}C NMR spectrum signals of the Dipp methyl protons overlap with the solvent signal and can therefore not be properly assigned. Furthermore, the carbene carbon atom could not be monitored. **ESI-MS** (positive ion mode, 3000 V, 300 °C): *m/z* 2251.4 {(NHC^{Dipp}Cu)$_2$[Ge$_9${P(N^{i}Pr$_2$)$_2$}$_3$]}$^+$. **Elemental analysis**: anal. calcd. for

$C_{63}H_{120}Cu_1Ge_9N_8P_3$: C, 42.04; H, 6.72; N,6.23; found: C, 41.80; H, 6.75 N; 6.12. **EDX**: calcd. Ge: 69 %, P: 23 %, Cu: 8 %; found Ge: 68(3) %, P 25(3) %, Cu 7(3) %. Analogue reaction with Cy_3PCuCl instead of the Cu-NHC complex did not result in unambiguous results yet.

$NHC^{Dipp}Cu[Ge_9\{P(N^iPr_2)^tBu\}_3]$ (4): Solid K_4Ge_9 (250 mg, 0.308 mmol, 1 eq.) was treated with an acetonitrile solution (8 mL) of $(^iPr_2N)^tBuPCl$ (138 mg, 0.616 mmol, 2 eq.). After stirring for 3h at r.t, remaining solids were removed by filtration obtaining a deep red solution. Dropwise addition of an acetonitrile solution (4 mL) of $NHC^{Dipp}CuCl$ (150 mg, 0.308 mmol, 1 eq.) led to the formation of a bright brownish precipitate. The reaction mixture was stirred for 15 min at room temperature. Subsequently, the orange supernatant solution was filtered off and the solid was washed with acetonitrile (2 x 4 mL) before it was dried in vacuo. The solid was extracted with toluene (8 mL), filtered to remove remaining solids and dried in vacuo to obtain the crude product as brown solid (137mg, 40 %). Purification by crystallization has not been successful to date. **^{1}H NMR** (400 MHz, 333 K, thf-d_8): δ [ppm] = 7.47-7.40 (m, 2H, $CH_{Ph(p)}$), 7.39-7.32 (m, 6H, CH_{Im} + $CH_{Ph(m)}$), 3.34 (brs, 6H, $CH_{(PNiPr)}$), 2.89 (m, 4H, $CH_{iPr(NHC)}$), 1.60 (d, $^3J_{HH}$ = 6.9 Hz, 12H, $Me_{iPr(NHC)}$), 1.22 (d, $^3J_{HH}$ = 6.9 Hz, 12H, $Me_{iPr(NHC)}$), 1.09 (brs, 63H, $Me_{(PNiPr)}$ + Me_{tBu}). **^{13}C NMR** (101 MHz, 298 K, thf-d_8): δ [ppm] = 180.31 (s, $C_{Carbene}$), 146.69 (s, $C_{Ph(iPr)}$), 136.17 (s, $C_{Ph}N$), 131.11 (s, $CH_{Ph(p)}$), 124.86 (s, $CH_{Ph(m)}$), 123.48 (s, CH_{Im}), 57.49 (brs, $CH_{(PNiPr)}$), 35.56 (d, $^1J_{CP}$ = 32.2 Hz, C_{tBu}), 30.71 (d, $^2J_{CP}$ = 7.7 Hz, Me_{tBu}), 30.53 (d, $^2J_{CP}$ = 7.7 Hz, Me_{tBu}), 29.86(s, $CH_{iPr(NHC)}$), 28.81 (d, $^2J_{CP}$ = 16.8 Hz, Me_{tBu}), 23.35 (brs, $Me_{(PNiPr)}$). **^{31}P NMR** (162 MHz, 298 K, thf-d_8): δ [ppm] = 91.44 (m, P_{Ge9}). In ^{13}C NMR spectrum signals of the Dipp methyl protons overlap with the solvent signal and can therefore not be properly assigned. **ESI-MS** (positive ion mode, 3000 V, 300 °C): *m/z* 2122.3 $\{(NHC^{Dipp}Cu)_2[Ge_9\{P(N^iPr_2)^tBu\}_3]\}^+$. Analogue reaction with Cy_3PCuCl instead of the Cu-NHC complex did not result in unambiguous results yet.

$(NHC^{Dipp}Cu)_2[Ge_9\{P(N^iPr_2)_2\}_2Cr(CO)_5]$ (5): Solid $(NHC^{Dipp}Cu)[Ge_9\{P(N^iPr_2)_2\}_3]$ (135 mg, 0.075 mmol, 1 eq.) was treated with a thf solution of $Cr(CO)_5$(thf) (prepared by irradiation of a $Cr(CO)_6$ (49.5 mg, 0.225 mmol) thf solution with an UV lamp at 300 nm). The resulting deep red reaction mixture was stirred for 2h at room temperature before the solvent was removed to yield a brownish residue. The solid was then extracted with toluene (6 mL) and filtered to remove insoluble materials. Subsequently, the toluene solution was concentrated to half of its original volume and stored in a freezer at -40°C for crystallization, obtaining black-block shaped crystals (30 mg, 20%) after one week. **^{1}H NMR** (400 MHz, 333 K, thf-d_8): δ [ppm] = 7.44-7.39 (m, 4H, $CH_{Ph(p)}$), 7.38 (s, 4H, CH_{Im}), 7.33-7.28 (m, 8H, $CH_{Ph(m)}$), 3.25 (m, 8H, $CH_{(PNiPr)}$), 2.75 (hept, $^3J_{HH}$ = 6.9 Hz, 8H, $CH_{iPr(NHC)}$), 1.51 (d, $^3J_{HH}$ = 6.9 Hz, 24H, $Me_{iPr(NHC)}$), 1.18 (d, $^3J_{HH}$ = 6.9 Hz, 24H, $Me_{iPr(NHC)}$), 1.13 (d, $^3J_{HH}$ = 6.6 Hz, 24H, $Me_{(PNiPr)}$), 0.98 (d, $^3J_{HH}$ = 6.6 Hz, 24H, $Me_{(PNiPr)}$). **^{13}C NMR** (101 MHz, 298 K, thf-d_8): δ [ppm] = 228.19 (s, CO_{eq}), 223.13 (s, CO_{ax}), 180.61 (s, $C_{Carbene}$), 146.36 (s, $C_{Ph(iPr)}$), 135.99 (s, $C_{Ph}N$), 130.80 (s, $CH_{Ph(p)}$), 125.12 (s, $CH_{Ph(m)}$), 123.55 (s, CH_{Im}), 52.12 (d, $^1J_{CP}$ = 10.9 Hz, $CH_{(PNiPr)}$), 29.81(s, $CH_{iPr(NHC)}$), 24.81 (m, $Me_{(PNiPr)}$). **^{31}P NMR** (162 MHz, 298 K, thf-d_8): δ [ppm] = 90.48 (m, P_{Ge9}). In ^{13}C NMR spectrum signals of the Dipp methyl protons overlap with the solvent signal and can therefore not be properly assigned. **IR** (crystal): *v* [cm^{-1}] = 2028 (s), 1911 (vs), 1877 (sh), 1860 (s). **Elemental analysis**: anal. calcd. for $C_{63}H_{120}Cu_1Ge_9N_8P_3$: C, 45.05; H, 5.83; N, 5.06; found: C, 45.24; H, 6.05 N; 4.85. **EDX**: calcd. Ge: 64 %, P: 14 %, Cu: 14 % Cr: 7 %; found Ge: 64(3) %, P 16(3) %, Cu 13(3) %, Cr: 7(3) %.

General Procedure for reactions of $K[Ge_9\{P(N^iPr_2)^tBu\}_3]$ with $M(CO)_5$(thf) (*M*: Cr, Mo, W)

$K[Ge_9\{P(N^iPr_2)^tBu\}_3]$ (0.075 mmol, 1 eq.) was dissolved in thf (1 mL) and cooled to -78 °C. Subsequently, a freshly prepared solution of $M(CO)_5$(thf) (0.300 mmol, 4 eq. based on the applied $M(CO)_6$ (*M*: Cr, Mo, W) complex) in 3-5 mL thf (also cooled to -78 °C) was added and the resulting deep red reaction mixture was stirred at -78 °C for 15 min before the cooling bath was removed and the mixture was stirred over night at room temperature. Subsequently, ESI-MS measurements were carried out with diluted aliquots of the respective reaction solutions monitoring multiple $M(CO)_5$ (*M*: Cr, Mo, W) coordinated $[Ge_9\{P(N^iPr_2)^tBu\}_3]^-$ species in the negative ion mode. **ESI-MS** (negative ion mode): (*M*: Cr) *m/z* 1601.5 $\{[Ge_9\{P(N^iPr_2)^tBu\}_3]\{Cr(CO)_5\}_2\}^-$, *m/z* 1793.5 $\{[Ge_9\{P(N^iPr_2)^tBu\}_3]\{Cr(CO)_5\}_3\}^-$. (*M*: Mo): *m/z* 1633.5 $\{[Ge_9\{P(N^iPr_2)^tBu\}_3]\{Mo(CO)_4\}_2\}^-$, *m/z* 1661.5 $\{[Ge_9\{P(N^iPr_2)^tBu\}_3]\{Mo(CO)_4\}\{Mo(CO)_5\}\}^-$, *m/z* 1689.5 $\{[Ge_9\{P(N^iPr_2)^tBu\}_3]\{Mo(CO)_5\}_2\}^-$. (*M*: W): *m/z* 1865.5 $\{[Ge_9\{P(N^iPr_2)^tBu\}_3]\{W(CO)_5\}_2\}^-$.

SUPPORTING INFORMATION

Results and Discussion

Crystallographic data

Table S1. Crystallographic data of compounds **3** and **5**.

Compound	**3**	**5**
formula	$C_{63}H_{120}CuGe_9N_8P_3$·tol	$C_{83}H_{128}CrCu_2Ge_9N_8O_5P_2$·4.5 tol
fw [g·mol^{-1}]	1891.56	2626.86
space group	*Pnma*	*P-1*
a [Å]	15.8197(3)	15.2381(5)
b [Å]	21.2584(4)	15.9171(6)
c [Å]	25.9998(7)	26.1995(9)
α [°]	90	95.245(3)
β [°]	90	91.952(3)
γ [°]	90	89.808(3)
V [Å^3]	8743.8(3)	6324.3(4)
Z	4	2
T [K]	123	123
λ [Å]	Mo *Kα*	Mo *Kα*
ρ_{calcd} [g·cm^{-3}]	1.437	1.379
μ [mm^{-1}]	3.379	2.591
collected reflections	255892	110430
independent reflections	8840	24827
R_{int} / R_{δ}	0.0787/0.0240	0.0518/0.0364
parameters / restraints	632/36	1316/60
R_1 [$I > 2\,\sigma(I)$ / all data]	0.0335/0.0475	0.0358/0.0535
wR_2 [$I > 2\,\sigma(I)$ / all data]	0.0693/0.0765	0.0794/0.0886
goodness of fit	1.167	1.059
max./min. diff. el. density [e / Å^{-3}]	0.62/-0.46	1.07/-0.46
CCDC	1826974	1826975

Table S2. Selected bond lengths in compound **3**.

bond	distance [Å]
Ge1-Ge2	2.8669(5)
Ge1-Ge4	2.5174(4)
Ge2-Ge2^{I}	2.8131(6)
Ge2-Ge3	2.5025(5)
Ge2-Ge4	2.5027(5)
Ge3-Ge6	2.5706(5)
Ge4-Ge5	2.5694(5)
Ge4-Ge6	2.5818(5)
Ge5-Ge6	2.6415(6)
Ge6-Ge6^{I}	2.6392(7)
Ge3-P1	2.352(1)
Ge3-P4	2.37(3)
Ge4-P2	2.380(1)
Ge4-P3	2.363(3)
Ge1-Cu	2.5441(7)
Ge2-Cu	2.4958(5)
Ge1-Ge5	3.343(7)
Ge2-Ge6	3.387(8)

Atoms marked with (I) are symmetry generated.

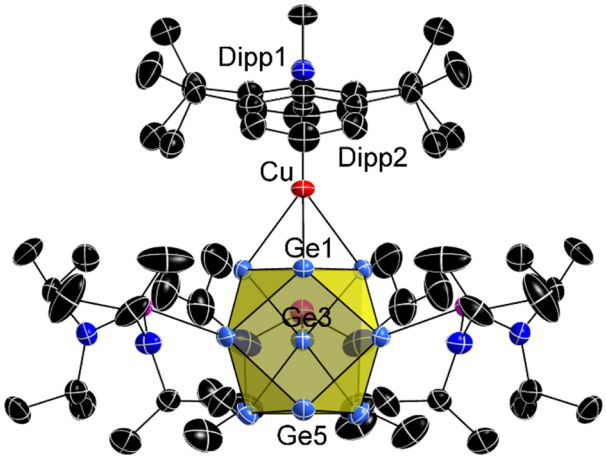

Figure S1. Labelled full ellipsoid crystal structure of compound **3** (without disorder; only major phosphine individuals are shown). Ellipsoids are shown at a 50 % probability level. For clarity reasons all protons and the solvent toluene molecule are omitted.

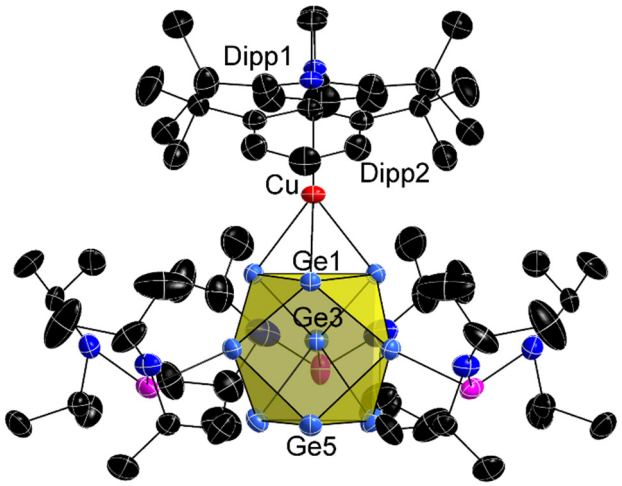

Figure S2. Labelled full ellipsoid crystal structure of compound **3** (without disorder; only minor phosphine individuals are shown). Ellipsoids are shown at a 50 % probability level. For clarity reasons all protons and the solvent toluene molecule are omitted.

Table S3. Selected bond lengths in compound **5**.

bond	distance [Å]
Ge1-Ge2	2.8086(5)
Ge1-Ge3	2.8032(5)
Ge1-Ge4	2.5171(4)
Ge1-Ge5	2.5317(5)
Ge2-Ge3	2.8871(5)
Ge2-Ge5	2.5525(5)
Ge2-Ge6	2.5494(5)
Ge3-Ge4	2.5459(5)
Ge3-Ge6	2.5527(5)
Ge4-Ge7	2.5266(5)
Ge4-Ge9	2.5676(5)
Ge5-Ge7	2.5189(4)
Ge5-Ge8	2.5478(5)
Ge6-Ge8	2.5723(5)
Ge6-Ge9	2.5623(5)
Ge7-Ge8	2.7898(5)
Ge7-Ge9	2.8169(5)
Ge8-Ge9	2.8194(5)
Ge4-P1	2.3721(9)
Ge5-P2	2.3756(9)
Ge6-Cr1	2.5140(6)
Ge1-Cu1	2.4241(5)
Ge2-Cu1	2.5312(5)
Ge3-Cu1	2.5457(5)
Ge7-Cu2	2.4295(5)
Ge8-Cu2	2.5443(5)
Ge9-Cu2	2.5654(5)
Ge1-Ge7	3.571(6)
Ge2-Ge8	3.025(2)
Ge3-Ge9	3.108(1)
P1-N5	1.687(3)
P1-N6	1.694(3)
P2-N7	1.698(3)
P2-N8	1.689(3)

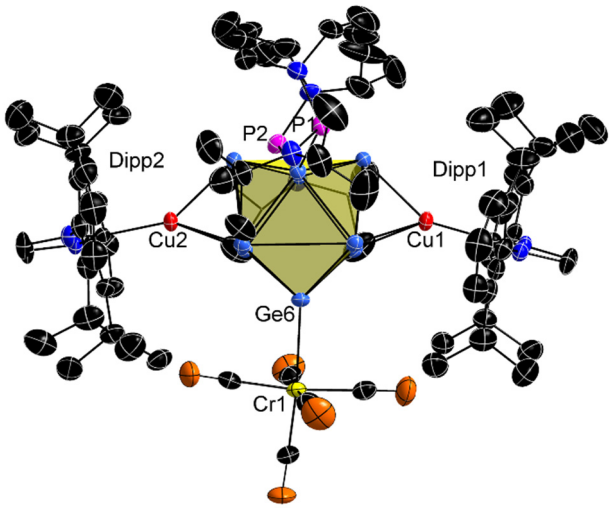

Figure S3. Labelled full ellipsoid crystal structure of compound **5**. Ellipsoids are shown at a 50 % probability level. For clarity reasons all protons and the solvent toluene molecule are omitted.

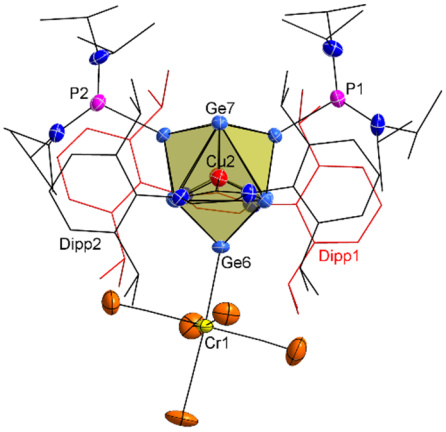

Figure S4. Top view on triangular cluster face of **5** which is coordinated by Cu2, showing ecliptic orientation of the NHC^{Dipp} moieties towards each other and staggered orientation towards the two phosphine groups and the $Cr(CO)_5$ moiety attached at the capping atoms of the trigonal prism. Ellipsoids are shown at a 50 % probability level. For clarity reasons carbon atoms are represented as wire sticks and all protons, as well as the solvent toluene molecule are omitted. Furthermore, the NHC^{Dipp} ligand in the back (Dipp 1) is represented in red colour.

SUPPORTING INFORMATION

NMR spectra

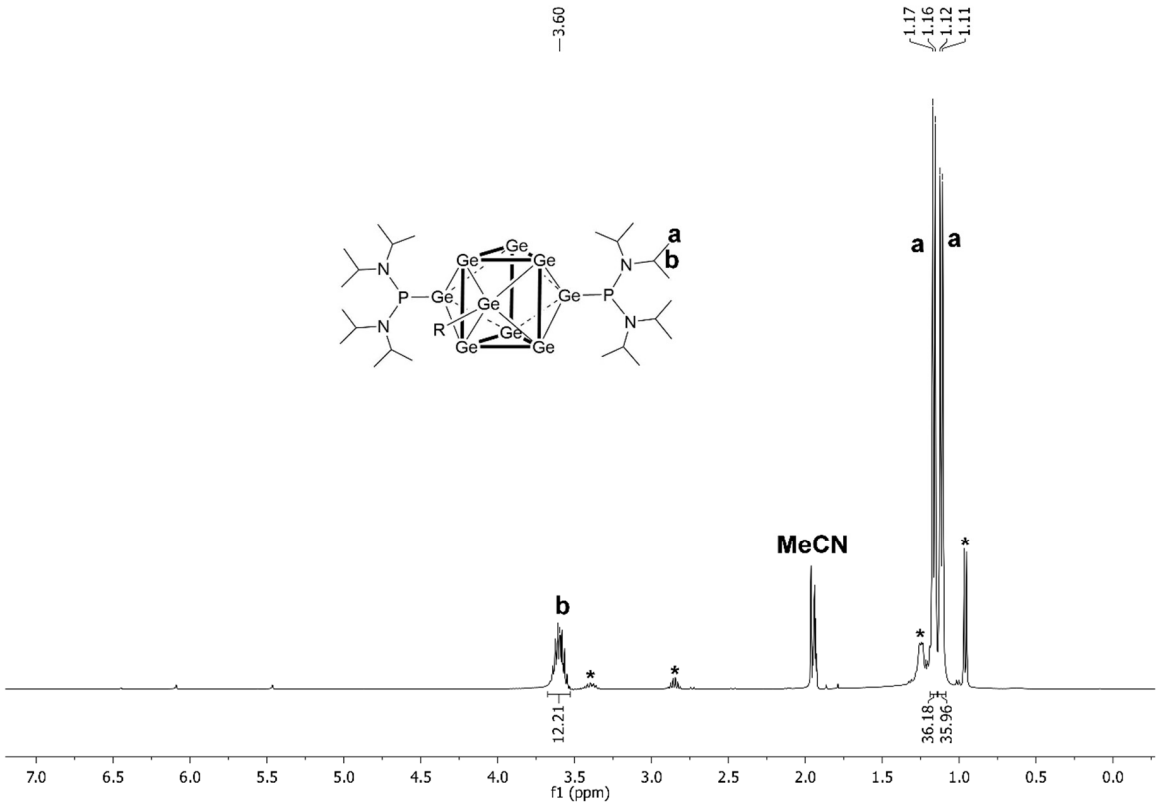

Figure S5. ^{1}H NMR spectrum of compound **1** acquired in MeCN-d_3. Signals caused by impurities are asterisked.

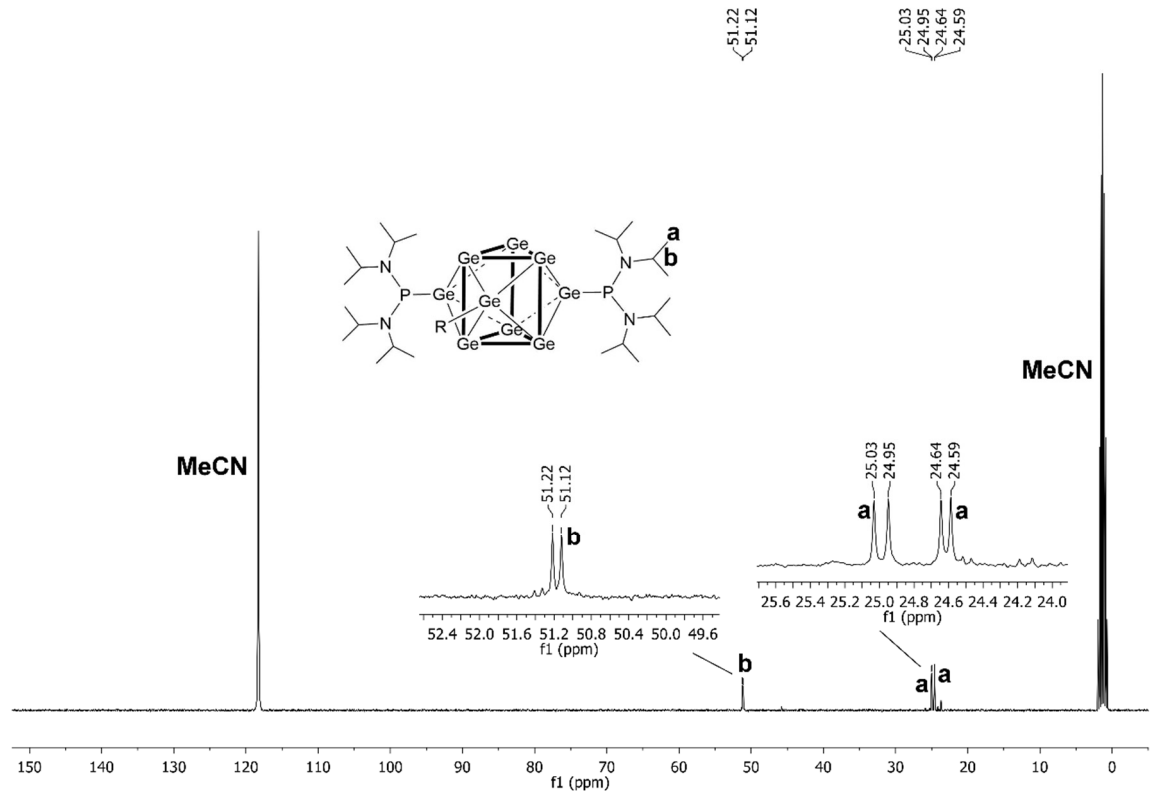

Figure S6. ^{13}C NMR spectrum of compound **1** acquired in MeCN-d_3.

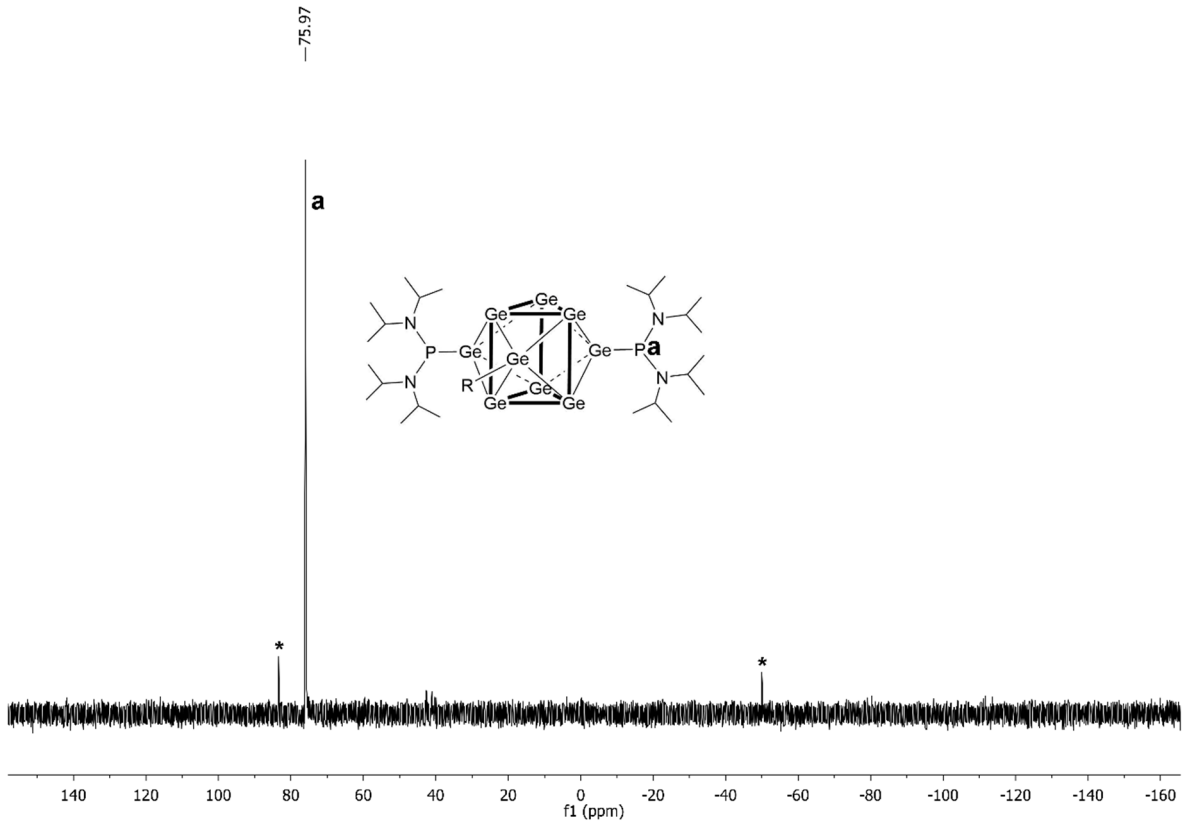

Figure S7. ^{31}P NMR spectrum of compound **1** acquired in MeCN-d_3. Signals caused by impurities are asterisked.

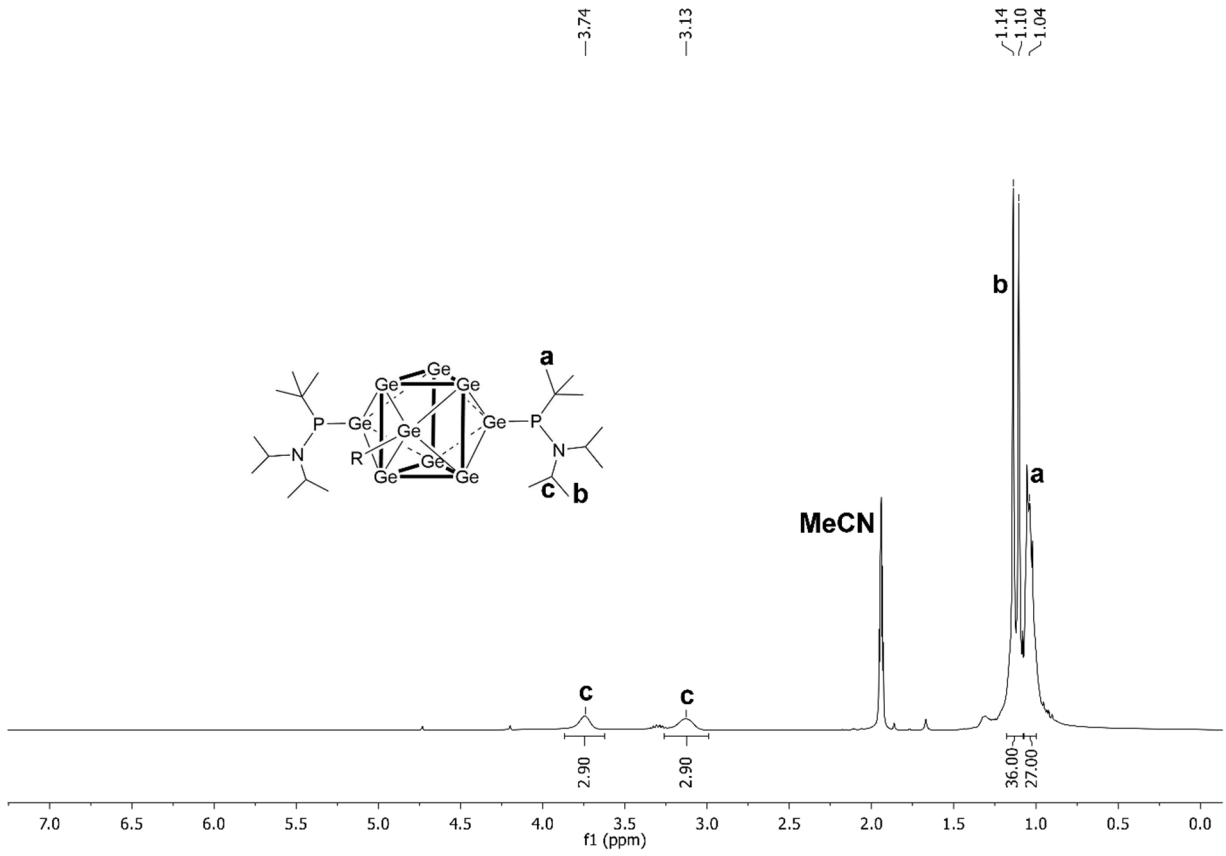

Figure S8. ^{1}H NMR spectrum of compound **2** acquired in MeCN-d_3.

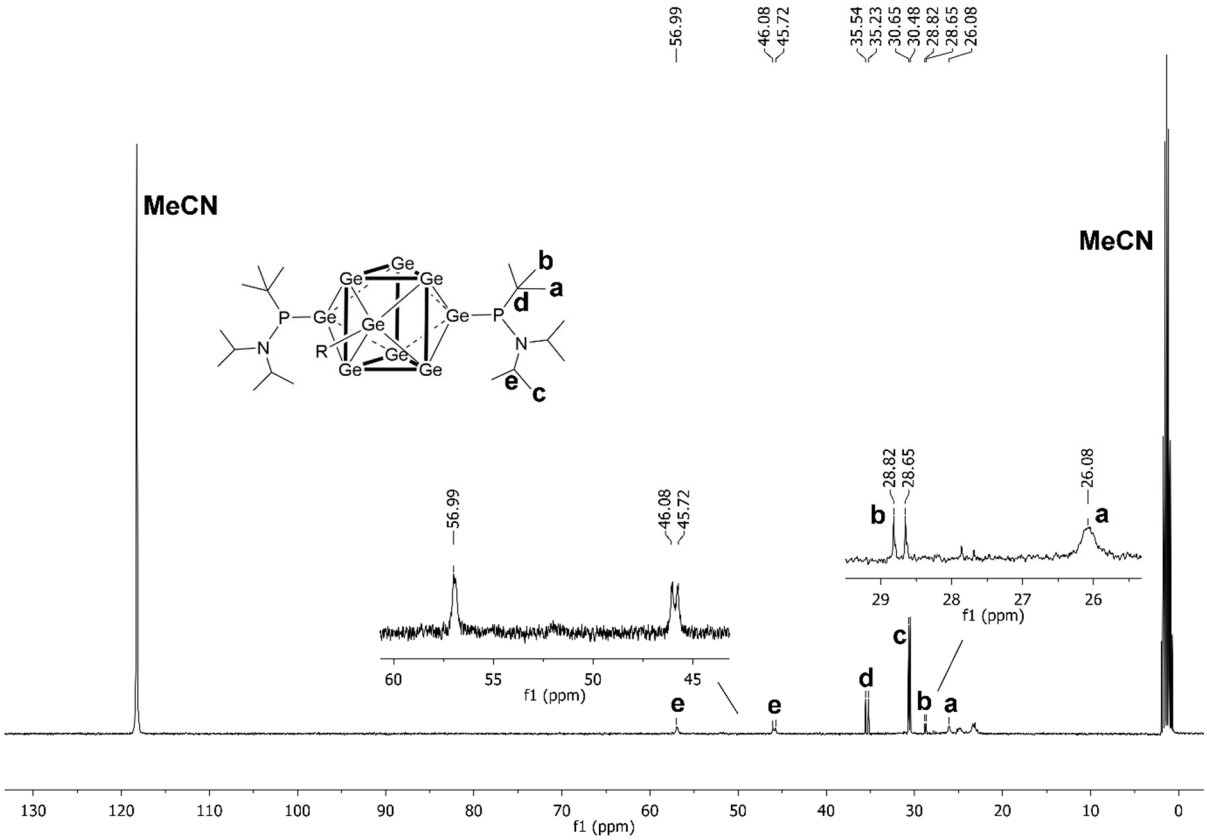

Figure S9. ^{13}C NMR spectrum of compound **2** acquired in MeCN-d_3.

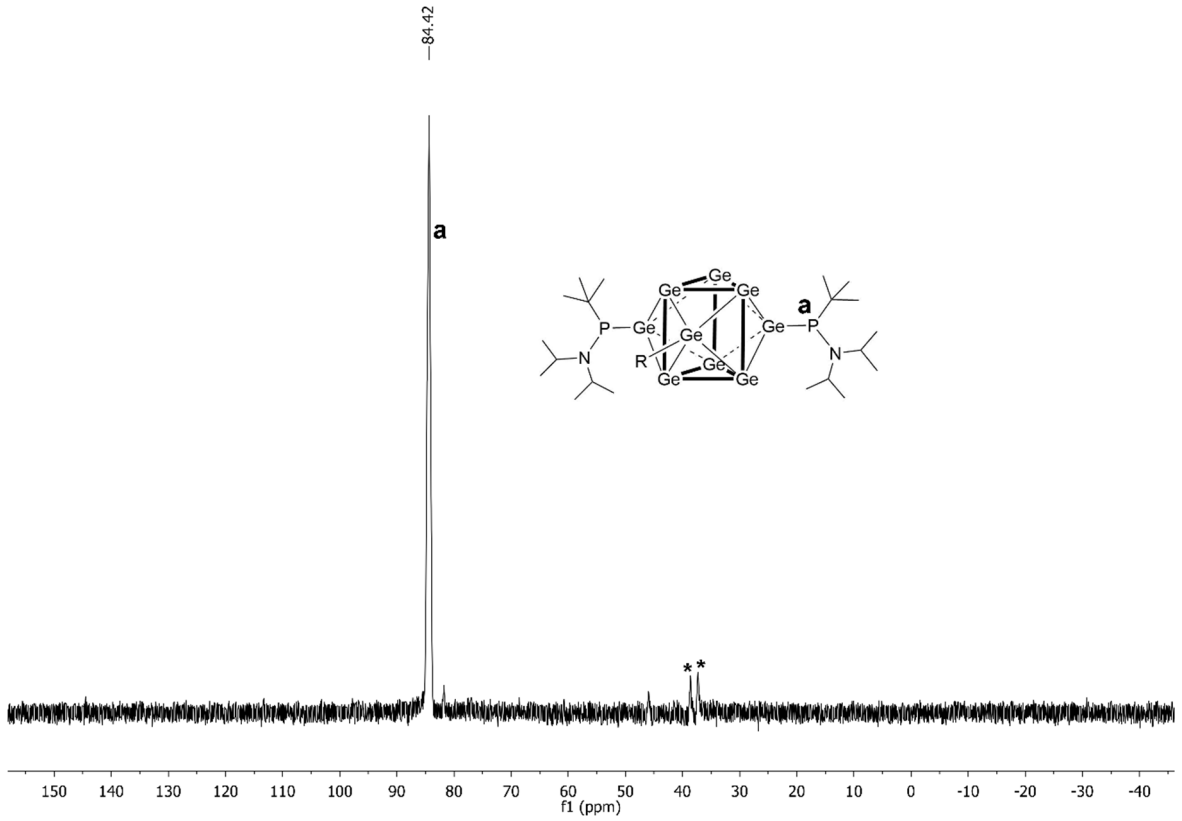

Figure S10. ^{31}P NMR spectrum of compound **2** acquired in MeCN-d_3. Signals caused by impurities are asterisked.

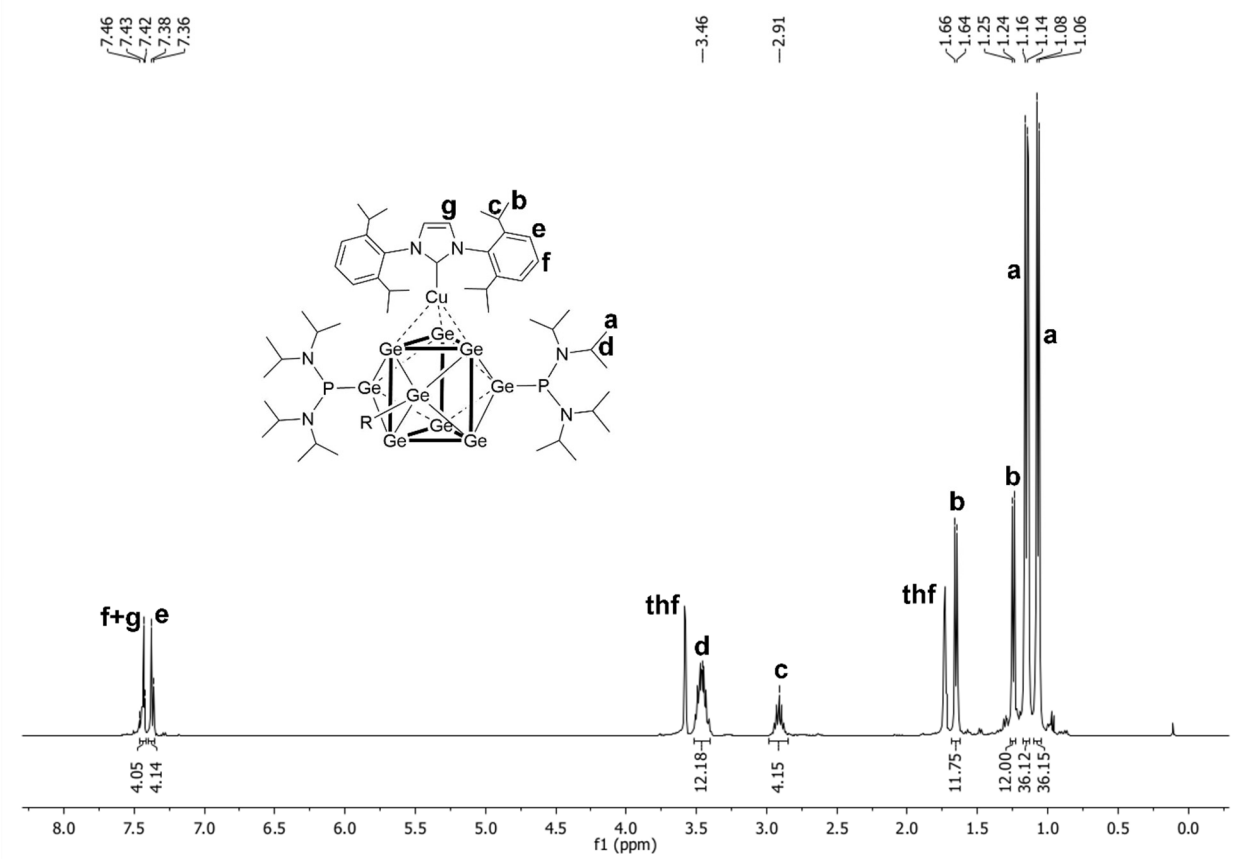

Figure S11. ^{1}H NMR spectrum of compound **3** acquired in thf-d_8.

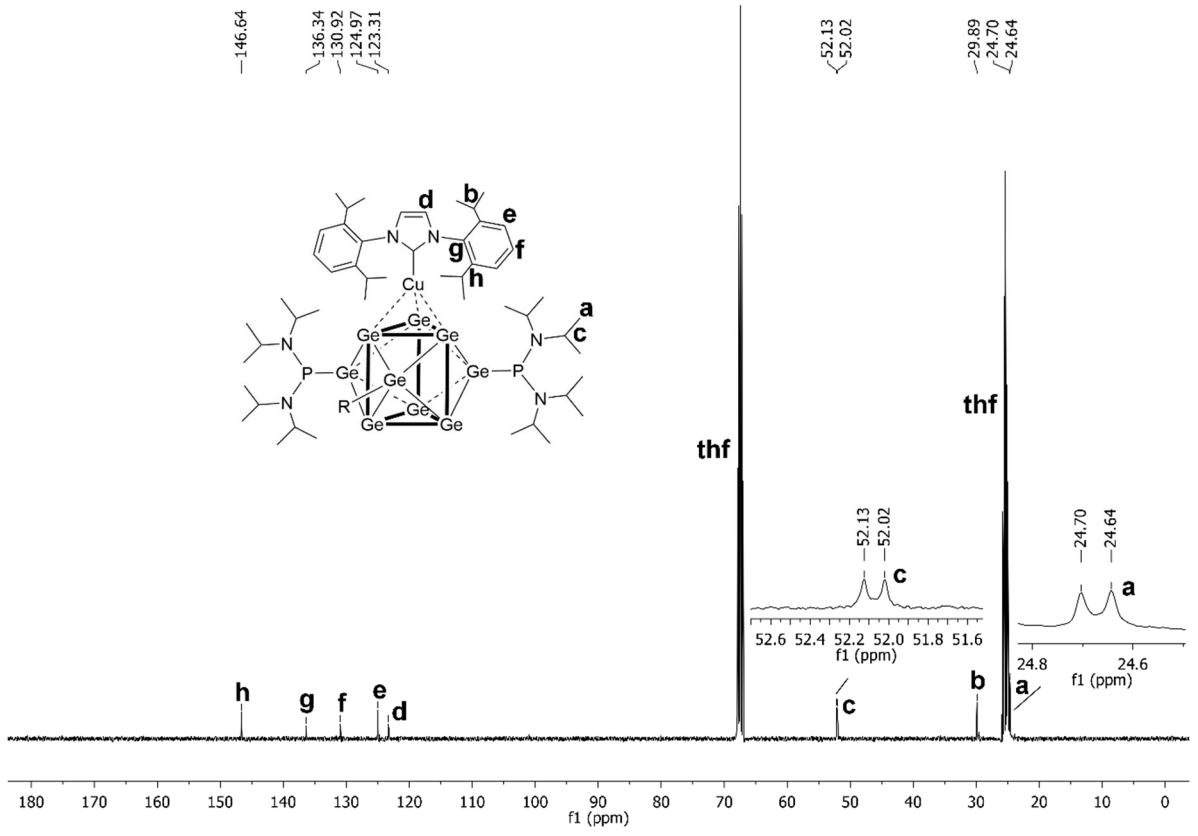

Figure S12. ^{13}C NMR spectrum of compound **3** acquired in thf-d_8.

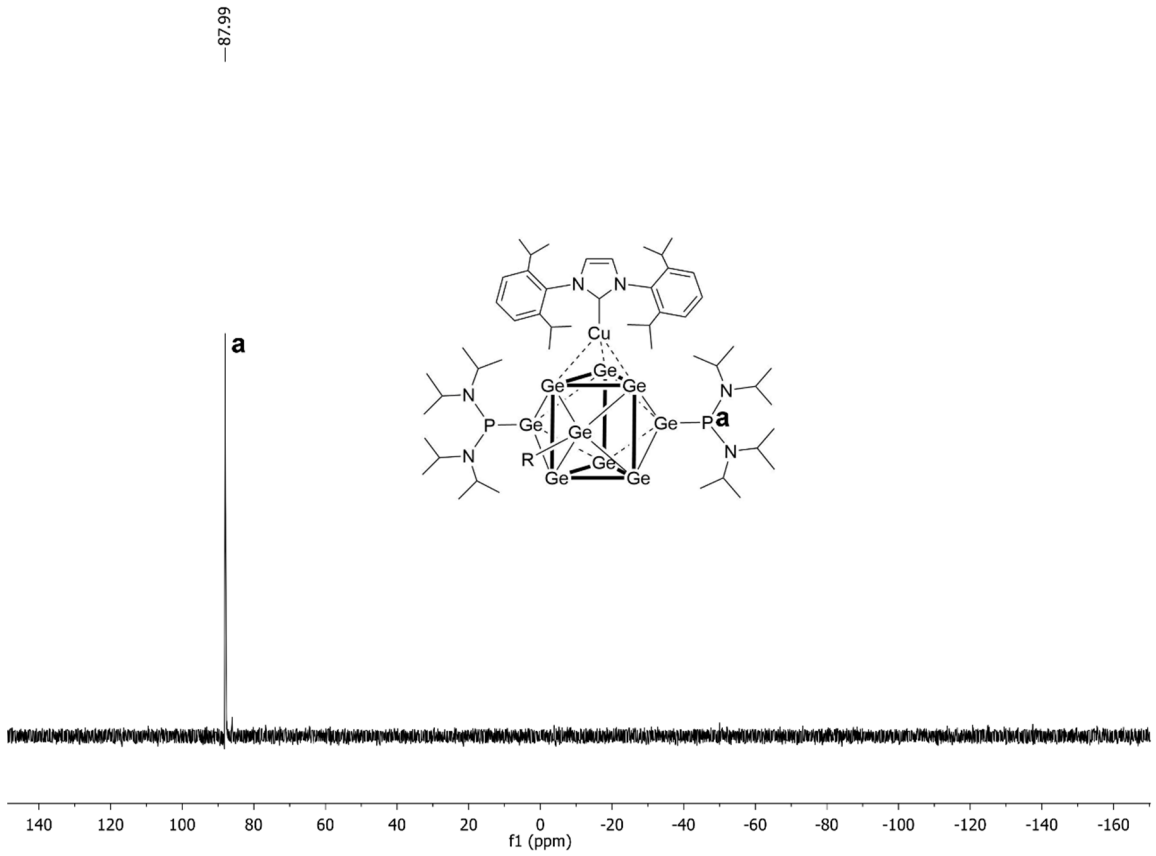

Figure S13. ^{31}P NMR spectrum of compound **3** acquired in thf-d_8.

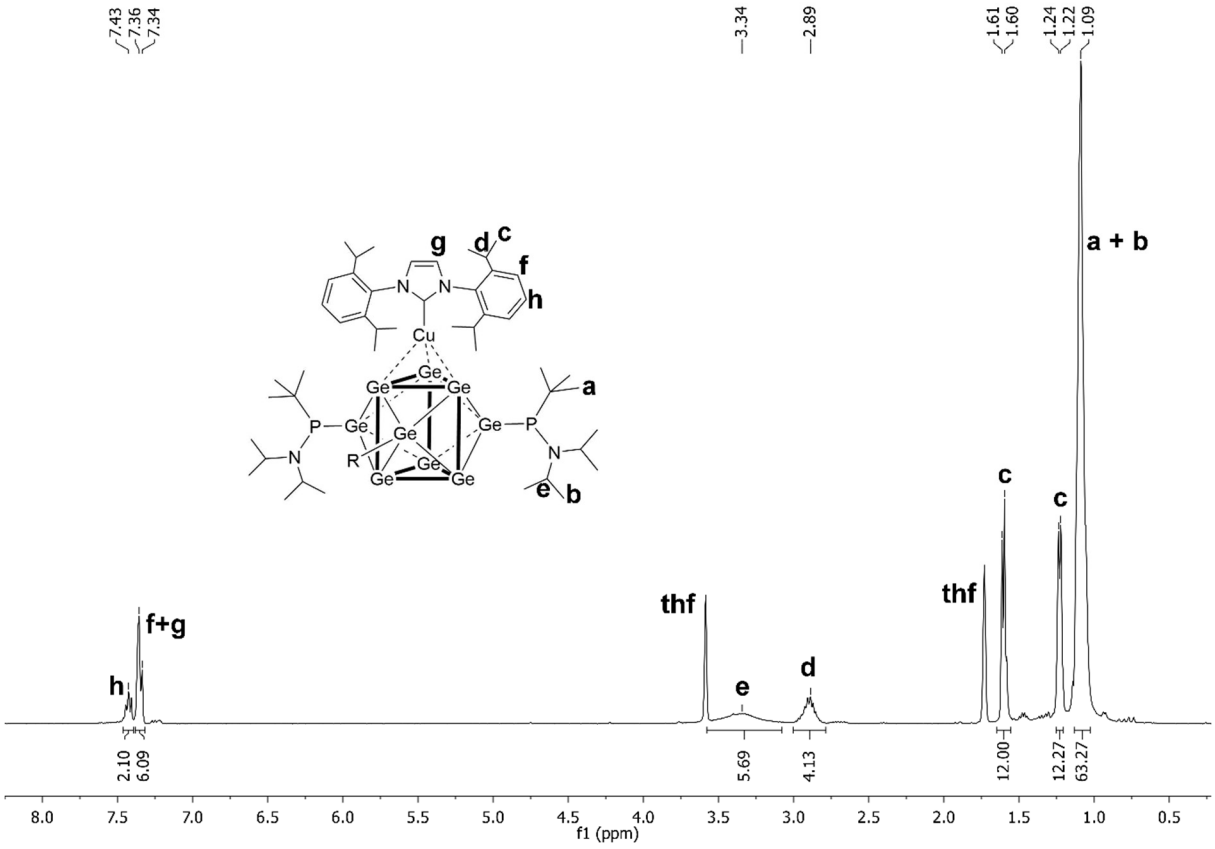

Figure S14. ^{1}H NMR spectrum of compound **4** acquired in thf-d_8. Spectrum was acquired at 333 K.

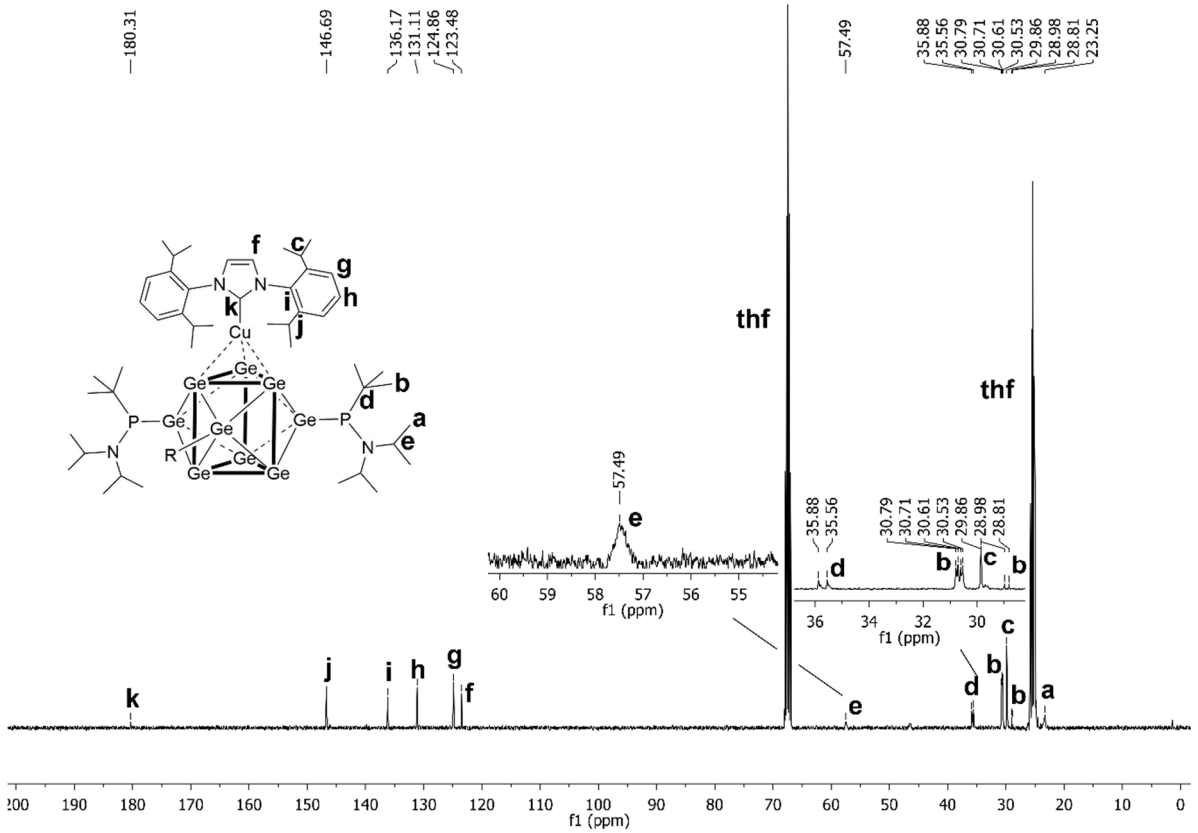

Figure S15. ^{13}C NMR spectrum of compound **4** acquired in thf-d_8. Spectrum was acquired at 298 K.

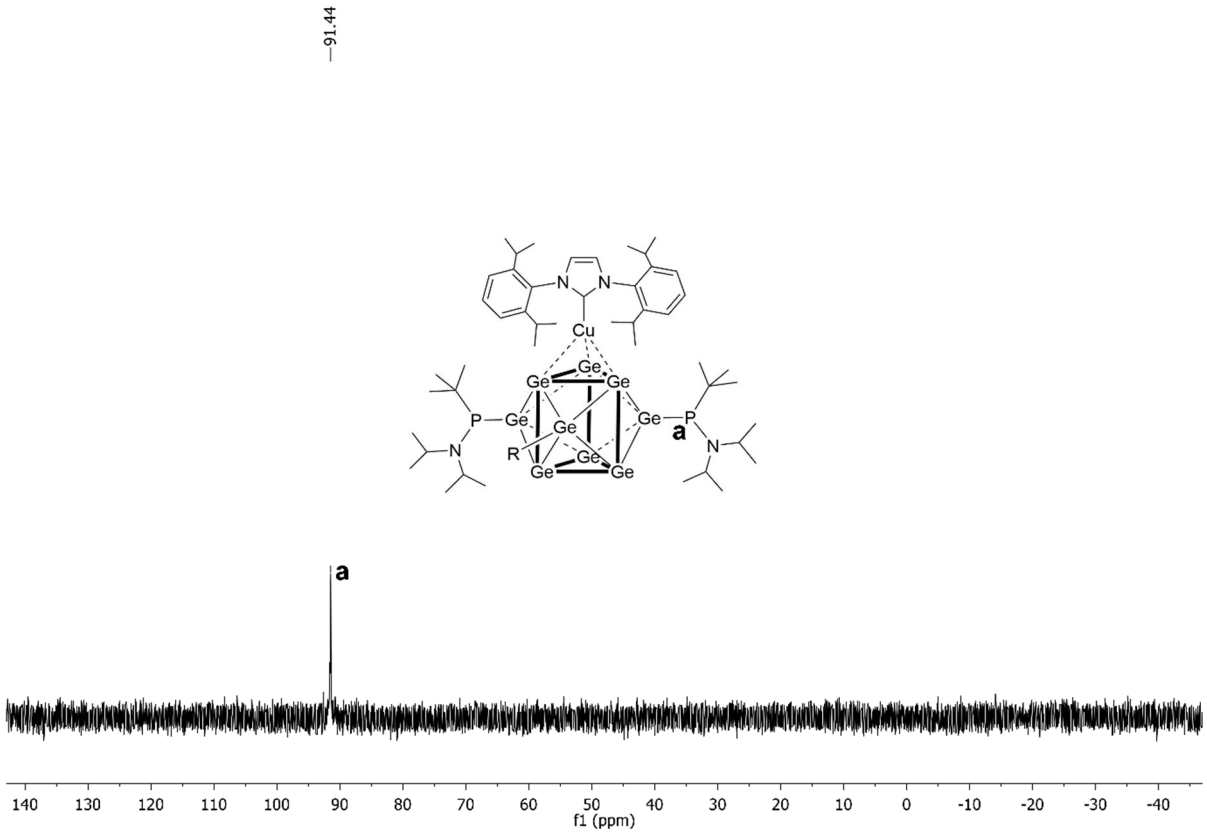

Figure S16. ^{31}P NMR spectrum of compound **4** acquired in thf-d_8. Spectrum was acquired at 333 K.

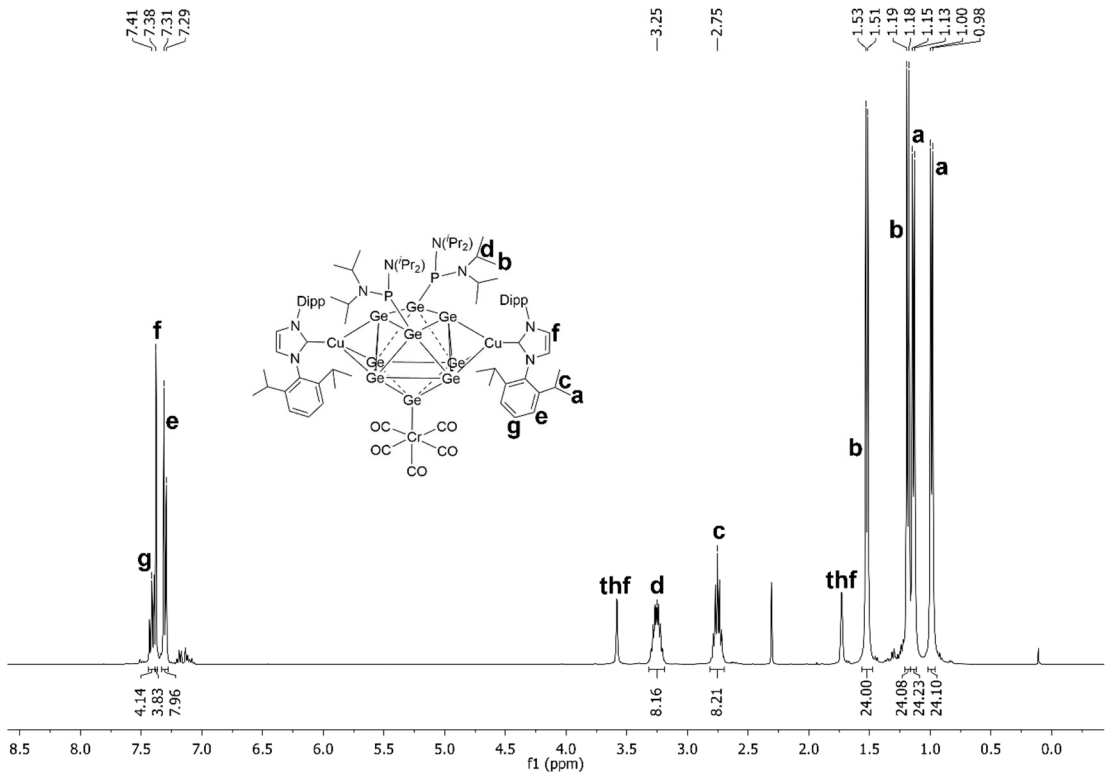

Figure S17. ^{1}H NMR spectrum of compound **5** acquired in thf-d_8.

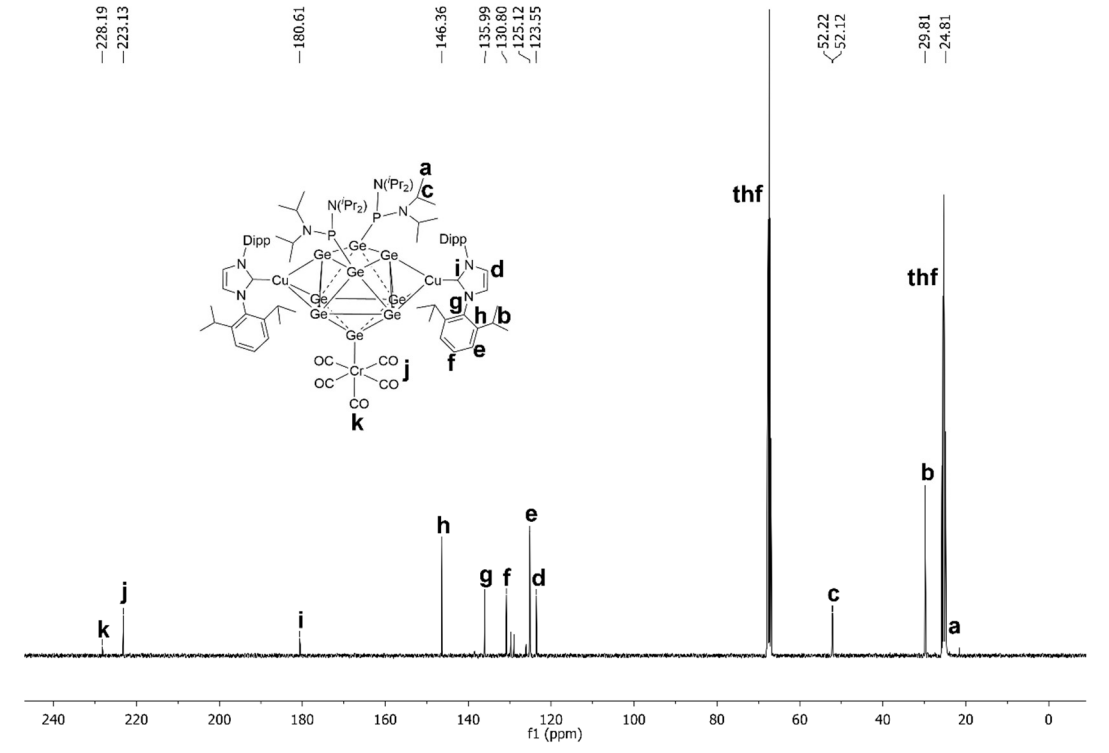

Figure S18. ^{13}C NMR spectrum of compound **5** acquired in thf-d_8.

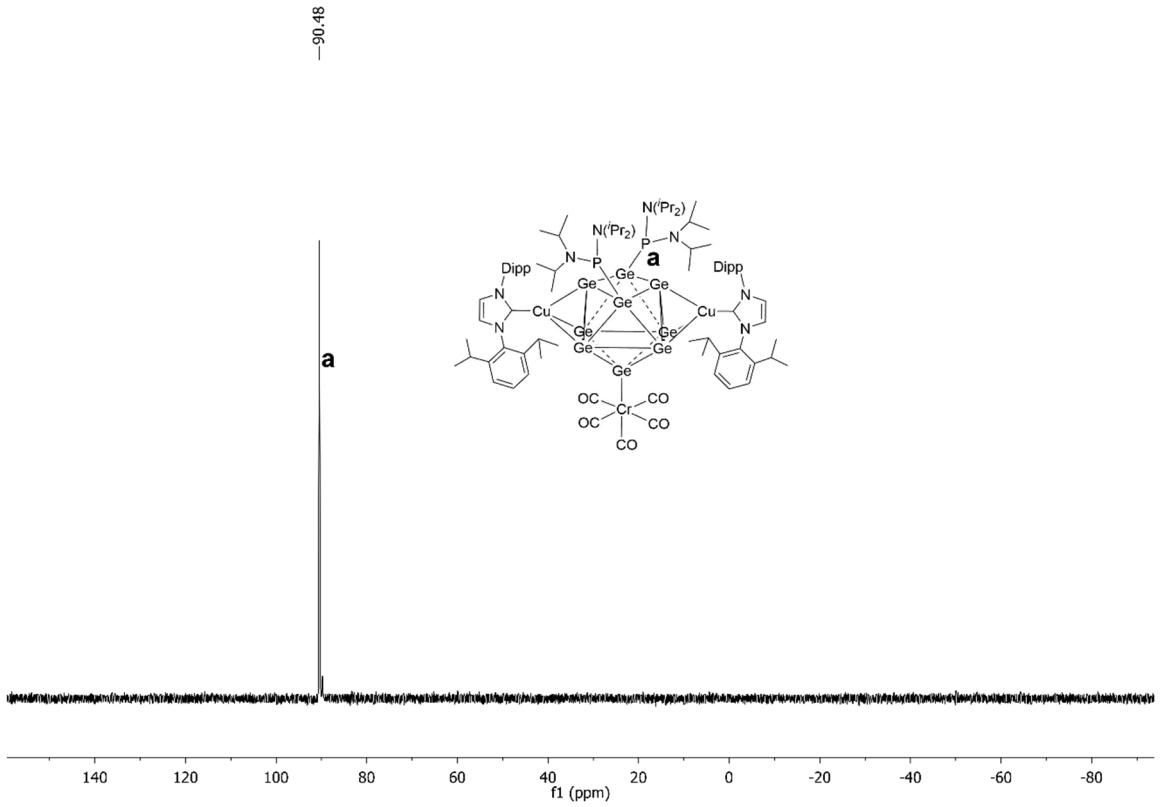

Figure S19. ^{31}P NMR spectrum of compound **5** acquired in thf-d_8.

ESI-MS spectra

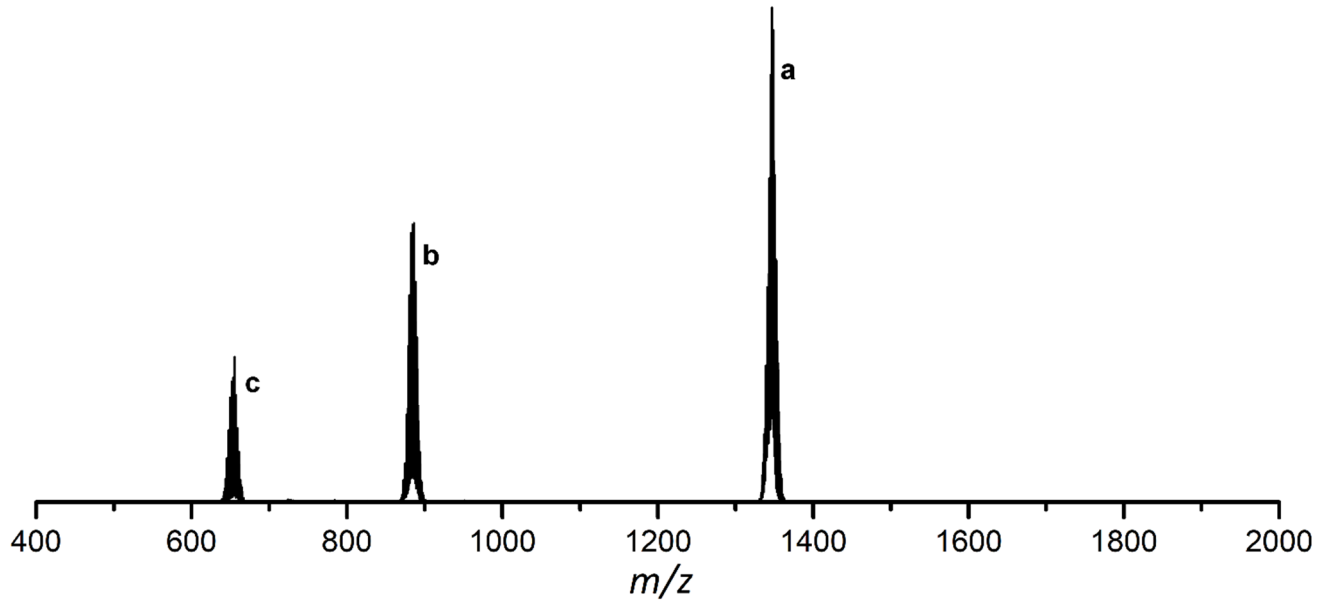

Figure S20. ESI-MS spectrum (negative mode, 3500 V, 300 °C) obtained upon examination of an acetonitrile solution of $[Ge_9\{P(N^iPr_2)_2\}_3]^-$ (**1a**). Besides the signal at *m/z* 1347.1 $[Ge_9\{P(N^iPr_2)_2\}_3]^-$ (a) two further signals at *m/z* 884.5 $\{[Ge_9\{P(N^iPr_2)_2\}_1]\}^-$ (b) and *m/z* 653.7 $[Ge_9]^-$ (c) are detected. Species (b) and (c) are formed upon cleavage of phosphine substituents from the $[Ge_9]$ cluster core during the ionization process. A detailed picture of the signal of anion **1a** is provided in the manuscript (Figure 1), a detailed representation of signal (b) can be found in Figure S21.

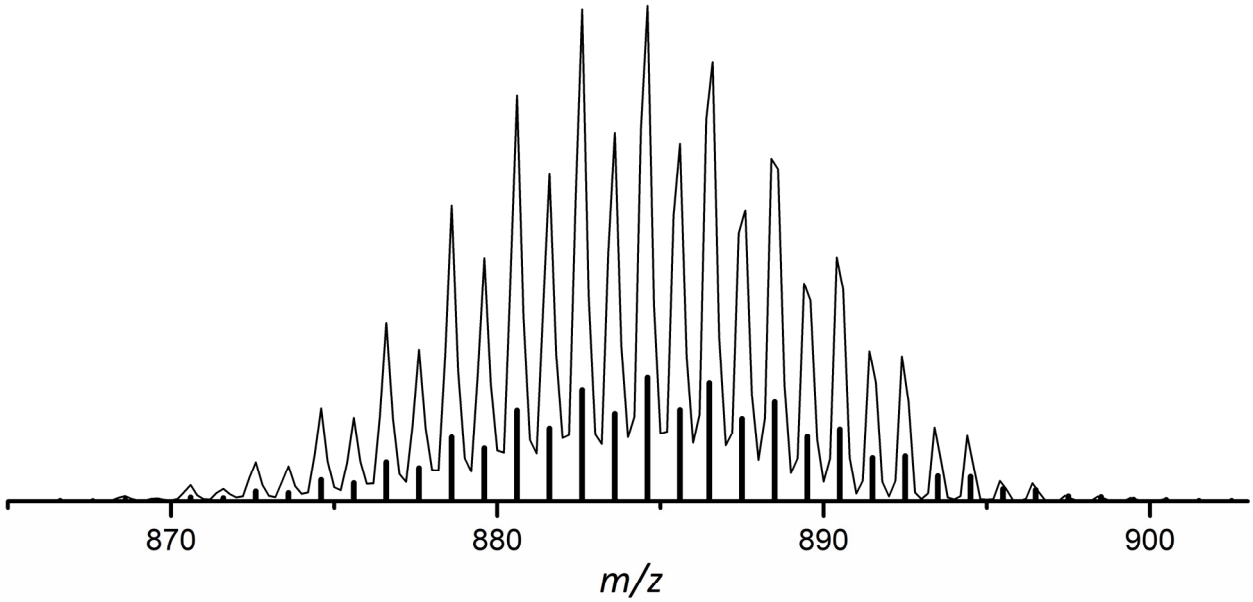

Figure S21. Detail view of ESI-MS signal of $[Ge_9\{P(N^iPr_2)_2\}_1]^-$ detected in the examination of an acetonitrile solution of $[Ge_9\{P(N^iPr_2)_2\}_3]^-$ (**1a**) upon cleavage of two phosphine substituents from the $[Ge_9]$ cluster core during the ionization process. Calculated spectrum is represented as black bars.

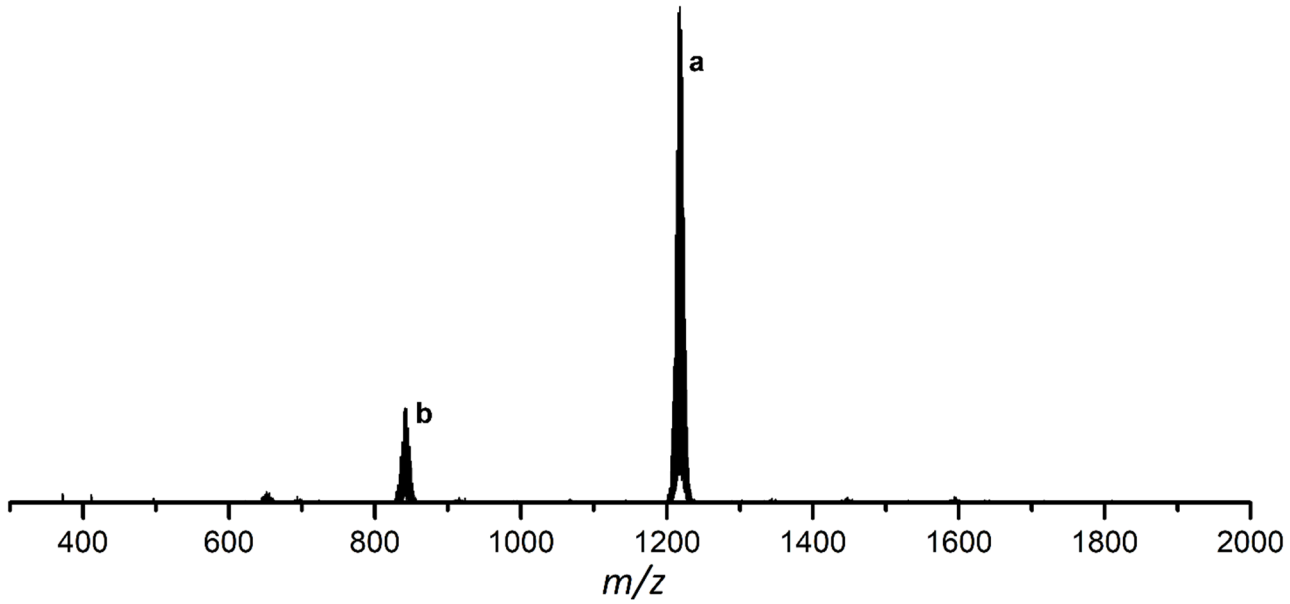

Figure S22. ESI-MS spectrum (negative mode, 3500 V, 300 °C) obtained upon examination of an acetonitrile solution of $[Ge_9\{P(N^iPr_2)^tBu\}_3]^-$ (**2a**). Besides the signal at *m/z* 1218.5 $[Ge_9\{P(N^iPr_2)^tBu\}_3]^-$ (a) a further signal at *m/z* 841.5 $[Ge_9\{P(N^iPr_2)^tBu\}_1]^-$ (b) is detected. Species (b) is formed upon cleavage of two phosphine substituents from the $[Ge_9]$ cluster core during the ionization process. A detailed view of signal of anion **2a** is shown in the manuscript (Figure 1), a detailed view of species b is presented in Figure S23.

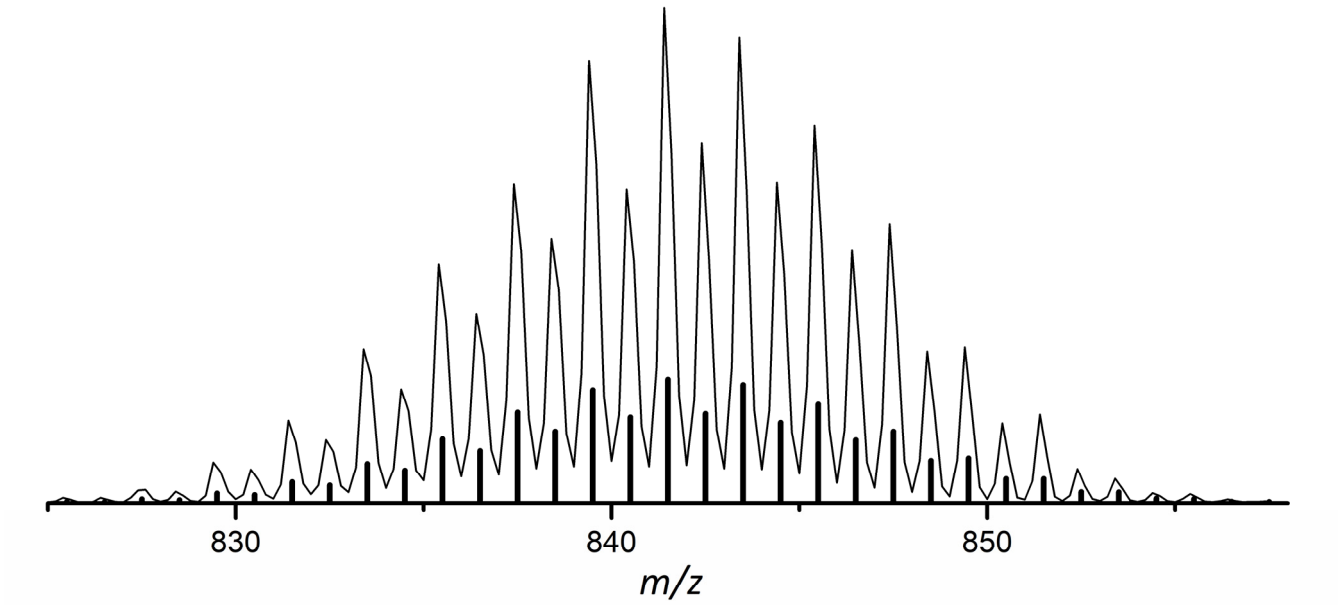

Figure S23. Detail view of ESI-MS signal of $[Ge_9\{P(N^iPr_2)^tBu\}_1]^-$ detected in the examination of an acetonitrile solution of $[Ge_9\{P(N^iPr_2)^tBu\}_3]^-$ (**2a**) upon cleavage of two phosphine substituents from the $[Ge_9]$ cluster core during the ionization process. Calculated spectrum is represented as black bars.

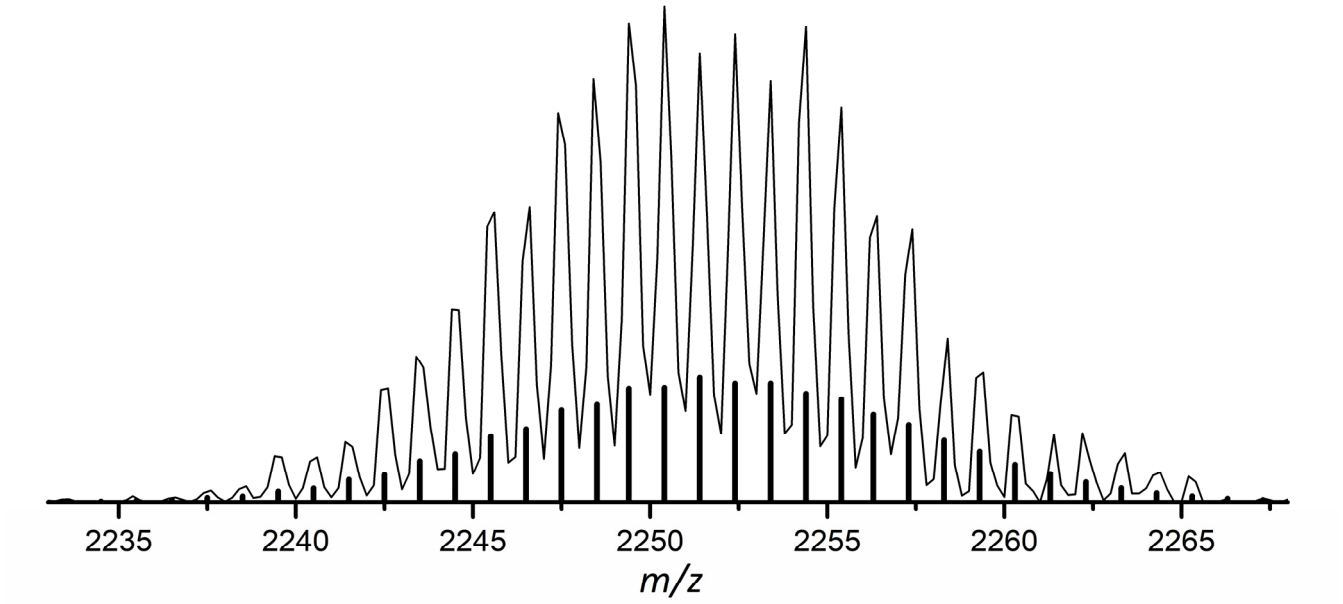

Figure S24. ESI-MS signal (positive ion mode, 3000 V, 300 °C) at *m/z* 2251.4, which can be assigned to $\{(NHC^{Dipp}Cu)_2[Ge_9\{P(N^iPr_2)_2\}_3]\}^+$ (**3-CuNHC^{Dipp}**), detected in the examination of a thf solution of $(NHC^{Dipp}Cu)[Ge_9\{P(N^iPr_2)_2\}_3]$ (**3**). The detected species is formed upon coordination of a positively charged $[Cu\text{-}NHC^{Dipp}]^+$ fragment to the neutral compound **3** during the ionization process. Calculated spectrum is represented as black bars.

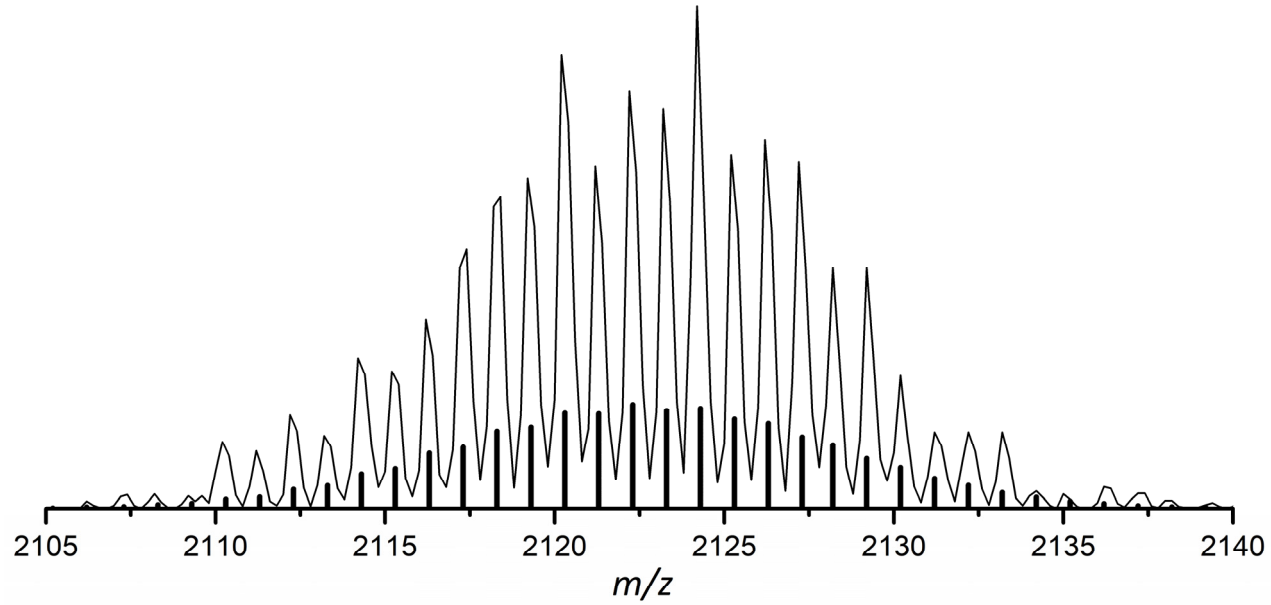

Figure S25. ESI-MS signal (positive ion mode, 3000 V, 300 °C) at *m/z* 2122.3, which can be assigned to $\{(NHC^{Dipp}Cu)_2[Ge_9\{P(N^iPr_2)^tBu\}_3]\}^+$ (**4-CuNHC^{Dipp}**), detected in the examination of a thf solution of $(NHC^{Dipp}Cu)[Ge_9\{P(N^iPr_2)^tBu\}_3]$ (**4**). The detected species is formed upon coordination of a positively charged $[Cu\text{-}NHC^{Dipp}]^+$ fragment to the neutral compound **4** during the ionization process. Calculated spectrum is represented as black bars.

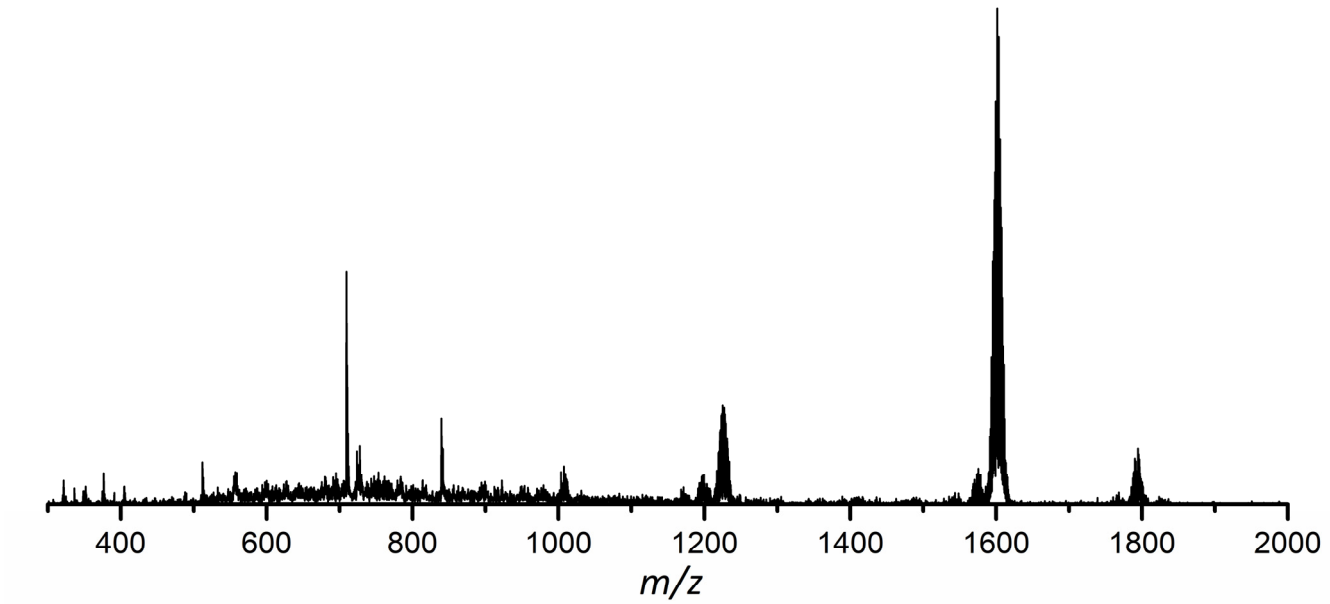

Figure S26. ESI-MS spectrum (negative ion mode, 3000 V, 300 °C) obtained upon examination of a thf reaction solution of $[Ge_9\{P(N^iPr_2)^tBu\}_3]^-$ (**2a**), with $Cr(CO)_5$(thf), revealing the presence of multiple $Cr(CO)_5$-fragment substituted **2a**. The signal at *m/z* 1601.5 can be assigned to twofold coordinated species $\{[Ge_9\{P(N^iPr_2)^tBu\}_3]\{Cr(CO)_5\}_2\}^-$ and the signal at *m/z* 1793.5 to the threefold substituted species $\{[Ge_9\{P(N^iPr_2)^tBu\}_3]\{Cr(CO)_5\}_3\}^-$. Detailed views of the signals are provided in Figures S27 and S28.

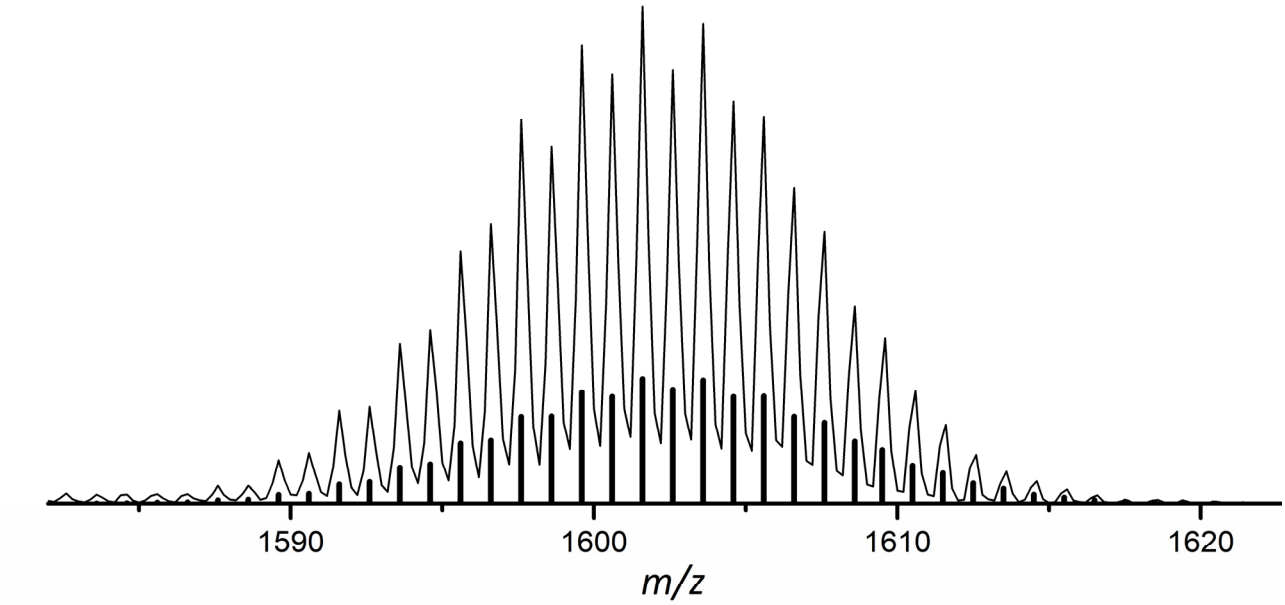

Figure S27. ESI-MS signal (negative ion mode, 3000 V, 300 °C) at *m/z* 1601.6, which can be assigned to$\{[Ge_9\{P(N^iPr_2)^tBu\}_3]\{Cr(CO)_5\}_2\}^-$ detected from thf solution upon reaction of $[Ge_9\{P(N^iPr_2)^tBu\}_3]^-$ (**2a**) with $Cr(CO)_5$(thf). Calculated spectrum is represented as black bars.

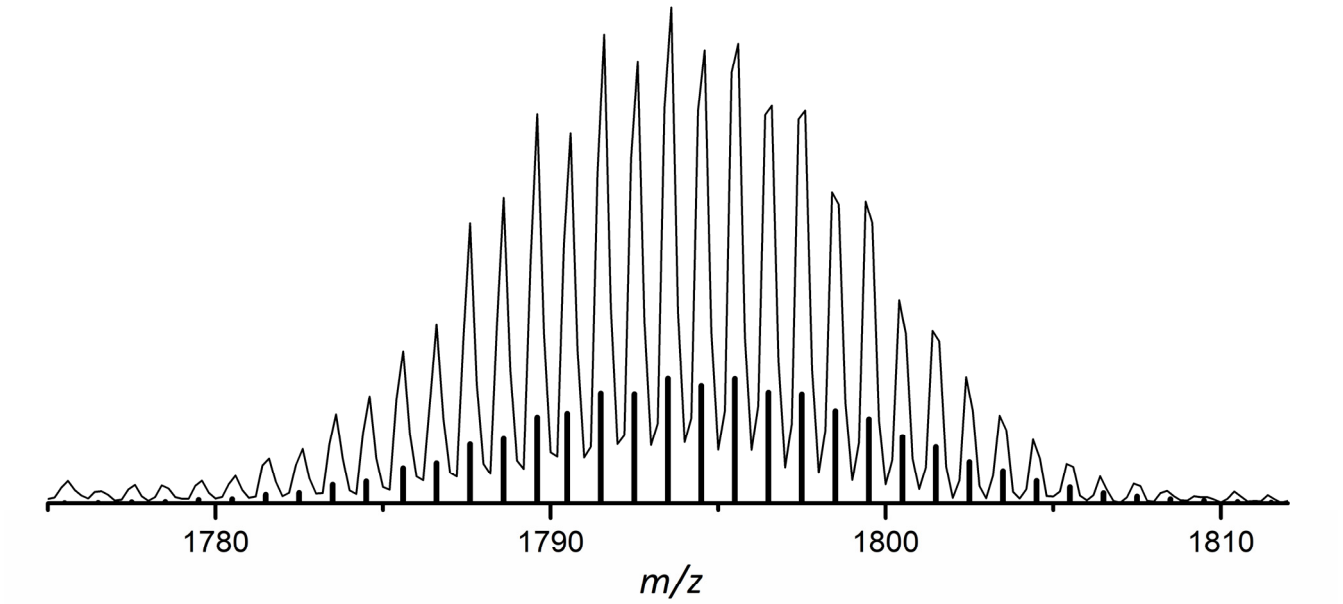

Figure S28. ESI-MS signal (negative ion mode, 3000 V, 300 °C) at *m/z* 1793.5, which can be assigned to $\{[Ge_9\{P(N^iPr_2)^tBu\}_3]\{Cr(CO)_5\}_3\}^-$ detected from thf solution upon reaction of $[Ge_9\{P(N^iPr_2)^tBu\}_3]^-$ (**2a**) with $Cr(CO)_5$(thf). Calculated spectrum is represented as black bars.

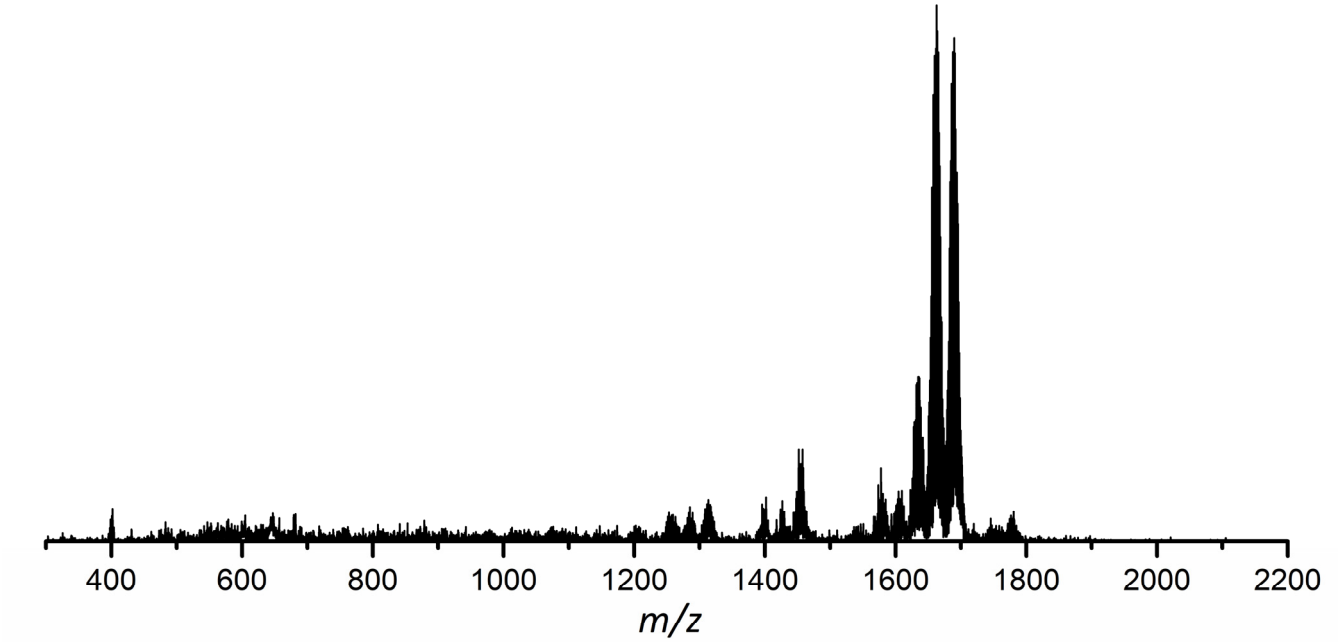

Figure S29. ESI-MS spectrum (negative ion mode, 3000 V, 300 °C) obtained upon examination of a thf reaction solution of $[Ge_9\{P(N^iPr_2)^tBu\}_3]^-$ (**2a**), with $Mo(CO)_5$(thf), revealing the presence of multiple $Mo(CO)_5$-fragment substituted **2a**. The signal at *m/z* 1689.5 can be assigned to twofold coordinated species $\{[Ge_9\{P(N^iPr_2)^tBu\}_3]\{Mo(CO)_5\}_2\}^-$. The signals at *m/z* 1661.5 and *m/z* 1633.5 can be assigned to species occurring upon gradual cleavage of CO ligands. Detailed views of the signals are provided in Figures S30-S32.

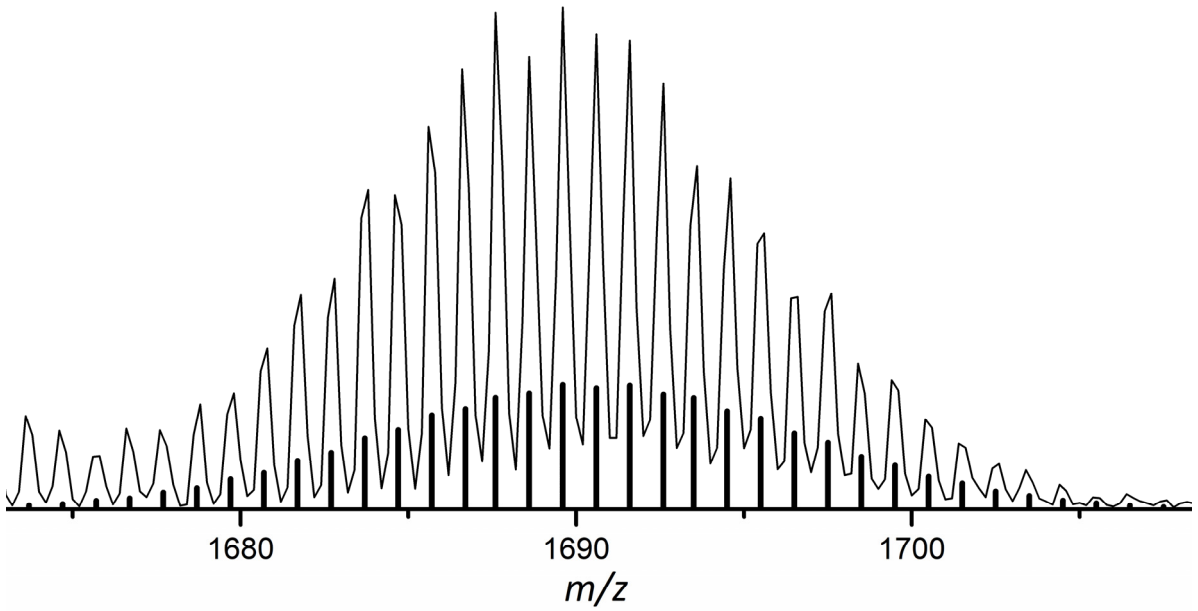

Figure S30. ESI-MS signal (negative ion mode, 3000 V, 300 °C) at *m/z* 1689.5, which can be assigned to $\{[Ge_9\{P(N^iPr_2)^tBu\}_3]\{Mo(CO)_5\}_2\}^-$ detected from thf solution upon reaction of $[Ge_9\{P(N^iPr_2)^tBu\}_3]^-$ (**2a**) with $Mo(CO)_5$(thf). Asymmetry of isotope pattern is caused by signal overlap. Calculated spectrum is represented as black bars.

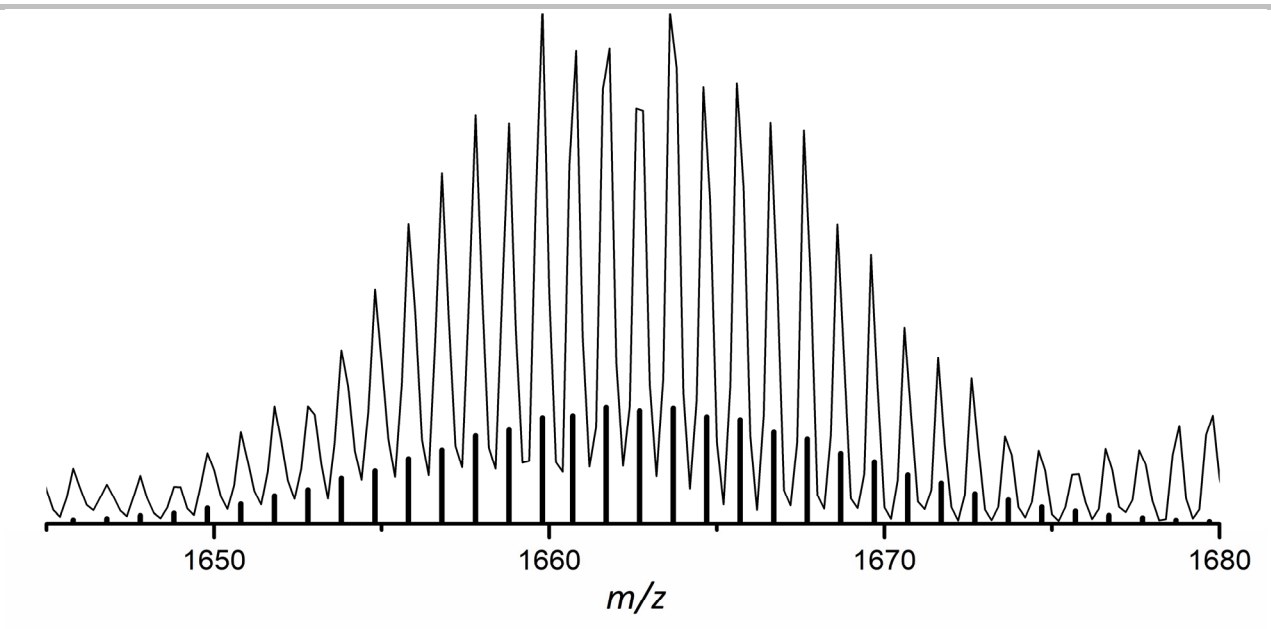

Figure S31. ESI-MS signal (negative ion mode, 3000 V, 300 °C) at *m/z* 1661.5, which can be assigned to $\{[Ge_9\{P(N^iPr_2)^tBu\}_3]\{Mo(CO)_4\}\{Mo(CO)_5\}\}^-$ detected from thf solution upon reaction of $[Ge_9\{P(N^iPr_2)^tBu\}_3]^-$ (**2a**) with $Mo(CO)_5$(thf). Asymmetry of isotope pattern is caused by signal overlap. Calculated spectrum is represented as black bars.

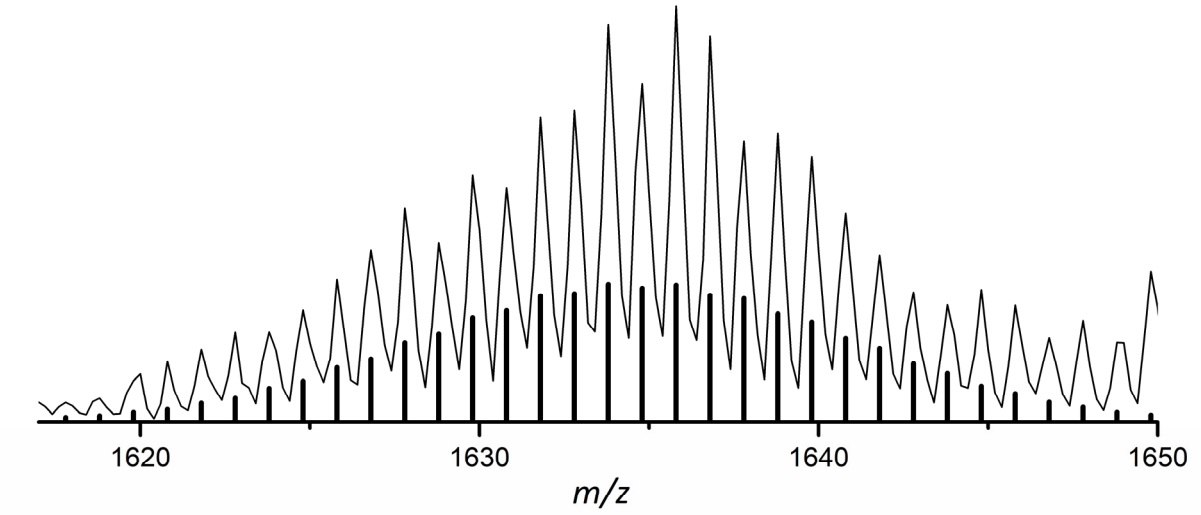

Figure S32. ESI-MS signal (negative ion mode, 3000 V, 300 °C) at *m/z* 1633.5, which can be assigned to $\{[Ge_9\{P(N^iPr_2)^tBu\}_3]\{Mo(CO)_4\}_2\}^-$ detected from thf solution upon reaction of $[Ge_9\{P(N^iPr_2)^tBu\}_3]^-$ (**2a**) with $Mo(CO)_5$(thf). Asymmetry of isotope pattern is caused by signal overlap. Calculated spectrum is represented as black bars.

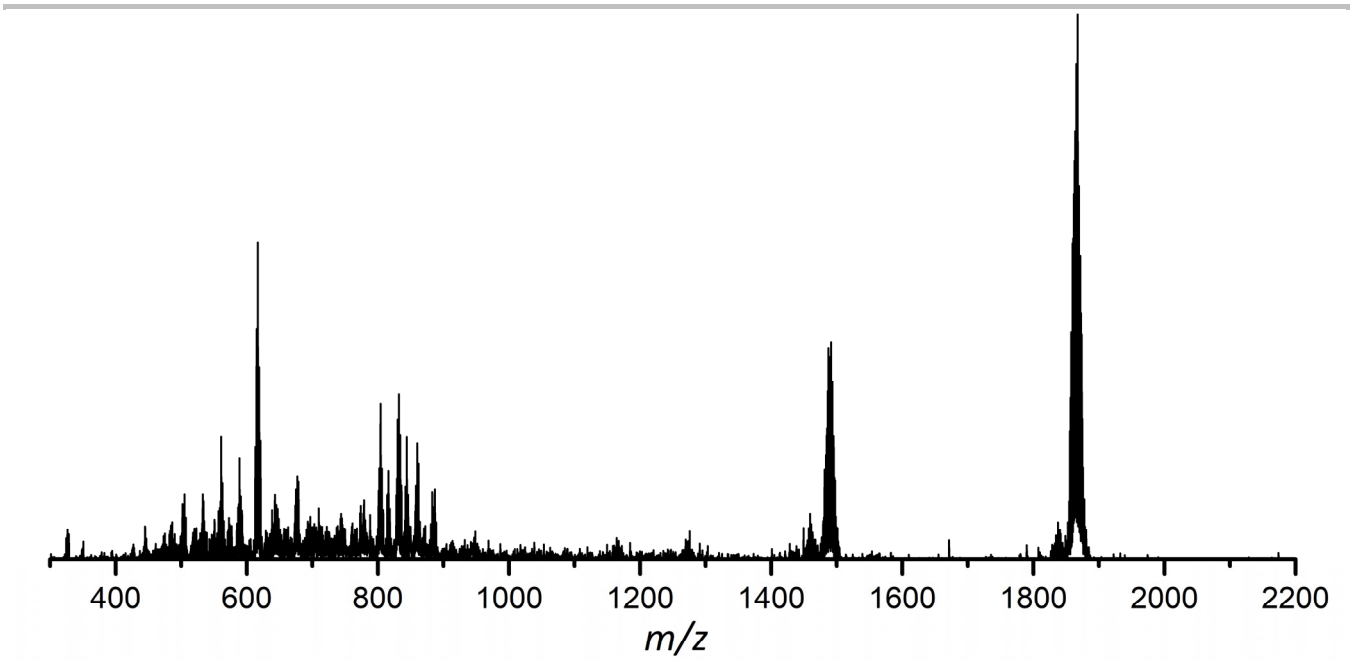

Figure S33. ESI-MS spectrum (negative ion mode, 3000 V, 300 °C) obtained upon examination of a thf reaction solution of $[Ge_9\{P(N^iPr_2)^tBu\}_3]^-$ (**2a**), with $W(CO)_5$(thf), revealing the presence of multiple $W(CO)_5$-fragment substituted **2a**. The signal at *m/z* 1865.5 can be assigned to twofold coordinated species $\{[Ge_9\{P(N^iPr_2)^tBu\}_3]\{W(CO)_5\}_2\}^-$. A detailed view of the signals is provided in Figures S26. The signal at approx. m/z 1500 also revealing a typical isotope pattern for $[Ge_9]$ species could not be assigned to a defined species yet.

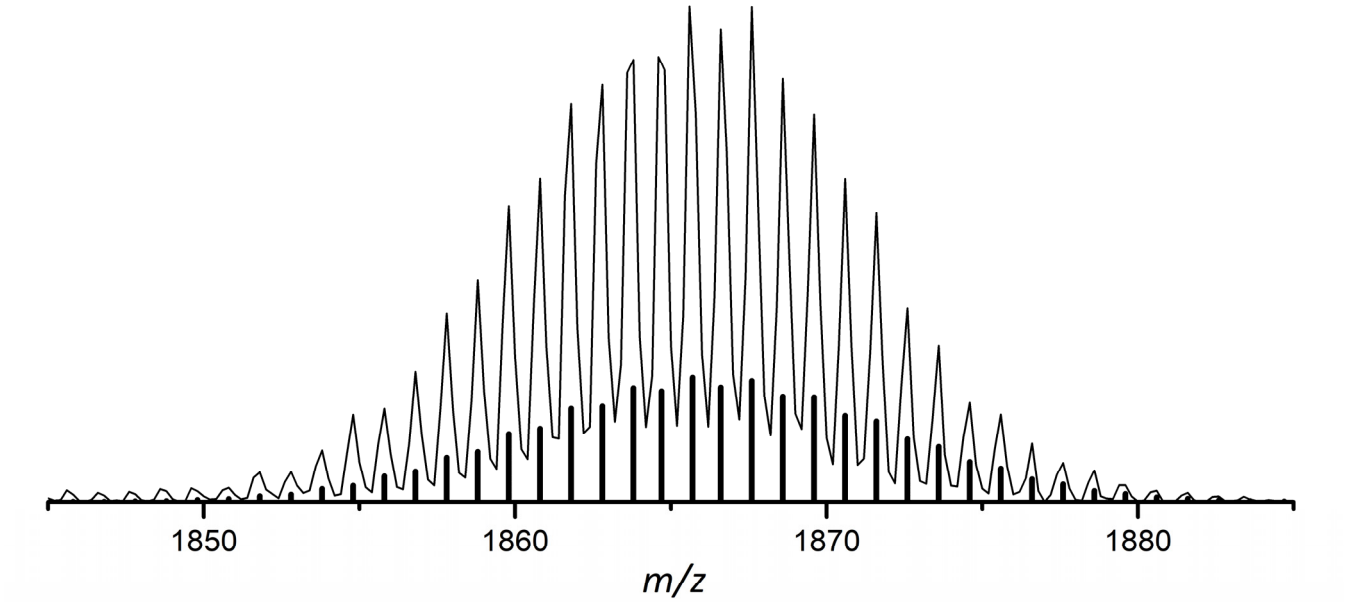

Figure S34. ESI-MS signal (negative ion mode, 3000 V, 300 °C) at *m/z* 1865.5, which can be assigned to $\{[Ge_9\{P(N^iPr_2)^tBu\}_3]\{W(CO)_5\}_2\}^-$ detected from thf solution upon reaction of $[Ge_9\{P(N^iPr_2)^tBu\}_3]^-$ (**2a**), with $W(CO)_5$(thf). Calculated spectrum is represented as black bars.

IR spectra

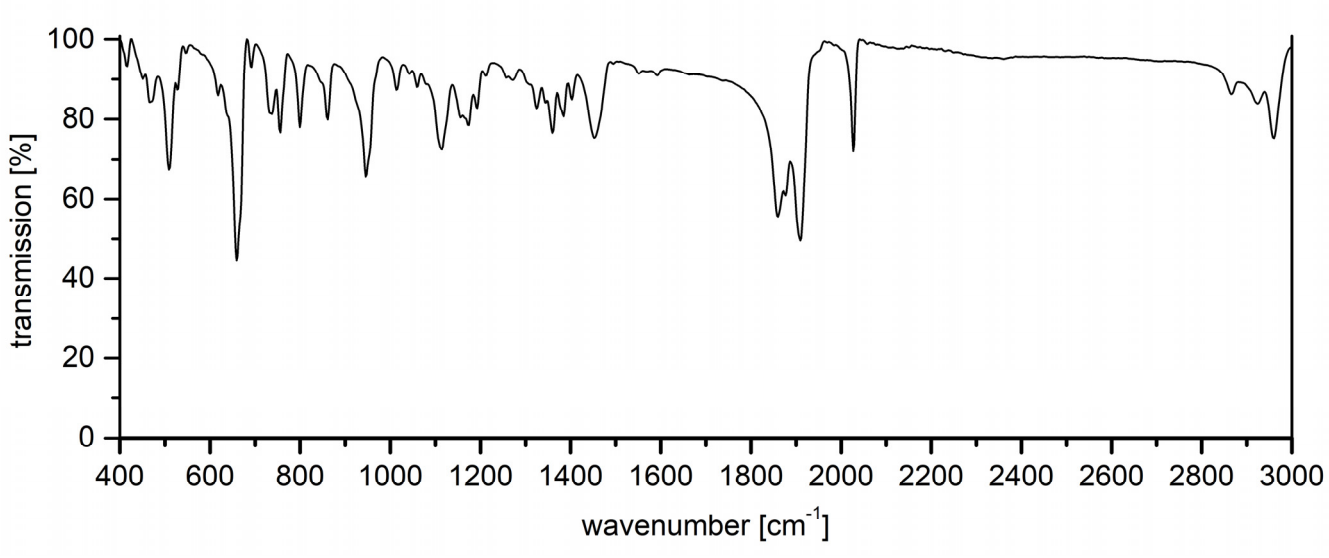

Figure S35. Complete IR spectrum of compound **5** acquired by measurement of an isolated crystal. A detailed view on the carbonyl vibrations area is provided in Figure S36.

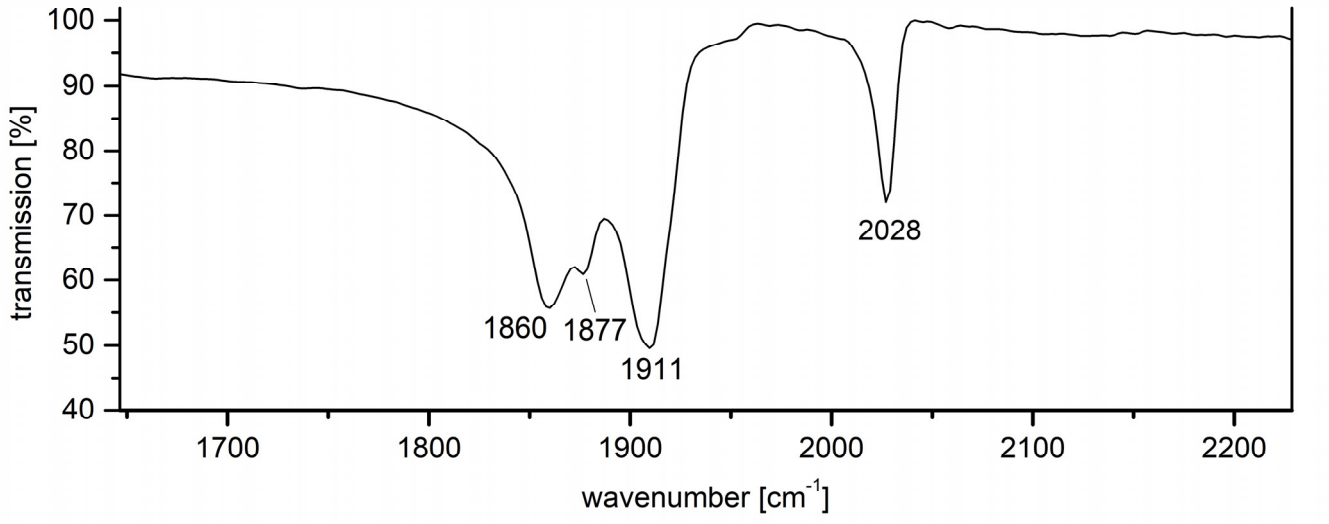

Figure S36. Detailed view of CO vibrations area in IR spectrum of compound **5** acquired by measurement of an isolated crystal.

SUPPORTING INFORMATION

References

[1] B. Wrackmeyer, C. Köhler, W. Milius, J. M. Grevy, Z. García-Hernández, R. Contreras, *Heterat. Chem.* **2002**, *13*, 667.
[2] L. Hintermann, *Beilstein J. Org. Chem.* **2007**, *3*, 22.
[3] O. Santoro, A. Collado, A. M. Z. Slawin, S. P. Nolan, C. S. J. Cazin, *Chem. Commun.* **2013**, *49*, 10483.
[4] G. Sheldrick, *Acta Cryst. Sect. C* **2015**, *71*, 3.
[5] G. R. Fulmer, A. J. M. Miller, N. H. Sherden, H. E. Gottlieb, A. Nudelman, B. M. Stoltz, J. E. Bercaw, K. I. Goldberg, *Organometallics* **2010**, *29*, 2176.

Author Contributions

Experimental work, as well as evaluation of the obtained data and writing of the original draft was done by Felix S. Geitner. Dr. Wilhelm Klein did parts of the crystal structure refinements. Prof. Dr. Thomas F. Fässler is principle investigator and was responsible for funding acquisition and project administration.

6 Complete List of Publications

Publications

[1] **F. S. Geitner**, W. Klein, T. F. Fässler, „*Synthesis and Reactivity of Multiple Phosphine-Functionalized Nonagermanide Clusters*", *Angew. Chem. Int. Ed.* **2018**, *57*, 14509.

[2] **F. S. Geitner**, C. Wallach, T. F. Fässler, „*On the Variable Reactivity of Phosphine-Functionalized [Ge_9] Clusters – Zintl Cluster-substituted Phosphines or Phosphine-substituted Zintl Clusters*", *Chem. Eur. J.* **2018**, *24*, 4103.

[3] **F. S. Geitner**, T. F. Fässler, „*Low oxidation state silicon clusters – synthesis and structure of [$NHC^{Dipp}Cu(\eta^4\text{-}Si_9)]^{3-}$*", *Chem. Commun.* **2017**, *53*, 12974.

[4] **F. S. Geitner**, J. V. Dums, T. F. Fässler, „*Derivatization of Phosphine Ligands with Bulky Deltahedral Zintl Clusters – Synthesis of Charge Neutral Zwitterionic Tetrel Cluster Compounds [$(Ge_9\{Si(TMS)_3\}_2)^tBu_2P]M(NHC^{Dipp})$ (M: Cu, Ag, Au)"*, *J. Am. Chem. Soc.* **2017**, *139*, 11933.

[5] **F. S. Geitner**, M. A. Giebel, A. Pöthig, T. F. Fässler, „*N-Heterocyclic Carbene Coinage Metal Complexes of the Germanium-Rich Metalloid Clusters $[Ge_9R_3]^-$ and $[Ge_9R^I_2]^{2-}$ with $R = Si(^iPr)_3$ and $R^I = Si(TMS)_3$*", *Molecules* **2017**, *22*, 1204.

[6] **F. S. Geitner**, W. Klein, T. F. Fässler, „*Formation of the intermetalloid cluster $[AgSn_{18}]^{7-}$ – the reactivity of coinage metal NHC compounds towards $[Sn_9]^{4-}$*", *Dalton Trans.* **2017**, *46*, 5796.

[7] L. J. Schiegerl, **F. S. Geitner**, C. Fischer, W. Klein, T. F. Fässler, „*Functionalization of [Ge_9] with Small Silanes: $[Ge_9(SiR_3)_3]^{3-}$ (R: iBu, iPr, Et) and the Structures of $(CuNHC^{Dipp})[Ge_9\{Si(iBu)_3\}_3]$, $(K\text{-}18c6)Au[Ge_9\{Si(iBu)_3\}_3]_2$, and $(K\text{-}18c6)_2[Ge_9\{Si(iBu)_3\}_2]$"*, *Z. Anorg. Allg. Chem.* **2016**, *642*, 1419.

[8] **F. S. Geitner**, T. F. Fässler, „*Introducing Tetrel Zintl Ions to N-Heterocyclic Carbenes – Synthesis of Coinage Metal NHC Complexes of $[Ge_9\{Si(SiMe_3)_3\}_3]^-$*", *Eur. J. Inorg. Chem*. **2016**, 2688.

Conference Contributions

[1] Low Oxidation State Silicon Clusters – Synthesis and Structure of $[NHC^{Dipp}Cu(\eta^4\text{-}Si_9)]^{3-}$
F. S. Geitner, T. F. Fässler
Poster, 18th International Symposium on Silicon Chemistry 2017 in Jinan, China.

[2] Reactivity of tetrel *Zintl* Cluster Anions towards Coinage Metal NHC Compounds
F. S. Geitner, T. F. Fässler
Poster, 18. Vortragstagung der Wöhler-Vereinigung für Anorganische Chemie 2016, Berlin.